

PROCEEDINGS
VETERINARY PATHOLOGY SERVICE
WEDNESDAY SLIDE CONFERENCE
2015-2016



JOINT PATHOLOGY CENTER
SILVER SPRING, MD 20910
2016

JOINT PATHOLOGY CENTER
VETERINARY PATHOLOGY SERVICE

Joint Pathology Center
Wednesday Slide Conference 2015-2016

Conference 1		9 September 2015				
Case	JPC No.	Slide ID No.	Species	Lesion / condition	Tissue	Page
1	3167631	09-A-471	NHP, Rhesus macaque	Mucinous adenocarcinoma	Colon	1
2	4066309	15-0022	NHP, African green monkey	Mesenteritis, abdominal abscess (<i>Klebsiella pneumoniae</i>)	Mesentery/ abdomen	6
3	4065942	14-144	Sheep	Venous thrombophlebitis (<i>Pseudomonas aeruginosa</i>)	Jugular vein	10
4	4049056	D12-33071	Dog	Hydatid cysts (<i>E. multilocularis</i> larvae)	Liver	15
Conference 2		16 September 2015				
1	4050459	B15-894	Dog	Sertoli tumor and squamous metaplasia	Testicle/Prostate	23
2	3164421	S09-1502	Cat	Herpesvirus pneumonia	Lung	26
3	3169265	08-2379-7	Cat	Tularemia	Spleen	31
4	4066360	B14-182	Dog	Fungal mastitis; (<i>Zygomycetes</i> or <i>Pythium</i>)	Mammary	34
Conference 3		23 September 2015				
1	4066661	8482-15	Ox/Calf	Brucellosis abortion	Placenta	38
2	3165093	NCAH 2010-2	Deer	<i>Pasteurella multocida</i> pneumonia	Lung	42
3	4032719	13-11676	Elk	Myonecrosis	Skeletal muscle	45
4	4066795	21-Jan-09	Horse	Pulmonary silicosis	Lung	49
Conference 4		30 September 2015				
1	4066007	15H672	Cat	Adenocarcinoma	Trachea	54
2	4066222	13-338	Dog	<i>Neospora caninum</i> encephalitis	Cerebellum / Brainstem	56
3	4065318	14-May-98	Cat	<i>Tritrichomonas foetus</i> colitis	Large intestine	61
4	4066091	D15-6096	Dog	Canine adenovirus 2	Pancreas / Lung	63
Conference 5		7 October 2015				
1	4065817	060377-1	Horse	Squamous cell carcinoma	Prepuce	71
2	4066859	14-42715	Cat	Pulmonary fibrosis	Lung	75
3	4032912	12-269-84	Rat	<i>Capillaria hepatica</i>	Liver	79
4	4066359	N14-367	Pig	Porcine reproductive and respiratory syndrome	Lung	84
Conference 6		28 October 2015				
1	4018127	NCAH-2012B	Raccoon	Cystic endometrial hyperplasia	Uterus	89
2	4048928	E274/14	Parrot	<i>Chlamydia psittaci</i> hepatitis	Liver	93
3	4066233	A	Duck	<i>Leukocytozoon</i> spp. encephalitis	Brain	96
4	4066459	N2015-0172 (Digital)	Toad	Nephroblastoma and <i>Mycobacterium</i> spp.	Kidney	101
Conference 7		4 November 2015				
1	4066676	2014 #1	Horse	<i>Trypanosoma evansi</i> encephalitis	Brain	106
2	4067274	E 4992/14	Horse	Mast cell tumor	Skin	113
3	4048653	E-6398-14	Horse	Equine herpesvirus-1	Lung, liver, adrenal gland	117
4	4001093	Case III	Horse	Interstitial and glomerulonephritis	Kidney	121
Conference 8		10-Nov-15				
1	4066249	14-292	Horse	<i>Clostridium novyi</i> hepatitis	Liver	129
2	4019891	TAMU-02 2012	Ox	Rabies virus	Brainstem	133
3	3133960	30334-08	Dog	Suprasellar germ cell tumor	Cerebrum	137
4	4067882	N 1241	Dog	Hereditary / Familial glomerulonephropathy	Kidney	142
Conference 9		18 November 2015				
1	4001570	E305-08A	Sheep	Ricketts	Rib bone	149
2	4052870	W361-13	Donkey	Osteopetrosis	Long bone	154
3	4053418	13073102	Rat	Intervertebral disc disease	Spinal column	160
4	4066452	26-Feb-83	Giraffe	Pigmented villonodular Tenosynovitis	Joint	165
Conference 10		2 December 2015				
1	4067275	S 696/14	Dog	Neuronal ceroid lipofuscinosis	Cerebellum	173
2	4048842	49052	Dog	Fibrocartilagenous emboli	Spinal cord	179

Joint Pathology Center
Wednesday Slide Conference 2015-2016

3	4048788	13-526	Cat	Hypertensive neuronal degeneration	Cerebrum	186
4	4067774	15 0160-21	Ox	White matter degeneration (dysmyelinogenesis)	Cerebellum	190
Conference 11	9 December 2015					
1	4066457	24-Sep-34	Deer	Follicular dysplasia	Skin	194
2	4066087	3140429021	Cat	Auricular chondritis	Pinna / skin	198
3	4033565	N9619660	Ferret	Piloileiomyosarcoma	Skin	202
4	4073336	B14-15532 (digital)	Dog	Post Grooming Furunculosis	Skin	205
Conference 12	6 January 2016					
1	3164430	A10-9691	Guinea pig	Teratoma	Ovary	209
			NHP, Cynomolgus macaque	Myocardial degeneration, cardiomyopathy	Heart	212
2	4001216	AFIP2				
3	4019441	870/2	Hare	<i>Yersinia pseudotuberculosis</i>	Cecum, liver	219
4	4066314	F1473713 (digital)	Rabbit	Phacitis, uveitis, <i>Encephalitozoon cuniculi</i>	Eye	222
Conference 13	13 January 2016					
		N2015-5055 (Digital)	Tetra	Dermocystidium spp. dermatitis	Skin	227
1	4066453					
2	4068374	35139	Atlantic Salmon	Amoebic gill disease	Gills	232
3	4067883	15-0816	Lumpfish	Microsporidiosis, <i>Nucleospora cyclopteri</i>	Kidney	238
4	4052876	10-9030	Goldfish	Cyprinid herpesvirus 2 renal necrosis	Kidney	244
Conference 14	20 January 2016					
1	4032259	AFIP case#1	Guinea pig	Myocardial mineralization, Vitamin D toxicity	Heart	248
2	4019884	CRL2	Rabbit	Enteritis; <i>E. coli</i> , coccidiosis	Cecum, small/large intestine	252
3	4033747	12A-892 (Digital)	NHP, Rhesus macaque	Simian virus 40 encephalitis	Cerebrum	256
4	4070249	RT13-623	Rat	Glomerulonephropathy	Kidney	261
Conference 15	27 January 2016					
1	4002480	33177-A	Red Cardinal	Trematode, <i>Collyriclum faba</i> dermatitis	Skin	267
2	4066922	15-0608	Opossum	Leptospirosis nephritis, Besnoitia spp. protozoal cysts	Kidney	271
3	4068934	V15-04651	Iguana	Bacterial endocarditis (<i>Neisseria meningitidis</i>)	Heart	275
4	4066312	E6400/14	Harbor seal	Bronchointerstitial pneumonia; influenza A, bacterial, larval nematodes	Lung	280
Conference 16	3 February 2016					
1	4065722	15-0021	NHP, Rhesus macaque	Cytomegalovirus radiculitis	Spinal cord	287
2	4070246	MK14-5429	NHP, Patas monkey	Exogenous lipid pneumonia	Lung	291
3	3167218	S 1215/09	Rabbit	Herpes simplex virus encephalitis	Cerebrum	295
4	4068766	14-062 (Digital)	Mouse	Pulmonary botryomycosis & eosinophilic crystalline pneumonia	Lung	299
Conference 17	10 February 2016					
1	4033379	TAMU-1-2013	Horse	Neonatal isoerythrolysis	Liver	304
2	4065767	A15-9631 (Digital)	Horse	Serum hepatitis / Theilers disease	Liver	309
3	4066679	705-14	Dog	Leishmaniasis	Spleen / Bone marrow	313
4	4066536	21966 (Digital)	Dog	Malignant neoplasm, (Balloon cell melanoma)	Gingival mass cytology	321
Conference 18	23 March 2016					
1	4017817	12 599	Chicken	<i>Clostridium perfringens</i> necrotizing enteritis,	Small intestine	325
2	4066088	T15-9947	Dog	<i>Hepatozoon americanum</i> myocarditis	Heart	328
3	4069358	14183	Cat	Nephritis; Lily toxicity	Kidney	332
4	4070541	0561-15	Cat	Gastric eosinophilic sclerosing fibroplasia	Stomach	337
Conference 19	30 March 2016					

Joint Pathology Center
Wednesday Slide Conference 2015-2016

1	4002877	11-996	Dog	Hepatocutaneous syndrome	Liver	341
2	3174957	H06-002960	Horse	Equine infectious anemia	Liver	345
3	4071582	R15/72	Cat	Metastatic melanoma	Liver	350
4	4019862	12-0011	Cat	Cholangiocellular carcinoma	Liver	355
Conference 20	30 March 2016					
1	4048070	13-870	Dog	Cholesterolosis bulbi, retinal atrophy	Eye	362
2	4048848	9650463	Dog	Granulomatous / Necrotizing scleritis	Eye	365
3	4066796	12B2550	Cat	Chondrosarcoma (post traumatic ocular sarcoma)	Eye	370
4	4035591	NTU20-12-1750	Dog	Orbital meningioma	Eye	374
Conference 21	13 April 2016					
1	4070542	1888-15	Dog	Granulomatous meningoencephalitis	Brain, spinal cord	380
2	4035763	UFMG 1	Dog	Necrotizing meningoencephalitis	Cerebrum	385
3	4018117	11-123787	Deer	Neuroendocrine carcinoma	Brain	391
4	4067276	WHL 14317601 (Digital)	Squirrel	Bromethalin toxicity	Cerebrum, cerebellum	397
Conference 22	27 April 2016					
1	4017222	NIEHS-087	Mouse	Necrosuppurative hepatitis (<i>Burkholderia cepacia</i>)	Liver	403
2	4032917	AR07-025012	Rat, Fischer 344	Testicular interstitial cell tumor and LGL / mononuclear cell leukemia	Testicle	407
3	4067775	15-V587 (Digital)	Rat	Squamous papilloma of the Zymbals gland	Head, transverse section	412
4	4069626	EX 109	Rat	Pituitary adenoma; mammary fibroadenoma	Pituitary & mammary glands	415
Conference 23	7 May 2016					
1	4003029	G10-083313	Turkey	<i>Erysipelothrix rhusiopathiae</i> hepatitis	Liver	422
2	4035761	UFMG-2	Coimbra's titi / new world primate	<i>Entamoeba histolytica</i> colitis	Intestine	425
3	4066096	D14-043814	Yak	Renal lead toxicity	Kidney	430
4	4033979	PA5050	Goat	Polioencephalomalacia	Cerebrum	437
Conference 24	11 May 2016					
1	4069824	JPC WSC 1	Ox	Clostridial myocarditis (blackleg)	Heart	442
2	4017089	NF-11-604	Sheep	Mannheimia hemolytica pneumonia	Lung	448
3	4066678	2014 #2	Ox	<i>Actinomyces bovis</i> ; lumpy jaw	Maxilla	454
4	4066085	N14-17	Horse	<i>Actinobacillus equilli</i> nephritis	Kidney	459
Conference 25	18 May 2016					
1	4021637	H11-003673	Turkey	Turkey Hemorrhagic enteritis virus necrotizing splenitis	Spleen	463
2	3167330	10-01139	Cat	Feline infectious peritonitis pulmonary vasculitis	Lung	468
3	4048846	S 307/14	Dog	Canine distemper virus; <i>Nocardia veterana</i> encephalitis	Cerebellum, brainstem	474
4	4032260	11N2549	Dog	Canine parvovirus enteritis	Small intestine	481



WEDNESDAY SLIDE CONFERENCE 2015-2016

Conference 1

9 September 2015

CASE I: 09-A-471 (JPC 3167631).

Signalment: 26 year old intact male rhesus macaque (*Macaca mulatta*).

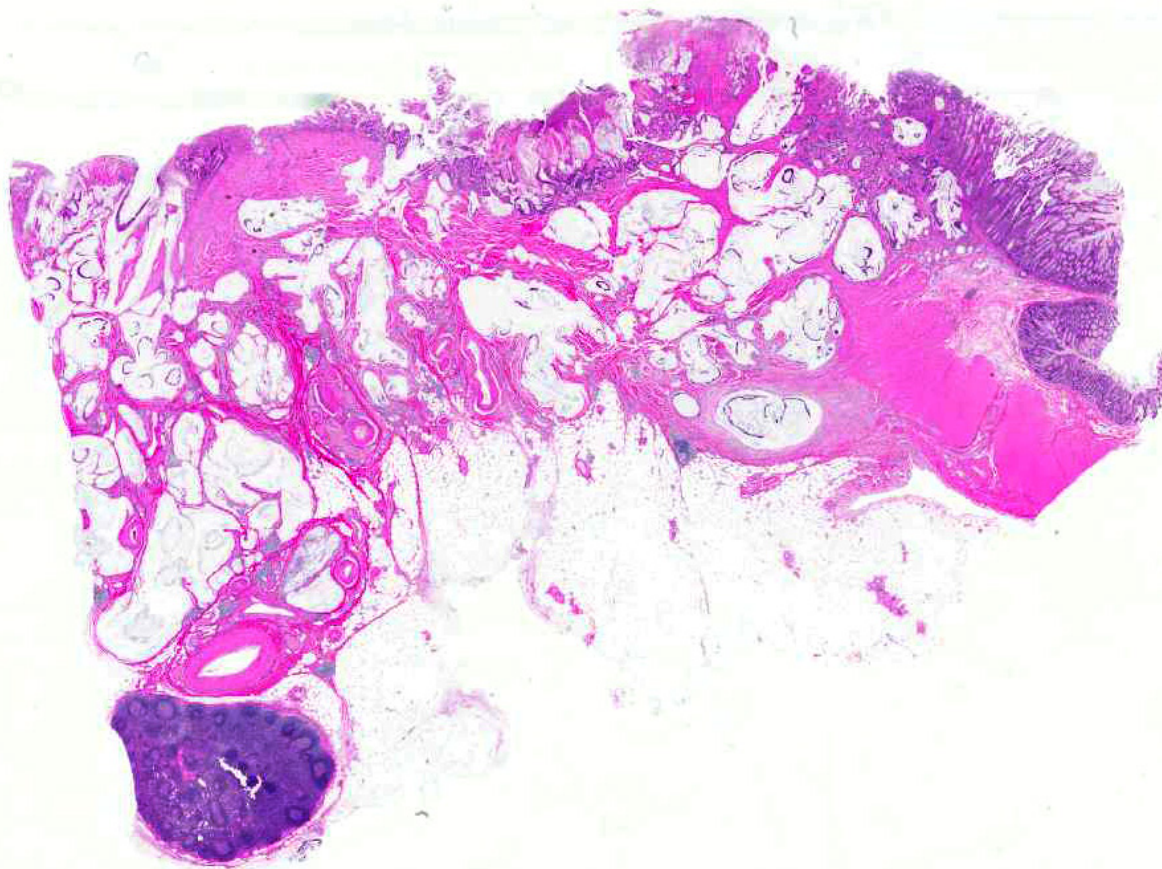
History: This animal was born at Oregon National Primate Research Center (ONPRC). A cardiac murmur and mild to moderate cardiomegaly were noted approximately one year prior to necropsy. Four months prior to necropsy, weight loss was reported and thickening of the cecocolic junction was noted on abdominal palpation. Hematology results demonstrated an iron deficiency anemia.

Gross Pathology: At necropsy, the animal was in good nutritional condition. The apex of the heart was rounded. The left atrium was pale and enlarged twice normal size.

The left atrioventricular valve was multifocally thickened with smooth, shiny, white nodules (endocardiosis). The endocardial surface of the left atrium was opaque, white and leathery. A pendulous red cystic mass was attached to the serosal surface of the jejunum and contained approximately 10 ml of blood. A white irregular mass was seen inside the cyst near



1-1. Circumferential thickening of intestinal wall by colonic adenocarcinoma resulted in narrowing of lumen. Note the mucosal ulceration and hemorrhage. (Photo courtesy of: Oregon National Primate Research Center <http://onprc.ohsu.edu>)



1-2 Colon, rhesus monkey. The colon is transmurally infiltrated by a multicystic epithelial neoplasm. (HE, 4X)

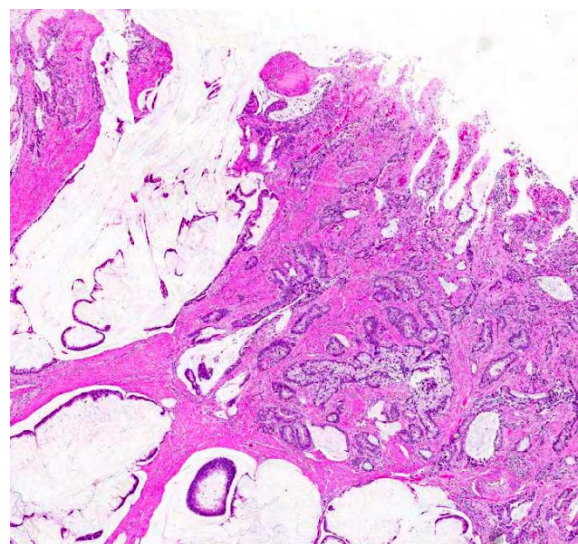
the point of attachment to the intestinal wall. A neoplasm measuring 2.5 cm in greatest dimension was present within the ascending colon. It narrowed the lumen and expanded the wall circumferentially and segmentally. The mucosa was multifocally ulcerated and hemorrhagic

intestinal wall is an unencapsulated, poorly circumscribed modestly cellular neoplasm. It is composed of epithelial cells arranged in tubules surrounded by a moderate reactive stroma (desmoplasia). Many neoplastic

Laboratory

Results:

	Value	Ref. Interval
WBC	6.5 x 10 ³ /μL	3.8 – 12.6 x 10 ³ /μL
RBC	5.34 x 10 ⁶ /μL	4.5-6.4 x 10 ⁶ /μL
MCV	60 fL	67-77 fL
MCH	18.4 pg	22.1- 25.84 pg
MCHC	30.6 g/dl	32.2 – 34.0 g/dl



1-2 Colon, rhesus monkey. Neoplastic glands which contain abundant mucus multifocally efface the disorganized and ulcerated mucosa. (HE, 35X)

Contributors Histopathologic Description:

Disrupting the mucosal epithelium, expanding and transmurally infiltrating the

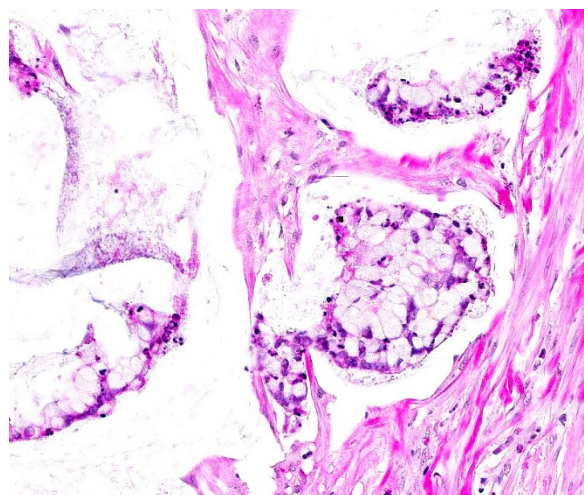
tubules are disrupted and appear as attenuated ribbons amid large lakes of mucin. The neoplastic cells exhibit marked anisocytosis and anisokaryosis, have distinct cell borders and a moderate amount of granular, eosinophilic cytoplasm. Nuclei are irregularly round to oval and vesiculate with one or two distinct nucleoli. The mitotic rate ranges from 1-3/HPF. There is extensive single cell necrosis of the neoplastic cells. An inflammatory infiltrate composed of lymphocytes, plasma cells, eosinophils and fewer neutrophils is associated with the neoplasm. The overlying mucosa is focally ulcerated. The mucosa adjacent to the neoplasm is proliferative with goblet cell hyperplasia. Multifocally crypts are dilated and contain moderate numbers of neutrophils.

Microscopic diagnoses of tissues not submitted:

Jejunum: Leiomyoma.

Heart:

1. Endocardiosis, right and left atrioventricular valves.
2. Myocardial necrosis, degeneration, mineralization, fibrosis.
3. Atrial subendocardial fibroelastosis, bilateral with jet lesion.



1-4. Colon, rhesus monkey. Neoplastic glands are lined by or contain a single layer of columnar epithelium admixed with abundant mucus and cellular debris. (HE, 256X)

Contributor's Morphologic Diagnosis:

Colon:

1. Adenocarcinoma, mucinous.
2. Colitis, proliferative, lymphoplasmacytic, eosinophilic, multifocal, marked with goblet cell hyperplasia and crypt abscesses.

Contributor's Comment: The primary findings in this case were mucinous colonic adenocarcinoma, jejunal leiomyoma and fibrosing myocardial necrosis. The hypochromic, microcytic anemia noted clinically was attributed to the hemorrhage in the ulcerated mucosa overlying the neoplastic mass.

The intestinal adenocarcinomas are classified according to histological features and include:

1. Papillary adenocarcinoma
2. Tubular adenocarcinoma
3. Mucinous adenocarcinoma
4. Signet ring cell adenocarcinoma

Intestinal adenocarcinoma is the most frequently diagnosed tumor of older macaques.^{4,5,11,12,15} A high prevalence of intestinal tumors at the ileocecal junction in aged animals (over 20 years) has been documented.^{11,12,13,14}

Intestinal neoplasms are rare in large animal species. Intestinal adenocarcinomas in dogs are seen in the proximal small intestine and large intestine. Regional metastasis to mesenteric lymph nodes may occur. Distant metastasis to the liver, spleen and lungs occurs less frequently. Boxers, collies, poodles and German shepherds are predisposed.²

In cats, intestinal adenocarcinoma is less common than lymphosarcoma. In sheep, the occurrence of intestinal adenocarcinomas is associated with ingestion of bracken fern and certain weeds. In cattle, intestinal adenocarcinoma is associated with bracken

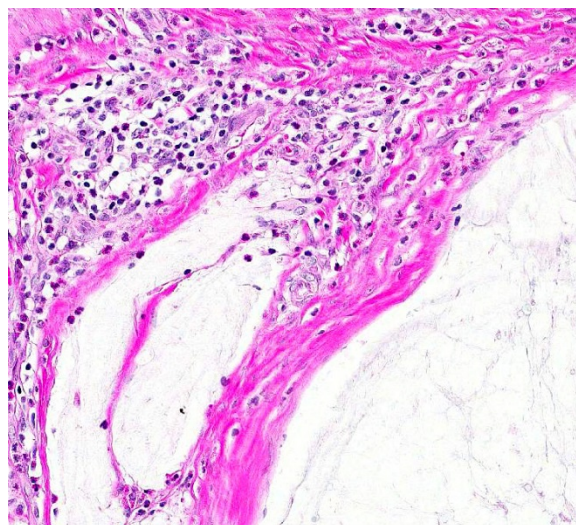
fern ingestion and bovine papillomavirus-4 infection and frequently metastasize to liver, lung, kidney, uterus and ovaries.² In contrast to other simian species, colonic carcinomas are frequently seen in cotton-top tamarins^{1,8} and has been linked to the high prevalence of chronic colitis in these animals.⁹

Although, the tumorigenesis has not been completely studied in non-human primates, long term feeding of a high-fat, low-fiber diet has been shown to cause pre-malignant alterations in African green monkeys.¹¹ A novel *Helicobacter* sp. has been isolated from inflamed colons of cotton-top tamarins, which are predisposed to developing inflammatory bowel disease (IBD) and colon cancer.¹³ Also, the colonic adenocarcinoma in rhesus monkeys has been linked to *Helicobacter macacae*.⁹ Mutation in *K-ras* has been observed in approximately 40 % of colonic adenocarcinoma of humans; however, no such mutations were recorded in macaques with intestinal adenocarcinoma.¹¹

JPC Diagnosis: Colon: Mucinous adenocarcinoma.

Conference Comment: Conference participants agreed that the histologic appearance of this neoplasm is distinctive, due in part to the presence of large lakes of mucin, and does not lend itself to a long differential diagnosis list; however, two candidate conditions for consideration include endometriosis and simian retrovirus induced peritoneal fibromatosis. Detailed features of the neoplastic cells were discussed with special mention of the basally located nuclei and prominent apical globules present within the cytoplasm. In addition to the description of the neoplastic cells, conference participants described the numerous secondary changes present within the colon including extensive goblet cell hyperplasia, inflammatory infiltrates within the colonic mucosa, as well as areas of ulceration and the presence of crypt abscesses.

Large intestine (LI) adenocarcinomas share many characteristics with their human counterparts and a recent study characterized the immunohistochemical profile of these tumors in the rhesus macaque. LI adenocarcinomas demonstrated a modification in the expression of one or more of the following markers: CD10, β -catenin, sirtuin 1, cytokeratin 17, and p53. Additionally, this study described the histologic characteristics of LI adenocarcinoma as having abundant mucin deposition, transmural spread and lymphatic invasion, the first two of which



I-5. Colon, rhesus monkey. Neoplastic glands are lined by or contain a single layer of columnar epithelium admixed with abundant mucus and cellular debris. (HE, 256X)

were described in this case.⁴

Participants also discussed the classic gross description of intestinal adenocarcinoma as having a “napkin ring-like” appearance due to constriction caused by the desmoplastic response elicited by the neoplasm, which is present in the excellent gross image provided by the contributor. The desmoplastic response is related to the interaction of tumor cells with the surrounding stroma via many types of mediators including cytokines and growth factors. One such mediator is platelet derived growth factor (PDGF), which stimulates fibroblasts and results in excessive production of collagen,⁷ often referred to as a scirrhous response. Tumor cells can have

various effects on stromal fibroblasts including causing them to differentiate into other types of mesenchymal cells, such as myofibroblasts, and inducing the production of cytokines that stimulate tumor growth, as well as stimulating them to de-differentiate and produce abnormal extracellular matrix. Growth factors are also sequestered within the stroma, and the actions of tumor cells can control their release.⁷ Intestinal adenocarcinoma is described in humans¹² and domestic animal species² as having a similar gross appearance, and the mucinous variant is indicative of a poorer prognosis due the mucinous excretions facilitating invasion through the intestine wall.¹²

As mentioned by the contributor, intestinal adenocarcinoma in sheep is thought to be at least partially related to the ingestion of bracken fern, or may be related to the application of fertilizers or herbicides.^{2,6} Bracken fern affects grazing animals throughout the world and causes a variety of syndromes ranging from neurologic and cardiac conditions in horses and pigs to enzootic hematuria in cattle and sheep. Bracken fern-induced neoplasia is most commonly associated with the urinary bladder and upper alimentary tract and is most often described in cattle, where it may also be associated with bovine papillomavirus-2. All parts of the plant are considered toxic and contain multiple toxins, including a thiaminase as well as multiple carcinogens, ptaquiloside being the most common.¹⁰ There is also a recent report of intestinal adenocarcinoma in farmed sika deer where bracken fern may have played a role, in combination with other factors.⁶ Intestinal carcinomas in sheep are more commonly located in the small intestine, and less commonly in the colon, and they are also associated with luminal constriction and a marked desmoplastic response. Intestinal adenocarcinomas in large domestic species other than sheep, and other than those associated with bracken fern or papillomavirus, are uncommon.²

Contributing Institution:

Oregon National Primate Research Center
<http://onprc.ohsu.edu>

References:

1. Barack M. Intestinal carcinomas in two tamarins (*Saguinus fuscicollis*, *Saguinus oedipus*) of the German Primate Center. *Lab. Anim.* 1988; 22(2): 14-147.
2. Brown CC, Baker DC, Barker IK. Alimentary system. In: Maxie MG, ed. *Jubb, Kennedy and Palmer's Pathology of Domestic Animals*. 5th ed. Vol 3. Philadelphia, PA: Saunders, Elsevier; 2007:1-106.
3. DePaoli A, McClure HM. Gastrointestinal neoplasms in nonhuman primates: a review and report of eleven new cases. *Vet Pathol Suppl.* 1982;7:104-25.
4. Harbison CE, Taheri F, Knight H, Miller AD. Immunohistochemical characterization of large intestinal adenocarcinoma in the rhesus macaque (*Macaca mulatta*). *Vet Pathol.* 2015;52(4):732-740.
5. Johnson EH, Morgenstern SE, Perham JM, Barthold SW. Colonic adenocarcinoma in a rhesus macaque (*Macaca mulatta*). *J Med Primatol.* 1996;25:435-8.
6. Kelly PA, Toolan D, Jahns H. Intestinal adenocarcinoma in a herd of farmed sika deer (*cervus nippon*): a novel syndrome. *Vet Pathol.* 2015;52(1): 193-200.
7. Kusewitt DF. Neoplasia and Tumor Biology. In: Zachary JF, McGavin MD, eds. *Pathologic Basis of Veterinary Disease*. 5th ed. St. Louis, MO: Elsevier; 2012:303-304.
8. Liu CH, Chen YT, Wang PJ, Chin SC. Intestinal adenocarcinoma with pancreas and lymph node metastases in a captive cotton-top tamarin (*Saguinus oedipus*). *J Vet Med Sci.* 2004; 66:1279-1282.
9. Marini RP, Muthupalani S, Shen Z, Ellen M, Buckley EM, Alvarado C, et al. Persistent infection of rhesus monkeys with *Helicobacter macacae* and its isolation from an animal with intestinal adenocarcinoma. *J Med Microbiol.* 2010 Aug;59(Pt 8):961-9.

10. Newman SJ. The Urinary System. In: Zachary JF, McGavin MD, eds. *Pathologic Basis of Veterinary Disease E edition*. 5th ed. St. Louis, MO: Elsevier; 2012:652.
11. O'Sullivan MG, Carlson CS. Colonic adenocarcinoma in rhesus macaques. *J Comp Path*. 2001; 124:212-215.
12. Rodriguez NA, Garcia KD, Fortman JD, Hewett TA, Bunte RM, Bennett BT. Clinical and histopathological evaluation of 13 cases of adenocarcinoma in aged rhesus macaques (*Macaca mulatta*). *J Med Primatol*. 2002; 31:74-83.
13. Saunders KE, Shen Z, Dewhirst FE, Bruce J, Paster BJ, Dangler CA, et al. Novel intestinal *Helicobacter* species isolated from cotton-top tamarins (*Saguinus oedipus*) with chronic colitis. *J Clin Microbiol*. 1999; 37(1):146-151.
14. Uno H, Alsum P, Zimbric ML, Houser WD, Thomson JA, Kemnitz JW. Colon cancer in aged captive rhesus monkeys (*Macaca mulatta*). *Am J Primatol*. 1998; 44:19-27.
15. Valverde CR, Tarara RP, Griffey SM, Roberts JA. Spontaneous intestinal adenocarcinoma in geriatric macaques (*Macaca* sp.). *Comp Med*. 2000; 50:540-4.

CASE II: 15-0022 (JPC 4066309).

Signalment: Two-year-old, intact male African green monkey (*Cercopithecus aethiops*).

History: The animal was wild caught on St. Kitts. It was part of a group of 22 African green monkeys brought to the institution on 12/17/2014. Health records from vendor indicated heavy growth of *Klebsiella pneumoniae*. All were treated with enrofloxacin at the vendor. The first quarantine exam on 12/22/14 was unremarkable. Decreased appetite was noted on 12/30/14, and it continued to decrease with marked weight loss. Physical examination on 1/2/14 revealed a large, firm mass in the right cranial abdomen. Abdominal fluoroscopy

and CT scan revealed a loss of serosal detail mid-abdomen, with a mass effect with intestines displaced cranially and caudally.

Gross Pathology: A 4.5 x 3.5 x 2.2 cm firm, tan, irregular mass was present in the mesentery and involved the ileocecolic junction. Loops of duodenum, jejunum and colon were adhered to the mass and to themselves multifocally. The serosa of the intestinal loops was roughened, with multifocally light red discolorations. On cut section, 80% of the mass was firm, and tan to yellow. Multifocally, there were half a dozen irregular cavitations, which varied in size from 3-8mm in diameter. These were filled with mucoid white to yellow material. On the left medial lobe of the liver, along the diaphragmatic surface, there was a focal, 15x5 mm pale tan, irregular, flat and friable area.

A 4.5 cm x 1 mm tan nematode was present free within the stomach (*Physaloptera* sp, presumptive).

Embedded within the mucosa of the cecum were half a dozen tan nematodes, 4.5-5cm x 0.5mm diameter with anterior filamentous ends (consistent with *Trichuris* sp).

Laboratory Results: The CBC was within normal limits with the exception of moderate numbers of reactive lymphocytes and moderate numbers of neutrophils with basophilic cytoplasm. The chemistry panel was within normal limits. Urinalysis revealed moderate blood, ketonuria, mild proteinuria, and large numbers of calcium oxalate crystals.

Hypermucoviscosity (HMV) variant of *Klebsiella pneumoniae* was isolated from the abscess and rectal and oropharyngeal swabs.



2-1. Peritoneal mass, African green monkey. A 4.5 x 3.5 x 2.2 cm firm, tan, irregular mass was present in the mesentery and involved the ileoceco-colic junction. Loops of duodenum, jejunum and colon were adhered to the mass (left). At right is a closer view of the excised mass. (Photo courtesy of: Laboratory of Comparative Pathology, Memorial Sloan-Kettering Cancer Center (www.mskcc.org/research-areas/programs-centers/comparative-medicine-pathology)).

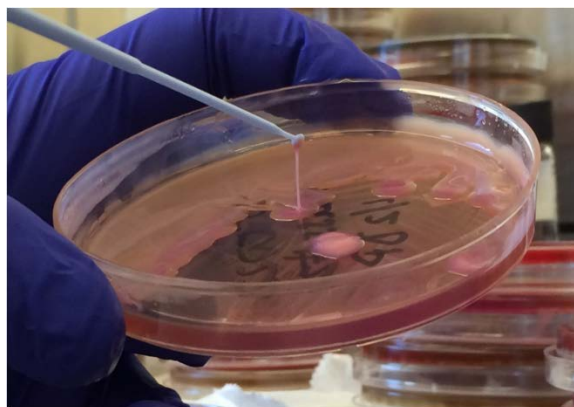
Histopathologic Description: Abdominal mass: The muscularis and serosa of the intestinal sections and adjoining mesenteric fat are obliterated and expanded by large areas of liquefaction necrosis, infiltrates of large numbers of degenerate neutrophils, macrophages, foamy macrophages, moderate numbers of lymphocytes and plasma cells admixed with eosinophilic proteinaceous material, fibrin, necrotic debris, and occasional hemorrhage and dissecting fibrosis. Many arteriolar walls in the mesentery are expanded by fibrillar eosinophilic material (fibrinoid necrosis). There are multifocal areas of liquefaction necrosis in the mesenteric lymph node, with infiltrates of large numbers of foamy macrophages and neutrophils (abscess), and proliferation of fibrous connective tissue that extend to the mesentery. Within the cytoplasm of macrophages and freely within the necrotic debris, there are large numbers of bacterial rods with a clear thick capsule.

The intestinal mucosa is multifocally infiltrated by moderate numbers of lymphocytes and plasma cells, with fewer eosinophils.

Contributor's Morphologic Diagnosis: Abdominal mass: Severe, locally extensive, chronic necrosuppurative and histiocytic mesenteritis, lymphadenitis and enterocolitis with abscess formation and myriad intrahistiocytic and extracellular encapsulated rod-shaped bacteria.

Contributor's Comment: Gross and microscopic examination revealed a locally extensive chronic abscess involving the mesenteric lymph nodes, small and large intestines and mesentery with large numbers of intrahistiocytic and free bacterial rods containing a thick capsule. Hypermucoviscosity (HMV) variant of *Klebsiella pneumoniae* was isolated from the abscess and rectal and oropharyngeal swabs. The invasive HMV phenotype of *Klebsiella pneumoniae* has been associated with multisystemic abscesses, and especially abdominal abscess in African green monkeys.^{10, 1}

Klebsiella pneumoniae is a gram-negative, aerobic, nonmotile bacillus and is a common

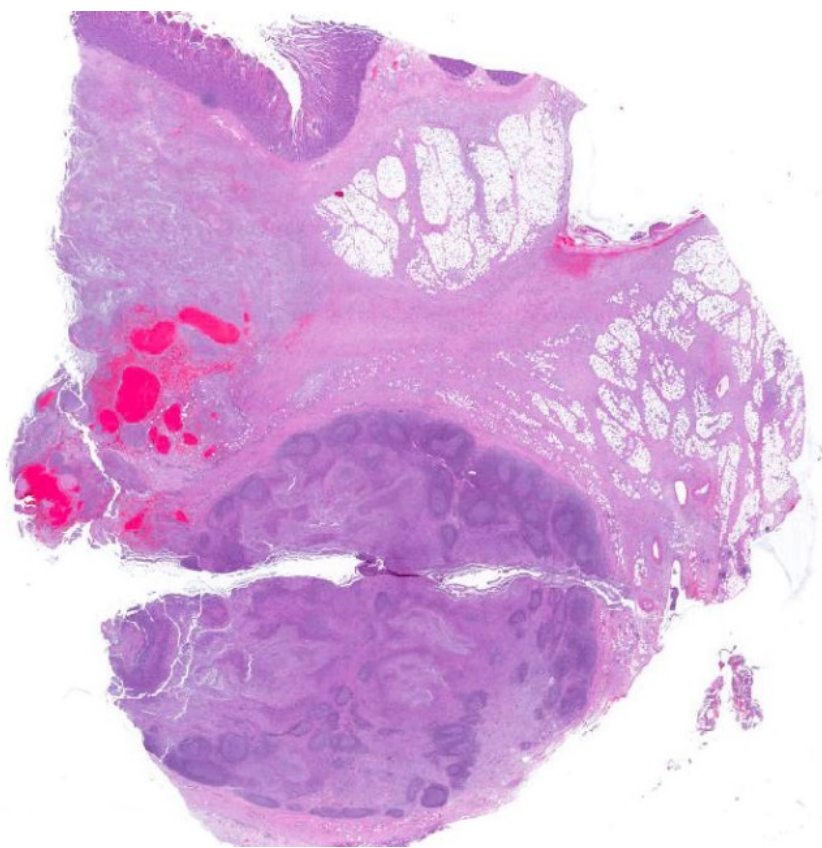


2-2 Bacterial culture, African green monkey. Demonstrating the “string test” associated with the hypermucoviscosity (HMV) variant of *Klebsiella pneumoniae*. (Photo courtesy of: Laboratory of Comparative Pathology, Memorial Sloan-Kettering Cancer Center (www.mskcc.org/research-areas/programs-centers/comparative-medicine-pathology)).

cause of a wide range of infections in humans and animals. In Old and New World monkeys, infection with *K. pneumoniae* causes pneumonia, meningitis, peritonitis, cystitis, and septicemia.⁸ *K. pneumoniae* also constitutes normal fecal and oral flora in many nonhuman primates. In the past 2 decades, a new type of invasive *K. pneumoniae* disease has emerged in humans in Taiwan and other Asian countries, and more recently from non-Asian countries, including the USA.⁴ Fatal human infections with invasive strains of *K. pneumoniae* involve pulmonary emboli or abscess, meningitis, endophthalmitis, osteomyelitis, or brain abscess.⁴ Recently, a highly invasive *K. pneumoniae* causing primary liver abscesses in humans has also been reported.⁵ These invasive, abscess-forming strains of *K. pneumoniae* are associated with the so-called hypermucoviscosity (HMV) phenotype, a bacterial colony trait identified by a positive string test (>5mm

string length).³ These *Klebsiella* spp. generally develop prominent polysaccharide capsules which increase virulence by protecting the bacteria from phagocytosis and preventing destruction by bactericidal serum factors.

The HMV phenotype is seen in *K. pneumoniae* expressing either the capsular serotypes K1 or K2. K1 serotypes of *K. pneumoniae* have 2 potentially important genes, *rmpA*, a transcriptional activator of colanic acid biosynthesis, and *magA*, which encodes a 43-kD outer membrane protein. K2 serotypes of *K. pneumoniae* also have *rmpA* but do not have *magA*. Capsular serotypes K1 and K2 are reported to play an important role in the invasive ability of HMV *K. pneumoniae*. The role of *rmpA* and *magA* in the pathogenesis of invasive *K. pneumoniae*, however, seems less certain.¹¹



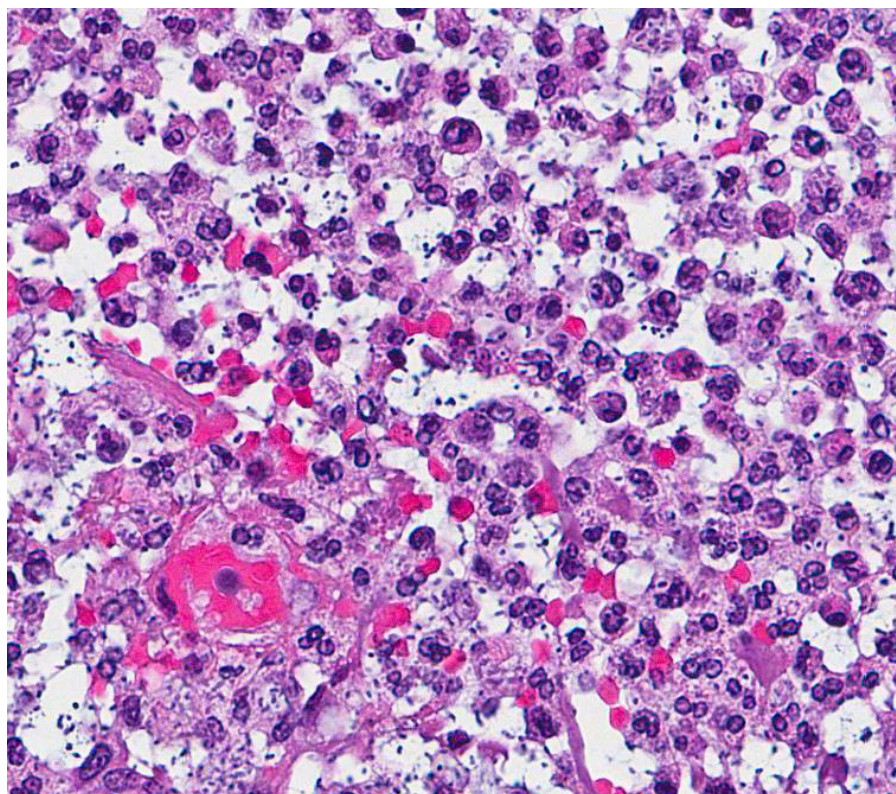
2-3. Peritoneal mass, African green monkey. A large adhesion incorporating the jejunum (top), mesentery, and mesenteric lymph node (bottom). There are multiple areas of necrosis and inflammation within the mesentery and lymph node (arrows.) (HE, 4X).

JPC Diagnosis: Intestine, lymph node, mesentery: Enterocolitis, lymphadenitis, peritonitis, pyogranulomatous and necrotizing, chronic-active, multifocal, marked with myriad intra and extracellular bacilli.

Conference Comment: Conference participants commented on slide variability with some slides containing a section of large intestine and others having small intestine. This is consistent with the excellent gross images provided by the contributor, consisting of overlapping sections of small and large intestine enmeshed within a focally extensive abscess. A gram stain was viewed during the conference, revealing histiocytes with abundant intracellular gram negative rods and a prominent capsule; however, in many cases similar features were readily visible on H&E. Participants discussed other stains which would facilitate visualization of the bacterial capsule, including mucicarmine. There was agreement the appearance of a gram negative bacillus with a large clear

capsule is distinctive for *Klebsiella* sp.; however, one differential diagnosis mentioned for this lesion was melioidosis. Melioidosis, caused by the gram negative bacterium *Burkholderia pseudomallei*, afflicts humans and many animal species including non-human primates, resulting in a wide range of disease manifestations. It is uncommon in North America, but has been associated with primates imported from endemic areas. Clinical and pathologic findings are often non-specific, resembling a bacterial septicemia, but abscesses can be seen in multiple tissues.⁹

Two conference participants (co-authors on the Twenhafel et al. manuscript) referenced below, discussed in detail the events surrounding the cases described in that publication. At the time of that report, African green monkeys presenting initially with extensive mid-abdominal abscessation (and less commonly in other body systems), caused by hypermuco-viscosity *K. pneumo-*



2-4. Mesentery, African green monkey. Areas of pyogranulomatous inflammation contain large numbers of bacilli which are surrounded by a thick capsule. Bacilli have been phagocytized by both neutrophils and macrophages. (HE, 400X).

niae was a novel finding.¹⁰ Since, work has been done to characterize the hypermucoviscosity variant of *K. pneumoniae* as discussed in the contributor's comment. The source of infection remains unclear and requires further epidemiologic studies. However, in at least one report in co-housed infected rhesus and cynomolgus macaques, transmission was thought to be fecal-oral and not from environmental contamination.¹ Like the source, the pathogenesis is still debatable particularly in light of extensive abscess formation in the mid-abdominal cavity in many cases. Participants dis-

cussed possible pathways to include septicemia or other methods of bacterial translocation from the intestine lumen. Regardless, the hypermucoid variant of *K. pneumoniae* is better able to resist innate immune defenses, including oxidative killing, and is more cytotoxic to blood monocytes in African green monkeys, compared to the non-hypermucoid variant, likely playing an important role in the pathogenesis.²

Conference participants also discussed infections caused by non-hypermucoviscosity *K. pneumoniae* in different animal species to include: Neonatal septicemia and pneumonia in foals and, abortion and stillbirth in mares;⁶ mastitis in cattle; urinary tract infections in dogs; bronchopneumonia and polyserositis in guinea pigs; enterotyphlitis in rabbits; bacteremia, liver and kidney abscesses, pneumonia and myocarditis in mice; and abscesses in multiple locations in rats.⁷

Contributing Institution:

Laboratory of comparative pathology,
Memorial Sloan-Kettering cancer center

<https://www.mskcc.org/research-areas/programs-centers/comparative-medicine-pathology>

References:

1. Burke RL, Whitehouse CA, Taylor JK, Selby EB. Epidemiology of Invasive *Klebsiella pneumoniae* with Hypermucoviscosity Phenotype in a Research Colony of Nonhuman Primates. *Comp. Med.* 2009;59(6):589-597.
2. Cox BL, Schiffer H, Dagget G Jr, et al. Resistance of *Klebsiella pneumoniae* to the innate immune system of African green monkeys. *Vet Microbiol.* 2015;176(1-2):134-42.
3. Fang CT, Chuang YP, Shun CT, et al. A novel virulence gene in *Klebsiella pneumoniae* strains causing primary liver abscess and septic metastatic complications. *J Exp Med.* 2004;199: 697–705.
4. Lau YJ, Hu BS, Wu WL, et al. Identification of a major cluster of *Klebsiella pneumoniae* isolates from patients with liver abscesses in Taiwan. *J Clin Microbiol* 2000;38(1):412-414.
5. Lederman ER, Crum NF. Pyogenic liver abscess with a focus on *Klebsiella pneumoniae* as a primary pathogen: An emerging disease with unique clinical characteristics. *Am J Gastroenterol* 2005;100(2):322-31.
6. Maxie MG. *Jubb, Kennedy and Palmer's Pathology of Domestic Animals*. 5th ed. Vol 2. Philadelphia, PA: Saunders, Elsevier; 2007:131,632.
7. Percy DH, Barthold SW. *Pathology of laboratory rodents and rabbits*. 3rd ed. Ames, IA: Blackwell; 2007:64, 152, 229, 275.
8. Pisharath HR, Cooper TK, Brice AK, et al. Septicemia and Peritonitis in a colony of common marmosets (*Callithrix jacchus*) secondary to *Klebsiella pneumoniae* infection. *American association for laboratory animal science* 2005;44(1): 35-37.
9. Ritter JM, Sanchez S, Jones TL, et al. Neurologic melioidosis in an imported pigtail macaque (*Macaca nemestrina*). *Vet Pathol.* 2013;50(6):1139-44.
10. Twenhafel NA, Whitehouse CA, Stevens EL, et al. Multisystemic abscesses in African green monkeys (*Chlorocebus aethiops*) with invasive *Klebsiella pneumoniae*: identification of the hypermucoviscosity phenotype. *Vet Pathol* 2008;45:226–231.
11. Yeh KM, Kurup A, Siu LK, et al. Capsular serotype K1 or K2, rather than magA and rmpA, is a major virulence determinant for *Klebsiella pneumoniae* liver abscess in Singapore and Taiwan. *J Clin Microbiol.* 2007;45:466–471.

CASE III: 14-144 (JPC 4065942)

Signalment: 4 month old Dorset cross ewe (*Ovis aries*)

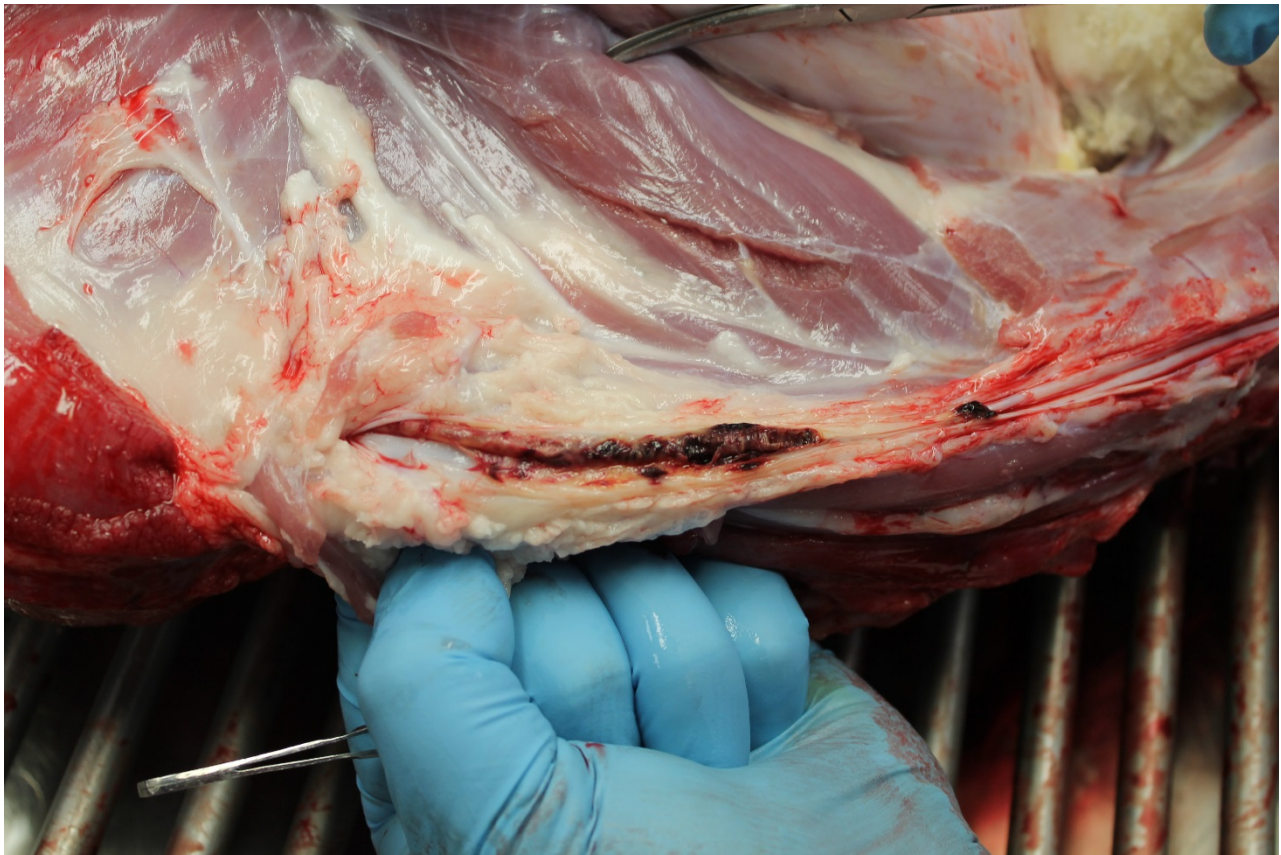
History: As part of an IACUC-approved experimental protocol, this lamb had a long term IV catheter in the right jugular vein. Catheter care included frequent bandage changes and cleaning of the catheter site with a chlorhexidine based solution. The catheter was replaced several times during the study, with aerobic bacterial cultures of the catheter tip when removed.

Gross Pathology: At necropsy, the right jugular catheter was encased in a thick coat of fibrin with enmeshed erythrocytes, which merged into the jugular wall (thrombophlebitis, figure 3-1). In the right caudal lung lobe, an adherent fusiform shiny tan thromboembolus, approximately 4 x 4 x 30

mm, largely occluded the lumen of the large pulmonary artery (figure 3-2).

Laboratory Results: There were multiple negative blood cultures and catheter cultures during the study (duration approximately 90 days). Two weeks prior to necropsy, the removed catheter grew a heavy pure culture of *Pseudomonas aeruginosa*. Additional cultures of blood surfaces at necropsy were positive for heavy pure growth of *P. aeruginosa*.

Histopathologic Description: Submitted tissue is right jugular vein (cross-section, opened longitudinally) and adjacent soft tissues. Adherent to the intima are two large nodular organizing septic thrombi, one with a central ovoid defect (catheter sheath). The two thrombi occlude >50% of the lumen. The thrombi contain large numbers of predominantly degenerate neutrophils and



3-1. Right jugular vein, sheep. The right jugular vein contains an indwelling catheter encase in a thick coat of fibrin. (Photo courtesy of: Department of Comparative Medicine, Penn State College of Medicine, Penn State Hershey Medical Center, <http://www.hmc.psu.edu/comparativemedicine/>)



3-2. Lung, sheep. A large thrombus (arrow), occludes the pulmonary artery within the right caudal lung lobe. (Photo courtesy of: Department of Comparative Medicine, Penn State College of Medicine, Penn State Hershey Medical Center, <http://www.hmc.psu.edu/comparativemedicine/>)

karyorrhectic debris as well as bacterial rods, often forming discrete lamellations separated by fibrin with abundant enmeshed erythrocytes. A Brown and Hopps tissue Gram stain identifies the rods as gram-negative, and they are often present in very large numbers. At the peripheral margins of both thrombi there is ingrowth of plump fibroblasts with scant immature collagenous matrix as well as new small caliber blood vessels lined by plump endothelium

(angiogenesis). There is partial and incomplete re-endothelialization of both thrombi. The venous wall is largely effaced by fibroplasia, with extension into adjacent adnexa. In some sections there is focally extensive recent hemorrhage in the venous media. Histology of the pulmonary artery thromboembolus (not submitted) was similar, including central canal.

Contributor's Morphologic Diagnosis:

Jugular vein: Thrombophlebitis, chronic-active, focally extensive, severe with Gram negative rods.

Contributor's Comment:

Inflammation or infection of the venous wall (phlebitis) is frequently complicated by thrombosis. Thrombosis results from antemortem intravascular coagulation, and must be differentiated from post-mortem clotting.^{2,5} Predisposing factors are described by the classic Virchow's triad of endothelial damage, turbulence or stasis of flow, and hypercoagulability. In this case, the presence of the catheter may potentially cause endothelial damage by direct physical injury, as well as turbulence by interrupting laminar flow. Both inflammation as well as endotoxin from gram-negative bacteria may



3-3 Right jugular vein, sheep. A large lamellated thrombus (arrow) is attached to the wall of the markedly thickened vein. (HE, 6X)



3-4. Right jugular vein, sheep. Higher magnification of the attached thrombus, showing lines of Zahn, as well as the central empty space where the catheter was located. There is extensive fibrin attaching this thrombus to the underlying wall of the vessel, and the endothelial lining is diffusely lost. (HE, 28X)

activate the coagulation cascade. Resolution of thromboemboli can occur by thrombolysis, organization (fibrosis and contracture) with re-endothelialization, and/or re-canalization.²

Jugular thrombophlebitis can be a significant problem in ruminants, both related to catheterization as well as perivascular administration of irritating solutions (such as 5% dextrose for ketosis or calcium gluconate for milk fever). Broken off fragments from the jugular site were able to travel to the right heart before lodging in a pulmonary artery (thromboembolism). The distinction between bland and septic thromboemboli can be of critical importance, as the latter may give rise to additional foci of infection, including embolic pneumonia or nephritis.

The inherent resistance of *Pseudomonas aeruginosa* to chlorhexidine-based disinfectants is well-documented.^{3,4} *Pseudomonas aeruginosa* is a normal inhabitant of water systems, and is therefore nearly ubiquitous in distribution. The organism is a significant cause of hospital acquired infections, often with a poor prognosis related both to the resistance of the organism to treatment as well as co-morbidities in the

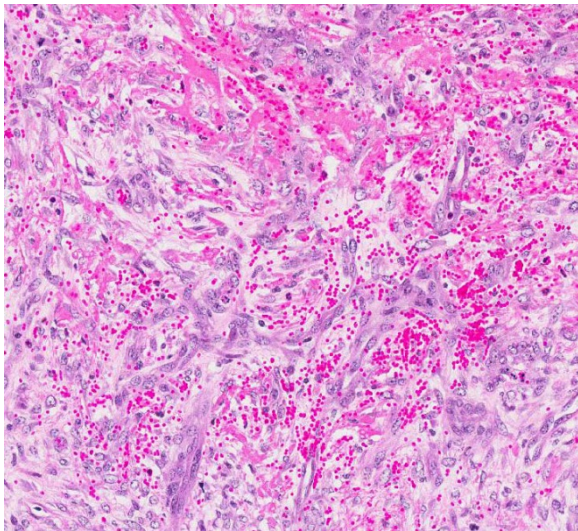
patients. *Pseudomonas aeruginosa* colonization of medical devices is facilitated by pili and fimbriae as well as biofilm formation, the latter making antibiotic treatment unrewarding.¹ Single blood cultures are frequently negative in cases of bacteremia, and frequent repeated large volume blood cultures have the

best success.

JPC Diagnosis: Jugular vein: Thrombophlebitis, fibrinosuppurative, chronic-active, focally extensive, with marked mural granulation tissue.

Conference Comment: Conference participants were impressed by the level of detail within the organizing thrombus, including the presence of lines of Zahn. These are more characteristically present in arterial thrombi and refer to the laminated appearance of the thrombus due to alternating layers of platelets and fibrin with enmeshed erythrocytes and leukocytes.² Most participants misinterpreted the vessel as an artery due to the thickness of the wall. Although they did not see an internal elastic lamina to confirm the vessel as an artery, most believed the vessel wall was too expanded by mural granulation tissue to allow its visualization. Participants described the clear area within the center of the larger thrombus but did not readily associate it with a catheter, and most agreed that while they considered the possibility of bacteria within the lesion, the abundant karyorrhectic debris made identification of microorganisms exceedingly difficult.

Hemostasis was reviewed in detail during the conference including a discussion of initiating events. While turbulent blood flow, a component of Virchow's triad, is clearly present with the placement of an intraluminal catheter, endothelial injury is also a very important factor in the formation of a thrombus. Endothelial injury results in the exposure of tissue factor, and other subendothelial components such as collagen, resulting in platelet aggregation and the initiation of coagulation. The release of tissue factor, located within the plasma membrane of activated endothelium, results in the initiation of the extrinsic coagulation



3-5. Right jugular vein, sheep. The wall of the jugular vein is diffusely thickened by granulation tissue. (HE, 240X)

pathway; the intrinsic pathway is initiated by collagen and other subendothelial components coming into contact with prekallikrein, high molecular weight kininogen and factors XII and XI (contact group of coagulation factors).² When tissue factor comes into contact with factor VII, it forms a complex which along with calcium, activates factor X to initiate the common pathway. While conceptually it is easier to learn and discuss the coagulation cascade as two separate pathways which combine to form the common pathway, the in vivo process is more commonly considered a single intertwined set of events that begins with the exposure of tissue factor.²

Participants reviewed the basic steps in the hemostatic process starting with vasoconstriction and formation of a platelet plug, followed by coagulation and formation of a fibrin meshwork, followed by fibrinolysis and finally tissue repair, and the role of platelets in this process was discussed. Platelets adhere to exposed subendothelial collagen and von Willebrand's factor is released by local activated endothelium, which provides a more secure connection between the collagen and platelets via platelet receptor GPIb. Platelets then release the contents of their α -granules and produce other mediators which continue to promote hemostasis. The release of adenosine diphosphate (ADP) results in the binding of fibrinogen to platelet receptor GPIIb-IIIa, and the fibrinogen forms a scaffold as the platelets aggregate, eventually covering the defect. Factors released from the aggregated platelets, such as platelet derived growth factor, stimulate fibroblast recruitment which can eventually result in fibrosis at the thrombus location, as occurred in this case.²

Contributing Institution:

Department of Comparative Medicine
Penn State College of Medicine
Penn State Hershey Medical Center
<http://www.hmc.psu.edu/comparativemedicine/>

References:

1. Laverty G, Gorman SP, Gilmore BF: Biomolecular Mechanisms of *Pseudomonas aeruginosa* and *Escherichia coli* Biofilm Formation. *Pathogens* 2014;3(3):596-632.
2. Mosier DA: Vascular Disorders and Thrombosis. In: McGavin MD, Zachary JF, eds. *Pathologic Basis of Veterinary Disease*. Fourth ed. St. Louis, Mo: Mosby Elsevier; 2007: 61-87.
3. Nakahara H, Kozukue H: Isolation of chlorhexidine-resistant *Pseudomonas aeruginosa* from clinical lesions. *J Clin Microbiol* 1982;15(1):166-168.

4. Oie S, Kamiya A: Microbial contamination of antiseptics and disinfectants. *Am J Infect Control* 1996;24(5):389-395.

5. van Vleet JF, Ferrans VJ: Cardiovascular System. In: McGavin MD, Zachary JF, eds. *Pathologic Basis of Veterinary Disease*. Fourth ed. St. Louis, MO: Mosby Elsevier; 2007: 559-611.

CASE IV: D12-33071 (JPC 4049056)

Signalment: 4 year-old, spayed female, Labrador retriever dog (*Canis lupis familiaris*)



4-1. Liver, dog. The liver was 2-3 times normal size and contained numerous cysts ranging up to 15cm within the hepatic parenchyma. (Photo courtesy of: Prairie Diagnostic Services (PDS) and Department of Veterinary Pathology, Western College of Veterinary Medicine, 52 Campus Drive, University of Saskatchewan, Saskatoon, Saskatchewan, S7N, 5B4, CAN www.usask.ca/wcvm/vetpath)

History: The dog presented to its primary care veterinarian for a two-month history of gradual, progressive weight loss and inappetence. In the two weeks prior to presentation, the owner had noted marked abdominal distention. On physical examination by the primary care veterinarian, the dog was reasonably bright but very thin, with severe muscle wasting. The abdomen was markedly distended and a fluid wave could be ballotted. In-house routine bloodwork revealed a mild anemia and

hypoalbuminemia. Abdominal ultrasonography revealed an intra-abdominal mass of mixed echogenicity that appeared to occupy several areas within the liver. Ultrasound-guided fine needle aspiration (FNA) cytology of the suspect hepatic lesion was attempted twice and yielded only necrotic debris. The primary care veterinarian was highly suspicious of a hepatic malignancy and referred the dog to a veterinary specialty center for further evaluation and probable exploratory laparotomy.

At the referral center, the dog was again noted to be thin (BCS 2/9) with severe muscle wasting. The abdomen was markedly distended by free fluid and there was a palpable fluid wave. The degree of abdominal distension hampered abdominal palpation for organomegaly. Three-view thoracic radiographs revealed mild lymphadenomegaly of the sternal lymph nodes. Presurgical routine blood work was performed (see results under 'Laboratory Results'). A coagulation profile was unremarkable.

An exploratory laparotomy was performed through a ventral midline incision and 3.5 liters of a red-tinged abdominal fluid was removed.

The liver was two to three times the normal size; firm to friable; and mottled red-brown and



4-2 Liver, dog. Fluid aspirated from the hepatic cysts. (Photo courtesy of: Prairie Diagnostic Services (PDS) and Department of Veterinary Pathology, Western College of Veterinary Medicine, 52 Campus Drive, University of Saskatchewan, Saskatoon, Saskatchewan, S7N, 5B4, CAN www.usask.ca/wcvm/vetpath)

tan. Multiple, variably sized, often raised nodules were present on the hepatic surface and extended into the hepatic parenchyma. The largest nodule was approximately 15.0 cm in diameter and involved almost the entirety of the right lateral liver lobe. A partial lobectomy was performed on the left lateral liver lobe. Not all of the abnormal hepatic tissue could be removed. Multiple, small, white nodules were present in the omentum, and the wall of proximal duodenum was thickened. A hepatic biopsy; the excised portion of the left lateral liver lobe; a section of omentum; and a full-thickness duodenal biopsy were submitted for histopathologic examination.

The dog recovered uneventfully from surgery and was discharged four days after the surgery to the primary care veterinarian for continued supportive therapy and monitoring.

Following the histopathologic diagnosis of alveolar echinococcosis, a fecal sample from the patient was submitted for fecal flotation examination. Parasite eggs were not identified.



4-3 Liver, dog. A wet mount prep of material aspirated from the cysts revealed protoscolices with an armed rostellum as well as aggregates of mineralized material (calciferous bodies) (400X)

The dog received a single treatment of albendazole after it returned to the primary care veterinarian. Unfortunately the dog's condition continued to decline and it died nine days after it was discharged. The owners gave their consent for a full postmortem examination.

Strict safety precautions were observed during the whole necropsy procedure. On gross examination, the body condition of the dog was poor with marked generalized muscle wasting; accentuation of all bony prominences (i.e. zygomatic arch, spine of scapula, ribs, tuber coxae); and depletion of subcutaneous and visceral adipose stores.

Gross Pathology: The gastrointestinal tract was removed after gross external examination and was frozen at -70° for three weeks to inactivate *Echinococcus* spp. eggs. It was thawed, dissected and the intestinal contents were examined for *Echinococcus* spp. Adult cestodes were not seen.

There was approximately one litre of serosanguinous fluid in the abdomen and small amounts of fibrin on the serosal surface of the intestines. Approximately 75% of the liver was replaced by multifocal to coalescing, variably raised, firm, yellow to brown masses that on cut section effaced the parenchyma, were occasionally cystic, and exuded moderate amounts pale yellow viscous fluid with white sand-like material (interpreted to be 'hydatid sand'; see mages 4-1 and 4-2). The hepatic lymph nodes, pancreas, and the adjacent mesentery contained numerous, small (approximately 4-mm in diameter) translucent cysts. The sternal, tracheobronchial, hepatic and mesenteric lymph nodes were moderately enlarged and dark black in color

Laboratory Results: A wet mount preparation of the viscous fluid from one of the cysts was examined microscopically and revealed metacestode larva and aggregates of mineralized material (calciferous bodies).

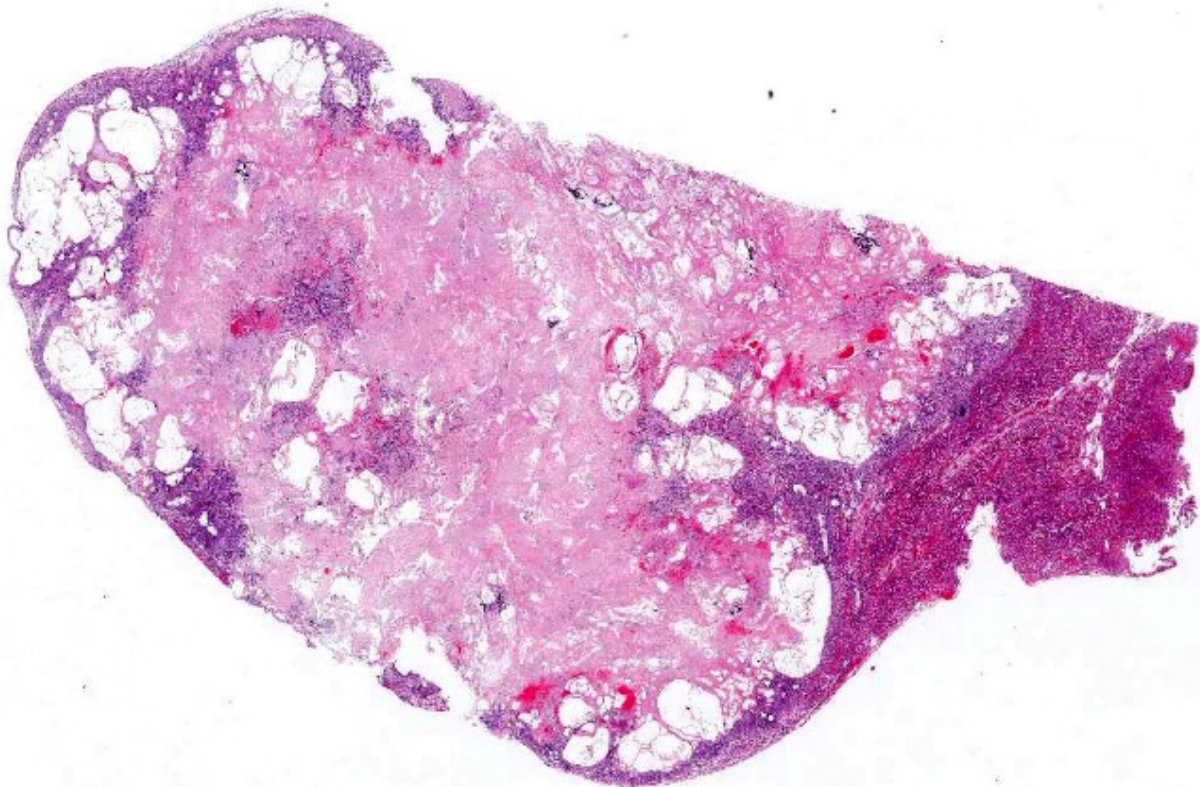
The cyst contents and abdominal fluid were submitted for PCR. Based on the band size, PCR for both of these samples was considered positive for *Echinococcus multilocularis*. PCR amplification and sequencing was performed on liver tissue using in-house primers developed by Dr. Karen Gesy for the *cob*, *cox1* and *nad2* mitochondrial genes; the alveolar hydatid cyst of *Echinococcus multilocularis* found in this dog grouped with European-type strains of the cestode.

Histopathologic Description:

Liver: Effacing and replacing approximately 70-90% of the examined sections were optically vacant areas with multiple hydatid cysts that were lined by a thin bladder wall and contained numerous calciferous bodies and metacestode protoscoleces that had a parenchymatous body, calcareous corpuscles, and rostellar hooks which were variably surrounded by large numbers of epithelioid macrophages, foreign body and Langhans-type giant cells, neutrophils, hemorrhage,

necrotic hepatocytes, and extensive areas of fibrosis. Multifocally, large numbers of degenerate neutrophils and necrotic cellular debris surrounded the hydatid cysts and occasional cysts were mineralized. In the surrounding parenchyma, hepatocytes frequently contained granular and globular intracytoplasmic, gold-brown material (interpreted to be hemosiderin and/or bile, respectively), clear vacuoles (vacuolar degeneration) and were separated and individualized by bands of fibrous connective tissue (fibrosis) and foamy and streaming eosinophilic material admixed with postmortem bacteria (autolysis artifact).

Lymph node (hepatic): Approximately 50-70% of the cortex and medulla in the examined sections were replaced and distorted by large optically vacant areas with small numbers of hydatid cysts containing metacestode protoscoleces and were surrounded by fibroblasts and collagen. There were marked numbers of hemosiderophages



4-4. Liver, dog. Approximately 80% of the section is replaced by a degenerate multilocular cyst characteristic of *Echinococcus multilocularis*. (HE, 4X)

in the subcapsular sinus and throughout the trabecular and medullary sinuses.

Mesentery: Multifocally, there were small numbers of collapsed hydatid cysts associated with extensive areas that were infiltrated by large numbers of fibroblasts, macrophages, giant cells, neutrophils, and fewer lymphocytes and plasma cells.

Pancreas: There were large optically vacant spaces and small numbers of protoscoleces were seen in these spaces.

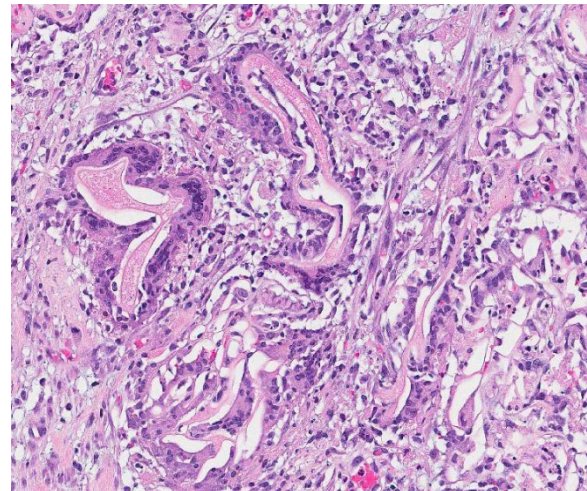
Contributor's Morphologic Diagnosis:

Left lateral liver lobe and liver biopsy: Multiple, intrahepatic, multilocular cysts with rare metacestode larva of *Echinococcus* spp. and accompanying macrophagic to mixed inflammation, necrosis and fibrosis.

Contributor's Comment: *Echinococcus multilocularis* is a zoonotic tapeworm and the cause of alveolar hydatid disease (aka: Alveolar echinococcosis) in people, dogs and other abnormal hosts; includes domestic and wild pigs, horses, and monkeys.^{5,7} *E. multilocularis* is found in Canada, the United States and Europe.^{5,7} The worldwide importance of the parasite has increased due to global travel and trade as well as changes in climate, landscape and wildlife-human interactions.⁵

The life cycle of *E. multilocularis* involves wild canids and rodents.⁷ The adult tapeworms live in the intestines of a carnivore (primarily foxes and to a lesser extent coyotes, wolves and wild felids) and produce eggs that are shed in the feces. Eggs passed in the feces of the definitive host are immediately infective for the intermediate hosts. Rodents (typically voles, lemmings and deer mice), the intermediate hosts, ingest the eggs which develop into a multilobed larval form (metacestode stage; hydatid cyst) in the liver and abdomen. The metacestode stage consists of aggregations of small vesicles (cysts) in which protoscoleces are

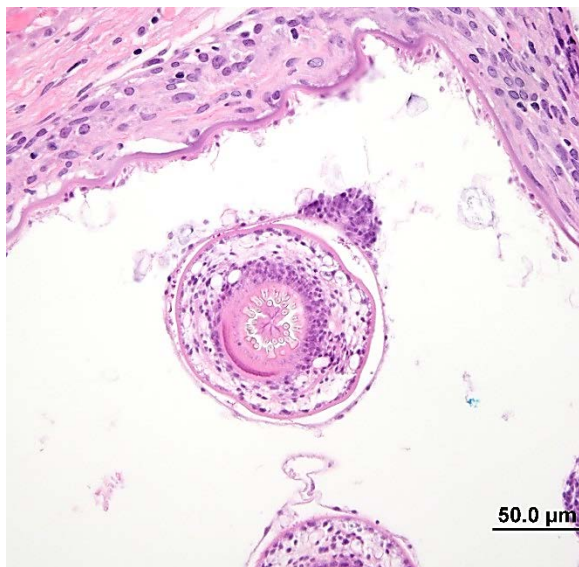
produced by the germinal layer in natural intermediate hosts. The cyst aggregates form alveolar structures composed of numerous cysts of irregular shapes with dimensions between less than 1 and 10mm (in some hosts up to 20–30 mm). The cysts contain a highly variable number of protoscoleces or they may be sterile (no protoscolex formation) and partially calcified. Progressive budding and expansion of the cyst causes severe tissue damage and may result in the spread of metacestodes to other tissues, as present in this case, where the metacestode stage was



4-5. Liver, dog. The hyaline wall of collapsed cysts are surrounded by multinucleated foreign body macrophages as well as numerous epithelioid macrophages. (HE, 196X)

found in the local lymph nodes, pancreas, and mesentery. The life cycle is completed when a carnivore ingests a rodent infected with the cyst stage of the parasite. Dogs, and less commonly cats, can be definitive hosts (i.e. adult tapeworm develops in the small intestine) when they ingest an infected rodent. Rarely, as in this case, the dog can act as an intermediate host (develop the metacestode larval stage) likely by ingesting eggs shed in the feces of wild carnivores, pets or even their own feces. People become infected with the larval stage when they ingest eggs in the soil; food or water contaminated with feces of wild carnivores or pets; or less commonly, through close association with infected animals.

Until 2009, *E. multilocularis* was considered to be endemic in wildlife in only two regions of Canada: the northern tundra zone of the Canadian territories and the southern Prairie Provinces, Manitoba, Saskatchewan and Alberta.^{3,8,9} Cases involving domestic dogs had not been reported in Canada. In 2009, hepatic alveolar hydatid disease (HAD) was diagnosed in a 3-year-old dog that had lived only in the British Columbia.^{8,9} In 2012, a second case of HAD was diagnosed in a 2-year-old dog that had resided in only two parts of southern Ontario.² This dog is the third case to be reported in a domestic dog in Canada. The dog was acquired from a breeder in north-eastern Alberta and lived most of its life in southern Alberta. The dog had brief visits to British Columbia (Vancouver Island) and Manitoba. At the time of its death the dog had been residing in southern Manitoba for a couple of months. While in southern Alberta the dog had plenty of opportunity to come in contact with the feces of wild carnivores. It is likely the dog acquired the infection while residing in southern Alberta.



4-6. Liver, dog. Rare viable cysts are lined by a 3-4μm hyaline wall, germinal epithelium, and protoscolices containing an armed rostellum. (Photo courtesy of: Prairie Diagnostic Services (PDS) Department of Veterinary Pathology, Western College of Veterinary Medicine, 52 Campus Drive, University of Saskatchewan, Saskatoon, Saskatchewan, S7N 5B4, Canada www.usask.ca/wcvm/vetpath) (HE, 200X)

Genetic analysis of tissue from the dogs in British Columbia and Alberta grouped with strains of *E. multilocularis* from west-Central Europe. The origin of the European-type strains of *E. multilocularis* in these Canada dogs is unclear but appears to be associated either with the importation of domestic dogs into Canada from Europe, since cestode treatment at the time of importation is not required or the historic importation of red foxes into North America from Europe for hunting and the fur trade.⁸

In Canada, human cases of alveolar hydatid disease are rare with a single case being reported in Manitoba in the 1930's. There is currently no evidence to suggest cases of alveolar hydatid disease are occurring in people in Canada. However, cases of alveolar hydatid disease in domestic dogs are not only of clinical interest, but also of epidemiological importance as they are indicators of environmental contamination with *E. multilocularis* eggs and likely represent the main infection route for humans in North America.^{5,7,6}

The antemortem diagnosis of alveolar hydatid disease in dogs is difficult. Spontaneously excreted proglottids are very small and are only occasionally detected on the surface of fecal samples by the animal owner or at laboratory examination. By flotation techniques taeniid eggs may be detected in fecal samples, but morphological differentiation of the eggs of *E. multilocularis*, *E. granulosus* and the *Taenia* species inhabiting the intestine of domestic dogs and cats is not possible.⁷ In routine practice, abdominal masses of unclear origin in dogs and other animals can be assessed by fine needle aspiration cytology for tumour identification or exclusion. In this case, ultrasound-guided fine needle aspiration cytology did not confirm a metacestode infection. Molecular diagnostics performed on fresh and formalin-fixed tissues, abdominal fluid and fluid samples from the

hepatic cysts did help to establish the diagnosis in this case and may be useful in establishing the antemortem diagnosis.

The post mortem diagnosis of alveolar hydatid disease in aberrant hosts is based on pathognomonic macroscopic and histopathologic findings, and in doubtful cases, on results of immunological and molecular tests. Although alveolar hydatid disease of the liver is rare in dogs, it should be considered as a possible differential diagnosis in cases of space-occupying lesions in the liver, even in a young dog.

JPC Diagnosis: Liver: Multilocular hydatid cysts, with granulomatous hepatitis and hepatocellular atrophy, Labrador retriever dog, canine.

Conference Comment: Conference participants mentioned the variability between slides, with only a few sections containing cysts with protoscolices. Most of the slides did have aggregates of germinal epithelium along the inner margin of the cyst wall, and there was speculation these structures represented parts of developing capsules which would contain protoscolices. Others considered the possibility that the cysts were sterile due to the dog being a non-traditional intermediate host for this cestode.

The differential diagnosis discussed by participants included cysticercosis, denoting the larval form of many *Taenia* genera cestodes, although most agreed the multiloculated nature of the cysts and the appearance of the laminated cyst wall was fairly distinctive for hydatid cysts despite the absence of protoscolices. Cysticerci (second stage taeniid larva) have a thick fluid filled bladder (hence the name “bladderworm”), one or more scolices which are usually inverted, and are often surrounded by a fibrous capsule formed by the intermediate host. The structure has a series of hooks and suckers that allow it to attach to host tissue.¹ See the table below for a list of taeniid

tapeworms with larval stages commonly found in mammalian intermediate hosts.

Echinococcus granulosus typically parasitizes wild canids as the definitive host, but the intermediate host is usually a large domestic species, such as cattle, sheep and horses among others. Wild canids pass the proglottids in areas where these animals graze, and upon ingestion the embryos develop into hydatid cysts. The cysts are most commonly found in the liver and lungs, although other organs can be infected; they may never result in clinical disease, but can result in carcass condemnation at time of slaughter.⁴ In contrast to *E. multilocularis*, hydatids of *E. granulosus* are unilocular in nature and do not infiltrate but rather expand and compress adjacent tissue as space occupying structures, and may rupture or leak fluid, causing a hypersensitivity reaction.¹ Hydatid sand refers to the cyst fluid containing free protoscolices from ruptured brood capsules, of which the contributor provides an excellent image.

Contributing Institution:

Prairie Diagnostic Services (PDS) and Department of Veterinary Pathology, Western College of Veterinary Medicine, 52 Campus Drive, University of Saskatchewan, Saskatoon, Saskatchewan, S7N 5B4, Canada. Websites: www.pdsinc.ca and www.usask.ca/wcvm/vetpath

References:

1. Bowman DD. *Georgis' Parasitology for Veterinarians*. 9th ed. St. Louis, MO: Saunders Elsevier; 2009:132, 140-145, 388-391.
2. Brooks A, Skelding A, Stalker M, et al. Alveolar hydatid disease (*Echinococcus multilocularis*) in a dog from southern Ontario. *AHL Newsletter*. Mar 2013;17(1)8.
3. Catalano S, Lejeune M, Liccioli S, et al. *Echinococcus multilocularis* in urban coyotes, Alberta, Canada. *Emerg Infect Diseases*. 2012;18(10):1625-1628.

4. Cullen JM, Brown DL. Hepatobiliary system and exocrine pancreas. In: Zachary JF, McGavin MD, eds. *Pathologic Basis of Veterinary Disease E edition*. 5th ed. St. Louis, MO: Elsevier; 2012:436.
5. Deplazes P and Eckert J. Veterinary aspects of alveolar echinococcosis- a zoonosis of public health significance. *Vet Parasitol* 2001;98:65-87.
6. Deplazes P, van Knapen F, Schweiger A, Overgaauw PAM. Role of pet dogs and cats in the transmission of helminthic zoonoses in Europe, with a focus on echinococcosis and toxocarosis. *Vet Parasitol*. 2011;182:41– 53.
7. Eckert J, Gemmell MA, Meslin FX, Pawłowski ZS. *WHO/OIE Manual on Echinococcosis in Humans and Animals: a Public Health Problem of Global Concern*. Paris:World Organisation for Animal Health (Office International des Epizooties; OIE) and World Health Organization (WHO); 2001.
8. Jenkins EJ, Peregrine AS, Hill JE, et al. Detection of European Strain of *Echinococcus multilocularis* in North America. Letter to editor. *Emerg Infect Diseases*. 2012;18(6):1011-1012.
9. Peregrine AS, Jenkins EJ, Barnes B, et al. Alveolar hydatid disease (*Echinococcus multilocularis*) in the liver of a Canadian dog in British Columbia, a newly endemic region. *Can Vet J*. 2012;53:870-874.

Cestodes of veterinary importance with gross and/or histologically identifiable larval stages (not comprehensive)				
ADULT CESTODE	DEFINITIVE HOST	LARVAL STAGE	INTERMEDIATE HOST (IH)	COMMON SITE for IH
<i>Taenia saginata</i>	humans	<i>Cysticercus bovis</i>	cattle	muscle
<i>Taenia solium</i>	humans	<i>Cysticercus cellulosae</i>	pig	muscle
<i>Taenia (Multiceps) multiceps</i>	canids	<i>Coenurus cerebralis</i>	sheep, cattle	CNS
<i>Taenia hydatigena</i>	canids	<i>Cysticercus tenuicollis</i>	sheep, cattle, pig	peritoneum
<i>Taenia ovis</i>	canids	<i>Cysticercus ovis</i>	sheep	muscle
<i>Taenia pisiformis</i>	canids	<i>Cysticercus pisiformis</i>	rabbit	peritoneum, liver
<i>Taenia serialis</i>	canids	<i>Coenurus serialis</i>	rabbit	Subcutis, connective tissue
<i>Taenia taeniaeformis</i>	cats	<i>Cysticercus fasciolaris</i> (<i>strobilocercus</i>)	rodents	liver
<i>Taenia krabbei</i>	canids	<i>Cysticercus tarandi</i>	Reindeer, wild ruminants	muscle
<i>Echinococcus granulosus</i>	domestic and wild canids	<i>Unilocular hydatid cyst</i>	sheep, cattle, swine, horses	Liver, lung
<i>Echinococcus multilocularis</i>	domestic and wild canids	<i>Multilocular hydatid cyst</i>	Mice and rats	liver



WEDNESDAY SLIDE CONFERENCE 2015-2016

Conference 2

16 September 2015

CASE I: B15-894 (JPC 4050459).

Signalment: 12-year-old, male (intact), Labrador retriever (*Canis familiaris*)

History: Little clinical history was provided with the case. The non-retained testicle was described as “small.”

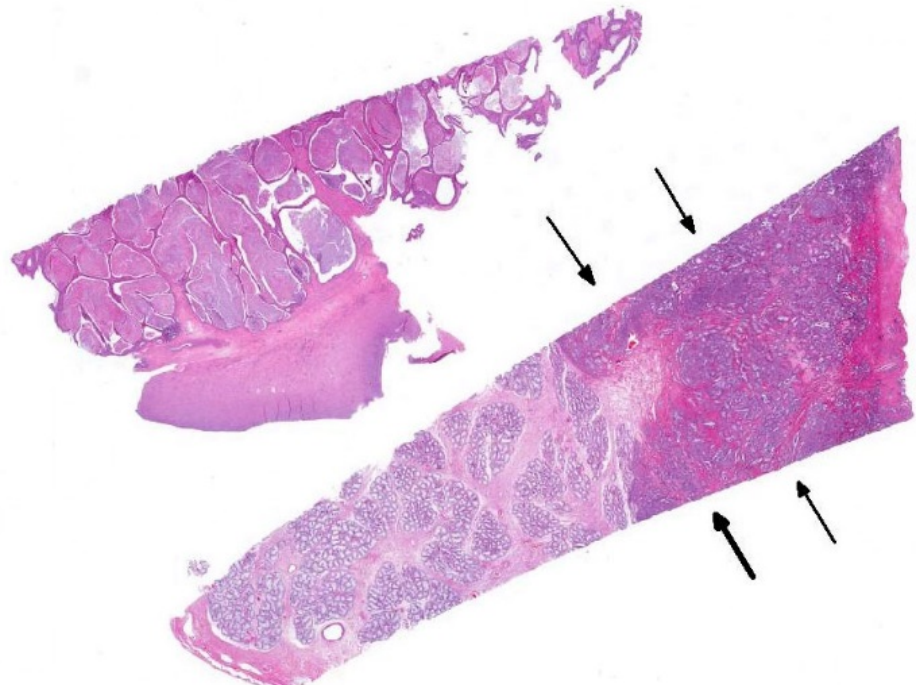
Gross Pathology: Received in two formalin filled jars, labeled prostate and retained testicle, were three pieces of firm, mottled, dark brown to grey tissue, up to 2.0 x 2.0 x 0.5 cm and a 4.0 x 3.5 x 2.0 cm testicle with epididymis, respectively. Near the tail of the epididymis, the testicle contained a well demarcated, approximately 2.5 cm, oval, firm, white to tan mass that compressed the adjacent parenchyma and bulged from the cut surface.

Laboratory Results: None.

Histopathologic

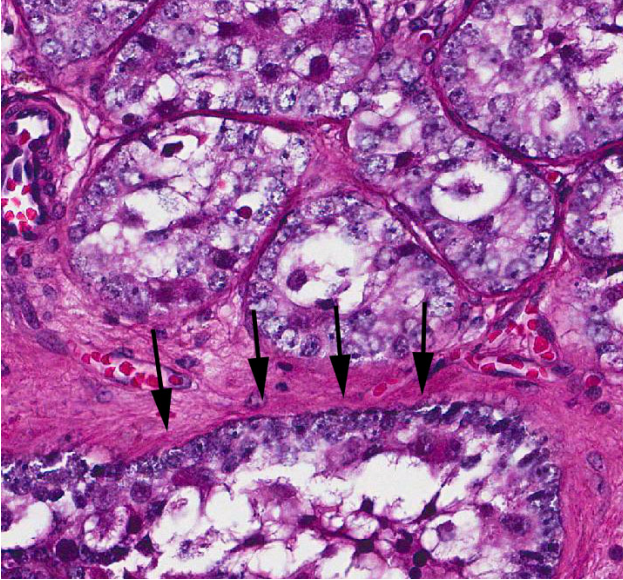
Description: Testicle: Compressing adjacent seminiferous tubules is a variably encapsulated, poorly demarcated, densely

cellular mass. Neoplastic cells are closely packeted into tubule-like nests and cords, within a dense fibrovascular stroma. Neoplastic cells frequently line the fibrous stroma in palisades and occasional pile to form islands. Neoplastic cells are round, to polygonal, to elongate, with indistinct cell borders, and moderate amounts of eosinophilic, flocculent to vacuolated cytoplasm. Nuclei are centrally located and oval to elongate, with vesicular chromatin and 1-3 basophilic nucleoli. The center of packets frequently contain similar cells with hyper eosinophilic cytoplasm,



Retained test and prostate, dog: 50% of the testis (arrows) is replaced by a well-demarcated neoplasm composed of tubules. (HE, 4X)

rounded nuclei, and prominent, magenta nucleoli. Small numbers of necrotic neoplastic



Retained testis, dog. The neoplasm is composed of neoplastic Sertoli cells which often fill tubules. Neoplastic cells palisade along the basement membrane of affected tubules (arrows). (HE, 220X)

cells are scattered throughout the section. Mitotic figures are less than one per ten 40x HPF. Anisocytosis and anisokaryosis are moderate. Remaining tubules are characterized by complete lack of spermatogenesis and increased prominence of Sertoli cells.

Prostate: Prostatic acini are diffusely and severely distended by abundant mixtures of keratinaceous debris, sloughed epithelial cells, granular debris, and acicular clefts. The normal glandular epithelium is diffusely replaced by a well-differentiated, 3-4 cell thick, stratified squamous epithelium (metaplasia). In some sections, scattered acini are ruptured and infiltrated by numerous foamy macrophages and neutrophils.

Contributor's Morphologic Diagnosis:

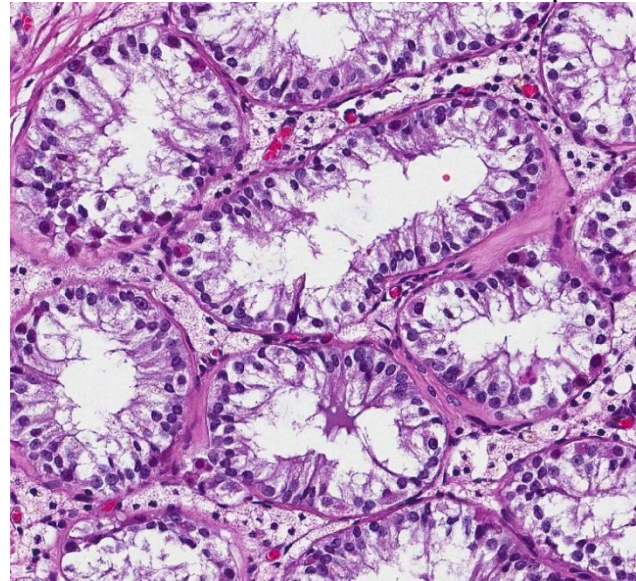
Retained testicle: Sertoli cell tumor

Prostate: Squamous metaplasia, diffuse, severe

Contributor's Comment: Microscopic features of the neoplasm in this retained testicle are consistent with Sertoli cell tumor, a neoplasm derived from supporting cells within seminiferous tubules. Additional findings included

severe, prostatic squamous metaplasia and tubular atrophy in the non-retained testicle. Sertoli cell tumors have been reported from most domestic species, but are uncommon in all but the dog. Grossly, the tumors are white, irregularly ovoid, lobulated, bulge when cut, and may be cystic. Their abundant fibrous stroma makes them firm to hard, a useful differentiating feature not found in seminomas or interstitial cell tumors. Their presence may cause marked distortion of the testicle, but most remain within the tunica albuginea.

Growth of Sertoli cell tumors may be intratubular, as in this case, or diffuse. Microscopic characteristics of intratubular neoplasms include a dense collagenous stroma surrounding seminiferous tubule-like structures that contain polygonal to elongate cells, with eosinophilic, foamy to vacuolated cytoplasm. In some areas, the neoplastic cells palisade along the stroma. Mitotic figures are few. Cells appear discrete and spherical in diffuse tumors and show little or no tendency to palisade. The dense stroma and palisading cells usually differentiates Sertoli cell tumors from seminomas or interstitial cell tumors. In well differentiated tumors, neoplastic

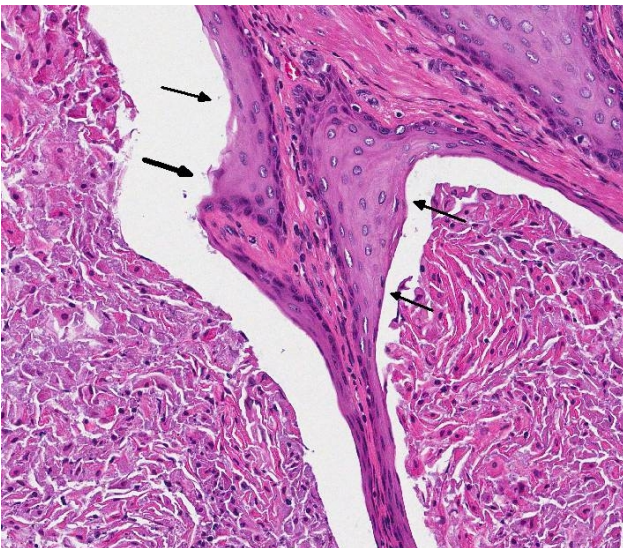


Retained testis, dog. Seminiferous tubules in the unaffected portion of the section are hypoplastic, lacking spermatogonia and shrunken. Intervening interstitial cells are small and degenerate. (HE, 164X)

cells resemble normal Sertoli cells, with basally located nuclei and frequent cytoplasmic lipid

droplets and globules. Cells of less differentiated tumors exhibit disordered growth and increased pleomorphism.

The incidence of Sertoli cell tumors is 20 times higher in cryptorchid dogs and up to 30% of affected dogs manifest signs of hyperestrinism. Especially with larger tumors, production of excessive estrogen and inhibin result in feminization, including attraction of male dogs, reduced libido, testicular and penile atrophy, preputial swelling, perineal hernia, gynecomastia, redistribution of fat, and symmetrical, often ventral, alopecia. Squamous metaplasia of the prostate gland and suppurative prostatitis may lead to dysuria. Estrogenic depression of bone marrow can result in anemia, thrombocytopenia and granulocytopenia, predisposing the dog to hemorrhage and infection. Castration of affected dogs generally results in recovery and regression of associated changes. Most Sertoli cell tumors are benign, but metastasis can occur to regional lymph nodes and distant organs. Metastatic tumors can also be hormonally active.



Prostate gland, dog. Glands are markedly dilated and lined by squamous epithelium (arrows). Glandular lumina contain abundant keratinized epithelium and squamous debris. (HE, 140X)

JPC Diagnosis: Testicle: Sertoli cell tumor.
Testicle, seminiferous tubules and interstitial cells: Hypoplasia, diffuse, severe.

Prostate: Squamous metaplasia, diffuse, severe.

Conference Comment:

Differential diagnosis discussed in this case included the various testicular neoplasms including interstitial cell tumors and seminoma which arise from the interstitial endocrine cells and germ cells respectively. Other less common types of germ cell testicular tumors include teratoma and embryonal carcinoma. Like Sertoli cell tumors, interstitial cell tumors and seminomas are most often considered benign with metastasis being uncommon.¹ With regard to retained testes, Sertoli cell tumors are more common in abdominal testes and seminomas more common in inguinal testes. Interestingly, the contralateral testis is also at increased risk of tumor development.¹ Seminomas have a firm texture with a homogenous appearance and a pink-grey color grossly. Microscopically they are characterized as having round cells with a small amount of cytoplasm, a large nucleus with prominent nucleolus, an elevated mitotic rate, and can be diffuse or intratubular with infiltration of lymphocytes being common.¹ Interstitial cell tumors, being the most common testicular neoplasm in the dog, grossly have a distinctive tan or yellow-orange color due to their high lipid content and frequently contain areas of hemorrhage. Microscopically, they can be solid-diffuse with cells arranged in sheets or cords and separated by fine bands of fibrous connective tissue or cystic in nature with cords of cells surrounding fluid filled areas that may contain erythrocytes. The tumor cells can vary in shape, but the cytoplasm is almost always finely or coarsely vacuolated.⁴

The feminizing effect of Sertoli cell tumors was also discussed during the conference and mentioned above by the contributor. Inhibin inhibits the release of GnRH from the hypothalamus, and ultimately the release of LH and FSH from the anterior pituitary, which affects the production of estrogen and testosterone, resulting in the feminizing effects.¹ In addition to squamous metaplasia of the prostate gland, glandular hyperplasia can also

occur. The squamous metaplasia is not considered to be a pre-neoplastic change in this case, unlike in other locations with other causes, such as the lung of smokers. In metaplastic tissue, specialized epithelium is frequently replaced by less specialized epithelium, it is often a reversible change, and the mechanism varies with cause. Another example of squamous metaplasia occurs in the esophageal glands of various avian species in response to vitamin A deficiency, the exact mechanism of which is unclear.⁶

Following discussion of the neoplasm in this section, participants discussed the non-neoplastic portion of the testicle. The lack of developing spermatogonia, small volume of remaining seminiferous tubules and decreased numbers of interstitial cells were considered to be hypoplastic changes due to the abdominal location of the testis, although the hormonal contribution of the Sertoli cell tumor was considered as a contributing factor non-viability of the adjacent seminiferous tubules.

Slide variation was noted with some slides demonstrating more prominent acicular cholesterol clefts and degree of inflammation.

Contributing Institution:

Department of Pathology, University of Georgia (www.vet.uga.edu/VPP)

References:

1. Foster RA. Male reproductive system. In: McGavin MD, Zachary JF, eds. *Pathologic Basis of Veterinary Disease*. 5th ed. St. Louis, MO: Mosby Elsevier; 2012:1130-1145.
2. Foster RA. Male reproductive system. In: McGavin MD, Zachary JF, eds. *Pathologic Basis of Veterinary Disease*. 4th ed. St. Louis, MO: Mosby Elsevier; 2007:1317-1348.
3. Foster RA, Ladds PW. Male genital system. In: Maxie MG, ed. *Jubb, Kennedy and Palmer's Pathology of Domestic Animals*. 5th ed. Philadelphia, PA: Elsevier Saunders; 2007:565-619.
4. Kennedy PC, Cullen JM, Edwards JF et al. *World Health Organization Histological*

classification of tumors of the genital system of domestic animals. Washington DC: Armed Forces Institute of Pathology; 1998:15-18.

5. MacLachlan NJ, Kennedy PC. Tumors of the genital systems. In: Meuten DJ, ed. *Tumors in Domestic Animals*. 4th ed. Ames, IA: Blackwell Publishing; 2002:547-573.

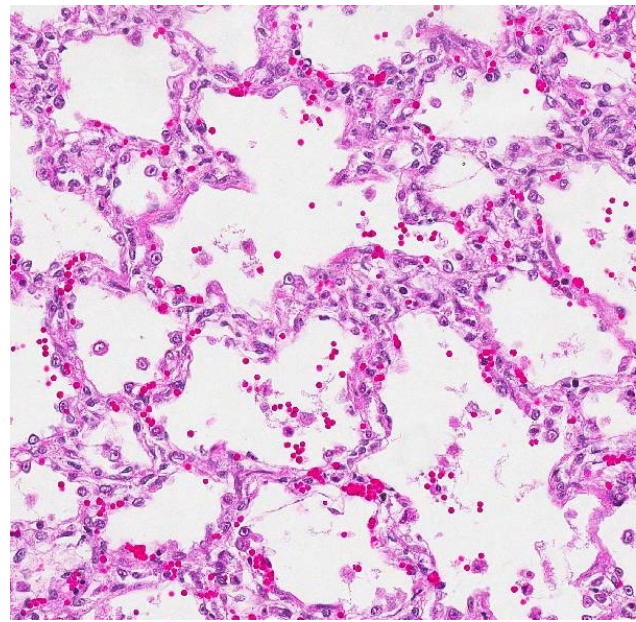
6. Myers RK, McGavin DM, Zachary JF. Cellular adaptations, injury, and Death: Morphologic, biochemical and genetic bases. In: McGavin MD, Zachary JF, eds. *Pathologic Basis of Veterinary Disease*. 5th ed. St. Louis, MO: Mosby Elsevier; 2012:29-30.

CASE II: S09-1502 (JPC 3164421).

Signalment: Feline, Norwegian forest cat, 2 weeks of age, male (*Felis catus*).

History: All animals from a litter of two week old kittens were treated with infusion and ampicillin, but all kittens died.

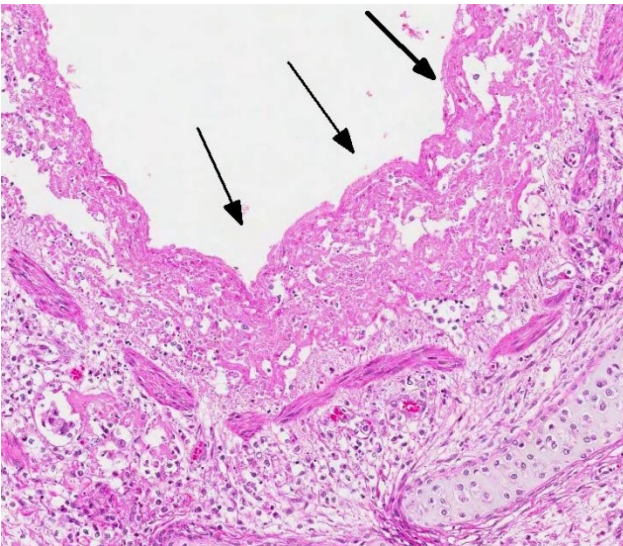
Gross Pathology: Lung: pink and whitish mosaic pattern on surface and in the parenchyma, diffusely increased texture.



Lung, kitten: Alveolar septa are diffusely and markedly expanded throughout the section by a mix of cellular infiltrate as well as fibrin and edema. (HE 196X)

Laboratory Results: Immunohistochemistry positive for FeHV-antigen.

Histopathologic Description: Lung: Throughout the organ bronchi and bronchioli are necrotic or degenerating. The bronchiolar epithelium is replaced by karyorrhectic and pyknotic cell debris and eosinophilic material (necrosis), infiltrated with numerous degenerating neutrophils and fewer macrophages. In some of the remaining viable epithelial cells eosinophilic intranuclear inclusion bodies are visible, only in some slides syncytia cell formation with eosinophilic intranuclear inclusion bodies can be seen. In the lumina of the bronchi/bronchioli and in most alveolar spaces cell debris and a slightly fibrillar eosinophilic material as well as numerous degenerating neutrophils showing karyopyknosis and karyorrhexis, macrophages and some erythrocytes can be found. The interstitial walls are still viable but thickened due to a moderate infiltration of the alveolar walls with macrophages and neutrophils and activation of pneumocytes type II. In the lumina of these alveolar spaces moderate amounts of macrophages, few neutrophils and some erythrocytes (acute bleeding) are visible. Peribronchiolar and perivascular tissue is edematous, moderate amount of degenerating neutrophils, few lymphocytes and macrophages are diffusely visible in the edematous tissue. In this region some bronchiolar gland epithelia



Lung, kitten: Airway epithelium in bronchioles and bronchi is diffusely necrotic (arrows.). (HE 144X)

degenerate and in few intranuclear eosinophil inclusion bodies can be seen.

Contributor's Morphologic Diagnosis: Lung: Pneumonia, bronchointerstitial, severe, necrotizing, subacute, multifocal to coalescing, with epithelial intranuclear inclusion bodies (FeHV-1).

Contributor's Comment: Feline herpesvirus 1 (FeHV-1) – feline rhinotracheitis virus, is a double-stranded DNA virus belonging to the subfamily of alpha-herpesvirus (family herpesviridae). FeHV-1 infections are ubiquitous and occur throughout the world, but clinical disease is much less frequent. Carrier cats are either latently or actively infected. Latent carriers do not shed infectious virus unless the genome is activated due to stress or corticoid administration. Clinically apparent disease is more frequent within a population of high density.

Infection can occur in utero, neonatally or in the 2-12 week age range when maternal immunity wanes. Virus is infectious on all mucous membranes but requires contact with nasal or ocular secretions, airborne spread only occurs over short distances.

Infections normally happen intranasal followed by a rapid cytolytic infection of nasal epithelium under an optimal replication-temperature of 37°C and then a secondary spread to conjunctival sac, oropharynx, trachea, bronchi and bronchioli. The typical incubation period is two to four days. Microscopically intranuclear inclusion bodies can be seen in epithelial cells of the described organs named above, but only from the second to seventh day after infection. Transient viremia may occur but is not a prominent feature. Latent infections develop in as many as 80% of infected cats, where the virus is distributed in several tissues of the head. The virus persists in the trigeminal nerve, ganglia of the optic nerve, olfactory bulb and cornea.

Latent carriers have been converted to active virus shedders by giving them corticosteroids for several days or by stress. Also parturition and lactation are stressful events that may trigger

activation, which may be an important source of infection for kitten.

The classical rhinotracheitis occurs in kitten within an age range of 6-12 weeks. Severity of clinical signs varies greatly. The most consistent manifestation is rhinitis associated with sneezing and nasal exudation. Low-grade fever occurs but usually clinical signs disappear in 7-14 days. Some kitten can manifest rhinitis, pharyngitis, glossitis, tracheitis, pneumonia, high fever, depression, anorexia and drooling. Mortality occurs among this group of animals.

Besides the classical rhinotracheitis other clinical syndromes can be attributed to FeHV-1 infection. Those may belong to the complex of respiratory diseases as recurrent rhinitis in older cats as a result of reinfection or activation of a latent infection. Also a chronic sinusitis with opportunistic bacteria and mycoplasma that follows an acute upper respiratory infection of FeHV-1 with permanent turbinate and mucosal

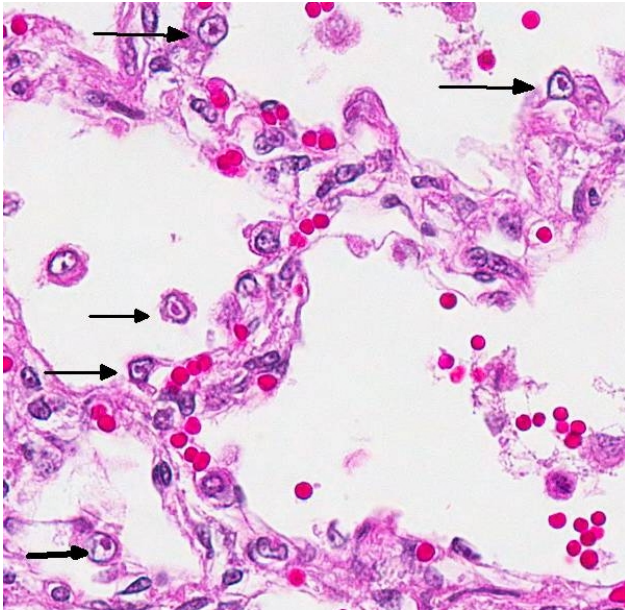
damage can be seen. Another manifestation can be a chronic conjunctivitis and keratitis that can last for months and is usually mild and bilateral but can become copious and purulent with time. Photophobia is particularly characteristic. Acute or chronic herpetic corneal ulcers can be a troublesome complication or herpesvirus ulcerative dermatitis.^{1,3,6}

Also problems in context of reproductive events can occur as abortion, which is probably a non-specific phenomenon, and neonatal disease associated with queens that fail to provide maternal immunity or infect their young at birth. There the kitten shows pneumonia without upper respiratory disease after a short period of fading away.^{1,6} In our case, the two week old kitten didn't show pathologic changes in the upper but in the lower respiratory tract.

<i>Alphaherpesvirinae:</i> <i>focal lesions in skin and mucosa of respiratory and genital tract; abortion; neonates: necrosis in multiple organs, latency in nerves</i>	Equine herpesvirus 1: Equine herpesviral abortion, rhinopneumonitis, neurologic disease	horse
	Equine herpesvirus 3: Equine coital exanthema	horse
	Equine herpesvirus 4: Equine rhinopneumonitis	horse
	BHV-1: infectious bovine rhinotracheitis/infectious pustular vulvovaginitis/infectious balanoposthitis	cattle
	BHV-2: bovine mammillitis virus (bovine herpes mammillitis)	cattle
	BHV-5: bovine herpesvirus encephalitis	cattle
	SHV-1: Aujeszky's disease, Pseudorabies	pig>others
	Canine herpesvirus 1:	dog
	Feline herpesvirus 1: upper respiratory tract disease (rhinotracheitis) and conjunctivitis (ulcers)	cats
	Feline herpesvirus 1: feline herpesvirus ulcerative dermatitis	cats
Gallid herpesvirus-1: Infectious laryngotracheitis (ILT)	chicken	

	Gallid herpesvirus-2: Marek's disease	chicken
	Psittacine herpesvirus: Pacheco's disease	psittacines
	Anatid herpesvirus-1: Duck plaque/Duck virus enteritis	ducks, geese, swan
	Simplexvirus: HSV-1, HSV-2, HBV, BHV-2	
	Herpesvirus simplex, type 1/type 2	human & nonhuman primates
	Herpesvirus simiae/Herpes B/Cercopithecine HV	rhesus macaques
	Simian varicella virus	macaques, AGM, Patas monkeys
Betaherpesvirinae: <i>no cell lysis, karyomegaly, latency in secretory glands, lymphoreticular organs, kidney</i>	HHV-5, HHV-6, MCMV-1	humans
	Porcine herpesvirus 2: porcine cytomegalovirus disease/Inclusion body rhinitis	porcine
	Cytomegalovirus	humans + nonhuman primates
Gammaherpesvirinae: <i>primates: lymphoproliferative disease, latency in lymphoid tissue</i>	EHV-2	
	EHV-5	
	BHV-4: bovine herpes mammary pustular dermatitis	cattle
	OHV-2/AHV-1: malignant catarrhal fever	various ruminants
	Epstein-Barr virus (lymphocryptovirus-gamma 1)	primates
	Kaposi-sarcoma-associated herpesvirus/human herpesvirus-8 (KSHV/HHV8) (Rhadinovirus-gamma 2)	primates
Deltaherpesvirinae	Anatid herpesvirus-1: duck plague	
	SHV-2: Einschlusskörperchenkrankheit	pig
	Karpfenpocken	fish
?	Koi-herpesvirus (KHV, carp nephritis and gill necrosis virus, CNGV, Cyprinid-Herpesvirus-3, CyHv-3)	fish

JPC Diagnosis: Lung: Bronchointerstitial pneumonia, fibrinonecrotic, diffuse, marked with eosinophilic intranuclear inclusion bodies.



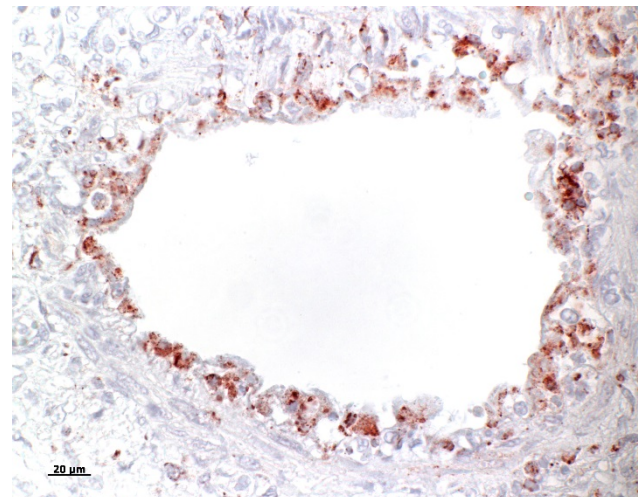
Lung, kitten: Intranuclear viral inclusions consistent with herpesvirus are present in macrophages and pneumocytes (arrows) as well as epithelium of airways and submucosal glands (not shown) (HE 400X)

Conference Comment:

This excellent case of feline herpesviral (FHV) pneumonia clearly demonstrates viral intranuclear inclusion bodies, a histologic finding typically seen in the acute phase of the disease, and not often visualized in most animals that succumb to the disease in the subacute or chronic phase. There was extensive discussion during the conference regarding the location of the intranuclear inclusions. Most agreed viral inclusions were present in macrophages and endothelial cells; but they were also identified in bronchiole glandular epithelium, due in part to the prominence of feline bronchiole glands. Participants also briefly discussed differentiating a prominent activated nucleolus from an intranuclear inclusion. Although both have a similar eosinophilic staining pattern, the herpesviral intranuclear inclusions were generally larger and peripheralized the chromatin. Slide variation was noted with a few slides having a focally extensive area of coagulative necrosis, an uncommon presentation for this entity. Other histologic changes

discussed include the discontinuous alveolar septa, alveolar and interstitial edema, and relatively fewer numbers of type II pneumocytes than anticipated.

Differential diagnosis discussed for this lesion included feline calicivirus and high pathogenicity avian influenza, although viral inclusions are not a histologic feature of either entity. Feline calicivirus (FCV), in addition to causing rhinitis, stomatitis and conjunctivitis, can also cause an interstitial pneumonia and necrotizing bronchiolitis with secondary bacterial infection. The clinical and pathologic findings in FHV and FCV are similar in some aspects, and together account for the majority of feline respiratory diseases. FCV can also result in a transient lameness due to a self-limiting arthritic condition, termed “limping kitten syndrome.” There is a virulent form of FCV, described as a systemic hemorrhagic syndrome with high mortality⁵, in which cats present clinically with diarrhea, pneumonia, edema and hemorrhage. Unlike the more virulent strain where viral antigen is present systemically in both endothelial cells and epithelial cells, in the less virulent more ubiquitous form, viral antigen is generally only present in oral mucosa and respiratory epithelium.⁷



Lung, kitten: Attenuated bronchiolar epithelium is multifocal strongly positive for FHV-1 antigen. (anti-FHV1, 400X)

Cats can also become infected with highly pathogenic avian influenza virus (HPAI) H5N1 from infected wild birds. The primary

respiratory lesions in H5N1-infected cats includes bronchointerstitial pneumonia and bronchiolar necrosis, but significant disease outside the respiratory system, including multifocal hepatic necrosis, is also a noted and described finding.^{4,8} To date, horizontal transmission between domestic cats has not been documented in the wild⁴ but has been demonstrated experimentally with excretion from both the respiratory and digestive tracts.⁸ Additionally, cats have also been shown to be susceptible to other forms of influenza virus such as H1N1 from humans as well as low pathogenicity avian influenza viruses.²

Contributing Institution:

Institute of Veterinary Pathology, Vetsuisse Faculty, CH-8057 Zurich, Switzerland
www.vetpathology.unizh.ch

References:

1. Appel, MJG. *Virus infections of carnivores*. Amsterdam, The Netherlands: Elsevier Science Ltd; 1987.
2. Driskell EA, Jones CA, Berghaus RD, et al. Domestic cats are susceptible to infection with low pathogenic avian influenza viruses from shorebirds. *Vet Pathol*. 2012;50(1):39-45.
3. Gross TL, Ihrke PJ, Walder EJ, Affolter VK. *Skin Diseases of the Dog and Cat. Clinical and Histopathological Diagnosis*. 2nd ed. Ames, IA: Blackwell; 2005.
4. Klopfleisch R, Wolf PU, Uhl W et al. Distribution of Lesions and Antigen of Highly Pathogenic Avian Influenza Virus A/Swan/Germany/R65/06 (H5N1) in Domestic Cats after Presumptive Infection by Wild Birds. *Vet Pathol*. 2007;44:261-268.
5. Lopez A. Respiratory system, mediastinum, and pleurae. In: McGavin MD, Zachary JF, eds. *Pathologic Basis of Veterinary Disease*. 5th ed. St. Louis, MO: Mosby Elsevier; 2012:472-474.

6. Maxie MG. *Jubb, Kennedy and Palmer's Pathology of Domestic Animals*. 5th ed. Philadelphia, PA: Elsevier Saunders; 2007.

7. Pesavento PA, Murphy BG. Common and emerging infectious disease in the animal shelter. *Vet Pathol*. 2014;51(2):478-491.

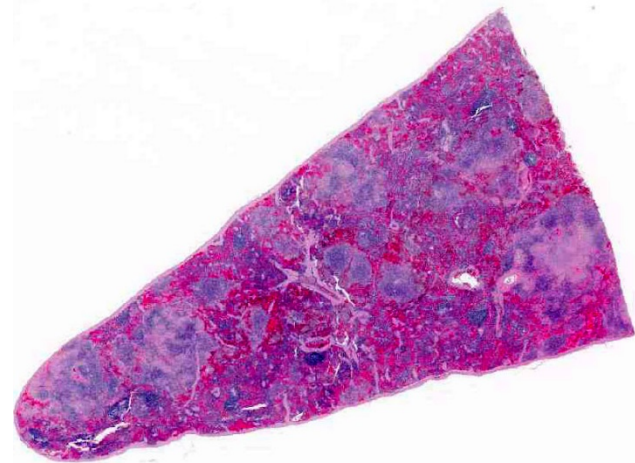
8. Rimmelzwaan GF, van Riel D, Baars M, et al. Influenza A virus (H5N1) infection in cats causes systemic disease with potential novel routes of virus spread within and between hosts. *Am J Pathol*. 2006;168(1):176-83.

CASE III: 08-2379-7 (JPC 3169265).

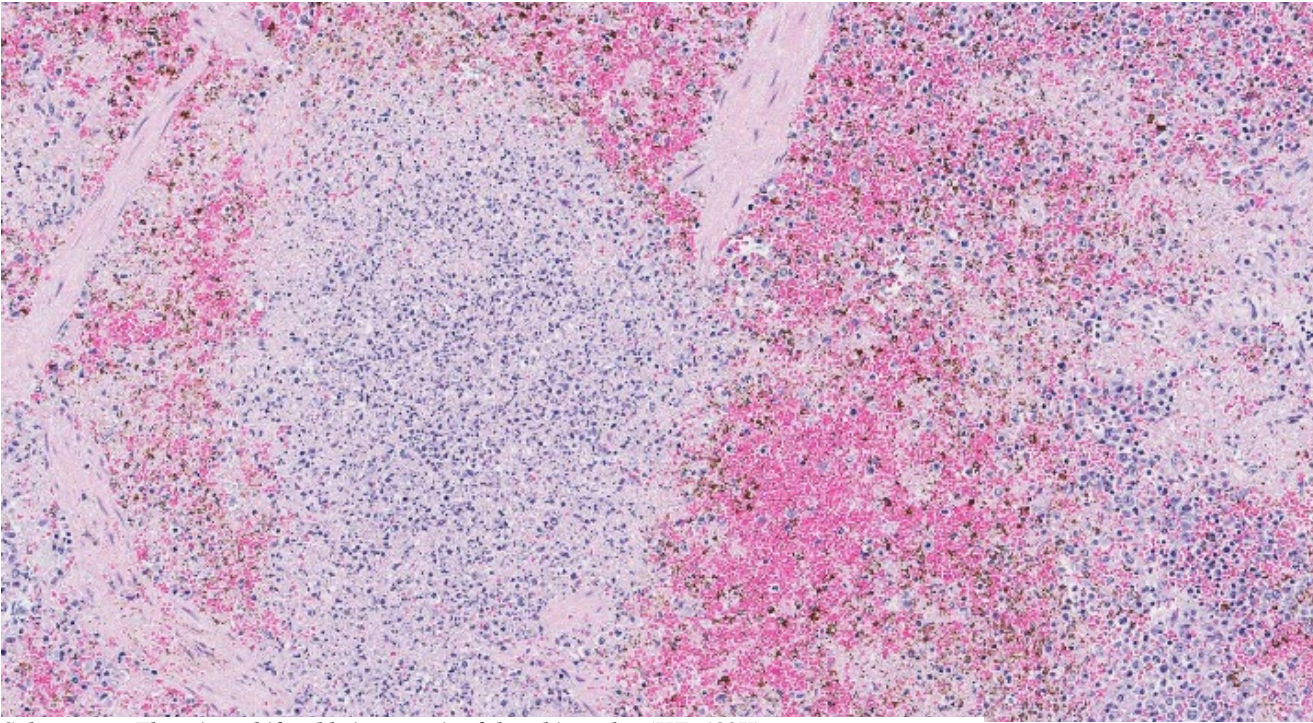
Signalment: 12-year-old male castrated domestic shorthaired cat (*Felis catus*).

History: Presented to the referring veterinarian with a history of anorexia, pyrexia, lethargy, diarrhea and oral ulcers of seven days duration.

Gross Pathology: The mesenteric and mandibular lymph nodes were markedly enlarged, and the corticomedullary architecture was effaced by friable, pinpoint yellow-white raised nodules. The pulmonary parenchyma contained several slightly raised, white nodules which were miliary to 2 mm in diameter. 10 and



Spleen, cat. There is diffuse necrosis focused on white pulp, which extends into the surrounding red pulp. (HE, 6X)



Spleen, cat. There is multifocal lytic necrosis of the white pulp. (HE, 198X)

20 ml of clear, yellow-red fluid was found in the abdominal cavity. The livers were yellowish-brown and the hepatic parenchyma contained several white, slightly raised nodules which were miliary to 2 mm in diameter and evenly distributed through the parenchyma. The spleens contained multiple white, round, raised nodules and were approximately 1-2 mm in diameter.

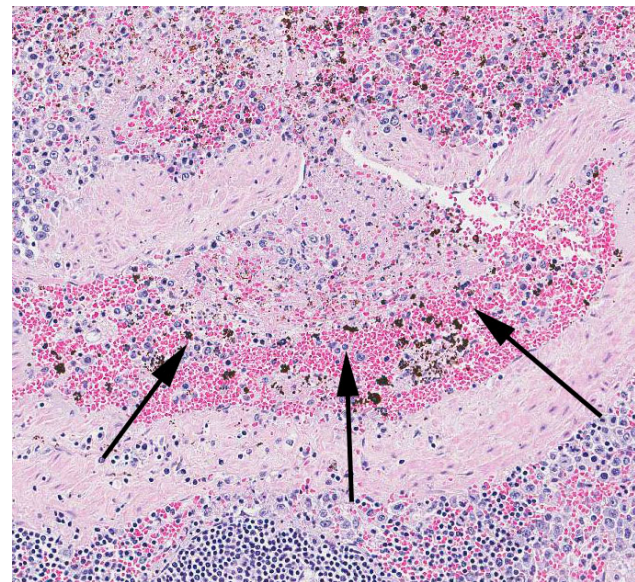
Laboratory Results: Specimens of spleen, liver, and lung submitted for culture, PCR and DNA sequencing were positive for *Francisella tularensis*.

Histopathologic Description: Spleen: The parenchyma is disrupted by multiple nodules composed of degenerate neutrophils, and macrophages and varying amounts of amorphous to slightly fibrillar eosinophilic material (fibrin) and basophilic cellular and nuclear debris (liquefactive necrosis) with loss of lymphoid tissue from the areas surrounding these nodules. Overall, there is a moderate degree of depletion of the periarterial lymphoid sheaths. Erythrocyte and myeloid precursors are scattered throughout the splenic parenchyma with rare megakaryocytes (extramedullary hematopoiesis).

Contributor's

Morphologic Diagnosis: Moderate to severe multifocal acute necrosuppurative splenitis

Contributor's Comment: *Francisella tularensis*, the causative agent of tularemia, is an aerobic, gram-negative coccobacillus. The two most common biovars are *F. tularensis* biovar *tularensis* and *F. tularensis* biovar *palaeartica*. *F. tularensis* biovar *tularensis* biovar is more



Spleen, cat. Splenic vessels occasionally contain non-occlusive fibrinocellular thrombi. (HE, 220X)

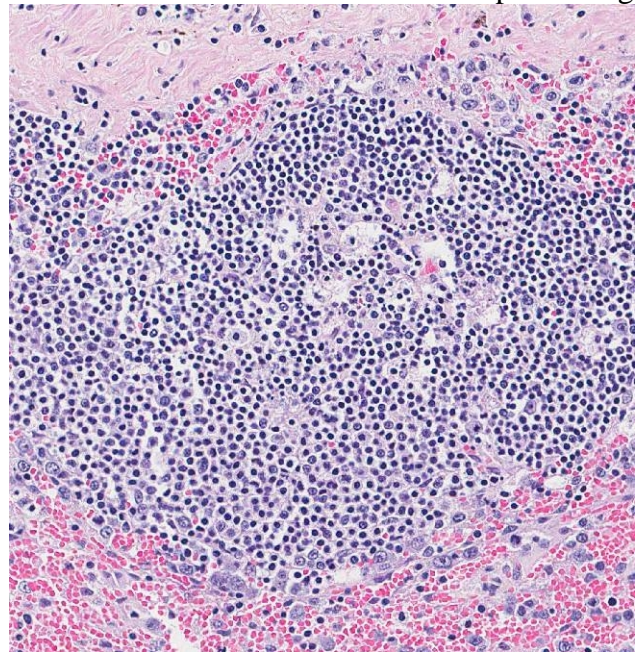
common in North America.^{1, 10, 6, 2, 8} *F. tularensis* biovar *tularensis* has been the only biovar identified in fatal systemic infections in cats.² Infections have been reported in cats, rabbits, rodents, dogs, cattle, sheep, horses, non-human primates, and humans with cats, rabbits, rodents, and sheep appearing to be the most susceptible to natural infection.^{1, 6, 2} Tularemia is transmitted via bites of infected arthropods (most often ticks or flies), ingestion of infected rabbits and or rodents, inhalation, and mucous membrane exposure.^{1, 10, 6, 8} Clinical signs commonly associated with tularemia include fever, anorexia, lymphadenopathy, hepatosplenomegaly, dehydration, and neutrophilia or neutropenia with toxic change. Common gross findings with tularemia include multifocal splenic, hepatic, lymphoid, and pulmonary necrosis, oral and gastrointestinal ulceration, and enterocolitis.^{1, 10, 6, 2, 8} Microscopic findings typically include necrotizing inflammation in multiple organs (spleen, liver, lungs, lymph nodes, and gastrointestinal tract common) with varying numbers of associated neutrophils and macrophages. Colonies of intralosomal gram negative coccobacilli may be visualized as well.^{1, 6, 2} Definitive diagnosis is based on successful isolation of *F. tularensis* from specimens obtained from affected animals,^{1, 10, 6, 2, 8} fluorescent antibody reaction and agglutination with *F. tularensis* anti-serum,^{1, 10, 6} immunohistochemistry on formalin fixed paraffin embedded tissues,^{2, 8} or PCR and DNA sequencing.⁸

JPC Diagnosis: Spleen: Splenitis, necrotizing, multifocal, marked with lymphoid depletion, fibrin thrombi and extramedullary hematopoiesis.

Conference Comment: Conference participants agreed both red and white pulp are affected by necrosis, but the lesions are centered on the white pulp, with severe lymphoid depletion. Participants described the abundant fibrin thrombi within the section, but noted they are non-occlusive with no evidence of infarction. Differential diagnoses which were discussed included *Yersinia pseudotuberculosis*, *Yersinia*

enterocolitica and *Salmonella* spp. infection, which share many gross and histologic characteristics with tularemia, as well as *Yersinia pestis*. The history provided is typical for both plague and tularemia infection. However, *Yersinia enterocolitica* and *pseudotuberculosis* are generally associated with large colonies of gram-negative bacilli visible histologically, and *Salmonella* spp. infection is less commonly seen in domestic cats. Special stains that can be used to identify *F. tularensis* include Gram stains as well as both Giemsa and Warthin-Starry. In this case Gram stains did not help identify organisms in the section.

Tularemia has been reported in nearly all 50 states except Hawaii, and in 2015 is on the rise in North and South Dakota, Colorado, Wyoming, and New Mexico. More common modes of infection in humans include cleaning/skinning infected lagomorphs and arthropod bites, but also include infectious from contaminated water supplies as well as consumption of contaminated undercooked meat. Sporadic outbreaks of tularemia are known to occur in sheep resulting



Spleen, cat. The white pulp is hypocellular and contains tangible body macrophages and cellular debris, suggesting lymphocytolysis. (HE, 280X)

in late term abortion and may be associated with abundant tick populations.⁵ In some cases of small mammal infection, classic lesions may not

be present grossly or histologically. Additionally, in wildlife species, autolysis and freeze artifact may interfere with evaluation of gross lesions. Subclinical infections are known to occur, but the role of subclinically infected animals in disease transmission is unclear, which serves to highlight the importance of taking appropriate safety precautions when working with the carcasses of deceased wildlife in endemic areas.⁴

The agent is highly infectious with as few as 10-50 organisms capable of causing an infection and it is classified as a category A bioterrorism agent. Experimentally induced lesions from inhalation in African green monkeys included necrotizing pyogranulomatous lesions which targeted the lung and lymphoid tissue.⁹ The organisms are most commonly located intracellularly in macrophages, in both the inhalation form in primates⁹ as well as in small mammals, but may also be present extracellularly in exudates and necrotic debris as well as in other cell types.³ *F. tularensis* is able to evade the immune system by infecting and replicating in macrophages and disseminating to distal organs in the acute phase of the disease without being detected. It prevents activation of macrophages that would result in an appropriate host innate immune response, which is important in survival in infections with virulent *F. tularensis*.⁷

Contributing Institution:

Department of Veterinary Biosciences
College of Veterinary Medicine
The Ohio State University
1925 Coffey Road
Columbus, OH 43210
<http://vet.osu.edu/biosciences.htm>

References:

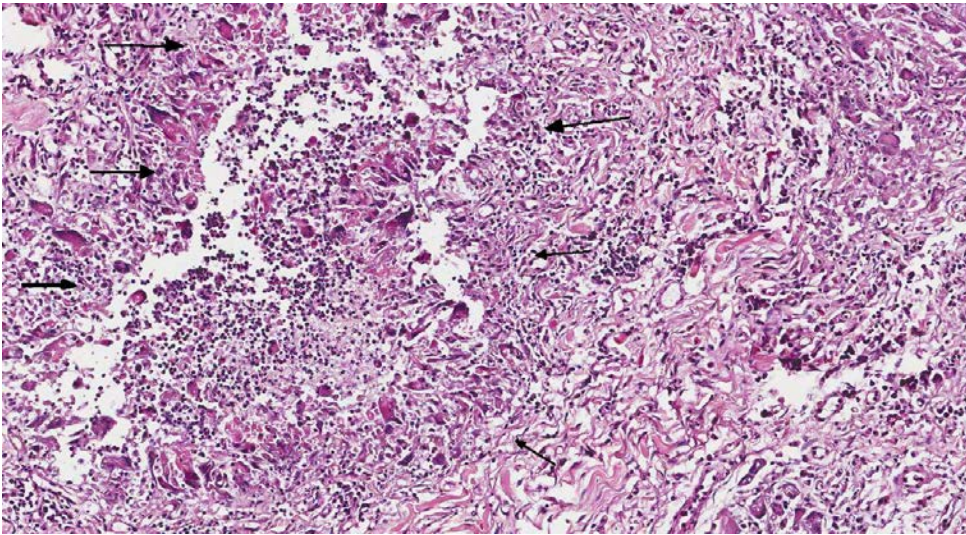
1. Baldwin CJ, Panciera RJ, Morton RJ, Cowell AK, Waurzyniak BJ. Acute tularemia in three domestic cats. *JAVMA* 1991;199:1602-1605.
2. DeBey BM, Andrews GA, Chard-Bergstrom C, Cox L. Immunohistochemical demonstration of *Francisella tularensis* in lesions of cats with tularemia. *J Vet Diagn Invest.* 2002; 14:162-164.

3. Gyuranecz M, Szeredi L, Makrai L et al. Tularemia of European Brown Hare (*Lepus europaeus*): A pathological, histopathological, and immunohistochemical study. *Vet Pathol.* 2010;47(5):958-63.
4. Nelson DD, Halderson GJ, Stanton JB. *Francisella tularensis* infection without lesions in gray tree squirrels (*Sciurus griseus*): a diagnostic challenge. *J Vet Diagn Invest.* 2014;26(2):312-315.
5. O'Toole D, Williams ES, Woods LW et al. Tularemia in range sheep: An overlooked syndrome? *J Vet Diagn Invest.* 2008;20(4):508-513.
6. Rhyan JC, Gahagan T, Fales WH. Tularemia in a cat. *J Vet Diagn Invest.* 1990; 2:239-241.
7. Russo BC, Brown MJ, Nau GJ. MyD88-Dependent signaling prolongs survival and reduces bacterial burden during pulmonary infection with virulent *Francisella tularensis*. *Am J Pathol.* 2013;183(4):1223-32.
8. Spletstoeser WD, Tomaso H, Al Dahouk S, Neubauer H, Schuff-Werner P. Diagnostic procedures in Tularemia with special focus on molecular and immunological techniques. *J. Vet. Med.* 2005;52:249-261.
9. Twenhafel NA, Alves DA, Purcell BK. Pathology of inhalational *Francisella tularensis* spp. *tularensis* SCHU S4 infection in African green monkeys (*Chlorocebus aethiops*). *Vet Pathol.* 2009;46:698-706.
10. Woods JP, Crystal MA, Morton RJ, Panciera RJ. Tularemia in two cats. *JAVMA.* 1998; 212:81-83.

CASE IV: B14-182 (JPC 4066360).

Signalment: 2 years of age, female, neutered, Springer Spaniel canine (*Canis lupus familiaris*).

History: The animal was admitted to the Tuskegee University teaching hospital for a mass in the right mammary chain and a mass in the left mammary chain. The animal swam in a pond less than 1 week after a laparotomy. Both masses were warm to the touch and ulcerated. There was a draining swollen area on the medial surface of the right stifle joint and a swollen area on caudal

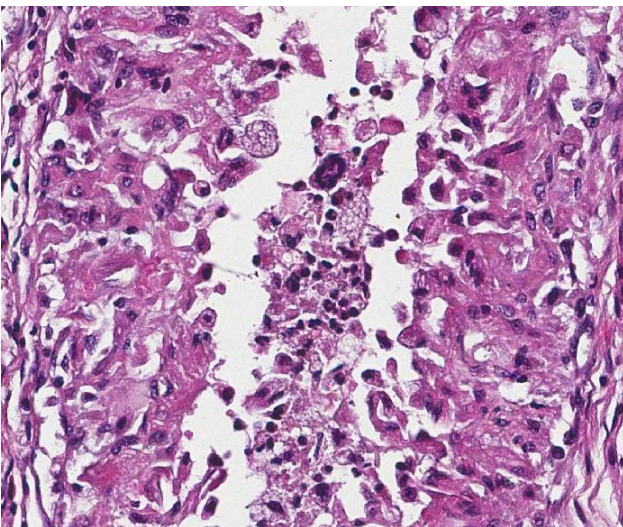


Mammary tissue, dog: The tissue is effaced by multiple poorly formed granulomas surrounding a central necrotic core (arrows).. (HE. 120X)

aspect of the left carpus. The two mammary gland masses were surgically excised and submitted for microscopic evaluation.

Gross Pathology: Both mammary masses were irregularly shaped, firm, ulcerated and contained several draining tracts. The mass in the right mammary gland was 22 cm X 5 cm and the mass in the left mammary gland was 15 cm X 5 cm. The right stifle joint swelling and the swelling on the left carpus were round to oval, 4 – 5 cm in diameter, hard, ulcerated and exuded serosanguinous fluid.

Laboratory Results: None.



Mammary tissue, dog: Granulomas are lined by a layer of mildly pleomorphic epithelioid macrophages. (HE. 196X)

Histopathologic

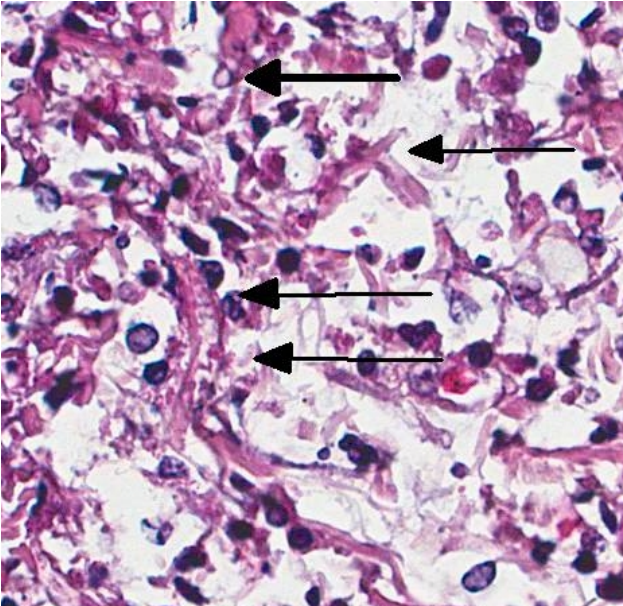
Description: Several sections from the mammary masses were examined microscopically. Microscopic lesions are similar in all tissues. All sections submitted were from the 2 mammary masses.

In all tissues, normal architecture is obscured by variably-sized coalescing cellular nodules that are often separated by thick bands of fibrous connective tissue. Nodules often have centers comprised of cellular debris, few to moderate neutrophils and few eosinophils. Macrophages, epithelioid cells, multinucleated giant cells, Langhans giant cells, few to moderate lymphocytes, plasma cells, and fibroblasts surround these necrotic centers. Other nodules lack necrotic centers and are comprised of variable combinations and concentrations of plasma cells, macrophages, epithelioid cells, multinucleated and Langhans giant cells. Giant cells often contain intracytoplasmic round, 2-4 micron structures with clear centers and thick eosinophilic walls. Within cellular masses, the periodic acid-Schiff stain reveals numerous non-parallel hyphae with thick walls. Hyphae are poorly septate, 6-12 micron wide with occasional non-dichotomous branching (Fig. 1).

Contributor's Morphologic Diagnosis: Mammalitis, granulomatous, diffuse, severe with intralesional fungi.

Contributor's Comment: The lesions in both mammary glands were induced by *Zygomycetes* or *Pythium insidiosum*. The location of lesions, morphology, size of the organism, and inflammatory reaction are features consistent with both zygomycosis and pythiosis. Staining of the organism with the periodic acid -Schiff stain (PAS) and not the Gomori's methenamine silver stain (GMS) is more consistent with

zygomycosis; however, the history of swimming in a pond several days after a laparotomy is more consistent with a diagnosis of pythiosis.



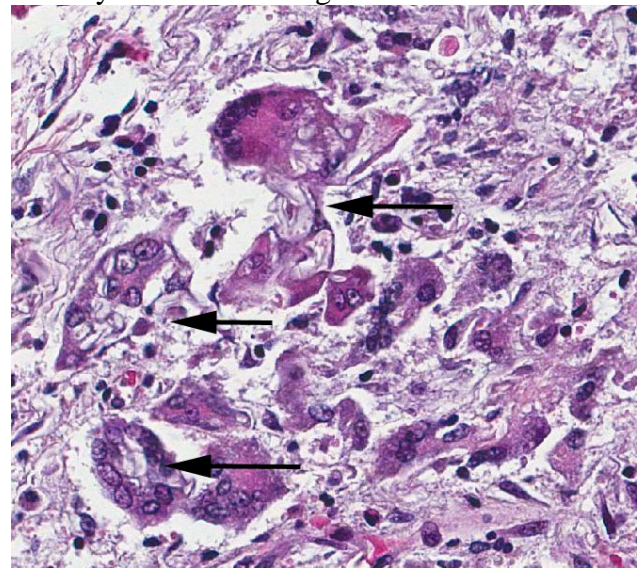
Mammary tissue, dog: Within necrotic cores, cross- and tangential sections of hyphae may be occasionally visualized in negative relief (HE, 280X)

Dogs with compromised immune systems are highly susceptible to both conditions. These infections are usually obtained via inhalation or ingestion with primary sites in the respiratory and gastrointestinal systems. Cutaneous infections in both immunosuppressed and immunocompetent dogs are often secondary to open skin wounds. *Pythium insidiosum* may be present in water, and when animals with open skin wounds enter contaminated bodies of water, they are susceptible to these infections. Skin lesions are typically characterized by nodules that are frequently ulcerated with necrotic centers and granulomatous and or pyogranulomatous inflammation. Hyphae with non-septate or poorly septate, non-parallel walls, and non-dichotomous branches are present in nodule centers. Hyphae are 4-16 micron wide. These features are beneficial in distinguishing *Zycomycetes* and *Pythium* from their primary differential diagnoses of aspergillosis and candidiasis. *Aspergillus* sp. is septate and 2-3 micron wide and *Candida* sp. is 2-3 micron wide with pseudohyphae.² Drugs that are effective against fungal infections are ineffective for

treatment of *Pythium* species, which is not a fungus but a member of the phylum Oomycota.³

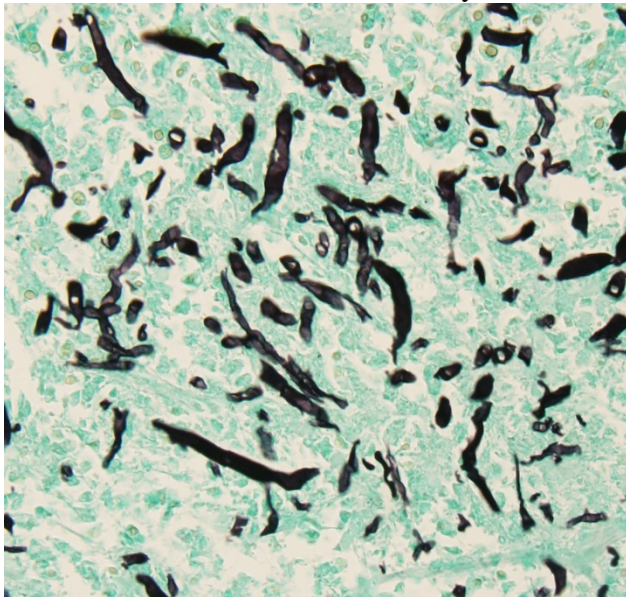
JPC Diagnosis: Mammary gland (per contributor): Panniculitis, granulomatous and eosinophilic, chronic-active, diffuse, marked with numerous hyphae, Springer spaniel, canine.

Conference Comment: Tissue identification was particularly challenging in this case, with a mix of interpretations by conference participants; considerations included glandular tissue, pancreas, intestine, and uterus. Many conference participants commented on the presence of eosinophils in the inflammatory milieu and profound fibrosis, indicating chronicity. Serial tissue sections subjected to silver staining by the Grocott methenamine silver (GMS) method and periodic-acid Schiff (PAS) reaction were viewed and discussed during the conference; while hyphae were demonstrated with both stains, the GMS method proved superior in highlighting the hyphae. In our experience, even with special histochemical stains, the infectious organisms of *Pythium insidiosum*, *Lagenidium* species, Oomycetes, and Zygomycetes are problematic to differentiate histologically, and ancillary laboratory testing, such as microbial culture or PCR assay, is often required to definitively identify the infectious agent.



Mammary tissue, dog. Often, hyphae are surrounded by robust multinucleated foreign body giant cells. (HE, 360X)

Pythium insidiosum and *Lagenidium* species Oomycetes are dimorphic water molds (previously thought to be fungi) found in tropical or subtropical areas such as the southern United States. Infection is primarily cutaneous or subcutaneous, but systemic, gastrointestinal and vascular sites can occur in domestic animals and humans. Infection occurs when the host comes into contact with standing or stagnant water containing the motile aquatic flagellate zoospores; this infectious form of the organism is attracted to injured mammalian tissue. Infections in domestic animals are most commonly reported in the limbs, ventral thorax and abdomen of horses. In horses, the organisms cause large granuloma like mass lesions that may contain a purulent discharge and clinically resemble cutaneous habronemiasis, neoplasia, and exuberant granulation tissue.¹ The cutaneous condition in the dog is less common than the gastrointestinal form, where the condition is also often progressive and refractory to medical therapy; the lesion starts as a dermal nodule that may resemble a lick granuloma and expands into the subcutis, spreads peripherally, may ulcerate and develop draining tracts and is often associated with an eosinophilia. Infection in cats and cattle has been reported, but is less common in these species. *Lagenidium* species cutaneous/subcutaneous infection is very similar to



Mammary tissue, dog. Hyphae range from 4-12 μ m in diameter with non-parallel walls and lack septations. (GMS, 400X)

pythiosis clinically, and is equally aggressive, but has only been reported in dogs.¹

Zygomycosis is caused by fungi in the class *Zygomycetes* which is divided into the two orders, *Mucorales* and *Entomophthorales*. The hyphae are described as being infrequently septate and their broad nature allows them to be differentiated from other fungal organisms. Like pythiosis, zygomycosis most commonly occurs in horses and the cutaneous lesions resemble those of pythiosis. However, zygomycotic cutaneous lesions in horses are usually found on the lateral neck, trunk or head, are smaller than those of pythiosis, and often have no association with standing water.¹

Contributing Institution:

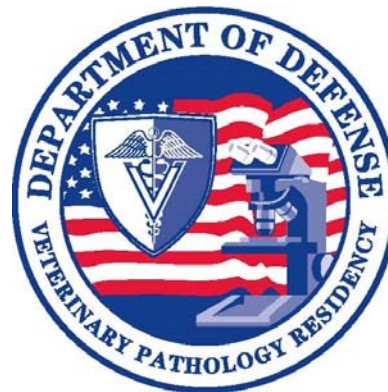
Tuskegee University

College of Veterinary Medicine, Nursing and Allied Health

http://www.tuskegee.edu/academics/colleges/cv_mnah/school_of_veterinary_medicine.aspx

References:

1. Ginn PE, Mansell JEKL, Rakich PM. Skin and appendages. In: Maxie MG, ed. *Jubb, Kennedy and Palmer's Pathology of Domestic Animals*. 5th ed. Philadelphia, PA: Elsevier Saunders; 2007:700-709.
2. Ribes JA, Vanover-Sams CL, Baker CL. Zygomycetes in Human Disease. *Clin Microbiol Rev*. 2000;13:236-301.
3. Wim G, Len JA, et al. *Pythium insidiosum*: An Overview. *Veterinary Microbiology*. 2010; 146:1-16.



WEDNESDAY SLIDE CONFERENCE 2015-2016

Conference 3

23 September 2015

Dr. Donal O'Toole, MVB, Ph.D., Diplomate ECVF, FRCPath
Pathologist, Wyoming State Veterinary Laboratory
Professor, University of Wyoming

CASE I: 8482-15 (JPC 4066661).

Signalment: Bovine neonate, male, Angus (*Bos taurus*).

History: Fourteen-month-old heifer had been bred while still with her dam. Not knowing she was pregnant, she was vaccinated against brucellosis on January 15, 2015, using RB51 vaccine strain of *Brucella abortus*. The fetus was expelled April 9, 2015. The attending veterinarian and an assistant had been exposed to the fetus and fetal fluids.

Gross Pathology: None reported

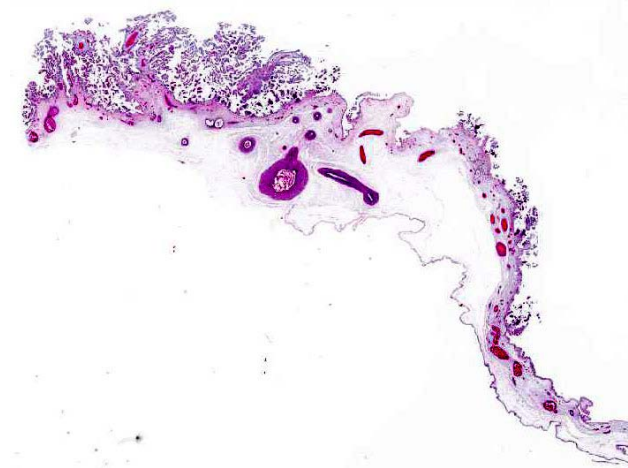
Laboratory Results: Bacterial cultures of placenta were positive for *Brucella abortus*. The isolate was confirmed as strain RB51 with PCR by the USDA-APHIS National Veterinary Services Laboratory.

Histopathologic Description: Sections of cotyledon are characterized by multiple foci of necrosis of villi. Numerous degenerate inflammatory cells are present in the necrotic foci. Variable numbers of neutrophils can be seen scattered throughout the lamina propria.

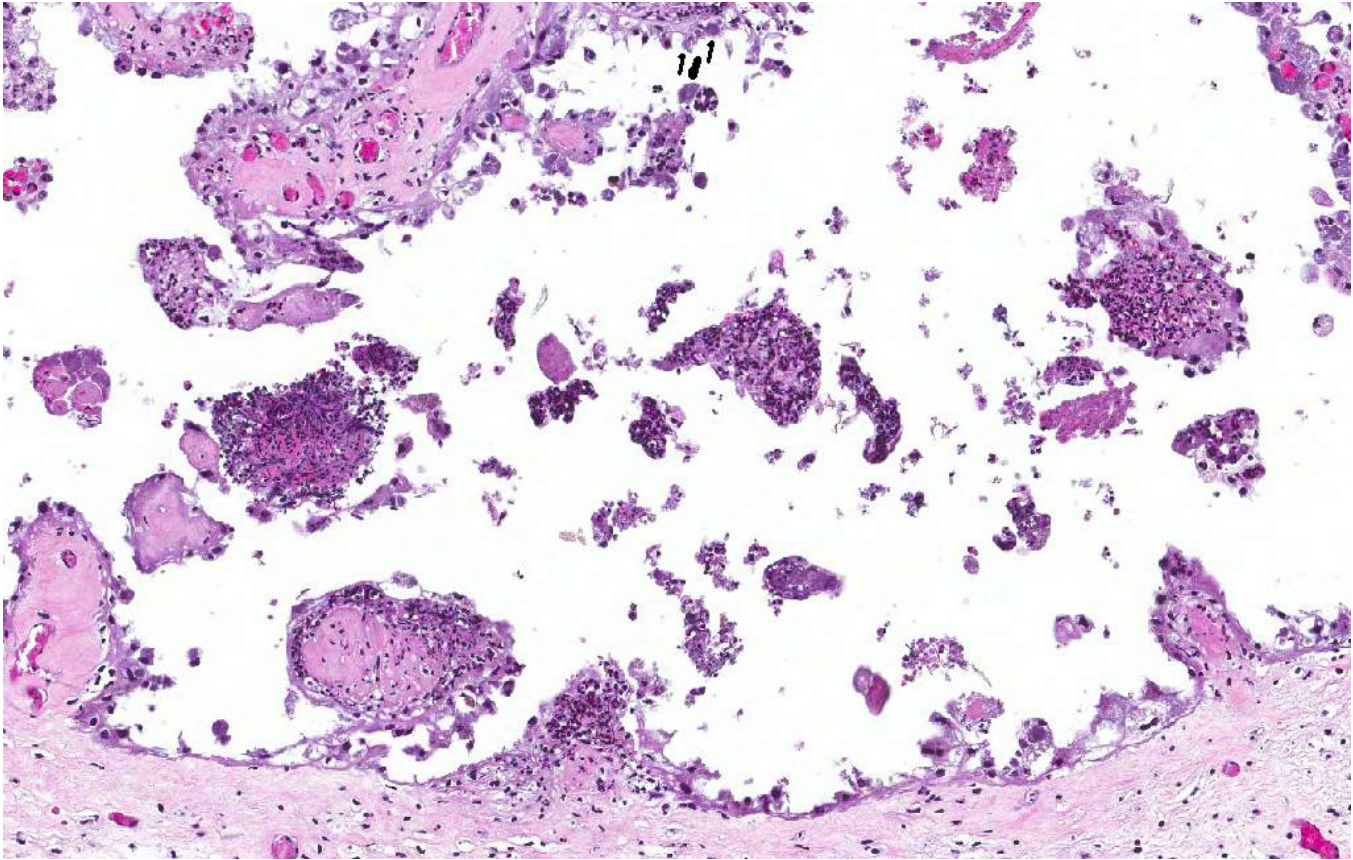
Margination of neutrophils as well as exocytosis is observed in blood vessels in the lamina propria. Occasional fibrin thrombi are present. Cytoplasm of many remaining trophoblasts is distended with coccobacilli.

Contributor's Morphologic Diagnosis:

1. Marked multifocal subacute necrotic and neutrophilic placentitis with intralesional coccobacilli.



The submitted section is composed of cotyledon (upper left), chorion, and allantois.



There is multifocal necrosis of chorionic villi infiltration of moderate numbers of neutrophils. (HE, 80X)

2. Moderate to marked multifocal subacute neutrophilic vasculitis.

Contributor's Comment: Bovine brucellosis is a disease for which the United States Department of Agriculture has implemented an eradication program due to its zoonotic potential. Vaccination plays a major role in the control strategy for brucellosis. The most recently developed vaccine utilizes strain RB51. RB51 is a spontaneous rough mutant of *B. abortus* 2308 that lacks a homopolymer of perosamine as the O-chain component of LPS.⁸ The O-chain is an immunodominant antigen that can cause problems related to serologic diagnosis of vaccinated animals and is expressed in smooth colony types of *B. abortus*.⁸ In addition to lacking the O-side chain of LPS, this isolate is less virulent compared to known virulent strains and is protective against infection with virulent *B. abortus*, making it a suitable vaccine candidate.⁸ During infection, the majority of the organisms localize in cotyledons, placental membranes, and in allantoic fluid. Early infection of the placenta

begins in intercotyledonary erythrophagocytic trophoblasts followed by replication in adjacent chorioallantoic trophoblasts.¹ After replication, there is necrosis of trophoblasts with release of massive numbers of organisms into the uterine lumen.¹ The usual source of infection for cattle is ingestion of organisms from an aborted fetus or placenta, or contaminated uterine discharge.⁷

This case is unusual in that abortion was the result of administration of the vaccine strain (RB51) of *B. abortus*. It has been shown that vaccinating pregnant cattle with RB51 can result in rare placentitis and preterm expulsion of the fetus.⁵ Vaccination of pregnant cattle is ill-advised. Therefore, vaccination is limited to young, non-pregnant cattle. In spite of recommendations, instances of fetal wastage occur.² In the present case, the fact the pregnancy status was unknown resulted in fetal loss. It should be noted that animal workers are at risk of infection by *B. abortus* when assisting parturition or handling infected tissues from these animals.

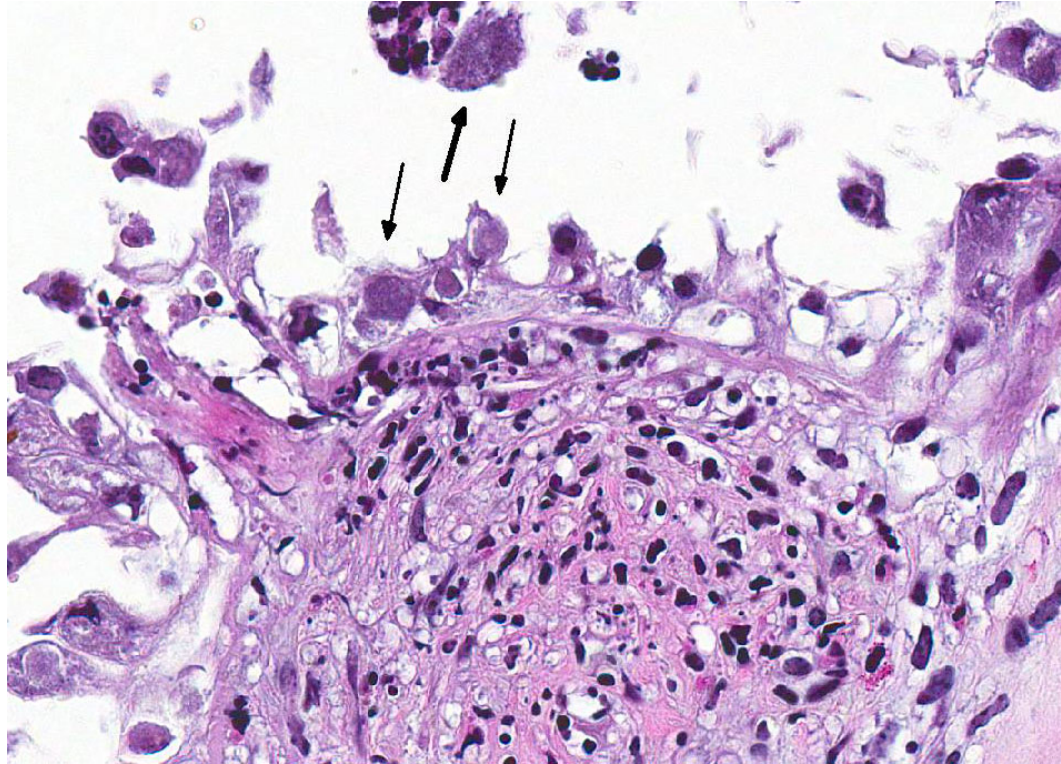
JPC Diagnosis: Placenta, chorionic villi: Placentitis, necrotizing, multifocal to coalescing, mild with mild vasculitis and numerous intratrophoblastic bacilli.

Conference Comment: Conference participants were struck by the low degree of vascular and trophoblastic changes in the section of chorioallantois and speculated the mild nature of lesions was related to abortion being caused by vaccine strain (RB51) of *B. abortus*. The vasculitis was discussed as well as the importance of recognizing vasculitis in placental lesions and cases of abortion, which can help differentiate causes

such as brucellosis and chlamydiosis from other etiologies. Participants described vessels as being infiltrated by low numbers of lymphocytes, plasma cells and neutrophils as well as the presence of fibrin and hemorrhage, accompanied by hypertrophic endothelium, but agreed the overall changes were mild. Vascular changes would also be expected in maternal tissues. Other common lesions seen with *B. abortus* infection include fetal pneumonia, which can vary in severity, as well as microscopic granulomas in the liver, spleen and lymph nodes.

Necrotizing placentitis with intratrophoblastic bacteria is typical for, but not unique to, *B. abortus*, and would be expected to be much more severe in naturally occurring disease. Gross lesions commonly consist of a necrotizing placentitis with thick brown and/or bloody exudates. In general, gross and microscopic

lesions can be very similar with the various agents of bacterial abortion. Differential diagnosis for bacterial placentitis with intratrophoblastic bacteria include other gram negative organisms such as *Coxiella burnetii*, where infected trophoblasts typically have a

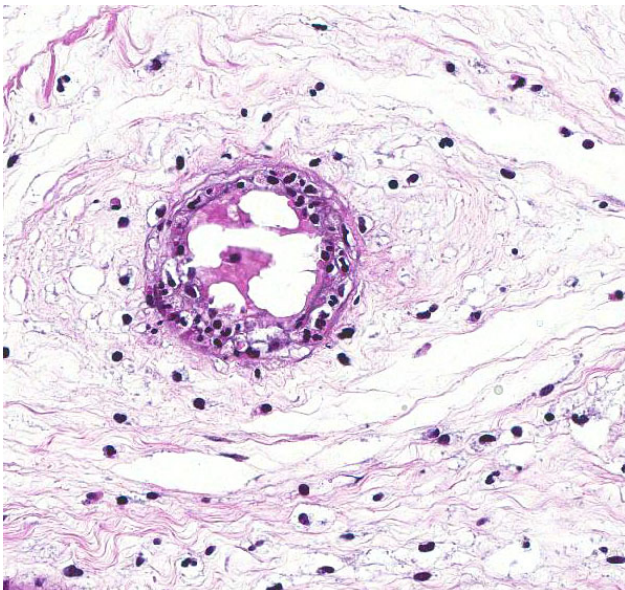


Trophoblasts lining necrotic villi contain numerous bacilli within their cytoplasm. (HE, 400X)

more foamy vacuolated appearance, and *Chlamyphila abortus*, where placental vasculitis would be very prominent. *C. burnetii* is more common in goats and is rare in the U.S., and *C. abortus* is more common in sheep. The gram-positive organism *Listeria monocytogenes* was also discussed, which, in addition to abortion, results in fetal septicemia and the presence of foci of necrosis in many organs. Other bacterial causes of abortion include leptospirosis, which would not result in necrotizing placentitis; and *Campylobacter* sp., which more commonly results in early embryonic death but can result in abortion with similar gross and histologic placental lesions as brucellosis, but lesions are generally less severe.³

There are both smooth and rough strains of *Brucella* spp., with rough strains lacking the expression of O side chain on the lipo-

polysaccharide (LPS), and include the RB51 vaccine strain. Smooth and rough strains enter phagocytic cells, preferably macrophages, differently and the rough strain is more rapidly targeted to the phagolysosomal compartment and is generally unable to replicate, whereas smooth strains are capable of intracellular replication within the phagosome. Virulent *Brucella* spp. employ multiple mechanisms to detoxify free radicals in order to survive in the phagosome, including expression of superoxide dismutases. *Brucella* spp. have also adapted mechanisms to avoid the innate immune system, such as decreased stimulatory activity of TLR4 receptors, being devoid of structures such as pili, fimbriae and capsules that would stimulate pattern recognition receptors (PRRs), as well as prevention of phagosome-lysosome fusion and inhibition of macrophage apoptosis.⁴ Primary routes of infection are considered to be oral exposure to contaminated fetal membranes and aborted fetuses, and ingestion of contaminated milk. Once the infection is localized within lymph nodes, bacteremia results in extension of infection into multiple organs including the uterus, placenta and mammary glands. When the infection reaches the fetal membranes, bacteria replicate within trophoblast cells, and there is extensive necrosis and exudates as well as endometritis, and abortion is the eventual result.⁴



A mild vasculitis affects small vessels within the chorion. (HE, 300X)

Contributing Institution:

Veterinary Diagnostic Center, University of Nebraska-Lincoln, Lincoln, NE.
vbms.unl.edu/nvdl

References:

1. Anderson TD, Cheville NF, Meador VP. Pathogenesis of placentitis in the goat inoculated with *Brucella abortus*. II. Ultrastructural studies. *Vet Pathol.* 1986; 23:227-239.
2. Fluegel Dougherty AM, Cornish TE, O'Toole D, Boerger-Fields AM, Henderson OL, Mills KW. Abortion and premature birth in cattle following vaccination with *Brucella abortus* strain RB51. *J Vet Diagn Invest.* 2013; 25: 630-635.
3. Foster RA. Female reproductive system and mammary gland. In: McGavin MD, Zachary JF, eds. *Pathologic Basis of Veterinary Disease.* 5th ed. St. Louis, MO: Mosby Elsevier; 2012:1110-1115.
4. Olson SC, Palmer MV. Advancement of Knowledge of *Brucella* over the past 50 years. *Vet Pathol.* 2014;51(6):1076-1089.
5. Palmer MV, Cheville NF, Jensen AE. Experimental infection of pregnant cattle with the vaccine candidate *Brucella abortus* strain RB51: pathologic, bacteriologic, and serologic findings. *Vet Pathol.* 1996; 33:682-691.
6. Poester FP, Goncalves VS, Paixao TA, Santos RL, Olsen SC, Schurig GG, Lage AP. Efficacy of strain RB51 vaccine in heifers against experimental brucellosis. *Vaccine.* 2006; 24: 5327-5334.
7. Schlafer DH, Miller RB. Female genital system. In: Maxie MG, ed. *Jubb, Kennedy, and Palmer's Pathology of Domestic Animals.* Vol 3. 5th ed. Philadelphia, PA: Elsevier Saunders; 2007: .
8. Schurig GG, Roop RM, Bagchi T, Boyle S, Buhrman D, Sriranganathan N. Biological properties of RB51; a stable rough strain of *Brucella abortus*. *Vet Microbiol.* 1991; 28:171-188.

CASE II: 2010-2 (JPC 3165093).

Signalment: Six yearling white-tailed deer (*Odocoileus virginianus*), male and female.

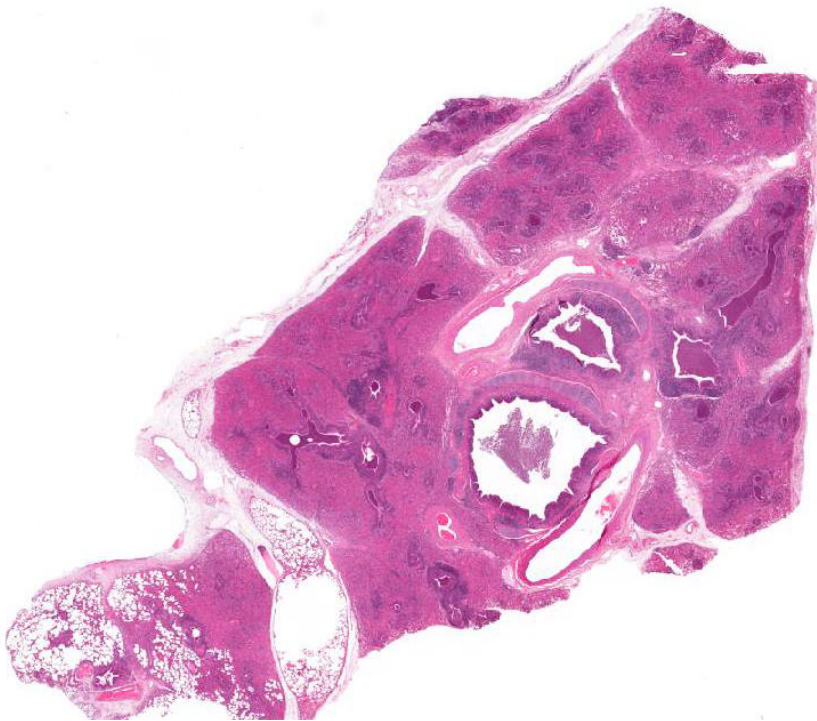
History: Over a period of 6-9 months 6 of 20 white-tailed deer confined to a small pasture developed weight loss, increased respiratory rate, intermittent nasal discharge, and labored breathing, with coughing upon forced exercise. The six affected deer were isolated in a sick pen and treated orally with antibiotics. In spite of antibiotic treatment and ad lib feed, minimal improvement was noted and all 6 deer were euthanized and examined.

Gross Pathology: Deer were thin, in poor body condition with minimal fat stores. Lesions were similar in all deer and varied only in degree of severity. Pulmonary lesions consisted of red to purple discoloration and atelectasis of cranial lung lobes with variable involvement of middle and caudal lung lobes. Discolored and atelectatic lung was sharply demarcated from less affected lung which generally remained pink and inflated. Affected lung was firm and on cut surface

airways oozed purulent exudate. Affected lung did not float in formalin. Tracheal mucosa was diffusely reddened and contained intraluminal mucopurulent exudate. Tracheobronchial and mediastinal lymph nodes were moderately enlarged and edematous.

Laboratory Results: Bacteriologic culture of fresh lung from all deer yielded heavy, pure growth of *Pasteurella multocida*.

Histopathologic Description: Submitted sections of lung are from different animals and differ slightly in degree of involvement and severity. Multifocally, bronchi and bronchioles are variably filled with large numbers of degenerate and non-degenerate neutrophils, small amounts of fibrin, and detached epithelial cells. In the most severely affected airways, epithelium is characterized by multifocal areas of degeneration and necrosis with attenuation of remaining epithelial cells. Moderate numbers of neutrophils are seen within airway epithelium. Affected airways and vessels are surrounded by variable cuffs of lymphocytes, plasma cells and macrophages. The most pronounced lymphoid cuffs contain lymphoid follicles. In the remainder of affected lung alveolar interstitium is congested and alveoli contain neutrophils, erythrocytes and small amounts of fibrin with alveoli near bronchi/bronchioles being most severely affected. Interlobular regions are expanded by clear space due to edema and there are multifocal, mild infiltrates of neutrophils with the pleura.



Airways diffusely contain a cellular exudate and surround alveoli are consolidated and atelectatic. (HE, 6.0X)

Contributor's Morphologic Diagnosis: Lung, bronchopneumonia, fibrinosuppurative, multifocal to focally extensive, acute to subacute, moderate, with multifocal airway epithelial necrosis and interlobular edema.

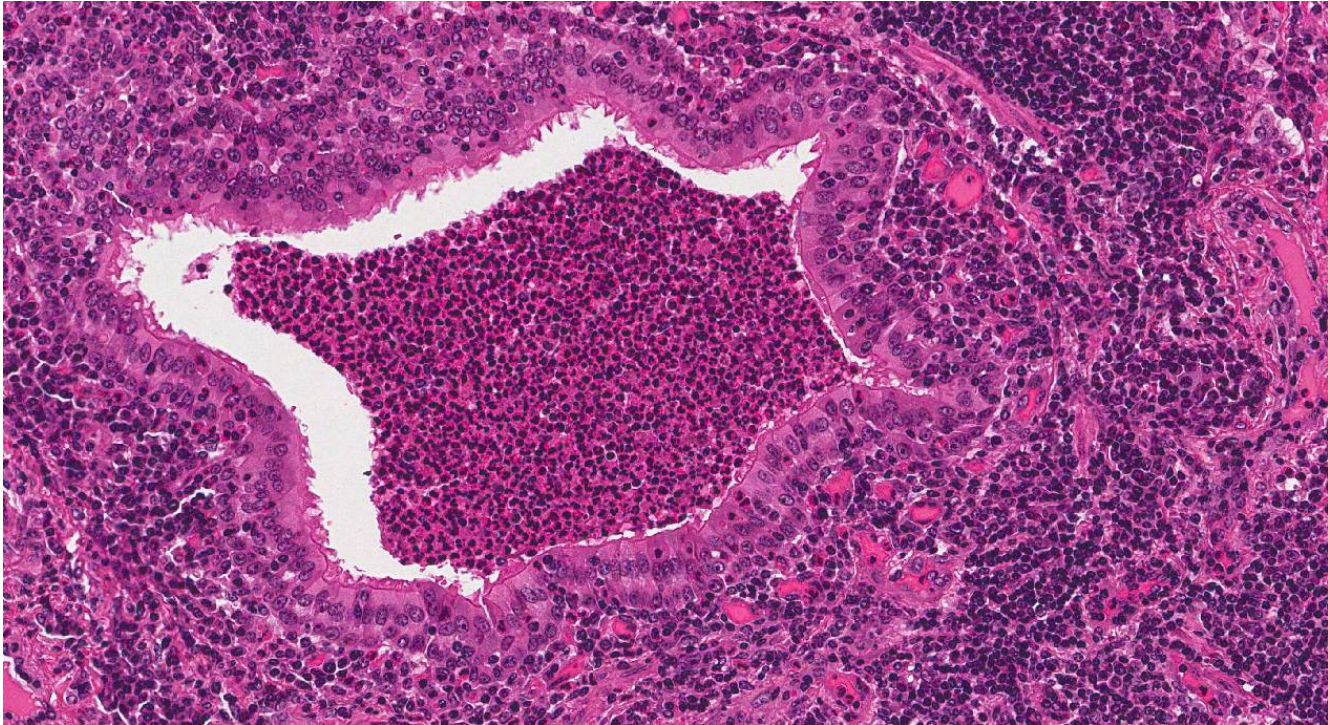
Contributor's Comment: *Pasteurella* organisms are

nonmotile, nonsporeforming, aerobic, fermentative, gram-negative coccobacilli. *Pasteurella* spp. are distributed worldwide and are a common etiology of diseases in cattle, bison, water buffalo, sheep, goats, domestic and wild birds, rabbits, laboratory animals and marine mammals.^{2,4,5,7}

Pasteurella multocida is a common commensal organisms of the tonsil and nasopharynx in healthy ruminants.² Transition from infection to disease may be facilitated by stressors such as

of serogroups D and A, respectively. Serogroup F strains are predominately isolated from diseased poultry.⁴

Pasteurellosis has been recorded in many species of deer including axis, black-tailed deer, mule deer, fallow, red, roe, sambar, reindeer, elk and white-tailed deer.^{4,5,7} Disease generally presents as either hemorrhagic septicemia or pneumonia. Hemorrhagic septicemia has been responsible for outbreaks with high mortality in elk and fallow deer.^{4,5} The pneumonic form, as seen in this case,



Characteristic of *P. multocida* infection, airways are filled with viable neutrophils without necrotic changes in the lining epithelium (HE, 140X)

transport, intercurrent disease, climatic changes, social changes, or changes in feed or management.²

P. multocida has traditionally been classified into 5 capsular groups (A,B,D,E and F). Worldwide, serogroup A isolates are major causes of bovine respiratory disease. Serogroups A, and to a lesser extent D, cause fowl cholera in birds. Serogroups B and E are associated with hemorrhagic septicemia in cattle and water buffaloes in tropical regions of Africa and Asia. Serogroups B and E are rarely isolated from cattle in North America. In pigs, atrophic rhinitis and pneumonia are associated with toxigenic strains

is characterized by fibrinosuppurative bronchopneumonia, with or without necrosis and hemorrhage.

While *Mannheimia haemolytica* (formerly *P. haemolytica*) can cause severe, acute fibrinonecrotic pneumonia and is an important component of the bovine respiratory disease complex, *P. multocida* is associated with less fulminating fibrinous to fibrinopurulent bronchopneumonia with limited lung necrosis.²

JPC Diagnosis: Lung: Bronchopneumonia, suppurative, chronic-active, diffuse, severe with intralobular edema and emphysema.

Conference Comment: This case nicely characterizes bronchopneumonia in a deer and allowed conference participants to discuss the neutrophil-rich, bronchial- and bronchiolar-centric nature of the disease process. Though all agreed that the extensive bronchopneumonia was most consistent with an infectious (most likely bacterial) etiology, most participants determined that infectious organisms were difficult, if not impossible, to visualize by routine histologic examination. Gram stains did not aid in identifying organisms. Additional histologic features discussed included type II pneumocyte hyperplasia, segmental atelectasis, and prominent bronchus-associated lymphoid tissue (BALT) hyperplasia, a finding that varied in severity between slides. Despite the slide variation, the presence of BALT hyperplasia along with the bronchial- and bronchiolar-centric inflammatory process lead conference participants to include *Mycoplasma bovis* as the main differential diagnosis. However, most agreed that the lack of well-differentiated nodules of necrosis made this diagnosis less likely. Another differential diagnosis discussed included *Mannheimia hemolytica*. However, “oat cells,” fibrin rich exudate, and extensive necrosis, characteristic histologic features of *M. hemolytica*, were not present in this case. Additionally, bacterial aggregates are often easy to visualize in pneumonic manheimiosis. The typical gross findings of *M. hemolytica* and *P. multocida* were compared as well. The classic gross postmortem findings of *M. hemolytica* including fibrin, hemorrhage, necrosis, and pleuritis with extensive “marbling” (due interlobular edema) particularly affecting the cranioventral lung regions were key features discussed in making the distinction between *M. hemolytica* and *P. multocida*. Other bacterial agents of respiratory disease in ruminants include *Histophilus somni*, *Trueperella* (formerly *Arcanobacterium*) *pyogenes*, and *Bibersteinia trehalosi*.

Compared to *M. hemolytica*, bacterial pathogenicity is reduced in *P. multocida* infection resulting in a slower onset of disease with absence of necrosis, vasculitis and exudation of

abundant fibrin. In *P. multocida*, injury to cells of the respiratory system results from infiltration of inflammatory cells and release of their mediators and enzymes.⁹ In contrast, *M. hemolytica* causes injury by release of bacterial toxins, such as leukotoxin, in addition to the effects of inflammatory mediators released from leukocytes, which results in a more necrotizing and fibrinous lesion. The leukotoxin, which is a member of the RTX group of toxins, is *M. hemolytica*'s most important virulence factor, and can be directly toxic to cells as well as enhances the overall acute inflammatory response through activation of leukocytes and the complement system. Additionally, *M. hemolytica* has other virulence determinants such as polysaccharide in the capsule which can facilitate bacterial adherence and colonization, and inhibit their phagocytosis.⁹ Environmental stressors and concurrent viral infection with agents such as bovine respiratory syncytial virus, bovine viral diarrhea, and infectious bovine rhinotracheitis virus result in increased susceptibility to infection by the bacterial agents.

P. multocida hemorrhagic septicemia is a reportable condition which occurs in cattle and water buffalo in Asia and Africa, and uncommonly in wild ruminants in the United States as previously mentioned by the contributor.^{4,5} In this condition, the bacteria disseminate hematogenously to multiple organs resulting in congestion and hemorrhages in the respiratory, gastrointestinal and urinary tracts.¹ It is a high mortality condition with death being rapid,⁶ and infection is thought to occur by inhalation or ingestion. Natural infections also occur in goats, but this species is considered more resistant to the infection.⁸

Contributing Institution:

National Centers for Animal Health; Ames, IA
<http://ars.usda.gov/>

References:

1. Annas S, Zamri-Saad M, Jesse FF, Zunita Z. Comparative clinicopathological changes in

buffalo and cattle following infection by *Pasteurella multocida* B:2. *Microb Pathog*. 2015;88:94-102.

2. Confer AW: Update on bacterial pathogenesis in BRD. *Anim Health Res Rev*. 2009;10:145-148.

3. Dabo SM, Taylor JD, Confer AW: *Pasteurella multocida* and bovine respiratory disease. *Anim Health Res Rev*. 2008;8:129-150.

4. Eriksen L, Aalbaek B, Leifsson PS, Basse A, Christiansen T, Eriksen E, Rimler RB: Hemorrhagic septicemia in fallow deer (*Dama dama*) caused by *Pasteurella multocida*. *J Zoo Wild Med*. 1999;30:285-292.

5. Franson JC, Smith BL: Septicemic pasteurellosis in elk (*Cervus elaphus*) on the United States National Elk Refuge, Wyoming. *J Wild Dis*. 1988; 24:715-717.

6. Lopez A. Respiratory system, mediastinum and pleurae. In: McGavin MD, Zachary JF, eds. *Pathologic Basis of Veterinary Disease*. 5th ed. St. Louis, MO: Mosby Elsevier; 2012:500-520.

7. Mackintosh C, Haigh JC, Griffin F: Bacterial diseases of farmed deer and bison. *Rev Sci Tech Off Int Epiz*. 2002;21:249-263.

8. Shafarin MS, Zamri-Saad M, Khairani BS, Saharee AA. Pathological Changes in the Respiratory Tract of Goats infected by *Pasteurella multocida* B:2. *J Comp Path*. 2009;140:194-197.

9. Zachary JF. Mechanisms of microbial infections. In: McGavin MD, Zachary JF, eds. *Pathologic Basis of Veterinary Disease*. 5th ed. St. Louis, MO: Mosby Elsevier; 2012:170-180.

CASE III: 13-11676 (JPC 4032719).

Signalment: 1-year-old female Roosevelt elk (*Cervis canadensis roosevelti*)

History: A one-year-old female Roosevelt elk (*Cervis canadensis roosevelti*) from an elk farm in Oregon received pour-on dewormer in a stanchion on April 20, 2013. Three days later, the animal appeared unstable on its front legs and subsequently became recumbent. Between April 23 and its euthanasia on May 7, the animal was seen by a veterinarian twice, once on April 26 and once on May 3 and received antibiotics and

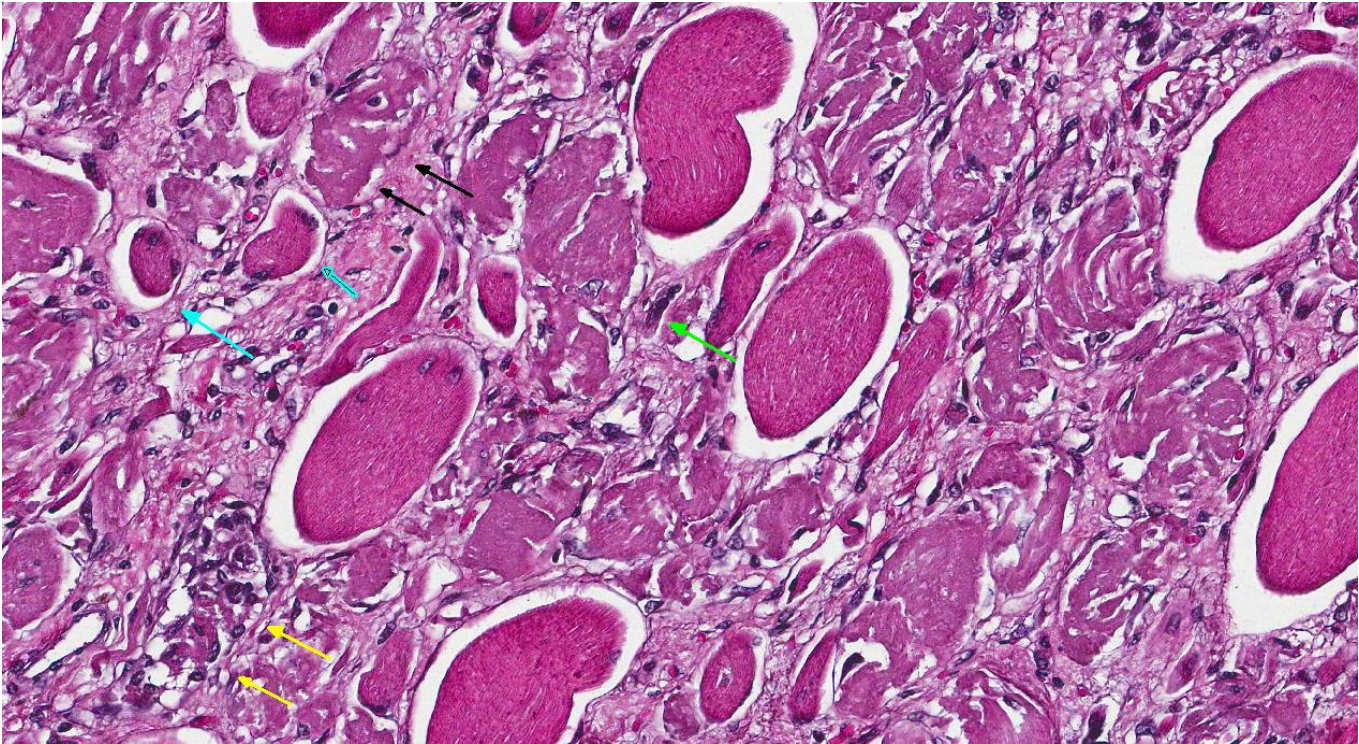
cortisol. The animal was not observed to stand during this entire period.

Gross Pathology: The animal was in good body condition with minimal post-mortem autolysis. Multifocal muscles within the caudal aspect of the left pelvic limb were firm and mottled pale white-tan to pink. The lesions frequently affected entire muscle bellies, but they appeared grossly to be restricted to the left pelvic limb. Similar lesions were not observed in the thoracic limbs, or anywhere else on the body.

Laboratory Results: None.

Histopathologic Description: Up to eighty percent of muscle fibers in examined sections are severely fragmented with a loss of cross striations and hypereosinophilia. These fibers are frequently difficult to distinguish from the extensive fibrous connective tissue in the perimysium. The remaining muscle fibers are markedly varied in size and there is extensive to complete loss of cross-striations. They also undergo one or more of the following changes: formation of contraction bands, hypereosinophilia, vacuolation or milder fragmentation of sarcoplasm, or centralization of nuclei. There is prominent proliferation of satellite cells at the periphery of myocytes. There are frequent centralized nuclei in large, mature muscle fibers.

There is extensive loss of myofibers with replacement by variably dense fibrous connective tissue that expands the epimysium and the perimysium. This fibrous connective tissue occasionally contains rare scattered macrophages and lymphocytes, but active inflammation is mild to absent overall. There are frequent, scattered hemosiderin-laden macrophages. Frequently surrounding or within areas of fibrosis there are multifocal elongated, narrow myocytes with lightly basophilic cytoplasm containing multiple centralized nuclei arranged in a row (strap cells).



This polyphasic skeletal muscle lesion shows many different forms of myocyte injury, including contraction band necrosis (black arrows), infiltration of macrophages (yellow arrows), atrophy (blue arrows), and myocyte regeneration with internalization of satellite nuclei (green arrow). (HE, 120X)

Multiple vessels, particularly small and medium caliber arterioles (but also some large veins) contain fibrin thrombi. Most of these thrombi are older and embedded in circumferential, proliferative spindle-shaped cells with foamy cytoplasm. This proliferation occurs in one to all layers of affected vessels and occludes the lumen, but there are small capillaries present with some red blood cells (recanalization). There is occasionally perivascular hemorrhage. Peripheral nerve bundles within the fascial planes tend to have the epineurium expanded by prominent myxomatous matrix.

Some slides contain myofibers expanded by well-demarcated, ovoid cysts filled with innumerable basophilic organisms (*Sarcocystis* species, suspected) that are not associated with inflammation.

Contributor's Morphologic Diagnosis:

Skeletal muscle: Locally extensive multiphasic myocyte degeneration, regeneration, necrosis, and loss with extensive fibrosis.

Small to medium caliber veins and arteries: Multifocal fibrin thrombi with transmural spindle cell proliferation and recanalization.

Contributor's Comment: Initially—particularly since Oregon has high rates of selenium deficiency in its farmed animals—the top differential diagnosis for this case was nutritional myopathy (white muscle disease). Liver samples were submitted to the Michigan State University Diagnostic Center for Population and Animal Health for selenium testing. The resulting liver selenium content of 3.6 is above the reference range of 0.7 to 2.5 micrograms per gram established for cattle. A previous study of 447 female farmed elk in Oregon found that liver selenium ranged from 0.002-3.15ppm. 42% of these animals had liver selenium levels considered low by cattle standards¹. Although this animal's selenium

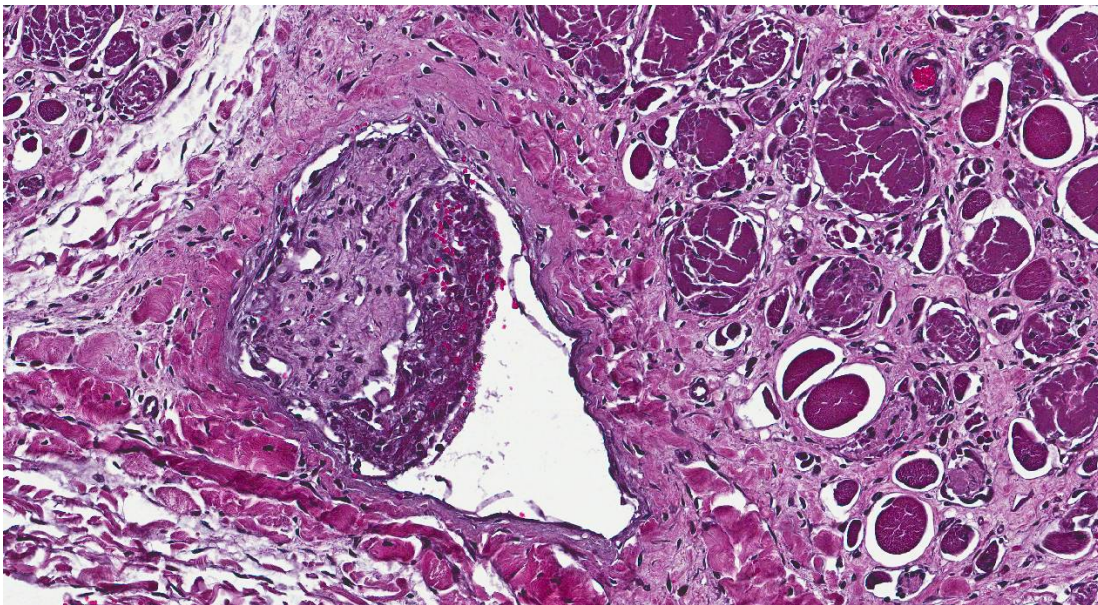
value does not necessarily rule out the presence of a vitamin E or selenium deficiency, the extremely localized nature of the lesion along with the history of being in a stanchion three days prior to the development of symptoms led us to consider the strong possibility of capture myopathy in this case.

Microscopically, the myocyte degeneration and regeneration in the lesion is multiphasic. This is not consistent with a traditional capture myopathy resulting from a single incident. Capture myopathy is thought to result from a combination of local hyperthermia and lactic acidosis coupled with altered blood flow due to massive catecholamine release when an animal (particularly a non-domesticated animal) struggles while being restrained. The resulting combination of hyperthermia, acidosis, and altered blood flow results in localized myonecrosis that can produce a number of distinct syndromes depending on the duration of stress, the extent of the lesion, and the nature of recuperation².

This lesion is problematic with regards to capture myopathy for two reasons: a case with a single reported capture event should produce a monophasic myonecrosis and vascular lesions are not considered a consistent aspect of capture

myopathy. Upon extensive discussion among pathologists in the diagnostic laboratory, we felt that a possible explanation for the observed lesions was an initial incidence of capture myopathy or trauma (or any other possible reason for the initial bout of recumbency). Following the animal being recumbent, and perhaps due an initial exertional rhabdomyolysis, the pressure of the animal's weight on the limb likely produced a localized pressure ischemia.

Shifting of the animal's weight could have produced various incidences of ischemia and reperfusion over the course of disease, resulting in multiple incidences of muscle damage over time, which could explain the multiphasic nature of the myocyte degeneration and regeneration. The vascular lesions could indicate that the initiating injury could have been an infarct, but in the absence of a source of inflammation or thrombosis anywhere else in the body, it seems more likely that the proliferative and thrombotic vascular lesions are secondary to a combination of pressure ischemia and altered blood flow. Of course, the development of thrombi due to stagnation of blood in the vessels likely resulted in infarcts later on in the course of disease, adding to the ischemic lesions produced by pressure on the limb.



Multifocally, vessels contain organizing fibrin thrombi. (HE, 78X)

Another interesting aspect of this case was the absence of an active pigmentary nephrosis in this animal. Although there were a few chronic infarcts in the kidneys along with a few dilated tubules, there were no pigment casts present in the tubules. Despite the fact that the

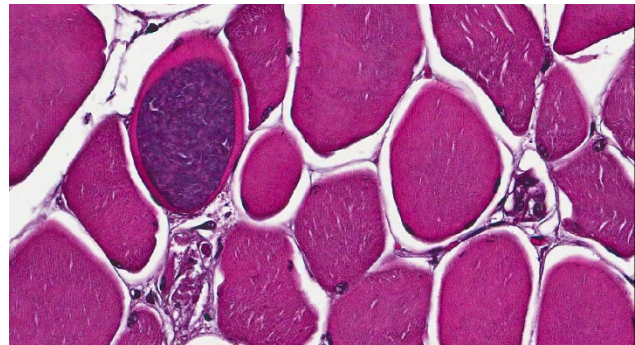
lesions in the limb were likely ongoing, one can speculate that the myocyte degeneration in the limb was not severe enough to produce an active myoglobinuria.

JPC Diagnosis: 1. Skeletal muscle: Degeneration, necrosis and atrophy, diffuse, severe, with regeneration.
2. Skeletal muscle: Sarcocysts, multiple.
3. Skeletal muscle, vessels: Thrombosis, acute and chronic, multifocal, moderate.

Conference Comment: Conference participants agreed that there were confounding factors in this case and it is difficult to determine a specific etiology and chain of events due to the combination of vascular lesions, acute necrosis, atrophy and the presence of variable amounts of fibrous connective tissue. The combination of acute necrosis and atrophy is indicative of a polyphasic process, and participants agreed there is likely more than one event or process which contributed to this lesion. There was discussion regarding the amount of fibrous connective tissue within the section; some participants thought the fibrous connective tissue appeared prominent because of atrophy of surrounding muscle and not necessarily due to excessive fibrosis. Masson's trichrome stain demonstrated the amount of fibrous connective tissue is actually quite variable within the sections, with some areas being dominated by fibrous connective tissue and others having only small amounts, which is likely indicative of the polyphasic and dynamic nature of this lesion. Most agreed the precise cause of the vascular lesions, as well as their role in the pathogenesis of the muscular changes is unclear.

The size of the vessels and duration of obstruction play important roles in determining the size and nature of vascular-origin myofiber necrosis. Blockage of smaller capillaries results in less severe injury due to abundant vascular anastomoses, but can cause segmental myofiber necrosis along with regeneration and, if the cause is ongoing, the lesion would be polyphasic. This is in contrast to blockage of a large artery, where a large section of ischemic muscle would present

as acutely necrotic and as a monophasic lesion, and which would eventually be replaced by fibrosis.³ Causes of muscle ischemia and necrosis that may apply in this case include external muscle pressure and vascular obstruction (due to being recumbent), and swelling of a muscle confined within non-expandable fascia (i.e. compartment syndrome). Additionally, reperfusion injury can result when the animal is moved, which may also cause myofiber necrosis. Muscular injuries in "downer cows" can be either monophasic or polyphasic depending on duration of recumbency.³



Rare myocytes contain intracytoplasmic sarcocysts. (HE, 116X)

Following myocyte necrosis, remaining myofiber nuclei are unable to divide and rely on activation of adjacent satellite cells, which are more resistant to injury than myocytes. These cells divide and become activated myoblasts in order to regenerate the damaged segment of muscle. During the regenerative process, myoblast nuclei can be seen within the center of regenerating myofibers, which is a key finding indicative of regeneration. Success of regeneration depends on whether the basal lamina is intact and whether viable satellite cells are present. In the case of significant muscle trauma, there is often disruption of the basal lamina and most healing will, therefore, occur by fibrosis.³

Upon consultation, JPC physician neuromuscular pathologists did not believe there was a vascular or neurogenic contribution to the histologic changes.

There was slide variation with some sections having low numbers of sarcocysts which

contained numerous bradyzoites. Participants agreed that the presence of the sarcocysts did not contribute to the muscular lesion.

Contributing Institution:

Oregon State University Veterinary Diagnostic Laboratory

<http://vetmed.oregonstate.edu/diagnostic>

References:

1. Stussy SJ, Findholt SL, Johnson BK, Noyes JH. Selenium levels and productivity in three Oregon elk herds. *Northwest Science*. 74:2. 2000. 97-101.
2. Spraker TR. Stress and capture myopathy in artiodactylids. In *Zoo and Wild Animal Medicine: Current Therapy 3*. Fowler ME, ed. WB Saunders Company. 1993. 481-488.
3. Valentine BA, McGavin DM. Skeletal muscle. In: McGavin MD, Zachary JF, eds. *Pathologic Basis of Veterinary Disease*. 5th ed. St. Louis, MO: Mosby Elsevier; 2012:879-898.

CASE IV: 3309 (JPC 4066795).

Signalment: 12-year-old, thoroughbred mare (*Equus caballus*).

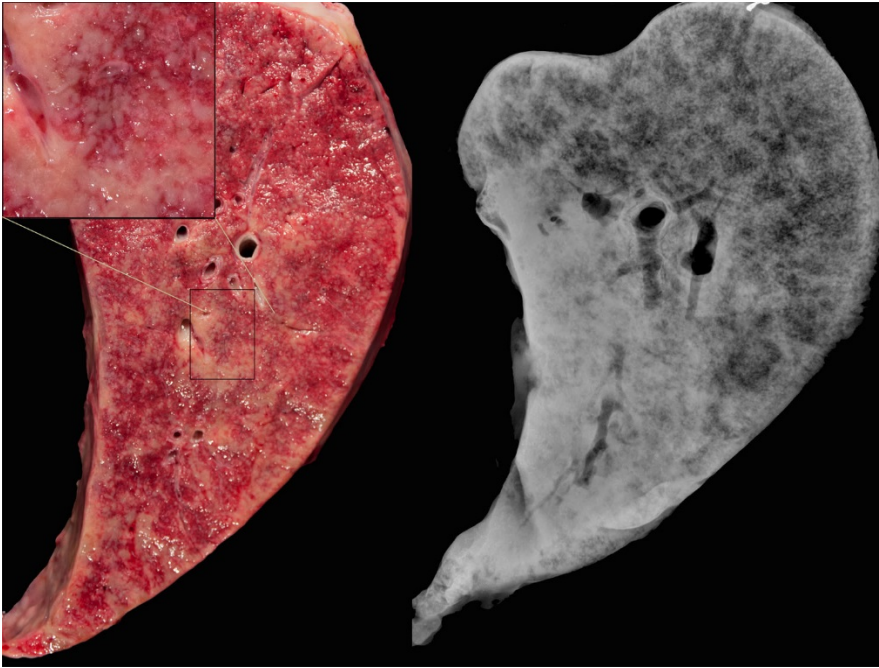
History: This horse lived in Monterey County, California for at least 2 years. She had a six month history of progressive exercise intolerance, cough and tachypnea. On physical examination, the horse had frequent coughing within minimal exercise (e.g. walking) and markedly increased respiratory rate with abdominal effort and nasal flaring at rest. The horse also had moderate, generalized, decreased muscling. No nasal discharge or pyrexia was noted. Euthanasia was elected due to the severity and progression of the clinical signs.

Gross Pathology: Tan, pinpoint nodules, fibrous tracks and coalescing areas of firm consolidation replaced approximately 75% of pulmonary parenchyma. The nodules bulged on cut surface.

Fibrous tracks and consolidated regions frequently extended into the pleural surface. Gritty particles were encountered upon full thickness, serial sectioning of the lung. The pelvis had thickening of the right ilial body and abundant dense fibrous tissue in the area of ischiatic spine (healing fracture callus).

Laboratory Results: Post-mortem radiographs of serial sections of the left lung revealed severe consolidation in the central and ventral lung fields. Small foci of radio-dense material were scattered throughout the lung. Complete blood count (CBC) analysis demonstrated mild fibrinogenemia 500 mg/dL (ref 100-400mg/dL); mild leukocytosis due to neutrophilia 12,155/ μ L (ref 2600-6800/ μ L) with slight toxicity; and mild monocytosis 541/ μ L (ref 0-500/ μ L). Severely compromised pulmonary parenchyma likely contributed to changes in the serum chemistry analysis that included elevated anion gap at 19mmol/L (ref 7-17mmol/L) with low normal bicarbonate at 23mmol/L (ref 23-32). A qPCR analysis for equine herpes virus 5 was negative on section of affected lung.

Histopathologic Description: There are multifocal to coalescing and nodular aggregates of inflammation and fibrosis that efface ~75% of the parenchyma; these aggregates consistently surround bronchioles and are also scattered within the alveolar parenchyma. Fibrosis diffusely thickens the visceral pleura. Nodules comprise aggregates of large foamy macrophages with fewer lymphocytes and plasma cells. Central areas of coagulation or liquefactive necrosis are occasionally present and mineralized. Multinucleated giant cells are

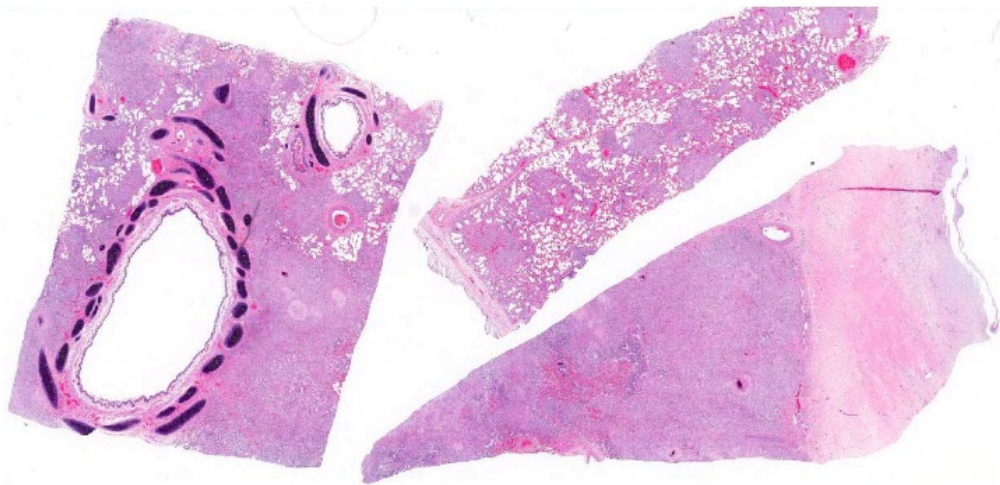


Side by side comparison of the gross (left) and radiographic (right) appearance of a transverse section through the left lung lobe. Approximately 75% of pulmonary parenchyma has multifocal to coalescing, and frequently nodular, regions of inflammation and fibrosis that frequently extended to the pleural surface (gross image, left). The magnified insert of the affected region of the lung demonstrates the tan, inflammatory nodules bulging on cut surface. The radiograph reveals a diffuse, military interstitial pattern with severe ventral consolidation. Only few large bronchi contain air and the rest are obliterated by inflammation and fibrosis. (Image courtesy of: University of California Davis, Department of Pathology, Microbiology, Immunology I Garrod Dr, UC Davis, Davis CA 95616)

occasionally present. Macrophages frequently contain small numbers of refractile, birefringent, and angular crystals that are approximately one micron in diameter and smaller. Bronchiole lumina are occasionally collapsed and contain proteinaceous, granular debris. Small-caliber blood vessels are generally congested.

Contributor's Morphologic Diagnosis:

Lung: Severe, generalized, multinodular to confluent granulomatous pneumonia with intralesional crystals, parenchymal and pleural fibrosis, necrosis and mineralization



There is multifocal to coalescing areas of inflammation which are primarily centered on small airways, as evidenced by the middle section. (HE, 6X)

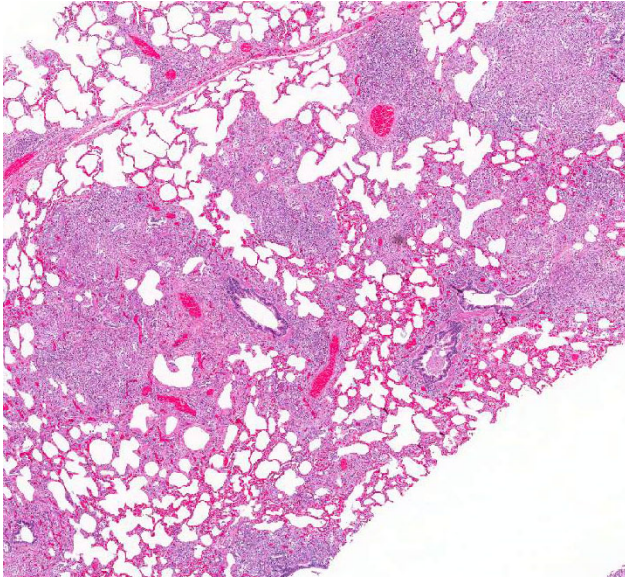
Tracheobronchial, cervical, mediastinal, thoracic aortic lymph nodes (not submitted): Necrotizing and fibrosing granulomatous lymphadenopathy with mineralization and intralesional crystals

Contributor's Comment:

Approximately 75% of lung parenchyma was effaced by generalized granulomatous and fibrosing pneumonia, which is consistent with the history of respiratory compromise, tachypnea, cough and exercise intolerance. The morphology of these lesions with intralesional crystals, combined with the exposure to cristobalite in Monterey County, CA, is consistent with pulmonary silicosis (PS). PS is defined as silicate pneumoconiosis and accompanying pulmonary fibrosis.¹ Lesions are caused by inhalation of cytotoxic silica

dioxide (SiO₂) crystal polymorphs including quartz, cristobalite, and tridymite.¹ PS is seen with increased frequency in horses from the Monterey, Carmel, Napa and Sonoma regions of California where soils have high levels of

cristobalite.⁶ Although PS occurs commonly in the aforementioned areas, a few cases have been reported outside of this region.²

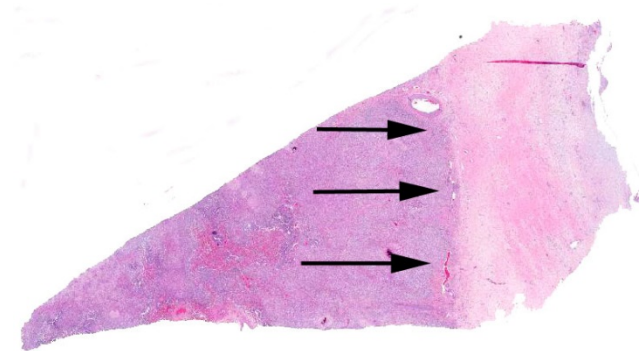


Higher magnification demonstrates the bronchiolocentricity of the inflammation in this section of lung. (HE, 12X)

Common presenting signs in horses with silicosis include weight loss, exercise intolerance, respiratory distress, or increased respiratory effort.² Typical pulmonary radiographic findings in cases of PS have been described in detail, and are characterized by a diffuse, interstitial pattern ranging in distribution from miliary to micronodular to linear; alveolar consolidation is commonly seen.² Gross lesions in uncomplicated cases of PS are usually limited to the pulmonary system. Histologically, lesions are similar to the case presented here with lesions being limited to the pulmonary system and draining lymph nodes. PS is sometimes observed concurrently with bone fragility syndrome. Lesions of the latter have been statistically correlated to pulmonary silicosis; in these cases, the term silica-associated osteoporosis has been proposed (SAO).³ Gross lesions of SAO reflect systemic osteoporosis and are most apparent in the axial skeleton, particularly the scapulae, ribs, spine and pelvis. For example, bowing of the scapulae and irregular thickening of the scapular spine is one of the prominent features of advanced SAO. Multiple pathological fractures in the ribs and regional expansion of the cortex with porous bone in the axial skeleton are common post

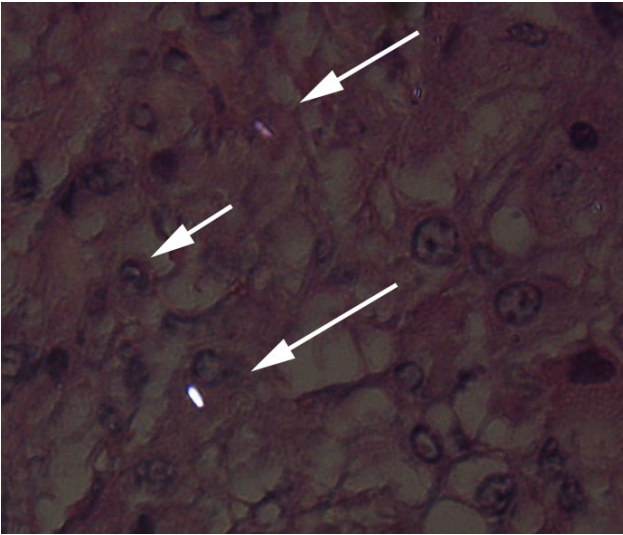
mortem findings. Pathological fractures of the scapulae, pelvis and vertebrae are common as well.¹ Osteolytic foci and loss of cortical bone definition are variably observed radiographically in the bones of the axial skeleton and proximal portion of the appendicular skeleton.¹ Increased, heterogeneous radiopharmaceutical uptake associated with increased bone turnover are commonly found in cervical vertebrae, scapulae, ribs, sternbrae and pelvis (Optional JD. Anderson et al 2008). The histological feature of SAO are numerous, large osteoclasts with supernumerary nuclei and foamy cytoplasm that excessively resorb trabecular and cortical bone within osteolytic lesions.¹ Large cavities and thin disordered trabeculae commonly replace parent cortical and trabecular bone. Additionally, disordered osteonal formation results in a mosaic pattern of lamellar bone packets.¹ The etiopathogenesis of SAO is unknown.¹

In this case, definitive silicosis-associated skeletal lesions were not identified. Although the mare had a healing fracture callus in the pelvis, which is commonly seen in cases of SAO, typical osteoporotic lesions were not observed grossly or radiographically. This case represents an uncomplicated case of PS without confirmed SAO.



One section of lung shows a thick band of pleural fibrosis. (HE 6X)

JPC Diagnosis: Lung: Pneumonia, nodular and granulomatous, multifocal to coalescing, severe, with pleural fibrosis and edema, and scattered intrahistiocytic birefringent crystals.

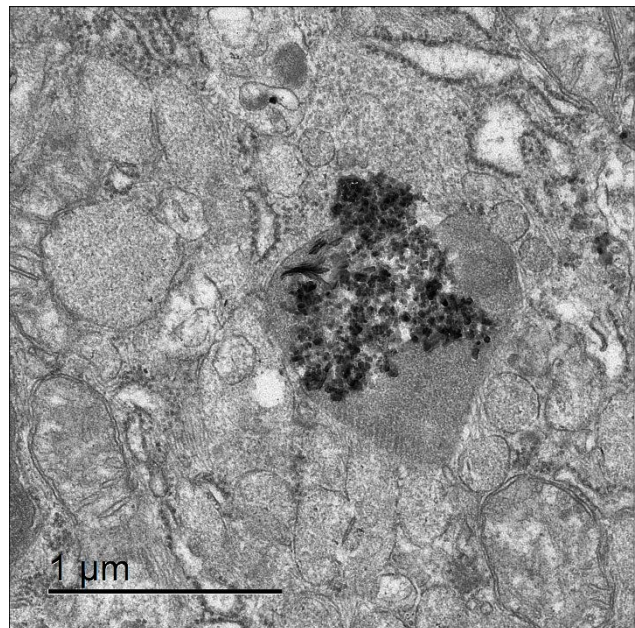


Histiocytes scattered throughout the section occasionally contain small birefringent crystals. (HE, 400X)

Conference Comment: This very interesting case generated lively discussion among participants following review of the history, signalment, and contributor's findings and proposed etiology. Like the contributor, most conference participants agreed the pulmonary changes are centered on small airways and dominated by granulomatous inflammation and fibrosis. Other histologic features discussed included the secondary pleural changes of fibrosis, subpleural edema and mesothelial hypertrophy, as well as the few areas of dystrophic mineralization. That said, participants also commented on the severity of the pathologic changes seen in the sections available for evaluation, which seem excessive in comparison to the relatively low number of birefringent crystals present in most areas of the lesion.

This case was additionally studied in consultation with the Department of Pulmonary and Mediastinal Pathology, whose pathologists have more familiarity and experience with the pathology of pulmonary silicosis, a common occupational exposure in humans. Similar to the contributor and conference participants, the pathologists described the lesions in this case as being centered on small airways (bronchiolocentric), an observation more apparent in the less affected areas of the lung. Specific changes they described include airway constriction, distortion, obliteration and

metaplasia secondary to granulomatous inflammation; the bronchiolocentric nature of the lesions indicates the airway as the route of injury. That said, they interpreted the pattern of the granulomatous inflammation as more commonly associated with an infectious etiology versus pulmonary silicosis, such as that from a fungal or mycobacterial agent; in humans, the inflammatory pattern can also occur with inhaled antigens. In their evaluation, the histologic changes in this horse would be atypical for pulmonary silicosis, as the condition in humans typically consists of well-circumscribed nodules with a central area of lamellated collagen bundles surrounded by a thick rim of histiocytes. Furthermore, the nodules seen in human cases of pulmonary silicosis most often contain many more birefringent crystals compared with the extremely low number seen in this individual. Various tissue histochemical stains of submitted unstained serial sections did not demonstrate microbial organisms in this horse.



Transmission electron microscopy of affected cell with a ruptured organelle containing crystals. (Image courtesy of: University of California Davis, Department of Pathology, Microbiology, Immunology, 1 Garrod Dr, UC Davis, Davis CA 95616)

In addition to pulmonary silicosis, conference participants also included equine herpes virus 5 (equine multinodular pulmonary fibrosis) and mycobacterial infection in the differential

diagnosis. Equine multinodular pulmonary fibrosis is histologically characterized by marked interstitial fibrosis with alveolar like architecture lined by cuboidal epithelial cells. Macrophages and neutrophils are present in airways in variable numbers, and intranuclear inclusion bodies are occasionally seen in macrophages.⁷ Mycobacterial agents known to cause granulomatous pneumonia in horses include *Mycobacterium avium complex*, *Mycobacterium tuberculosis* and *Mycobacterium bovis*. Unlike ruminants, the granulomas in horses typically do not have prominent caseous necrosis or calcification in the center of lesions, and extensive fibrosis is seen with chronicity, giving the lesions a sarcomatous appearance.⁴

We thank the contributor for providing excellent supporting materials with the case submission, which immensely increased the teaching and learning value of this very interesting case, including the superb gross and electron microscopy images, radiographs and clinical pathology data.

Contributing Institution:

University of California Davis
Department of Pathology, Microbiology,
Immunology
1 Garrod Dr
UC Davis
Davis CA 95616

References:

1. Arens AM, Barr B, Puchalski SM, *et al.* Osteoporosis associated with pulmonary silicosis in an equine bone fragility syndrome. *Vet Pathol.* 2011;48:593-615.
2. Berry CF, O'Brien TR, Madigan J, Hager DA. Thoracic radiographic features of silicosis in 19 horses. *J Vet Intern Med.* 1991;5:248-256.
3. Durham MG, Armstrong CM. Fractures and bone deformities in 18 horses with silicosis. *AAEP Proc.* 2006;52:1-7.
4. López A. Respiratory system, mediastinum and pleurae. In: McGavin MD, Zachary JF, eds.

Pathologic Basis of Veterinary Disease. 5th ed. St. Louis, MO: Mosby Elsevier; 2012:501-509.

5. Myers RK, McGavin MD, Zachary JF. Cellular adaptations, injury, and death: Morphologic, biochemical and genetic bases. In: McGavin MD, Zachary JF, eds. *Pathologic Basis of Veterinary Disease.* 5th ed. St. Louis, MO: Mosby Elsevier; 2012:39-43.
6. Schwartz LW, Knight HD, Whittig LD, Malloy RL, Abraham JL, Tyler NK. Silicate pneumoconiosis and pulmonary fibrosis in horses from the Monterey-Carmel peninsula. *Chest.* 1981;80:82-85.
7. Williams KJ. Gammaherpesviruses and pulmonary fibrosis: Evidence from humans, horses and rodents. *Vet Pathol.* 2014;51(2):372-384.



WEDNESDAY SLIDE CONFERENCE 2015-2016

Conference 4

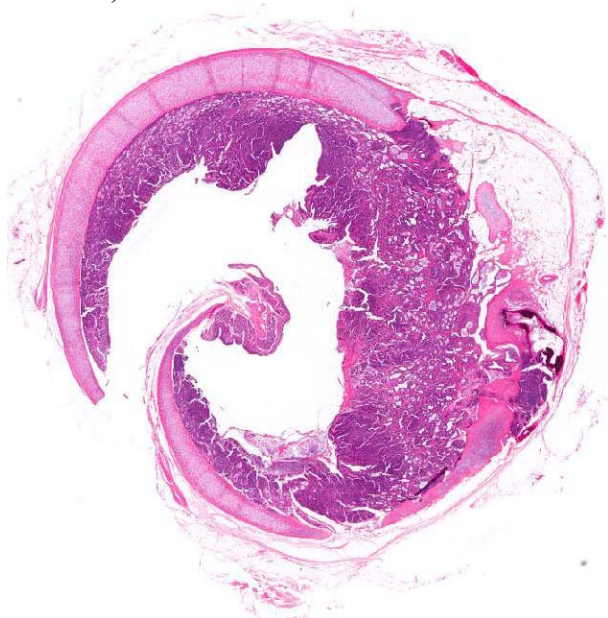
30 September 2015

CASE I: 15H672 (JPC 4066007).

Signalment: 10 year old neutered male domestic short hair cat (*Felis catus*).

History: The cat presented for chronic history of respiratory distress. Mass identified in trachea.

Gross Pathology: Focally extensive thickening/protrusion of the tracheal mucosa that partially occluded the lumen (1.5 cm x 1 cm x 0.25 cm).



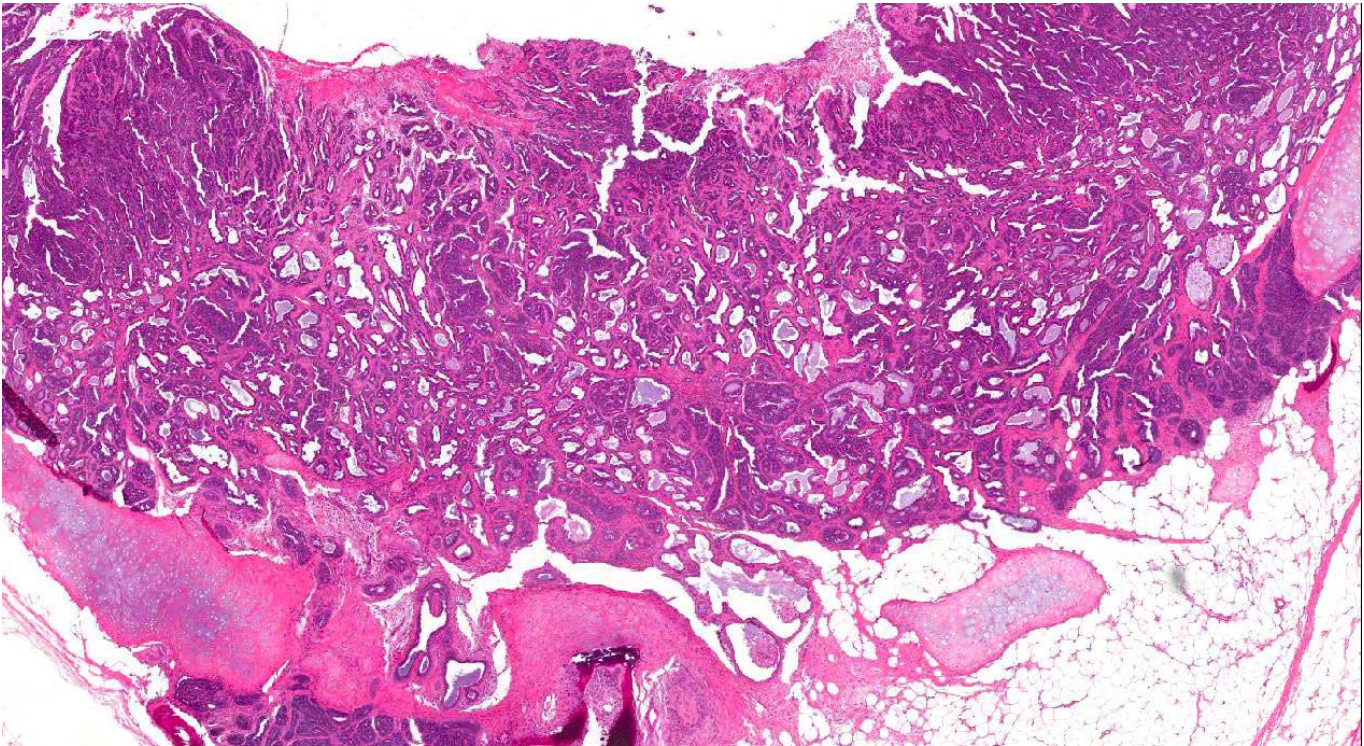
1An infiltrative, well-demarcated neoplasm circumferentially thickens and effaces the tracheal submuco, multifocally infiltrating into the cartilage of the tracheal rings. (HE 4X)

Laboratory Results: None

Histopathologic Description: Sections of trachea in which there are marked thickening/expansion of the mucosal area by a partly delineated and nonencapsulated mass within the subepithelial/lamina propria area that contains submucosal glands. The mass is composed of cells arranged in numerous variably-sized acini and small cysts with occasional dense clusters in one area supported by a fine fibrovascular stroma. The cysts are lined by one to several layers of cells that are cuboidal with modest amounts of basophilic cytoplasm and a single oval nucleus with finely dispersed chromatin. Mitoses are not seen. Some of the acini and cysts contain small amounts of eosinophilic secretion product. Surrounding many of the cysts are minimal multifocal infiltrates of lymphocytes. A few cells of the mass extend into the subjacent tracheal cartilage in an area.

Contributor's Morphologic Diagnosis:
Trachea: Mucosal adenocarcinoma

Contributor's Comment: The mass appears to have arisen from glands of the tracheal mucosa and, as described, protrudes into the tracheal lumen and extends at least in one area into the subjacent tracheal cartilage. Mitotic figures are



2The infiltrative neoplasm is composed of variably-sized tubules and acini which are often lined with mucin. (HE, 20X)

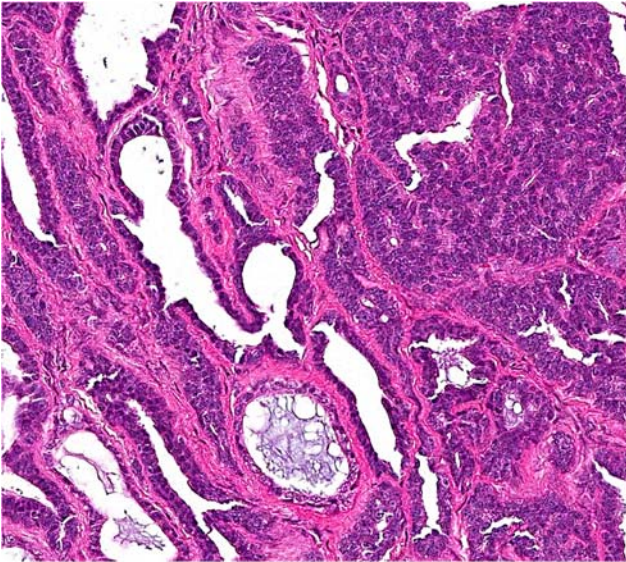
not common and there is little nuclear atypia; therefore, an adenoma is a consideration. However, the mass appears to be expansile replacing the mucosa in areas and, as indicated, extends to the tracheal cartilage. Tumors of the trachea are very rare in dogs and cats. One publication describes a tracheal tumor in a cat.³ It is unlikely that the mass is metastatic since: a) Metastasis to the trachea is rare, and b) other neoplastic masses were not identified in the animal. Other types of neoplasms that can occur in the trachea include: Squamous cell carcinoma (especially in humans that smoke), adenoid cystic carcinoma, papilloma, chondroma, hemangioma, and carcinoid. This location of the mass has similarities to adenoid cystic carcinoma seen in humans.⁵

JPC Diagnosis: Trachea: Mucosal adenocarcinoma.

Conference Comment: Characteristics of this unique neoplasm which generated discussion during the conference include the focal area of infiltration into tracheal cartilage (may not be present in all slides) and the fact that it was

circumferential in nature, affecting the entirety of tracheal mucosa. Participants noted frequent piling of cells and the focal invasion as two characteristics indicative of a more malignant phenotype. Most agreed the neoplasm was likely primary in the trachea due to the resemblance of the neoplasm to tracheal glands and the fact that another primary tumor was not reported in this animal.

Other primary tracheal neoplasms reported in domestic species, not listed above, include undifferentiated carcinoma, plasmacytoma, leiomyoma, fibrosarcoma, mast cell tumor, rhabdomyosarcoma, osteochondroma, osteosarcoma,⁷ and primary intratracheal lymphosarcoma.² Epithelial tumors and osteo-chondroma are the most common tumors of the feline and canine trachea, respectively.⁴ Laryngeal tumors are also considered rare, but occur more frequently than tracheal tumors. Papillomas and squamous cell carcinomas are the most common laryngeal tumors in dogs, and laryngeal lymphomas are occasionally seen in cats.⁶ Neoplasms can be extraluminal or intra-



Higher magnification of the neoplasm showing the marked variation in size of neoplastic acini, as well as the dense fibrous supporting stroma.(HE, 88X)

luminal and cause swelling in the neck and/or tracheal obstruction, respectively, depending on location; dyspnea, cough and dysphagia are common associated clinical signs. Studies have suggested an association between tobacco smoke and oral squamous cell carcinoma in cats,¹ but the precise relationship between tobacco smoke and respiratory tract tumors in cats is unclear, although it can be postulated, based on secondhand smoke being a known human carcinogen.

Contributing Institution:

College of Veterinary Medicine, Iowa State University, Ames, Iowa 50010
Iowastateuniversity.com

References:

1. Bertone ER, Snyder LA, Moore AS. Environmental and lifestyle risk factors for oral squamous cell carcinoma in domestic cats. *J Vet Intern Med.* 2003; 17(4):557-62.
2. Brown MR, Rogers KS, Mansell KJ, Barton C. Primary intratracheal lymphosarcoma in four cats. *J Am Anim Hosp Assoc.* 2003;39(5):468-472.
3. Cain GR, Manley P. Tracheal adenocarcinoma in a cat. *JAVMA.* 1983;182(6):614-616.

4. Carlisle CH, Biery DN, Thrall DE. Tracheal and laryngeal tumors in the dog and cat: Literature review and 13 additional patients. *Vet Radiol.* 1991;32:229-235.
5. Hu Z, Meng Y, Wu H, Shen J, Bi Y, Luo Y, et al. Adenoid cystic carcinoma of the tracheobronchial tree: Clinico-pathologic and immunohistochemical studies of 21 cases. *Int J Clin Exp Pathol.* 2014;7(100):7527-7535.
6. Lopez A. Respiratory system, mediastinum, and pleurae. In: McGavin MD, Zachary JF, eds. *Pathologic Basis of Veterinary Disease.* 5th ed. St. Louis, MO: Mosby Elsevier; 2012:480.
7. Ramirez GA, Altimira J, Vilafranca M. Cartilaginous tumors of the larynx and trachea in the Dog: Literature review and 10 additional cases (1995-2014). *Vet Pathol.* 2015; Apr 16, Epub: 1-

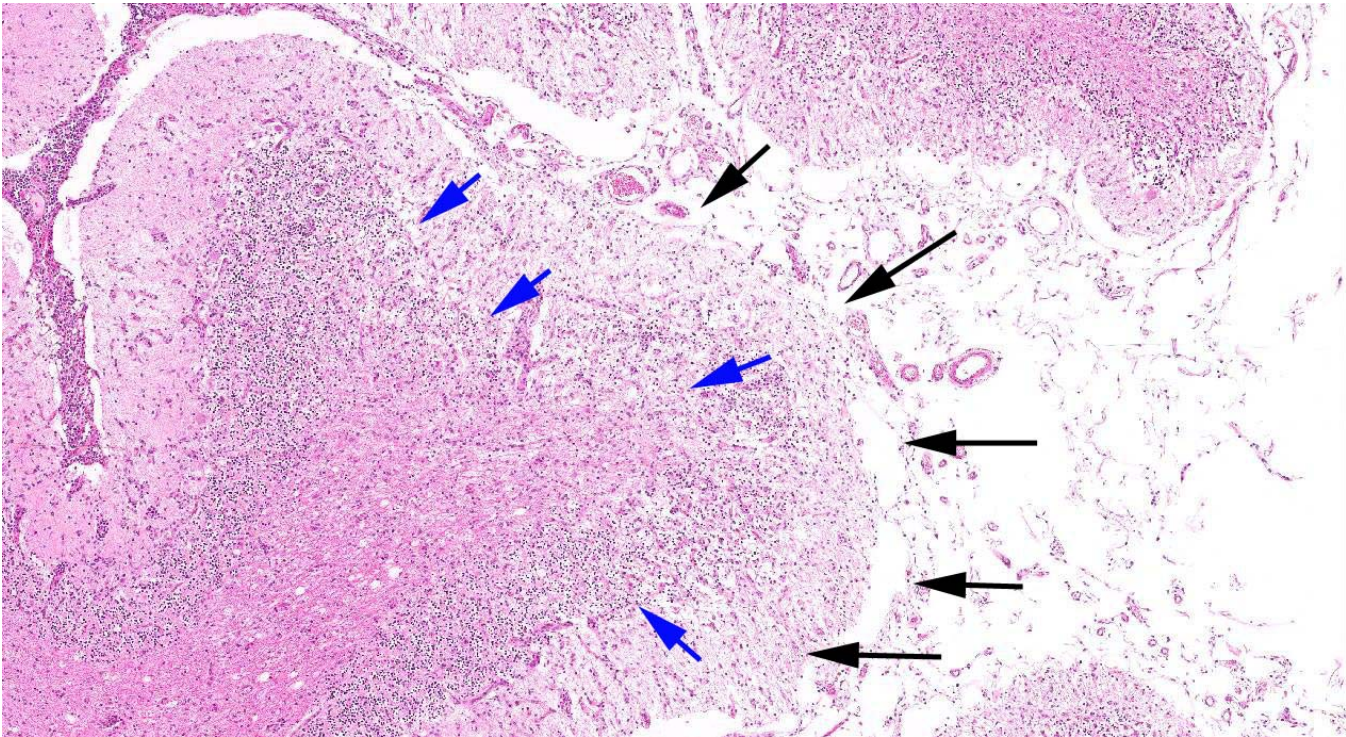
CASE II: 13-338 (JPC 4066222).

Signalment: 5-month-old, female, Labrador retriever, canine (*Canis familiaris*).

History: Approximate 3-month history of progressively abnormal gait and ataxia. Neurological examination revealed mild to moderate tetraparesis and mild proprioceptive ataxia in the pelvic limbs. Evaluation of the spinal reflexes showed reduced flexion in all four limbs and also reduced muscle tone in the pelvic limbs. The patellar reflexes were reduced bilaterally. MRI findings indicated cerebellar atrophy.

Gross Pathology: Examination of the brain reveals mildly increased amounts of clear cerebrospinal fluid surrounding the brain. The cerebellum is diffusely small relative to the cerebrum and medulla with the caudal aspect of the fourth ventricle extending beyond the caudal margin of the vermis. The folia appear diffusely thin with widening of the sulci and moderate congestion of the meninges. The remaining carcass is grossly unremarkable.

Laboratory Results: Cytological examination of the cerebrospinal fluid shows moderate mixed

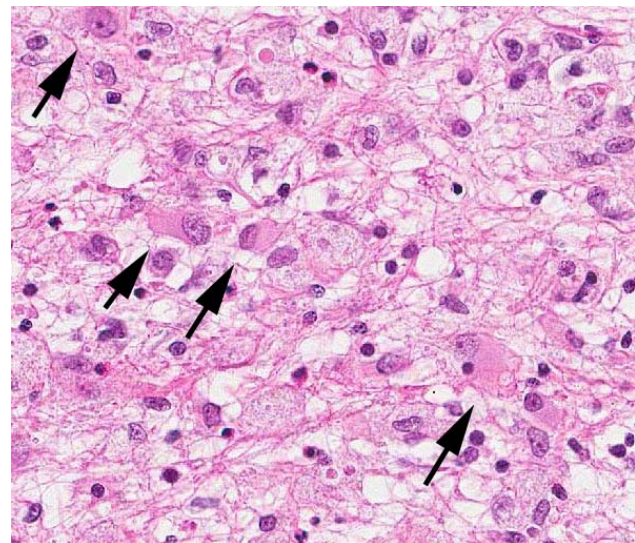


There is marked pallor (necrosis) of the submeningeal gray matter of the cerebellar folia (black arrows). The necrosis extends into the underlying molecular layer, which is now hypocellular due to extensive neuronal necrosis (blue arrows). (HE, 37.5X)

pleocytosis. Samples of brain tissue are PCR positive for *Neospora caninum* and PCR negative of canine herpesvirus, canine parvovirus, *Toxoplasma gondii*, and *Sarcocystis sp.*

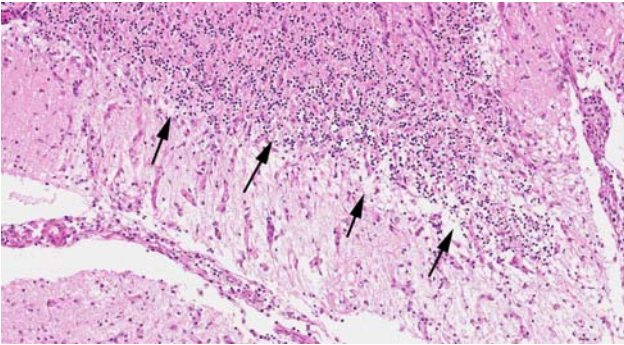
Histopathologic Description: Brain (cerebellum and brainstem): The cerebellar folia are partially to extensively disrupted by multifocal to coalescing foci of neuropil rarefaction, loss and collapse with marked Gitter cell infiltration and fibrous astrocyte proliferation, gliosis, and proliferation of small caliber vessels lined by reactive endothelium. Low to moderate numbers of plasma cells, lymphocytes, fewer eosinophils and neutrophils are interspersed amongst the collapsed folia, expand the overlying meninges, and distend perivascular spaces within the subjacent cerebellum and brainstem. Smaller, randomly scattered foci of gliosis, nonsuppurative inflammation, and mild rarefaction are scattered randomly within the cerebellar peduncles and brainstem. Within the foci of inflammation, and randomly distributed within the neuropil, are variably frequent protozoal tissue cysts that measure up to 113 μm in diameter. These cysts have a 2 - 3 μm thick

cyst wall and contain numerous 8 x 2 μm basophilic bradyzoites (**Figure 4**). Sporadic foci of axonal swelling, digestion chambers containing few debris-filled Gitter cells, and occasional spheroids are noted throughout the white matter.



Necrotic gray matter contains numerous astrocytes with abundant eosinophilic cytoplasm (gemistocytic astrocytes). (HE, 228X)

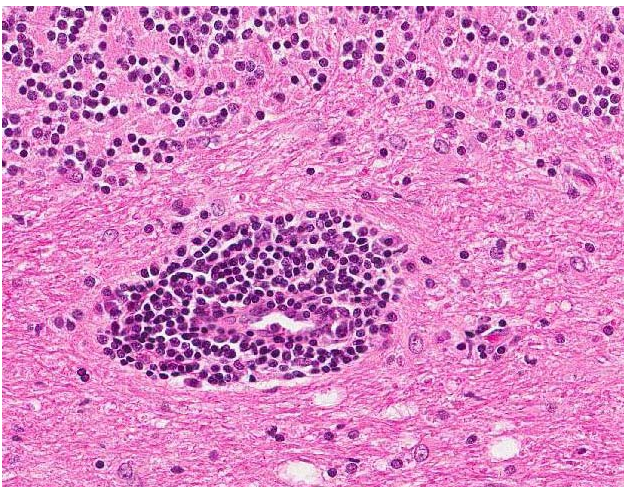
In tissues not included for conference material, also contain similar lesions and protozoal tissue cysts. These lesions were noted in the cerebrum, midbrain, thalamus, and spinal cord with mild infiltration of the spinal nerve roots.



Regionally, there is extensive loss of Purkinje cells (black arrows). (HE, 44X)

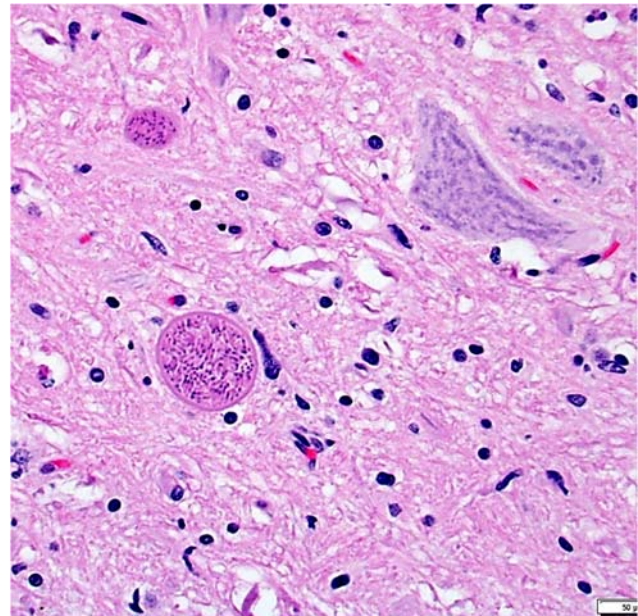
Contributor's Morphologic Diagnosis: Brain (cerebellum and brainstem): Meningoencephalitis, lymphoplasmacytic, histiocytic, necrotizing, subacute to chronic, multifocal, moderate to marked with protozoal tissue cysts (consistent with *Neospora caninum*)

Contributor's Comment: Additional findings that were not present in all slides include rare clusters of free 2 x 6 μm , spindle-shaped tachyzoites within the neuropil and fibrinoid degeneration scarcely noted within the walls of arterioles. Overall, the microscopic findings and PCR results confirm the etiologic diagnosis of *Neospora* encephalitis as the underlying cause



There is multifocal marked lymphohistiocytic perivascular cuffing within the underlying white matter. (HE, 150X)

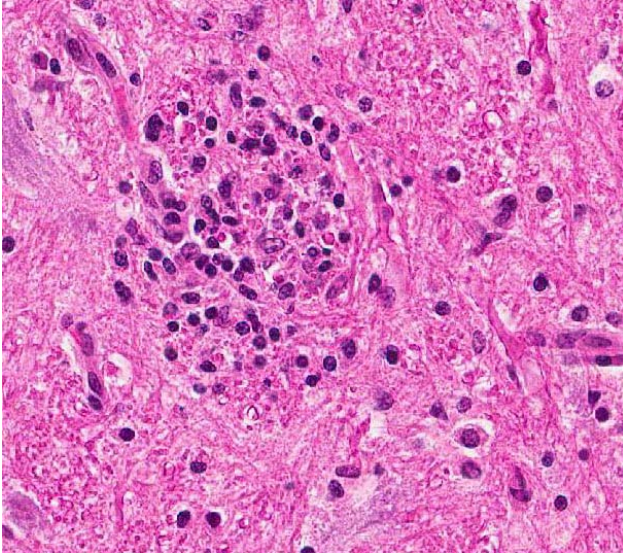
for the progressive ataxia in this 5-month-old Labrador retriever puppy. *Neospora caninum* is a protozoan parasite of animals and can cause serious neuromuscular and polysystemic disease in dogs,^{2,6} as well as significant disease in cattle,^{6,9} small ruminants, horses, and wildlife.⁵ Infection can be fatal in dogs of any age, but disease is most severe in puppies less than 6 months of age and those that are congenitally infected.^{5,7,8} Based on the literature, there is an apparent age-related variation in lesion distribution in the canine. Young dogs and puppies typically develop lesions in the skeletal muscles and spinal nerve roots with resultant ascending paralysis, which tends to be most severe in the hind limbs.¹ Lesions may also be found in multiple organs including the central nervous system, lungs, heart, and liver.^{1,8}



Randomly distributed throughout both necrotic and unaffected areas are numerous apicomplexan cysts ranging up to 130 μm . (HE, 400X) (Image courtesy of: University of Calgary Faculty of Veterinary Medicine, Clinical Skills Building, 11877 85th St NW, Calgary, AB T3R 1J3 <http://vet.ucalgary.ca>)

Infection in adult dogs can result in polymyositis, polysystemic infection, or multifocal central nervous system involvement.^{8,10} Several reports describe necrotizing cerebellitis and cerebellar atrophy as a significant lesion associated with *Neospora* encephalitis in adult dogs.^{3,11,12} This particular case is unique in that significant the necrotizing cerebellar lesions were found in a puppy. Transmission of *N. caninum* in dogs may

occur both vertically and horizontally. Vertical transmission is well recognized in the dog with data suggesting that transmission from the dam to puppies occurs transplacentally, during the terminal stages of gestation, or postnatally via



Ruptured Neospora cysts are replaced by glial nodules (HE, 320X)

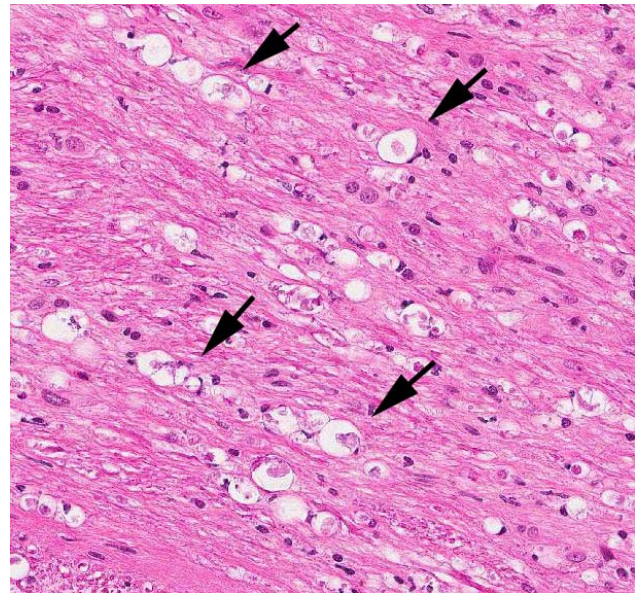
milk.⁹ Horizontal transmission also occurs in the dog through ingestion of infected tissues.⁹ Further communications with the breeder revealed that the dam of this puppy, as well as 10 other dogs from the same kennel, was fed a diet of raw beef and deer. Additional serological testing revealed that dam, as well as 4 other dogs, tested positive for *Neospora caninum*. The diet of raw tissues were the likely source of infection in the dam with subsequent horizontal transmission this puppy. Given that most puppies do not develop clinical signs until over 4 weeks of age,⁸ it is difficult to determine if transplacental or postnatal infection occurred in this case.

JPC Diagnosis: Cerebellum and brainstem: Necrotizing polioencephalitis, subacute, multifocal to coalescing, moderate with lymphocytic and neutrophilic meningitis and apicomplexan schizonts.

Conference Comment: Central nervous system (CNS) changes in the slide due to *Neospora* infection were profound and conference participants noted the protozoal schizonts were often found in less affected areas of the section;

the precise reason for this discordant finding is unclear but not uncommon. Conference participants agreed that the most prominent change in the cerebellum was necrosis and loss of cerebellar grey matter extending into the adjacent white matter. The molecular and granular cell layers were reduced in thickness and there was loss of Purkinje cells with occasional empty baskets in the most severely affected areas. Glial nodules and prominent spheroids were described, as well as inflammatory infiltration of the meninges with extension into, and prominent expansion of, Virchow-Robin spaces. The inflammatory infiltrate was primarily mononuclear, dominated by lymphocytes, plasma cells and gitter cells; the latter being most noticeable in areas of necrosis and neuroparenchymal loss.

Differential diagnosis considered for this case included *Toxoplasma gondii* as well as *Sarcocystis* spp. Many features of toxoplasmosis and neosporosis are similar including the presence of the proliferative tachyzoite and tissue cyst phases. However, *N. caninum* does not develop in a parasitophorous vacuole and has a thicker cyst wall than *T. gondii*. The differences cannot be reliably differentiated by light microscopy, and require the use of electron microscopy or immunohistochemistry in many cases.¹⁴ Ultrastructural differences include



Multifocally, within the folial white matter, there is axonal damage with swelling and formation of digestion chambers. (HE, 320X)

greater number of micronemes and rhoptries with *N. caninum*, in addition to a thicker cyst wall.¹² *N. caninum* is more commonly reported in the CNS where the tissue cysts are most commonly found; although *T. gondii* has a CNS form causing similar histologic changes. *N. caninum* seems to have an affinity for cells of the monocyte macrophage system, although many cell types can be infected, and it likely spreads to the CNS via leukocyte trafficking.¹⁴ Toxoplasmosis seems to affect a wider variety of mammalian species

Although very uncommon, both *Sarcocystis canis* and *Sarcocystis neurona* have been documented to cause CNS disease in dogs,¹² In one documented case of *S. neurona* the affected dog was receiving immunosuppressive therapy and developed widespread encephalitis, predominantly in the grey matter, with brainstem, cerebellum and cerebrum being involved. The lesions also consisted of intense areas of inflammation, which was most pronounced in the cerebellum.⁴ The dividing schizonts of *S. neurona* form distinct rosettes of merozoites, arranged around a prominent residual body and their schizonts differ from other protozoa in that the merozoites lack rhoptries.¹⁴ Encephalomyelitis due to *S. neurona* infection has also been described in cats, which along with many other mammals including harbor seals and nonhuman primates, can serve as intermediate hosts for *S. neurona*.¹²

Contributing Institution:

University of Calgary Faculty of Veterinary Medicine (vet.ucalgary.ca)

References:

1. Barber JS, Trees AJ. Clinical aspects of 27 cases of neosporosis in dogs. *Vet Rec.* 1996; 139(18): 439-443.
2. Bjerkas I, Mohn SF, Presthus J. Unidentified cyst-forming sporozoon causing encephalomyelitis and myositis in dogs. *Z Parasitenkd.* 1984; 70(2): 271-274.
3. Cantile C, Arispici M. Necrotizing cerebellitis due to *Neospora caninum* infection in an old dog. *J Vet Med A Physiol Pathol Clin Med.* 2002; 49(1):47-50.
4. Cooley AJ, Barr B, Rejmanek D. Sarcystis neurona encephalitis in a dog. *Vet Pathol.* 2007;44:956-961.
5. Dubey JP. Recent advances in Neospora and neosporosis. *Vet Parasitol.* 1999; 84(3-4): 349-367.
6. Dubey JP: Review of *Neospora caninum* and neosporosis in animals. *Korean J Parasitol.* 2003; 41(1): 1-16.
7. Dubey JP, Carpenter JL, Speer CA, et al.: Newly recognized fatal protozoan disease of dogs. *J Am Vet Med Assoc.* 1988; 192(9): 1269-1285.
8. Dubey JP, Lindsay DS: A review of *Neospora caninum* and neosporosis. *Vet Parasitol.* 1996; 67(1-2): 1-59.
9. Dubey JP, Schares G, Ortega-Mora LM: Epidemiology and control of neosporosis and *Neospora caninum*. *Clin Microbiol Rev.* 2007; 20(2): 323-367.
10. Gaitero L, Anor S, Montoliu P, et al. Detection of *Neospora caninum* tachyzoites in canine cerebrospinal fluid. *J Vet Intern Med.* 2006; 20(2): 410-414.
11. Garosi L, Dawson A, Couturier J, et al. Necrotizing cerebellitis and cerebellar atrophy caused by *Neospora caninum* infection: magnetic resonance imaging and clinicopathologic findings in seven dogs. *J Vet Intern Med.* 2010; 24(3): 571-578.
12. Greene CE. *Infectious diseases of the dog and cat.* 4th ed. St. Louis, MO: Elsevier Saunders; 2012:825, 836-838.
13. Lorenzo V, Pumarola M, Siso S. Neosporosis with cerebellar involvement in an adult dog. *J Small Anim Pract.* 2002; 43(2): 76-79.
14. Zachary JF. Nervous system. In: McGavin MD, Zachary JF, eds. *Pathologic Basis of Veterinary Disease.* 5th ed. St. Louis, MO: Mosby Elsevier; 2012:809, 841.

CASE III: 1423851 (JPC 4065318).

Signalment: 8 year old male neutered domestic short-haired cat (*Felis catus*).

History: This cat lived in a colony used for long term nutritional studies. It was noted to be icteric and inappetent, and subsequently euthanized.



There is a focally extensive area of ulceration and necrosis within the colonic wall extending into the muscular tunics. (HE, 4X)

Gross Pathology: No gross lesions were noted by the prosector, who submitted multiple fixed tissues for microscopic examination, including colon.

Laboratory Results: The spleen was positive for feline coronaviral antigens. Fungal stains on the lesion in the colon were negative.

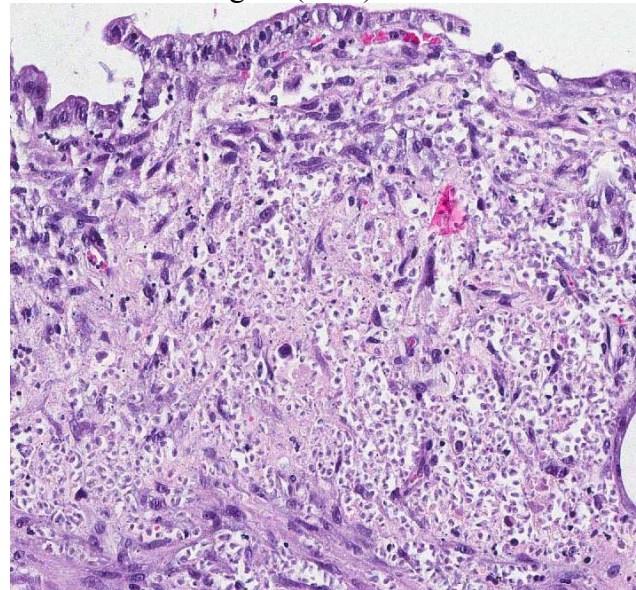
Histopathologic Description: Segments of colonic crypts contain abundant small protozoal organisms that are teardrop to crescent-shaped, have eosinophilic cytoplasm and round hyperchromatic nuclei. Cellular debris is associated with their presence. The mucosal surface is altered by erosions and ulcerations, while neighboring glands are lined by hypertrophic and hyperplastic enterocytes exhibiting increased mitotic activity and loss of goblet cells. The neighboring lamina propria and submucosa also contains numerous organisms, associated with moderate numbers of macrophages, neutrophils, lymphocytes and fewer plasma cells. Mixed inflammation extended into the muscularis in a few areas, but

with fewer protozoa. Similar organisms were found in the ileal crypts.

In lesions not shown, this animal also had an exocrine pancreatic adenocarcinoma, with surrounding inflammation. Vacuolar change was discovered in the liver, along with bile stasis. Pyogranulomas were found in the spleen and were immunohistochemically positive for FIP antigens.

Contributor's Morphologic Diagnosis: Colon: Colitis, necrotizing and suppurative, locally transmural, with numerous protozoal organisms consistent with *Tritrichomonas foetus*.

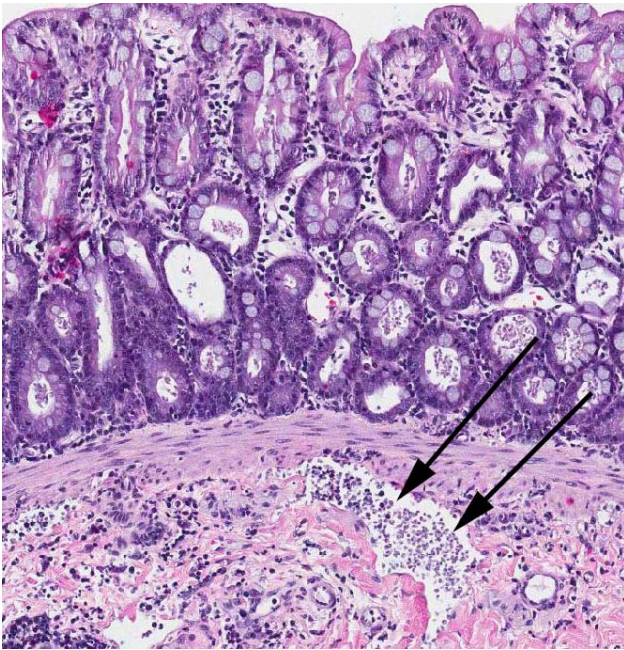
Contributor's Comment: *Tritrichomonas foetus* is an important cause of chronic large bowel diarrhea in cats, as well as an important venereal pathogen of cattle, causing early abortion and infertility. It is a commensal inhabitant of the nasal and GI tract of pigs. Diarrhea generally affects young, densely housed animals, and has been described as a frequent pathogen of purebred animals.⁹ Catteries with purebred cats positive for *Tritrichomonas foetus* infection have fewer square feet per cat.² Cats infected with this organism had diarrhea for mean duration 135 days (range 1-288 days). Other signs included anorexia (22%), depression (24%), and weight loss or failure to gain (20%).¹ Of 45 cats treated



3Ulcerated areas of the mucosa contain innumerable trichomonads within the mucosa and submucosa. (HE, 92X)

with ronidazole, the only antibiotic effective against this organism, 36% had partial or no improvement or relapsed, but some animals had concurrent *Giardia*.¹⁰

PCR is the test capable of identifying the greatest number of cats (34/36), versus culture (in pouch 24/36 or Diamond's media (5/36)).² Other tests can include wet mount smears of loop samples from the rectum and chromogenic in situ hybridization.⁴ A confounding factor is the presence of *Pentatrichomonas hominis*.³



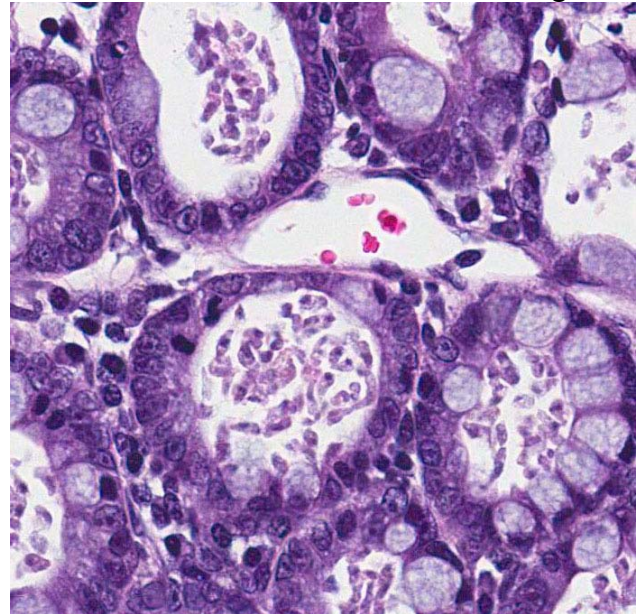
Numerous trichomonads are present within glands in the adjacent, less affected mucosa, as well as in the submucosa, as well as within submucosal lymphatics (black arrows). (HE, 120X).

In sections from spontaneously infected cats, lesions included an increase in lymphocytes and plasma cells in the lamina propria as measured across the width of the villi, and a few infiltrating neutrophils. Trichomonads were tear-shaped to crescentic organisms; flagella were not visible. Organisms were on the mucosa and less frequently in crypts. Organisms were visible only in 56% of sections in colon and 6 sections were needed to have 95% confidence of seeing them. Some cats, such as this one, had ulcers containing trichomonads as well.¹⁰

Initial infection of naïve cats with a feline isolate of *T. foetus* produced persistent infection in all cats and resulted in diarrhea that resolved after 7 weeks.⁷ Experimental infection of cats with 2 bovine isolates resulted in colonization of the intestine and lesions that varied in severity with the isolate.⁶ Conversely heifers inoculated with a feline organism developed similar endometritis to that caused by a bovine isolate and organisms were recovered over an 11 week period.³ Some authors believe the bovine and feline pathogens are separate species.^{5,8}

JPC Diagnosis: Large intestine: Colitis, necrotizing, multifocal to coalescing, severe with numerous intra- and extracellular tritrichomonads.

Conference Comment: The sheer number of organisms present in the sections was impressive with tritrichomonads filling colonic gland lumina in the superficial and deeper mucosa, both intra- and extracellular, as well as being present in dilated submucosal lymphatics. The deep invasion in this case is unusual in that organisms are reported to be most consistently found in close association with the mucosal surface, although invasion of deeper layers is known to occur.¹⁰ There is effacement of colonic glands



Higher magnification of numerous elliptical trichomonads which are present within colonic glands. There is a mild decrease in goblet cells as well as a lymphoplasmacytic colitis which separates and surrounds colonic glands. (HE, 360X)

and crypts with attenuation and crypt abscesses in the remaining crypts. The presence of mitotic figures provide evidence of regeneration. Conference participants commented on the goblet cell hyperplasia in some areas in contrast with the loss of goblet cells in regenerative areas.

Two trichomonads have been identified as inhabiting the intestinal tract of cats, *Tritrichomonas foetus* and *Pentatrichomonas hominis*, with *T. foetus* being considered the cause of large bowel diarrhea and *P. hominis* being considered a commensal.⁴ Although most commonly considered an infection of kittens, older cats may be asymptotically infected with *T. foetus* as well.⁹ Generally thought to be the same organism which causes diarrhea in cats as well as venereal disease in cattle, recent studies have suggested the organisms may indeed be different species. A new species, *Tritrichomonas blagburni* n.sp., has been suggested as the cause of intestinal tritrichomonas in cats.⁸

Giardia sp. trophozoites can be difficult to distinguish from those of *T. foetus*. Differentiating features of *T. foetus* includes a distinct undulating membrane, lack of cyst formation and being refractory to treatment with common antiprotozoals used for treatment of giardia. Pathogenicity of *T. foetus* may be related to alterations in normal host flora, epithelial adherence and elaboration of cytotoxins. An important consideration in obtaining biopsy samples for evaluation is sampling from multiple locations, as literature indicates organisms may not be present in all samples.¹⁰

Contributing Institution:

Veterinary Medical Diagnostic Laboratory,
University of Missouri
vmdl.missouri.edu

References:

- Gookin JL, Levy MG, Law JM, et al. Experimental infection of cats with *Tritrichomonas foetus*. *Am J Vet Res*. 2001;62:1690-1897.
- Gookin JL, Stebbins ME, Hunt E, et al. Prevalence of and risk factors for feline *Tritrichomonas foetus* and *Giardia* infection. *J Clin Microbiol*. 2004;42:2707-2710.
- Levy MG, Gookin JL, Poore M, et al. *Tritrichomonas foetus* and not *Pentatrichomonas hominis* is the etiologic agent if feline trichomal diarrhea. *J Parasitol*. 2003; 89:99-104.
- Mostegl MM, Wetscher A, Richter B, et al. Detection of *Tritrichomonas foetus* and *Pentatrichomonas hominis* in intestinal tissue specimens of cats by chromogenic in situ hybridization. *Vet Parasitol*. 2012;183:209-214.
- Šlapeta J, Muller N, Stack CM, et al. Comparative analysis of *Tritrichomonas foetus* (Riedmuller 1928) cat genotype, *T. foetus* (Riedmuller 1928) cattle genotype and *Tritrichomonas suis* (Davaine, 1875) at 10 DNA loci. *Int J Parasitol*. 2012;42:1143-1149.
- Stockdale HD, Dillon AR, Newton JC, et al. Experimental infections of cats (*Felis catus*) with *Tritrichomonas foetus* isolated from cattle. *Vet Parasitol*. 2008;154:156-161.
- Stockdale HD, Rodning S, Givens M, et al. Experimental infection of cattle with a feline isolate of *Tritrichomonas foetus*. *J Parasitol*. 2007;93:1429-1434.
- Walden HS, Dykstra C, Dillon A, et al. A new species *Tritrichomonas* (Sarcomastigophora: Trichomonida) from the domestic cat (*Felis catus*). *Parasitol Res*. 2013;112: 2227-2235.
- Xenoulis PG, Lopinski DJ, Read SA, et al. Intestinal *Tritrichomonas foetus* infection in cats: a retrospective study of 104 cases. *J Feline Med Surg* 2013; 15: 1098-1103.
- Yaeger MJ, Gookin JL. Histologic features associated with *Tritrichomonas foetus*-induced colitis in domestic cats. *Vet Pathol* 2005;42: 797-804.

CASE IV: D15-6096 (JPC 4066091).

Signalment: 4-month-old, intact female, Rottweiler mix dog (*Canis familiaris*).

History: The puppy had a recent history of increased respiratory rate and effort progressing to dyspnea. A bronchointerstitial pattern on chest radiographs was noted. There was a lack of response to antifungals and antibiotics. The dog had a one week history of prednisone use for

suspected protein-losing enteropathy. The dog had a longer history of pyoderma, chronic diarrhea, ascites, and microhepatica. The puppy had been administered two DHPP vaccines sometime prior to 2 months of age. The puppy died at home two days after being discharged.

Gross Pathology: The puppy was moderately thin with muscle wasting. There was periocular dermatitis, inflammation centered on the mucocutaneous junction, and ventral abdominal pyoderma. The lungs were mottled pale pink to dark pink with multifocal to coalescing, white to beige, flat to slightly raised, semi-firm areas in a branching pattern. The lesions were most prominent in the hilar and mid lobe regions intermixed with slightly sunken, non-crepitant, dark pink to red irregular areas of parenchyma (atelectasis). There were multifocal, fairly well-demarcated, dark red, irregular foci, 1-3 mm in diameter, throughout the lung parenchyma (hemorrhage). On cut section the lungs were mottled dark red to red to pink to beige and semi-firm. The liver was friable and mottled pale pink to dark pink. A delicate fibrin membrane was adherent to the liver capsule. The intestines were moderately dilated with watery to viscous contents. The lymphatics overlying the pancreas

and associated with the duodenum and proximal jejunum were prominent.

Bacteriology

Lung (2 specimens) - No growth and no significant growth, respectively

Liver - No growth

Spleen- Staphylococcus intermedius group (mixed culture, 1+)

Immunohistochemistry (IHC)

Canine adenovirus type 2 – lung (respiratory epithelium, pneumocytes, alveolar macrophages), exocrine pancreas, and labial glands in the oral mucocutaneous junction - **positive**

Canine adenovirus type 2 – small intestine - inconclusive

Canine distemper virus – lung - negative

Canine parvovirus – small intestine - negative

Virology

Virus isolation – lung - **Canine adenovirus isolated**



Lungs - Mottled pale pink to dark pink with multifocal to coalescing, white to beige, flat to slightly raised, semi-firm areas in a branching pattern admixed with areas of atelectasis. (Image courtesy of: University of Minnesota Veterinary diagnostic Laboratory, <http://www.vdl.umn.edu>)

Electron Microscopy

Negative stain – lung - **Adenovirus**

Molecular Diagnostics

Canine Respiratory Panel (PCR) – Lung - Canine distemper virus - **positive**

Canine influenza virus - negative

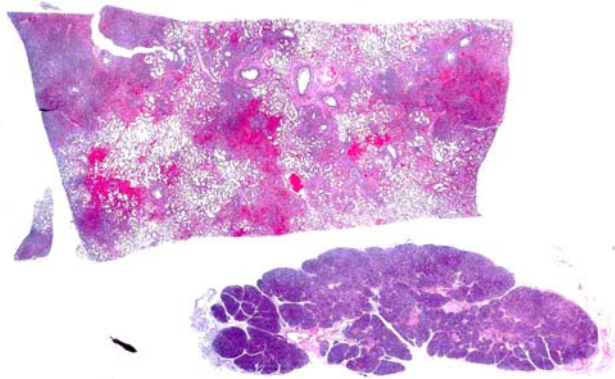
Canine parainfluenza virus - negative

Canine respiratory coronavirus - negative

Canine Adenovirus 2 - positive

Canine *Bordetella bronchiseptica* - negative

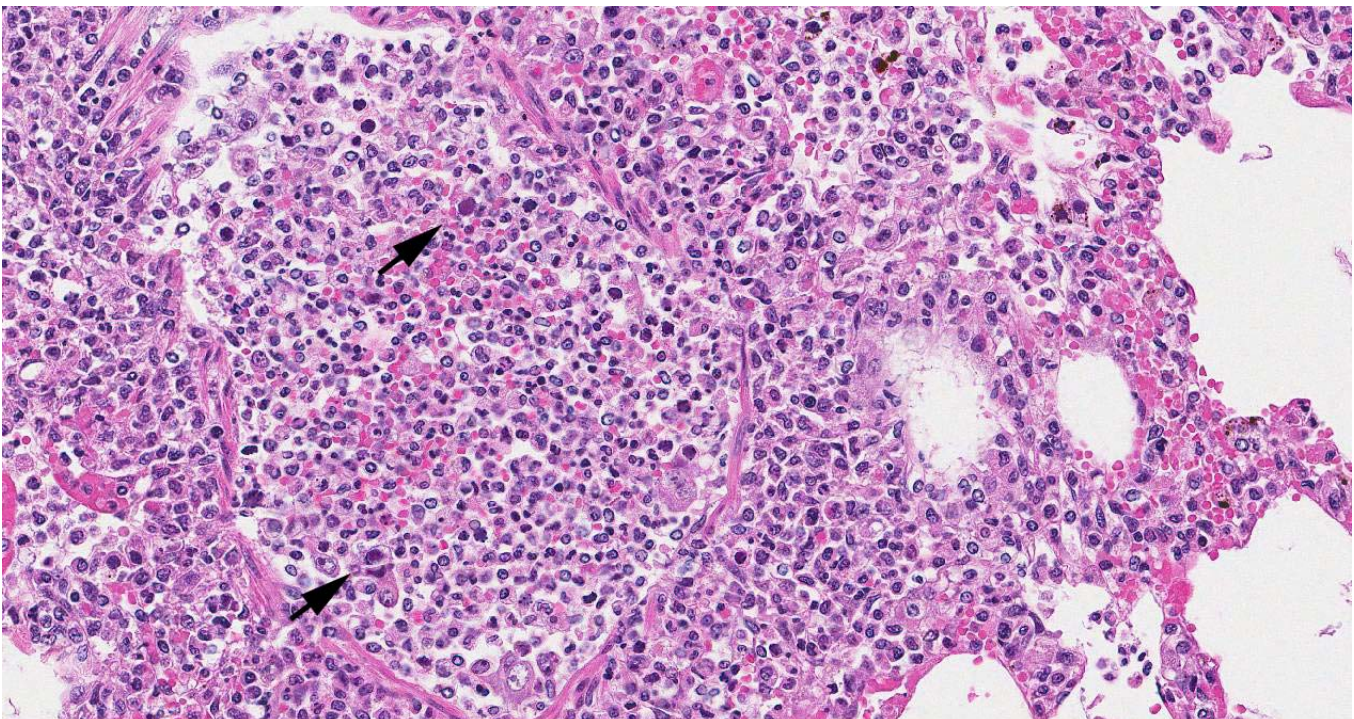
Streptococcus equi subsp *zooepidemicus* –
negative



Submitted tissues include lung and liver. The lung contains multiple confluent foci of hemorrhage and necrosis centered on airways. (HE, 4X)

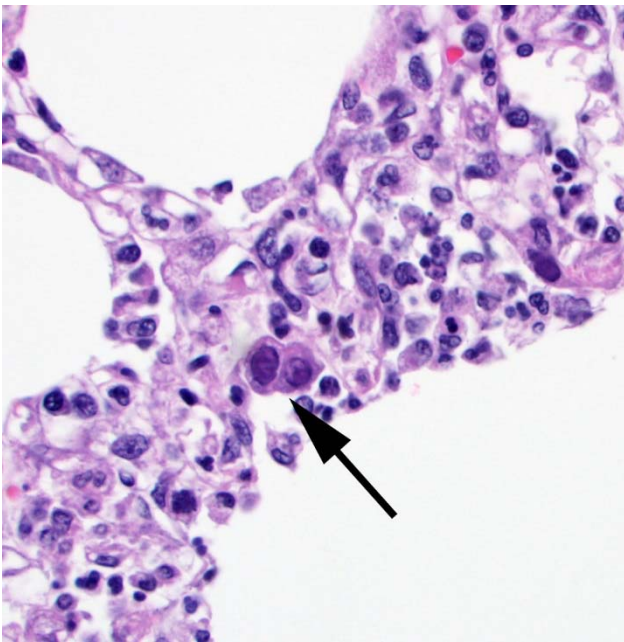
Histopathologic Description: Lung – Multifocally affecting ~50% of the section there are geographic areas of alveoli filled with neutrophils and alveolar macrophages admixed with accumulations of fibrin, hemorrhage, and siderophages centered around bronchi and bronchioles. The bronchi and bronchioles are lined by mildly to moderately hyperplastic respiratory epithelium and are filled with degenerate and non-degenerate neutrophils and

sloughed epithelial cells. Occasionally the bronchial and bronchiolar walls are disrupted by inflammatory infiltrates as previously described and necrotic debris. Within these bronchi and bronchioles, a small to moderate number of scattered epithelial cells, sloughed epithelial cells, bronchial gland epithelium, and rarely pulmonary macrophages have swollen, enlarged nuclei that contain a large, 5-15µm, ovoid to round, smudgy, basophilic to amphophilic intranuclear inclusion that typically completely fills the nucleus but occasionally has a thin clear rim (halo) between the inclusion and margined chromatin. There are moderate to large numbers of lymphocytes and plasma cells, neutrophils and macrophages within the bronchial submucosa and surrounding bronchial glands with mild edema. There are infrequent thrombi within adjacent vessels. There is moderate perivascular edema around large caliber vessels within these areas. The alveolar septa multifocally are mildly expanded by neutrophils, macrophages, lymphocytes, infrequent fibrin, and rarely lined by few plump type II pneumocytes. Within affected alveoli, there are scattered pneumocytes, which are often sloughed, as well as alveolar



Higher magnification of an affected bronchiole. There is extensive necrosis and sloughing of airway epithelium; within the luminal exudate, sloughed epithelial cells contain adenoviral intranuclear inclusions. (HE, 110X)

macrophages that contain intranuclear inclusion bodies as described in the bronchial epithelium. Pancreas – The exocrine pancreatic cells in randomly distributed foci are pale with loss of zymogen granules, occasionally vacuolated (degeneration), or faded and shrunken. Nuclei of these cells are frequently absent and the cells are admixed with amorphous cellular debris (necrosis). There are low numbers of neutrophils, macrophages, and lymphocytes and plasma cells within these areas and in the interstitium. Moderate numbers of acinar cells in these areas have an enlarged nucleus with marginated chromatin and an eosinophilic to basophilic inclusion similar to that described in the bronchial epithelial cells in the lung. Multifocally large areas of the surrounding adipose tissue are hypereosinophilic with absent nuclei and concentric flocculent to amorphous eosinophilic material within the adipocytes or between them (fat necrosis). There are small numbers of macrophages, neutrophils, and lymphocytes along the periphery of these areas.



4Lung. (H&E) There are large basophilic intranuclear inclusion bodies in two adjacent pneumocytes lining the alveolar septa. The septa wall is thickened by infiltrates of macrophages, lymphocytes, and neutrophils. (HE, 400X) (Image courtesy of: University of Minnesota Veterinary diagnostic Laboratory, <http://www.vdl.umn.edu>)

Mucocutaneous junction (not included): Multifocally there is mild parakeratotic

hyperkeratosis, acanthosis, infrequent spongiosis, and occasional areas of ulceration. There are multifocal neutrophilic intracorneal pustules and superficial serocellular crusts composed of serum proteins and degenerate and non-degenerate neutrophils. There are multifocal areas in some sections of glabrous skin, with moderate numbers of lymphocytes and plasma cells, macrophages and neutrophils surrounding the labial glands. The labial glands are often absent, degenerative, or replaced by necrotic debris and sloughed cells with few intraluminal neutrophils and debris. Rarely within these glands the nuclei are enlarged with marginated chromatin and contain a large ovoid basophilic inclusion body.

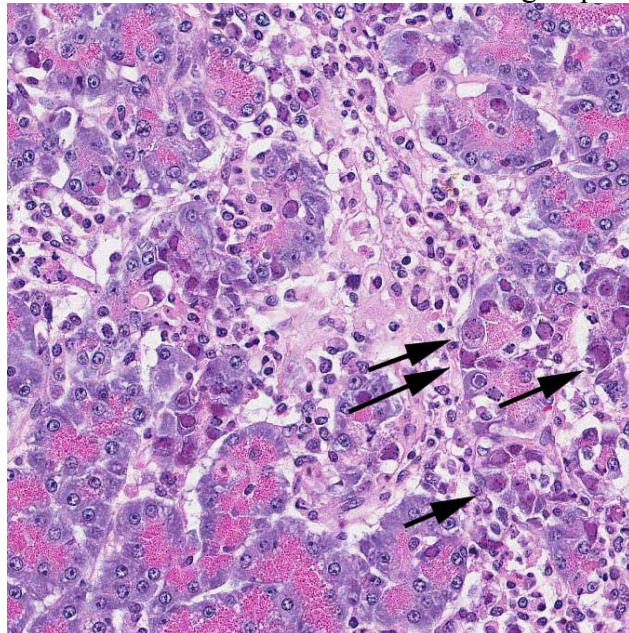
Contributor's Morphologic Diagnosis:

1. Lung: Necrosuppurative and lymphoplasmacytic bronchitis/bronchiolitis and bronchointerstitial pneumonia, multifocal to coalescing, moderate to marked, subacute with mild bronchial epithelial hyperplasia and intraepithelial intranuclear inclusion bodies (consistent with canine adenovirus type 2).

2. Pancreas: Necrotizing and lymphohistiocytic pancreatitis, multifocal, moderate, subacute with intraepithelial intranuclear inclusion bodies (consistent with canine adenovirus type 2).

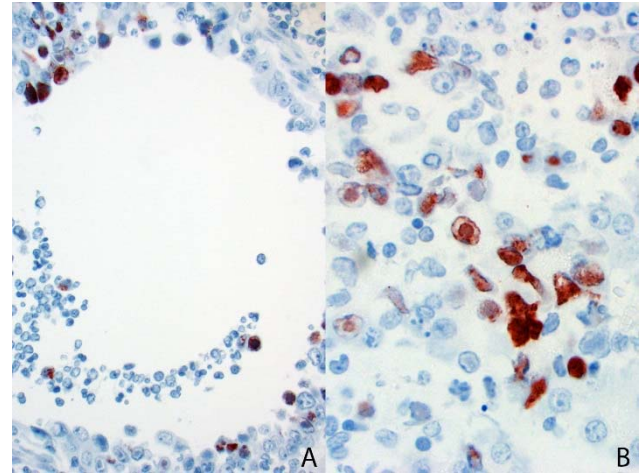
Contributor's Comment: Canine adenovirus (CAV) is a non-enveloped icosahedral double stranded DNA virus found worldwide that belongs to the genus *Mastadenovirus* and family *Adenoviridae*. In addition to affecting domestic dogs, other carnivores such as foxes, coyotes, otters, and wolves are susceptible to CAV infection and antibodies have been detected in fishers, polar and black bears, sea lions, and walruses.^{4,8} There are two serotypes of adenovirus, canine adenovirus type 1 (CAV1) and canine adenovirus type 2 (CAV2), that are genetically and antigenically similar yet divergent enough to allow differentiation with various diagnostic methods. The similarities allow vaccination with a parenteral modified live attenuated CAV2 in dogs to provide cross-protection against CAV1 while avoiding the

well-known side effects of using a modified live CAV1 vaccine.^{8,13} In countries with established systematic vaccination in the domestic dog population, circulation of the virus is limited and thus prevalence of disease is low. In unvaccinated and wild canid populations, seroprevalence is variable but significant (between 30-70% worldwide) indicating exposure to this virus is common.^{5,6,8,15} CAV1 is a systemic infection that targets hepatocytes and endothelial cells and mostly affects young dogs with mortality rates between 10-30%. In contrast, CAV2 is typically limited in extent and virulence resulting in a respiratory infection that is often asymptomatic in otherwise healthy dogs. This virus is one of the organisms involved in canine infectious respiratory disease (CIRDC) complex (also called canine infectious tracheobronchitis or kennel cough) that typically occurs after exposure to other dogs (boarding, shelter, dog parks, etc.). CAV2 replicates most readily in non-ciliated bronchiolar and bronchial epithelium as well as the epithelial cells of the tonsillar crypts, pharynx, nasal mucosa, mucus cells of the trachea and bronchi, and occasionally type 2 pneumocytes.¹³ In addition, replication can occur to a limited extent in the intestinal epithelial cells and CAV2 has been previously associated outbreaks of diarrhea in one group of



Within the pancreas, there is multifocal degeneration and necrosis of acinar tissue. Numerous acinar epithelial cells contain intranuclear viral inclusions (arrows). (HE, 100X)

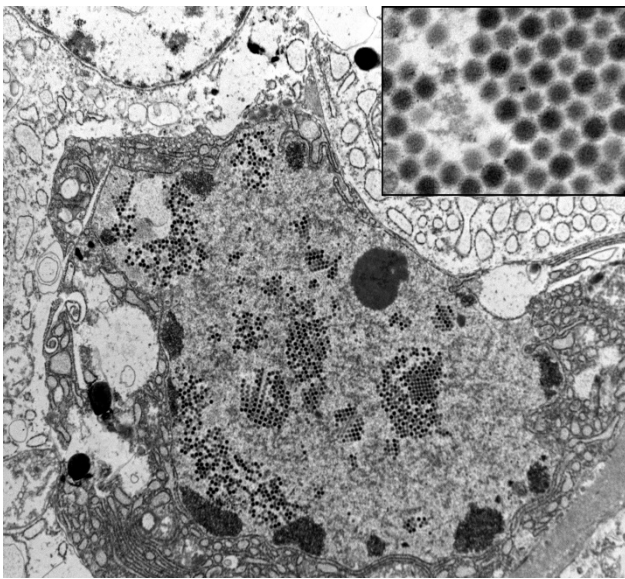
dogs.⁶



Immunohistochemistry - Canine adenovirus type 2. A. Lung, bronchiole. B. Pancreas. (Image courtesy of Univ. of Minnesota Veterinary Diagnostic Lab, <http://www.vdl.umn.edu>)

The extensive pulmonary infection with CAV2 resulting in dyspnea and respiratory failure in this puppy in the absence of a secondary bacterial infection is unusual. Additionally the extent of infection in this puppy including the oral labial glands at the mucocutaneous junction and exocrine pancreatic acinar cells is rare. The pattern of tissue involvement is reminiscent of that described in some immunodeficient Arabian foals with equine adenoviral infection¹⁰ and, to the authors' knowledge, involvement of the pancreas with CAV2 infections in the dog has not been previously described in the literature. However, less typical locations to identify adenoviral inclusions have been noted previously in the splenic macrophages and hepatocytes in a bulldog puppy with systemic CAV2 infection.¹ In a separate report, detection of CAV2 via in situ-hybridization in the liver and spleen and via polymerase chain reaction in the brain was noted in a puppy without inclusion bodies present in any of these tissues.³ The exact cause of the histologic pattern in this puppy is unclear and although mutations have been noted to occur in CAV³, this virus is generally considered genetically stable⁸ while the significance of mutations in terms of virulence or cell tropism is unknown.

Clinical and severe pulmonary infection with CAV2 is typically attributed to an immunocompromised status or complication with other viruses or bacteria.¹ Co-infections with CIRDC are common of which infections with multiple respiratory viruses appears to be more common than previously believed.^{12,14} In this puppy, both canine distemper virus (CDV) and adenovirus were detected by PCR of lung tissue but interestingly there was no immunoreactivity noted in the lung on CDV IHC and a lack of viral inclusions consistent with CDV. Although PCR and IHC testing of CDV has not been directly compared, the higher sensitivity of PCR over IHC has been noted in another veterinary infectious disease² and inclusion bodies were only found in 25% of CDV cases confirmed by other methods in another report⁷ which may explain the findings in this case. The contribution of CDV in this case is unknown and assuming that the lack of histologic or immunohistochemical detection suggests a low viral load, one of two following scenarios is likely: 1. Early infection prior to significant viral



Transmission electron microscopy of pancreatic acinar cell (15000x). There are numerous intranuclear adenoviral particles forming paracrystalline arrays. Inset (100000x): Magnified view of adenoviral particles. (Image courtesy of the University of Minnesota Veterinary Diagnostic Laboratory, <http://www.vdl.umn.edu>)

replication and cytopathic effects, or 2. Late infection after significant but incomplete clearance of the virus. With either of these

scenarios, the degree of virus-induced immunosuppression can be questioned as the former is before the lymphoid destruction that induces immunosuppression and the latter would imply enough recovery of the immune system to allow significant clearance of the virus. Other reasons for possible immunosuppression also existed in this puppy including recent steroid usage and others conditions including marked lymphangiectasia with hypoproteinemia and evidence of an intrahepatic portosystemic shunt. The occurrence of clinical infection in this vaccinated puppy is likely attributable to interference of maternal antibodies which typically persist until 12-14 weeks of age (2-4 weeks beyond this puppies last vaccine) rather than emergence of a variant strain.^{8,13}

JPC Morphologic Diagnosis:

1. Lung: Pneumonia, bronchointerstitial, necrotizing, multifocal to coalescing, severe with numerous intraepithelial intranuclear viral inclusion bodies, Rottweiler mix, canine.
2. Pancreas: Pancreatitis, necrotizing, multifocal to coalescing, moderate with numerous intraepithelial intranuclear viral inclusion bodies.
3. Adipose tissue, peripancreatic and mesenteric: Fat necrosis, multifocal to coalescing, with saponification.

Conference Comment:

In the lung, conference participants readily identified intranuclear inclusion bodies within intact and sloughed epithelial cells, both bronchiolar and type II pneumocytes. Along with expansion of alveolar septa with inflammatory cells and foci of alveolar septal necrosis, and megakaryocytes are also occasionally found in alveolar capillaries. Multifocally, alveoli contain a macrophage-rich exudate and there is type II pneumocyte hyperplasia. Participants also described segmental necrosis of bronchiolar epithelium, epithelial attenuation, and sloughing of epithelial cells into the lumina. Changes identified by participants in the pancreas mirrored those of the contributor and include degeneration and necrosis of pancreatic acinar epithelium; loss of zymogen granules; expansion of the interlobular

areas with fibrin and edema; and presence of intranuclear inclusion bodies in the acinar epithelial cells. Other changes include necrosis and mineralization (saponification) of the peripancreatic fat.

Canine adenovirus type 2 is most often associated with mild respiratory disease, although more severe fatal disease has been documented.¹ This dog's history included vaccination only up to 8 weeks, as well as administration of corticosteroids, both of which were suggested as playing a role in the pathogenesis in this case. The differential diagnosis for viral pneumonia in the dog discussed by participants included: canine morbillivirus, canine influenza virus, canine coronavirus and canine parainfluenza virus. In this case, the intranuclear viral inclusion bodies within epithelial cells are considered distinctive for canine adenovirus type 2, making other viral etiologies less likely. Some participants speculated that a secondary bacterial infection also may have contributed to the pulmonary changes in this dog.

Viruses are well-known to play a role in the pathogenesis of bacterial pneumonias by damaging the respiratory epithelium, inhibiting bacterial clearance and facilitating bacterial adhesion. Other participants commented that a contributing bacterial etiology likely would have resulted in a more neutrophil-rich inflammatory component in the lung. Bacterial agents of canine infectious respiratory disease include *Bordetella bronchiseptica*, *Mycoplasma* spp., and *Streptococcus equi* sp. *zooepidemicus*.¹⁴

The pancreatic involvement in this case is uncommon in typical infections with canine adenovirus. Pancreatitis due to adenovirus infection is well documented in nonhuman primates; adenoviral infection in a number of non-human primate species can result in pancreatic necrosis and fibrosis with chronic-active inflammation. Pancreatic involvement typically occurs in more clinically severe cases, typically with underlying immunosuppression; other lesions also include hepatitis and nephritis. Adenovirus infection in immunocompetent

nonhuman primate hosts usually presents as self-limiting respiratory and gastrointestinal infections.⁹ Fowl adenovirus, a common disease in chickens, results in necrotizing pancreatitis, gizzard erosion, and inclusion body hepatitis.¹¹

We appreciate the excellent supporting materials with the submission, including laboratory data, gross, immunohistochemistry, and electron microscopy images. These additional materials greatly enhances the teaching value of this case.

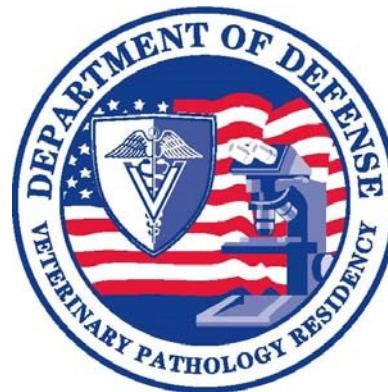
Contributing Institution:

University of Minnesota Veterinary Diagnostic Laboratory. <http://www.vdl.umn.edu>

References:

1. Almes KM, Janardhan KS, Anderson J, Hesse RA, Patton KM. Fatal canine adenoviral pneumonia in two litters of Bulldogs. *J Vet Diagn Invest.* 2010;22: 780–784.
2. Baszler TV, Gay LJ, Long MT, Mathison BA. Detection by PCR of *Neospora caninum* in fetal tissues from spontaneous bovine abortions. *J Clin Microbiol.* 1999;37: 4059–4064.
3. Benetka V, Weissenbock H, Kudielka I, Pallan C, Rothmüller G, Möstl K. Canine adenovirus type 2 infection in four puppies with neurological signs. *Vet Rec.* 2006;158: 91–94.
4. Brown CC, Baker DC, Barker IK. Alimentary system. In: Maxie MG, ed. *Jubb, Kennedy and Palmer's Pathology of Domestic Animals.* 5th ed. Vol. 2. Philadelphia, PA: Elsevier Saunders; 2007:166.
5. Bulut O, Yapici O, Avci O, Simsek A, Atli K, Dik I, Yavru S, Hasircioglu S, Kale M, Mamak N. 2013 The Serological and Virological Investigation of Canine Adenovirus Infection on the Dogs. *The Scientific World Journal* 2013 Sep 24;2013:587024. doi: 10.1155/2013/587024. eCollection 2013.
6. Buonavoglia C, Martella V. Canine respiratory viruses. *Vet Res* 2007;38: 355–373.

7. Damián M, Morales E, Salas G, Trigo FJ. Immunohistochemical Detection of Antigens of Distemper, Adenovirus and Parainfluenza Viruses in Domestic Dogs with Pneumonia. *J Comp Pathol* 2005;133; 289–293.
8. Decaro N, Martella V, Buonavoglia C. Canine Adenoviruses and Herpesvirus. *Vet Clin North Am Small Anim Pract* 2008;38; 799–814.
9. Mansfield KG, Sasseville VG, Westmoreland SV. Molecular localization techniques in the diagnosis and characterization of nonhuman primate infectious diseases. *Vet Pathol*. 2014;51(1);1101-26.
10. McChesney AE, England JJ, Adcock JL, Stackhouse LL, Chow TL. Adenoviral infection in suckling Arabian foals. *Vet Pathol* 1970;7; 547–564.
11. Ono M, Okuda S, Yazawa Y et al. Adenoviral gizzard erosion in commercial broiler chickens. *Vet Pathol*. 2003;40; 294-303.
12. Rodriguez-Tovar LE, Ramírez-Romero R, Valdez-Nava Y, Nevárez-Garza AM, Zárate-Ramos JJ, López A. Combined distemper-adenoviral pneumonia in a dog. *Can Vet J*. 2007;48; 632–634.
13. Sykes JE. Canine Viral Respiratory Infections. In: Sykes JE, ed. *Canine and Feline Infectious Diseases*. 1st ed. Philadelphia, PA: Elsevier Saunders; 2013:170-181.
14. Viitanen SJ, Lappalainen A, Rajamäki MM. Co-infections with Respiratory Viruses in Dogs with Bacterial Pneumonia. *J Vet Intern Med*. 2015;29; 544–551.
15. Wright N, Jackson FR, Niezgoda M, Ellison JA, Rupprecht CE, Nel LH. High prevalence of antibodies against canine adenovirus (CAV) type 2 in domestic dog populations in South Africa precludes the use of CAV-based recombinant rabies vaccines. *Vaccine*. 2013;31; 4177–4182.



WEDNESDAY SLIDE CONFERENCE 2015-2016

Conference 5

6 October 2015

CASE I: 060377 (JPC 4065817).

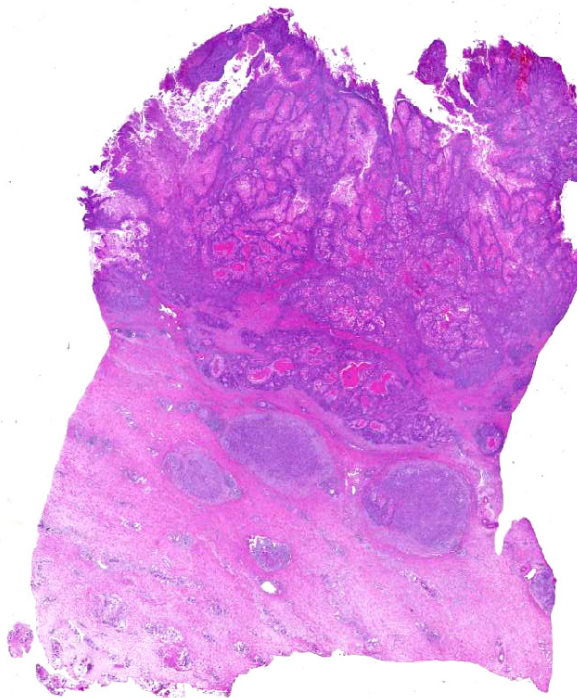
Signalment: 20-year-old quarter horse (*Equus ferus caballus*) gelding.

History: This 20-year-old gelding horse had been part of a small herd that was used for antibody production against various antigens. It suddenly presented with muddy-red fluid discharge from the prepuce and physical examination revealed a large, proliferative mass within the sheath that was bleeding and friable. The animal was anesthetized for a more thorough exploration of the mass. The mass was determined to be deep within the prepuce, palpable up to, and involving, the body wall. Due to the location and infiltrative nature of the mass, resection was not possible and the animal was euthanized. A full necropsy was not performed; only the penis and prepuce was removed for post mortem examination.

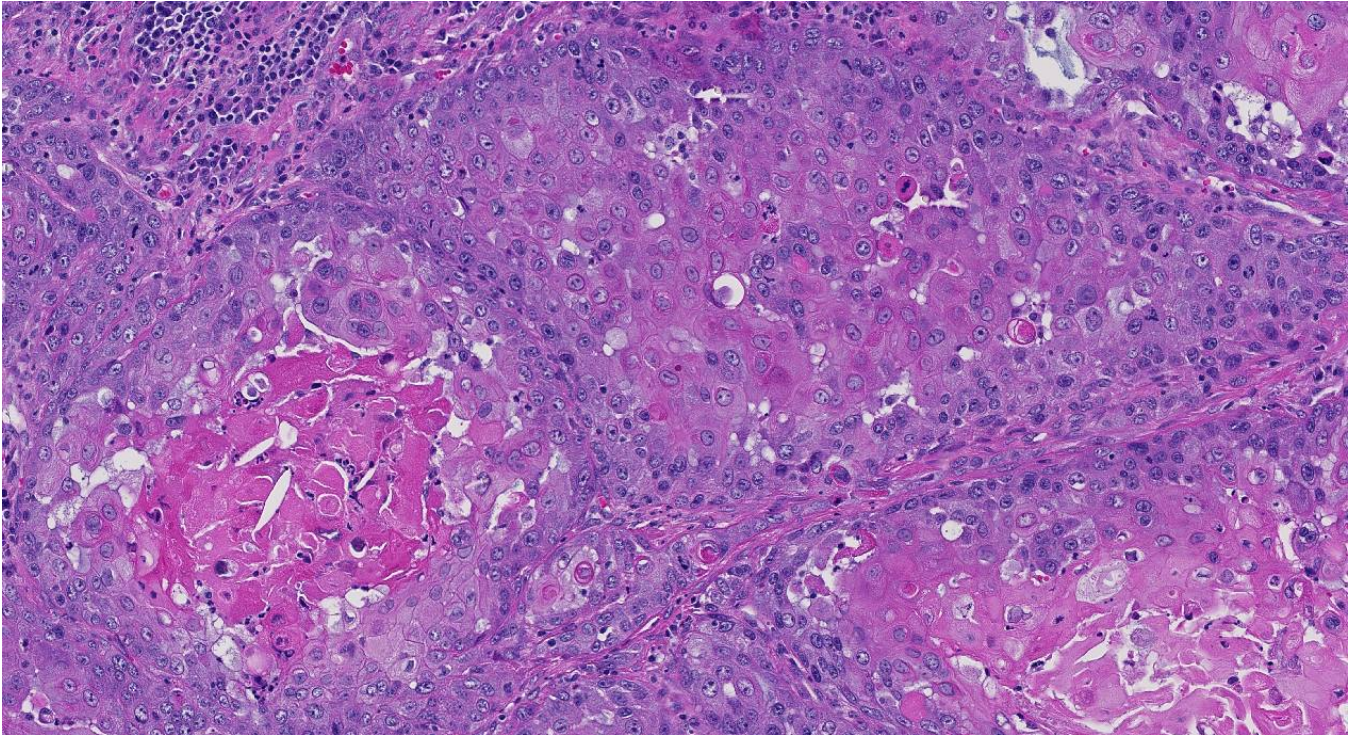
This animal was part of a research project conducted under an IACUC approved protocol in compliance with the Animal Welfare Act, PHS Policy, and other federal statutes and regulations relating to animals and experiments involving animals. The facility where this research was conducted is accredited by the Association for Assessment and Accreditation of Laboratory Animal Care, International and adheres to principles stated in the Guide for the Care and

Use of Laboratory Animals, National Research Council, 2011.

Gross Pathology: Extending from the base of the glans penis, involving the surrounding prepuce, and extending deep to the body wall is a 13x13x12 cm friable, proliferative, ulcerated mass.



The preputial mucosa is replaced by an exophytic multilobular infiltrative mass composed of islands of keratinizing squamous epithelium. (HE,6X)



The neoplasm is composed of lobules and nests of epithelial cells which exhibit central abrupt keratinization. Nuclei are markedly anisokaryotic. (HE, 240X)

Laboratory Results: N/A

Histopathologic Description: Prepuce: Multifocally, effacing and replacing normal tissue architecture, affecting approximately 70% of the tissue section, extending to cut borders, is an unencapsulated, infiltrative, well-demarcated, moderately cellular neoplasm composed of polygonal cells arranged in nests and packets, often surrounding variably sized areas composed of keratin, admixed with degenerate neutrophils, necrotic cellular debris, sloughed, often necrotic, neoplastic cells, and hemorrhage, on a moderately dense desmoplastic stroma. Neoplastic cells have distinct cell borders, moderate to abundant amounts of brightly eosinophilic cytoplasm, a round to oval nucleus with finely stippled chromatin, and up to 4 variably distinct nucleoli. The mitotic rate is brisk, with up to 5 mitotic figures in some high-powered fields. Anisocytosis and anisokaryosis are marked. Neoplastic cells at the periphery of nests and packets occasionally surround concentric lamellations of brightly eosinophilic material (keratin pearls), and often exhibit dyskeratosis and single cell necrosis.

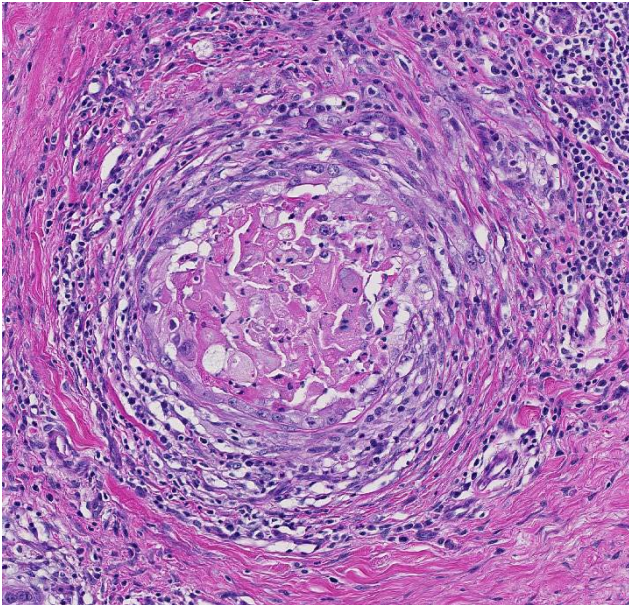
Multifocally, neoplastic cells are found within expanded lumens of lymphatics. There are multifocal aggregates of lymphocytes and plasma cells that infiltrate the neoplasm and surrounding fibrovascular connective tissue. The surrounding connective tissue is edematous with dilated lymphatics.

Contributor's Morphologic Diagnosis:
Prepuce: Squamous cell carcinoma.

Contributor's Comment: Squamous cell carcinoma (SCC) is the most common genital malignant tumor in horses and is considered a "classic" neoplastic lesion in the study of veterinary pathology.^{1,5} SCCs are epithelial neoplasms that arise from keratinocytes, and often develop at mucocutaneous junctions, such as the eyelids, perineum, anus, and external genitalia in stallions and geldings.^{2,3,4,9} Gross lesions are often proliferative and may exhibit ulceration, hemorrhage, necrosis, and infection.^{2,3} Histologically, neoplastic cells are usually well-differentiated, keratinization is almost always present, and the neoplasm is frequently infiltrated by neutrophils and/or

eosinophils.³ Historically, potential promoters such as ultraviolet light, chronic inflammation, and smegma accumulation have been associated with development of the neoplasm, although the role of these elements remains unclear.⁵

There are numerous recent reports that reveal increasing evidence to support a potential causal relationship between equine papillomavirus type 2 (EcPV2) and equine penile squamous cell carcinoma (SCC).^{1,4,5,8} Studies have suggested that equine penile papillomas, in situ carcinomas, and invasive carcinomas belong to a continuum of papilloma-induced disease, which is supported by detection of EcPV2 DNA in horses with characteristic SCC lesions, and in various lesions of the penis in a proportional number of control cases.⁶ When comparing the levels of EcPV2



Nests of neoplastic squamous epithelium infiltrated the underlying submucosa, often surrounded by concentric layers of proliferating fibroblasts and collagen (desmoplasia). HE, 80X

viral load in equine SCC lesions, penile non-SCC, or precursor disease lesions, and tissues without observable lesions from SCC-prone sites on clinically normal horses, EcPV2 DNA was present significantly more often, and in higher copy numbers, in the equine penile SCC lesions than the others. The presence of EcPV2 DNA has also been demonstrated in anal lesions, a lymph node, and contact metastases.¹ Additionally, in one report, viral mRNA was

detected in all examined EcPV2 DNA positive lesions, while only 2.6% of specimens from healthy horses had detectable mRNA.⁷ This finding provides evidence of intralesional viral transcriptional activity which further supports an active role of the virus in equine SCC disease.⁹

Note: Opinions, interpretations, conclusions, and recommendations are those of the authors and are not necessarily endorsed by the U.S. Army.

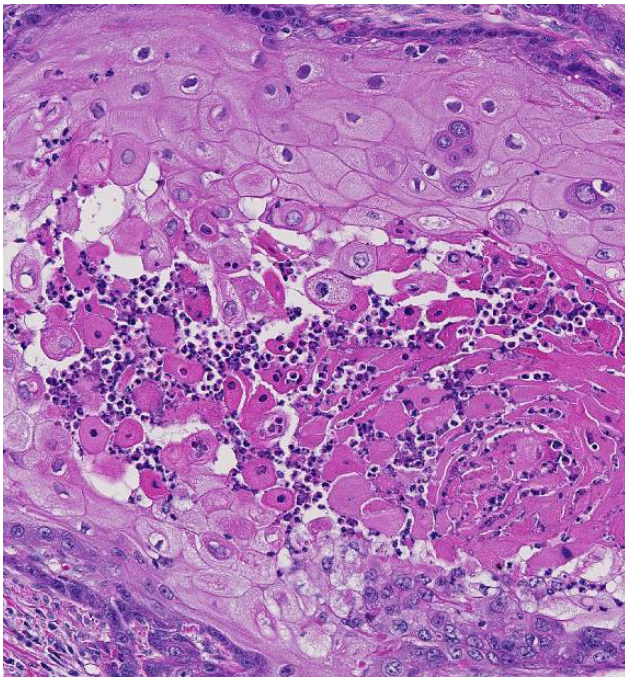
JPC Diagnosis: Prepuce: Squamous cell carcinoma.

Conference Comment: Conference discussion included a review of neoplastic features of malignancy observed within this neoplasm, including marked anisocytosis and anisokaryosis, invasion of lymphatics, elevated mitotic rate, infiltrative pattern, and desmoplasia. As noted by the contributor, additional features included dyskeratosis, areas of necrosis, infiltration of a mixed population of inflammatory cells as well as few areas of mineralization. Although the specific anatomic location could not be determined histologically in this case, participants briefly discussed common locations for SCC in horses, including the urogenital area, ocular/periorcular regions, and the stratified squamous portion of the stomach. Locations for squamous cell carcinoma in other species include the nares, pinnae and lips of white cats, the vulva of sheep and goats and the nonglandular stomach of rodents and pigs.

In addition to horses, squamous cell carcinomas of the eyelid epithelium occur in other species, most commonly cattle, cats, and dogs. Squamous cell carcinomas develop through a stepwise process, often consisting of precancerous stages and the formation of a papilloma. Tumor development begins with initiation, which is an irreversible genetic change typically caused by solar radiation. The next step is promotion, which includes the growth of genetically altered or initiated cells within a favorable environment. Promotion is followed by progression, which results in increasing malignancy of the developing tumor and involves both genetic and

epigenetic changes to tumor cells.⁷ Ultraviolet radiation induced squamous cell carcinoma of the eyelid occurs most commonly in Hereford cattle which have nonpigmented eyelids.⁷ The ultraviolet radiation induces DNA damage and subsequent mutation; of the three wavelengths of ultraviolet light, UVB is thought to be most associated with development of cutaneous neoplasms. The energy in UV light absorbed is by DNA and results in covalent crosslinking of pyrimidine bases and the formation of pyrimidine dimers, preventing proper base pairing. It is postulated that nucleotide excision repair mechanisms are overwhelmed with continued UV exposure, which may result in the propagation of cells with genomic mutations.⁶

As mentioned by the contributor, recent evidence supports an association between equine penile



Aggregates of neutrophils are scattered throughout the neoplasm as a result of liberated keratin. (HE, 100X)

squamous cell carcinoma and equine papillomavirus 2 (EcPV2). The expression of two proteins, E6 and E7, has been demonstrated in the human papillomavirus associated with cervical cancer, which interact with proteins associated with cell cycle regulation.¹⁰ Zhu et al. demonstrated that a subset of equine penile squamous cell carcinomas contained the E6/E7

nucleic acid of EcPV2, and a majority of neoplastic cells contained virus, providing additional evidence for the role of EcPV2 in penile and preputial SCCs in horses. Additionally, in that study the E6/E7 oncogenes of EcPV2 were present in metastatic SCCs. There was also evidence of solar damage in cases of penile and preputial SCC not associated with EcPV2.¹⁰

Contributing Institution:

USAMRIID

Pathology Division

1425 Porter Street, Frederick, MD 21702-5011

<http://www.usamriid.army.mil/>

References:

1. Bogaert L, Willemsen A, Vanderstraeten E, et al. EcPV2 DNA in equine genital squamous cell carcinomas and normal genital mucosa. *Vet Microbiol.* 2012;158:33-41.
2. Brinsko SP, Blanchard TL, Varner DD. Male Reproductive Disorders. In: Smith BP, ed., *Large Animal Internal Medicine*, 4th ed. St. Louis, MO: Mosby Elsevier; 2009;1475-1476.
3. Foster RA, Ladds PW. Neoplasms of the penis and prepuce. In: Maxie MG, ed., *Jubb, Kennedy and Palmer's Pathology of Domestic Animals*, Vol 3. 5th ed. Philadelphia, PA: WB Saunders Co; 2007:617-619.
4. Knight C, Dunowska M, Munday JS, Peters-Kennedy J, Rosa BV. Comparison of the Levels of *Equus caballus* papillomavirus type 2 (EcPV-2) DNA in equine squamous cell carcinomas and non-cancerous tissues using quantitative PCR. *Vet Microbiol.* 2013;166:257-262.
5. Knight CG, Munday JS, Peters J, Dunowska M. Equine penile squamous cell carcinomas are associated with the presence of equine papillomavirus type 2 DNA Sequences. *Vet Pathol.* 2011;48:1190-4.
6. Kumar V, Abbas AK, Aster JC. *Pathologic basis of disease*. 9th ed. Philadelphia, PA: Elsevier Saunders, 2015: 324-325.

7. Kusewitt DF. Neoplasia and Tumor Biology. In: McGavin MD, Zachary JF, eds. *Pathologic Basis of Veterinary Disease*. 5th ed. St. Louis, MO: Mosby Elsevier; 2012:298-299, 315.

8. Lange CE, Tobler K, Lehner A, et al. EcPV2 DNA in equine papillomas and in situ and invasive squamous cell carcinomas supports papillomavirus etiology. *Vet Pathol*. 2012;50:686-692.

9. Sykora S, Samek L, Schonhaler K, et al. EcPV-2 is transcriptionally active in equine SCC but only rarely detectable in swabs and semen from healthy horses. *Vet Microbiol*. 2012;158:194-198.

10. Zhu KW, Affolter VK, Gaynor AM, Dela Cruz FN, Pesavento PA. Equine genital squamous cell carcinoma: In situ hybridization identifies a distinct subset containing *Equus caballus* papillomavirus 2. *Vet Pathol*. Online first May 12, 2015:1-6.

CASE II: 14-42715 (JPC 4066859).

Signalment: 10 year old, male neutered, domestic shorthair cat, feline (*Felis catus*).

History: The cat was diagnosed with suspected idiopathic pulmonary fibrosis approximately eleven months prior to date of death. On the morning of the cat's death, the owner found their German shepherd dog standing over the cat's body, and there were numerous puncture wounds on the cat's dorsum and limbs.

Gross Pathology: The animal was in fair nutritional condition evidenced by scant visceral and subcutaneous adipose tissue stores. There was a cutaneous puncture wound on the right dorsal trunk, and another ventral to the right scapula. There were multiple sites of subcutaneous hemorrhage over the trunk and appendages.



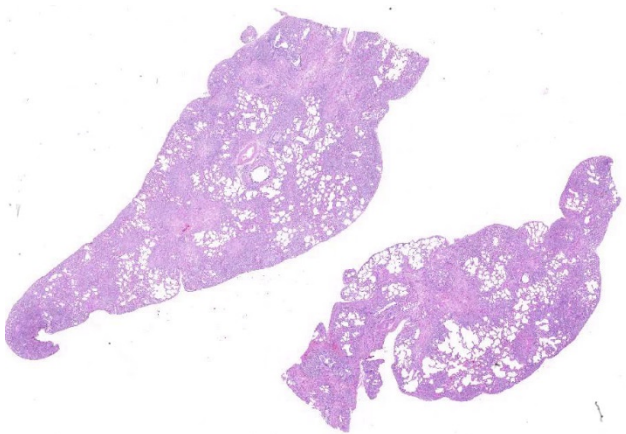
All lung lobes display a prominent nodular pattern. (Image courtesy of University of Illinois College of Veterinary Medicine Department of Pathobiology and Veterinary Diagnostic Laboratory. <http://vetmed.illinois.edu/path/>)

All lung lobes were firm and displayed a prominent nodular pattern, with nodules ranging from 0.2 cm to 0.5 cm in diameter. The pancreas consisted of discrete, multifocal, 3 mm diameter and smaller, white to tan nodules. The splenic capsule contained few, multifocal, 2 mm diameter white to tan, firm, slightly raised patches. The right thyroid gland was moderately enlarged relative to the left.

Laboratory Results: No virus was detected via virus isolation of lung tissue. Rare to very rare coliforms, *Streptococcus* (Group D), and *Trueperella pyogenes* bacteria were isolated from lung samples.

Histopathologic Description: Lung. Effacing 70% of the lung parenchyma, mostly located subpleurally and around large airways, are multifocal to coalescing areas of fibrosis. The subpleural foci of fibrosis are retracted and efface the normal lung parenchyma architecture. These foci of fibrosis are composed of aggregates of mature fibroblasts admixed fewer lymphocytes and plasma cells, and with a marked accumulation of collagen. In these areas the pleural mesothelial cells are multifocally hyperplastic. At the periphery of foci of fibrosis are some areas with less mature fibroblasts piling and arranged in parallel (foci of fibroplasia), producing small amounts of collagen. In between these areas of fibrosis are

variably distended and confluent alveoli with ruptured septa (emphysema, honey combing aspect) giving the lung a nodular architecture.



Approximately 80% of the section is replaced by fibrous connective tissue primarily focused on airways. (HE 4X)

Terminal bronchiolar smooth muscles are frequently markedly hyperplastic and remaining alveoli often filled with foamy macrophages and fewer lymphocytes, plasma cells and rare neutrophils. Alveoli are also often lined by plump cuboidal pneumocytes (type II pneumocyte hyperplasia).

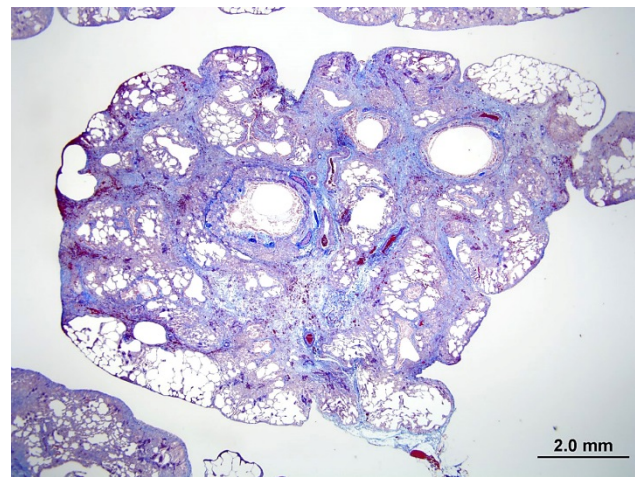
Within bronchiolar and bronchial lumens, is abundant basophilic, slightly fibrillar material (mucus) admixed basophilic nuclei and nuclear debris (necrotic neutrophils). Bronchial glands are mildly hyperplastic. The tunica media of vessels is markedly thickened (hyperplastic).

Contributor's Morphologic Diagnosis: Lung, chronic, severe, multifocal to coalescing interstitial fibrosis, with alveolar honeycombing, mild chronic histiocytic, lymphocytic, and plasmacytic interstitial pneumonia, and chronic moderate catarrhal and suppurative bronchitis.

Contributor's Comment: Idiopathic pulmonary fibrosis (IPF), also known as cryptogenic fibrosing alveolitis, is a form of interstitial lung disease (ILD), and is the most prevalent idiopathic interstitial pneumonia in humans.⁴ Human IPF is defined as a specific form of chronic, progressive fibrosing interstitial pneumonia of unknown cause, occurring

primarily in older adults, and limited to the lungs. It is further characterized by progressive worsening of dyspnea, and carries a poor prognosis.⁴ A consensus published in 2000 by a joint collaboration between the American Thoracic Society (ATS) and the American College of Chest Physicians (ACCP) classified human IPF as a distinct clinical entity with the histologic appearance of usual interstitial pneumonia (UIP), which includes a patchwork distribution of fibrosis leading to honeycombing (predominantly in the subpleural/paraseptal regions), smooth muscle metaplasia or hyperplasia, and the presence of fibroblastic foci.²

Diagnosis of human IPF relies on the exclusion of other known causes of interstitial lung disease (ILD), the presence of a UIP pattern on high resolution CT scans (HRCT), or specific combinations of HRCT and lung biopsy patterns in patients where lung biopsy samples are obtained.⁴

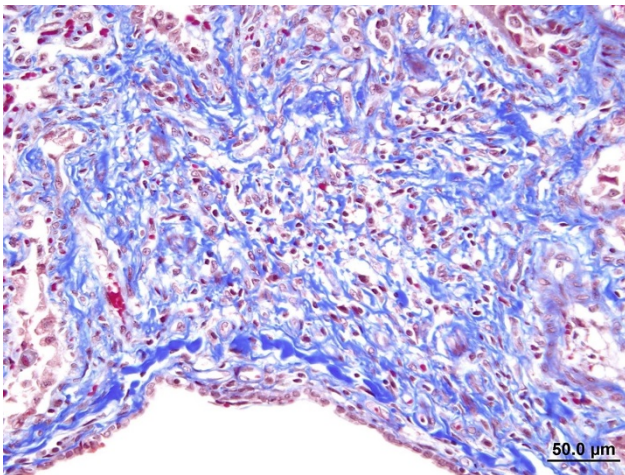


A Masson's trichrome stain demonstrates the amount of collagen present within this section of lung. (HE, 10X) (Image courtesy of University of Illinois College of Veterinary Medicine Department of Pathobiology and Veterinary Diagnostic Laboratory. <http://vetmed.illinois.edu/path/>)

Human IPF carries a variable and unpredictable natural history, and remains a poorly understood. While an exact etiology for human IPF remains unknown, several risk factors have been identified, including cigarette smoking, environmental exposures (metal and wood dusts, farming, raising birds, hairdressing, stone polishing), microbial agents (Epstein-Barr virus,

hepatitis C virus), and gastroesophageal reflux.⁴ Genetic factors have also been identified in the context of human IPF. For example, strong associations with familial IPF have been identified with mutations in the surfactant protein C gene.⁶

Animal models used to study IPF often fail to mimic morphological changes seen in human IPF, nor do they follow a similar progression of disease.⁷ Beginning in 1996, IPF has been recognized in cats,¹ characterized as a novel spontaneous chronic, progressive respiratory disease with morphologic features of UIP.² One study found that the average age of onset is 8.7 years, and average duration between onset of disease and death/euthanasia is 5.5 months.⁷ The disease in cats shares critical features with human IPF in the context of gross pathology, histopathology, cell differentiation markers, and ultrastructural details.^{5,7} No other spontaneous disease of induced animal model is able to reproduce the criteria for UIP as in feline IPF.²



Large areas of fibrosis focus on and efface airways throughout the section. (HE, 20X) (Image courtesy of University of Illinois College of Veterinary Medicine Department of Pathobiology and Veterinary Diagnostic Laboratory. <http://vetmed.illinois.edu/path/>)

Grossly, lungs are mottled tan to red, and display a distinct cobblestone appearance on pleural surfaces that typically involves large regions of the lungs. Additionally, the extensive areas of fibrosis typically form plaque-like regions that are discernible from normal lung tissue and extend deep into the parenchyma. Grossly

discernable honeycombing is an uncommon finding.⁷

The histopathologic hallmark (and most important diagnostic criterion) is that of a heterogeneous appearance at low magnification, characterized by fibrosis with scarring and honeycomb change that alternate with regions of less affected or even normal parenchyma.^{3,4,5,7} Other changes include foci of fibroblasts/myofibroblasts, and interstitial smooth muscle hyperplasia.^{1,2} The amount of inflammation is variable, but not a prominent feature, however, large foci of alveolar macrophages is a common finding. In some (69%) cats, mucous cell metaplasia is noted. In cats that do not demonstrate mucous cell metaplasia, the lining cells are either type II pneumocytes (well differentiated) or columnar cells of an unknown phenotype.⁷

In typical cases, lesions are often patchy or multinodular, rather than diffuse. The histopathologic changes often preferentially affect the subpleural and paraseptal parenchyma.^{3,4} This case is atypical in that lesions efface the entire pulmonary parenchyma, with virtually no normal tissue remaining. Similar cases have been documented by other authors, with the conclusion that the disease was too advanced to appreciate any temporal heterogeneity.³ Similarly, this case likely represents advanced disease, as this animal survived approximately one year after detection of clinical signs (average duration is 5.5 months). This animal died after a traumatic encounter with a dog. Thus, the cause of death was concluded to be respiratory compromise in the face of increased respiratory demand due to the traumatic incident.

JPC Diagnosis:

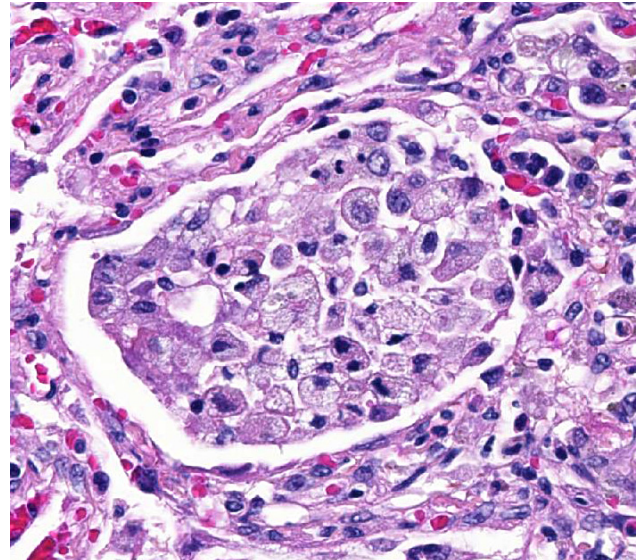
Lung: Fibrosis, interstitial, multifocal to coalescing, marked with smooth muscle hypertrophy and hyperplasia, type II pneumocyte hyperplasia, and moderate alveolar histiocytosis.

Lung: Bronchitis and bronchiolitis, chronic-active, multifocal, moderate with squamous metaplasia.

Conference Comment: The conference description was aligned very closely with the contributor's description. The nodularity of the fibrosis, especially in subpleural areas correlates well with the contributor's high quality gross image. The overall cellularity of the interstitial fibrous component, albeit variable in severity in some areas, was also a major discussion point. Conference participants speculated on the presence of myofibroblasts in some areas, which are thought to be an important cellular component of feline idiopathic pulmonary fibrosis.⁷ Important ancillary changes described included alveolar macrophages variably filling alveolar lumina, prominent alveolar epithelial lining cells (in this case, interpreted as type II pneumocyte hyperplasia), luminal narrowing of arteries, pleural mesothelial hypertrophy, and an inflammatory component within bronchi and bronchioles that varied between slides.

Most agreed that the mostly neutrophilic inflammatory infiltrate within the larger airways along with mucous exudation was a secondary process and may have been related to the positive bacterial culture in the lungs.

The precise pathogenesis of feline idiopathic pulmonary fibrosis is unclear, but current scientific literature suggests a defect in type II pneumocytes and alveolar repair are precursory findings. The loss of these cells may have an important role in the development of pulmonary fibrosis.⁷ Chronic interstitial inflammatory stimulation resulting in fibrosis has also been implicated in cases of interstitial fibrosis. However, in feline idiopathic pulmonary fibrosis, inflammation may not have an essential role and the primary defect and stimulus may involve the type II pneumocytes. In this case, conference participants noted that, overall, interstitial inflammation was mild at best and not a significant feature. Additionally, ultrastructural changes suggest surfactant protein C may play a role in the disease.⁷



Many alveoli are expanded and filled with numerous foamy macrophages. (HE, 320X)

This case was submitted to the Department of Pulmonary and Mediastinal Pathology at the Joint Pathology Center (JPC) for comparative pathology consultation regarding idiopathic pulmonary fibrosis in humans. Their consultation revealed similar histologic features as those discussed in the conference, but proposed an alternative interpretation to these changes. Their interpretation is that of an “organizing pneumonia characterized by airway luminal, airspace, and interstitial loose fibroblastic connective tissue”. Though difficult to discern due to overwhelming and diffuse injury, they favored an airway-centered process and described organizing pneumonia, in general terms, as a subacute process that is most commonly the sequelae of infection and, in many cases, difficult/impossible to document. The larger cartilaginous airways were described as showing “submucosal and adventitial chronic inflammation with varying degrees of destruction including complete obliteration of the small airways.” In their opinion, this case resembles progression of subacute organizing pneumonia to non-specific interstitial pneumonia (with fibrosis) with the histomorphologic features less consistent with unusual interstitial pneumonia (UIP) as it occurs in people. However, also noted in their detailed consultation, interstitial pulmonary fibrosis in cats (i.e. a novel spontaneous

chronic, progressive respiratory disease with morphologic features of UIP in humans) may have variations in histologic appearance as compared to humans suggesting possible species differences.

Contributing Institution:

University of Illinois College of Veterinary Medicine Department of Pathobiology and Veterinary Diagnostic Laboratory.
<http://vetmed.illinois.edu/path/>

References:

1. Caswell JL, Williams KJ. Respiratory system. In: Maxie, MG ed. Jubb, Kennedy, and Palmer's Pathology of Domestic Animals. Vol 2. 5th ed. Philadelphia, PA: Saunders Elsevier; 2007:570.
2. Cohen LA *et al.* Identification and Characterization of an Idiopathic Pulmonary Fibrosis-Like Condition in Cats. *J Vet Intern Med.* 2004; 18: 632-641.
3. LeBodec K, Roady P, O'Brien RT. A Case of Atypical Diffuse Feline Fibrotic Lung Disease. *Journal of Feline Medicine and Surgery.* 2014; 16(10): 858-863.
4. Raghu *et al.* An Official ATS/ERS/JRS/ALAT Statement: Idiopathic Pulmonary Fibrosis: Evidence Based Guidelines for Diagnosis and Management. *Am J Respir Crit Care Med.* 2011; 183: 788-824.
5. Rhind SM and Gunn-Morre, DA. Desquamative Form of Cryptogenic Fibrosing Alveolitis in a Cat. *J Comp Path.* 2000; 123: 226-229.
6. Thomas AQ, *et al.* Heterozygosity for a Surfactant Protein C Gene Mutation Associated with Usual Interstitial Pneumonitis and Cellular Nonspecific Interstitial Pneumonia in One Kindred. *Am J Respir Crit Care Med.* 2002; 165: 1322-1328.
7. Williams K *et al.* Identification of Spontaneous Feline Idiopathic Pulmonary Fibrosis: Morphology and Ultrastructural

Evidence for a Type II Pneumocyte Defect. *Chest.* 2004; 125: 2278-2288.

CASE III: 12-269-84 (JPC 4032912).

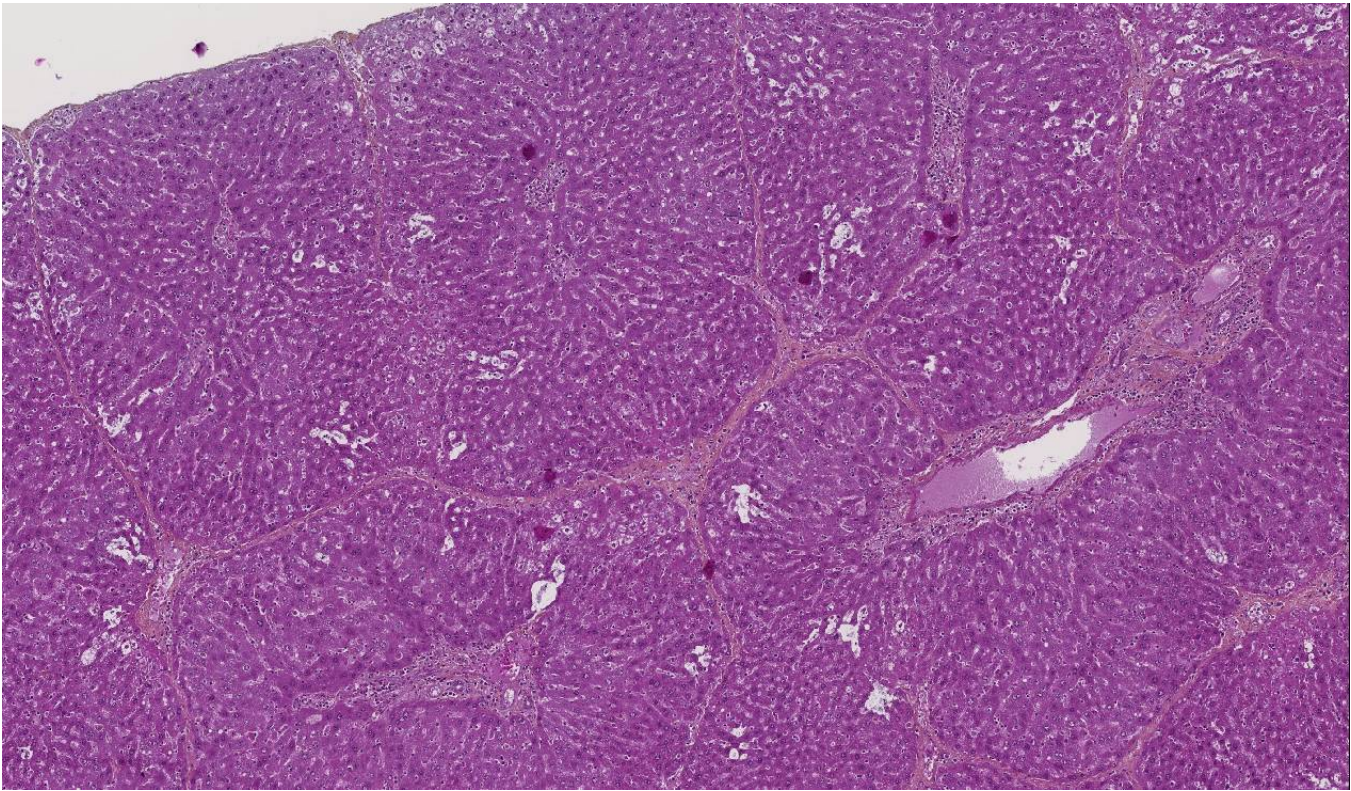
Signalment: Black rats (*Rattus rattus*) (unknown age and gender).

History: In November 2011, a trapping campaign was organized in a French zoological park to assess the prevalence of capillariasis in wild rodents. The campaign was initiated after the diagnosis of capillariasis in a primate from the zoo. Eighty rats were trapped and their livers were sampled and fixed in 10% buffered formalin.

Gross Pathology: Most livers were grossly unremarkable. In a few cases, livers had a slightly irregular surface and, in some areas, contained tightly packed pinpoint yellow foci and small irregular tracts.

Laboratory Results: None

Histopathologic Description: There is some variability between slides regarding the severity and the type of lesions. Livers show various degrees of bridging fibrosis characterized by fine fibrous septae connecting portal tracts to portal tracts or to centrilobular spaces (the so-called *septal fibrosis*). As a consequence, in the most affected areas, the architecture is reminiscent of the porcine liver. This pattern is highlighted with Masson's trichome stain. In addition, there are various degrees of lymphoplasmacytic and, to a lesser extent, eosinophilic infiltration in septae and around portal tracts and centrilobular veins. Sections usually have one or two aggregates of parasitic eggs surrounded by macrophages and multinucleated giant cells, and a peripheral rim of fibrosis with lymphocytes, plasma cells and eosinophils (granulomas). In older granulomas, eggs are mainly surrounded by fibrosis. Eggs are typically barrel-shaped, about 80 µm in length, bi-operculate and have a thick shell, the inner layer of which is refractile and the outer layer



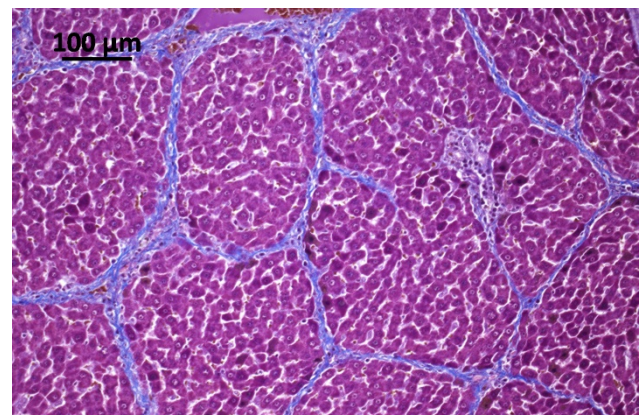
There is mild bridging portal fibrosis present diffusely throughout the section which separates and surrounds individual hepatic lobules. (HE, 76X)

striated (**Fig. 3**). The content is eosinophilic and granular (morphology consistent with unembryonated eggs of *Capillaria hepatica*). Some granulomas also contain areas of necrosis and/or dystrophic mineralization. Some slides show sections of adult worms: they measure 100-150 μm in diameter, have a pseudocoelom and a digestive tract (nematodes), a polymyarian-coelomyarian musculature and two bacillary bands (hypodermal bands with nuclei) (aphasmid nematodes) (**Fig. 4**). This morphology is consistent with adults of *Capillaria hepatica*. Some worms are surrounded by numerous eosinophils and macrophages.

Contributor's Morphologic Diagnosis: Liver: Hepatitis, granulomatous and eosinophilic, chronic, multifocal, moderate, with intralesional eggs and adult nematodes consistent with *Capillaria hepatica* (adults are not present on all slides).

Liver: Porto-portal and porto-central bridging fibrosis, multifocal, moderate to severe (septal fibrosis).

Contributor's Comment: *Capillaria hepatica* (also known as *Calodium hepaticum*), the cause of hepatic capillariasis, is an aphasmid nematode that mainly infects rodents and lagomorphs, and occasionally other vertebrates such as dogs or primates (including humans).^{8,11} Rodents of the genus *Rattus* are considered the main reservoir. As such, they tend to be highly infected and are

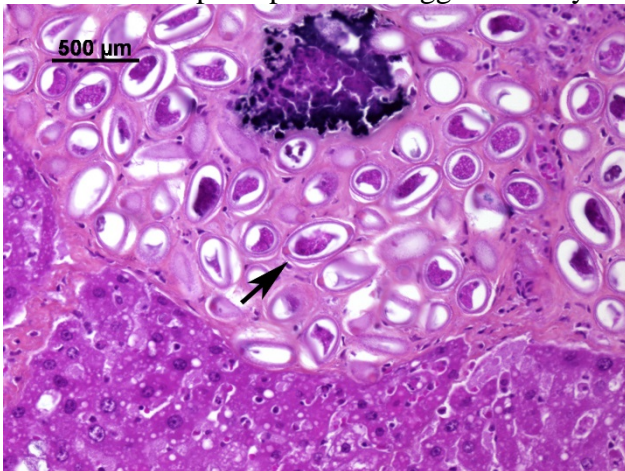


A Masson's trichrome stains highlights the degree of bridging fibrosis. (Masson's trichrome, 100X) (Image courtesy of: Unité d'Histologie, Embryologie et Anatomie pathologique, Département des Sciences Biologiques et Pharmaceutiques Ecole Nationale Vétérinaire d'Alfort, France www.vet-alfort.fr)

often the only source of parasites in urban environments.^{9,10} Infection of other mammals and humans results from incidental ingestion of water or food contaminated by embryonated eggs.¹⁰

Capillaria hepatica is the only known nematode with a direct life cycle requiring death of the host to be completed. Following their ingestion, embryonated eggs hatch in the intestine and release first stage larvae that cross the cecal barrier and reach the liver through mesenteric and portal veins. The migration of larvae within the hepatic parenchyma produces areas of hepatic necrosis.^{10,11} After three weeks, mature females start to lay eggs around portal tracts until they die (up to seventy days later). After their death, adults progressively disintegrate. Eggs elicit a mixed inflammatory response composed of macrophages, multinucleated giant cells, lymphocytes, plasma cells and eosinophils that leads to the formation of granulomas.^{10,11}

The peculiarity of hepatic capillariasis is that eggs are kept within the hepatic parenchyma instead of being released through the biliary tract as for other hepatic parasites. Eggs can only be



Throughout the section, fibrotic areas contain numerous 80-100µm thick-shelled *Capillaria* eggs. (HE 200X) (Image courtesy of: Unité d'Histologie, Embryologie et Anatomie pathologique, Département des Sciences Biologiques et Pharmaceutiques Ecole Nationale Vétérinaire d'Alfort, France www.vet-alfort.fr)

released in the environment after death and

decomposition of the host or after its ingestion by a predator. This predator represents a paratenic host that, although not necessary for completing the cycle, greatly promotes the maturation and the dissemination of the eggs.^{10,11}

A peculiar finding in rats infected with *Capillaria hepatica* is the development of septal fibrosis, a type of bridging fibrosis in which portal tracts are connected to portal tracts (or rarely to centrilobular spaces) by thin strands of connective tissue containing collagen, fibroblasts and lymphocytes. This pattern gives the hepatic parenchyma a porcine liver-like architecture. In humans, septal fibrosis is an important, frequent and non-specific finding in chronic liver diseases. For this reason, rats infected with *Capillaria hepatica* represent a good model for hepatic fibrosis. It has been shown that in this model, septal fibrosis is not preceded by hepatic necrosis or overt chronic inflammation. The first step of septal fibrosis appears to be star-shaped expansions of portal spaces containing fibroblasts and blood vessels that sprout from periportal spaces. The presence of proliferating blood vessels is a characteristic feature.^{2-3,5,7}

In the present case, other rodent species (ex: Greater white-toothed shrew (*Crocidura russula*)) have been trapped and revealed to be infected by *Capillaria hepatica* but only rats developed septal fibrosis. For veterinary pathologists, this example illustrates how different can be the patterns of tissue reaction among species, even with the same initiating cause. Another well-known example for that is tuberculosis.¹

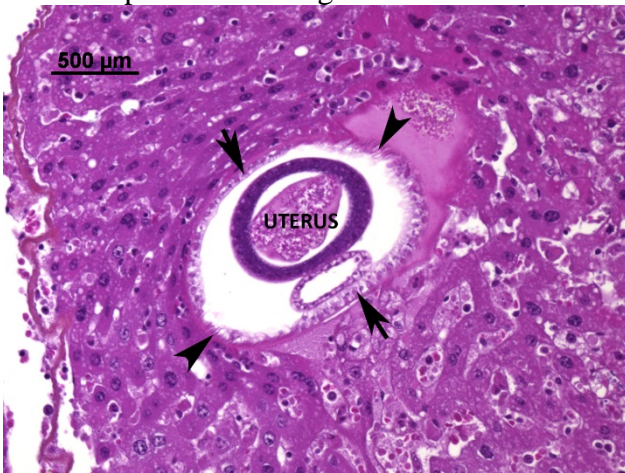
Table 1. Hepatic parasites in Domestic Species

PARASITE	DEFINITIVE (DH) OR INTERMEDIATE (IH) HOSTS	LOCATION / COMMENT
WANDERING LARVAE (NUMEROUS SPECIES)		
<i>Cysticercus tenuicollis</i> (<i>Taenia hydatigena</i>)	IH: sheep, goat, cattle, squirrel, swine	Cysts in peritoneal cavity / Fatal hepatic hemorrhages in lambs severely infected. Associated with Black disease
<i>Cysticercus pisiformis</i> (<i>Taenia pisiformis</i>)	IH: rabbit, squirrel, small rodents	Cysts in liver capsule
<i>Cysticercus fasciolaris</i> (<i>Taenia teaniaeformis</i>)	IH: rodents, rabbit	Cysts in liver / Associated with the development of fibrosarcoma
Larvae of <i>Ascaris suum</i>	DH: swine	Causes milk-spotted liver. Adults in intestine
Larvae of <i>Stephanurus dentatus</i>	DH: swine	Adults in urinary system
Larval strongyles (<i>Strongylus edentatus</i> , <i>S. equi</i> , <i>S. vulgaris</i>)	DH: horse	Causes villous perihepatitis
CESTODES		
<i>Stilesia hepatica</i>	DH: ruminants (Africa)	Only cestodes that inhabit the bile ducts
<i>Thysanosoma actinioides</i>	DH: ruminants (America)	
<i>Echinococcus granulosus</i>	IH: humans, cattle, swine, sheep, deer, horse, small rodents, moose etc.	Liver
<i>Echinococcus multilocularis</i>	IH: humans, cattle, swine, sheep, deer, horse, small rodents, moose etc.	Liver
<i>Mesocestoides corti</i> / <i>M. lineatus</i>	IH: dog, cat, other mammals, reptiles, rodents	Liver, peritoneal and pleural cavities, lungs, other organs
NEMATODES		
<i>Capillaria hepatica</i>	DH: small rodents, rabbit, humans etc.	Liver
TREMATODES		
<i>Fasciola hepatica</i>	DH: ruminants, dog, cat, horse	Bile ducts / Associated with Black disease and bacillary hemoglobinuria.
<i>Fasciola gigantica</i>	DH: cattle, sheep	Bile ducts
<i>Fascioloides magna</i>	DH: cattle, sheep, horse, pig	Liver
<i>Dicrocoelid flukes</i>		
<i>Eurytrema pancreaticum</i>	DH: sheep, goat, cattle	Pancreatic and bile ducts and duodenum
<i>Concinnum procyonis</i>	DH: raccoon, fox, cat	Pancreatic and bile ducts
<i>Dicrocoelium dendriticum</i>	DH: sheep, goat, dog, pig, deer	Bile ducts / Associated with Black disease.
<i>Dicrocoelium hospes</i>	DH: cattle (Countries south to the Sahara)	Bile ducts
<i>Platynosomum fastosum</i>	DH: cat (North America and Amazonia)	Liver, bile ducts
<i>Athesmia foxi</i>	DH: New World monkeys	Bile ducts
<i>Opisthorchid flukes</i>		
<i>Metorchis albidus</i>	DH: dog, cat, fox	Bile ducts
<i>Metorchis conjunctus</i>	DH: cat, dog, fox, mink	Bile ducts

	(North America)	
<i>Metorchis bilis</i>	DH: red fox	Bile ducts
<i>Opistorchis felinus</i>	DH: cat, dog, fox (Europe, Russia)	Bile ducts
<i>Opistorchis sinensis</i>	DH: dog, cat, pig, humans, fox	Bile duct and duodenum. Associated with cholangiocarcinoma in humans.
<i>Opistorchis tenuicollis</i>	DH: dog, cat, fox, pig	Pancreatic and bile ducts
<i>Pseudamphistomum truncatum</i>	DH: dog, cat, fox	Bile ducts
<i>Paramphistomatidae</i>		
<i>Gigantocotyle explanatum</i>	DH: cattle, buffalo	Bile ducts
<i>Schistosomatidae</i>		
<i>Schistosoma japonicum</i> , <i>S. mansoni</i> , <i>S. bovis</i> , <i>S. spindale</i> etc.	DH: various species (humans, monkey, cat, dog, ruminants etc.)	Adults reside in veins (portal v., mesenteric v. etc.)

JPC Diagnosis: Liver: Hepatitis, granulomatous and eosinophilic, chronic, multifocal, moderate with bridging fibrosis and adult nematodes and eggs.

Conference Comment: Conference participants also noted slide variation as mentioned above, with absence of adult nematodes in some sections and variation in the degree and type of inflammation around nematodes. Eosinophilic inflammation is present in some sections and others are dominated by granulomatous inflammation. The stichosome, which is a row of basophilic esophageal gland cells surrounding the esophagus and is one of the most distinctive characteristics of aphasmid nematodes,⁴ is seen only in a few sections and the eggs are described as being unembryonated. Other ancillary changes described include the pitted and undulating surface of the liver as well as the hepatocellular degeneration and necrosis



Cross-sections of adult nematodes include a low polymyarian-coelomyarian musculature (arrowheads), intestine lined by low cuboidal epithelium (arrow), and a centrally placed uterus (HE, 400X)

directly surrounding adult nematodes in some sections.

Aphasmid nematodes derive their name from the lack of a tiny set of sensory papillae (phasmids) on their caudal end, which are not identifiable histologically, but differentiate them from the phasmid nematodes (i.e. strongyles, rhabditoids, ascarids, oxyurids, rhabditoids and spirurids). Histologically visible characteristics that help distinguish them from the phasmids include absence of lateral cords, the presence of hypodermal/bacillary bands, and as mentioned above, the presence of a stichosome, which would only be seen in sections with esophagus. The eggs of some species are bipolar plugged / bioperculate as seen in this case, but may be embryonated or unembryonated depending on the specific parasite species.⁴

As mentioned above by the contributor, portal bridging fibrosis is a prominent feature of this entity. However, unlike many other types of portal fibrosis, hepatic stellate cells do not seem to participate in the pathogenesis of this lesion. Experimentally, septa are visible around the 23rd and 27th day after rat inoculation with embryonated eggs, and prominent angiogenesis precedes deposition of collagen, which is a key component in the development of hepatic fibrosis. The earliest changes are seen in portal areas, which may be located some distance away from the location of the actual nematodes,⁷ and may emanate from multiple portal areas simultaneously.³ In addition to angiogenesis, studies have found that proliferating cells

responsible for the formation of prominent septa include fibroblast like cells⁷ as well as pericytes and myofibroblasts.³ Other cells, such as eosinophils, may also be present, but evidence for involvement of hepatic stellate cells is absent.⁷ Interestingly, angiogenesis also seems to play a role in regression of fibrosis as it occurs in rats infected with *C. hepatica*.³

Contributing Institution:

Unité d'Histologie, Embryologie et Anatomie pathologique, Département des Sciences Biologiques et Pharmaceutiques Ecole Nationale Vétérinaire d'Alfort, France www.vet-alfort.fr

Reference

1. Caswell JL: Tuberculosis. In: Maxie, MG ed. *Jubb, Kennedy, and Palmer's Pathology of Domestic Animals*. Vol 2. 5th ed. Philadelphia, PA: Saunders Elsevier; 2007:606-610.
2. Ferreira LA, Andrade ZA. *Capillaria hepatica*: a cause of septal fibrosis of the liver. *Mem Inst Oswaldo Cruz*. 1993; 88: 441–447.
3. Gaban L, Ramos CDL, Barbosa Júnior AA, Souza MM de, Andrade Z de A. Dynamics of *Capillaria-hepatica*-induced hepatic septal fibrosis in rats. *Rev Soc Bras Med Trop*. 2010; 43: 643–646.
4. Gardiner CH, Poynton SL. *An Atlas of Metazoan Parasites in Animal Tissues*. Washington, DC: Armed Forces Institute of Pathology; 1999:40-43.
5. Gomes AT, Cunha LM, Bastos CG, Medrado BF, Assis BC, Andrade ZA. *Capillaria hepatica* in rats: focal parasitic hepatic lesions and septal fibrosis run independent courses. *Mem Inst Oswaldo Cruz*. 2006; 101: 895–898.
6. Jones TC, Hunt RD, King NW. Diseases caused by parasitic helminths and arthropods. In: *Veterinary Pathology*. Wiley-Blackwell; 2007:601–667.
7. Maria De Souza M, Tolentino M, Assis BCA, Cristina De Oliveira Gonzalez A, Maria Correia Silva T, Andrade ZA. Pathogenesis of septal fibrosis of the liver. (An experimental study with a new model). *Pathol Res Pr*. 2006; 202: 883–889.
8. Mowat V, Turton J, Stewart J, Lui KC, Pilling AM. Histopathological features of

Capillaria hepatica infection in laboratory rabbits. *Toxicol Pathol*. 2009 37: 661–666.

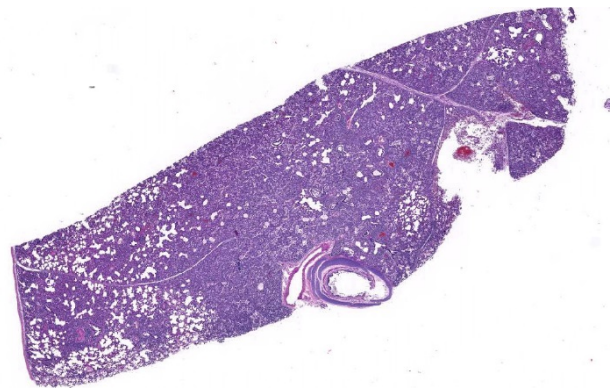
9. Redrobe SP, Patterson-Kane JC. *Calodium hepaticum* (syn. *Capillaria hepatica*) in captive rodents in a zoological garden. *J Comp Pathol*. 2005; 133: 73–76.

CASE IV: N14-367 (JPC 4066359).

Signalment: 4 weeks of age, male, Duroc porcine (*Sus scrofa domesticus*)

History: The submitted animal was one of approximately 20 pigs displaying respiratory distress. This pig died enroute to the veterinary clinic. This animal came from a 600-head porcine facility in Puerto Rico.

Gross Pathology: A male red porcine in adequate body condition (BCS 3.5/5) presented in a mild state of autolysis. A 6 cm wide area of alopecia was present on the dorsal aspect of the body extending from the neck to the base of the tail. Alopecia was also noted around the snout



There is diffuse consolidation of the lung as a result of severe interstitial pneumonia. (HE, 4X)

and the left dorsal carpal region had a focal circular hairless area of 3x3 cm. The lungs were markedly thickened with a meaty consistency and did not collapse or float in formalin solution (interstitial pneumonia). They were diffusely

mottled pink to red and contained multifocal to coalescing dark red circular areas ranging from 2.5x 2 cm to 2x1 cm. The right caudal lung lobe had a 4x1 cm dark red area at its border. Blood oozed from cut surfaces of the lung (congestion). The pericardial sac contained 5-6 ml of transparent amber colored fluid. The myocardium was diffusely pale. The nasal turbinates were diffusely hyperemic. The spleen surface had multiple circular plum colored areas measuring 1.5 cm in diameter, which extended into the parenchyma. The small and large intestine were diffusely gas-distended.

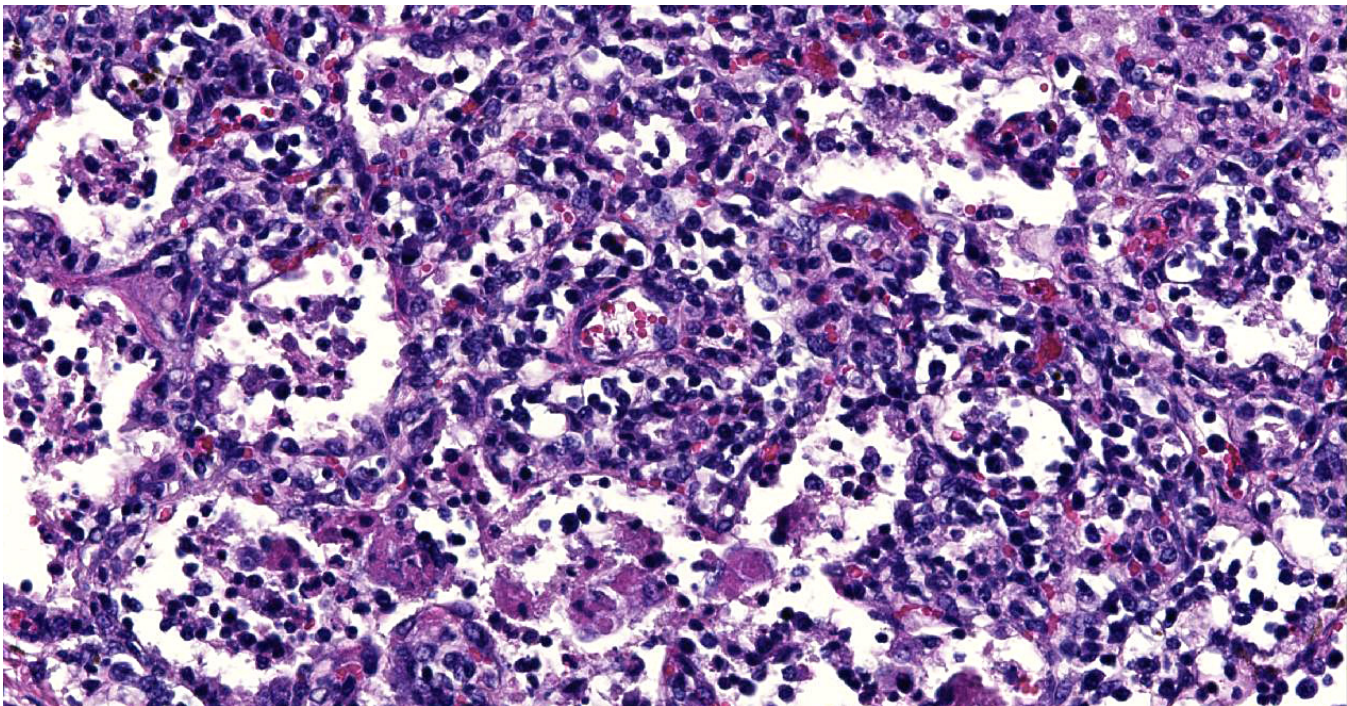
Laboratory Results: Bacteriology was assessed in-house and samples for virology and nutritional analyses were sent to the Diagnostic Center for Population and Animal Health at Michigan State University.

Virology: Lung tissue was positive for PRSSV by PCR. Samples were negative for Swine influenza virus and pseudorabies virus.

Culture and Sensitivity: *Streptococcus pyogenes* was isolated from the lung. The isolate was susceptible to carbenicillin, and not

susceptible to tobramycin, norfloxacin, vancomycin, gentamycin, sulfa/trimethoprim and erythromycin. Nutritional analysis for vitamin E levels in the liver were normal. Trace nutrient analysis of the liver revealed adequate levels of selenium, zinc and copper. Iron levels were slightly elevated at 674 micrograms/gram (normal reference interval is 300-600). Cobalt and molybdenum were also analyzed, but reference values for pigs were unavailable.

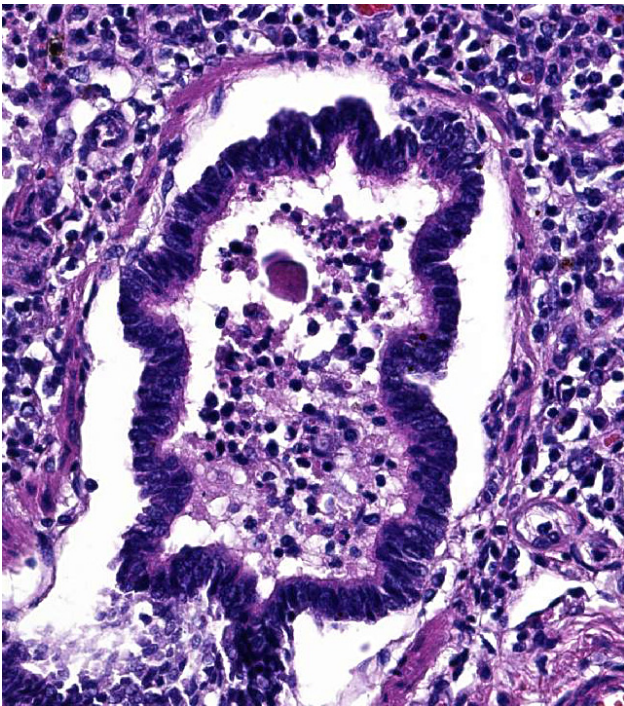
Histopathologic Description: Lung: Diffusely, the interstitium is moderately to markedly expanded by predominantly macrophages, lesser lymphocytes and plasma cells, and few neutrophils. Alveolar lumina are markedly distended with fibrin and proteinaceous karyorrhectic cellular debris, numerous viable and degenerate neutrophils, macrophages, and lesser lymphocytes and plasma cells. Greater than 80% of alveolar walls are necrotic characterized by loss or replacement with fibrinoid necrosis. There is also scattered type II pneumocyte hyperplasia. In severely affected areas, bronchiolar lumina contain moderate amounts of fibrillar to homogenous eosinophilic material (fibrin and protein) with karyorrhectic



There is diffuse septal necrosis, and remaining alveoli and mixed cellular infiltrate, fibrin, and hyperplastic Type II pneumocytes. (HE, 208X)

necrotic cellular debris and neutrophils, macrophages, lymphocytes and plasma cells (Fig. 3). Occasional vessels contain fibrin thrombi. There is BAL hyperplasia and interstitial congestion in less inflamed areas.

Heart: The subendocardium contains a locally extensive area of myocardial hemorrhage with a mild infiltrate of lymphocytes (Fig. 4). Within this area and the adjacent myocardium there is myofiber separation due to expansion of the interstitial space (edema). There is moderate perivascular edema around multiple epicardial vessels.



2 Airways contain an exudate of viable and degenerate neutrophils admixed with fibrin, edema, and abundant cellular debris. (HE, 210X)

Haired skin: There is mild to moderate superficial perivascular edema and infiltrates of small number of lymphocytes and plasma cells. There is moderate to marked orthokeratotic hyperkeratosis. The stratum corneum is lined by few small accumulations of ovoid 2x3 micrometer, pale basophilic yeasts (*Candida* sp.). There are few small accumulations of coccoid bacteria that are often in pairs or small clusters (*Streptococcus* and/or *Staphylococcus* sp.). These organisms are often associated with small

numbers of neutrophils, lymphocytes and plasma cells.

Contributor's Morphologic Diagnosis:

Lung: Severe diffuse lymphohistiocytic and necrotizing interstitial pneumonia, etiology PRRSV.

Lung: Mild to moderate multifocal suppurative bronchointerstitial pneumonia.

Heart: Mild focally extensive lymphocytic and hemorrhagic myocarditis.

Lymph node and Peyer's patches: Severe diffuse lymphoid hyperplasia.

Haired skin: Moderate to severe diffuse orthokeratotic hyperkeratosis with intracorneal yeasts and bacteria and mild suppurative crusting.

Haired skin: Mild superficial perivascular lymphoplasmacytic dermatitis.

Contributor's Comment: The cause of death in this pig was a severe interstitial pneumonia associated with porcine reproductive and respiratory syndrome (PRRS) virus, as identified in lung tissue by PCR. Porcine reproductive and respiratory syndrome is caused by an arterivirus in the family Arteriviridae.

There are 2 clinical manifestations of PRRS: A reproductive phase and a respiratory phase. The reproductive form of the disease typically lasts 1-4 months, and is characterized by increased numbers of stillborn and mummified fetuses, late term abortion, and weak-born piglets. Anorexia and agalactia are also often present further contributing to preweaning mortality. Suckling piglets characteristically develop a "thumping" respiratory pattern. The respiratory form of the disease is characterized by a chronic interstitial pneumonia clinically associated with dyspnea with no associated cough. Post-weaning pigs are primarily affected and have a significant reduction in daily weight gain and increased mortality up to 10-25%.¹ Secondary bacterial infections are common. Histologically, the virus results in a severe necrotizing interstitial pneumonia with sparing of the bronchiolar epithelium. Alveolar septa are thickened by infiltrates of lymphocytes and macrophages,

which also infiltrate the alveolar lumina, along with small numbers of neutrophils. Scattered alveoli will contain karyorrhectic cellular debris. There may be variable type II pneumocyte hyperplasia. Lymphoid hyperplasia is a characteristic feature of PRRSV infection, along with scattered apoptosis of follicular lymphocytes. Perivascular infiltrates of lymphocytes, plasma cells and macrophages may be present in several organs including the nasal mucosa, heart, kidney, and brain.

This virus is very contagious among pigs, and is transmitted via several routes of exposure including parenteral, intranasal, intramuscular, oral, vaginal and intrauterine. The virus replicates in monocyte-derived cells and is shed in blood, semen and oral fluids. Subclinical carriers are common, attributing to the endemic nature of the disease and difficulty in eradication once it has been introduced into a herd.⁵

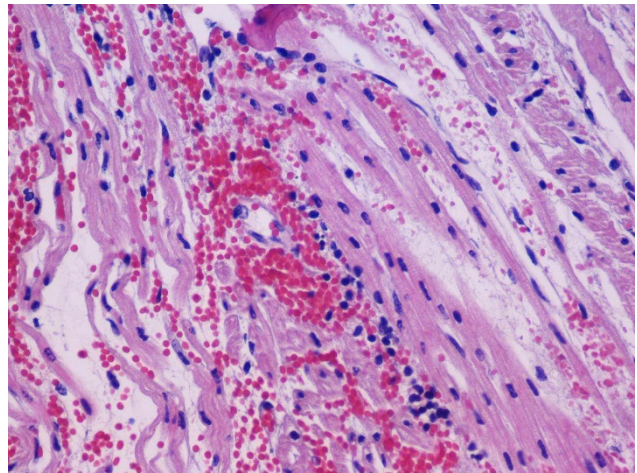
In this case, the suppurative bronchointerstitial pneumonia is secondary to opportunistic bacterial invasion. *Streptococcus pyogenes* was isolated from the lung in this case. This is a human pathogen, warranting consideration of this being a potential zoonosis or a possible contaminant. The lesions in the heart are likely a sequela to the PRRS virus. Another differential to rule-out for this lesion is encephalomyocarditis virus. This animal had a rough hair coat and areas of alopecia, which were histologically associated with hyperkeratosis and intracorneal coccoid bacteria and yeasts, suggestive of *Candida sp.* Similar mycotic agents and numerous rod bacteria were also present in the lumen of the intestine. The overgrowth of yeasts and bacteria is likely due to an immunosuppressive state of the animal secondary to viral infection. Prolonged antibiotic use can also cause a similar overgrowth of yeast.

JPC Morphologic Diagnosis:

1. Lung: Pneumonia, interstitial, necrotizing, subacute, diffuse, marked with type II pneumocyte hyperplasia.
2. Lung: Bronchopneumonia, neutrophilic, acute, multifocal, moderate.

Conference Comment:

The slide description and conference discussion of the histologic features in the submitted section of lung closely aligned with those by the contributor. Most conference participants agreed the process likely began in the alveolar interstitium with septal degeneration and necrosis, and subsequently progressed to loss of alveolar septa and the influx of inflammatory cells. Hyaline membranes are prominent in some areas secondary to exudation of fibrin; rare syncytial cells are also observed. Although BAL hyperplasia is not a prominent feature in most slides, there is slide variation and some participants felt BAL hyperplasia was an important microscopic finding when present. Additionally, a secondary process affecting medium and large airways is present. Bronchioles contain variable numbers of viable and degenerate neutrophils, admixed with fewer sloughed epithelial cells. Participants attributed the inflammatory lesions of the conducting airways to secondary bacterial infection, most likely due to *Streptococcus pyogenes* based on the contributor's laboratory information and comments above. The differential diagnosis considered in this case included *Mycoplasma hyopneumoniae* and swine influenza virus.



There are multifocal areas in the myocardium of hemorrhage, edema, and infiltration by small numbers of lymphocytes. (HE, 200X). (Image courtesy of: Tuskegee University College of Veterinary Medicine, Nursing and Allied Health, 1200 Old Montgomery Rd., Tuskegee, AL 36088 http://www.tuskegee.edu/academics/colleges/cvmnah/school_of_veterinary_medicine.aspx)

The PRRS virus results in significant economic losses in the swine industry worldwide, with annual cost estimates around \$600 million in the United States alone. It is a species specific virus that has a high mutation rate, which may result in outbreaks in previously vaccinated herds. As mentioned above, routes of transmission and shedding are diverse and duration of infection and shedding may vary depending on virus strain. Additionally, prolonged infection is a key feature of the virus, as with other arteriviruses.³

Clinically, PRRS disease typically occurs in clinical stages, the first beginning with viral infection and replication in alveolar macrophages followed by spread to alveolar pneumocytes, most likely via leukocyte trafficking. The virus appears to have a predilection for infection of macrophages. The presence of infected alveolar macrophages results in alveolar damage and acute interstitial pneumonia. Degeneration and necrosis of pneumocytes occur as a result of the acute inflammatory response. Being an enveloped virus, the agent is able to infect the cell without causing cell death. However, both infected and non-infected macrophages release proinflammatory cytokines, recruiting additional inflammatory cells, and causing significant tissue damage. Histologically, the results of the cytokine cascade are seen as alveoli filled with inflammatory cells and debris, as observed in this pig case. Infected macrophages drain to regional lymph nodes where they infect lymphocytes and other macrophages, resulting in clinically large, firm, grossly edematous nodes. In the second clinical stage of disease, the virus spreads to other organ systems and becomes a persistent infection. This typically results in more generalized infection of lymph nodes and the reproductive organs, among other tissues such as tonsil and spleen.

At the molecular level, the PRRS virus is able to prevent infected macrophages/monocytes from functioning properly during phagocytosis, antigen presentation and cytokine release, thus hampering the immune response.⁴ Specifically, infection results in impaired expression of cytokines such as TNF α , IL-12 and IFN γ .² Additionally, the virus increases the release of IL-10 from infected cells, which is immunosuppressive, affecting both the innate and adaptive immune response.⁴

References:

1. Cahn CM, Line S. *The Merck Veterinary Manual*. 10th ed. Whitehouse Station, NJ: Merck & Co., Inc.; 2010:661-663.
2. Garcia-Nicolas O, Quereda JJ, Gomez-Laguna J et al. Cytokines transcript levels in lung and lymphoid organs during genotype 1 porcine reproductive and respiratory syndrome virus (PRRSV) infection. *Vet Immunol Immunopathol*. 2014;160(1-2):26-40.
3. Perez AM, Davies PR, Goodell CK. Lessons learned and knowledge gaps about the epidemiology and control of porcine reproductive and respiratory syndrome virus in North America. *JAVMA*. 2015;246(12):1304-1317.
4. Zachary JF. Mechanisms of Microbial infection. In: McGavin MD, Zachary JF, eds. *Pathologic Basis of Veterinary Disease*. 5th ed. St. Louis, MO: Mosby Elsevier; 2012:214-215.
5. Zimmerman JJ, Karriker LA, Ramirez A, et al. *Diseases of Swine*. 10th ed. Wiley-Blackwell; 2012: 461-480.



WEDNESDAY SLIDE CONFERENCE 2015-2016

Conference 6

2 November 2015

Dr. Michael Garner, DVM, PhD, DACVP
Pathologist and Proprietor, Northwest ZooPath
Snohomish, WA

CASE I: NCAH-2012B (JPC 4018127).

Signalment: 77 month old female raccoon (*Procyon lotor*).

History: This individual was used as a negative control in a transmissible spongiform encephalopathy (TSE) transmission study. This animal died 68 months after the experimental cohorts in the study were inoculated with a TSE.

Gross Pathology: The uterus was markedly distended, appearing to occupy the majority of the abdominal cavity. The wall of the uterus was uniformly thin, and contained approximately 300mL of a clear, thin liquid (hydrometra). The oviducts were moderately thickened, and the ovaries appeared small. The stomach was moderately distended, containing approximately 50mL of dark black mucoid material and had multifocal hemorrhages. The intestinal tract appeared compressed and did not contain any ingesta. Microscopic lesions were bilateral and confined to the uterus and oviducts.

Laboratory Results: None

Histopathologic Description: Uterus: Endometrial glands are variably dilated by clear

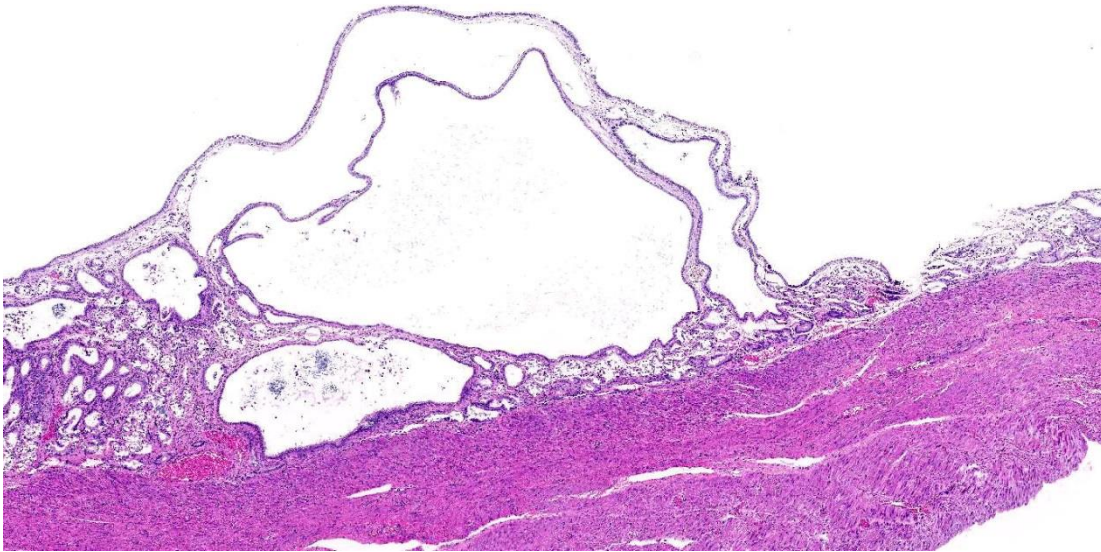


Uterus, raccoon. The mucosa is studded with multifocal cystic endometrial glands. (HE, 6X)

space and scant to moderate amounts of eosinophilic fluid and/or viable and degenerate epithelial cells or cystic, up to 4 mm in diameter. Glands are haphazardly arranged and the epithelium lining glands and cysts are short to tall columnar, occasionally with intact cilia, line rare papillary projections, or are occasionally piled up four to five cells thick. Nuclei are round to oval with finely stippled basophilic chromatin and a single lum magenta nucleolus. Small to moderate numbers of viable and degenerate neutrophils are rarely present in the loose connective tissue of the submucosa, which is atrophied. The myometrium is variably thin (section variation) and myometrial blood vessels are dilated by red blood cells (congestion).

Contributor's Morphologic Diagnosis: Uterus: Endometrial hyperplasia, cystic, diffuse, chronic, mild to moderate.

Contributor's Comment: Endometrial hyperplasia is common in domestic canines, often involves cystic distension of endometrial glands (cystic endometrial hyperplasia, CEH) and may result in bacterial infection (pyometra). A variety of sterile substances have been placed in the uterine lumen of bitches during the luteal (sometimes referred to as secretory or progestational) phase, which resulted in endometrial hyperplasia and remodeling. Another theory suggests a low-grade, subclinical bacterial infection during the luteal phase results in endometrial proliferation. CEH can affect a single or just a few glands, affect glands segmentally, or diffusely affect the entire endometrium.



Uterus, raccoon: Cystic endometrial glands range up to 2mm in diameter. (HE, 20X)

Some species develop endometrial hyperplasia as a result of excessive and prolonged estrogenic stimulation. Estrogen contributes to the pathogenesis of endometrial hyperplasia by priming the endometrium, via estrogen receptors, to induce the synthesis of intracellular receptors for progesterone.¹¹ Progesterone, from ovarian corpora lutea (CL), then induces the proliferation

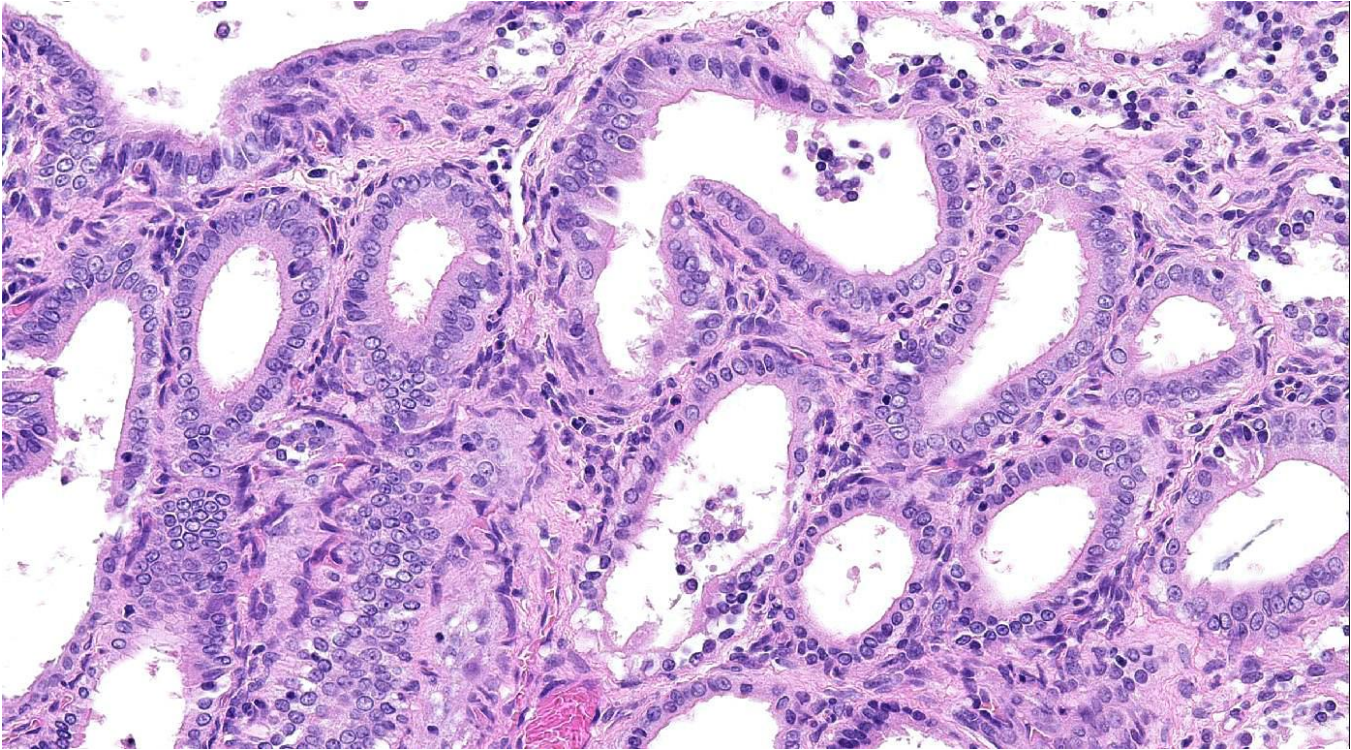
and secretion of the endometrium.⁶ In addition to the normal estrous cycle, estrogen sources may be endogenous, as with granulosa cell tumors, or exogenous, as with phytoestrogens.¹¹ Exogenous sources of progesterone can be found in melengestrol acetate (MGA), megestrol acetate, and medroxyprogesterone.⁷

Chronically hyperplastic endometrial glands lead to the gross accumulation of mucoid fluid. Mucometra and hydrometra are considered by some to be variations of the same condition, their difference lying in hydration of the mucin secreted by the endometrium. In addition to the accumulation of fluid concurrent with endometrial hyperplasia, it may also result from the obstruction of a segment of the uterus, cervix, or vagina. If muco/hydrometra persists, the pressure caused by the accumulating fluid results in the attenuation/atrophy of the endometrium

and thinning of the uterine wall.¹¹

In addition to domesticated animals, cystic endometrial hyperplasia has also been described in raccoons,^{3,4} Asian and African elephants,¹ African hunting dogs (*Lycaon pictus*),⁶ a chinchilla,² and multiple zoo

canid species.⁷ With the exception of one primiparous individual, all elephants with CEH (15 total) were nulliparous. Asian elephants had a significantly greater risk of developing CEH while the risk for both Asian and African elephants increased with age.¹ The three African hunting dogs were multiparous; two had CLs and two had ovarian granulosa cell tumors.⁶ The chinchilla was nulliparous and had a history of



Mildly dilated gland contain small amounts of sloughed cells, protein, and cell debris. Lining cells are tall, columnar, and lack the characteristic vacuolation of cells under progesterone influence. (HE, 168X)

blood being found sporadically in its cage.² Zoo canids that had been treated with MGA as a contraceptive were significantly more likely to develop CEH than non-treated canids.⁷

Of the four female raccoons used in the study, three developed endometrial hyperplasia; the uterus of the fourth was not examined. None of these raccoons had received any exogenous hormone therapy nor were any ovarian cysts/tumors or uterine, cervical, or vaginal obstructions identified. Finally, all of the raccoons were nulliparous.⁴ The likely pathogenesis of cystic endometrial hyperplasia and resultant mucometra in this case may therefore be similar to that of domestic carnivores (i.e. driven by prolonged and/or repeated estrogen priming followed by progesterone stimulation).

JPC Diagnosis:

1. Uterus: Multiple endometrial cysts.
2. Uterus, muscular tunic: Adenomyosis, multifocal.

Conference Comment: Conference participants' histologic description was largely aligned with the contributor's description. Additional features discussed included infiltration of the uterine stroma by low numbers of lymphocytes and macrophages, a scant amount of mineral admixed with the sloughed epithelial cells and few multifocal areas of uterine adenomyosis. Although the lesion was initially interpreted as cystic endometrial hyperplasia by conference participants, the moderator offered an alternative interpretation. Although admittedly within the current literature, cysts within endometrium are almost universally described with reference to cystic endometrial hyperplasia, the moderator noted that CEH is generally more of a proliferative lesion, and in this case the lesion was minimally proliferative and predominantly only cystic. Thus, this lesion may represent an age-related change which occurs in mammals and is unrelated to estrogenic stimulation and development of hyperplastic uterine mucosa. Schlafer and Gifford have accurately stated that describing and interpreting proliferative and cystic lesions within the endometrium is often "difficult, frustrating and

potentially confusing,”¹⁰ which serves to highlight the potential for contention in a case such as this.

There are two patterns of cystic endometrial hyperplasia described in the bitch: generalized CEH and pseudoplacental endometrial hyperplasia (PEH), also referred to as localized endometrial hyperplasia of pseudopregnancy. Both may result in accumulation of secretions within the uterus, but in PEH there will also be cellular debris present from necrosis of the superficial endometrium, which may be confused with pyometra.⁹ Additionally, in PEH the proliferation is highly organized and histologically similar to placentation sites seen in pregnancy.¹⁰ In contrast to CEH, noncystic endometrial hyperplasia is generally only recognized microscopically and characterized by irregular proliferation and arrangement of uterine glands. The stroma is generally edematous, the mucosal epithelium hypertrophied, and adenomyosis may be present.⁹ Adenomyosis refers to endometrial tissue located within the muscular layers of the uterus. It often appears like normal uterine glands which may be associated with secretory material, or the glandular epithelium may be atrophied leaving only connective tissue and resulting in a cyst like structure in the myometrium.¹⁰

In the cow CEH is associated with granulosa cell tumors, ovarian follicular cysts as well as exposure to exogenous sources of estrogen.^{9, 11} In the mare and camelids it is considered very uncommon and not associated with granulosa cell tumors.⁹ CEH has also been observed as a common lesion in miniature pigs, which are often kept as pets and therefore live longer than domestic pigs. In the sow CEH has also been associated with the mycotoxin zearalenone.⁵ CEH has also been described in sheep associated with ingestion of estrogen containing plants as well as in goats without association with ingestion of estrogenic plants.⁸

Contributing Institution:

National Centers for Animal Health, Ames, IA
www.nadc.ars.usda.gov

References:

1. Agnew DW, Munson L, Ramsay EC. Cystic endometrial hyperplasia in elephants. *Vet Pathol.* 2004; 41:179-183.
2. Granson HJ, Carr AP, Parker D, Davies JL. Cystic endometrial hyperplasia and chronic endometritis in a chinchilla. *J Am Vet Med Assoc.* 2011; 239: 233-236.
3. Hamir AN, Klein L. Polycystic kidney disease in a raccoon (*Procyon lotor*). *J Wildl Dis.* 1996; 32: 674-677.
4. Hamir AN, Kunkle RA, Miller JM, Cutlip RC, Richt JA, Kehrl ME, Jr., Williams ES. Age-related lesions in laboratory-confined raccoons (*Procyon lotor*) inoculated with the agent of chronic wasting disease of mule deer. *J Vet Diagn Invest.* 2007; 19:680-686.
5. Ilha MRS, Newman SJ, van Amstel S, et al. Uterine lesions in 32 female miniature pet pigs. *Vet Pathol.* 2010; 47(6):1071-1075.
6. Jankowski G, Adkesson MJ, Langan JN, Haskins S, Landolfi J. Cystic endometrial hyperplasia and pyometra in three captive African hunting dogs (*Lycaon pictus*). *J Zoo Wildl Med.* 2012;43:95-100.
7. Moresco A, Munson L, Gardner IA. Naturally occurring and melengestrol acetate-associated reproductive tract lesions in zoo canids. *Vet Pathol.* 2009;46:1117-1128.
8. Radi ZA. Endometritis and cystic endometrial hyperplasia in a goat. *J Vet Diagn Invest.* 2005; 17:393-395.
9. Schlafer DH, Foster RA. Female genital system. In: Maxie GM, ed. *Jubb, Kennedy and Palmer's Pathology of Domestic Animals.* Vol 3. 6th ed. St. Louis, MO: Elsevier; 2016:382-383.
10. Schlafer DH, Gifford AT. Cystic endometrial hyperplasia, pseudo-placental endometrial hyperplasia, and other cystic conditions of the canine and feline uterus. *Theriogenology.* 2008;70(3):349-358.
11. Schlafer DH, Miller RB: Female genital system. In: Maxie GM, ed. *Jubb, Kennedy, and Palmer's Pathology of Domestic Animals.* Vol 3. 5th ed. St. Louis, MO: Elsevier; 2007:429-564.

CASE II: E274/14 (JPC 4048928).

Signalment: Juvenile, female bronze-winged Parrot (*Pionus chalcopterus*).

History: Numerous birds of a flock with various parrots died spontaneously or after a short episode of unspecific symptoms.



Section of liver from a bronze-winged parrot. (HE, 4X)

Gross Pathology: Necropsy revealed hepatomegaly and multifocal randomly distributed white foci in the liver. Spleen and kidneys were swollen and moderate numbers of adult *Ascaridae* were present in the duodenum.

Laboratory Results: PCR tested negative for avian bornavirus. Ziehl-Nielsen staining of a liver imprint failed to identify acid-fast bacteria.

Histopathologic Description: Liver: The liver architecture is multifocally disrupted by randomly distributed areas up to 0.1 cm in diameter characterized by loss of cellular detail, karyorrhexis, karyolysis, and deposition of cellular debris (necrosis). Foci are surrounded by moderate numbers of degenerated and viable heterophils and macrophages. Occasionally hepatocytes and Kupffer cells contain intracytoplasmic grey indistinct granular structures. Increased numbers of aforementioned cells are also present within the sinusoids. Multifocally, most often surrounding bile ducts are moderate numbers of mainly lymphocytes, plasma cells, and fewer macrophages. Multifocally, bile ducts are minimal hyperplastic

and occasionally ectatic. Additionally, the liver is diffusely congested.

Giemsa staining revealed multifocal dark purple cytoplasmic inclusions in both hepatocytes and macrophages.

Contributor's Morphologic Diagnosis: Liver: Hepatitis, chronic-active, multifocal, random, necrotizing and granulomatous, moderate to severe, with intracellular bacteria consistent with *Chlamydophila psittaci*, bronze-winged parrot (*Pionus chalcopterus*), avian.

Contributor's Comment: The members of the order *Chlamydiales* are obligate intracellular, gram-negative bacteria depending on the host cells energy resources (ATP). They have a biphasic life cycle with the infectious form that enters the cell (elementary body, EB), the intracellular, metabolic active, replicating form (reticulate body, RB) and the intermediate body (IB) with morphologic characteristics between EB and RB.

Infection with *C. psittaci* occurs primarily via inhalation, ingestion or conjunctival exposure to contaminated feather dust or faeces. The bacteria spread to lung, air sacs and pericardial sac within few hours. EBs attach to microvilli of the host cell membrane and are internalized via invagination.⁴ Bacteria-containing endocytic vesicles are called inclusions. They proceed to the nuclear area where EBs differentiate into RBs. A role of snapin (a part of the SNARE complex) connecting chlamydial inclusions with the microtubule network by interacting with both IncB and dynein has been proposed.¹ RBs replicate via binary fission and reorganize, through IBs, into new EBs. New EBs are released from host cell via cell lysis or exocytosis. In high pathogenic serotypes the inclusion membrane degrades mainly during the active multiplication, releasing the bacteria into the cytoplasm, leading to cell lysis.⁷ The rapid multiplication leads to bacteraemia within 48 hours. Infectious EBs are spread via cloaca and/or nasal turbinates into the environment.

Typical clinical findings include diarrhoea and excretion of green to yellow-green urate. Severely affected birds may become anorectic and produce sparse, dark green droppings, followed by emaciation, dehydration and death.

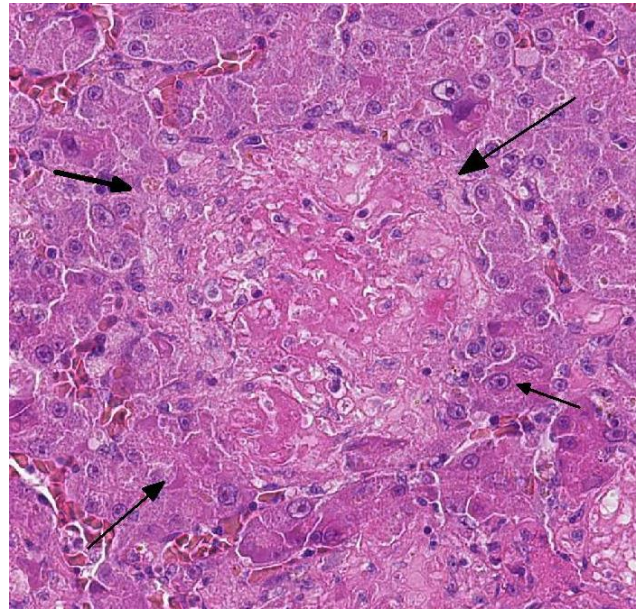
Typical gross findings are hepatomegaly and splenomegaly with or without necrotic foci, often accompanied by fibrinous airsacculitis, pericarditis and peritonitis and serous to purulent conjunctival exudate.

The genus *Chlamydophila* contains six species: *C. abortus* (ruminants), *C. caviae* (guinea pigs), *C. felis* (felidae), *C. pecorum* (ruminants, swine, koalas), *C. pneumonia* (humans, marsupialia and amphibia) and *C. psittaci* (birds). *Chlamydophila* spp. are known to infect at least 469 domestic, free-living or pet bird species in 30 orders.³ Of the nine known “outer membrane protein A” (ompA) subtypes of *C. psittaci*, seven are known to naturally infect birds (A – F and E/B) and two to infect mammals (M56 – muskrat and snowshoe hare, WC – cattle). Each avian serotype seems to be associated with a different group or order of birds.² Furthermore, strains of *C. psittaci* fall into two general categories: highly or less virulent strains. Highly virulent strains or toxigenic strains (e.g. serotype D) are isolated most often from turkeys and occasionally from clinically inapparent wild birds. In natural and experimental hosts, they are responsible for a rapid and fatal disease progression characterized by extensive vascular congestion and inflammation of vital organs. Veterinarians and poultry workers are especially at risk of becoming infected with serovar D strains. Strains of low virulence (e.g. serotype B and E) cause slowly-progressing epidemics with a mortality rate of less than 5% and neither develop severe vascular damage nor severe clinical signs.⁶ They are routinely isolated from pigeons and ducks. Chlamydiosis may be accompanied by concurrent infection with *Salmonella* spp, especially in pigeons, ducks and some psittacine birds. Avian strains can infect humans and may lead to severe pneumonia. However, cases of human-to-human transmission rarely occur. Immunity to chlamydia is generally poor and

short-lived. Older birds are often more susceptible to clinical signs than younger ones.

JPC Diagnosis:

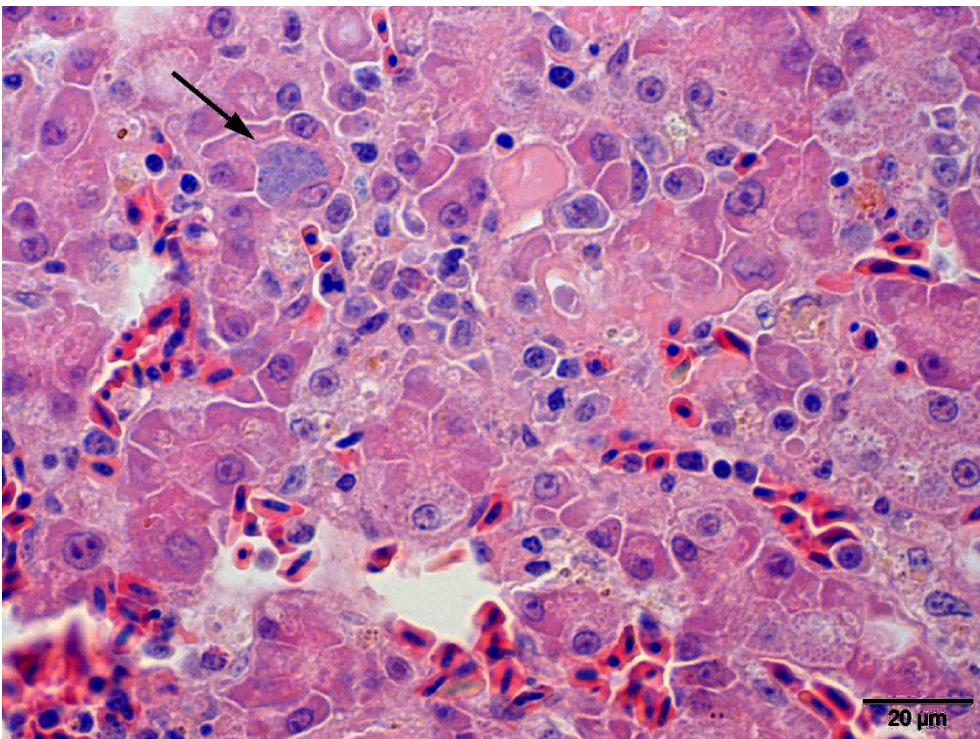
Liver: Hepatitis, necrotizing, random, multifocal, moderate with diffuse hepatocellular degeneration.



Liver, parrot. Multiple foci of coagulative necrosis are scattered throughout the section. Older foci are infiltrated by low numbers of heterophils and macrophages. (HE, 144X)

Conference Comment: Multifocal and random foci of coagulative and lytic necrosis effacing hepatic parenchyma were the predominant histologic features observed by conference participants. In less affected/non-necrotic parenchyma, changes indicative of hepatocellular degeneration including hepatocyte swelling, pallor, and centrilobular to midzonal vacuolar change were also described. Bile ducts containing blood and inflammatory cells were noted; however, this finding was deemed incidental and, in this case, unrelated to the pathogenesis of *C. psittaci*. Conference participants rarely identified 1-2µm, pale basophilic to amphophilic, intracellular organisms in macrophages and hepatocytes, most consistent with *C. psittaci* organisms. Slide variation regarding presence of organisms, was noted amongst conference participants.

Although not available for this conference, participants discussed various histochemical stains including Macchiovello and Gimenez stains, to identify and/or better highlight organisms in *C. psittaci*-suspect tissues. Common postmortem findings in *C. psittaci*-infected birds include hepatomegaly and splenomegaly, both which were observed grossly in this case. Histologically, the spleen is another primary organ to identify lesions and organisms. This infection is very common in Amazon parrots, which will demonstrate clinical illness. Pigeons and doves are common carriers, but do not become ill; however, they may facilitate zoonosis.



Liver, parrot. Rare hepatocytes are expanded by aggregates of basophilic bacterial consistent with *Chlamydia*. Many of the hepatocytes show evidence of cellular degeneration characterized by the presence of large granules within their cytoplasm. (HE, 20X). (Photo courtesy of: Department of Veterinary Pathology, Freie Universitaet Berlin <http://www.vetmed.fu-berlin.de/en/einrichtungen/institute/we12/index.html>)

All genotypes / subtypes of *C. psittaci* can be transmitted to people and cause psittacosis (i.e. parrot fever), a disease originally named when infection was thought to be only transmitted from psittacine birds. Most cases of human psittacosis are related to contact with psittaciformes; however, it is also an occupational hazard for

those working in the poultry industry and others in close contact with different avian species.⁸ Infection in humans can result in a wide range of disease from asymptomatic infections to mild influenza-like symptoms, to severe disease with pulmonary and extrapulmonary involvement including gastrointestinal, hepatic, cardiac and neurologic signs.

C. psittaci infection in poultry production operations is most commonly associated with turkey or duck farms, but has also been documented in chickens, more commonly broilers. In chickens, both the *ompA* genotypes B and the more pathogenic D can cause clinical infection consisting of respiratory symptoms. However, as described above for other avian species, respiratory symptoms are generally more severe in genotype D infected chickens and it may also result in anorexia and mortality. Additionally, genotype D shows significantly higher bacterial replication in infected tissues and may demonstrate systemic dissemination. It is found to be excreted in the cloaca and from the pharynx in infected chickens as seen in other avian species.⁹

Atherosclerosis is frequently seen in captive psittacine birds and is considered the most common vascular disease of birds. Interestingly, it has been associated with the presence of *C. psittaci* antigen in blood vessels indicating infection may be a risk factor for development of atherosclerosis.⁵ However, the exact role of *C. psittaci* infection in the pathogenesis of atherosclerosis, regarding severity and strain, is unclear.

Contributing Institution:

Department of Veterinary Pathology, Freie Universitaet Berlin
<http://www.vetmed.fuberlin.de/en/einrichtungen/institute/we12/index.html>

References:

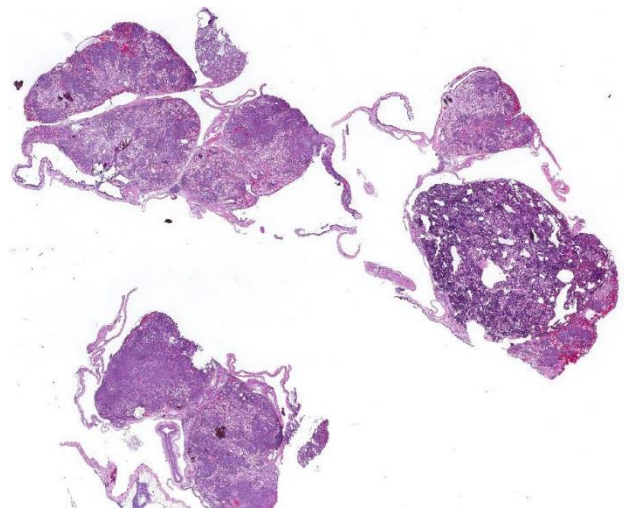
1. Böcker S, Heurich A, Franke C, et al. *Chlamydia psittaci* inclusion membrane protein IncB associates with host protein Snapin. *Int J Med Microbiol.* 2014;304(5-6):542-53.
2. Geens T, Desplanques A, Van Loock M, et al. Sequencing of the *Chlamydomphila psittaci* ompA gene reveals a new genotype, E/B, and the need for a rapid discriminatory genotyping method. *J Clin Microbiol.* 2005;43(5):2456-61.
3. Kaleta EF, Taday EMA. Avian host range of *Chlamydomphila* spp. based on isolation, antigen detection and serology. *Avian Pathol.* 2003;32(5):435-462.
4. Hodinka RL, Wyrick PB. Ultrastructural study of mode of entry of *Chlamydomphila psittaci* into L-929 cells. *Infect Immun.* 1986;54(3):855-63.
5. Pilny AA, Quesenberry KE, Bartick-Sedrish TE, et al. Evaluation of *Chlamydomphila psittaci* infection and other risk factors for atherosclerosis in pet psittacine birds. *J Am Vet Med Assoc.* 2012;240(12): 1474-80.
6. Tappe JP, Andersen AA, Cheville NF. Respiratory and Pericardial Lesions in Turkeys Infected with Avian or Mammalian Strains of *Chlamydomphila psittaci*. *Vet Pathol.* 1989;26(5):386-395.
7. Vanrompay D, Charlier G, Ducatelle R, et al. Ultrastructural changes in avian *Chlamydomphila psittaci* serovar A-, B-, and D-infected Buffalo Green Monkey cells. *Infect Immun.* 1996;64(4): 1265-71.
8. Vanrompay D, Harkinezhad T, van de Walle M, et al. *Chlamydomphila psittaci* transmission from pet birds to humans. *Emerg Infect Dis.* 2007;13(7):1108-1110.
9. Yin L, Lagae S, Kalmar I, et al. Pathogenicity of low and highly virulent *Chlamydomphila psittaci* isolates for specific-pathogen-free chickens. *Avian Diseases.* 2013;57(2):242-247.

CASE III: N2015-0172 (JPC 4066459).

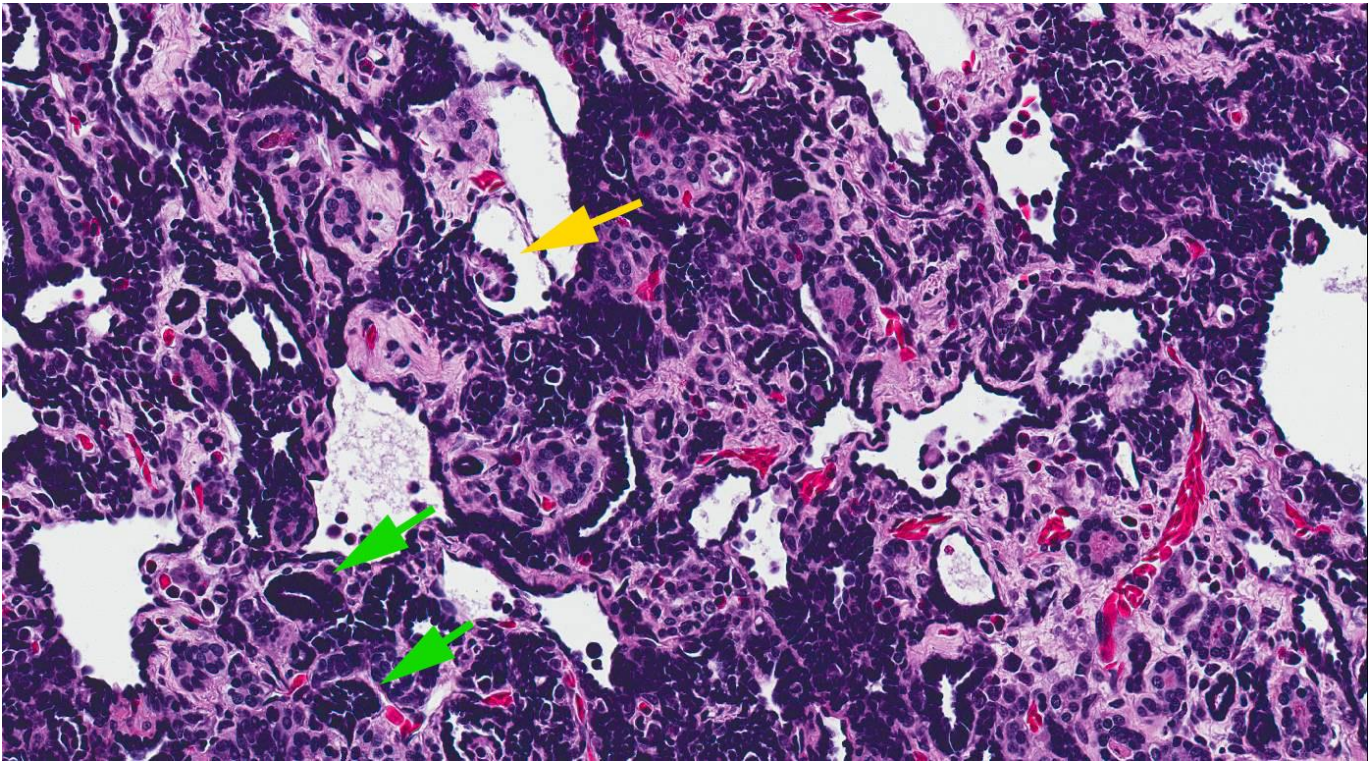
Signalment: 14.5 year old, male, Colorado River toad (*Incilius alvarius*).

History: This individual was found dead with no premonitory signs. Post-traumatic necrotic hindlimb digits were removed approximately 7 months prior to death and the animal was reportedly normal in the interim.

Gross Pathology: Examined is a 243.6 g adult female Colorado River toad in fair body and good postmortem condition. There are numerous, discrete, round to oval wounds consisting of epidermal loss with red discoloration of the exposed tissue. Most are on the medial and ventral aspect of the left proximal hindlimb, left perianal area and caudal ventrum, but are also present on the right ventral brachium and antebrachium, near the elbow. Compression of the right forelimb results in expression of purulent material from one of these wounds. The distal aspect of all digits of the left hindlimb are absent, with only 1.0 mm to 2.0 mm remaining. The kidneys are diffusely mottled maroon and pink and have slightly nodular surface.



Multiple sections of kidney, adrenal, and interrenal glands are submitted. (HE, 6X)



Kidney, toad. Renal tissue is multifocally effaced by ribbons of blastemal cells which often form tubule-like structures (green arrows), and often become cystic. In some cystic tubules a polypoid proliferation of blastema, resembling glomeruli, bulge into the tubular lumina (yellow arrow). (HE, 120X)

There is a small amount of clear watery fluid in the ventral lymph sacs and a large amount of similar fluid in the coelomic cavity. Coelomic fat bodies are large and slightly pink to tan.

Laboratory Results: Aerobic culture (skin wounds): *Pseudomonas aeruginosa*, *Aeromonas* spp.

Anaerobic culture (skin wounds): *Fusobacterium* spp., *Bacteriodes* spp., unidentified Gram positive rods.

Histopathologic Description: Kidney and interrenal gland: Throughout the renal parenchyma and into the interrenal gland are variably sized, fairly discrete foci of inflammation composed of predominantly macrophages with fewer lymphocytes and granulocytes and admixed with abundant karyorrhectic debris. These granulomas often compress the surrounding parenchyma. Similar infiltrates multifocally expand Bowman's space and occasionally completely efface glomerular tufts. There are variably dense inflammatory infiltrates predominated by granulocytes

traversing the renal interstitium and are of highest densities surrounding granulomas. Tubules throughout the kidneys contain granular eosinophilic material admixed with karyorrhectic debris. Tubular epithelial cells frequently contain brown globular cytoplasmic pigment and there is rare intratubular crystalline material. This material is pale yellow and birefringent with polarized light (presumed oxalates). A focal ureteral branch contains abundant mineralization.

Kidney: There is a focal, unencapsulated, well-demarcated neoplasm composed of variably differentiated epithelial cells and blastemal cells set in a loose collagenous stroma. Blastemal cells have indistinct cell borders, scant to inapparent cytoplasm, and ovoid nuclei with hyperchromatic to finely stippled chromatin are present in dense clusters. Epithelial cells range from embryonal, with similar appearance to those above, forming ribbon-like strands and branching tubules, to more differentiated cuboidal to columnar cells forming mature, discrete tubules. These cells have distinct cell borders with a moderate

amount of eosinophilic cytoplasm that occasionally contains prominent granules. The nuclei are round to slightly ovoid, often basilar, with coarsely clumped chromatin. In some areas, tufts of cells protrude from primitive tubule walls into the lumen, resembling embryonic glomeruli. Mitotic figures are rare and only identified in blastemal populations. The stroma of this neoplasm is composed of loose aggregate of collagen interspersed with spindle to wavy cells. The interstitium contains few granulocytes, lymphocytes and macrophages.

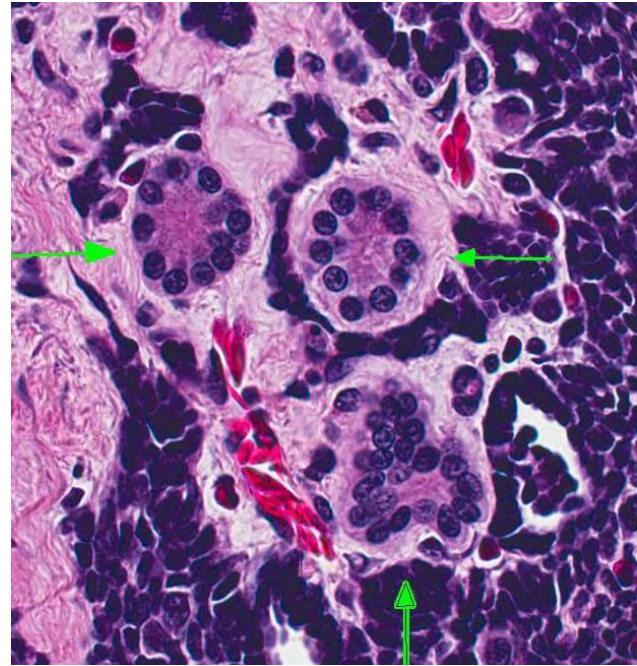
Contributor's Morphologic Diagnosis:

1. Kidneys and interrenal gland:
Glomerulonephritis and adrenalitis, granulomatous, necrotizing, subacute, multifocal to coalescing, severe, with abundant intralesional acid-fast bacteria and renal architectural effacement
2. Kidney: Nephroblastoma

Contributor's Comment: Death of this Colorado River toad was the result of systemic mycobacteriosis. The most severe lesions were in the kidney, with granulomatous and necrotizing inflammation and containing abundant intralesional acid-fast and faintly Gram positive bacilli. There were numerous open skin wounds which, histologically, were chronic and also contained acid-fast bacteria. Given these findings, the wounds were considered to be the likely site of origin. Other tissues involved in the systemic infection included the interrenal gland, liver, heart and brain.

Mycobacteriosis in amphibians often presents as a disease of the integument, attributable to skin wounds and the organisms' common presence in water. Multiple non-tuberculous *Mycobacterium* species have been reported to cause disease in amphibians, including *M. marinum*, *M. chelonae*, *M. fortuitum*, *M. xenopi*, *M. abscessus*, *M. avium*, and *M. szulgai*; *M. marinum*, *M. xenopi* and *M. fortuitum* are reported as the most common isolates.⁶ Dissemination to multiple organs is a common feature of amphibian mycobacteriosis, and is grossly identified as pale nodules within the parenchyma or grey patches on mesothelial surfaces. Associated inflammation is typically

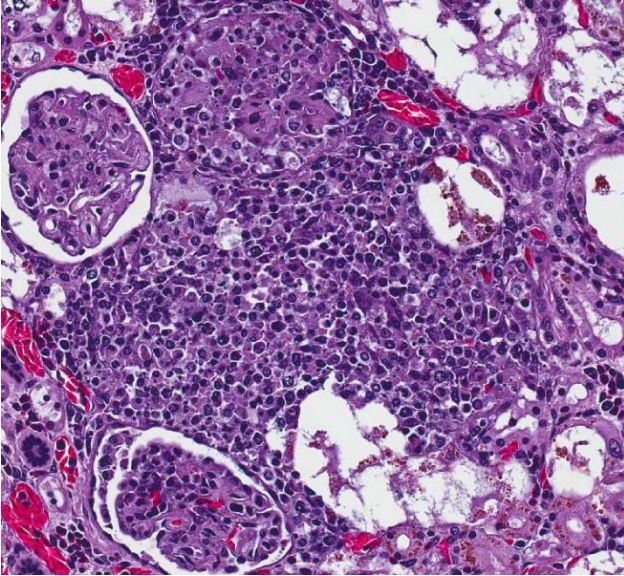
described as granulomatous, although the nature of the infiltrate depends on the stage of infection and can range from a mixture of granulocytes and macrophages in more acute lesions to more typical granulomas with macrophages centrally and lymphocytes peripherally in chronic lesions.¹ In this individual, the most severe lesions were in the kidney and consisted of discrete, but otherwise disorganized granulomas, suggestive of a subacute time course. Renal severity may be directly related to the location of the skin wounds, as hindlimb lesions in amphibians have been reported to spread directly to the kidneys.¹



Kidney, toad. Pre-existent chromaffin cells (green arrows) are scattered through the neoplasm. (HE, 200X)

In addition to disseminated inflammation throughout the kidneys, there was a large, focal, unilateral renal neoplasm. The morphologic appearance of this tumor was consistent with a nephroblastoma (e.g. Wilms tumor, embryonal nephroma). Classically, nephroblastomas consist of three embryonal cell populations. These include an epithelial component which forms irregular tubules and immature glomerular tufts, a mesenchymal component forming a loose stroma, and an undifferentiated blastemal component dispersed throughout the tumor.^{4,5} Differentiation of the mesenchymal component into muscle, bone and/or cartilage is common in

some species, but has not been reported in amphibians. In this case, there were few glomerular structures and the tumor was predominated by blastemal and epithelial cells, and no differentiation of the mesenchymal component. As in a previously described



Kidney, toad. In other sections of the kidney, renal parenchyma is effaced by poorly-formed granulomas composed of large numbers of macrophages, admixed with fewer lymphocytes. (HE, 120X)

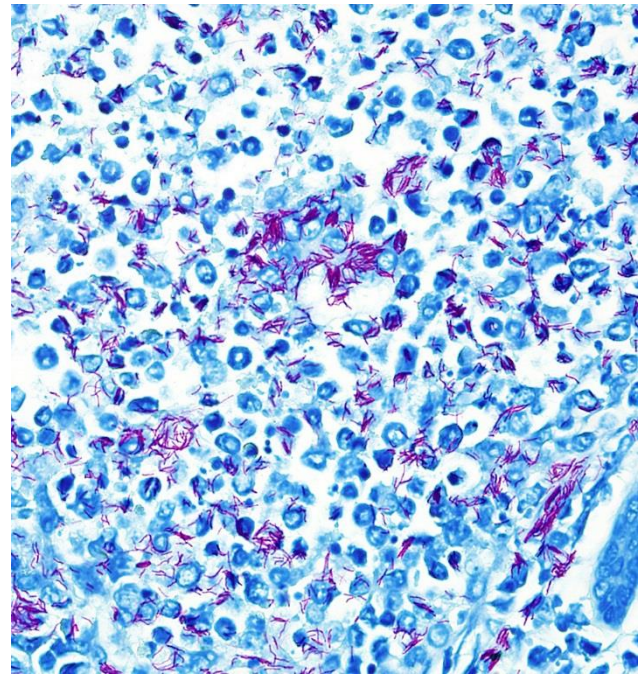
amphibian nephroblastoma,³ tubules in this case were variably differentiated, with some neoplastic tubular cells containing eosinophilic granular cytoplasm. In mammals, birds and reptiles, nephroblastomas arise from the metanephric blastema, either from neoplastic transformation during nephrogenesis, or from persistent nephrogenic rests.⁵ In amphibians and fish, which contain functional mesonephri throughout life, the tumor is thought to arise from mesonephric tissue. Rare in amphibians, nephroblastomas have been previously reported in an African clawed frog (*Xenopus laevis*), a fire-bellied newt (*Cynops pyrrhogaster*), a giant Japanese salamander (*Andrias japonicus*), and as an induced lesion in ribbed newts (*Pleurodeles waltl*).^{2,3} Nephroblastoma can be confirmed in humans and other mammals by immunohistochemical identification of Wilms tumor protein 1 within neoplastic cells. This has been attempted in amphibians in only one of the previously reported cases, and neither tumor cells nor internal controls were positive.³

Immunohistochemistry was not pursued in this case.

JPC Diagnosis:

1. Kidney, testis, and interrenal gland: Nephroblastoma.
2. Kidney: Nephritis, granulomatous, multifocal to coalescing, moderate with intra- and extracellular acid fast bacilli.
3. Collecting duct: Nephrolith.

Conference Comment: In discussing the nephroblastoma, conference attendees noted the presence of well differentiated mesenchymal and epithelial elements, as well as embryonal elements. Islands of chromaffin cells were identified in one section of tissue, indicating the tumor had invaded and effaced the adrenal gland. Within the section of kidney affected by the mycobacterium infection, both degeneration and regeneration of renal tubule epithelial cells was

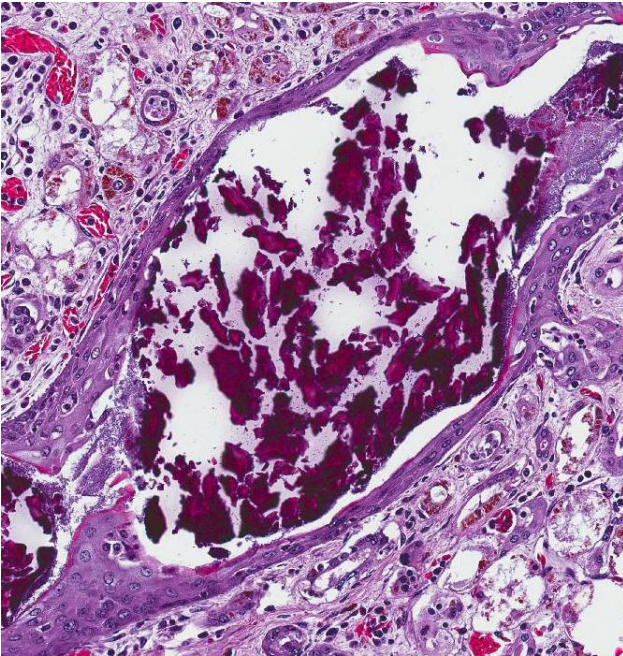


Kidney, toad. Granulomas contain numerous 3-5µm acid-fast bacilli (Ziehl-Nielsen, 100X) (Photo courtesy of: Wildlife Conservation Society, Wildlife Health Center, 2300 Southern Blvd., Bronx, NY 10460 <http://www.wcs.org>)

noted, as well as the presence of cellular debris in ectatic tubule lumina. Overall, participants

agreed this was an excellent case and a challenging description.

In general mycobacteria can be classified into three groups: 1) Organisms that produce tubercles such as *M. tuberculosis* and *M. bovis*, 2) organisms that result in lepromatous inflammation such as *M. leprae* and 3) the atypical or non-tuberculous mycobacteria that may be opportunistic or primary pathogens; included in the third group are the mycobacterial organisms that infected the toad in this case. Many of the agents such as *M. marinum*, which is often the agent seen in amphibian infections, are zoonotic and can be important human pathogens in immunosuppressed and even non-immunosuppressed individuals. The organisms can be transmitted through direct contact with the animals or indirectly through the water.⁷



Kidney, toad. Collecting ducts throughout the renal sections are filled with crystalline mineral (nephroliths). (HE, 110X)

Internal organs commonly infected in amphibian mycobacteriosis include the liver, spleen, kidney as seen in this case, and intestines. Mycobacterial lesions may be misdiagnosed as lymphosarcoma in cases of amphibian mycobacteriosis but should be suspected in amphibians with granulomatous, lymphocytic or pyogranulomatous nodular inflammation in internal organs. Treatment is often ineffective and requires culling of affected individuals.

Mycobacterial infections are not uncommon in captive amphibians and can infect a number of species. Infections are less common in reptiles but have been reported in snakes, lizards, turtles and crocodiles. Lesion locations in reptiles include the liver, lung, spleen, kidney, oral cavity, joints and subcutis. In snakes, lesions may be seen in the oral cavity and lungs; in lizards disease is more commonly reported to be disseminated; and in chelonians mycobacteriosis may include pulmonary, hepatic, plastron and skin lesions.⁶

Contributing Institution:

Wildlife Conservation Society

www.wcs.org

References:

1. Green DE. Pathology of Amphibia. In: Wright KM, Whitaker BR, eds. *Amphibian Medicine and Captive Husbandry*. Malabar, FL, USA: Krieger Publishing Company; 2001:401-485.
2. Green DE, Harshbarger JC. Spontaneous neoplasia in amphibian. In: Wright KM, Whitaker BR, eds. *Amphibian Medicine and Captive Husbandry*. Malabar, FL, USA: Krieger Publishing Company; 2001:335-400.
3. Kawasumi T, Kudo T, UNE Y. Spontaneous nephroblastoma in a Japanese giant salamander (*Andrias japonicus*). *J Vet Med Sci*. 2012;74:673-675.
4. Maitra A. Diseases of Infancy and Childhood. In: Kumar V, Abbas AK, Fausto N, Aster JC, eds. *Pathologic Basis of Disease, Eighth Edition*. Philadelphia, PA, USA: Saunders Elsevier; 2010:447-483.
5. Meuten DJ. Tumors of the Urinary System. In: Meuten DJ, ed. *Tumors in Domestic Animals, Fourth Edition*. Ames, IA, USA: Blackwell Publishing; 2002:509-546.
6. Reavill DR, Schmidt RE. Mycobacterial lesions in fish, amphibians, reptiles, rodents, lagomorphs, and ferrets with reference to animal models. *Vet Clin Exot Anim*. 2012;15:25-40.

7. Bercovier H, Vincent V. Mycobacterial infections in domestic and wild animals due to *Mycobacterium marinum*, *M. fortuitum*, *M. chelonae*, *M. porcinum*, *M. farcinogenes*, *M. smegmatis*, *M. scrofulaceum*, *M. xenopi*, *M. kansasii*, *M. simiae* and *M. genavense*. Rev sci tech Off Epiz. 2001;20(1):265-290.

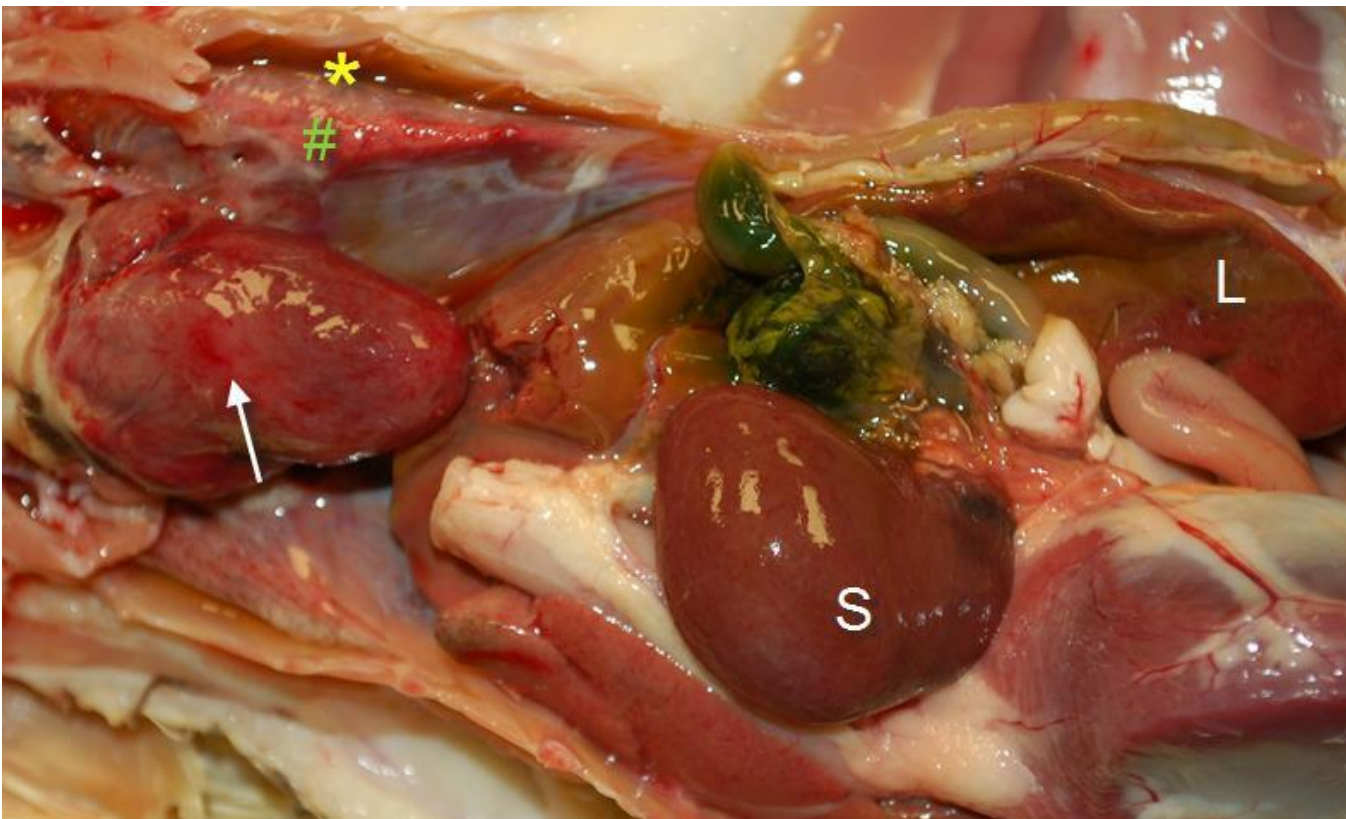
CASE IV: A (JPC 4066233).

Signalment: Six week-old, Welsh Harlequin Ducks (*Anas platyrhynchos domesticus*).

History: A group of eleven Welsh Harlequin ducklings hatched in Northern Ontario in late June were housed indoors until approximately 4-5 weeks of age, and then were allowed access to an outdoor enclosure during the day. Other than green watery diarrhea, the ducks were clinically normal. However in mid-August, at six weeks of age, one of the ducks became inappetent and

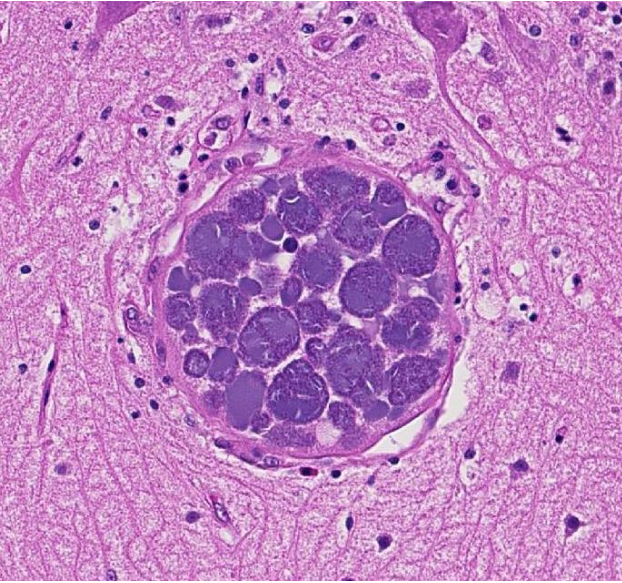
lethargic, exhibited labored breathing, and died overnight. In the following two days, three more ducks died, the last two exhibiting similar clinical signs as the first. In total, the owner lost 5 of the 11 ducks; two recovered following intensive supportive care. Chickens were also maintained on the same property but housed in a separate enclosure and suffered no morbidity or mortality. Pens were cleaned every 1-2 days; feed and water were always available and refreshed daily.

Gross Pathology: Two ducks were received for postmortem examination. Both ducks had similar findings and were in good body condition with good muscle mass, external and internal fat stores but the tissues were generally pale. There was mild generalized subcutaneous edema and focal hemorrhage in the caudal pectoral muscle. The lungs were very edematous, pink/purple, and pleural spaces of the lateral margins of the lungs contained small amounts of clear fluid. There was focal hemorrhage on the epicardium. The spleen was very enlarged and soft. The liver was



There is focal hemorrhage on the epicardium (arrow). The spleen (S) was very enlarged and soft. The liver (L) was enlarged, tan/red and soft. There was mild generalized subcutaneous edema (*) and focal hemorrhage in the caudal pectoral muscle (#). (Photo courtesy of: Animal Health Laboratory, University of Guelph, Guelph, Ontario, Canada <http://ahl.uoguelph.ca>)

enlarged, tan/red and soft. The esophagus and proventriculus were empty; the gizzard contained grit and the intestine contained only a small amount of bile. Kidneys and bone marrow were pale.



Cerebellum, duck: Scattered throughout all sections of the brain, endothelial cells are swollen up to 100um by megaloschizonts with numerous cytomeres. There is mild edema and gliosis of adjacent neuropil. (HE, 188X)

Laboratory Results: No bacterial pathogens were isolated from Duck A spleen and Duck B heart blood. RT-PCR testing of lung/trachea and cecal tonsil pools for Avian influenza virus (AIV) and avian paramyxovirus-1 (APMV-1), and pooled brain/kidney for West Nile virus (WNV) and Eastern equine encephalitis virus (EEEV) were negative.

Histopathologic Description: BRAIN (Slide A): Variable numbers of large protozoal megaloschizonts containing enlarged host nuclei and numerous cytomeres and infrequently degenerate/ruptured megaloschizonts are present in the brain, occasionally within distended endothelial cells filling capillary lumens, infrequently rimmed by a small amount of hemorrhage with a few mononuclear cells and granulocytes in the surrounding parenchyma. The ruptured megaloschizonts are often surrounded by larger numbers of inflammatory cells, including multinucleated cells and released merozoites. Numerous small vessels are

infiltrated and surrounded by narrow cuffs of mononuclear cells and granulocytes. Hypertrophied astrocytes and reactive microglia are present within the parenchyma surrounding affected vessels, and also in close proximity to infrequent small foci of acute parenchymal necrosis.

LIVER (Tissue not provided): Within the liver, there is widespread multifocal to coalescent acute hepatic necrosis with mild to marked hemorrhage and hepatic dissociation. Sinusoids and vessels contain numerous red blood cells with eccentric compressed nuclei and round cytoplasmic structures morphologically compatible with protozoal gametocytes (Figure 2). Kupffer cells are enlarged and contain pale orange pigment, cellular debris and occasionally phagocytized erythrocytes.

Contributor's Morphologic Diagnosis:

Brain: Mild encephalitis with vasculitis and perivascularitis, mild multifocal necrosis with numerous intraparenchymal megaloschizonts

Liver: Marked acute multifocal to coalescent hepatic necrosis with numerous intraerythrocytic gametocytes and mild erythrophagocytosis

Contributor's Comment: The megaloschizonts with the enlarged host nuclei found only in the brain in these ducks are characteristic of *Leukocytozoon* spp.; *Leukocytozoon simondii* is the species that infects ducks and geese. The vector for *L. simondii* is the blackfly (*Simuliidae* spp.) and infective sporozoites carried in the salivary gland are introduced into the circulation of the bird at the time of the insect bite.^{1,3} The sporozoites travel to the liver, enter hepatocytes and develop into first-generation meronts. These enlarge, go through multiple rounds of nuclear division, and form sections called cytomeres which are multinucleated. These further develop into uninucleate merozoites and multinucleate syncytia.^{1,3} Some of the merozoites re-enter hepatocytes for a second round of merogony, while some merozoites and syncytia enter the circulation. The merozoites penetrate erythrocytes and develop into round gametocytes, and the intravascular syncytia

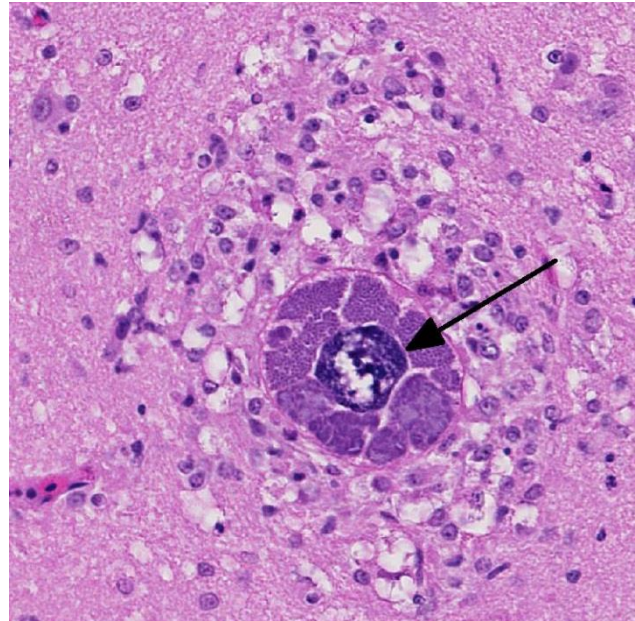
travel to various organs where they are phagocytized by reticuloendothelial cells, including macrophages, and develop into second generation meronts called megalomeronts or megaloschizonts because of their large size (100 to 200 μm).^{1,3} A megaloschizont characteristically contains a markedly enlarged centrally located host nucleus and numerous cytomeres.¹ *L. simondi* megaloschizonts can be found in many tissues including brain, lung, spleen and heart.¹ When the megaloschizonts mature, they release large numbers of tiny merozoites that enter erythrocytes or leukocytes and develop into round or fusiform gametocytes.^{1,3} The infective gametocytes are ingested by a biting fly, undergo sexual reproduction, produce a zygote that becomes a motile ookinete. Upon entering the small intestinal epithelium, the ookinete transforms into an oocyst, undergoes sporogony to produce sporozoites which then relocate to the salivary gland of the biting fly to complete the life cycle.^{1,3}

The principal clinical effect of *Leucocytozoon* spp. infection is intravascular hemolytic anemia, thought to relate to the release of an antierythrocyte factor produced either by the meronts or their host cells rather than the primary mechanical destruction of the red blood cells by the protozoa, since the lowest hematocrit values occur before the parasitemic spike.⁴

In discussions with the referring veterinarian, the black fly population in the area appeared to be very low in early August, but in susceptible ducks, very limited exposure to infected blackflies is sufficient for the intravascular introduction of sufficient sporozoites to cause mortality. The prepatent period for *L. simondi* infection is approximately two weeks, so this fits well with the length of time from the initial release of the ducks into the outside enclosure and the onset of mortality. The producer has been advised that leukocytozoonosis is one disease that will have to be managed if they wish to continue to raise susceptible ducks in Northern Ontario.

JPC Diagnosis: Brain: Intraendothelial hemoprotezoal megaloschizonts, multifocal,

moderate, with intraerythrocytic gametocytes and minimal perivascular inflammation.

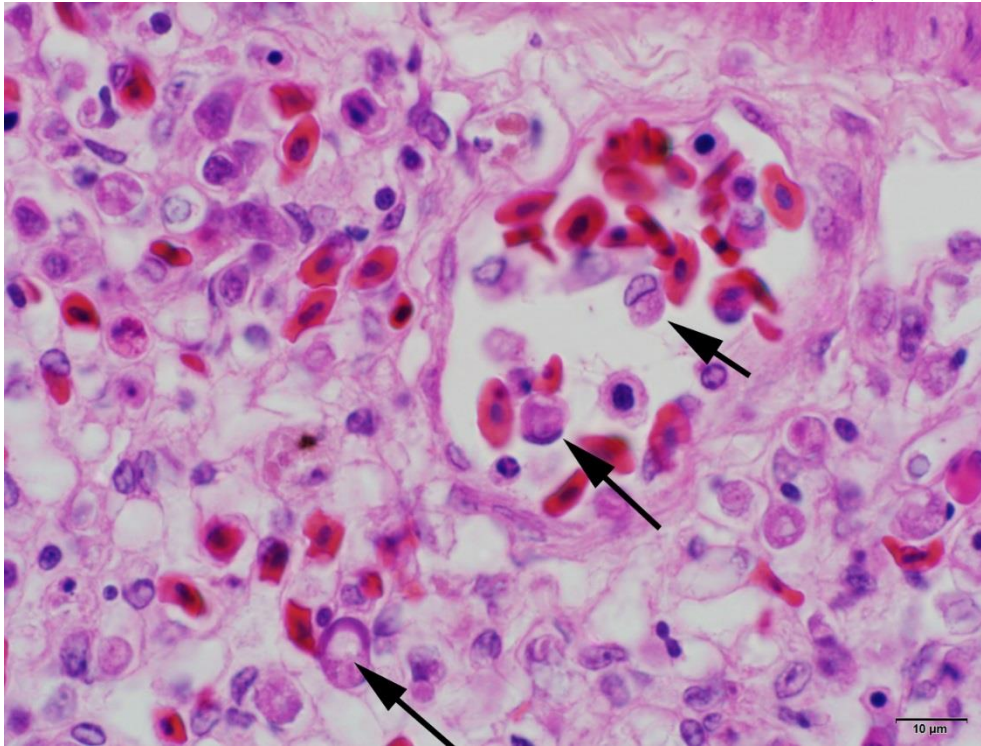


Cerebellum, duck: Occasional parasitized endothelial cells exhibit hypertrophic nuclei surrounded by cytomeres. (HE, 188X)

Conference Comment: The histologic features discussed during the conference were very similar to the contributor's histologic description. Slide variability was noted with some slides containing sections of pineal gland. Participants also discussed the ecology of avian hemoparasites and how it relates to host pathology. Infection with hemoparasites in the reservoir host is very common and often an incidental finding, resulting in minimal pathology. However, when an aberrant host is infected, the megaloschizonts can cause marked tissue damage, often in the liver and spleen, resulting in clinical signs and death in severe cases.

Avian blood parasites include three *Haemosporidia* genera which are closely related: *Plasmodium*, *Haemoproteus* and *Leucocytozoon*. All are transmitted by a variety of biting insect vectors, which vary depending on the specific parasite, geographic location and distribution. The majority of bird species can become infected, but some species are more susceptible to infection than others (i.e. waterfowl, wild turkeys and penguins are commonly infected, but

infection is less common in migratory shorebirds).



1Cerebrum, duck: Erythrocytes contain clear vacuoles (gametocytes) which displace the nucleus to the periphery. (HE, 400X). (Photo courtesy of: Animal Health Laboratory, University of Guelph, Guelph, Ontario, Canada <http://ahl.uoguelph.ca>)

In general, *Plasmodium* and *Leucocytozoon* species are capable of causing more severe disease, and species of *Haemoproteus* are considered less pathogenic. Hepatomegaly and splenomegaly may be seen in infection with all three genera, but *Plasmodium* and *Haemoproteus* infection results in production of hemozoin pigment from digestion of hemoglobin, which can be seen in the liver, spleen and other organs, and may impart a black or brown appearance to the organs grossly. *Leucocytozoon* infection does not result in production of hemozoin pigment, so organs will not have the dark discoloration. A presumptive diagnosis can be made based on microscopic examination of a blood film, and the appearance of the parasite in red blood cells (RBC). *Leucocytozoon* results in the most dramatic change in RBC structure, with enlargement and elongation of RBCs and formation of hornlike extensions at each end of the cells; splitting of the nucleus may also be seen. With *Haemoproteus* and *Plasmodium*, less

dramatic changes are seen and include slight enlargement of the cells, lateral displacement of the nucleus, hemozoin pigment, and the presence of the small schizonts or gametocyte nuclei.² Because the different hemoprotozoa can cause similar lesions, both grossly and histologically, PCR is often necessary to reach a precise etiologic diagnosis.⁵

There are many species of *Leucocytozoon*, but not all are pathogenic. The species of *Leucocytozoon* which are pathogenic to wild birds include *L. simondi* (waterfowl), *L. marchouxi* (doves and pigeons) and *L. toddi* (raptors). The species which may cause disease in domestic birds include *L. simondi* (waterfowl; U.S., Canada, Europe), *L.*

smithi (turkeys; U.S., Canada), *L. macleani* (chickens; S.E. Asia), *L. struthionis* (ostriches; S. Africa), *L. schoutendeni* (chickens; sub-Saharan Africa, S.E. Asia) and *L. caulleryi* (chickens; south and S.E. Asia).¹

In *Leucocytozoon* infection, gross lesions seen in infected birds include splenomegaly, hepatomegaly, tissue pallor and thinning of the blood. Histologically, capillaries may be distended by gametocytes with absence of host tissue reaction. The large megaloschizonts, which are often associated with small vessels, typically elicit a mononuclear inflammatory reaction but the meronts may or may not be associated with an inflammatory response. After the megaloschizonts rupture they may be filled with eosinophilic debris and mononuclear cells. Severe centrilobular hepatic necrosis may be seen along with periportal hepatitis and pigment laden macrophages / Kupffer cells. The enlarged spleen is congested, with loss of normal

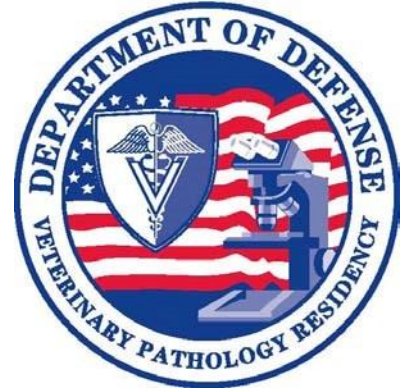
architecture, and contains large macrophages distended with pigment and cellular debris. Lymphocytic and histiocytic infiltration may be seen in other organs such as the lung and myocardium.¹

Contributing Institution:

Animal Health Laboratory, University of Guelph, Guelph, Ontario, Canada
<http://ahl.uoguelph.ca>

References:

1. Forrester DJ, Greiner EC. Leucocytozoonosis. In: Atkinson CT, Thomas NJ, Hundter DB, eds. *Parasitic Diseases of Wild Birds*. Ames, Iowa: Blackwell Publishing; 2008:54-107.
2. Friend M, Franson JC, Ciganovich EA. *Field manual of wildlife diseases, general field procedures and diseases of birds*. Washington DC: U.S. Department of the Interior, U.S. Geological survey; 1999:193-200.
3. Gardiner CH, Fayer R, Dubey JP. Leucocytozoon. In: *An Atlas of Protozoan Parasites in Animal Tissue*. USDA Agricultural Research Service. Agriculture Handbook # 651; 1988:72.
4. Kocan R. Anemia and Mechanism of Erythrocyte Destruction in Ducks with Acute Leukocytozoon Infections. *J Protozol.* 1968;15(3):455-462.
5. Schmidt RE, Reavill DR, Phalen DN. *Pathology of pet and aviary birds*. Ames, IA: Wiley Blackwell; 2015:109-110.



WEDNESDAY SLIDE CONFERENCE 2015-2016

Conference 7

9 November 2015

CASE I: 2014 #1 (JPC 4066676).

Signalment: 4-year-old, castrated male, crioulo horse (*Equus caballus*).



In this herd, affected animals displayed a 14-day course of ataxia, incoordination, and wobbling affecting the hindlimbs. (Photo courtesy of: Faculdade de Veterinária – UFRGS, Setor de Patologia Veterinária Av. Bento Gonçalves 909091540-000 Porto Alegre RS, Brazil.)

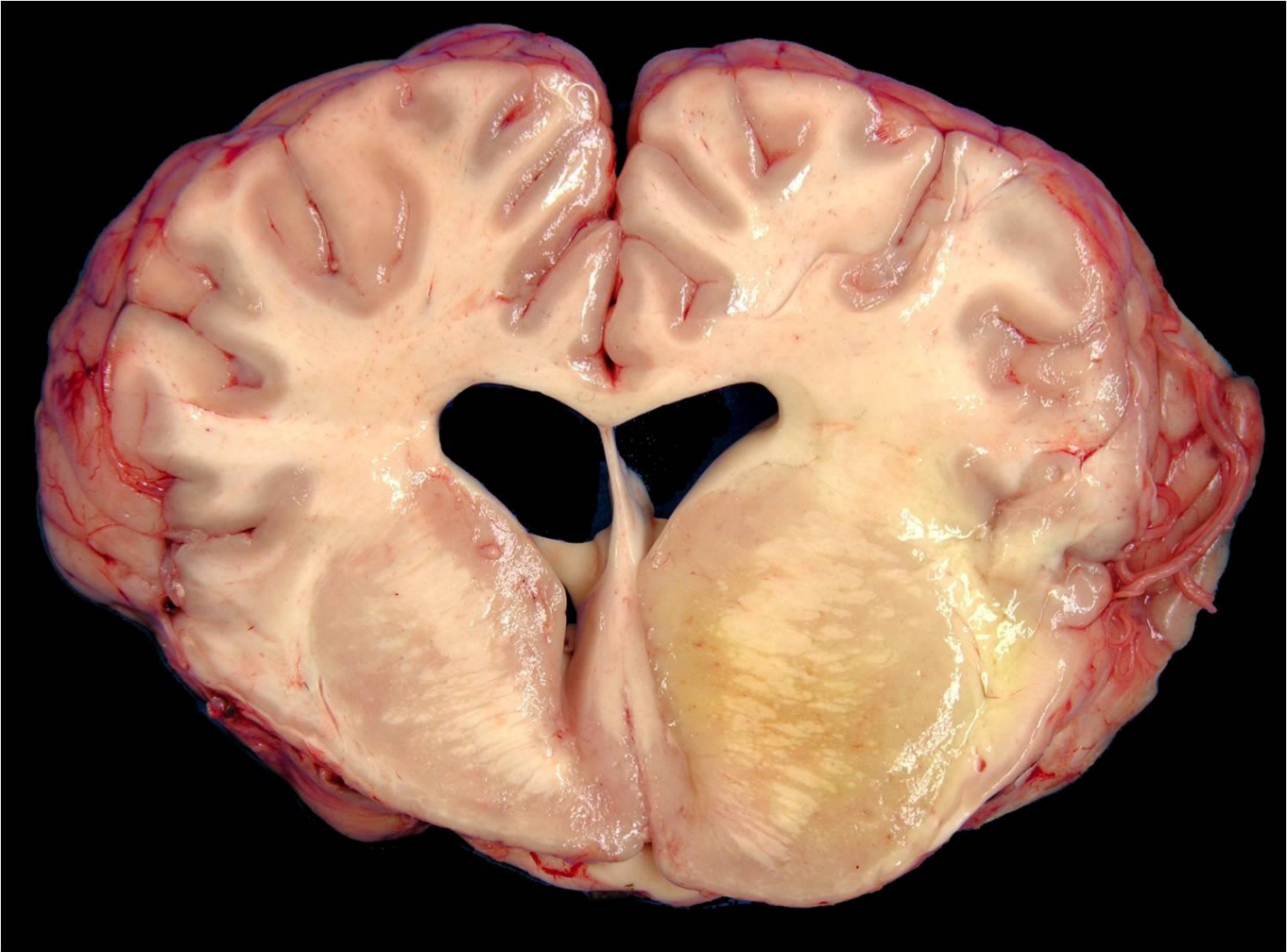
History: During the summer of 2003, approximately 200 horses on 3 bordering farms, as well as 10 mares from a fourth farm that were sent to one of the 3 farms for breeding, were

maintained near the banks of a river. Farm employees reported that capybaras (*Hydrochoerus hydrochaeris*) were affected by a similar disease and died at the time horses were affected

but we were unable to confirm this information. However, we could confirm that several horses in one of the farms had been treated with a common needle early in the outbreak.

Approximately one month after their arrival in the farm, many of the horses presented with marked weight loss, muscle atrophy, and incoordination. Within 2 to 3 months, and extending through the rest of the year and into 2004, approximately 100 horses died. We did evaluate clinically and necropsied 15 of these horses, 22 of

which presented a chronic wasting form of the disease. The horse of this report is one of a group in which the onset of disease was insidious and



There is asymmetrical necrosis and gelatinous edema within the thalamus. (Photo courtesy of: Faculdade de Veterinária – UFRGS, Setor de Patologia Veterinária, Av. Bento Gonçalves 909091540-000 Porto Alegre RS, Brazil. <http://www.ufrgs.br/patologia/>)

characterized by progressive weight loss (despite voracious appetite), lethargy, incoordination, gait instability (wobbling) involving the pelvic limbs (mal das cadeiras = disease of the hip), atrophy of heavy muscles of the hindquarters, difficulty in rising, muscle weakness, pallor of mucous membranes, subcutaneous edema of the ventral portions of the trunk and limbs. Additionally to above described signs that ran a course of 14 days, encephalic neurologic clinical signs including marked ataxia (Fig. 1), blindness, circling, hyperexcitability, somnolence, proprioceptive deficits, head tilt, and paddling movements were observed and ran a course of 20 days.

Gross Pathology: There were marked hindquarter muscle atrophy, splenomegaly, and lymphadenomegaly. Gross lesions in the brain

included asymmetric swelling of the cerebral hemispheres with flattening of gyri. The white matter of the parietal, temporal, and frontal lobes was unilaterally yellow, gelatinous, and friable due to severe edema and malacia. Similar lesions were observed in the basal nuclei, thalamus, and mesencephalon.

Laboratory Results: Hematologic findings included normocytic normochromic anemia, with leukocytosis due to lymphocytosis. Erythrophagocytosis and protozoa identified as *T. evansi* were seen in the peripheral blood. High titers against *T. evansi* (optical density, 1,422) were detected in the serum of this horse.

Histopathologic Description: Histologically, lymphoid organs had marked follicular hyperplasia, erythrophagocytosis, and hemosi-

derosis. In the liver there was moderate lymphoplasmacytic periportal hepatitis, Kupffer cell hypertrophy, and hemosiderosis.



Thalamus, horse. Even at very low magnification, blood vessels are highlighted by prominent perivascular cuffs. (HE, 5X)

The brain lesions affected mainly the white matter and were characterized by moderate to severe perivascular lymphoplasmacytic meningoencephalitis, edema and necrosis. Lymphocytes and plasma cells, often with intracytoplasmic Russell bodies (Mott cells), greatly expanded the Virchow-Robin spaces and extended into the surrounding neuropil. Lesions in the spinal cord tended to wane from cranial to caudal. Organisms of *T. evansi* were not detected in the HE stained sections of brain, but numerous *T. evansi* organisms or fragments of these organisms were detected in formalin-fixed, paraffin-embedded sections of the brain by immunohistochemistry through avidin-biotin-peroxidase complex immunoperoxidase method using rabbit anti-*T. evansi*, diluted 1:1000 as the primary antibody (the immunohistochemistry tests were performed at the Prairie Diagnostic Service, University of Saskatchewan, Western College of Veterinary Medicine). The parasites were observed in the perivascular spaces and in the neuropil.

Contributor's Morphologic Diagnosis:

Lymphoplasmacytic encephalitis, moderate to severe, 4-year-old, castrated male, crioulo, *Equus caballus*, horse.

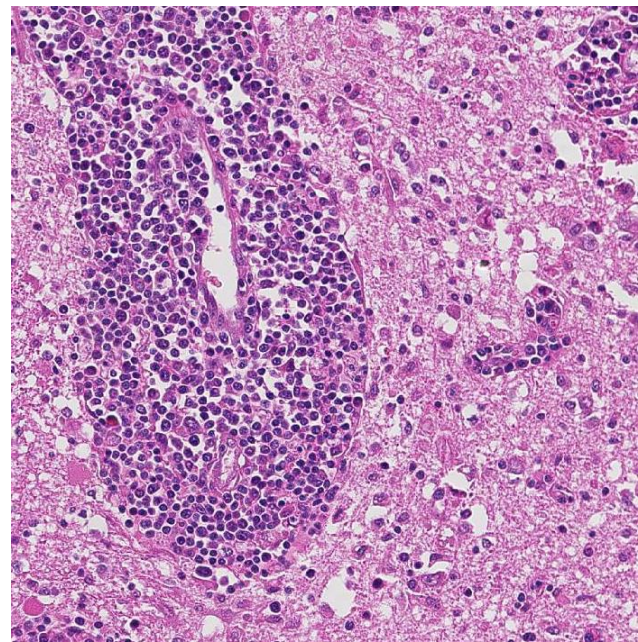
Etiologic diagnosis: Protozoal encephalitis

Etiology: *Trypanosoma evansi*

Name of the condition: Trypanosomiasis

Contributor's Comment: *Trypanosoma evansi* is a flagellate protozoan parasite that causes disease in several mammalian species. The hind limb weakness of equine trypanosomiasis gave rise to denomination "mal das cadeiras" or "mal de caderas" respectively in Brazil and in many of Spanish speaking countries of South America. Other denominations for the same disease are murrina (Panama) and surra (Asia). In South America, capybaras (*Hydrochoerus hydrochaeris*) coatis (*Nasua nasua*) small marsupials (e.g., *Monodelphis* spp.), and armadillos (*Dasypus* spp.) are possible reservoirs for *T. evansi*. Unlike the African *Trypanosoma* species that cause nagana in animals and "sleeping sickness" in human beings, *T. evansi* does not require development stages within its the vector, and is mechanically transmitted through the bite of insects, especially tabanids and stomoxids, by the South American vampire bat (*Desmodus rotundus*) and, possibly, by ticks.^{3,6}

Trypanosomiasis in horses is characterized by intermittent fever, anemia, progressive



Thalamus, horse. Virchow-Robins space is expanded by up to 15 layers of lymphocytes with fewer histiocytes and rare plasma cells (HE, 144X).

weakness, loss of body condition, and unstable gait.²¹ Neurologic signs have been described occasionally in horses in the terminal phase of natural infection by *T. evansi*.²¹ Trypanosomiasis by *T. evansi* is enzootic in horses from the Midwestern Brazil, mainly the Pantanal region.^{3,4,6,9,22, 23}

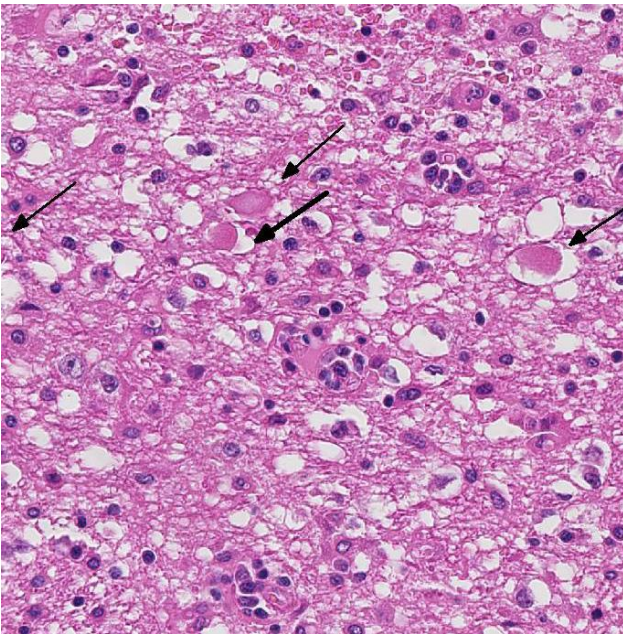
T. evansi induces a wasting disease with a protracted clinical course²⁸ associated with anemia and instability of pelvic limbs in horses, camels, and dogs.⁴ Natural infection by *T. evansi* rarely is recognized as a cause of encephalitis in horses.²¹ Neurologic signs have been reported in cattle²⁷ and hog deer²⁶ naturally infected by *T. evansi*; however, the histopathologic changes in the brain of these species were not fully described. Mild lymphoplasmacytic meningoencephalitis was reported in horses, donkeys, dogs, goats,² coatis (*Nasua nasua*),⁹ and buffalo²⁵ experimentally infected by *T. evansi*. The horse of this report and the other necropsied horses in the current outbreak had a severe lymphoplasmacytic meningoencephalitis with marked edema and variable necrosis. The lesions in the brain of these horses resembled those described in horses infected by *Trypanosoma brucei brucei*,^{14,17} which causes a disease known as nagana, and those described for human trypanosomiasis caused by *Trypanosoma brucei gambiense* and *Trypanosoma brucei rhodesiense*.^{13,16}

T. evansi antigen was detected by immunohistochemistry in the brain of 8 of 9 horses affected in the outbreak, including the brain of the horse of this report. The protozoa were detected within blood vessels, in perivascular spaces, and in the brain parenchyma. This suggests that trypanosomes invaded the brain parenchyma and were responsible for the lesions observed here. The pathogenesis of cerebral necrosis was not elucidated since thrombosis was absent. Neither the mechanism by which trypanosomes entered the neuroparenchyma was determined. The introduction of *T. evansi* into a naïve population, as was the case here, could explain the development of fatal trypanosomiasis with severe encephalitis. The reason for the sudden

appearance of the disease in this region of Brazil, where it was previously unreported, is unknown, but it could have been introduced by transportation of infected horses or migration of capybaras from regions where trypanosomiasis is enzootic in this country. A factor that may have contributed to the development of severe encephalitis was that these affected horses were treated with subtherapeutic doses of diminazene aceturate and other antitrypanosomal drugs.^{19,20} Several studies have demonstrated that the use of subtherapeutic doses of diminazene aceturate may prolong survival of horses experimentally infected by *T. brucei* spp. however this faulty procedure results in subsequent invasion of the central nervous system by the organisms which induce necrotizing encephalitis.^{8,10,11,15,18,24} Diminazene aceturate clears trypanosomes from tissues except those localized on the central nervous system,¹⁹ because the drug does not cross the blood-brain barrier^{11,17} allowing trypanosomes harbored in the central nervous system to survive antitrypanosomal therapy; a change in these organisms surface glycoproteins favor recurrent parasitemias by variants of the organism.²⁰

How trypanosomes penetrate the blood-brain barrier is not clear, but several mechanisms have been proposed: (i) entrance through sites where the blood-brain barrier is incomplete, such as sensory ganglia and circumventricular organs;¹⁶ (ii) increase in vascular permeability due deposition of immune complexes in the choroid plexus; and (iii) opening of intercellular tight junctions of the ependymal lining of the ventricular system by toxins released by the parasite.¹² It is believed that invasion of the central nervous system by trypanosomes occurs where the blood-brain barrier has been disrupted, either directly by the parasites or by release of chemical mediators, such as cytokines and proteases.^{7,13,15} An interaction between the trypanosomes and the host response could promote tissue damage and facilitate the entry of parasites into the central nervous system.¹³ This scenario is supported by the histopathologic changes and immunohistochemistry observe in the horse of this report. Trypanosomiasis due to

T. evansi should be considered in the differential diagnosis of encephalitis in horses in regions where the disease is enzootic.



Thalamus, horse. Within affected white matter, there are frequent swollen axons (spheroids) (arrows). (HE, 168X)

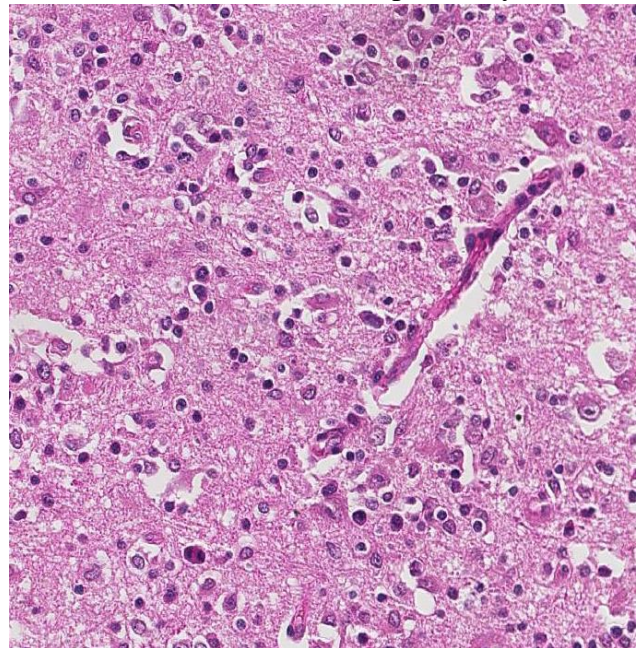
The list of differentials should include equine herpesvirus type 1 myeloencephalopathy, Eastern equine encephalitis, Western equine encephalitis, Venezuelan equine encephalitis, equine protozoal myeloencephalitis, West Nile virus infection, and rabies. The nature and distribution of lesions in the central nervous system of horses with naturally occurring *T. evansi* infection should help to distinguish trypanosomiasis from viral or other protozoal infections.

JPC Diagnosis: Telencephalon: Meningo-encephalitis, lymphoplasmacytic and histiocytic, diffuse, severe with vasculitis, spongiosis and gliosis.

Conference Comment: Conference participants were struck by the marked degree of perivascular cuffing and described the presence of edema, lymphocytes, and macrophages (Gitter cells) expanding Virchow-Robin spaces. They also described lymphocytic infiltration, gliosis, gemistocytes and neuronal degeneration and necrosis in the surrounding neuropil. The

meninges were also expanded by a lymphoplasmacytic infiltrate and edema. Some sections contained areas of vascular damage with the presence of cellular debris, protein and hemorrhage in vessel walls and therefore some participants also described vasculitis. Multifocally, there are hypertrophied endothelial cells in the less affected vessels.

T. evansi is the causative agent of “surra,” which originated in Africa, but is also present across the Middle East, Asia, in Central and South America and has also been reported in Russia. It is thought to derive from genetic modification (a deletion) in *T. brucei*. It has a wide host range, indeed the widest among salvarian trypanosomes, including camels, dogs, horses, deer, llamas, cattle, sheep, goats, cats, pigs, and elephants among others. Disease is particularly devastating in camels and horses, often proving fatal in the absence of treatment. Clinical signs can vary dramatically between species and even between individuals of the same species. Infection in camels can occur acutely as in horses, but often has a more protracted course with signs such as intermittent fever, weakness, anorexia, weight loss, abortion, anemia, edema and petechial and ecchymotic hemorrhages. All age groups are affected and the course of the disease can be up to 2-3 years. The



Thalamus, horse. There is marked gliosis in affected areas within the grey matter. (HE, 168X).

urine of infected camels apparently has a specific odor, which may allow diagnosis of the disease. Dogs are also highly susceptible to infection and death may result at 1-4 weeks post infection. i

Trypanosomes have developed mechanisms which allow them to both evade the immune system and cause immunosuppression. This includes antigenic variation in main membrane surface glycoproteins, variant surface glycoprotein (VSG), which forces the host to constantly redevelop their humoral response. The immunosuppressive effects of *T. evansi* infection are not fully understood but may involve modulation of macrophage activity, decreased responsiveness of lymphocytes, and/or changes in the CD4:CD8 lymphocyte ratio; they may even be capable of eliminating memory B cells. The complex immunosuppressive or immunomodulatory mechanisms of *T. evansi* have created significant barriers in developing effective vaccines and maintaining effective treatments.⁵

Contributing Institution:

Setor de Patologia Veterinária, UFRGS
<http://www.ufrgs.br/patologia/>

References:

1. Camargo RE, Uzcanga GL, Bubis J. Isolation of two antigens from *Trypanosoma evansi* that are partially responsible for its cross-reactivity with *Trypanosoma vivax*. *Vet Parasitol.* 2004;123:67-81.
2. Dargantes AP, Campbell RSF, Copeman DB, et al. Experimental *Trypanosoma evansi* infection in the goat. II. Pathology. *J Comp Pathol.* 2005;133:267-276.
3. Davila AMR, Silva RAMS. Animal trypanosomiasis in South America. Current status, partnership, and information technology. *Ann N Y Acad Sci.* 2000;916: 199-212.
4. Davila AMR, Souza SS, Campos C, Silva RA. The seroprevalence of equine trypanosomiasis in the Pantanal. *Mem Inst Oswaldo Cruz* 1999;94:199-202.
5. Desquesnes M, Holzmuller P, Lai DH, Dargantes A, Lun ZR, Jittaplapong S. *Trypanosoma evansi* and surra: a review and perspectives on origin, history, distribution, taxonomy, morphology, hosts, and pathogenic effects. *Biomed Res Int.* 2013;194176:1-22.
6. Franke CR, Greiner M, Mehlitz D. Investigations on naturally occurring *Trypanosoma evansi* infections in horses, cattle, dogs and capybaras (*Hydrochaeris hydrochaeris*) in Pantanal de Poconé (Mato Grosso, Brazil). *Acta Trop.* 1994;58:159-69.
7. Girard M, Bisser S, Courtioux B, Vermot-Desraches C, Bouteille B, Wijdenes J, Preud'homme JL, Jauberteau MO. In vitro induction of microglial and endothelial cell apoptosis by cerebrospinal fluids from patients with human African trypanosomiasis. *Int J Parasitol.* 2003;33:713-720.
8. Grab DJ, Nikolskaia O, Kim YV, Lonsdale-Eccles JD, Ito S, Hara T, Fukuma T, Nyarko E, Kim KJ, Stins MF, Delannoy MJ, Rodgers J, Kim KS. African trypanosome interactions with an in vitro model of the human blood-brain barrier. *J Parasitol.* 2004;90:970-979.
9. Herrera HM, Dávila AMR, Norek A, Abreu UG, Souza SS, D'Andrea PS, Jansen AM. Enzootiology of *Trypanosoma evansi* in Pantanal, Brazil. *Vet Parasitol.* 2004;125:263-275.
10. Keita M, Bouteille B, Enanga B, et al. *Trypanosoma brucei brucei*: a long-term model of human African trypanosomiasis in mice, meningoencephalitis, astrocytosis, and neurologic disorders. *Exp Parasitol.* 1997;85:183-192.
11. Kennedy PGE, Rodgers J, Jennings FW, et al. A substance P antagonist, RP-67, 580, ameliorates a mouse meningoencephalitic response to *Trypanosoma brucei brucei*. *Proc Natl Acad Sci USA* 1997;94:4167-4170.
12. Lambert PH, Berney M, Kazyumba G. Immune complexes in serum and in

- cerebrospinal fluid in African trypanosomiasis. Correlation with polyclonal B cell activation and with intracerebral immunoglobulin synthesis. *J Clin Invest.* 1981;67:77-85.
13. Lonsdale-Eccles JD, Grab DJ. Trypanosome hydrolases and the blood-brain barrier. *Trends Parasitol* 2002;18:17-19.
14. Losos GJ, Ikede BD. Review of pathology of diseases of domestic and laboratory animals caused by *Trypanosoma congolensis*, *T. vivax*, *T. brucei*, *T. rhodesiense* and *T. gambiense*. *Vet Pathol* 1972;9(Suppl):1-71.
15. Masocha W, Robertson B, Rottenberg ME, et al. Cerebral vessel laminins and IFN- γ define *Trypanosoma brucei brucei* penetration of blood-brain barrier. *J Clin Invest.* 2004;114:689-694.
16. Mhlanga JDM, Bentivoglio M, Kristensson K. Neurobiology of cerebral malaria and African sleeping sickness. *Brain Res Bull* 1997;44:579-589.
17. Moulton JE. Relapse after chemotherapy in goats experimentally infected with *Trypanosoma brucei*: pathological changes in central nervous system. *Vet Pathol.* 1986;23:21-28.
18. Ouwe-Missi-Oukem-Boyer O, Mezui-MeNdong J, Boda C, et al. The vervet monkey (*Chlorocebus ethiops*) as an experimental model for *Trypanosoma brucei gambiense* human African trypanosomiasis: a clinical, biological and pathological study. *Trans R Soc Trop Med Hyg.* 2005;100:427-436.
19. Rodrigues A, Figuera RA, Souza TM, et al. Surtos de tripanossomíase em eqüinos no Rio Grande do Sul: aspectos epidemiológicos, clínicos, hematológicos e patológicos. *Pesq Vet Bras.* 2005;25:239-249.
20. Rodrigues A, Figuera R. A., Souza TM, et al. Neuropathology of naturally occurring *Trypanosoma evansi* infection of horses. *Vet Pathol.* 2009;46:251-258.
21. Seiler RJ, Omar S, Jackson AR. Meningoencephalitis in naturally occurring *Trypanosoma evansi* infection (surra) of horses. *Vet Pathol.* 1981;18:120-122.
22. Silva RAMS, Herrera HM, Domingos LBS, et al. Pathogenesis of *Trypanosoma evansi* infection in dogs and horses: hematological and clinical aspects. *Ciência Rural* 1995;25:233-238.
23. Silva RAMS, Seidl A, Ramirez L, Dávila AMR. *Trypanosoma evansi* e *Trypanosoma vivax*: Biologia, Diagnóstico e Controle. Embrapa Pantanal, Corumbá, Brazil, 2002.
24. Sternberg JM, Rodgers J, Bradley B, Maclean L, Murray M, Kennedy P. Meningoencephalitic African trypanosomiasis: brain IL-10 and IL-6 are associated with protection from neuro-inflammatory pathology. *J Immunol.* 2005;167:81-89.
25. Sudarto MW, Tabel H, Haines DM. Immunohistochemical demonstration of *Trypanosoma evansi* in tissues of experimentally infected rats and a naturally infected water buffalo (*Bubalus bubalis*). *J Parasitol.* 1990;76:162-167.
26. Tuntasuvan D, Mimapan S, Sarataphan N, et al. Detection of *Trypanosoma evansi* in brains of the naturally infected hog deer by streptavidine-biotin immunohistochemistry. *Vet Parasitol.* 2000;87:223-230.
27. Tuntasuvan D, Sarataphan N, Nishikawa H. Cerebral trypanosomiasis in native cattle. *Vet Parasitol.* 1997;73:357-363.
28. Ventura RM, Takata CSA, Silva RAMS, et al. Molecular and morphological studies of Brazilian *Trypanosoma evansi* stocks: the total absence of kDNA in trypanosomes from both laboratory stocks and naturally infected domestic and wild mammals. *J Parasitol.* 2000;86:1289-1298.

CASE II: E 4992/14 (JPC 4067274).

Signalment: 5-year-old gelding horse (*Equus ferus caballus*).

History: A solitary, non-painful, superficial mass in the skin over the left scapula was recognized by the owner. Only minimal growth was apparent during the last six months.

Gross Pathology: One sample measuring 7.1 x 5.5 x 1.7 cm with a well demarcated mass of 5.2 x 4.5 x 1.7 cm was submitted for histopathological examination.

Laboratory Results: None

Histopathologic Description: Subcutis (per contributor, connective tissue and skeletal muscle): Expanding the subcutis and infiltrating, separating and surrounding collagen bundles and skeletal muscle fibers is a mostly unencapsulated, poorly circumscribed mass. It is composed of small nests of round cells with distinct cell borders and moderate amounts of amphophilic cytoplasm that occasionally contains small basophilic granules (mast cells). Nuclei are centrally located, mostly round with finely stippled chromatin and indistinct nucleoli. Mitotic rate is low with less than one mitotic figure in ten high power fields (400x). Mast cell islands are separated by abundant fibrovascular stroma with thick bundles of collagen and high numbers of variable sized eosinophilic granulomas. Granulomas are characterized by central accumulation of partly degenerated eosinophils and peripherally bordered by few macrophages, variable numbers of fibroblasts / fibrocytes, abundant collagen fibers and few lymphocytes and plasma cells. Occasionally central debris is mineralized (deposition of fine granular basophilic material) and collagen bundles are hyalinized (collagenolysis). Intermingled between mast cell islands and granulomas are high numbers of viable eosinophils and fewer extravasated erythrocytes. Rarely, vessel walls are severely thickened by edema and few migrating eosinophils.

Contributor's Morphologic Diagnosis:

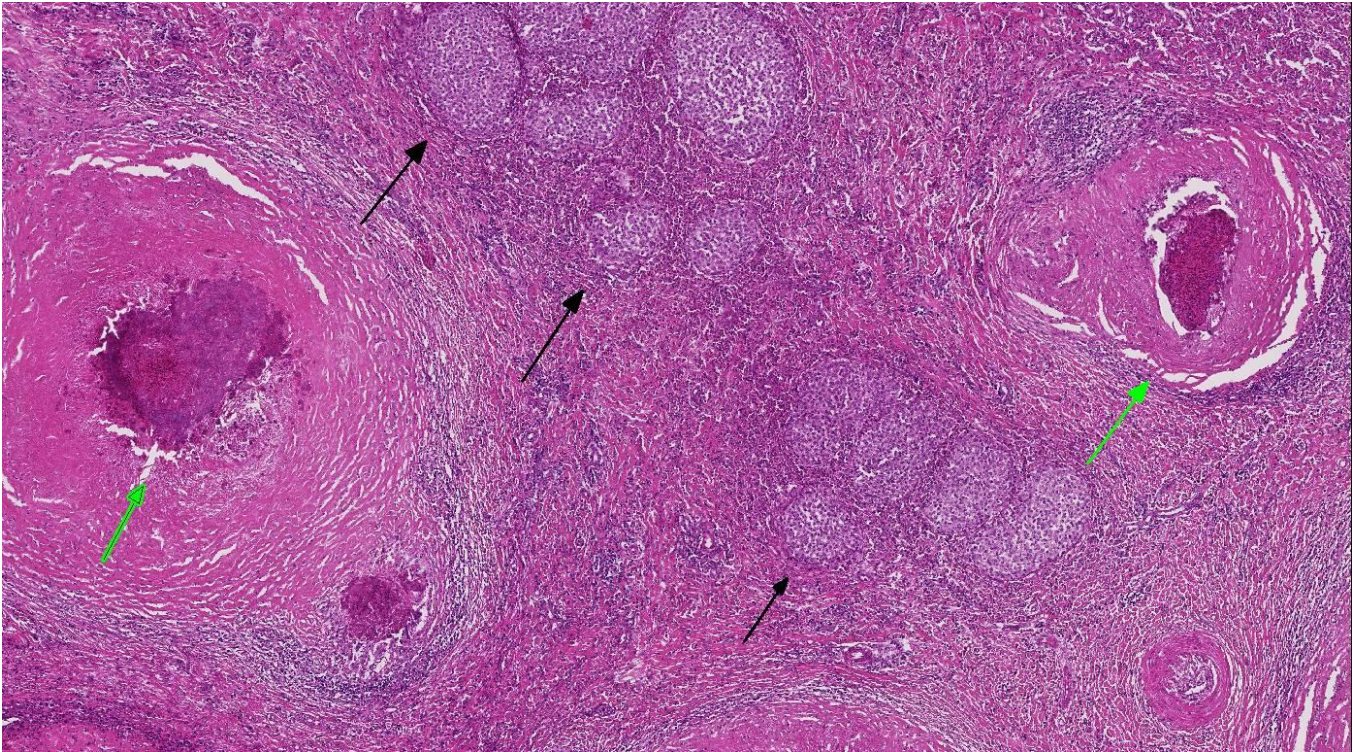
Subcutis (per contributor): Mast cell tumor



Skin, horse. A section of subcutis with attached underlying skeletal muscle is submitted for examination. (HE, 6X).

Contributor's Comment: Mast cell tumors are common dermal neoplasms especially of dogs and also cats, but occur in all domestic species including horses, ruminants, pigs, and ferrets. Depending on affected site and species the biological behavior is variable. Besides the skin, mast cell tumors occasionally arise in parenchymal organs like the spleen, liver, intestine, or as mast cell leucosis affecting the bone marrow. Additionally, metastasis from a cutaneous site may manifest in regional lymph nodes or generalize to diverse locations.

Mast cells are involved in numerous inflammatory conditions, especially type I hypersensitivity. After binding of IgE to membrane receptors and cross-linking of immunoglobulins on these receptors by specific antigens, degranulation of stored primary mediators and de novo synthesis of secondary mediators occurs. Granules contain, among others, primary mediators like biogenic amines (histamine, adenosine and serotonin), chemotactic factors (eosinophil chemotactic factor and neutrophil chemotactic factor) and multiple enzymes. Secondary mediators include leukotrienes, prostaglandins, platelet activating factor and several cytokines (TNF-alpha, IL-1, 3, 4, 5 and 6). In summary, these mediators generate edema, mucus secretion, smooth muscle spasm, and the recruitment of additional leukocytes, especially eosinophils.



Skin, horse. The neoplasm is composed of nests of neoplastic round cells (black arrows) and eosinophilic granulomas (green arrows) scattered throughout a dense collagenous stroma. (HE, 25X)

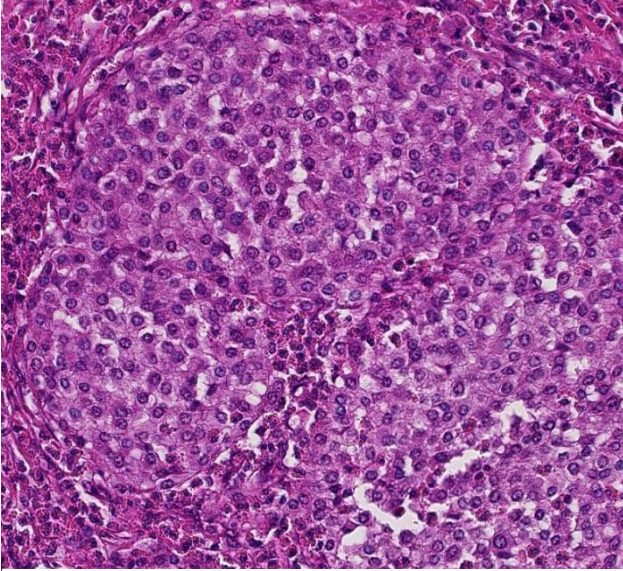
In the dog, mast cell tumors are common, accounting for 15 – 20 % of all skin tumors, being additional the most frequent malignant or potentially malignant cutaneous neoplasia.² Well differentiated neoplastic cutaneous mast cells typically form diffuse loose sheets or densely packed cords with intermingled mature eosinophils. They are never encapsulated or even well demarcated. Ulceration may occur in large tumors after traumatization due to pruritus triggered by mediators degranulated from mast cells. The proto-oncogene c-KIT has been discussed as a possible prognostic factor in canine cutaneous mast cell tumors with mutations or aberrant expression of c-KIT turned out to be poor predictors.¹³

In horses, mast cell tumors are relatively rare, covering only 3 – 7% of cutaneous and mucocutaneous neoplasms.¹¹ Commonly affected horses are male without an apparent breed predilection and the mean age is 7 - 11 years with a range from 1 to 30 years.^{1, 5, 6} In a recent large study Arabians were affected more frequently.¹ Tumors typically present as solitary immovable nodules on the head, trunk, neck, and limbs,

where they are often found close to joints.¹¹ The tumors may be hyperpigmented, alopecic or ulcerated.³ Nevertheless, most tumors are neither painful nor pruritic.³ Usually, mast cell tumors in the horse behave benign and excision is curative as recurrence is uncommon.⁵

Histologically, cutaneous mast cell tumors in horses often differ from their counterparts in the dog. Foci of necrosis, severe eosinophilic infiltration with subsequent collagenolysis, reactive fibrosis and dystrophic mineralization are often present. In this respect mast cell tumors may resemble equine collagenolytic granulomas or verminous dermatitis due to onchocerciasis or habronemiasis.² Typically, neoplastic mast cells are well-differentiated and arranged in multifocal small nests or coalescing nodules.¹¹ Malignant tumors are rare, presenting with loss of cellular differentiation and high mitotic index.⁸ Local but not visceral metastasis has been documented.^{8, 9} In contrast to canine mast cell tumors, neither changed c-KIT staining pattern nor histologic features were associated with an unfavorable clinical course.¹

JPC Diagnosis: Subcutis and skeletal muscle:
Mast cell tumor.

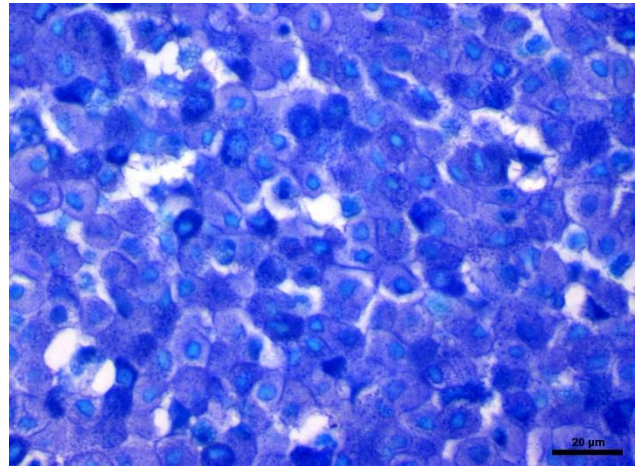


Skin, horse. Neoplastic mast cells have abundant poorly granular cytoplasm with centrally-placed nuclei (HE, 196).

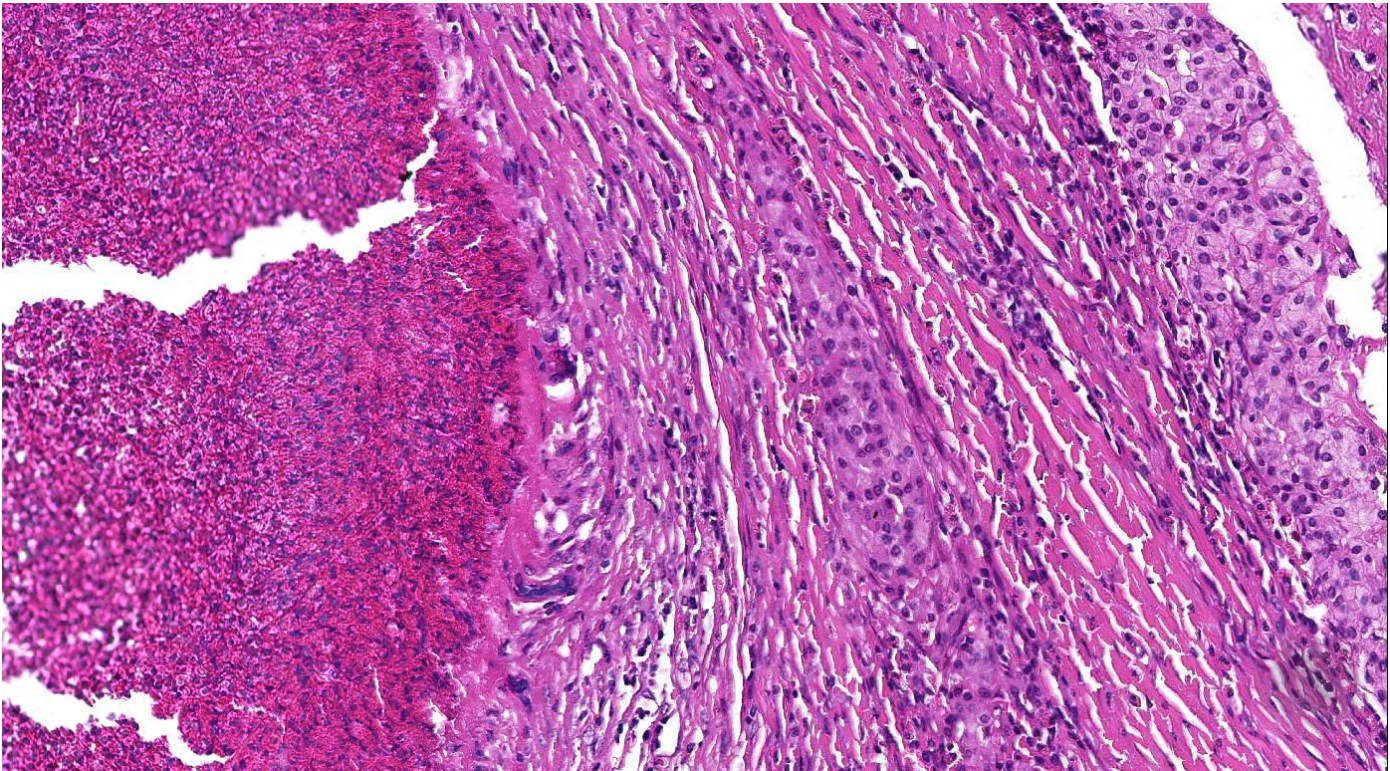
Conference Comment: This was a challenging slide for many conference participants with the histologic description largely focusing on the presence of eosinophilic granulomas. Other differential diagnosis considered for this lesion included equine nodular collagenolytic granuloma, cutaneous habronemiasis, cutaneous pythiosis and multisystemic eosinophilic epitheliotropic disease. At sub gross the eosinophilic granulomas were the most prominent feature, and due to the paucity and/or inconspicuous nature of the equine mast cell granules the cells were easily overlooked and/or misinterpreted.

In canine mast cell tumors, the proto-oncogene *c-kit* encodes for the transmembrane receptor tyrosine kinase (RTK) KIT, which normally plays a role in transcription of genes that control mast cell growth and survival, but also plays a role in tumor development in some tumors. A percentage of canine mast cell tumors demonstrate mutations in *c-kit*, including internal tandem duplication (ITD) mutations in exon 11, which result in activation of KIT in the absence of ligand binding, as well as point mutations in *c-kit* extracellular domains at exons 8 and 9.

Specific mutations in the gene that encodes the KIT RTK results in constitutive activation of the RTK (via tyrosine phosphorylation) and cell proliferation in the absence of growth factor stimulation. In general tumors with ITD mutations in *c-kit* exon 11 are known to behave more aggressively.⁷ However, the presence of these specific mutations also results in a more favorable response to treatment with tyrosine kinase inhibitors (TKIs) as compared to mast cell tumors without these specific mutations. Additionally, it has also been demonstrated that *c-kit* mutations are conserved between the primary tumor and lymph node metastasis, indicating that both can be used for mutational testing to select patients that will respond to favorably to TKIs.⁴ Mutations in KIT genes may also result in changes in cellular proteins involved in motility and the cytoskeleton.¹⁰ To our knowledge, analogous studies on equine mast cell tumors and their response to TKI therapy have not been published at the time of this conference. Additionally, another study of canine mast cell tumors showed that in addition to KIT, cellular expression patterns of the RTK vascular endothelial growth factor receptor 2 (VEGFR2) may also be predictive of a poorer prognosis.¹²



Skin, horse. A Toluidine blue stain demonstrates few intracytoplasmic granules within equine mast cells. (Photo courtesy of: Department of Veterinary Pathology, Freie Universitaet Berlin, <http://www.vetmed.fu-berlin.de/en/einrichtungen/institute/we12/index.html>)



Skin, horse. The eosinophilic granuloma at left is bounded by a layer of epithelioid and foreign body type giant cells and concentric lamellations of collagen, which entrap trabeculae of neoplastic mast cells at center and right. (HE, 100X)

Contributing Institution:

Department of Veterinary Pathology, Freie Universität Berlin, Germany,
<http://www.vetmed.fu-berlin.de/en/einrichtungen/institute/we12/index.html>

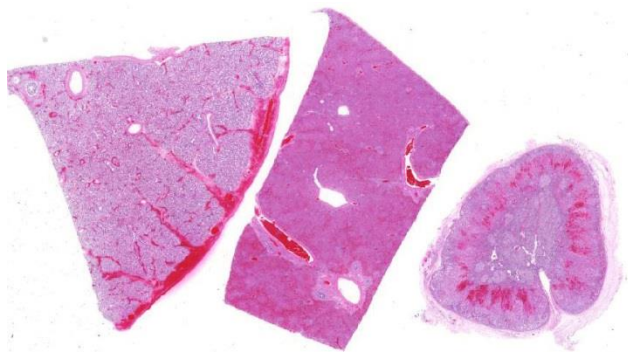
References:

- Clarke L, Simon A, Ehrhart EJ, Mulick J, Charles B, Powers B, Duncan C. Histologic characteristics and KIT staining patterns of equine cutaneous mast cell tumors. *Vet Pathol.* 2014;51: 560-562.
- Ginn PE, Mensett JEKL, Rukich PM. In: Maxie GM, ed. *Jubb, Kennedy, and Palmer's Pathology of Domestic Animals*. 5th ed. Edinburgh: Elsevier Saunders; 2007:553-781.
- Mair TS, Krudewig C. Mast cell tumours (mastocytosis) in the horse: A review of the literature and report of 11 cases. *Equine Veterinary Education.* 2008; 20:177-182.
- Marconato L, Zorzan E, Giantin S, et al. Concordance of c-kit mutational status in matched primary and metastatic cutaneous canine mast cell tumors at baseline. *J Vet Intern Med.* 2014;28:547-553.
- McEntee MF: Equine cutaneous mastocytoma: morphology, biological behavior and evolution of the lesion. *J. Comp Pathol.* 1991;104:171-178.
- Millward LM, Hamberg A, Mathews J, Machado-Parrula C, Premanandan C, Hurcombe SDA, Radin MJ, Wellman ML: Multicentric mast cell tumors in a horse. *Vet Clin Pathol.* 2010;39:365-370.
- Letard S, Yang Y, Hanssens K, et al. Gain-of-function mutations in the extracellular domain of KIT are common in canine mast cell tumors. *Mol Cancer Res.* 2008;6(7): 1137-1145.
- Reppas GP, Canfield PJ. Malignant mast cell neoplasia with local metastasis in a horse. *New Zealand Veterinary Journal.* 1996;44: 22-25.

9. Riley CB, Yovich JV, Howell JM. Malignant mast cell tumors in horses. *Australian Veterinary Journal*. 1991;68:346-347.
10. Schlieben P, Meyer A, Weise C, et al. Tandem duplication of KIT exon 11 influences the proteome of canine mast cell tumours. *J Comp Path*. 2013;148:318-322.
11. Scott D, Miller W. *Equine Dermatology*. St. Louis, MO: Elsevier;2003.
12. Thompson JJ, Morrison JA, Pearl DL, et al. Receptor tyrosine kinase expression profiles in canine cutaneous and subcutaneous mast cell tumors. *Vet Pathol*. Oct 12, 2015; online first:1-14.
13. Webster JD, Yuzbasiyan-Gurkan V, Miller RA, Kaneene JB, Kiupel M. Cellular proliferation in canine cutaneous mast cell tumors: Associations with c-KIT and its role in prognostication. *Vet Pathol*. 2007; 44: 298-308.

CASE III: E-6398-14 (JPC 4048653).

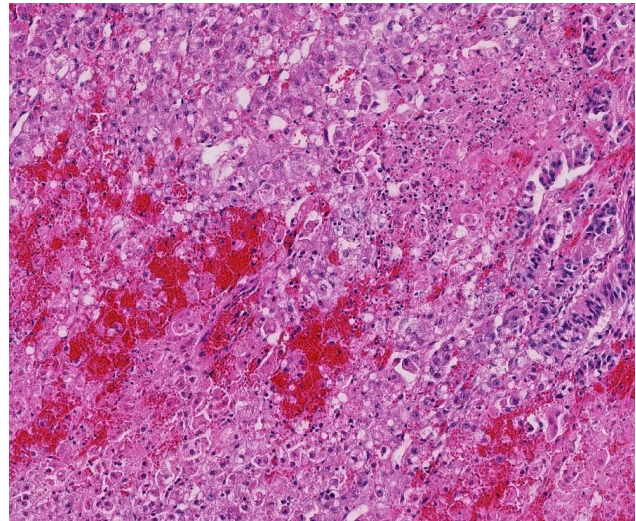
Signalment: 5 day-old, male, Quarterhorse (*Equus caballus*).



A section of lung, liver, and adrenal gland are submitted. (HE, 5X)

History: The foaling was not witnessed but there were no obvious signs of dystocia or distress. The colt was not seen drinking colostrum but was seen nursing the next morning. By 36 hrs of age, he became depressed, weak and stopped nursing. His condition progressively worsened and he was

presented to the veterinary teaching hospital at 48 hrs of age. Bloodwork performed at that time revealed severe leukopenia, azotemia, hypoproteinemia, severe dehydration, hypoxemia, hypercapnia, and acidosis. After 48 hrs in hospital, the colt developed thrombocytopenia. Despite fluid therapy, oral mucous membranes and coronary bands became severely hyperemic and the extremities became cool. He then broke with severe watery, yellow diarrhea. He died early on the morning of his third day of hospitalization.



Adrenal gland, horse. There are confluent areas of necrosis and hemorrhage throughout the adrenal cortex. (HE, 92X)

Gross Pathology: The carcass was in fair body condition having small body fat stores. Oral mucous membranes, the conjunctiva and most soft tissues were faintly yellow. Approximately 1 L of cloudy, yellow brown fluid filled the thorax. Approximately 200 mls of similar fluid was noted in the pericardial sac. The thymus was pale and contained many petechia. The lungs were diffusely dark red, very heavy, wet and rubbery. Sections sunk when placed in formalin. There were multifocal to coalescing petechia and ecchymoses on the epi- and endocardial surfaces of the heart.

The abdomen contained approximately 500-700 mls of yellow-brown cloudy fluid. The liver was diffusely dark red-brown with slightly rounded edges with many, small, randomly scattered, pinpoint white foci scattered throughout. The

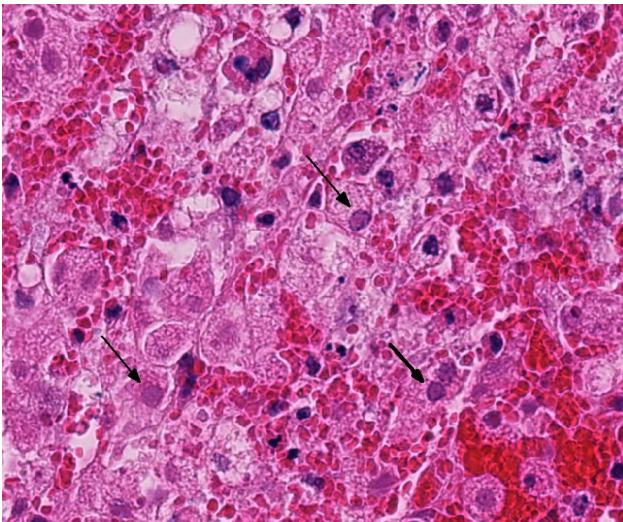
spleen was moderately enlarged, dark red-black and oozed blood on cut surface. Frequent tiny petechia were scattered on the serosa of the gastro-intestinal tract.

Laboratory Results: Antemortem blood cultures - *Actinobacillus equuli* and *Streptococcus sp.* were isolated.

Fecal culture (antemortem sample) - no *Salmonella sp.* isolated

Aerobic cultures of lung and liver (postmortem samples) - no microbial growth

RT-PCR on pooled liver and lung samples - positive for Equine herpesvirus-1



Adrenal gland, horse. Numerous cells within necrotic areas of the cortex contain intranuclear herpesviral inclusions (arrows). (HE, 280X)

Histopathologic Description: Sections of lung were diffusely moderately congested. The adventitia surrounding medium to large caliber arteries were diffusely expanded with pale edema fluid and frequent foci of hemorrhage. Alveoli were diffusely distended with pale edema fluid, and sometimes contained small flakes of aspirated keratin and/or small amounts of pale proteinaceous debris. Interlobular septa and the pleura were often moderately to markedly expanded due to edema and variably sized, sometimes large areas of hemorrhage. Occasionally randomly scattered within the parenchyma were small pale foci of acute necrosis where alveoli contained small aggregates of fibrin, few neutrophils and sparse

cell debris which partially obscured interalveolar septa. Rare cells in and around these foci (assumed to be alveolar pneumocytes) contained pale, pink, intranuclear inclusion bodies (INIB) which margined chromatin.

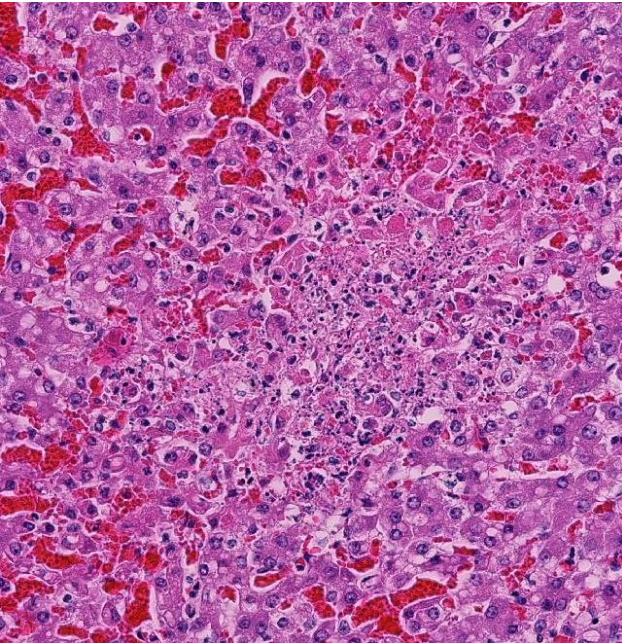
Hepatic sinusoids were often mildly congested. Frequent, randomly scattered foci of lytic necrosis were present throughout the sections. Within these foci, hepatocytes were replaced by pale proteinaceous debris admixed with sparse karyorrhectic debris. Hepatocytes at the margins of these foci sometimes contained pale pink, intranuclear inclusions. Rare dense aggregates of bacteria were noted within sinusoids.

There were frequent, multifocal to coalescing areas of hemorrhage and lytic necrosis within the adrenal cortex. Adrenocortical cells at the periphery of areas of necrosis also often contain INIBs similar to those described above. Small foci of acute lytic necrosis were noted in the spleen and thymus.

Contributor's Morphologic Diagnosis:

1. Lung: Severe, diffuse, acute, pulmonary congestion and edema with frequent foci of hemorrhage and occasional, mild, multifocal (embolic), fibrinonecrotizing, pneumonia with rare intranuclear inclusion bodies (INIBs).
2. Liver: Moderate, acute, multifocal and random, necrotizing hepatitis with intrahepatocellular INIBs.
3. Adrenal gland: Severe, acute, multifocal to coalescing, necrotizing and hemorrhagic, adrenalitis with INIBs.

Contributor's Comment: Equine herpesvirus-1 (EHV-1) is a common cause of respiratory disease, neurologic disease, and abortion in horses. The virus is widespread with a worldwide distribution. Abortions may occur several weeks to months after exposure and usually occur in the last 3-4 months of gestation. There is generally no premonitory clinical signs in the dam with rapid expulsion of a fresh, minimally autolyzed fetus. Abortions may occur



Liver, horse. There are randomly scattered areas of necrosis throughout the liver. (HE, 188X)

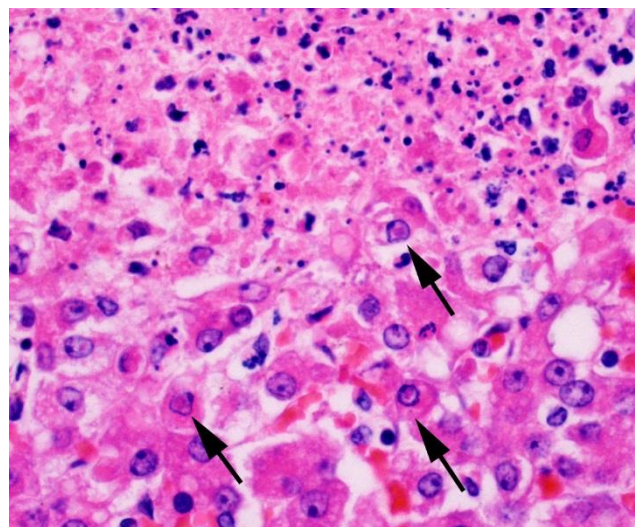
sporadically within a herd or as outbreaks typically affecting multiple mares over a short period of time.^{3,2}

Generalized neonatal disease, as demonstrated in this case, is also reported where foals infected in utero may be born alive. As in this case, infected foals generally die in the first few days of life due to acute interstitial pneumonia, pulmonary edema, and secondary septicemia. *Actinobacillus equuli* and *Streptococcus sp.* are commonly isolated agents. Interestingly, one reference² indicated that while areas of hepatic necrosis are common in aborted fetuses, such lesions are generally not present in neonatal foals succumbing to systemic EHV-1 infection. However, in this 5 -ay old foal, hepatic necrosis with INIBs was a prominent finding.

In natural disease conditions, EHV-1 infects epithelial cells in the upper respiratory tract which may cause mucosal damage, predisposing affected horses to infection with other respiratory pathogens (bacteria, fungi, etc). Subsequent infection of circulating leukocytes (typically monocytes and T cells) enables the virus to disseminate to other organs including the uterus and central nervous system. Infection of endothelial cells in the gravid uterus and CNS (in neurologic cases) may result in vasculitis and

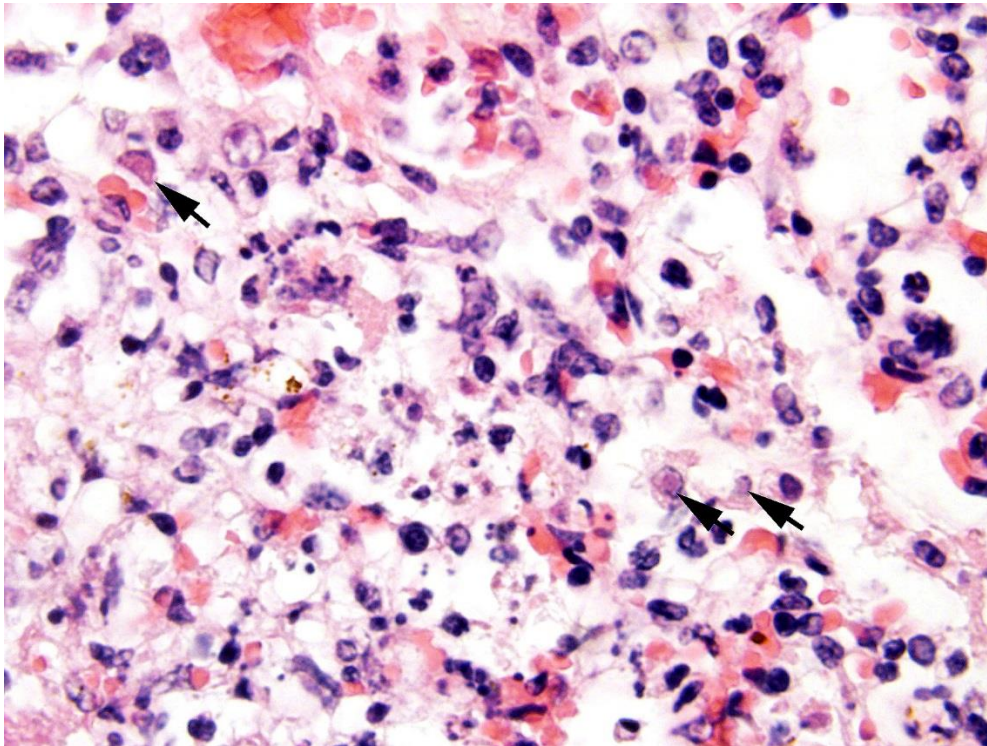
thrombosis. Acute and severe disruption of placental circulation is likely responsible for the sudden death and expulsion of fresh fetuses which is characteristic of EHV-1 abortion.¹

Exposure to EHV-1 is very common in most horse populations. Horses, including foals and young horses, in large breeding/training facilities are often seropositive for EHV-1, with or without any signs of respiratory disease.¹ Infections are usually acquired via nasal secretions from the dam, other foals, pasture mates, and/or from contact with fomites. Latent infections are common; the virus may be harbored in the trigeminal ganglia or in lymphoid cells. Latently infected horses do not shed virus and are clinically normal. However, under certain conditions, there may be reactivation of the virus and recrudescence of infection. The virus can be reactivated experimentally in horses by administration of high doses of glucocorticoids. Stressful situations such as transport, sales, competitions, or mixing of horses, as well as immunocompromise due to concurrent disease, are thought to be factors leading to recrudescence of disease. In closed herds, abortions due to EHV-1 infection are often attributed to recrudescence of infection in individuals, which may or may not be accompanied by clinical disease, and who subsequently may shed virus and act as a source of infection to other exposed, susceptible horses.¹ There was frequent move-



Liver, horse: Hepatocytes on the periphery of the areas of necrosis contain intranuclear herpesviral inclusions. (HE, 300X).

ment of horses within the barn that this mare and foal originated from, so both late gestational infection and/or recrudescence of infection in the mare are possibilities in this case.



Lung, horse. Type 1 pneumocytes within areas of septal necrosis in the lung contain intranuclear herpesviral inclusions (arrows). (HE, 320X)

and few conference participants reported identifying rare syncytia within the section. The septal and subpleural hemorrhage within the section of lung is impressive. Some participants reported inclusion bodies within the endo-

thelium, and the degree and nature of vascular damage in both the lung and liver is necrotizing, though more prominent in the lung. There is also septal necrosis and infiltration of inflammatory cells into the interstitium in the section of lung. Other differential diagnosis discussed for these lesions included equine adenovirus, equine arterivirus and African horse sickness; although the nature and distribution of lesions and characteristic alpha herpesviral inclusion bodies made for a less ambiguous diagnosis.

JPC Diagnosis:

Adrenal gland: Adrenalitis, necrotizing and hemorrhagic, multifocal to coalescing, severe with intranuclear viral inclusion bodies.

Liver: Hepatitis, necrotizing, multifocal and random, marked with intranuclear viral inclusion bodies.

Lung: Pneumonia, interstitial, necrotizing, diffuse, mild with necrotizing vasculitis and intranuclear viral inclusion bodies.

Conference Comment: The adrenal gland has linear areas of hemorrhage and lytic necrosis within the zona reticularis and zona fasciculata, with the presence of both degenerate (vacuolated) and necrotic adrenal cortical cells which contain characteristic alpha herpes viral inclusions. The lytic necrosis within the liver is random with the presence of fewer inclusion bodies in degenerate and necrotic hepatocytes,

Equine herpesvirus infection within the central nervous system is less common than the respiratory and abortive manifestations of EHV-1, only occurring in a small percentage of infected horses. However, the neurologic form can be particularly devastating, ultimately resulting in a vascular origin myeloencephalitis, which begins with an upper respiratory infection as described above. The precise factors determining why some horses develop neurologic signs is not well understood, but may be related to infection with certain virus strains. In contrast to CNS herpes viral infections in some other domestic species (bovine – IBR, porcine – pseudorabies), EHV-1 is not neuronotropic, although neurons and astrocytes may become infected, and the CNS form of the disease is more commonly seen in adult horses. Circulating infected cells, primarily T lymphocytes and monocytes, spread the virus to endothelial cells

of small vessels of the CNS resulting in vasculitis, thrombosis and infarction of tissues supplied by those vessels. Lesions can occur throughout the CNS, including the spinal cord, but inclusion bodies within the CNS are generally not seen.⁵ Gross lesions consist of randomly distributed areas of malacia with accompanying hemorrhage and edema,⁴ reflecting the vascular nature of the lesion.

Contributing Institution:

Department of Pathology/Microbiology
Atlantic Veterinary College, University of Prince
Edward Island
www.avc.upei.ca

References:

1. Njaa, BL. Disorders of horses. Viral causes of abortion and neonatal loss. In: *Kirkbride's Diagnosis of Abortion and Neonatal Loss in Animals*. 4th ed. West Sussex, UK: Wiley-Blackwell;2012:154-157.
2. Maxie MG. Equid herpesvirus 1 abortion in horses. In: Maxie MG ed. *Jubb, Kennedy, and Palmer's Pathology of Domestic Animals*. 5th ed. Vol 3. Philadelphia, PA: Elsevier Saunders; 2007:532-533.
3. Dunowska M. A review of equid herpesvirus 1 for the veterinary practitioner. Part B: Pathogenesis and epidemiology. *N Z Vet J*. 2014;62(4):179-188.
4. Zachary JF. Mechanisms of Microbial Infections. In: McGavin MD, Zachary JF, eds. *Pathologic Basis of Veterinary Disease*. 5th ed. St. Louis, MO: Mosby Elsevier; 2012:228-229.
5. Zachary JF. Nervous System. In: McGavin MD, Zachary JF, eds. *Pathologic Basis of Veterinary Disease*. 5th ed. St. Louis, MO: Mosby Elsevier; 2012:840-841.

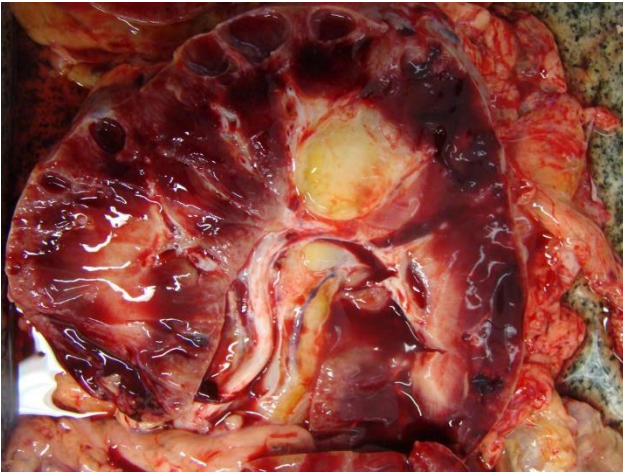
CASE IV: Case III (JPC 4001093).

Signalment: 17-year-old, female, intact Brasileiro de Hipismo equine (*Equus caballus*).

History: A 17-year-old, female, Brasileiro de Hipismo equine was presented to the Equine Hospital of the Faculty of Veterinary Medicine and Zootechny, University of São Paulo (FMVZ-USP), São Paulo, Brazil with the history of acute progressive weight loss, hyporexia and selective appetite in the last 15 days. Food intake had been declining progressively and presently the horse was anorexic. No difficulties in prehension or mastication had been noticed. At the veterinary hospital, the animal was treated with ringer lactate and 5% glucose fluid/ IV. Physical examination was unremarkable except for an increased rectal temperature (39.2°C) in the first day and at rectal examination the left kidney was enlarged. The clinical course followed to depression, emaciation (486 Kg), prostration, ataxia, labial and hindlimb edema, epistaxis and mildly pasty diarrhea. Samples of blood, serum and urine were collected for lab analysis. Renal failure was confirmed by marked increased blood urea nitrogen (BUN) and creatinine, and those levels were 400 mg/dL and 14.4 mg/dL, respectively. The hematology showed leukocytosis and neutrophilia (13.617/ mm³). Urine analysis revealed low normal specific



Kidney, horse. The right kidney was enlarged and tan with a irregular capsular surface and numerous cysts visible through the capsule. (Image courtesy of: Faculdade de Medicina Veterinária e Zootecnia, Departamento de Patologia, Av. Prof. Dr. Orlando Marques de Paiva, 87, Cep – 05508-000)



Kidney, horse. On cut section, there are numerous subcapsular cysts and the calyx is markedly distended. (Image courtesy of: Faculdade de Medicina Veterinária e Zootecnia, Departamento de Patologia, Av. Prof. Dr. Orlando Marques de Paiva, 87, Cep – 05508-000)

gravity (1.015), pH 8.0, moderate amount of hemoglobin (++) and moderate amount of protein (++)). Microscopic examination of the sediment allowed identification of a moderate increase in leukocytes.

The percutaneous abdominal ultrasonography revealed an enlargement in both kidneys with multiple cystic cavities filled with anechoic fluid. A larger cyst, measuring 6.7 cm in diameter, was found in the left kidney. The right kidney was enlarged but smaller than the left and also displayed multiple cysts. The animal presented a rapid decrease in its general condition due to renal failure, and the lack of improvement to initial fluid therapy indicated a poor prognosis and euthanasia was advised after five days. The necropsy was performed a few hours later in the same day.

Gross Pathology: The animal was extremely thin, with ribs, lumbar vertebrae and pelvic bones easily visible. The pericardial sac, thoracic and abdominal cavity presented serous yellowish translucent free liquid of 100ml, 1L and 8L, respectively. There was a marked mesenteric and subcutaneous fat atrophy. The left kidney showed a marked increase in size, irregular brownish outer surface with multiple cystic cavities, measuring up to 2.0 cm in diameter and was filled by a yellowish turbid liquid, and no capsular adhesion. A large cyst was observed in

the left cranial kidney pole, measuring about 6.5 cm in diameter and draining a reddish-yellow turbid liquid. Corticomedullary ratio was slightly increased and the kidney was irregular grayish tan. The consistency of the parenchyma was firm. The right kidney was also enlarged, presenting a brownish, irregular outer surface with multiple cystic cavities and without capsular adhesion. The corticomedullary ratio was increased, and there was a dilation of the renal pelvis and calyces, caused by the presence of yellowish firm sandy structures (calculi) measuring up to 2mm in diameter. The urinary bladder was moderately distended and contained translucent urine with fine sandy structures, and its mucosa was irregular, red and thickened. The aglandular gastric mucosa presented multiple ulcers, measuring up to 2.1 x 1.7cm, and there was a marked thickening (3.0 cm) of the glandular mucosa wall and dilated, congested and varicose vessels in the serous gastric membrane. The other organs were unremarkable.

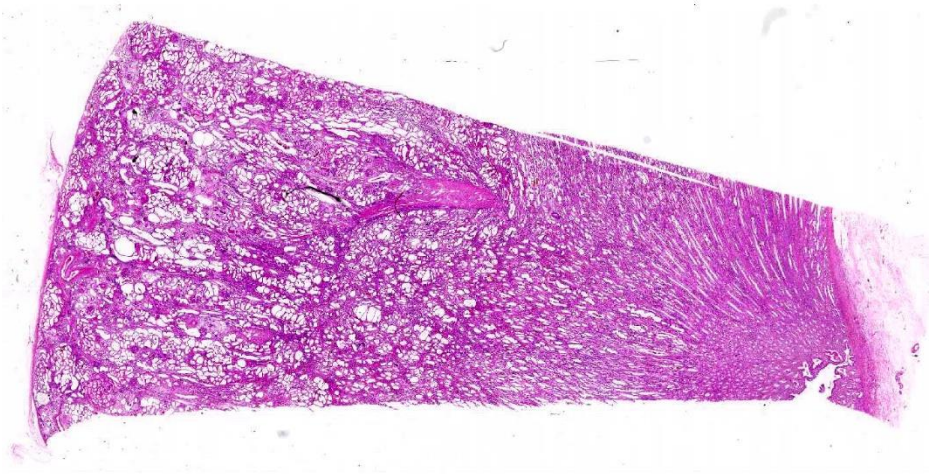
Laboratory Results:

Hematology (ref. values):

RBC 6,7 x 106/mm³ (6.8 – 12,9 x 106/mm³)
 Hematocrit 30 % (32-53%)
 Hemoglobin 10.5 mg/ dL (11-19mg/dL)
 MCV 44.78 fl
 MCHC 35 %
 WBC 15300 /mm³ (5400-14300 /mm³)
 Neutrophils 89% (13.617) (2260-8580/ mm³)
 Bands 0
 Basophils 2% (306) (0-100/mm³)
 Lymphocytes 7% (1071) (1500-7700/mm³)
 Monocytes 0 (0-1000/mm³)
 Eosinophils rare (0-800/ mm³)

Serum chemistry (ref. value):

Creatinine: 14,4 mg/dL (1.2-1.9 mg/dL)
 BUN: 400 mg/dL (21.4-51.36 mg/dL)
 Triglycerides: 807 mg/dL (22.9-46.0 mg/dL)
 Cholesterol: 258.7 mg/dL (61-112 mg/dL)
 Total protein: 6.4 mg/dL (5.2-7.9 g/dL)
 Albumin: 2.9 mg/dL (2.65–3.69g/dL)
 Ca e P: not measured



Kidney, horse. At low magnification, cortical tubules as well as Bowman's capsules are markedly dilated (HE, 4X)

Abdominal ultrasonography: showed hyper-echoic, bilateral polycystic kidneys with the biggest cyst measuring 6.7 cm located in the left kidney cranial pole.

Urine culture (at necropsy): *Klebisella pneumoniae*

Pericardial fluid (at necropsy): pH 7.5, specific gravity 1014, protein 1.2g/ dL, 200 nucleated cells/ mm³, without bacteria.

Abdominal fluid (at necropsy): pH7.5, specific gravity 1012, protein 0,8g/ dL, 600 nucleated cells/ mm³, without bacteria.

Histopathologic Description: The main alteration of the kidney histopathology is the presence of diffuse tubule and glomeruli cystic cavities of different sizes with a marked renal architectural loss. The cysts involve the corticomedullary tubules and most of them are in the cortex rather than in the medulla. Cysts are lined by flattened or cuboidal to columnar epithelium and some are divided by thin trabeculae or have papillae lumen projection. Few cysts have amorphous eosinophilic plugs (tubular proteinuria) in the lumen and were located in the cortex and medulla; some were associated with multifocal presence of crystals, and some showed hyaline plugs mix with degenerated leukocytes in the lumen. The

glomeruli were generalized diffusely changed and the main features were basal membrane thickening and cellular proliferation, i.e. marked diffuse chronic membranoproliferative glomerulonephritis. There was glomerular crescent formation, glomerulosclerosis and several foci of glomerular obsolescence which can be characterized by shrunken, eosinophilic and hypocellular glomeruli. Occasionally, few glomeruli had cystic dilation and had glomerular tuft

atrophy. These main features of cysts and glomeruli can be easily seen using Periodic Schiff Acid (PAS) and Masson's Trichrome stain (special stains were not sent). Mild tubular proteinuria (PAS-positive plugs) and moderate interstitial fibrosis were also clearly seen. There are also hemorrhagic foci and moderate suppurative interstitial nephritis. In addition, brownish granules consistent with hemosiderin pigmentation were observed in the tubular epithelium close to congestion areas and mild diffuse medial hypertrophy of small arteries could be seen. In some slide sections, small foci of mononuclear infiltrate were found in the collagenous capsule of a larger cyst (not present in all slides). Other findings consisted of moderate lymphoplasmacytic portal hepatitis associated with moderate vacuolization of hepatocytes and marked fibrosis, as showed by Masson's trichrome stain (not present in the slide). Marked medial hypertrophy and presence of small thrombi were also noticed in small arteries and capillaries of the spleen and liver (not present in the slide).

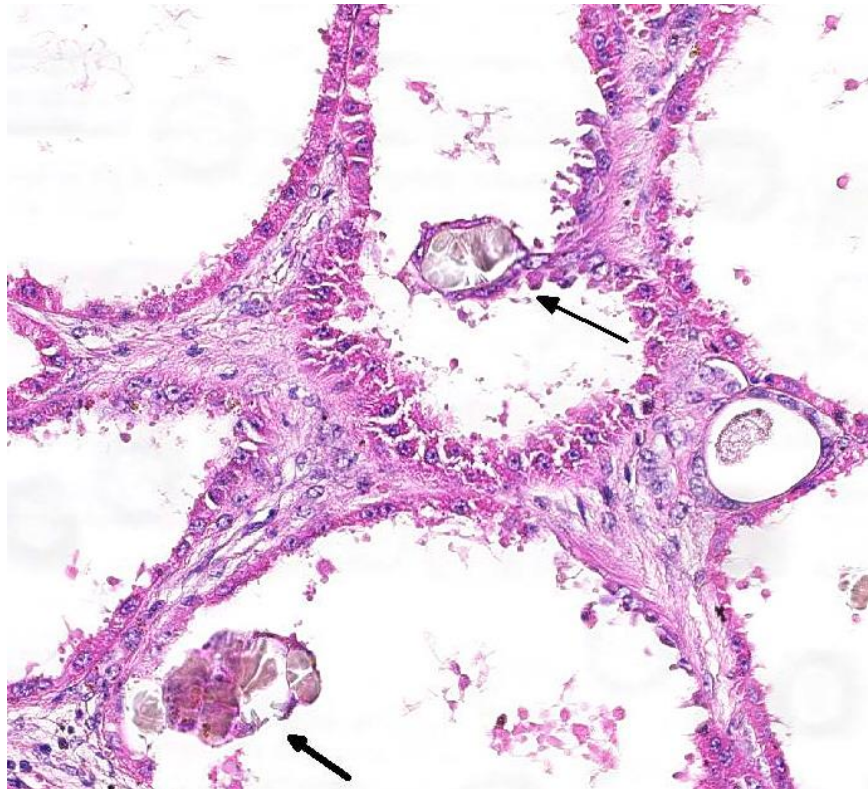
Contributor's Morphologic Diagnosis: Kidney: Tubular and glomeruli cysts, multiple, diffuse, marked associated with chronic membranoproliferative glomerulonephritis, glomerulosclerosis, and chronic interstitial nephritis with moderate interstitial fibrosis (polycystic kidney disease).

Contributor's Comment: Polycystic kidney disease (PKD) is described in several domestic and laboratory animal species as well as in humans. There were only few case reports published of PKD in exotic or wildlife species, including young springboks (*Antidorcas marsupialis*), young and adult slender lorises (*Loris lydekkerianus*), and adult Brazilian agoutis (*Dasyprocta leporina*).

Cystic diseases of the kidney include various conditions characterized by one or more grossly visible cystic cavities in the renal parenchyma. Cysts can arise during organogenesis, and may be associated with histological criteria of renal dysplasia. In general, PKD is described as either 1) a congenital form or 2) an adult form. The congenital form is known to occur in dogs, cats, horses, cattle, sheep, pigs, several laboratory animal species, and humans. In humans, this congenital form is based on an autosomal recessive trait caused by mutation on the PKHD1 gene encoding fibrocystin, which is a receptor protein. It is proof that this genetic mutation follows an autosomal recessive trait similar to the

childhood form of PKD in humans is also responsible for polycystic kidney disease in Persian kittens, lambs, and West Highland White and Cairn terrier puppies, whereas the inheritance of congenital PKD in other species is unknown.

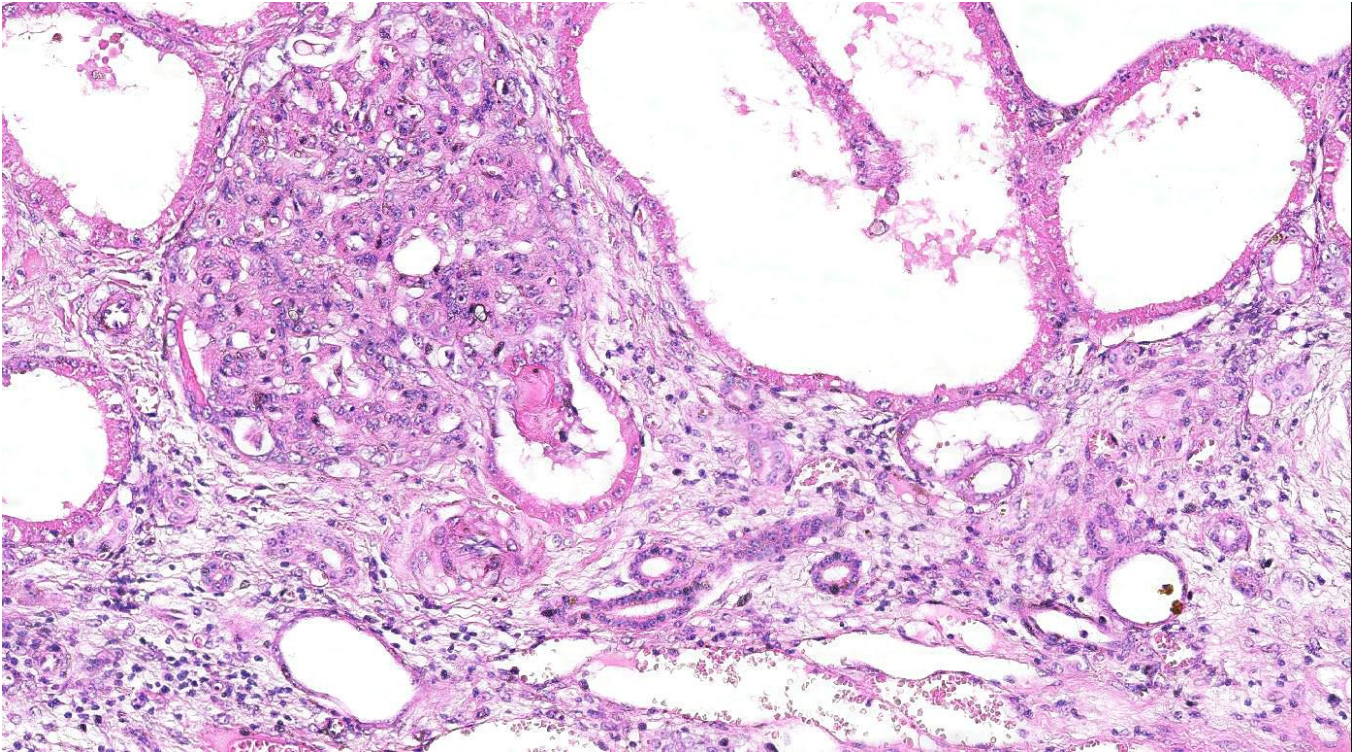
Cysts can develop in any part of the nephron, including the glomerular space, or in the collecting system. In glomerulocystic disease, they only develop in Bowman's space, but this exclusivity is exceptional. There is no evidence that cysts are caused by a failure of nephrons to unite with the collecting system. Analysis of their content indicates that they are part of functional nephrons, and that their activity is consistent with their location in the nephron. Three mechanisms, which are not mutually exclusive, may lead to the formation of renal cysts. The pathogenesis of cyst formation in PCKD is thought to represent a combination of altered cell growth, fluid secretion and altered composition of the extracellular matrix.



Dilated tubules are lined by hyperplastic epithelium containing numerous protein droplets, and often contain sheave-like birefringent oxalate crystals. (HE, 45X)

Nevertheless, the gross and histopathological similarities of the lesions together with the progressive nature of lesions resulting in presentation in middle to old age is similar to these entities, implying a similar pathogenesis. As such, it would appear most likely that equine PCKD results from a random genetic defect resulting in downstream malformation of distal tubules/collecting ducts within the kidneys, ultimately culminating in effacement of normal renal architecture by progressively enlarging space occupying fluid-filled cysts.

Renal cysts can be subdivided into congenital or acquired lesions. Solitary renal cysts occur in many species, most commonly in pigs and cattle, and are essentially incidental findings. Renal cysts become clinically significant when multiple and bilateral; such cases are named



Glomeruli are decreased in number and markedly hypercellular with numerous synechiae. Surrounding tubules are markedly atrophic, and the interstitium is markedly expanded with loosely arranged fibrous connective tissue. (HE, 180X)

polycystic kidneys. Polycystic kidney disease (PCKD) is best characterized in man with further subdivision into autosomal dominant and autosomal recessive forms.

Autosomal recessive PCKD is rare and usually is associated with disease in childhood that is often severe. Those patients who do survive may progress to the development of hepatic fibrosis. In veterinary species, a similar entity has been described in Cairn terriers, characterized by juvenile onset and multiple cysts in both kidneys and liver.

Polycystic kidneys are uncommon in horses; to our knowledge, there have been only five previous cases of PCKD in mature horses. In those cases, clinical signs (severe weight loss and anorexia) were similar to our case, although some author had related hematuria as the main clinical sign. Both kidneys were presented enlarged, containing multiple cystic structures that distorts the normal renal architecture are the classical gross findings.

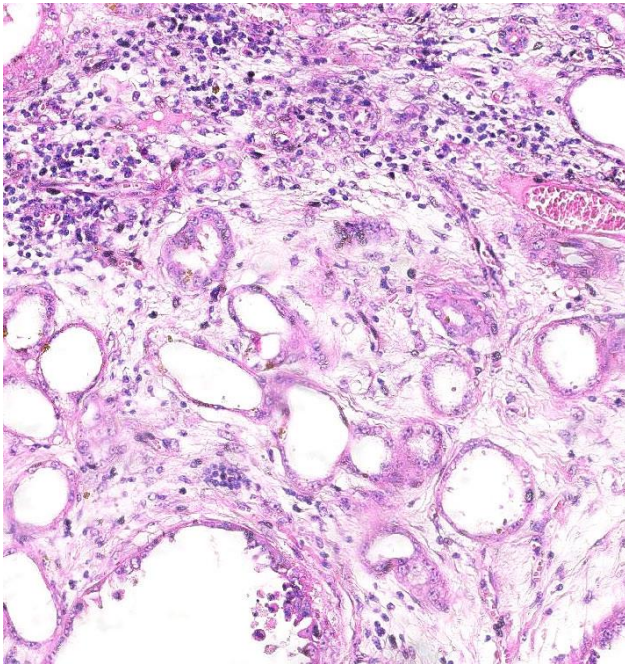
Studies in man and Persian cats have been carried out in attempt to identify the segment of the nephron which is involved in cyst development. In man, the cysts have been identified as focal dilations of proximal or distal convoluted tubules of the nephron, with occasional involvement of glomeruli. The cysts result from initial epithelial proliferation which then becomes separated from the tubule lumen and is filled not only by glomerular filtrate but also by a dysfunction of epithelial fluid absorption and secretion.

With regard to hematological and biochemical parameters, major biochemical abnormalities include consistently increased urea and creatinine levels, as would be expected with a chronic renal disease resulting in progressive reduction of renal function. Anemia was reported in cases where hematuria was a clinical finding but not in the present one and in those who this clinical sign was absent; therefore, this abnormality may reflect blood loss rather than

diminution of erythropoietin production by the peritubular interstitial tissue of the kidney.

Although secondary hyperparathyroidism due to chronic renal failure is a common sign, it was not found in the present case.

Despite the morphological similarity of the lesion seen in man and Persian cats, it is unlikely that a similar familial genetic defect is responsible for the disease in horses, given the paucity of reported cases and lack of evidence of familial association disease. Nevertheless, the gross and histopathological similarity between lesions together with the progressive nature of lesions resulting in presentation in middle to old age is similar to these entities, implying a similar pathogenesis. As such, it would appear most likely that equine PCKD results from a random genetic defect resulting in downstream malformation of distal tubules/collecting ducts within the kidneys, ultimately culminating in effacement of normal renal architecture by progressively enlarging space occupying fluid-filled cysts. Immunohistochemistry can be performed in order to clarify the segment of epithelium in cyst formation. A combination of



Kidney, horse The renal interstitium is markedly expanded by loosely arranged collagen and moderate numbers of lymphocytes and plasma cells. Tubules are ectatic and lined by attenuated epithelium (HE 140X)

vimentin and a specific anticytokeratin antibody direct against cytokeratin 18 showed to be useful to characterized collect tubule involvement.

JPC Diagnosis: Kidney: Nephritis, interstitial, chronic, diffuse, severe, with cystic tubular dilation, membranoproliferative glomerulonephritis, synechia formation, neutrophilic tubulitis and marked interstitial fibrosis.

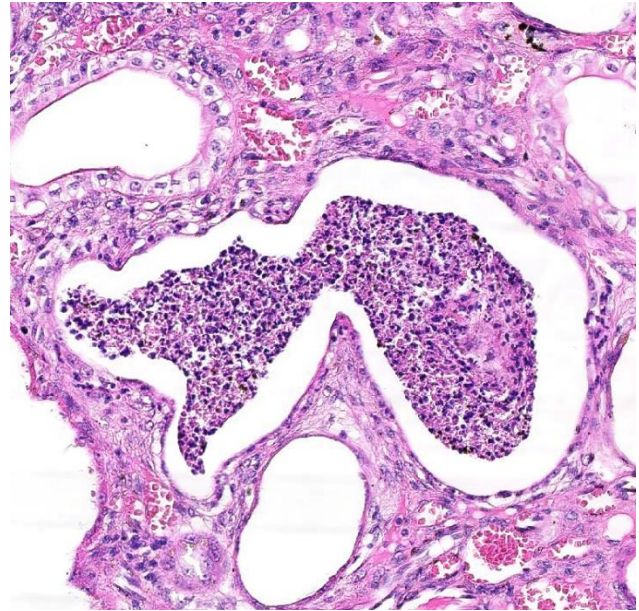
Conference Comment: Conference participants unanimously agreed that this case provided a superb descriptive challenge, with heterogeneous changes in nearly all sections of the nephron, but expressed varying interpretations as to the underlying pathogenesis and etiologic diagnosis. Most participants initially focused on the glomerular changes, including membrano-proliferative glomerulonephritis, crescent formation, synechia and periglomerular fibrosis as described by the contributor. Participants agreed that the cortical tubules are markedly ectatic and/or cystic, and some participants felt strongly that there was significant tubular loss somewhat obscured by dilation of remaining tubules. Nearly all participants observed cellular casts, cellular debris, inflammatory cells and oxalate crystals within tubular lumina, with fibrosis and chronic inflammation in the adjacent interstitium. Some participants described shrunken, obsolescent glomerular tufts within a dilated urinary space; others interpreted the same finding as nodular proliferations of hyperplastic tubular epithelium projecting into the lumina of dilated tubules. Most participants interpreted the renal changes, including the markedly dilated tubules, as an acquired or secondary lesion vice a primary underlying congenital condition.

This case was studied by Dr. Rachel Cianciolo at the Ohio State University, who has extensive experience and a keen interest in veterinary nephropathology; she interprets the renal changes as representing two simultaneous ongoing processes: 1) obstructive nephropathy with tubular dilatation and hyperplastic renal pelvis epithelium, which may be related to the evidence of urolithiasis described grossly, and the presence of oxalate crystals in the tubules; and 2)

proliferative and sclerosing glomerulonephropathy, which may or may not be immune complex-mediated. She also observes that there is “protracted tubular epithelial degeneration and necrosis with secondary interstitial edema and inflammation that could be due to either of the above processes.” She further elaborates that polycystic kidney disease, as it occurs in human medicine, specifically refers to hereditary syndromes, either autosomal dominant or autosomal recessive; polycystic kidney is most appropriately applied when the specific genetic mutation has been identified or there is support for a heritable process. In this case, the tubular dilation, degeneration and necrosis are likely related to urolithiasis / crystalluria, and which is aligned more closely with an “acquired cystic disease.”

This case was additionally studied in consultation with the Departments of Genitourinary and Nephropathology at the Joint Pathology Center, whose medical pathologists are familiar with polycystic kidney disease as described in humans. They indicated the renal lesions in this case are not consistent with polycystic kidney disease, at least as it occurs in humans. Similar to conference participants, the medical pathologists identified dilated tubules with atrophic tubular epithelium, including within collection ducts, and a mesangioproliferative glomerulonephritis with decreased numbers of glomeruli. They characterize the lesion as chronic tubulointerstitial disease, and also describe arteriolar and arterial sclerosis. They also commented on the birefringent, smooth-surfaced crystals within tubules and within the interstitium and stated that, by light microscopy, the crystals are consistent with calcium oxalate. They also mentioned the presence of basophilic non-birefringent crystals vicinity the renal pelvis, consistent with calcium phosphate.

The underlying cause of the glomerular changes remains uncertain in this case. Typically, glomerulonephritis is described as an immune mediated disease and the proliferative (or mesangioproliferative) form occurs most commonly in horses. Glomeruli can also be non-specifically



Kidney, horse. Largely within the medulla, ectatic tubules contain moderate to large numbers of neutrophils (tubulitis) (HE, 30X)

involved in association with other renal conditions, such as tubulointerstitial disease,⁴ which may have caused the glomerular changes in this case vice an immune mediated process. Other non-immune mediated causes of glomerular injury include hypertension and coagulation secondary to endothelial injury.⁴

That said, the glomerular lesions in this case were severe enough to result in crescent formation, a finding which generally occurs as a response to fibrin exudation into the urinary space, followed by invasion of mononuclear cells, proliferation of parietal epithelium, and production of collagen by fibroblasts.⁴ Additionally, the presence of synechia, which occurs with loss of podocytes and adhesion of the glomerular basement membrane to the parietal epithelium, is another indicator of severe glomerular damage. Glomerulonephritis in horses is apparently not uncommon, but progression to renal failure is reported as rare. Infectious causes in horses include equine infectious anemia and *Streptococcus equi*. The contributor’s necropsy observations of a urinary bladder with thickened, irregular red mucosa and reported urine culture of *Klebsiella pneumonia* provide further plausible explanation for acquired renal tubular disease with simultaneous glomerular lesions.

Contributing Institution:

Faculdade de Medicina Veterinária e Zootecnia
 Departamento de Patologia
 University of São Paulo
 São Paulo, Brazil

References:

1. Aguilera-Tejero E., Estepa J.C., López I., Bas S, Rodriguez M. Polycystic kidneys as a cause of chronic renal failure and secondary hypoparathyroidism in a horse. *Equine Vet J.* 2000;32:167-169.
2. Biller DS, DiBartola SP, Eaton KA, Pflueger S, Wellman ML, Radin MJ Inheritance of Polycystic Kidney Disease in Persian Cats. *J Hered.* 1996;87:1-5.
3. Cowley BD, Gudapaty S, Kraybill AL, Barash BD, Harding M A, Calvet, J P, Gattone VH. Autosomal-dominant polycystic kidney disease in the rat. *Kidney Int.* 1993;43: 522-534.
4. Maxie MG, Newman SJ. Urinary System. In: Maxie MG ed. *Jubb, Kennedy, and Palmer's Pathology of Domestic Animals.* 5th ed. Vol 2. Philadelphia, PA: Elsevier Saunders; 2007:442-462.
5. Igarashi P, Somlo S. Genetics and pathogenesis of polycystic kidney disease. *J Am Soc Nephrol.* 2002;13:2384–2398.
6. Iverson W.O., Fetterman,G.H., Jacobson E.R., Olsen J.H., Senior D.F., Schobert EE. Polycystic kidney and liver disease in Springbok. 1. Morphology of the lesions. *Kidney Int.* 1982; 22:146–155.
7. Muller DWH, Szentiks CA, Wibbelt G. Polycystic Kidney Disease in Adult Brazilian Agoutis (*Dasyprocta leporina*). *Vet Pathol.* 2009;46:656–661.
8. Plesker R., Schulze H. Polycystic nephropathy in slender lorises (*Loris lydekkerianus*). *Am J Primatol.* 2006;68:838–844.
9. Rhind SM, Keen JA. Polycystic kidney disease in a mature horse: report and review of previously reported cases. *Equine Vet Educ.* 2004;16:178-183.
10. Takahashi H, Calvet J P, Dittmore-Hoover D, Yoshida K, Grantham JJ, Gattone VHA. Hereditary Model of Slowly Progressive Polycystic Kidney Disease in the Mouse. *J Am Soc Nephrol.* 1991;1:980-989.
11. Torre VE, Harris PC. Mechanisms of disease: autosomal dominant and recessive polycystic kidney diseases. *Nat Clin Pract Nephrol.* 2006;2(1):40-55.



WEDNESDAY SLIDE CONFERENCE 2015-2016

Conference 8

11 November 2015

CASE I: 14-292 (JPC 4066249).

Signalment: 20-year-old female pony
(*Equus caballus*)

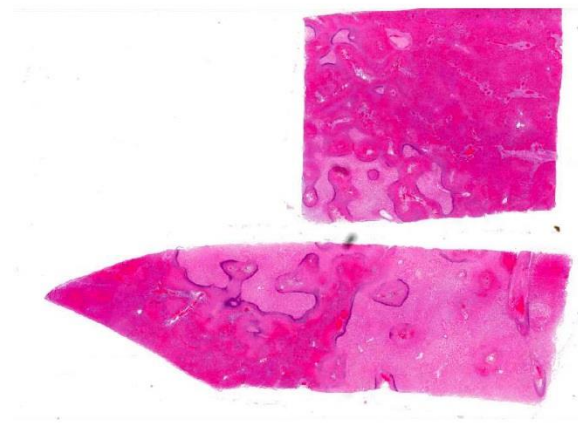


Liver, pony: Multifocally, the hepatic parenchyma is dry, malodorous, and has small pockets of emphysema. (Photo courtesy of: Photo courtesy of: University of Calgary Faculty of Veterinary Medicine, Clinical Skills Building, 11877 85th St NW, Calgary, AB T3R 1J3. <http://www.vet.ucalgary.ca/>)

History: A 20-year-old female pony presented to the referring veterinarian with a history of acute onset depression, decreased appetite, and separation from herdmates. On initial presentation, the pony was tachycardic, tachypneic, and mildly febrile. Over a 2-day period the pony deteriorated with development of a high fever and marked icterus. Complete blood count revealed lymphopenia, mild monocytosis and mild thrombocytopenia. Marked increases in SDH, AST, ALP and GGT were noted on

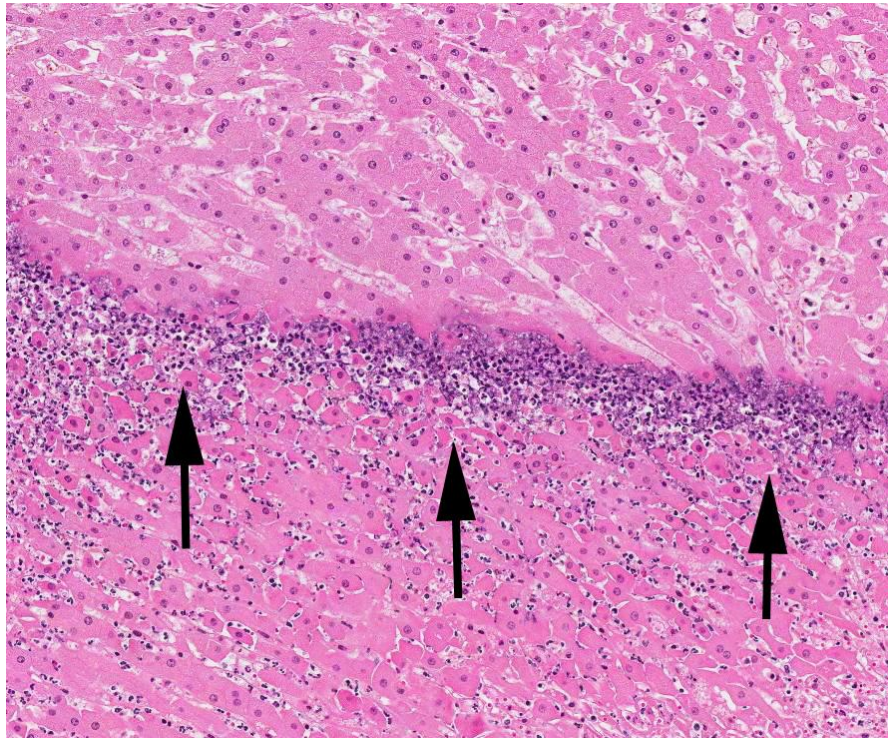
chemistry. Abdominal ultrasound showed multifocal, hyperechoic areas within the liver and a 4 cm mass in close proximity to the spleen. Treatments included intravenous fluids, antibiotics, and anti-inflammatories. The pony was humanely euthanized 3 days after initial presentation.

Gross Pathology: At necropsy, the body was fresh, in good nutritional condition and there was no evidence of dehydration. There was severe icterus. Within the peritoneal cavity there were liters of opaque, red fluid. On the serosal surface of the small intestines there were numerous petechiae and ecchymoses. Primarily located within the left side of the liver, there was an extensive, mo-



Liver, pony: Two sections of liver exhibit confluent areas of coagulative necrosis. (HE, 5X)

derately well-defined, approximately 35 cm in diameter focus where the parenchyma was swollen, firm and dark red to tan. This area was accompanied by a thick layer of fibrin on the capsular surface with adhesion to the diaphragm and spleen. On cut section, there were multifocal to coalescing areas of pallor and reddening interpreted to be necrosis and hemorrhage, respectively. The hepatic parenchyma was dry, lusterless, and malodorous with multiple small pockets of air (emphysema). Large thrombi were observed



Liver, pony. Areas of coagulative necrosis (top) are delineated by a border of degenerate neutrophils and abundant cellular debris. (HE, 80X)

within blood vessels.

Laboratory Results: Fluorescent antibody testing was negative for *Clostridium chauvoei*, *C. septicum*, *C. novyi* and *C. sordellii*. Significant organisms were not isolated on aerobic or anaerobic cultures. Immunohistochemistry was positive for *C. novyi*.

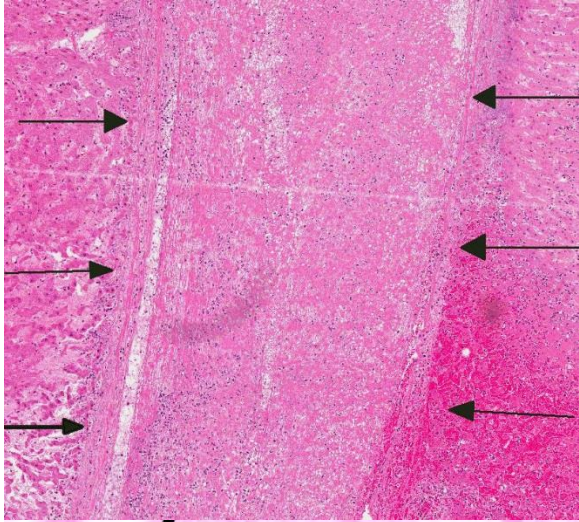
Histopathologic Description: Liver: Involving up to 80% of the hepatic parenchyma in one section, there are multifocal to confluent zones of acute coagulation necrosis which are characterized by hyper eosinophilia, loss of nuclear detail, and retention of the tissue architecture. Zones of coagulation necrosis are bordered by an intense band of basophilia which is composed of degenerate neutrophils and nuclear material. Multifocal areas of lytic necrosis are observed and are characterized

by eosinophilic cellular and karyorrhectic debris admixed with degenerate neutrophils, fibrin and hemorrhage. Frequently, the tunica media of blood vessels is disrupted by fibrin, nuclear debris, free red blood cells and neutrophils consistent with vasculitis. Affected blood vessels often contain thrombi. Within the zone of coagulation necrosis there are variable numbers of large (6 μ m x 1 μ m) bacilli reminiscent of *Clostridium* species. These organisms are gram-positive.

Contributor's Morphologic Diagnosis:

Liver: Hepatitis, necrotizing, extensive, severe, acute with emphysema, necrotizing vasculitis, thrombosis and gram positive bacilli

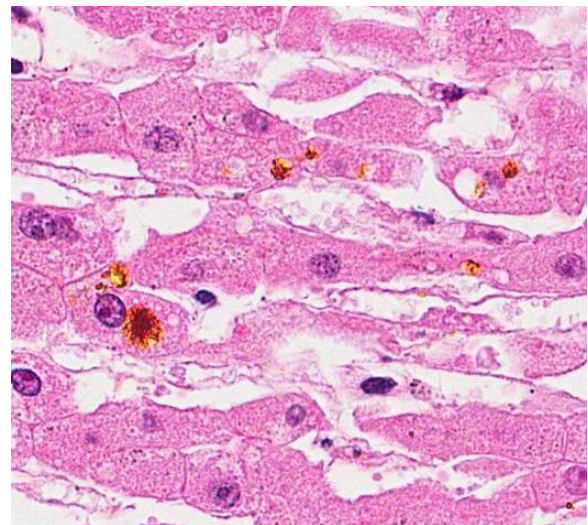
Contributor's Comment: The gross pathology and microscopic lesions in this pony were highly suggestive of clostridial hepatitis, a lesion commonly seen in ruminants, infrequently seen in swine, and rarely reported in equids. In ruminants,



Liver, pony. Blood vessels both within necrotic and viable areas of the parenchyma often contain fibrin thrombi (arrows). (HE, 80X)

Clostridium novyi group of bacteria: black disease (infectious necrotic hepatitis) and bacillary hemoglobinuria.^{5,6} There is considerable overlap in the gross pathology, histopathology and pathogenesis of these diseases. Black disease is caused by *C. novyi* type B, a bacterium that produces potent alpha and beta toxins. Bacillary hemoglobinuria is caused by *C. haemolyticum* (formerly *C. novyi* type D) which produces beta toxin only. Both diseases are characterized by acute hepatic necrosis and other systemic lesions associated with toxemia and generalized vascular damage.⁵ As the name suggests, bacillary hemoglobinuria is further characterized by intravascular hemolysis with anemia and hemoglobinuria.⁶ The pathogenesis of both diseases begins with the ingestion of environmental spores with seeding to histiocytes within the liver, spleen, and bone marrow. Spores lie dormant in the liver until the formation of a localized anaerobic environment allowing for germination of spores and the production of potent exotoxins by vegetative bacteria. In ruminants, migration of the common liver fluke, *Fasciola hepatica*, is thought to be the initiating event.⁶

To date, there are 7 reports of clostridial hepatitis in equids occurring in Australia, New Zealand, the United Kingdom, and the United States.^{3,4,6,7,9} Similar to the current case, clinical disease in horses is characterized by acute onset of depression, fever, abdominal pain, icterus, tachycardia, and tachypnea with rapid deterioration and death in 12-48 hours.^{7,9} Successful therapy has not been described and is not surprising given the rapid course of disease and difficulty in establishing an antemortem diagnosis. Reported necropsy findings include serosanguinous pericardial, pleural and peritoneal effusions, serosal hemorrhages, icterus, fibrinous peritonitis and hepatic necrosis.^{3,4,7,9} The inciting cause of the suitable anaerobic conditions for spore germination within the equine liver has not been definitively determined. Strongyle migration though the liver is an inconsistent finding and in the current case, there was no clear evidence of larval migration.^{5,9} Interestingly, many of the reported cases have a recent history of anthelmintic therapy prior to the onset of clinical signs.^{3,5,9} Recent use of anthelmintics was not reported in the current case.



Liver, pony. Within areas of necrosis, there are small to large aggregates of hematoidin. (HE, 200X)

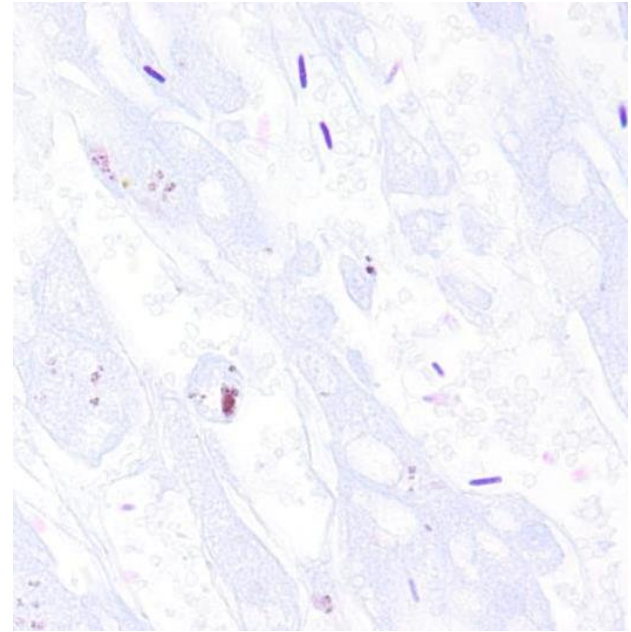
Arriving at an etiologic diagnosis was problematic in the current case. Liver was submitted to two laboratories for anaerobic culture and fluorescent antibody testing (FAT) for *Clostridium* spp. *Clostridium novyi* group organisms were not detected by FAT or by culture, highlighting the challenge at arriving at an etiologic diagnosis in cases of clostridial hepatitis. Both *C. novyi* and *C. haemolyticum* are extremely oxygen sensitive and fastidious in their nutritional requirements making culture challenging and an unreliable diagnostic tool.^{5,9} This diagnostic challenge is further highlighted by a report wherein *C. novyi* type A isolates were sent to 669 laboratories worldwide as part of an external quality control program. Only 3.5% of laboratories made a definitive identification of *C. novyi* type A.² In the current case, immunohistochemistry was positive for *C. novyi* and was instrumental in confirming the diagnosis.

JPC Diagnosis: Liver: Hepatitis, necrotizing, multifocal to coalescing, marked with vascular thrombosis.

Conference Comment: The conference histologic description was aligned very closely with the contributor's description, although few participants reported seeing bacilli. A mild amount of emphysema was seen within some sections, but this was not a prominent feature. Interestingly, the areas of coagulative necrosis often did not demonstrate the classic loss of differential staining in hepatocyte nuclei; however, the cells were swollen, pale and largely dissociated from normal hepatic cord architecture. Conference participants generally interpreted the lesion as acute or subacute, which corresponds with the clinical history, and the pattern appeared random rather than having a specific zonal distribution. Reaching an etiologic diagnosis in this case was particularly challenging for participants, with a

variety of possible etiologies discussed, ranging from infectious to toxic.

The differential diagnosis includes equine serum hepatitis, which is a common cause of acute liver failure in young horses. Grossly



Liver, pony. Clostridial bacilli are more easily visualized with a tissue Gram stain. (Gram, 400X) (Photo courtesy of: University of Calgary Faculty of Veterinary Medicine, Clinical Skills Building, 11877 85th St NW, Calgary, AB T3R 1J3. <http://www.vet.ucalgary.ca/>)

in this condition the liver is described as flaccid (“dishrag liver”) with a mottled or reticular pattern on cut section. Histology is characterized by extensive hepatic necrosis with stromal collapse; remaining hepatocytes often demonstrate fatty degeneration. This is typically not an acute process and mild fibroplasia is often present, which is in contrast to the liver seen in this case, although the clinical course has some similarities.¹ Not knowing the age of this animal, another infectious rule out is *C. piliforme*, the cause of Tyzzer’s disease, which is reported in young foals. In contrast to the lesion in this case, the microscopic lesion of Tyzzer’s consists of random foci of coagulative necrosis with neutrophilic infiltrates. The diagnosis depends on seeing the organisms at

the periphery of necrotic areas within degenerate and normal appearing hepatocytes, and the organisms often appear in bundles.¹ *Salmonella typhimurium* was also mentioned as a possibility, but again is most often seen in foals. Lesions are most commonly associated with the intestine, particularly in adult horses, but in cases of septicemia lesions may be seen in the liver.⁸

Since infectious organisms were not apparent in most slides, many conference participants considered a toxic etiology such as blue-green algae. Microcystin-LR is the most commonly referenced cyanobacterial hepatotoxin, found on ponds or other small bodies of water after a seasonal bloom. It is taken up into hepatocytes where it inhibits cytoplasmic protein phosphatases leading to necrosis, apoptosis, and perisinusoidal hemorrhage. The pattern of necrosis is most often centrilobular to massive, but can vary depending on the individual animal and amount of toxin ingested.¹ Overall, this was a challenging case with clinical, gross and histologic characteristics consistent with several potential etiologic agents.

Contributing Institution:

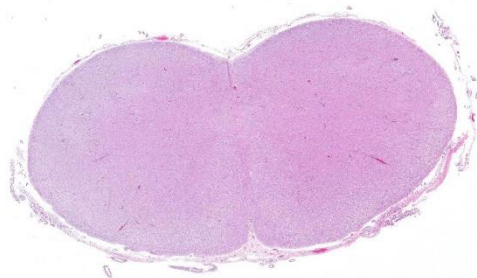
University of Calgary Faculty of Veterinary Medicine
<http://www.vet.ucalgary.ca/>

References:

1. Cullen JM, Stalker MJ. Liver and biliary system. In: Maxie MG, ed. *Jubb, Kennedy and Palmer's Pathology of Domestic Animals*. Vol 3. 6th ed. St. Louis, MO: Elsevier; 2016:312-331.
2. Finn SP, Leen E, English L, O'Briain DS. Autopsy findings in an outbreak of severe systemic illness in heroin users following injection site inflammation. *Arch Pathol Lab Med*. 2003; 127:1465-1470.
3. Gay CC, Lording PM, McNeil P, Richards WPC. Infectious necrotic hepatitis (black disease) in a horse. *Equine Vet J*. 1980;12(1):26-27.
4. Hollingsworth TC, Green VJD. Focal necrotizing hepatitis caused by *Clostridium novyi* in a horse. *Aus Vet J*. 1978;54:48.
5. Oaks JL, Kanaly ST, Fisher TJ, Besser TE. Apparent *Clostridium haemolyticum/Clostridium novyi* infection and exotoxemia in two horses. *J Vet Diagn Invest*. 1997;9:324-325.
6. Stalker MJ, Hayes MA. Liver and biliary system. In: Maxie MG, ed. *Jubb, Kennedy and Palmer's Pathology of Domestic Animals*. Vol 2. 5th ed. London, UK: Saunders Elsevier; 2007: 354-356.
7. Sweeny HJ. Infectious necrotic hepatitis in a horse. *Equine Vet J*. 1986;18(2):150-151.
8. Uzal FA, Plattner BL, Hostetter JM. Alimentary system. In: Maxie GM, ed. *Jubb, Kennedy and Palmer's Pathology of Domestic Animals*. Vol 3. 6th ed. St. Louis, MO: Elsevier; 2016:172-174.
9. Whitfield LK, Cypher E, Gordon SJG, et al. Necrotic hepatitis associated with *Clostridium novyi* infection (black disease) in a horse in New Zealand. *N Z Vet J*. 2015;63(3):177-179.

CASE II: TAMU-02 2012 (JPC 4019891).

Signalment: Yearling, black and white Holstein steer (*Bos taurus*)



A cross section of the brainstem was submitted for microscopic examination. (HE, 5X)

History: Neurologic signs for 6 days, circling, wandering, vocalizing prior to collapsing. Unable to stand, bilateral strabismus, decreased tongue tone.

Gross Pathology: No lesions

Laboratory Results: NA

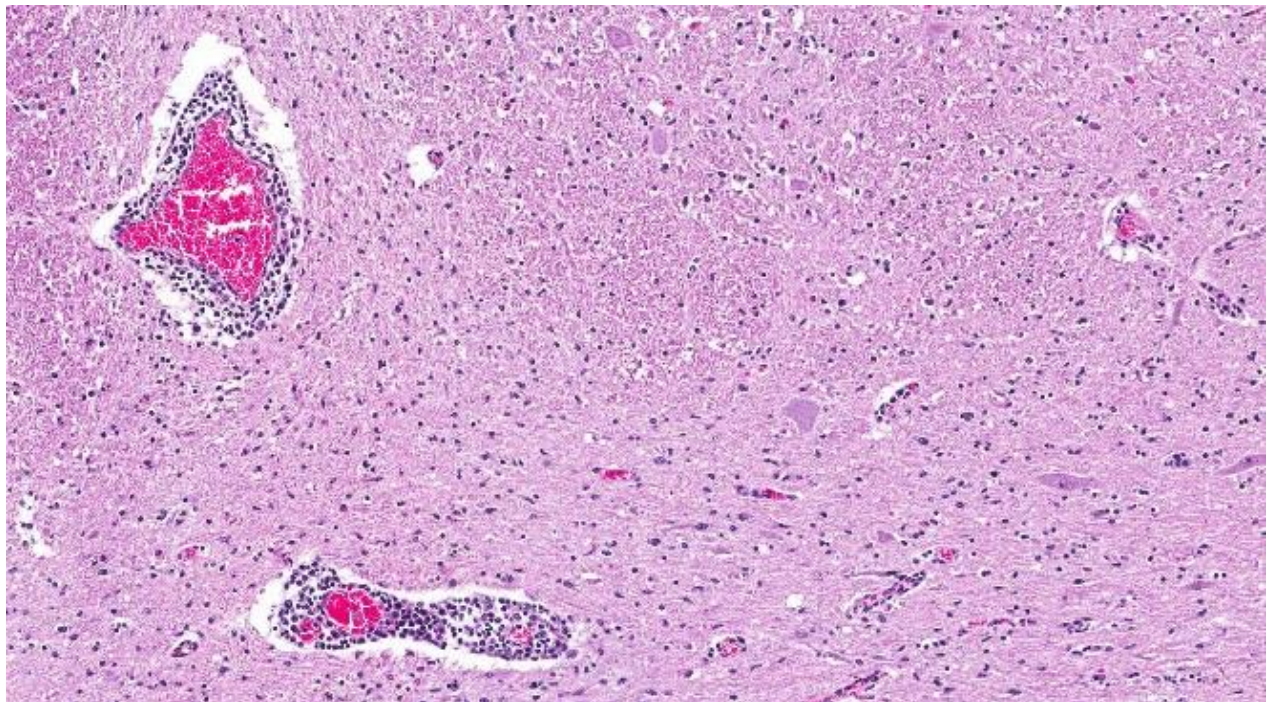
Histopathologic Description: A cross section of medulla oblongata is presented. Perivascular, especially perivenular, cuffs are widespread in the medulla and leptomeninges and vary from mild and single-cell thick to several layers thick. Gliosis is prominent in nuclei and perivascular where the glial cells almost form nodules. Many neurons contain 1-6, round to oval, homogeneous intracytoplasmic inclusions with a $<2\mu$ halo (Negri bodies).

Contributor's Morphologic Diagnosis:
Medulla oblongata: nonsuppurative

meningopolioencephalitis with gliosis and intracytoplasmic inclusions (Negri bodies).

Etiology: Lyssavirus of rabies

Contributor's Comment: The histologic lesion of rabies in cattle shows a wide range of variability in the polioencephalitis.^{8,9,10} Ganglionitis was severe in this cow, and it should be remembered that rabies virus is one of several that causes ganglionitis. It has been said that inflammation in bovine rabies is minimal compared to other species, but cases seen in our area are often florid like the present case. This may reflect the fact that animals are clinically ill for at least 6 days. Early sacrifice is thought to result in milder lesions. The presence of Negri bodies is thought to be inversely related to the degree of inflammation. Regardless, the presented case had significant inflammation and widespread Negri bodies throughout the brain as well as in the Purkinje cells, a common site in cattle.



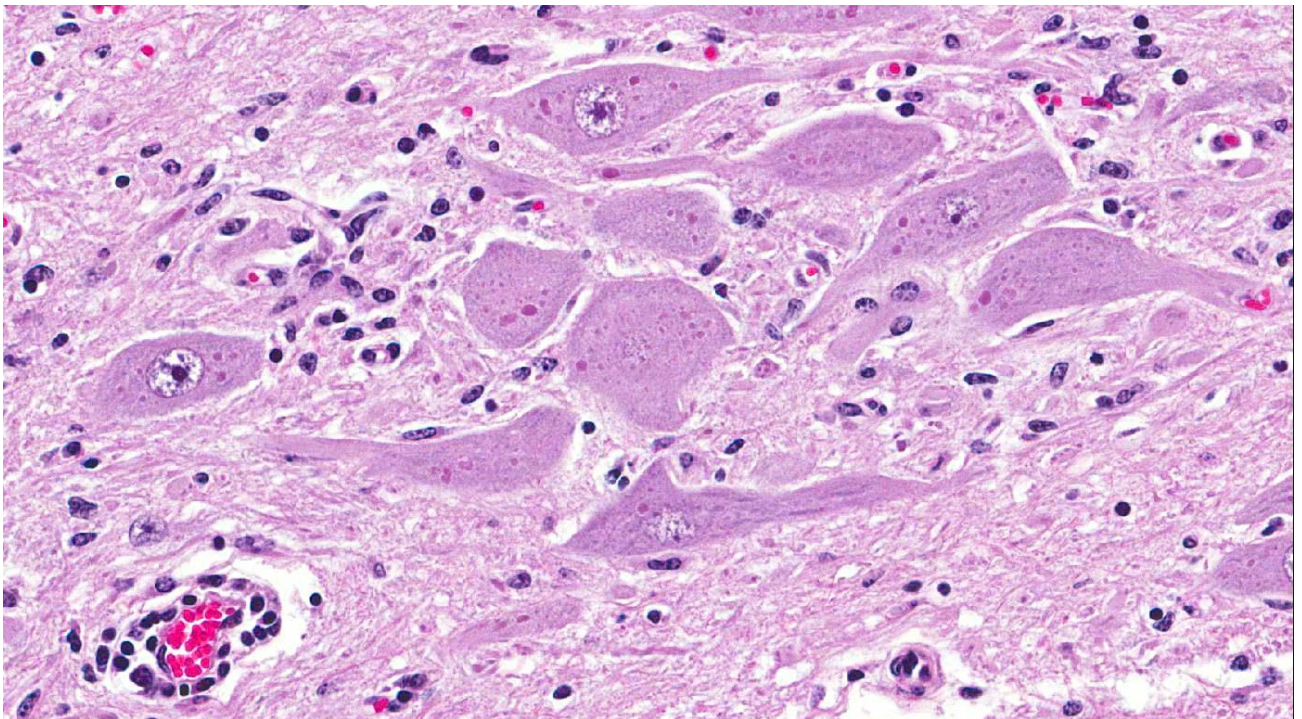
Grey matter vessels are cuffed by five to six layers of lymphocytes with diffuse gliosis of the grey matter. (HE, 80X)

Texas is setting records in rabies cases with several hundred cases reported in the counties adjacent to our laboratory. Because of baited vaccination of wildlife, we have now got less fox and coyote rabies and lots of skunk rabies.⁷ Nonhematophagous bats are also commonly infected.¹

The history was classic (6, and being forewarned, all precautions were taken in taking samples to confirm rabies, as well as completing a complete necropsy. While papers about the virtues of immunohistochemical (IHC) techniques are touted, we must conform to the use of our State's official test that is a direct immunofluorescent (DIF) test on chilled brain. That may be a good thing in view of a comparison of diagnostic tests on 26 naturally infected cows in Brazil where IHC detected only 92.4% of cases.⁶ The official sample in Texas is a transverse section of the brain extending caudally from the colliculi to the level of and

including the midcerebellar cortex. Previous sampling used a midsagittal half of the entire brain, or half of a transverse section of the brain at the level of the cerebellar roof nuclei and the hippocampus (This allowed us to store the other half of these sections in the event of loss of sam-ples.). The previous sites were based on the belief that the cerebellum was best for ruminants while the hippocampus was best for other species. Our State lab has had rare cases where the brain was positive on one side; therefore, we now include transverse pieces of entire brainstem. Otherwise, we will not get an official "negative" test. Our greatest liability challenges are not dealing with positive cases; rather, things get exciting with getting neither negative or positive results due to improper sampling or sample submission.

Historically, diagnosis of rabies has involved a variety of tests. Direct immunofluorescence, direct immunohistochemistry,



Neurons within brainstem nuclei contain numerous 2-4um brightly eosinophilic intracytoplasmic viral inclusions (Negri bodies). (HE, 360X)

mouse inoculation and the demonstration of meningoencephalitis with Negri bodies have been used. A recent comparison of techniques in diagnosis of bovine rabies supported the belief that the cerebellum was an area of 100% positivity with mouse inoculation and direct immunofluorescence; however, the pons, spinal cord and thalamus were also good. Negri bodies were seen 82% of the time in the cerebellum.⁽⁴⁾ Similar results were found in a second study.⁽²⁾ A recent immunohistochemical study of archival tissues of rabies in a variety of species concluded “the best site for rabies virus detection in dogs and cats was the hippocampus, but in cattle, viral antigen was most prominent in the brainstem, followed by the cerebellum. In horses, the cervical spinal cord and adjacent brainstem were the optimal sites for detecting rabies virus antigen. In raccoons and skunks, labeling was dispersed more widely; thus, tissue site selection might be less important for these wildlife reservoir species.”⁹

It is always difficult to compare results using different techniques conducted in different laboratories, but I hope whoever examines tongue tone in cattle showing the sign of this cow wears proper PPE!

JPC Diagnosis: Brainstem: Meningoencephalitis, nonsuppurative, diffuse, moderate, with gliosis and neuronal intracytoplasmic inclusion bodies.

Conference Comment: Conference participants described the inflammatory infiltrate as mild to moderate in severity, composed of lymphocytes, plasma cells, and macrophages, expanding Virchow-Robin spaces up to five times normal thickness, as well as being present surrounding vessels in adjacent meninges. The endothelium of affected vessels is multifocally hypertrophied, and there are prominent areas of

gliosis as described by the contributor. There was slide variation in the number of Negri bodies present, with some slides having an abundance, most prominently in brainstem nuclei.

Rabies virus testing was discussed during the conference in the context of working in areas of the world where high ambient temperatures and lack of refrigeration may present challenges that make the fluorescent antibody test less feasible, and the use of other methods such as immunohistochemistry (IHC) more practical. However, as mentioned above by the contributor, the accuracy of IHC can be less than 100%; nonetheless, some studies have shown the accuracy of IHC to be very similar to fluorescent antibody testing, indicating it may be a feasible alternative in some cases. Important considerations for IHC include the species of mammal being tested in regard to the area of brain sampled as discussed above, the type of antibody used (polyclonal vs. monoclonal) and the time the tissue remained in formalin.⁹ Reverse transcription-PCR for rabies diagnosis has been developed and has been shown to have similar results when compared with the fluorescent antibody test;³ and in some cases has been shown to be superior when there is significant decomposition in the sample.⁵

Besides more commonly implicated wildlife species such as foxes, skunks and raccoons, bats are also an important wildlife rabies reservoir, capable of transmitting the virus to domestic species and humans. Bats are one of the most commonly infected wildlife species in Texas and were indeed the most commonly infected species between 2006 and 2010.⁴ A great deal is unknown regarding the complex pathogenesis of rabies in bats, and although uncommon, adaption of bat rabies virus variants into other mammals has occurred.⁴ Bats may be exposed to the virus

multiple times in their lives, via different routes, which can influence outcome in future exposures. Clinical outcome can vary significantly in infected bats, from rapid clinical progression to survival for several months after infection, and route of infection may play a role in how the disease progresses and the bats' ability to transmit the disease.² Rabies remains an important public health problem in the United States and worldwide; understanding testing methodology and pathogenesis, in order to facilitate prompt diagnosis in cases of human exposure and to help control infection in domestic species, remains important for public health officials and pathologists alike.

Contributing Institution:

Dept of Veterinary Pathobiology
College of Veterinary Medicine and
Biomedical Sciences
Texas A&M University
College Station, TX, 77843-4467

References:

- Blanton JD, Palmer D, Dyer J, Rupprecht CE. Rabies surveillance in the United States during 2010. *J Am Vet Med Assoc.* 2011;239:773-83.
- Davis AD, Jarvis JA, Pouliott CE, et al. Susceptibility and pathogenesis of little brown bats (*Myotis lucifugus*) to heterologous and homologous rabies viruses. *J Virol.* 2013;87(16):9008-15.
- Dupuis M, Brunt S, Appler K, et al. Comparison of automated quantitative reverse transcription-PCR and direct fluorescent antibody detection for routine rabies diagnosis in the United States. *J Clin Microbiol.* 2015;53(9):2983-9.
- Mayes BC, Wilson PJ, Oertli EH, et al. (2001-2010). *J Am Vet Med Assoc.* 2013;243(8):1129-1137.
- McElhinney LM, Marston DA, Brookes SM. Effects of carcass decomposition on rabies virus infectivity and detection. *J Virol Methods.* 2014;207:110-113.
- Pedroso PM, Leal JS, Dalto AG, Oliveira LGS, Driemeier D. Bovine rabies diagnosed in the Veterinary Pathology Department of the Universidade do Rio Grande do Sul, Porto Alegre, RS, Brasil from 2002 to 2007. *Acta Scientiae Veterinariae.* 2010;40(1):1015-20.
- Shwiff SA, Kirkpatrick KN, Sterner RT. Economic evaluation of an oral rabies vaccination program for control of a domestic dog-coyote rabies epizootic: 1995-2006. *J Am Vet Med Assoc.* 2008;233:1736-41.
- Silva MLCR, Riet-Correa F, Galiza GJN, Azevedo SS, Afonso JAB, Gomes AAB. Distribution of rabies virus in the central nervous system of naturally infected ruminants. *Pesq Vet Bras.* 2010;30:940-944.
- Stein LT, Rech RR, Harrison L, Brown CC. Immunohistochemical study of rabies virus within the central nervous system of domestic and wildlife species. *Vet Pathol.* 2010;47(4):630-636.
- Summers BA, Cummings JF, de Lahunta A. *Veterinary Neuropathology.* St Louis, MO: Mosby; 1995:95-100.

CASE III: 30334-08 (JPC 3133960).

Signalment: 3-year-old, neutered, hermaphrodite, Pug (*Canis familiaris*)

History: The dog was seen at an animal hospital clinic on 8/8/08 with a high

temperature, anxious appearance, tense abdomen and painful in the lumbar area. CBC, Chemistry panel, urinalysis and radiographs of the spine, abdomen and thorax were within normal limits. It was treated for vertebral disk syndrome. No improvement



Dog, hypothalamus. An infiltrative neoplasm extends up into the thalamus. (HE, 4X).

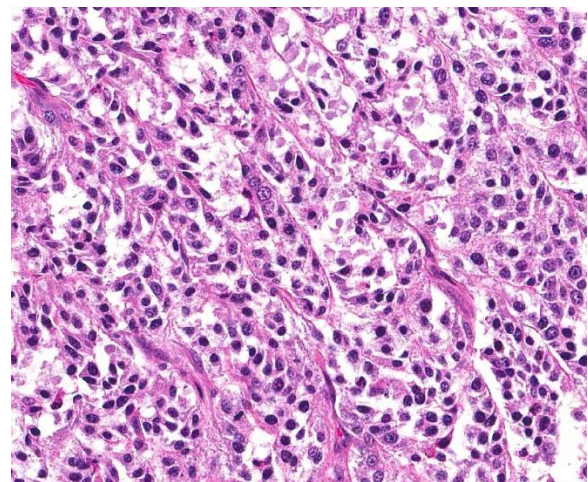
was noted after initial treatment with dexamethasone. After 12 days post presentation the dog's condition deteriorated and was hospitalized. Abnormal physical findings included anorexia, knuckling of the rear legs, circling to the left, dilated right pupil, constricted left pupil, semi consciousness, protruding tongue, lateral recumbency and lack of response to stimuli. The dog became unconscious before death.

Gross Pathology: The ventral surface of the brain has a large irregular mass destroying the pituitary gland, most of the thalamus and the optic chiasma. The mass extended along the base of the skull and measured approximately 7 X 1.5 X 3 cm. On longitudinal section, the brain has an approximately 1.3 cm in diameter, granular,

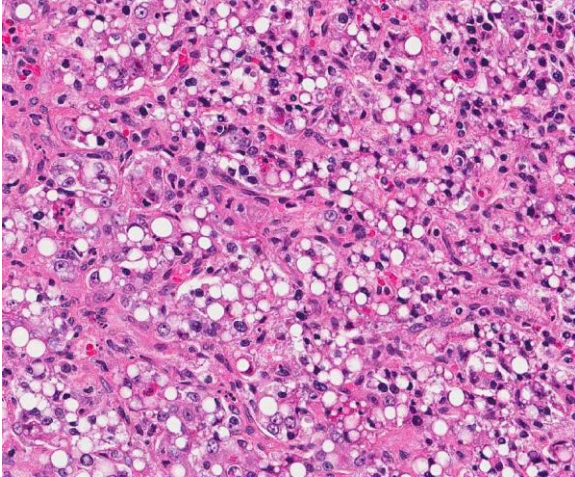
greenish colored, irregular round mass primarily within the thalamus and third ventricle.

Laboratory Results: Immunohistochemistry stains for vimentin (VM) and cytokeratin (CK) are positive. Within the neoplasm, the small cell population constantly strongly stained with CK. On the other hand, the large cell population was mostly stained with (VM). Stains for NSE, S100 and GFAP are negative.

Histopathologic Description: Brain and meninges: Within the meninges and extending into the gray and white matter is a poorly circumscribed, expansile, invasive, densely cellular neoplasm subdivided in lobules and packets by a fibrovascular stroma. The neoplasm is composed of two populations of pleomorphic cells and three patterns. One cell population consists of large polygonal cells arranged in pseudorosettes, occasionally around a central vascular core, and cords separated by fine fibrovascular stroma. These cells have distinct cell borders and moderate to abundant, wispy eosinophilic (hepatoid-like appearance), frequently vacuolated (signet ring-like appearance)



The primary cell population are small poorly differentiated polygonal germ cells with scant cytoplasm which are arranged in nests and packets. (HE, 200X)



Adjacent to nests of germ cells is a second populations of cells with prominent clear cytoplasmic vacuoles, also in nests and packets. (HE, 200X)

cytoplasm. Occasionally hepatoid type cells have apical brush borders. The nuclei are large, vesicular, irregularly round, central or peripherally located with finely stippled chromatin and one or two nucleoli. The second population of cells is smaller (round and epithelial type) and they are scattered throughout the neoplasm. These cells have scant eosinophilic cytoplasm, indistinct cell borders and round nuclei with clumped chromatin. Mitotic figures range from 3-5 per 400X field in some areas. There is marked anisocytosis and anisokaryosis, and individual cell necrosis. There are extensive areas of necrosis characterized by cellular and eosinophilic debris, mild hemorrhage, degenerate neutrophils, plasma cells and MOTT cells interspersed between neoplastic cells. Within the adjacent gray and white matter, there is multifocal moderate gliosis with occasional glial nodules, satellitosis and scattered neuronal necrosis.

Contributor's Morphologic Diagnosis: Suprasellar germ cell tumor

Contributor's Comment: Germ cells give rise to spermatogonia in the testis and oogonia in the ovary. Gonadal germ cell

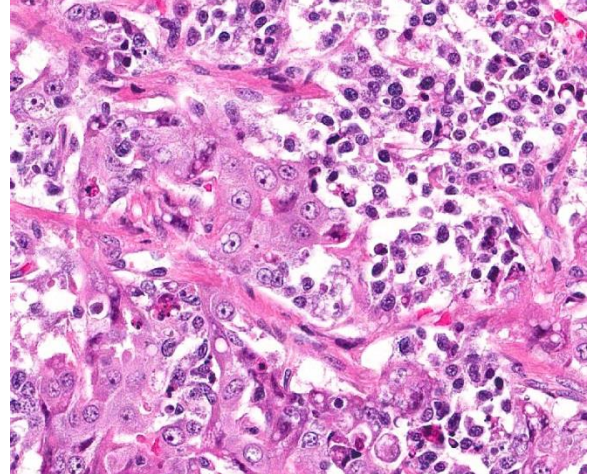
tumors more commonly reported in domestic animals include seminomas, teratomas, embryonal carcinomas, and mixed germ cell-sex cord stromal tumors. However, extragonadal tumors have been reported including the intracranial suprasellar germ cell tumor and mixed germ cell tumor in the eye and spinal cord of dogs.^{2,6} Suprasellar germ cell tumors or germinomas are very rare neoplasms in man (children and adolescents) and young dogs presumed to arise from ectopic migration of germinal epithelium from the yolk sac (embryonic stages) and its persistence at these novel sites. A recent genetic study of intracranial germ cell tumor in man suggests that these tumors are derived from cells that retain, at least partially, an embryonic stem cell-like phenotype, which is a hallmark of primordial germ cells.³ The preferred location of these tumors, as the name refers, is the pineal and hypothalamus region above the sella turcica. Microscopically, these tumors vary in cell morphology and patterns; primarily from large polygonal cells with hepatoid-like or vacuolated signet-like appearances forming cords and pseudo-rosettes (similar to hormone-producing cells or gonadal teratomas) to small cells with small amounts of cytoplasm forming nests scattered throughout the neoplasm (similar to a neuroendocrine pattern or resembling seminomas).⁸ Few foci of epithelial cells (cuboidal or squamous epithelial cells) can be seen within the tumor. Neoplastic cells are very pleomorphic making difficult to establish the difference between two or more populations of neoplastic cells. However, other authors described three populations of cells: round cells with a large round to ovoid nucleus and indistinct borders arranged in clusters, large hepatoid cells with distinct borders and compact or vacuolated cytoplasm arranged in trabeculae and epithelial cells (columnar or cuboidal, occasional squamous cell differentiation) forming tubuloacinar structures.²

Immunohistochemically, these tumors express alpha-fetoprotein, vimentin and keratin. Alpha-fetoprotein is a positive marker for germ cell tumors in humans and dogs, and is produced by yolk sac tumors, enteric elements of teratomas and some embryonal carcinomas.⁶ The diagnosis of the suprasellar germ cell tumor is based on three criteria: 1) midline suprasellar location, 2) presence within the tumor of several distinct cell types (histomorphology), and 3) positive staining for alpha-fetoprotein, VM and CK. Within the sellar region, the WHO classification of tumors from the nervous system of domestic animals has four tumors that include pituitary adenoma, pituitary carcinoma, craniopharyngioma and suprasellar germ cell tumor.⁴

The neoplasm was considered as a suprasellar germ cell tumor as a primary differential based on the pleomorphism of the neoplastic cells with different patterns and gross location. However, alpha-fetoprotein, which is an important marker for this type of tumor, was unavailable in the laboratory. In addition, this tumor was highly cellular and invasive with extensive areas of necrosis and frequent mitotic figures. Anaplastic meningioma was also considered as differential diagnosis since the microscopic location is associated with the meninges, the tumor has features of malignancy and the neoplastic cells are CK and VM positive. However, meningiomas are usually present in middle aged to older dogs. Furthermore, anaplastic astrocytoma and craniopharyngioma should also be considered since they share several histomorphological features with suprasellar germ cell tumor. Craniopharyngioma has areas resembling ameloblastoma and usually the mitotic rate is low.

JPC Diagnosis: Cerebrum: Suprasellar germ cell tumor.

Conference Comment: Overall the conference histologic description was similar to the contributor's description. Many thought there were only two populations of cells, but some participants described three: 1) polygonal cells arranged in tubules, acini and/or rosettes, 2) polygonal cells arranged in small islands and cords, and 3) round to polygonal cells arranged in loose sheets, with the third population having multifocal areas

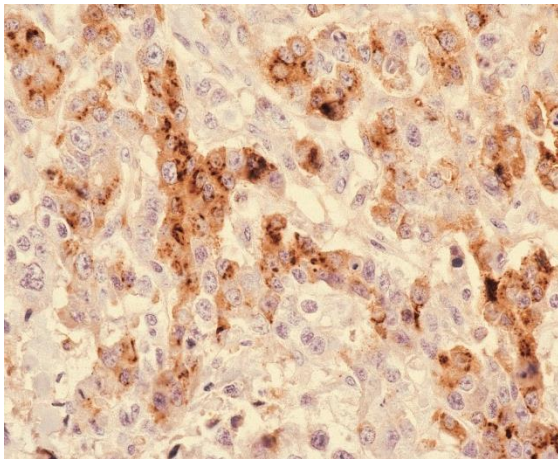


A third population of polygonal epithelial-like cells is scattered throughout the mass. (HE, 200X)

of individual cell necrosis. The different cell populations were described as being haphazardly intermingled, making specific patterns difficult to discern. There was discussion regarding the presence of “epithelial-like” cells, though some participants thought this population was not a prominent feature of the neoplasm. Participants also described deeply basophilic amorphous material and focally extensive areas of lytic necrosis. Immunohistochemical stains evaluated included alpha-fetoprotein, vimentin and pancytokeratin; there was multifocal cytoplasmic immunoreactivity in each with the strongest positivity demonstrated with pancytokeratin.

The differential diagnosis list for neoplasms in the suprasellar region were discussed including craniopharyngioma. This tumor arises from remnants of Rathke's pouch.

Craniopharyngiomas are composed of polygonal to columnar cells arranged in solidly cellular areas but may also be seen arranged in cysts or tubules. These tumors generally have areas of squamous differentiation and ciliated cells lining cystic spaces, neither of which were present in the tumor in this case. They can have multifocal areas of necrosis, and cholesterol crystals may be seen. Pituitary adenoma and pituitary carcinoma were also discussed. Pituitary adenomas are composed of polygonal to spindle shaped cells which can be arranged in solidly cellular areas as well as a sinusoidal pattern, and they lack the characteristic of multiple cell types as seen in the tumor in this case. The nuclei in pituitary adenomas are vesiculate, similar to the tumor in this case, but the cells have a moderate to abundant amount of granular cytoplasm. Pituitary carcinomas are similar to adenomas but are more invasive with greater cellular atypia and higher mitotic rate.⁴



Cytoplasm of the epithelial-like cells strongly positive for alpha fetoprotein. (anti-AFP, 200X)

Grossly, suprasellar germ cell tumors are grey-white in color, located on midline and usually obscure the pituitary and compress overlying neuroparenchyma. Pituitary tumors are white to brown in color and can be quite large, also compressing the adjacent neuroparenchyma.⁴ Craniopharyngiomas are

also large tumors that grow along the ventral brain, but may extend dorsally into the neuroparenchyma.⁵ Each of these is a reasonable gross differential diagnosis for a mass located in the most ventral region of the brain, on midline and caudal to the optic chiasm.

Contributing Institution:

The University of Georgia
Veterinary Diagnostic and Investigational
Laboratory
Tifton, GA 31793
www.vet.uga.edu/dlab/tifton/index.php

References:

1. Barnhart KF, Wojcieszyn J, Storts RW. Immunohistochemical staining patterns of canine meningiomas and correlation with published immunophenotypes. *Vet Pathol.* 2002; 39:311-321.
2. Ferreira AJA, Peleteiro MC, Carvalho T, Correia JMJ, Shulman FY and Summers BA. Mixed germ cell tumor of the spinal cord in a young dog. *J Small Anim Pract.* 2003; 44(2):81-84.
3. Høi-Hansen CE, Sehested A, Juhler M, Y-FC Lau, Skakkebaek NE, Laursen H and Rajpert-De Meyts E. New evidence for the origin of intracranial germ cell tumors from primordial germ cells: expression of pluripotency and cell differentiation markers. *J. Pathology.* 2006; 209 (1):25-33.
4. Koestner A, Bilzer T, Fatzer R, Schulman FY, Summers BA, Van Winkle TJ. *Histological Classification of Tumors of the Nervous System of Domestic Animals.* 2nd series. Vol. V. Washington DC: Armed Forces Institute of Pathology; 1999:30-36.
5. Koestner A, Higgins RJ. Tumors of the nervous system. In: Meuten DJ, ed. *Tumors*

in Domestic Animals. 4th ed. Ames, IA: Blackwell Publishing Professional; 2002:623-626,728.

6. Patterson-Kane JC, Shulman FY, Santiago N, McKinney L and Davis CJ. Mixed germ cell tumor in the eye of a dog. *Vet Pathol*. 2001; 38(6):712-714.
7. Summers BA, Cummings and de Lahunta A. Tumors of the central nervous system. In: Summers BA, Cummings and de Lahunta A, eds. *Veterinary Neuropathology*. St. Louis, MO: Mosby; 1995:384-385.
8. ACVP meeting, neuropathology mystery slides, case # 5. Presented by Dr. Amanda Fales-Williams (Iowa State University).

CASE IV: N 1241 (JPC 4067882).

Signalment: Thirteen-month-old male neutered orange roan English Cocker Spaniel dog (*Canis familiaris*) weighing 9.1 kg.

History: One month history of weight loss, severe azotemia [creatinine 740 mg/dL (0.3-1.7 mg/dL)] and marked proteinuria [urine protein to creatinine ratio UP:UC of 22 (<0.5)]. Lethargy and anorexia. Euthanasia.

Gross Pathology: The animal presented 24 hours after euthanasia and showed a relatively poor body condition. There was a moderate subcutaneous edema mainly affecting the ventral abdominal and inguinal area. Approximately 150 ml of yellow-red transparent liquid was found within the abdomen (ascites) and 100 ml of similar fluid within the thorax (hydrothorax). The lungs were moderately oedematous. Both kidneys were diffusely pale tan and presented with a diffusely rough and granular appearing surface with several multifocal small (up to 2 x 1 cm) pitted. On incision, the cortex

showed a generalized punctiform or granular appearance.

Laboratory Results:

DNA was extracted from hair follicles collected at necropsy. PCR amplifying exon 3 of gene *COL4A4* for detecting a single nucleotide substitution (A → T) at the base 115 (1) showed that the animal was a mutated homozygous at this position (PCR performed by ANTAGENE, France).

Histopathologic Description: Kidney: All glomeruli show a marked segmental to global damage accompanied by a mild to moderate multifocal interstitial inflammation and fibrosis. Most of the glomeruli contain abundant brightly eosinophilic extracellular homogenous (proteinaceous) material, which appears to be mainly within the Bowman's space. This proteinaceous material is stained bright red with Masson's trichrome, purple with Periodic acid Schiff (PAS) and unstained with Congo red stain. Often, glomeruli show multifocal to diffuse thickening of the Bowman's capsule, segmental to global thickening of capillary basement membranes and mild to moderate increase in cellularity. Adhesions between glomerular tuft and Bowman's capsule (synechia) and periglomerular fibrosis are common. Some glomeruli are sclerotic and obsolescent. There is a mild to moderate interstitial, often periglomerular, lymphoplasmacytic inflammation, and mild to moderate interstitial fibrosis which often extends from the cortex to the medulla forming radial streaks. Tubules are frequently mildly to moderately distended with intraluminal eosinophilic extracellular homogenous material (protein) and scant cellular debris and lined by flattened epithelial cells. Within the cortex, the interstitium appears moderately hypercellular (suspected reactive fibroblasts and/or immature mesenchymal cells).

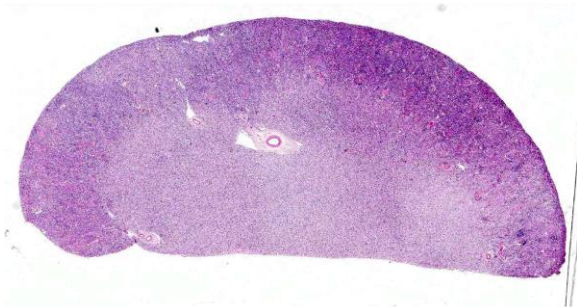


Kidneys, dog. Both kidneys are very pale and show a diffusely rough and granular appearing surface and cortex with moderate multifocal to coalescing pitting. (Photo courtesy of: School of Veterinary Medicine and Science, University of Nottingham, UK <https://www.nottingham.ac.uk/vet/servicesfortheveterinaryprofession/pathology.aspx>)

Contributor's Morphologic Diagnosis:

Kidney: Severe, generalized, segmental to global, chronic membranoproliferative glomerulonephritis with glomerulosclerosis and proteinuria.

Condition: Hereditary nephropathy / Familial nephropathy

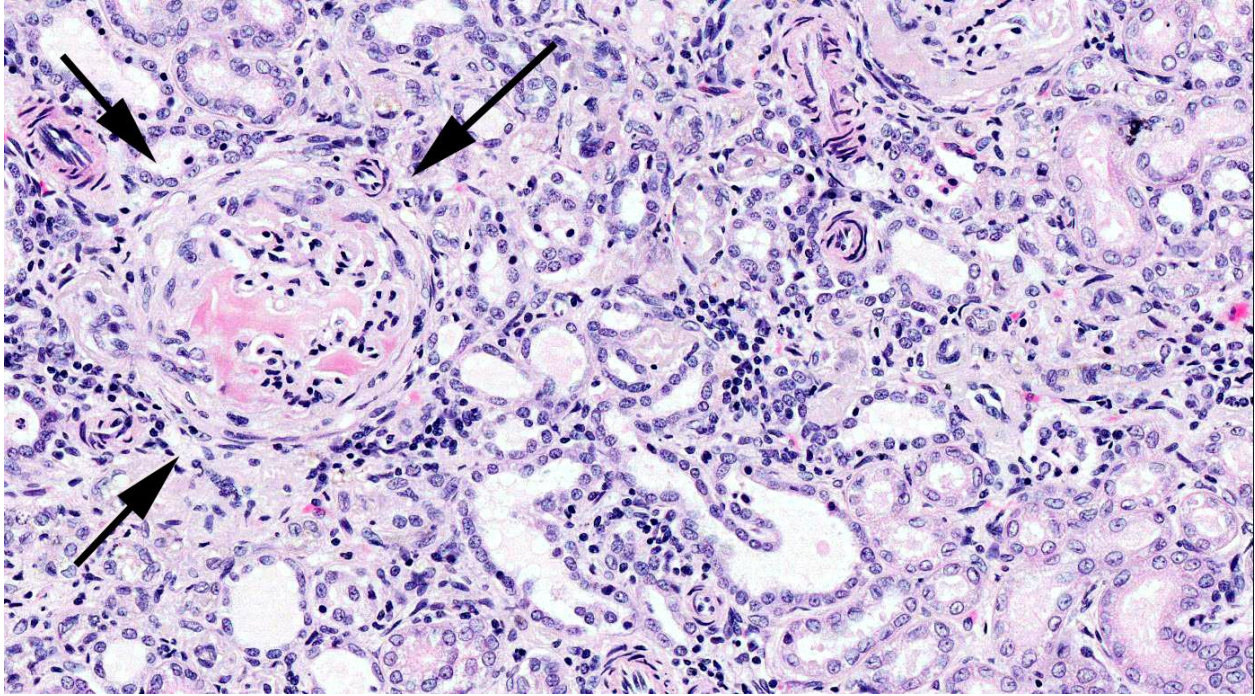


1Kidney, dog. The kidney has multifocal areas of pallor and an undulant capsular surface (HE, 5X).

Contributor's Comment: The clinical presentation and the lesions observed in the kidneys indicated a renal failure. The edema

observed in multiple organs and body cavities was very likely secondary to the proteinuria.

Hereditary nephropathy (HN) (also called Familial Nephropathy or Hereditary Nephritis) is the most commonly used name for kidney diseases that occur in dogs due to genetic type IV collagen abnormalities.^{2,7,10} This group of diseases is considered analogous to human Alport nephropathy, although the latter presents usually with ocular and/or hearing abnormalities which have not been reported in dogs.^{9,3-6} To date, 4 different collagen IV gene mutations have been identified in dogs with HN (table 1). HN in the English Cocker Spaniel is an invariably progressive and ultimately fatal renal disease, which typically causes renal failure between 6 months and 2 years of age. The disease is inherited as an autosomal recessive trait and based on a genetic defect caused by a single base substitution in the exon 3 of *COL4A4*



Kidney, dog. There are changes at all levels of the nephron. Glomeruli (arrows) are hypercellular with synechiae formation, abundant protein within Bowman's space, and marked periglomerular fibrosis. Tubules are decreased in number, ectatic, and often lined by attenuated cuboidal epithelium. The interstitium is expanded and infiltrated by moderate numbers of lymphocytes and plasma cells. (HE, 60X).

gene (A \rightarrow T).² Collagen (type IV) defects cause severe structural and functional alterations in glomerular basement membranes (GBM).^{7,4,5} Unlike most collagens, type IV collagen occurs only in the basement membranes (BM) and comprises up to six genetically distinct α -chains (designated as $\alpha 1(IV)$ to $\alpha 6(IV)$) encoded by 6 genes (*COL4A1* to *COL4A6*).⁶ Three defined trimer combinations ($\alpha 1\alpha 1\alpha 2$, $\alpha 3\alpha 4\alpha 5$ and $\alpha 5\alpha 5\alpha 6$) are formed from the six $\alpha(IV)$ chains.⁵⁻⁷ The $\alpha 1$ and $\alpha 2$ chains are present in the BM of all tissues, whereas the other four chains have restricted tissue distribution during the development.^{5,6} The expression of collagen IV chains is also subjected to temporal regulation.⁶ In the GBM, genes encoding the $\alpha 1$ and $\alpha 2$ chains are expressed during embryonic development, but their levels gradually decrease as the expression of genes encoding the $\alpha 3$, $\alpha 4$, and $\alpha 5$ chains starts. This switch explains why the affected animals are born apparently

healthy and have an early onset of disease. In affected English Cocker Spaniel dogs, the mutation in *COL4A4* prevents a normal synthesis of $\alpha 4$ chains and therefore inhibits a normal assembly of $\alpha 3\alpha 4\alpha 5$ collagen type IV heterotrimers in mature glomeruli. Instead, these heterotrimeric units are replaced by others lacking $\alpha 4$, which are suggested to be structurally weaker or less resistant to proteolytic degradation. These structural changes in the GBM lead to glomerular damage due to abnormal cell-cell and matrix-cell interactions, and a progressive tubule-Interstitial injury.⁷

Affected English Cocker Spaniel puppies typically present with proteinuria as their first clinical manifestation of the disease at the age of 2 to 8 months. Renal damage progresses and end-stage renal disease is often present at 12 months of age (ranging from 6 to 18 months), as was the case in the dog here presented.⁷

Breed	Mode of inheritance	Gene affected	Location within gene	Specific mutation	Reference
Samoyed	X-Linked	COL4A5	Exon 35	Single nucleotide substitution (G→T)	9
Mixed breed from Navasota, Texas (USA)	X-Linked	COL4A5	Exon 9	10-base pairs deletion	10
English Cocker Spaniel	Autosomal recessive	COL4A4	Exon 3	Single nucleotide substitution (A→T)	1
English Springer Spaniel	Autosomal recessive	COL4A4	Exon 30	Single nucleotide substitution (C→T)	11

Table 1. Genetic collagen IV defects identified in dogs (adapted from Ref. 2).

Contributors were unable to investigate a possible familiar occurrence of renal disease in the kindred of the dog presented here, since no information about it could be obtained.

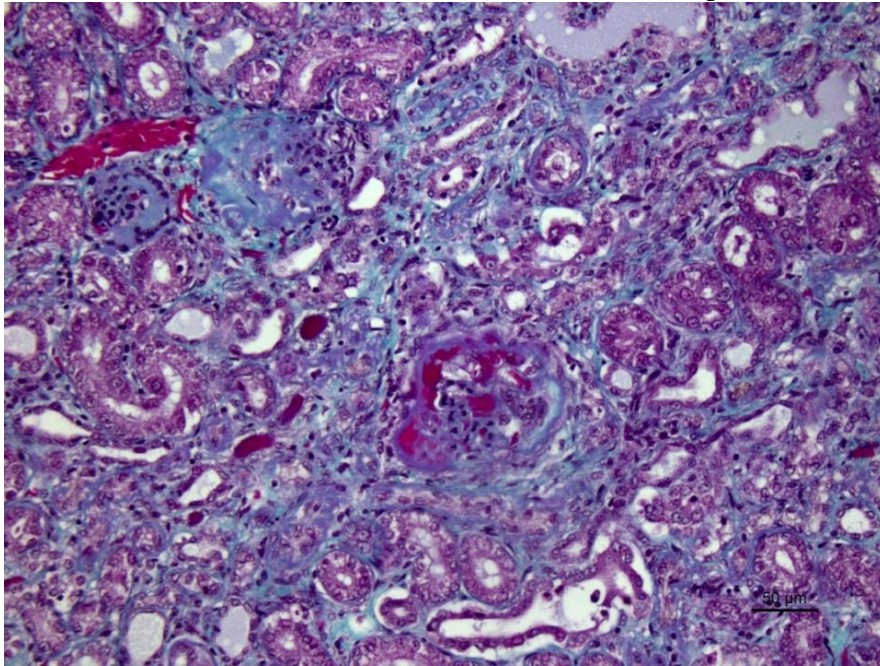
The light microscopic lesions in the kidney of HN-affected dogs are reported to be segmental thickening of GBMs and mesangial expansion, progressing through glomerular and periglomerular fibrosis and glomerulosclerosis. Usually, these lesions are accompanied by tubulointerstitial nephritis, interstitial fibrosis and tubular atrophy.^{7,10} All these light histological features were observed in the present case. The striking presence of extracellular material observed within the Bowman's spaces of most glomeruli is unusual in the contributors' opinion. Based on its appearance in hematoxylin and eosin (HE) and the performed special stains, the contributors interpret this material as a very protein-rich glomerular filtrate.

Immunohistochemistry (IHC) and transmission electron microscopy (TEM) are useful techniques to further characterize the lesion,

but they were not performed in the present case. Normal mature GBM is known to strongly express $\alpha 3$, $\alpha 4$ and $\alpha 5$ chains of type IV collagen. In English Cocker Spaniels with HN, however, the expression of those chains is either absent ($\alpha 4$) or greatly reduced ($\alpha 5$). Additionally, there is increased expression of three other chains ($\alpha 1$, $\alpha 2$, and $\alpha 6$) that would normally only be minor components of the mature GBM and therefore weakly expressed.⁷ Ultrastructural GBM changes are common to all the genetically characterized examples of HN. The principal change is an irregular thinning or thickening of GBM with splitting and fragmentation of its lamina densa. There is also often fusion of visceral epithelial cell foot processes and wrinkling of glomerular capillary walls.^{7,8} In this case, the definite diagnosis was based on a DNA test offered by ANTAGENE in France. Genetic tests are recommended in cases of suspected HN in English Cocker Spaniels and are widely available (OptiGen, Laboklin, Genetic Technologies, ANTAGENE, Genindexe, Genomia, Van Haeringen)

(www.thekennelclub.org.uk/media/14688/dn)

[atestsworldwide.pdf#sthash.eQZ2iMgB.dpu](#)
f).



Kidney, dog. There is moderate interstitial, periglomerular and glomerular fibrosis (stained in blue). The extracellular (proteinaceous) material present within glomerular Bowman's space stains bright red. Masson's trichrome, 200X). (Photo courtesy of: School of Veterinary Medicine and Science, University of Nottingham, UK <https://www.nottingham.ac.uk/vet/servicesfortheveterinaryprofession/pathology.aspx>)

JPC Diagnosis: Kidney: Membrano-proliferative glomerulonephritis, diffuse, marked with tubular atrophy and loss, and interstitial nephritis with fibrosis.

Conference Comment: The conference histologic description was very similar to the contributor's description. However, without knowledge of the signalment, history, or access to special stains, nearly all participants placed amyloidosis at the top of the differential diagnosis. Indeed, the histologic features of this entity when viewed only on an HE-stained section share many features with amyloidosis. The microscopic findings in cases of hereditary nephropathy (HN) are indicative of glomerular disease, but are not specific for or unique to HN.⁷ In addition to the above changes, moderate numbers of glomeruli were described as undergoing

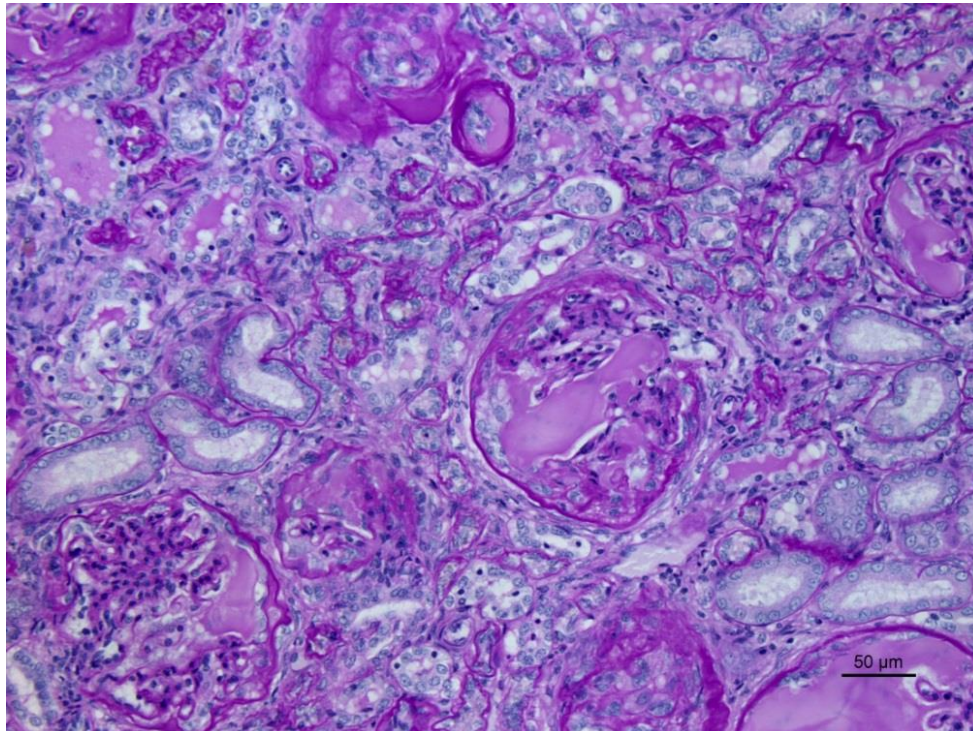
cystic glomerular atrophy with a characteristic small glomerular tuft and expanded Bowman's space.

Nonspecific changes which occur in the tubules and interstitium in glomerular disease include tubular degeneration, atrophy, interstitial fibrosis and nephritis, as was described in this case. These secondary changes tend to increase in severity as the primary glomerular disease progresses. Although the exact mechanism resulting in the tubular and interstitial changes in this condition is not completely understood, the underlying process is presumed to be similar for the development of tubular lesions in other

glomerular disorders.⁷ Blood is supplied to the tubules via the vasa recta from the efferent glomerular arteriole; in cases of glomerulosclerosis, this blood flow through the vasa recta is decreased, resulting in hypoxia and subsequent tubular epithelial cell death. Damaged tubules thereupon become lined by cuboidal or squamous cells which do not have a brush border and lack normal tubule cell function. Chronic proteinuria is also reported to damage tubular epithelium.¹¹

In the initial stages of HN, biopsies from affected dogs presenting with proteinuria can be normal. Early histologic changes include mild focal and segmental mesangial expansion, and the lesions eventually progress to global glomerulosclerosis as described above. The distinctive features of

this entity are demonstrated via electron microscopy, as well as with IHC that is specific for the different types of type IV collagen alpha chains. Tissue IHC is necessary to demonstrate the presence of the abnormal collagen chains because not all dogs that have ultrastructural changes consistent with HN have evidence of abnormal type IV collagen. Although proteinuria is a classic clinical manifestation of this condition and moderate hypoalbuminemia is seen, affected animals usually do



Kidney, dog. There is moderate thickening of the Bowman's capsule and basement membranes of glomerular capillaries and renal tubules (stained purple). The extracellular (proteinaceous) material present within the Bowman's space stains purple. (Periodic acid Schiff, 200X) (Photo courtesy of: School of Veterinary Medicine and Science, University of Nottingham, UK <https://www.nottingham.ac.uk/vet/servicesfortheveterinaryprofession/pathology.aspx>)

not have nephrotic syndrome or hypertension, but rather develop a worsening uremia as the condition progresses.⁷

Contributing Institution:

School of Veterinary Medicine and Science,
University of Nottingham, UK
<https://www.nottingham.ac.uk/vet/servicesfortheveterinaryprofession/pathology.aspx>

References:

1. Cox ML, Lees GE, Clifford EK, Murphy KE. Genetic cause of X-linked Alport syndrome in a family of domestic dogs. *Mamm Genome*. 2003;14(6):396-403.
2. Davidson AG, Bell RJ, Lees GE, Kashtan CE, Davidson GS, Murphy KE. Genetic cause of autosomal recessive hereditary nephropathy in the English Cocker Spaniel. *J Vet Intern Med*. 2007;21(3):394-401.
3. Deltas C, Pierides A, Voskarides K. Molecular genetics of familial hematuric diseases. *Nephrology Dialysis Transplantation*. 2013;28(12):2946-60.
4. Gubler MC. Inherited diseases of the glomerular basement membrane. *Nat Clin Pract Nephrol*. 2008;4(1):24-37.
5. Heidet L, Cai Y, Guicharnaud L, Antignac C, Gubler M-C. Glomerular Expression of Type IV Collagen Chains in Normal and X-Linked Alport Syndrome Kidneys. *Am J Pathol*. 2000;156(6):1901-1910.
6. Khoshnoodi J, Pedchenko V, Hudson BG. Mammalian collagen IV. *Microsc Res Tech*. 2008;71(5):357-70.

7. Lees GE. Kidney diseases caused by glomerular basement membrane type IV collagen defects in dogs. *J Vet Emerg Crit Care*. 2013;23(2):184-93.
8. Lees GE, Wilson PD, Helman RG, Homco LD, Frey MS. Glomerular ultrastructural findings similar to hereditary nephritis in 4 English cocker spaniels. *J Vet Intern Med*. 1997;11(2):80-5.
9. Longo I, Porcedda P, Mari F et. al. COL4A3/COL4A4 mutations: from familial hematuria to autosomal-dominant or recessive Alport syndrome. *Kidney Int*. 2002;61(6):1947-56.
10. Maxie GM and Newman SJ. Urinary system. In: *Pathology of Domestic Animals*. Jubb, Kennedy, and Palmer's. 5th edition, Saunders Elsevier. 2007; Vol.2, p. 460.
11. Newman SJ. Urinary System. In: McGavin MD, Zachary JF, eds. *Pathologic Basis of Veterinary Disease*. 5th ed. St. Louis, MO: Mosby Elsevier; 2012:590-627.
12. Nowend KL, Starr-Moss AN, Lees GE, Berridge BR, Clubb FJ, Kashtan CE, Nabity MB, Murphy KE. Characterization of the Genetic Basis for Autosomal Recessive Hereditary Nephropathy in the English Springer Spaniel. *J Vet Intern Med*. 2012;26(2):294-301.
13. Zheng K, Thorner PS, Marrano P, Baumal R, McInnes RR. Canine X chromosome-linked hereditary nephritis: a genetic model for human X-linked hereditary nephritis resulting from a single base mutation in the gene encoding the alpha 5 chain of collagen type IV. *Proc Natl Acad Sci U S A*. 1994;91(9):3989-3993.



WEDNESDAY SLIDE CONFERENCE 2015-2016

Conference 9

18 November 2015

Dr. Julie Engiles, DVM, PhD, DACVP
Associate Professor, University of Pennsylvania
New Bolton Center, Kennett Square PA

CASE I: E305-08A (JPC 4001570).

Signalment: 23-month-old female
Corriedale sheep (*Ovis aries*).

History: The sheep was in good condition, but had been showing increasing reluctance to rise over the previous weeks. The front limbs were extremely bowed, and there was pronounced thoracic lordosis. This sheep was part of an embryo transfer trial using semen and ovum from sheep affected with suspected inherited rickets. The sheep were

on good quality pasture with high soil phosphorus levels.

Gross Pathology: On post-mortem examination there was segmental thickening of the distal radial physis, and enlargement of the costochondral junctions of ribs 5-10. The radius showed dorsal and valgus curvature. All the long bones had thickened cortices, and enthesiophytes were present around the carpal and tarsal joints.



Ribs, sheep. there was diffuse enlargement of the costochondral junction of ribs 5-10. (Photo courtesy of: Institute of Veterinary, Animal and Biomedical Sciences, Massey University, Tennant Drive, Palmerston North, New Zealand)

Laboratory Results: Calcium 1.97 mmol/L (2.0-2.7)
Phosphate: 0.73 mmol/L (1.3-2.7)
25-hydroxyvitamin D₃: 36 nmol/L (no difference compared with control sheep)
1,25-dihydroxyvitamin D₃: 154 pmol/L (no difference compared with control sheep)

Histopathologic Description: The physal lesion is characterized by irregular segmental thickening of the hypertrophic zone and dis-



Ribs, sheep. Transverse sectioning of affected ribs demonstrate obvious irregularities within the growth plate with visible retention of cartilage cores extending into the flared metaphysis. (Photo courtesy of: Institute of Veterinary, Animal and Biomedical Sciences, Massey University, Tennant Drive, Palmerston North, New Zealand)

organization of chondrocyte columns. Tongues and islands of persistent hypertrophic chondrocytes extend from the physis into the metaphysis. The cartilage matrix in some areas is eosinophilic and interspersed with fibrin. The metaphysis consists of thickened, disorganized trabeculae of woven bone, fibrous connective tissue, degenerate cartilage matrix, fibrin and hemorrhage merging into thick trabeculae of lamellar bone. In some sections osteoclastic resorption cavities are present in the cortex, and occasionally within trabeculae. Wide osteoid seams line some trabeculae.

Contributor's Morphologic Diagnosis:

Rib: Osteodystrophy with physal thickening and unmineralized osteoid seams.

Contributor's Comment: Rickets is a metabolic bone disease, most commonly due

to either phosphorus deficiency or vitamin D deficiency. The classical lesions of rickets include: Segmental thickening of growth plates (particularly of rapidly growing bones), enlargement of costochondral junctions (the so-called rachitic rosary), and spontaneous fractures.¹⁰ In cattle, pigs and sheep collapse of subchondral bone of the humeral head is also described. Impaired mineralization of the physis and newly formed osteoid leads to islands and tongues of hypertrophic chondrocytes extending into the metaphysis, disorganization of the primary spongiosa, thick osteoid seams lining trabeculae and microfractures.¹⁰

Rarely, rickets may be due to inherited defects in vitamin D metabolism or renal tubular function. See the recent review on



Radius, sheep. The growth plate of the distal radius is also segmentally expanded and there is a retained cartilage core extending toward the metaphysis. (Photo courtesy of: Institute of Veterinary, Animal and Biomedical Sciences, Massey University, Tennant Drive, Palmerston North, New Zealand)

vitamin D metabolism and rickets for further details.⁴

In Corriedale sheep with autosomal recessive inherited rickets,^{3,5} a novel nonsense mutation in the non-collagenous bone protein, dentin matrix protein 1 (DMP1), leading to a premature stop codon and truncation of the protein has been found (personal communication, K. Dittmer). The equivalent form of this disease in humans is called autosomal recessive hypophosphataemic rickets I. The mutation in DMP1 leads to increased serum fibroblast growth factor 23 (FGF23) concentration. FGF23 inhibits the renal NPT-2a co-transporter (a Na-P co-transporter) and CYP27B1 (1 α -hydroxylase) activity in the kidney, altering phosphate reabsorption in the renal tubules, and inhibiting 1,25(OH)₂D₃ production. Consequently, humans with this condition have hypophosphataemia, phosphaturia, inappropriately normal serum 1,25(OH)₂D₃ concentrations and rickets.⁶

The thickened cortices seen in the long bones of affected sheep² and enthesiophytes are a feature of X-linked hypophosphataemic

rickets in humans.⁹ The pathogenesis of this is unclear. However in the sheep, we hypothesize that the enthesiophytes are the result of strain on ligament/tendon attachments to weakened, poorly mineralised bone. Likewise, the thickened cortices are a consequence of bone being deposited at sites of strain in order to decrease deformation associated with mechanical loading, as described by Wolff's law or the mechanostat model.^{7,8}

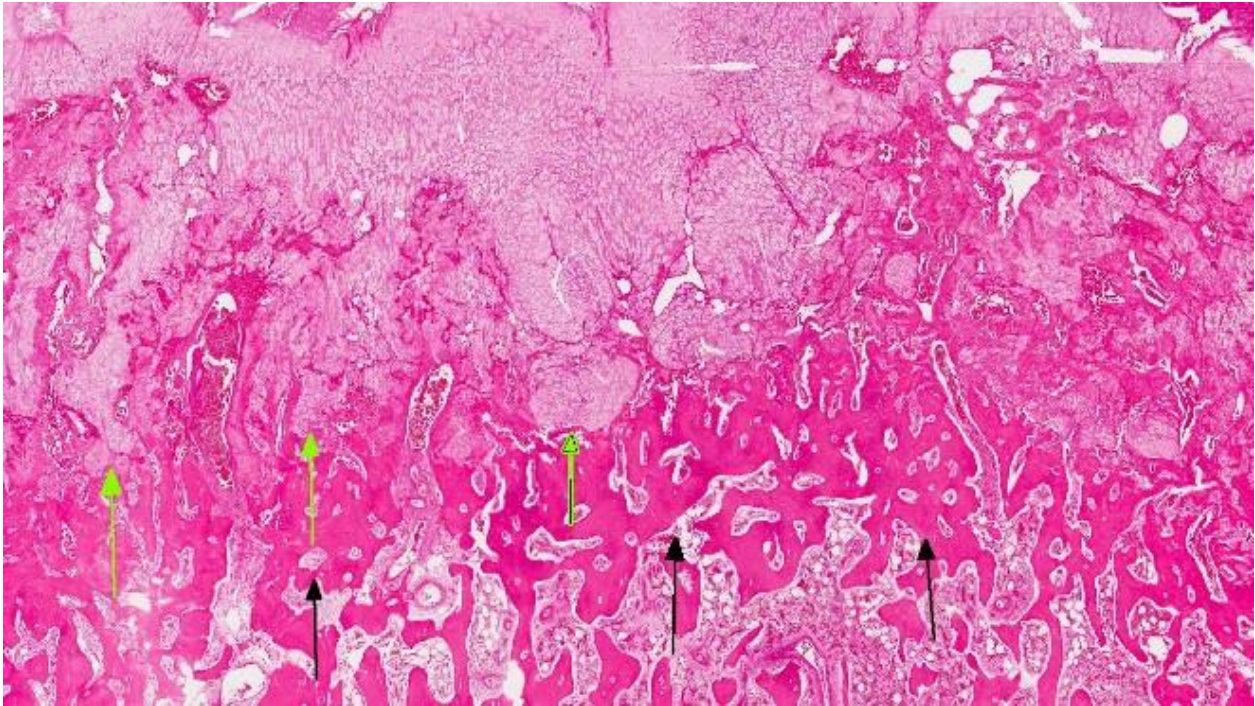
This inherited disease has the potential to be widespread in Corriedale sheep worldwide. A test for heterozygous animals has been developed.

JPC Diagnosis: Rib bone: Physeal chondrodysplasia, diffuse with excessive proliferation of the zone of hypertrophy, retained cartilage cores, lack of mineralization and myelofibrosis.

Conference Comment: The histologic description given in conference was very similar to the contributor's description. The absence of mineralized cartilage and decreased number of normal osteoclasts, along with the abnormal distribution of chondrocytes into disorganized clusters (rather than forming organized columns or rows) with scattered chondrocyte necrosis were also described and discussed. Some conference participants noted the presence of



Rib, sheep. Even at low magnification, long tongues of unremodeled cartilage are visible, extending from the growth plate into the metaphysis. (HE, 4X)



Rib, sheep. Failure of physal chondroclasis has resulted in retention of long, irregularly shaped cores of unmineralized, unre modeled cartilage (green arrows), as well as irregularly, often horizontally anastomosing trabeculae of primary spongiosa. (HE, 14X)

enthesiophytes at sites of tendon/ligament attachment, although this was not a feature present in all slides. This observation led to specific discussion of how enthesiophyte formation relates to the pathogenesis of inherited rickets, as addressed in the contributor's comment above.

The lesions of rickets result from failure of mineralization, which includes both impaired endochondral ossification and failed mineralization of osteoid. This results in the presence of excess osteoid as well as the prominent nodular thickenings of cartilage which are apparent grossly. The enlarged irregular physis is composed of increased numbers of disorganized chondrocytes, as seen in this case. The metaphyses are flared secondary to impaired osteoclast removal of cartilage and unmineralized bone (osteoid) from the cutback zones. Osteoclasts cannot bind unmineralized matrix, impairing remodeling and resulting in accumulation of

unmineralized osteoid and cartilage.¹ Naturally occurring rickets is uncommon in sheep, cattle, horses, dogs, and cats; llamas and alpacas are highly susceptible and pigs are susceptible when they don't receive adequate feed supplementation. There is also a genetic form in pigs which is similar to a condition that occurs in people.⁴ Like rickets, the pathogenesis of osteomalacia also involves defective mineralization, but is a condition that occurs in adult animals after the growth plates have closed and therefore does not involve growth plates. Osteomalacia results in increased amounts of unmineralized osteoid at sites of pressure or stress.

Vitamin D₃ is formed in the skin and can also be absorbed in the diet, as can vitamin D₂. It is stored in fat or transported to the liver where it must undergo the first step of activation, hydroxylation. Once hydroxylated in the liver, 25-hydroxycholecalciferol

[25(OH)D₃], which is the primary form of vitamin D in circulation, must again be hydroxylated in the kidney by 1 α -hydroxylase, to form 1, 25-dihydroxycholecalciferol [1,25(OH)₂D₃], the metabolically active form of vitamin D. Formation of this metabolically active form in the kidney is regulated by serum phosphorus and calcium concentrations and parathyroid hormone. The metabolically active form of vitamin D acts to mobilize calcium from bone in order to maintain serum calcium concentration, by maturation and activation of osteoclasts. The precise mechanism by which vitamin D influences bone growth is not completely understood, but may be indirectly through calcium and phosphorus concentration, or through direct interaction with osteoblasts and chondrocytes.⁴

Contributing Institution:

Institute of Veterinary, Animal and Biomedical Sciences, Massey University, Tennant Drive, Palmerston North, New Zealand

References:

1. Carlson CS, Weisbrode SE. Bones, joints, tendons and ligaments. In: McGavin MD, Zachary JF, eds. *Pathologic Basis of Veterinary Disease*. 5th ed. St. Louis, MO: Mosby Elsevier; 2012:946-949.
2. Dittmer KE, Firth EC, Thompson KG, Marshall JC, Blair HT. Changes in bone structure of Corriedale sheep with inherited rickets: A peripheral quantitative computed tomography assessment. *The Veterinary Journal*. 2011;187: 369-373.
3. Dittmer KE, Howe L, Thompson KG, Stowell KM, Blair HT, Cockrem JF. Normal vitamin D receptor functions with increased expression of 25-hydroxyvitamin D₃-24-hydroxylase in Corriedale sheep with

inherited rickets. *Res Vet Sci*. 2011;91(3):362-369.

4. Dittmer KE, Thompson KG. Vitamin D Metabolism and Rickets in Domestic Animals: A Review. *Vet Pathol*. 2011;48:389-407.
5. Dittmer KE, Thompson KG, Blair HT. Pathology of inherited rickets in Corriedale sheep. *J Comp Path*. 2009;141:147-155.
6. Lorenz-Depiereux B, Bastepe M, Benet-Pages A, Amyere M, Wagenstaller J, Muller-Barth U, Badenhop K, Kaiser SM, Rittmaster RS, Shlossberg AH, Olivares JL, Loris C, Ramos FJ, Glorieux F, Vikkula M, Juppner H, Strom TM. DMP1 mutations in autosomal recessive hypophosphatemia implicate a bone matrix protein in the regulation of phosphate homeostasis. *Nature Genetics*. 2006;38:1248-1250.
7. Pearson OM, Lieberman DE. The aging of Wolff's "law": Ontogeny and responses to mechanical loading in cortical bone. *Yearbook of Physical Anthropology*. 2004;47: 63-99.
8. Rauch F. Material matters. A mechanostat-based perspective on bone development in osteogenesis imperfecta and hypophosphatemic rickets. *Journal of Musculoskeletal and Neuronal Interactions*. 2006;6:142-146.
9. Reid IR, Hardy DC, Murphy WA, Teitelbaum SL, Bergfeld MA, Whyte MP. X-linked hypophosphatemia: A clinical, biochemical, and histopathologic assessment of morbidity in adults. *Medicine*. 1989;68:336-352.
10. Thompson KG. Bones and joints. In: Maxie MG, ed. *Jubb, Kennedy, and Palmer's Pathology of Domestic Animals*. 5th ed.

Vol1. Philadelphia, PA: Elsevier Saunders; 2007:1-184.

CASE II: W361-13 (JPC 4052870).

Signalment: Neonatal female donkey foal (*Equus africanus asinus*).



Mandible, donkey: This donkey foal exhibits marked brachygnathism inferior. (Photo courtesy of: Faculty of Veterinary Science, University of Melbourne www.vet.unimelb.edu.au)

History: A middle-aged donkey jenny was presented to the University of Melbourne for imminent parturition. The sire of the foal was unknown. Foaling was routine and the foal was bright and vigorous, but approximately one hour post-parturition the foal suffered a fracture of the right tibia during an attempt to stand. Radiographs indicated a displaced spiral fracture of the distal tibial diaphysis and metaphysis. The tibia and femur also had radiographic evidence of reduced medullary cavity size, thickened mid-diaphyseal cortices, and conical metaphyseal bone extending toward the mid-diaphysis. Due to the suspicion of underlying bone disease, the foal was euthanized with owner consent.

Gross Pathology: The animal displayed marked brachygnathism inferior and failure of dental eruption. All bones were brittle and

easily cut with a knife. There was an acute spiral fracture extending along the left tibia, as well as a non-displaced fracture of the right transverse process of the L2 vertebrae. Focal bone thickenings (callouses) and hemorrhages were present over the midpoint of the ribs bilaterally from T6-T13, and the orientation of the ribs was deviated. On sectioning, all long bones displayed thickened cortices and large cores of intramedullary trabecular bone that extended along the diaphysis from both the proximal and distal metaphysis, with severe reduction in medullary space.

Laboratory Results: None

Histopathologic Description:

Long bone, metaphysis: Extending from the growth plate through the medullary cavity of the metaphysis there is a marked increase in the extent of metaphyseal trabeculae. Trabeculae are disorganized and are composed of irregular cores of retained cartilage derived from the hypertrophic zone of the physis, overlaid and interspersed by mineralized bone. Towards the diaphysis there is a progressive decrease in trabecular size and number, and



Mandible, donkey: Radiographs of the head demonstrate that the teeth are present, but have failed to erupt. (Photo courtesy of: Faculty of Veterinary Science, University of Melbourne www.vet.unimelb.edu.au)

intertrabecular medullary spaces contain foci of hematopoietic cells within loose fibroadipose connective tissue. The cortex is markedly thickened and poorly compacted, with cortical bone arranged in longitudinal lamellae separated by loose fibrovascular and adipose tissue with occasional sparse bone marrow infiltration. Osteoclast numbers throughout the section are markedly decreased, and there is no evidence of reversal lines or Howship's lacunae within the section.



Tibia, donkey: Radiographs of long bones of the hindlimb show a markedly increased density of the diaphysis. (Photo courtesy of: Faculty of Veterinary Science, University of Melbourne www.vet.unimelb.edu.au)

Contributor's Morphologic Diagnosis: Bone: Osteopetrosis, diffuse, donkey (*Equus africanus asinus*).

Contributor's Comment: Osteopetrosis (AKA marble bone disease) is a heterogeneous disease process characterized by defective osteoclastic bone resorption, resulting in failure of bone

remodeling and dense, fragile bones that fracture readily. The condition has been reported in a number of species, including Angus, Hereford and Simmental cattle, Peruvian Paso and Appaloosa horses, white-tailed deer, rabbits and several dog breeds.¹² To the author's knowledge, this is the first case observed in a donkey. Brachygnathia inferior is a common finding in affected animals, reflecting failure of mandibular growth, and dental eruption is typically impaired, as this process requires bone resorption. Anemia has also been reported in some cases, as well as leukopenia and immune deficiencies such as hypoglobulinaemia.^{1,6} Anemic animals often display hepatosplenomegaly due to prominent extramedullary hematopoiesis. Hematological assessment was not performed in the present case, but the presence of abundant hematopoietic tissue within the medullary cavity, as well as a lack of extramedullary hematopoiesis in the liver and spleen, suggest that marrow function was adequate. In humans, failure of bone remodeling has also been associated with nerve entrapment and compression, most commonly manifesting as blindness and



Ribs, donkey: Calluses and hemorrhages, representing previous fractures were seen on ribs 6-13. (Photo courtesy of: Faculty of Veterinary Science, University of Melbourne www.vet.unimelb.edu.au)



Long bones, donkey: Large cores of intramedullary trabecular bone that extended along the diaphysis from both the proximal and distal metaphysis, with severe reduction in medullary space. (Photo courtesy of: Faculty of Veterinary Science, University of Melbourne www.vet.unimelb.edu.au)

deafness, though these feature have not been noted in domestic species.

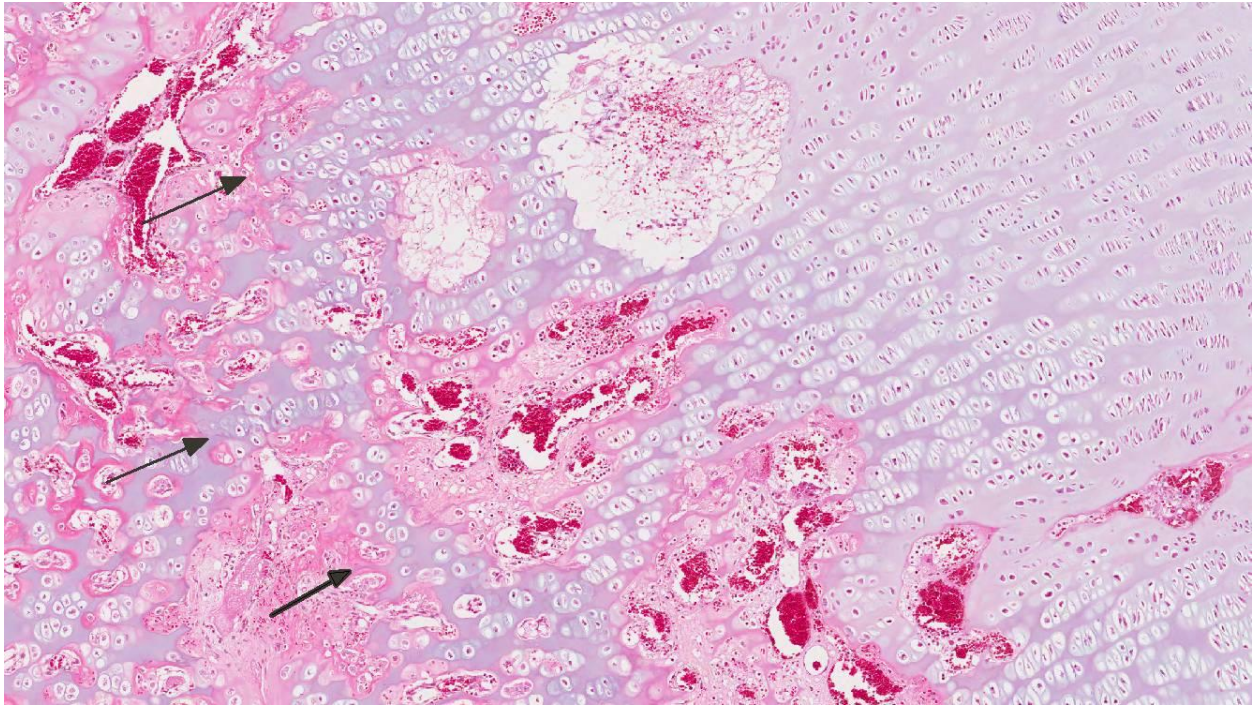
Osteopetrosis occurs in various forms, but the disease typically reflects either functional osteoclast impairment (such as defects in carbonic anhydrase or the H⁺-ATPase proton pump)¹³ or depletion of the osteoclast cell population. Many cases in domestic species are suspected to represent genetic defects with autosomal recessive heritability, but the specific mutation has so far only been identified in Angus cattle, which display a deletion mutation of the *SLC4A2* anion exchanger.⁸ The *SLC4A2* defect results in

failure of acidification at the sites of remodeling and defective bone demineralization. Osteoclasts are rare in the Angus form of disease, but animals with functional osteoclast defects typically have adequate or increased osteoclast numbers, though the osteoclasts may display morphological abnormalities such as hypertrophy, increased numbers of nuclei or absence of a ruffled border.

Osteopetrosis caused by failure of osteoclast development is rare, but osteoclast-poor disease with autosomal recessive heritability exists in humans. Osteoclast differentiation is dependent on RANK/RANKL (Receptor Activator of Nuclear Factor- κ B/ Receptor Activator of Nuclear Factor- κ B Ligand) signaling, and mutations in genes responsible for this receptor/ligand pair (*TNFRSF11A* and *TNFRSF11*, respectively) lead to the profound osteoclast deficiency.^{11,5} In mouse models, osteopetrosis is also observed with defects in a range of other genes associated with osteoclast differentiation, but these



Tibia, donkey. A total lack of physcal remodeling has resulted in a thick core of unremodeled primary spongiosa extending into the diaphysis. (HE, 4X)



Tibial physis, donkey. There is marked persistence of the physal zone of hypertrophy. Cartilage cores bridge in a horizontal fashion (arrows) as well as laterally, and there are large areas of degenerate cartilage with minimal osteoid deposition or mineralization. (HE, 35X)

have not been described in natural disease.³ The depletion of osteoclasts in the present case suggests it may be a different form of osteopetrosis to that described in most other equine cases, which typically display normal to increased osteoclast numbers. However, a single case of osteoclast-poor osteopetrosis has been reported in a Peruvian Paso foal.⁸

Acquired osteopetrosis-like disease has been reported secondary to a number of viral infections, presumably reflecting viral osteoclast tropism and cell depletion. Zonal lesions consistent with osteopetrosis have been reported with bovine viral diarrhoea virus in cattle,⁹ and similar features have been identified in the metaphyseal region of dogs with distemper and cats infected with feline leukaemia virus.¹² Osteosclerotic disease similar to osteopetrosis has also been reported associated with

hypervitaminosis,⁶ lead poisoning,¹² and exogenous oestrogen⁵ and glucocorticoid administration.⁴ Cases of rickets may display retention of cartilaginous metaphyseal trabeculae overlaid by osteoid, similar to those observed in osteopetrosis. In rickets, however, the trabeculae are poorly mineralized, while the bone in cases of osteopetrosis undergoes normal mineralization.

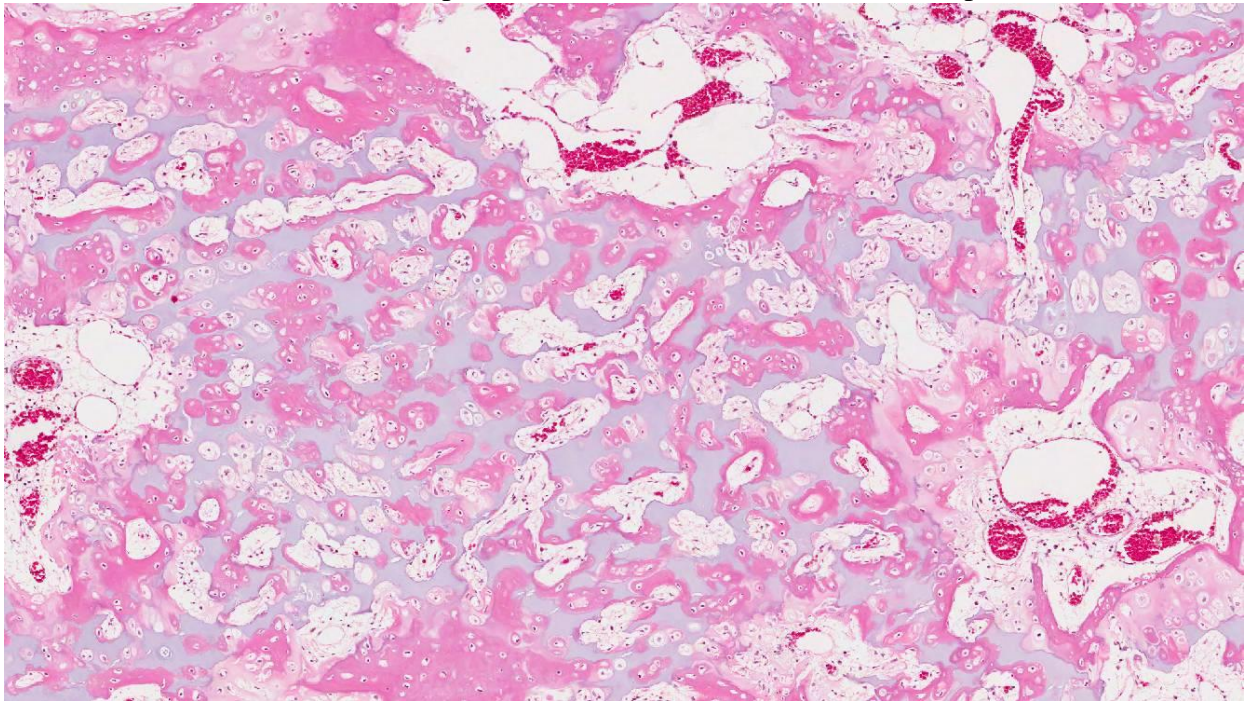
JPC Diagnosis: Long bone: Physal dysplasia, diffuse, severe with osteoclast depletion, failure of chondroclasis, cortical osteopenia and diffuse medullary osteosclerosis (osteopetrosis).

Conference Comment: The histologic description discussed in conference was very similar to the contributor's. The noted primary features included increased bony trabeculae arranged in disorganized transverse and longitudinal arrays with

persistent cartilage cores, absence of osteoclasts, decreased bone marrow elements, absence of a cutback zone and cortical osteopenia. The physal zones involved in endochondral ossification appear histologically normal until subjacent to the zone of hypertrophy, where osteoclasts would normally be present remodeling mineralized cartilage, but in this case are absent. Cortical osteopenia, including multiple thin, widely separated longitudinal bands of bone, was also described and discussed as a feature not commonly associated with osteopetrosis, and there was speculation it may reflect a secondary process. The gross images were viewed during conference, and there was discussion regarding the multiple callouses and hemorrhages on the ribs being secondary to in utero fracture.

There are two main forms of osteopetrosis described in humans: a recessively inherited lethal form in which lesions are present at

birth, and a dominant form which manifests in adults.² Osteopetrosis in Red Angus calves with a deletion mutation in the gene *SLC4A2*, which encodes the anion exchanger for carbonate and chloride, has recently been compared to the recessive form which occurs in children, and aspects of the craniofacial lesions were found to be similar. Craniofacial lesions in affected calves include dorsoventrally compressed brains with depressions of the parietal cortex due to thickening of the parietal bone; compression of the cerebral hemispheres with vermis herniation through the foramen magnum; chromatolysis in multiple cranial nerve nuclei; optic nerve atrophy; loss of retinal ganglion cells; and dysplastic changes in the molar and premolar teeth. There was also corpora amylacea in the thalamus, basal nuclei and midbrain, and mineralization in vessels of the thalamus. One important difference noted between the condition in Red Angus calves and the recessive lethal form in humans is the presence of increased



Tibial diaphysis, donkey. There is extensive unremodeled and degenerating primary spongiosa with thin lining osteoid seams within the diaphysis. Marrow spaces are markedly decreased in volume and lack hematopoietic precursors. (HE, 35X)

numbers of osteoclasts in people, while decreased numbers of osteoclasts were present in the long bones of affected calves. Osteoclast numbers in calves, however, were more normal in bones of the head. Affected calves died in utero or shortly after birth and were either homozygous or heterozygous for the *SLC4A2* mutation, respectively.⁹ Long bone lesions in affected calves included dense unresorbed bony trabeculae from the metaphysis to the central diaphysis, similar to what is present in other species.²

The specific type of osteoclast defect present influences the number of osteoclasts, whether increased, decreased, or absent, in various types of osteopetrosis. For example, in mutations involving the chloride channel (*CICN7*) or the proton pump (*ATP6i*), osteoclasts may be present in increased numbers but are nonfunctional; however, in mutations involving the *RANKL* gene, necessary for proper osteoclast differentiation, osteoclasts are decreased or absent. Osteopetrosis in Hereford and Simmental breeds of cattle is similar to the condition in Angus calves. One difference is the presence of thickened frontal bones with cystic spaces, creating a domed forehead that can be mistaken for hydrocephalus. Osteopetrosis is described in Belgian Blue cattle in Europe in combination with abnormal skull formation and mandibular gingival hamartomas. A mutation was identified in the chloride / proton exchanger lysosomal anion transporter *CICN7* in affected calves. Osteopetrosis is also described in inbred Polypay sheep and white-tailed deer, both of which also have brachygnathia inferior, a common finding in many affected species. The white-tailed deer also have calluses on several ribs, similar to the disease in horses, suggesting in utero rib fractures. Osteopetrosis has been documented in dogs but is poorly characterized.²

Contributing Institution:

Faculty of Veterinary Science, University of Melbourne

www.vet.unimelb.edu.au

References:

1. Berry CR, House JK, Poulos PP, et al. Radiographic and pathologic features of osteopetrosis in two Peruvian Paso foals. *Veterinary Radiology & Ultrasound*. 1994;35:355-361.
2. Craig LE, Dittmer KE, Thompson KG. Bones and Joints. In: Maxie MG, ed. *Jubb, Kennedy, and Palmer's Pathology of Domestic Animals*. 6th ed. Vol1. St. Louis, MO: Elsevier; 2015:49-53.
3. Del Fattore A, Cappariello A, Teti A. Genetics, pathogenesis and complications of osteopetrosis. *Bone*. 2008;42:19-29.
4. Glade MJ, Krock L. Glucocorticoid-Induced inhibition of osteolysis and the development of osteopetrosis, osteonecrosis and osteoporosis. *Cornell Vet*. 1982;72:76-91.
5. Guerrini MM, Sobacchi C, Cassani B, et al. Human osteoclast-poor osteopetrosis with hypogammaglobulinemia due to TNFRSF11A (RANK) mutations. *Am J Hum Genet*. 2008;83:64-76.
6. Kramers P, Fluckiger MA, Rahn BA, et al. Osteopetrosis in Cats. *Journal of Small Animal Practice*. 1988;29:153-164.
7. Meyers SN, McDanel TG, Swist SL, et al. A deletion mutation in bovine *SLC4A2* is associated with osteopetrosis in Red Angus cattle. *BMC Genomics*. 2010;11:337.
8. Nation PN, Klavano GG. Osteopetrosis in two foals. *Can Vet J*. 1986;27:74-7.
9. O'Toole D, Swist S, Steadman L, Johnson GC. Neuropathology and

craniofacial lesions of osteopetrotic Red Angus calves. *Vet Pathol.* 2012;49(5):746-754.

10. Scruggs OW, Fleming SA, Maslin WR, et al. Osteopetrosis, anemia, thrombocytopenia, and marrow necrosis in beef calves naturally infected with bovine virus diarrhea virus. *J Vet Diagn Invest.* 1995;7:555-9.

11. Sobacchi C, Frattini A, Guerrini MM, et al. Osteoclast-poor human osteopetrosis due to mutations in the gene encoding RANKL. *Nat Genet.* 2007;39:960-2.

12. Thompson K. Diseases of Bones and Joints. In: Maxie MG, ed. *Jubb, Kennedy and Palmer 's Pathology of Domestic Animals.* 5th ed. Vol1. Philadelphia, PA: Elsevier Ltd; 2007:24-40, 75-80.

13. Tolar J, Teitelbaum SL, Orchard PJ. Osteopetrosis. *N Engl J Med.* 2004;351:2839-49.

CASE III: 13073102 (JPC 4053418).

Signalment: 24 week-old male Lewis rat (*Rattus norvegicus*)

History: The L5 lumbar intervertebral disc was subjected to surgical puncture. Necropsy and tissue collection were performed two months post-procedure.

Gross Pathology: No description provided

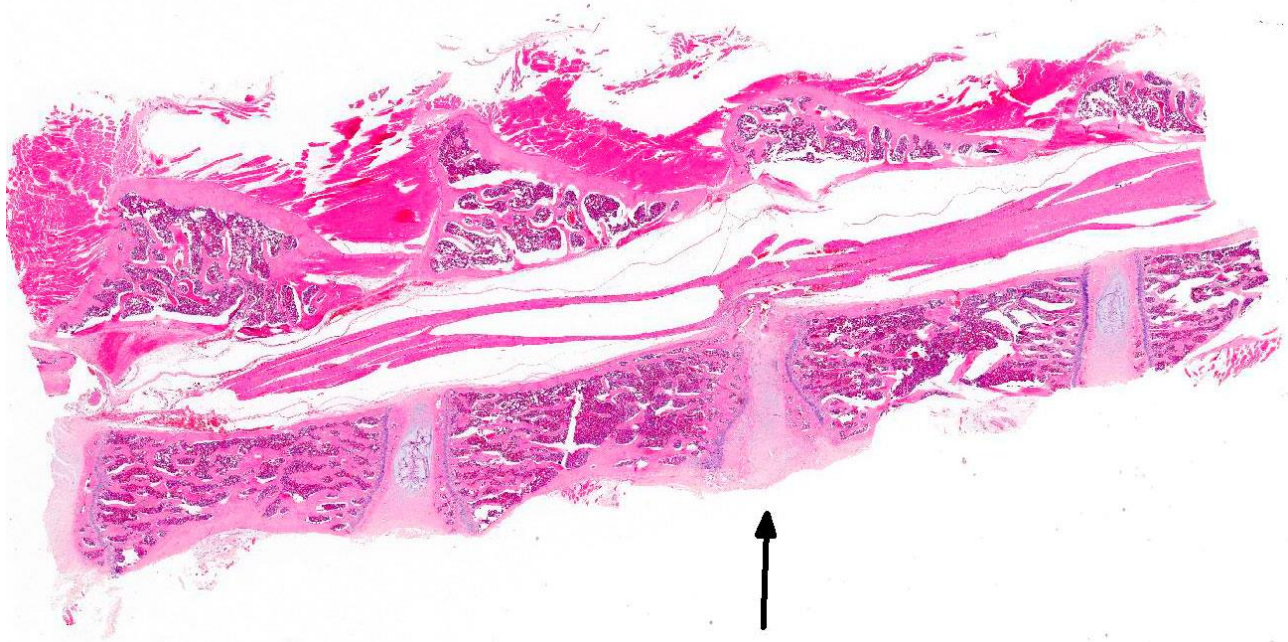
Laboratory Results: N/A

Histopathologic Description: Located centrally within this parasagittal section of decalcified lumbar spinal column is a degenerate intervertebral disc flanked by two normal discs. The degenerate disc exhibits loss of the central nucleus pulposus and

replacement of the normal lamellar arrangement of the annular fibrosus by disorganized fibrocartilage and hyaline cartilage (Figure 1). In particular, the dorsal annulus has been replaced by a mass of disorganized hyaline cartilage capped by proliferating fibrovascular tissue and metaplastic woven bone that bulges into the spinal canal and compresses overlying degenerating cauda equine nerves. On one side of the degenerate disc, epiphyseal lamellar bone and portions of physeal cartilage have been replaced by disorganized hyaline cartilage containing zones of granular degenerate matrix (Figure 2). Residual physeal cartilage is variably disorganized and there is mildly increased thickness of adjacent metaphyseal trabecular bone (osteosclerosis).

Contributor's Morphologic Diagnosis: Intervertebral disc: Degeneration, focal, chronic, with focal osseous metaplasia and compressive cauda equina nerve degeneration.

Contributor's Comment: Vertebral disc degeneration is a serious condition in humans that may occur during aging or be induced through injury. Vertebral disc degeneration results in a diminished load carrying capacity leading to the inability to perform basic tasks.³ Several animal models have been developed to mimic human vertebral disc degeneration (Table 1), often involving mechanical interventions such as altered loading, altered motion, or incited disc injury, and are used to explore disease pathogenesis and to test possible treatments. Important considerations for the selection of the model system and interpretation of experimental results are related to differences in anatomy, physiology, and biomechanics between humans and the various model species.¹ The



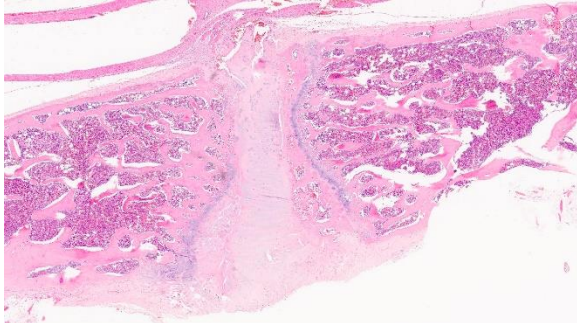
Thoracic spine, rat. One vertebral space is compressed (arrow) due to removal of the nucleus pulposus. (HE, 5X).

case presented here involves a rat model of vertebral disc degeneration in which a minor needle puncture injury to the annulus fibrosus causes degenerative changes in the intervertebral disc and adjacent vertebrae.

The normal intervertebral disc is avascular and primarily aneural. It is comprised of a dynamic extracellular matrix as well as a fibrocartilaginous network that maintains tensile strength. Importantly, there is normally a clear morphological distinction between the peripheral annulus fibrosus (AF) and inner nucleus pulposus (NP).⁹ The composition of the outer AF is primarily type I collagen fibers that are aligned at approximately 30° angles to the longitudinal axis of the spine. The direction of the type I fibers alternates in each concentric layer of the disc in an orientation designed to provide maximal strength. These collagen fibers also align with the cells of the AF, which are fibroblast-like with elongated nuclei. The inner layer of the disc, the nucleus pulposus

(NP), contains a viscous proteoglycan gel, a small amount of type II collagen, and (in humans; see more below) chondrocyte-like, rounded cells.⁵ The proteoglycan gel is primarily composed of aggrecan, which is extremely hydrophilic. The aggrecan absorbs water and creates a swelling pressure responsible for maintaining tissue hydration and balancing the osmolarity of the disc.⁹ Consequently, a hydrostatic pressure is created within the nucleus, which is contained by the lamellae of the annulus, and distributes loads evenly across the underlying/adjacent vertebrae.³

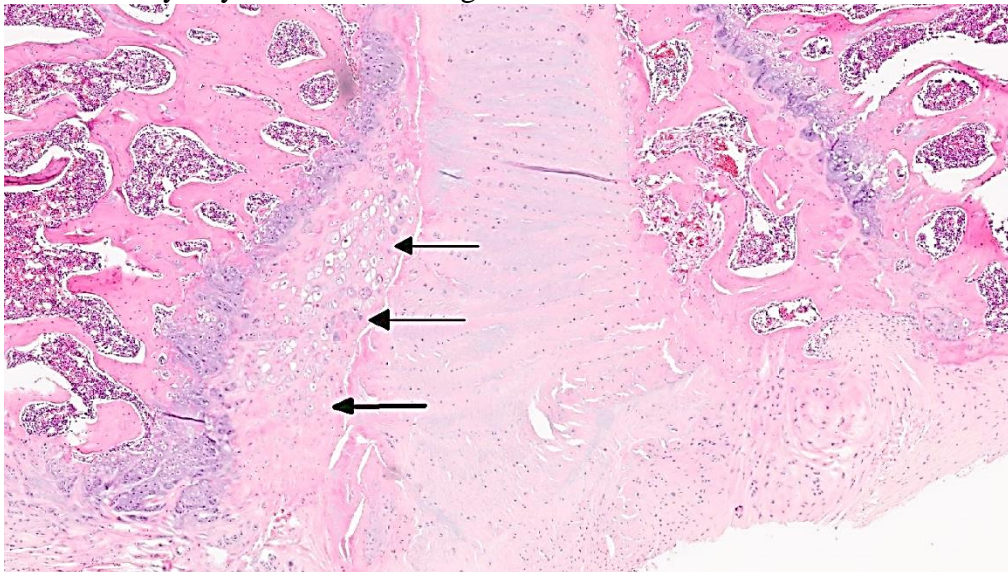
Vertebral disc injury causes a degradative cascade that leads to both physiological and morphological changes. The degenerative changes involve increased breakdown of matrix, altered matrix synthesis, and cell loss through apoptosis. Fissures in the outer annulus may cause bulging of the disc⁴ and aggrecan degeneration of the nucleus pulposus leads to infiltration of nerve endings and blood vessels into the normally avascular



Higher magnification of the anuclear disk space. (HE, 8X)

disc, resulting in pain. Loss of aggrecan also causes a decrease in hydration and swelling pressure, causing decreases in disc height and alterations in load carrying capacity.⁹

In a damaged disc, there eventually is no clear morphologic distinction between the AF and the NP. Over time, the organization of the chondrocyte-like NP cells is lost as these cells are replaced by fibrosis characterized by decreased type II collagen and increased type I and type X collagen.^{4,5} The predictable pattern of the AF cells becomes disorganized as cells are lost or become arranged in clusters.⁹ Finally, disc injury also causes the recruitment of inflammatory cytokines and degradative



There is remodeling and thickening of the vertebral endplate to the compressed disk space. The remodeled endplate contains disordered chondrones of proliferating chondrocytes. (HE, 39X)

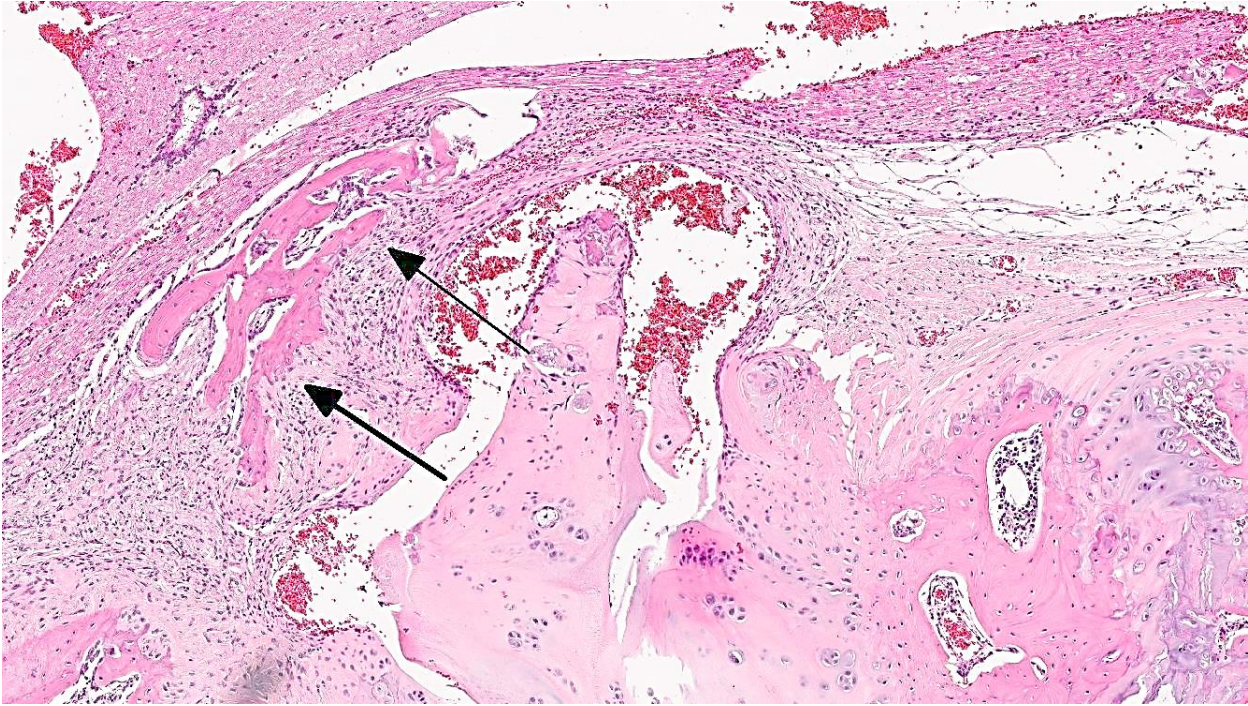
enzymes. IL-1, the primary cytokine in the damaged disc, inhibits the production of the extracellular matrix and stimulates additional cytokine production.⁵ As additional cytokines are recruited to the damaged disc, apoptotic cell death ensues.

There are several differences in the development, cell composition, anatomy, physiology, and mechanical properties of intervertebral discs between humans and animals.¹ The composition of the nucleus pulposus and the organization of the cartilage endplates are two notable examples of differences between humans and many animal species. Throughout the life of rats the nucleus pulposus is composed of notochordal cells, which are large, highly vacuolated, loosely arranged, produce large quantities of hyaluronin, and influence the metabolism of other cell types within the disc. In contrast, numbers of notochordal cells decrease rapidly in the nucleus pulposus of young humans and in adults are replaced by chondrocytic cells.

In rats and many other species the secondary ossification centers of the vertebral body

form a complete osseous epiphyseal plate between the intervertebral disc and the vertebral body physis and this persists throughout the life of the animal. In

humans, however, the epiphysis from the secondary ossification center exists as a ring adjacent to the outer



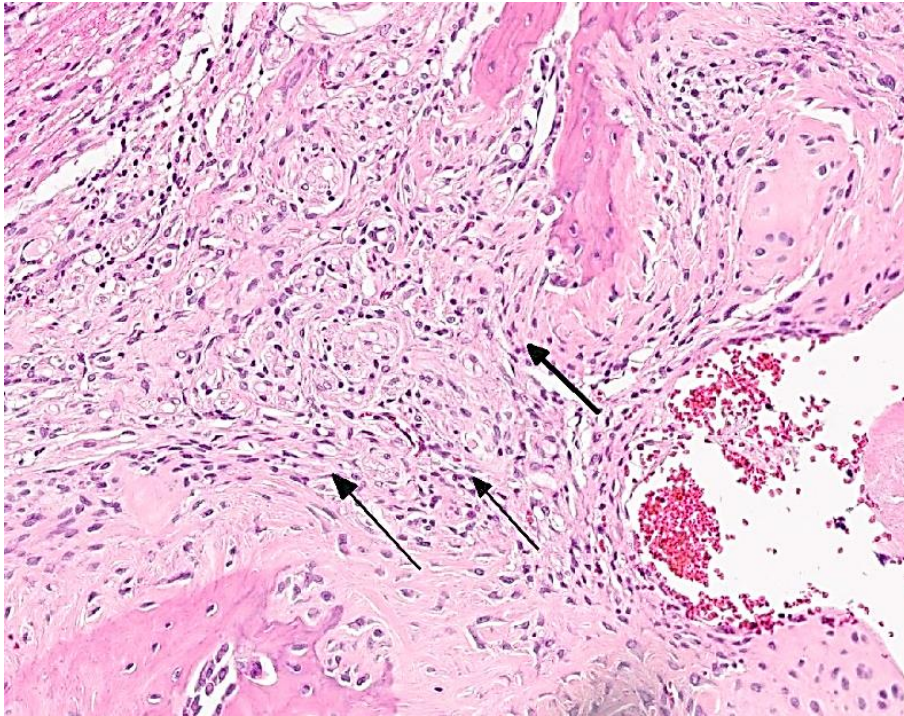
The degenerating annulus fibrosus (surrounded by a venous sinus) is prolapsed dorsally against the ventral longitudinal ligament. There is an osteophyte of woven bone embedded within a focus of fibrosis involving spinal nerves and the ventral longitudinal ligament adjacent to the prolapsed disk (HE, 50X).

annulus fibrosus rather than as a complete plate adjacent to the disc and the physis closes at about 25 years of age. Because of this the base of the cartilage endplate acts as the growth region for the vertebral body in humans while in most other species vertebral body growth occurs via the epiphyseal plates. The relevance and translatability to humans of results obtained from studies of disc degeneration using animal models must consider the potential impact of differences such as these.

JPC Diagnosis: Intervertebral disc: Disc rupture and prolapse with degeneration of the annulus fibrosus, end plate collapse, vertebral osteophytosis and mild focal spinal nerve compression and degeneration.

Conference Comment: The contributor provides a thorough histologic description which is very similar to the description given during the conference. There was

speculation as to whether the small section of bone dorsal to the vertebral body represents an osteophyte or is bone fractured during the surgical puncture procedure. Additionally, a focal area with interwoven streams and bundles of spindle cells adjacent to this area of bone has a distinct neural morphology, and there was conjecture whether this may represent an incipient traumatic neuroma. The chondrocytes were described as being hypertrophied, hyperplastic and reactive, manifesting as multiple large chondrocytes trapped within a single lacuna. There were also areas of chondrocyte necrosis and the vacuolated, degenerate chondrocytes. The moderator led a discussion on how bone reacts to injury, demonstrated in this case as epiphyseal endplate merger with the annulus fibrosus, a manifestation of degenerative intervertebral disc disease. Please note, the digital image is upside down and must be flipped vertically for the proper anatomic orientation.



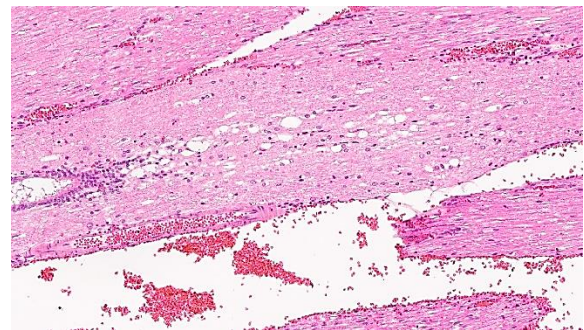
There is a focal proliferation of small nerve bundles (neuroma) immediately adjacent to the dorsal aspect of the prolapsed disk. (HE, 65X)

Degeneration of intervertebral discs is a particularly important disease not only in people, but also in dogs. It occurs in all dog breeds but there are significant differences in the pathogenesis between chondrodystrophic and nonchondrodystrophic breeds. Chondrodystrophic breeds have an increased expression of fibroblast growth factor 4 (FGF4), which affects not only appendicular skeleton formation, but also the composition of the nucleus pulposus (NP) in their intervertebral discs. In these breeds the NP contains a much greater content of collagen than proteoglycan, and collagen content can increase over time in the degeneration process, decreasing water content and the disc's ability to adequately absorb mechanical forces. The NP begins to degenerate very early in life, and microscopically this is seen as chondrocyte proliferation and lobulation of the NP. These changes occur in all intervertebral discs. Eventually the NP with higher collagen content begins to degenerate, harden and may

mineralize, becoming friable, and the inner aspects of the annulus fibrosis (AF) can also begin to degenerate and tear, allowing fragments of NP to enter the AF. These changes can extend through the AF, resulting in a Hansen type I intervertebral disc herniation, with fragments of degenerate NP extending through the dorsal longitudinal ligament into the spinal canal. This most frequently results in local myelomalacia in the affected spinal cord region with

accompanying inflammation, but can result in ascending myelomalacia in some severe cases.²

Nonchondrodystrophic breeds do not suffer the same type of degeneration and mineralization of the NP as chondrodystrophic breeds. The NP in their intervertebral discs may undergo degeneration and fibrous metaplasia, but it occurs later in life and generally only affects a single disc or few discs are involved, and



Dorsal to the prolapsed annulus fibrosis, the spinal cord contains low to moderate numbers of dilated myelin sheaths. (HE, 75X)

the degeneration is thought to be related to trauma and disruption of the annulus fibrosus. These changes result in a Hansen type II herniation which refers to partial herniation of the NP through the AF, bulging of the AF, and compression of the dorsal longitudinal ligament, which may then impinge on the spinal cord. Type II herniations in general result in less severe disease. Disc herniations most commonly occur dorsally or dorso-laterally, but can also occur ventrally, cranially and caudally. Cranial and caudal herniation of the nucleus pulposus into the vertebral body creates a lesion known as a Schmorl's node within the vertebral endplate. Intervertebral disc herniations are rare in other species but have been documented in the cervical region of horses, similar to type II lesions in dogs. Sows and boars have also been documented to have degenerative intervertebral disc changes, but not dorsal herniation of the NP.²

Contributing Institution:

Eli Lilly and Company, Investigational Pathology, Indianapolis, IN 46285
www.lilly.com

References:

1. Alini M, Eisenstein SM, Ito K, et al. Are animal models useful for studying human disc disorders/degeneration? *Eur Spine J.* 2008; 17:2-19.
2. Craig LE, Dittmer KE, Thompson KG. Bones and Joints. In: Maxie MG, ed. *Jubb, Kennedy, and Palmer's Pathology of Domestic Animals*. 6th ed. Vol1. St. Louis, MO: Elsevier; 2015:142-147.
3. Ferguson SJ, Steffen T. Biomechanics of the aging spine. *Eur Spine J.* 2003; 12:S97.103.
4. Keorochana G, Johnson J, Taghavi C, et al. The effect of needle size inducing generation in the rat caudal disc: evaluation

using radiograph, magnetic resonance imaging, histology, and immunohistochemistry. *The Spine Journal.* 2010; 10: 1014-1023.

5. Kepler C, Ponnappan R, Tannoury C, et al. The molecular basis of intervertebral disc degeneration. *The Spine Journal.* 2013: 318-330.
6. Phillips FM, Reuben J, Wetzel FT. Intervertebral disc degeneration adjacent to a lumbar fusion: an experimental rabbit model. *J Bone Joint Surg Br.* 2002; 84: 239-294.
7. Singh K, Masuda K, An H. Animal models for human disc degeneration. *The Spine Journal.* 2005; (5): 267S-279S.
8. Sun F, Qu J, Zhang Y. Animal models of disc degeneration and major genetic strategies. *Pain Physician.* 2013; (16): E267-E275.
9. Urban J, Roberts S. Degeneration of the intervertebral disc. *Arthritis Research and Therapy.* 2003; (5): 120-130.

CASE IV: 66898 (JPC 4066452).

Signalment: 7-year-old, female intact, reticulated giraffe (*Giraffa camelopardalis reticulata*).

History: This adult female reticulated giraffe was born and housed at the Maryland Zoo in Baltimore. In 2011, the animal had an acute onset of right front limb lameness with swelling of the right front fetlock. Traumatic injury was suspected. Although the animal improved slightly with multiple courses of treatment (topical and systemic non-steroidal anti-inflammatory medications, chondroprotective supplements, analgesics and topical steroids), lameness and swelling in the right front fetlock persisted with episodes of acute



Carpal joint, giraffe. Upon opening, the carpometacarpal joint has extensive proliferation of hemorrhagic tissue within the joint, as well as marked thickening of the joint capsule. (Photo courtesy of: Department of Molecular and Comparative Pathobiology, Johns Hopkins University, 733 N. Broadway, Suite 811, Baltimore, MD 21205)

worsening of clinical signs over a 3-year period. Ultrasonography and thermography of the fetlock in early 2012 showed changes consistent with chronic osteoarthritis. Intra-articular injections of hylartin and depomedrol were performed with minimal improvement. Ultimately, the animal was euthanized in 2014 at the age of 17 due to progression of chronic lameness.

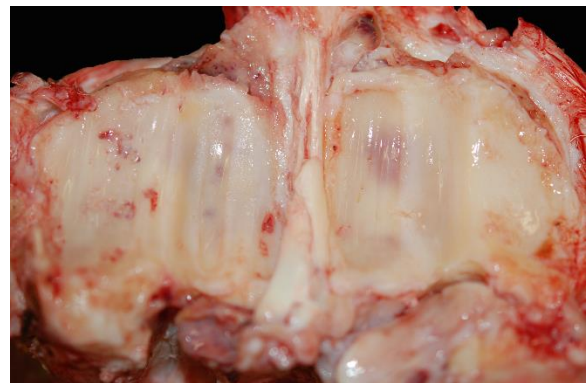
Gross Pathology: At necropsy, the right front fetlock was severely swollen and soft on palpation. Aspiration of the affected joint yielded a large amount of turbid red fluid with low viscosity. Joint fluid cytology revealed many non-degenerate neutrophils, with occasional lymphocytes and macrophages on a proteinaceous background. Aerobic bacterial culture of joint fluid was negative. The articular surface of the carpometacarpal joint contained multiple variably-sized areas of cartilage fibrillation and erosion, and in several areas there was exposure and eburnation of the underlying subchondral bone. The periarticular cartilage contained numerous small osteophytes. The synovial lining was diffusely thickened and discolored red to tan, with numerous small pinpoint areas of hemorrhage. On the palmar aspect of the fetlock, deep to the deep digital

flexor tendon, the tendon sheath was multifocally adhered to the underlying fascia by abundant, dark red-brown granulation tissue. Within this reactive tissue and also multifocally throughout the joint capsule were multiple variably sized firm yellow-tan smooth nodules, which were well demarcated and encapsulated.

Additional gross findings in this animal included mild to moderate, chronic active osteoarthritis in multiple joints with varying degrees of fibrinous effusion and synovial hyperplasia, multifocal renal cortical fibrosis, severe dental disease, and a benign ovarian tumor.

Laboratory Results: None

Histopathologic Description: Submitted slides may contain sections of synovium and tendon sheath or just tendon sheath. Arising from the flexor tendon sheath is a well-demarcated, partially encapsulated, densely cellular mass. The majority of cells within the mass resemble well-differentiated macrophages and fibroblasts on an intervening dense collagenous stroma. A low number of cells (less than 10% of the cell



Carpal joint, giraffe. The articular surface of the carpometacarpal joint contained extensive cartilaginous fibrillation and erosion, with multifocal exposure and eburnation of the underlying subchondral bone. (Photo courtesy of: Department of Molecular and Comparative Pathobiology, Johns Hopkins University, 733 N. Broadway, Suite 811, Baltimore, MD 21205.)

mass) are characterized by abundant eosinophilic finely vacuolated cytoplasm, large size (up to 200µm), and contain up to 50 nuclei arranged centrally within the cell. There is mild multifocal hemorrhage throughout the mass, and macrophages frequently contain abundant brown granular pigment, which stains positively with Prussian blue (hemosiderin). The mass is diffusely infiltrated by moderate numbers of neutrophils along with fewer lymphocytes and plasma cells, and is almost entirely surrounded by a dense fibrous connective tissue capsule.



Joint capsule, giraffe: The synovium of the affected joint is thrown into thick frond-like villar projections. (HE, 5X)

The synovium of the affected fetlock is diffusely and markedly hyperplastic with numerous thick frond-like villous projections. The synovium is expanded by a large population of mixed inflammatory cells with large numbers of neutrophils, and moderate granulation tissue. Occasionally, hyperplastic synovial villi contain large multinucleated cells, which are morphologically identical to those seen within the nodule in the adjacent tendon sheath.

Immunohistochemically, large multinucleated cells all exhibit strong, cytoplasmic reactivity for cathepsin K and moderate cell membrane reactivity for IBA-1 (ionized

calcium-binding adapter molecule 1). Multinucleated cells were negative for lysozyme immunostaining. Mononuclear, macrophage-like cells throughout the mass exhibit strong cytoplasmic reactivity for cathepsin K, while a smaller proportion of mononuclear cells showed moderate cytoplasmic reactivity for IBA-1 and lysozyme.

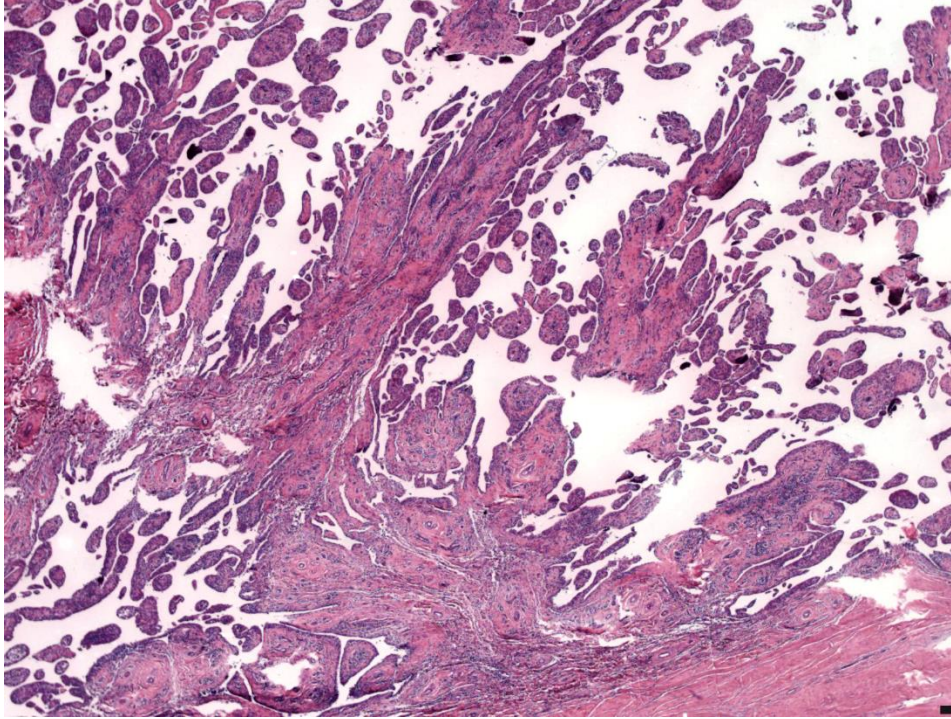
Contributor's Morphologic Diagnosis:

Fetlock, pigmented villonodular tenosynovitis, diffuse, chronic-active, severe with moderate neutrophilic inflammation, hemorrhage, and moderate intrahistiocytic hemosiderin.

Contributor's Comment:

Gross and histologic findings in this case are consistent with a diagnosis of pigmented villonodular tenosynovitis (PVNS), a condition which occurs in humans and has been reported in a range of animal species including dogs, horses, and a European lynx.^{3, 5, 7} Nodules seen in this condition are characterized histologically by abundant connective tissue, heavy macrophage and fibroblast infiltration, and large multinucleated giant cells which morphologically resemble osteoclasts. The pigmented appearance of these nodules is the result of intrahistiocytic hemosiderin accumulation thought to be secondary to recurrent intra-articular hemorrhage. This syndrome belongs to a group of histologically similar conditions that likely represent a spectrum of the same process. Localized forms are also sometimes referred to as "localized nodular tenosynovitis" or "benign giant cell tumor of tendon sheath."

The etiology of this condition is uncertain, with debate over whether these lesions represent a primarily neoplastic or inflammatory process. Although these lesions are considered almost universally benign, rare reports of distant metastasis have occurred,¹ and localized forms may exhibit local recurrence after surgical excision.⁸



Joint capsule, giraffe. Higher magnification of the villar synovial proliferation. (HE,40X) (Photo courtesy of: Department of Molecular and Comparative Pathobiology, Johns Hopkins University, 733 N. Broadway, Suite 811, Baltimore, MD 21205.)

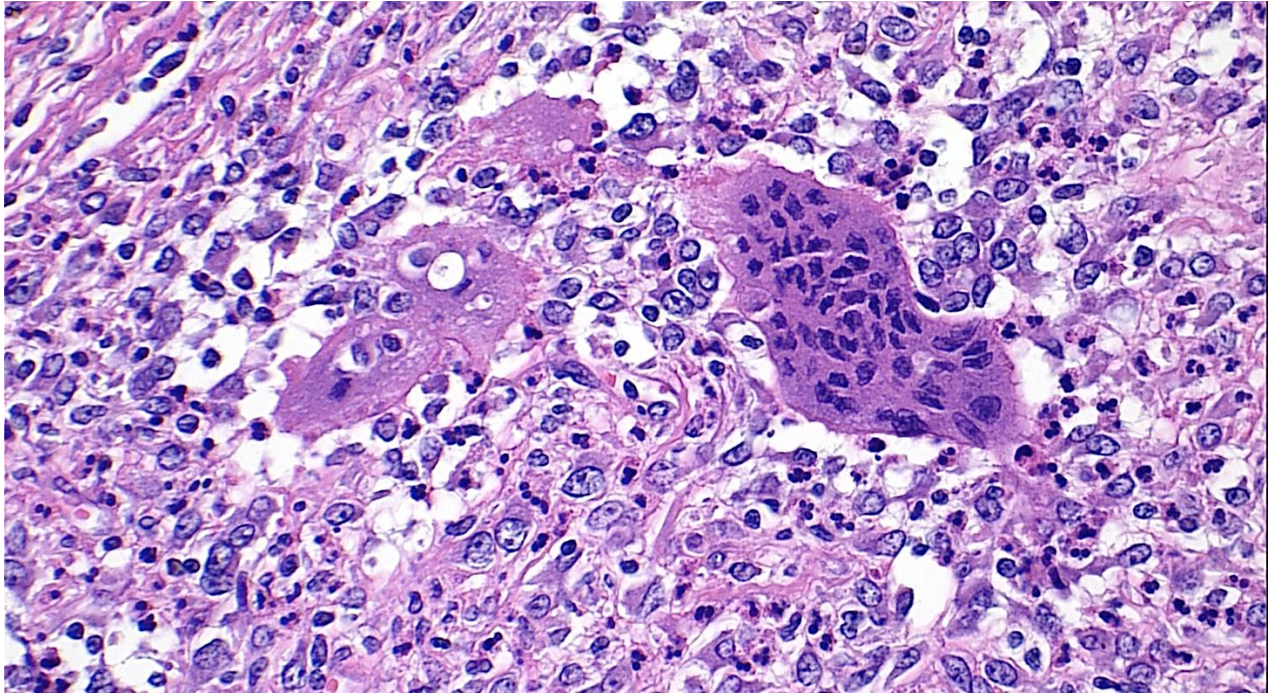
Genetic analysis of human cases of PVNS has revealed a cluster of non-random clonal chromosomal translocations, with multiple cases sharing similar breakpoints on several chromosomes.⁶ Interestingly, a majority of lesions share a break in the region of chromosome 1 which encodes macrophage colony stimulating factor (CSF1), a cytokine important for macrophage differentiation and proliferation. CSF1 is known to play an important role in the pathogenesis of numerous inflammatory arthritides, including rheumatoid arthritis. Recent theories on PVNS suggest a “landscaping effect” as part of the pathogenesis, with a low number of neoplastic cells overexpressing CSF1, resulting in recruitment of large numbers of mononuclear inflammatory cells which make up the bulk of the lesion.^{4,9}

In humans, 40-75% of PVNS cases have a history of previous trauma to the affected joint.⁵ Similar to this giraffe, lesions in people occur most frequently in high-use

joints of the distal limbs, and are more frequently associated with the flexor surface. In this giraffe, no evidence of trauma was found grossly or radiographically at necropsy. However, based on the extended history, an episode of previous acute trauma or repetitive microtrauma cannot be excluded. Cultures of the synovial fluid from the affected joint were negative, and special stains of microscopic

specimens were all negative for infectious organisms, making an infectious etiology unlikely.

The histogenesis of the large multinucleated cells remains elusive. Several cell types of origin have been proposed, including synovial mesenchyme, synoviocytes, tissue macrophages, and cells of osteoclastic lineage. In the case of this animal, IHC yielded inconclusive results as to the origin of these unusual cells, with multinucleated cells expressing IBA1 (a cytoplasmic marker of macrophages) predominantly along the cell membrane, and showing diffuse strong cytoplasmic positivity for cathepsin K (a cysteine protease responsible for matrix-degradation). While cathepsin K has traditionally been used as an osteoclast marker, recent reports have shown expression is not limited to osteoclasts. Cathepsin K expression has also been demonstrated in conditions resulting in high macrophage



Joint capsule, giraffe. The synovium is expanded by a mixed inflammatory population of numerous polygonal and spindle histiocytes, fewer neutrophils, and low numbers of multinucleated giant cells. (Photo courtesy of: Department of Molecular and Comparative Pathobiology, Johns Hopkins University, 733 N. Broadway, Suite 811, Baltimore, MD 21205.) (HE, 400X)

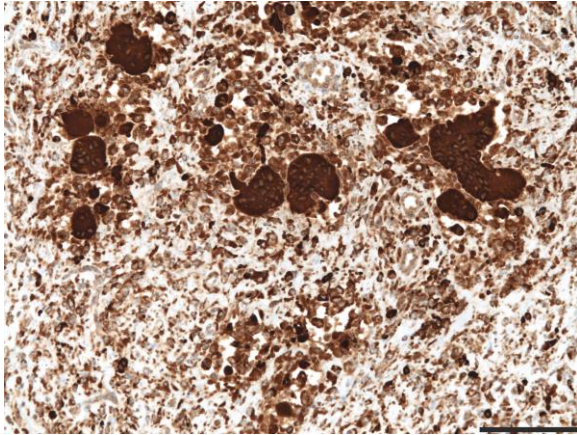
activation, such as granulomatous diseases (tuberculosis and foreign-body granulomas), sarcoidosis and sarcoid-like lesions, and is expressed by both macrophages and multinucleated giant cells in these conditions.² In the case of this giraffe, high expression of cathepsin K by cells in the tendon sheath and synovium may have contributed to osteoarthritic changes.

Inflammation and degenerative changes were also seen in other joints – namely, the contralateral fetlock, both hocks, and the right stifle. Lesions were characterized by a range of changes, from multifocal cartilage fibrillation and erosion to focal chondromalacia, effusive synovitis/bursitis with fibrin and synovial villous hyperplasia. These lesions likely represent the effects of chronic forelimb lameness resulting in altered weight bearing in the other limbs as a compensatory response.

JPC Diagnosis: Synovium and adjacent tendon: Synovitis and tenosynovitis, neutrophilic and histiocytic, villous and nodular, diffuse, severe with multinucleate giant cells and hemosiderophages.

Conference Comment: Conference participants agreed this was a very interesting and challenging case, and there was significant slide variation which increased the level of difficulty. One subset of slides contains only a section of the nodular tissue, making tissue identification enigmatic. Three important aspects of the description in this case included tissue identification based on the presence of tendon on the slide, the villous proliferation of synovium, and the formation of “pigmented” nodules containing fibrovascular tissue and inflammatory cells encased in a dense fibrous capsule. Only a small subset of slides contains all three fea-

tures and many slides contain only the pigmented nodule surrounded by fibrous tissue. The section containing all features is scanned online and it is recommended conference contributors view the virtual slide online to gain a better appreciation of the villous synovial proliferation and tendon changes.

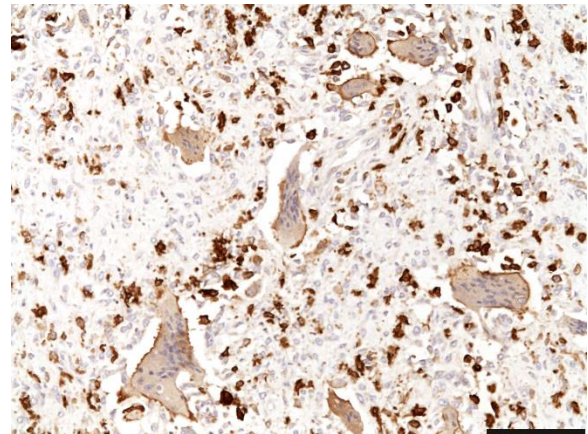


Joint capsule, giraffe. Macrophages and multinucleated giant exhibit strong cytoplasmic positivity for cathepsin K. (Photo courtesy of: Department of Molecular and Comparative Pathobiology, Johns Hopkins University, 733 N. Broadway, Suite 811, Baltimore, MD 21205.)

Conference participants described the nodular mass as fibrovascular tissue containing numerous inflammatory cells including neutrophils, macrophages, many with hemosiderin, and multinucleate giant cells with fewer lymphocytes and plasma cells. The nodule also has multifocal areas containing fibrin, hemorrhage and edema. Fibroblasts or fibroblast-like cells are hypertrophic and multifocally hyperplastic, and the collagenous stroma is haphazardly arranged and appears fibrillated in many areas; some participants described the histologic features of the nodular mass as pseudoneoplastic. Within sections of tendon histologic findings include degeneration and loss of nuclei, areas of hypercellularity, fraying of fibers, and side-to-side fusion and necrosis, all indicative of degeneration. The synovium is observed as proliferative and inflamed; the conference moderator

discussed that because the synovium lines both tendons and joint spaces, that a reactive and inflamed synovium can result in the formation of adhesions. Conference participants speculated as to whether the villous proliferation of synovium originated from synovium lining a tendon, or from the synovium lining the joint space; ultimately participants concluded it was difficult to determine with certainty in this case.

This interesting case also was studied in consultation with the Department of Soft Tissue Pathology at the Joint Pathology Center, whose medical pathologists are familiar with tenosynovial giant cell tumor as described in humans. The medical pathologists agreed the histomorphologic features from the lesion in this giraffe resemble those of tenosynovial giant cell tumor as it occurs in humans; they also observed sheets of plump polygonal cells admixed with osteoclast type giant cells in a collagenized stroma. The medical pathologists also observed a neutrophilic and plasma cell infiltrate in the lesion, and commented that this is not a typical finding of tenosynovial giant cell tumor in people. They speculated that in the case of this



Joint capsule, giraffe: Macrophages show cytoplasmic reactivity and MNGCs show membrane reactivity to IBA-1. (Photo courtesy of: Department of Molecular and Comparative Pathobiology, Johns Hopkins University, 733 N. Broadway, Suite 811, Baltimore, MD 21205.)

giraffe, the inflammatory component may be indicative of an unrecognized infection, an autoimmune component, or possibly inflammatory recruitment by the tumor cells.

This is an interesting case in that the nature, origin and cause of the nodular lesion is unclear. As described above, there is indeed uncertainty in the literature regarding whether this is a neoplastic or inflammatory lesion. As seen in this case and described in others, the nodular proliferation is histologically distinct and different from the adjacent reactive hyperplastic villous synovium. When described as a neoplasm, many different patterns have been described in the literature, with the common thread being the presence of multinucleated giant cells.⁷ The nodules have been described as proliferations of synovial cells, admixed with inflammatory cells including multinucleate giant cells,³ with the cell of origin described as synoviocytes without anaplastic features⁷ or synovioblastic mesenchyme.⁵ In other reports, the giant cells have been described as a proliferation of neoplastic epithelioid to pleomorphic mononuclear cells admixed with fibroblast like cells.⁵ In this giraffe it is unclear if the nodules viewed histologically originated from the tendon sheath, the joint capsule, or from both locations; at necropsy, nodules were described grossly by the contributor as associated with both the tendon sheath and the joint capsule. Exact anatomic origin or location within or adjacent to the joint may not be critical, as it is recognized that there is an overlap in the appearance of lesions whether described as giant cell tumor of tendon sheath, localized nodular tenosynovitis, or pigmented villonodular synovitis of joints.⁷

Contributing Institution:

Department of Molecular and Comparative Pathobiology
Johns Hopkins University

References:

1. Asano N, Yoshida A, Kobayashi E, Yamaguchi T, Kawai A. Multiple metastases from histologically benign intraarticular diffuse-type tenosynovial giant cell tumor: a case report. *Hum Pathol.* 2014;45: 2355–2358.
2. Bühling F, et al. Cathepsin K--a marker of macrophage differentiation? *J Pathol.* 2001;195: 375–382.
3. Campbell MW, Koehler JW, Weiss RC, Christopherson PW. Cytologic findings from a benign giant cell tumor of the tendon sheath in a dog. *Vet Clin Pathol.* 2014;43: 270–5.
4. Cupp J S *et al.* Translocation and expression of CSF1 in pigmented villonodular synovitis, tenosynovial giant cell tumor, rheumatoid arthritis and other reactive synovitides. *Am J Surg Pathol.* 2007;31: 970–976.
5. Malatesta D. *et al.* Benign giant cell tumour of tendon sheaths in a European lynx (*Lynx lynx*). *J Vet Med Ser A.* 2005;52:125–130.
6. Nilsson M. *et al.* Molecular cytogenetic mapping of recurrent chromosomal breakpoints in tenosynovial giant cell tumors. *Virchows Arch.* 2002;441:475–480.
7. Pool RR, Thompson KG. Tumors of joints. In: Meuten DJ ed. *Tumors of Domestic Animals.* 4th ed. Ames, IA:Iowa State Press; 2002: 201-209.
8. Rao AS, Vigorita V J. Pigmented villonodular synovitis (giant-cell tumor of the tendon sheath and synovial membrane), A review of eighty-one cases. *J. Bone Joint Surg.* 1984;66:76–94.

9. West R B, *et al.* A landscape effect in tenosynovial giant-cell tumor from activation of CSF1 expression by a translocation in a minority of tumor cells. *Proc. Natl. Acad. Sci.* 2006;103:690–695.



WEDNESDAY SLIDE CONFERENCE 2015-2016

Conference 10

2 December 2015

Mark Butt, DVM, , DACVP

Tox Path Specialists, LLC
Frederick, MD

CASE I: S 696/14 (JPC 4067275).

Signalment: Canine, Staffordshire terrier, 3.5 years (*Canis lupus familiaris*)

History: The dog had developed progressive neurological and behavioral dysfunction for the last six months. The dog was finally euthanized with severe ataxia.

Gross Pathology: Necropsy revealed no relevant lesions; the central nervous system and vertebral column appeared normal.

Laboratory Results: None

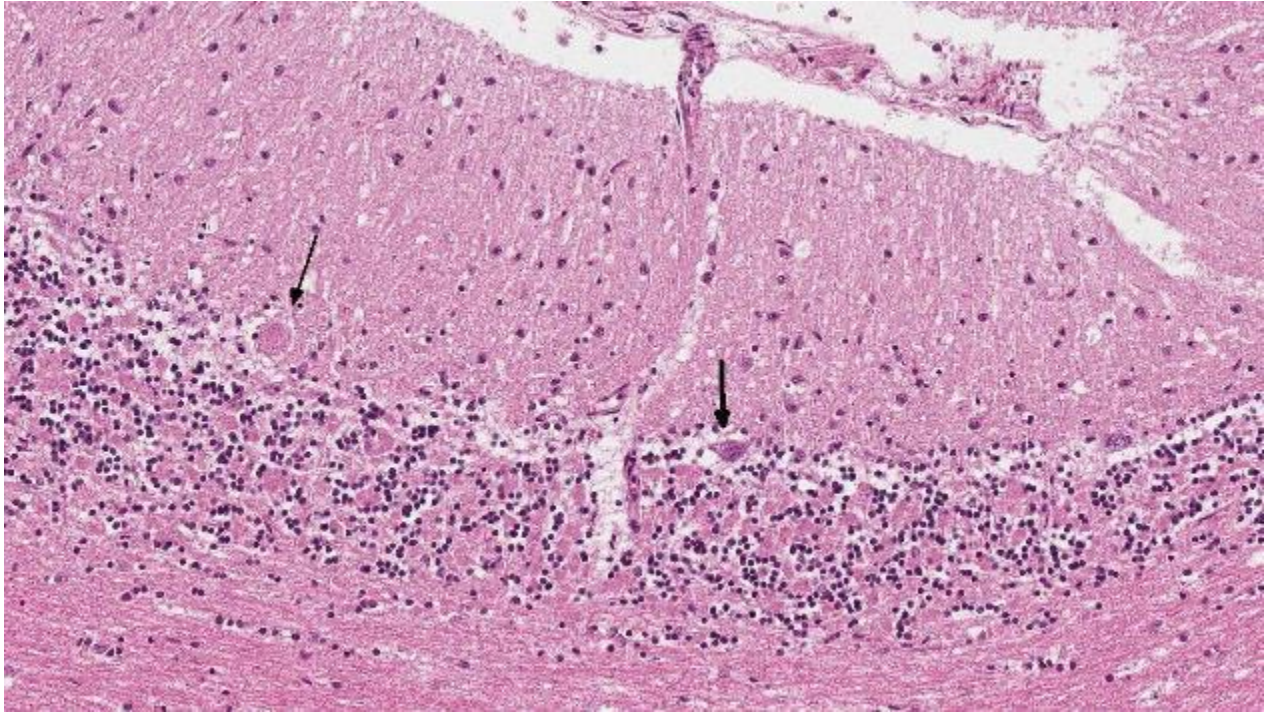
Histopathologic Description: Cerebellum: There is marked diffuse loss of Purkinje cells with remaining Purkinje cells containing abundant, lightly eosinophilic to amphophilic, granular to globular, cytoplasmic material, which often displaces the nuclei peripherally. Multifocally, Purkinje cells and neurons of the deep cerebellar nuclei are shrunken, hypereosinophilic and angular or swollen and rounded, with hyperchromatic or pyknotic nuclei (neuronal degeneration and necrosis). Rarely, large round clear spaces in the

Purkinje cell layer (empty baskets) are present. Almost diffusely, the granular cell layer is hypocellular (neuronal atrophy).

Contributor's Morphologic Diagnosis: Cerebellum: Purkinje cell degeneration, necrosis and loss, multifocal, moderate, with cerebellar atrophy and abundant neuronal intracytoplasmic granular pigment.

Contributor's Comment: The neuronal ceroid-lipofuscinoses are inherited lysosomal storage diseases also referred to as Batten's disease. In humans they represent the most common group of progressive encephalopathies in children. In addition to humans, the disease is documented in sheep,²⁹ goats,⁷ cattle,¹³ horses,³¹ mice,⁸ cats³³ and several breeds of dogs.¹⁶ Table 1 summarizes published cases.

The disease is characterized by accumulation of granules in the cytoplasm of most nerve cells and, to a lesser extent, of many other cell types. The granules are autofluorescent, periodic acid-Schiff (PAS), Luxol Fast Blue and Sudan black B positive and resistant to lipid solvents. Consequences include



Cerebellum, dog. Rare Purkinje cells remain (arrow), and the underlying granular cell layer is markedly hypocellular. (HE, 78X)

progressive selective neuronal loss with secondary astrocytic proliferation and hypertrophy as well as infiltration by macrophages.

The disease is clinically classified by age of onset into early (up to 1.5 years) and late (up to 9 years) onset forms. It is additionally categorized according to the defective genes associated with the disease (see Table 1). All forms result in progressive neurodegeneration of the central nervous system, but clinical symptoms are variable depending on breed, age and individual factors. Affected dogs change their behavior, become blind, and suffer from progressive proprioceptive and motor deficits, seizures and ataxia.

Gross lesions are often absent; especially in cases with early onset, marked cerebral atrophy may be apparent with often a brown tinge in severely affected areas.

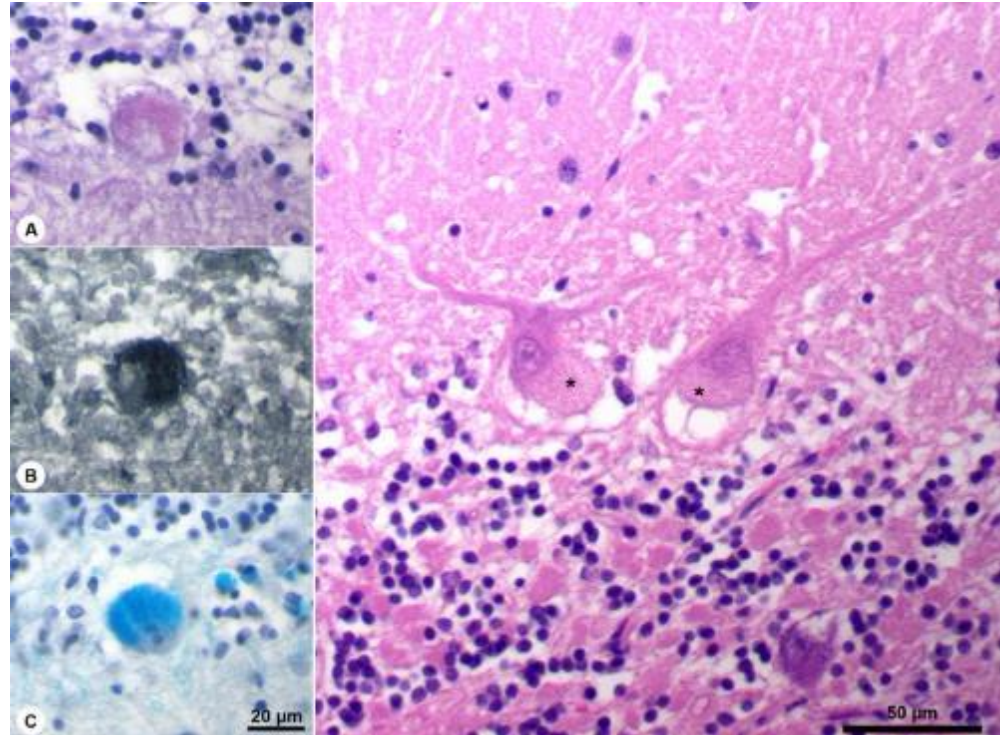
JPC Diagnosis: Cerebellum, brainstem: Purkinje cell degeneration and loss, diffuse, marked with intracellular ceroid accumulation and granular cell loss.

Conference Comment: The primary lesion in this case, as described by conference participants, is the striking (70-80%) loss of Purkinje cells, and overall the conference description was similar to the contributor's description. In addition to the change described above, hypocellularity within the granular cell layer, spongiosis within the white matter and the presence of spheroids were also described. There was discussion regarding the presence of dilated axons within the granular cell layer and whether they truly represent dilated axons or only appear dilated due to the loss of granular cells. The moderator noted the presence and function of Bergmann glial cells, proliferation of which may be seen within the granular and Purkinje cell layers in cases of Purkinje cell loss or injury; their processes

can be visualized within these areas using the glial fibrillary acidic protein (GFAP) stain.

Storage diseases comprise a heterogeneous group of conditions that result from the accumulation of material within the cell, which is unable to be metabolized or further broken down, either due to resistance to cellular processing or excessive

accumulation that exceed the cell's capacity to process it. Many of the storage diseases involve lysosomes, and in animals nearly all of the inherited storage diseases are lysosomal in nature. They often affect neurons due to the long-lived nature of these cells, which provides a longer period over which material can be accumulated as compared to cells with short turnover times.

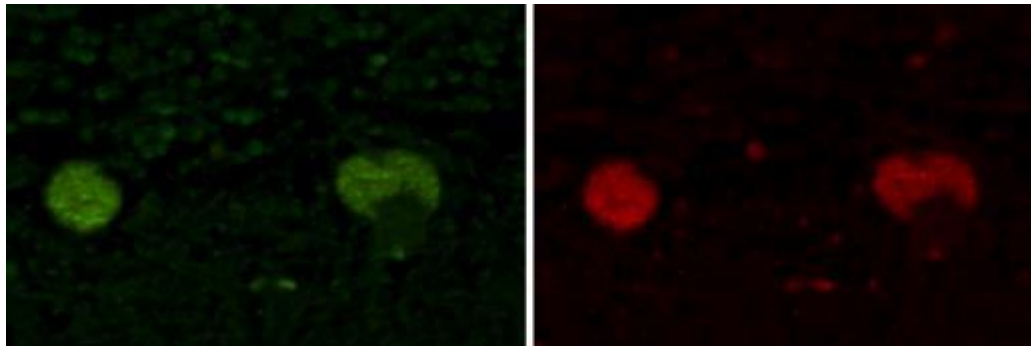


Cerebellum, dog.. Intracytoplasmic granules (right) is positive on periodic acid-Schiff (A), Sudan black (B), and Luxol fast blue (C). (Image courtesy of Department of Veterinary Pathology, Freie Universität Berlin, Germany,

<http://www.vetmed.fu-berlin.de/en/einrichtungen/institute/we12/index.html>

Defects in lysosomal processing may involve defects in a specific enzyme or lysosomal hydrolase due to a genetic defect, and can include defects in post-translational processing, production, or trafficking. Non-inherited mechanisms of storage disease include ingestion of an exogenous toxin which inhibits a lysosomal enzyme, with the result being similar to those involving genetic

defects. This is the case with ingestion of “locoweed” which produces the phytotoxin swainsonine. Resistance of the accumulating material to cellular



Cerebellum, dog: Intracytoplasmic granules exhibit autofluorescence. (Image courtesy of Department of Veterinary Pathology, Freie Universität Berlin, Germany,

<http://www.vetmed.fu-berlin.de/en/einrichtungen/institute/we12/index.html>

Breed	Reference	Gene	Onset	Age
American Bulldog	4,34	CTSD	Early	1 – 3 Years
American Staffordshire Terrier	1	ARSG	Late	1.5 – 9 Years
Australian Cattle Dog	28		Early	12 Month
Australian Shepherd	17,23	CLN6	Early	18 – 21 Month
Border Collie	19	CLN5	Early	15 Month
Chihuahua	21		Early	1 – 2 Years
Chinese Crested dog	12	MFSD8	Early	19 Month
Cocker Spaniel	20		Late	1.5 – 6 Years
Dachshund	3,27	TPP1 (CLN2)	Early	6 – 12 Month
Dachshund	26	CLN1	Early	9 Month
Dachshund	32		Late	4.5 – 7 Years
Dalmatian	9,10		Early	6 – 12 Month
English Setter	18	CLN8	Early	1 – 1.5 Years
Labrador Retriever	25		Late	7 Years
Miniature Schnauzer	15,24		Late	2 – 4 Years
Mixed breed (Australian Shepherd / Blue Heeler)	11	CLN8	Early	8 Month
Polski Owczarek Nizinny (PON)	22		Early-late	0.5 – 4.5 Years
Retriever	30		Late	3 Years
Saluki	2		Early	12 Month
Tibetan Terrier	6,35	ATP13A2	Late	4 – 8 Years
Welsh Corgi	14		Late	6 – 8 Years

Table 1: Dog breeds with neuronal lipofuscinosis and, if known, the affected gene (ARSG: Arylsulfatase G, ATP13A2: ATPase type 13A2, CTSD: Cathepsin D, CLN: Ceroid-lipofuscinosis neuronal, MFSD8: Major facilitator superfamily domain containing 8, TPPI: tripeptidyl peptidase 1)

processing may also be due to specific alterations in the substrate, either exogenous or endogenous, and not due to a processing enzyme defect per se. The detailed mechanisms involved in cellular dysfunction and death, secondary to the accumulation of undigested material, in most cases are unclear.⁵

In the veterinary literature neuronal ceroid-lipofuscinoses (NCL) is best characterized in sheep and dogs, and as described in the above chart, the condition in dogs is generally classified by age of onset and course of disease.²¹ The actual defect resulting in abnormal accumulations may not only involve lysosomal enzymes, but also

mitochondrial defects or other defects in protein processing involving the endoplasmic reticulum. The variation in gene mutations and resulting defects likely play a role in the variation in clinical presentations and histologic findings. The storage material seen within the Purkinje cell cytoplasm can be present in multiple organs, but is particularly damaging in neurons, and may be seen in the cerebral cortical and retinal neurons in addition to Purkinje cells. Severe blindness may be the primary clinical presentation in which case retinal atrophy would likely be the primary lesion, whereas other animals will present with gait abnormalities, aggression, seizures or dementia with loss of Purkinje cells and/or

neurons within other regions of the brain (hippocampus, cerebrum, brainstem).⁵ Lipofuscin accumulates in many cells throughout the body as part of the normal aging process, and in the retina is normally only seen in the retina pigment epithelium. Autofluorescent material within other retinal cells, including ganglion and Mueller cells, is diagnostic for neuronal ceroid lipofuscinosis.¹¹

Contributing Institution:

Department of Veterinary Pathology, Freie Universität Berlin, Germany,
<http://www.vetmed.fu-berlin.de/en/einrichtungen/institute/we12/index.html>

References:

1. Abitbol M, Thibaud J-L, Olby NJ, Hitte C, Puech J-P, et al. A canine Arylsulfatase G (ARSG) mutation leading to a sulfatase deficiency is associated with neuronal ceroid lipofuscinosis. *PNAS*. 2010;107:14775-14780.
2. Appleby EC, Longstaffe JA, Bell FR. Ceroid-lipofuscinosis in two Saluki dogs. *J Comp Path*. 1982; 92: 375-380.
3. Awano T, Katz ML, O'Brien DP, Sohar I, et al. A frame shift mutation in canine TPP1 (the ortholog of human CLN2) in a juvenile Dachshund with neuronal ceroid lipofuscinosis. *Molec Genet Metab*. 2006; 89: 254-260.
4. Awano T, Katz ML, O'Brien DP, Taylor JF, et al. A mutation in the cathepsin D gene (CTSD) in American bulldogs with neuronal ceroid lipofuscinosis. *Molec Genet Metab*. 2006; 87: 341-348.
5. Cantile C, Youssef S. Nervous System. In: Maxie MG, ed. *Jubb, Kennedy, and Palmer's Pathology of Domestic Animals*. Vol 1. 6th ed. St. Louis, MO: Elsevier; 2015:284-292.
6. Farias FHG, Zeng R, Johnson GS, Winger FA, et al. A truncating mutation in ATP13A2 is responsible for adult-onset neuronal ceroid lipofuscinosis in Tibetan terriers. *Neurobiology of Disease*. 2011; 42: 468-474.
7. Fiske RA, Storts RW. Neuronal ceroid-lipofuscinosis in Nubian goats. *Vet Pathol*. 1988; 25: 171-173.
8. Gao HL, Boustany RMN, Espinola JA, Cotman SL, et al. Mutations in a novel CLN6-encoded transmembrane protein cause variant neuronal ceroid lipofuscinosis in man and mouse. *Am J Hum Genet*. 2002; 70: 324-335.
9. Goebel HH, Bilzer T, Dahme E, Malkusch F. Morphological studies in canine (Dalmatian) neuronal ceroid-lipofuscinosis. *Am J Med Genet Suppl*. 1988; 5: 127-139.
10. Goebel HH, Dahme E. Ultrastructure of retinal pigment epithelial and neural cells in the neuronal ceroid-lipofuscinosis affected Dalmatian dog. *Retina*. 1986; 6: 179-187.
11. Guo J, Johnson GS, Brown HA, Provencher ML. A CLN8 nonsense mutation in the whole genome sequence of a mixed breed dog with neuronal ceroid lipofuscinosis and Australian shepherd ancestry. *Molec Genet Metab*. 2014; 112: 302-309.
12. Guo JY, O'Brien DP, Mhlanga-Mutangadura T, Olby NJ. A rare homozygous MFSD8 single-base-pair deletion and frameshift in the whole genome sequence of a Chinese crested dog with neuronal ceroid lipofuscinosis. *BMC Vet Res*. 2015;10:960.
13. Harper PAW, Walker KH, Healy PJ, Hartley WJ, et al. Neurovisceral ceroid-lipofuscinosis in blind Devon cattle. *Acta Neuropathologica*. 1988; 75: 632-636.
14. Jolly RD, Palmer DN, Studdert VP, Sutton RH, et al. Canine ceroid-lipofuscinoses: A review and classification. *Journal of Small Animal Practice*. 1994; 35: 299-306.

15. Jolly RD, Sutton RH, Smith RIE, Palmer DN. Ceroid-lipofuscinosis in miniature schnauzer dogs. *Aust Vet J.* 1997; 75: 67-67.
16. Karli P, Karol A, Oevermann A. The canine neuronal ceroid-lipofuscinosis: A review. *Schweizer Archiv Fur Tierheilkunde.* 2014;156: 417-423.
17. Katz ML, Farias FH, Sanders DN, Zeng R. A missense mutation in canine CLN6 in an Australian shepherd with neuronal ceroid lipofuscinosis. *J Biomed Biotechnol.* 2011; 2011:198042.
18. Katz ML, Khan S, Awano T, Shahid SA, et al. A mutation in the CLN8 gene in English Setter dogs with neuronal ceroid-lipofuscinosis. *Biochem Biophys Res Commun.* 2005; 327: 541-547.
19. Melville SA, Wilson CL, Chiang CS, Studdert VP. A mutation in canine CLN5 causes neuronal ceroid lipofuscinosis in border collie dogs. *Genomics.* 2005; 86: 287-294.
20. Minatel L, Underwood SC, Carfagnini JC. Ceroid-lipofuscinosis in a Cocker spaniel dog. *Vet Pathol.* 2000; 37: 488-490.
21. Nakamoto Y, Yamato O, Uchida K, Nibe K. Neuronal Ceroid-Lipofuscinosis in longhaired chihuahuas: Clinical, pathologic, and MRI findings. *J Am Anim Hosp Assoc.* 2011; 47: E64-E70.
22. Narfstrom K, Wrigstad A, Ekestén B, Berg AL. Neuronal ceroid lipofuscinosis: clinical and morphologic findings in nine affected Polish Owczarek Nizinny (PON) dogs. *Vet Ophthalmol.* 2007; 10: 111-120.
23. O'Brien DP, Katz ML. Neuronal ceroid lipofuscinosis in 3 Australian shepherd littermates. *J Vet Intern Med.* 2008; 22: 472-475.
24. Palmer DN, Tyynela J, vanMil HC, Westlake VJ, Jolly RD. Accumulation of sphingolipid activator proteins (SAPs) A and D in granular osmiophilic deposits in miniature schnauzer dogs with ceroid-lipofuscinosis. *J Inherit Metab Dis.* 1997; 20: 74-84.
25. Rossmeisl JH, Duncan R, Fox J, Herring ES, Inzana KD. Neuronal ceroid-lipofuscinosis in a Labrador retriever. *J Vet Diag Invest.* 2003; 15: 457-460.
26. Sanders DN, Farias FH, Johnson GS, Chiang V. A mutation in canine PPT1 causes early onset neuronal ceroid lipofuscinosis in a dachshund. *Molec Genet Metab.* 2010; 100: 349-356.
27. Sanders DN, Kanazono S, Winger FA, Whiting REH. A reversal learning task detects cognitive deficits in a dachshund model of late-infantile neuronal ceroid lipofuscinosis. *Genes Brain and Behavior.* 2011; 10: 798-804.
28. Sisk DB, Levesque DC, Wood PA, Styer EL. Clinical and pathologic features of ceroid lipofuscinosis in two Australian cattle dogs. *J Am Med Assoc.* 1990; 197: 361-364.
29. Tammen I, Houweling PJ, Frugier T, Mitchell NL, et al. A missense mutation (c. 184C > T) in ovine CLN6 causes neuronal ceroid lipofuscinosis in Merino sheep whereas affected South Hampshire sheep have reduced levels of CLN6 mRNA. *Biochim Biophys Acta.* 2006;1762: 898-905.
30. Umemura T, Sato H, Goryo M, Itakura C. Generalized lipofuscinosis in a dog. *Japanese J Vet Sci.* 1985; 47: 673-677.
31. Url A, Bauder B, Thalhammer J, Nowotny N, et al. Equine neuronal ceroid lipofuscinosis. *Acta Neuropathologica.* 2001; 101: 410-414.
32. Vandeveld M, Kristensen B, Braund KG, Greene CE. Chronic canine distemper virus encephalitis in mature dogs. *Vet Pathol.* 1980; 17: 17-28.
33. Weissenboeck H, Rossel C. Neuronal ceroid-lipofuscinosis in a domestic cat: Clinical, morphological and immunohistochemical findings. *J Comp Path.* 1997; 117: 17-24.
34. Woehlke A, Droegemueller C, Distl O. Canine ceroid lipofuscinosis in American bulldogs. *Tieraerztliche Praxis Ausgabe Kleintiere Heimtiere.* 2007; 35: 351.

35. Woehlke A, Philipp U, Bock P, Beineke A, et al. A one base pair deletion in the canine ATP13A2 gene causes exon skipping and late-onset neuronal ceroid lipofuscinosis in the Tibetan terrier. *PLoS Genet.* 2011; 7(10): e1002304.

CASE II: 49052 (JPC 4048842).

Signalment: 5-year-old, 9.3 kg, tricolor, female, intact Beagle mix (*Canis familiaris*)

History: The patient presented to the Neurology Service with a 3-week history of peracute onset paraplegia. There was no known trauma and no therapy was undertaken. At the time of presentation, the dog was paraplegic with pain sensation and severe extensor rigidity of the hind limbs. She had an MRI performed which showed a locally extensive intramedullary myelopathy from the level of L2 extending caudally. There was minimal to no contrast enhancement with T2 hyperintensity of the gray matter (irregularly shaped and undulating) from L2 to the conus medullaris. Due to poor prognosis for return to function, the owner elected euthanasia.

Gross Pathology: Nervous: The brain and spinal cord are removed and fixed whole in formalin. The brain is externally grossly normal. The lumbar spinal cord exhibits moderate, locally extensive swelling, such that the diameter of the majority of the segment approaches that of the intumescence. The fixed spinal cord is dissected. A locally extensive segment of the lumbar spinal cord from L2 to L7 exhibits severe cavitation of the grey matter and diffuse swelling (myelomalacia and edema). Extensive grey matter cavitation is also noted on longitudinal sections.



MRI Longitudinal section of the spinal cord, T2W image. A well-margined, irregular, undulating T2 hyperintensity is present from L2-3 to the conus medullaris. (Photo courtesy of: Animal Medical Center, 510 East 62nd St. New York, NY 10065 <http://www.amcnv.org/>)

MRI report: Fairly well margined, irregularly shaped and undulating T2 hyperintensity is within the spinal cord from the level of L2-3 caudally to the conus medullaris (T2W, Figure 1). This area remains heterogeneously hyperintense on flair images and is hypointense on T1 weighted images without evidence of contrast enhancement. There is no evidence of signal voids on the FFE sequences. The spinal cord is increased in diameter over this region. The disc spaces are essentially normal with only a minimal amount of narrowing to the nucleus pulposus of 4-5.

Diagnosis: Locally extensive intramedullary myelopathy, from L2 caudally.

Comments: Consideration is given to noncontrast enhancing neoplasia. Another perhaps less likely differential could include intramedullary cyst formation. The persistent hyperintensity on flair images makes a cyst alone unlikely.



Cross sections (A) and Longitudinal sections (B) of the fixed spinal cord, showing severe grey matter cavitation and overall edema. (Photo courtesy of: Animal Medical Center, 510 East 62nd St. New York, NY 10065 <http://www.amcnv.org/>)

Histopathologic Description: Three cross sections and two longitudinal sections of lumbar spinal cord are examined. In all sections, multifocal to coalescing, asymmetric and symmetric regions of predominantly grey matter undergo necrosis, characterized by sharply defined parenchymal loss and replacement by myriad Gitter cells with formation of cavitated, cystic spaces (infarction). Infarcted regions measure up to 5 x 6 mm and comprise approximately 50 – 75% of the spinal cord parenchyma. Within and at the periphery of these regions of necrosis, within the regional grey and white matter and less frequently the leptomeninges, multiple arterioles contain amorphous amphophilic hyaline material which partially or fully occludes the lumen

(fibrocartilaginous emboli). Multifocally, emboli are covered by endothelial cells (organization). Few neurons in the surrounding grey matter exhibit cell swelling with cytoplasmic pallor, dispersed or absent Nissl substance and nuclear fading (chromatolysis). Predominantly ventral, but also lateral and dorsal funiculi contain multifocal dilated myelin sheaths with digestion chamber formation and Gitter cell infiltration. Axons are multifocally enlarged (swollen) and eosinophilic (spheroids), (Wallerian degeneration). In the regional parenchyma, increased populations of glial cells are also present, including microglia, which exhibit rod morphology, and astroglia with gemistocytic astrocytosis. Ventral spinal nerves are hypercellular with myelin sheath dilation, myelin loss, macrophage infiltration and Schwann cell proliferation (Büngner's bands). Spinal nerves also contain scattered inflammatory populations including lymphocytes and plasma cells. Emboli stain magenta with PAS and blue with Alcian blue.

Contributor's Morphologic Diagnosis:

Lumbar spinal cord (L2-L7): Poliomyelomalacia, severe, locally extensive with intralesional fibrocartilaginous emboli, Gitter cell infiltration and cavitation (infarction), consistent with fibrocartilaginous embolic myelopathy (FCEM)

Lumbar spinal cord (L2-L7): Myelin vacuolation, ventral, lateral and dorsal funiculi myelin vacuolation with Gitter cell infiltration, axonal spheroid formation, (Wallerian degeneration) and gliosis with gemistocytic astrocytosis

Lumbar spinal cord (L2-L7): Myelin vacuolation and loss, spinal nerves with Schwann cell proliferation (Büngner's bands,

Wallerian degeneration) and neuritis, multifocal lymphoplasmacytic, mild

Contributor's Comment: Fibrocartilagenous embolic myelopathy (FCEM) is defined by the presence of occlusive, intravascular material histologically and histochemically similar to the nucleus pulposus of the intervertebral disc resulting in ischemic necrosis of the spinal cord.^{2,3} FCEM is most commonly reported in large and giant breed dogs, however, small breed dogs can also be affected.²⁻⁶ Some studies have found that approximately 80% of dogs with FCEM had a body weight greater than 20 kg.⁴ Male predominance has been found in some studies, whereas others find no sexual predilection. Ages can range from 2 months to 11 years, with a median of 5-6 years in the majority of studies.³ In many cases, clinical signs are associated with exercise or trauma.^{2,3} Neurologic signs are typically peracute in onset (less than 6 hours), as in this case, and are often asymmetric, nonprogressive and nonpainful after the first 24 hours.^{3,5} Maximal neurologic deterioration occurs within the first 6 to 24 hours and is followed by gradual improvement or stabilization of signs.³ Progression beyond 24 hours may be secondary to additional embolizations or secondary spinal cord injury. The distribution of lesions is in the location of the infarction. The most commonly affected spinal cord segments have been reported to occur in the regions of L4-S3 and C6-T2 in dogs with a histologic diagnosis of FCEM and L4-S3 and T3-L3 in dogs with an antemortem diagnosis.^{2,3} Relative sparing of the thoracic spinal cord may be due to protective effects of the intercapital ligament overlying the intervertebral discs or the fewer and smaller radicular arteries and anastomotic surface vessels.²

The embolizing material has been identified as fibrocartilage histologically and is histochemically identical to the nucleus pulposus of the intervertebral disc. There are multiple hypotheses to explain how the fibrocartilagenous material enters the spinal vessels.³ The pathophysiology of this process is controversial and the exact mechanism is poorly understood.⁴

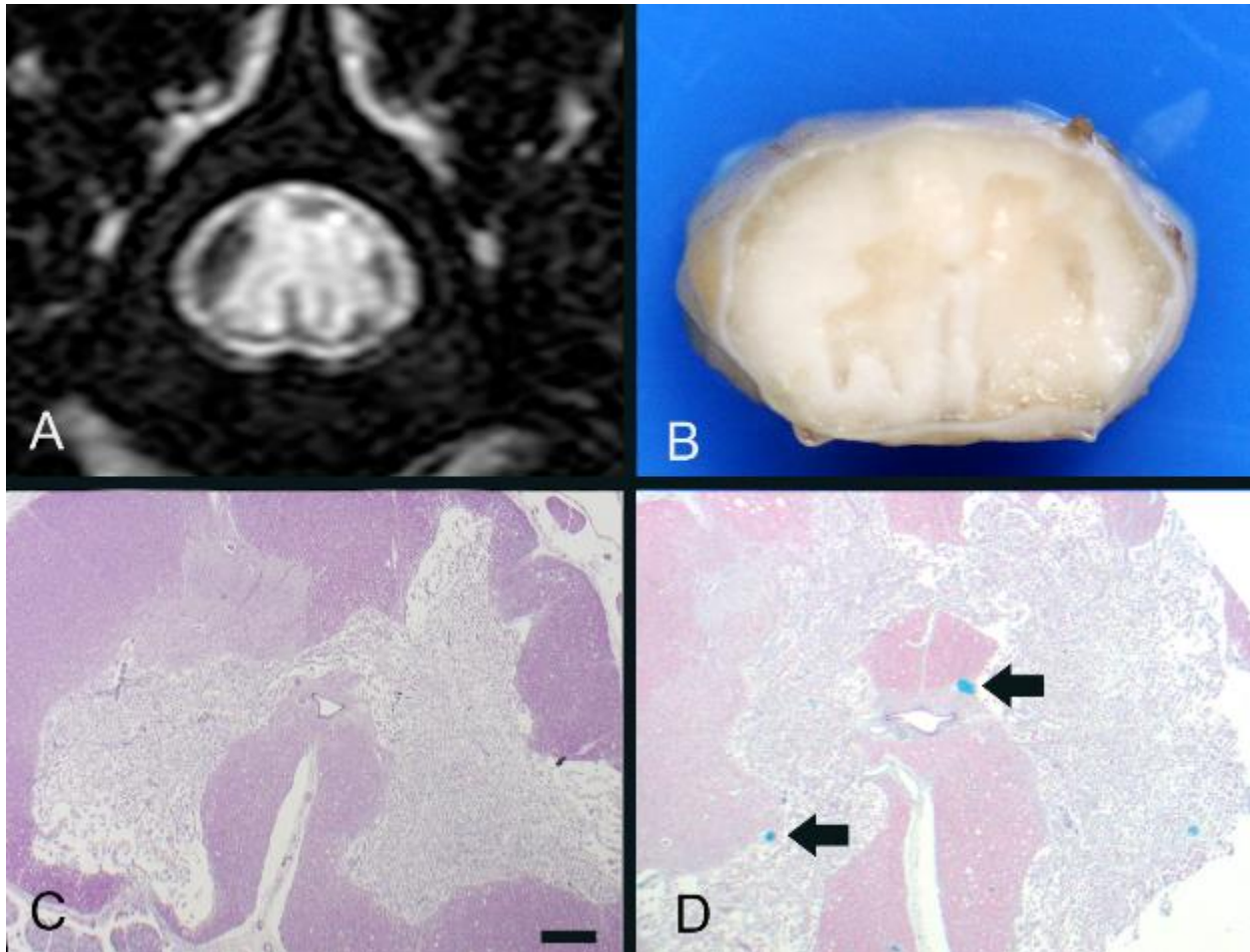
- 1) Direct penetration of nucleus pulposus fragments into spinal cord or vertebral vessels. Penetration into thin walled veins is considered more likely, however, injection entrance or arteriovenous anastomoses could explain the presence of emboli in arteries. In large breed and non-chondrodystrophoid dogs, the nucleus pulposus remains soft for a longer period of time, which may predispose to mechanical vascular injection with type II disc disease.^{2,4,6}
- 2) Chronic inflammatory neovascularization of the degenerated intervertebral disc, with penetration of nucleus pulposus fibrocartilage into the newly formed vessels after a sudden rise of intervertebral disc pressure.³
- 3) Remnant embryonic vessels within the nucleus pulposus, which is normally avascular in adults.³
- 4) Mechanical herniation into the vertebral bone marrow sinusoidal venous channels with retrograde entrance into the basivertebral vein and internal vertebral venous plexus. In humans, this hypothesis is supported by the presence of Schmorl's nodules (masses of fibrocartilage within the vertebral body cancellous bone), however, these are extremely rare in dogs.³

- 5) Fibrocartilage may arise from vertebral growth-plate cartilage in immature dogs or metaplasia of the vascular endothelium, which ruptures into the lumen and embolizes within the spinal cord intrinsic vasculature.³

Other types of material which can occlude vessels include thrombi, bacterial, parasitic, neoplastic or fat emboli. FCEM should be differentiated from noncompressive nucleus pulposus extrusion, in which nondegenerated nucleus pulposus extrudes during strenuous exercise or trauma, causes a spinal cord contusion and dissipates within the epidural

space. Other differential diagnoses are compressive intervertebral disc extrusion, infectious and immune mediated myelitis, neoplasia and intra- and extramedullary hemorrhages.³

Definitive diagnosis of FCEM can only be obtained with histologic examination of the affected spinal cord segments, which demonstrates fibrocartilaginous material in spinal vessels within or near an area of focal myelomalacia.³⁻⁵ The infarcted region is most severe at the center of the lesion and tends to taper off in adjacent cranial and caudal segments.⁵ The distribution reflects the supply of the occluded vessels, and is



Cross section of lumbar spinal cord. MRI image (A), fixed spinal cord, L4 (B), H&E low magnification view of L4, 20x, bar is 500 μ m (C), and Alcian Blue (D). Well delineated grey matter necrosis with replacement by Gitter cells (infarction) is observed. (Photo courtesy of: Animal Medical Center, 510 East 62nd St. New York, NY 10065 <http://www.amcn.org/>)

typically asymmetric. As in this case, grey matter is generally more severely affected than white matter, and lesion margins are typically well delineated.^{3,4} At gross examination, the spinal cord is commonly swollen and may appear grey or hemorrhagic.⁵ Severely malacic regions can be replaced by large sheets of macrophages embedded within a vascular network,⁴ or with cavitation. Infarction within a spinal funiculus will result in focal axonal swelling and spongy ballooning of myelin at its margins. If the ventral horn grey matter is infarcted, Wallerian degeneration develops in its neuronal projections in the ventral funiculus and in the ventral spinal roots.^{4,5}

Fibrocartilagenous material can be observed in both arteries and veins. In some cases, it can be difficult to identify the type of vessel occluded due to attenuation of the wall by the embolism. Emboli are amphophilic in H&E sections, magenta with PAS (Figure 4C) and blue with Alcian blue stains (Figures 3D, 4D). Attempts at organization are manifest as endothelial coverage, also observed in these sections.⁵

In order to produce infarction of the spinal cord parenchyma, multiple intramedullary tributaries must be occluded.⁵ The ventral spinal artery (VSA) extends along the ventral median fissure for the entire length of the

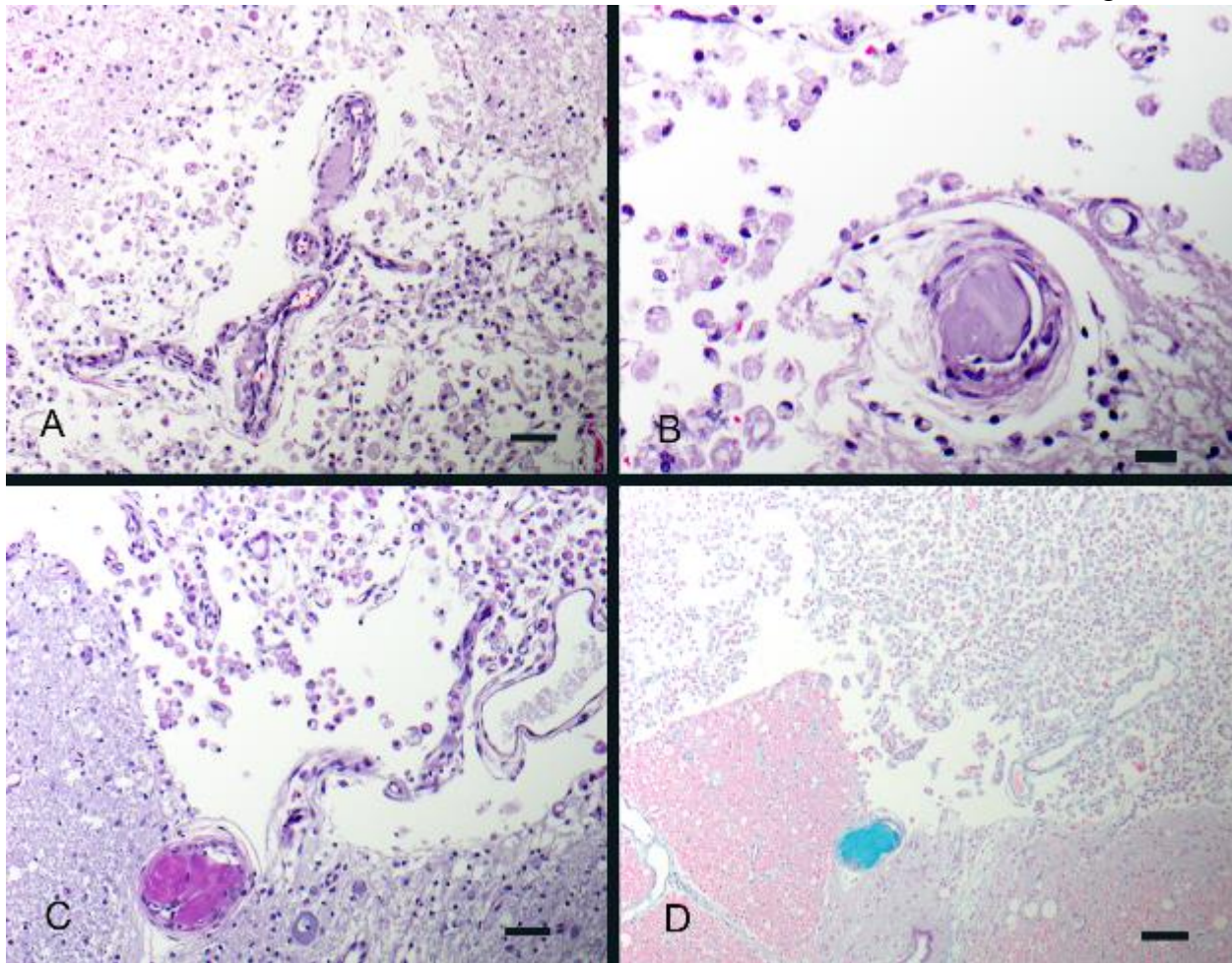
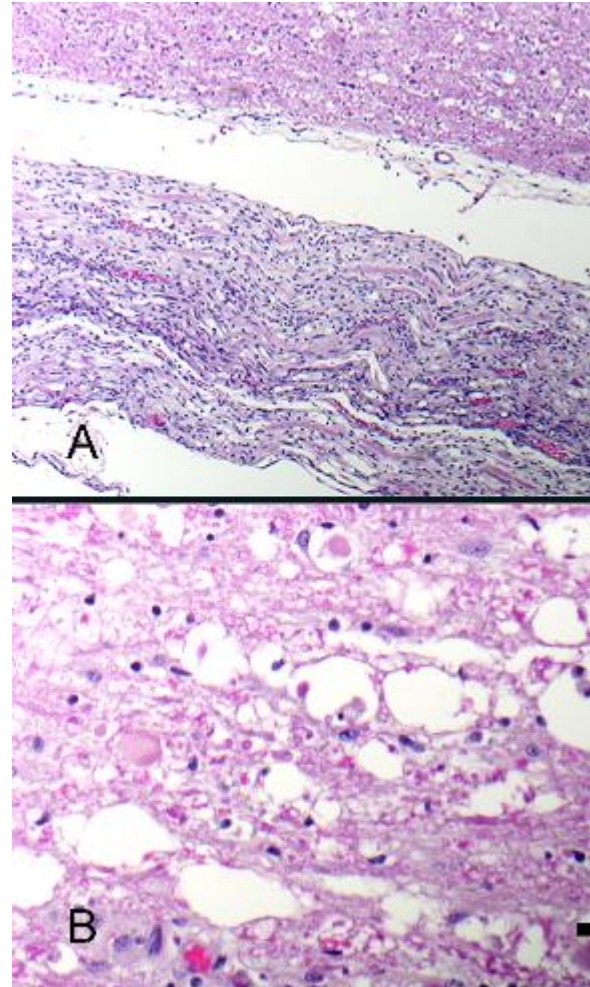


Figure 4. Cross section of lumbar spinal cord. MRI image (A), fixed spinal cord, L4 (B), H&E low magnification view of L4, 20x, bar is 500 μ m (C), and Alcian Blue (D). Well delineated grey matter necrosis with replacement by Gitter cells (infarction) is observed. (Photo courtesy of: Animal Medical Center, 510 East 62nd St. New York, NY 10065 <http://www.amcnv.org/>)

spinal cord, and is the largest in diameter in the cervical and lumbar regions.³ The VSA gives rise to the central arteries, which supply most of the grey matter and part of the lateral and ventral white matter of the spinal cord, with asymmetric distribution at several spinal cord segments.³ The dorsal spinal arteries are also continuous throughout the spinal cord, have the largest diameter in the cervical and lumbar regions and supply the dorsal white and grey matter. The anastomotic plexus on the surface of the spinal cord gives rise to radial arteries that enter the spinal cord and supply the lateral and ventral white matter.³ In our case, the central arteries were most frequently occluded vessels, resulting in severe ischemic necrosis of predominantly the grey matter.

Prognosis is dependent upon severity and extent of the ischemic injury. One study found that 84% of dogs had either complete clinical recovery or partial recovery with return to normal function as a pet. The lesion length-vertebral length ratio has been associated with outcome. This is the ratio between the length of the intramedullary hyperintensity on mid-sagittal T2 weighed images and the length of the vertebral body (C6 in dogs with cervical lesions or L2 in dogs with thoracolumbar lesions). Dogs with a lesion-length vertebral length ratio (LL:VL) greater than 2.0 or a percent cross sectional area of the lesion of 67% or greater were significantly more likely to have an unsuccessful outcome than those with lower values.³ In this case, the LL:VL was 7 (11.12/1.6) and the percent cross sectional area of the lesion was 75%. Lower motor neuron signs have been correlated with a poor prognosis, but distinction between upper and lower motor neuron signs was not found to be statistically significant in one case series, in which extension of the lesion appeared to be a more important prognostic factor than localization.⁴ Absence of deep pain

perception was significantly associated with dogs that were later euthanized, and was determined by some authors to be the most important negative prognostic factor observed.⁴ This change is likely associated with severe, bilateral grey and white matter damage. Additional negative prognostic factors were involvement of intumescences and symmetrical clinical signs. Immediate



Spinal nerves are hypercellular with myelin loss and Schwann cell proliferation (Büngner's bands), (100x, bar is 100um, A). The spinal cord surrounding the infarcted regions undergoes myelin vacuolation with digestion chamber formation, Gitter cell infiltration, gliosis and axonal swelling (spheroids, Wallerian degeneration), (400x, bar is 500um, B). (Photo courtesy of: Animal Medical Center, 510 East 62nd St. New York, NY 10065 <http://www.amcnv.org/>)

physiotherapy and hydrotherapy had a major positive influence on the recovery rate.⁴

Figure 5: Spinal nerves are hypercellular with myelin loss and Schwann cell proliferation (Büngner's bands), (100x, bar is 100um, A). The spinal cord surrounding the infarcted regions undergoes myelin vacuolation with digestion chamber formation, Gitter cell infiltration, gliosis and axonal swelling (spheroids, Wallerian degeneration), (400x, bar is 500um, B).

JPC Diagnosis: Spinal cord: Poliomyelomalacia, extensive, multifocal, marked with cavitation, spinal nerve demyelination and intravascular fibrocartilagenous emboli.

Conference Comment: The conference histologic description was similar to the contributor's very thorough description. For complete histologic examination of the spinal cord, the moderator discussed the benefits of examining both transverse and longitudinal sections. Ascending and descending tracts are readily visualized with transverse sections but axonal changes are difficult to evaluate. In contrast, axonal changes are much easier to appreciate with longitudinal sections, but invariably not all tracts will be seen. Therefore, the conference moderator highly recommended that conference participants evaluate an oblique and a transverse section and considered such evaluation as the optimal method to evaluate spinal cord segments. In addition to the aforementioned thorough histologic description, histologic evidence of chronicity in this case was discussed including the degree of cavitation and re-endothelialization around emboli.

The contributor provides an excellent review of FCEM in dogs. In addition to being reported in dogs, FCEM (though much less

common) has also been reported in other species including horses, pigs, turkeys and cats. Of note, FCEM usually occurs in middle aged to older cats, with equal representation between males and females, and most commonly occurring at the C6-T2 spinal cord segments.² Interestingly, Horner's syndrome has also been associated with FCEM in cats when the lesion is localized to the T1-T3 spinal cord segments.¹

Contributing Institution:

Animal Medical Center
<http://www.amcnny.org/>

References:

1. Barker EN, Schofield E, Granger NP. What is your Neurologic Diagnosis? *J Am Vet Med Assoc.* 2014;245(1):49-51.
2. Cauzinille L, Kornegay JN. Fibrocartilagenous embolism of the spinal cord in dogs: review of 36 histologically confirmed cases and retrospective study of 26 suspected cases. *J Vet Intern Med.* 1996;10(4):241-245.
3. DeRisio L, Platt SR. Fibrocartilagenous embolic myelopathy in small animals. *Vet Clin Small Anim.* 2010;40:859-869.
4. Gandini G, Cizinauskas S, Lang K, Fatzer R, Jaggy A. Fibrocartilagenous embolism in 75 dogs: clinical findings and factors influencing the recovery rate. *J Sm Anim Prac.* 2003;44:76-80.
5. Summers BA, Cummings JF, de Lahunta A. Degenerative diseases of the central nervous system. In: *Veterinary Neuropathology.* St. Louis, MO: Mosby; 1995:246-249.
6. Thompson K. Bones and Joints. In: Maxie MG, ed. *Jubb, Kennedy, and Palmer's Pathology of Domestic Animals.* 5th ed. Vol. 1. Philadelphia, PA: Elsevier Saunders; 2007:156-157.

Zachary JF. Cardiovascular System and Lymphatic Vessels. In: McGavin MD, Zachary JF, eds. *Pathologic Basis of Veterinary Disease*. 5th ed., St. Louis, MO: Mosby Elsevier; 2012:585-586.

CASE III: 13-526 (JPC 4048788).

Signalment: Adult, 8-year-old, female spayed, DLH cat (*Felis catus*)

History: Presented to an emergency clinic with acute onset of blindness and inappetence. Owner had noted subtle change in behavior the previous day and believed the cat had been drinking and urinating more in the past 2 weeks. Physical examination: mentally dull and anxious, severely hypertensive (230 mmHg systolic on Doppler). Ophthalmic examination: no menace response, palpebral reflex present, sluggish bilateral pupillary light reflex, equivocal dazzle reflex. Hospitalized to treat (amlodipine besylate) and monitor hypertension. Tonic-clonic seizure developed 4 hours later, resolved with diazepam, but the cat remained stuporous and showed anisocoria. Euthanasia was elected.

Gross Pathology: Gross findings were very nonspecific. Tissues throughout the body were hyperemic with marked congestion seen in large abdominal veins (caudal vena cava, renal veins). Renal capsular surfaces were irregularly depressed overlying wedge-shaped pale areas extending to the corticomedullary junction (chronic infarcts).

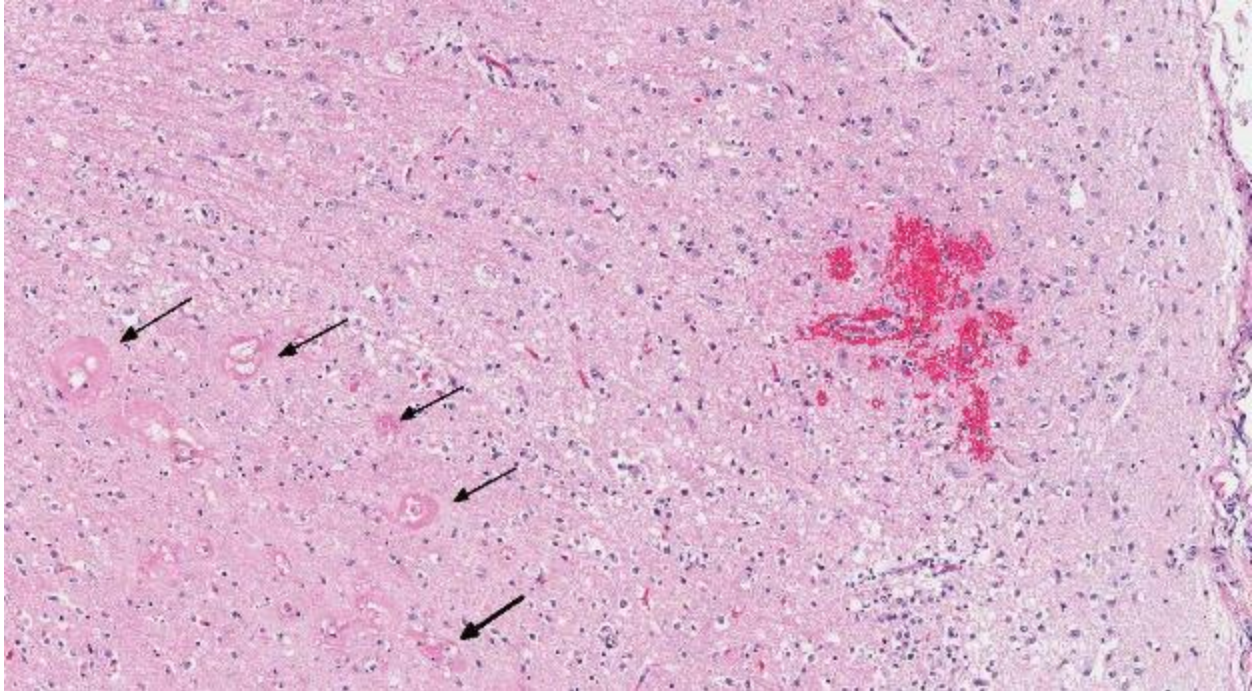
Laboratory Results:

Clinical pathology: Hematology: low platelets with clumping observed; Serum biochemistry: mild hyperglycemia (stress), mild hyponatremia (pressure natriuresis); Urinalysis: glucosuria, negative for protein, USG 1.010 (isosthenuria consistent with pressure diuresis).



Cerebrum, cat. There is mild pallor in the parietal lobe (lower right), barely visible on low magnification. (HE, 5X)

Histopathologic Description: Brain: There is a large poorly demarcated wide area of pallor within each dorsal parietal lobe extending from deep white matter and encompassing full thickness of the associated overlying grey matter. Pallor is caused by marked separation and accentuation of the linear myelin sheaths in white matter and marked vacuolation (spongiform change) in the overlying grey matter. Severe neuronal degeneration, necrosis and loss is seen with shrunken, eosinophilic and angular neurons, scattered nuclear debris (karyorrhexis) and heavy complement of glial cells, gitter cells and reactive astrocytes. Occasionally, glial cells replace neurons. There are a few microhemorrhages within the area of edema and necrosis in the grey matter. Vessels within the area of pallor show severe effacement of architecture by amorphous eosinophilic material and small amount of nuclear debris (fibrinoid change). These vessels are surrounded by large clear vacuoles (perivascular edema). Blood vessels with intact walls are often lined by hypertrophic (reactive) endothelial cells and surrounded by low numbers of neutrophils, macrophages, lymphocytes and plasma cells. Multifocally throughout the section, Virchow-Robin space is markedly expanded by clear space transected by fine eosinophilic strands (edema). Leptomeninges overlying the affected gyrus are mildly expanded by edema and low numbers of mixed



Cerebrum, cat. Walls of arterioles within the affected parietal lobe are necrotic, and diffusely expanded by pale by extruded protein (fibrinoid necrosis). (HE, 96X)

inflammatory cells, mostly mononuclear with occasional neutrophils. Pial arteriolar walls often contain amorphous eosinophilic droplets or circumferentially (protein leakage).

Contributor's Morphologic Diagnosis:

Brain, cerebrum, parietal lobes, bilateral, edema with neuronal degeneration, necrosis and loss, locally extensive, acute, severe associated with arteriolar fibrinoid change, acute, severe.

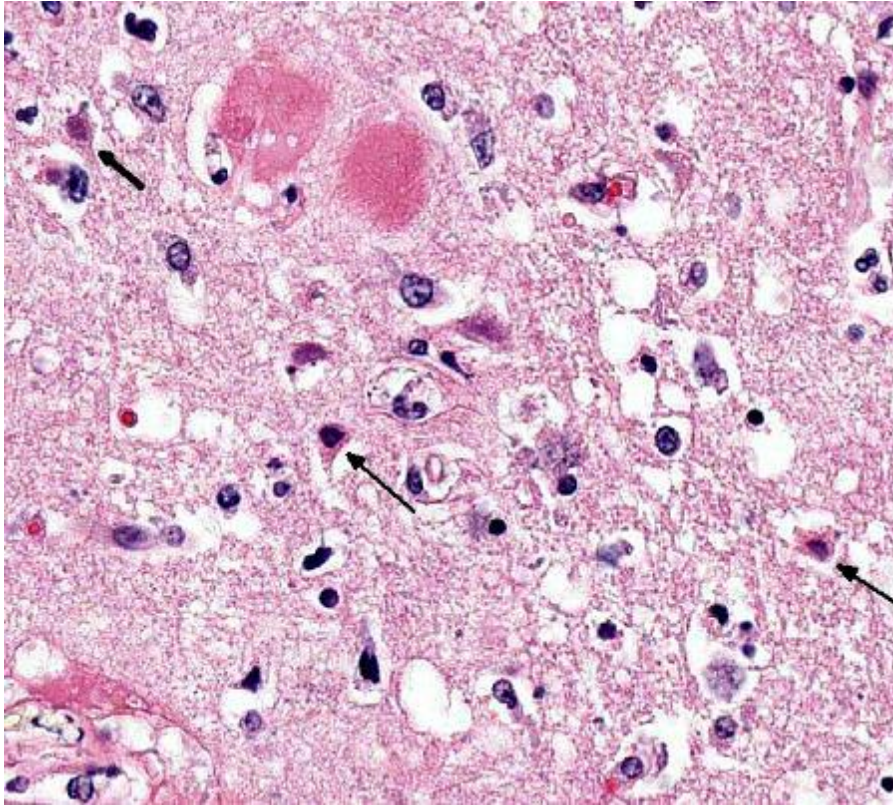
Contributor's Comment: Systemic hypertension as a clinically important condition in domestic cats was initially described in 1986.⁴ It has been defined as a sustained increase in systolic blood pressure ≥ 160 -170 mmHg.² Three clinical categories are recognized and defined as:

- Stress-induced ("white coat") hypertension: transitory artifactual increase (median rise of 17.6 ± 5.9

mmHg) secondary to activation of the sympathetic nervous system in the classical "fight or flight" response;

- Secondary hypertension: most common and associated with systemic diseases or treatments including chronic renal disease, hyperthyroidism, primary hyperaldosteronism, pheochromocytoma, diabetes mellitus and erythropoietin treatment; and
- Idiopathic (primary or essential) hypertension: about 20% of hypertension in cats occurs in the absence of other demonstrable disease conditions.

Target organ damage (TOD) is a risk in the face of uncontrolled hypertension with the heart, brain, eyes and kidneys being at greatest risk. The cat of this report showed



Cerebrum, cat. In the affected area, neurons are necrotic as a result of ischemia (arrows). (HE, 284X)

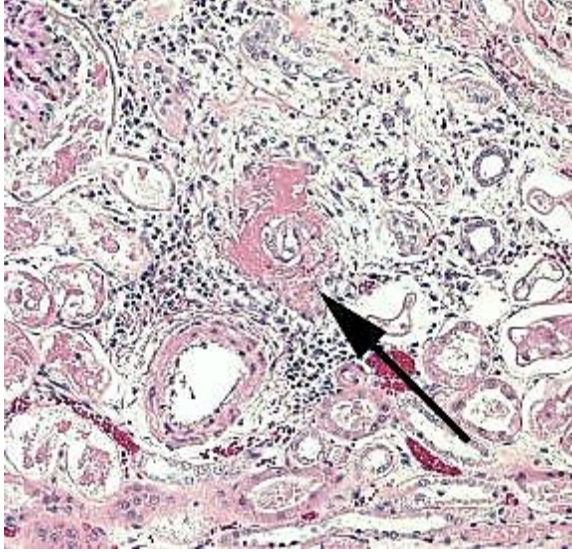
TOD in the brain as described above. Changes in the eyes and kidneys were also focused largely on vascular structures, specifically arterioles, with similar effacement by amorphous eosinophilic material with small amounts of nuclear debris, commonly known as fibrinoid change or necrosis. This cat presented with acute onset of blindness and an anxious demeanor with rapid deterioration to seizing and stupor. This is a classical presentation for target organ damage in a hypertensive cat with the first noted sign often being acute blindness associated with catastrophic effusive retinal detachment (Fig. 2). Sudden onset of intracranial neurological signs is also common. Renal and cardiac changes are generally more insidious. Accelerated progression of chronic kidney disease and development of congestive heart failure associated with left ventricular hypertrophy,

respectively, are reported.³ Pathogenesis of the insidious conditions is poorly understood, particularly regarding cause and effect.

The risk of target organ damage rises as the blood pressure rises.^{4,5} Risk is minimal at <150mmHg, mild at 150-159mmHg, moderate at 160-179mmHg and severe at >180mmHg. This cat had a recorded pressure of 230mmHg at presentation. The vascular lesions in the brain, eyes and kidneys are acute suggesting a relatively short course of hypertension in this cat. There is no evidence to suggest hyperplastic

vascular changes that would be seen as a response to sustained hypertension. It has been suggested that vascular remodeling can occur within 14 days of onset of hypertension.¹

Hypertension in this cat was considered idiopathic despite being younger than reported age of >12 years for development of idiopathic hypertension.⁵ Complete histological evaluation did not show pathology consistent with any of the conditions associated with secondary hypertension. Secondary hypertension is most commonly seen in cats with chronic kidney disease (CKD) or with hyperthyroidism. Many cats with systemic hypertension show some degree of CKD. It is often unclear whether the hypertension initiates renal damage or systemic hypertension develops as a consequence of reduced renal function.



Kidney, cat: There is fibrinoid necrosis of renal arterioles and ischemic damage of surrounding parenchyma. (Photo courtesy of: University of Calgary Faculty of Veterinary Medicine, 3280 Hospital Dr. NW Calgary, AB Canada, T2N 4Z6 <http://vet.ucalgary.ca/>)

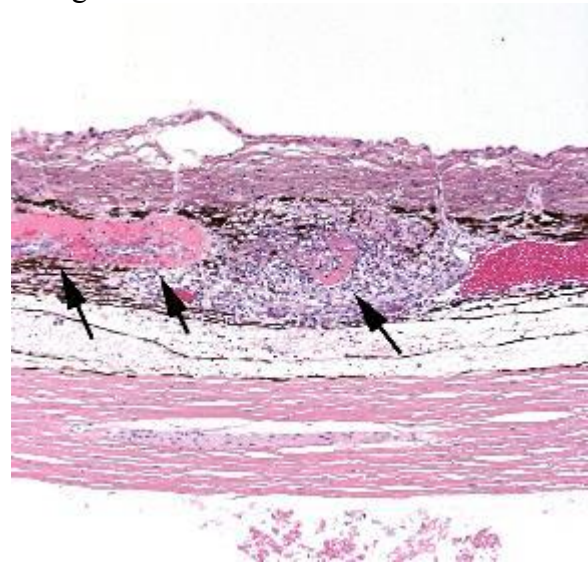
Hyperthyroidism has been considered a risk factor for systemic hypertension with recent information suggesting this risk may be overstated.³

JPC Diagnosis: Cerebrum: Fibrinoid vascular necrosis, multifocal, moderate with neuronal necrosis and edema.

Conference Comment: This was a challenging case for most conference participants with many focusing the majority of their description on the vascular changes. Most participants described an asymmetric fibrinoid vasculitis and listed various etiologic differential diagnosis, such as feline ischemic encephalopathy, FIP, FeLV as well as hypertension. The moderator and many conference attendees stated they had not previously seen a CNS case similar to this, with the unique asymmetric fibrinoid change within vessels, and some speculated that an infarction may result in a similar lesion, although the contributor provided a convincing workup and description of a

hypertension induced lesion / TOD. The lesion was described as focally extensive within the white matter, but also extending into the grey matter with areas of spongiosis, hemorrhage and neuronal necrosis. The affected vessels were described as having indistinct vessel walls and endothelium, largely obscured by dense eosinophilic debris with expansion of Virchow-Robin space by edema, similar to the contributor's description above. Low numbers of mitoses were described within vessel endothelium.

The moderator discussed duration of injury as determined by relative populations of glial cells. It generally takes approximately 4-5 days to see a prominent astrocyte response; in this case there is a mild increase in the number of astrocytes, and a much more prominent increase in the number of microglial cells. Microglial cells respond more rapidly to CNS injury, generally increasing in number within 24 hours, and consequently there was speculation this lesion was approximately 2-3 days duration, which corresponds to the contributor's comment above regarding the acute nature of changes in the br



Eye, cat: There is fibrinoid necrosis of retinal vessels and marked perivascular inflammation. (Photo courtesy of: University of Calgary Faculty of Veterinary Medicine, 3280 Hospital Dr. NW Calgary, AB Canada, T2N 4Z6 <http://vet.ucalgary.ca/>)

Autoregulation of cerebral blood flow normally prevents excesses of pressure and flow within the brain that can result in excess pressure related damage; however, there are upper limits on this autoregulatory mechanism. When this mechanism fails in cases of prolonged and/or excessive systemic blood pressure, vessels become distended and endothelial tight junctions open, resulting in extravascular leakage of fluid, and edema is the end result. Depending on the severity, cerebral edema may be visible grossly along with widening and flattening of the cerebral gyri, and caudal herniation of the cerebellum through the foramen magnum due to increased intracranial pressure.

Histologically, as seen in this case, vacuolation of the neuropil is present, and may be predominantly in the white matter. Vascular lesions can include arteriolar hyalinosis, which may reflect endothelial damage, and leakage of fibrin and other plasma components into the vessel wall and extravascular space; this change may occur prior to onset of fibrinoid vascular necrosis. Hyperplastic arteriosclerosis, microhemorrhages and perivascular cuffing by inflammatory cells may also be seen depending on degree and duration of hypertension.^{1,4}

Contributing Institution:

University of Calgary Faculty of Veterinary Medicine
3280 Hospital Dr. NW
Calgary, AB Canada
T2N 4Z6
<http://vet.ucalgary.ca/>

References:

1. Brown CA, Munday JS, Mathur S and Brown SA. Hypertensive encephalopathy in cats with reduced renal function. *Vet Pathol.* 2005;42:642-649.

2. Brown S, Atkins C, Bagley R, et al. ACVIM consensus statement: Guidelines for the identification, evaluation, and management of systemic hypertension in dogs and cats. *J Vet Intern Med.* 2007;21:542-558.

3. Jepson R. Feline hypertension: Classification and pathogenesis. *J Feline Med Surg.* 2011;13:25-34.

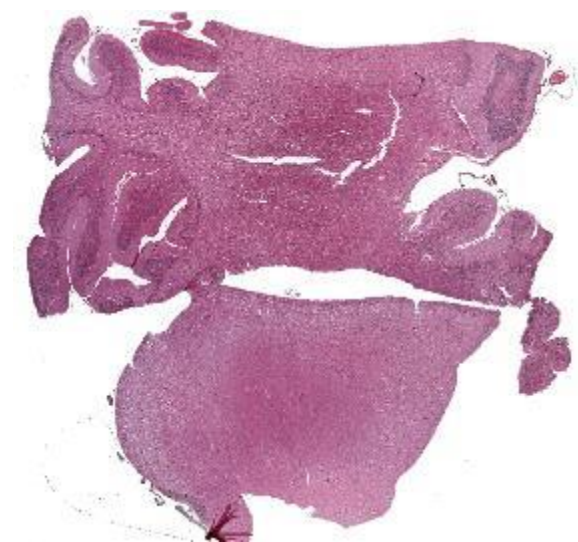
4. Kent M. The cat with neurological manifestations of systemic disease: Key conditions impacting on the CNS. *J Feline Med Surg.* 2009;11:395-407.

5. Stepien RL. Feline hypertension: Diagnosis and management. *J Feline Med Surg.* 2011;13:35-43.

CASE IV: 15 0160-21 (JPC 4067774).

Signalment: Bovine, Charolais (*Bos taurus*), male, 3 years old

History: This three-year-old, charolais bull was presented for a two-month history of chronic posterior paresia. Clinical examination showed right hock stiffness with right leg mobility reduction.



Cerebellum, brainstem, ox: No abnormalities are visible at subgross examination. (HE, 4X)

Gross Pathology: No lesions were observed on macroscopic examination

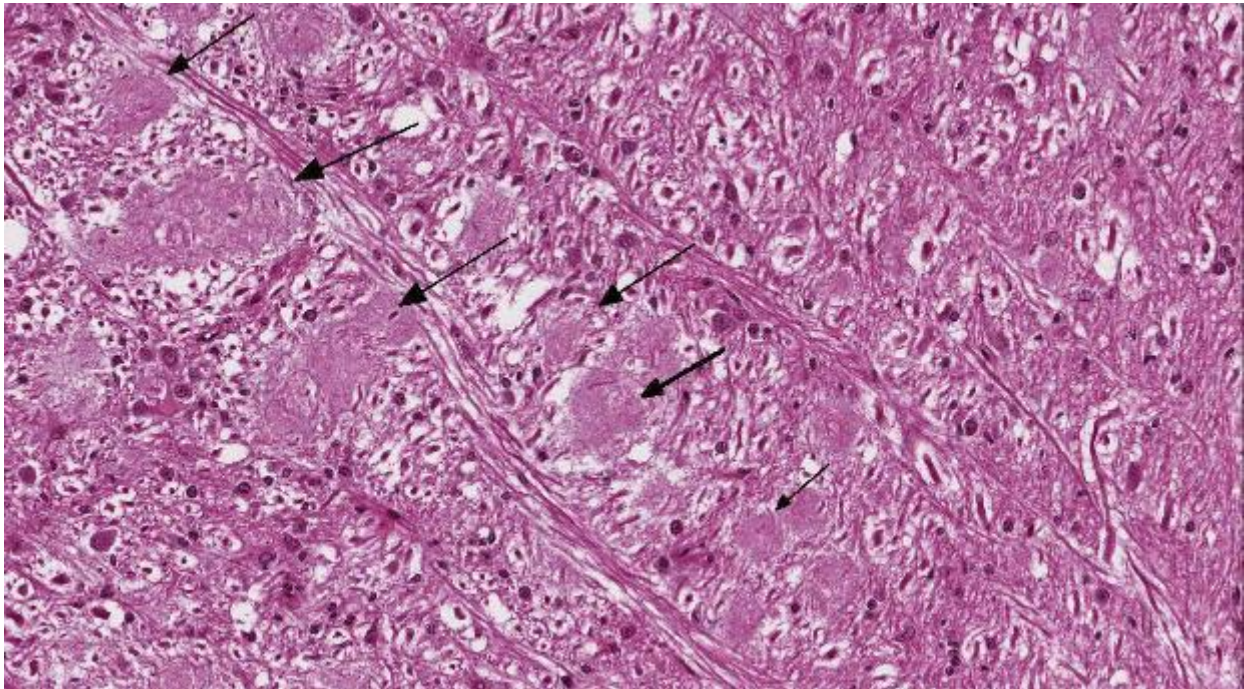
Laboratory Results: No biochemical abnormalities ante mortem were found. Cerebrospinal fluid cytological examination was normal.

Histopathologic Description: Brain, cerebellum: Multifocally in the white matter can be found numerous 20-100 μm diameter eosinophilic, acellular, granular to fibrillar, round to ovoid-shaped plaques, haphazardly distributed. The rest of the white matter contains multifocal, intra- and intercellular, optically empty, vacuolation (spongiosis). A mild, non-suppurative, inflammatory reaction can be found within and around the pathological areas, characterized by discrete lymphocytic perivascular cuffing and mild gliosis with increased number of oligodendrocytes and hyperacidophilic astrocytes (reactive astrocytes).

Kluver and Barerra stains showed the material was bright blue (consistent with myelin). No PAS positive material was observed.

Contributor's Morphologic Diagnosis: Brain, cerebellum, white matter, eosinophilic plaques, multifocal, severe with mild spongiosis and discrete gliosis in a Charolais bull, characteristic of progressive ataxia of Charolais cattle.

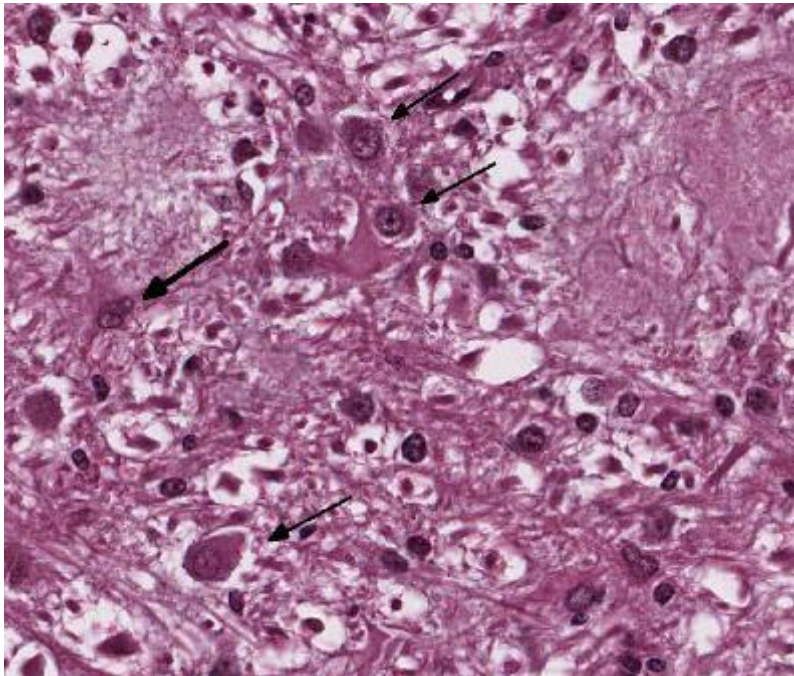
Contributor's Comment: Progressive ataxia is a condition seen in purebred and crossbred Charolais cattle. It is a genetic disease suspected to be of autosomal recessive transmission.^{2,6} The chromosomal locus containing the gene coding the basic myelin protein is likely to be involved in this condition.¹ However studies are still ongoing to identify the causal mutation. It is a slowly progressive disease affecting Charolais cattle from 6 months to two years or more. Clinically, the animal will generally present



There are numerous round densely packed plaques of fibrils arranged in columns throughout the brainstem and cerebellum white matter. (HE, 284X)

a progressive hindlimb stiffness evolving into incoordination and dysuria. All other neurological functions are not thought to be affected.^{2,6} The pathogenesis of the disease is an oligodendroglial dysmyelinogenesis. It is thought that the defect of production and maintenance of myelin sheaths in white matter, leading to widening of the node of Ranvier and subsequent poor saltatory nerve impulse conduction causing the nervous symptoms observed.

Ultrastructurally, the disease is characterized by hypertrophic and hyperplastic oligodendrocytes emitting numerous and disorganized small processes around the node of Ranvier, leading to myelin sheaths malformation in the white matter. The histological examination displays haphazard, multifocal, pale, eosinophilic, granular to fibrillar, 20-100 μm plaques which are pathognomonic for this disease, along with mild oligodendroglial hyperplasia, discrete



Brainstem, ox: Markedly hypertrophic oligodendroglial cells (arrows) are present adjacent to plaques. The plaques are composed of tangled processes of these cells. (HE, 320X).

astrocytosis, lymphocytic infiltration and cuffing.^{2,4,5,6}

This condition has not been described in man. However, a similar condition has been reported in two bull-mastiff dogs.³ In this case, the lesions are characterized by an oligodendroglial dysplasia forming small eosinophilic plaques of 20 μm around axons. Identically to the bovine species, there were only rare and small GFAP positive processes, excluding an astrocytic origin for those plaques.

JPC Diagnosis: Cerebrum and cerebellum, white matter: Dysmyelinogenesis, multifocal, moderate, with fibrillary plaques and oligodendroglial hypertrophy.

Conference Comment: The conference description was very similar to the contributor's description above. Participants discussed the appearance of the fibrillary plaques as having a distinctive structure, often forming columns in certain regions of the section, and being absent of nuclei. The formation and origin of the plaques was discussed as originating from processes of hypertrophied oligodendrocytes, and not from the accumulation of abnormal myelin. This is a unique entity in that there are few known genetic diseases which affect oligodendrocytes. There is some slide variation, but lesion characteristics appear similar in all sections.

This condition is reported in both sexes of Charolais cattle, and has also been reported in three-quarter crossbred as well as purebred animals. Gross lesions are absent, but the microscopic

lesions are unique and distinctive. Axons are found to traverse the plaques with mostly normal myelin and no sign of degradation or phagocytosis of the myelin. Evidence of axonal degeneration, when found, is mild. As mentioned above, ultrastructural examination suggests the abnormality lies within the paranodal region of axons. Younger plaques are characterized by axons wrapped with hypertrophied oligodendrocyte processes, in a thin myelin sheath, near the nodes of Ranvier. In older plaques the axons may be demyelinated and surrounded by more abundant oligodendrocyte processes. The defect lies in the inability of oligodendrocytes to maintain the paranodal myelin structure with resultant oligodendrocyte hypertrophy.²

There are two types of oligodendrocytes within the CNS, interfascicular oligodendrocytes and satellite cells. The interfascicular oligodendrocytes are responsible for myelination of axons and normally they appear as small cells with hyperchromatic nuclei; special - staining techniques, such as myelin basic protein, are normally required to visualize their processes. The nuclei of oligodendrocytes are often seen aligned in rows parallel to myelinated axons, where they maintain the internodal segments of the myelin sheath.⁷

Contributing Institution: Unité d'Histologie, Embryologie et Anatomie pathologique, Département des Sciences Biologiques et Pharmaceutiques.

Ecole Nationale Vétérinaire d'Alfort, FRANCE
www.vet-alfort.fr

References:

1. Duchesne A, Eggen A. Radiation hybrid mapping of genes and newly identified microsatellites in candidate regions for

bovine arthrogryposis-palatoschisis and progressive ataxia based on comparative data from man, mouse and rat. *J Anim Breed Genet.* 2005;122(Suppl.1):28-35.

2. Maxie MG, Youssef S. The nervous system. In: Maxie MG ed. *Jubb, Kennedy and Palmer's Pathology of Domestic Animals*. 5th ed. Vol 1. Edinburgh, UK: Saunders Elsevier; 2007:381-385.

3. Morrison JP, Schatzberg SJ, De Lahunta A, Ross JT, Bookbinder P, Summers BA. Oligodendroglial dysplasia in two Bullmastiff dogs. *Vet Pathol.* 2006 ;43:29-35.

4. Parodi AL. Progressive ataxia in cattle study of histologic lesions. *Recueil de Medecine Veterinaire de l'Ecole d'Alfort.* 1981 ; 339-345. (in French)

5. Patton CS. Progressive ataxia in Charolais cattle. *Vet Pathol.* 1977;14:535-537.

6. Vandeveld M, Higgins R, Oevermann A. *Veterinary Neuropathology: Essentials of Theory and Practice*. Chichester, UK: Wiley-Blackwell; 2012:176-177.

7. Zachary JF. Nervous System. In: McGavin MD, Zachary JF, eds. *Pathologic Basis of Veterinary Disease*. 5th ed. St. Louis, MO: Mosby Elsevier; 2012:777-778.



WEDNESDAY SLIDE CONFERENCE 2015-2016

Conference 11

9 December 2015

Elizabeth Mauldin, DVM, , DACVP
Associated Professor of Pathology and Dermatology
University of Pennsylvania School of Veterinary Medicine
Philadelphia, PA

CASE I: N1400608 (JPC 4066457).

Signalment: Mature gravid female white-tailed deer (*Odocoileus virginianus*).

History: This doe was found dead, but was observed alive in the same yard the previous evening.

Gross Pathology: Approximately 95% of the skin was alopecic, hyperpigmented, and covered by small coalescing crusts. A small

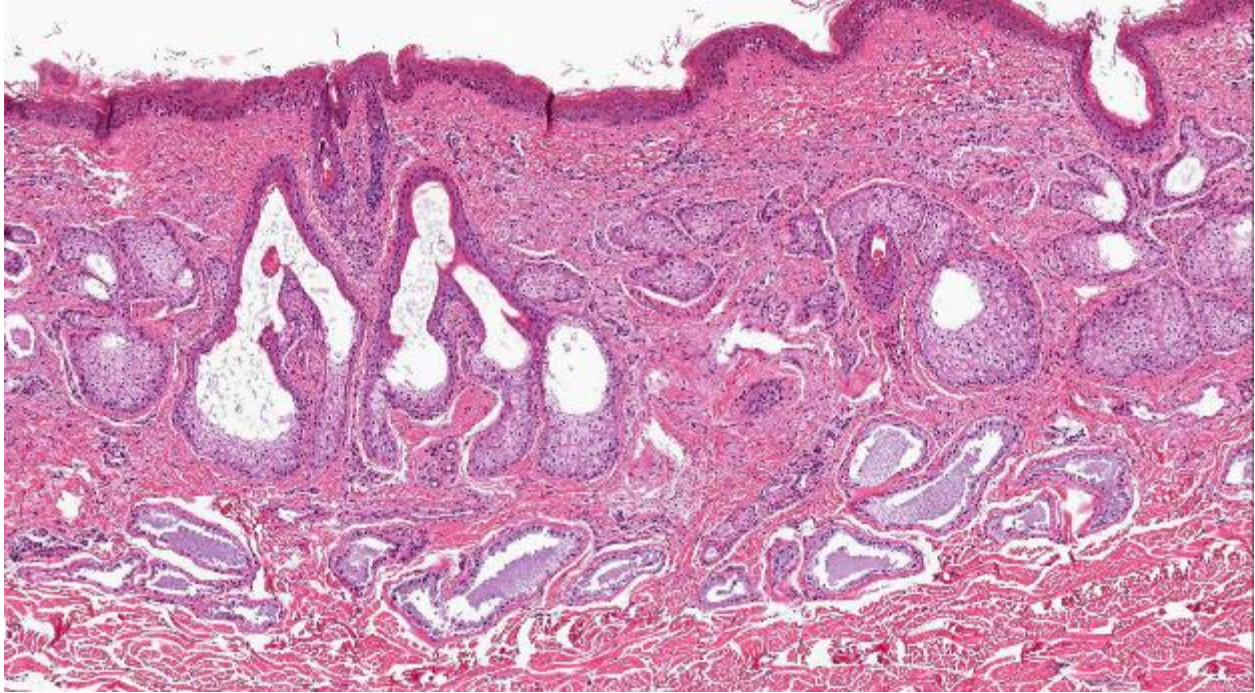


Skin, white-tailed deer. Approximately 95% of the skin was alopecia and hyperpigmented with small amounts of hair remaining over the inguinal, axillary, and perianal regions as well as the distal extremities. (Photo courtesy of: University of Pennsylvania, School of Veterinary Medicine, Department of Pathobiology, <http://www.vet.upenn.edu/research/academic-departments/pathobiology/pathology-toxicology>)

amount of hair remained over the inguinal, axillary, and perianal regions and the distal extremities. There was consolidation and dark red to black discoloration of the right cranial lung lobe. The remainder of the thoracic and abdominal viscera was grossly normal.

Laboratory Results: None

Histopathologic Description: Diffusely, there is a defect in hair development. Hair shafts are frequently absent from follicles; remaining hair shafts are angular or kinked, attenuated, and fragmented, and rarely extend to follicular ostia at the skin surface. The hair cortex is composed of hyaline, relatively thinned keratin. Follicular infundibula



Haired skin, white-tailed deer. Hair follicles are empty or contain fragmented, poorly formed hair shafts and keratin debris. Diffusely sebaceous glands are hyperplastic, and apocrine glands are dilated by excessive secretory product. HE, 55X).

are multifocally dilated and misshapen, and some are filled with excessive orthokeratin. Occasional hair bulbs and inferior portions of hair follicles are present at the level of the infundibular-isthmic junction. Sebaceous glands are multifocally hyperplastic, with ectatic ducts that contain fragments of keratin debris. There is mild dermal inflammation with few scattered lymphocytes and histiocytes. The epidermis is variably mildly acanthotic and hyperpigmented.

Contributor's Morphologic Diagnosis:

Haired skin: Follicular dysplasia, diffuse

Name of disease: Toothpaste hair disease of white-tailed deer

Contributor's Comment: Toothpaste hair disease of the white-tailed deer is a rare condition sporadically affecting individuals with features of widespread alopecia and multifocal crusts. Previous cases have

reportedly arisen in the Great Lakes region and the Mississippi Valley.⁵ Despite there being some knowledge of this entity for decades, little has been determined as to a cause, including an underlying genetic defect. Moreover, to date there are no cases described in the primary literature, and there are no similar reports in other cervid species.⁵ The likely cause of death in this case was attributed to the regional bronchopneumonia.

This condition calls into question the distinction between follicular dystrophy and dysplasia. A true follicular dystrophy suggests a degenerative process and possible association with 'malnutrition' of hair follicle cells.⁷ The result is defective and impaired development of hair in spite of a structurally normal hair follicle. In contrast, follicular dysplasias not only feature abnormal hairs but are also accompanied by abnormal hair follicles.⁵ While this entity has been classified as a form of follicular dystrophy in the past, we consider a

diagnosis of follicular dysplasia appropriate in this case given the occasional abnormal morphology of hair bulbs, and their often aberrant location within the superficial dermis. In prior cases of toothpaste hair disease, a direct link with malnutrition, though suspected, has not been confirmed. A nutrient/mineral assay was not performed on tissues from the present case.

Follicular dysplasias are not uncommon in veterinary medicine. Color dilution alopecia and black hair follicular dysplasia are well-described conditions in various breeds of dog and cattle.¹ The former has also been reported in the horse.⁴ Non-color dependent follicular dysplasias have also been reported for various dog breeds including Siberian huskies, Irish water spaniels, and Portugese water dogs amongst others. The hairlessness trait of the Sphynx cat and Chinese crested and Mexican hairless dogs is another widely recognized form of follicular dysplasia (congenital hypotrichosis) brought about by the intentional propagation of spontaneous genetic mutations.¹ Hair cycle disorders (including cyclic flank alopecia and follicular arrest) are also classified by some to be follicular dysplasias.

Follicular dystrophies are comparatively quite rare. There are several well-characterized follicular dystrophies in mice. Recently, a spontaneous autosomal recessive mutation was discovered on mouse chromosome 2, termed follicular dystrophy (*fold*), affecting the P/J mouse strain.³ A primary follicular dystrophy has also been described in a substrain of B6 mice.¹¹ The phenotype is one of focal alopecia progressing to ulcerative dermatitis and scarring, and is attributed to polymorphism in alcohol dehydrogenase (*Adh4*) and differential expression of epithelial retinol dehydrogenase (*DHRS9*), leading to the impaired removal of excess retinol. Yet

another follicular dystrophy phenotype has been defined in B6.C mice, resulting from the Angora mouse mutation brought about by a deletion in fibroblast growth factor 5 (*Fgf5*) gene.¹⁰

Humans are also subject to follicular dystrophies. An entity known as acquired progressive kinking of hair is an androgen-dependent disorder that causes affected hairs



daired skin, white-tailed deer. Dysplastic follicles occasionally contain small, misformed hair shafts which lack a distinct cuticle, cortex, and medulla. (HE, 268X)

of the scalp to resemble pubic hair in morphology.⁹ A subset of follicular dystrophies are known to stem from deficiencies in one of various nutrients, including copper (Menke's kinky hair syndrome), sulfur (trichothiodystrophy), and amino acids (Netherton's syndrome).⁵

JPC Diagnosis: Haired skin and subcutis: Follicular dysplasia with sebaceous gland hyperplasia, duct dilation and hyperkeratosis.

Conference Comment: The conference description focused on the numerous empty and/or keratin filled, malformed, ectatic hair follicles as well as disorganization and hyperplasia of the sebaceous glands and ectatic sebaceous gland ducts. The moderator was careful to point out that dilated sebaceous gland ducts should not be

confused with dilated hair follicles as both are present in this case. Participants also noted the presence of dilated apocrine glands, malformed hair bulbs and shrunken, fragmented, malformed and hypereosinophilic hair shafts, with absence of normal hair shaft architecture, which led to interpretation as a form of congenital hypotrichosis.

Although uncommon, a similar condition has been reported previously in white tailed deer. In the other reported case, hair follicle density was normal, follicles were ectatic and either empty or contained keratin debris and hair shaft fragments, and apocrine ducts were dilated and hair bulbs were abnormal, similar to what was seen in this case. In that case there was normal hair present on the ventral thorax and sebaceous gland hypertrophy and hyperplasia was variably present. There was also mild epidermal hyperplasia and hyperpigmentation, similar to what is seen in this case. The authors of that manuscript went on to discuss the types of congenital hypotrichosis described in cattle including forms which are lethal, forms associated with dental abnormalities and viable hypo-trichosis, which shares many similarities with this case.¹² Viable hypotrichosis is reported to affect Guernsey, Jersey, Holstein and Hereford cattle with an autosomal recessive mode of inheritance resulting in dysplastic hair follicles that don't produce hair shafts, generalized alopecia and cystic apocrine glands. Ectodermal defects resulting in congenital alopecia can be restricted to the hair follicle, or also be associated with other ectoderm derived tissues (i.e. teeth, nails).⁶

Formation of a hair follicle and hair shaft involves complex molecular signaling pathways that begin with formation placode, a condensed mesodermal structure which lies just below an epidermal invagination.

The placode grows down into the mesenchyme which is followed by differentiation of the follicular mesenchyme, and formation of the dermal papilla and connective tissue sheath, which leads to formation of the hair bulb. The hair bulb is responsible for formation of the hair shaft. When the mesenchymal cells of the dermal papilla become enclosed by keratinocytes, formation of the hair shaft begins. Hair shaft formation is accomplished by the matrix keratinocytes of the hair bulb. Hair shafts are composed of a cortex, which is covered by a cuticle protecting the hair from damage, and many hair shafts have a pigmented medulla. Surrounding the hair shaft is the inner root sheath, which disappears at the level of the follicular infundibulum. The outer root sheath forms at the same time as the inner root sheath and hair follicle, but is not derived from matrix keratinocytes. Downgrowth of the outer root sheath pushes the hair bulb toward the subcutis while matrix keratinocytes are producing the hair shaft and inner root sheath, which grow toward the skin surface. As mentioned above by the contributor, hair follicle dysplasias, which involve defects in the hair follicle and shaft, are often differentiated from the alopecic conditions where the hair follicle appears normal, but the shaft itself is abnormal. Additionally, it is important to differentiate between alopecic conditions with a decreased number of relatively normal hair follicles, vs. alopecic conditions with a normal number of abnormal follicles. Congenital forms of alopecia may involve the epithelial and mesenchymal cells of the hair follicle, but may also involve follicular melanocytes, derived from neuroectoderm, and include color dilution alopecia and black hair follicular dysplasia in dogs.⁶

Contributing Institution:

University of Pennsylvania, School of Veterinary Medicine, Department of Pathobiology
<http://www.vet.upenn.edu/research/academic-departments/pathobiology/pathology-toxicology>

References:

1. Ginn PE, Mansell JEKL, Rakich PM. Skin and appendages. In: Maxie MG, ed. *Jubb, Kennedy and Palmer's Pathology of Domestic Animals*. Vol 1. 5th ed. Philadelphia, PA: Elsevier Limited; 2007:582-585.
2. Gross, Ihrke, Walder, and Affolter. Skin diseases of the dog and cat. 2nd ed. Ames, IA: Blackwell Science; 2005:518-530.
3. Harris BS, Ward-Bailey PF, Johnson KR, Bronson RT. Follicular dystrophy: a new skin and hair mutation on mouse Chromosome 2. The Jackson Laboratory. Mouse mutant resource. 2013.
4. Henson FMD and Stidworthy MF. Alopecia due to colour-dilute follicular dysplasia in a horse. *Equine Veterinary Education*. 2003; 15(6): 288-290.
5. Joint Pathology Center. Wednesday Slide Conference; No. 26. April 7, 1999. <http://www.askjpc.org/wsc/wsc/wsc98/98wsc26.htm>. Accessed April 10, 2015.
6. Mecklenburg L. An overview on congenital alopecia in domestic animals. *Vet Dermatol*. 2006;17(6):393-410.
7. Mecklenburg L, Linek M, Tobin, DJ, eds. *Hair loss disorders in domestic animals*. Wiley-Blackwell; 2009:83-85.
8. Miller WH, Griffin CE, Campbell KL. Muller and Kirk's small animal dermatology. 7th ed. St. Louis, MO:

Elsevier; 2013:597-599.

9. Mortimer PS, Gummer C, English J, Dawber RP. Acquired progressive kinking of hair. Report of six cases and review of literature. *Arch Dermatol*. 1985; 121(8):1031-3.

10. Sundberg JP, Rourk MH, Boggess D, Hogan ME. Angora mouse mutation: altered hair cycle, follicular dystrophy, phenotypic maintenance of skin grafts, and changes in keratin expression. *Vet Pathol*. 1997; 34(3):171-9.

11. Sundberg JP, Taylor D, Lorch G, Miller J, et al. Primary follicular dystrophy with scarring dermatitis in C57BL/6 mouse substrains resembles central centrifugal cicatricial alopecia in humans. *Vet Pathol*. 2011; 48(2): 513-524.

12. Zimmerman TJ, Jenks JA, Holler LD, Jacques CN, Morlock WW. Congenital hypotrichosis in a white-tailed deer fawn from South Dakota. *J Wildl Dis*. 2004;40(1):145-149.

CASE II: 3140429021 (JPC 4066087).

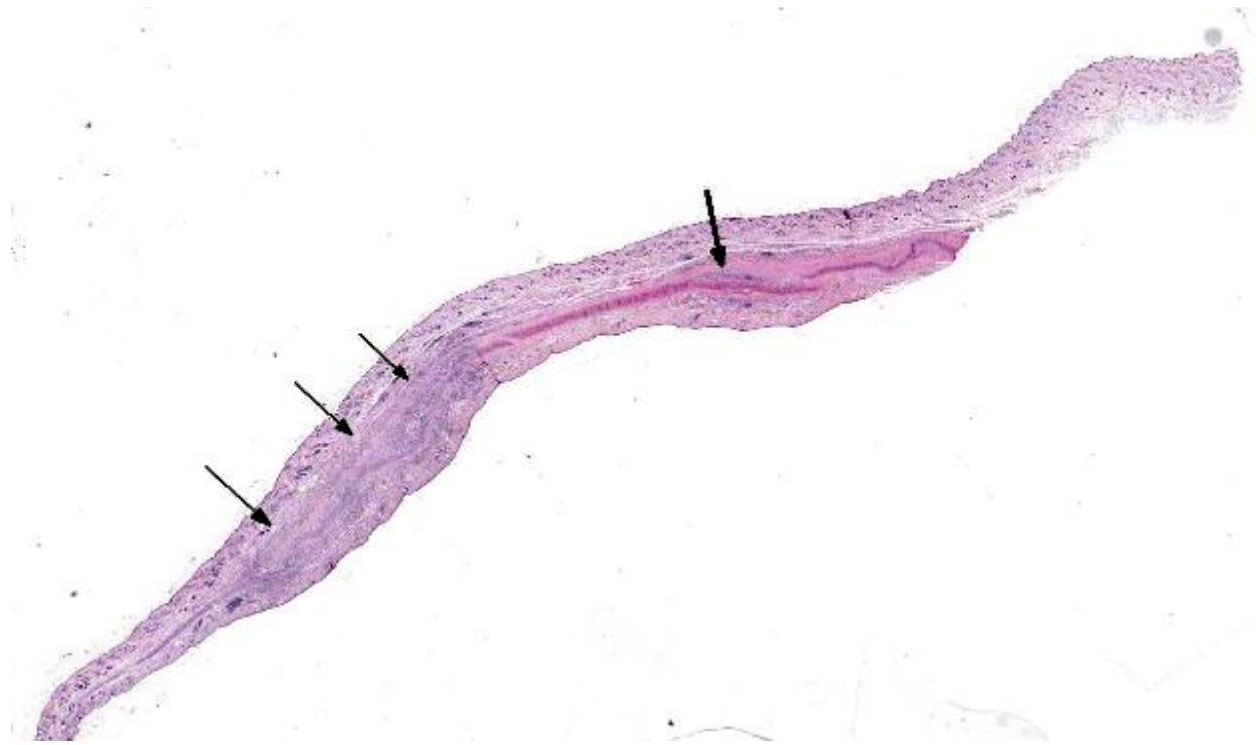
Signalment: 8-year-old, male, European shorthair domestic cat (*Felis catus*).

History: Firm, plaque-like thickening of the pinna which is growing.

Gross Pathology: The cut surface of the pinnal thickening is beige and firm.

Laboratory Results: None

Histopathologic Description: Pinna: The deep dermis of the pinna is multifocally thickened by large numbers of neutrophils and fewer lymphocytes and plasma cells in the dermis surrounding the abnormal auricular cartilage. The inflammatory in-



Pinna, cat. Multifocally, the pinnal cartilage is surrounded and infiltrated by a cellular infiltrate which extends into the surrounding dermis (arrows). (HE, 6X)

filtrate sometimes extends into the cartilage, which in some sections is occasionally split. The chondrocytes in these areas show degeneration and necrosis characterized by cytoplasmic hypereosinophilia and pyknotic or karyorrhectic nuclei. The necrotic cells are occasionally surrounded by small numbers of lymphocytes. Multifocally the cartilage is expanded by nodular areas that lack the normal architecture and are occasionally surrounded by dense connective tissue (fibrocartilagenous noduli). The deep dermis shows mild to moderate oedema, with dilation of dermal lymphatics, and there is multifocal proliferation of fibroblasts. The superficial dermis shows a moderate perivascular and periadnexal lymphoplasmacytic infiltrate with scattered neutrophils and mast cells. There is hyperemia of dermal capillaries.

Contributor's Morphologic Diagnosis:

Pinna: Marked multifocal, chronic

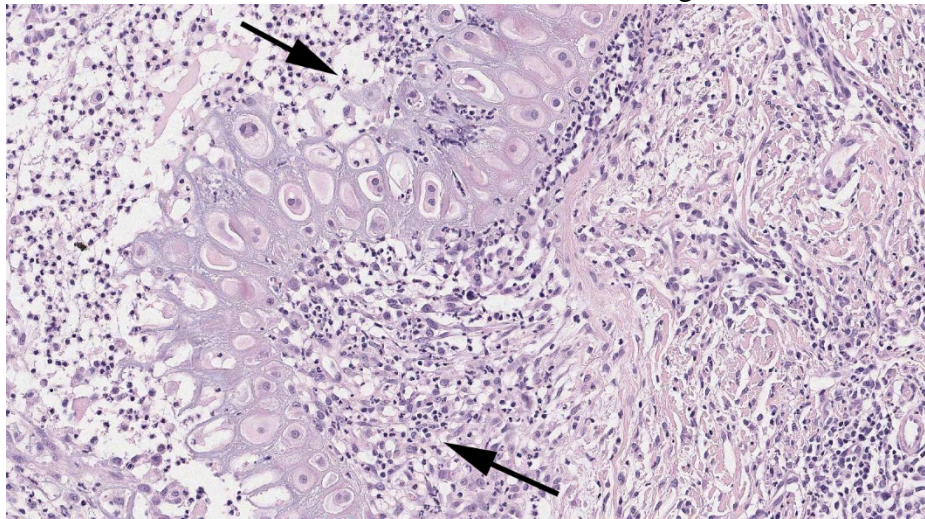
lymphoplasmacytic and neutrophilic chondritis and dermatitis with degeneration splitting and necrosis of auricular cartilage.

Contributor's Comment:

Auricular chondritis has been reported in rats, mice, cats, dogs, in a horse and very rarely in cattle.¹ It has been classified among the immune-mediated diseases due to similarities to rheumatoid arthritis and lupus erythematosus as well as its favorable response to immunomodulatory therapy.⁵ In humans, it manifests as part of relapsing polychondritis complex, a rare systemic autoimmune disease characterized by episodic destructive inflammation of cartilaginous tissues throughout the body especially those of the ear, nose, joints and respiratory tract.⁶ It has been reported rarely in cats and dogs and both ears are typically affected. Clinical signs include pain, swelling, erythema and deformation of the pinnae. Other organs such as joints, eyes and

heart may be present as well. Histologically, lesions consist of lymphoplasmacytic infiltrates and loss or necrosis of cartilage.^{3,6}

In cattle, one case report characterizes the lesions by lymphoplasmacytic infiltrates and presence of few macrophages within the cartilaginous plate of the pinna, which can



Pinna, cat. Numerous neutrophils and fewer histiocytes breach the fibrous perichondrium and infiltrate the distorted cartilaginous plates. (HE, 144X)

be expanded by multiple basophilic cartilaginous nodules, vascularization and perivascular fibrosis. Chondrocytes in the center of the cartilaginous nodules may be swollen and found in clusters (proliferation). Rarely, low numbers of spindle cells surrounded by lacuna were present within these dense collagenous bundles (interpreted as early osseous metaplasia).⁶ In humans, histologically similar lesions may involve the pinnae, nose, trachea, joints, eyes and heart.^{3,6}

JPC Diagnosis: Ear pinna: Auricular chondritis, chronic-active, multifocal, moderate with cartilage degeneration.

Conference Comment: The conference histologic description of this well characterized lesion was very similar to the

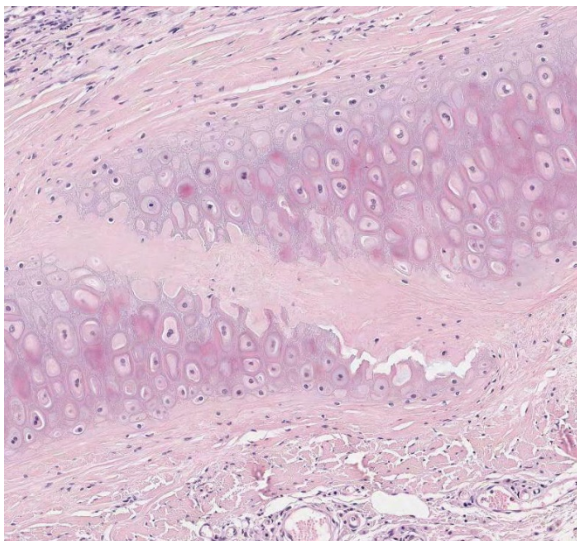
contributor's description and emphasized the targeting of auricular cartilage. The cartilage was described as discontinuous, pale, degenerate and deformed with infiltration by a mixed inflammatory cell population, dominated by neutrophils. Multifocal thick-ening of the dermis and perichondral fibrous tissue coupled with granulation tissue associated with and

surrounding foci of the most affected cartilage (a histologic feature that varies between slides) resulted in a brief discussion amongst conference participants regarding the chronicity of the lesion. In this case, the term "chronic-active" used in the JPC diagnosis denotes the chronic degenerative changes associated with the auricular cartilage as well as the

active, on-going acute inflammatory component consisting heavily of neutrophils and lesser numbers of mononuclear cells.

Feline relapsing polychondritis, more commonly known as auricular chondritis, is an uncommon condition in cats with no sex predilection affecting predominantly young to middle aged cats, although the lesion has been documented in older cats as well. The current published veterinary literature is unclear regarding whether additional cartilage tissues may be involved; although there has been speculation regarding the presence of joint, ocular lesions and cardiac involvement which is documented in the corresponding human condition as discussed above.⁴ There is a case reported by Baba et al. which involved systemic joint and cartilage inflammation. In that case, the

histologic ear lesions were similar to other cases reported in the literature. Additionally, costal cartilages were swollen, laryngeal cartilages thickened, and the articular cartilage of most peripheral joints eroded. There was also destruction of the subchondral bone, lymphocytic inflammation in the trachea and larynx and chondrolysis of the thyroid cartilage with associated inflammation. The costal cartilages were described as “irregularly hypertrophic” with bone formation and mixed inflammatory infiltration. Involvement of the respiratory tract and costal cartilage was not previously reported in cats. Uveitis was also reported in that case. Overall, the lesions described in Baba et al.’s case report were more similar to human relapsing polychondritis than other cases of feline auricular chondritis previously reported. However, there were also discrepancies with the human condition, including the nature of the joint lesions, which were more consistent with, and diagnosed as chronic progressive arthritis. Additionally, the cat also had lymphoma, which was considered as a possible cause of the inflammatory lesions in the joints / cartilage.²



Pinna, cat. Participants discussed the apparent cleft in the pinnal cartilage, as to whether it might represent a

previous focus of quiescent inflammation, or a function of cut through a cartilaginous ostium. (HE, 88);

Histologic lesions in this case are similar to cases described in the veterinary literature and include inflammation and loss of basophilic staining of the ear cartilage with degeneration and necrosis. Fibroblast and capillary endothelial cell proliferation surrounding inflamed cartilage is also described, and is consistent with the presence of granulation tissue as previously discussed. The condition is most often bilateral, fever is reported in some cases and there has been no documented association with FeLV or FIV; unlike the condition in humans, it does not seem to have a relapsing nature. In some cases, cats have been documented to improve without treatment. Due to the rarity of the condition and the lack of thorough follow up in documented cases, the prognosis is unclear.⁴

Contributing Institution:

Utrecht University
Department of Pathobiology
www.uu.nl/faculty/veterinarymedicine/EN/abs_services/vpdc

References:

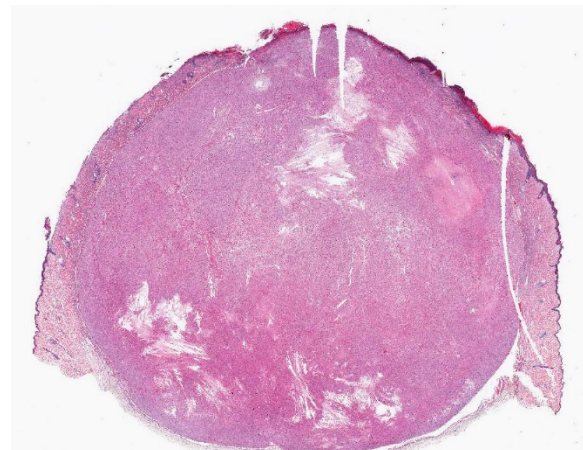
1. Adissu HA, Baird JD, Wood GA. Case Report: A Case of Bilateral Auricular Chondritis in a Heifer. *Case Reports in Veterinary Medicine*. 2014; Article ID 929075. Hindawi Publishing. <http://dx.doi.org/10.1155/2014/929075>. Accessed June 2, 2015.
2. 6. Baba T, Shimizu A, Ohmuro T, Uchida N, et al. Auricular chondritis associated with systemic joint and cartilage inflammation in a cat. *J Vet Med Sci*. 2009;71(1):79-82.
3. Delmage DA, Kelly DF. Auricular chondritis in a cat. *J Small Anim Pract*. 2001;42(10):499-501.

4. Gerber B, Crottaz M, von Tschamer C, Scharer V. Feline relapsing polychondritis: two cases and a review of the literature. *J Feline Med Surg*. 2002;4(4):189-94.
5. Griffin, C. Dermatologic diseases of the auricle. 2006. International Veterinary Information Service; WSAVA lecture. www.ivis.org/proceedings/wsava/2006/lecture26/Griffin4.pdf - 2011-11-28. Accessed June 2, 2015.
6. Torres SMF. Miscellaneous Diseases of the Pinna. *The Merck Veterinary Manual*. Whitehouse Station, NJ: Merck and Co.;2009-2015. http://www.merckvetmanual.com/mvm/eye_and_ear/diseases_of_the_pinna/miscellaneous_diseases_of_the_pinna.html. Accessed June 2, 2015.

CASE III: N9619660 (JPC 4033565).

Signalment: 2-year-old male ferret (*Mustela putorius furo*).

History: Soft subcutaneous mass on head caudal to the right ear growing over 2 months. Otherwise healthy.



Ferret, head. A 2cm expansile nodule is present within the dermis caudal to the right ear.(HE, 5X)

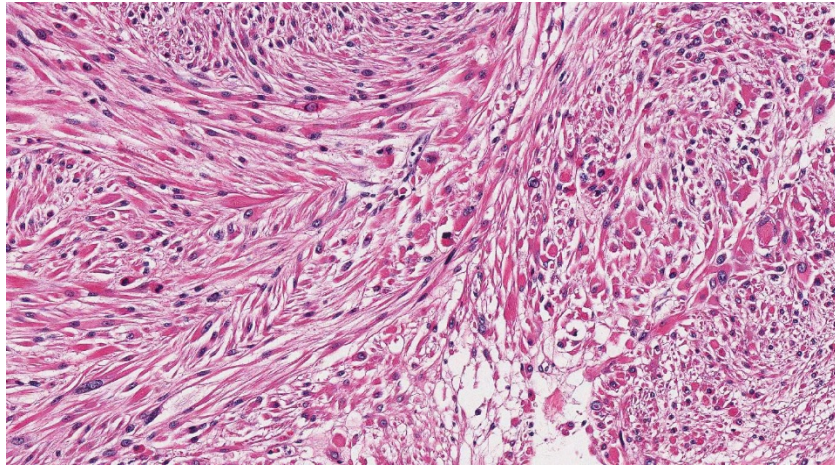
Gross Pathology: 2 cm in diameter firm white-tan mass with overlying ulcer.

Laboratory Results: Fine needle aspirate of mass consisted only of blood.

Histopathologic Description: Expanding the dermis and subcutis, there is a well-demarcated, expansile proliferation of neoplastic spindle cells surrounded by a pseudocapsule of compressed adjacent connective tissue. Neoplastic cells are arranged in long interwoven bundles and streams supported by a fine collagenous stroma. Cells are spindle-shaped to strap-shaped with moderate to abundant eosinophilic fibrillar cytoplasm and an oval to irregular nucleus with coarsely clumped chromatin, occasional nuclear vacuoles, and one to multiple prominent nucleoli. There is moderate anisocytosis and severe anisokaryosis with occasional binucleation or multinucleation with lining up of nuclei, and the mitotic index varies depending on the section from 2-5 per 10 high power fields. There are few coalescing large areas of necrosis within the tumor (<50% of the neoplasm) and in some sections, there are small aggregates of lymphocytes within the peripheral aspect of the neoplastic proliferation. There is an overlying ulcer covered by a serocellular crust with fibrin and within the subjacent dermis, there are numerous necrotic and viable neutrophils. The surgical margins are clean (present in the majority of tissue sections).

Immunohistochemistry (Figure 2A and 2B): Nearly all of the neoplastic cells have diffuse strong cytoplasmic immunoreactivity for smooth muscle actin and approximately 60% of the neoplastic cells have weak to moderate cytoplasmic immunoreactivity for desmin.

Contributor's Morphologic Diagnosis:
Skin and subcutis (head): Pilo leiomyosarcoma.



Head, ferret. Elongate neoplastic cells are arranged in broad streams and bundles. (HE, 77X)

Contributor's Comment: The histopathology is consistent with a mesenchymal neoplasm and the cellularity, pleomorphism and mitotic activity are consistent with a sarcoma. Based on the histomorphology and growth pattern of the cells, the immunohistochemistry findings, and the location within the dermis and subcutis, this tumor is consistent with a pilo leiomyosarcoma. Pilo leiomyosarcomas are neoplasms arising from the arrector pili muscles, which are the smooth muscle bundles supporting the hair follicle and allowing for piloerection. Tumors arising from the arrector pili muscles have been reported in ferrets,^{1,5,7} as well as in dogs and cats.¹⁻³ The majority of cases in ferrets have been pilo leiomyosarcomas, with fewer reports of benign pilo leiomyomas.⁴

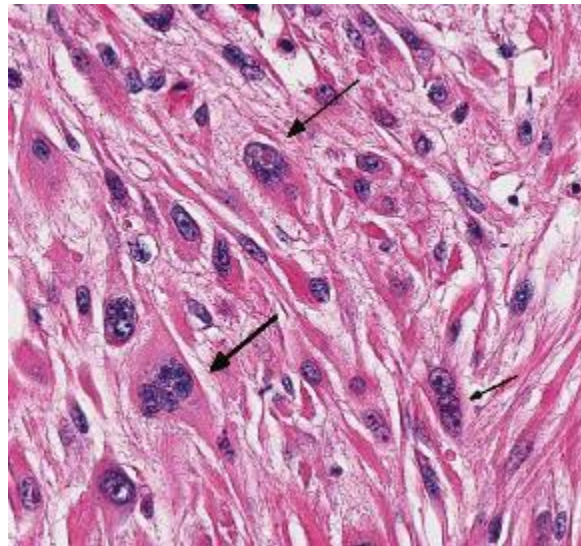
In ferrets, pilo leiomyosarcomas most commonly arise from the head and trunk, with fewer cases from the limbs, and may have surface ulceration.^{5,7} Histologically, despite being well-demarcated, the neoplastic cells have significant nuclear pleomorphism, and reports vary regarding mitotic activity, which may be uncommon (1-2 per 10 high power fields)⁷ or more

frequent (≥ 2 per 10 high power fields).⁵ The nuclear pleomorphism or increased mitotic activity (mitotic index of ≥ 2)⁵ are the foundation for the diagnosis of malignancy in these cases.

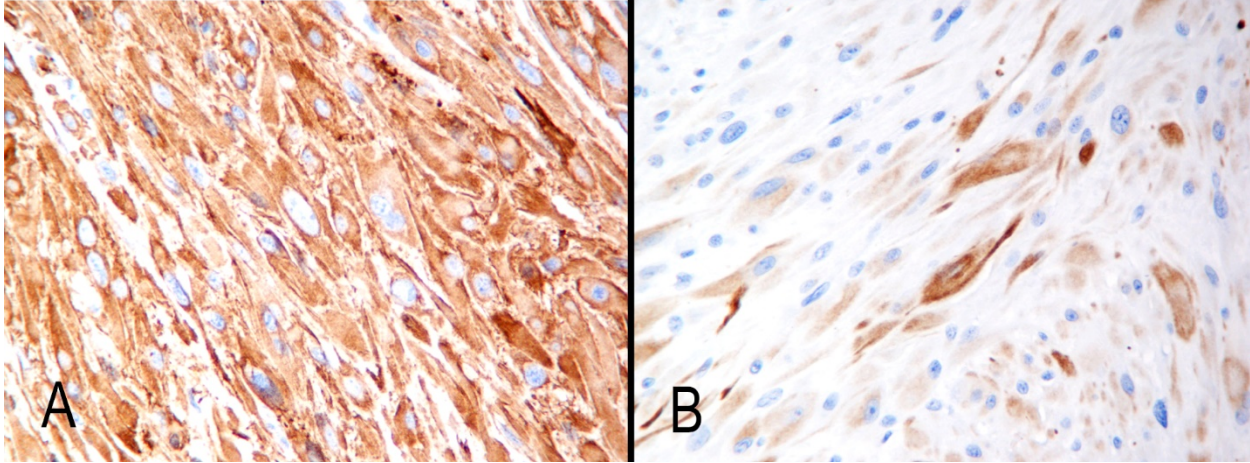
Foci of lymphocytes may be seen at the periphery of the neoplasm⁷ and areas of necrosis within the tumor may be identified,⁵ as in the current case. Direct connection of the tumor with the adjacent arrector pili muscles may or may not be

found,^{5,7} and is not clearly present in this case. The majority of

pilo leiomyosarcomas in ferrets are positive for desmin and smooth muscle actin with immunohistochemistry^{5,7} (Figure 2A and 2B). The prognosis for pilo leiomyosarcomas in ferrets is good following complete surgical excision with no reports of metastasis and good long-term survival in those cases with follow-up.^{5,7} Follow-up is not available for the present case.



Ferret, head. Neoplastic smooth muscle cells exhibit marked anisocytosis and anisokaryosis as well as multinucleation. (HE, 320X)



*Neoplastic cells show strong diffuse cytoplasmic positivity for desmin (A), and multifocal moderate cytoplasmic positivity for smooth muscle actin. (Photo courtesy of: Animal Medical Center, 510 East 62nd Street, New York, NY 10065
www.amcny.org*

In dogs and cats, general criteria to support a diagnosis of cutaneous leiomyosarcoma, as compared to a benign leiomyoma, include mitotic index of ≥ 1 , evidence of invasion, and/or necrosis within the tumor.¹ In dogs and cats, piloleiomyomas and piloleiomyosarcomas are considered likely to be cured by complete excision, and local recurrence or metastasis of cutaneous leiomyosarcomas in general is uncommon.¹⁻³ In humans, leiomyosarcomas arising from the arrector pili muscles have a moderate local recurrence rate of 30% and metastasis is not reported.⁷

In conclusion, this case is a classic example of a piloleiomyosarcoma in a ferret and has many of the characteristic gross and histologic features reported with this entity.

JPC Diagnosis: Haired skin and subcutis: Piloleiomyosarcoma.

Conference Comment: The conference description was very similar to the contributor's histologic description above. The neoplastic cell nuclei were described as cigar shaped with blunted ends and the cells themselves were described as strap-shaped, which is often a feature used to describe

rhabdomyosarcomas. Eosinophilic nuclear vacuoles were also discussed and described as cytoplasmic invaginations, although their actual nature/origin is unclear. There was spirited discussion on the designation of the neoplasm as a piloleiomyosarcoma as opposed to piloleiomyoma. While the cellular characteristics of malignancy, such as binucleation, multinucleation, anisocytosis/anisokaryosis, and a high mitotic rate is evident in this neoplasm and well-documented in the literature, metastatic potential is extremely low, and has not been described in the literature.

Cutaneous smooth muscle tumors can also arise from vascular smooth muscle and deep dermal smooth muscle of the genital area. Vascular origin smooth muscle tumors are termed angioleiomyoma/angioleiomyosarcoma. Regardless of origin, the tumors have similar histologic characteristics. Anatomic location can help differentiate these tumors, such as location in the genital area, or other features such as entrapment of hair follicles within the neoplasm, contiguity with erector pili muscle, or the presence/absence of a prominent vascular component may also be helpful.⁵ Other neoplasms involving the skin of ferrets include mast cell tumors, basal cell tumors and neoplasms of apocrine sweat

glands. Mast cell tumors are most common on the head, neck, shoulders and trunk but can occur at any location. Tumors of basal cell origin (most commonly sebaceous epithelioma of the skin) can also occur at any location and are benign. The most common malignancy of the skin of the ferret are those of apocrine glands, which are most often seen around the prepuce and vulva, but may also be seen on the head and neck. Other less common tumors in the skin of ferrets include squamous cell carcinoma, cutaneous lymphoma, hemangioma/hemangiosarcoma, and fibroma/fibrosarcoma.⁶

Contributing Institution:

Animal Medical Center
510 East 62nd Street
New York, NY 10065
www.amcny.org

References:

1. Cooper BJ, Valentine BA. Tumors of muscle. In: *Tumors in Domestic Animals*. Ames, IA: Iowa State Press; 2002:319-363.
2. Goldschmidt MH, Shofer FS. Uncommon skin tumors. In: *Skin Tumors of the Dog and Cat*. New York, NY: Butterworth Heinemann; 1998:291-295.
3. Liu SM, Mikaelian I. Cutaneous smooth muscle tumors in the dog and cat. *Vet Pathol*. 2003; 40:685-692.
4. Mialot M, Prata D, et al. Multiple progressive piloleiomyomas in a ferret (*Mustela putorius furo*): a case report. *Vet Dermatol*. 2010; 22:100-103.
5. Mikaelian I, Garner MM. Solitary dermal leiomyosarcomas in 12 ferrets. *J Vet Diagn Invest*. 2002;14:262-265.
6. Orcutt C, Tater K. Dermatologic diseases. In: Quesenberry KE, Carpenter JW, eds. *Ferrets, rabbits, and rodents clinical medicine and surgery*. 3rd ed. St. Louis, MO: Elsevier Saunders; 2012:127-130.
7. Rickman BH, Craig LE, Goldschmidt MH. Piloleiomyosarcoma in seven ferrets. *Vet Pathol*. 2001; 38:710-711.

CASE IV: B14-15532 (4073336).

Signalment: 1-year-old spayed female golden retriever (*Canis familiaris*).

History: The dog has an acute history of skin lesions that were noticed 12 to 14 hours prior to examination by a veterinary dermatologist. One week prior to presentation, the local veterinarian gave the dog a rabies vaccine, and no abnormalities were noted on physical exam. Three days prior to presentation, the dog was routinely bathed at a commercial grooming facility. On physical examination, the dog was febrile (104°F), lethargic, and painful and had a mild neutrophilia with left shift. Two 6-mm punch biopsies were taken from the dorsolumbar skin via local anesthesia.

Gross Pathology: Coalescing erythematous to hemorrhagic papules and pustules on the dorsal midline.

Laboratory Results: None

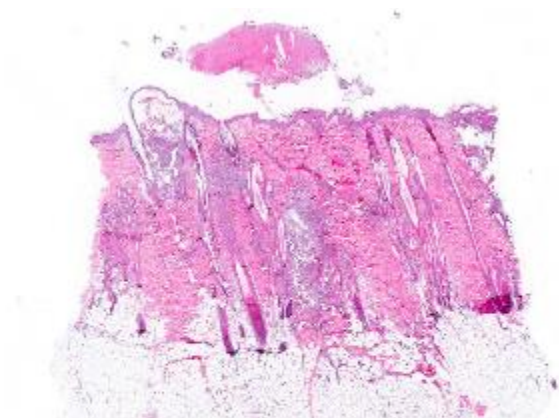


Haired skin, dog. The skin of the dorsal midline was covered with hemorrhagic papules and pustules. (Photo courtesy of: University of Pennsylvania, School of Veterinary Medicine, Department of Pathobiology <http://www.vet.upenn.edu/diagnosticlabs>)

Histopathologic Description: The main histologic change is multifocal outer root sheath necrosis with suppurative inflammation and acute hemorrhage in the superficial and mid-dermis. Dense localized aggregates of neutrophils and fewer macrophages surround adnexal units and are admixed with free keratin and erythrocytes. The suppurative aggregates form large subepidermal pustules. The epidermis is expanded by spongiosis with mild acanthosis. There is mild superficial dermal edema.

Contributor's Morphologic Diagnosis: Furunculosis, necrosuppurative and hemorrhagic, acute, multifocal, severe.

Etiologic diagnosis: Bacterial furunculosis



Haired skin, dog. A punch biopsy contains numerous areas of dermal inflammation and overlying serocellular crust. (HE, 6X).

Name of disease: Post-grooming furunculosis

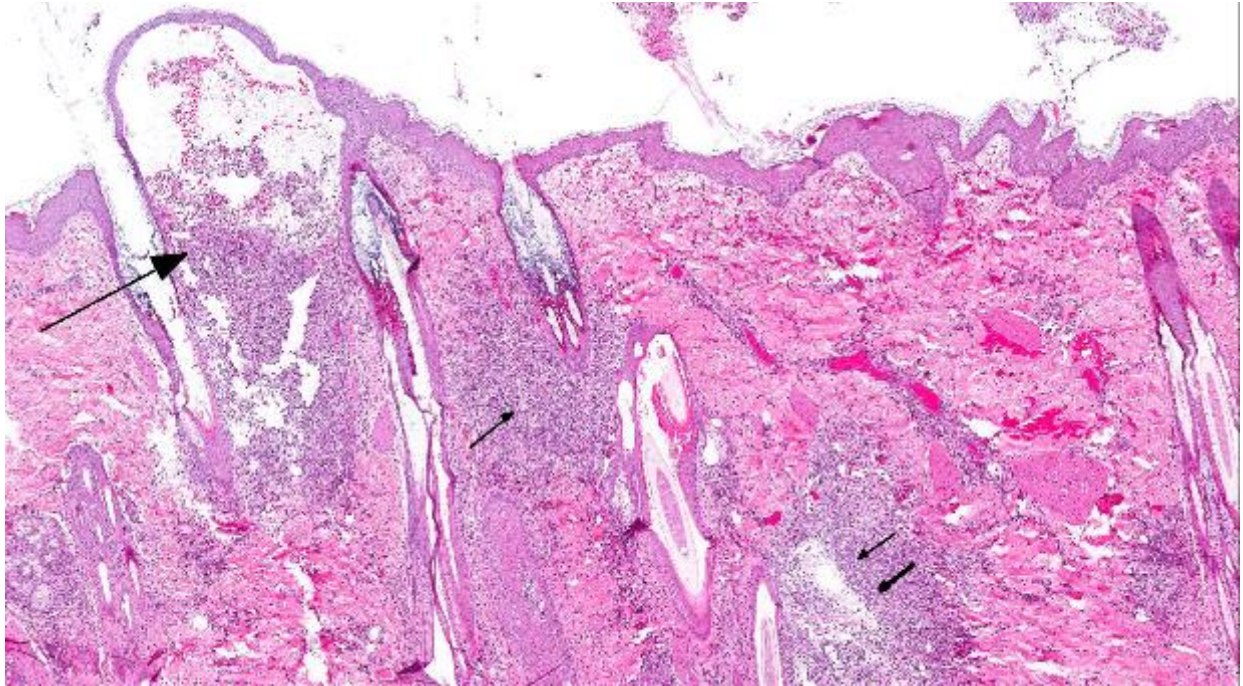
Contributor's Comment:

The clinical and histologic features are typical of "post-grooming furunculosis" (PGF). This acute and severe inflammatory reaction is associated with the use of contaminated grooming products. While contaminated shampoos or conditioners are the most common causes, vigorous brushing (e.g. coat stripping), whirlpools, and contaminated surgical scrub have also been documented. *Pseudomonas* spp. is the most common isolate from the skin. In some cases, the bacteria can be cultured from both the skin and the affected product.

The clinical lesions typically arise on the dorsal midline as hemorrhagic pustules and crusts. The dogs may be febrile and very painful on thoracolumbar palpation. In dogs with a dense or thick haircoat (e.g. Golden retriever), the lesions may be missed on initial examination. In fact, some patients have been worked up for discospondylitis, back pain, tick borne diseases or pancreatitis.

In contrast to other causes of furunculosis (e.g. demodicosis, dermatophytosis, staphylococcal infection), PGF is acute. The outer root sheath is necrotic rather than hyperplastic and the rupture occurs in the superficial dermis. Furthermore, the inflammation is hemorrhagic and fibri-nosuppurative rather than pyogranulomatous. Bacteria may be difficult to discern on H&E and Gram stain as they are often small gram negative bacilli.

JPC Diagnosis: Haired skin: Furunculosis, superficial, necrosuppurative and hemorrhagic, acute, multifocal to coalescing, marked.



There is furunculosis resulting from the destruction of follicles throughout the section (arrows). The superficial nature of the inflammation at left (large arrow) is a characteristic feature of post-grooming furunculosis. (HE, 30X)

Conference Comment: The presence of erector pili muscles allows localization of the section to skin of the back/dorsum. At subgross magnification, a distinctive histologic pattern is identified characterized by inflammation targeting the hair follicle in the superficial dermis. A coagulum of predominantly degenerate neutrophils, fibrin, hemorrhage and debris overlies the epidermis; folliculosebaceous units are infiltrated by neutrophils with fewer macrophages and plasma cells admixed with hemorrhage and edema within the superficial dermis and extending into the mid dermis. The infiltrate results in a mural folliculitis with progression to furunculosis. The inflammatory milieu associated with the corresponding furunculosis contains basophilic fragmented material, interpreted as keratin, along with free necrotic keratinocytes which can be differentiated from macrophages by the distinctive rounded cellular margins in the former. The moderator noted that in many inflammatory conditions targeting the hair follicle, the

follicular epithelium is typically hyperplastic which is not a microscopic feature observed in cases of PGF.

The superficial nature of the lesions, acute onset, hemorrhage and lesions isolated to the dorsal trunk can help differentiate this condition from other causes of folliculitis and furunculosis in dogs. The predilection for lesions over the dorsum in PGF is postulated to be associated with the nature of grooming or bathing activities that may concentrate brushing and shampooing efforts on this area. The dorsum also has increased hair density and hair shaft size. Cytologic features of impression smears may include neutrophils and macrophages with or without eosinophils, red blood cells, and intracellular or extracellular bacteria. Clinicopathologic abnormalities associated with this condition may include neutrophilia, with or without a left shift, monocytosis, lymphopenia and mild thrombocytopenia. These abnormalities, when

considered with the presence of fever, may suggest a systemic inflammatory response.¹

Pseudomonas aeruginosa, a gram negative bacillus, is the most common bacterial agent associated with post-grooming furunculosis. *Pseudomonas aeruginosa* is a common bacterial contaminant associated with water and can survive in the presence of some disinfectants. Other bacteria, such as *Serratia marcescens* and *Burkholderia cepacia*, are associated with this condition. In the veterinary setting, *S. marcescens* has been implicated as a contaminant of intravenous catheters, and *B. cepacia* has been documented as a contaminant of ear cleaning solutions.¹

Contributing Institution:

University of Pennsylvania, School of Veterinary Medicine, Department of Pathobiology
<http://www.vet.upenn.edu/diagnosticlabs>

References:

1. Baxter CG, Vogelnest LJ. Multifocal papular deep bacterial pyoderma in a Boxer dog caused by *Pseudomonas aeruginosa*. *Aust Vet J*. 2008;86:435–439.
2. Cain C, Mauldin EA. Clinical and histopathologic features of dorsally oriented furunculosis in dogs following water immersion or exposure to grooming products. *J Am Vet Med Assoc*. 2015; 246(5):522-9.
3. Hillier A, Alcorn JR, Cole LK, et al. Pyoderma caused by *Pseudomonas aeruginosa* infection in dogs: 20 cases. *Vet Dermatol*. 2006;17:432–439.
4. Ihrke PJ, Gross TL. Warning about postgrooming furunculosis. *J Am Vet Med Assoc*. 2006;229:1081–1082.

Joint Pathology Center
Veterinary Pathology Services



WEDNESDAY SLIDE CONFERENCE 2015-2016

Conference 12

6 January 2016

Moderator:

Tim Cooper, DVM, Ph.D, DACVP
Associate Professor
Department of Comparative Pathology
Penn State Hershey Medical Center
Hershey, PA

CASE I: A10-9691 (JPC 3164430).

Signalment: Adult female guinea pig (*Cavia porcellus*).

History: This underweight adult guinea pig was found abandoned with truncal alopecia and a palpable abdominal mass. Age was estimated at 3 years. Ovariohysterectomy was performed in preparation for adoption.



Ovary, guinea pig. The right ovary was enlarged at 3.5 cm x 4 cm x 3.5 cm. (Photo courtesy of: Purdue University Animal Disease Diagnostic Laboratory: <http://www.addl.purdue.edu/> and Department of Comparative Pathobiology: <http://www.vet.purdue.edu>.)

Gross Pathology: The right ovary was enlarged at 3.5 cm x 4 cm x 3.5 cm.

Numerous fluid-filled cysts up to 7-8 mm in diameter were evident on cross-section. Extensive stromal calcification or ossification necessitated decalcification before histologic processing.

Laboratory Results:

No ancillary testing performed.

Histopathologic Description: A few viable follicles are in the periphery of the mass, but most of the specimen lacks recognizable ovarian tissue and instead is composed of neoplastic tissue from all 3 germ layers. The endodermal component includes tubuloacinar glands (lobules of serous acini formed by pyramidal cells with bright eosinophilic cytoplasmic granules) and cystic spaces lined by respiratory type epithelium with numerous ciliated cells and mucus-filled goblet cells. The ectodermal component consists of neuroectodermal tissue with axons, glial cells, and neuronal cell bodies; no skin, hair follicles or cutaneous adnexal glands are observed. The mesodermal

component consists mainly of fibrous tissue with scattered plates of well differentiated bone. No lesions were detected in the left ovary or in the uterus.

Contributor's Morphologic Diagnosis:
Ovary: Ovarian teratoma

Contributor's Comment: The presence of all 3 germ layers in a neoplastic gonadal mass was the basis for the diagnosis of teratoma. Reproductive tract tumors account for about 25% of neoplasia in the guinea pig. Though not considered common, teratoma is the most frequently reported tumor of the guinea pig ovary, occurring in juveniles and adults, and accounting for all but 6 of 29 ovarian tumors reviewed in a 1976 book chapter.³ Interestingly, testicular teratomas seem not to have been reported in the guinea pig.

One of two ovarian teratomas reported by Willis⁷ spread to peritoneal surfaces. Of 10 cases of ovarian teratoma found at necropsy of about 13,000 guinea pigs over an 8-year period,⁶ none had metastasized, though some cases had resulted in abdominal hemorrhage.



Ovary, guinea pig. Numerous fluid-filled cysts up to 7-8 mm in diameter were evident on cross-section (Photo courtesy of: Purdue University Animal Disease Diagnostic Laboratory: <http://www.addl.purdue.edu/> and Department of Comparative Pathobiology. <http://www.vet.purdue.edu/cpb/>)

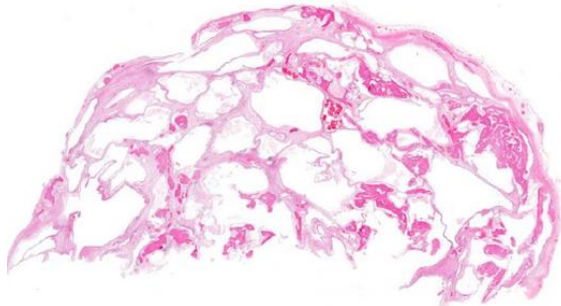
Tissues from at least 2 germ layers were found in all 10 tumors; most tumors had all 3 germ layers, and nervous tissue tended to be the dominant ectodermal component. Nervous tissue also figured prominently as the ectodermal component in another case of ovarian teratoma that had spread to the peritoneal surface of the diaphragm.¹

Granulosa cell tumor is reported far less commonly than ovarian teratoma in guinea pigs;³ however, because of its potentially cystic nature, it should be included in the differential diagnosis for an ovarian mass along with cystic rete ovarii.⁴ Though distant metastasis has not been recorded in ovarian teratomas in guinea pigs, a few cases have seeded peritoneal surfaces. In this guinea pig, no recurrence or spread of the teratoma was clinically evident at 10 weeks after ovariohysterectomy. The alopecia had resolved, and the guinea pig had gained weight.

JPC Diagnosis: Ovary: Teratoma.

Conference Comment: Conference participants agreed with the contributor that there is a lack of recognizable ovarian tissue on the slide aside from a small section of oviduct at the margin. The neoplasm is large, encapsulated and expansile with haphazardly arranged ectodermal, mesodermal and endodermal elements. Ectodermal elements described and discussed include neurons, neuropil and glia; mesodermal elements include woven bone with osteoclasts, mineralized hyaline cartilage, periosteum and lymphocytes; endodermal elements include ciliated respiratory epithelium with goblet cells, bronchial glands, exocrine pancreatic acini with zymogen granules, and occasional intestinal crypts (not present in all sections). Other features described include hemorrhage, hemosiderin-laden macrophages and large, polyhedral, intensely eosinophilic crystals tentatively identified as hemoglobin crystals.

Alzarin red or Dunn-Thompson stains can be used to confirm the crystals as hemoglobin origin. Other tissue types that can be seen in



Ovary, guinea pig. The subgross view demonstrates numerous cysts as well as large trabeculae of bone (arrows). (HE, 5X)

teratomas which were not present in this example include ectodermal components such as hair, tooth enamel, sebaceous glands and cornified squamous epithelium. Other mesodermal elements can include adipose tissue, bone marrow, skeletal/cardiac/smooth muscle, embryonic mesenchyme and tooth structures including dentin and pulp. Other endodermal components include salivary gland epithelium, renal epithelium and thyroid gland (when thyroid tissue predominates the neoplasm is referred to as “struma ovarii” – literally, “goiter of the ovary”).

Other species in which teratoma is common include 129 strain mice where the tumor most commonly occurs in the testis, but can also occur in extragonadal locations such as along the midline. Ovarian teratomas in mice are uncommon,⁴ however; malignant teratoma has been documented in the ovary of transgenic mice. Teratomas are also common in cryptorchid testis of male horses. They are uncommon in other domestic/lab animal species, but have been documented in ferrets, dogs, cats, cattle, sheep and domestic poultry.² As a general rule, malignant teratomas are far less common in all species than their benign counterparts.

Ovarian neoplasms can be broadly divided into three groups: a) sex-cord stromal tumors which include granulosa-theca cell tumors, and thecoma/luteoma; b) tumors of the epithelial surface which include papillary adenoma/carcinoma and cystic adenoma; and c) germ cell tumors which include dysgerminoma and teratoma. Teratomas arise from totipotential germ cells that have differentiated along two or more somatic lines. Dysgerminomas, in contrast have not undergone somatic differentiation and still resemble germ cells, similar to their testicular counterpart, the seminoma. Other rare germ cell tumors include yolk sac carcinoma, choriocarcinoma and embryonal carcinoma.⁵

Contributing Institution:

Purdue University

Animal Disease Diagnostic Laboratory:

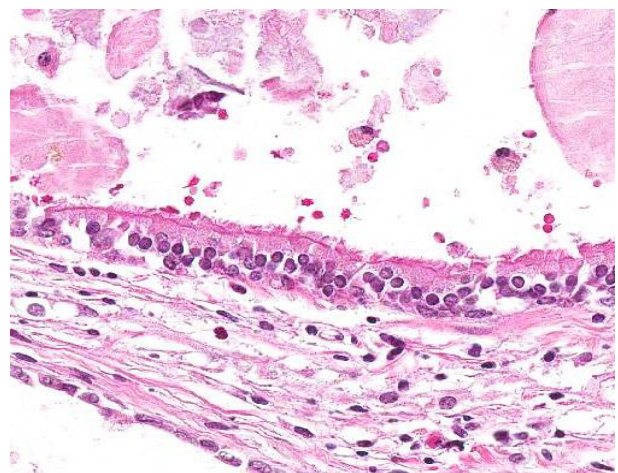
<http://www.addl.purdue.edu/>

Department of Comparative Pathobiology:

<http://www.vet.purdue.edu/cpb/>

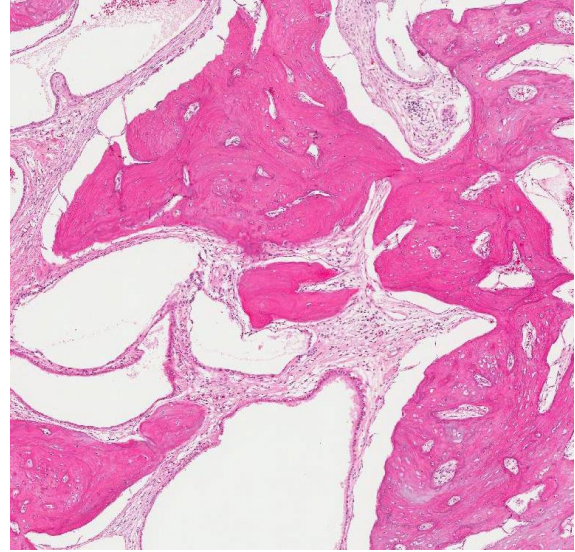
References:

1. Frisk CS, Wagner JE, Doyle RE. An ovarian teratoma in a guinea pig. *Lab Anim Sci.* 1978; 28:199-201.



Ovary, guinea pig. Cysts are primarily lined by a single layer of tall columnar ciliated epithelium and contain a moderate amount of eosinophilic secretory material and sloughed cells in their lumina. (HE, 200X)

2. Leylek RA, Blankenship-Paris TL, Boyle MC. Pathology in practice. Malignant teratoma of the left ovary of a mouse. *J Am Vet Med Assoc.* 2014; 245(2):191-193.
3. Manning PJ. Neoplastic diseases. In: Wagner JE, Manning PJ, Eds. *The Biology of the Guinea Pig.* New York: Academic Press; 1976:211-225.
4. Percy DH, Barthold SW. *Pathology of Laboratory Rodents and Rabbits.* 3rd ed. Ames, IA: Blackwell; 2007:121, 248-251.
5. Schlafer DH, Foster RA. Female genital system. In: Maxie GM, ed. *Jubb, Kennedy and Palmer's Pathology of Domestic Animals.* Vol 3. 6th ed. St. Louis, MO: Elsevier; 2016:375-377.
6. Vink HH. Ovarian teratomas in guinea-pigs: A report of ten cases. *J Pathol.* 1970; 102:180-182.
7. Willis RA. Ovarian teratomas in guinea-pigs. *J Pathol Bacteriol.* 1962; 84:237-239.



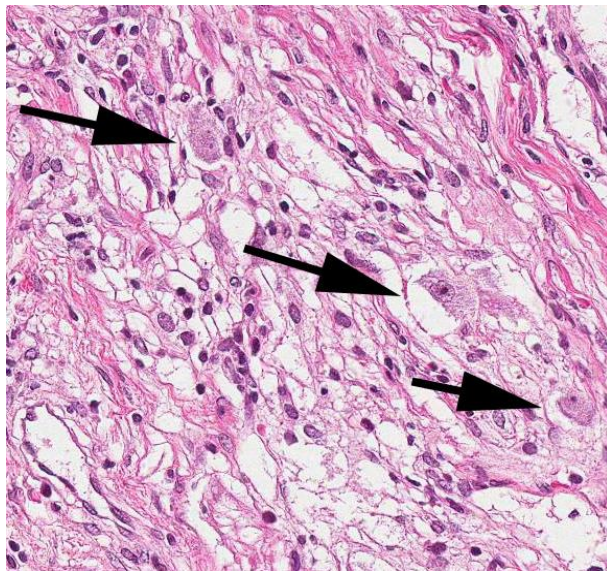
Ovary, guinea pig. Trabeculae of well-differentiated bone are scattered throughout the neoplasm. (HE, 36X)

CASE II: AFIP2 (JPC 4001216).

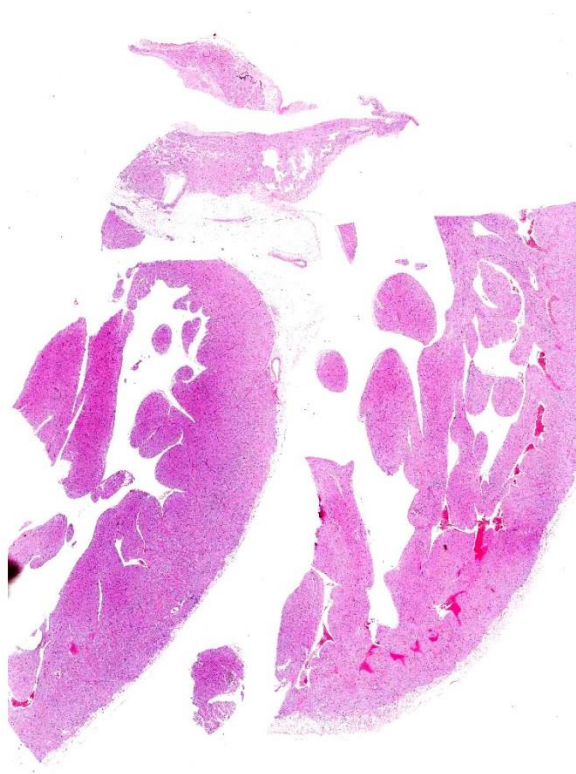
Signalment: Four-year-old, male cynomolgus macaque (*Macaca fasciculata*)

History: Ten months before this animal was euthanized, it showed depression and loss of appetite. After a complete clinical examination, the electrocardiogram revealed an inverted QRS complex on lead II, consistent with a Grade III heart block. Thoracic radiographs showed an enlarged heart. During a second electrocardiogram, retrograde polarization and wide QRS were noted. Days before the euthanasia, the animal was markedly depressed. On a third electrocardiogram, heart block was diagnosed.

Gross Pathology: The left ventricle of the heart was dilated and pale. There was



Ovary, guinea pig. The stroma between cysts contains large areas of neural tissue with occasional neurons (arrows). (HE, 200X)



Heart, cynomolgus macaque: Subgross view of the markedly thinned left ventricle. (HE, 5X)

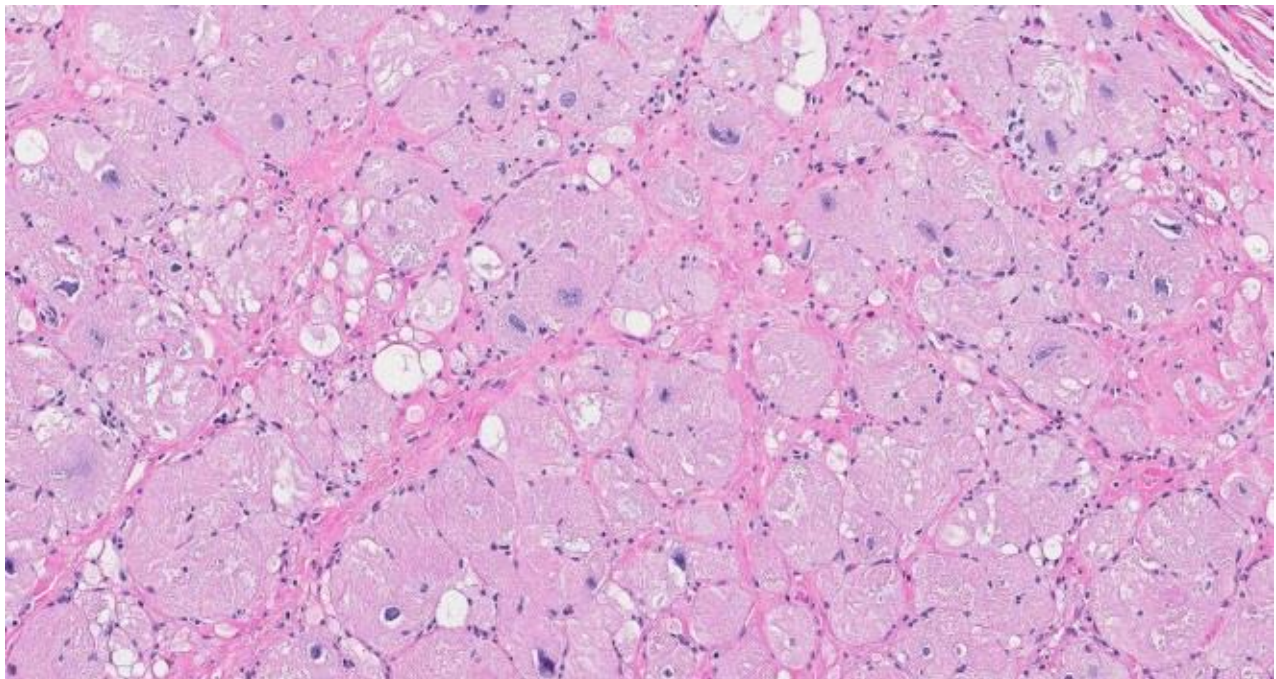
excessive fluid around the heart (pericardial effusion). There was an abnormal surface to

the entire liver and there was an adhesion between the left and right medial lobes. Based on the necropsy findings and clinical observations, a preliminary diagnosis of cardiomyopathy was made and routine histology sections were processed.

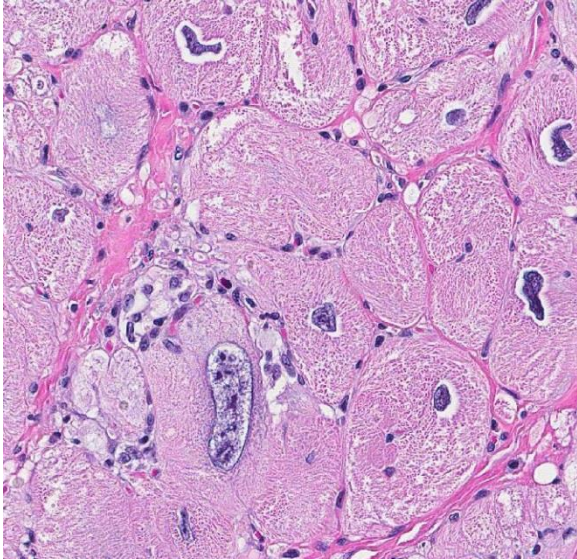
Laboratory Results:

Hemogram and blood chemistry:
Unremarkable.

Histopathologic Description: Heart: The left ventricle is markedly dilated and the wall is thin. In the left ventricular wall, myocardial bundles are haphazardly arranged, with multifocal fascicles of dense fibrous connective tissue (myocardial fiber disarray and fibrosis). There is locally extensive enlargement of myocardial cells with coarse, clear cytoplasmic vacuoles and enlarged, bizarrely shaped nuclei. Occasionally, nuclei have central condensation of the chromatin (caterpillar cells). There are multifocal shrunken, hypereosinophilic myocardiocytes with pyknotic nuclei (necrotic cardiomyocytes). Associated with multiple



Heart, cynomolgus macaque: There is massive cyto- and karyomegaly of cardiac myocytes. Wow! (HE, 124X)



Heart, cynomolgus macaque. Nuclei are often markedly enlarged and pleomorphic. (HE, 220X)

aggregates of mononuclear cells (lymphocytes and macrophages) and lesser numbers of eosinophils. In the interventricular septum, there are similar, but less severe changes as described in the left ventricle. There are discrete segments of endocardial fibrosis with minimal mononuclear infiltrates. In the left auricle, there are focal areas of contraction band necrosis, characterized by the presence of

dense hypereosinophilic bands in the sarcoplasm of cardiomyocytes, with pyknotic nuclei. Occasionally, there are focal areas of coagulative necrosis surrounded by inflammatory aggregates.

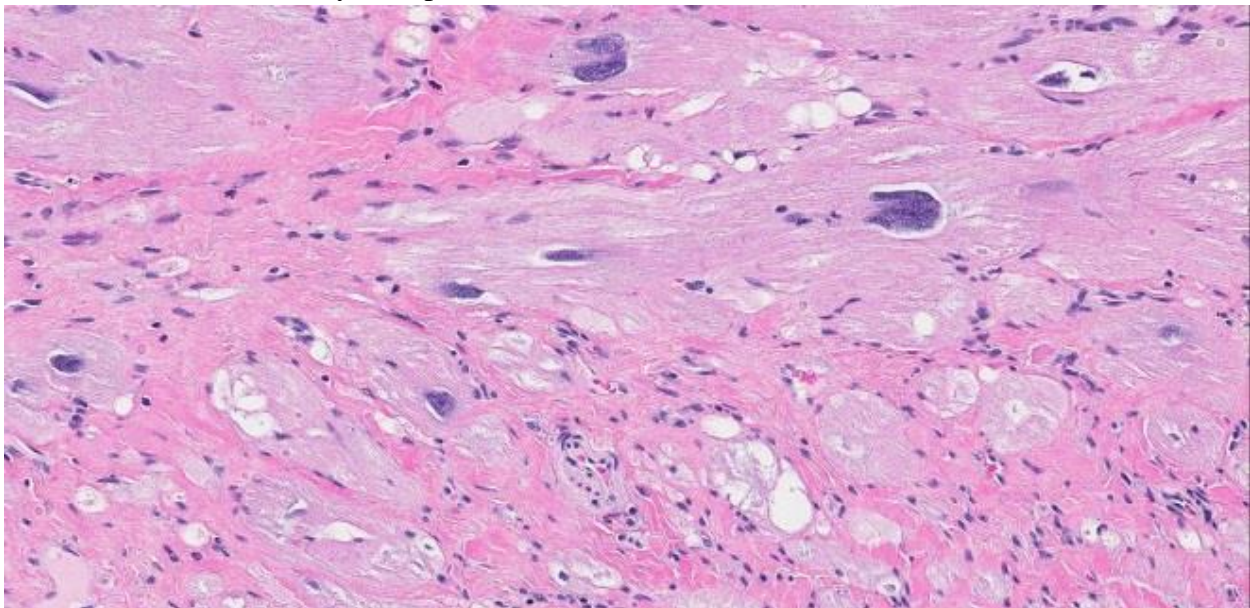
The right ventricle (not submitted) has minimal aggregates of mononuclear cells in the myocardial interstitium. No histological findings were present in the right auricle.

Other findings include passive congestion of the liver, mild hepatic capsular fibrosis, with subcapsular atrophy and focal hemorrhages.

Desmin immune histochemistry demonstrated altered distribution in enlarged cardiomyocytes of the left ventricle, with focal decreased labeling of intercalated discs and Z bands and pale granular cytoplasmic staining, especially in areas of myocardial disarray.

Contributor's Morphologic Diagnosis:

Heart: Myocardial degeneration and disarray, severe, locally extensive, with necrosis, fibrosis, myocardial vacuolation, and karyomegaly, consistent with the dilated

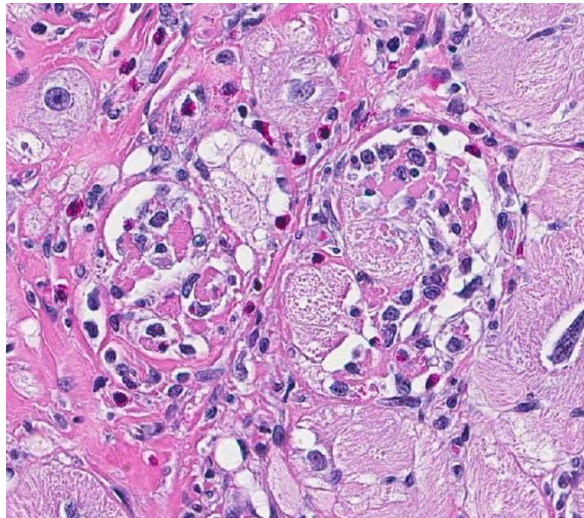


Heart, cynomolgus macaque. There is multifocal to coalescing areas of myofibers loss with replacement with mature collagen. (HE, 164X)

phase of left ventricular hypertrophic cardiomyopathy.

Contributor's Comment: The term cardiomyopathy originated from a group of myocardial diseases in humans with unknown origin or pathogenesis. Generally, cardiomyopathy is characterized by cardiomegaly, mural thrombosis and fibrosis of the myocardium and can be subdivided in a) dilated; b) hypertrophic; and c) restrictive.⁸

The primary differential diagnoses for this case are dilated cardiomyopathy and the dilated phase of hypertrophic cardiomyopathy. In dogs and cats, dilated cardiomyopathy frequently affects all chambers of the heart, with thickened, fibrotic endocardium, myocardial hypertrophy and focal areas of myocardial fibrosis and necrosis. In Holstein cattle, dilated cardiomyopathy most often affects both the right and left ventricles, with similar histological findings as dilated cardio-



Heart, cynomolgus macaque. Scattered throughout the myocardium, there are fragmented and necrotic myofibers undergoing phagocytosis. (HE, 324)

myopathy in dog and cats.^{8,11}

Hypertrophic cardiomyopathy can affect all chambers or be restricted to the left ventricle. Common histologic features include

myocardial disarray, myocardial hypertrophy and vesicular nuclei, as well as diffuse interstitial fibrosis.^{8,11} In general, domestic species have dilated cardiomyopathy and the dilated phase of hypertrophic cardiomyopathy have similar histologic features, which do not indicate etiology or the underlying mechanism of disease process. Histopathology by itself is not a definitive method of differentiation between these two diagnoses. In humans, hypertrophic cardiomyopathy is characterized by similar histological changes as described above in domestic animals. Myocardial disarray is considered a cardinal diagnostic feature of hypertrophic cardiomyopathy in humans when it occupies 20% of one or more tissues blocks.⁴ The dilated phase of hypertrophic cardiomyopathy is usually associated with left ventricular myocardial fibrosis and remodeling, thinning of the ventricular wall and dilatation of the chamber, resembling macroscopic morphologic features of dilated cardiomyopathy.⁵ Fibrosis is often associated with dysplastic changes in the media of small intramyocardial arteries.²

An important feature in human cases of hypertrophic cardiomyopathy is the immunohistochemical expression of desmin. Desmin is an intermediate filament found in muscle tissue, which forms a network around Z-bands, intercalated discs and myofibrils in cardiomyocytes.^{3,4} In the case of this nonhuman primate, desmin immunostain displayed altered distribution in enlarged cardiomyocytes of the left ventricle, with granular cytoplasmic staining and decreased labeling of intercalated discs and Z bands, especially in the disarrayed myocardial fibers compared to unaffected areas in the same section. It was proposed that the lack of proper binding between defective myosin and other sarcomeric filaments causes defective sarcomere formation and myofibrillar disorganization, resulting in disarray and compensatory hypertrophy of cardiac

myocytes in cats.⁶ Based on this postulate, this author and others conclude that altered expression of desmin might serve as a possible immunohistochemical marker for hypertrophic cardiomyopathy.^{3,4}

The electrocardiogram for this nonhuman primate revealed an inverted QRS complex on lead II, diagnostic of a Grade III heart block. Heart block can be the result of several disease states, including myocardial degeneration, necrosis and inflammation, when it occurs in close proximity of the conduction system (J&K). In humans, high grade ventricular block is a rare complication of hypertrophic cardiomyopathy although mild alterations of electrical conduction are commonly observed.¹⁰ In non-human primates, cardiomyopathy has a fairly infrequent occurrence and there is a lack of literature regarding common ECG findings during the clinical course of disease.

Interestingly, in both human and animals, histological changes of myocardial fibrosis and cardiomyocyte disruption have been reported secondary to stress cardiomyopathy, myocardial infarction, hypertension, cardiac hypertrophy and heart failure. Particularly in stress-induced cardiomyopathy (also known as Takotsubo cardiomyopathy), the literature includes descriptions of contraction band necrosis, leukocyte infiltrates and edema. In this condition, left ventricular dysfunction and wall abnormalities are described in the apical and midventricular myocardium, but the basal myocardium is spared.⁷

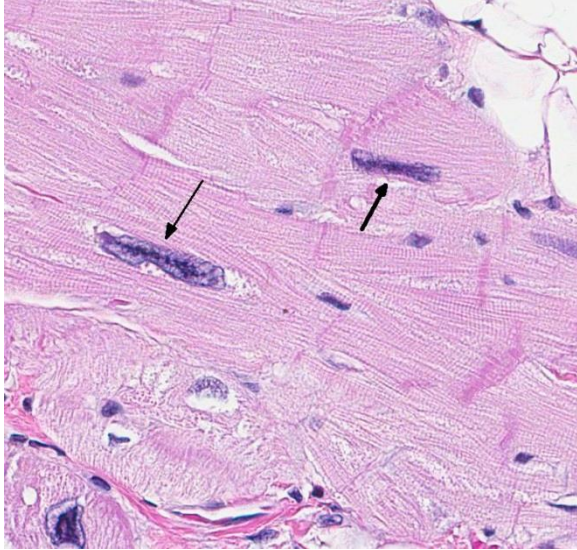
In cynomolgus monkeys, the most common spontaneous finding in the heart is focal mononuclear infiltrates in the interstitium or in perivascular regions, often from the subendocardium, with or without minimal myocardial degeneration and necrosis. This histologic change is not associated with any clinical condition and is considered incidental. Other less common spontaneous

findings in macaques include mineralization of myocardium and/or blood vessels, endocarditis, pericarditis, eosinophilic infiltrates and fibrosis.¹

Spontaneous cardiomyopathy was recently described in cynomolgus monkeys.¹² In this case series, there were no clinical or gross abnormalities. Findings were mainly histological, with extensive areas of myocardial disarray, interstitial fibrosis, vacuolation of perimyseal connective tissue, and disrupted myocytes containing vacuolated sarcoplasm and enlarged nuclei (karyomegaly). Despite the appearance of altered cardiomyocytes, this condition was not associated with active cardiomyocyte damage. In the present case, occasional infiltrates of mononuclear cells occurred in the right ventricle and were considered separate from the cardiomyopathy. In the left ventricle, inflammatory infiltrates (containing lymphocytes, macrophages and eosinophils) were the result of myocardial degeneration and necrosis with chronic remodeling, myocardial disarray and fibrosis. We believe that the case presented here is a completely separate entity that shares some of the histological features described by Zabka et al (2009)¹², but has a different clinical outcome and pathophysiology.

The main findings in this case are: a) electrocardiographic evidence of grade III heart block; b) the presence of a dilated and thin left ventricular free wall; c) myocardial disarray in histopathology, and d) decreased and granular sarcoplasmic desmin expression demonstrated by immunohistochemistry. Altogether, these findings support the diagnosis of dilated phase of hypertrophic cardiomyopathy in this cynomolgus macaque.

JPC Diagnosis: Heart, left ventricle: Myocyte cytomegaly and karyomegaly, diffuse, severe with myocyte vacuolation, degeneration, necrosis and loss, and diffuse, severe myocardial fibrosis.



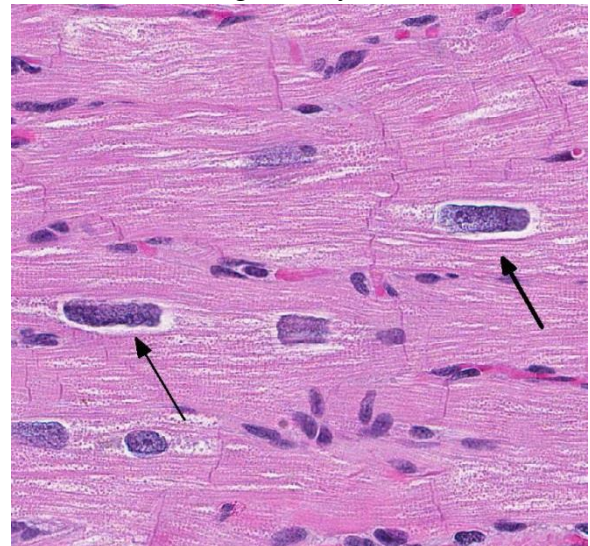
Heart, cynomolgus macaque. Occasionally, myocardial nuclei have linear chromatin condensations "caterpillar cells". (HE, 320X)

Conference Comment: Participants agreed that this is an excellent illustration of this condition, and the moderator commented on the elevated level of difficulty in describing and interpreting the slide in the absence of experience reviewing macaque hearts.

Approximately 60% of the myocardium is affected in the section. The most obvious change is the markedly cytomegalic and karyomegalic cardiac myocytes, varying in size from 10-100 times the normal macaque cardiomyocyte, with evidence of both hypertrophy and degeneration. A Masson's trichrome stain highlights the severe and diffuse (rather than subendocardial) myocardial fibrosis, and the moderator discussed the fibrosis as being a separate distinctive process. In the moderator's opinion, transverse sections of myocardium are best to evaluate for non-parallel orientation of cardiomyocytes (myofiber

disarray); in this case he would grade the degree of disorganization as mild to moderate. The moderator led a discussion comparing hypertrophic cardiomyopathy (HCM) with cardiac hypertrophy, and in this case many participants were not able to reach a definitive diagnosis of HCM based on the histologic sections and information provided, although it was certainly considered with the differential diagnosis.

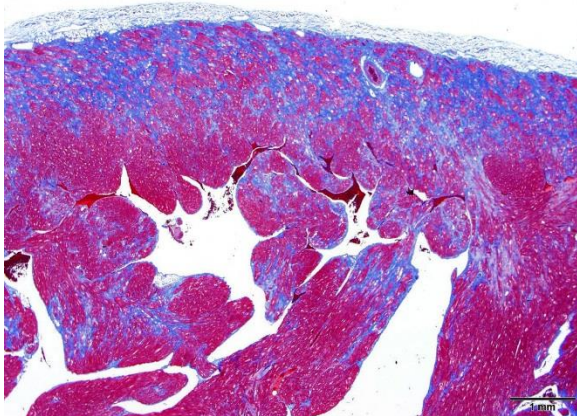
The cytologic appearance of the myocyte in this case is consistent with both HCM and myocardial hypertrophy but other differentiating histologic features were not identified. While myofiber disarray is the most significant diagnostic criteria for HCM, it is a relative rather than absolute change, and minor disarray can be evident with other cardiac diseases and even in normal hearts. Additionally, because there is usually asymmetric hypertrophy of the interventricular septum in HCM, concurrent evaluation of the IVS (not submitted) would aid in diagnosis. Fibrointimal dysplasia of small and medium mural coronary arteries is often a feature of HCM (particularly in the IVS), but was not evident in the examined section. HCM is generally considered to be a



Heart, cynomolgus macaque. Myocardial nuclei often display an enlarged rectangular profile ("boxcar nuclei") (HE, 320X)

makes diagnosis more challenging. Contraction band necrosis was described by participants in the atrial myocardium, but was not a prominent feature, and is distinguished from hypercontraction artifact.

A subtle feature pointed out by the moderator is small tags of fibrous tissue extending from the pericardium, which provides evidence of pericardial effusion. Pericardial effusion and passive congestion in the liver are both features of right sided heart failure, and in this case the right ventricle (not submitted) was described by the contributor as having minimal changes. It is postulated that the marked degree of left ventricular hypertrophy likely compressed the right ventricular lumen, impairing function and resulting in pericardial effusion and passive congestion.



Heart, cynomolgus macaque. A Masson's trichrome stain demonstrates the amount of fibrosis within the left ventricle, primarily in the subepicardial region. (Masson's, 40X)

increases in both pressure and volume. Volume overload may also result in dilation of the ventricle lumen. Both mechanical stimuli and trophic stimuli can initiate pathologic hypertrophy, and result in changes such as increased protein synthesis and myocyte hypertrophy, which result from changes in gene expression. However, myocardial changes that occur in pathologic hypertrophy, including impaired contractility and relaxation, eventually limit the benefit of

the compensatory hypertrophic response. Once hypertrophy is no longer able to compensate for the increased workload, degenerative changes occur in the myocardium secondary to factors such as poor vascular supply. Interstitial fibrosis may also result, leading to deterioration of function and eventual failure. Concentric hypertrophy typically results from increases in afterload and eccentric hypertrophy (dilated chamber) results from increases in preload.⁹ Myofiber disarray is generally not a prominent feature of cardiac hypertrophy.

Contributing Institution:

Pfizer Inc.
Global Research and Development
Groton/New London Laboratories
Eastern Point Road MS 8274-1330
Groton, CT.
Phone: 860-441-4498
www.pfizer.com

References:

1. Chamanza R, Parry NMA, Rogerson P, Nicol JR, Bradley AE. Spontaneous lesions of the cardiovascular system in purpose-bred laboratory non-human primates. *Toxicol Pathol.* 2006; 34:357-363.
2. Davies MJ, McKenna WJ. Hypertrophic cardiomyopathy. Pathology and pathogenesis. *Histopathology.* 1995; 26:493-500.
3. Francalanci P, Gallo P, Bernucci P, Silver MD, d'Amati G. The pattern of desmin filaments in myocardial disarray. *Human Pathol.* 1995; 26:262-266.
4. Gallo P, d'Amati G. Cardiomyopathies. In: Silver MD, Gotlieb AI and Schoen FJ, eds. *Cardiovascular pathology.* 3rd ed. pp. 285-

325. Philadelphia, PA: Churchill Livingstone; 2001:285-325.

5. Hamada T, Kubo T, Kitaoka H, Hirota T, et al. Clinical features of the dilated phase of hypertrophic cardiomyopathy in comparison with those of dilated cardiomyopathy. *Clin Cardiol.* 2010; 33:E24-E28.

6. Hayman R, Une Y, Nomura Y. Desmin as possible immunohistochemical finding for feline hypertrophic cardiomyopathy. *J Vet Med Sci.* 2000; 62:343-346.

7. Lyon AR, Rees PSC, Prasad S, Poole-Wilson PA, Harding SE. Stress (Takotsubo) cardiomyopathy – a novel pathophysiological hypothesis to explain catecholamine-induced acute myocardial stunning. *Nat Clin Pract Cardiovasc Med.* 2008; 5:22-29.

8. Maxie MG, Robinson WF. Cardiovascular system. In: Maxie MG, ed. *Jubb, Kennedy and Palmer's Pathology of Domestic Animals.* Vol 3. 5th ed. Philadelphia, PA: Elsevier; 2007: 44-50.

9. Robinson WF, Robinson NA. Cardiovascular System. In: Maxie MG, ed. *Jubb, Kennedy, and Palmer's Pathology of Domestic Animals.* Vol 3. 6th ed. St. Louis, MO: Elsevier; 2015:7-10, 45-47.

10. Tamura M, Harada K, Ito T, Enoki M, Takada G. Abrupt aggravation of atrioventricular block and syncope in hypertrophic cardiomyopathy. *Arch Dis Child.* 1995; 73:536-537.

11. Van Vleet JF, Ferrans VJ. Myocardial diseases of animals. *Am J Pathol.* 1986; 124:98-178.

12. Zabka TS, Irwin M, Albassam MA. Spontaneous cardiomyopathy in *Cynomolgus* monkeys (*Macaca fascicularis*). *Toxicol Pathol.* 2009; 37:814-818.

CASE III: 15-0816 (JPC 4067883).

Signalment: Juvenile (< 1yr), male, European brown hare (*Lepus europaeus*)

History: Found dead in a forest in January

Gross Pathology: The hare was in a good body condition. The spleen was moderately enlarged, swollen, dark (weight

3.4 g). The distal part of the caecum (vermiform appendix) was distended; the wall was swollen and hemorrhagic. On cross section, multiple white foci could be seen in the wall. Similar foci were seen in intestinal lymph nodes. The lungs had large hemorrhages. No gross lesions were observed in the liver.

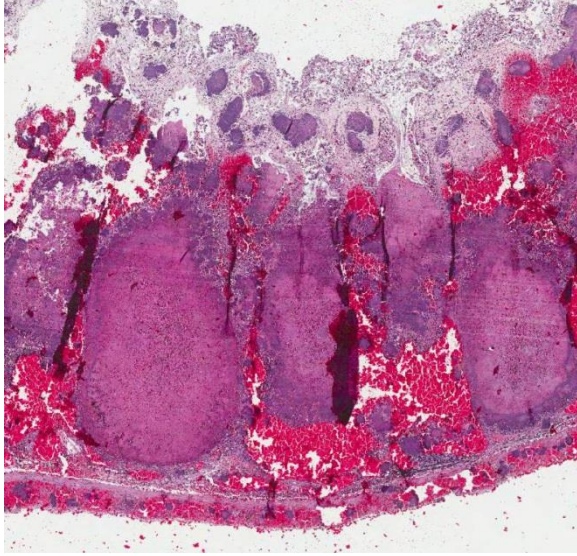


Appendix and liver, hare. Subgross view. (HE, 5X)

Laboratory Results:

Bacteriology: aerobic culture on blood agar: *Yersinia pseudotuberculosis* in lung, liver, spleen, intestinal lymph node and caecum.

Histopathologic Description: Caecum: The mucosa and the normal lymphatic tissue are mostly replaced by large hemorrhages and large focal areas of necrotic debris, mixed inflammatory cells and colonies of rod bacteria. The lesions extend to the submucosa, muscular layer and serosa.



Appendix, hare. There is transmural necrosis of the colonic wall which focuses on lymphoid tissue of the cecal tonsil. There is marked hemorrhage of the intervening lamina propria. Scattered throughout the tissue but most visible in the overlying autolytic mucosa are numerous colonies of large bacilli. (HE, 23X)

Liver: There are multiple, small, often coalescent necrotic foci with colonies of rod bacteria in the middle. Bacterial emboli are also present widely in hepatic sinuses.

Contributor's Morphologic Diagnosis: Severe, subacute, bacterial typhlitis, hepatitis and splenitis consistent with *Yersinia pseudotuberculosis* septicemia.

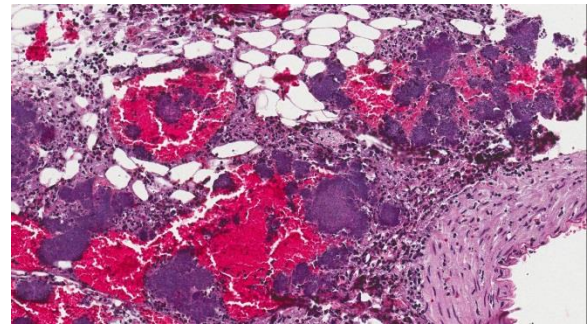
Contributor's Comment: *Y. pseudotuberculosis* is a gram-negative rod or coccobacillus closely related to *Y. pestis*, the etiological agent of sylvatic plague.² Wild hares (*Lepus* spp.) are known to be susceptible to *Y. pseudotuberculosis* infection.⁴ Birds and rodents are considered as reservoirs of the bacterium. Infection is acquired orally by fecally contaminated food or water and bacteria invade the intestinal epithelium in the jejunum or ileum.² Bacteria can infiltrate the liver and spleen and less commonly also other organs (lungs, kidneys, bone marrow). Infection can be acute, subacute or chronic. The disease typically occurs in nature in the cold season. In

humans, *Y. pseudotuberculosis* has caused outbreaks of food poisoning related to contaminated vegetables.⁷

JPC Diagnosis:

Appendix: Appendicitis, necrotizing, transmural and hemorrhagic, diffuse, severe with marked lymphoid necrosis, vasculitis and numerous large colonies of gram negative bacilli.

Liver: Hepatitis, necrotizing, multifocal to coalescing, severe with numerous large colonies of gram negative bacilli.



Appendiceal serosa and adjacent mesentery, hare. Large colonies of small bacilli are present both within vessels and in the surrounding tissue. (HE, 168X)

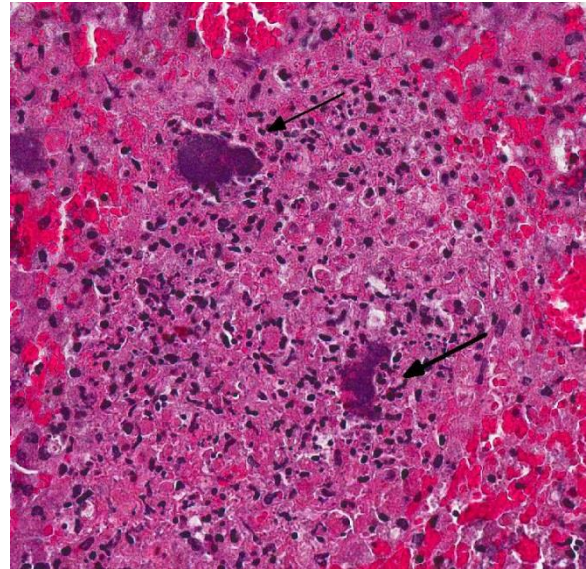
Conference Comment: Enteropathogenic *Yersinia* species bacteria are primarily thought to be contracted via oral infection which is followed by colonization of intestinal lymphoid tissue/Peyer's patches; entry is facilitated through the membrane protein invasin, attaching to $\beta 1$ integrins expressed on M cells. Bacteria can then spread to regional lymph nodes and to the liver and spleen. Virulence factors include a type III secretion system which plays a role in delivering the *Yersinia* outer proteins (YOPS) to target cells such as macrophages and neutrophils, which interferes with

signaling pathways, phagocytosis and the inflammatory response.¹

The bacteria also produce other proteins such as YadA and Ail that protect against phagocytosis and the host immune response. *Yersinia* largely resides extracellularly as small colonies in suppurative foci in the lamina propria of the intestine as well as in lymph nodes, but may also be found intracellularly.⁹

Aside from rabbits, other small mammals such as hamsters and guinea pigs can also become infected with *Y. pseudotuberculosis*. Additionally, virulent strains have been demonstrated experimentally to cause persistent infection in the cecum of asymptomatic mice, and are shed in the feces.¹ Gross lesions in the acute form of *Y. pseudotuberculosis* include pale, yellow-white nodules in the intestinal wall with mucosal ulceration in the distal small intestine and cecum. In subacute and chronic forms of the infection caseous and/or miliary lesions may be seen in the liver, spleen, mesenteric lymph nodes and lungs.⁶ *Y. pseudotuberculosis* is often grouped with *Y. enterocolitica* as “Yersiniosis” as infections with these two organisms cannot be reliably distinguished without culture. The disease has also been described in large animal species including sheep, cattle, deer, goats, pigs as well as nonhuman primates. Similar to small mammals, the intestine, mesenteric lymph nodes and liver may be affected and microscopic lesions include abundant colonies of gram negative coccobacilli in the distal small intestine, especially at Peyer’s patches, as well as in the large intestine. As infection progresses, suppurative foci eventually replace Peyer’s patches and multifocal microabscesses may be seen in the lamina propria of the intestine. Microabscesses or pyogranulomatous foci may also be seen in mesenteric lymph nodes.⁹

Other genera of bacteria to include on the differential diagnosis list for large colonies of bacteria seen microscopically include *Actinomyces*, *Actinobacillus*, *Trueperella*, *Corynebacterium*, *Staphylococcus*, and *Streptococcus*.



Liver, hare. Numerous foci of necrosis throughout the section contain large colonies of bacilli (arrows). (HE, 246 X)

In conference, the section of appendix was described as being diffusely and transmurally effaced by focally extensive areas of lymphoid necrosis centered on lymphoid tissue. Hemorrhage, edema and multifocal venous fibrin thrombi were also described, and the presence of large colonies of short bacterial rods was a key feature in this case. The liver was described as being approximately 15-20% affected by random foci of lytic necrosis. Affected areas contain a mixed inflammatory cell population, predominantly degenerate and viable heterophils, as well as colonies of short bacterial rods and venous fibrin thrombi. The sections of liver and appendix are moderately autolytic, which is not uncommon in rabbits/hares due in part to post mortem production and retention of heat.

Many participants described the section of appendix as cecum or colon, not recognizing the unique appearance of the rabbit appendix. The terminal portion of the cecum is known as the vermiform appendix, a thick-walled blind-ended tube which contains abundant large, expansive, lymphoid follicles which span the depth of the appendix wall, and in this case are characterized by extensive lymphoid necrosis. A morphologically similar structure is present at the entrance to the cecum and is known as the sacculus rotundus.^{5,8} These structures are important lymphoid organs in the rabbit and hare, which play a role in the development of B lymphocyte diversification.³

Contributing Institution:

Finnish Food Safety Authority Evira
www.evira.fi

References:

1. Fahlgren A, Avican K, Westermarck L, Nordfelth R, Fallman M. Colonization of cecum is important for development of persistent infection by *Yersinia pseudotuberculosis*. *Infect Immun*. 2014; 82(8):3471-82.
2. Gasper PW, Watson RP. Plague and Yersiniosis. In: Williams ES, Barker IK, eds. *Infectious diseases of wild mammals*. 3rd ed. London, UK: Manson Publishing Ltd; 2001:313-329.
3. Hanson NB, Lanning DK. Microbial induction of B and T cell areas in the rabbit appendix. *Dev Comp Immunol*. 2008; 32(8):980-991.
4. Mair NS. Yersiniosis in wildlife and its public health implications. *J Wildl Dis*. 1973; 9:64-71.
5. Manning PJ, Ringler DH, Newcomer CE. *The biology of the laboratory rabbit*. 2nd ed. San Diego, CA: Academic Press; 1994:53.
6. Percy DH, Barthold SW. *Pathology of laboratory rodents and rabbits*. 3rd ed. Ames, IA: Blackwell publishing; 2007:192, 226, 283.
7. Rimhanen-Finne R, Niskanen T, Hallanvuo S, Makary P, et al. *Yersinia pseudotuberculosis* causing a large outbreak associated with carrots in Finland. *Epidemiol Infect*. 2006; 137(3):342-347.
8. Snipes RL. Anatomy of the Rabbit Cecum. *Anat Embryol*. 1978; 155:57-80.
9. Uzal FA, Plattner BL, Hostetter JM. Alimentary system. In: Maxie MG, ed. *Jubb, Kennedy, and Palmer's Pathology of Domestic Animals*. 6th ed. Vol2. St. Louis, MO: Elsevier; 2015:176-177.

CASE IV: F14371301 (JPC 4066314).

Signalment: 6-month-old, male intact, double-maned lionhead rabbit (*Oryctolagus cuniculus*)

History: The 1.49 kg rabbit was seen by the exotics service at the veterinary teaching hospital for evaluation of redness, swelling and excessive watery discharge from the left eye. General physical examination was normal except for the ocular abnormalities. The rabbit was referred for an ophthalmology consult where severe anterior uveitis, iris bombe and a complete cataract (visualized through miotic pupil) were diagnosed. A course of prednisolone acetate, tropicamide (1%) and flurbiprofen (0.03%) eye drops and oral meloxicam (1.5 mg/ml) were prescribed to suppress inflammation and pain. Clinical progression of anterior uveitis, adverse side effects of continued corticosteroid and NSAID therapy, and a high index of suspicion for *Encephalitozoon cuniculi* prompted enucleation of the left eye. The left eye was submitted for histopathological examination.



Eye, rabbit. The iris is inflamed and red, and a mature cataract is visible through the contracted pupil. (Photo courtesy of: Department of Microbiology, Immunology, and Pathology, Colorado State University, Ft. Collins, CO. <http://csu-cvmb.colostate.edu>)

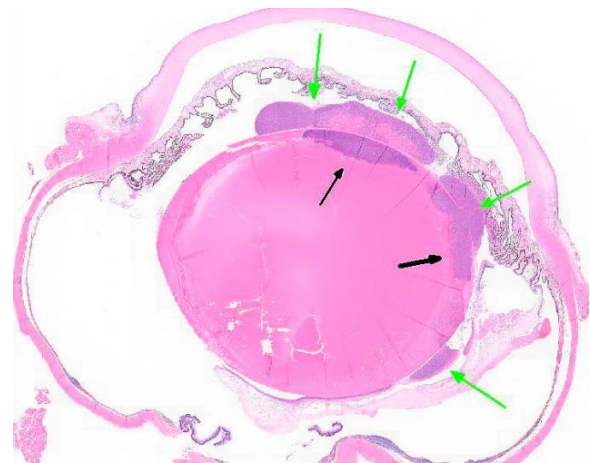
Histopathologic Description: Eye, OS: The equatorial lens capsule is ruptured with edges of the fragmented lens capsule retracted and coiled outward. The anterior segment is flooded with copious foamy macrophages admixed with heterophils, lenticular fragments, and necrotic debris extruding from the lens. There are myriad lenticular spherical microorganisms (2-3 micron). Lenticular architecture is also altered by torn, fibrillated, and denatured lens proteins forming Morgagnian globules and bladder cells. The lens epithelium is undergoing fibrous metaplasia forming a subcapsular fibrous plaque (consistent with cataract). Rafts of inflammatory cells and necrotic debris in the anterior segment are associated with adherence of the iris to the lens (posterior synechiae). The filtration angle is collapsed and the trabecular meshwork is infiltrated by previously described inflammatory cells. Diffusely, the iris is edematous and infiltrated by significant numbers of heterophils and fewer lymphocytes, plasma cells and histiocytes. The anterior face of the iris is covered with mixed inflammatory cells and fibrin. Similarly, the posterior segment is filled with previously described inflammatory cells, necrotic debris, fibrin and extravasated erythrocytes. The choroid is obscured by

diffuse lymphoplasmacytic infiltrate. There is diffuse retinal pigment epithelium hypertrophy associated with diffuse retinal detachment, thinning and atrophy of the photoreceptor layer. The conjunctiva is edematous with congested vessels lined by reactive endothelium and cuffed by heterophils and lymphocytes.

Lenticular spherical (2-3 micron) microorganisms are highlighted with Giemsa stain.

Contributor's Morphologic Diagnosis:

Eye, OS: Phacitis, pyogranulomatous with lens capsule rupture, cataract, anterior uveitis, posterior synechiae, lymphoplasmacytic choroiditis, retinal detachment and intralenticular spherical microorganisms, etiology consistent with *Encephalitozoon cuniculi*.

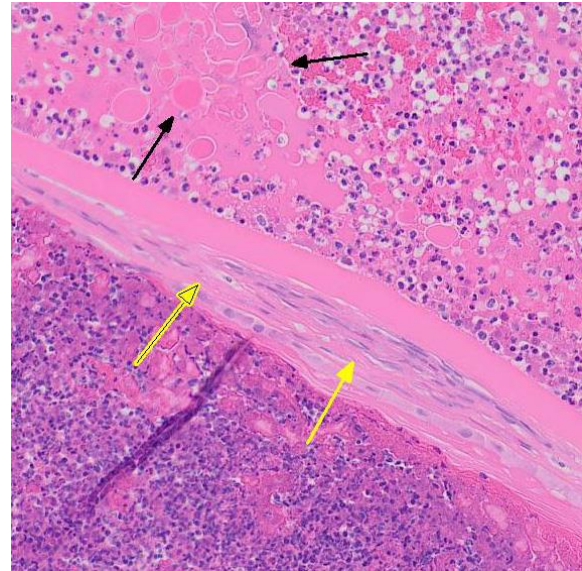


Eye, rabbit. There is a marked cellular exudate with the posterior chamber and posterior segment (green arrows). There is additionally an infiltrate within the peripheral aspect of the lens itself (black arrows). (HE, 7X)

Contributor's Comment: *Encephalitozoon cuniculi* is a spore-forming microsporidian obligate intracellular parasite with a simple, direct life cycle that infects a wide range of species. The phylum *Microspora* has a unique organelle, the polar filament, which remains coiled inside the spore.¹⁰ Ill-defined environmental cues cause unwinding and extrusion of the polar filament from the spore and injection of infectious sporoplasm into

the host cell.¹⁰ Ingestion or inhalation of spores shed in the urine, feces and mucus secretions are the primary routes of transmission. Once intracellular infection is established, division of the sporoplasm yields proliferative meronts that differentiate and mature (sporogony) within parasitophorous vacuoles.¹⁰ Swollen parasitophorous vacuoles cause the host cell to lyse, releasing spores into the extracellular space and completing the life cycle.¹⁰

E. cuniculi primarily infects rabbits (Type I genotype), including research colonies used in experimental models of human disease resulting in lesions of *E. cuniculi* being confused and misinterpreted as lesions associated with more serious human conditions.¹⁰ While seroprevalence for the organism is high in rabbits, infection is often subclinical and associated with incidental renal lesions at necropsy.⁶ Seropositive rabbits with clinical manifestations of encephalitozoonosis exhibit signs of vestibular disease (head tilt, ataxia), azotemia with nonspecific anorexia, lethargy and weight loss, and white intraocular masses (granulomas), cataracts and uveitis resulting in enucleation.⁵ Microscopic lesions include focal to segmental granulomatous interstitial nephritis (early), fibrosing lymphoplasmacytic interstitial nephritis (chronic) and nonsuppurative granulomatous meningoencephalomyelitis.⁶ Rabbits with neurological deficits have a more favorable prognosis than those presenting with clinical signs of renal insufficiency.⁵ Dwarf rabbits are especially prone to ocular lesions associated with *E. cuniculi* including white intraocular masses (granulomas), cataracts and phacoclastic uveitis resulting in enucleation.⁶



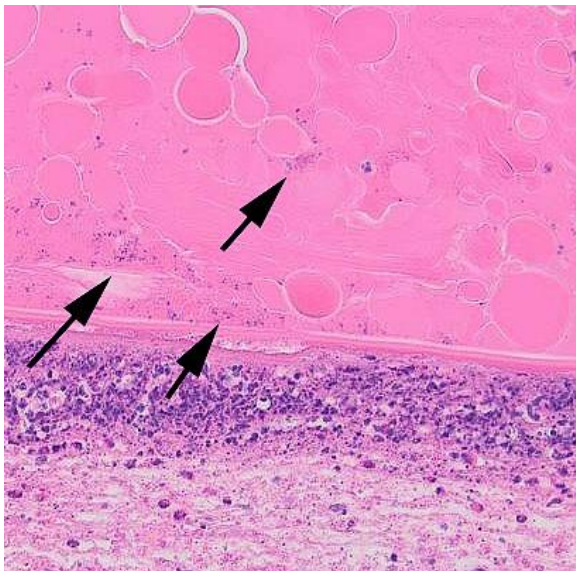
Eye, rabbit. The lens is infiltrated by innumerable degenerate heterophils and cellular debris (bottom left.) There is fibrous metaplasia of the subcapsular lens fibers (yellow arrows) and numerous viable and degenerate heterophils in the posterior chamber admixed with brightly eosinophilic granular and globular (black arrows) extruded lens material. (HE, 200X)

Ocular lesions are mostly unilateral, and rabbits with ocular disease generally do not suffer extra-ocular clinical abnormalities.⁵ Intrauterine infection is the proposed route of transmission with ocular encephalitozoonosis. The organism permeates the developing lens resulting in cataract formation, spontaneous rupture of the lens capsule and extrusion of lens substance inciting phacoclastic uveitis characterized by granulomatous inflammation intimately associated with the lens capsule.⁵ Posterior synechia, phthisis bulbi and secondary glaucoma are not uncommon sequelae.^{2,4,8} Early in the course of ocular disease associated with the organism, phacoemulsification can be used to treat the condition.² The tendency of nearly complete lens regeneration from lens epithelial cells requires large capsulectomy to suppress lens regrowth.¹ The prognosis for treatment of phacoclastic uveitis is poor, and enucleation is almost invariable.

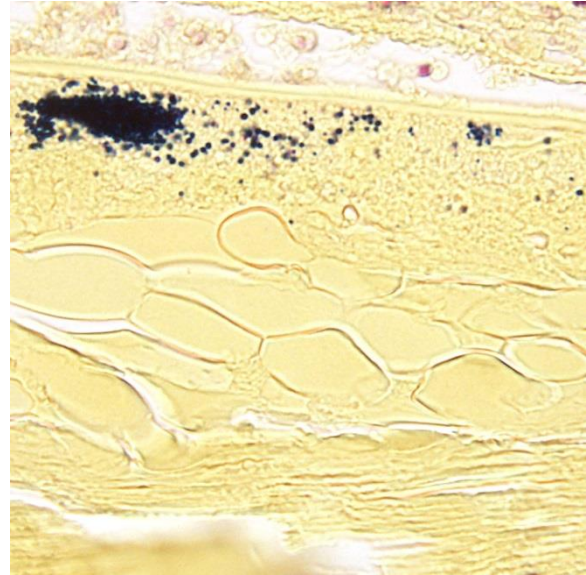
Visualization of small (2-3 micron) spores is challenging with routine H&E stains. Gram, Giemsa, carbon fuschin and Ziehl-Neelsen acid fast stains permit greater visualization of the spores. Immunohistochemical detection of intralenticular *E. cuniculi* organisms and PCR of liquefied lens substance is especially effective in organism detection.^{4,5}

Subclinical chronic infections in lagomorphs (Type I genotype) and dogs (Type III genotype) and the risk for zoonoses in immunocompromised individuals require appropriate precautions and biosecurity when working with infected or at risk populations of these species.^{3,9} Disseminated encephalitozoonosis in the kidney, sinuses, lung, brain and conjunctiva is well-recognized in AIDS patients.

JPC Diagnosis: Eye: Endophthalmitis, fibrinosuppurative, diffuse, severe with posterior synechiae, cataract, lens rupture, retinal detachment and intralenticular microsporidia.



Eye, rabbit. Lens fibers at the posterior face of the lens are degenerate, with loss and liquefaction of lens protein (Morgagnian globules). There are aggregates of microsporidian spores scattered throughout the posterior aspect of the lens (arrows)

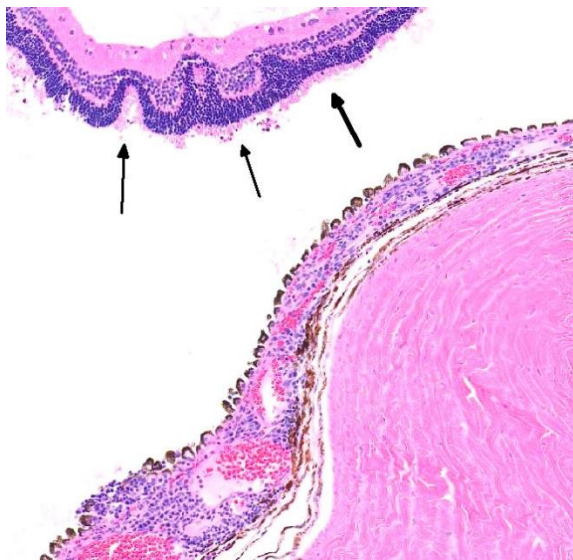


2Eye, rabbit. Moderate numbers of gram-positive microsporidium spores are present within the subcapsular lens. (Brown-Brenn, 1000X)

Conference Comment: Based upon phylogenetic analysis and the presence of chitin within the spore, microsporidia are classified as fungi or at least closely related to fungi. *E. cuniculi* infection has been documented in many mammalian species including rats, mice, squirrel monkeys, horses and foxes.¹¹

Although clinical and subclinical *E. cuniculi* infections were once common in laboratory rabbits, the agent is excluded from most modern facilities. Spores are transmitted primarily by ingestion and inhalation (or transplacentally), and they are shed in the urine of infected animals. *E. cuniculi* is capable of causing disease in dogs as discussed above, where lesions are most common in the brain and kidney. The organism targets vascular endothelium resulting in segmental vasculitis. Once infected, animals often remain permanently infected as macrophages are incapable of clearing the organism, although organisms

can be difficult to find in chronic lesions. Within the kidney, they are most common in the renal tubular epithelium and glomerular capillaries. Gross kidney lesions include nonsuppurative interstitial nephritis.¹ In addition to nephritis and meningoencephalitis, *E. cuniculi* infections have also been associated with placentitis in horses, squirrel monkeys, blue foxes and an alpaca.¹¹ One of the primary differential diagnosis for *E. cuniculi* is toxoplasmosis. The following characteristics can help differentiate the two organisms: *T. gondii* is not birefringent, *E. cuniculi* spores are; *T. gondii* does not stain with gram, acid fast or Luna stains; *T. gondii* stains more readily in H&E sections; *T. gondii* is a larger organism, measuring approximately 3-6µm.



Eye, rabbit. The retina (arrows) is detached, with hypertrophy ("tombstoning") of the underlying pigmented retinal epithelium. The underlying choroid is congested and moderate expanded by lymphocytes and fewer plasma cells. (HE, 144X)

Conference participants agreed that this is an excellent descriptive slide, and the conference histologic description was aligned closely with the contributor's description above. The inflammation and necrotic debris surrounding the lens was

described as containing degenerate eosinophils and heterophils, macrophages and lymphocytes. Within the ruptured lens Morgagnian globules were described as relatively abundant and bladder cells as uncommon. The corneal endothelium is infiltrated with leukocytes, and there is neovascularization and inflammation within the corneal stroma. Microsporidian spores were described as being present extracellularly between lens fibers and rarely within macrophages. Some discussion centered on the nature of the proliferative fibrovascular tissue at the lens margin, i.e. whether the spindled cells represent hyperplastic response or metaplastic lens epithelium. In addition to tissue gram and acid-fast stains, another histochemical stain that can be used to visualize *E. cuniculi* organisms includes the Luna method.⁷

Contributing Institution:

Colorado State University

<http://csu->

[cvmb.colostate.edu/academics/mip/pages/default.aspx](http://csu-cvmb.colostate.edu/academics/mip/pages/default.aspx)

References:

1. Cantile C, Youssef S. Nervous System. In: Maxie MG, ed. *Jubb, Kennedy, and Palmer's Pathology of Domestic Animals*. 6th ed. Vol 1. St. Louis, MO: Elsevier; 2015:385.
2. Felchle LM, Sigler RL. Phacoemulsification for the management of *Encephalitozoon cuniculi*-induced phacoclastic uveitis in a rabbit. *Vet Ophthalmol*. 2002; 5:211-215.
3. Fournier S, Liguory O, Sarfati C. Disseminated infection due to *Encephalitozoon cuniculi* in a patient with AIDS: case report and review. *HIV Med*. 2000; 1:155-161.

**Joint Pathology Center
Veterinary Pathology Services**



WEDNESDAY SLIDE CONFERENCE 2015-2016

C o n f e r e n c e 13

13 January 2016

Jeff Wolf, DVM, DACVP
Experimental Pathology Laboratories, Inc.
Sterling, Virginia

CASE I: N2015-5055 (JPC 4066453).

Signalment: Adult female cardinal tetra fish (*Paracheirodon axelrodi*)

History: This animal was one of 15 cardinal tetra (*Paracheirodon axelrodi*) in a 220 gallon heated freshwater tank. The tank contained a total of 29 species of tropical fish. Additional species included firehead tetra (*Hemigrammus bleheri*), rummy nose tetra (*Hemigrammus rhodostomus*), yellow phantom tetra (*Hyphessobrycon roseus*), serpae tetra (*Hyphessobrycon eques*), red phantom tetra (*Hyphessobrycon sweglesi*), bleeding heart tetra (*Hyphessobrycon erythrostigma*), Savanna tetra (*Hyphessobrycon stegemanni*), blue emperor tetra (*Inpaichthys kerri*), silver tetra (*Ctenobrycon spilurus*), white finned rainbowfish (*Bedotia leucopteron*), snakeskin barb (*Puntius rhomboocellatus*), cherry barb (*Puntius titteya*), three-striped glass catfish (*Eutropiellus debauwi*), glass catfish (*Kryptopterus bicirrhis*), diagonal-

stripe catfish (*Corydoras melini*), slant bar catfish (*Corydoras loxozonus*), Napo catfish (*Corydoras napoensis*), eartheater (*Geophagus megasema*), Leopold's angelfish (*Pterophyllum leopoldi*), freshwater angelfish (*Pterophyllum scalare*), blue butterfly cichlid (*Mikrogeophagus ramirezi*), Bolivian ram (*Mikrogeophagus altispinosus*), slender hemiodus (*Hemiodopsis gracilis*), green knifefish (*Eigenmannia virescens*), festivum (*Mesonauta mirificus*), spotted platyfish (*Xiphophorus maculatus*), chessboard cichlid (*Crenicara filamentosa*) and panchax (*Pachypanchax spp.*).

Three adult cardinal tetra from the group of 15 were presented for clinical examination due to white foci noted on the skin surface. On examination each animal was alert, active and in good body condition with no evidence of fin fraying or increased opercular rate and the animals were reported to have no change in appetite. Numerous (between 10 and 20) 2 to 3 mm diameter transparent raised nodules on the skin surface that centrally contained a coiled to elongate approximately



Numerous 2- to 3mm diameter transparent raised nodules were present on the skin surface. Each contained a prominent coiled to elongate approximately 2 mm long and 0.1 mm diameter white vermiform structure. (Photo courtesy of: Wildlife Conservation Society, New York Aquarium, Zoological Health Program, Aquatic Animal Medicine & Pathology Department, <http://www.wcs.org>)

2 mm long and 0.1 diameter white vermiform structure were present on all three animals. Further investigation found 6 out of 15 cardinal tetra exhibited similar skin lesions, and the remaining 9 animals showed varying degrees of diffuse pallor with patchy to loss of their characteristic red and blue iridescent coloration. No other species in the tank exhibited similar lesions. Skin scrapings were performed on the 3 tetra presented for clinical examination and one representative of each of the other species present in the tank. Following skin scrape cytology results, two cardinal tetra were euthanized for histopathology and ancillary testing. The remaining 13 animals were removed from the tank and placed into isolation.

Gross Pathology: Similar lesions to those noted clinically were apparent on both of the euthanized animals. Numerous (between 10 and 20) 2 to 3 mm diameter transparent raised

nodules were present on the skin surface. Each contained a prominent coiled to elongate approximately 2 mm long and 0.1 mm diameter white vermiform structure. Both animals were in otherwise good body condition and were reproductively active based on gonad development. Cytology findings are presented below.

Laboratory Results: Skin scrapings and wet mounts from both clinical and necropsy cases contained numerous elongate mesomycetozoal cysts that were approximately 100 um diameter and

tapered at one end to a 5 um diameter thin projection. The cysts were often ruptured at one end and were filled with innumerable approximately 5 to 7 um diameter spores. Individual spores had a prominent large central to eccentric refractile vacuole (refractile body). These findings were consistent with *Dermocystis-tidium* spp. infection. Skin scrapings from the representative animals of each of the 28 other species in the tank were negative for mesomycetozoal cysts. One frozen tetra was submitted for 18s small subunit rRNA PCR to confirm the pathomorphologic diagnosis

and provide species identification but results are not available at this time.

Histopathologic Description: Histologically, the dermis is multifocally expanded and the overlying scales are elevated in multiple locations by 100 to 200 μm diameter by 1000 to 2000 μm long tubular mesomycetozoal cysts that have a 1 to 2 μm thick eosinophilic laminated wall and contain innumerable 3 to 7 μm diameter round spores. Individual spores have a prominent large eosinophilic central to eccentric vacuole (retractile body) that is surrounded by a rim of weakly eosinophilic to clear cytoplasm containing a peripheralized deeply basophilic nucleus. There is a mild to moderate associated inflammatory infiltrate within the dermis composed primarily of granulocytes and macrophages. Cysts are occasionally captured as they penetrate the overlying epidermis and protrude from the epidermal surface. At the base of the anal fin, where the inflammatory cell infiltrate is most severe, moderate numbers of pyriform to ovoid holotrich ciliates (approximately 40 x 80 μm) infiltrate the dermis and are admixed with the inflammatory cells and mesomycetozoal cysts and spores.

Contributor's Morphologic Diagnosis:

1. Skin, dorsum, ventrum, base of anal and caudal fins: Dermatitis, granulocytic, histiocytic, multifocal, subacute, mild to moderate with multiple intralesional mesomycetozoal cysts and luminal spores (*Dermocystidium* spp.)
2. Skin, base of anal fin: Dermatitis, granulocytic, histiocytic, focal, subacute, moderate with intralesional protozoa (*Tetrahymena* spp.)

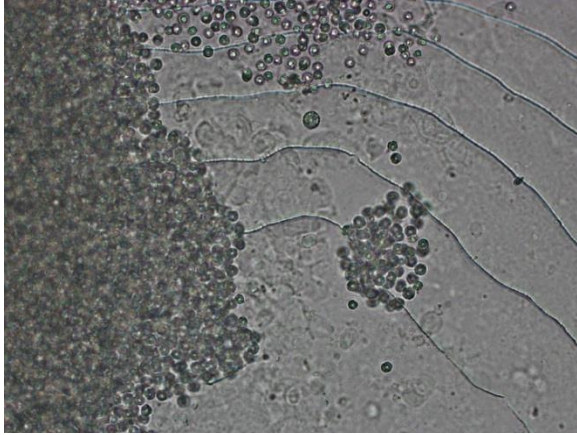


Skin scrapings and wet mounts from both clinical and necropsy cases contained numerous elongate mesomycetozoal cysts that were approximately 100 μm diameter and tapered at one end to a 5 μm diameter thin projection. (Photo courtesy of: Wildlife Conservation Society, New York Aquarium, Zoological Health Program, Aquatic Animal Medicine & Pathology Department, <http://www.wcs.org>)

Contributor's Comment: *Dermocystidium* is a member of the class *Mesomycetozoea* (previously known as the DRIP clade), which contains organisms that lie at the boundary between animals and fungi.

Phylogenetic analysis of the 18s small subunit rDNA genes indicates this class contains 10 different genera of parasitic and saprophytic microbes including: *Amoebidium*, *Anurofeca*, *Dermocystidium*, *Ichthyophonus*, *Pseudoperkinsus*, *Psorospermium*, *Rhinosporidium*, *Sphaerosoma* and two currently unnamed agents "clone LKM51" and "rosette agent."²

The majority of mesomycetozoea are pathogens of aquatic species, specifically fishes and invertebrates with *Rhinosporidium* a notable exception. The life cycles of these organisms have not been completely documented. In vitro, both *Dermocystidium* and the rosette agent develop unflagellated zoospores which could serve as a method of transmission and infection.² Waterborne transmission of *Dermocystidium* has been documented.⁴

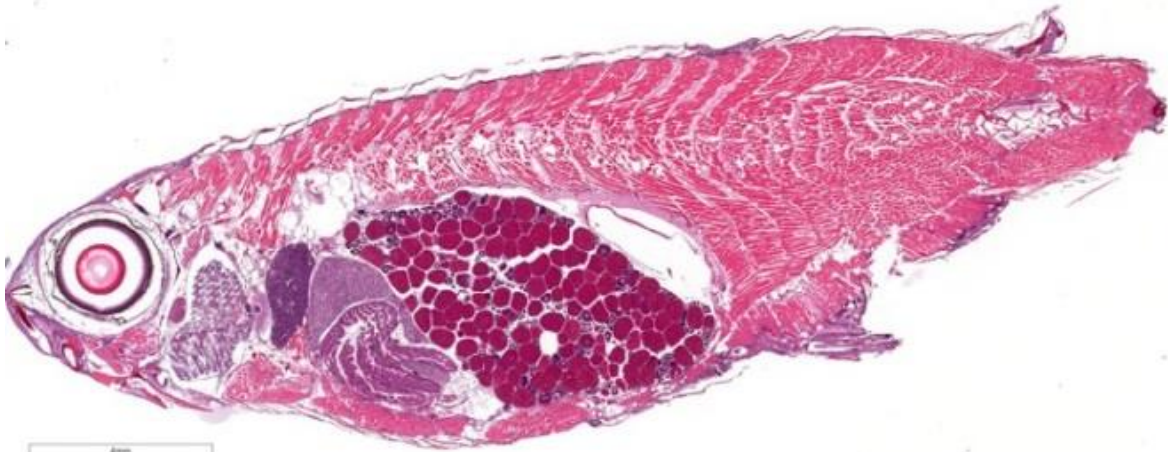


The cysts were often ruptured at one end and were filled with innumerable approximately 5 to 7 μ m diameter spores. Individual spores had a prominent large central to eccentric refractile vacuole (refractile body). (Photo courtesy of: Wildlife Conservation Society, New York Aquarium, Zoological Health Program, Aquatic Animal Medicine & Pathology Department, <http://www.wcs.org>)

There are currently 14 recognized species of *Dermocystidium* which all cause pathogenic infection in fishes and aquatic invertebrates.⁷ The skin and gills are the primary sites of infection, though visceral lesions have also been reported.⁵ The most diagnostic feature on cytology and histology is the presence of cysts (sporocysts) containing the characteristic spherical spore (endospore) stage with a large central vacuole (refractile body).³ There are four previous reports of *Dermocystidium* infection in *Paracheirodon* genus fishes (cardinal tetra, *Paracheirodon axelrodi* and neon tetra, *P. innesi*) with two providing histopathology similar to what is presented in this case.^{1,6} In the two most recent

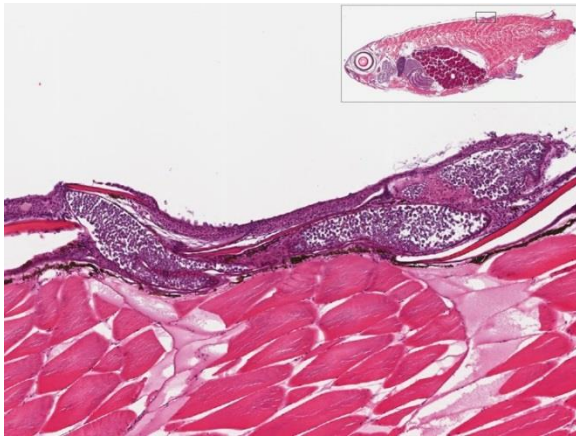
reports the agent was confirmed by 18S rDNA PCR to be *Dermocystidium salmonis*, a pathogen previously reported in Pacific salmon species. Both reported lesions to be predominantly epidermal and most severe along the anterior body and fins.^{1,6} The histologic lesions and distribution of the infection in the fish presented here are similar to these two previous reports, which suggests *Dermocystidium salmonis* infection in this group of cardinal tetra. One cardinal tetra from this group was submitted for 18S rDNA PCR and diagnostic confirmation; however, results were not available at the time of case submission. In recent case reports as well as in this case infection occurred in mixed species tanks, but only *Paracheirodon* genus fishes were affected. This may indicate a sensitivity of this genus to *Dermocystidium* infection. A source for infection was not clear in the current case. There were no recent changes in water source and there was no prior history of this infection in other tanks. There had been recent (6 weeks prior) addition of other genera of fishes to the impacted tank following 30 day quarantine, however there had not been a recent introduction of *Paracheirodon* spp. It is not clear from the current literature if a carrier state in other fishes is possible. The focal *Tetrahymena* infection in this case was believed to be opportunistic and incidental.

JPC Diagnosis: Skin: Dermatitis, ulcerative and granulocytic, subacute, multifocal, moderate with multiple mesomycetozoan cysts and ciliates.



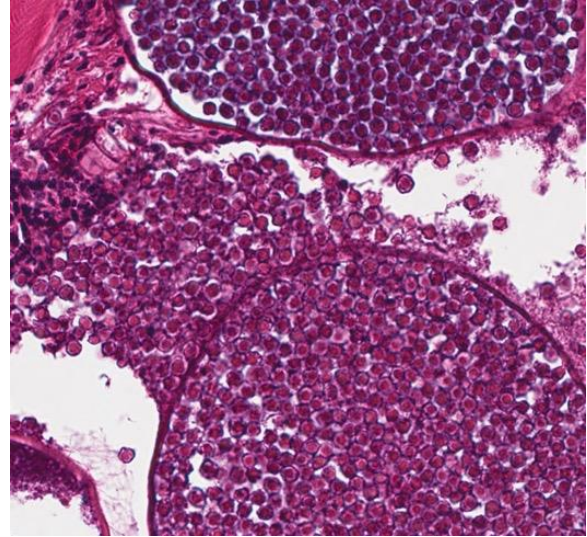
A sagittal section of an entire tetra was submitted for examination. (HE, 5X)

Conference Comment: The conference histologic description was aligned very closely with the contributor's description above. Participants commented on the excellent quality of the digital slide and parasagittal section. Participants were careful to point out the shape of the cysts located dorsally as being elongated, versus the cysts located ventrally which are round to ovoid; this is an important component to the description and can aid in identification of the organism. The contributor provided excellent gross images and the moderator led a discussion regarding the difficulty in identifying the mesomycetozoan tubular, opaque cysts grossly due to their resemblance to nematodes. Another important point raised by the moderator included recognizing the fish contains abundant eggs, which is indicative of good body condition and lack of debilitation.



Scaled skin, tetra. Multifocally, the dermis is expanded by elongate mesomycetozoal cysts. (HE, 200X)

Some conference participants identified the ciliate as a trichodinid due to its similar size compared with a tetrahymenid, but as the moderator pointed out, *Trichodina* spp. don't penetrate the skin whereas tetrahymenids do. Trichodinids, while also ciliates, generally cause a relatively mild disease in healthy fish but can result in significant losses in young fish, particularly when secondary bacterial

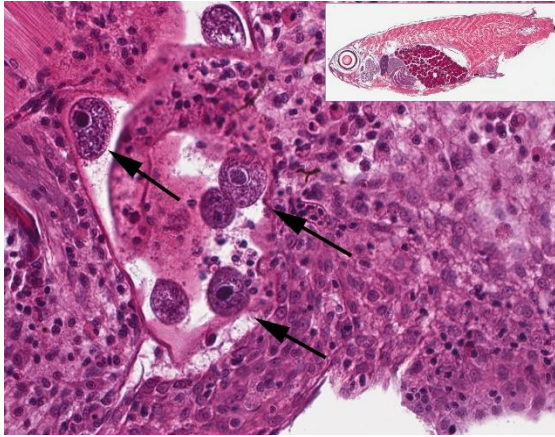


Scaled skin, tetra. The cysts are filled with numerous round spores with a central to eccentric vacuole and a peripheralized nucleus. Occasional cysts are ruptured and spores are extruded into the surrounding dermis. (HE, 400X)

infections are present or in cases of debilitation due to other causes. Tetrahymenids are often opportunistic invaders, as seen in this case, but can also invade internal organs and result in lethal infections in severe cases. Infection has been referred to as "guppy disease" due to its preference for infecting guppies. *Tetrahymena* sp. can also cause disease in catfish, common carp, and rainbow trout secondary to skin damage and invasion of internal organs.³

Contributing Institution:

Wildlife Conservation Society - New York Aquarium
 Zoological Health Program – Aquatic
 Animal Medicine & Pathology Department
www.wcs.org



Scaled skin, tetra. In areas of ulceration, several ciliates with prominent hyperchromatic nuclei have invaded the dermis. (HE, 400X)

References:

1. Langenmayer MC, Lewisch E, Gotesman M, et al. Cutaneous infection with *Dermocystidium salmonis* in cardinal tetra, *Paracheirodon axelrodi* (Schultz, 1956). *J Fish Dis.* 2014; 38(5):503-506.
2. Mendoza L, Taylor JW, and Ajello L. The Class *Mesomycetozoea*: Heterogeneous group of microorganisms at the animal-fungal boundary. *Ann Rev Microbiol.* 2002; 56:315-355.
3. Noga EJ. *Fish Disease: Diagnosis and treatment.* 2nd ed. Ames, IA: Wiley-Blackwell; 2010: 137-141, 174-175.
4. Olson RE, Dungan CF, and Hold RA. Water-borne transmission of *Dermocystidium salmonis* in the laboratory. *Dis Aquat Org.* 1991; 12:41-49.
5. Roberts RJ. The mycology of teleosts. In: Roberts RJ, ed. *Fish Pathology.* Chichester, UK: Wiley-Blackwell; 2012: 383-401.
6. Westmoreland LSH, Hadfield CA, Clayton LA, et al. *Mesomycetozoea* in cardinal tetras (*Paracheirodon axelrodi*) and green neon tetras (*Paracheirodon simulans*). In:

Proceedings of the IAAAM, 46th Annual Conference. Chicago: April 6-10, 2015.

7. Index Fungorum; www.indexfungorum.org. Accessed January 13, 2016.

CASE II: 35139 (JPC 4068374).

Signalment: Adult, unknown gender, Atlantic salmon (*Salmo salar*)

History: This case was submitted as part of a sample of 10 fish from a sea cage in which fish were presenting with rapid breathing and increased mortalities.

Gross Pathology: There were moderate numbers of poorly defined, multifocal to coalescing, white to grey, swollen plaques over the lamellae of all gill arches.

Laboratory Results: N/A

Histopathologic Description: These are sections of gill. There is mild multifocal telangiectasis (euthanasia artifact – expect slide variation). Approximately 60-80% of the filament surface has variably sized plaques of lamellar hyperplasia. These are characterized by interlamellar accumulation of haphazardly arranged cells (lamellar epithelial hyperplasia). There are occasional interlamellar spaces (lacunae) in areas of hyperplasia, and at the edge of these areas, there are frequent lamellar synechia. Within these interlamellar spaces, as well as on the surface of the lamellae, there are variable (mostly small) numbers of amoebic organisms. These are 15-20um round, with a vacuolated cytoplasm, and a small nucleus containing a dense, basophilic aggregate. Gram stains did not reveal any Gram positive organism in any of the sections examined.



Gill, salmon. There is marked hyperplasia of lamellar epithelium, primarily at the tips of the gill filaments (HE, 40X)

Contributor's Morphologic Diagnosis:

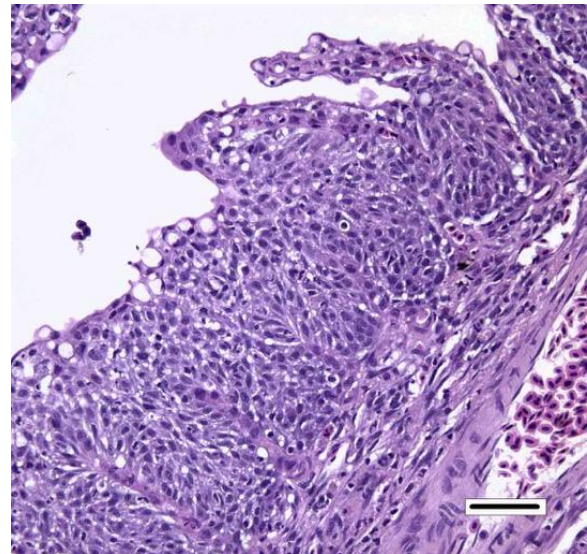
Gill: Moderate, multifocal to coalescing, lamellar hyperplasia with synechiae and lacunae formation, and intralesional amoebic organisms.

Contributor's Comment: The gross and histological presentation of this case is consistent with Amoebic gill disease (AGD). AGD is caused by *Neoparamoeba perurans*.³² Koch's postulates have been recently confirmed by culture of *N. perurans* and challenge of naïve *Salmo salar*,⁸ disproving the aetiological role previously ascribed to *Neoparamoeba pemaquidensis*.²¹ Work on the virulence factors of *N. perurans* is ongoing, and a protease-like exotoxin has been associated with a cytotoxic effect of amoeba.⁷ This may be associated with the epithelial necrosis noted ultrastructurally in AGD affected *S. salar* gills.¹⁶ It is noteworthy that *N. perurans* has been reported to lose virulence in culture, and this has been postulated to occur due to lack of attachment and/or the absence of an extracellular product.⁵

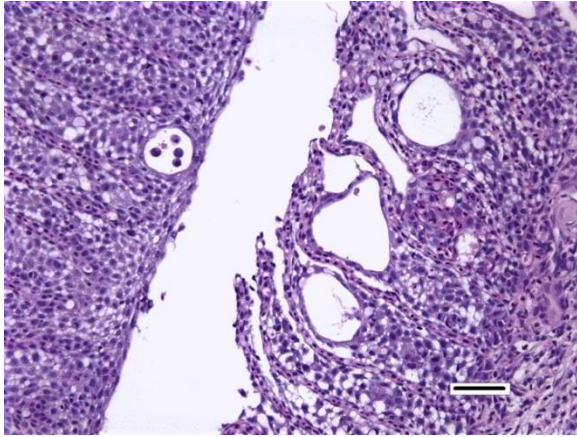
AGD affects salmonids, turbot (*Scophthalmus maximus*), ayu (*Plecoglossus altivelis*), European seabass (*Dicentrarchus labrax*), sharpshout seabream (*Diplodus puntazzo*), and ballan wrasse (*Labrus bergylta*).^{12,21} In this review, we will focus on

Atlantic salmon (*Salmo salar*), as this is the species in which this disease has the highest economic impact. In *S. salar*, the downstream effects of AGD include reduced growth, increased susceptibility to other pathogens and, if untreated, mortality. Its economic burden is large; in Tasmania (where AGD has been endemic since 1980) costs have been estimated at ~\$1 AUS/kg salmon (not cited). Disease occurs at temperatures 12-20°C and high salinity (35‰).¹⁷ However, there is variability on this presentation and in Scotland outbreaks may happen as low as 8°C.

Grossly, AGD presents as multifocal white to grey swollen areas on the gills, associated with excess of mucus.¹⁷ Lesion distribution favours gill areas with lower water flow (i.e. at the dorsal aspect of the gill arches).³ Several gross scoring systems have been developed, with diverse focus on aspects of the severity and distribution of AGD-associated lesions.^{2,30} These scoring systems have been used to predict expected mortality levels of AGD affected fish if left untreated³⁰. There is moderate to good agreement



Gill, salmon. Lamellar epithelium is hyperplastic to the extent that there is fusion and effacement of individual secondary lamellae. (HE, 100X)



Gill, salmon. Focal fusion of adjacent lamellae (lamellar synechiae) results in the formation of dilated pseudocysts. (HE, 100X)

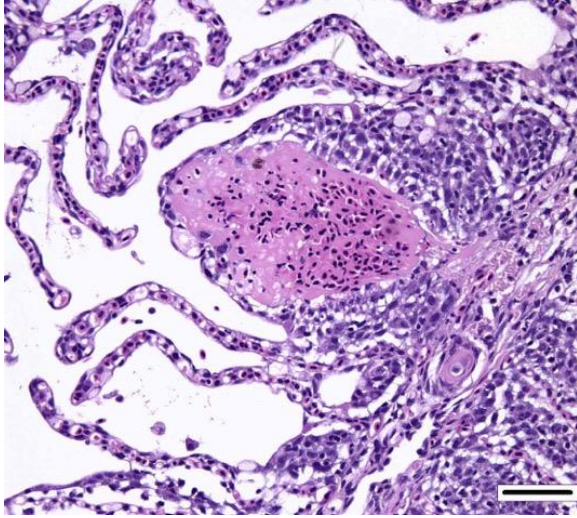
($\kappa=0.52-0.74$) between the gross signs of AGD and the histological presentation, and regions with gross lesions are those with histological signs.¹ However, this agreement is not ideal, with multiple instances of disagreement depending on the AGD stage, other pathogens, assessor, sampling method, histological technique and histological experience.¹

Histologically, AGD presents with lamellar epithelial hyperplasia and fusion (with creation of small interlamellar vesicles/lacunae), which are variably associated with interbranchial lymphoid tissue area increase, filament fusion, changes in chloride cells, and haemorrhage.^{4,17,22} Gill epithelial hyperplasia is a stereotypical feature of gill damage, but in AGD it has been postulated that it may be a result of the effect of the cytotoxic protease of the amoeba.⁷ Whether this is true or not, gill lamellar hyperplasia in AGD is associated with proliferating cell nuclear antigen (PCNA) increase², and p53 downregulation¹⁸ in lamellar epithelial cells. Amoebic organisms are noted in close association with the epithelium of lamellae and filaments, and often around the margins of the hyperplastic plaques.⁴ There is no description of epithelial invasion and these amoeba are considered

ectoparasites.¹⁶ In field studies, Adams et al.² first detected histological lesions at 13 week post transfer, with three distinct phases: (1) Primary attachment/interaction associated with extremely localized host cellular alterations, juxtaposed to amoebae, including epithelial desquamation and oedema; (2) Initial focal hyperplasia of undifferentiated epithelial cells; and (3) lesion expansion, squamation–stratification of epithelia at lesion surfaces and variable recruitment of mucous cells to these regions. A pattern of preferential colonization of amoebae at lesion margins was apparent during stage 3 of disease development.

There is a significant body of work on the systemic host response during AGD. Early work on innate immunity changes in *S. salar* recorded an increased chemotactic response of head kidney macrophages, with paradoxical reduction in head kidney phagocyte respiratory burst.¹¹ Overall, there is debate on the protective role of adaptive immunity in AGD.²⁶ There is evidence of anti- *N.perurans* antibodies circulating post exposure, but the response is considered poor.^{10,31} A field study on the adaptive immune response to AGD revealed that even though there is increase of seropositivity against *N. perurans* (with predominance of carbohydrate epitopes over peptide epitopes), there was no evidence to support that these antibodies were protective.²⁹ Subsequently, Vincent et al.³¹ noted reduced mortality in the second exposure which may support the existence of a protective acquired immune response. Interestingly this reduction in mortality was not associated with reduction in the severity of the gill lesions.

At the gill level, there is increased mRNA expression of IL-1 β , TCR-alpha chain, CD8, CD4, MHC-II α , MHC-I, IgM and IgT in AGD-challenged salmon at 10 days post-1,



Gill, salmon. There is multifocal aneurysmal dilation of lamellar capillaries; thrombosis of these vessels shows that it is not a postmortem change. (HE, 100X)

inoculation.²³ This suggests that an acquired immune response is present at the local level which is further supported by the presence of MHC class II+ cells within gill lesions.¹⁹ An interesting pattern has been noted with the role of IL-1 β in AGD, which is overexpressed in advanced AGD, despite an absence of marked inflammation.⁶ This may be due to reduced transcription of the receptor IL-1R-I, although this effect is not complete, as IL1R-II is expressed at normal levels.²⁰

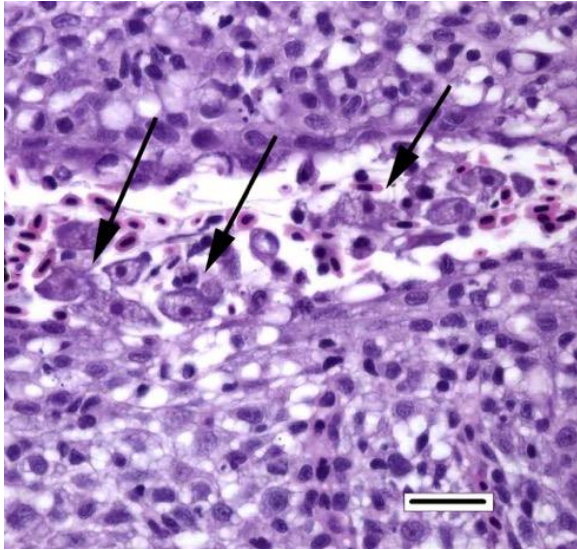
The pathogenic effect of AGD on *S. salar* has also been studied, and includes cardiovascular compromise, osmoregulatory changes, and ion regulation changes. AGD results in cardiovascular compromise, which is noted even with light AGD lesions.^{13,15} This may explain why mortalities can occur with light lesions, as it happens in the field, and could be related to individual variation in the ability to cope with acute and chronic increases in cardiovascular demand. In AGD, cardiovascular compromise may be the result of increased afterload, characterized by elevation of dorsal aortic pressure and systemic circulation resistance (systemic hypertension), without derangement of the

renin-angiotensin system.^{13,15,25} The increased afterload is coupled with cardiac morphological changes in chronic AGD. In a field study using gross lesion scores and number of freshwater baths required to assess clinical severity, *S. salar* with severe “AGD history” had increased ventricle length: axis length and ventricular width:axis length/height and thickened compact myocardium at the expense of the spongiosa, when compared with fish with “light AGD history”.²⁷

Very interestingly, the cumulative findings of several studies do not support respiratory failure as the main mechanism of AGD-induced mortality. This may be due to gill reserve capacity and reduction in mucus density, despite an increased amount of mucus.^{26,28} AGD results in hyperplasia of the lamellar epithelium, with consequent reduction on respiratory-efficient gill surface area due to multifocal increase in blood water diffusion distance.² However, this is coupled with reduction on mucus density, which reduces the blood-water diffusion barrier resistance.²⁸ During AGD, there is increase in the rate and amplitude of opercular movements,⁹ but this is not coupled with reduction in oxygen uptake.²⁶ Other respiratory changes are noted, however, and CO₂ plasma pressure is increased in AGD-affected fish, with reduced pH consistent with mild respiratory acidosis from 7dpi.²⁴, preceded by early alkalosis (48hpi), which could be the result of hyperventilation.¹⁴

JPC Diagnosis: Gill: Branchitis, proliferative, subacute, multifocal, moderate with fusion and adhesion of secondary lamella, dilation and thrombosis of lamellar capillaries and moderate numbers of intra- and extracellular amoeba.

Conference Comment: The contributor provides an excellent histopathologic



Gill, salmon. Low to moderate numbers of amoebae with a prominent macronucleus are present within the interlamellar space. (arrows). (HE, 350X)

description and overview of amoebic gill disease (AGD). Conference participants described lamellar epithelial hyperplasia with fusion as a primary feature, as well as mild edema and goblet cell hyperplasia. The majority of organisms are present on surface areas of fused lamellar epithelium, and rarely are they seen within phagocytic cells. The moderator cautioned participants to avoid over-interpreting lamellar changes such as blunting, particularly when lamella are not oriented parallel to the plane of section. The moderator also explained a finding often termed “epithelial lifting” – it can represent lamellar edema, especially if the space beneath the epithelium contains proteinaceous or flocculent material, but it can also be a tissue handling (e.g., fixation) artifact. AGD can be a challenging diagnosis due to similarities in appearance between sloughed epithelial cells and the organisms. Organisms are most commonly seen in areas of lamellar fusion and, in some cases, may be small and shrunken. Geimsa stain is effective at staining the organisms purple on a blue background, aiding the diagnosis.

The moderator also discussed the differences between lamellar fusion and lamellar adhesion. In cases of lamellar fusion, there is filling of lamellar sulci from the bottom and it is most often associated with inflammation and epithelial proliferation. With lamellar adhesions, there is adherence of two or more lamella and there may be an absence of proliferation or inflammation. In this case, there are examples of both with lamellar fusion near the base of lamella and adhesions toward the top.

Dilated capillaries within secondary lamellae were described as either telangiectasia or aneurysmal dilation by conference participants. The moderator indicated this vascular change can be a perimortem event, or a non-specific change in certain diseases. In many cases, distinguishing between peri- and antemortem telangiectasis is difficult. However, in this case, the presence of organizing fibrin thrombi indicates the telangiectatic changes are antemortem.

Contributing Institution:

The Royal (Dick) School of Veterinary Studies, Easter Bush Campus, Midlothian, UK

References:

1. Adams MB, Ellard K, Nowak BF. Gross pathology and its relationship with histopathology of amoebic gill disease (AGD) in farmed Atlantic salmon, *Salmo salar* L. *J. Fish Dis.* 2004; 27:151-161.
2. Adams MB, Nowak BF. Amoebic gill disease: sequential pathology in cultured Atlantic salmon, *Salmo salar* L. *J. Fish Dis.* 2003; 26: 601-614.
3. Adams MB, Nowak BF. Distribution and structure of lesions in the gills of Atlantic salmon, *Salmo salar* L., affected with

- amoebic gill disease. *J. Fish Dis.* 2001; 24:535-542.
4. Adams MB, Nowak BF. Sequential pathology after initial freshwater bath treatment for amoebic gill disease in cultured Atlantic salmon, *Salmo salar* L. *J. Fish Dis.* 2004; 27:163-173.
 5. Bridle AR, Davenport DL, Crosbie PB, Polinski M, Nowak BF. Neoparamoeba perurans loses virulence during clonal culture. *Int J Parasitol.* 2015; 45(9-10):575-8.
 6. Bridle AR, Morrison RN, Cupit Cunningham PM, Nowak BF. Quantitation of immune response gene expression and cellular localisation of interleukin-1beta mRNA in Atlantic salmon, *Salmo salar* L., affected by amoebic gill disease (AGD). *Vet Immunol Immunopathol.* 2006; 114: 121-134.
 7. Butler R, Nowak BF. In vitro interactions between Neoparamoeba sp. and Atlantic salmon epithelial cells. *Journal of Fish Diseases.* 2004; 27: 343-349.
 8. Crosbie PB, Bridle AR, Cadoret K, Nowak BF. In vitro cultured Neoparamoeba perurans causes amoebic gill disease in Atlantic salmon and fulfils Koch's postulates. *Int J Parasitol.* 2012; 42:511-515.
 9. Fisk DM, Powell MD, Nowak BF. The effect of Amoebic Gill Disease and hypoxia on survival and metabolic rate of Atlantic salmon (*Salmo salar*). *Bull Eur Assoc Fish Pathol.* 2002; 22: 190-194.
 10. Gross K, Carson J, Nowak B. Presence of anti-Neoparamoeba sp. antibodies in Tasmanian cultured Atlantic salmon, *Salmo salar* L. *J. Fish Dis.* 2004; 27: 81-88.
 11. Gross KA, Powell MD, Butler R, Morrison RN, Nowak BF. Changes in the innate immune response of Atlantic salmon, *Salmo salar* L., exposed to experimental infection with Neoparamoeba sp. *J. Fish Dis.* 2005; 28: 293-299.
 12. Karlsbakk E, Olsen AB, Einen A-CB, Mo TA, Fiksdal IU, Aase H, Kalgraff C, Skår S-Å, Hansen H: Amoebic gill disease due to Paramoeba perurans in ballan wrasse (*Labrus bergylta*). *Aquaculture.* 2013; 412–413: 41-44.
 13. Leef MJ, Harris JO, Hill J, Powell MD. Cardiovascular responses of three salmonid species affected with amoebic gill disease (AGD). *J Comp Physiol B.* 2005; 175: 523-532.
 14. Leef MJ, Harris JO, Powell MD. Respiratory pathogenesis of amoebic gill disease (AGD) in experimentally infected Atlantic salmon *Salmo salar*. *Diseases of Aquatic Organisms.* 2005; 66: 205-213.
 15. Leef MJ, Hill JV, Harris JO, Powell MD. Increased systemic vascular resistance in Atlantic salmon, *Salmo salar* L., affected with amoebic gill disease. *J. Fish Dis.* 2007; 30: 601-613.
 16. Lovy J, Becker JA, Speare DJ, Wadowska DW, Wright GM, Powell MD. Ultrastructural Examination of the Host Cellular Response in the Gills of Atlantic Salmon, *Salmo salar*, with Amoebic Gill Disease. *Vet Pathol.* 2007; 44: 663-671.
 17. Mitchell SO, Rodger HD. A review of infectious gill disease in marine salmonid fish. *J. Fish Dis.* 2011; 34: 411-432.
 18. Morrison RN, Cooper GA, Koop BF, Rise ML, et al. Transcriptome profiling the gills of amoebic gill disease (AGD)-affected Atlantic salmon (*Salmo salar* L.): a role for tumor suppressor p53 in AGD pathogenesis? *Physiol Genomics.* 2006; 26: 15-34.
 19. Morrison RN, Koppang EO, Hordvik I, Nowak BF. MHC class II+ cells in the gills of Atlantic salmon (*Salmo salar* L.) affected

by amoebic gill disease. *Vet Immunol Immunopathol.* 2006; 109: 297-303.

20. Morrison RN, Young ND, Nowak BF. Description of an Atlantic salmon (*Salmo salar* L.) type II interleukin-1 receptor cDNA and analysis of interleukin-1 receptor expression in amoebic gill disease-affected fish. *Fish Shellfish Immunol.* 2012; 32:1185-1190.

21. Munday BL, Zilberg D, Findlay V. Gill disease of marine fish caused by infection with *Neoparamoeba pemaquidensis*. *J. Fish Dis.* 2001; 24: 497-507.

22. Norte dos Santos CC, Adams MB, Leef MJ, Nowak BF. Changes in the interbranchial lymphoid tissue of Atlantic salmon (*Salmo salar*) affected by amoebic gill disease. *Fish Shellfish Immunol.* 2014; 41: 600-607.

23. Pennacchi Y, Leef MJ, Crosbie PB, Nowak BF, Bridle AR. Evidence of immune and inflammatory processes in the gills of AGD-affected Atlantic salmon, *Salmo salar* L. *Fish Shellfish Immunol.* 2014; 36: 563-570.

24. Powell MD, Fisk D, Nowak BF. Effects of graded hypoxia on Atlantic salmon infected with amoebic gill disease. *J Fish Biol.* 2000; 57: 1047-1057.

25. Powell MD, Forster ME, Nowak BF. Apparent vascular hypertension associated with Amoebic Gill Disease affected Atlantic salmon (*Salmo salar*) in Tasmania. *Bull Eur Assoc Fish Pathol.* 2002; 22: 328-333.

26. Powell MD, Leef MJ, Roberts SD, Jonesk MA. Neoparamoebic gill infections: host response and physiology in salmonids. *J Fish Biol.* 2008; 73: 2161-2183.

27. Powell MD, Nowak BF, Adams MB. Cardiac morphology in relation to amoebic

gill disease history in Atlantic salmon, *Salmo salar* L. *J. Fish Dis.* 2002; 25: 209-215.

28. Roberts SD, Powell MD. The viscosity and glycoprotein biochemistry of salmonid mucus varies with species, salinity and the presence of amoebic gill disease (vol 175, pg 1, 2004). Erratum in: *J Comp Physiol B.* 2005; 175: 219-219.

29. Taylor RS, Crosbie PB, Cook MT. Amoebic gill disease resistance is not related to the systemic antibody response of Atlantic salmon, *Salmo salar* L. *J. Fish Dis.* 2010; 33: 1-14.

30. Taylor RS, Muller WJ, Cook MT, Kube PD, Elliott NG. Gill observations in Atlantic salmon (*Salmo salar*, L.) during repeated amoebic gill disease (AGD) field exposure and survival challenge. *Aquaculture.* 2009; 290: 1-8.

31. Vincent BN, Morrison RN, Nowak BF. Amoebic gill disease (AGD)-affected Atlantic salmon, *Salmo salar* L., are resistant to subsequent AGD challenge. *J. Fish Dis.* 2006; 29:549-559.

32. Young ND, Crosbie PBB, Adams MB, Nowak BF, Morrison RN. *Neoparamoeba perurans* n. sp., an agent of amoebic gill disease of Atlantic salmon (*Salmo salar*). *Int J Parasitol.* 2007; 37: 1469-1481.

CASE III: 15-0816 (JPC 4067883).

Signalment: Approximately 6-month-old, gender unknown, lumpfish (*Cyclopterus lumpus*)

History: A corporate aquarium group undertook a captive breeding program to supply multiple aquaria within the group with juvenile lumpfish for display. All of the fish

were bred in a single facility, and after being grown, juvenile fish were dispersed to their new facilities at around 3 to 4 months. Over the course of the next few months, elevated mortality rates were observed in juvenile lumpfish in multiple locations. Typically, fish were either found dead or were observed to become lethargic, pale, and to develop buoyancy problems. In many fish, significant coelomic or generalized swelling was reported prior to death or euthanasia. Some cases displayed exophthalmos. Ongoing losses from affected groups proved unsustainable, and after a few months the entire originating group and dispersed populations were culled and restocked.



Kidney, lumpfish. The kidney is massively enlarged by an interstitial proliferation of lymphoid and phagocytic cells. (HE, 6X).

Gross Pathology: Postmortem examinations were typically undertaken at aquaria by aquarists, although some smaller fish were submitted whole in neutral buffered formalin to the laboratory. Typical gross findings included generalized or gill pallor, generalized “whole body” edema giving the fish a “jelly-like” consistency, marked intracelomic accumulations of clear watery fluid, exophthalmos and enlargement and mottling of the kidneys and occasionally spleen. Routine skin scrapes and gill presses undertaken on-site by aquarists were usually reported to be negative, with occasional

identifications of amoebae from gills, or scuticociliates from skin.

Laboratory Results: In most cases, no clinicopathologic data was available. In one fish, air-dried celomic fluid smears and blood smears were submitted for cytological examination. The hematocrit was also measured in this fish, and was 14%. In this individual, aerobic cultures of coelomic fluid yielded a sparse growth of *Bacillus* species and light growth of alpha-hemolytic *Streptococcus*.

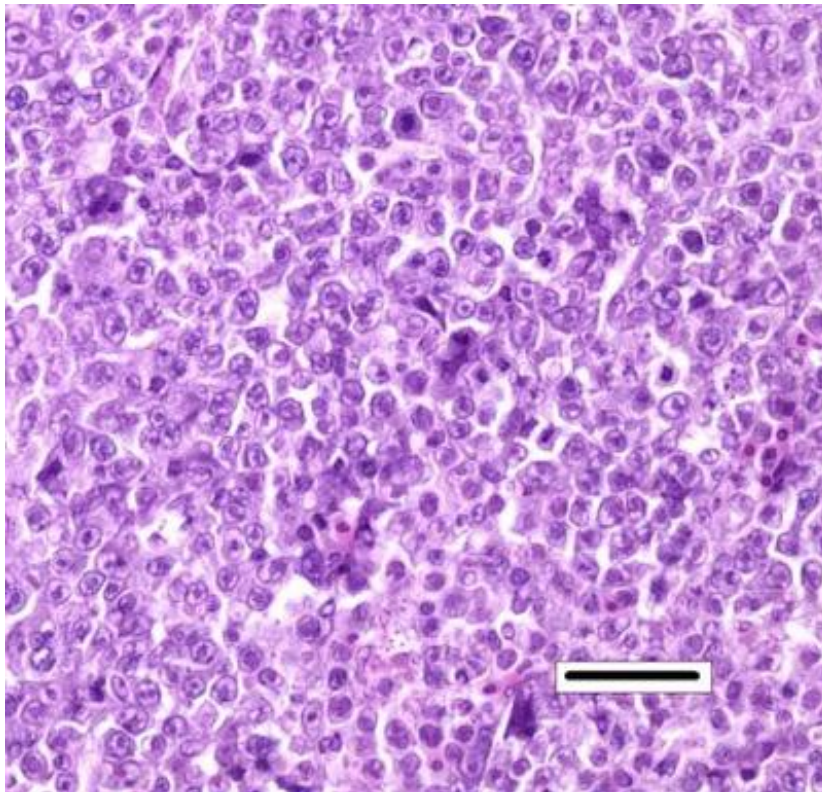
Cytologic description: Blood smear: Significant artifactual changes are present, resulting in poor cytoplasmic preservation of red cells, and abnormal chromatin staining. Assessment of red cell parameters is unreliable for this reason. This fish has a significant monocytosis, and lymphocytes also appear increased in number. In addition, significant numbers of the monocytic cells, and occasional presumptive lymphocytes, have intranuclear clusters of multiple (regularly 8 in some cells, occasionally more) elliptical refractile spores, consistent with intranuclear microsporidia.

Coelomic fluid: Moderately cellular smears in which mononuclear cell/macrophages and lymphocytes predominate. Cellular morphology is shrunken and nuclei are more condensed than in the blood smears. Intranuclear microsporidia are abundant within the mononuclear populations, and aggregates of similar spores within cytoplasmic fragments are also a feature

Histopathologic Description: Submitted material is derived from two different fish demonstrating similar histopathological changes.

Kidney: Hematopoietic kidney is massively expanded and normal architecture effaced by densely cellular sheets of mononuclear round cells, whose morphology is suggestive of

lymphoid/lymphoblastic origin. There is no intervening stroma, but small numbers of remnant tubules are present within the cell sheets. A subpopulation of cells have condensed aggregations of multiple (typically around 4 to 8) pale eosinophilic faintly refractile circular to ovoid spores (each approximately 1 x 3 μm) contained within their nuclear membranes (Figure 3a), and more numerous cells with intranuclear eosinophilic vacuoles/cytoplasmic folds are present. Varying numbers of spores are present in the extracellular milieu as a result of nuclear/cellular rupture, with phagocytosis by intermingled macrophages. Spores are most abundant in small multifocal areas of necrosis. There is extension of lymphoblastoid infiltrates into paravertebral striated muscle groups and connective tissue, spinal ganglia and spinal cord meninges.



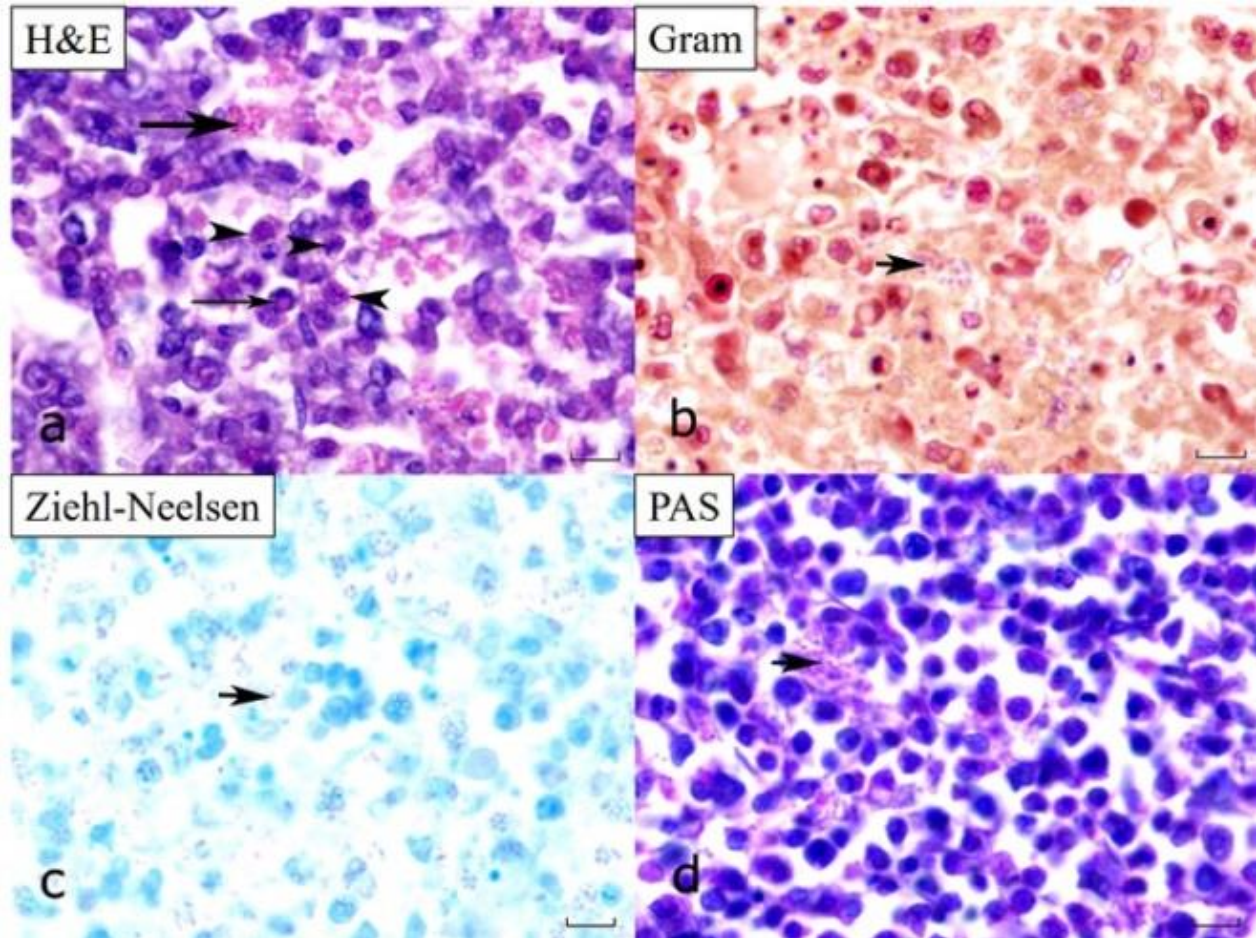
Kidney, lumpfish. The interstitium is profoundly expanded by a monomorphic population of blast lymphocytes with large nuclei, nucleoli, and a moderate mitotic rate. (HE, 400X).

Similar cells are also present within the lumina of blood vessels. Spores stain weakly gram-positive, focally Ziehl-Neelsen positive and weakly PAS-positive.

Contributor's Morphologic Diagnosis: Lymphoproliferative and minimally necrotizing interstitial nephritis, diffuse, chronic, with intranuclear microsporidia (*Nucleospora cyclopteri*), kidney, lumpfish (*Cyclopterus lumpus*).

Contributor's Comment: Intranuclear microsporidiosis has recently emerged in wild Icelandic fisheries of lumpfish (*Cyclopterus lumpus*, also known as lumpsuckers) and been described and speciated as a novel species, *Nucleospora cyclopteri*.² There are earlier clinical, histopathological and ultrastructural

descriptions of intranuclear microsporidiosis from captive lumpfish in Canada.⁶ Based on ultrastructural comparisons, it is suspected that the same parasite is implicated in these historical cases and the recent Icelandic cases.³ Definitive confirmation of this awaits molecular studies of material from the Canadian cases.² The recent Icelandic cases were found in wild fish harvested for their eggs, which are a traditional caviar substitute. Although the prevalence of infection was relatively high (parasites were recognized at 12 out of 43 sites sampled around the Icelandic coast), and clinical disease was seen in 18 of 77 fish (presenting with enlarged pale kidneys), many



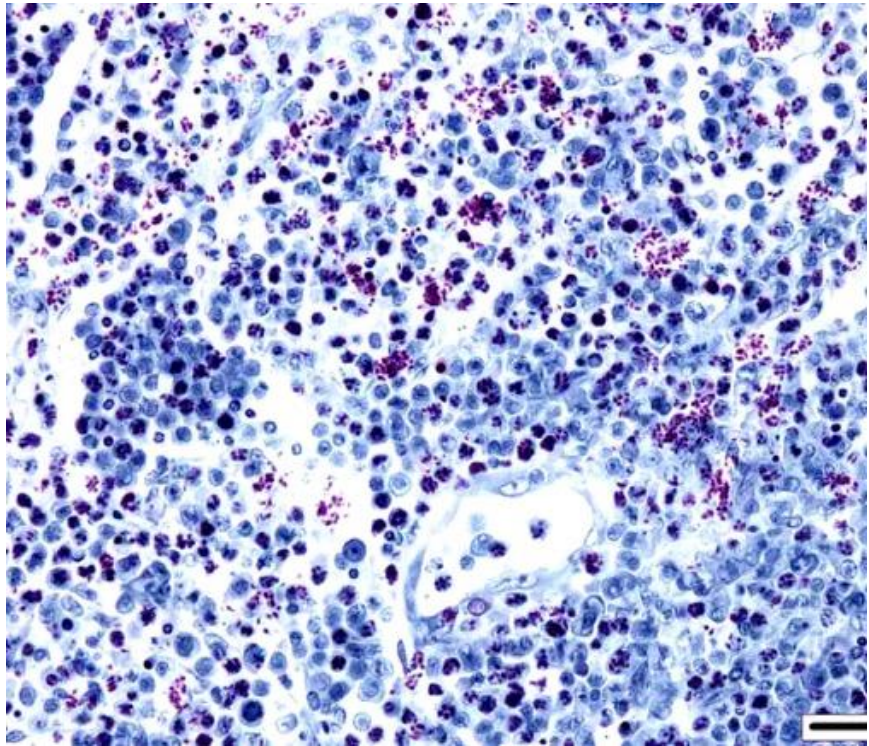
Kidney, lumpfish. Spores stain weakly gram-positive, focally Ziehl-Nielsen positive, and weakly PAS-positive. (Photo courtesy of: International Zoo Veterinary Group, Pathology Station House, Parkwood Street, Keighley, West Yorkshire, BD21 4NQ, United Kingdom, <http://www.izvg.co.uk>)

other fish were clinically unaffected.² A very recent report describes co-infection by *Nucleospora cyclopteri* and *Kudoa islandica* in farmed lumpfish in Norway.¹

In the last 2 years in the United Kingdom we have recognized this infection as a significant cause of mortality in aquarium-bred colonies of lumpfish destined for public aquaria, and in research colonies used for experimental studies into lumpfish husbandry. Along with wrasse, lumpfish are increasingly employed as cleaner fish for the control of sea lice in Atlantic salmon aquaculture, and there is an increasing interest in their susceptibility to diseases, particularly those to which salmonids may potentially be susceptible.

On cytological examination, cells in the coelomic fluid and monocytes/lymphocytes within blood smears contain numerous distinct intranuclear microsporidial spores. They are easier to see in this context than in the more shrunken nuclei of histological sections. Enhanced visualization may have been possible with a Peterson-Luna stain.⁸ In histological sections, infiltrates of proliferating lymphocyte-like cells with intranuclear organisms expand the hematopoietic kidney early in the course of the disease, before disseminating (consistent with the presence of spores in circulating monocytes in the blood smears) into multiple organs (including in advanced cases gastrointestinal tract, meninges, spleen,

gonads and coelomic and cutaneous connective tissues). Sheets of infiltrating cells contain foci of necrosis and there is extracellular liberation of spores, which are frequently phagocytosed by admixed populations of reactive macrophages. The identity of the proliferating cells is difficult to determine with certainty based on morphology alone, but the most recent publication suggests that they are lymphocytes and monocytic precursor cells^{2, 3} and the earlier report describes the affected cells as lymphocyte-like.⁶



Kidney, lumpfish. A Luna stain demonstrates the microsporidian spores admirably. (Luna, 100X).

Although formerly classified as protozoans, microsporidia are now considered to be more closely related to fungi. They are obligate intracellular spore-forming organisms with a pan-taxonomic distribution, and commonly infect fish, typically causing xenomas in a range of tissues depending on host and parasite⁶. However, intranuclear microsporidia are also recognised in fish, in particular a closely-related parasite, *Nucleospora* (formerly *Enterocytozoon*) *salmonis*, which is distributed worldwide, and has been recorded in several salmon species, causing anemia and lymphoblastosis.⁴ The precise mode of transmission of *N. cyclopteri* remains uncertain, but many microsporidia, including *N. salmonis*, have a direct life cycle. The possibility of vertical transmission has also been discussed.² In fish, intranuclear microsporidia have also been described infecting enterocytes in Tanzanian killifish (*Nothobranchius rubripinnis*) and, most

recently, infecting enterocytes leading to a wasting syndrome in farmed gilthead sea bream (*Sparus aurata*).⁷

JPC Diagnosis: Kidney, hematopoietic tissue: Necrosis, diffuse with marked hyperplasia, multifocal infarction, and intranuclear, intracytoplasmic and free microsporidia.

Kidney: Nephritis, histiocytic, diffuse, marked with tubular degeneration, necrosis and loss and intranuclear, intracytoplasmic and free microsporidia.

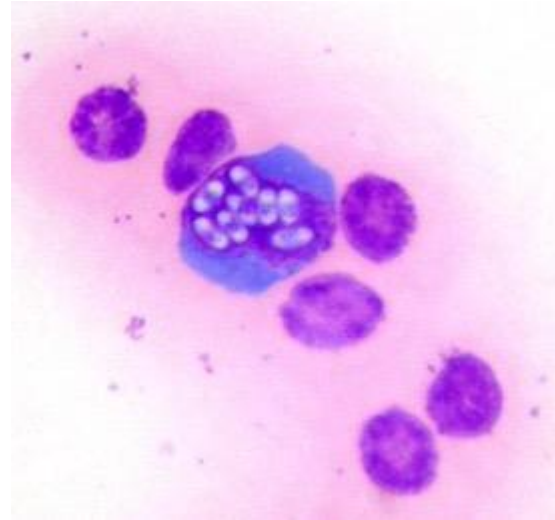
Conference Comment: Conference participants described the kidney as approximately 50% affected, with necrosis and hyperplasia of hematopoietic tissue being the most remarkable features. Participants also described mild, multifocal degeneration and necrosis of tubular epithelium with

aggregation of debris in tubule lumina (tubular casts) and tubular loss. The moderator pointed out glomeruli and tubule density varies between species and it is therefore useful to review a normal control animal before describing glomerular and tubular loss. There is slide variability with some sections having a focally extensive area of coagulative necrosis which participants postulated is an infarction. An excellent quality cytology image is provided by the contributor and participants commented on the unique intranuclear nature of this microsporidian.

The expansion of hematopoietic tissue was striking in this case, characterized by sheets of large blastic cells reminiscent of a lymphoproliferative neoplasm, admixed with a second population of smaller phagocytic round cells. Two additional alternate diagnoses in this case were discussed: lymphoproliferative neoplasia and *Exophiala* sp. infection. *Exophiala* sp. fungal infections can cause disease in both freshwater and marine species including channel catfish, lake and cutthroat trout as well as Atlantic salmon and cod among others. Lesions can be both cutaneous and visceral with areas of necrosis and chronic granulomatous inflammation, and in some cases infection has a predilection for the kidney with the presence of renomegaly and involvement of other visceral organs.⁹ Fungal infection characteristically results in lesions with vasculitis, thrombosis, and infarction.

Contributing Institution:

International Zoo Veterinary Group
Pathology
Station House, Parkwood Street
Keighley
West Yorkshire
BD21 4NQ
United Kingdom
www.izvg.co.uk



Coelomic fluid, lumpfish. Cells in the coelomic fluid and monocytes/lymphocytes within blood smears contain numerous distinct intranuclear microsporidian spores. (Photo courtesy of: International Zoo Veterinary Group, Pathology Station House, Parkwood Street, Keighley, West Yorkshire, BD21 4NQ, United Kingdom, <http://www.izvg.co.uk>)

References:

1. Alarcón, M., Thoen, E., Poppe, T. T., Bornø, G., et al. Co-infection of *Nucleospora cyclopteri* (Microsporidia) and *Kudoa islandica* (Myxozoa) in farmed lumpfish, *Cyclopterus lumpus* L., in Norway: a case report. *J Fish Dis.* 2015, Apr 10; doi: 10.1111/jfd.12372. E pub ahead of print.
2. Freeman, M. A., Kasper, J. M., & Kristmundsson, Á. *Nucleospora cyclopteri* n. sp., an intranuclear microsporidian infecting wild lumpfish, *Cyclopterus lumpus* L., in Icelandic waters. *Parasit Vectors.* 2013; 6:49.
3. Freeman, M. A. & Kristmundsson, Á. Ultrastructure of *Nucleospora cyclopteri*, an intranuclear microsporidian affecting the Atlantic lumpfish (*Cyclopterus lumpus* L.). *Bulletin of the European Association of Fish Pathologists.* 2013; 33(6):194-198

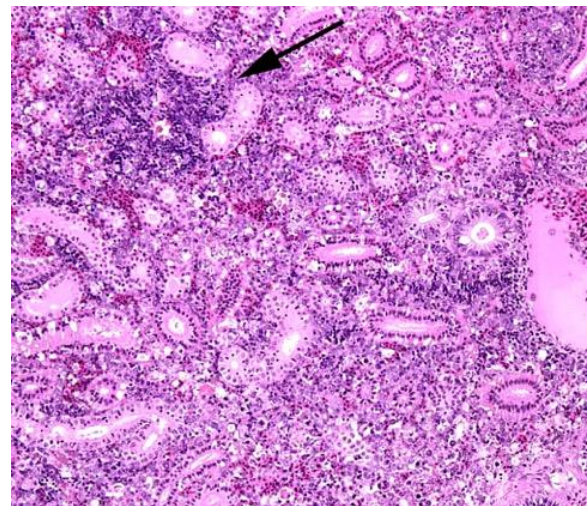
4. Hedrick, R. P., Groff, J. M., & Baxa, D. V. Experimental infections with *Enterocytozoon salmonis* Chlmonczyk, Cox, Hedrick (Microsporea): an intranuclear microsporidium from chinook salmon *Oncorhynchus tshawytscha*. *Dis Aquat Organ*. 1991; 10:103-108.
5. Lom, J., & Dyková, I. Microsporidian xenomas in fish seen in wider perspective. *Folia Parasitologia*. 2005; 52:69-81.
6. Mullins, J. E., Powell, M., Speare, D. J., & Cawthorn, R. An intranuclear microsporidian in lumpfish *Cyclopterus lumpus*. *Dis Aquat Organ*. 1994; 20:7-13.
7. Palenzuela, O., Redondo, M. J., Cali, A., Takvorian, P. M., et al. A new intranuclear microsporidium, *Enterospora nucleophila* n. sp., causing an emaciative syndrome in a piscine host (*Sparus aurata*), prompts the redescription of the family Enterocytozoonidae. *Int J Parasitol*. 2014; 44:189-203.
8. Peterson TS, Spitsbergen JM, Feist SW, Kent ML. Luna stain, an improved selective stain for detection of microsporidian spores in histologic sections. *Dis Aquat Organ*. 2011; 95(2):175-80.
9. Sindermann CJ. *Principal diseases of marine fish and shellfish*. 2nd ed. Vol. 1. San Diego: Academic press; 1990:71-72.

CASE IV: 10-9030 (JPC 4052876).

Signalment: Seven, 6- to 8-inch long goldfish (*Carassius auratus*)

History: In June 2010, a fish kill occurred at a lake in south east South Dakota. This pond's primary function is a storm sewer retention basin, and the kill occurred a couple days after a big rain event. The rain event was likely the stressor that started the die off. The

die off involved a high percentage of goldfish, but dead bullheads and crappies were also seen. Mortality in these other species is common during the transition from spring to summer in our natural lakes and ponds. The goldfish first appeared in the lake about two years before the die off. The exact source of the goldfish is not known; however, it is assumed that someone released their pet fish. Dead goldfish were submitted to Animal Disease Research and Diagnostic Laboratory at South Dakota State University by the South Dakota Department of Game Fish and Parks for diagnostic workup due to concern with possible viruses that attack species such as koi, carp, and goldfish.

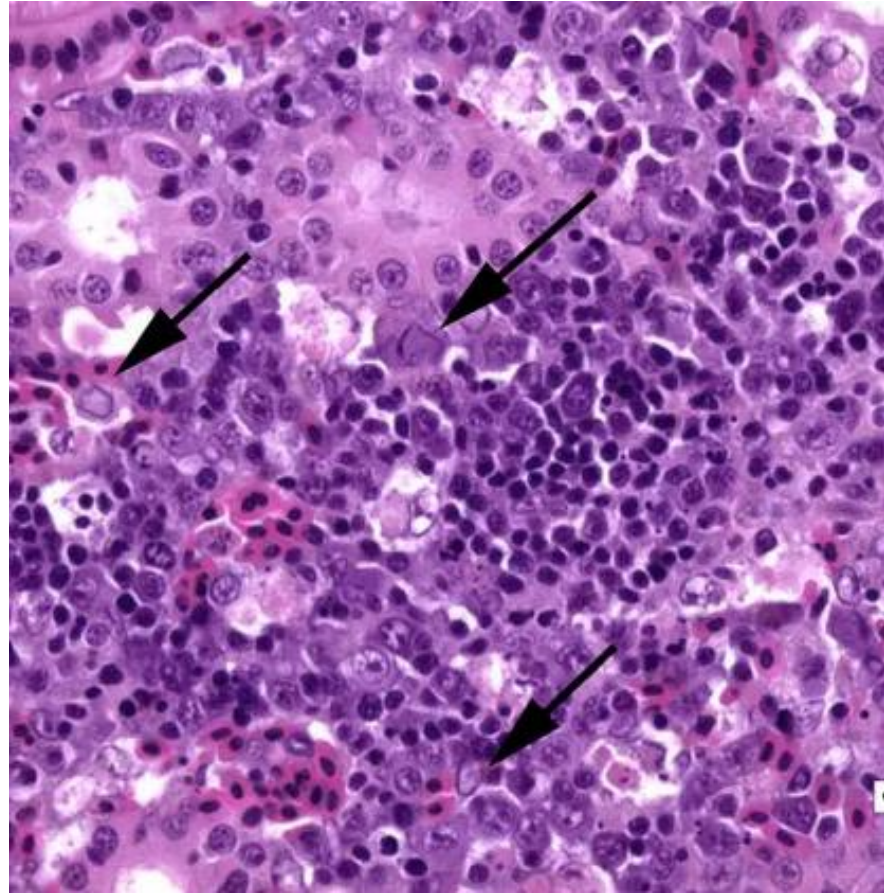


Kidney, goldfish. Nephrons are markedly separated by hyperplastic hematopoietic tissue. The pallor of this tissue is the result of diffuse necrosis; one focus of apparently normal tissue remains (arrow). (HE, 40X)

Gross Pathology: Some of the dead goldfish gills had limited multifocal hemorrhages and pale foci that appear to be necrosis. All fish had empty stomachs and full gallbladders. A couple of fish had edema and reddening of the lateral skin.

Laboratory Results: Pools of gill, liver, and spleen were cultured and large growths of

Aeromonas hydrophilia were isolated from all pools. Viral examination included the collection of kidney, gill, and spleen from the goldfish, and after processing, inoculating EPC cells at 15°C for VHS (viral hemorrhagic septicemia); and EPC cells at 25°C for SVCV (spring viremia of carp virus), LMBV (largemouth bass virus), or KHV (koi herpes virus). After a week the EPC cells at 25°C had cytopathic effect (CPE). Supernatant from the cell culture was filtered and put on EPC cells again and CPE was present again at a week. These cells were harvested and polymerase chain reaction (PCR) for VHS and SVCV was run and was



Kidney, goldfish. Nuclei of hematopoietic tissue are occasionally enlarged by a single glassy, amphophilic intranuclear viral inclusion. (HE, 360X)

found to be negative. Kidney, spleen, and gill homogenate was sent to Veterinary Diagnostic Laboratory at the University of Minnesota; it was examined for koi herpes virus with PCR and found to be negative. Minnesota also put homogenate on KF-1 cells at 15°C and 25°C for 42 days being passed on day 14 and day 28 and the results were negative. Finally, pools of kidney, spleen, gill, liver, and intestine were sent to Department of Medicine and Epidemiology, School of Veterinary Medicine, University of California, Davis; they were positive for Cyprinid Herpesvirus 2 (CHV-2) using PCR.

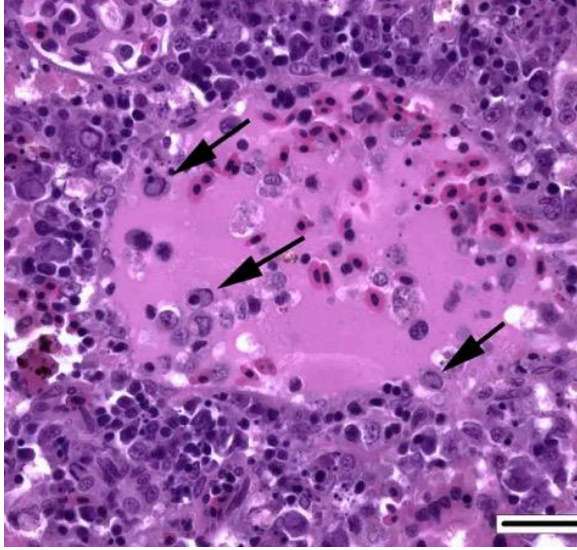
Histopathologic Description: The gills have severe pleocellular inflammation with some proliferation and multifocal necrosis. There is severe multifocal meningoencephalitis. The inflammation is most extensive in the

meninges and the ventricles. The head kidney, kidney, and spleen have severe multifocal to coalescing necrosis of hematopoietic tissue. Many intranuclear basophilic inclusion bodies are present.

Contributor's Morphologic Diagnosis: Submitted kidney slides: Acute severe multifocal to coalescing necrotizing interstitial nephritis with intranuclear inclusion bodies.

Etiology: Cyprinid Herpesvirus 2, confirmed by PCR.

Contributor's Comment: Herpesviral hematopoietic necrosis (HVHN) is a disease of goldfish *Carassius auratus auratus*. It is caused by Cyprinid herpesvirus 2 (CyHV-2), a member of the cyprinid herpesvirus group that includes carp pox (CyHV-1) and koi herpesvirus (CyHV-



Kidney, goldfish. Circulating leukocytes also contain intranuclear viral inclusions. (HE, 360X)

3). Cyprinid Herpesvirus 2 is found worldwide. Most goldfish populations carry the virus and disease outbreaks are sporadic and brought on by stress. Mortality associated with HVHN can approach 100 percent. The virus causes severe necrosis of hematopoietic tissue. Necrosis and inflammation is also found in the gills.^{3,5}

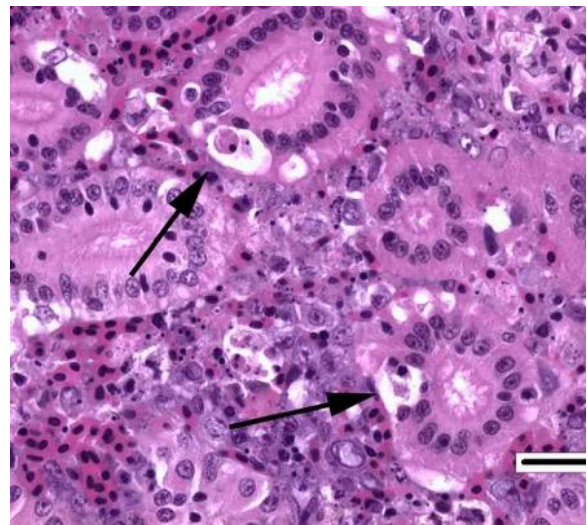
JPC Diagnoses: 1. Kidney, hematopoietic tissue: Necrosis, diffuse, with moderate hyperplasia and numerous intranuclear inclusion bodies.

2. Kidney, tubules: Degeneration, necrosis and loss, diffuse, with rare intranuclear inclusion bodies.

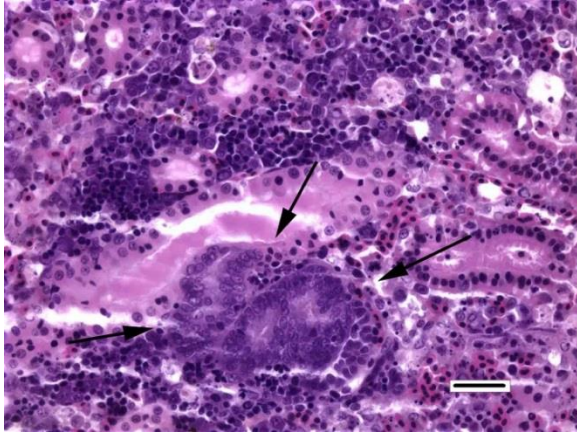
Conference Comment: Infection and goldfish mortality associated with CyHV-2 has been described throughout the world including in North America, Japan, Australia, the United Kingdom, Italy,² China and France; global fish trade is an important pathway for viral spread. Outbreaks are triggered by handling stress, transportation, and variations in water temperature.¹

The three cyprinid herpesviruses are closely related to anguillid herpesvirus 1; all 4 viruses are grouped within the genus *Cyprinivirus*. Cyprinid herpesvirus-3 (CyHV-3) is highly contagious and is also termed koi herpesvirus disease. It is an OIE reportable disease and is also present throughout the world due to global fish trade; it can be devastating to the production of koi and common carp. Characteristic signs of disease include erratic swimming, gasping for air, poor appetite, discoloration and fin erosions. Histologic lesions include gill, liver and renal necrosis with intranuclear inclusion bodies.

Hyperplasia of gastric gland epithelium, intestinal villi, and respiratory cells may also be seen, resulting in lamellar fusion. Survivors of CyHV-3 outbreaks and other unaffected fish species can act as carriers. The virus is transmitted horizontally and fish density may play a role in severity and spread of infection in an outbreak. Cyprinid herpesvirus-1 causes papillomatous skin lesions in infected koi; the virus is lethal in young fish, but is generally not lethal in adult koi.⁴



Kidney, goldfish. Multifocally, there is necrosis of tubule epithelium. (HE, 400X)



Occasional regenerative tubules are scattered throughout the section. (HE, 200X)

Consistent histopathologic findings in CyHV-2 infection include necrosis of hematopoietic tissue in the spleen and/or kidney (necrosis may or may not be present in both locations), with or without the presence of characteristic herpesviral inclusion bodies. Other reported microscopic findings include: branchial epithelial hyperplasia, necrosis^{1,2} and hypertrophy; necrosis and inflammation in the intestine; and lesions in the heart.¹ Viral DNA has been demonstrated in interstitium with eosinophilic cellular and demonstrated in subclinically affected animals with the presence of single cell necrosis in hematopoietic tissue, suggesting a possible role of latent infection in the pathogenesis of this disease.²

The most prominent lesion in these sections is the diffuse necrosis within the expanded renal hematopoietic tissue, and the presence of numerous prominent intranuclear inclusions within hematopoietic precursor cells and occasionally within renal tubule epithelium. The tunica media of few vessels is discontinuous and infiltrated by low numbers of inflammatory cells, however, the moderator pointed out that this is likely an “innocent bystander” lesion in areas of necrosis and not a true vasculitis. There is multifocal renal tubule epithelial

degeneration, necrosis and rare regeneration. Herpesviral intranuclear inclusion bodies are also present within circulating leukocytes, which can be seen in the lumen of several small vessels. The moderator also discussed the presence of mild compensatory hematopoietic tissue hyperplasia and erythrophagocytosis.

Contributing Institution:

Animal Disease Research and Diagnostic Laboratory

South Dakota State University

<http://www3.sdstate.edu/vs/adrdl/index.cfm>

References:

1. Boitard PM, Baud M, Labrut S, Boisseson C de, et al. First detection of Cyprinid Herpesvirus 2 (CyHV-2) in goldfish (*Carassius auratus*) in France. *J Fish Dis.* 2015; July, 14; E pub ahead of print. DOI 10.1111; jfd.12400.
2. Giovannini S, Vergman SM, Keeling C, Lany C, et al. Herpesviral Hematopoietic Necrosis in Goldfish in Switzerland: Early Lesions in Clinically Normal Goldfish (*Carassius auratus*). *Vet Pathol.* 2015; Nov 9; Online first. DOI: 10.1177/0300985815614974.
3. Goodwin AE, Khoo L, LaPatra SE, Bonar C, et al. Goldfish hematopoietic necrosis Herpesvirus (Cyprinid herpesvirus 2) in the USA: molecular confirmation of isolates from diseased fish. *J Aquat Anim Health.* 2006;18:11–18.

**Joint Pathology Center
Veterinary Pathology Services**



WEDNESDAY SLIDE CONFERENCE 2015-2016

C o n f e r e n c e 14

20 January 2016

Victoria Hoffman, DVM, DACVP
National Institutes of Health
Bethesda, MD

CASE I: AFIP case#1 (JPC 4032259).

Signalment: Seven male Hartley guinea pigs, 14 weeks-1.5 years of age (*Cavia porcellus*).

History: Tissues from several of 7 Hartley guinea pig boars, 14 weeks-1.5 years of age, found dead (4) or euthanized due to lethargy and hindlimb weakness (3) over a 3 week period. Animals were housed at an outside research institution, fed a commercial laboratory guinea pig diet, and used for several different research or training IACUC protocols by multiple investigators. Fixed tissues were received for histologic evaluation.

Gross Pathology: Hearts reported to have “severe multifocal to diffuse white infiltrates at several locations.” Heart weight-to-body weight ratios were reported for two animals, 0.779% and 0.737% (normal 0.422%).⁴

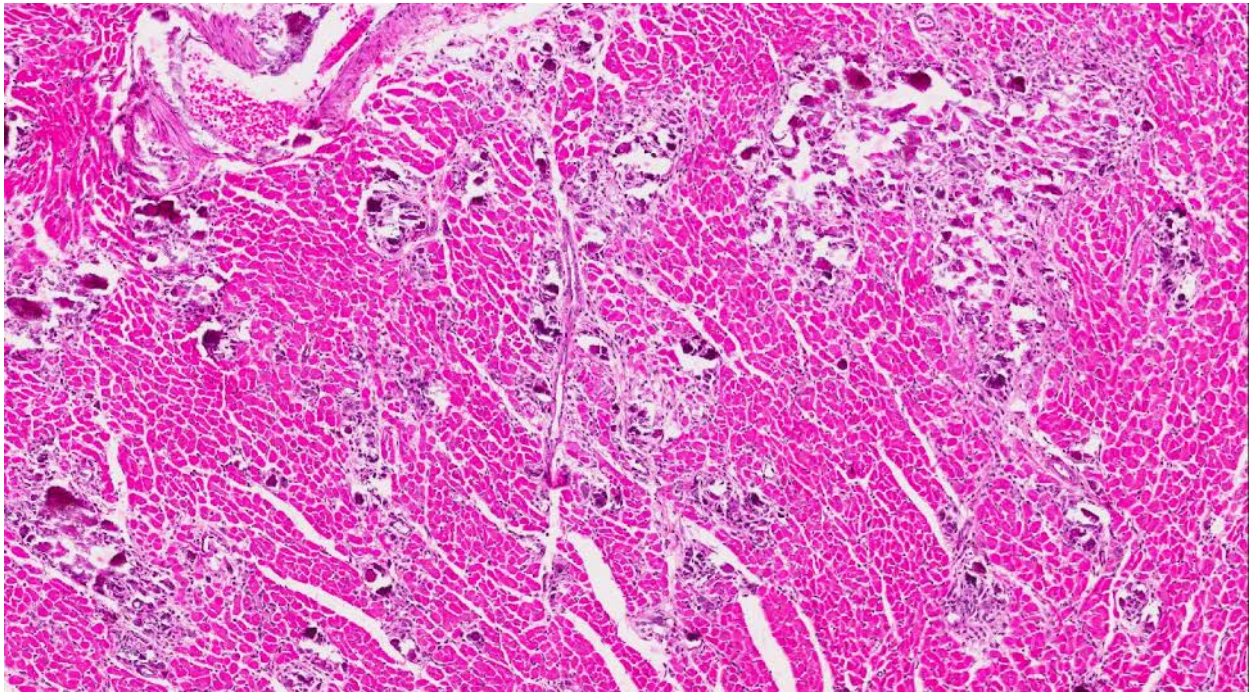
Laboratory Results: An independent analysis of the feed showed actual vitamin D3 levels to be 160 fold higher than the



Subgross of a sagittal section of the heart and great vessels. At low magnification, there are visible areas of myofibers loss, predominantly in the interventricular septum and left ventricular free wall. (HE, 5X)

label analysis reported. The specific lot of this diet was one of several later recalled for elevated vitamin D levels.

Histopathologic Description: Heart (longitudinal sections): Affecting from 30 to 70% of the ventricular myocardium (LVFW and IVS>RVFW) are multiple coalescing foci of clusters or less commonly individual cardiomyocytes notable for their intensely hyaline refractile amphophilic



Heart, guinea pig. In this higher magnification of the interventricular septum, there are multifocal to coalescing areas of myofiber loss, fibrosis, and mineralization. (HE, 63X)

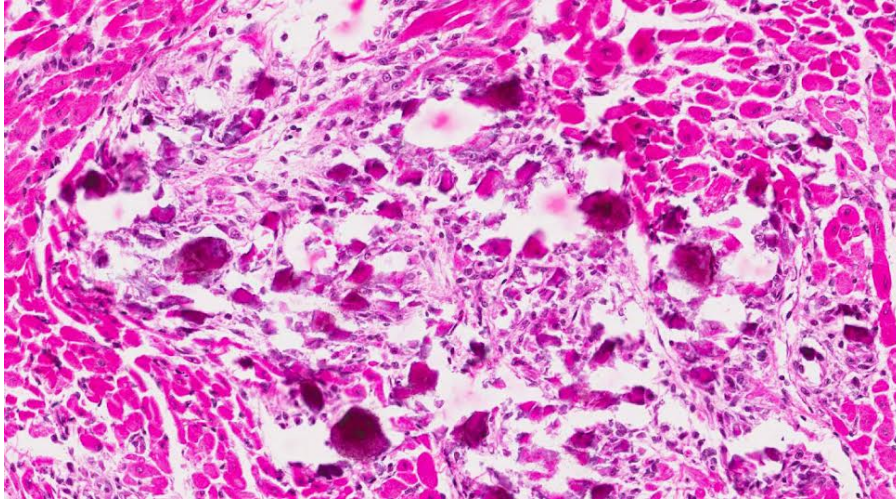
cytoplasm that is often fractured (mineralization). In some less affected cardiomyocytes, mineralization is finely punctate within the cytoplasm (mitochondrial mineralization). There is moderate to robust bland histiocytic to granulomatous inflammation, the latter including Langhans and foreign body type giant cells. There is significant organizing immature fibroplasia circumscribing inflammation and replacing cardiomyocytes. In some sections mineralization is also evident in the atrial myocardium as well as the intima and media of the aorta and pulmonary and coronary arteries. A von Kossa stain confirmed mineralization.

Mineralization of hepatocytes and renal tubular epithelium was also observed, and rarely the lung and spleen were mineralized (not submitted). In some animals there was centrilobular atrophy of the liver and

hemosiderin laden alveolar macrophages (heart failure cells) in the lungs.

Contributor's Morphologic Diagnosis: Heart, ventricular myocardium: Mineralization, multifocal to coalescing, subacute to chronic, severe, with granulomatous inflammation and organizing fibroplasia.

Contributor's Comment: In the summer of 2012, a laboratory animal feed manufacturer recalled several batches of feed, including the specific lot fed to these animals, because of excessively high vitamin D levels. Similar mortality nearly wiped out a small colony of a guinea pig model of human genetic disease at another institution.⁵ Interestingly, only one of 9 guinea pigs in that report had significant cardiac mineralization, and renal disease was the predominant manifestation.



Heart, guinea pig. Within affected areas, there is marked myofiber loss and replacement with fibrous connective tissue and crystalline mineral (which has fractured on sectioning.) Remaining myofibers are shrunken and atrophic, as well as at the periphery. (HE, 168X)

The major action of vitamin D ($1,25(\text{OH})_2\text{D}_3$) is to increase calcium and phosphorus absorption from the intestine via increased synthesis of calbindin by enterocytes.¹ Vitamin D also acts on the bone, stimulating osteoclastic resorption and making osteocytes responsive to parathyroid hormone. Vitamin D can stimulate calcium resorption in the kidney as well.

The major differential etiology for these lesions is metastatic mineralization, a poorly understood and likely multifactorial disease predominantly affecting male guinea pigs >1 year of age.^{3,7} Diet, particularly when high in phosphate and low in magnesium, is reported to be a significant factor. Only 4% of 140 animals examined in the Sparschu and Christie study had demonstrable cardiac mineralization, but lesion appearance and ventricular localization was similar (but less severe) than that reported herein. It is interesting to note that the guinea pigs in that study were given kale, a vitamin D rich plant.

The epizootic nature of the cases here combined with the young age (14 weeks) of

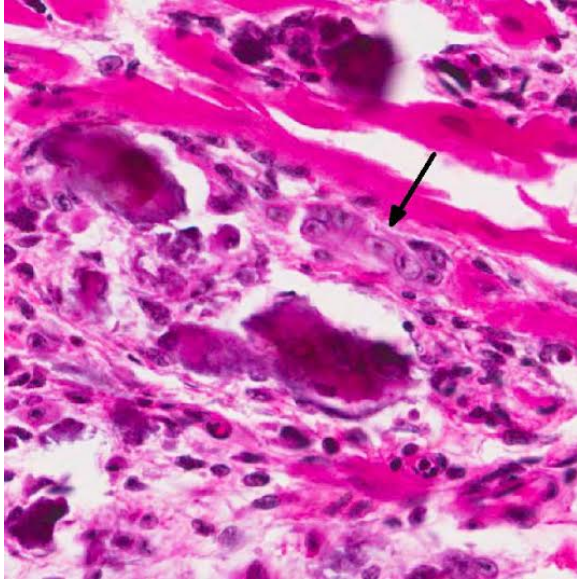
one of the guinea pigs suggested the probability of vitamin D toxicosis. Plants high in vitamin D glycosides include day blooming jessamine (*Cestrum diurnum*), *Trisetum flavescens*, and members of the *Solanum* (nightshade) family including *S. malacoxylon*.¹ The latter agent produces the disease *enteque seco* or *espichamento* in Argentina and Brazil. In addition to diet, accidental or deliberate rodenticide

poisoning should be ruled out.

JPC Diagnosis: 1. Heart, myocardium: Myocyte, degeneration, necrosis, atrophy and loss, multifocal to coalescing, severe with marked fibrosis, granulomatous myocarditis and mineralization.

2. Aorta: Mineralization, intimal and mural, multifocal, moderate.

Conference Comment: The initial steps in the synthesis of vitamin D involve the production of vitamin D_3 (cholecalciferol) in the skin via exposure to ultraviolet radiation but can also be obtained through dietary intake of vitamins D_2 or D_3 . In the liver, vitamins D_2 and D_3 are converted to 25-hydroxyvitamin $\text{D}_{2/3}$ which are found in circulation and can be measured. In the kidney, 25-hydroxyvitamin D is converted to the active form of vitamin D, which is known as calcitriol and abbreviated $1, 25(\text{OH})_2\text{D}$. Excess vitamin D can be ingested due to feed mixing errors as in this case, or via the ingestion of toxic plants, which is more commonly seen in ruminants. This condition results in elevated levels of



Heart, guinea pig. There are scattered attempts at myofiber regeneration throughout the section (arrow). (HE, 324X)

25-hydroxyvitamin D, while the active form, calcitriol is not elevated. It may be possible that when present at toxic levels, the inactive forms are involved in stimulation of the vitamin D receptor.⁴ The result of elevated vitamin D levels is an increase in calcium absorption in the intestine, increased resorption from bone and reduction in renal excretion followed by hypercalcemia, and hyperphosphatemia. In addition to the endocardium, other targets for mineralization include the kidneys, gastric mucosa, lungs and atrial walls.²

Gross lesions described by Holcombe et al. in a colony of guinea pigs similarly affected included white discoloration of multiple tissues including the gastrointestinal tract, skeletal muscle, and kidneys in addition to the cardiac muscle. Histologic lesions included varying degrees of mineralization in the tissues described grossly, as well as the lungs. Fibrosis and granulomatous inflammation were associated with mineralization, as seen in this case. Bone lesions were also demonstrated in affected guinea pigs, including osteosclerosis (most

prominently in the tibia), and changes in the articular cartilage. Additional lesions described in those cases included fatty change in the liver and chronic interstitial nephritis. Clinicopathologic changes included hyperphosphatemia and elevated serum alkaline phosphatase. Serum calcium levels (ionized and total) were not significantly elevated in affected guinea pigs, and are not a reliable indicator of vitamin D status in the guinea pig. However, the values of calcium multiplied by that of phosphorus was greater than 70 for the majority of affected animals in that study.⁴

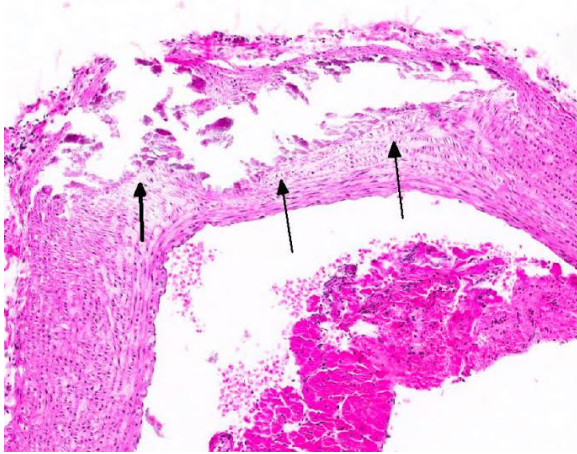
Conference participants described degeneration, necrosis and loss of cardiac myocytes secondary to mineralization. Participants discussed the differential diagnoses for metastatic calcification including renal disease, neoplasia such as lymphoma, multiple myeloma and tumors affecting the parathyroid gland resulting in primary hyperparathyroidism, as well as vitamin D toxicosis. Diagnostic techniques for investigating an outbreak of nutritional or toxic disease case involving multiple animals were also a point of discussion.

Contributing Institution:

Department of Comparative Medicine
Penn State Hershey Medical Center
<http://www.hmc.psu.edu/comparativemedicine>

References:

1. Capen CC. Endocrine glands. In: Maxie MG, ed. *Jubb, Kennedy, and Palmer's Pathology of Domestic Animals*, Vol 2. 5th ed. Edinburgh: Elsevier Saunders; 2007:325-428.



Aorta, guinea pig: There are large areas of mineralization within the arterial wall (arrows). (HE, 80X)

2. Craig LE, Dittmer LE, Thompson KG. Bones and Joints. In: Maxie MG, ed. *Jubb, Kennedy and Palmer's Pathology of Domestic Animals*. Vol 1. 6th ed. St. Louis, MO: Elsevier; 2016:89.
3. Galloway JH, Glover D, Fox WC. Relationship of diet and age to metastatic calcification in guinea pigs. *Lab Anim Care*. 1964; 14: 6-12.
4. Holcombe H, Parry NM, Rick M, Brown DE, et al. Hypervitaminosis D and metastatic calcification in a colony of inbred strain 3 Guinea pigs (*Cavia porcellus*). *Vet Pathol*. 2015; 52(4): 741-751.
5. Jensen JA, Brice AK, Bagel JH, Mexas AM, Yoon SY, Wolfe JH. Hypervitaminosis D in guinea pigs with alpha-mannosidosis. *Comp Med*. 2013; 63:156-162.
6. Joseph DR. The Ratio between the heart-weight and body-weight in various animals. *J Exp Med*. 1908; 10: 521-528.
7. Sparschu GL, Christie RJ. Metastatic calcification in a guinea pig colony: a pathological survey. *Lab Anim Care*. 1968; 18: 520-526.

CASE II: CRL2 (JPC 4019884).

Signalment: Approximately 6 week old, male, New Zealand White rabbit (*Oryctolagus cuniculus*).

History: The rabbit was clinically observed with diarrhea.

Gross Pathology: Cecal contents were thin and watery. There were few formed fecal pellets.

Laboratory Results:

Heavy growth of *Escherichia coli* from cecum

Parasitology: Positive for *Eimeria media* and *Eimeria perforans* by fecal analysis.



Enteron, rabbit. There are three sections on the slide – colon (upper right), cecum (center), and ileum (lower left) (HE 6X).

Histopathologic Description: Cecum: There is moderate, multifocal degeneration, necrosis and loss of epithelial cells, predominantly lining the luminal surface but occasionally extending deeper into the crypts. Along the apical surface of the intestinal epithelia, clusters of small

coccobacilli bacteria are tightly adhered. Bacteria are numerous and affect a large percentage of the epithelial surface. The mucosa and submucosa is mildly edematous. The lamina propria is infiltrated by mild to moderate numbers of heterophils and lesser numbers of lymphocytes. There are increased mitoses in the crypts, and epithelial cells are crowded and piled up at the tops of the crypts, indicative of a proliferative response to superficial cells loss.

Additional sections of small and large intestine may be present on the slide. These tissues are similarly affected. The ileum is additionally characterized by numerous intraepithelial protozoal forms consistent with coccidiosis.

Contributor's Morphologic Diagnosis:

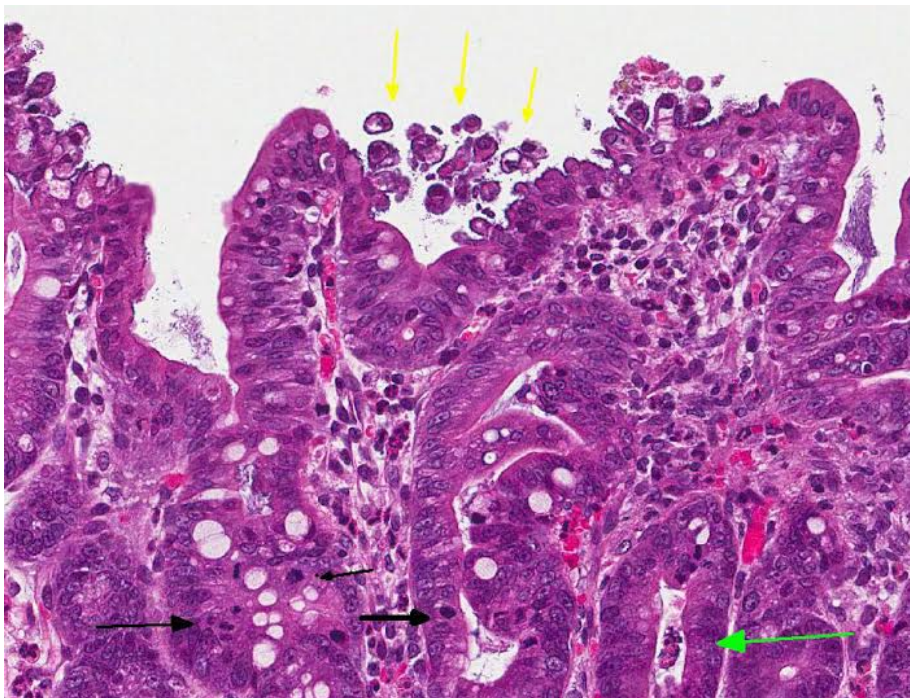
Cecum: Typhlitis, heterophilic and lymphocytic, moderate, diffuse with

moderate, multifocal adherent coccobacilli, consistent with *E. coli* infection.

Ileum: Enteritis, heterophilic, marked, diffuse with moderate adherent coccobacilli and coccidiosis.

Colon: Colitis, heterophilic and lymphocytic, mild, diffuse with mild multifocal adherent coccobacilli.

Contributor's Comment: Diarrhea in suckling and weanling rabbits can be a significant issue in rabbitries. Although diarrhea can be caused by a variety of factors, *Escherichia coli* is considered to be a common pathogen in young rabbits. *E. coli* can be classified into five categories: enterotoxigenic (ETEC), enteroinvasive (EIEC), enteropathogenic (EPEC), enteroadherent (EAEC), and enterohemorrhagic (EHEC).² Rabbits are usually affected with enteropathogenic *E. coli*, which does not produce toxins and does not invade the mucosa.⁴ Under normal circumstances, *E. coli* is not considered to be a part of the normal rabbit flora; or at least thought to be found in low numbers.^{5,6} While the mechanism of disease is not entirely clear, attachment and effacement of epithelial villi by the bacteria is thought to play a role with EPEC.³



Cecum, rabbit. There is necrosis and sloughing of luminal epithelium (yellow arrows), which are covered by a layer of short i. There are numerous mitotic figures (black arrows) in the underlying regenerative crypts. A single crypt abscess (green arrow) is present attesting to the necrotizing nature of this lesion. (HE, 204X)

In this case, the ileal, cecal and colonic epithelia have numerous adherent coccobacilli.

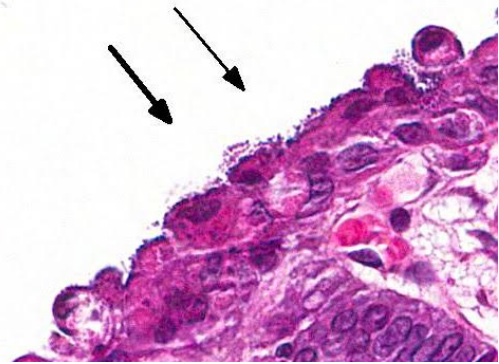
Gram staining revealed the bacteria to be gram-negative, and cultures of the intestines had heavy growth of *E. coli*. Concurrent coccidiosis may additionally contribute to *E. coli* proliferation in the intestines.

JPC Diagnosis: 1. Colon and cecum: Typhlocolitis, superficial and necrotizing, multifocal, mild with edema, crypt hyperplasia and moderate numbers of adherent mucosal bacilli.

2. Ileum: Enteritis, superficial and necrotizing, multifocal, mild, with edema, crypt hyperplasia, moderate numbers of adherent mucosal bacilli and moderate numbers of apicomplexan schizonts and gamonts.

Conference Comment: Classification of *E. coli* strains generally references the virulence factors and mechanisms which cause disease. Mechanisms of injury include alterations in cell membrane fluid / ion transport (enterotoxigenic forms) or necrosis of enterocytes caused by bacterial toxins and inflammatory mediators / enzymes (enteropathogenic and enterohemorrhagic forms). Enterohemorrhagic strains invade enterocytes but enteropathogenic and enterohemorrhagic forms do not. Enterohemorrhagic strains result in death of enterocytes, followed by inflammation and hemorrhage. Gross lesions in enterotoxigenic forms are often indistinct, in contrast to enteropathogenic and enterohemorrhagic forms where gross lesions can include a thickened granular appearing mucosa with hemorrhage and fibrin exudation, which varies in severity depending on strain. Enteroinvasive forms, which result in septicemic colibacillosis, begin as an intestinal infection and bacteria and enterotoxins gain access to systemic

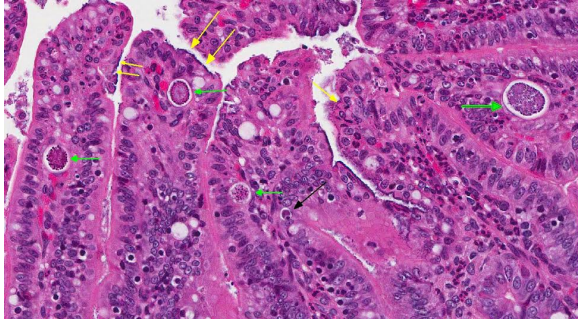
circulation through vessels in the lamina



*Cecum, rabbit. Overlying the edematous lamina propria, degenerate luminal epithelium is attenuated with lined by a layer of attached bacilli consistent with enteropathogenic *E. coli* (HE, 400X)*

propria underlying damaged mucosa.⁸

Enteropathogenic *E. coli* (EPEC), also referred to as attaching and effacing *E. coli* (AAEC), is often reported in rabbits but also affect other species such as calves, dogs and pigs. Bacteria attach to the microvillus border of intestinal epithelium by cups, which results in the formation of pedestals that can be seen ultrastructurally. Disruption of the microvillar border results in alterations in ion/fluid transport and a malabsorptive and maldigestive diarrhea; enterocyte death, fluid secretion and an inflammatory response also play a role in the pathogenesis.¹ Bacterial attachment is mediated by the protein intimin; EPEC also express fimbriae and EPEC adherence factor. EPEC produces bacterial proteins EspA, EspB, EspD, which enter cells and disrupt signal transduction pathways and microvilli. Some strains of EPEC produce a verotoxin which plays a role in the death of enterocytes and cells of the lamina propria.⁸ Infection of juvenile animals with EPEC / AAEC is often accompanied by co-infection with other intestinal pathogens such as rota or coronavirus, particularly in calves.¹



Ileum, rabbit. Within the epithelium, there are low numbers of developing coccidial gametocytes (green arrows) and a single developing schizonts (black arrow). There are numerous patches of aical epithelium which are lined by a dense band of enteropathogenic *E. coli* (yellow arrows). (HE, 400X)

Laboratory rabbit intestinal flora may include a wide variety of *E. coli* strains, including EPEC, which can be present in the absence of clinical signs; non-clinical animals may serve as reservoirs for infection. It has been suggested that inflamed intestine provides a favorable environment for pathogenic *E. coli* strains, which remain subclinical until other factors such as co-infections, stress or diet changes trigger an outbreak of clinical disease. Subclinical infection with various *E. coli* strains is important not only because of the reservoir potential, but also because many strains of *E. coli*, including EPEC, can be zoonotic.⁷

This case generated considerable discussion on different potential histologic diagnoses. Like the contributor, some conference participants preferred a mild to moderate typhlocolitis and enteritis; whereas others favored a more pathogenesis-oriented approach focused primarily on the EPEC-induced changes in the superficial mucosal epithelium (i.e. superficial mucosal epithelial necrosis) leading to the secondary lesions in lamina propria (i.e. inflammation, edema, and crypt hyperplasia). In sections of the small intestine intraepithelial protozoal schizonts and gamonts were described as

well as rare oocysts in the intestine lumen. Conference participants also noted the absence of adipose tissue in the small sections of mesentery that are present. Such mesenteric changes are suggestive of fat atrophy and could be related to this animal's nutritional status. However, the absence of adipose tissue could also be an incidental, age-related finding in a young rabbit.

Contributing Institution:

Charles River Labs Research Animal Diagnostic Services
CRIVER.COM

References:

1. Gelberg HB. Alimentary system and the peritoneum, omentum, mesentery and peritoneal cavity. In: McGavin MD, Zachary JF, eds. *Pathologic Basis of Veterinary Disease*. 5th ed. St. Louis, MO: Mosby Elsevier; 2012:809, 374-376.
2. Levine MM. Escherichia coli that cause diarrhea: enterotoxigenic, enteropathogenic, enteroinvasive, enterohemorrhagic, and enteroadherent. *The Journal of Infectious Diseases*. 1987; 155(3):377-389.
3. Moon HW, Whipp SC, Argenzio RA, Levine MM, Giannella RA. Attaching and effacing activities of rabbit and human enteropathogenic *Escherichia coli* in pig and rabbit intestines. *Infection and Immunity*. 1983; 41(3): 1340-1351.
4. Percy DH, Barthold SW. *Pathology of Laboratory Rodents and Rabbits*. 3rd ed. Ames, IA: Blackwell publishing; 2007:273-274.
5. Prescott JF. Escherichia coli and diarrhea in the rabbit. *Vet Pathol*. 1978; 15: 237-248.
6. Smith HW. Observations on the flora of the alimentary tract of animals and factors

affecting its composition. *J Pathol Bacteriol.* 1965; 89:95-122.

7. Swennes AG, Buckley EM, Madden CM, Byrd CP, et al. Enteropathogenic *Escherichia coli* prevalence in laboratory rabbits. *Vet Microbiol.* 2013; 163(3-4):395-398.

8. Zachary JF. Mechanisms of microbial infection. In: McGavin MD, Zachary JF, eds. *Pathologic Basis of Veterinary Disease.* 5th ed. St. Louis, MO: Mosby Elsevier; 2012:809, 165-167.

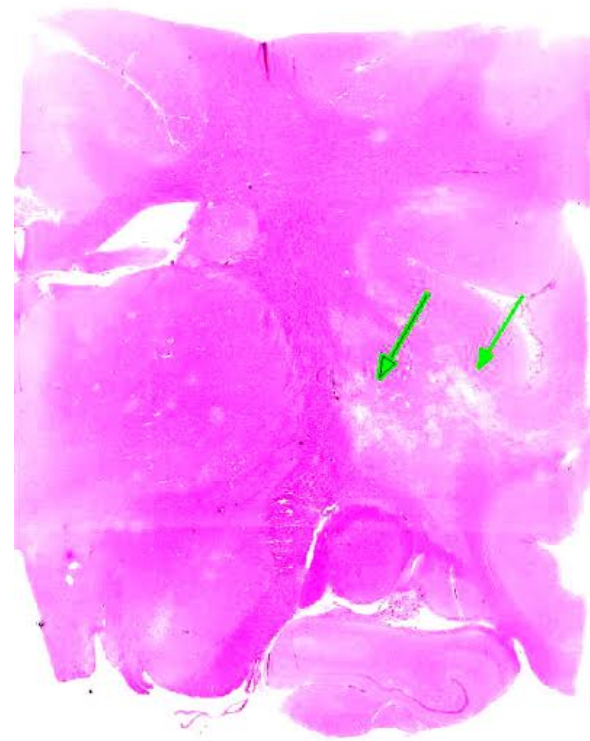
CASE III: 12A-892 (JPC 4033747).

Signalment: 11-year-old male Indian rhesus macaque (*Macaca mulatta*).

History: This animal was born at ONPRC and housed outdoors until 3 years of age, then kept indoors for the remainder of his life. He received two mucosal doses of SIV Mac239 approximately 5 years before his death. He was found deceased in the cage and was presented for necropsy the following day. He had been sedated multiple times for bronchoalveolar lavage over the course of the protocol. The most recent was performed 9 months prior to death. He had a history of intermittent epistaxis with the first report 10 months prior to death. On 12/29/2012 he was reported for epistaxis, not looking well, and hesitancy to stand. A cage side evaluation by a technician revealed a mild right head tilt and epistaxis. He took and ate treats readily when offered and was bright and interactive with the observer. He appeared slow-moving and hunched when ambulating. He was found dead in his cage the following day (12/30).

Gross Pathology: At necropsy, the animal was overweight (BCS 4/5). He had cyanotic oral mucous membranes, and epistaxis of

the right naris was evident. There was marked edema and congestion of all lung



Cerebrum, rhesus. At subgross magnification, there are areas of malacia within the white matter. (HE, 5X).

lobes with greater severity on the left side (found in left lateral recumbency). Sectioned surfaces of lung oozed blood-tinged fluid on palpation. Femoral bone marrow was diffusely dark red. Liver was rubbery, congested, enlarged, mottled dark red-brown with an enhanced reticular pattern. Gallbladder, cystic duct, and common bile duct were thickened and contained scant pale yellow bile. Renal cortices exhibited swelling and streaked pallor and renal medullae were streaked and congested. There was mild meningeal hemorrhage and congestion. Post-fixation, sections of the cerebellar peduncles have multiple, irregular foci of pale tan discoloration and are softer than the surrounding tissue.

Laboratory Results: Culture of the right naris grew *Pseudomonas* and *Staphylococcus aureus*. Culture of the lung grew Gram positive *Bacillus* spp. and α -hemolytic *Streptococcus* spp. His most recent complete blood count (1 month prior to necropsy) had only a minimal basophilia and the most recent serum chemistry (4 months prior to necropsy) was within normal limits.

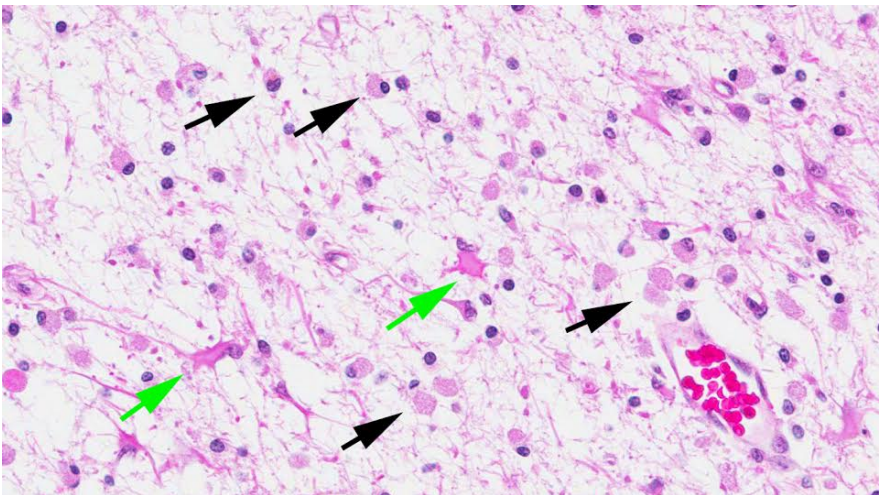
Immunohistochemistry of brain sections for SV40 antigen revealed moderate to strong staining of astrocyte nuclei and nuclei of (presumably) oligodendroglia within the white matter of the cerebrum and the cerebellum. Luxol fast blue staining of cerebrum and cerebellum highlighted loss of myelin with minimal myelin particulates in gitter cells.

Histopathologic Description: Within the cerebral white matter and extending into the white-gray matter junction are multifocal, irregular regions characterized by loss of neuropil and gliosis with prominent gemistocytic astrocytes that rarely contain glassy, intranuclear, amphophilic or granular, basophilic viral inclusions that

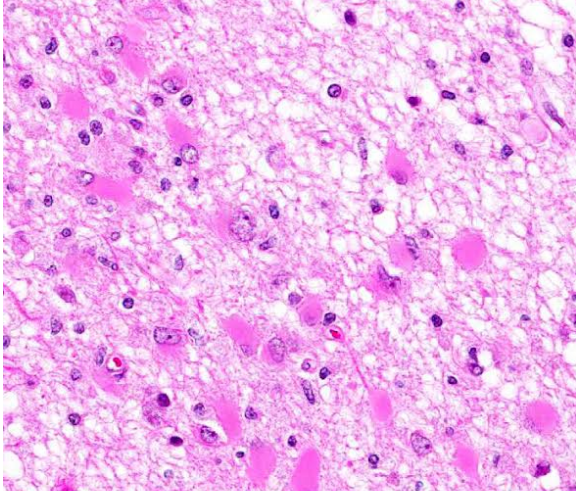
marginate the chromatin. Astrocytes are cyto- and karyomegalic, many with misshapen or bizarre nuclei and large or bizarre nucleoli. Affected areas are infiltrated by foamy gitter cells and fewer lymphocytes. In and around affected regions, Virchow-Robbins space of vessels is markedly expanded by clear space (edema) with variable numbers of lymphocytes, macrophages, and rare eosinophils. There is multifocal, minimal to mild extravasation of red blood cells into Virchow-Robbins space and rarely into surrounding parenchyma.

Contributor's Morphologic Diagnosis: Cerebrum: Leukoencephalitis, multifocal, chronic, severe with demyelination, gliosis, gitter cells, gemistocytic astrocytosis, and intranuclear viral inclusions within oligodendroglia and bizarre astrocytes.

Contributor's Comment: This case represents one manifestation of SV40 infection in immunosuppressed macaques. In this case, immunosuppression was due to experimental inoculation with SIV. The head tilt, posture, ambulation abnormalities, and death are attributable to brain lesions of SV40, while the epistaxis was unrelated and due to bacterial infection. Initial examination of the brain did not have grossly evident malacia, but multiple recuts of fixed tissue revealed discolored foci in the white matter. In addition to the characteristic histopathology, immunohistochemistry confirmed the presence of viral antigen within brain lesions.



Cerebrum, rhesus. At higher magnification, the areas of pallor are cavitations developing into glial scars. There is total loss of axons and myelin sheaths, with few remaining Gitter cells (black arrows). The remainder of the cells are astrocytes (green), whose proliferating processes are forming the glial scar. (HE, 400X). arrows



Cerebrum, rhesus. At the edge of the scar, there are numerous large astrocytes with abundant cytoplasm and large nuclei (gemistocytes). (HE, 256X).

Polyomaviruses are small, double-stranded DNA viruses and have been identified in birds, rodents, nonhuman primates, and humans. They were named for their propensity to cause tumors in either their natural host or atypical host(s), typically in differentiated cells. Much like herpesviruses, infection by polyomaviruses in their natural hosts typically causes an asymptomatic, life-long infection. The polyoma virion is divided into early and late-coding regions. The early region codes T antigens, the late codes capsid proteins. Small (t) and large (T) transforming/tumor antigens are conserved across all polyomavirus species and these proteins are fairly well-characterized. The small t antigen is not necessary for productive infection in cell culture, but the large T antigen is essential for production of progeny virions. T antigen plays a role in DNA replication as well as tumorigenesis. Some polyomaviruses, including SV40, have additional T antigens.¹

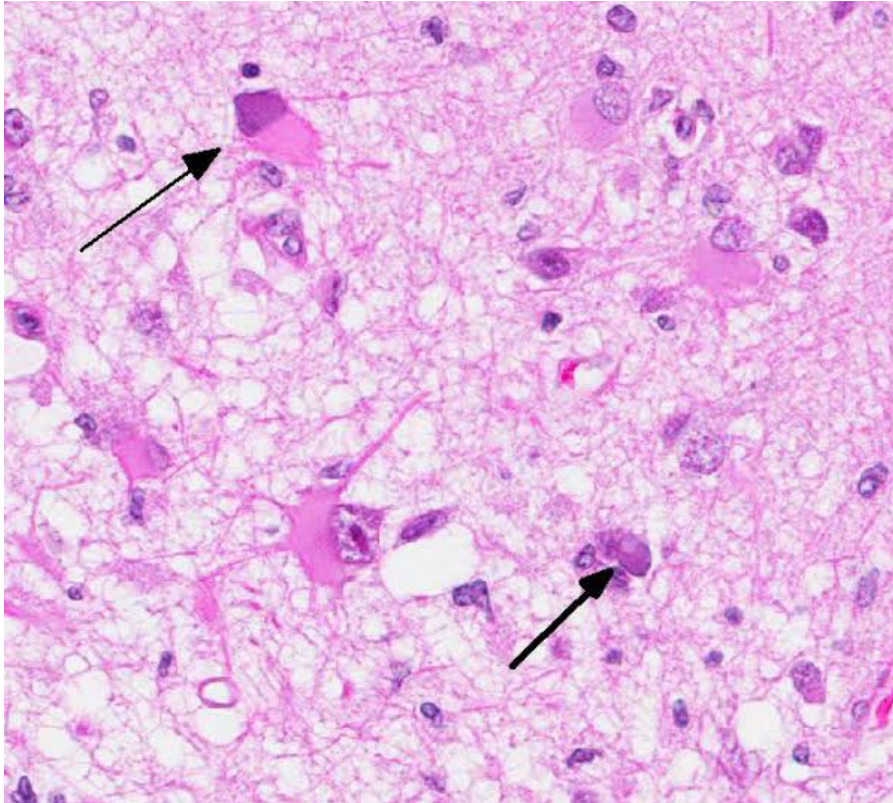
Simian virus 40 (SV40) is an endemic polyomavirus in captive and free-ranging macaques. Seroprevalence increases with age in socially-housed animals, and the

majority of animals are seropositive by 1 year of age.⁹ Infection does not cause lesions in immunocompetent animals, but immunosuppression, such as SIV infection or immunosuppressive drug regimens, allows reactivation of latent infections or primary infections to cause disease. Disease in immunosuppressed macaques can manifest as progressive multifocal leukoencephalopathy (PML), nephritis, or pneumonia.⁶

SV40 is of particular utility in research due to its comparative ease to grow in culture as well as it causing PML in SIV or SHIV-infected macaques similar to disease in human AIDS patients infected with JC virus. SV40 is potentially zoonotic, identified as a contaminant in early polio vaccines and is seroprevalent in people working with macaques.^{3, 4} There is public concern over SV40 vaccine contamination, and there has been extensive research into oncogenicity of SV40 in people as it is known to cause a host of neoplasms in hamsters.⁷

SV40 is of particular utility in research due to its comparative ease to grow in culture as well as it causing PML in SIV or SHIV-infected macaques similar to disease in human AIDS patients infected with JC virus. SV40 is potentially zoonotic, identified as a contaminant in early polio vaccines and is seroprevalent in people working with macaques.^{3, 4} There is public concern over SV40 vaccine contamination, and there has been extensive research into oncogenicity of SV40 in people as it is known to cause a host of neoplasms in hamsters.⁷

Neuropathology of SV40 can be PML or meningoencephalitis, though some overlap does occur.² PML is hypothesized to occur in animals with underlying SV40 infection that subsequently are immunosuppressed, while macaques with more inflammatory



Cerebrum, rhesus. Nuclei of both astrocytes and oligodendroglia are expanded by a glassy, basophilic viral polyomaviral inclusion (HE, 324X).

than demyelinating lesions were SV40-negative at the time of SIV infection with subsequent experimental SV40 infection.^{8, 2} PML occurs due to infection and subsequent loss or dysfunction of myelin-producing oligodendroglia. In addition to the demyelination, a unique histopathologic feature of PML in macaques are the gemistocytic astrocytes with abundant eosinophilic cytoplasm and bizarre nuclei.⁶ The gitter cell infiltration and gliosis are a secondary reaction to the breakdown of myelin. The more inflammatory manifestation of neurologic SV40 is characterized by leptomenigeal edema and perivascular and multifocal plaque-like infiltrates of lymphocytes and macrophages with extension of inflammatory cells into cortical gray matter.²

JPC Diagnosis: Cerebrum, subcortical white matter: Leukoencephalomalacia, multifocal, marked with demyelination, numerous pleomorphic gemistocytic astrocytes, and glial intranuclear inclusion bodies.

Conference Comment: The contributor provides an excellent review of SV40 infection and corresponding lesions above. There are seven polyomaviruses that have been identified in non-human primates. In addition to SV40 in

macaques, these include SV12 in baboons, B-lymphocyte papovavirus (LPV) in African green monkeys, *Polyomavirus papionis 2* in baboons, cynomolgus polyomavirus (CPV), SV40-CAL in macaques, and chimpanzee polyomavirus. These viruses are common as latent infections as seen with SV40 and discussed above.⁵ Renal lesions are associated with initial SV40 infection and the characterization of renal lesions and their relationship to the sequence of infection and immunosuppression vary between different polyomaviruses in non-human primates and humans.² With SV40 infection lesions include nonsuppurative tubulointerstitial nephritis with basophilic intranuclear inclusion bodies in tubule epithelial cells. Sloughed epithelial cells are present in tubule lumina and evidence of regeneration may be present. Pulmonary lesions secondary to SV40 infection may include interstitial pneumonia; other pulmonary

lesions may be also present and associated with immunosuppression, not secondary to SV40 infection.⁶

The pathogenesis of infection and corresponding CNS lesions in this case was also discussed. Recrudescence of the virus secondary to immunosuppression results in infection of oligodendrocytes and astrocytes, with loss of oligodendrocytes resulting in the demyelinating lesion seen histologically.

Multifocal to coalescing areas of necrosis and loss of the white matter constitute approximately 10% of the section, and are located primarily at the junction of the grey and white matter which contain numerous gemistocytic astrocytes and gitter cells. Additional characteristics include mild spongiosis and multifocal dilation of axon sheaths. There was a discussion regarding the chronicity of these lesions with some participants interpreting areas of pallor as having abundant astrocytic fibers, less debris and fewer gitter cells, indicating a developing astrocytic scar. Immunohistochemistry for glial fibrillary acidic protein proved that many of the filaments traversing these areas are indeed astrocytic processes.

Contributing Institution:

Oregon National Primate Research Center
<http://www.ohsu.edu/xd/research/centers-institutes/onprc/>

References:

1. An P, Sáenz Robles MT, Pipas JM. Large T antigens of polyomaviruses: amazing molecular machines. *Annu Rev Microbiol.* 2012. 66:213-236.
2. Axthelm MK, Koralnik IJ, Dang X, et al. Meningoencephalitis and demyelination are pathologic manifestations of primary polyomavirus infection in immunosuppressed rhesus monkeys. *J Neuropath Exp Neurol.* 2004. 63 (7): 750-758.
3. Engels EA. Cancer risk associated with receipt of vaccines contaminated with simian virus 40: epidemiologic research. *Expert Rev Vaccines.* 2005 Apr; 4(2):197-206.
4. Engels EA, Switzer WM, Heneine W, Viscidi RP. Serologic evidence for exposure to simian virus 40 in North American zoo workers. *J Infect Dis.* 2004 Dec 15; 190(12):2065-9.
5. Fahey MA, Westmoreland SV. Nervous system disorders of nonhuman primates and research models. In: Abee CR, Mansfield K, Tardif S, Morris T. eds. *Nonhuman Primates in Biomedical Research: Diseases.* 2nd ed. Vol 2. Waltham, MA: Elsevier; 2012: 739-741.
6. Horvath CJ, Simon MA, Bergsagel DJ et al. Simian Virus 40-induced disease in rhesus monkeys with simian acquired immunodeficiency syndrome. *Am J Pathol.* 1192 140(6): 1431-1440.
7. Qi F, Carbone M, Yang H, Gaudino G. Simian virus 40 transformation, malignant mesothelioma and brain tumors. *Expert Rev Respir Med.* 2011; 5(5):683-97. doi: 10.1586/ers.11.51.
8. Simon MA, Ilyinskii PO, Baskin GB, Knight HY, Pauley DR, Lackner AA. Association of simian virus 40 with central nervous system lesion distinct from progressive multifocal leukoencephalopathy in macaques with AIDS. *Am J Pathol.* 1992; 154: 437-446.
9. Verschoor EJ, Niphuis H, Fagrouch Z, et al. Seroprevalence of SV40-like polyomavirus infections in captive and free-ranging macaque species. *J Med Primatol.*

2008 Aug;37(4):196-201. doi:
10.1111/j.1600-0684.2007.00276.x. Epub
2008 Jan 9.

CASE IV: Rt13-623 (JPC 4070249).

Signalment: 9-month-old, female, Thicket Rat (*Grammomys surdaster*).

History: A thicket rat was inoculated with 200,000 *Plasmodium chabaudi* sporozoites intravenously and blood was collected for evaluation every other day. While blood was being collected, the rat died.

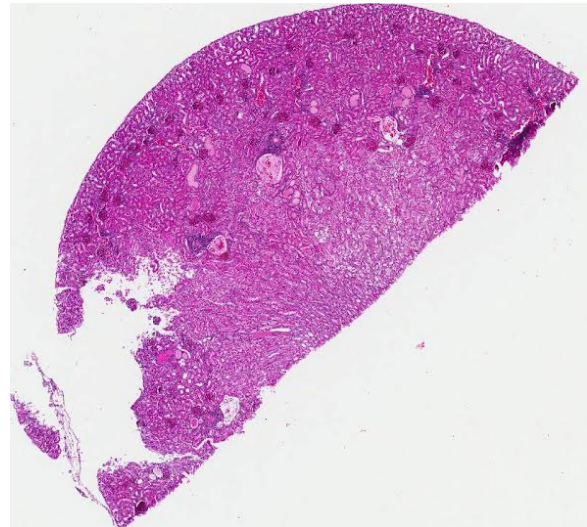
Gross Pathology: There was anasarca and approximately 1 ml of a clear pleural effusion. The spleen was very dark and was approximately four times normal size.

Laboratory Results: Parasitemia at time of death was 25.5%.

Histopathologic Description: Dark violet-red granules line capillary tufts in almost all glomeruli, with smaller granules in the mesangium and in the basement membrane of tubules. Some tubules are ectatic and contain protein casts. There are multifocal, perivascular lymphoid aggregates.

Other lesions included erythroid extramedullary hematopoiesis of the spleen, follicular hyperplasia of the splenic white pulp, multifocal nonsuppurative myocarditis, multifocal centrilobular hepatic lipidosis, and hemosiderophages in the liver, spleen, blood vessels, alveolar walls, and nasolacrimal ducts.

The granular material does not polarize and does not lose color when bleached.



Kidney, thicket rat. At subgross magnification, glomeruli are prominent due to their deep eosinophilia. (HE, 5X).

Special stains: Puchtler-Sweat and Perl's [Iron stains]: Blue granules were seen within tubular epithelium but not associated with the basement membrane. No staining was present in the glomeruli.

Masson's trichrome (-); PAS (-); and von Kossa and Alizarin Red (-).

Transmission Electron Microscopy:

Kidney, Glomerulus: Within the podocytes, there are 150-750 nm granular deposits adjacent to the basement membrane (white arrow). Similar but smaller deposits are seen within the basement membrane (black arrow). The foot processes are effaced with infrequent filter slits. The mesangium is moderately expanded without an increase in cellularity.

Kidney, Tubule: Small granules (<150 nm) are within the basement membrane (black arrow) and adjacent to the basement membrane (white arrow). There is a slight increase in lipid.

Elemental analysis of the granules was attempted but was inconclusive.

Contributor's Morphologic Diagnosis:

Kidney: glomerulonephropathy characterized by deposition of granular material along [capillary loops] glomerular basement membranes, diffuse, marked.

Kidney, tubules, basement membrane: granular pigmented material deposition.

Kidney: tubular proteinosis, multifocal, mild.

Kidney: chronic interstitial nephritis, multifocal, mild.

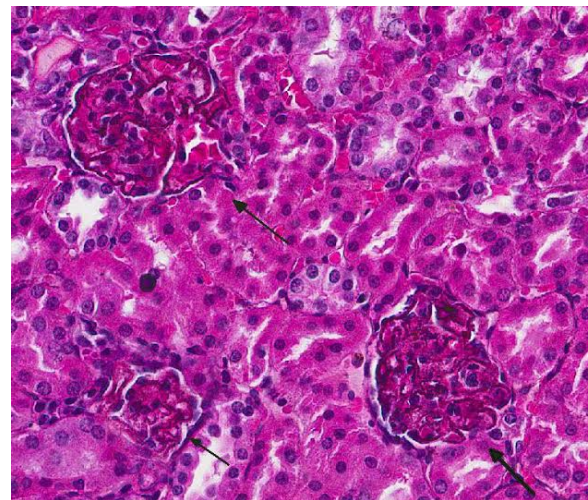
Contributor's Comment: According to the World Health Organization, there were approximately 198 million cases and 584,000 deaths due to malaria in 2014.¹² Although most of the cases are concentrated in (sub-Saharan) Africa, malaria can be found in Central and South America, India and Asia.¹¹ Mortality is highest in children under 5 years and in pregnant women.^{1,12} Humans are infected by *Plasmodium falciparum*, *P. malariae*, *P. ovale*, *P. vivax* and *P. knowlesi*. Anopheles mosquitoes serve as the vector.¹ Severe disease due to Acute kidney injury is found in less than 1% of cases of *Plasmodium falciparum* infection but the mortality rate can be as high as 45%.³ Few cases of kidney injury are also seen with *Plasmodium malariae* and *P. vivax* infection.³ Acute kidney injury is primarily seen in adults, older children, and those who live in areas with a low incidence of infection. Renal insufficiency may be part of multi-organ failure or the only clinical presentation.^{3,8} cerebral malaria or anemia is most often associated with *Plasmodium falciparum* infection.^{1,7}

If there is a full recovery, there is no progress to chronic kidney disease.³ Microscopic changes are variable, but

tubular degeneration and necrosis predominate. Parasitized erythrocytes are sequestered in glomerular and interstitial vessels, and hemosiderin in tubular epithelium, hemoglobin casts, mild glomerular changes, and interstitial nephritis may also be present. Immune-mediated glomerulonephritis is not associated with acute kidney injury.^{3,7} Renal changes may be due to obstruction and sequestration of infected erythrocytes, glomerular and tubular inflammatory changes, fluid loss, and altered renal circulation.³

There have been reports of a “quartan malarial nephrotic syndrome” due to immune complex disease in children in Nigeria that was thought to be related to *Plasmodium malariae* infection.⁶ Subsequent papers have suggested that renal disease in children in Nigeria, as well as Uganda and Ivory Coast, was associated with, but not caused, by *Plasmodium malariae* infection.^{3,4}

Thicket rats found in sub-Saharan Africa are natural hosts for chronic *Plasmodium chabaudi*, *P. berghei*, *P. vinckei*, and *P. yoelii* infection and model chronic *Plasmodium falciparum* disease in man. Anopheles mosquitos serve as vectors for the both human and rodent plasmodial



Kidney, thicket rat. A deeply eosinophilic granular pigment is deposited within glomeruli. (HE 296).

infection. Although no one species mimics *Plasmodium falciparum* infection completely, there are enough similarities, especially with *Plasmodium chabaudi*, to make them a valuable tool for comparative study. In both *Plasmodium chabaudi* and *Plasmodium falciparum*, symptoms develop as parasitemia increases and then resolve when parasitemia decreases. Infected rodents develop anemia secondary to dyserythropoiesis, suppression of hematopoiesis, and thrombocytopenia as seen in man. Red blood cells sequester in the placenta, which serves as a model of malaria-related fetal and neonatal abnormalities. In several ways, *Plasmodium chabaudi* is not representative of infection by *Plasmodium falciparum*. Unlike *Plasmodium falciparum* in man, the organ of sequestration is the liver, and not the brain. Infected animals develop hypothermia instead of fever. Although there is splenomegaly, it is not correlated with level of parasitemia or sequestration.¹⁰

In a recent report, mice infected with *Plasmodia berghei* ANKA developed renal failure accompanied by increased inflammatory cytokines, expression of adhesion molecules, and products of oxidation. Resulting changes in the vascular endothelium led to interstitial edema and, over time, mice developed acute tubulointerstitial nephritis. Although there was no deposition of brown granular material apparent by examination of H&E slides, there was deposition of polarizable crystals identified as hemozoin in glomeruli and endothelium.⁵

The degree of pigment deposition in the glomeruli was unusual. Analysis by special stains, electron microscopy, and elemental analysis did not reveal the composition of the granular material. Given the high level

of parasitemia, we felt the material was directly related to infection with malaria.

JPC Diagnosis: 1. Kidney, cortex, glomerular and tubular basement membranes: Immune complex deposition, diffuse.

2. Kidney, cortex: Tubular ectasia and proteinosis, multifocal, mild.

3. Kidney: Cortical perivascular lymphocytic infiltrates, multifocal, mild.

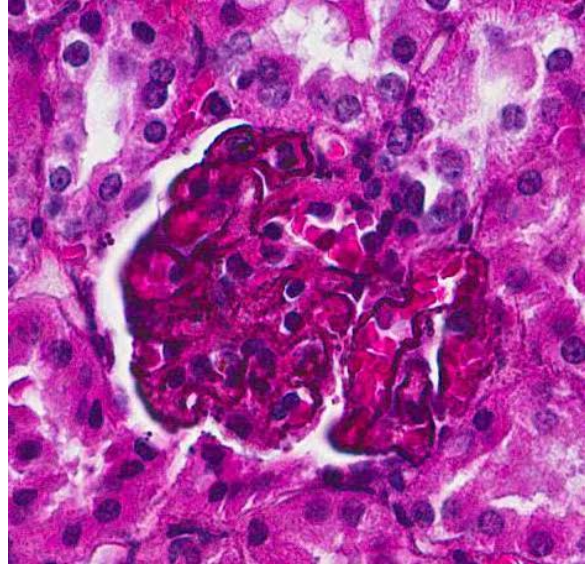
Conference Comment: This case was studied in consultation with Dr. Rachel Cianciolo co-director of the International Veterinary Renal Pathology Service; she interpreted the renal changes in the submitted microscopic slide as most consistent with immune complex-mediated membranous glomerulonephropathy and commented it is very unusual to observe the actual immune complex deposits with hematoxylin and eosin staining alone. This case was also studied in consultation with the Department of Nephropathology at the Joint Pathology Center, whose medical pathologists are familiar with glomerular disease as described in humans; they similarly postulated that the deposits may be immunoglobulin or complement, as would occur with membranous glomerulonephropathy, and further noted that, in humans, the index of suspicion would be elevated for lupus nephritis in this case.

A definitive diagnosis of immune-mediated glomerulonephropathy requires immunofluorescent or immunohistochemical confirmation of immunoglobulin and complement components in glomerular tufts. Ultrastructurally, electron-dense deposits may be seen in mesangial, subepithelial or subendothelial locations. Glomerulonephritis results following the deposition of immune complexes within the glomeruli or

following the formation of antibodies to antigens present in the basement membrane (anti-GBM disease). Immune complex glomerulonephritis is a sequela to persistent infections of various etiologies including viral, bacterial and parasitic infections, as well as autoimmune disease. Antigen-antibody complexes form in the presence of antigen excess or when antigen-antibody quantities are equal. The complexes deposit in glomerular capillaries, fix complement, and cause basement membrane damage, which is enhanced by the ensuing inflammatory response. Factors that can determine the extent of deposition include the size and charge of complexes, glomerular permeability and the antigen-antibody avidity. Small and intermediate complexes are the most damaging, as larger complexes are removed from circulation by the mononuclear phagocytic system.⁹

Glomerular lesions described in human malaria patients do include prominent mesangial proliferation with occasional basement membrane thickening and deposition of an eosinophilic granular material along capillary walls, within the mesangium and in Bowman's capsule.^{2,3} The origin/nature of this material is not well described. Other findings include immunofluorescence demonstration of IgM and C3 in mesangial capillary walls, although other studies have found immune complex deposition was not seen in basement membranes or the mesangium of glomeruli and clinical / clinical pathology findings apparently don't necessarily support the presence of immune complex deposits in all cases of acute renal failure related to malaria infection.³ However, in other reports in the literature glomerulonephritis is described in cases of acute renal failure in malaria infection and a distinction is made between chronic progressive glomerulopathy which occurs in

quartan malaria in Africa, versus acute renal failure associated with falciparum malaria in Southeast Asia, India and sub-Saharan Africa.² Ultrastructural findings described in human cases include subendothelial and



Kidney, thick-tailed rat. At higher magnification, the granular pigment outlines capillary basement membranes, and granular deposits are present within the mesangium as well. (HE, 400X).

mesangial electron dense deposits with the presence of granular, fibrillary and amorphous material.^{2,3} The absence of a prominent glomerular inflammatory response in this case leads to speculation regarding the role of the glomerular deposits in renal function.

In this case, diffusely and globally within glomeruli there are 1-2µm, prominent, eosinophilic globules lining capillaries and slight increase in cellularity within the mesangium. There are multifocal glomerular synechia, and the parietal epithelium is mildly hypertrophied. The eosinophilic material is also seen within the basement membrane of adjacent tubules, and there is tubular ectasis, proteinosis and attenuation of tubular epithelium with few areas of tubular epithelial degeneration and necrosis. During the conference, there was discussion

regarding the origin of the eosinophilic globules, including calcium, hemosiderin, lipofuscin, and melanin. A battery of histochemical stains performed by the contributor did not shed further light as to the nature the basement membrane deposits.

Nephrotic syndrome is well-documented in human malarial infection, and various histologic patterns of glomerular lesions are reported in the literature, including focal segmental glomerulosclerosis (FSGS), membranoproliferative glomerulonephritis, minimal change disease, and membranous glomerulonephritis, among others [Asinobi AO – 2015]. In a 1967 study of the histologic features of nephrotic syndrome in 77 people with quartan malaria (infection with *Plasmodium malariae*), approximately half had detectable malarial organisms, and all but one had glomerulonephritis, including nine cases histologically classified as membranous glomerulonephritis [Kibukamusoke JW-1967], which corresponds with the preferred diagnosis offered by Dr. Rachel Cianciolo in this case. In the same study, 63% of the patients were children, thus presumably “non-immune”, and had a higher incidence of parasitemia as compared to adults. A more recent review article on the topic provided by the contributor summarizes the clinicopathologic findings of malaria-induced renal damage in people, including the various forms of malarial nephropathy and their association with a specific malarial etiology and the patient anamnesis⁴. General observations in the review included the finding that non-immune (naïve) patients have a higher risk of developing acute renal failure than semi-immune people (those living in endemic areas); in quartan malaria (*Plasmodium malariae*) cases originating from Nigeria and the Ivory Coast, the primary glomerular lesion with light microscopic examination was characterized as membranous nephron-

pathy; and fatal acute renal failure occurs in cases of falciparum malaria in up to 40% of non-immune patients with high parasitemia above 5% of parasitized erythrocytes.

During the conference, the moderator disclosed that this thickset rat was one of several in an experimental group that either died or was euthanized with similar clinical and histopathologic findings as the one presented in this case. The glomerular lesions, gross findings indicative of nephrotic syndrome (anasarca and pleural effusion), and the clinical history of an immunologically naïve animal with a high parasitemia lends to the possibility of an emerging animal model for malarial acute nephrotic syndrome/renal failure. Interestingly, glomerulonephritis is described in both rat and mouse models infected with variants of *Plasmodium berghei*, with primarily mesangial deposition of immunoglobulins (e.g. IgM, IgG, C3, among others) and malarial antigen. [George CR 1976; Ehrlich JH – 1981). In the rat, the renal lesions were transitory and appeared to resolve within one to three months, unlike the lethal course of disease that occurred in this thickset rat.

Contributing Institution:

National Institutes of Health

9000 Rockville Pike

14A, Room 120

Bethesda, MD 20892

<http://www.ors.od.nih.gov/sr/dvr/Pages/default.aspx>

References:

1. Autino B, Corbett Y, Castelli F, et al. Pathogenesis of malaria in tissues and blood. *Mediterr J Hematol Infect Dis*. 2012; 4(1):e2012061.

2. Barsoum RS. Malarial acute renal failure. *J Am Soc Nephrol.* 2000; 11:2147-2154.
3. Das BS. Renal failure in malaria. *J Vector Borne Dis.* 2008; 45:83-97.
4. Ehrich JHH, Eke FU. Malaria-induced renal damage: facts and myths. *Pediatr Nephrol.* 2007; 22(5):626-37.
5. Elias RM, Correa-Costa M, Claudiene RB, et al. Stress and Modification of Renal Vascular Permeability Are Associated with Acute Kidney Injury During P. berghei ANKA Infection. *PLOS One.* 2012; 7(8):e44004.
6. Hendrickse RG, Adeniyi A, Eddington GM, et al. Quartum Malarial Nephrotic Syndrome. *Lancet I.* 1972; 1(7761):1143-1149.
7. McAdam AJ, Sharpe AH. Infectious diseases. In Kumar V, Abbas A K, Fausto N eds. *Robins and Cotran Pathological Basis of Disease.* 8th ed. Philadelphia, PA: Elsevier Saunders: 2010:386-388.
8. Mishra SK, Das BS. Malaria and acute kidney injury. *Semin Nephrol.* 2008; 28(4):395-408.
9. Newman SJ. The Urinary System. In: McGavin MD, Zachary JF, eds. *Pathologic Basis of Veterinary Disease.* 5th ed. St. Louis, MO: Mosby Elsevier; 2012:620-622.
10. Stephens R, Culleton RL, Lamb TJ. The contribution of Plasmodium chabaudi to our understanding of malaria. *Trends Parasitol.* 2012; 28(2):73-82.
11. Schwartz DA, Genta RM, Bennett, DP, Pomerantz RJ. Infectious and parasitic diseases. In Rubin R, Strayer DS eds. *Rubin's Pathology.* 5th ed. Baltimore, MD: Lippincott Williams & Wilkins: 8:359-362.
12. World Health Organization. World Malaria Report. 2014:2-3.

Joint Pathology Center
Veterinary Pathology Services



WEDNESDAY SLIDE CONFERENCE 2015-2016

Conference 15

27 January 2016

Timothy Walsh, DVM, DACVP
National Zoological Park

CASE I: 33177-A (JPC 4002480).

Signalment: 2nd year adult, intact male, red cardinal (*Cardinalis cardinalis*).

History: This wild-caught cardinal presented with a large crusted mass within the skin of the cloacal region and poor body condition. Euthanasia was elected and a necropsy was performed by the referring veterinarian. Formalin-fixed organ/tissue samples were subsequently submitted for histological examination.

Gross Pathology: Focally within the skin and subcutis of the dorsal cloacal region,

there is a large crusted mass composed of multiple small (up to approximately 6 mm in diameter), individual, cystic structures containing a soft brownish, amorphous material. Each cyst contains one to two, light grey to tan and roughly ovoid trematode parasites with a concave ventral surface. Each fluke measures 4-6mm long x 4-6mm diameter and is characterized by prominent vitelline glands and an extensively convoluted, white to tan uterus. The mass is focally contiguous with the overlying skin surface via a single, pinpoint pore. No other gross lesions were identified.



Cloaca, cardinal. The skin and subcutis of the dorsal cloacal region contains a large mass of individual cystic structures. (Photo courtesy of: University of Minnesota, Veterinary Diagnostic Laboratory, 1333 Gortner Ave, St Paul, MN, 55108 <http://www.vdl.umn.edu/>)

Laboratory Results:

Parasite identification: Trematode parasites extracted from the dermal pseudocysts were identified as *Collyriclum faba*.

Histopathologic Description: Skin and subcutis (dorsal cloacal region): The dermis and subcutis are expanded by a focal cluster of 3-6mm diameter, spherical to ovoid pseudocysts individually separated and surrounded by thick bands of compressed dermal fibrous connective tissue. The pseudocysts are enclosed by a variably thick (2-40um diameter) collagenous capsule and contain one to two, 3-5mm diameter (in cross section) adult trematodes. These trematodes are characterized by the following features: a 5-7um thick pale eosinophilic cuticle containing numerous brightly eosinophilic spines in pairs or small groups; an anterior sucker and pharynx; prominent vitellaria; a coiled uterus containing large numbers of 20um x 10um, ovoid, brown-shelled eggs (containing miracidia); testes containing numerous basophilic spermatozoa and ovaries. The surrounding thickened dermal and subcuticular connective tissue contains mild to moderate, multifocal to coalescing infiltrates of heterophils, macrophages and lesser numbers of lymphocytes and plasma cells. Occasionally scattered within these regions, there are dense, multifocal infiltrates of macrophages (including multinucleated macrophages) surrounding small clusters of trematode eggs. Overlying the pseudocyst cluster, the skin is multifocally ulcerated and covered by a thick serocellular crust composed of large amounts of eosinophilic and basophilic cellular and keratinaceous debris with entrapped viable and degenerate heterophils, small colonies of basophilic coccoid bacteria and small numbers of trematode eggs.



Cloaca, cardinal. Cystic structures are up to 6mm in diameter. (Photo courtesy of: University of Minnesota, Veterinary Diagnostic Laboratory, 1333 Gortner Ave, St Paul, MN, 55108 <http://www.vdl.umn.edu/>)

Blood vessels throughout the section contain large numbers of blood cells parasitized by protozoal organisms (e.g. *Leukocytozoon* sp. and/or *Hemoproteus* sp.). In one field, a skeletal muscle myofiber is expanded by a large sarcocyst containing numerous bradyzoites.

Contributor's Morphologic Diagnosis:

- 1) Skin and subcutis (dorsal cloacal region): Parasitic pseudocysts, multifocal, with ulcerative and granulocytic dermatitis and intralesional mature adult flukes and fluke ova, etiology consistent with *Collyriclum faba*
- 2) Skeletal muscle: Sarcocystosis, mild
- 3) Protozoal parasitemia, marked

Contributor's Comment: *Collyriclum faba* is a digenetic trematode which uncommonly infects passeriform and galliform birds of Eurasia and North and South America.^{1,5,7} The adult trematodes are uniquely located within the peri-cloacal skin and subcutis and less commonly, the skin of the ventrum, limbs, head and neck.⁷ The parasites form discrete encapsulated pseudocysts containing paired, juxtaposed adult forms. Macroscopically, compared with most



Cloaca, cardinal. Cross section of the cloacal mass, showing several closely apposed pseudocysts. (HE, 4X).

trematodes, *Collyriclum faba* is dorsally convex and ventrally flattened with a dorsal rather than ventral sub-terminal oral sucker.¹ The histological characteristics of the trematodes include: a thick pale eosinophilic, poorly muscular cuticle containing numerous brightly eosinophilic spines in pairs or small groups; a dorsal sucker; bifurcated intestinal crura; prominent vitellaria; a coiled uterus containing operculated brown-shelled eggs; reproductive organs.^{1,7}

The life cycle of this parasite is incompletely understood, however, birds are thought to become infected following ingestion of metacercariae in the putative snail or dragonfly intermediate hosts.^{3,7} Fluke eggs are thought to be released from a pore in the dermal pseudocysts of the avian host upon immersion in water where they then infect the intermediate hosts.^{3,6} This phenomenon has been demonstrated by rubbing wet gauze over the pseudocysts in live avian patients.³ *Collyriclum faba* is not usually associated with clinically significant disease, though it has been associated with cloacal obstruction and emaciation in some cases.³

JPC Diagnosis: 1. Glabrous skin: Multiple trematode pseudocysts with mild heterophilic and granulomatous dermatitis.

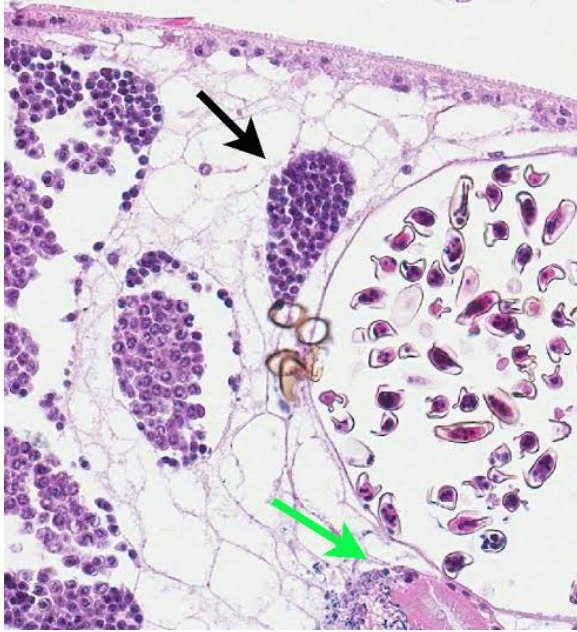
2. Skeletal muscle: Sarcocysts, multiple (some sections).

3. Circulating erythrocytes: Intracytoplasmic protozoa.

Conference Comment: The prevalence of infection and specificity of *C. faba* for certain bird species is thought to be related to the distribution of intermediate hosts and diet of the definitive host. *C. faba* has been identified in both wild avian species as well as domestic poultry.³ The first intermediate host, a small freshwater snail, has a relatively limited distribution, while the second intermediate host, various species of mayfly, as well as the definitive avian hosts, have a larger range. As mentioned above by the contributor, adults of *C. faba* form pseudocysts, which are located in the subcutis and occur in pairs. Birds will most often harbor up to four cysts, and as mentioned above are not generally associated with clinical disease; however, heavily parasitized birds may be anemic, emaciated, have problems defecating and eventually die. The parasitism may occur in combination with viral disease such as West Nile virus, in which case severity of infection is increased.⁴ Increased numbers of



Cloaca, cardinal. Each pseudocyst contains cross sections of two flukes (arrows). (HE, 10X)



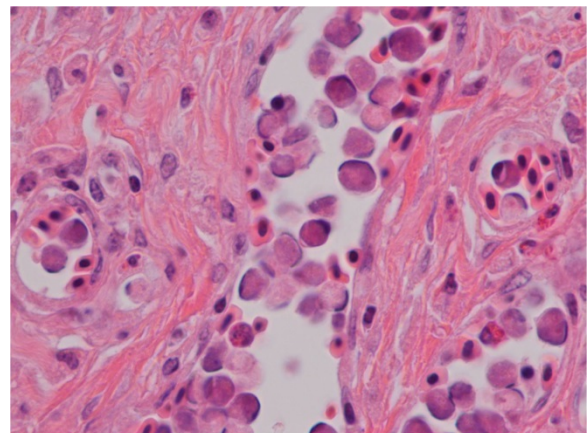
Cloaca, cardinal. The flukes have a thin serrated cuticle, a large uterus containing brown-shelled eggs, cross sections of a testis containing spermatocytes (black arrows) and ceca (green arrow) (HE, 120X).

cysts can also be associated with increased morbidity and mortality.⁵

There is slide variability with few sarcocysts being present in skeletal muscle in some sections. *Sarcocystis* spp. protozoan parasites are common incidental findings in various mammalian and avian species. Infective sporocysts are shed in the feces of the definitive host, which are ingested by the intermediate host, where asexual reproduction occurs resulting in the formation of cysts in the skeletal muscle. One common species which infects birds is *S. falcatula*; the Virginia opossum is the definitive host and many different species of birds serve as intermediate hosts. The birds ingest infective sporocysts in the opossum's feces, or by ingesting transport hosts such as cockroaches. In addition to skeletal muscle, sarcocysts may also be found in cardiac muscle and the central nervous system. The definitive host is infected by ingesting a bird which contains sarcocysts. The cysts are

digested and zoites invade the intestinal epithelium of the definitive host, developing into gamonts. Fertilization occurs, resulting in the formation of oocysts, which sporulate and are shed as the infective form in the feces. The intermediate host ingests feces with sporocysts; once the sporocysts are ingested, the sporozoites are released in the intestine, where they migrate to blood vessels, eventually developing into meronts. Merozoites are eventually liberated from the meronts and enter circulation, resulting in their migration to cardiac, skeletal muscle and nervous tissue where they develop into sarcocysts, containing metrocytes that produce bradyzoites, which are infective to the definitive host.²

The conference histologic description was very similar to the contributor's thorough description above. Multiple sections of a small tubular structure, lined by cuboidal to columnar epithelium and surrounded by smooth muscle, are present at the periphery of the section and these structures were tentatively identified as the vas deferens. The excellent gross images submitted with this case were also discussed. Conference participants commented on the nodular and ulcerative nature of the lesion as well as the



Cloaca, cardinal. The vast majority of leukocytes in the peripheral blood contain a single glassy intracytoplasmic hemogregarine schizont which peripheralizes the nucleus. (HE, 600X)

feather loss and poor body condition, indicated by keel prominence and the absence of subcutaneous fat. The dark brown foci seen grossly overlying the pseudocysts were postulated to be foci of ulceration secondary to rupture and release of eggs. Although difficult to resolve even at high power, the egg shells have small hyalinized spines. Conference participants discussed the different hemoprotozoan genera including *Plasmodium*, *Haemoproteus* and *Leucocytozoon* but agreed it was not possible to definitively determine which organism is present in this case.

Contributing Institution:

University of Minnesota
<http://www.vdl.umn.edu/>

References:

1. Blankespoor HD, Wittrock DD, Aho J, Esch GW. Host-parasite interface of the fluke *Collyriclum faba* (Bremser in Schmalz, 1831) as revealed by light and electron microscopy. *Z Parasitenkd.* 1982; 68:191-199.
2. Gardiner CH, Fayer R, Dubey JP. *An atlas of protozoan parasites in animal tissues.* Washington D.C.: Armed Forces institute of pathology; 1998:41.
3. Grove DM, Zajac AM, Spahr J, Duncan RB, Sleeman JM. Combined infection by avian poxvirus and *Collyriclum faba* in an American crow (*Corvus brachyrhynchos*). *J. Zoo Wildl. Med.* 2005;36: 111-114.
4. Heneberg P, Faltynkova A, Bizos J, Mala M, et al. Intermediate hosts of the trematode *Collyriclum faba* (Plagiochiida: Collyriclidae) identified by an integrated morphological and genetic approach. *Parasit Vectors.* 2015; 8:85.
5. Literak I, Honza M, Haman A, Pinowska B, Pcola S. Cutaneous trematode

Collyriclum faba in wild birds in the central European Carpathians. *J. Parasitol.* 2003; 89: 412-416.

6. Parker D. What is your diagnosis? *J. Avian Med. Surg.* 2009; 23:159-161.
7. Taylor MA, Coop RL, Wall RL. *Veterinary Parasitology.* 3rd ed. Ames, IA: Blackwell Publishing; 2007:521.

CASE II: 15-0608 (JPC 4066922).

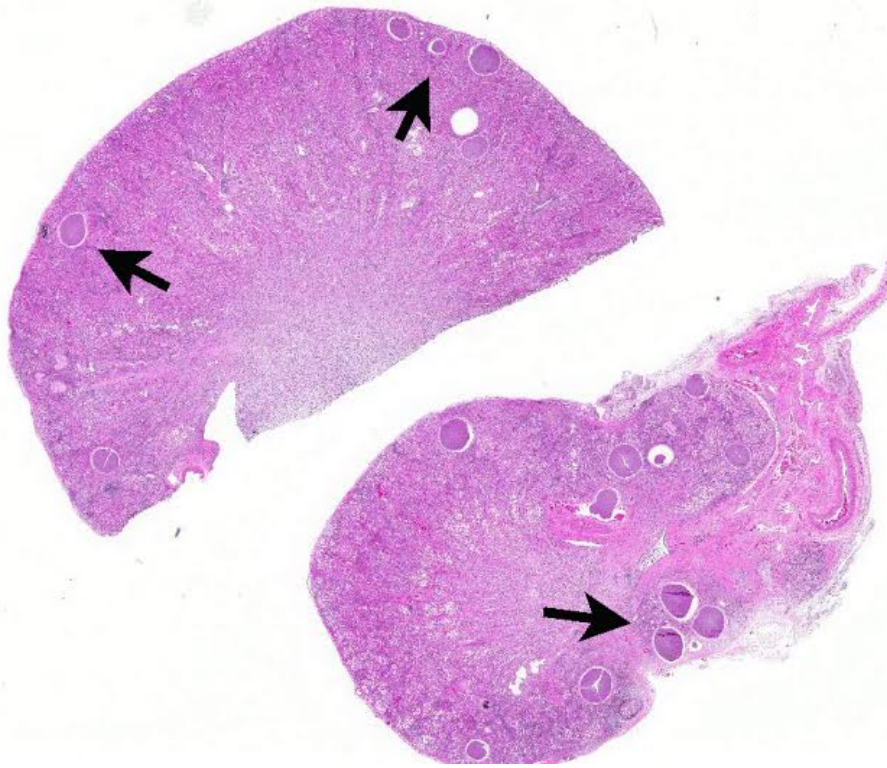
Signalment: Adult female opossum (*Didelphis virginiana*).

History: A Good Samaritan found this opossum on a road side and transported it to a wildlife rehabilitation center. The attending veterinarian examined the opossum and found the following: emaciation and dehydration; an abrasion on the right dorsum; a scab with protruding bone at the tail tip; a bruised and swollen left elbow; and numerous small white nodules in the skin of the muzzle, ears and anus. Radiographs revealed a fracture of the left ulna. The opossum died while under isoflurane anesthesia and the attending veterinarian performed a necropsy.

Gross Pathology: There were numerous 1mm in diameter white nodules in the kidney, adrenal glands, spleen, heart, ovary, and haired skin and subcutis.

Laboratory Results: NA

Histopathologic Description: Kidney: Multifocally, throughout the cortex, there are many round protozoal cysts up to 850-1000 µm in diameter that compress adjacent nephrons. The cysts are composed of densely packed crescentic bradyzoites that are 4 µm long surrounded by a 3-8 µm thick rim of host cell cytoplasm which is enclosed



Kidney, opossum. There are multiple round apicomplexan cysts within the renal cortex. (HE, 5X).

in 20-40 μm thick, hyaline capsule. Multifocally, extending from the cortex to the medulla, the interstitium is disrupted and expanded by aggregates of moderate numbers of lymphocytes admixed with fewer plasma cells, and neutrophils. Multifocally, cortical tubules are dilated with attenuated epithelium and contain proteinaceous fluid admixed with few sloughed cells and cellular debris. There are few tubules lined with swollen vacuolated epithelial cells (degeneration). There is also loss of tubules with replacement by fibrous connective tissue. Multifocally, few glomerular tufts are expanded by an eosinophilic homogeneous material.

Contributor's Morphologic Diagnosis:

Kidney: Protozoal cysts, numerous, etiology consistent with *Besnoitia* spp.

Kidney: Nephritis, interstitial, lymphoplasmacytic and neutrophilic, chronic,

multifocal, marked, with membranous glomerulonephritis, and interstitial fibrosis.

Not submitted:

Haired skin, ovary, adrenal gland, spleen, and heart: Protozoal cysts, numerous, etiology consistent with *Besnoitia* spp.

Lung:

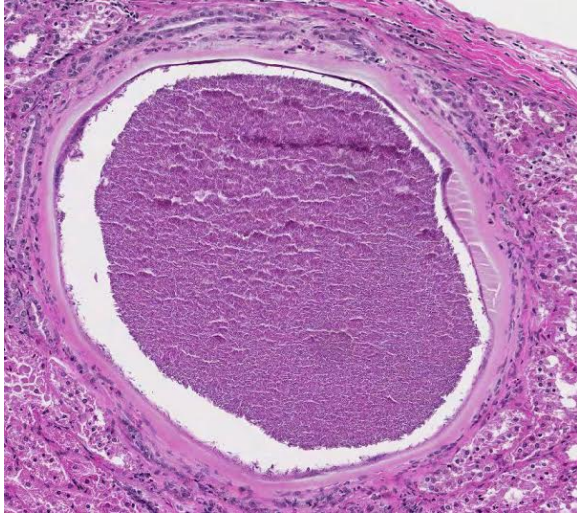
Bronchopneumonia, granulomatous, multifocal, marked, with adult nematodes, larvae and eggs, etiology consistent with *Capillaria* spp. and

Didelphostrongylus spp.

Spleen: Amyloidosis,

multifocal, marked.

Contributor's Comment: The role that the *Besnoitia* parasitism played in the pathology of the kidney is not clear. There are *Besnoitia* cysts surrounded by inflammatory cells and some without, and there are aggregates of inflammatory cells not associated with cysts. The cysts are predominantly intact. *Besnoitia* is not typically associated with clinical disease in the opossum, though cases with morbidity have been reported.^{1,6} While the cause of the chronic interstitial nephritis is not apparent in the submitted sections, this opossum was likely stressed, immunosuppressed and experiencing chronic antigenic stimulation. The open tail wound, the fractured ulna, the skin abrasion, the bronchopneumonia, and the *Besnoita* all likely contributed to the chronic antigenic



Kidney, opossum. Apicomplexan cysts measure up to 40um with a thick hyaline capsule and large numbers of zoites. (HE, 40X)

stimulation which resulted in the glomerular changes in the kidney and amyloid deposition in the spleen.

Besnoitia is a protozoal parasite in the phylum *Apicomplexa*.³ *Besnoitia* spp. require two hosts (heteroxenous life cycle).^{1,6} The domestic cat has been demonstrated to act as a definitive host for *Besnoitia darlingi* (species associated with opossums), in which infectious oocysts develop and are shed.⁷ Opossums and other species act as intermediate hosts, in which oocysts develop into tissue cysts.^{2,7} Opossums become infected by ingestion of oocysts from cats or tissue cysts by consumption of infected tissue from other intermediate hosts.^{2,6,7}

JPC Diagnosis: 1. Kidney: Tubulo-interstitial nephritis, neutrophilic and histiocytic, chronic diffuse, marked with intratubular leptospores.

2. Kidney: Amyloidosis, interstitial, multifocal, mild.

3. Kidney: Apicomplexan cysts, multiple.

Conference Comment:

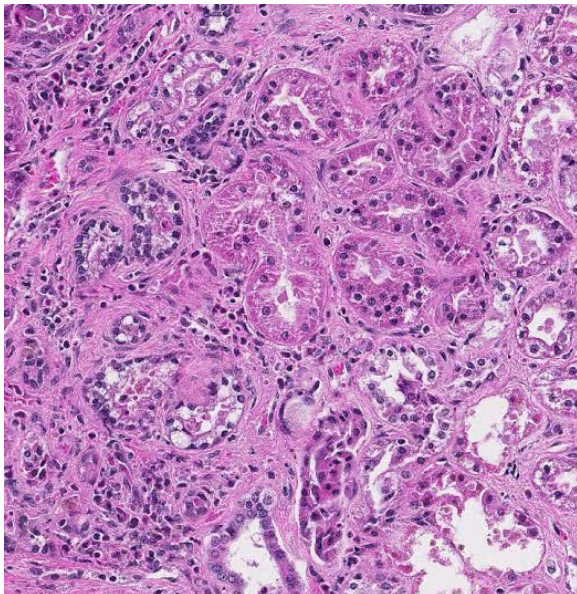
Besnoitia spp. protozoan parasites infect a wide variety of both wild and domestic mammalian species. The cysts are most commonly seen in visceral organs, skin, and skeletal muscle. As mentioned above, *Besnoitia* spp. infection in the opossum generally does not produce clinical disease; however, cases with significant lesions and clinical disease have been reported. Clinical disease is generally associated with immunosuppression, stress, and young age. The precise reason some opossums are afflicted by more severe disease is unclear, but other comorbidities may also play a role. In reported clinical cases, protozoal cysts presenting as white nodules at multiple locations in both eyes and nodules throughout the skin were predominant findings; varying degrees and types of ocular pathology were also observed. White nodules were also reported in the oral cavity, lungs, skeletal muscle and heart, specifically in the myocardium where protozoal cysts, foci of mineralization and inflammation were noted. Mineralized hyperechoic



Kidney, opossum. Higher magnification of the apicomplexan cyst. (HE, 100X).

nodules were also reported in the kidneys as well as varying degrees of interstitial nephritis and tubular changes. Foci of mineralization were also described in various other tissues.¹ Another study reported protozoal cysts in other organs such as the liver, spleen, stomach and lung. In that same study, debilitated adult female opossums were the most affected subgroup, the ear was the most frequently reported site for protozoal cysts, and the majority of infections were seen in the summer season.²

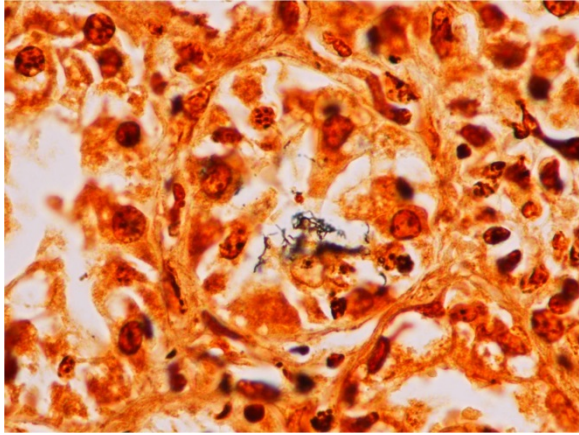
Histologically, the cysts consist of a single enlarged host cell, within which abundant crescent-shaped bradyzoites are packed into a parasitophorous vacuole, which fills the enlarged host cell. The host cell cytoplasm is present as a thin rim at the margin of the enlarged cell. Elongated host cell nuclei may be seen as an inner cyst membrane. The outer layer of the cyst, which forms the capsule, is seen as a variably thick, hyalinized layer of collagen fibers² which stains blue with Masson's trichrome stain.⁵



Kidney, opossum. Chronic changes in the remainder of the kidney include marked interstitial fibrosis with tubular degeneration and atrophy. (HE, 260X).

Mineralization of cysts may be seen as well as varying degrees of host inflammatory reaction.² *Besnoitia* spp. infections are well documented in other mammalian species, including cattle which may become infected with *B. besnoiti*. Recently, a new cyst nomenclature has been proposed for that species, due to historical inconsistencies in cyst descriptions consisting of the following: Hypertrophied host cell, enlarge nuclei, intracytoplasmic parasitophorous vacuole which contains bradyzoites, an inner cyst wall that may be vacuolated and an outer cyst wall in better developed cysts., and includes tissue cysts This entire structure is referred to as a tissue cyst. In cattle, the condition occurs in acute, subacute and chronic stages. The acute stage is associated with endothelial infections and resultant vascular damage. In subacute and chronic stages, tissue cysts are seen in mesenchymal host cells and are described in a variety of tissues, including being frequently described in the skin.⁵

In this case, the primary lesions, aside from the cysts, include interstitial nephritis, fibrosis, and both tubular and glomerular damage. The interstitial infiltrate is diverse, ranging from predominantly lymphocytes and plasma cells in some areas to being neutrophil- and eosinophil-rich in others. There is mild multifocal intratubular inflammation with tubular degeneration and necrosis. Glomerular changes include membranoproliferative glomerulonephritis and glomeruli range from essentially normal to obsolescent; periglomerular fibrosis is striking in some areas. Amyloid is present in small amounts multifocally within the medullary interstitium, and during the conference, was confirmed with Congo red staining and green birefringence under polarization. The moderator also discussed the presence of extramedullary myelo-



Kidney, opossum: Leptospire in the lumen of a proximal convoluted tubule. (Warthin-Starry 4.0, 1000X)

poiesis, which is multifocal and extensive in some areas of the cortical interstitium.

In light of the interstitial nephritis and tubular changes, conference participants considered leptospirosis as a primary differential diagnosis. A Warthin-Starry stain identified low numbers of leptospire in the lumen of renal tubules. The opossum has been documented as a reservoir for multiple leptospirosis serovars. Renal lesions due to leptospirosis vary with virulence of the infecting serovar and stage of infection, but generally consist of varying degrees of tubulointerstitial nephritis and tubular necrosis. Subacute or chronic cases have an increased degree of interstitial inflammation and fibrosis may be extensive.⁴

Contributing Institution:

Walter Reed Army Institute of Research
www.wrair.army.mil

References:

1. Ellis AE, Mackey E, Moore PA, Divers SJ, et al. Debilitation and mortality associated with besnoitiosis in four Virginia

opossums (*Didelphis virginiana*). *J Zoo Wildl Med.* 2012; 43:367-374.

2. Elsheikha HM, Mansfield LS, Fitzgerald SD, Saeed MA. Prevalence and tissue distribution of *Besnoitia darlingi* cysts in the Virginia opossum (*Didelphis virginiana*) in Michigan. *Vet Parasitol.* 2003; 115:321-327.

3. Gardiner CH, Fayer R, Dubey JP, Service USAR. *An Atlas of Protozoan Parasites in Animal Tissues.* U.S. Department of Agriculture, Agricultural Research Service. 1988.

4. Greene CE, Sykes JE, Brown CA, Hartmann K. Leptospirosis. In: Greene CE. Ed. *Infectious diseases of the dog and cat.* 3rd ed. St. Louis, MO: Saunders Elsevier; 2006:402-415.

5. Langenmayer MC, Gollnick NS, Majzoub-Altweck M, Scharr JC. Naturally acquired bovine Bestoitis: Histological and immunohistochemical findings in acute, subacute and chronic disease. *Vet Pathol.* 2015; 52(3):476-488.

6. Shaw S, Grasperge B, Nevarez J, Reed S. *Besnoitia darlingi* infection in a Virginia opossum (*Didelphis virginiana*). *J Zoo Wildl Med.* 2009; 40: 220-223.

7. Smith DD, Frenkel JK. *Besnoitia darlingi* (Apicomplexa, Sarcocystidae, Toxoplasmatinae): transmission between opossums and cats. *J Protozool.* 1984; 31:584-587.

CASE III: V15-04651 (JPC 4068934).

Signalment: Three-year-old female green iguana / common iguana (*Iguana iguana*)

History: The owner raises green iguanas as well as multiple other species of iguanas.



Heart, green iguana. Multiple cross-sections of the heart demonstrate a fibrinopurulent exudate filling the right ventricle and extending into the myocardium. Photo courtesy of: New Mexico Department of Agriculture Veterinary Diagnostic Services, 1101 Camino de Salud NE Albuquerque, NM 87102 www.nmda.nmsu.edu

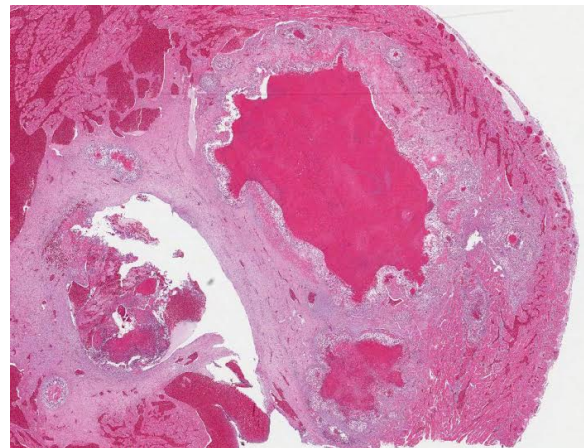
The three green iguanas consisted of two females and a male that were housed together. The green iguanas would fight amongst themselves with two of the iguanas developing cutaneous abscesses. The female iguana presented for necropsy became acutely ill and was dead on arrival at the submitting veterinary clinic.

Gross Pathology: The iguana was in good body condition with mild postmortem decomposition. There was a 1.8 x 1.8 cm subcutaneous abscess on the chin. The liver was enlarged and slightly pale. The spleen was enlarged. The urinary bladder contained large amounts of urates. The lungs contained a few multifocal pinpoint to 0.3 cm white foci. The pericardial sac contained moderate amounts of slightly cloudy light yellow fluid that contained free floating clots of fibrin. The pericardial sac was focally adhered to the epicardium of the left ventricle. The endocardium associated with the pericardial adhesion was thick and white. The lumen of the right ventricle was almost completely filled with a large, friable, yellow, fibrinopurulent exudate that was attached to the endocardium and multifocally extended into

the myocardium. The endocardium of the right ventricle was thickened and white.

Laboratory Results: *Neisseria iguanae* was cultured from the subcutaneous abscess and the exudate in the right ventricle of the heart.

Histopathologic Description: Heart: The lumen of the right ventricle contains a large thrombus consisting of fibrin, cellular debris, and rare macrophages and heterophils that is multifocally attached to the mural and valvular endocardium. The thrombus contains moderate numbers of small gram-negative cocci. The thrombus is surrounded by numerous epithelioid macrophages and multinucleated giant cells with lesser numbers of heterophils and lymphocytes. The endocardium of the right ventricle is markedly thickened by fibrous tissue that contains small numbers of granulomas characterized by a center of fibrin, necrotic debris and small cocci surrounded by epithelioid macrophages, multinucleated giant cells, heterophils, and lymphocytes. There are a few similar granulomas in the myocardium of the right ventricle. The epicardium is multifocally



Heart, green iguana. Transverse section of the heart with a large luminal thrombus in the right ventricle with associated endocardial and subendocardial fibrosis. (HE, 2X)

thickened by fibrous tissue, macrophages, heterophils, and lymphocytes.

Contributor's Morphologic Diagnosis:

1. Heart, right ventricle: Mural and valvular vegetative endocarditis with heterophilic and granulomatous inflammation and intralumenal small gram-negative cocci; etiology, *Neisseria iguana*
2. Heart, right ventricle: Myocardial granulomas

Contributor's Comment: *Neisseria* sp. are gram-negative bacteria that typically grow as diplococci in culture.^{5,7} The most well-known species of *Neisseria* are *N. gonorrhoeae* and *N. meningitidis*. *Neisseria*

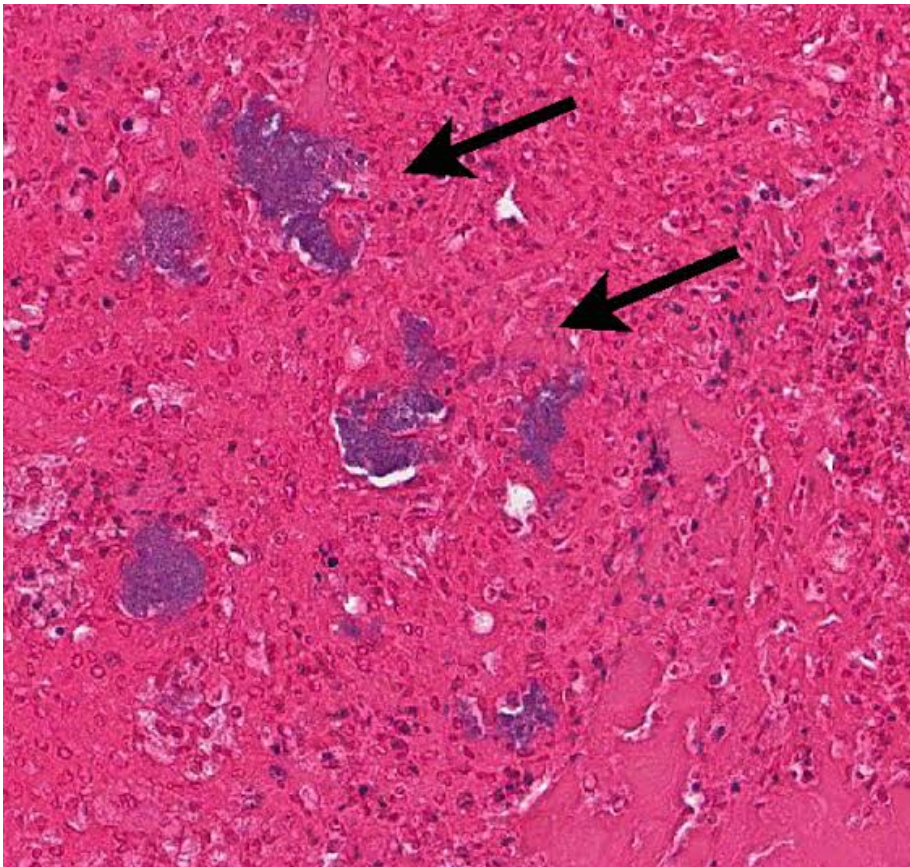
gonorrhoea is a venereal disease of humans. *Neisseria meningitidis* causes meningitis in people. However, most *Neisseria* species are commensal bacteria that are part of the normal oral and nasopharyngeal flora of mammals and the intestinal tract of birds.

In the 1980's, a syndrome of abscesses and septicemia in rhinoceros iguana and common iguana was identified at the National Zoological Park.⁷ The causative agent of the disease was classified as a new bacterium called *Neisseria iguanae*.¹ The bacterium was also isolated from the oral cavity from healthy animals in the collection. The cutaneous abscesses were believed to be the result of *N. iguanae* infection of the skin following bite wounds. One of the iguanas developed *N. iguanae* septicemia manifested as a liver abscess. In

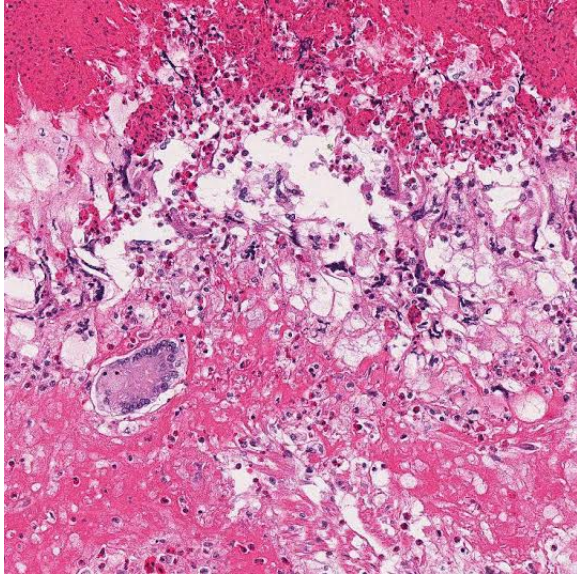
this case, the intraspecies aggression between the three common iguanas most likely resulted in the cutaneous abscess and mural and valvular endocarditis caused by *Neisseria iguanae* in this case.

The pathogenesis of bacterial endocarditis (also classified as infective endocarditis) is complex.^{4,8,9,10} The formation of infective endocarditis lesions involves the preparation of the endothelial layer for colonization, adherence of bacteria to the endothelial surface and survival of the bacteria with propagation of the thrombus.⁸ Intact

endothelium is believed to be resistant to bacterial



Heart, green iguana. Within the luminal thrombus, there are numerous colonies of short bacilli. (HE, 400X)



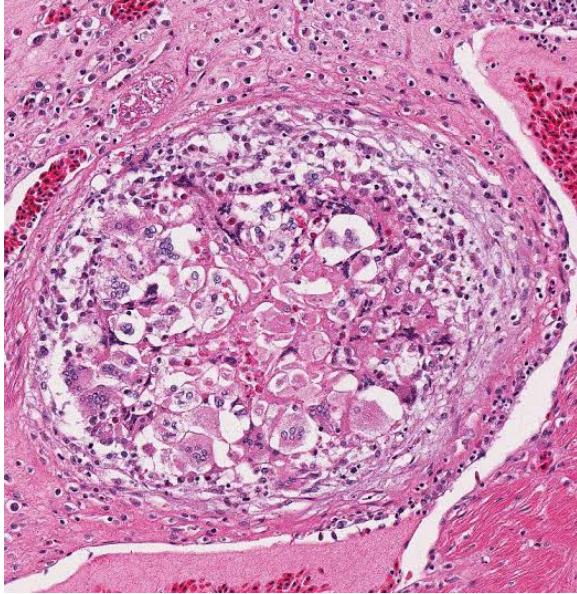
Heart, green iguana: The interface between the thrombus and adjacent endocardium contains numerous degenerating heterophils, epithelioid macrophages, foreign body type macrophages and abundant polymerized fibrin. (HE, 87X)

colonization.^{4,8,9,10} The resistant endothelial layer has to be disturbed in order for bacteria to adhere. The disturbance of the endothelial layer can be the result of mechanical forces or due to endothelial cell activation and damage as the result of local proinflammatory molecules such as IL-1.¹⁰ The endothelial cell damage causes activation of the coagulation cascade through the activity of tissue factor resulting in what is termed nonbacterial thrombotic endocarditis (NBTE). The resulting thrombus is colonized by bacteria that can adhere to damaged endothelial cells, platelets and adhesive extracellular matrix molecules such as fibrin and fibronectin. The bacteria adhere to the matrix molecules of the clot using a variety of surface molecules collectively called microbial surface component reacting with adhesive matrix molecules (MSCRAMMs).¹⁰ The proliferation of the thrombus of infective endocarditis involves the interaction of bacterial pathogens and the host immune and coagulation systems. Infective

endocarditis in the right side of the heart can result in emboli showering the lungs.⁹ Infective endocarditis in the left side of the heart can result in systemic embolism.

JPC Diagnosis: Heart: Endomyocarditis, granulomatous and heterophilic, focally extensive, marked with ventricular thrombosis and numerous bacterial colonies.

Conference Comment: *Neisseria* spp. are generally classified as obligate human pathogens, commensal organisms in humans and mammals and/or organisms that may cause opportunistic human infections. As mentioned above by the contributor *Neisseria* spp. bacteria are common oral flora of many mammals including *N. canis*, which has been isolated from the throats of cats and can be present in cat bite wound infections, and *N. weaver*, *N. zoodegmatidis*, *N. animaloris* which are normal oral flora of dogs and can be present in dog bite wound infections and in some cases can result in systemic infections in humans. Other species have been isolated from the oral cavity of guinea pigs, cows and rhesus monkeys. *Neisseria* spp. have also been isolated from the duodenum of healthy cats. Pathogenic *Neisseria* spp. utilize a number of adhesins, most commonly referenced with regard to human infections, and one of the best known is the type IV pilus which imparts twitching motility and facilitates uptake of foreign DNA. Most of the *Neisseria* spp. causing significant disease also possess a polysaccharide capsule, enabling avoidance of complement mediated killing and phagocytosis. Another feature which aids in resistance to antibody and complement mediated killing includes lipooligosaccharide (LOS), which is a membrane structure composed of lipid and oligosaccharide which is structurally different from lipopolysaccharide (LPS).³



Heart, green iguana. Within the fibrotic endocardium and adjacent myocardium, there are numerous well-formed granulomas. (HE, 58X).

Conference participants described this lesion as a severe granulomatous endocarditis with granuloma formation and fibrosis. The ventricle was described as being 100% occluded by a large, dense fibrin thrombus which contains numerous bacterial colonies as well as erythrocytes and necrotic debris, and is multifocally attached to the markedly thickened endocardium. Multiple granulomas are present in the superficial myocardium, near the epicardial–myocardial junction. Granulomas contain a dense core of eosinophilic debris (characteristic of reptile granulomas) surrounded by multiple macrophages with the presence of many multinucleate giant cells as well. The abundant white space surrounding the dense central core of debris is likely the result of retraction artifact. The granuloma's most peripheral layer is composed of dense fibrous connective tissue. The differential diagnosis discussed includes mycobacterial and fungal infections.

The moderator briefly discussed the structure of reptile hearts as there are

significant differences with mammalian hearts. Most reptiles have a single common ventricle and two atria. Three cavities or divisions are present in the ventricle, termed the *cavum pulmonale*, *cavum arteriosum* and *cavum venosum* and are partially separated by muscular septa. Blood flows from the right atrium, through the *cavum venosum* and into the *cavum pulmonale* and then enters the pulmonary circulation. Oxygenated blood flows from the pulmonary veins and reenters the heart through left atrium, flows into the *cavum arteriosum* during diastole, which channels blood into the *cavum venosum* which then flows into the aorta. Oxygenated and de-oxygenated blood is separated by pressure differences, outflow resistance and differential flow. Shunting and mixing of oxygenated and deoxygenated blood is variable depending on the reptile species and activity level. Nonetheless, blood flows are described as well separated within the ventricle (due to septa) and mixing of oxygen-poor and oxygen-rich blood is minimized.⁴

Contributing Institution:

New Mexico Department of Agriculture
Veterinary Diagnostic Services
www.nmda.nmsu.edu

References:

1. Barrett SJ, Schlater LK, Montali RJ, Sneath PHA. A new species of *Neisseria* from iguanid lizards, *Neisseria iguanae* sp. nov. *Lett Appl Microbiol.* 1994; 18:200-202.
2. Freedman LR. The pathogenesis of infective endocarditis. *J Antimicro Chemother.* 1987; 20(Suppl. A): 1-6.
3. Hung MC, Christodoulides M. The biology of *Neisseria* adhesins. *Biology.* 2013; 2(3):1054-1109.

4. Jensen B, van den Berg G, van den berg R, Oostra RJ et al. Development of the hearts of lizards and snakes and perspectives to cardiac evolution. *PLoS One*. 2013; 8(6):e63651.
5. Liu G, Tang CM, Exley RM. Non-pathogenic *Neisseria*: members of an abundant, multi-habitat, diverse genus. *Microbiology*. 2015; 161(7):1297-312.
6. Markey B, Leonard F, Archambault M, Cullinane A, Maguire D. Glucose non-fermenting, Gram-negative bacteria. In: *Clinical Veterinary Microbiology*. 2nd ed. London, UK: Mosby Elsevier; 2016: 375-379.
7. Plowman CA, Montali RJ, Phillips LG, Schlater LK, Lowenstine LG. Septicemia and chronic abscesses in iguanas (*Cyclura cornuta* and *Iguana iguana*) associated with *Neisseria* species. *J Zoo Anim Med*. 1987; 18(2-3): 86-93.
8. Sullman PM, Drake TA, Sande MA. Pathogenesis of endocarditis. *Am J Med*. 1985; 78 (Suppl. 6B): 110-115.
9. Thiene G, Basso C. Pathology and pathogenesis of infective endocarditis in native heart valves. *Cardiovasc Pathol*. 2006; 15: 256-263.
10. Widmer E, Que Y-A, Entenza JM, Moreillon P. New concepts in the pathophysiology of infective endocarditis. *Curr Infect Dis Rep*. 2006; 8(4): 271-279.

CASE IV: E6400/14 (JPC 4066312).

Signalment: Juvenile, male harbor seal (*Phoca vitulina*).

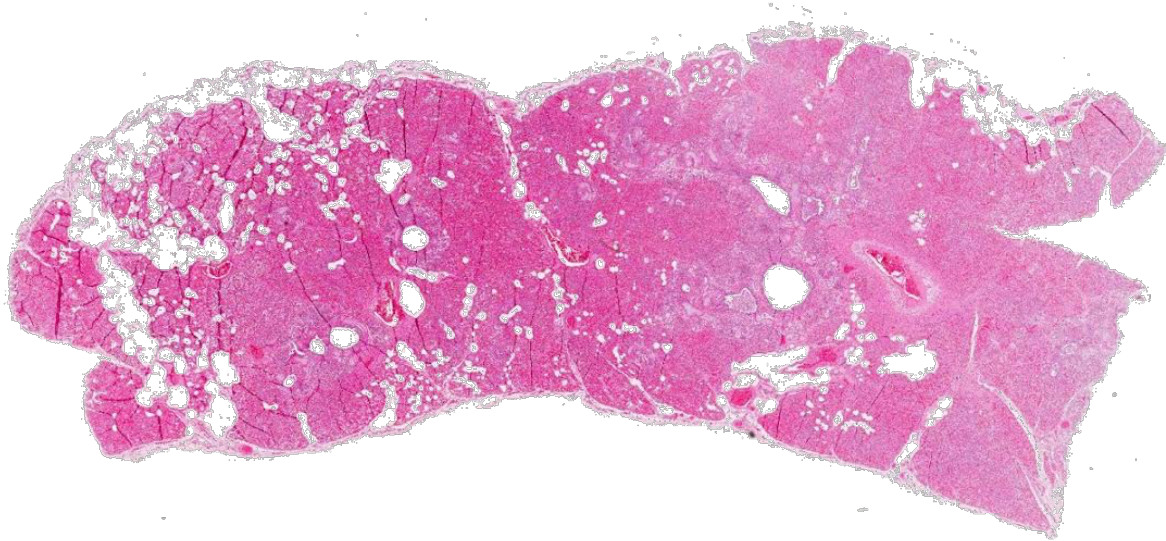
History: In 2014, an increased mortality occurred among harbor seals (*Phoca vitulina*) in northwestern European waters.

Hundreds of carcasses were washed up on the shores of Sweden, Denmark, and Germany.^{4, 10, 17} Along the Wadden sea coast of Lower Saxony, Germany, more than 320, and along the coast of Schleswig-Holstein, Germany, more than 2100 dead harbor seals were counted by the end of 2014.¹¹ The population size in the German part of the Wadden sea is approximately 12,000 animals.¹⁹ This necropsied seal was found moribund on the beach of the north Freisian coast close to the town of Büsum. The animal was euthanized humanely.

Gross Pathology: Necropsy revealed a poor nutritional status and severe generalized muscular atrophy. The poorly retracted lungs displayed severe congestion, diffuse consolidation, and multifocal firm nodular areas of gray-yellow discoloration with varying numbers of metazoan parasites. Additionally, there was severe, diffuse alveolar and interstitial emphysema. The pulmonary lymph nodes were markedly enlarged, and the tonsils were moderately swollen. There was no content in the stomach.

Laboratory Results: Lung tissue and tracheal swab were positive for influenza A virus using an influenza A-specific PCR for the matrix protein. Virus culture on embryonated chicken eggs and Madin-Darby canine kidney (MDCK) cells resulted in isolation of influenza A virus. Using specific primer sets for the hemagglutinin and neuraminidase genes with subsequent sequencing of the amplicons allowed classification into the subtype H10N7 of the influenza A virus.

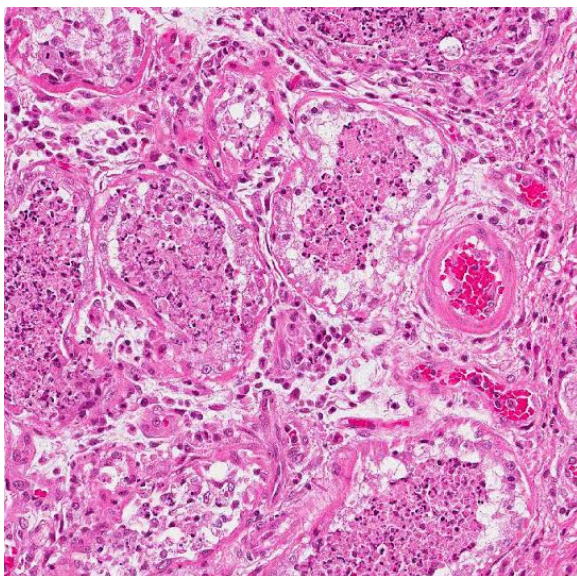
Immunolabeling of influenza A virus nucleoprotein revealed specific antigen staining in the respiratory tract.



Lung, harbor seal. At subgross inspection, there is diffuse consolidation and moderate segmental emphysema along the interlobular septa and pleura (HE, 4X).

Immunohistochemistry for morbillivirus nucleoprotein and reverse transcription PCR for morbillivirus were negative.

Microbiologically, moderate colony numbers of *Escherichia coli* and low numbers of *Acinetobacter pittii*, *Streptococcus phocae* and *Stenotrophomonas maltophilia* were isolated from the lung.



Lung, harbor seal. There is extensive necrosis within submucosal glands around large airways. (HE, 120X)

Parasitologically, the lung worms *Otostrongylus circumlitus* and *Parafilaroides gymnurus*, as well as the heartworm *Acanthocheilonema* (previously termed *Dipetalonema*) *spirocauda*, were identified in the lungs.

Histopathologic Description: The tissue from the lung displays a mild diffuse hyperplasia of bronchial epithelial cells with loss of cilia. There are mildly scattered karyopyknotic cells (necrosis) within the epithelial lining of the deep airways associated with few intraepithelial lymphocytes and occasional mitotic figures. Bronchial lumina are partially filled with cellular debris, neutrophils, foamy macrophages and desquamated epithelial cells. Bronchial glands show severe hydropic swelling, karyorrhexis and pyknosis of epithelial cells (degeneration and necrosis) with accumulation of cellular debris within the lumina. In the peribronchial and perivascular interstitium, there is a moderate to severe infiltration of lymphocytes, plasma cells and macrophages extending multifocally into the interalveolar interstitium. Most alveolar lumina are filled either with macrophages and desquamated

pneumocytes or neutrophils and macrophages. Occasionally, few to moderate numbers of erythrocytes are present in alveolar lumina. Furthermore, accumulation of eosinophilic homogenous or fine fibrillar material is present in alveoli (fibrin), sometimes in a membranous shape, along the alveolar wall. Inter-alveolar capillaries are engorged with red blood cells. Multifocally, venous vessels show partial occlusion by eosinophilic material attached to the vascular wall with infiltrating fibroblasts and endothelial lining on the surface. Multifocally, there are cross and longitudinal sections of larval nematode structures with a diameter of up to 50 μm and a length of about 200 μm surrounded by a cuticle. In the body cavity, a digestive tract is present. Restricted to few lobules, there are distended alveoli with ruptured inter-alveolar septae as well as distended interlobular septae.

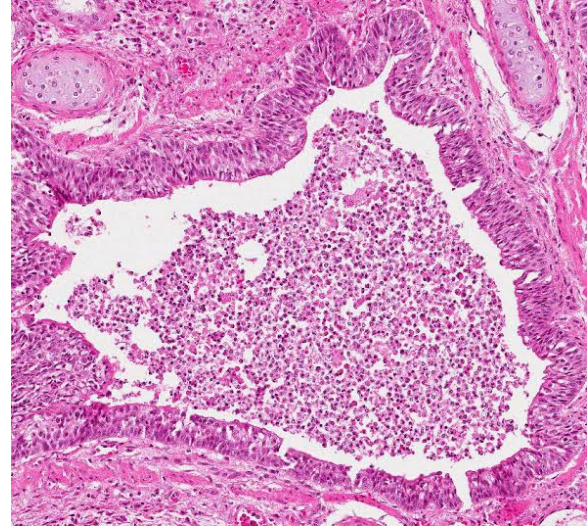
Contributor's Morphologic Diagnosis:

Lung: Pneumonia, broncho-interstitial, moderate, chronic, multifocal, lymphohistiocytic and plasmacytic with hyperplasia of bronchial epithelium; bronchitis, moderate, acute, multifocal, necrotizing with necrotizing adenitis of bronchial glands; pneumonia, suppurative, multifocal, moderate; multifocal subtotal vascular thrombosis; pulmonary endoparasitosis with larval stages of nematodes.

Contributor's Comment: The seal suffered from severe pneumonia caused by a concurrent infection with influenza A virus H10N7, pulmonary endoparasites, and several bacterial species. Besides the lung, morphologic changes associated with the influenza A virus infection were present only in the upper respiratory tract characterized by acute necrotizing rhinitis and tracheitis. Immunohistologically, influenza A virus nucleoprotein was

demonstrated intralesionally in the cytoplasm and nuclei of epithelial cells of bronchi and bronchial glands. Additionally, it was present in nasal and tracheal respiratory epithelium.

Avian influenza A viruses are known to cross species barriers and infect various mammalian species, including man and pinnipeds.^{2, 4, 9, 10, 13} Different influenza virus

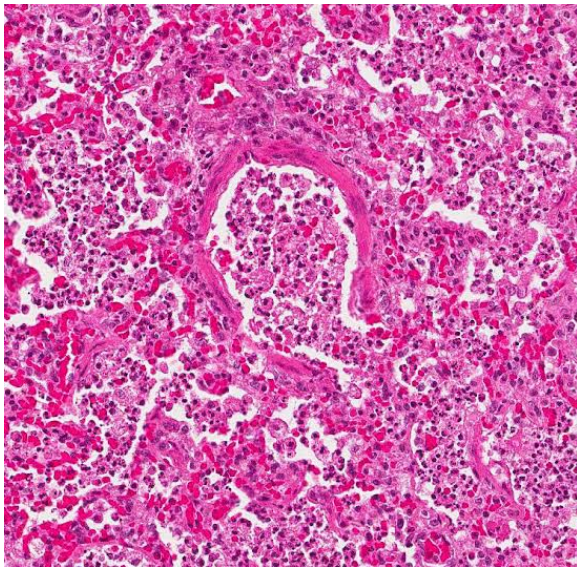


Lung, harbor seal. Large airways are filled with a cellular exudate composed of sloughed epithelium, histiocytes and neutrophils admixed with cellular debris (likely representing reflux from surrounding alveoli). There is mild hyperplasia of airway epithelium, which is infiltrated by low numbers of neutrophils. (HE, 87X).

A subtypes have previously been reported to cause fatal mass mortalities of harbor seals, including subtypes H5N1, H3N8 and H5N4.^{2, 4, 9, 13} However, subtype H10N7 has not been isolated from seals before. Infections with the subtype H10N7 have been reported in man in Egypt and Australia,^{3, 7} and various avian species including chicken,^{3, 14} ducks,¹⁴ mallards,¹⁷ and wild birds.¹⁶ According to the predicted amino acid sequence, this subtype is regarded as a low pathogenic avian influenza (LPAI) strain with a low zoonotic potential.^{11, 17} However, virus detection has been reported in spleen samples of affected seals from Denmark and a more virulent

potential of this H10N7 subtype cannot be excluded completely.¹¹

The influenza epidemic in 2014 in northern European waters started with an increased mortality among harbor seals in March in Sweden, and swapped in July to Denmark,¹¹ and reached Germany in October and The Netherlands in November. More than 2400 dead harbor seals were counted in German coastal waters.^{4, 12} The origin and mode of transmission of this avian influenza virus remains undetermined. Phylogenetic analysis revealed a close relationship to various influenza A viruses detected in wild birds. Specifically, the hemagglutinin and neuraminidase genes were genetically most

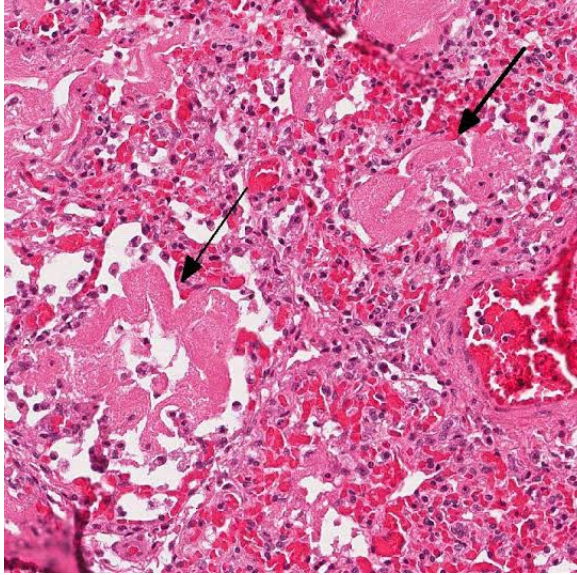


Lung, harbor seal. Alveolar septa are diffusely expanded by congestion, small amounts of edema and fibrin, circulating neutrophils, and patchy type 2 pneumocyte hyperplasia. (HE, 120X)

closely related to subtype H10N7 viruses recently found in migratory ducks in Georgia, Egypt, and the Netherlands.⁴ The seals may be infected oro-nasally with the virus through direct or indirect contact with wild birds or their droppings, because they

share the same shoreline habitats as waterfowl.^{11, 18} Hemagglutinin is the attachment protein of influenza viruses, binding to sialylated glycans on the host cell surface. Avian and swine influenza viruses bind to α 2,3 linked sialic acid. In contrast, human and several mammalian influenza A viruses bind to sialylated glycans with an α 2,6 linkage to galactose.^{1,2}

Virus-associated destruction of epithelial cells in the respiratory tract probably caused a predisposition for secondary bacterial infection resulting in suppurative pneumonia. Together with the parasitic burden in the lung, respiratory insufficiency is regarded as a main cause of death. Bacteriologically, *Escherichia coli*, *Acinetobacter pittii*, *Streptococcus phocae* and *Stenotrophomonas maltophilia* were isolated in the present case. *Acinetobacter pittii* and *Streptococcus phocae* are regarded as opportunistic pathogens. Similarly, *Streptococcus phocae* has been isolated from seals affected with phocine distemper, but has also been associated with starvation and abortion in Cape fur seals (*Arctocephalus pusillus pusillus*).⁷ Interestingly, bacteriological culture of lung samples from other seal carcasses with influenza A H10N7 infection resulted in isolation of bacteria, e.g. *Bordetella bronchiseptica* and *Streptococcus equi* ssp. *zooepidemicus* that were not isolated from lung samples of seal carcasses investigated during the annual health monitoring program. However, these bacterial species were exclusively isolated during the seal die-offs in 2002 and 2014 as a secondary pathogen (Siebert, pers. communication).



Lung, harbor seal. Multifocally, damaged alveolar septa have flooded the lumina with fibrin which has organized into thick hyaline membranes (arrows). (HE, 160X)

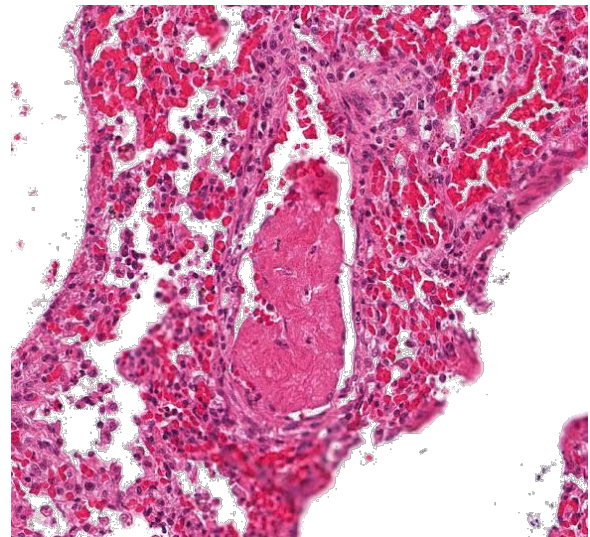
Commonly reported nematodes in the lung of harbor seals are *Parafilaroides gymnuris*, *Otostrongylus circumlitus*, and the heartworm *Acanthocheilonema* (previously termed *Dipetalonema*) *spirocauda*.¹⁵ Nematodic infections of the respiratory tract of harbor seals represent a common finding, particularly in juvenile individuals.¹⁵ The epithelial hyperplasia of deep airways, as well as the vascular thrombosis, may be related to the parasitic infestation in this case.

As differential diagnosis for infectious seal mass die-offs, phocine distemper virus (PDV) infection has to be considered. Phocine distemper was excluded in this case by reverse transcription PCR (RT-PCR) and immunohistochemistry. The total Wadden Sea seal population has reached a so far unprecedented population size of more than 39,000 animals. A serological survey revealed a lack of antibodies against phocine distemper indicating a high susceptibility for phocine distemper.⁶ The current prevalence of influenza virus antibodies in the German harbor seal population is unknown.

JPC Diagnosis: 1. Lung: Pneumonia, bronchointerstitial, necrotizing and fibrinous, diffuse, severe, with submucosal gland necrosis, alveolar and interlobular emphysema, and organizing fibrin thrombi.

2. Lung: Larval nematodes, few (variable across sections).

Conference Comment: Influenza A virus affects many species and waterfowl are considered the natural reservoir host for many subtypes. Subtypes which result in infection of mammals often occur through transmission from waterfowl. These viruses replicate in the intestinal tract of birds and fecal-oral transmission is the primary route of infection. In a rash of harbor seal deaths in Denmark reported in conjunction with the outbreak from which this case originated, (discussed above) animals were also affected with a necrotizing bronchopneumonia with the presence of bacteria in alveoli. Influenza virus A (H10N7) was also isolated in those cases; additionally, bacterial isolates included *Pseudomonas aeruginosa* with variable growth of *Streptococcus equi* subsp. *zooepidemicus*. The pulmonary lesions were attributed to



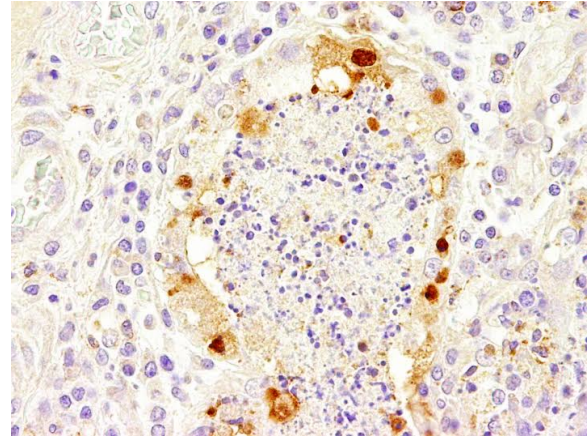
Lung, harbor seal. Occasionally vessels contain fibrin thrombi. (HE, 120X)

primary infection with influenza A, complicated by secondary bacterial infection, as seen in this case.¹¹

During the outbreak described above, which primarily resulted in seal deaths in Sweden, Denmark and Germany, only low numbers of seals were found dead in the Netherlands; the precise reason for variable mortality is unclear. A study measuring antibody levels of H10N7 (which in some references is termed seal influenza A) in captured or rehabilitated seals in the Netherlands found detectable antibodies in 41% of pups, 10% of weaners and 58% of adults or subadults, indicating infection with this virus may be widespread. Antibody titers were also found in adult grey seals. In subadult harbor and grey seals sampled prior to the 2014-2015 outbreak, only a small number had antibody titers against the virus, which may indicate absence of widespread herd immunity at the start of the outbreak.⁵

The conference histologic description was similar to the contributor's histologic description above. There was extensive discussion regarding the vascular changes in the section. There are distinctive fibrin thrombi partially occluding vessel lumina, but there are also vessels which appear to have near complete occlusion by fibroblasts and/or macrophages that are surrounded by concentric layers of fibrous tissue. Participants postulated the vascular changes may represent variable chronicity of the lesions, with the older, mature thrombi demonstrating partial to complete recanalization. Multifocally, hyaline membranes line the alveolar surface and are more prominent in the less atelectatic areas of the lung. Alveolar and interlobular septal emphysema were also described. Multifocally there is hyperplasia of bronchial and bronchiolar epithelium, with loss of cilia in many areas. The contributor

provides a detailed description and excellent history regarding the events surrounding this case.



Lung, harbor seal. Labeling of influenza A nucleoprotein in submucosal gland epithelium. (anti-influenza A with HE counterstain, 400X)

Contributing Institution:

Department of Pathology, University of Veterinary Medicine,
Hannover, Buenteweg 17, 30559 Hannover,
Germany.

<http://www.tiho-hannover.de/kliniken-institute/institute/institut-fuer-pathologie/>

References:

1. Air GM. Influenza virus-glycan interactions. *Curr Opin Virol.* 2014; 7:128–133.
2. Anthony SJ, St Leger JA, Pugliares K, et al. Emergence of fatal avian influenza in New England harbor seals. *MBio.* 2012; 3:e00166–12.
3. Arzey GG, Kirkland PD, Arzey KE, et al. Influenza Virus A (H10N7) in Chickens and Poultry Abattoir Workers, Australia. *Emerg Infect Dis.* 2012; 18:814–816.
4. Bodewes R, Bestebroer TM, van der Vries E, et al. Avian Influenza A (H10N7) Virus–Associated Mass Deaths among

- Harbor Seals. *Emerg Infect Dis.* 2015; 21:720–722.
5. Bodewes R, Garcia AR, Brasseur SM, Sancehz GJ, et al. Seroprevalence of antibodies against seal influenza A (H10N7) virus in harbor seals and gray seals from the Netherlands. *PLoS One.* 2015; 10(12):e0144899.
 6. Bodewes R, Morick D, van de Bildt MW, Osinga N, Rubio García A, Sánchez Contreras GJ, Smits SL, Reperant LA, Kuiken T, Osterhaus AD. Prevalence of phocine distemper virus specific antibodies: bracing for the next seal epizootic in north-western Europe. *Emerg Microbes Infect.* 2013;2(1):e3.
 7. de la Barrera CA, Reyes-Terán G. Influenza: Forecast for a Pandemic. *Arch Med Res.* 2005; 36:628–636.
 8. Henton MM, Zapke O, Basson PA. *Streptococcus phocae* infections associated with starvation in Cape fur seals. *J S Afr Vet Assoc.* 1999; 70:98–99.
 9. Hinshaw VS, Bean WJ, Webster RG, et al. Are seals frequently infected with avian influenza viruses? *J Virol.* 1984; 51:863–865.
 10. Jensen T, van de Bildt M, Dietz HH, et al. Another phocine distemper outbreak in Europe. *Science.* 2002; 297:209.
 11. Krog JS, Hansen MS, Holm E, et al. Influenza A(H10N7) virus in dead harbor seals, Denmark. *Emerg Infect Dis.* 2015; 21:684–687.
 12. Pund R, Huesmann J, Neuhaus H, et al. Auswirkungen des Influenza A-Infektionsgeschehens 2014/2015 auf den Seehundbestand in der Nordsee. *Natur- und Umweltschutz.* 2015; 14:13–17.
 13. Reperant LA, Rimmelzwaan GF, Kuiken T. Avian influenza viruses in mammals. *Rev Sci Tech.* 2009; 28:137–159.
 14. Serena Beato M, Terregino C, Cattoli G, et al. Isolation and characterization of an H10N7 avian influenza virus from poultry carcasses smuggled from China into Italy. *Avian Pathol.* 2006; 35:400–403.
 15. Siebert U, Wohlsein P, Lehnert K, et al. Pathological Findings in Harbour Seals (*Phoca vitulina*): 1996-2005. *J. Comp. Path.* 2007; 137:47–58.
 16. Siembieda JL, Johnson CK, Cardona C, et al. Influenza A viruses in wild birds of the Pacific flyway, 2005-2008. *Vector Borne Zoonotic Dis.* 2010; 10:793–800.
 17. Vittecoq M, Grandhomme V, Champagnon J, et al. High influenza A virus infection rates in Mallards bred for hunting in the Camargue, South of France. *PLoS One.* 2012; 7(8):e43974.
 18. Zohari S, Neimanis A, Härkönen T, et al. Avian influenza A (H10N7) virus involvement in mass mortality of harbour seals (*Phoca vitulina*) in Sweden, March through October 2014. *Euro Surveill.* 2014; 19(46).
 19. (http://www.waddenseasecretariat.org/sites/default/files/downloads/TMAP_downloads/Seals/harbour_seal_report_2014_b.pdf).

Joint Pathology Center
Veterinary Pathology Services



WEDNESDAY SLIDE CONFERENCE 2015-2016

Conference 16

3 February 2016

Micheal Eckhaus, VMD, DACVP
National Institutes of Health
Bethesda, MD

CASE I: 15-0021 (JPC 4065722).

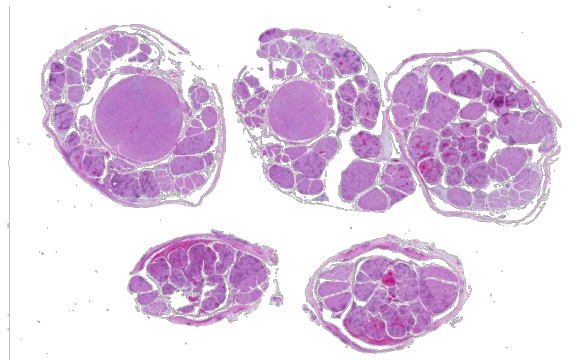
Signalment: 8-year-old male rhesus monkey (*Macaca mulatta*)

History: This SIV-infected monkey had a several day history of reduced cage movement and lower body stiffness. The animal was humanely sacrificed and submitted for necropsy evaluation.

Gross Pathology: The bladder was markedly distended at necropsy. Small areas of superficial congestion were noted from the meningeal surface in the distal lumbar cord and cauda equina region. On transection of fixed cord for trimming, more extensive punctate and focally extensive areas of hemorrhage were seen within the spinal nerves, especially in the more inferior cauda equina areas.

Laboratory Results: None

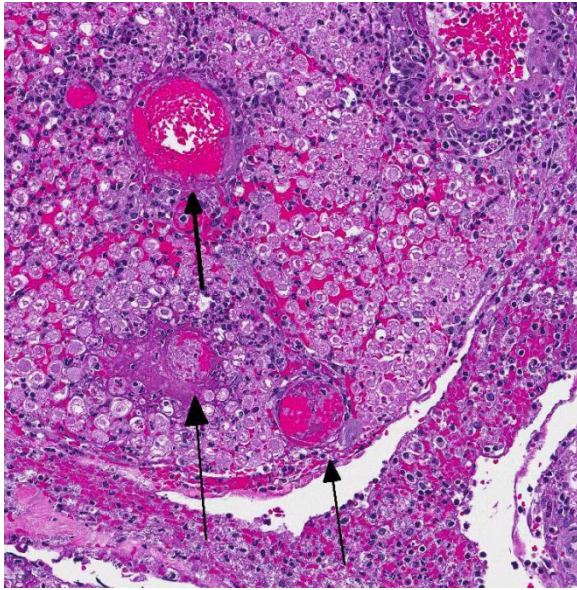
Histopathologic Description: Sections distributed and corresponding lesions vary somewhat as to the cord level present, with some slides containing only cauda equina



Cauda equina, rhesus macaque: Multiple cross sections at various levels of the cauda equine demonstrate hemorrhage and a cellular infiltrate within the spinal nerve roots and meningeal space. (HE, 5X)

tissue without distal lumbosacral spinal cord body. A patchy to focally extensive acute, necrotizing and inflammatory process is noted. Abundant neutrophilic inflammation is present within spinal nerves, admixed with macrophages and globular eosinophilic debris. Within some nerve roots (and some sections of cord), occasional swollen and/or fragmented axons are present. Numerous vessels are infiltrated by dense populations of neutrophils and fibrinoid necrosis and debris are frequently seen within and surrounding vascular walls. Associated with this angiitis are infrequent thrombi.

Scattered throughout the section are large, eosinophilic to amphophilic intranuclear inclusion bodies within enlarged (cytomegalic) Schwann cells and infrequently in endothelium. Also noted in most slides is patchy, necrotizing and fibrinous meningitis. Some sections contain mixed macrophage and granulocytic inflammatory debris within the distal aspect of the central canal.



Cauda equina, rhesus macaque: Within affected spinal roots, inflamed vessels are partially to totally thrombosed, and with hemorrhage and fibrin deposition within adjacent tissue. Large numbers of neutrophils, fibrin and hemorrhage are present within the spinal nerve and within the meningeal space (HE, 15X)

Contributor's Morphologic Diagnosis:

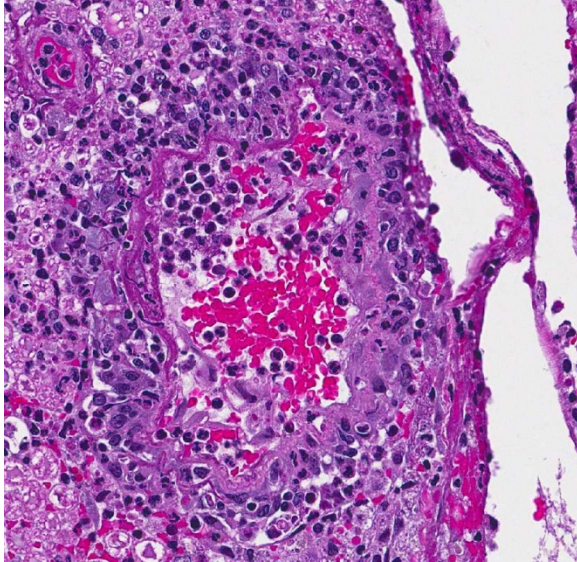
- 1) Radiculitis, necrotizing and fibrinous, acute, patchy to focally extensive, marked to severe with cytomegaly and intranuclear inclusion bodies, eosinophilic and amphophilic, (Cowdry type A)
- 2) Angiitis, necrotizing, neutrophil-rich, acute, multifocal with areas of fibrinoid change within and surrounding vessel walls and foci of thrombosis
- 3) Meningitis, necrotizing and fibrinous, patchy, mild-moderate (most sections)

- 4) Mixed inflammatory infiltrates, mild-moderate, central canal (some sections)
- 5) Nerve fiber degeneration, multifocal, mild (some sections)

Contributor's Comment: Immunohistochemical evaluation of sections was strongly positive for rhesus monkey cytomegalovirus (RhCMV) antigen. Rhesus monkey populations are infected with the beta herpesvirus RhCMV at an incidence approaching 100%, with seroconversion generally occurring within the first year of life.⁵ Viral shedding in urine and saliva continues throughout life.² Once infected, normal host immune response is generally able to control the virus, although not eradicate it.⁵ Immunosuppression such as that experienced with SIV infection leads to latent CMV reactivation. The developing rhesus macaque brain is also susceptible to RhCMV infection in the second trimester and intrauterine exposure result in neuropathic outcomes similar to those observed in human congenital CMV infection.⁷

Virus presence has been documented within the gastrointestinal tract, spleen, lung, central nervous system, liver, lymph nodes, testicles, spleen, intestine, nerves and arteries.⁴ It is the most frequently identified viral opportunistic pathogen in rhesus macaques.³ Either multifocal or diffuse interstitial pneumonitis is the most commonly detected lesion seen.² Unfortunately in this animal, other tissues were not submitted to determine the extent of organs involved. Infection may also lead to the formation of discrete proliferative masses in the gastrointestinal tract.³

From a comparative perspective, human CMV accounts for most HIV-related radiculitis, which in AIDS patients, tends to involve lumbosacral nerve roots, producing



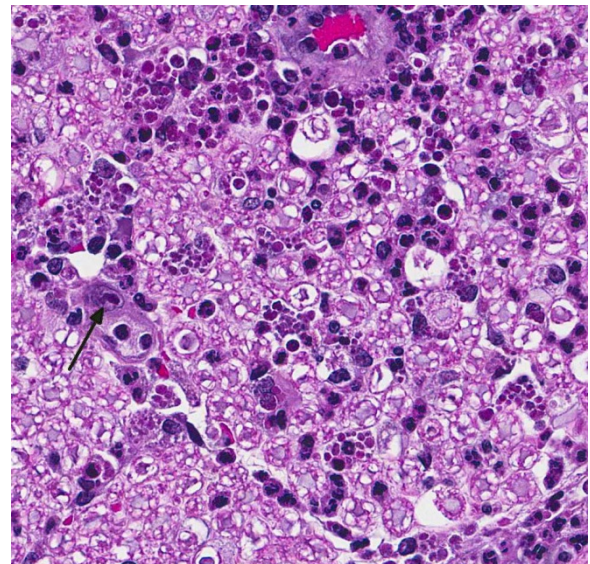
Cauda equina, rhesus macaque: The walls of inflamed vessels contain degenerate neutrophils, extruded fibrin, and moderate amounts of cellular debris, and are surrounded by low to moderate numbers of neutrophils and lymphocytes. (HE, 260X)

a rapidly progressive cauda equine syndrome with severe lower back pain.⁸ In humans, highly active antiretroviral therapy (HAART), first introduced in the mid 1990's has dramatically reduced the risk of opportunistic infections and improved the prognosis of patients with HIV infection. CMV disease has become a rare complication in AIDS patients.⁶

JPC Diagnosis: Lumbar spinal roots: Radiculitis, necrotizing and neutrophilic, multifocal to coalescing, with necrotizing vasculitis, fibrinohemorrhagic meningitis, and karyomegalic intranuclear viral inclusions.

Conference Comment: The most common opportunistic viral infection in SIV-infected rhesus macaques is rhesus cytomegalovirus (RhCMV). While it has been well documented to cause lesions in many organs including the leptomeninges and spinal nerve roots, as seen in this case, its role in peripheral neuropathies is less well-researched. A recent study of RhCMV

associated facial neuritis noted a mixed inflammatory population composed of neutrophils and macrophages, with macrophages containing intranuclear inclusion bodies.¹ Lesions were present in nerves of the tongue, lacrimal gland and other facial tissues. Axon loss was proportional to the degree of inflammation, the neuritis associated macrophages were infected with RhCMV and there was absence of evidence to support infection of Schwann cells.¹ Lesions were consistent with demyelination and loss of axons secondary to inflammation, supporting the study's assertion that nerve damage is likely related to inflammation rather than direct viral infection of Schwann cells in RhCMV peripheral neuropathies.¹ Lesions in those cases varied in severity from effacement of nerve architecture to milder lesions localized to the periphery. As mentioned above, human CMV (HCMV) is also associated with radiculoneuritis and lesions include peripheral neuritis, with the facial nerves



Cauda equina, rhesus macaque: Within the adjacent spinal nerve, myelin sheaths are occasionally dilated, often contain granular eosinophilic debris. The endoneurium is infiltrated by moderate numbers of viable neutrophils. Rare Schwann cells are karyomegalic, as a result of a large intranuclear viral inclusion (arrow). (HE, 400X)

being most commonly affected; however, in HCMV associated neuritis there is a demonstrated viral predilection for Schwann cells.¹

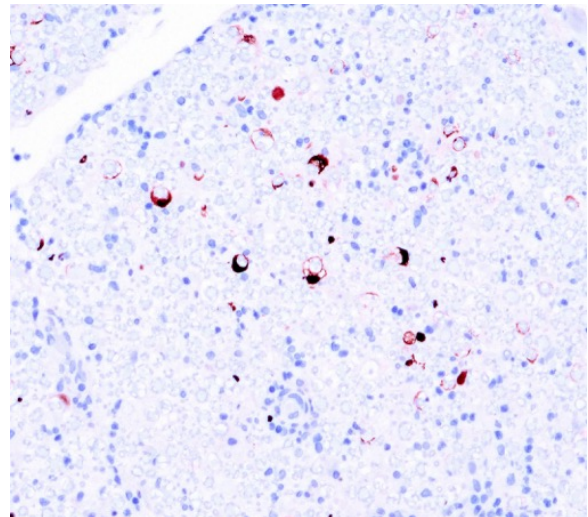
Conference participants noted that the spinal cord was largely unaffected and they described the inflammatory infiltrate and hemorrhage as extending from affected spinal nerves into adjacent perineural connective tissue and meninges. Additionally, the inflammatory infiltrate was identified as primarily neutrophilic. This is attributed to RhCMV induction of a CXC chemokine, which results in neutrophil chemoattraction.¹ Other microscopic features noted by participants included dilated myelin sheaths with numerous spheroids, variable numbers of gitter cells, and low numbers of cyto- and karyomegalic cells (most likely Schwann cells in this case), with large, darkly eosinophilic, intranuclear viral inclusion bodies. Other commonly affected tissues include the lung, gastrointestinal tract and the testes.

Contributing Institution:

Division of Laboratory Animal Resources,
University of Pittsburgh
<http://www.dlar.pitt.edu/>

References:

1. Assaf BT, Knight HL, Miller AD. Rhesus cytomegalovirus (*Macacine herpesvirus-3*) associated facial neuritis in a simian immunodeficiency virus infected rhesus macaques. *Vet Pathol.* 2015; 52(1):217-223.
2. Baskin G. Disseminated cytomegalovirus infection in immunodeficient rhesus monkeys. *Am J Pathol.* 1987; 129(2):345-352.



Cauda equina, rhesus macaque: Multifocally, Schwann cells are strongly immunopositive for RhCMV antigen. (antiRhCMV, 100X) (Image courtesy of: Division of Laboratory Animal Resources, University of Pittsburgh, Pittsburgh, Pa 15261 <http://www.dlar.pitt.edu/>)

3. Hendricks Hutto E, Anderson D, Mansfield K. Cytomegalovirus-associated discrete gastrointestinal masses in macaques infected with simian immunodeficiency virus. *Vet Pathol.* 2004; 41:691-695.
4. Kuhn E, Stolte N, Matz-Rensing K, Stahl-Hennig C. et al. Immunohistochemical studies of productive rhesus cyto-megalovirus infection in rhesus monkeys (*Macaca mulatta*) infected with simian immunodeficiency virus. *Vet Pathol.* 1999; 36:51-56.
5. Powers C, Frick K. Rhesus CMV: An emerging animal model for human CMV. *Med Microbiol Immunol.* 2008; 197:109-115.
6. Salzberger B, Hartmann P, Hanyes F, Uyanik B et al. Incidence and prognosis of CMV disease in HIV-infected patients before and after introduction of combination antiretroviral therapy. *Infection.* 2005; 33(5/6):345-349.
7. Tarantal A, Salmat M, Britt W, Lucaw P, et al. Neuropathogenesis induced by rhesus cytomegalovirus in fetal rhesus monkeys

(*Macca mulatta*). *J Infect Dis.* 1998; 177:446-450.

8. Tarulli A, Raynor E. Lumbosacral radiculopathy. *Neurol Clin.* 2007;25:387-405.

CASE II: MK14-5429 (JPC 4070246).

Signalment: 16 year old, intact female, Patas monkey (*Erythrocebus patas*)

History: End of Study. Focal area of consolidation in right caudal lung lobe noted. Submitted for histopathology.

Gross Pathology: Presented is a formalin-fixed pyramidal-shaped piece of lung with a partial cut through the middle. The 3 sides measure 2.5 cm and the base measures 1.5 cm. The tissue is firm and light gray except for one edge that is approximately 2mm x 5 mm that is purplish and somewhat aerated.

Laboratory Results: NA

Histopathologic Description: (slide variation of severity)

Multifocal to coalescing areas of varying sized infiltrates of macrophages and multinucleated giant cells engulfing and/or surrounding varying sized lipid droplets are observed primarily in alveolar airways. Many of these areas are also partially to completely surrounded by fibrous connective tissue with a mild to moderate lymphocytic and plasmacytic infiltrate. Extensive type II pneumocyte hyperplasia

and multiple moderately-sized lymphoid aggregates/nodules are observed. On some slides is an abundance of necrotic mineralizing debris admixed with small amounts of fibrin within a large bronchiole that has denuded mucosal epithelium and focal areas of mild to moderate smooth muscle hypertrophy. Some slides have multifocal areas of pleural fibrosis which extends into the pulmonary parenchyma.

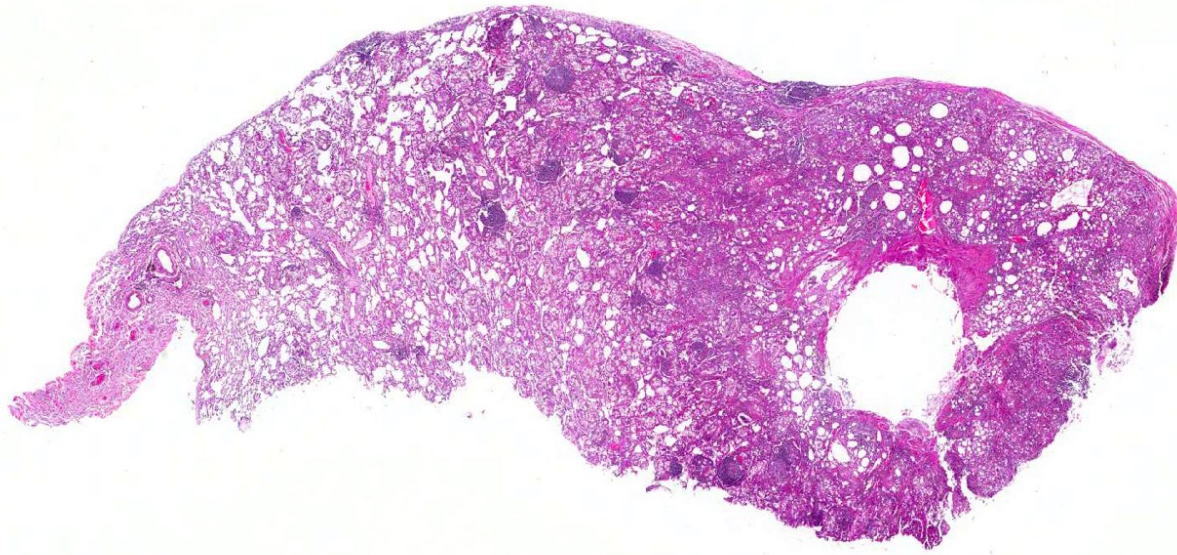
Contributor's Morphologic Diagnosis:

Lung: Pneumonia, granulomatous, multifocal to coalescing to diffuse, severe, chronic with abundant lipid accumulation and fibrosis

Contributor's Comment: The animal had what is known in the human literature as exogenous lipid pneumonia. This is a condition where a lipid or fat-like substance is inhaled or aspirated into the lungs eliciting a severe inflammatory response.

There are two types of lipid pneumonia: endogenous and exogenous. Endogenous lipid pneumonia has been described in rats²⁰ dog,^{5, 19} genet,¹⁸ cats,¹¹ mongoose,¹⁰ raccoons,⁹ llama,⁸ African grey parrot,⁶ opossums,³ Siberian tigers.¹ Exogenous lipid pneumonia has been induced experimentally in mice and rats,²⁰ and found in two cases of horses^{2, 15} and a cow.²¹

Lipid pneumonia is an uncommon form of pneumonia.⁷ It has been reported under different names, such as paraffinoma,²⁴ cholesterol pneumonia,²² oil granulomas of the lung,¹⁷ and lipid granulomatosis.



Lung, patas monkey: Subgross magnification reveals patchy consolidation and numerous lymphoid aggregates throughout the section. (HE, 5X)

Exogenous lipid pneumonia is more commonly reported in human literature⁷ whereas it is the least reported in the veterinary literature.¹¹ It is caused by the inhalation or aspiration of lipid substances: animal fats, vegetable oils or mineral oil. Animal fat/oils elicit a very active inflammatory response. Mineral oils are fairly inert because they have no fatty acids and are rapidly emulsified and consumed by pulmonary macrophages. Vegetable oils are emulsified and not hydrolyzed by the lung lipase.¹³ Aspiration may be due to age, psychiatric disorders, loss of consciousness,¹⁴ abnormality of deglutination (pharyngeal or esophageal) as well as gastro-esophageal reflux^{11,22} (oil floats on top of stomach fluids, thus oils may preferentially enter the airways).¹⁴ Most occur when oils are used for medicinal purposes (constipation, oral health, nasal drops, etc).^{12, 16, 17} A disproportionate population of fire breathers develop this type of pneumonia because of the liquid paraffin they use.²⁴

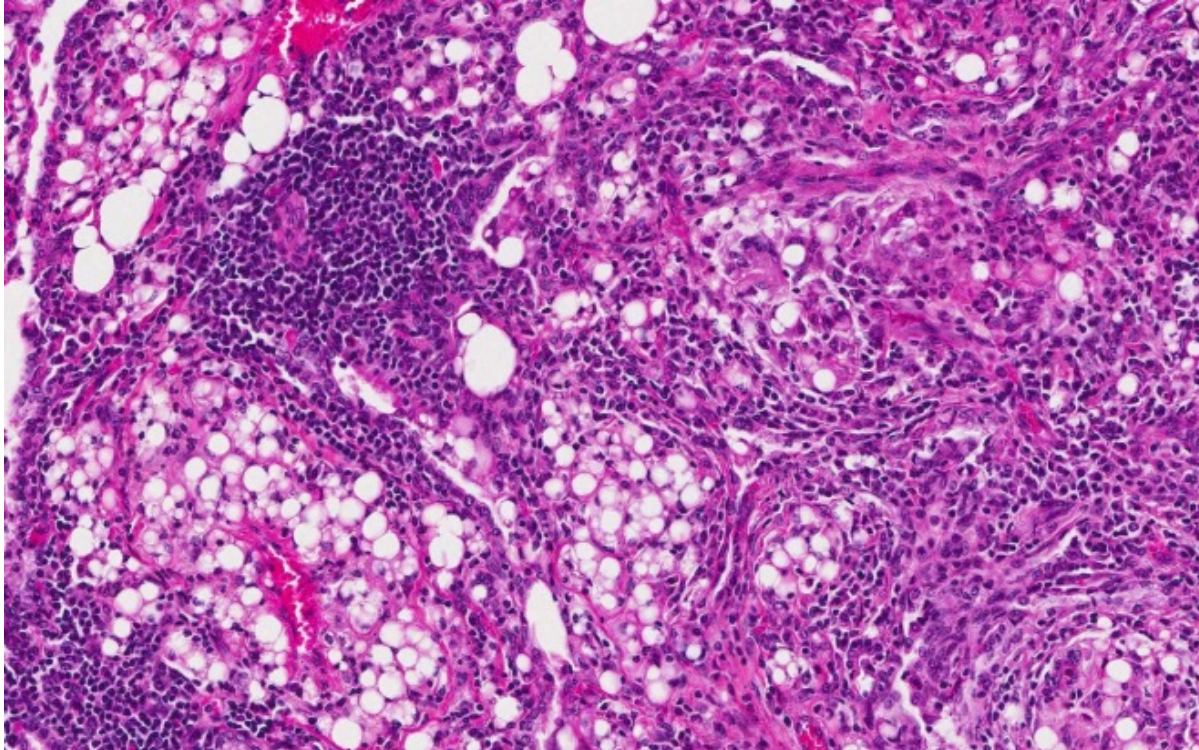
Many lipid substances are non-irritating, can enter the tracheobronchial tree without stimulating a gag or cough reflex, and impair the mucociliary transport system. The pathophysiology is that of a chronic foreign body reaction. Once lipids are in alveoli, they are emulsified and taken up by macrophages. These cells cannot metabolize the fatty substances, so cells die, oil is released and re-phagocytized. Over time, giant cell formation and fibrosis ensue. Diagnosis is made by the presence of large fat globules surrounded by macrophages and multinucleated giant cells as well as lipid-laden macrophages.²³

Endogenous lipid pneumonia, also called cholesterol or golden (accumulation of lipid in alveoli causing a yellow discoloration to the lungs) pneumonia, usually develop when lipids that normally reside in the lung tissue, most commonly cholesterol and its esters, escape from destroyed alveolar cell

membranes (surfactant) distal to an obstructing airway lesion or damaged by an inflammatory process. It can also occur with fat emboli to the lung, pulmonary alveolar proteinosis, and lipid storage disorders (Niemann-Pick disease).⁷ The pathogenesis is complex and may be related to retained epithelial secretions, cell breakdown, leakage from vessels, prolonged hypoxia, oxygen and carbon dioxide tension. It may be the result of transbronchial dissemination of breakdown products of cancer cells and secretions including mucin. Another though involves anoxic tissue injury stimulating phospholipases and mono-oxygenases, which in turn cause modification of low-density lipoprotein cholesterol. This cholesterol enhances lipid uptake by alveolar macrophages. Definitive diagnosis is demonstrating lipid-laden macrophages and cholesterol crystals.⁷

JPC Diagnosis: Lung: Pneumonia, interstitial, granulomatous, multifocal to coalescing, chronic, severe, with abundant intracytoplasmic lipid.

Conference Comment: Endogenous lipid pneumonia is described as an alveolar filling disorder, encompassing several conditions in which abnormal material accumulates within alveoli. This pulmonary lesion can be an incidental finding or responsible for clinical disease. Other alveolar filling disorders include alveolar proteinosis, alveolar histiocytosis, alveolar phospholipidosis, pulmonary hyalinosis and alveolar microlithiasis. Mild forms of alveolar histiocytosis are commonly seen in the dog and alveolar phospholipidosis occurs in rodents secondary to administration of certain types of drugs as well as in conditions where there is a mutation of surfactant protein D. Conditions which result in the accumulation of lipid-laden



Lung, patas monkey: At higher magnification, alveoli are filled with numerous macrophages and few multinucleated macrophages whose cytoplasm is markedly expanded by numerous, variably-sized lipid vacuoles. Affected alveoli are separated by large perivascular aggregates of lymphocytes. (HE, 200X)

foamy macrophages must be distinguished from other conditions which result in accumulation of macrophages with “foamy” appearing cytoplasm such as pneumocystis and histoplasmosis. In alveolar proteinosis, acellular eosinophilic or amphophilic material composed of surfactant proteins and phospholipids accumulates, but inflammation and fibrosis are not prominent features. Pulmonary hyalinoses, an incidental finding the lungs of aged dogs, is characterized by the accumulation of amorphous, laminated or hyaline material in macrophages and giant cells. In pulmonary alveolar microlithiasis, the accumulated material is extracellular and consists of laminated concretions in alveoli and can result in clinical disease depending on distribution of deposits.⁵

Conference participants described the lung as approximately 75% affected by a predominantly granulomatous infiltrate focused on variably sized lipid vacuoles within alveolar lumina. Other prominent features include extensive type II pneumocyte hyperplasia, fibrosis, and multifocal hyaline membrane formation. Conference participants also noted the multifocal nodular lymphoid aggregates which led to a brief discussion on their histogenesis (i.e. a chronic inflammatory response versus hyperplasia of preexisting bronchus/bronchiolar associated lymphoid tissue (BALT). The lipid expands the interstitium and prominently fills alveoli depending on location; in some areas, the precise location of the lipid, is difficult to determine due to fibrosis and inflammation. Additional histochemical stains used to highlight lipid include Oil Red O and Sudan black.

Contributing Institution:

Division of Veterinary Resources, National Institutes of Health

<http://www.ors.od.nih.gov/sr/dvr/Pages/default.aspx>

References:

1. Bolo E, Scaglione FE, Chiappino L, et al. Endogenous lipid (cholesterol) pneumonia in three captive Siberian tigers (*Panthera tigris altaica*). *J Vet Diag Invest.* 2012; 24:618-620.
2. Bos M, deBosschere H, Deprez P, et al. Chemical identification of the (causative) lipids in a case of exogenous lipoid pneumonia in a horse. *Eq Vet J.* 2002; 34:744-747.
3. Brown CC. Endogenous lipid pneumonia in opossums from Louisiana. *J Wildl Dis.* 1998; 24:214-219.
4. Carminato A, Vascellari M, Zotti A, et al. Imaging of exogenous lipoid pneumonia simulating lung malignancy in a dog. *Can Vet J.* 2011; 52:310-312.
5. Caswell JL, Williams KJ. Respiratory System. In: Maxie MG, ed. *Jubb, Kennedy, and Palmer's Pathology of Domestic Animals.* 6th ed. Vol 2. St. Louis, MO: Elsevier; 2015:517.
6. Costa T, Grifols J, Perpignan D. Endogenous lipid pneumonia in an African Grey Parrot (*Psittacus erithacus erithacus*). *J Comp Pathol.* 2013; 149:381-383.
7. Hadda V, Khilnani GC. Lipoid pneumonia: an overview. *Expert Rev resp Med.* 2010; 4:799-807.
8. Hamir AN, Andreasen CB, Pearson EG. Endogenous lipid pneumonia (alveolar histiocytosis) and hydrocephalus in an adult llama (*Llama glama*). *Vet Rec.* 1997; 141:474-475.
9. Hamir AN, Hanlon CA, Rupprecht CE. Endogenous lipid pneumonia (multifocal

alveolar histiocytosis) in raccoons (*Procyon lotor*). *J Vet Diagn Invest*. 1996; 8:267-269.

10. Hayashi T, Stemmermann GN. Lipid pneumonia in the Hawaiian feral mongoose. *J Pathol*. 1972; 108:205-210.

11. Jones DJ, Norris CR, Samii VF, Griffey SM. Endogenous lipid pneumonia in cats: 24 cases (1985-1998). *JAVMA*; 216:1437-1440.

12. Kim JY, Jung JW, Choi JC, et al. Recurrent lipid pneumonia associated with oil pulling. *Int J Tuberculosis Lung Dis*. 2014; 18:251-252.

13. Laurent F, Philippe JC, Vergier B, et al. Exogenous lipid pneumonia: HRCT, MR, and pathologic findings. *Eur Radiol*. 1999; 9:1190-1196.

14. Marchiori E, Zanetti G, Mano CM, Hochegger B. Exogenous lipid pneumonia. Clinical and radiological manifestations. *Resp Med*. 2011; 105:659-666.

15. Metcalfe L, Cummins C, Maischberger E, Katz L. Iatrogenic lipid pneumonia in an adult horse. *Ir Vet J*. 2010; 63:303-306.

16. Moreau E, Rerolle C, Deveaux M, et al. Exogenous lipid pneumonia as a contributory factor in a drug related death. *J Forensic Sci*. 2015; 60:514-517.

17. Papla B, Urbanczyk K, Gil T, et al. Exogenous lipid pneumonia (oil granulomas of the lung). *Pol J Pathol*. 2011; 4:269-273.

18. Perpignan D, Steffen D, Napier JE. Pulmonary adenocarcinoma and endogenous lipid pneumonia in a common genet (*Genetta genetta*). *J Zoo Wildl Med*. 2010; 41:710-712.

19. Raya AI, Marco F-D, Nunez A, Afonso JC, et al. Endogenous lipid pneumonia in a dog. *J Comp Pathol*. 2006; 135:153-155.

20. Romero F, Shah D, Duong M, et al. Chronic alcohol ingestion in rats alters lung metabolism, promotes lipid accumulation, and impairs alveolar macrophage functions. *Am J Respir Cell Mol Biol*. 2014; 51:840-849

21. Smith BL, Alley MR, McPherson WB. Lipid pneumonia in a cow. *New Zeal Vet J*. 1969; 17:65-67.

22. Spickard A, Hirschmann JV. Exogenous lipid pneumonia. *Arch Intern Med*. 1994; 154:686-692.

23. Wang C-W, Colby TV. Histiocytic lesions and proliferations in the lung. *Semin Diagn Pathol*. 2007; 24:162-182.

24. Weinberg I, Fridlender ZG. Exogenous lipid pneumonia caused by paraffin in an amateur fire breather. *Occupational Med*. 2010; 60:234-235.

CASE III: S 1215/09 (JPC 3167218).

Signalment: 1 ½ years, female, rabbit (*Oryctolagus cuniculus*)

History: The rabbit was presented with symptoms of salivation, seizures, somnolence and fever. Meningitis was suspected.

Gross Pathology: Yellowish covering of the eye's proximity; ulceration of the right cornea; edema of the mucosal-cutaneous intersections; slight enlargement and blood-reabsorption of the lymph nodes at the head; little yellowish dry mass in the outer ear canals; no abnormalities at the inner ears; slight lipidosis of the liver; dilated uterus, filled with white mucous.

Laboratory Results: Herpes simplex virus (HSV) was verified by polymerase chain reaction of paraffin-embedded, formalin-fixed brain material. Specificity of HSV-1, was confirmed by restriction enzyme digestion with BamHI and Sma-digestion (Institute of virology, TU Munich, Germany).

Histopathologic Description: Brain: multifocal moderate to severe perivascular accumulation of lymphocytes, plasma cells and histiocytes at meningeal and cortical blood vessels; multifocal extensive neuronal and glial necrosis at the cerebral cortex; detection of intranuclear eosinophilic to amphophilic inclusion bodies in cortical pyramidal neurons and glial cells, often filling the entire nucleus; electron microscopy showed high numbers of intra-nuclear particles of icosahedral nucleocapsids, consistent with the morphology of herpesvirus.



Cerebrum, rabbit: The submitted specimen is a transverse section of the frontal cortex, without visible lesion. (HE, 5X)

Eye (not on the slide): ulceration of the cornea; small foci of infiltrating lymphocytes and plasma cells at the limbus.

Contributor's Morphologic Diagnosis:

Brain: Meningoencephalitis, severe, multifocal, non-suppurative, with detection of numerous intranuclear inclusion bodies in neurons and glial cells.

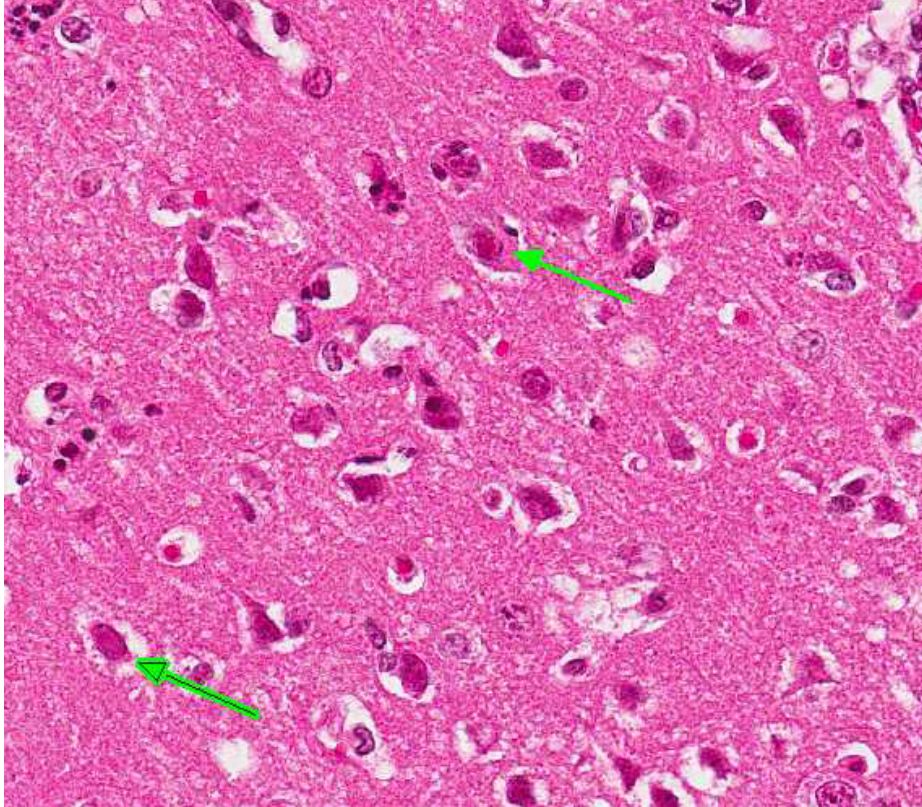
Contributor's Comment: Herpesvirus infection is an uncommon disease in domestic rabbits. *Herpesvirus sylvilagus* and *cuniculi* (formerly known as virus III or herpes-like virus) are known to be either only pathogenic for individual breeds or only slightly pathogenic for the domestic rabbit.^{5,2} A third, unclassified herpesvirus causes haemorrhagic dermatitis, pneumonia and necrotizing splenitis in rabbits.⁶

Naturally occurring encephalitis in domestic rabbits by herpes simplex virus infection has only been reported twice.^{9,1} In both reported cases a person with herpetic infection and close contact to the rabbit was suspected to be the source of infection for the animal.

Rabbits can be easily infected experimentally and act as an animal model for human herpes simplex infection.⁷ Trigeminally innervated areas, as for example the cornea, serve as the portal of entry for the human herpes simplex virus.⁷ Furthermore, nasal infection is known to lead to focal lesions in the brain.⁸

JPC Diagnosis: Cerebrum: Neuronal necrosis, multifocal, with intranuclear inclusion bodies and mild lymphocytic meningitis.

Conference Comment: Rabbits serve as experimental models for herpes simplex virus (HSV) type 1 (*human herpesvirus 1*)



Cerebrum, rabbit: There is extensive neuronal degeneration and necrosis within the superficial gray matter. Necrotic neurons are shrunken and angular, with occasionally pyknosis karyorrhexis; and occasionally abutted by one or more glial nuclei (satellitosis). Occasionally degenerating neurons (green arrows) contain eosinophilic intranuclear viral inclusions. (HE, 260X)

encephalitis in humans, and in rabbits, the infection is exclusively neurotropic. In humans, the intranasal route of infection is most important in development of encephalitis. Experimental intranasal inoculation in rabbits leads to migration via the olfactory nerves, leading into the frontal and temporal lobes. Intraocular inoculation of the virus in rabbits has also been used to study cell spread of HSV, and rabbits can present with neurologic signs as early as 2 days post infection; the disease is also known to progress quickly in spontaneous cases.³ Following intraocular inoculation, the virus travels through the optic nerve to the corpus geniculatum.^{1,3} Both ocular and nasal routes of inoculation can lead to seizures and death but the intranasal route has a higher mortality rate. Histologic

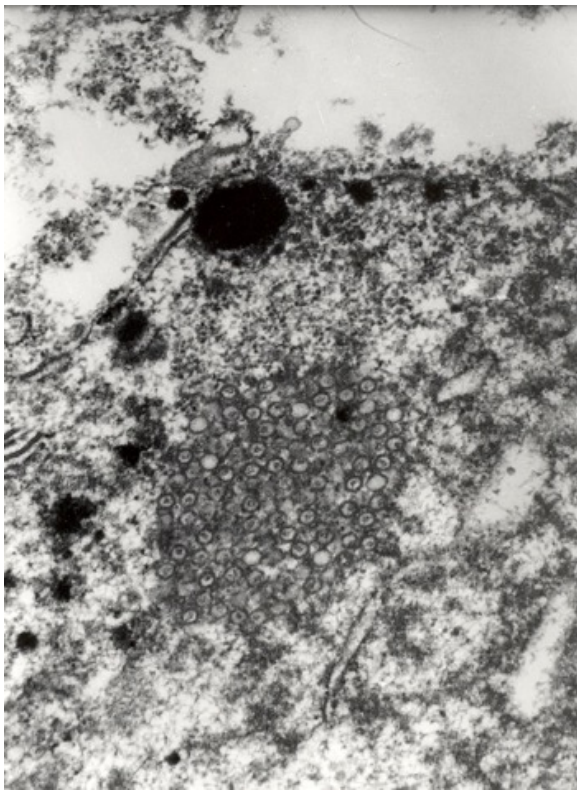
lesions described in other cases of both natural and experimental infection are similar to those seen in this case.^{1,3,9} Gross CNS lesions in rabbit HSV infections are uncommon which may be due in part to the rapid course of disease. In some reported cases of natural HSV infection in rabbits, humans in close contact were reported to have cold sores prior to the onset of clinical signs in the rabbit. Nonetheless, it is unclear if spontaneous HSV encephalitis in rabbits can arise from reactivation of latent infection or if disease only occurs shortly

after exposure.³

HSV can also result in fatal disease in nonhuman primates. In Old World primates, the course of HSV infection is comparable to humans with localization to the mucocutaneous tissues and relatively mild disease. However, New World primates (NWP) are considered highly susceptible and infection often leads to severe systemic disease and death with a rapid clinical course in many cases. In some NWPs such as owl monkeys and marmosets, they also develop ulceration of the oral mucous membranes but it is accompanied by hemorrhage and necrosis in the cerebral cortex as well as many other organs. In most of the reported cases in non-human primates, close contact with an infected human was found to

be the source of infection. The most characteristic lesions in HSV infection in NWP are oral ulcerations and lesions at the mucocutaneous junction, which cannot be grossly differentiated from lesions caused by herpesvirus T (*Herpes tamarinus*) infection. Molecular methods are needed to differentiate infections caused by the two viruses due to similarity of lesions.⁴

The conference description included multifocal, random areas of neuronal necrosis within the superficial gray matter accompanied by gliosis, satellitosis and low numbers of infiltrating heterophils. Perivascular cuffing by mononuclear cells is present multifocally within the gray matter and a similar mononuclear infiltrate as well



Neuron, rabbit. Ultrastructural evaluation demonstrates an aggregate of targetoid icosahedral nucleocapsids consistent with herpesviral particles within degenerating neurons. (Photo courtesy of Institute of Veterinary Pathology, Ludwig-Maximilians-University Munich, Veterinaerstrasse 13; D-80539 Munich, Germany, www.patho.vetmed.uni-muenchen.de)

as edema expand the meninges. The lack of neuronal degenerative changes such as swelling was noted by some participants; however, in some viral infections, neuronal necrosis (even in acute infection) may be the defining lesion.

Contributing Institution:

Institute of Veterinary Pathology, Ludwig-Maximilians-University Munich, Veterinaerstrasse 13; D-80539 Munich, Germany

www.patho.vetmed.uni-muenchen.de

References:

1. Grest P, Albicker P, Hoelzle L, Wild P, Pospischil A. Herpes simplex encephalitis in a domestic rabbit (*Oryctolagus cuniculus*). *J Comp Pathol.* 2002; 126: 308-11.
2. Hinze HC. New Member of the Herpesvirus Group Isolated from Wild Cottontail Rabbits. *Infect Immun.* 1971; 3: 350-354.
3. Nesburn AB. Isolation and characterization of a herpes-like virus from New Zealand albino rabbit kidney cell cultures: a probable re-isolation of virus 3 of Rivers. *J Virol.* 1969; 3: 59-69.
4. Matos R, Russell D, Van Alstine W, Miller A. Spontaneous fatal Human herpesvirus 1 encephalitis in two domestic rabbits (*Oryctolagus cuniculus*). *J Vet Diag Invest.* 2014; 26(5):689-694.
5. Mätz-Rensing K, Jentsch KD, Rensing S, Langenhuyzen S, et al. Fatal Herpes simplex infection in a group of common marmosets (*Callithrix jacchus*). *Vet Pathol.* 2003; 40:405-411.
6. Onderka DK, Papp-Vid G and Perry AW: Fatal herpesvirus infection in

commercial rabbits. *Can Vet J.* 1992; 33:539-543.

7. Paeivaerinta MA, Roeyttae M, Hukkanen V, Marttila RJ. Nervous system inflammatory lesions and viral nucleic acids in rabbits with herpes simplex virus encephalitis-induced rotational behaviour. *Acta Neuropathol.* 1994; 87: 259-68.

8. Stroop WG and Schaefer DC. Production of encephalitis restricted to the temporal lobes by experimental reactivation of herpes simplex virus. *J Infect Dis.* 1986; 153: 721-731.

9. Weissenboeck H, Hainfellner A, Berger J, Kasper I and Budka H. Naturally occurring herpes simplex encephalitis in a domestic rabbit (*Oryctolagus cuniculus*). *Vet Pathol.* 1997; 34: 44-7.

CASE IV: 14-062 (JPC 4068766).

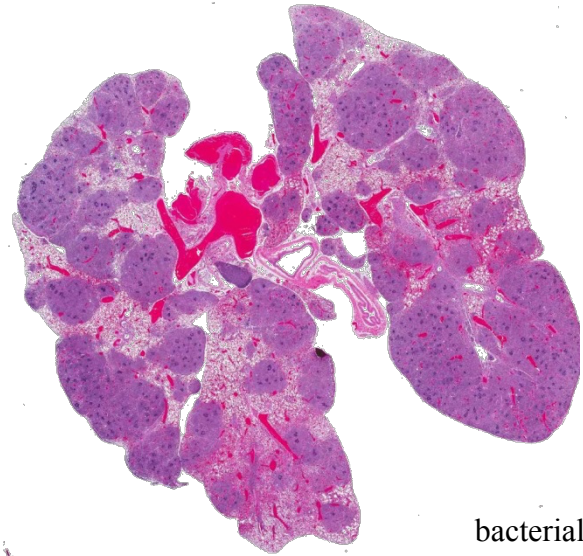
Signalment: 7 month-old, male, Cybb transgenic mouse, (*Mus musculus*)

History: Found dead in cage.

Gross Pathology: The lungs were described by the submitter as diffusely “mottled with multifocal masses throughout”; *Staphylococcus xylosum* infection was suspected.

Laboratory Results: None

Histopathologic Description: Lungs: Diffusely affecting greater than 90% of the section, multiple, coalescing pyogranulomas are effacing and replacing the normal architecture, compressing the adjacent parenchyma and occasionally distending bronchial and bronchiolar structures. Pyogranulomas are centered on large colonies of

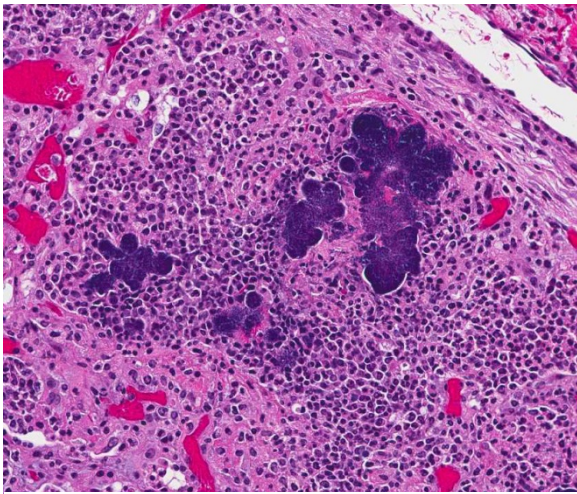


Lung, cybb mouse: All lung field contain coalescing nodular foci of inflammation. (HE, 6X).

cocci that are often embedded within hyalinized, eosinophilic material that also occasionally contains refractile, acicular crystalline structures. Bacterial colonies are surrounded by large numbers of viable and degenerate neutrophils admixed with variable amounts of amorphous, eosinophilic proteinaceous debris (necrosis) with large numbers of epithelioid macrophages, fewer scattered lymphocytes and plasma cells and rare multinucleated giant cells (Langhans-type). Within the adjacent parenchyma, alveoli are frequently expanded by large amounts of a similar inflammatory infiltrate containing brightly eosinophilic, refractile, needle-like to acicular crystalline material. The crystalline material is typically free within the alveolar spaces but is often found within the cytoplasm of alveolar macrophages and multinucleated giant cells (eosinophilic crystalline pneumonia). There is also diffuse vascular congestion, mild edema and peripheral emphysema.

Gram Stain:

Lung: Bacterial cocci are gram positive, consistent with *Staphylococcus sp.*



Lung, cybb mouse. Inflammatory nodules, which efface alveolar parenchyma, are composed of large, poorly formed pyogranulomas centered on large colonies of cocci. (HE, 200X)

Contributor's Morphologic Diagnosis:

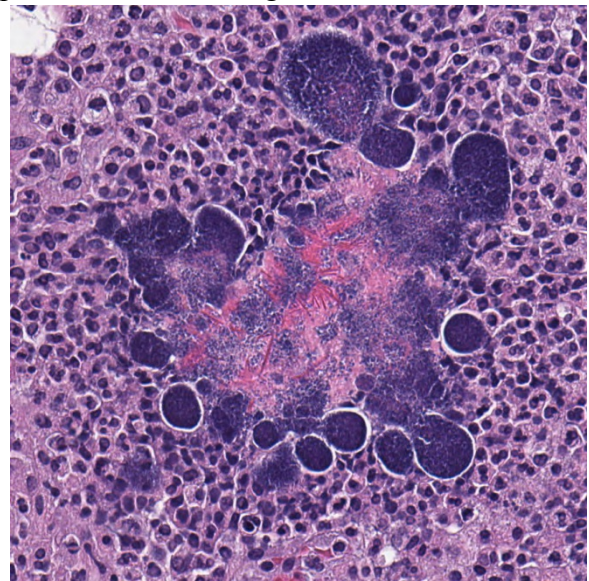
Lung: Diffuse, chronic-active, severe, pyogranulomatous pneumonia with intralesional bacteria (pulmonary botryomycosis).

Lung: Multifocal, subacute to chronic, moderate, eosinophilic crystalline pneumonia.

Contributor's Comment: Botryomycosis is a chronic infection caused by non-filamentous bacteria characterized by pyogranulomas that contain a central necrotic core with colonies of gram-positive cocci embedded within brightly eosinophilic, hyalinized material that occasionally forms club-shaped projections (Splendore-Hoeppli material). The condition is so named due to its resemblance to fungal pyogranulomas, and is not uncommon among domestic and laboratory animal species. Staphylococci are most commonly associated with botryomycosis, however, *Streptococcus sp.*, *Pseudomonas sp.*, *Actinobacillus sp.*, *Pasteurella sp.*, *Proteus sp.*, and *Escherichia sp.*, have also been isolated in reported cases.^{3,6,9} In mice, botryomycosis is typically caused by *Staphylococcus aureus* or *S. xylosus*, which are commensals of the skin and mucus membranes. In all species,

botryomycosis lesions are typically localized to the skin and subcutis but may extend to the underlying bone and muscle. Pulmonary botryomycosis, as seen in this case, is rare, but has been reported in horses, cattle and guinea pigs.⁶

Eosinophilic crystalline pneumonia, sometimes called "acidophilic macrophage pneumonia" or simply "intracellular eosinophilic crystals" is an idiopathic granulomatous pneumonia that occurs spontaneously in many strains of mice, namely the C57BL/6 and strains on a C57BL/6 background.^{5,10} This condition is also common among Swiss mice, B6C3F1 mice used by the National Institutes of Health and the National Toxicology Program and 129 strains, particularly the 129S4/SvJae strain in which severe cases resulting in respiratory distress or death have been reported.^{1,5,8} Largely considered a background lesion, eosinophilic crystalline pneumonia can range from subclinical to

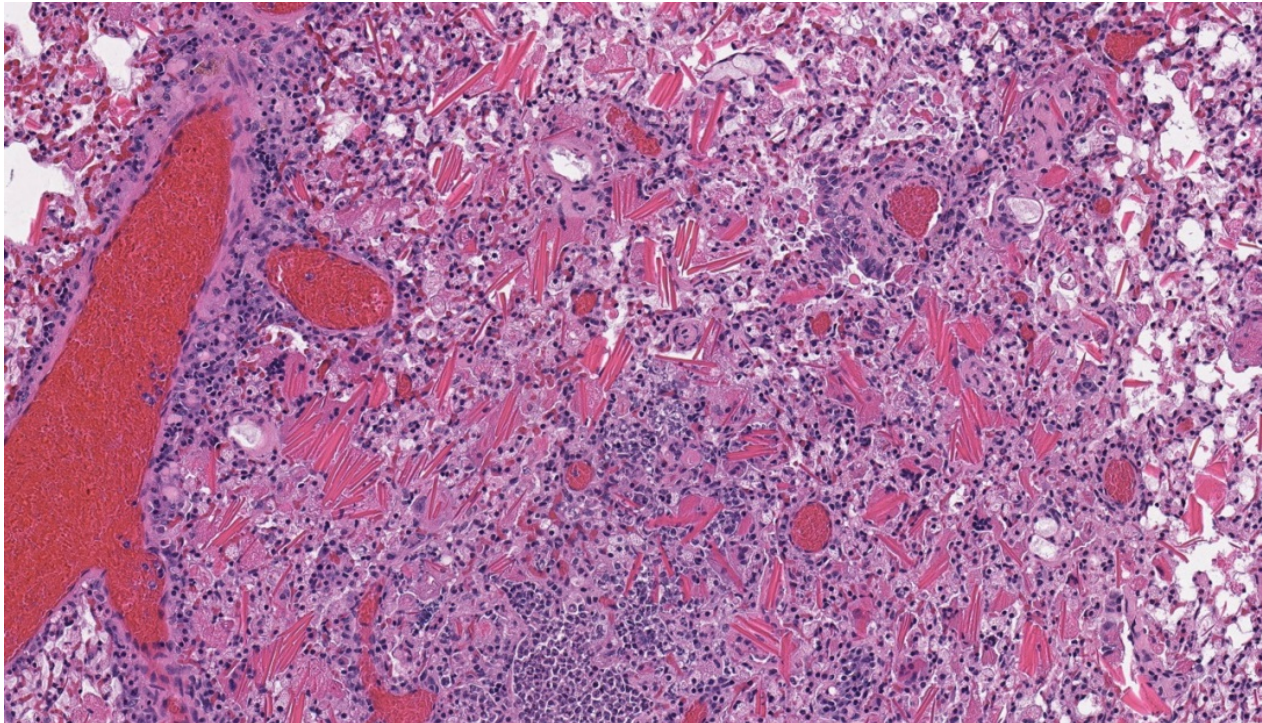


Lung, cybb mouse: Higher magnification shows that colonies of cocci are enmeshed in a brightly eosinophilic matrix which often contains specular acidophilic crystals. (HE, 400X) (Image courtesy of NIEHS/NTP, 111 T.W. Alexander Drive, Research Triangle Park, NC, 27709 <http://ntp.niehs.nih.gov/nnl/>)

fatal and is characterized by focal to diffuse accumulation of eosinophilic crystals composed predominantly of Ym1 protein, a chitinase-like protein expressed in neutrophil granule products and active macrophages. As in this case, crystals are readily apparent within macrophages, multinucleated giant cells, alveolar spaces and airways.^{1,5,8,10} The function of Ym1 protein is not completely understood, but may play a role in host immune defense, tissue repair and hematopoiesis.^{5,10}

The *Cybb* transgenic mouse was designed as a model for developing new treatments for chronic granulomatous disease (CGD); JAX developed this particular transgenic strain targeting the gene involved in X-linked CGD. As a result, male hemizygotes tend to have an increased susceptibility to infection with *S. aureus* due to a lack of phagocyte superoxide production.⁷ Given the strain-

specific increased susceptibility to bacterial infection and apparent pulmonary botryomycosis, staphylococcal infection is the most likely etiology in this case. Large colonies of Gram-positive cocci are consistent with *Staphylococcus sp.*, most likely *S. aureus* or *S. xylois*. We were unable to definitively identify the bacterial agent since bacterial culture was not performed. As previously mentioned, eosinophilic crystalline pneumonia is a common spontaneous lesion in the C57BL/6 mouse, which was the background strain used to manufacture this particular transgenic. However, since this condition may also occur in conjunction with other diseases, it is difficult to determine whether the eosinophilic crystalline pneumonia developed prior to the pulmonary botryomycosis, as a spontaneous disease possibly predisposing the animal to infection, or developed secondary to, or in



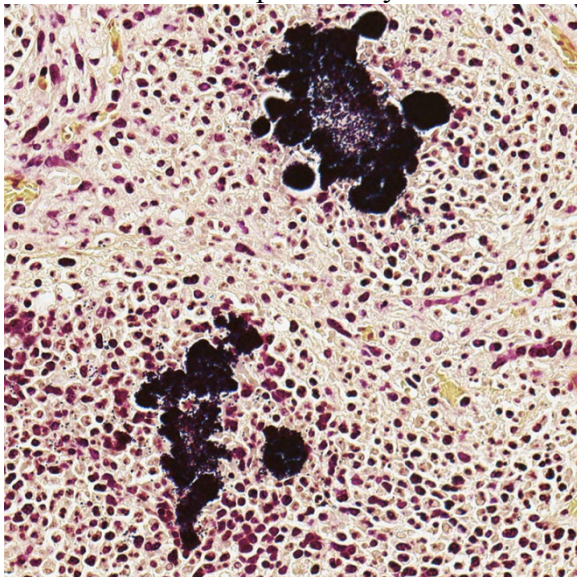
Lung, *cybb* mouse. Alveoli adjacent to pyogranulomatous nodules contain large numbers of alveolar histiocytes surrounding sheaves of brightly eosinophilic acidophilic crystals. *HE, 20X (Image courtesy of: NIEHS/NTP, 111 T.W. Alexander Drive, Research Triangle Park, NC 27709 <http://ntp.niehs.nih.gov/nnl/>)

conjunction with, the pulmonary botryomycosis.

JPC Diagnosis: 1. Lung: Pneumonia, pyogranulomatous, multifocal to coalescing, severe, with Splendore-Hoeppli material and numerous colonies of cocci.

2. Lung: Pneumonia, histiocytic, diffuse, moderate with extracellular and intra-histiocytic eosinophilic protein crystals.

Conference Comment: Botryomycosis also occurs in other species as a result of *Staphylococcus aureus* infection, including horses and pigs, and is most commonly associated with wound infection. The inflammatory reaction and lesions are similar to those seen in this case, consisting of pyogranulomatous inflammation and Splendore-Hoeppli reaction. In the skin and subcutis, it is often associated with nodular masses which progressively enlarge over time. The nodular structure is occasionally referred to as a pseudo-mycetoma. A



Lung, cybb mouse: Clusters of cocci within pyogranulomas are gram-positive. (Gram, 200X). (Image courtesy of: NIEHS/NTP, 111 T.W. Alexander Drive, Research Triangle Park, NC 27709 <http://ntp.niehs.nih.gov/nml/>)

similar inflammatory reaction is seen in *Actinobacillus lignieresii* (wooden tongue) and *Actinomyces bovis* (lumpy jaw) infections in cattle.¹¹ In many cases of botryomycosis, the bacteria will form yellow sulfur granules which can be seen grossly. The tissue granules consist of bacterial colonies surrounded by clubs of Splendore-Hoeppli material, which is generally regarded as being composed of antigen-antibody complexes.

The differential diagnosis for a nodular mass composed of pyogranulomatous inflammation includes filamentous bacterial or fungal infections, which result in the formation of a mycetoma.⁴ The organisms are not always readily visualized on H&E stained sections and therefore may require special histochemical stains for differentiation. Botryomycosis may also occur in the mammary gland of ruminants associated with staphylococcal mastitis, and in other large animals secondary to post castration staphylococcal infection.²

The conference description was very similar to that provided by the contributor. Additional features described and discussed include: multifocal expansion of alveolar septa by fibrous connective tissue; an exudate composed of neutrophils and histiocytes within larger airways, which may represent reflux from alveolar spaces; and the presence of Splendore-Hoeppli phenomenon within the center, rather than the periphery, of the bacterial colonies. Medullary sinuses of a hilar node contain numerous plasma cells, with few neutrophils and macrophages, which attest to the long-standing nature of this infection. There was discussion regarding the route of infection in this case; most participants favored an airway route, as the bronchi and bronchioles are particularly affected by the inflammatory process and the vessels are relatively spared.

Contributing Institution:

NIEHS/NTP

<http://ntp.niehs.nih.gov/nnl/>**References:**

1. Dixon D, Herbert RA, Sills RC, Boorman GA. Lung, Pleura, Mediastinum. In: Maronpot RR, ed. *Pathology of the Mouse*. Vienna, IL:Cache River Press; 1999:318.
2. Foster RA. Male reproductive system. In: McGavin MD, Zachary JF, eds. *Pathologic Basis of Veterinary Disease*. 5th ed. St. Louis, MO: Mosby Elsevier; 2012:1144.
3. Ginn PE, Mansell JEKL, Rakich PM. Skin and appendages. In: McGavin MD and Zachary JF, eds. *Pathologic Basis of Veterinary Disease*. 4th ed. Mosby Elsevier, St. Louis, MO; 2007:691.
4. Hargis AM, Ginn PE. The Integument. In: McGavin MD, Zachary JF, eds. *Pathologic Basis of Veterinary Disease*. 5th ed. St. Louis, MO: Mosby Elsevier; 2012:1034.
5. Hoenerhoff MJ, Starost MF, Ward JM. Eosinophilic Crystalline Pneumonia as a Major Cause of Death in 129S4/SvJae Mice. *Vet Pathol*. 2006; 43:682-688.
6. I-B02 - Botryomycosis - fibrovascular tissue – rat; Veterinary Systemic Pathology Online (VSPO); The Joint Pathology Center (JPC); http://www.askjpc.org/vspo/show_page.php?id=285; 2014; accessed: February 6, 2016.
7. Mouse strain datasheet, Strain Name: B6129S-Cybb^{tm1Din}/J; JAX Mouse Database. The Jackson Laboratory;

<http://jaxmice.jax.org/strain/002365.html>;
2016; accessed: February 6, 2016.

8. Percy DH and Barthold SW. Mouse: Acidophilic Macrophage Pneumonia/Epithelial Hyalinosis. In: Percy DH and Barthold SW, eds. *Pathology of Laboratory Rodents and Rabbits*. 3rd ed. Ames, IA: Blackwell Publishing; 2007:95.
9. Percy DH and Barthold SW. Mouse: Staphylococcal Infection. In: Percy DH and Barthold SW, eds. *Pathology of Laboratory Rodents and Rabbits*. 3rd ed. Ames, IA: Blackwell Publishing; 2007:74-76.
10. Renne R, Brix A, Harkema J, Herbert R, Kittel B, Lewis D, March T, Nagano K, Pino M, Rittinghausen S, Rosenbruch M, Tellier P, Wohrmann T. Proliferative and Nonproliferative Lesions of the Rat and Mouse Respiratory Tract. *Tox Pathol*. 2009; 37:5S-73S.
11. Valentine BA, McGavin MD. Skeletal muscle. In: McGavin MD, Zachary JF, eds. *Pathologic Basis of Veterinary Disease*. 5th ed. St. Louis, MO: Mosby Elsevier; 2012:892.

**Joint Pathology Center
Veterinary Pathology Services**



WEDNESDAY SLIDE CONFERENCE 2015-2016

C o n f e r e n c e 1 7

10 February 2016

Casey J. LeBlanc, DVM, PhD
Diplomate, ACVP
Clinical Pathologist & CEO
KDL VetPath
Knoxville, TN & Springfield, VA

CASE I: TAMU-1-2013 (JPC 4033379).

Signalment: 18-day-old thoroughbred colt
(*Equus caballus*)

History: A healthy newborn foal nursed and the next day, became lethargic and had hemoglobinuria. With progressive stupor, icterus, hyperbilirubinemia and anemia, the foal was presented to the clinic at 2 days of age.

Gross Pathology: Yellow mucous membranes and tissues (icterus); ~200ml abdominal transudate with fibrin strands; myocardial mottling grey and red (hemorrhage and necrosis) a small Thebsian vein in the noncoronary aortic sinus; urachus patent.

Laboratory Results:

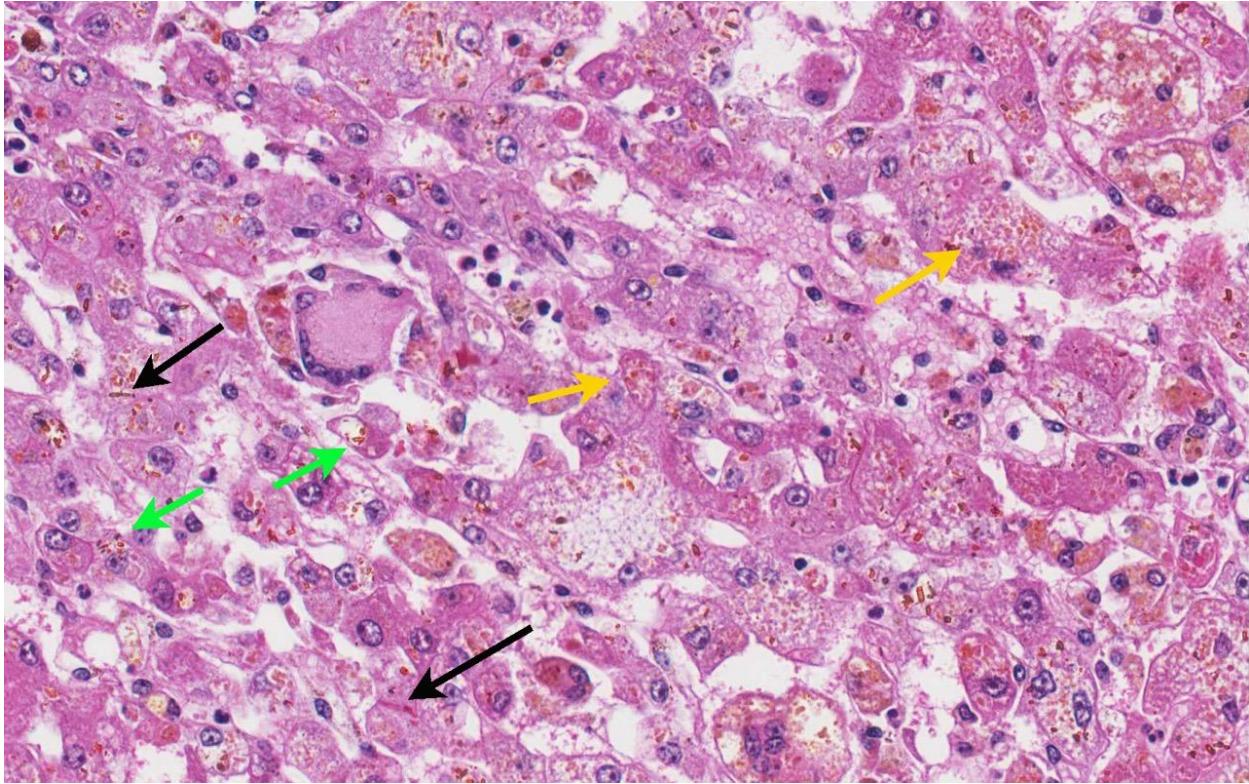
PCV=12 (32-53) no Nrbc's
Platelets 470,000/ul (100-350,000)
TP 4.7g/dl (5.3-7.3)



Mucous membranes, foal. The mucous membranes of this foal are extremely yellow, indicating icterus. (Photo courtesy of: Dept Vet Pathobiology, College Vet Med Texas A&M University, College Station, TX 77843-4467 <http://vetmed.tamu.edu/vtpb>)

Total bilirubin 14.5 mg/dl (0-1.9)
GGT 124U/L (0-53)
Alkaline phosphatase 553U/L (128-512)
ALT 850U/L (134-643)
Saline agglutination test positive
Mare serum Anti-Qab positive

Histopathologic Description: The section of liver has widespread atrophy of hepatocytes with hypertrophied and



Liver, foal. There is extensive pigment deposition throughout the section, to include brown granules in hepatocytes (lipofuscin- yellow arrows), brown spicular material (acid hematin – green arrows) and distended bile canaliculi (cholestasis – black arrows). Syncytial hepatocytes, often with peripheralized nuclei are scattered throughout the section. (HE, 40X)

occasionally binucleate nuclei. Some hepatocyte syncytia contain 6-8 nuclei. Often, the hepatocytes exhibit feathery degeneration, but centrilobular hepatocytes are degenerating or have individual cell necrosis. The spaces of Disse are expanded (edema), and sinus leukocytosis is common with leucocytes often concentrated in areas of hepatocyte loss. Scattered lipofuscin-laden macrophages are often near the pale staining triads, and bile casts and mild bile duct proliferation are noted. Throughout the section are syncytia similar to Langhan's type multinucleate giant cells with nuclei surrounding a tan, granular cytoplasm (lipofuscin). Erythrophagocytosis by Kupffer cells is noted, and iron-staining Kupffer cells are in sinusoids. Hepatic cords are disassociated (shock).

Contributor's Morphologic Diagnosis:

Liver: Subacute hepatopathy with centrilobular hepatocellular degeneration, necrosis and collapse; edema, lipofuscinosis, bile casts and mild bile duct proliferation; hepatocyte syncytia; erythrophagocytosis and hemosiderosis; multifocal neutrophilic hepatitis.

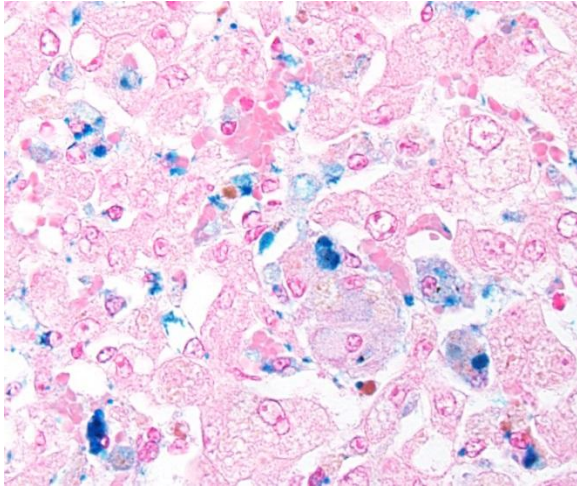
Contributor's Comment: This is a classic case of equine neonatal isoerythrolysis /isoimmune hemolytic anemia (NI). The animal was treated with dexamethasone, banamine, and antibiotics; clinical and post-mortem blood cultures were sterile. No organisms were noted with Gram or GMS stains. While there is inflammation in the lesion, it was felt to reflect secondary, cholestasis-induced hepatitis.

When reviewing the case with the resident, the pathologist commented that the giant cells were classically seen with NI; however, the resident noted that this lesion is not mentioned in textbooks as a lesion associated with NI. Young horse hepatocytes often form syncytia, and giant cell hepatopathies/ hepatidides are described; especially associated with leptospiriosis,^{13,20} but “idiopathic” hepatocyte syncytia have been described in 5-7 month-old, equine abortuses³ and have been seen by this contributor in leptospira PCR-negative cases. In human infants with jaundice, it was described as “giant cell hepatitis”¹⁷ or “syncytial giant cell hepatitis.”¹⁵ Initially, some considered it an expression of viral hepatitis, particularly serum hepatitis, in infancy. Some feel the lesion reflects a specific insult such as blood group incompatibility between mother and infant. It has been considered a nonspecific response of liver regeneration to any injury.^{10,19} Still others consider it a congenital defect in the formation of bile canaliculi or another genetically transmitted abnormality.^{5,14} Popper and Schaffner¹⁴ concluded hepatocyte giant cell formation was a feature of cholestasis in infancy, and that it may be associated with some inflammatory changes. Syncytial cell hepatitis has been reported in humans and is associated with bacterial sepsis (especially toxoplasmosis, syphilis listeriosis, tuberculosis), viral diseases (cytomegalovirus, herpes simplex, varicella, echovirus, parvovirus B19, enterovirus, rubella, human herpesvirus-6, human immunodeficiency virus, hepatitis types A, B and C, Marburg virus and paramyxovirus), liver transplantation and death from severe liver failure.^{8,16} However, in the neonatal period it is considered a non-specific reaction of immature hepatocytes to various forms of “aggression,”¹⁰ and the syncytia stain with nuclear proliferation and

growth factors.⁷ Just as in autoimmune hemolytic anemia in early childhood, syncytial cell hepatopathy has been reported in cases of equine NI.² It was noted in a case of NI presented in the WSC of 5-14-86. How does one explain the lack of the lesion description? Foal livers in fatal cases of NI are “busy,” and the syncytial cells, while typical, may be down-played in face of the catastrophic clinical and autopsy findings. Because our cases are often referral cases and are subacute to chronic, it may also be that syncytia are just more frequent in long-standing, fatal cases. Syncytia are characteristic. Foals seem prone to respond this way. Although neonatal infections may complicate clinical NI, infectious agents are not always documentable. We should remember that only recently a viral agent of equine Theiler’s disease has been identified,⁴ which may play a role (though I doubt it).

Kernicterus is always a concern in cases of prolonged unconjugated hyperbilirubinemia in neonates. This foal had no macroscopic lesions of kernicterus, the cortex did not fluoresce and no neuronal lesions were noted in the cerebral cortex, Purkinje cells or hippocampus, where it has been described in foals with NI.¹² It’s of interest that syncytia were not reported in any of their autopsy cases, even their chronic cases. There is a case report of NI in a three-day-old foal with kernicterus and neuronal necrosis represented macroscopically by yellow-discolored nuclei.⁶

For completeness, it is interesting that this colt had a persistent neutrophilia and developed a thrombocytosis. Alloimmune, neonatal neutropenia has been described in a foal with Ka antibodies in a recent report of NI.²¹ The most complete study of anti-erythrocyte antibodies in mare serum and colostrum was done in thoroughbred and



Liver, foal: There are moderate amounts of iron within Kupffer cells. (Perl's, 40X)

standardbred mares and Qa and Aa seemed to be the most common alloantibodies found at large;¹ however, these alloantibodies may not be the most common seen in clinical cases of NI.^{2,9} Alloantibodies to Qa antigens were found in the mare of our case. The colt of our study did not show a regenerative erythroid response. Over the 2-week hospitalization, no nucleated erythrocytes were noted and the bone marrow had erythrocytic hypoplasia. We wondered if this may have reflected a specific destruction of precursors of the erythroid series.

JPC Diagnosis: Liver: Hepatocellular degeneration and atrophy, diffuse, severe with Kupffer siderosis, cholestasis, and hepatocellular syncytial cell formation.

Conference Comment: Neonatal isoerythrolysis is a type II hypersensitivity reaction that results from antibodies directed against neonatal red blood cells, most frequently IgG or IgM. This leads to activation of complement component C1q and eventual formation of the membrane attack complex which lyses the red blood cell. Red blood cell lysis can also result

from opsonization of red blood cells by complement component C3b, or by antibody, followed by phagocytosis.¹⁸

Lipofuscin is an intracellular pigment thought to accumulate as a result of aging and cellular “wear and tear,” including processing of senescent cellular organelles and other material. It accumulates within lysosomes most significantly in post mitotic or slowly dividing cells as an end product of autophagy and is often seen as a perinuclear golden brown pigment. It looks very similar histologically to ceroid, which is more commonly associated with pathologic conditions such as severe malnutrition and vitamin E deficiency or can be seen in certain inherited conditions such as neuronal ceroid lipofuscinosis (see WSC 2015-16, conference 10, case 1). Ceroid is known to accumulate in both Kupffer cells and hepatocytes as well as other tissues and can be intracellular or extracellular. Lipofuscin is thought to accumulate slowly over the life of the animal, whereas ceroid usually accumulates rapidly depending on the associated condition. Histochemical techniques which can aid in identifying both ceroid and lipofuscin include Sudan black, oil-red-O, PAS and Ziehl-Neelsen stains. Although differences in content of the two pigments have been demonstrated by special histochemical techniques, it is not possible to differentiate the two pigments in standard H&E stained sections.¹¹

The primary histologic features in this case include hepatocyte degeneration and atrophy, with formation of syncytial cells. Extensive pigmentation of hepatocytes and Kupffer cells was present throughout the section prompting extensive discussion. . The brown granular to globular intracellular pigment within hepatocytes was interpreted as lipofuscin and within Kupffer cells as hemosiderin. An iron stain confirmed the presence of moderate amounts of hemo-

siderin within Kupffer cells and occasionally within hepatocytes. Viewing under fluorescence confirmed the presence of small amounts of autofluorescent pigment within hepatocytes consistent with lipofuscin. Abundant birefringent, yellow-brown spiculated material was ultimately identified as acid hematin. Numerous dilated bile canaliculi were also noted, indicating cholestatic disease. A Hall's stain for bile confirmed this finding.

We thank the contributor for providing clinical pathology data with the submission, which greatly adds to the teaching value of the case. One of the best indicators of regenerative anemia is reticulocyte count, but horses do not release reticulocytes. The absence of nucleated red blood cells may suggest a nonregenerative anemia; however, the best way to determine regenerative status would be a bone marrow sample. In this case, a bone marrow aspirate revealed erythrocytic hypoplasia, as indicated above in the contributor's comment. Conference participants briefly discussed bilirubin metabolism and the elevated total bilirubin in this case was interpreted as both pre-hepatic and hepatic, which fits with both the pathogenesis and histologic findings.

Contributing Institution:

Dept Vet Pathobiology, College Vet Med
Texas A&M University
<http://vetmed.tamu.edu/vtpb>

References:

1. Bailey E. Prevalence of anti-red blood cell antibodies in the serum and colostrum of mares and its relationship to neonatal isoerythrolysis. *Am J Vet Res.* 1982; 43:1917-21.
2. Boyle A, Magdesian KC, Ruby RE. Neonatal isoerythrolysis in horse foals and a mule foal: 18 cases (1988-2003). *J Am Vet Med Assoc.* 2005; 227: 1276-1283.
3. Car BD, Anderson WI. Giant cell hepatopathy in three aborted midterm equine fetuses. *Vet Pathol.* 1988; 25:389-91.
4. Chandriani S, et al. (2013) Identification of a previously undescribed divergent virus from the *Flaviviridae* family in an outbreak of equine serum hepatitis. *Proc Natl Acad Sci U S A.* 2013 Apr 9; 110(15):E1407-15. doi: 10.1073/pnas.1219217110.
5. Clayton PT, Disorders of bile acid synthesis. *J Inherit Metab Dis.* 2011; 34:593-604.
6. David JB, Byers TD, Braniecki A, Chaffin MK, Storts RW. Kernicterus in a foal with neonatal isoerythrolysis. *Comp Cont Educ Prac Veterinarian.* 1988; 20:517-20.
7. Fang JWS, González-Peralta RP, Chong SKF, Lau GM. Hepatic expression of cell proliferation markers and growth factors in giant cell hepatitis: Implications for the pathogenetic mechanisms involved. *JPGN.* 2010; 52:65-72.
8. Hicks J, Barrish J, Zhu SH. Neonatal syncytial giant cell hepatitis with paramyxoviral-like inclusions. *Ultrastructural Pathol.* 2001; 25:65-71.
9. MacLeay JM. Neonatal isoerythrolysis involving Qc and Db antigens in a foal. *J Am Vet Med Assoc.* 2001; 219:79-81.
10. Maggiore G, Sciveres M, Fabre M, Gori L, et al. Giant cell hepatitis with autoimmune hemolytic anemia in early childhood: Long-term outcome in 16 children. *J Pediat.* 2012; 159:127-132.
11. Myers RK, McGavin MD, Zachary JF. Cellular adaptations, injury and death: Morphologic, biochemical and genetic

bases. In: McGavin MD, Zachary JF, eds. *Pathologic Basis of Veterinary Disease*. 5th ed. St. Louis, MO: Mosby Elsevier; 2012:43-44.

12. Polkes AC, Giguere S, Lester GD, Bain FT. Factors associated with outcome in foals with neonatal isoerythrolysis (72 Cases, 1988 –2003). *J Vet Intern Med*. 2008; 22:1216-1222.

13. Poonacha KB, Smith BJ, Donahue JM, Tramontin RR. Leptospiral abortion in horses in central Kentucky. *Proc 36th Ann Convention Am Asso Eq Practitioners*. 1991; 36:397-402.

14. Popper H, Schaffner F. Pathophysiology of cholestasis. *Hum Pathol*. 1970; 1:1-24.

15. Portenza L, Luppi M, Barozzi P, Rossi G. HHV-6 in syncytial giant cell hepatitis. *NE J Med*. 2008; 359:593-602.

16. Raj S, Stephen T, Debski RF. Giant cell hepatitis with autoimmune hemolytic anemia: A case report and review of pediatric literature. *Clin Pediatr*. 2011; 50:357-9.

17. Shaffner F, Popper H. Morphologic studies in neonatal cholestasis with emphasis on giant cells. *Ann NY Acad Sci*. 1963; 111:358-374.

18. Snyder PW. Diseases of immunity. In: McGavin MD, Zachary JF, eds. *Pathologic Basis of Veterinary Disease*. 5th ed. St. Louis, MO: Mosby Elsevier; 2012:263-264.

19. Torbenson M, Hart J, Westerhoff M, Azzam RK. Neonatal giant cell hepatitis: Histological and etiological findings. *Am J Surg Pathol*. 2010; 34:1498-1503.

20. Wilke IW, Prescott JF, Hazlett MJ, Maxie MG, van Dreumel AA. Giant cell hepatitis in four aborted foals: A possible

leptospiral infection. *Can Vet J*. 1988; 29:1003-4.

21. Wong DM, Alcott CJ, Clark SK, Jones DE. Alloimmune neonatal neutropenia and neonatal isoerythrolysis in a Thoroughbred colt. *J Vet Diag Invest*. 2013; 24: 219-226.

CASE II: A15-9631 (JPC 4065767).

Signalment: 1-year-old, gelding, Arabian horse (*Equus ferus caballus*)

History: Forty days after being gelded, vaccinated (annual vaccines plus tetanus antitoxin), and de-wormed (ivermectin), this horse was acutely anorectic and ataxic in the morning with progression to recumbency by afternoon. On physical examination at the Veterinary Teaching Hospital later that day, the horse was recumbent in the trailer, depressed but responsive, and hypothermic (92.2 F). Other abnormal physical examination findings included hyperpnea (28 breaths per minute), intermittent vertical nystagmus, bilateral inconsistent menace response, mydriasis and delayed pupillary light reflex, prolonged capillary and jugular refill times, icterus, and dehydration.

Gross Pathology: Icterus, hemoabdomen, perirenal hemorrhage, subendocardial hemorrhage
Liver—pale yellow-brown, flaccid, 2.3 Kg (0.99% body weight)

Laboratory Results:

Test	Result	Reference Range
Packed cell volume (PCV)	58%	35-50%
Segmented neutrophils	0.4 x 10 ³ /μL	6.0-12.0 x 10 ³ /μL

Total Protein	7.6 g/dL	5.7-8.1 g/dL
Lactate	7.2 mmol/L	<2 mmol/L
Fibrinogen	112 mg/dL	115-289 mg/dL
Glucose	<20 mg/dL	73-124 mg/dL
Blood urea nitrogen (BUN)	3 mg/dL	8-27 mg/dL
Creatinine	2.0 mg/dL	0.6-1.8 mg/dL
TCO ₂	19 mmol/L	23-31 mmol/L
Anion gap	26.4 mmol/L	12-20 mmol/L
Aspartate aminotransferase (AST)	3,563 IU/L	206-810 IU/L
Alkaline phosphatase	933 IU/L	109-331 IU/L
γ-Glutamyl transferase (GGT)	158 IU/L	12-46 IU/L
Creatine kinase (CK)	9811 IU/L	88-453 IU/L
Bilirubin	21.1 mg/dL	0.10-2.60 mg/dL
Unconjugated	15.3 mg/dL	
Conjugated	5.8 mg/dL	
Blood ammonia	254.4 μmol/L	25.0-75.0 μmol/L

Aerobic and anaerobic bacterial culture: no significant growth.

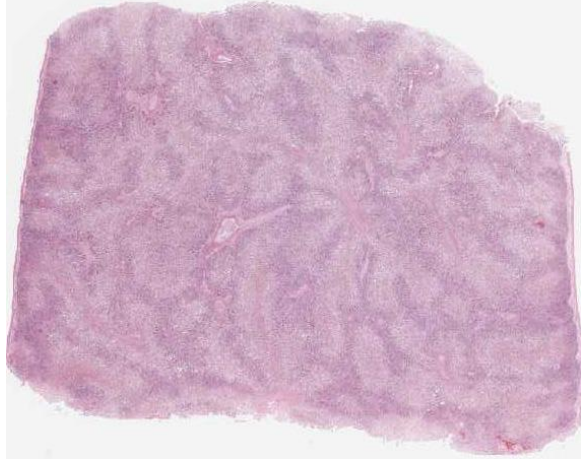
PCR for Theiler's disease-associated flavivirus (TDAV), Cornell University Animal Health Diagnostic Center: nNegative.

Histopathologic Description: Swelling, lysis, and drop-out of hepatocytes affected all hepatic lobules and were centrilobular to massive. Hepatocytes in lobular centers were generally not recognizable. In the lobular periphery, where viable parenchyma remained, hepatic plates were disrupted and hepatocytes had vacuolated cytoplasm. Brown crystals were in the cytoplasm of periportal hepatocytes. Brown granular pigment was in Kupffer cells. Inspissated bile was observed in a few canaliculi. There was patchy increase in fibrous tissue and mononuclear leukocytes (mainly lymphocytes) in portal tracts, but neither inflammation nor fibrosis was severe. Bile duct proliferation was not appreciated.

Changes in the cerebrum (slide not submitted to WSC) included increased space around vessels and cortical neurons with Alzheimer type II astrocytes (hypertrophied and hypochromatic nuclei). These changes were considered consistent with hepatic encephalopathy. In addition, many deep cortical neurons had ischemic change with a shrunken angular profile, intense cytoplasmic eosinophilia, and pyknosis.

Contributor's Morphologic Diagnosis:

Submassive hepatic necrosis



Liver, horse. The retiform pattern noted at subgross results from diffuse centrilobular and midzonal hepatocellular necrosis (pale areas), contrasted with the remaining viable periportal hepatocytes, which stain more intensely. (HE, 4X)

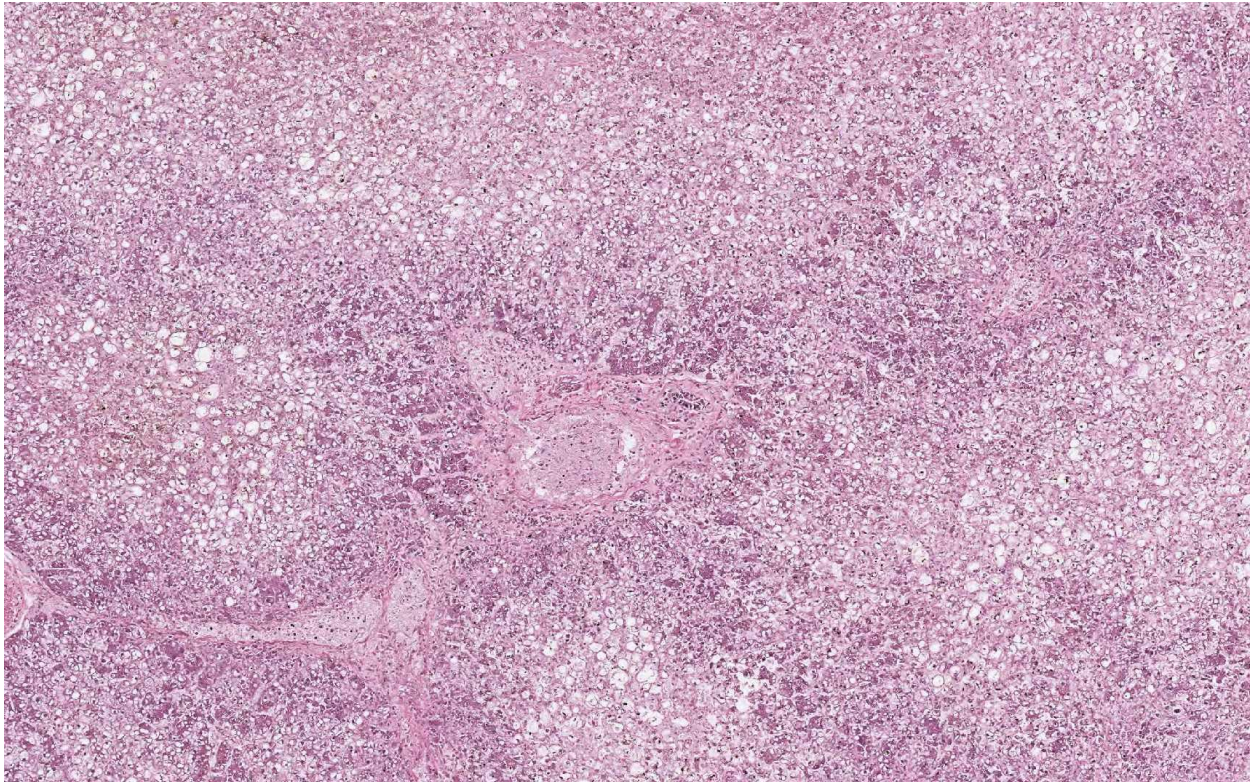
Contributor's Comment: The laboratory results—especially hypofibrinogenemia, decreased BUN, hypoglycemia, elevated hepatic enzyme activity, hyperbilirubinemia, and hyperammonemia—and the history and clinical signs all pointed to liver disease with hepatic encephalopathy as a likely explanation for the neurologic signs. The initial differential diagnosis included Theiler's disease (equine serum hepatitis), pyrrolizidine alkaloid or other hepatotoxicosis, ascending cholangiohepatitis, chronic hepatitis, and hepatic steatosis.

Postmortem gross and histologic lesions were typical of Theiler's disease, hence the PCR testing for Theiler's disease-associated virus (TDAV). This horse was negative by PCR for TDAV, but the serum was positive for a previously unreported non-flavivirus that is under investigation (personal communication, Drs. Bud Tennant, Tom Divers and colleagues at Cornell University and Columbia University).

Equine serum hepatitis or Theiler's disease was first described in 1919, when Arnold Theiler reported acute hepatic atrophy and hepatitis in South African horses vaccinated

against African horse sickness with an equine antiserum-containing live virus vaccine.⁶ Today, Theiler's disease is usually recognized in horses 4-10 weeks after injection with a product that contains equine serum or plasma, though some affected horses have no history of injection with equine blood-containing biologic products. Although the incubation period is long (42-90 days), clinical disease (subclinical cases are also recognized) is fulminating with acute hepatic failure and death within 24 hours in up to 90% of clinically ill horses. At autopsy, the carcass is icteric. The liver is generally close to normal size, but flaccid ("dish-rag" liver) due to massive necrosis with loss of so many hepatocytes. The histologic lesion is centrilobular to massive necrosis with mild, mainly lymphocytic, inflammation of portal tracts. Surviving periportal hepatocytes are swollen with vacuolated cytoplasm.

Theiler's disease has long been suspected to be a viral hepatitis, but the first candidate virus, Theiler's disease-associated virus (TDAV, a pegivirus in the Flaviviridae family), was only identified a few years ago in horses treated with equine antiserum to botulinum toxin.¹ Another pegivirus called equine pegivirus has been identified in horses, but has not been documented to cause hepatitis.⁴ The recently discovered non-primate hepacivirus (NPHV, equine hepacivirus) is another member of the Flaviviridae family that is hepatotropic and can result in transient or chronic infection with elevated hepatic enzymes and hepatitis in horses.³⁻⁵ Many horses (30-40%) have serum antibodies to NPHV; fewer horses have detectable viral RNA in the peripheral blood. The horse has been proposed as an animal model of viral hepatitis because NPHV is so closely related to the human hepatitis C virus.



Liver, horse. Higher magnification demonstrating the differential staining between hepatocytes in centrilobular and midzonal areas and those in the periportal areas. (HE 80X)

JPC Diagnosis: Liver: Necrosis, centrilobular to midzonal, diffuse with hepatocellular lipidosis.

Conference Comment: Although the majority of cases of equine serum hepatitis are associated with prior administration of equine biologics, cases have also been documented in horses with no history of prior injection. While Theiler's disease-associated virus has been proposed as an etiology for this condition,¹ additional research is necessary to prove definitive causation and fulfill Koch's postulates.² It is also unclear what percentage of horses develop subclinical hepatic disease after exposure to equine origin biologics as the disease is rarely diagnosed prior to development of hepatic failure; however, some animals have been known to survive after mild disease. Histologic findings often suggest a subacute process, which contrasts with the relatively acute clinical course of

disease. Lesions range from the presence of abundant degenerate and/or necrotic hepatocytes to complete loss of parenchymal cells. Many hepatocytes are often completely lost, leaving behind variable numbers of degenerate and lipid-filled hepatocytes, dilated congested sinusoids, and collapsed stromal remnants. Hemorrhage and acute necrosis are not typical findings. Other common features, albeit varying in severity, include low numbers of inflammatory cells, mild fibrosis in portal areas and an increase in bile duct profiles.²

In this case, conference participants described diffuse loss of hepatic cord architecture with hepatocellular degeneration, necrosis and loss. There is stromal collapse and mild portal bridging fibrosis. The brown pigment present within Kupffer cells and hepatocytes was interpreted as hemosiderin. The section is

moderately autolytic and there is abundant acid hematin present.

We thank the contributor for providing clinical pathology data with the submission, which greatly enhances the teaching and learning value of the case. Severe neutropenia is most commonly associated with endotoxemia, but the precise etiology is difficult to ascertain in this case. Elevated packed cell volume (PCV) is likely secondary to dehydration and the normal total protein is indicative of hypo-proteinemia in a dehydrated animal. Low fibrinogen, blood urea nitrogen, elevated ammonia and low glucose are indicators of liver failure. The profoundly low glucose is not compatible with life and may indicate some degree of artifact. The decreased TCO₂ and elevated anion gap are indicative of a metabolic acidosis and the unmeasured anions in this case include lactate and renal acids. Elevated AST is secondary to both myocyte and hepatocyte damage and elevated CK provides additional evidence of muscle damage. Elevated GGT and ALP are both indicators of cholestasis and the most common cause of elevated total bilirubin horses is anorexia. The hyperbilirubinemia in this case is higher than can be attributed to anorexia alone and, therefore; the remarkable hepatic changes likely contribute to the elevation. Elevated bilirubin can also be seen in cases of endotoxemia due to impaired excretion of conjugated bilirubin into the biliary tract.

Contributing Institution:

Purdue University

Animal Disease Diagnostic Laboratory:

<http://www.addl.purdue.edu/>

Department of Comparative Pathobiology:

<http://www.vet.purdue.edu/cpb/>

References:

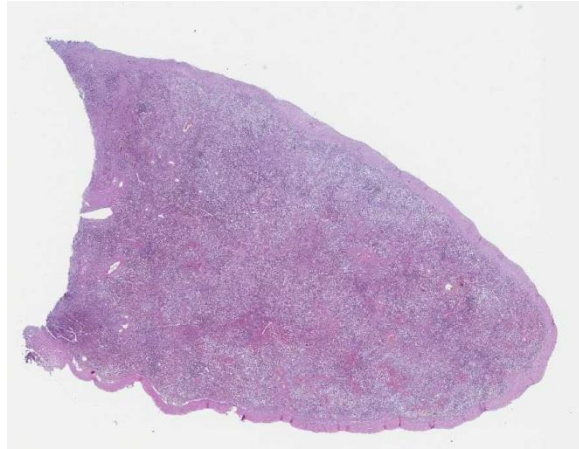
1. Chandriani S, Skewes-Cox P, Zhong W, Ganem DE, et al. Identification of a previously undescribed divergent virus from the Flaviviridae family in an outbreak of equine serum hepatitis. 2013. *Proc Natl Acad Sci USA*. 2013; 110(15):E1407-E1415.
2. Cullen JM, Stalker MJ. Liver and Biliary System. In: Maxie MG, ed. *Jubb, Kennedy, and Palmer's Pathology of Domestic Animals*. 6th ed. Vol 2. St. Louis, MO: Elsevier; 2015:312-313.
3. Pfaender S, Cavalleri JMV, Walter S, Doerrbecker J, et al. Clinical course of infection and viral tissue tropism of hepatitis C virus-like nonprimate hepaciviruses in horses. *Hepatology*. 2015; 61(5):447-459.
4. Ramsay JD, Evanoff R, Wilkinson TE, Divers TJ, et al. Experimental transmission of equine hepacivirus in horses as a model for hepatitis C virus. *Hepatology*. 2015; 61(5):1533-1546.
5. Scheel TKH, Kapoor A, Nishiuchi E, Brock KV, et al. Characterization of nonprimate hepacivirus and construction of a functional molecular clone. *Proc Natl Acad Sci USA*. 2015; 112:2192-2197.
6. Stalker MJ, Hayes MA. Liver and biliary system. In: Maxie MG, ed. *Jubb, Kennedy, and Palmer's Pathology of Domestic Animals*. 5th ed. Vol. 2. Elsevier, St. Louis, MO; 2007:297-388.

CASE III: 705-14 (JPC 4066679).

Signalment: 10-year-old, neutered female, dog, Pekingese (*Canis familiaris*)

History: The dog was presented to the veterinary hospital with a history of apathy and severe anemia. Due to a previous

diagnosis of hemolytic anemia, the dog received prednisolone (10 mg BID) and doxycycline (5 mg/kg IV bid), for two weeks, and a blood transfusion was performed 40 days prior to admission. One week after the admission, a blood sample was collected for total blood cell count and serological tests for detecting anti-



Spleen, dog. The spleen parenchyma is expanded by large numbers of macrophages, effacing the normal red and white pulp architecture. (HE, 5X).

Leishmania antibodies. At physical examination, the cornea of the left eye was diffusely opaque, and there was moderate exophthalmos. Ophthalmic examination revealed retinal detachment. The clinical condition of the dog was followed-up for two months, and total blood cell count was performed weekly. During this period, the dog received three blood transfusions. The animal died two and half months after the admission, despite medical treatment.

Gross Pathology: The dog was in good body condition. The cornea of the left eye was diffusely opaque and whitish. There was moderate exophthalmos of the left eye. The upper and lower incisor teeth were absent. The cervical, popliteal and mesenteric lymph nodes were enlarged. On the cut surface, these lymph nodes were diffusely light brown and soft (interpreted as hyperplasia and hemosiderosis). The spleen was markedly enlarged. The splenic capsule

was thickened by fibrosis and with several whitish plaques (1.0 to 3.0 mm in thickness) of chronic active inflammation (perisplenitis with multifocal hyperemia). On the cut surface, the splenic parenchyma protruded and it was firm (carnous) and reddish, with multiple small white foci. The liver was diffusely pale red with multifocal white foci (1.0 mm in diameter) in the parenchyma. The lungs were moderately congested and edematous. Mild myxomatous valvular degeneration was observed in the mitral valve. There were several petechiae in the epicardium of left ventricle and in the peritoneum. Dark red areas (approximately 2.0 cm in diameter), with sharp edge were observed in the parenchyma of the right and left kidney (acute infarction).

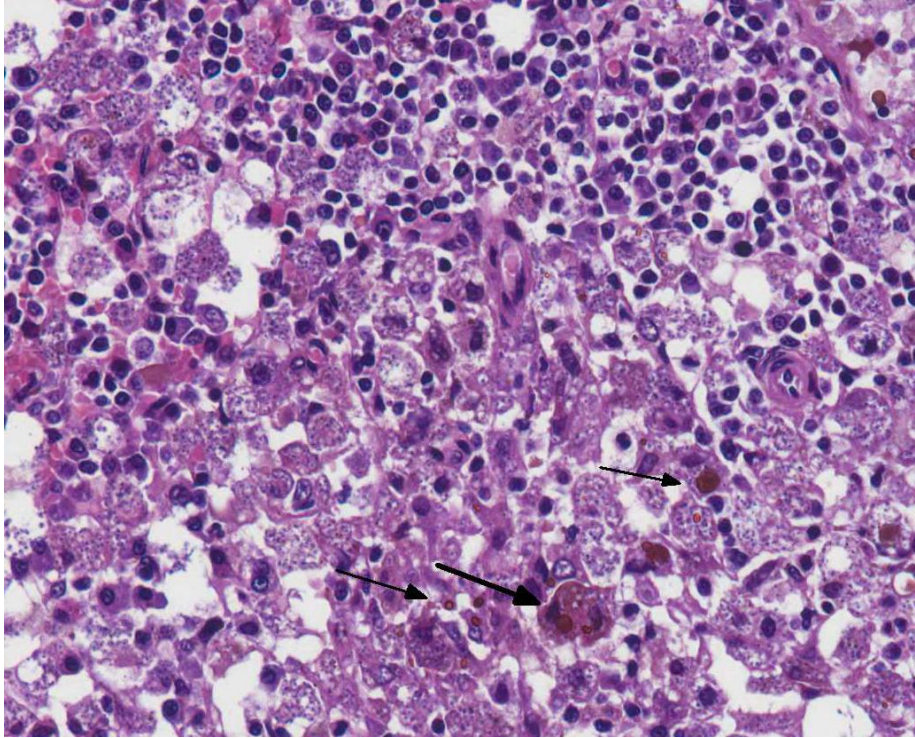
Laboratory Results: The initial serological tests resulted in positive indirect immunofluorescence reaction (RIFI) (1:40 dilution), and negative by ELISA, whereas the second serological tests were positive by both techniques (i.e. RIFI and ELISA).

The dog was observed for two months and total blood cell count analyses were performed weekly. Overall, the dog had marked anemia, leukopenia, and thrombocytopenia. Clinical pathology results are presented in Table 1.

After the last transfusion, i.e. 62 days after the first hematological evaluation, the RBC, HCT, and hemoglobin values were within the reference range.

Concomitantly with the fourth hematological evaluation, a bone marrow aspiration was performed. It was noticed the paucity of hematopoietic precursors, mainly from the erythroid lineage. Serological tests at this time resulted in positive ELISA and negative RIFI.

All hematological analyses revealed reduced numbers of platelets and lymphocytes. The numbers of monocytes remained below the



Spleen, red pulp. The red pulp is replaced by large numbers of amastigote-laden macrophages admixed with numerous plasma cells and fewer lymphocytes. Moderate numbers of macrophages (arrows) contain phagocytized erythrocytes.

reference range in most of the hematological exams.

Histopathologic Description: Spleen: The normal splenic architecture is markedly distorted due to complete replacement of the red and white pulp by numerous macrophages, moderate numbers of plasma cells, fewer lymphocytes, and occasional neutrophils, that expand the cords, fill the sinuses and invade the splenic trabeculae. Macrophages are enlarged and contain myriad of 2.0-4.0 μm , ovoid, intracytoplasmic amastigotes (Fig. 3) with a 1.0 μm nucleus, surrounded by a 1.0-2.0 μm clear zone and a kinetoplast perpendicular to the nucleus (compatible with amastigotes of *Leishmania* spp.). Multifocal areas of the capsule are expanded due to deposition of variable amounts of fibrous connective tissue and infiltration of scattered lymphocytes, plasma cells, and macrophages.

Occasional areas of neovascularization are within the capsule. There are scattered areas of karyorrhectic and cellular debris (lytic necrosis) containing occasional viable and degenerate neutrophils admixed with variable amounts of an eosinophilic beaded to fibrillar material (fibrin). There is multifocal histiocytic erythrophagocytosis, rare megakaryocytes, and numerous macrophages containing intracytoplasmic granular and brown pigment (hemosiderosis).

Bone marrow (proximal femur): The marrow parenchyma is completely replaced (myelophthisis) by numerous macrophages, moderate plasma cells and fewer lymphocytes. Macrophages contain myriad of basophilic structures similar to those described in the spleen (Fig. 4). Multifocally, are areas of karyorrhectic and cellular debris (lytic necrosis) containing occasional viable and degenerate neutrophils admixed with variable amounts of an eosinophilic beaded to fibrillar material (fibrin). There is multifocal hemosiderosis.

Tissues not submitted:

Lymph nodes present changes similar to those described in the spleen. Additionally, moderate lymphoid hyperplasia and increased plasma cell differentiation are observed. Macrophages containing myriad of amastigotes of *Leishmania* spp. are seen within lymphatic sinus, medullary cords,

cortical and paracortical regions. In the liver there are multiple areas with loss of hepatocytes and infiltration of macrophages, plasma cells and lymphocytes. Some macrophages are loaded with amastigotes of *Leishmania* spp. In both organs there is moderate multifocal hemosiderosis.

The kidneys presented with moderate membranous glomerulonephropathy. The Lumina of several tubules are ectatic, and contain aggregates of eosinophilic material (protein casts).

Amastigotes of *Leishmania* spp. were detected by immunohistochemistry (Streptavidin-biotin-peroxidase) in the spleen (Fig. 5) and in the bone marrow (Fig. 6 and 7).

Contributor's Morphologic Diagnosis:

Spleen: Splenitis and perisplenitis, histiocytic and plasmacytic, diffuse, severe, with myriad of intrahistiocytic amastigotes, etiology consistent with *Leishmania* spp.

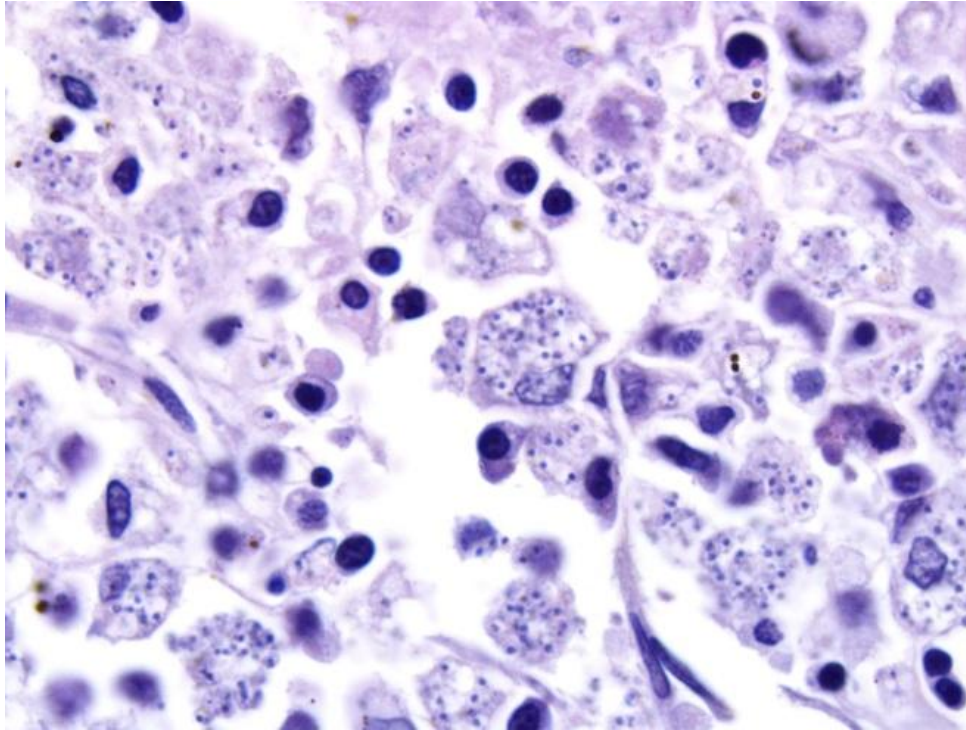
Bone marrow: Myelitis, histiocytic and lymphoplasmacytic, diffuse, severe, with myriad of intrahistiocytic amastigotes, etiology consistent with *Leishmania* spp.

Contributor's Comment: Canine leishmaniasis (CanL) is a major global zoonosis, potentially fatal to humans and dogs. Dogs are the main reservoir of the infection to humans.³ The disease is endemic in more than 70 countries in the world and occurs predominantly in the southern Europe, Africa, South and Central America.¹¹ While *Leishmania infantum* (synonym *L. chagasi*) occurs in Latin America, as well as in the Mediterranean climate regions of the Old World, *Leishmania donovani* infections are restricted to the (sub-) tropics of Asia and

Africa. In these former regions, transmission is mostly anthroponotic.⁹ In Latin America, approximately 90% of the cases of human visceral leishmaniasis are reported in Brazil, and occur in almost all of the states of the country. The higher incidence of the disease in humans takes place in the northeast region of the country (65% of the cases), followed by the southeast (14%) north (14%) and centerwest (14%).^{3,6} Currently, the disease is gradually spreading to the south and west regions of the country.^{3,10} Studies comparing the incidence or prevalence of the disease in dogs in different regions of the country are scarce. In Belo Horizonte, capital of the state of Minas Gerais, CanL is considered endemic with increasing seroprevalence in the canine population. From 1994 to 2000, this prevalence was estimated in 3.6% of all dogs of the county. In 2007, this index increased to 9.3%.^{3,8}

The life cycle of *Leishmania* spp. involves two hosts – a phlebotomine sand fly vector (genus *Lutzomyia* in the New World) and a mammal (including rodents, canids, or humans). *Leishmania* spp. occurs as flagellated, extracellular promastigotes in the gut of sand fly vectors. Infection occurs when a feeding sand fly deposits metacyclic promastigotes into the dermis of the host. In mammalian hosts, *Leishmania* spp. occur as amastigotes (2.0 to 3.0 µm in diameter) within mononuclear phagocytes in the skin, bone marrow, and visceral organs.¹¹ Although vector-borne is the most important route of transmission, CanL can also be transmitted in the absence of the invertebrate vector.¹³

CanL is manifested by a broad spectrum of clinical signs and degrees of severity. In the typical CanL case, history and physical examination include skin lesions, local or generalized lymphadenomegaly, emaciation,



Bone marrow. Macrophages, which largely replace immature erythropoietic elements, contain numerous 2-3µm amastigotes with a central nucleus and a rod-shaped kinetoplast. (HE, 400X)

cachexia, splenomegaly, anorexia or increased appetite, lethargy, temporal muscle atrophy, exercise intolerance, polyuria/polydipsia, ocular lesions, epistaxis, onychogryphosis, lameness, vomiting, and diarrhea.⁴ Serum biochemistry findings in dogs with clinical leishmaniasis include, most commonly, serum hypoproteinemia with hyperglobulinemia and hypoalbuminemia, resulting in a decreased albumin/globulin ratio. Mild increases of liver enzyme activities are frequent; however, grossly elevated liver enzyme activities, severe azotemia, or both, are found in only a minority of dogs with leishmaniasis. Proteinuria and some renal abnormalities develop in most dogs with this disease.¹

Hematological parameters and the serum biochemical profile in *L. infantum*-infected dogs have limited diagnostic value. However, they can be useful biomarkers for

evaluating the clinical progress of infected animals and may also contribute to the understanding of CanL pathogenesis. One the most remarkable characteristics of CanL-associated hematological disorders is anemia, characterized as non-regenerative normocytic or normochromic. The leucocyte alteration in the blood of symptomatic dogs

includes leucopenia characterized by monocytopenia, lymphopenia, and eosinopenia.¹ The pathogenesis of hematological changes in both red and white blood cells is often related to bone marrow disorders associated with diminished erythropoiesis due to intense bone marrow parasitism. In addition, anemia can be related to reduced plasma iron due to abnormal iron retention by macrophages and increased levels of hepcidin, typical of anemia of chronic diseases. Anemia could also be related to increased hemolysis in enlarged spleen and liver associated with inflammatory response to *L. infantum* and to decreased production of erythropoietin by damaged kidneys.⁷

Severely affected dogs are usually cachectic and suffer from muscle atrophy. The skin and hemolymphatic organs are primarily affected. Generalized lymphadenomegaly and splenomegaly are usually present. Hepatomegaly may be present, but is less

Hematology and biochemical parameters	First haematological evaluation	Second haematological evaluation (post transfusion)	Third haematological evaluation	Average of 11 haematological evaluations (4 th to 14 th) -mean(min-max)-	15 th haematological evaluation - 62 days after the first evaluation (post transfusion)	Reference range
Erythrocytes (million/mm ³)	2.16	2.35	1.57	3.06(1.45-4.13)	8.0	5.5-8.5
Hemoglobin (g%)	4.2	4.8	3.3	7.24(3.7-9.1)	19.3	12-18
Hematocrite (HCT) (%)	15	16	11	22.63(14-29)	53	37-55
VCM (fl)	69.44	68.09	70.06	75.47(62.11-96.55)	66.25	60-77
CHCM (%)	28.00	30.00	30	31.85(26.43-35.5)	36.42	31-36
HCM (pg)	19.44	20.43	21.02	23.88(22.03-26.67)	24.13	19.0-24.5
RDW (%)	17.8	16.8	17.9	15.12(13.6-17.6)	13.2	12-15
Metarubricytes (%)	16	16	18	20.81(4-47)	100	Absent
Total leukocytes (mm ³)	2672	2465	2347	5365(1544-11308)	1645	6000-17000
Bastonetes (mm ³)	106.88	49.30	140.82	560.58(33.53-2398)	Not performed	0-300
Neutrophils (mm ³)	1175.68	1972.00	1595.96	4121.39(218-10064.1)	1348.90	3000-11500
Lymphocytes (mm ³)	1336.0	345.10	563.28	553.29(54.5-1733.34)	197.40	1000-4800
Monocytes (mm ³)	53.44	98.60	46.94	312.31(30.88-1017.72)	65.80	150-1350
Eosinophils (mm ³)	Not performed	Not performed	Not performed	78.25(33.53-104.3)	32.90	
Platelets (mm ³)	38000	16000	44000	59272(16000-131000)	60000	175000-500000
Urea (mg/dL)	120.5	41.1	27.1	31.26(21.1-46.4)	24.7	20-56
Creatinin (mg/dL)	1.5	0.82	0.53	0.79(0.74-0.9)	0.6	0.5-1.5
Alanin aminotransferase (U/L)	124.5	136.5	151.7	75.88(40.85-130)	727.8	0-110
Aspartate aminotransferase (U/L)	168	90.3	130.7	59.30(41.6-75.5)	4.98	0-100
Alkaline Fosfatase (U/L)	315	403.5	264.5	214.6(85-529)	725.5	20-156
Gama-glutamil transpeptidase (U/L)	Not performed	Not performed	Not performed	6.26(1.2-20.1)	187.9	0-25
Glucose (mg/dL)	59.5	110.35	78.49	83.60(76.78-91.8)	81.54	76-119
Total proteins (g/dL)	6.9	6.5	6.8	6.77(6.2-7.3)	7.3	5.4-7.5

Table 1.

common. Small nodular foci of inflammation may develop in various organs, including the skin and the kidneys. Mucosal ulcerations in the nasal cavity, stomach, intestine, and colon are occasionally observed. The typical histopathologic finding in the majority of affected tissues is an inflammatory reaction associated with macrophages in the presence or absence of *Leishmania* amastigotes. Amastigote numbers may vary from very few organisms within macrophages to large numbers in rarer events. Lymphoplasmacytic inflammation is also common in dogs with leishmaniasis.¹ Additionally, renal disease due to glomerulonephritis and interstitial nephritis is commonly associated with CanL due to *Leishmania infantum*.

Diagnosis of canine leishmaniasis is based on the presence of clinical signs together with positive specific antibody assay. Infection can be confirmed by demonstration of the parasites (amastigotes) on

touch prep stained (Wright-Giemsa) slides or in cultures of tissue aspirates or biopsy specimens of the spleen, liver, bone marrow, or lymph nodes.¹ Immunohistochemistry is a useful tool that significantly increases the sensitivity of histopathology for detecting amastigotes, and it is a genus-specific assay to confirm the diagnosis.¹²

JPC Diagnosis: 1. Spleen, red pulp: Splenitis, histiocytic and plasmacytic, diffuse, marked with numerous intracellular amastigotes.

2. Spleen: Reticuloendothelial hyperplasia with erythrophagocytosis and hemosiderosis.

3. Spleen: Extramedullary hematopoiesis.

4. Bone marrow: Myelitis, histiocytic and plasmacytic, diffuse, marked with numerous intracellular amastigotes.

Conference Comment: *Leishmania* sp. organisms primarily infect the monocyte-

macrophage system and the visceral manifestation bears many similarities to histoplasmosis. *Leishmania* amastigotes are able to survive and reproduce in macrophage phagolysosomes due in part to an increase in pH, and macrophage destruction occurs secondary to proliferation of the protozoa.¹⁴ The immune response includes both T helper 1 (Th1) and T helper 2 (Th2) mediated mechanisms and tissue damage occurs via a variety of methods including granulomatous inflammation, immune complex deposition and the formation of autoantibodies. Inefficient killing of the organism by macrophages leads to the various immune responses, eventually resulting in damage to a variety of tissues and an array of clinical manifestations discussed above.² Resistance to infection is based on a strong Th1 response, whereas a strong Th2 response can be deleterious⁵ due to immune complex deposition, particularly in renal glomeruli. The level of parasite burden also appears to play a role in the immune response effectiveness against the invading organisms. In dogs with a high parasite load CD8+ T Cells are less effective at lysing infected macrophages. Genetic susceptibility also plays a role in outcome of infection with certain breeds such as the German Shepherd, cocker spaniel, and boxer being more susceptible.⁴ The most common clinical manifestations of disease include skin, renal and/or ocular disease as well as epistaxis, and the disease is broadly divided into cutaneous, mucocutaneous and visceral forms. Enlargement of the spleen is very common and nearly always occurs in cases of visceral leishmaniasis.¹⁴ While leishmaniasis is more common in Mediterranean countries and South America, endemic foci are also present in North America including in Texas, Oklahoma, Ohio and Michigan.⁵

The conference histologic description was aligned very closely with the contributor's

description above. Conference participants were struck by the marked degree of effacement of both the splenic red pulp and bone marrow.

We thank the contributor for providing clinical pathology data with the submission, which greatly enhances the teaching value of the case. Participants discussed the third hematological evaluation and whether the anemia is regenerative or nonregenerative, but without a reticulocyte count it is difficult to determine with certainty. The presence of nucleated red blood cells (metarubricytosis) can be indicative of regeneration with concurrent reticulocytosis, but nucleated red blood cells can also be present in other conditions such as bone marrow damage from inflammation or necrosis, lead poisoning and due to splenectomy among other things. A normal MCV would support a nonregenerative anemia; additionally, the pancytopenia and histologic changes in the bone marrow also provide support for a nonregenerative anemia. Elevated ALT and AST are indicative of mild hepatocellular damage, which correlates with the histopathologic description mentioned above by the contributor in the tissues not submitted. The total protein is normal but a decrease in albumin and increase in globulin is likely present in this case, based on the degree of infection and ongoing inflammation, which is a common pattern in dogs afflicted with leishmaniasis, as mentioned above by the contributor.

Contributing Institution:

Veterinary School. Universidade Federal de Minas Gerais

www.vet.ufmg.br

References:

1. Baneth G, Solano-Gallego L. Leishmaniasis. In: Greene CE, ed. *Infectious diseases of the dog and cat*. 4th ed. Philadelphia, US: Elsevier Saunders; 2012:735-748.
2. Cooper BJ, Valentine BA. Muscle and Tendon. In: Maxie MG, ed. *Jubb, Kennedy, and Palmer's Pathology of Domestic Animals*. 6th ed. Vol 1. St. Louis, MO: Elsevier; 2015:240.
3. Diniz SA, Silva FL, Carvalho Neta AV, et al. Animal reservoirs for visceral leishmaniasis in densely populated urban areas. *J Infect Dev Ctries*. 2008; 2:24-33.
4. Koutinas AF, Koutinas CK. Pathologic mechanism underlying the clinical findings in canine Leishmaniosis due to *Leishmania infantum/chagasi*. *Vet Pathol*. 2014;51(2):527-538.
5. Mauldin EA, Peters-Kennedy J. Integumentary system. In: Maxie MG, ed. *Jubb, Kennedy, and Palmer's Pathology of Domestic Animals*. 6th ed. Vol 1. St. Louis, MO: Elsevier; 2015:663.
6. Ministério da Saúde. *Manual de vigilância e controle da leishmaniose visceral*. Brasília, BR: Editora MS; 2006.
7. Nicolato RC, Abreu RT, Roatt BM, et al. Clinical forms of canine visceral Leishmaniasis in naturally *Leishmania infantum*-infected dogs and related myelogram and hemogram changes. *Plos One*. 2013;8(12):1-9.
8. Papa DN. Perfil epidemiológico da Leishmaniose Visceral em cães diagnosticados no Laboratório da Escola de Veterinária da Universidade Federal de Minas Gerais Belo Horizonte 2004 a 2008. Master's degree dissertation, Escola de Veterinária, Universidade Federal de Minas Gerais, 2010.
9. Ready PD. Epidemiology of visceral leishmaniasis. *Clin Epidemiol*. 2014; 6:147-154.
10. Romero GAS, Boelaert M. Control of visceral Leishmaniasis in Latin America – A systematic review. *Plos Negl Trop Dis*. 2010;4(1):1-17.
11. Solano-Gallego L, Miró G, Koutinas A, et al. LeishVet guidelines for practical management of canine leishmaniosis. *Parasite Vect*. 2011;4:86.
12. Tafuri WL, Santos RL, Arantes MRE, et al. An alternative immunohistochemical method for detecting *Leishmania* amastigotes in paraffin-embedded canine tissues. *J Immunol Methods*. 2004; 292:17-23.
13. Turchetti AP, Souza TD, Paixão TA, Santos RL. Sexual and vertical transmission of visceral leishmaniasis. *J Infect Dev Ctries*. 2014; 8:403-407.
14. Valli VEO, Kiupel M, Bienzle D. Hematopoietic System. In: Maxie MG, ed. *Jubb, Kennedy, and Palmer's Pathology of Domestic Animals*. 6th ed. Vol 3. St. Louis, MO: Elsevier; 2015:1

CASE IV: 21966 (JPC 4066536).

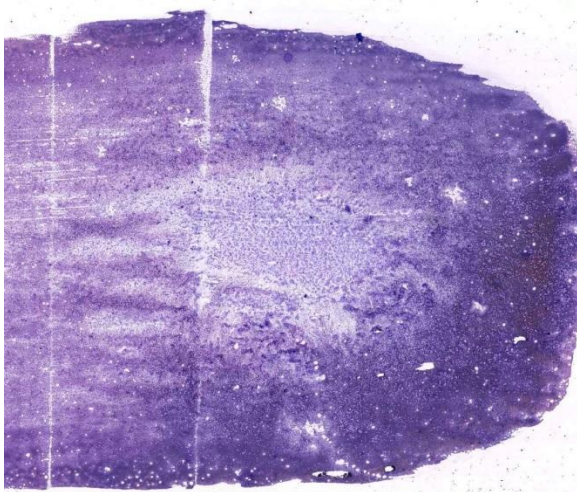
Signalment: 10-year-old spayed female Miniature Dachshund dog, (*Canis familiaris*)

History: The dog was presented with a gingival mass on right maxilla, which had been enlarging for 2 to 3 weeks. Both right and left mandibular lymph nodes were enlarged by palpation. Thoracic CT scan revealed no metastasis in the lung.

Gross Pathology: The mass measured 3.7 x 2.4 x 1.1 cm and was partly red and black.

Laboratory Results: None

Cytologic description: Fine-needle aspiration of the mass was performed. The smear was highly cellular and consisted of monomorphic cells, most of which are in clusters. The cells had a round nucleus in pale abundant cytoplasm. The cytoplasm was mild to moderately vacuolated and small black pigment noted in a few cells. Cells showed mild to moderate anisocytosis and anisokaryosis, and mitotic figures were rarely seen.



Fine needle aspirate, oral mass, dog. A densely cellular, fine needle aspirate was submitted digitally for examination. (Wright's-Giemsa, 4X).

From the left mandibular lymph node, similar morphologic cells were mainly acquired, and several small lymphocytes, plasma cells, and eosinophils were noted. On the smear of right mandibular lymph node, lymphoid cells, predominantly small mature lymphocytes with some lymphoblasts and plasma cells were seen. Scattered melanophages were also observed.

Contributor's Interpretation:

1. Gingival mass: Malignant melanoma with metastasis to the left mandibular lymph node was suspected.
2. Right mandibular lymph node: Reactive lymph node.

Histologic result: The mass was partly resected for histopathology. On histologic examination, the neoplastic cells invaded almost all of the mass and were arranged in nests supported by a fine fibrovascular stroma. The neoplastic cells had clear abundant cytoplasm and round to oval nucleus. The cytoplasm was vacuolated and small amount of brown pigment were observed in several cells. A few mitotic figures are noted. Both left and right mandibular lymph nodes were removed and submitted for the histopathology. Neoplastic cells infiltrated both lymph nodes, and especially in the left lymph node, they spread across a wide area.

Contributor's Comment: Tumors of melanocytic origin are relatively common in the dog. The malignancy of melanoma greatly depends on anatomic location, and oral melanoma is highly aggressive. Cytologic morphology of melanoma is various, showing the feature of epithelial cells, mesenchymal cells or discrete round cells. Balloon cell melanoma, which is a rare variant of melanocytic tumor, has been

reported in human, dog and cat.^{1, 3,8,9,10,11} Microscopically, the neoplastic cells are amelanotic and cytoplasm is vacuolated. Sebaceous carcinoma, liposarcoma, other clear cell neoplasm and granulomatous inflammation are listed as differentials. In this case, sebaceous carcinoma and liposarcoma were unlikely due to the location. The malignant neoplasia was more suspicious than inflammatory disease because of the morphologic atypia. Due to the small amount of granules that can be melanin pigments, melanoma was the primary rule-out; immunohistochemistry such as Melan-A is helpful for further diagnosis.

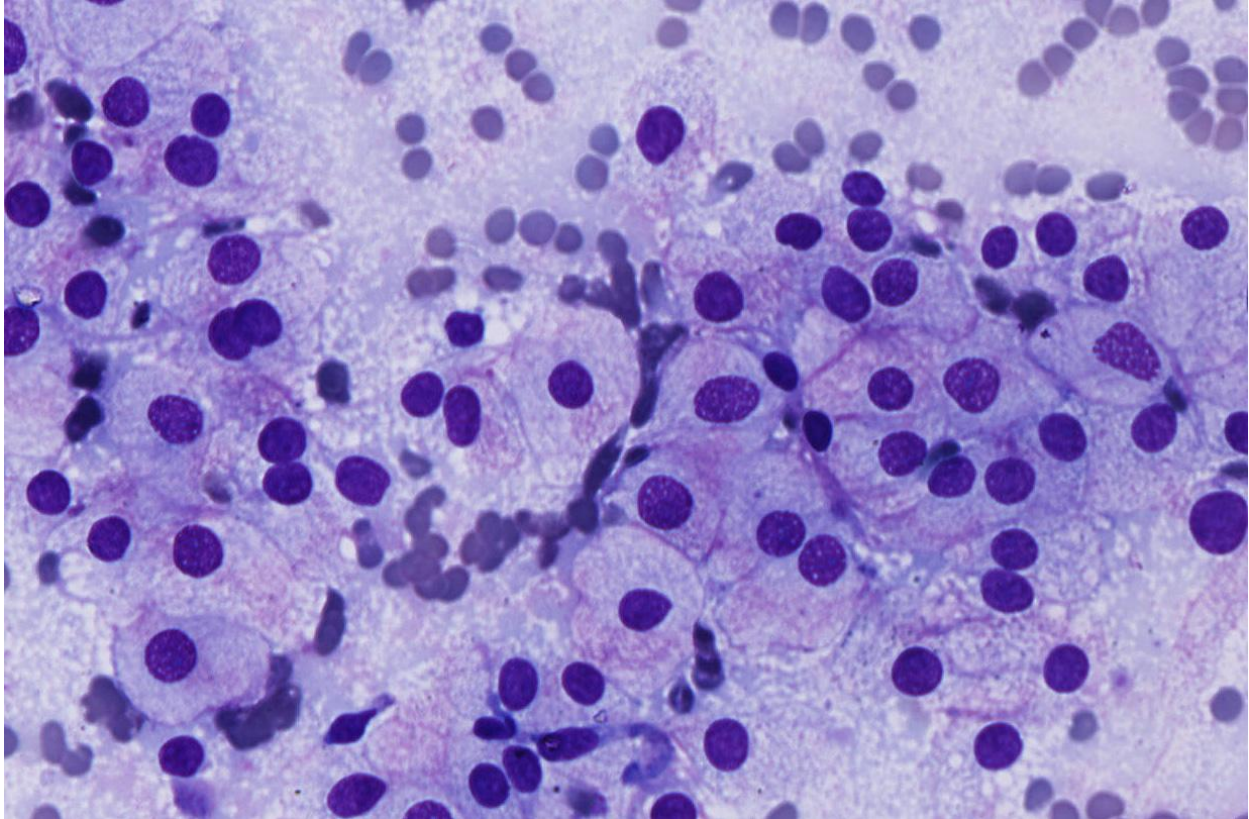
JPC Diagnosis: Fine needle aspirate, oral mass: Malignant neoplasm; differentials include amelanotic melanoma (balloon cell), rhabdomyoma, granular cell tumor, and oncocytoma.

Conference Comment: The neoplastic cells are round to spindled and arranged individually and in small aggregates; the cytoplasm is amphophilic and indistinctly vacuolated and a low to moderate subset of cells contain a pale, granular eosinophilic material in the cytoplasm, the origin of which is unclear. The cells have a single, central, round to oval nucleus with finely stippled chromatin, and 1-2 variably distinct nucleoli. Anisocytosis is mild and anisokaryosis is moderate, and the N:C is low; rare mitoses are observed. Other salient features include nuclear molding, a central fold in the nuclear membrane of few cells, and rare multinucleate cells. Features of malignancy are not striking in this sample, but the anisokaryosis, nuclear molding and presence of mitoses warrants a malignant interpretation. Many conference participants commented melanomas are usually more aggressive looking, particularly

in the oral cavity. A search for melanin was largely unrewarding, particularly with the digital slide only being scanned to 20X, but small amounts are seen in images of the histologic section provided by the contributor. Aside from the differential diagnoses listed above, conference participants remarked the cells resemble hepatocytes in animals with steroid hepatopathy, suggesting glycogen or another similar substrate may be present within the cytoplasm.

Differential diagnoses discussed include balloon cell melanoma, rhabdomyoma, granular cell tumor and oncocytoma. A definitive diagnosis is not possible without the use of immunohistochemistry, which was not performed by the contributor.

Balloon cell melanoma is an uncommon variant of melanoma most commonly described in the skin in both domestic animals and humans, and in cats is often localized to the head. The cells are described as epithelioid, large and round, with abundant finely vacuolated cytoplasm that generally lacks pigment.^{6,11} Glycogen (PAS positive) and lipid rich variants have been described, primarily in humans. Although the balloon cells may contain substances other than glycogen and other similar appearing non-melanocytic tumors may contain glycogen,¹¹ warranting a cautious interpretation of cytoplasmic features. The background of glycogen rich neoplasms is occasionally described as "tigroid," referring to a vague tiger striping pattern imparted by background constituents.⁴ Ultrastructural findings in balloon cell melanomas indicate the cytoplasmic vacuoles represent enlarged melanosomes. In addition to Melan A, balloon cell melanomas may stain for S-100 and neuron-specific enolase.^{1,11}



Fine needle aspirate, oral mass, dog. Neoplastic cells are polygonal with distinct cell borders, abundant vacuolated amphophilic cytoplasm with adherent pink fibrillar matrix. Nuclei exhibit rosy chromatin with mild anisokaryosis, and binucleated cells are frequent. (HE, 120X)

Rhabdomyomas, oncocytomas and granular cell tumors have a similar cytologic appearance with eosinophilic granular material in the cytoplasm, comparable to what is seen in a subset of cells in this case. The similar cytoplasmic appearance in oncocytomas and rhabdomyomas is related to the presence of large numbers of mitochondria, and in granular cell tumors is postulated to be due to metabolic abnormalities and accumulation of lysosomes.⁵ Rhabdomyomas are benign tumors of striated muscle and may occur in the larynx and tongue of domestic animals. Cells may have abundant cytoplasmic glycogen, suggested by PAS positivity.⁷ Oncocytomas are epithelial or neuroendocrine origin neoplasms which arise from oncocytes or oxyphil cells, and are described in the larynx of young dogs. The exact origin of granular cell tumors is unclear but they primarily occur in the oral

cavity and have been conjectured to be of Schwann cell origin. Rhabdomyomas and oncocytomas have benign behavior, and the behavior of granular cell tumors is not well defined. Both rhabdomyoma and oncocytoma have large pale cells with granular or foamy cytoplasm. The nucleus of oncocytoma is central, while the nucleus of rhabdomyoma may be central or peripheral and both have finely clumped chromatin and a single indistinct nucleolus. Multinucleate cells may be seen in rhabdomyoma. The indistinct nucleolus is a feature which may help distinguish them from balloon cell melanoma. Granular cell tumors are variably sized but typically have abundant granular eosinophilic cytoplasm and an eccentric nucleus. Pleomorphism may be moderate in each of the three tumors. Additional diagnostics which may help differentiate the tumors include desmin positivity in

rhabdomyoma, cytokeratin positivity in oncocytoma and PAS positivity (diastase resistance) in granular cell tumor.²

Contributing Institution:

Laboratory of Comparative Pathology and Department of Diagnostic Pathology, Graduate School of Veterinary Medicine, Hokkaido University, Japan

<http://www.vetmed.hokudai.ac.jp/>

References:

1. Blanchard TW, Bryant NJ, Mense MG. Balloon cell melanoma in three dogs: a histopathological, immunohistochemical and ultrastructural study. *J Comp Pathol.* 2001; 125:254-261.
2. Burkhard MJ. Respiratory Tract. In: Raskin RE, Meyer DJ, eds. *Canine and Feline Cytology*. 3rd ed. St. Louis, MO: Elsevier; 2016:155-156.
3. Cangul IT, van Garderen E, van der Linde-Sipman JS, van den Ingh TS, Schalken JA. Canine balloon and signet-ring cell melanomas: a histological and immunohistochemical characterization. *J Comp Pathol.* 2001; 125:166-173.
4. DeMay RM. *The Art and Science of Cytopathology*. Vol 2. 2nd ed. Hong Kong: American Society for Clinical Pathology; 2012:592.
5. Dunbar MD, Ginn P, Winter M, Miller KB, Craft W. Laryngeal rhabdomyoma in a dog. *Vet Clin Pathol.* 2012; 41(4):590-593.
6. Goldschmidt MH, Dunstan RW, Stannard AA, Tschanner CV, et al. *Histological classification of epithelial and melanocytic tumors of the skin of domestic animals*. Vol III. 2nd series. Washington D.C.: Armed Forces Institute of Pathology. 1998:38-39.
7. Hendrick MJ, Mahaffey EA, Moore FM, Vos JH, Walder EJ. *Histological classification of mesenchymal tumors of the skin and soft tissues of domestic animals*. 2nd series. Washington D.C.: Armed Forces Institute of Pathology. 1998:21.
8. Kao GF, Helwig EB, Graham JH. Balloon cell malignant melanoma of the skin. A clinicopathologic study of 34 cases with histochemical, immunohistochemical, and ultrastructural observations. *Cancer.* 1992; 69:2942-2952.
9. Mowat A, Reid R, Mackie R. Balloon cell metastatic melanoma: an important differential in the diagnosis of clear cell tumors. *Histopathology.* 1994; 24:469-472.
10. van der Linde-Sipman JS, de Wit MM, van Garderen E, Molenbeek RF, et al. Cutaneous malignant melanomas in 57 cats: identification of (amelanotic) signet-ring and balloon cell types and verification of their origin by immunohistochemistry, electron microscopy, and in situ hybridization. *Vet Pathol.* 1997; 34:31-38.
11. Wilkerson MJ, Dolce K, DeBey BM, Heeb H, et al. Metastatic Balloon Cell Melanoma in a Dog. *Vet Clin Pathol.* 2003; 32(1):31-6.

Joint Pathology Center
Veterinary Pathology Services



WEDNESDAY SLIDE CONFERENCE 2015-2016

Conference 18

23 March 2016

CASE I: 12 599 (JPC 4017817).

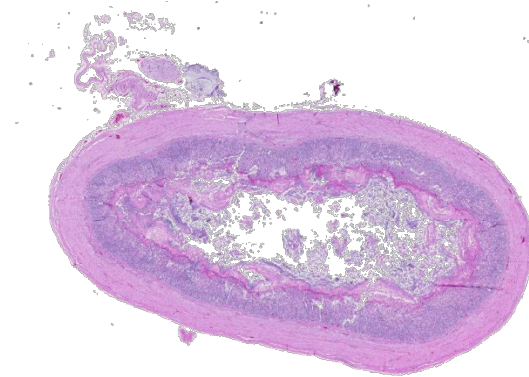
Signalment: 3-week-old female chicken (*Gallus gallus*)

History: This farm has two groups of 50 chicks each. One group is fed regular, non-medicated feed and the other group is fed organic feed. Twenty-five birds on the organic feed have died. The only clinical sign is a lack of interest in eating. The group fed regular feed is has no clinical signs.

Gross Pathology: The bird is emaciated with no body fat present. The crop and ventriculus contain a small amount of green feed material. The small intestinal mucosa is necrotic.

Laboratory Results: None

Histologic description: The small intestine has diffuse coagulative necrosis of the upper third of the mucosa including the villi, which forms a pseudomembrane over the surface. Numerous gram- positive bacilli are within the necrotic tissue.



Intestine, chicken. Cross section of jejunum in which the proximal 33% of the mucosa is necrotic and brightly eosinophilic. (HE, 6X)

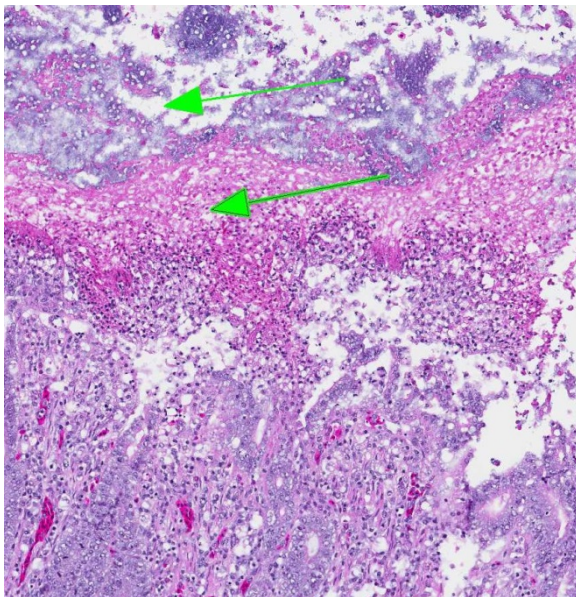
Contributor's Morphologic Diagnosis:
Small intestine: Necrotic enteritis

Contributor's Comment: Necrotic enteritis is an enterotoxemia caused by *Clostridium perfringens* types A and C. The disease affects domestic poultry, primarily birds 2-5 weeks of age, but older birds are also affected.

C. perfringens is normally found in the environment and is part of the normal flora

of birds. Disease occurs following an alteration in the intestinal microflora or a condition that results in damage to the mucosa (coccidia, salmonella, ascarid larva, mycotoxins). Diets high in indigestible, water-soluble, non-starch polysaccharides (wheat, rye, oats, and barley) are risk factors for the disease in birds.³ The organic feed in this case may have contained some of these carbohydrates and would explain why only birds fed this diet were affected.

Necrotic enteritis usually manifests as an acute disease with a sudden increase in flock mortality. There is also a subclinical form of the disease in which birds have reduced weight gain and poor feed conversion ratios due to poor digestion and absorption from the damaged intestinal mucosa.³ This bird was emaciated and may have had the subclinical form of the disease followed by the acute clinical disease terminally.

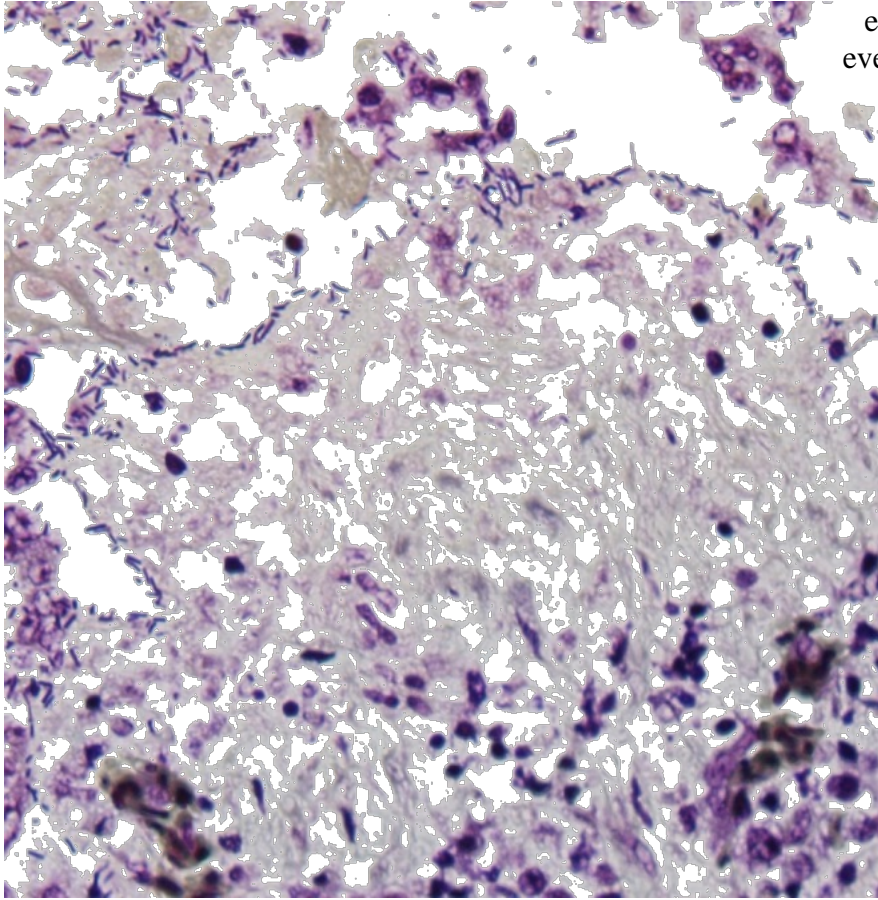


Intestine, chicken. The proximal 33% of the villi are replaced by an eosinophilic coagulum (lower arrow) which is covered by a thick blue layer of bacterial colonies. (HE, 100X)

JPC Diagnosis: Small intestine: Enteritis, necrotizing, circumferential, diffuse, severe with numerous mucosa-adherent bacilli.

Conference Comment: *Clostridium perfringens* is a rapidly growing, gram-positive anaerobe that specializes in tissue destruction and nutrient acquisition classically resulting in extensive necrosis. It has the potential to cause disease in most domestic animal species including cattle sheep, goats, pigs and horses, and often begins as an enterotoxemia, as seen in so-called “pulpy kidney” disease in sheep. The injurious mechanisms of *C. perfringens* are mediated through the actions of many toxins including α , β , ϵ and ι toxins as well as several other degradative enzymes that have cytotoxic effects on endothelial cells, enterocytes, extracellular matrix components and other tissues. The ultimate result is death of enterocytes and/or endothelial cells followed by absorption of toxins into the circulatory system where they can cause cell damage and disease in distant tissues such as the kidney and brain.⁴ *C. perfringens*-induced necrotic enteritis (NE), caused by *C. perfringens* type A (and in some cases) type C, is the most common clostridial enteric disease of poultry. It is most commonly seen in broiler chickens 2-6 weeks of age, but also occurs in many other avian species including turkeys and waterfowl as well as in older broiler chickens. Diagnosis is based on clinical and pathological findings; isolation of the organism and toxin does not prove causation as they can both also be found in the intestine of healthy birds. Other clostridial organisms which can cause disease in birds include *Clostridium colinum* which causes ulcerative enteritis, as well as *Clostridium difficile*, *Clostridium fallax* and *Clostridium baratii*.¹

A key element in the pathogenesis of *C. perfringens* induced NE in chickens is the pore-forming NetB toxin (which has some similarities to *C. perfringens* beta toxin). It creates a hole in the cell membrane that



Intestine, chicken. There are numerous robust bacilli lining the necrotic villi and remaining crypts (at left) and admixed within the overlying cellular debris. (Brown-Brenn, 600X)

results in leakage of cell contents and cell death and is apparently a central factor in disease pathogenesis. Strains of *C. perfringens* positive for the *netB* gene also carry additional virulence genes for toxins, other nutritional/metabolic factors related to fitness, and adhesins, which contributes to their ability to proliferate rapidly and cause disease. It is suggested the NetB toxin is a key initiating factor in the pathogenesis of NE, and may actually target endothelial cells in the lamina propria and not the intestinal epithelium. Key initiating events include colonization of the intestinal mucosa and degradation of the mucous layer, which allows toxins access to the enterocytes.²

Histologic lesions are characterized by extensive mucosal necrosis which may

extend into the submucosa or even the muscularis in severe cases. There is a sharp line of demarcation between necrotic and viable tissue and bacilli are seen trapped in fibrinonecrotic debris.¹ A key histologic feature in NE includes the presence of abundant large *C. perfringens* bacilli at the margin of the submucosa once the superficial mucosa has become necrotic and is sloughed, which may represent biofilm formation and be related to disease pathogenesis or progression.² Gross lesions are typically isolated to the small intestine, but may also be

seen in the ceca. The intestine is thin-walled, gas-distended and filled

with a dark brown, grey, and/or yellow-green fluid, while the mucosal surface is typically covered by a necrotic coagulum. Thickening of the intestinal wall may be seen in chronic cases and some affected chickens may develop cho-langiohepatitis.

The differential diagnosis includes coccidiosis, which may precede NE and can be differentiated by the presence of blood in the intestinal tract (which is not typically seen in cases of NE), and the presence of coccidial organisms. Ulcerative enteritis caused by *C. colinum* and histomoniasis are other diagnostic considerations.¹

Contributing Institution:

College of Veterinary Medicine
Virginia Tech

Blacksburg, VA 24061
www.vetmed.vt.edu

References:

1. Cooper KK, Songer JG, Uzal FA. Diagnosing clostridial enteric disease in poultry. *J Vet Diagn Invest.* 2013; 25(3):214-27.
2. Prescott JF, Parreira VR, Mehdizadeh GI, Lepp D, Gong J. The pathogenesis of necrotic enteritis in chickens: What we know and what we need to know. Review. *Avian Pathol.* 2016; Jan26 Epub: 1-21.
3. Timbermont L, Haesebrouck F, Ducatelle R, Van Immerseel F. Necrotic enteritis in broilers: an updated review on the pathogenesis. *Avian Pathol.* 2011; 40:341-347.
4. Zachary JF. Mechanisms of microbial infection. In: McGavin MD, Zachary JF, eds. *Pathologic Basis of Veterinary Disease.* 5th ed. St. Louis, MO: Mosby Elsevier; 2012:170.

CASE II: T15-9947 (JPC 4066088).

Signalment: Five-year-old Beagle mix, intact female dog (*Canis familiaris*)

History: The patient suddenly became anorectic, lethargic, and had increased body temperature (105.6°F), high white blood cell count (WBC), and was azotemic.

Gross Pathology: There were multifocal areas of hemorrhage on the epicardium.

Laboratory Results: Laboratory tests for Lyme disease and *Ehrlichia*, and fluorescent antibody (FA) tests for canine parvovirus

and canine adenovirus were negative. Aerobic culture yielded heavy growth of *Candida albicans* from the intestine and a few colonies from lungs and liver.

Histologic description: Scattered “onion skin” cysts were present between myocardial fibers of the sections of heart. In some sections, multifocal mild to moderate granulomatous to pyogranulomatous myocarditis was observed. Similar cysts were present in the diaphragm, skeletal muscle, pancreas, liver, small intestine and abdominal fibroadipose tissue (sections not included in the slide). Additionally, multifocal areas of necrosis and vascular thrombi were observed in the sections of liver and spleen. Moderate to severe mineralization was present in various tissues including the renal tubules, lungs and intestinal mucosae. Other secondary lesions observed include diffuse, severe amyloidosis in the small intestine, pancreas and renal glomeruli.

Contributor’s Morphologic Diagnosis: Myocardium: “onion skin cysts” (consistent with cysts of *Hepatozoon americanum*) with multifocal mild to moderate granulomatous to pyogranulomatous myocarditis; and dissemination of the cysts to various tissues.

Contributor’s Comment: *Hepatozoon* spp that infect domestic dogs in the United States include *H. canis* and *H. americanum*. *Hepatozoon canis* and *H. americanum* differ in numerous aspects including geographic distribution, definitive tick hosts, sites of merogony and clinical syndromes in canine intermediate hosts, treatment approaches, and regions of 18S rRNA gene sequence. *H. americanum* gamonts are found in circulating leukocytes of dogs, as are those of *H. canis*. Ultrastructural and immunohistochemical evidence indicates that the host cell for *H. americanum* during



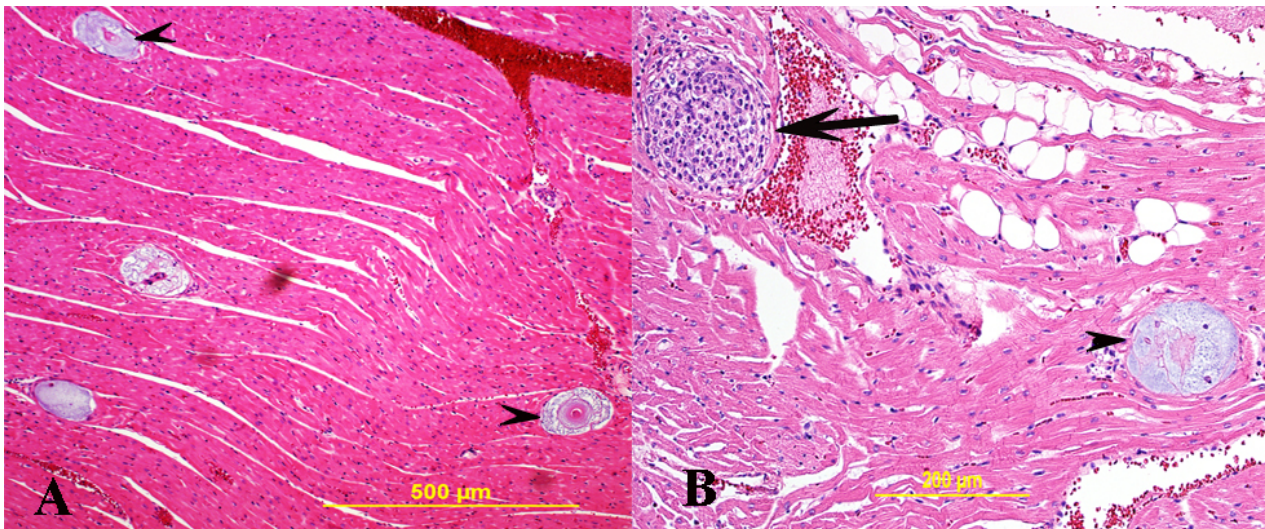
Heart, dog. A cross section of the myocardium is submitted. Small cysts and foci of cellular infiltrates are scattered throughout the section but difficult to pick up at this magnification. (HE, 5X)

merogony and gamogony is a monocyte, rather than a neutrophil, which is considered the favored host cell for *H. canis*. Also, merogony of *H. americanum* takes place in a host cell that is lodged primarily between individual striated muscle fibers whereas the asexual process for *H. canis* occurs in a wide variety of sites, especially in hemolymphatic tissues and visceral organs. The meronts of *H. americanum* are usually found within “onion skin” cysts that are created by layers of mucopolysaccharide-rich material that is apparently elaborated by

the host cell. Such characteristic lesion is not associated with the *H. canis* meront, which is rarely found in muscle and has its own characteristic morphologic feature referred to as a “wheel spoke” arrangement of merozoites within the meront.^{1,4}

Hepatozoon americanum causes American canine hepatozoonosis, which is a highly debilitating, tick-borne disease of dogs mainly in the south-central and south-eastern USA⁴ although documented in other regions of the USA.¹ It is caused by *Hepatozoon americanum*, a protozoan parasite, the definitive host of which is the tick *Amblyomma maculatum*.³ In the United States, *A. maculatum* was traditionally endemic in states bordering the Gulf Coast and several states bordering the Atlantic coast including Georgia, Florida, and the southern portion of South Carolina. However, current data report establishment of the Gulf Coast tick in states farther inland including Oklahoma, Kansas, Arizona, Arkansas, Missouri, Indiana, Kentucky, and Tennessee and additional states along the Atlantic coast including Maryland, Virginia, and West Virginia.^{1,4} Dogs get the disease by ingesting infected ticks.^{3,4}

Clinically, infected dogs are often febrile,



Heart, dog. Sections of myocardium containing scattered “onion skin” cysts (arrow heads) and a focal pyogranulomatous myocarditis (arrow). (HE, 100x). (Photo courtesy of: The University of Georgia, College of Veterinary Medicine, Department of Pathology, Tifton Veterinary Diagnostic and Investigational Laboratory, Tifton, GA 31793, <http://www.vet.uga.edu/dlab/tifton/index.php>)

stiff, lethargic, and depressed. Wasting of body mass, marked in temporal muscles, and periosteal bone proliferation (hypertrophic osteopathy) are documented in dogs with chronic disease. Microscopically, trophozoite within macrophage-like cells in many tissues, mainly in striated muscles, apparently transforms the host cell into a mucopolysaccharide-producing entity that builds structures commonly called “onion skin” cysts. Parasite-containing cysts and lesions can be found in many tissues, but are consistently found in striated muscles.⁴ Adipose and loose connective tissues are less commonly affected; rarely, other organs/ tissues such as lymph nodes, spleen, liver, and pancreas may be affected.^{5,6} Mature meronts of a well-developed cyst of *H. americanum* release merozoites, which

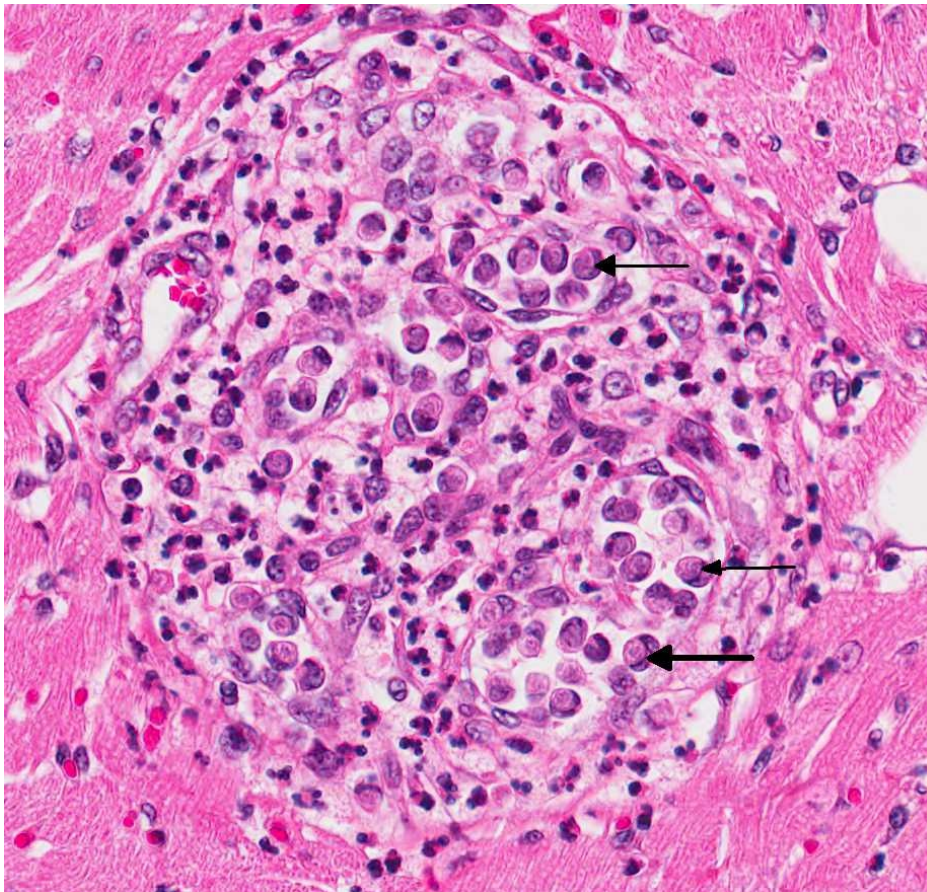
incite local inflammation such as pyogranulomatous myositis, and are associated with a systemic reaction and overt illness.⁴ Dogs may die due to secondary amyloidosis, glomerulonephritis⁸ and associated other secondary lesions such as mineralization.

JPC Diagnosis: Heart: Myocarditis, histiocytic and lymphoplasmacytic, multifocal, mild with apicomplexan cysts and intrahistiocytic and extracellular merozoites.

Conference Comment: Once and infected tick is ingested, the sporocysts excyst and release sporozoites, which penetrate the intestinal mucosa, disseminate systemically, and reproduce asexually (merogony) in cells located within striated muscle.⁴ It is unclear

if the sporozoites travel to target tissues in the extracellular milieu or are ingested by leukocytes and thereupon disseminate hematogenously.¹ The cells, which are parasitized in both the “onion skin” cyst form in striated muscle as well as in peripheral blood, are of monocyte lineage and protect the developing organism from host defenses.³

Merogony results in the production of merozoites that eventually give rise to gamonts that circulate in the blood where



Heart, dog. Foci of pyogranulomatous inflammation represent ruptured meronts, and macrophages often contain phagocytized merozoites (arrows).

ticks can ingest them.⁴ When merozoites are released from the cyst form, they incite a marked, localized, acute inflammatory response that eventually results in formation of a granuloma, but infected mononuclear cells are able to escape the granuloma.³ The cysts are actually located between muscle fibers and contain a host cell, within which is the developing zoite stage. The host cell is surrounded by the lamellated structure composed of muco-polysaccharide in the “onion skin cyst” stage. Collagen fibers, fibroblasts and capillaries may be embedded within or closely associated with the lamellated cyst wall; but inflammatory cells are generally not associated with the large cysts. The developing parasites within the host cell, inside the cyst, bear ultrastructural features of developing apicomplexan trophozoites, although a parasitophorous vacuole is not observed. Both the merozoite asexual stage and the gamont sexual stage may be observed within different macrophages present in the granulomas which form after the tissue cysts rupture.³

As mentioned above, *H. americanum* infection can result in periosteal bone proliferation. Most commonly, periosteal bone proliferation occurs in the diaphyseal regions of proximal limb bones but may also manifest in other locations such as the vertebrae. This finding is in contrast to hypertrophic osteopathy which occurs in the distal limb. Histologically, *H. americanum*-induced periosteal bone lesions are often symmetric, resemble hypertrophic osteopathy, and characterized by trabeculae of woven bone oriented perpendicular to the cortex. The lesions may be widespread and in locations unassociated with presence of the organism, suggesting a systemic effect of the infection as opposed to a local condition.² As compared above, *H. americanum* generally results in more severe disease than *H. canis* and is often fatal.

Infection with *H. americanum* results in a profound neutrophilia and anemia, although the organisms may not be seen on a blood smear. In addition to muscle atrophy and bone pain, other clinico-pathologic findings in affected dogs include hyperglobulinemia, mucopurulent ocular discharge and uveitis. The disease may follow a waxing and waning course over time with periods of relapse correlating with release of merozoites and associated inflammation.^{1,7}

Conference participants described the “onion skin cysts” as 200um in diameter, composed of lamellations of mucinous material, and separating cardiac myocytes. Small characteristic granulomas, present in some slides, were described as foci of macrophages containing tachyzoites which peripheralize the nucleus, with few neutrophils at the margin. A subset of slides also contains small foci of fibrosis, which is populated with low numbers of hemosiderin laden macrophages, lymphocytes and plasma cells. Multifocal areas of hemorrhage are also present. Rare foci of mineralization and myofiber degeneration are present in some sections.

Contributing Institution:

The University of Georgia, College of Veterinary Medicine, Department of Pathology, Tifton Veterinary Diagnostic and Investigational Laboratory Tifton, GA 31793, <http://www.vet.uga.edu/dlab/tifton/index.php>

References:

1. Allen, KE, Johnson EM, Little SE. Hepatozoon spp Infections in the United States. *Vet Clin Small Anim.* 2011; 41: 1221–1238.
2. Craig LE, Dittmer KE, Thompson KG. In: Maxie MG, ed. *Jubb, Kennedy, and Palmer's Pathology of Domestic Animals.*

6th ed. Vol 1. St. Louis, MO: Elsevier; 2016:94.

3. Cummings CA, Panciera RJ, Kocan KM, Mathew JS, Ewing SA. Characterization of Stages of *Hepatozoon americanum* and of Parasitized Canine Host Cells. *Vet Pathol.* 2005; 42:788-796.

4. Ewing SAE, Panciera RJ. American Canine Hepatozoonosis. *Clin Microbiol Rev.* 2003; 16: 688–697.

5. Panciera RJ, Ewing SA, Cummings CA, Kocan AA, Breshears MA, Fox JC. Observations on tissue stages of *Hepatozoon americanum* in 19 naturally infected dogs. *Vet Parasitol.* 1998; 78:265–276.

6. Potter TH, Macintire, DK. *Hepatozoon americanum*: an emerging disease in the south-central/southeastern United States. *J Vet Emer Critical Care.* 2010; 20: 70-76.

7. Valli VEO, Kiupel M, Bienzle D. Hematopoietic system. In: Maxie MG, ed. *Jubb, Kennedy, and Palmer's Pathology of Domestic Animals.* 6th ed. Vol 3. St. Louis, MO: Elsevier; 2016:109-111.

8. Van Vleet JF, Valentine BA. Muscle and tendons. Hepatozoonosis. In Maxie MG, ed. *Jubb, Kennedy and Palmer's pathology of domestic animals.* 5th ed. Vol 1. Elsevier Saunders; 2007: 270-271.

CASE III: 14183 (JPC 4069358).

Signalment: Four-year-old, male, crossbreed, feline (*Felis catus*)

History: The cat was admitted to a veterinary facility for lethargy and vomiting. The owner reported that the cat had ingested

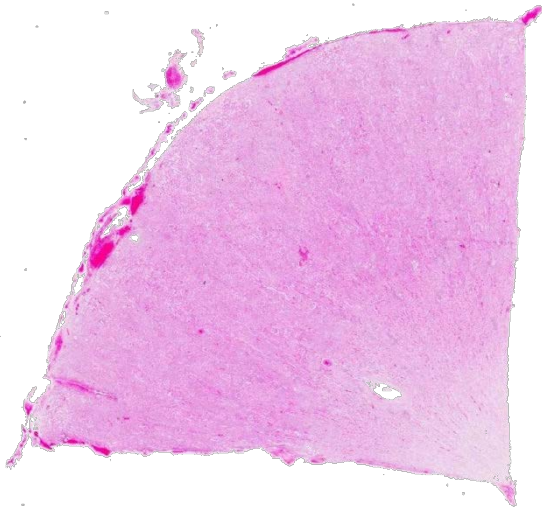
some leaves of lily (*Lilium* sp.). At admission, it was anuric and vomited frequently.

Gross Pathology: Renal congestion with swollen kidneys and perirenal hemorrhages and edema were found. Pulmonary congestion, gastrointestinal congestion, and paleness of the liver were seen. The stomach and intestine was empty.

Laboratory Results: None

Histologic description: In lily toxicosis, severe renal tubular degeneration accompanied by luminal accumulation of cellular and proteinaceous debris is a common finding. Both hyaline and granular casts often occlude the collecting ducts.

The epithelium of most tubules has undergone varying degrees of degeneration and necrosis. Cortical tubules were more severely affected than medullary tubules, and proximal convoluted tubules were more severely affected than straight tubules, thin segments, or ducts. Degenerate epithelial cells had swollen, irregularly vacuolated cytoplasm. Necrotic epithelial cells had granular eosinophilic cytoplasm and either lacked a nucleus or exhibited pyknosis and karyorrhexis. The lumens of many tubules and ducts contained eosinophilic, granular remnants of desquamated, necrotic epithelial cells, granular casts, or homogeneously eosinophilic material (hyaline casts). Lymphocytes and some macrophages had accumulated in the interstitium.



Kidney, cat. A triangular section of renal cortex is submitted. (HE, 5X)

Contributor's Morphologic Diagnosis:

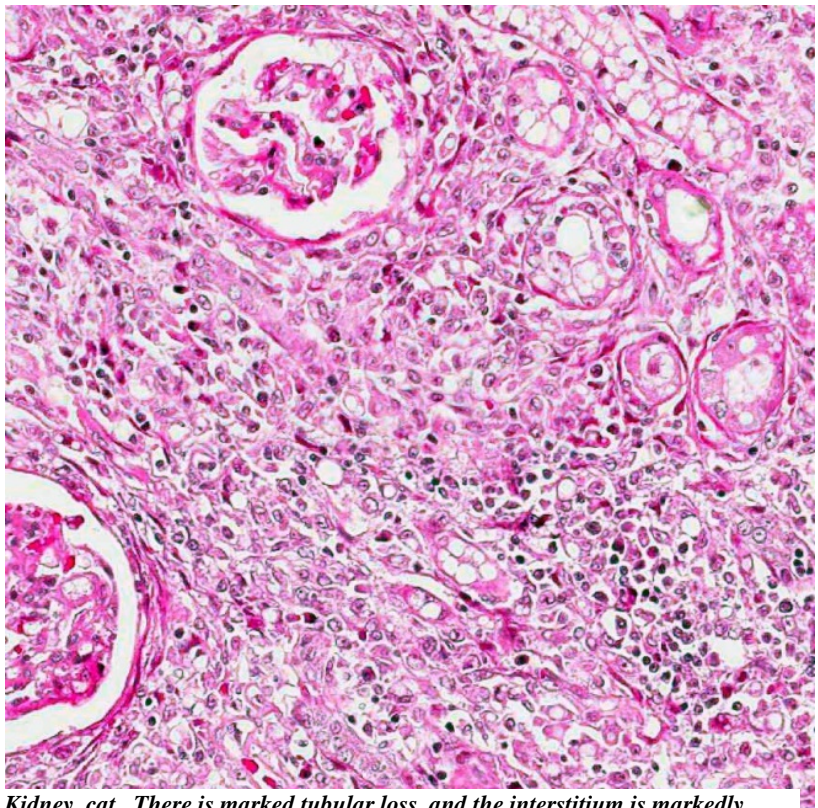
Kidney: Tubular degeneration and necrosis diffuse.

Kidney: Interstitial histio-lymphocytic diffuse subacute nephritis.

Contributor's Comment: The *Liliaceae*, or lily family, is composed of 280 to 300 genera made up of 4000 to 4600 different species. The numbers vary because botanists differ in how to classify this diversity based on flowering type, ovary position, and distribution. There are ornamental plants within the group (lilies, tulips, hyacinths, daffodils, and amaryllis); food plants (onions, garlic, asparagus, leeks, shallots, and chives); and a variety of toxic species in the family, some of which are quite deadly. It must be remembered that the common name "lily" is applied to many species of multiple

genera within and without this group. *Lilium* plants are mainly sold for indoor use as potted plants or as floral arrangements but are also planted outdoors in flower gardens.⁵

The genera *Lilium* (Madonna lily, white lily, tiger lily, rubrum lily, Japanese show lily, devil lily, Easter lily, trumpet lily, leopard lily, panther lily, stargazer lily, Asiatic lily, wild yellow lily, and Turk's cap lily) and *Hemerocallis* (the "day" lilies with flowers lasting only one day) are the groups considered potentially nephrotoxic to cats. For the purposes of our discussion, we will limit our investigation to the genera *Lilium* and *Hemerocallis* which cause nephrotoxicity. Nevertheless, it must be kept in mind that a wide variety of plants are in the lily family or are called "lilies" (and hybrids exist), and within this group there is a similar diversity in the potential toxicological effects.³



Kidney, cat. There is marked tubular loss, and the interstitium is markedly expanded by numerous macrophages and fewer neutrophils, lymphocytes and rare plasma cells. (HE, 100X)

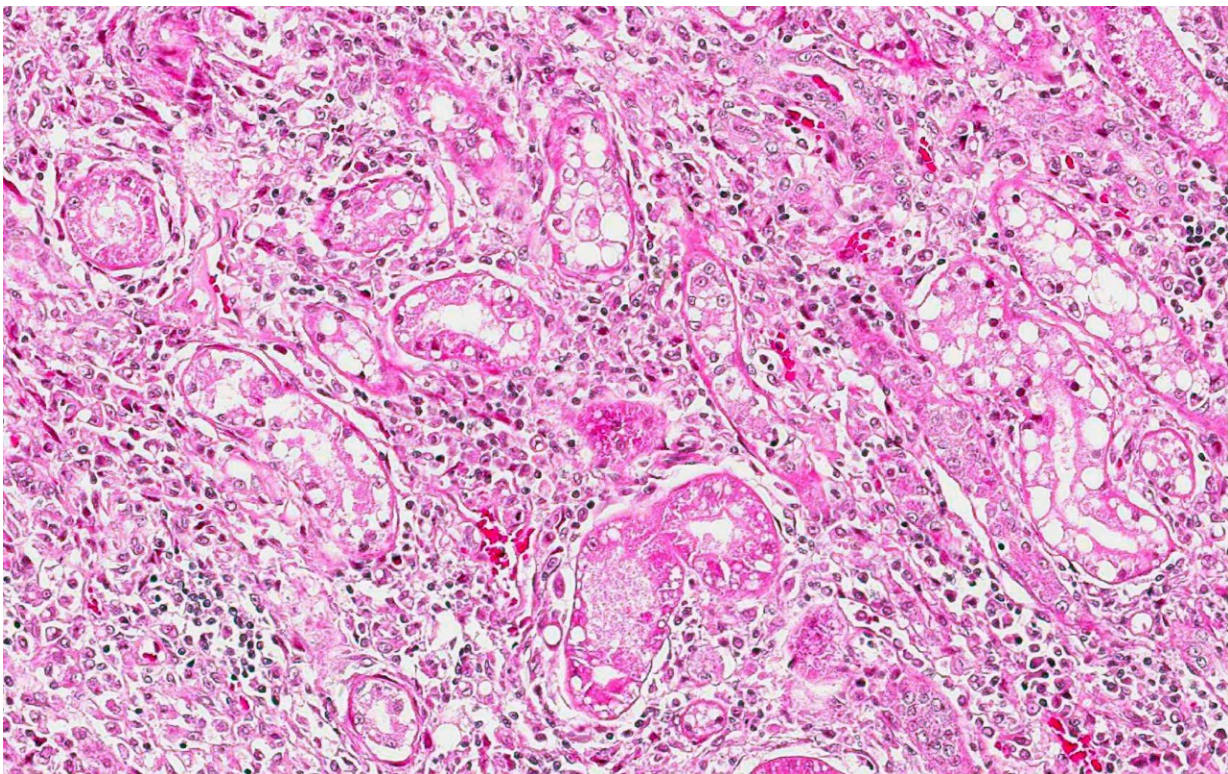
Various members of the *Lileaceae* family of plants can cause acute tubular necrosis in animal species, for example, *Narthedum ossifragum* (bog asodel) in ruminants, several lilies, and their hybrids (*Lilium* spp.)³ Most pet owners know little about the danger these plants pose to cats. Although cats are finicky eaters, for some unknown reason they eat the leaves and flowers of *Lilium* plants. Both leaves and flowers are reportedly toxic. Ingestion of one or two leaves or one whole flower has caused dead in cats.^{3,5}

Cats are really sensitive to ingestion of certain species of lilies; no age, sex, or breed predilection has been identified.³ The mortality rate from Easter lily toxicosis is reported to be as high as 50–100%, depending on the time symptomatic treatment is initiated. High mortality rate is reported if treatment is not initiated before onset of anuric renal failure, which occurs 18–24 hours after exposure.⁵ Nephrotoxic

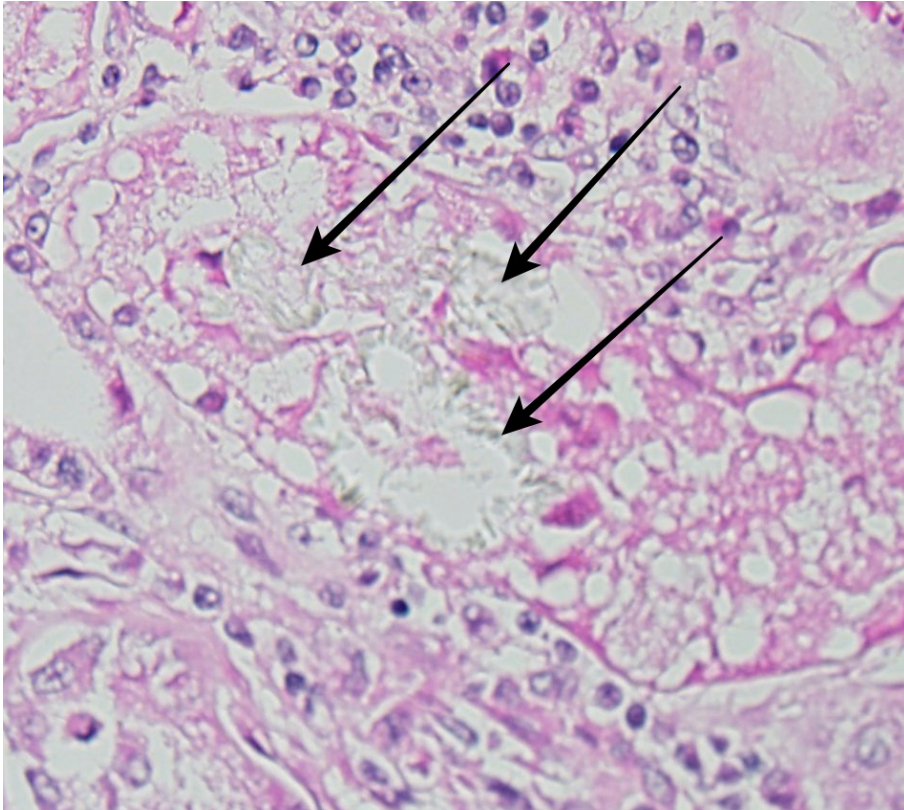
damage cannot be duplicated in rats, mice, or rabbits. In dogs, only vomiting and gastrointestinal signs can be seen after lily ingestion in dogs even when fed large amounts of these plants.³

The exact mechanism of action of lily poisoning, specifically lily-induced nephrotoxicity is unknown. The rapid onset of clinical signs after ingestion of culprit species indicates rapid absorption rate for the poison. The toxins damage renal tubular epithelial cells resulting in cell death and sloughing of damaged renal cells. The insult to the kidney is severe, leading initially to polyuric kidney failure. This polyuric kidney failure leads to extreme dehydration. If this dehydration progresses far enough or goes on long enough, anuric renal failure and complete renal shutdown can develop.³

In this case, microscopic lesions in the kidney were compatible with nephrotoxic tubular necrosis of a few days duration. Nephrotoxic tubular necrosis is not a



Kidney, cat. There is marked tubular loss, and remaining tubules show degenerative changes, including celling into the lumen, the presence of numerous discrete clear vacuoles, brightly eosinophilic cytoplasmic granules. Few epithelial cells are pyknotic and rarely sloughed into the lumen. (HE X)



Kidney, cat. Rarely, degenerating tubules contain birefringent fan-shaped oxalate crystals (arrows) (HE, 400X)

specific diagnosis and can result from a variety of nephrotoxins, such as aminoglycoside antibiotics (e.g., gentamicin), metals (e.g., lead, arsenic, mercury), or metabolites of ethylene glycol.² In this case, the lily was the probable source of the nephrotoxin and the whole renal lesions.

At present, there is no “gold standard” test for analysis and verification of lily ingestion. The most positive confirmations involve the observation of the animal ingesting the lily, compatible clinical syndrome signs, compatible clinicopathological findings, and supportive postmortem lesions in cats that die. Even if postmortem lesions are suggestive of lily poisoning, positive verification of lily ingestion cannot be made unless ingested plant material observed within the gastrointestinal tract. Despite no specific test existing to verify this poisoning, if the index of suspicion for lily intoxication is high,

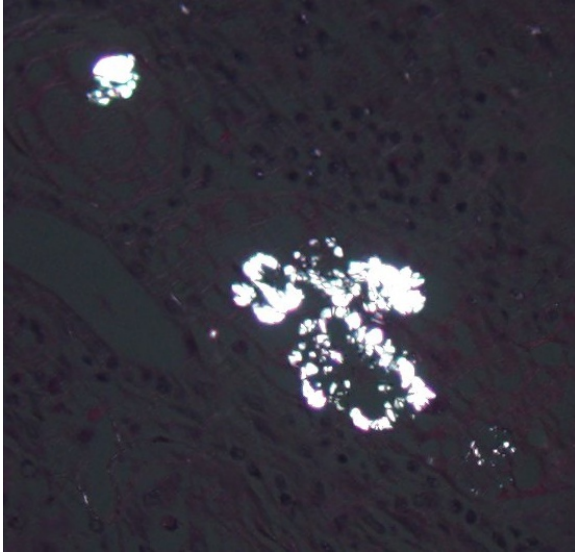
initiation of appropriate fluid therapy should begin to prevent anuric renal failure from developing.³

JPC Diagnosis:
Kidney: Tubular degeneration, necrosis and, diffuse, marked with loss with mild atrophy and regeneration, marked lymphoplasmacytic nephritis, protein casts and rare oxalate crystals.

Conference
Comment: The contributor has provided an excellent discussion of lily

toxicosis in the cat. Although not commonly described in association with lily toxicosis, pancreatic lesions may also be seen. Changes include cytoplasmic vacuolation affecting the majority of acinar cells which is interpreted as a degenerative change. Pancreatitis has also been reported to result from Easter lily ingestion. Changes in the pancreatic islet cells are not reported.

Seizures are also reported in addition to the renal and pancreatic changes and may occur within 8 hours after exposure.⁵ The flowers of lily plants are more toxic than its leaves but ingestion of either may result in the renal changes described above. Changes within the kidney occur initially in the inner cortex, and as the condition progresses, tubules within the outer cortex succumb to damage as well. Ultrastructural changes include mitochondrial swelling in renal proximal tubule epithelium and the formation of megamitochondria, which may result from either enlargement of individual mit-



Kidney, cat. Luminal oxalate crystals are easily identified, even at lower magnification.) (HE, 400X)

ochondria or fusion of mitochondria. Other ultrastructural changes that have been described include pyknotic nuclei and lipid infiltration.⁵

The conference histologic description included many of the tubular features described above by the contributor. The primary findings in this case are tubule degeneration and necrosis and the inflammation is considered a secondary finding. There was discussion regarding the origin of the inflammation and whether it was a process unrelated to the tubular necrosis, and perhaps present prior to the onset of nephrotoxic tubular changes; however, a consensus opinion was not reached in this regard and thus it was included in the morphologic diagnosis with the tubular changes. Additional features include tubule regeneration and atrophy, mild glomerular changes including thickened parietal and visceral epithelium and low numbers of sloughed epithelium within the urinary space. Low numbers of birefringent crystals are also seen within tubule lumina when viewed under polarized light. The capsule is mildly expanded by

hemorrhage and inflammatory cells. Although mild, the presence of glomerular lesions also lends evidence to another process taking place in the kidney as glomerular lesions are not commonly reported in cases of lily intoxication. Other nephrotoxic plants which affect domestic animal species that were discussed during the conference include *Isotropis* toxicity in ruminants, oak toxicity in ruminants and horses, *Amaranthus retroflexus* (pigweed) toxicity in swine and cattle, *Lantana camara* toxicity in cattle, and oxalate containing plant (i.e. *Rumex* spp., *Oxalis cernua*, *Halogeton glomeratus*, etc.) toxicity in cattle and sheep.²

Contributing Institution:

Animal Pathology Department / Veterinary Diagnostic Laboratory, Veterinary Faculty; Federal University of Pelotas. 96010-900 Pelotas, RS, Brazil.

<http://wp.ufpel.edu.br/sovet/>

<http://www.ufpel.edu.br/fvet/lrd/>

References:

1. Brady MA, Janovitz EB. Nephrotoxicosis in a cat following ingestion of Asiatic hybrid lily (*Lilium* sp.). *J Vet Diagn Invest.* 2000; 12:566–568.
2. Cianciolo RE, Mohr FC. Urinary system. In: Maxie MG, ed. *Jubb, Kennedy, and Palmer's Pathology of Domestic Animals.* 6th ed. Vol 2. St. Louis, MO: Elsevier; 2016:421-428.
3. Fitzgerald K T. Lily Toxicity in the Cat. *Top Companion Anim Med.* 2010; 25(4):213-217.
4. Maxie MG, Shelley JN. Urinary system. In: Maxie MG, ed. *Jubb, Kennedy and Palmer's Pathology of Domestic Animals.*

5th ed. Vol. 2. Philadelphia, PA: Elsevier; 2007: 472-473.

5. Rumbelha WK, Francis JA, Fitzgerald SD, Nair MG, Holan K, Bugyei KA, Simmons H. A Comprehensive Study of Easter Lily Poisoning in Cat. *J Vet Diagn Invest* 2004 16: 527-541.

CASE IV: 0561-15 (JPC 4070541).

Signalment: 9-month-old, intact female Persian cat (*Felis catus*)

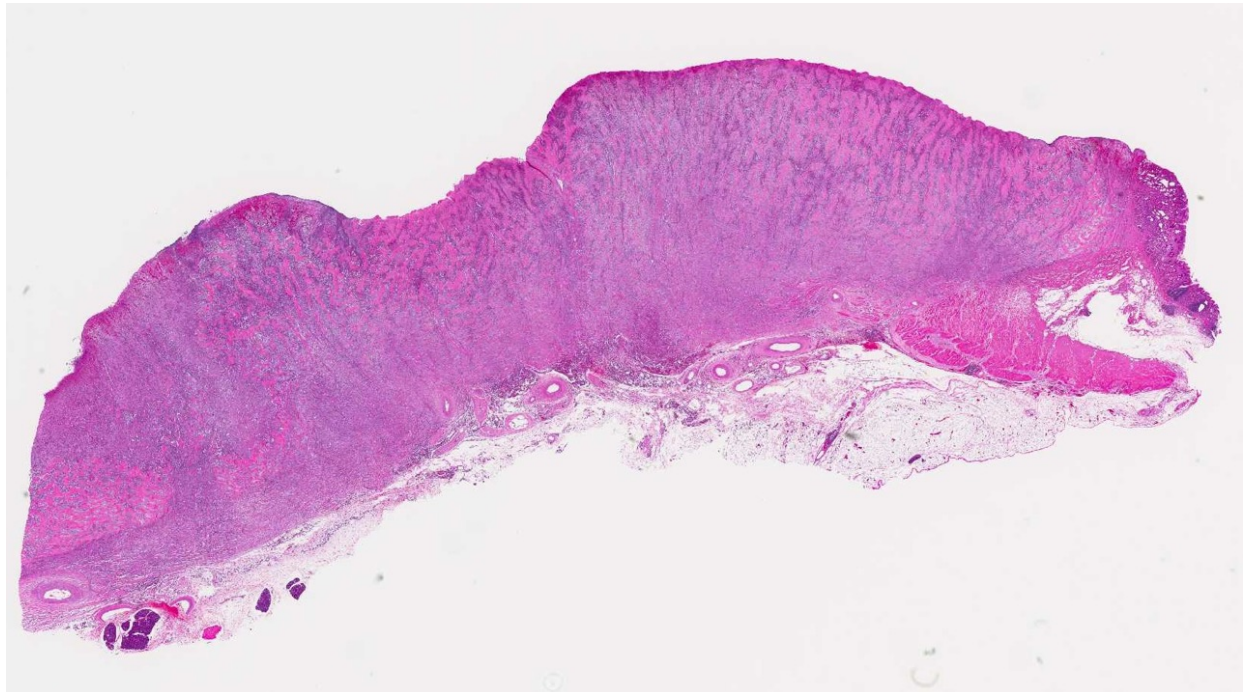
History: The cat had a history of intermittent vomiting and failure to gain weight. Radiographs revealed a mass at the gastric pylorus and an exploratory laparotomy was performed.

Gross Pathology: The gastric pylorus region had thickened wall with roughened

mucosa surface.

Laboratory Results: None

Histologic description: Expanding and effacing the architecture of the gastric mucosa, submucosa and tunica muscularis at the pyorus is a transmural proliferation of a fibroproliferative mass with surface necrosis and ulceration. The lesion affects all layers of the gastric wall, and is comprised of branching and anastomosing cords and trabeculae of dense collagen separated and surrounded by a dense population of fibroblastic cells intermixed with large numbers of eosinophils, plasma cells, regionally dense neutrophils, lesser histiocytes, mast cells and lymphocytes. Toward the serosal surface, the fibroblastic proliferation is necrotic and overlain by edematous, loose fibrovascular proliferation and above described inflammatory cells. There is obliteration of mucosal epithelium, further covered by necrotic cell debris, and dense aggregates of neutrophils that are occasionally centered on small clusters of



Pylorus, cat. The submitted section of pylorus is largely effaced by an infiltrative mass. A small section of pancreas is present in the lower left. (HE 6X).

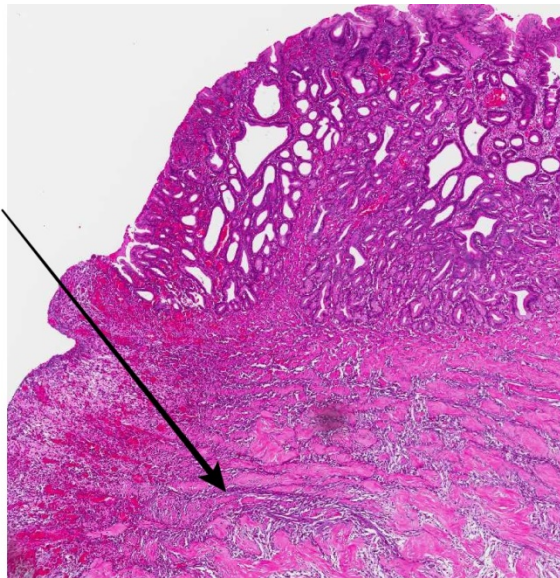
cocci, as well as hair shafts in cross and tangential section .

A Gram stain of the lesion revealed myriad gram-positive rods and gram-negative coccobacilli (often associated with degenerate collagen) on the ulcerated surface.

Periodic acid-Schiff stains failed to demonstrate fungi present within the lesion.

Contributor's Morphologic Diagnosis:

Stomach: 1. Feline gastrointestinal eosinophilic sclerosing fibroplasia
2. Marked surface necro-suppurative gastritis, with intralesional hair shafts and bacteria



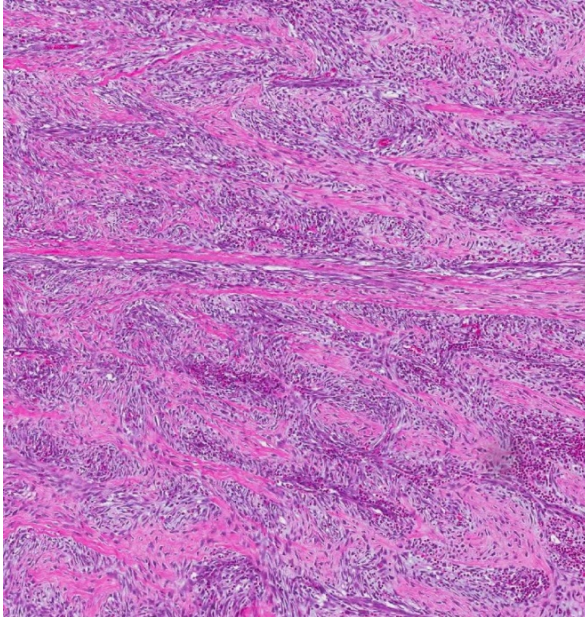
Pylorus, cat. Higher magnification of the interface between the pylorus (top, with dilated glands), and the mass below (arrow). (HE, 45X)

Contributor's Comment: Feline gastrointestinal eosinophilic sclerosing fibroplasia is a recently described disease in cats characterized by a nodular, non-neoplastic, proliferative, fibrosing and eosinophilic lesion that effaces the stomach wall of cats.² The disease tends to affect middle-aged cats and typical clinical signs include decreased appetite, weight loss, vomiting, and diarrhea.³

Reported breeds include Ragdoll, domestic shorthair, domestic longhair, Siamese, Maine Coon, Himalayan, Persian and Scottish fold.^{2,3,4} The disease is most often seen at the pyloric sphincter, ileocecolic junction or colon, often involving the regional lymph node, and can be associated with peripheral eosinophilia.² The etiopathogenesis of this condition is not clearly defined, with migrating foreign body, genetic predisposition and eosinophil dysregulation, herpesvirus infection, and food hypersensitivity are all speculated in the pathogenesis.³

The condition has previously been confused with sclerosing mast cell tumor, which is a neoplasm that tends to occur in the small intestine, unassociated with peripheral eosinophilia and extensive fibroproliferation, and less commonly forms palpable masses in the stomach.³ While bacteria are seen within lesions of feline gastrointestinal eosinophilic sclerosing fibroplasia in some reports, antimicrobial therapy is not effective.² Neither feline coronavirus, feline herpes virus nor any individual bacterial agent have been linked as an etiologic agent.³

A single case report indicated an association between phycomycetes and this disease entity in a domestic cat.⁵ The disease has been reported in United States, Australia, Europe, Japan and New Zealand^{3,4} and this represents this as a first case from Singapore. Prognosis of affected cats is typically grave, and there is no conclusive single conclusive treatment regime.³ Cats treated with prednisolone have a significantly longer survival period and a combination treatment approach of surgical resection, prednisolone, antimicrobial therapy and immune modulation may help improve clinical outcome.³



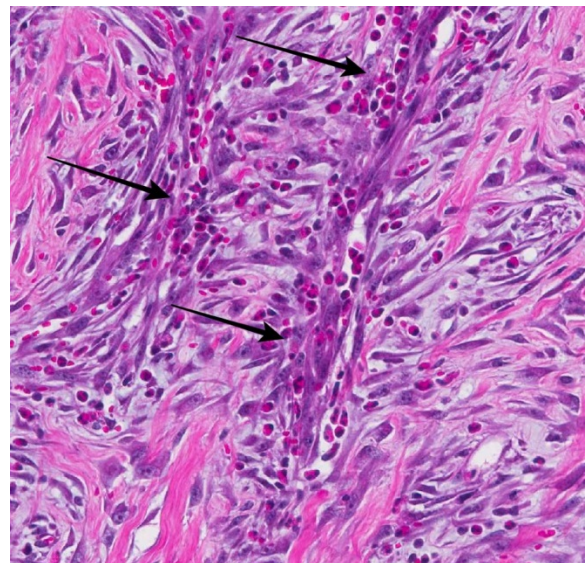
Pylorus, cat. The mass is composed of large numbers of fibroblasts which produce a herringbone pattern of mature collagen. (HE, 200X)

JPC Diagnosis: Stomach: Gastritis, ulcerative, eosinophilic and mastocytic, sclerosing, transmural, severe, with entrapped hair shafts and extracellular bacilli.

Conference Comment: The mass lesion present in feline gastrointestinal eosinophilic sclerosing fibroplasia has been described as hard, non-painful and easily palpable. Upon fine needle aspiration or biopsy the lesions are firm, described as ‘gritty,’ and are heterogeneous when sectioned at necropsy or at time of surgery.³ Histologically, it is not uncommon to find bacteria within the lesions, as seen in this case; fungal organisms and nematode infections have also been associated with these lesions.^{3,5} Secondary infections are proposed to play a role in perpetuation of the inflammatory lesion. The broad trabeculae of fibroplasia intermixed with foci of inflammation is characteristic of the lesion, as conspicuously observed in this case. The histologic differential diagnosis includes fibrosarcoma and mast cell tumor; and malignant

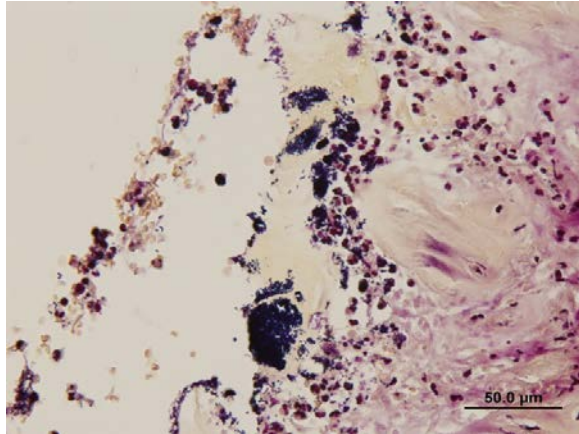
lymphoma is also a consideration at the macroscopic level.

Eosinophils are presumed to play a primary role in the pathogenesis of this fibroplastic lesion. Eosinophils are most commonly called in from the bloodstream in response to chemoattractants, such as in parasitic and allergic conditions, and are often seen as a component of subacute and chronic inflammation. Eosinophils contain several different types of granules, including large specific granules, small granules, primary granules, and secondary granules, which elaborate a wide variety of cytokines, chemokines and degradative enzymes that can perpetuate and enhance the inflammatory response, stimulate fibrosis, and result in significant host tissue damage, including cell and extracellular matrix components. Eosinophil chemottractants originate from a variety of sources such as epithelial cells, parasites, mast cells and eosinophils themselves and include CCL-5 (RANTES), C5a, CCL-11 (eotaxin), IL-4, IL-5 and IL-13.¹ One important mediator is



Pylorus, cat. The mass diffusely contains large numbers of eosinophils (arrows) as its primary inflammatory component. (HE, 400X)

major basic protein, which is present within large specific granules; the protein is toxic to helminths, as well as adjacent host cells, and causes histamine release from mast cells as well as activating neutrophils.



Pylorus, cat. Multifocally, colonies of mixed bacilli are present within the inflammatory mass. (Photo courtesy of: Institute of Molecular and Cell Biology, 61 Biopolis Drive, Proteos Building Level 6 Singapore, (<http://www.imcb.a-star.edu.sg/php/ittid-i-histo.php>)

In this lesion, eosinophils compose a major component of the inflammatory cell population, with mast cells being relatively fewer in number. Extracellular bacteria can be visualized without the aid of Gram stains. Multifocal areas of inflammation, composed of neutrophils, macrophages and multinucleate giant cells, surround free hair shafts.

Contributing Institution:

Advanced Molecular Pathology Laboratory
Institute of Molecular and Cell Biology
61 Biopolis Drive, Proteos
Singapore 138673

References:

1. Ackermann MR. Female reproductive system and mammary gland. In: McGavin MD, Zachary JF, eds. *Pathologic Basis of*

Veterinary Disease. 5th ed. St. Louis, MO: Mosby Elsevier; 2012:102.

2. Craig LE et al. Feline gastrointestinal eosinophilic sclerosing fibroplasia. *Vet Pathol*. 2009 Jan; 46(1):63-70.

3. Linton M et al. Feline gastrointestinal eosinophilic sclerosing fibroplasia: 13 cases and review of an emerging clinical entity. *J Feline Med Surg*. 2015 May; 17(5):392-404.

4. Suzuki M, Onchi M, Ozaki M. A case of feline gastrointestinal eosinophilic sclerosing fibroplasia. *J Toxicol Pathol*. 2013 Mar; 26(1):51-3.

5. Grau-Roma L, Galindo-Cardiel I, Isidoro-Ayza M, Fernandez M, Majó N. A case of feline gastrointestinal eosinophilic sclerosing fibroplasia associated with phycomycetes. *J Comp Pathol*. 2014 Nov; 151(4):318-21.

**Joint Pathology Center
Veterinary Pathology Services**



WEDNESDAY SLIDE CONFERENCE 2015-2016

Conference 19

30 March 2016

John M. Cullen, VMD, PhD, DACVP, FIATP
Professor, Anatomic Pathology
NCSU College of Veterinary Medicine, Raleigh, NC

CASE I: 11-966 (JPC 4002877).

Signalment: 12-year-old male neutered Chihuahua, canine (*Canis familiaris*).

History: Initially, the animal was presented to the referring veterinarian (rDVM) for abdominal enlargement due to ascites. Exploratory laparotomy was performed and the liver was described as having numerous yellow nodules over the entire surface. Clinically, the rDVM was concerned about neoplasia. After the biopsies were reviewed, the rDVM was contacted and some additional information was obtained. The animal had crusty lesions on all four footpads and multifocally on all four limbs. The dog's owners had recently moved to a new residence and they thought the skin issues were due to flea infestation. The animal was euthanized three weeks after surgery and was submitted for necropsy. Samples submitted for the slide conference originated from the original surgical biopsy and necropsy tissue.

Gross Pathology: Footpads on all four limbs are covered by flaky golden-brown crusts. Crusts are either firmly adhered or easily peel away from the digital, metacarpal and metatarsal pads. The skin over the distal left lateral forelimb and left cubital region have similar areas of crusting and mild alopecia which measure 7 mm in diameter and 18 x 4 x 1 mm, respectively. Crusts are also present bilaterally over both hocks and measure 20 x 10 x 1 mm (left) and 22 x 12 x 1 mm on the (right). The subcutaneous tissues are expanded and ooze clear fluid (edema). The abdomen contains 1220 mL of golden serous fluid. The liver is 3.7% of total body weight (after removal of abdominal fluid). The liver contains innumerable widespread variably sized brown-red nodules separated by depressed tan areas (parenchymal collapse). The nodules range in size from 3 mm diameter up to 2.5 cm diameter.

Laboratory Results: No laboratory diagnostic results were provided by referring veterinarian.



Liver, dog. The liver represented 3.7% of the dog's body weight, and grossly, was covered with numerous 3mm-2.5cm hepatocellular nodules. The intervening parenchyma is yellow-orange and collapsed. (Photo courtesy of: University of Tennessee College of Veterinary Medicine, Department of Pathobiology, 2407 River Drive, Room A201, Knoxville, TN 37996 <http://www.vet.utk.edu/>)

Histopathologic Description: Liver: At low power, there is multifocal to coalescing collapse and loss of hepatic parenchyma. The areas of collapse separate variably sized unencapsulated nodules of well differentiated hepatocytes (regenerative hyperplasia). In areas of collapse, there are heavily vacuolated and swollen hepatocytes, increased bile duct profiles, plugs of golden material (bile) in canaliculi (canalicular cholestasis), and low numbers of lymphocytes, plasma cells, and neutrophils. Multifocally, within the areas of collapse, there are occasional areas containing mildly increased fibrous tissue (confirmed with trichrome). There are multifocal clusters of macrophages containing golden brown pigment.

There is some variation among slides because some samples were from the original biopsy while others were obtained during necropsy 3 weeks later.

Contributor's Morphologic Diagnosis:

Liver: Severe chronic multifocal to coalescing parenchymal loss and nodular regeneration with fatty change, biliary hyperplasia and canalicular cholestasis

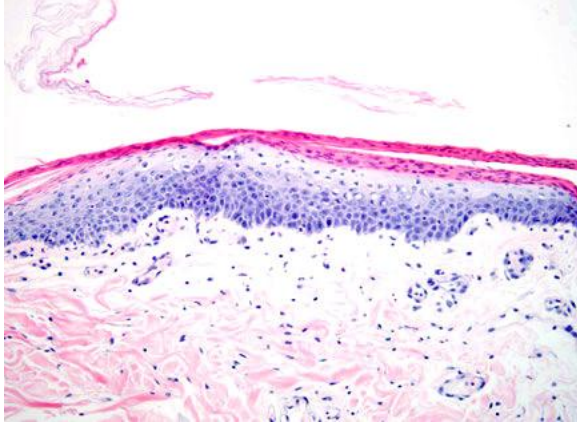
Footpad: Marked chronic basal cell hyperplasia, intracellular edema (stratum spinosum), and parakeratotic hyperkeratosis (*slide not included*)

Contributor's Comment: Gross and histologic changes in the liver and skin are consistent with hepatocutaneous syndrome. Most animals present clinically for the skin lesions; however, in this case the animal presented for the hepatic disease because the owners mistakenly associated the cutaneous lesions with fleas.

Hepatocutaneous syndrome has been reported in humans, dogs, cats, and the black rhinoceros.^{1,2,5-7} Older small breed dogs are primarily affected. The long-term prognosis for animals with hepatocutaneous syndrome is very poor. In cases of hepatocutaneous syndrome, the liver has a gross appearance resembling cirrhosis. Histologically, there



Footpads, dog. Digital, metacarpal, and metatarsal footpads are covered by flaky golden-brown crusts. (Photo courtesy of: University of Tennessee College of Veterinary Medicine, Department of Pathobiology, 2407 River Drive, Room A201, Knoxville, TN 37996 <http://www.vet.utk.edu/>)



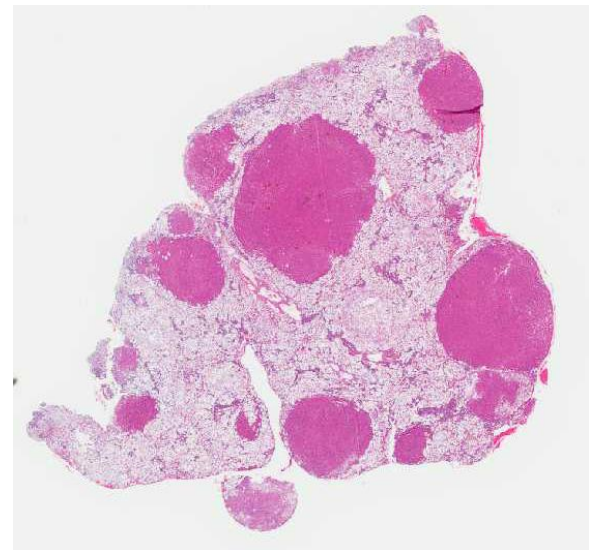
Footpads, dog. Histologic examination of the footpad lesion should a superficial “red” zone of parakeratotic hyperkeratosis, a “white” zone of underlying intracellular edema of the cells within the stratum spinosum, and at bottom, a “blue” zone of basal cell hyperplasia (HE, 200X) Photo courtesy of: University of Tennessee College of Veterinary Medicine, Department of Pathobiology, 2407 River Drive, Room A201, Knoxville, TN 37996 <http://www.vet.utk.edu/>

are foci of regenerative nodular hyperplasia separated by areas of parenchymal collapse containing heavily vacuolated hepatocytes. Hepatic changes are considered idiopathic, but have been suggested to be due to an underlying metabolic, hormonal, or toxic etiology. The pathogenesis of the associated skin lesions is unknown, but hepatic dysfunction with derangement of glucose and amino acid metabolism have been suggested.^{1,2,7}

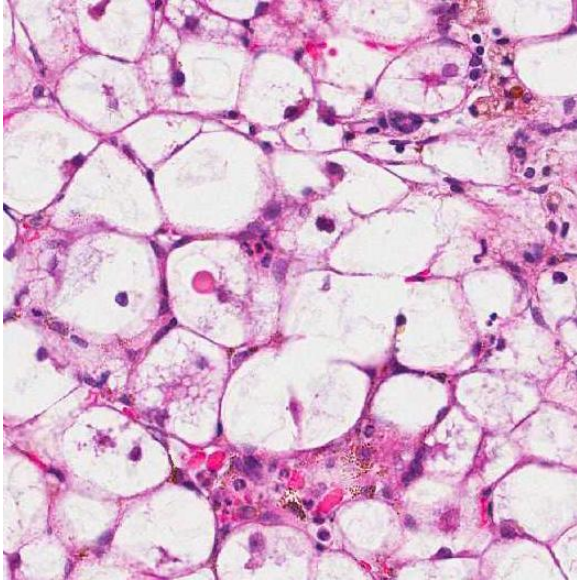
This disorder produces characteristic cutaneous changes that typically occur on the footpads, mucocutaneous junctions, and pressure points. Gross changes may include crusting, erosion/ulceration, erythema, alopecia, and exudation. The histologic appearance is often referred to as “red, white and blue.” (The “red” corresponds to superficial parakeratotic hyperkeratosis; “white” corresponds to pallor in the stratum spinosum which is due to intracellular edema; “blue” corresponds to basal cell hyperplasia.² Depending on the duration of the disease, all of the classical components of the histologic lesion may or may not be

seen and could also be obscured by secondary changes (e.g. erosion, ulceration, infection). Superficial necrolytic dermatitis (SNE), necrolytic migratory erythema (NME), and metabolic epidermal necrosis (MEN) have been terms used to refer to the cutaneous syndrome in humans.¹ The majority of canine cases are associated with liver disease, whereas human cases are typically associated with a functional pancreatic glucagonomas. However, in animals, the cutaneous lesions have also been associated with glucagon secreting tumors, diabetes mellitus, pancreatic carcinoma, gastric carcinoma and thymic amyloidosis.^{5,7}

Other differential diagnoses to consider for parakeratotic skin diseases include zinc-responsive dermatosis, generic dog food dermatosis, lethal acrodermatitis of bull terriers, irritant contact dermatitis, and thallium toxicosis.^{1,2} The signalment, clinical history, and ancillary diagnostic tests, in combination with histologic findings, should easily differentiate between these potential differentials.



Liver, dog. Subgross of the submitted tissue exhibits nodules of hyperplastic hepatocytes with few to a single portal area. The intervening parenchyma is collapsed, with loss of lobular architecture. (HE, 5X)



Liver, dog. Hepatocytes within the majority of the stroma are swollen with abundant hepatocellular glycogen and small amounts of fat (HE, 400X)

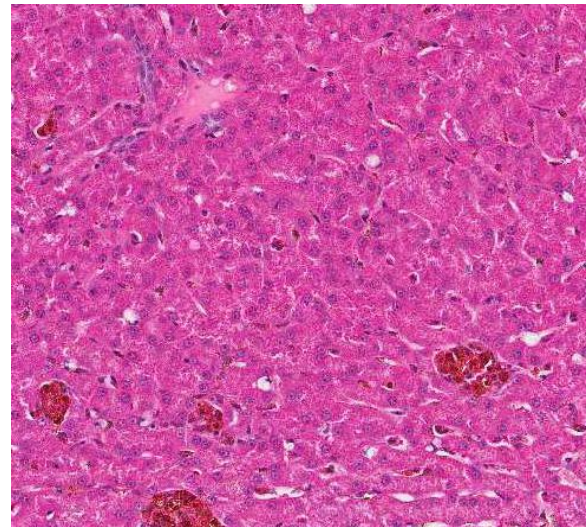
JPC Diagnosis: Liver: Hepatocellular glycogenosis and lipidosis diffuse, severe with foci of regeneration.

Conference Comment: Hepatic lesions in canine hepatocutaneous syndrome tend to diffusely affect the liver and are non-inflammatory in nature. Lesions are often described as a degenerative hepatopathy with formation of cytoplasmic vacuoles, eventually leading to parenchymal collapse. Histologically, affected hepatocytes demonstrate severe ballooning (both glycogen and/or lipid, micro- and macro-vesicular, vacuolar degeneration). Hepatic nodular regeneration is also an important component of the histologic lesions and the pattern is usually multifocal to coalescing and random. Bile duct proliferation may also be seen. A “honeycomb” appearance to the liver is described ultrasonographically.³ Common clinicopathologic abnormalities include elevated hepatic enzymes and non-regenerative anemia which may be microcytic. Other less common but reported abnormalities include hyperglycemia, thrombocytosis and elevated total bilirubin.

Low plasma amino acid concentrations are also reported.³ Therapy is generally not effective and most dogs succumb to the disease within months of developing skin lesions.^{1,3} Although many dogs are presented initially due to cutaneous lesions, some may only have hepatic lesions at the time of initial diagnosis and present with non-specific signs of lethargy and inappetence, have elevated hepatic enzymes and/or signs of hepatic encephalopathy.³

The moderator commented that this syndrome is very difficult to diagnose correctly based solely on the histologic hepatic lesions. The conference histologic description was very similar to the contributor’s description above. There is a sharp line of demarcation between degenerative and regenerative areas; sinusoids are compressed and largely obscured in the areas of vacuolar degeneration. Low numbers of binucleate hepatocytes, as well as rare mitoses within the foci of hepatocellular regeneration.

The moderator commented on the atypical appearance of the regenerative nodules,



Liver, dog. Nodules of hyperplastic hepatocytes contain aggregates of siderophages, few portal areas, and lack the fibrosis often seen in regenerative nodules. (HE, 75X)

noting that in regeneration, hepatic cords are most often arranged in double rows, while in this case they are singly arranged. The presence of one portal area per regenerative nodule is typical and is seen in some of the regenerative foci in this case. Conference participants also commented on the relative absence of fibrosis in the H&E stained section. The excellent gross image provided by the contributor was also discussed and the moderator noted that the gross “cluster of grapes” appearance imparted by the regenerative nodules is classic for this condition.

Similar cutaneous lesions may be seen (without liver lesions), with glucagon-secreting pancreatic tumors. There is also a single case report of superficial necrolytic dermatitis associated with an insulin producing tumor in a dog.⁴

Contributing Institution:

University of Tennessee College of
Veterinary Medicine
Department of Pathobiology
2407 River Drive
Room A201
Knoxville, TN 37996
<http://www.vet.utk.edu/>

References:

1. Byrne KP. Metabolic epidermal necrosis-hepatocutaneous syndrome. *Vet Clin North Am Sm Anim Pract.* 1999; 29(6):1337-1355.
2. Gross TL, Ihrke PJ, Walder EJ, Affolter VK. *Skin Diseases of the Dog and Cat.* 2nd ed. Ames, IA: Blackwell Publishing Professional; 2005:86-91.

3. Hall-Fonte DL, Center SA, McDonough SP, Peters-Kennedy J et al. Hepatocutaneous syndrome in Shih Tzus: 31 cases (1996-2014). *J Am Vet Med Assoc.* 2016; 248(7):802-813.

4. Isidoro-Ayza M, Lloret A, Bardagi M, Ferrer L, Martinez J. Superficial necrolytic dermatitis in a dog with an insulin-producing pancreatic islet cell carcinoma. *Vet Pathol.* 2014; 51(4):805-808.

5. Kimmel SE, Christiansen W, Byrne KP. Clinicopathological, ultrasonographic, and histopathological findings of superficial necrolytic dermatitis with hepatopathy in a cat. *J Am Anim Hosp Assoc.* 2003; 39:23-27.

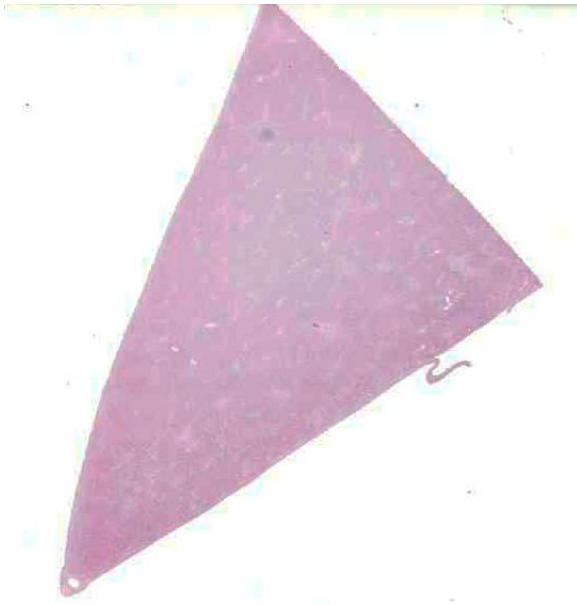
6. Munson L, Koehler JW, Wilkinson JE, Miller RE. Vesicular and ulcerative dermatopathy resembling superficial necrolytic dermatitis in captive black rhinoceroses (*Diceros bicornis*). *Vet Pathol.* 1998; 35:31-42.

7. Stalker MJ, Hayes MA. Liver and biliary system. In: Maxie MG, ed. *Jubb, Kennedy, and Palmer's Pathology of Domestic Animals.* 5th ed. Philadelphia, PA: Elsevier Saunders; 2007:332.

CASE II: H06-002960 (JPC 3174957).

Signalment: 11 year old, female, thoroughbred, equine (*Equus caballus*).

History: Mare with recurring anemia, edema of the ventrum, weight loss and lethargy. The animal previously had a positive Coggin's test.



Liver, horse. A triangular, pale-staining section of liver is presented for evaluation. (HE,5X)

Gross Pathology: Subcutaneous and visceral adipose tissue reserves were reasonable. Approximately 10 ml of clear fluid was recovered from the pericardial sac. The liver was enlarged and dark red. Splenomegaly was evident with petechiae evident over the capsule. Similar petechiation was noted over the small intestinal serosa and kidney capsules. The medullary bone marrow is diffusely red and translucent.

Laboratory Results: Positive Coggin's test.

Histopathologic Description: Periacinar necrosis of the liver with attendant, predominantly periportal, infiltration by admixed lymphocytes and macrophages, including hemosiderophages. Hemosiderin-containing Kupffer cells and erythrophagocytosis evident.

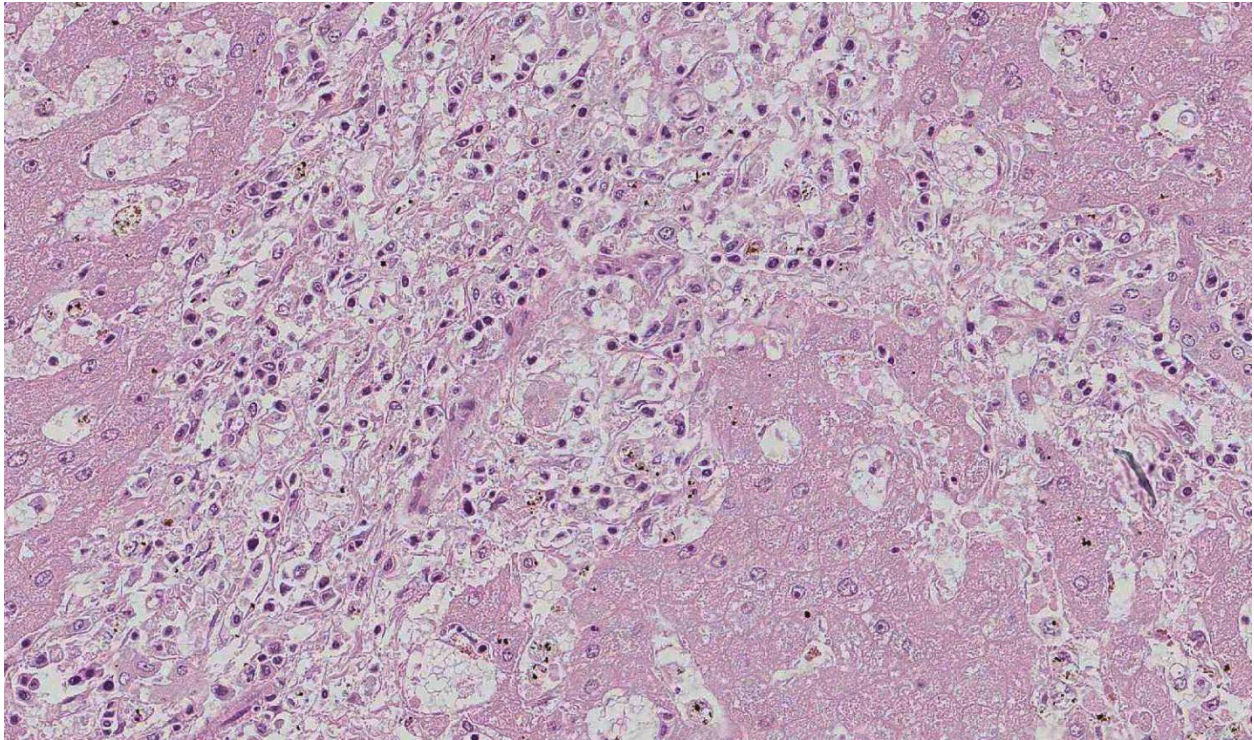
Additionally, there was lymphohistiocytic interstitial nephritis and similar infiltrates noted within the capsular and sub-capsular regions of the adrenal gland. Congestion, focal hemorrhage, lymphoid depletion and

medullary histiocytic infiltration (including hemosiderophages) were evident in lymph nodes. Hemosiderophages present in alveolar septa.

Contributor's Morphologic Diagnosis: Lymphohistiocytic hepatitis, chronic, periportal, moderate-severe with periacinar necrosis and occasional erythrophagocytosis.

Contributor's Comment: Equine infectious anaemia (EIA) virus is a lentivirus of the Retroviridae family with a worldwide distribution. EIA, or 'swamp fever', affects all species of Equidae, causing pyrexia, edema, splenomegaly and tissue petechiation.^{5,6} Transmission occurs via the mechanical transfer of blood by contaminated medical equipment or biting insects and the resulting infection can persist with cyclic recurrence.^{5,6} Viral replication occurs primarily in tissue macrophages of the liver, spleen and lymph nodes, and to a lesser extent in the kidney, and lung. A persistent, life-long viremia may result in clinical relapses when the viral load is high.^{5,6}

The lentivirus causing EIA is considered to have little direct cytopathic effect and with the pathogenesis involving indirect effects of the immune response.⁶ Anemia corresponds with the appearance of circulating antibody, which is complement-fixing but not initially virus-neutralizing. C3 appears on erythrocyte membranes, and probably explains the erythrophagocytosis. Antibodies are believed to react with virus adsorbed to erythrocytes which results in complement activation and red cell destruction of the "innocent bystander" type. The lifespan of red blood cells is typically shortened by up to 65% and the hemolysis that occurs is largely intracellular. The bone marrow is initially highly responsive but ultimately becomes hypoproliferative.⁶



Liver, horse. Portal areas are expanded by abundant fibrosis and infiltration of low to moderate number of lymphocytes and plasma cells. (HE, 320X)

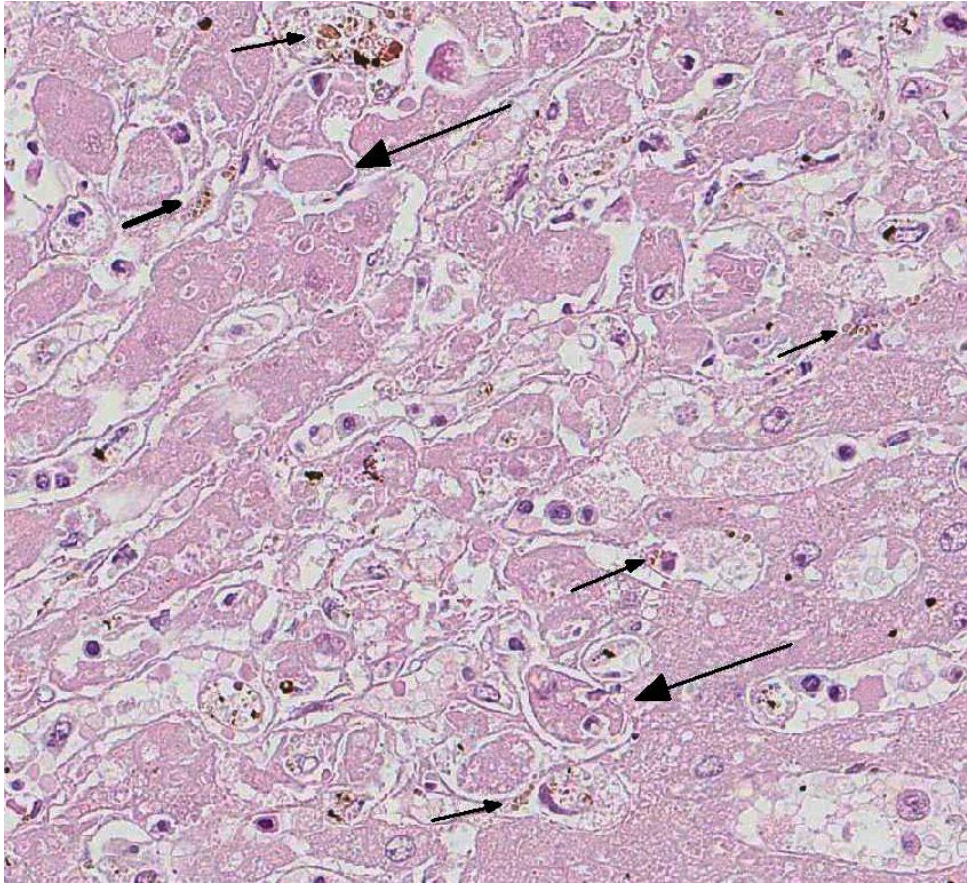
In 2006, an outbreak of EIA occurred in the Republic of Ireland in four foals following administration of contaminated hyperimmune plasma imported from Italy. The disease spread by iatrogenic transmission, resulting in 38 cases.³ Disease was confirmed by agar gel immunodiffusion, ELISA, immunoblot and using a novel PCR technique.¹ This outbreak highlighted the threat posed to animal populations by the use of unregulated veterinary medicines.

JPC Diagnosis: Liver: Hepatitis, lymphoplasmacytic, portal, diffuse, moderate with centrilobular fibrosis, erythrophagocytosis, hemosiderosis and mild hepatocellular degeneration and loss.

Conference Comment: Equine infectious anemia (EIA) evades the immune system by escaping the antibody response, resulting in a chronic infection. This retroviral disease

in horses serves as a model to study lentiviral immune escape mechanisms. Recrudescence of infection after a period of inactivity is related to antigenic variation of surface glycoproteins. Studies have shown that selection pressure against the predominant virus strain, namely via virus neutralizing antibody in this case, results in increased antibody escape by viral variants.⁴ This seems to indicate a more effective immune response against the primary infecting strain, and increases the likelihood of escape by a viral variant.

In addition to anemia, thrombocytopenia is also a component of equine infectious anemia, sharing the same mechanism as the anemia. The thrombocytopenia may be reflected in acute cases where petechial hemorrhages are evident under the tongue and on the ocular and vulvar mucosa. The majority of hemolysis is intravascular and during acute disease may be severe enough



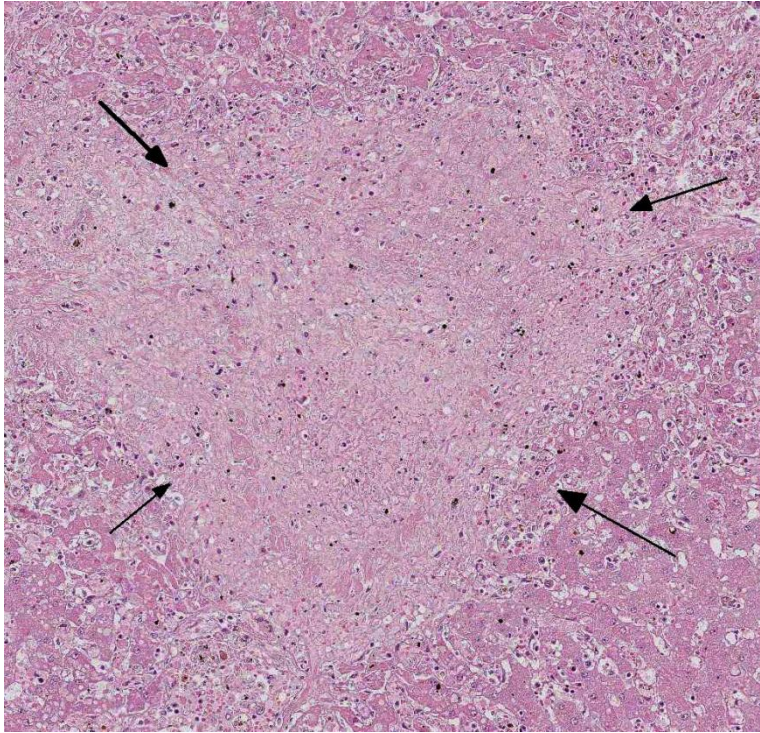
Liver, horse. Throughout the section, individual hepatocytes are rounded up, effacing plate architecture (large arrows). Kupffer cells diffusely contain abundant hemosiderin pigment (small arrows). (HE, 360X)

to result in debilitation and death. During the initial stages of infection, the anemia is regenerative but eventually becomes non-regenerative.⁷ The anemia is due to hemolysis from secondary antibody and complement fixation as described above; but is also due to inhibition of erythropoiesis, and impaired bone marrow response is likely due in part to mechanisms associated with anemia of inflammation.² Leukopenia and a relative monocytosis may also be seen, as well as erythrophagocytosis, a feature noted in this case. Chronically, the bone marrow is hypoplastic and there is sinusoidal expansion imparting a grossly red appearance to the bone marrow. A plasmacytosis may also be seen within the bone marrow in chronic cases.⁷

hepatic chords and sinusoidal dilation, increased periportal connective tissue, and Kupffer cell hyperplasia. Hemorrhage and necrosis may be seen in centrilobular areas in acute cases and hepatocellular vacuolar degeneration in subacute cases. Regardless of the stage of infection, whether quiescent or in clinical relapse, the presence of increased hemosiderin laden macrophages provides evidence of infection. Splenic follicles may be enlarged but appear hypocellular and, acutely, the spleen will be congested.⁷

In this case, there is increased pallor of portal areas at subgross histologic examination due to the presence of increased fibrous connective tissue; multifocally,

Gross lesions include splenomegaly, ventral edema, petechial hemorrhage in the kidneys, and degree of reddening within the bone marrow noted to be in direct proportion to disease duration.⁷ Capsular hemorrhage may be seen on both the liver and spleen; the liver may also have a fine lobular pattern. Microscopic lesions vary with duration but can be seen in most tissues. The hepatic changes vary in range and severity and include periportal infiltrates (as seen in this case), atrophy of



Liver, horse: Centrilobular necrosis is present throughout the section (and often bridging) as a result of long-standing anemia. (HE, 140X)

portal areas are also infiltrated by lymphocytes and macrophages. Low to moderate numbers of periportal hepatocytes are necrotic and mild hepatocellular vacuolar degeneration is present at the margin of affected areas. Cholestatic bile canaliculi and occasional erythrophagocytosis are also histologic features noted in this case. Multifocally within centrilobular areas, there is hepatocellular necrosis, as well as fibrosis; these findings reflect a degree of hypoxemia most likely secondary to anemia.

During the conference, the moderator commented on the uncommon nature of active hepatitis in the horse liver; and some conference participants described vasculitis as a prominent component in this section of liver leading some to list equine viral arteritis virus (the causative agent of equine viral arteritis) as their main differential diagnosis. Vasculitis can be seen in cases of

EIA. Other features described and discussed during the conference include mild portal to centrilobular bridging fibrosis and mesothelial hypertrophy.

Contributing Institution:

UCD Veterinary Sciences Centre
UCD School of Agriculture, Food
Science and Veterinary Medicine
University College Dublin
Belfield
Dublin 4
Ireland
www.ucd.ie

References:

1. Cullinane A, Quinlivan M, Nelly M, Patterson H et al. Diagnosis of equine infectious anaemia during the 2006 outbreak in Ireland. *Vet Rec.* 2007; 161: 647-652.
2. Grimes CN, Fry MM. Nonregenerative Anemia: Mechanisms of decreased or ineffective erythropoiesis. *Vet Pathol.* 2015; 52(2):298-311.
3. More SJ, Aznar I, Bailey DC, Larkin JF, et al. An outbreak of equine infectious anaemia in Ireland during 2006: Investigation methodology, initial source of infection, diagnosis and clinical presentation, modes of transmission and spread in the Meath Cluster. *Eq Vet J.* 2008; 40: 706-708.
4. Schwartz EJ, Nanda S, Mealey RH. Antibody escape kinetics of Equine infectious anemia virus infection of horses. *J Virology.* 2015; 89(13):6945-695.
5. Sellon DC, Perry ST, Coggins L, Fuller FJ. Wild-type equine infectious anemia virus replicates in vivo predominantly in

tissue macrophages, not in peripheral blood monocytes. *J Virol.* 1992; 66:5906-5913.

6. Valli VEO: Hematopoietic system. In: Maxie MG, ed. Jubb, Kennedy and Palmer's Pathology of Domestic Animals. 5th ed. Vol 3. Philadelphia, PA: Elsevier; 2007: 235-239.

7. Valli VEO, Kiupel M, Bienzle D. Hematopoietic system. In: Maxie MG, ed. Jubb, Kennedy, and Palmer's Pathology of Domestic Animals. 6th ed. Vol 3. St. Louis, MO: Elsevier; 2016:114-116.

CASE III: R15/72 (JPC 4071582).

Signalment: Domestic cat, 5 years and 8 months old, male, castrated. (*Felis silvestris catus*).

History: The cat was brought to the clinic with hypotension and icteric mucous membranes. All lymph nodes were slightly prominent. Radiograph showed an enlarged, pendulous abdomen with hepatomegaly and severe splenomegaly. The ultrasound examination revealed that the liver is covered with hypo echoic, nodule-like structures. The visible mesenteric lymph nodes were enlarged. Laboratory tests: Coagulation time was significantly prolonged. Liver-associated values were as well significantly altered. Because of poor prognosis the animal was euthanized.

Gross Pathology: Right eye: Buphthalmos. A brownish, 0.5 cm mass is present laterally on the sclera.

Liver: Diffusely severely enlarged, with disseminated white-green and black, up to



Liver, cat. The liver is diffusely enlarged and covered with raised green and black nodules ranging up to 5mm in diameter. Nodules contain central areas of necrosis. (Photo courtesy of: University of Bern, Vetsuisse faculty, Institute for Animal Pathology (ITPA), Laenggassstrasse 122, CH – 3012, Switzerland, <http://www.itpa.vetsuisse.unibe.ch/>)

5mm nodules which are multifocally slightly raised and show central necrosis.

Spleen: Diffusely severely enlarged. Multifocally are up to 4 cm nodules present that are dark red and slightly firm.

Laboratory results (See Table 1, next page)

Histopathologic Description: Liver: Extending to all cut borders, infiltrating the sinusoids and disrupting the architecture of the hepatocellular cords, there is a diffuse, densely cellular, non-demarcated and non-encapsulated neoplasm consisting of neoplastic cells that are arranged in sheets

Area	Parameter	Unit	Reference	
Hematology	Hematocrit	l/l	0.27-0.47	0.19
	HB total	g/l	82-153	62
	Erythrocytes	10e12/l	5.9-11.2	3.43
	MCV	fl	37.0-55.0	54.7
	MCH	pg	11.3-17.2	18.2
	MCHC	g/l	263-359	332
	RDW	%	13.8-21.1	28.1
	Retikulocytes %	%	0.05-1.17	6.35
	Retikulocytes	10e9/l	3.7-94.1	217.7
	CHr	pg	>14.2	20.7
	MCVr	fl	47.6-72.8	83.2
	Thrombocytes	10e9/l	180-430	52
	MPV	fl	10.2-25.8	25.2
	Leukocytes	10e9/l	6.5-15.4	13.14
	Leukocytes corrected	10e9/l	6.5-15.4	10.81
Chemistry	Hemolitic Index		<15	29
	Icterus Index		<10	10
	Lipemia index		<100	30
	Na	mmol/l	144-159	146
	K	mmol/l	3.11-4.93	4.93
	Cl	mmol/l	110-130	103
	Ca	mmol/l	2.22-2.92	1.98
	P	mmol/l	0.82-1.91	4.05
	Glucose	mmol/l	3.17-5.71	6.96
	Total protein	g/l	55-76	45.3
	Albumin	g/l	30.3-40.5	25.5
	Urea	mmol/l	6.46-12.20	72.79
	Creatinine	μmol/l	52-138	658
	Bilirubin	μmol/l	0-6.2	155.4
	ALAT (GPT)	IU	12-77	4231
	AP	IU	0-93	122
	ASAT (GOT)	IU	12-61	7146
	CK	IU	0-596	4095
	gGT	IU	0-2	4
	GLDH	IU	0-3	2279
Serum Amyloid A	μg/ml	<5	121.3	
Coagulation	PT (Quick)	sec	9.4-13.1	27.8
	PTT	sec	12.0-16.3	58.2
	TT	sec	16.5-25.1	42.3
	Fibrinogen	mg/dl	150-300	19



Liver and spleen, cat. Cross sections of the spleen (left) and liver (right) exhibit poorly defined, pigmented nodules, which range up to 4cm in diameter. (Photo courtesy of: University of Bern, Vetsuisse faculty, Institute for Animal Pathology (ITPA), Laenggassstrasse 122, CH – 3012, Switzerland, <http://www.itpa.vetsuisse.unibe.ch/>)

and vague packets. The cells are round to polygonal, up to 25 μm in diameter with moderately distinct cell borders and abundant basophilic, finely granular cytoplasm that multifocally contains brownish pigment (melanin). The cells contain a round to oval, central nucleus with finely vesicular chromatin and mostly one prominent, basophilic nucleolus. There are abundant multinucleated, up to 100 μm giant cells with up to 8 nuclei. Anisokaryosis and anisocytosis are severe. Mitoses range from 3 to 6 per 400x HPF. The neoplastic cells are in large numbers present in almost all blood vessels and lymphatics (vascular invasion, Figure 3). Multifocally there are large areas of necrosis, surrounded by hemorrhage, edema and an inflammatory infiltrate consisting mostly of degenerate neutrophils, macrophages and some lymphocytes and plasma cells. The adjacent hepatocytes are rounded, have an eosinophilic and vacuolated cytoplasm (degeneration). Single cell necrosis is

present. Multifocally bile plugs are present in the canaliculi and yellow to brown pigment in the hepatocytes (cholestasis). There is diffuse congestion present.

Masson-Fontana: Many of the neoplastic cells contain variable amounts of intracytoplasmic, agyrophilic, granular material (melanin).

Immunohistochemistry: The neoplastic cells stain positive with 'Melan A' and 'PNL-2' (Melanoma).

Contributor's Morphologic Diagnosis:
Liver: Melanoma, metastatic

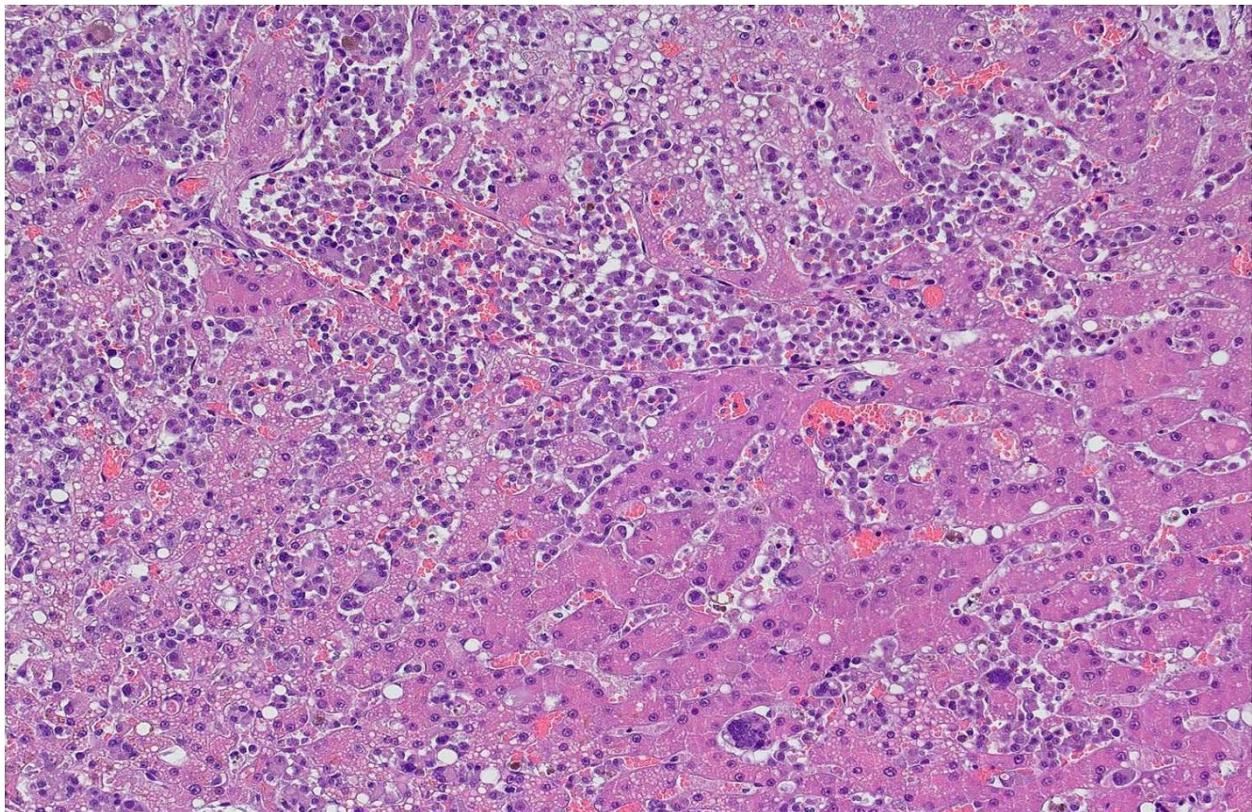
Contributor's Comment: The present case describes a rare case of metastatic conjunctival melanoma in the liver and spleen of an adult spayed, domestic shorthair cat, presented because of jaundice and an enlarged, pendulous abdomen. The hematology, blood chemistry and coagulation values were severely abnormal

(see Table 1). The primary tumor was found in the eye as a small conjunctival, brownish nodule. In the clinic, because of the exclusive conjunctival involvement and no evidence of iridial or corneal involvement, the mass was diagnosed as a conjunctival melanoma. This mass was not clinically relevant and was surgically removed before the clinical symptoms occurred.

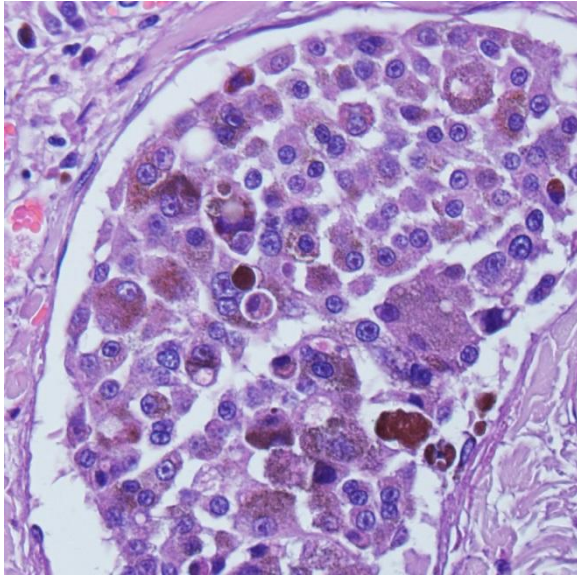
Malignant melanomas are generally tumors of older animals; however, they have been reported in juvenile animals of many species.² They are common in the dog and uncommon in other domestic species. In cats, they are uncommon and occur mainly in older cats showing no sex predisposition. Malignant melanomas can be composed of a variety of cell morphologies including spindle cells, epithelioid cells, a mixture of spindle cells and epithelioid cells, singlet-

ring cells or balloon cells. In addition they can be heavily pigmented or amelanotic.³ The present metastatic mass in liver and spleen is considered as an epithelioid type and is pigmented. Metastasis occurs commonly with spread via lymphatics to regional lymph nodes and lungs. It is not uncommon for malignant melanomas to spread to other body sites, including unusual locations such as the brain, heart and spleen.³

Ocular melanoma in cats occurs in a variety of sites. The vast majority of feline ocular melanomas arise diffusely from the anterior uvea (iris, ciliary body).⁵ Conjunctival melanomas in dogs and cats are in general rare.³ One study reported in a comparison study of 19 feline ocular melanomas that 16 were intraocular, while only three were



Liver, cat. Sinusoids and hepatic vessels are expanded by numerous neoplastic cells, some multinucleated. Hepatocytes often contain numerous discrete lipid vacuoles. (HE, 200X) (Photo courtesy of: University of Bern, Vetsuisse faculty, Institute for Animal Pathology (ITPA), Laenggassstrasse 122, CH – 3012, Switzerland, <http://www.itpa.vetsuisse.unibe.ch/>)



Liver, cat. Neoplastic cells contain abundant intracytoplasmic melanin pigment. (HE, 400X)

conjunctival.⁴ In another study by Schobert et al. (2010), in 13 cases of conjunctival melanoma in cats with adequate follow-up information, only three reported metastasis (14%). Of those three cases, two had metastasized to the submandibular lymph nodes, while in the third case, an abdominal mass was detected.⁵ Interesting about our case is that two abdominal organs (liver, spleen) were severely infiltrated and that the neoplastic cells were present in the lymphatics and blood vessels diffusely within the spleen and liver.

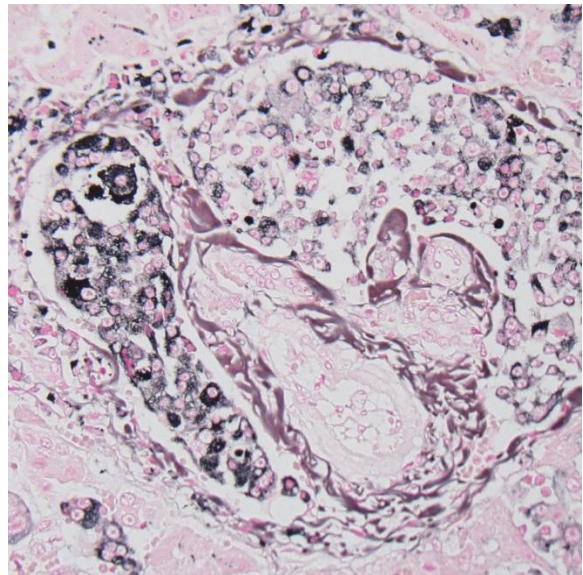
JPC Diagnosis: Liver: Metastatic melanoma.

Conference Comment:

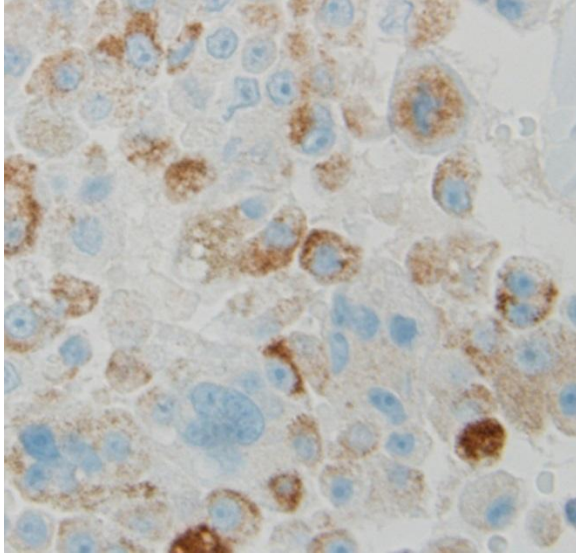
The most common location for feline conjunctival melanoma is on the bulbar conjunctiva with extension into the orbital tissues, and abundant pigmentation is seen in the majority of tumors. The presence of multinucleated tumor cells is common and may explain the presence of multinucleated

neoplastic cells in the metastatic disease in the liver in this case. Conjunctival melanoma in cats has a poorer long term prognosis than the same neoplasm in dogs.⁵ In general, melanomas are less common in cats than dogs but the eye is the most common site, and melanoma is the most common intraocular neoplasm in cats. Non-ocular melanomas occur in cats as well but are considered rare and metastasis was present in 30% of cases in one study.¹ In general non-ocular melanoma is a disease of older cats, with the exception of auricular melanoma which occurs in a significantly younger population.¹ Non-ocular melanomas often occur on the head of cats and have a similar distribution as squamous cell carcinoma. Amelanotic melanomas in cats carry a poorer prognosis and are often negative for Melan A but most are positive for S100.¹

This was a challenging case for conference participants with the majority diagnosing this lesion as histiocytic sarcoma due in large part to the presence of multinucleated cells. Cholestasis, as seen in this case, is also a common feature of hepatic histiocytic



Liver, cat. Neoplastic melanocytes exhibit strong positivity with a Fontana-Masson's stain. (Fontana Masson, 240X)



Liver, cat. Neoplastic melanocytes exhibit diffuse strong reactivity against Melan A. (anti-Melan, 360X).

sarcoma. The moderator commented this is an unusual case and he had not previously seen a case like this one. Additional features described and discussed included vascular thrombosis and, interestingly, rare mitoses were noted in hepatocytes in the absence of regenerative nodules. The moderator pointed out the collar of connective tissue surrounding the central vein, which is a normal feature in the feline liver that distinguishes it from other species. The areas of hepatocyte necrosis and loss surrounding the central vein are presumed secondary to hypoxia from obstruction of sinusoids by tumor emboli. The excellent gross image and the laboratory data provided by the contributor greatly enhanced the learning / teaching value of this case.

Contributing Institution:

University of Bern, Vetsuisse faculty
 Institute for Animal Pathology (ITPA)
 Laenggassstrasse 122
 CH - 3012
 Switzerland
<http://www.itpa.vetsuisse.unibe.ch/>

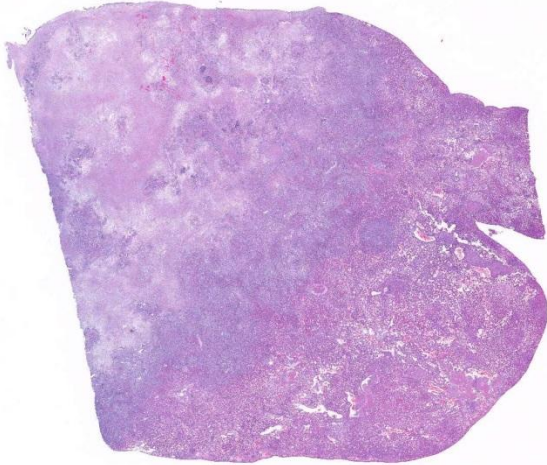
References:

1. Chamel G, Abadie J, Albaric O, Labrut S. Non-ocular melanomas in cats: a retrospective study of 30 cases. *J Feline Med Surg.* 2016; Jan 14(E pub):1-7.
2. Ginn PE, Mansell JEKL, Rakich PM. Skin and appendages. In: Maxie MG, ed. *Jubb, Kennedy, and Palmer's Pathology of Domestic Animals.* 5th ed. Vol 1. Philadelphia, PA: Elsevier Saunders; 2007:760.
3. Meuten DJ. *Tumors in Domestic Animals.* 4th ed. Iowa State Press; 2002.
4. Patnaik AK, Mooney S. Feline melanoma: a comparative study of ocular, oral, and dermal neoplasms. *Vet Pathol.* 1988; 25: 105-112.
5. Schobert CS, Labelle P, Dubielzig RR. Feline conjunctival melanoma: histopathological characteristics and clinical outcomes. *Veterinary Ophthalmology.* 2010;

CASE IV: 12-0011 (JPC 4019862).

Signalment: 12-year-old, female spayed, domestic shorthair cat, feline (*Felis domesticus*).

History: The cat was presented to an animal shelter with a history of vomiting and anorexia. Upon physical examination, she was thin with pale mucous membranes. The abdomen was distended, and hepatomegaly was palpated. The cat underwent exploratory laparotomy, and representative samples of liver, as well as the lesions in the greater omentum and parietal peritoneum were collected for histopathologic evaluation. However, the cat was euthanized due to poor prognosis.



Liver, cat. An infiltrative, partially necrotic neoplasm replaces 50% of the section (HE, 5X)

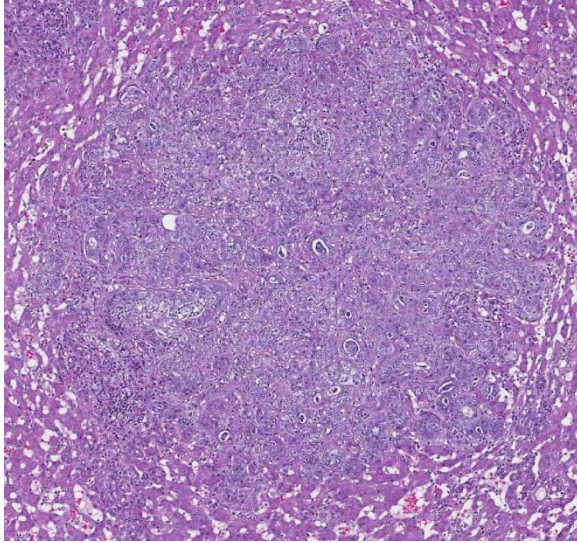
Gross Pathology: The abdominal cavity contained blood, and clotted blood and fibrin tags covered the surface of the liver. Hepatic architecture was also extensively effaced and expanded by multiple, coalescing, umbilicated, firm, pale tan nodules (5-20mm diameter) that extended across the surface and throughout the parenchyma. Firm, pale tan, coalescing nodular lesions (3-10mm diameter) also extended to involve the greater omentum and parietal peritoneum.

Laboratory Results: Serum biochemistry abnormalities: Total protein 8.9 g/dL (5.8-8.1); Albumin 1.8 g/dL (2.6-4.0); Alanine aminotransferase 240 U/l (15-52); Aspartate aminotransferase 112 U/l (14-42); Bilirubin 4.5 mg/dL (0-0.6).

Hematologic abnormalities: Hematocrit 18% (24-45); Hemoglobin 6.5 g/dL (8.0-15.0); Red blood cell count 4.37 M/ μ L (5.0-10.0).

Histopathologic Description: Liver: The hepatic parenchyma is extensively necrotic and effaced by focal to coalescing proliferations of neoplastic cells that differentiate toward biliary epithelium and form acini, tubules, and packets. Cells are low cuboidal to columnar with indistinct borders, and pale amphophilic, vacuolated cytoplasm. Nuclei are large, round to oval, and contain one or two prominent nucleoli. There are 2-4 mitotic figures per ten 40x objective fields. Neoplastic ducts and acini contain luminal neutrophils, proteinaceous fluid, and cell debris, and are embedded within an extensive background collagenous stroma (scirrhous response). Neoplastic cells are present in lymphatics, and along the capsular surface in some regions (not present in all sections). Blood vessels and sinusoids contain fibrin thrombi. Scattered neutrophils are present throughout the necrotic tissue. Mesothelial cell proliferation is also seen along the capsular surface.

Within the adjacent remaining parenchyma, portal regions are expanded by moderate proliferations of lymphocytes & plasma cells, with bile duct proliferation, and periductular fibrosis. Some bile ducts are lined by attenuated epithelium and contain luminal or periductal neutrophils.



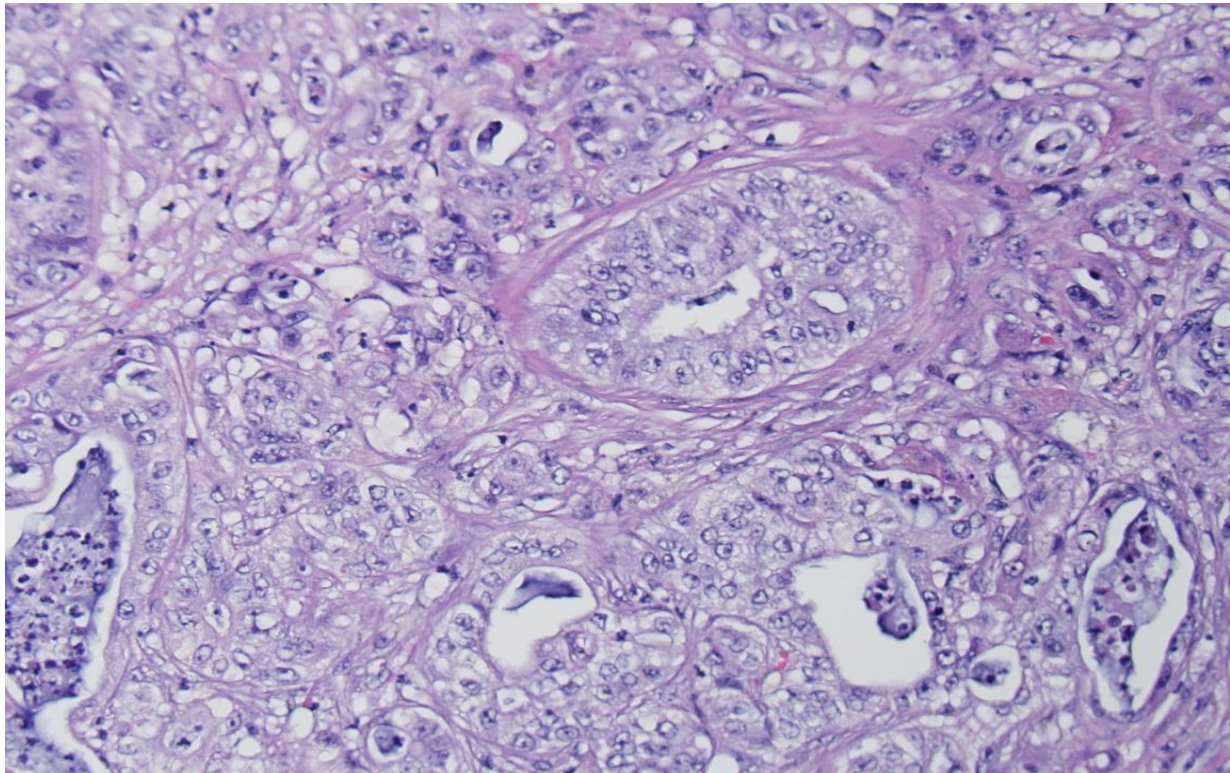
Liver, cat. Well-demarcated, often coalescing neoplastic nodules are distributed throughout the section. (HE, 70X)

Contributor's Morphologic Diagnosis:

Liver: Cholangiocellular carcinoma with lymphatic invasion; Chronic fibrosing, lymphoplasmacytic portal hepatitis, domestic shorthaired cat, feline.

Contributor's Comment: Cholangiocellular carcinomas are malignant neoplasms that can occur in all species. They arise from bile duct epithelium, predominantly from intrahepatic ducts, although extrahepatic ducts can be involved also. These neoplasms can present either in the form of a mass or as coalescing, umbilicated, nodular proliferations on the surface of the liver and throughout the parenchyma.^{7,11}

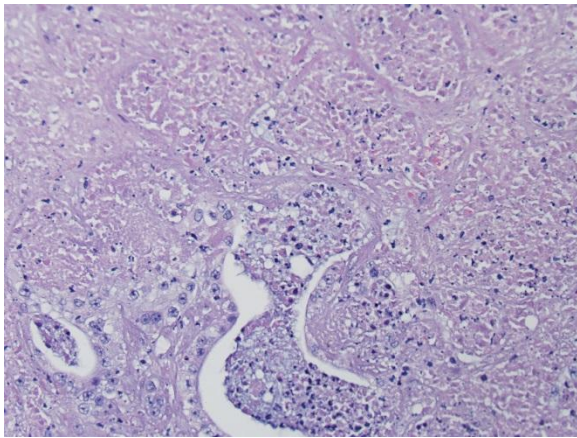
Although primary hepatobiliary tumors are rare in cats, cholangiocellular carcinoma represents the most common non-hematopoietic, hepatic malignancy in this species.¹ This is a locally aggressive neoplasm with a high metastatic potential, and metastases are documented in up to 80% of necropsy cases.⁸ Extrahepatic metastasis is common, especially to cranial abdominal lymph nodes and lung, and seeding of tumor into the abdominal cavity is not uncommon, with lesions extending throughout the



Liver, cat. The neoplasm is composed of epithelial cells forming cell differentiated tubules and acini. (HE, 200X)

mesentery and visceral peritoneal surfaces.¹¹

In cats, cholangiocellular carcinomas are typically found in animals of 9 years of age and older.¹ There are no breed predilections, and although there are some suggestions that this tumor is more commonly diagnosed in male cats,¹ other studies do not demonstrate such a gender difference.⁶ The prognosis is poor, with a life expectancy of less than 6 months.⁶



Liver, cat. Large areas of the neoplasm are necrotic. (HE, 200X)

As compared with cats with benign tumors of the biliary tract, cats with cholangiocellular carcinoma are more likely to exhibit clinical signs, and lethargy, anorexia, and vomiting are most commonly reported.¹ Upon physical examination, the most common finding is the presence of a cranial abdominal mass or hepatomegaly, while ascites and icterus are less common.¹

Hematologic and biochemical profiles are often nonspecific.¹ Leukocytosis is sometimes reported, and alanine aminotransferase, aspartate aminotransferase, and total bilirubin levels may be elevated.⁶

Microscopically, these tumors are usually distinctly adenocarcinomatous, comprising proliferations of cells that differentiate toward biliary epithelial cells, and form acini, tubules, and papillary projections.

More poorly differentiated forms may be composed of solid epithelial proliferations, with or without the formation of islands, cords, or packets of cells, and foci of squamous differentiation. Numerous mitotic figures are present. A variable connective tissue stroma is present, often with marked collagen deposition, the so-called scirrhous response. Areas of necrosis are also common.^{7,11}

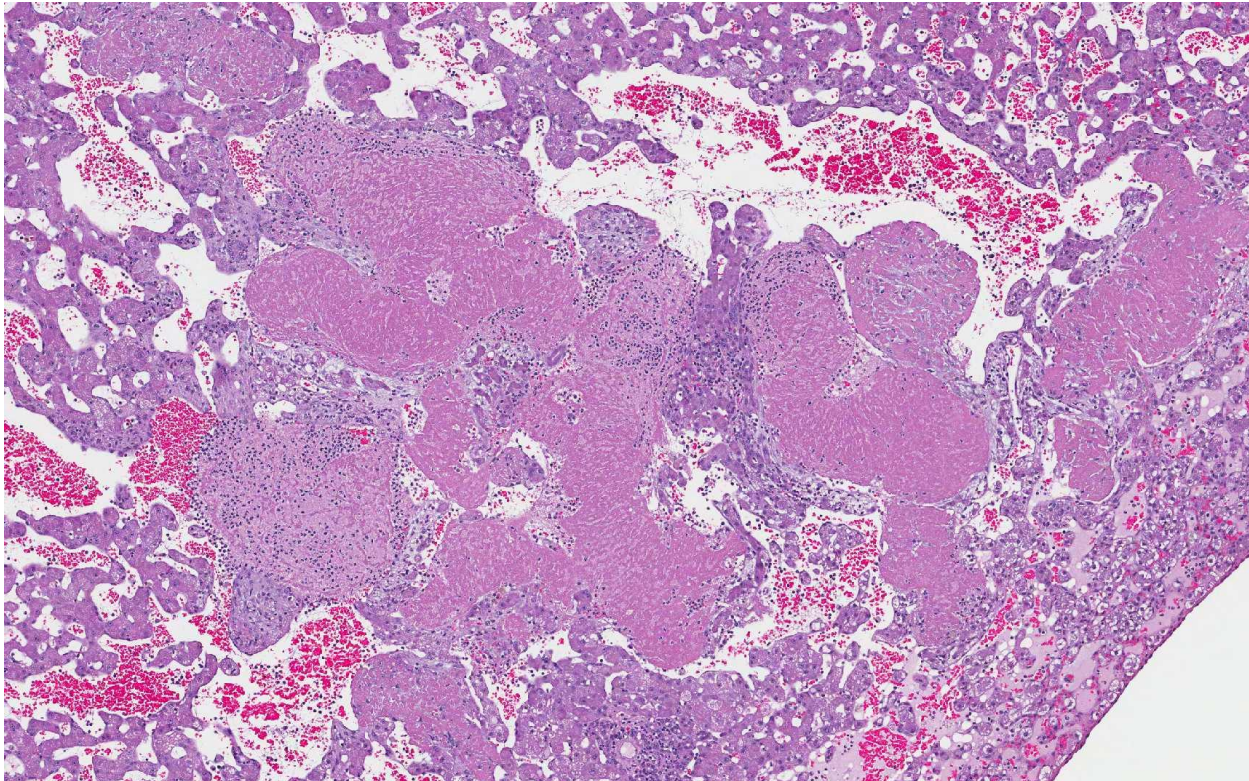
Paraneoplastic alopecia has also been associated with cholangiocellular carcinoma, as well as pancreatic adenocarcinoma in cats. This presents as bilaterally symmetrical alopecia of the ventrum and limbs, sometimes with a shiny appearance to the alopecic skin. Histologically, skin changes comprise follicular and adnexal atrophy with hypoplasia of the stratum corneum.⁹

In people, cholangiocellular carcinoma is the second most common hepatic malignancy after hepatocellular carcinoma, accounting for more than 7% of cancer deaths throughout the world. In the United States, it accounts for 3% of all cancer deaths, and its prevalence is highest in Hispanics. Although most cholangiocellular carcinomas in the western world arise without evidence of antecedent disease, chronic hepatobiliary inflammatory conditions can predispose patients to development of these tumors. The incidence rates of this malignancy are highest in Southeast Asia, where a major risk factor is chronic infection of the biliary tract with the liver fluke *Opisthorchis sinensis*. Additional predisposing risk factors for development of cholangiocellular carcinoma in people, include: primary sclerosing cholangitis; infection with hepatitis B or C; and congenital diseases of the biliary tract, such as choledochal cysts or Caroli's syndrome.^{4,5} However, no definitive association between inflammatory hepatobiliary disease, or other antecedent conditions, has been established in cats.

JPC Diagnosis: 1. Liver: Cholangiocellular carcinoma.

2. Liver: Cholangiohepatitis, suppurative, multifocal, severe, with septic thrombi and telangiectasis.

and parasite excretory products found within host cholangiocytes which have the ability to drive cell proliferation. The fluke *O. viverrini* is capable of secreting extracellular vesicles, which are small membrane bound structures released from different types of helminths. The vesicles are taken up by



Liver cat: Large sinusoidal fibrin thrombi are present in one edge of the section; adjacent sinusoids are massively dilated due to altered blood flow. (HE, 70X)

Conference Comment: As mentioned above, in certain regions of Southeast Asia there is a link between cholangiocellular carcinoma in people and infection with liver flukes, including *Opisthorchis viverrini*. The fluke is classified as a group 1 carcinogen, and the infective stage can be transmitted by consumption of undercooked fish. Once in the digestive tract of the definitive host, the parasites migrate to the bile ducts where they feed on biliary epithelium. The carcinogenicity of fluke infection is driven by multiple factors, including mechanical damage to biliary epithelium, inflammatory processes driven by cytokines such as IL-6,

cholangiocytes resulting in both inflammatory and protumorigenic changes providing a mechanism by which the parasite is able to drive tumorigenesis. Vesicle uptake is documented to result in dysregulation of protein expression involved in wound healing, tumor cell invasion and the proteasome complex.² Liver fluke carcinogenesis has not been documented in domestic food animals, such as sheep and cattle; this may be due to interspecies differences in immunomodulatory mechanisms or uptake of procarcinogenic secretory products, or perhaps because of differences in lifespan. Infection with the biliary fluke

Platynosomum fastosum in cats, which results in varying degrees of inflammation, fibrosis and hyperplasia within the biliary tract, has been found concurrently with cholangiocarcinoma in some animals.³

In this slide, the lobular hepatic architecture is approximately 75% effaced. Concentric fibrosis surrounding bile ducts is a prominent feature, and the moderator commented this feature is secondary to cholestasis, and neutrophilic cholangitis is, in turn, the result of biliary stasis.

Fibrin thrombi within sinusoids and blood vessels contain enmeshed epithelioid macrophages and other inflammatory cells. In this slide, large areas of sinusoidal dilation border fibrin thrombi. These areas of dilation may represent local blood flow change or, in the normal liver, would often be interpreted as foci of telangiectasis, a common histologic finding in the liver of the cat.

Additionally, two important diagnostic features in this case include the scirrhous reaction and mucous within ducts / tubules, which are not seen in hepatocellular carcinoma. In domestic animal species, metastatic neoplasia in the liver is more common than primary neoplasia.¹⁰

Contributing Institution:

Massachusetts Institute of Technology
16-849, Division of Comparative Medicine
77 Massachusetts Avenue
Cambridge, MA 02139
<http://web.mit.edu/comp-med/>

References:

1. Balkman C. Hepatobiliary neoplasia in dogs and cats. *Vet Clin North Am Small Anim Pract.* 2009; 39:617-25.

2. Chaiyadet S, Sotillo J, Smout M, Cantacessi C, et al. Carcinogenic liver fluke secretes extracellular vesicles that promote cholangiocytes to adopt a tumorigenic phenotype. *J Infect Dis.* 2015; 212(10):1636-45.

3. Cullen JM, Stalker MJ. In: Maxie MG, ed. *Jubb, Kennedy, and Palmer's Pathology of Domestic Animals.* 6th ed. Vol 2. St. Louis, MO: Elsevier; 2016:322.

4. Friman S. Cholangiocarcinoma – current treatment options. *Scand J Surg.* 2011; 100:30-34.

5. Kumar V, Abbas AK, Fausto N, Aster JC. *Robbins and Cotran, Pathologic Basis of Disease.* 8th ed. Elsevier; 2010:880-881.

6. Lawrence HJ, Erb HN, Harvey HJ. Nonlymphomatous hepatobiliary masses in cats: 41 cases (1972 to 1991). *Vet Surg.* 1994; 23:365–368.

7. Maxie MG. *Jubb, Kennedy, and Palmer's Pathology of Domestic Animals.* 5th ed. Vol 2. Philadelphia, PA: Elsevier; 2007:385-386.

8. Patnaik AK. A morphological and immunocytochemical study of hepatic neoplasms in cats. *Vet Pathol.* 1992; 29:405–415.

9. Tasker S, Griffon DJ, Nuttall TJ, et al. Resolution of paraneoplastic alopecia following surgical removal of a pancreatic carcinoma in a cat. *J Small Anim Pract.* 1999; 40:16-19.

10. World Small Animal Veterinary Association. *Standards for the Clinical and Histologic Diagnosis of Canine and Feline Liver Diseases.* Philadelphia, PA: Saunders Elsevier; 2006.

11. Zachary JF, McGavin MD. *Pathologic Basis of Veterinary Disease*. 5th ed. St. Louis; Mosby Elsevier; 2012:444.

Joint Pathology Center
Veterinary Pathology Services



WEDNESDAY SLIDE CONFERENCE 2015-2016

Conference 20

6 April 2016

Amy C. Durham, MS, VMD, DACVP
Assistant Professor, Anatomic Pathology
University of Pennsylvania
School of Veterinary Medicine

CASE I: 13-870 (JPC 4048070).

Signalment: 11-year-old female spayed miniature schnauzer (*Canis familiaris*)

History: The dog presented for evaluation of a cataract and it was discovered that the dog is blind in this eye and has a probable retinal detachment. An enucleation was performed.

Gross Pathology: The interior of the eye is filled with an opaque white material that obscures all internal structures.

Laboratory Results: None

Histopathologic Description:

The vitreous and the anterior and posterior chambers are filled with a proteinaceous material containing many cholesterol crystals. A mild mixed inflammation of macrophages and lymphocytes is present at the margins of the fluid and a few macrophages are within the fluid. The retina has mild atrophy of the inner layers, a partial

detachment, and a diffuse, mild inflammation of lymphocytes and plasma cells. The back of the iris is covered with a fibrous layer containing many lymphocytes. A few lens fibers are round, swollen and vacuolated. The lens is not present in all slides.

Contributor's Morphologic Diagnosis:

1. Cholesterosis bulbi
2. Retinal atrophy, partial detachment and lymphoplasmacytic retinitis
3. Cataract

Contributor's Comment: Cholesterosis bulbi is the accumulation of cholesterol within a degenerate vitreous humor that has become liquefied (syneresis). The condition may also involve the anterior and posterior chambers as in this case. It occurs in eyes that have suffered previous hemorrhage, inflammation or other degenerative changes.² The cause in this case is unknown but the cataract is a possibility.



Globe, dog. The posterior chamber of the eye is filled with an opaque white material which obscures internal structure. (Photo courtesy of: College of Veterinary Medicine, Virginia Tech, Blacksburg, VA 24061, www.vetmed.vt.edu)

JPC Diagnosis: Eye, Globe: Panuveitis, lymphoplasmacytic and histiocytic, diffuse, moderate with protein and cholesterol-rich exudate, retinal detachment and atrophy, and drainage angle closure.

Conference Comment: Cholesterolosis bulbi is an uncommon condition and not well-documented in the professional veterinary literature. Although it is more well-documented in human medicine, it is still uncommon may also be referred to as “synchysis scintillans”. The lesion is typically found in the vitreous and common causes include trauma and degenerative ocular disease, which may be associated with chronic inflammation and/or longstanding retinal detachment. The cholesterol crystals are thought to be derived from the breakdown of intraocular erythrocytes and, may also be found within the anterior chamber.^{1,4} In people, cholesterolosis bulbi may be associated with a condition known as Coats’ disease, which includes retinal telangiectasis with intra and

subretinal exudation.⁴ In cases of cholesterolosis in the absence of intraocular hemorrhage, it has been suggested that cholesterol crystals may enter eye through breaks in the retina and originate from the cholesterol rich subretinal fluid. Phacolysis has also been proposed as a source of cholesterol crystals.³

In addition to the proteinaceous, cholesterol-laden fluid filling most segments of the globe, conference participants noted retinal degeneration and atrophy, mild keratitis, uveal inflammation and choroidal edema. Fragmentation and fibrillation as well as cataractous changes were also described within the lens (not present in all sections), although the moderator cautioned against over-interpreting lens rupture due to the fragile nature of the lens and its tendency to fracture during sectioning. Specific retinal changes included retinal detachment, hypertrophy and hyperplasia of the retinal pigment epithelium, vacuolation of the nerve fiber layer, and degeneration of the ganglion

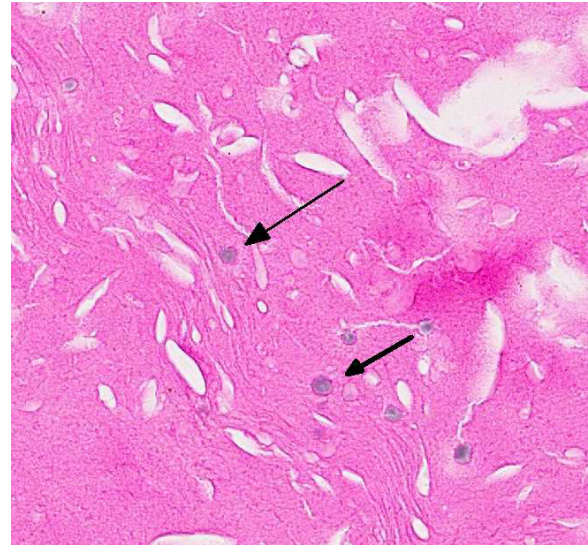


Globe, dog. The posterior chamber, and to a lesser extent, the anterior chamber is filled by a flocculent brightly eosinophilic proteinaceous exudate. (HE, 5X)

cell and plexiform layers. The moderator commented on the rare nature of cholesterosis bulbi, citing several potential underlying causes such as trauma and hemorrhage, although it should be noted that intraocular hemorrhage is a relatively common finding not specific to this uncommon condition. Asteroid hyalosis was also present and is typically characterized by the presence of 4-10µm pale basophilic granules / globules within the posterior segment, consisting of lipids embedded in a matrix of calcium and phosphorus, and attached to the vitreous. The asteroid bodies appear as amorphous globules, are PAS positive and contain small birefringent crystals when viewed under polarized light. Diabetes mellitus is a risk factor in people for the development of asteroid hyalosis as are hypertension and atherosclerosis.⁵

Contributing Institution:

College of Veterinary Medicine
Virginia Tech
www.vetmed.vt.edu



Globe dog. The exudate in the posterior chamber contains numerous acicular cholesterol clefts as well as numerous 10-20 µm amphiphilic globules (asteroid hyalosis). (HE, 320X)

References:

1. Brodsky MC. Synchrony scintillans in a child. *JAMA Ophthalmol.* 2015; 133(7):e150793.
2. Grahn BH, Peiffer RL. Veterinary ophthalmic pathology. In: Gelatt KN, Gilger BC, Kern TJ, eds. *Veterinary Ophthalmology*. 5th ed. Hoboken NJ: Wiley-Blackwell; 2013:490.
3. Park, J, Lee H, Kim YK, Chae JD, Lee HJ. A case of cholesterosis bulbi with secondary glaucoma treated by vitrectomy and intravitreal bevacizumab. *Korean J Ophthalmol.* 2011;25(5):362-365.
4. Stacey AW, Borri M, Francesco SD, Antenore AS, et al. A case of anterior chamber cholesterosis due to Coats' disease and a review of reported cases. *Open Ophthalmol J.* 2016. Feb 29;10:27-32.
5. Yanoff M, Sassani JW. *Ocular Pathology*. 6th ed. Mosby Elsevier; 2009:486-487.

CASE II: 9650463 (JPC 4048848).

Signalment: 9-year-old male neutered Labrador retriever dog (*Canis familiaris*).

History: Chronic glaucoma of the left eye for approximately 1 year with pain and blindness. Glaucoma is poorly controlled with medical management and history of cataract with cataract surgery in the same eye 1.5 years prior.

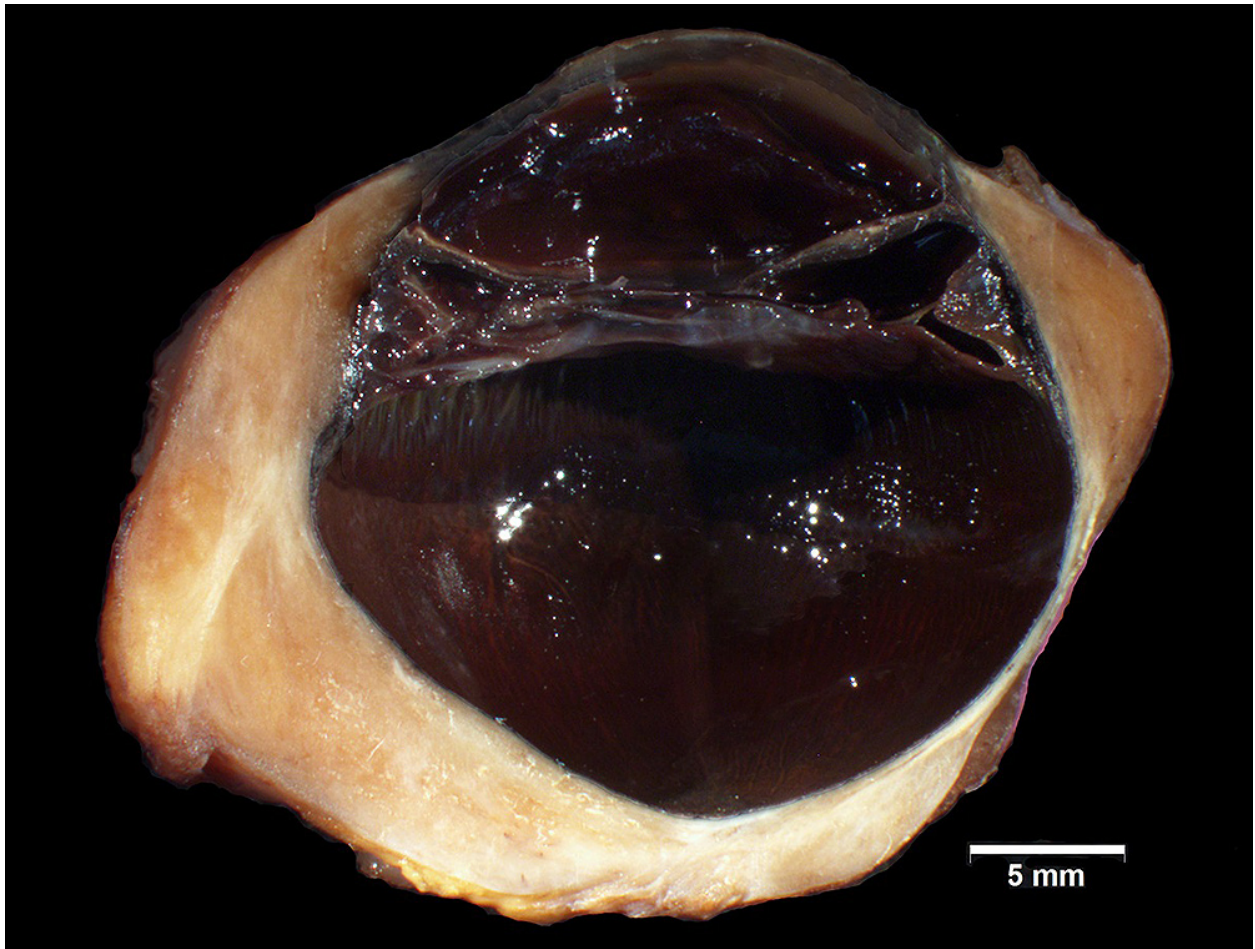
Gross Pathology: The globe is enlarged and there is multifocal nodular to coalescing severe thickening of the sclera at the limbus and extending nearly circumferentially around the globe, measuring up to 0.7 cm in

the thickest areas. There is intraocular blood and there is corneal opacity.

Laboratory Results: Results of complete blood count and chemistry panel are within reference interval.

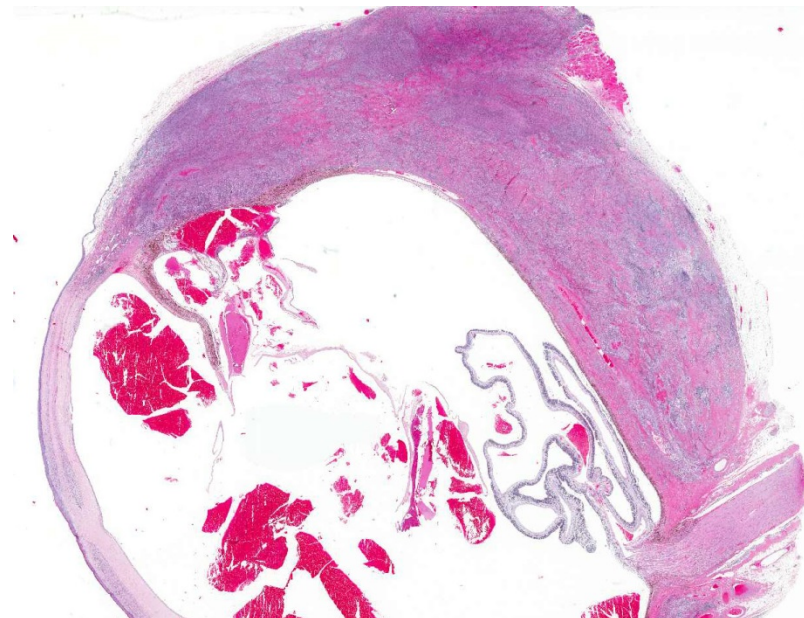
Histopathologic Description: Please note that the section available for participants contains the majority of the scleral lesion, but may not contain all of the internal lesions within the globe.

The globe is enlarged and severely expanding the sclera at the limbus and extending nearly circumferentially, there is a nodular to diffuse inflammatory infiltrate with extensive fibroplasia and fibrosis. The



Globe, dog. The sclera of this enlarged globe is thickened segmentally, up to 0.7cm in some areas. The retina is detached. (Photo courtesy of: Animal Medical Center, 510 East 62nd Street, New York, NY 10065, www.amcny.org)

inflammation is composed of predominantly epithelioid macrophages, lymphocytes, and plasma cells, with fewer neutrophils. There are occasional discrete granulomatous foci with central altered collagen that is hypereosinophilic and smudged (“collagenolysis”), surrounded by a rim of epithelioid macrophages. There is extensive collagen deposition within the inflammatory lesion, and in some areas the collagenous tissue is in a storiform-like pattern that multifocally has central similarly altered collagen that is hypereosinophilic with smudging (“collagenolysis”). The inflammatory lesion and collagen deposition extends from the nodular area of the limbus posteriorly to adjacent to the optic nerve,



Globe, dog. Subgross image of the eye, showing the profound fibrosis and inflammatory change of the sclera. The retina is diffusely detached and there is hyphema with in the anterior and posterior chambers. There is multifocal inflammatory infiltrates within the cornea (HE, 5X)

and extends outward into the adjacent extraocular skeletal muscle.

Within the cornea, there is hyperplasia of the epithelium with irregular rete ridge formation, and within the stroma, there is fibrosis, neovascularization, and a mild inflammatory infiltrate, composed of lymphocytes, plasma cells, and neutrophils. There

is a focal break in Descemet’s membrane (corneal stria) filled in with fibroplasia and fibrosis. Within the anterior uvea, there is iris and ciliary body atrophy, a pre-iridal fibrovascular membrane that spans across the filtration angle, and a mild to moderate perivascular accumulation of lymphocytes and plasma cells. There is blood within the anterior and posterior chambers, as well as in the vitreous. A fragment of lens is present, which includes lens capsule, and the lens fibers are fragmented, hypereosinophilic, and have occasional Morgagnian globules and bladder cells. There is a fibrovascular membrane adhered to the posterior aspect of the lens capsule.

There is diffuse retinal detachment with hypertrophy of the retinal pigmented epithelium, and there is mild atrophy of the inner nuclear and ganglion cell layers of the retina.

Masson’s trichrome: There is segmental red staining of the lesional collagen with Masson’s trichrome.

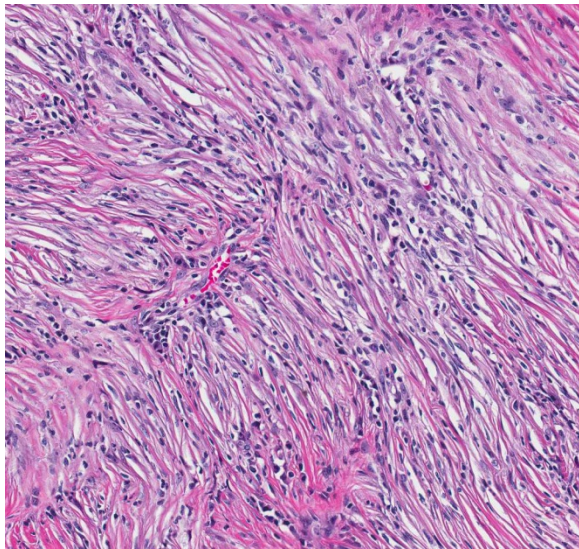
Contributor’s Morphologic Diagnosis:

Eye (left):

1. Severe granulomatous scleritis with altered collagen, consistent with necrotizing scleritis (also known as granulomatous scleritis).

2. Buphthalmia; corneal fibrosis, neovascularization, keratitis, and focal rupture of Descemet’s membrane (corneal stria); mild lymphoplasmacytic anterior uveitis with pre-iridal fibrovascular membrane, occlusion of filtration angle and hyphema; retinal detachment with inner retinal atrophy; and lens cataractous change.

Contributor's Comment: The scleritis in this case is consistent with the disease entity known as necrotizing scleritis. The most diagnostic features are the formation of discrete granulomas within the inflammatory lesion, as well as the altered collagen appearance, which is often referred to as "collagenolysis" or "collagen necrosis." Necrotizing scleritis is discussed in more detail below. The other intraocular lesions described in this globe, as well as the clinical glaucoma, may be secondary to the scleritis², although the granulomatous inflammation does not extend into the intraocular structures in this case. Another possible pathogenesis for the glaucoma is a lens-induced uveitis or other idiopathic or immune-mediated lymphoplasmacytic uveitis leading to formation of a pre-iridal fibrovascular membrane and subsequent occlusion of the filtration angle. Histologic evidence supporting the clinical diagnosis of



Globe, dog. The sclera is expanded by abundant mature collagen, throughout which is an infiltrate of large numbers of macrophages and lymphocytes. (HE, 200X)

secondary glaucoma includes the buphthalmia, iris and ciliary body atrophy, keratitis with focal rupture of Descemet's membrane (corneal stria), retinal detachment

with retinal pigmented epithelial hypertrophy, and inner retinal atrophy.

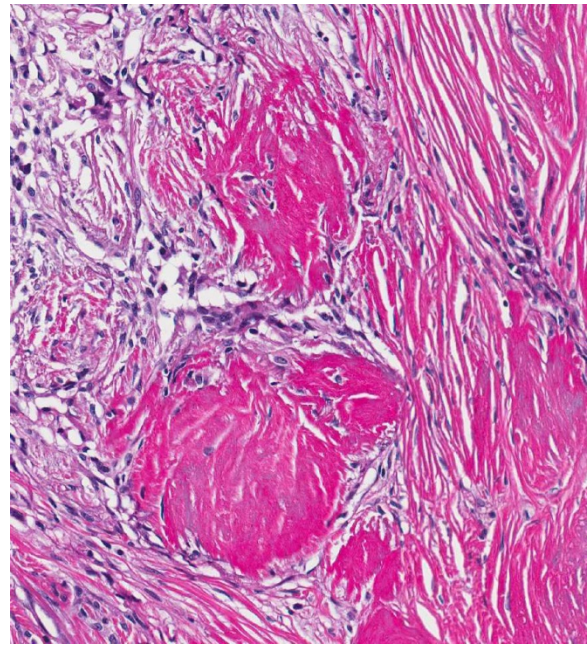
The majority of scleral disease in dogs is inflammatory in nature and is most often the result of secondary involvement of the sclera with either intraocular inflammation or extension from an orbital cellulitis,⁷ as with a penetrating foreign body, trauma, or infectious etiology.⁵ Primary scleral/episcleral inflammation can be clinically divided into unilateral versus bilateral, nodular versus diffuse, and scleral versus episcleral categories, but there is often overlap in the clinical presentation of these entities and of secondary scleritis/episcleritis.⁵ One of the most common primary inflammatory diseases of the sclera/episcera is nodular granulomatous episcleritis, while necrotizing scleritis is rare in comparison.

Nodular granulomatous episcleritis, not present in this case, is also referred to as ocular nodular fasciitis, among other names, and is a proliferative nodular inflammatory lesion at the limbus of the eye that behaves somewhat like a neoplasm in its locally infiltrative growth.⁷ The histologic lesion consists of a proliferation of histiocytes, spindle cells and lymphocytes and plasma cells. The inflammation has a diffuse granulomatous pattern, but discrete granulomatous foci are not present, and collagenolysis is not a feature.⁷

Necrotizing scleritis, the disease entity in the present case, is also an inflammatory and proliferative process within the sclera, and has more recently been referred to by some as granulomatous scleritis.^{1,3} For the remainder of the discussion, this entity will be referred to as necrotizing scleritis, the more well-known name for the condition. In necrotizing scleritis, there is a similar composition of inflammatory cell types to that identified in cases of nodular gran-

ulomatous episcleritis, including histiocytes, lymphocytes, plasma cells and spindle cells. Some lesions also have a neutrophilic component, as in the present case, or an eosinophilic component.⁶ The two main distinguishing features of necrotizing scleritis from nodular granulomatous episcleritis are the formation of discrete granulomatous foci, and the presence of altered collagen (“collagenolysis”).^{6,7} The altered collagen is often surrounded by epithelioid macrophages to form the discrete granulomas. Altered collagen may have an abnormal tinctorial staining quality with Masson’s trichrome,² which is identified in the present case as segmental red-staining of the collagen rather than the usual blue. The terms collagenolysis and collagen necrosis are somewhat controversial since collagen is considered inert and therefore cannot technically become “necrotic.” There is also often a granulomatous vasculitis, but this is not present in every case³. In the current case, although the inflammation appears somewhat vasocentric in some areas, overt vasculitis is not identified.

In necrotizing scleritis, the inflammation and spindle cell proliferation typically begins in the anterior sclera and slowly spreads circumferentially and posteriorly with eventual progression to involvement of the uvea and retina.⁷ On gross evaluation, the sclera is severely thickened and bright white.³ Staphyloma, which is a protrusion of uveal tissue through a weakened portion of the sclera, is a possible sequela in some cases, along with disinsertion of the extraocular muscles.^{4,5} Necrotizing scleritis is most commonly bilateral, but the second eye may not be affected until later in the course of the disease.^{3,7} It is critical to alert clinicians to the likelihood of involvement of the contralateral eye, given the important prognostic implications for vision³. The treatment for necrotizing scleritis is



Globe, dog. Scattered throughout the fibrous and inflammatory infiltrates are focal areas of brightly eosinophilic, degenerate collagen referred to in the literature as “collagenolysis”. (HE, 172X)

aggressive life-long anti-inflammatory or immunosuppressive therapy, but complete remission is rare and medical management fails in many cases, leading to enucleation of the affected eye(s).^{5,7}

The pathogenesis of necrotizing scleritis is not well-understood. No etiologic agents have been identified in these cases,⁷ although necrotizing scleritis has been reported in dogs with ehrlichiosis.³ An immune-mediated pathogenesis has been suggested, particularly due to the comparable lesion in humans, which is an autoimmune disease process, as well as the partial response to immunosuppressive therapy in dogs.^{1,2,5} Most cases reported appear to be localized to the eye, with rare reports that have evidence for other systemic immune-mediated disease, which is the case for humans with necrotizing scleritis.¹ There is some evidence for a type III and type IV hypersensitivity mechanism to the pathogenesis of necrotizing scleritis in dogs, but there is variability in the literature as to whether T- or B-lymphocytes predominate

in the lymphocytic component of the inflammation.^{1,2} Some pathologists have made the comparison between necrotizing scleritis and systemic reactive histiocytosis in dogs and consider that these entities may be related (personal communication, R. Dubielzig). This is in particular due to the vasocentric nature of the cellular infiltrate in necrotizing scleritis (personal communication, R. Dubielzig).

In conclusion, this case is a classic example of necrotizing scleritis in the eye of a dog, highlighting the characteristic histologic features of this condition including the granulomatous inflammation and the altered collagen within the lesion.

JPC Diagnosis:

1. Eye, sclera: Scleritis, granulomatous and sclerosing, focally extensive, severe with optic nerve demyelination.
2. Eye: Panuveitis, lymphoplasmacytic, chronic, diffuse, moderate with hyphema, pre and post iridial fibrovascular membranes, retinal detachment and atrophy, and hypermature cataract.

Conference Comment: The contributor provides a comprehensive and very informative review of this entity. The conference analysis of this case included separating the ocular lesions into two separate processes as alluded to in the contributor's discussion. The first process, the scleritis with formation of vague granulomas, includes a tremendous fibroblastic response (fibrosis) initiated by inflammation and necrosis. The second, primarily intraocular process is quite extensive, and encompasses the corneal changes (squamous metaplasia of the corneal epithelium and a break in Descemet's membrane), cataract, pre- and post-iridal fibrovascular membrane

formation with drainage angle obstruction, changes in the ciliary body and iris, intraocular hemorrhage, and retinal detachment. The moderator cautioned against over interpreting retinal degenerative changes particularly in a detached retina that has been artifactually folded and distorted. Some sections contain optic nerve in which moderate to severe degenerative changes (i.e. axonal degeneration and gitter cells) are seen.

Contributing Institution:

Animal Medical Center
510 East 62nd Street
New York, NY 10065
www.amcny.org

References:

1. Day MJ, Mould JRB and Carter WJ. An immunohistochemical investigation of canine idiopathic granulomatous scleritis. *Vet Ophthalmol.* 2008;11:11-17.
2. Denk N, et al. A retrospective study of the clinical, histological, and immunohistochemical manifestations of 5 dogs originally diagnosed histologically as necrotizing scleritis. *Vet Ophthalmol.* 2012; 15:102-109.
3. Dubielzig RR. Diseases of the cornea and sclera. In: *Veterinary Ocular Pathology a comparative review.* Saunders Elsevier: New York, NY; 2010: 232-234.
4. Grahn BH, Cullen CL and Wolfer J. Diagnostic ophthalmology, Necrotic scleritis and uveitis. *Can Vet J.* 1999; 40:679-680.
5. Grahn BH and Sandmeyer LS. Canine episcleritis, nodular episclerokeratitis, scleritis, and necrotic scleritis. *Vet Clin Small Anim.* 2008;38:291-308.

6. Njaa BL and Wilcock BP. The ear and eye. In: Zachary and McGavin, ed. *Pathologic Basis of Veterinary Disease*. 5th ed. Mosby Elsevier: St. Louis, MO; 2012:1153-1244.

7. Wilcock BP. Eye and ear. In: Maxie, MG, ed. *Jubb, Kennedy and Palmer's Pathology of Domestic Animals*. 5th ed. Vol. 1. Saunders Elsevier: Philadelphia, PA; 2007:459-552.

CASE III: 12B2550 (JPC 4066796).

Signalment: 12-year-old intact domestic short hair cat (*Felis catus*)

History: Corneal perforation of unknown duration in the right eye (OD). Suspect cataracts and anterior lens luxation OD. Presented to ophthalmologist for enucleation OD. Eye was submitted to the referring institution for biopsy.

Gross Pathology: The entire right globe was received. The globe was 1.9 cm in nasolateral diameter, and had a white-tan, raised mass at 3-6 o'clock. On cut section, the mass was firm to slightly gritty, and obscured the ciliary body and a portion of the iris. The lens was opaque, and slightly irregular. The retina was detached, and the peripheral iris was irregular segmentally.

Laboratory Results: N/A

Histopathologic Description: Examined is a parasagittal section of the globe, in which there is a discrete, unencapsulated, mesenchymal mass filling the posterior chamber, abutting the equator of the lens, and partially obliterating the anterior uvea.

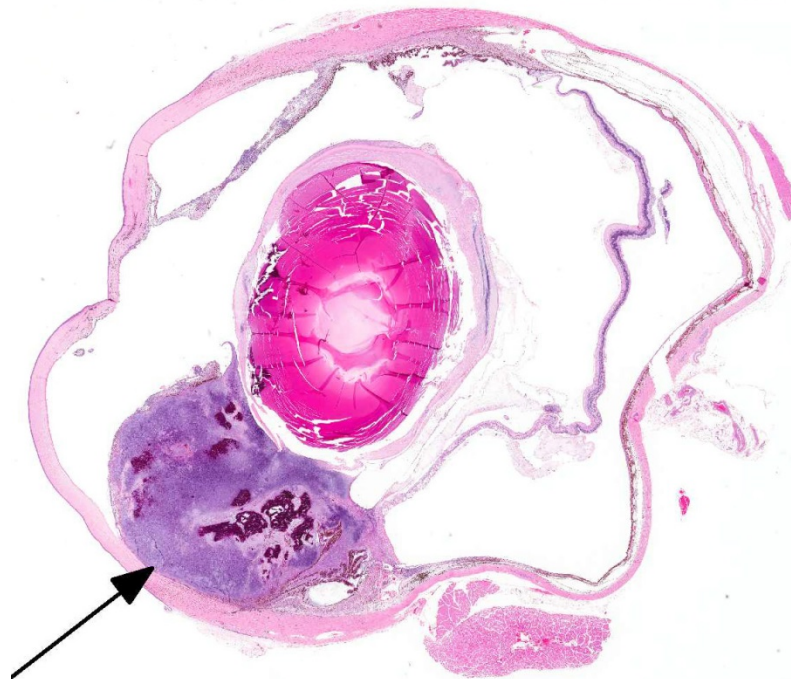
The cornea is distorted axially by implanted uveal pigment, fibrosis, and segmental rupture of Descemet's membrane. Portions of smooth muscle, iris pigment epithelium, and nodules of lymphocytes and plasma cells are also adherent to the exposed posterior stroma. The surrounding stroma is densely eosinophilic and slightly hypercellular (fibrosis), and the epithelium is hyperplastic. Peripherally, the stroma lacks clefting (edema) and the epithelium is thinned. The posterior chamber/uveal mass is composed of irregular clusters of chondrocytes, sheets of spindle to stellate cells, and abundant granular to hyaline basophilic chondroid matrix, which abuts the posterior cornea and is intermittently covered by extensions of an inflamed fibrovascular membrane; there is a segment of Descemet's membrane surrounded by this membrane. The cells have scant amounts of amphophilic cytoplasm, and distinct borders.



Globe, cat. The globe contains a white mass which obscures the ciliary body, prolapses the ventral iris leaflet, and opposes the lens. The lens is opaque, and the retina is segmentally detached. (Photo courtesy of: University of California Davis, Department of Pathology, Microbiology, Immunology, 1 Garrod Dr, UC Davis, Davis CA 95616)

Nuclei are plump and oval, with coarse chromatin and prominent nucleoli. There is moderate anisocytosis and anisokaryosis, and about 35 mitotic figures per 10 400x fields. There are many scattered cells that are shrunken and hyper eosinophilic, and there are several regions of mineralization. The mass and associated matrix is contiguous with the break in the lens capsule and the variably cellular layer of fibrous tissue that lines the inner capsule that replaces the cortex; there are foci of cartilage within the lens. The lens nucleus lacks fiber definition, and has a few swollen fibers and irregular clefts. Fibrous tissue with moderate nuclear atypia and scattered mitotic figures surround the outer capsule, as well.

The unaffected iris leaflet is expanded by edema and mononuclear inflammation, and the iridocorneal angle is collapsed. Reactive



Globe, cat. Subgross magnification of the affected globe, with a cartilaginous neoplasm within the posterior segment (arrow). There is circumferential spindle cell metaplasia subjacent to the lens capsule, a detached retina, and the dorsal iris leaflet is adhered to the cornea (anterior synechia). (HE, 5X)

fibrovascular tissue lines the inner ciliary body. The entire retina is detached, with variable outer retinal atrophy, minimal subretinal exudate, and diffuse hypertrophy of the retinal pigmented epithelium. Peripherally, the full thickness of the retina is disorganized with fluid filled clefts/cavities. The inner retina is largely devoid of ganglion cells, particularly the non tapetal aspect. There is perivascular retinal infiltration by lymphocytes and plasma cells. The optic nerve head is vacuolated and anteriorly displaced. The optic nerve parenchyma is essentially normal. There are a few foci of lymphocytes and plasma cells in the sclera.

Contributor's Morphologic Diagnosis:

1. Right eye: Lens capsule rupture with uveal chondrosarcoma (post traumatic ocular sarcoma)
2. Right eye: Lymphonodular panuveitis
3. Right eye: Iridocorneal angle collapse with inner retinal atrophy (chronic glaucoma)
4. Right eye: Complete chronic retinal detachment and chronic retinitis
5. Right eye: Mild to moderate chronic keratitis with focal Descemet's membrane rupture and uveal implantation

Contributor's Comment: Taken together, the constellation of lesions (corneal rupture with uveal incorporation, lens capsule rupture, and ocular sarcoma) are classic for feline post-traumatic ocular sarcoma (FPTOS). The relationship of the chondrosarcoma to the lens and to the lenticular rupture was highlighted, as was the extent of

retinal and optic nerve lesions. There was no evidence of extra-ocular extension in examined sections, which suggests that recurrence/extension is unlikely following enucleation in this case.

Feline ocular sarcomas are malignant, intraocular neoplasms that are usually associated with evidence of trauma (i.e. FPTOS) from the clinical history and/or histologic findings (e.g. lens capsule rupture, retinal detachment, and corneal perforation). The time from trauma to the development of FPTOS varies widely, uncommonly in as little as 2 months, and more commonly several years; up to 10 years of latency has been reported.³ The average time between trauma and enucleation is 7 years.³ Extra-ocular invasion can occur and is typically at the limbus through the sclera, or at the optic nerve.^{2,5} For this reason, prophylactic enucleation of a feline eye after trauma should be considered if the eye is nonvisual.³ Metastasis is uncommonly reported in this disease, but current studies are small and/or have limited follow up.

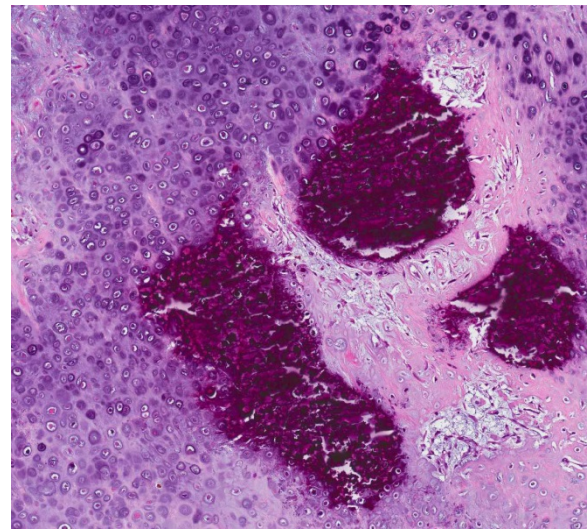
FPTOS have a typical distribution. Tumors commonly occupy the posterior iris with expansion to the posterior chamber, posterior lenticular capsule, retina, and choroid.² Invariably the lens is destroyed, either from initiating trauma or from tumor invasion, and significant inflammation accompanies these tumors (i.e. lens-induced uveitis).^{2,7} There are three variants of FPTOS, the most common of which is the spindle cell variant, followed by round cell variant, and lastly osteosarcoma/chondrosarcoma.³ The cell of origin in spindle cell variants is likely lenticular epithelium.^{3,7}

The phenomenon of FPTOS is similar to vaccine-associated feline sarcomas. The latter is associated with vaccination of cats

for infectious diseases, most commonly rabies and feline leukemia virus.⁵ Vaccine-associated feline sarcomas are most commonly fibrosarcomas, but many different sarcoma variants have been reported, similar to FPTOS.^{5,7} Although the pathogenesis of both types of tumors is unknown, inflammation is an antecedent feature, suggesting a causal relationship is possible.

JPC Diagnosis:

1. Eye, globe: Chondrosarcoma (post-traumatic ocular sarcoma).
2. Eye, lens: Lenticular rupture with subcapsular chondroid metaplasia.
3. Eye: Anterior uveitis, lymphoplasmacytic, multifocal, mild.



Globe, cat. Neoplastic cells within the chondrosarcoma are well differentiated and present within lacuna with a dense blue (glycosaminoglycan-rich matrix.) There is multifocal mineralization within the matrix as well. (HE, 124X)

Conference Comment: Interestingly, studies in rabbits, macaques and human infants have shown that when a cataractous lens is removed, but the lens capsule and lens epithelium (which cover the anterior surface of the lens) are left intact, they result

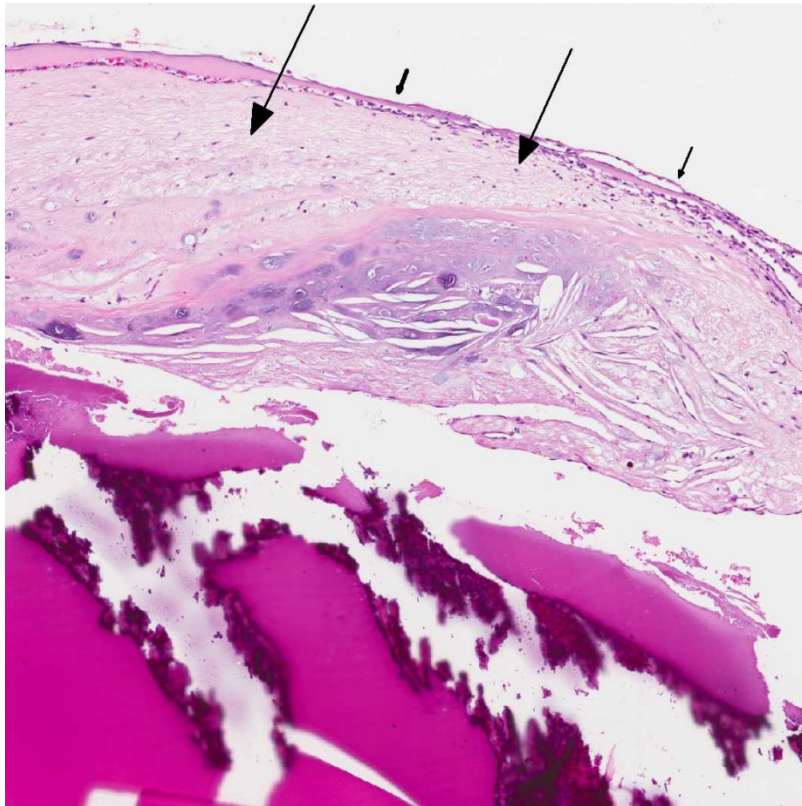
in functional lens regeneration - indicating these epithelial cells (or a subpopulation thereof) have stem cell / progenitor cell properties.⁶ This may explain their ability to undergo mesenchymal neoplastic transformation in the cat. A subset of feline post traumatic intraocular sarcomas have been found to arise from the lens epithelium, although this phenomenon has not been documented to occur in people or dogs.⁷ Features of FPTOS that support a lens epithelial origin include the frequent presence of lens capsule rupture, tumor development around the lens, lens capsule basement membrane being present around the neoplasm and alpha A crystallin positivity.³

Aside from cats, intraocular sarcoma has also been documented in rabbits with a history of chronic intraocular inflammatory

disease. The two documented cases in rabbits were negative for *E. cuniculi* and bacterial infection via histochemical staining and polymerase chain reaction. The neoplasms expressed vimentin but were negative for smooth muscle actin, desmin, cytokeratin and S100. The neoplasms consisted of a population of anaplastic mesenchymal cells with the presence of lens fragments in the tumor. Trauma was not documented in the rabbits but the neoplasms were particularly aggressive and they were associated with the lens, similar to what is seen in many cases of FPTOS. Neoplastic cells extended through the sclera into adjacent extraocular tissues as well.⁴ Non-trauma related feline intraocular chondrosarcoma has been documented in cats, although it is very uncommon. Given that mammals do not have cartilage within the globe, the tissue origin in non-trauma

related intraocular sarcoma is unclear. It is proposed to arise from multipotent mesenchymal stem cells which may be present within the trabecular meshwork, cancer stem cells, or potentially from vascular pericytes. In all four documented cases in cats the neoplasm was contained within the globe.¹

Conference participants discussed the spatial association of the neoplastic mass with the lens and how it may relate to the pathogenesis of this neoplasm, as well as the origin of the mass of cartilage distant from the neoplasm at the posterior aspect of the lens. A possible origin for this area is spindle cell and chondroid metaplasia of subcapsular lens fibers separate from the neoplastic transformation on-going elsewhere.



Lens, cat. Subjacent to the lens capsule (small arrows) is a thick layer of spindle cell metaplasia of lens fibers with a focal area of chondroid metaplasia, acicular cleft formation, and mineralization of lens fibers. (HE, 120X)

The trabecular meshwork of the iridocorneal angle was described as being collapsed and/or obscured by anterior uveitis, and glaucomatous changes were described in the retina including loss of ganglion cells as described above, as well as retinal atrophy. Anterior uveitis is a common finding in the cat with quite a number of potential etiologies, and its connection to the neoplasm in this case could not be definitively proven. There are also areas with normal retina in this case, and the most severe thinning and loss of nuclei are present in the non-tapetal region.

Contributing Institution:

University of California Davis
Department of Pathology, Microbiology,
Immunology
1 Garrod Dr.
UC Davis
Davis, CA 95616

References:

1. Beckwith-Cohen B, Teixeira LBC, Dubielzig RR. Presumed primary intraocular chondrosarcoma in cats. *J Vet Diagn Invest.* 2014; 26(5):664-668.
2. Dubielzig RR, Everitt J, Shaddock JA, Albert DM. Clinical and morphologic features of post-traumatic ocular sarcomas in cats. *Vet Pathol.* 1990; 27:62-65.
3. Dubielzig RR. Non-surgical trauma. In: Dubielzig RR, Ketring KL, McLellan GJ, Albert DM, ed. *Veterinary Ocular Pathology: A Comparative Review.* Philadelphia, PA: Saunders Elsevier; 2010:81-114.
4. Morrison WB, Starr RM. Vaccine-associated feline sarcomas. *J Am Vet Med Assoc.* 2001; 218:697-702.
5. McPherson L, Newman SJ, McLean N, McCain S, et al. Intraocular sarcomas in two rabbits. *J Vet Diagn Invest.* 2009; 21:547-551.
6. Lin H, Ouyang H, Zhu J, Huang S, et al. Lens regeneration using endogenous stem cells with gain of visual function. *Nature.* 2016; 531:323-328.
7. Zeiss CJ, Johnson EM, Dubielzig RR. Feline intraocular tumors may arise from transformation of lens epithelium. *Vet Pathol.* 2003; 40:355-362.

CASE IV: NTU20-12-1750 (JPC 4035591).

Signalment: 7-year-old neutered female Maltese, dog (*Canis familiaris*)

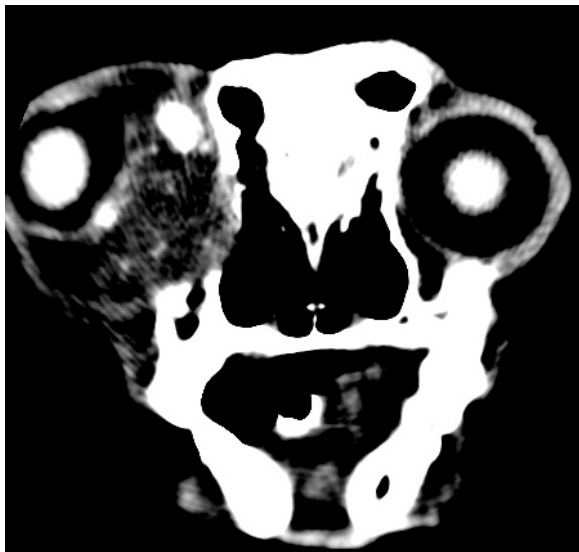
History: The animal presented signs of exophthalmos in the right eye, with mucopurulent discharge, for over half a year. Computed tomography scan revealed an irregular, retrobulbar, space-occupying mass with osteolytic lesion. A retrobulbar



Dog. The dog has a one-year history of exophthalmos with a mucous discharge. (Photo courtesy of: Graduate Institute of Molecular and Comparative Pathobiology, School of Veterinary Medicine, National Taiwan University, No. 1, Sec. 4, Roosevelt Road, Taiwan 106-17, Taiwan (ROC))

tumor was highly suspected. After five months of follow-up, the patient was presented for enucleation to relieve the discomfort, poor condition of right eye, and blindness. Right eye transconjunctival exenteration was performed and submitted for histopathological examinations.

Gross Pathology: The submitted specimens included (1) the right eye and periorbital mass, (2) right eyelids, (3) third eyelids, and (4) the mass in deep orbit. The periorbital mass, which was solitary, firm, yellowish, and space-occupying, encompassed and surrounded the globe. On cross section, the mass was multilobulated, leading to deformation of eyeball, but the delineation of eyeball was still identified. There was also a solitary, firm, and brownish tissue of irregular shape and with uneven surface along with the globe. Pieces of the eyelid displayed a firm and solitary appearance, partially containing haired skin coat. The third eyelid with an uneven surface was meaty, brownish, solitary and



CT of head, dog: Computed tomography scan revealed an irregular, retrobulbar space-occupying mass with osteolytic lesion. (Photo courtesy of: Graduate Institute of Molecular and Comparative Pathobiology, School of Veterinary Medicine, National Taiwan University, No. 1, Sec. 4, Roosevelt Road, Taipei 106-17, Taiwan (ROC))

firm. The tissues obtained from the deep orbit comprised several solitary and firm tissues of variable shape and size. Submitted specimens were trimmed and selected for histopathological examination.

Laboratory Results: N/A

Histopathologic Description:

The periorbital mass, which is located behind the globe, is unencapsulated and poorly demarcated, and is causing the deformation of globe. The neoplastic cells are arranged in islands, small lobules and tight whorls or bundles, and are separated by a delicate fibrous stroma. These tumor cells have epithelioid appearance with ample eosinophilic cytoplasm, fairly distinct cell margins, and large open-faced nucleoli. Mitoses are rare. Islands of chondroid and osseous metaplasia, and varied size of vacuolation resembling adipose tissue, are present in the tumor area. The neoplasm invades the peripheral adipose tissues and extra-ocular muscles. Tumor cells infiltrate the lamina propria of the bulbar conjunctiva and partially replace the outer sclera. Multifocal necrosis is remarkable in the tumor area, but may be rare in the tissue of the submitted slide. Aggregations of lymphocytes and hemorrhage are also noted at the marginal area of the tumor. Retinal detachment, with remarkable hypertrophy of retinal pigment epithelium and degeneration of ganglion cells, is noted. Edema is present in the conjunctival epithelia. At the area behind the globe, the tumor cells encompassed an obscure nerve bundle with degenerative changes, suggestive of an orbital nerve.

By tissue immunohistochemistry tumor cells are immunopositive for vimentin, S-100 and neuron-specific enolase (NSE), and are immunonegative for cytokeratin (CK), desmin, glial fibrillary acidic protein (GFAP), Melan-A, and neurofilament (-).

The epithelia of eyelid and third eyelid demonstrate severe hyperplasia, and the lamina propria displays extensive plasmacytic infiltration and hemorrhage. The tissues from the deep mass display numerous aggregates of lymphocytes, edema, hemorrhage, and necrosis, with presence of suspected neoplastic cells as described.

Contributor's Morphologic Diagnosis:

Orbit: Orbital meningioma, excisional biopsy, right eye, dog

Contributor's Comment: Although meningiomas are common tumors in the central nervous system of dogs, orbital meningioma is rare. Orbital meningiomas can arise from secondary extension of an intracranial neoplasm along the optic nerve or, as in the case of primary orbital tumors, from neoplastic transformation of arachnoid cap cells outside the optic nerve sheath.³ Orbital meningiomas in dogs and humans

usually grow slowly, compress the peripheral connective tissues, and may involve bilateral optic nerves with rare extracranial metastasis.^{3,6,7} On immunohistochemistry, they may show variable positivity for S-100 and vimentin, but are generally negative for cytokeratin.³ It is reported that an orbital meningioma with extracranial metastasis to the lung and heart in a dog demonstrated intracytoplasmic PAS+ granules.⁷

The histological features of meningiomas can be classified as meningotheliomatous, fibromatous, psammomatous or transitional pattern. In a study from the Comparative Ocular Pathology Laboratory of Wisconsin,³ in 22 canine orbital meningiomas collected from 1981-1997, most of them were meningotheliomatous with rare fibromatous foci. The tumors characteristically have large epithelial-like neoplastic cells with nuclei containing disperse chromatin and prominent nucleoli. Psammoma bodies, which are commonly found in intracranial meningiomas, were not found in this study. In addition, islands of bone and cartilage

metaplasia, which are very rare in the intracranial meningiomas, are very commonly present.³ Metaplasia is very rare in human and canine meningiomas, but is more common in the orbital meningioma, which can be a diagnostic aid for both histologic and ultrasound analysis.³ In the present case, the histology findings are very similar to the Wisconsin's study; nevertheless, prominent



Eye, dog: Grossly, a large fibrous multilobular retroorbital neoplasm occupies much of the orbit, pushing the globe forward and transversely compresses it. (Photo courtesy of: Graduate Institute of Molecular and Comparative Pathobiology, School of Veterinary Medicine, National Taiwan University, No. 1, Sec. 4, Roosevelt Road, Taipei 106-17, Taiwan (ROC))

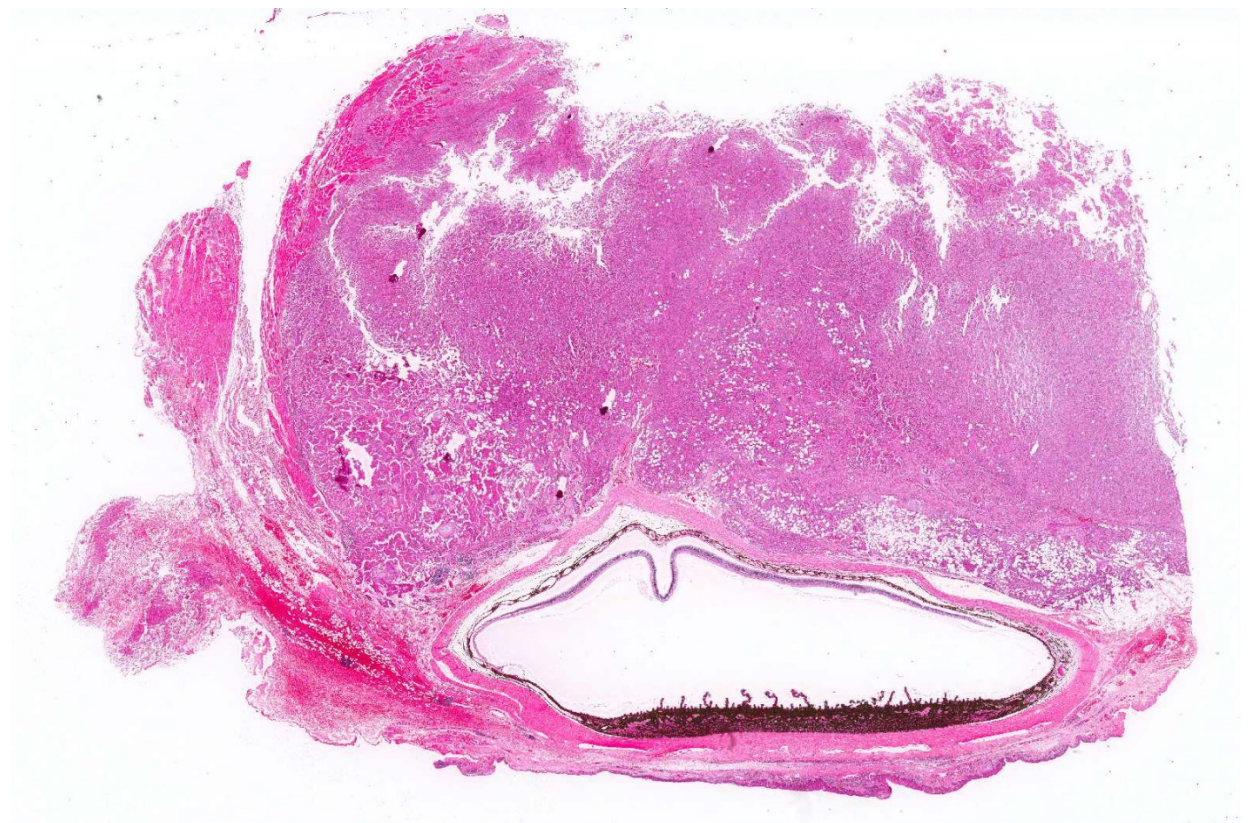
local invasion suggesting malignancy is noted in our case.

In the present case, due to the overlapping expression of neural markers, the diagnosis should rely on histologic findings of classic chondroid and osseous metaplasia with myxomatous changes. It's reported that canine meningiomas reveal variable positive results for neural markers, such as S-100 and NSE.² Correlated to the location, morphology, and IHC results, the differential diagnosis should include an epithelioid variant of malignant peripheral nerve sheath tumor. The orbital meningioma classically shows that epithelioid tumor cells envelope the optic nerve, expand into the peripheral adipose and loose connective tissues with myxomatous stroma, and chondroid and osseous metaplasia is present.⁶ In the veterinary literature, epithelioid malignant PNST involving

multiple organs with a mixture of spindle and epithelioid cells histologically has been reported.⁴

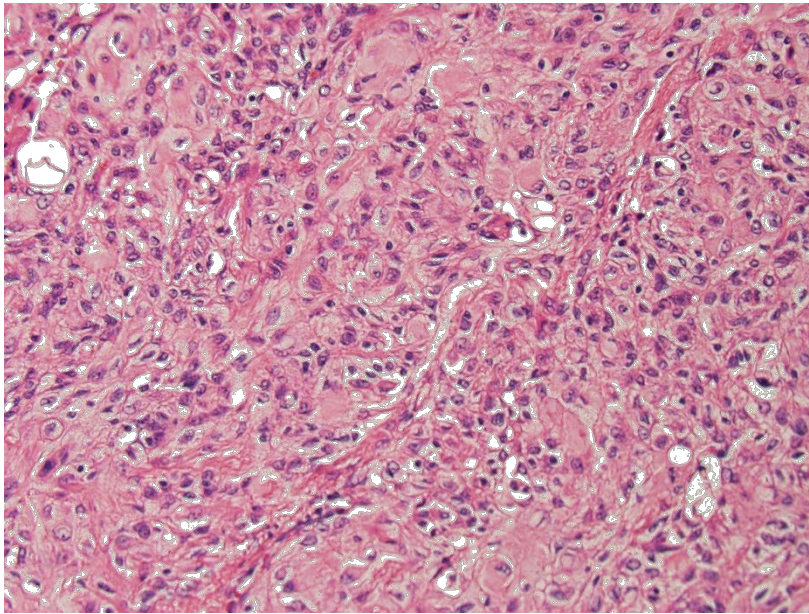
JPC Diagnosis: Eye, extraocular tissues:
Orbital meningioma.

Conference Comment: Orbital meningiomas are generally regarded as slow growing and benign, but intraocular invasion may occur and metastasis has also been documented. Local recurrence is seen with intermediate frequency due in part to the difficulty in obtaining complete excision. The tumors are often found to be closely associated with the optic nerve and may appear to originate from the optic nerve sheath.⁶ Fine needle aspiration or diagnostic imaging may be included in the initial diagnostic process. The cytologic appearance of meningioma cells upon



Eye, dog: Subgross magnification of the retro-orbital neoplasm. (HE, 5X)

aspiration may include round to polygonal to indistinctly shaped spindle cells which have moderate to abundant pale blue to grey cytoplasm, round to ovoid nuclei, mild anisokaryosis, a granular chromatin pattern, and small or indistinct nucleoli.^{8,10} The features may be consistent with a mesenchymal neoplasm without prominent signs of malignancy, but may also present a diagnostic challenge due to the variable appearance of cells. Cells of the adjacent retina may also be obtained during aspiration and various components of the retina, including pigment epithelium, rods and cones, and nerve fibers, which have a distinctive cytologic appearance, should not be interpreted as part of the neoplasm.¹⁰ Central blindness has been found to develop in the opposite eye in some cases of orbital meningioma, which suggests infiltration of the tumor along the optic nerve to the level of the optic chiasm.⁶ Aside from being reported in dogs and cats, orbital



Eye, dog: The neoplasm is composed of tightly arranged streams and bundles of polygonal to spindle cells which are arranged in various planes. There is mild anisokaryosis and a low mitotic rate. (HE, 400X)

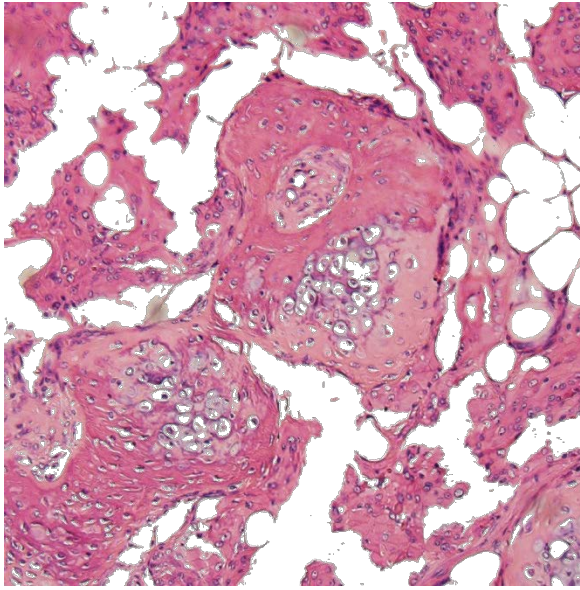
meningioma has also been reported in large animals, such as cattle, although much less commonly.⁹

The moderator discussed the classic appearance of orbital meningioma in dogs and suggested that in an orbital neoplasm composed of large polygonal to spindle cells containing areas of cartilaginous and osseous differentiation, meningioma should be the first consideration. The differential diagnosis for orbital tumors in the dog includes multilobular tumor of bone, a mesenchymal neoplasm which also contains areas of cartilage and bone; these tumors have a characteristic lobulated pattern, and lobules are surrounded by spindle cells embedded in a rich collagenous matrix. Soft tissue sarcoma is an additional consideration for an orbital spindle cell neoplasm containing abundant collagen; these tumors typically lack bone and cartilage; however, and in dogs, morphologically low-grade but biologically high-grade fibrosarcoma would be the primary concern. Other considerations for orbital neoplasia include

lymphoma, osteosarcoma, lacrimal or salivary gland adenocarcinoma, hemangiosarcoma, liposarcoma (including hibernoma) and canine lobular orbital adenoma. Microscopically, the presence of osteoid would be the discriminating feature for osteosarcoma; and the presence of strap cells, rowed nuclei, and cross striations are characteristic features of rhabdomyosarcoma.³

Macroscopically, canine orbital multilobular adenoma has a discriminating appearance and texture that may help differentiate it from other neoplasms, including the

presence of friable, translucent lobules with a delicate capsule and often found to be challenging to manipulate and remove



Eye, dog. Scattered throughout the neoplasm are small nodules of cartilage and bone. Adipocytes likely represent remnants of the infiltrated retro-orbital fat. (HE, 200X)

during surgery. Histologically, multilobular adenoma consists of well-differentiated lacrimal or salivary gland tissue with the absence of ducts, and may have PAS positive material within the cytoplasm.⁵

Contributing Institution:

Graduate Institute of Molecular and Comparative Pathobiology, School of Veterinary Medicine, National Taiwan University

<http://www.vm.ntu.edu.tw/CompPathol/>

References:

1. Adamo P, Forrest L, Dubielzig R: Canine and Feline Meningiomas: Diagnosis, Treatment, and Prognosis. *Compendium*. 2004; December(26):951-966.
2. Barnhart KF, Wojcieszyn J, Storts RW. Immunohistochemical staining patterns of canine meningiomas and correlation with published immunophenotypes. *Vet Pathol*. 2002;39:311-321.
3. Dubielzig RR, Ketring KL, McLellan GJ, Albert DM. *Veterinary Ocular Pathology: A Comparative Review*. Philadelphia, PA: Saunders Elsevier; 2010:126-141.
4. Garcia P, Sanchez B, Sanchez MA, Gonzalez M, Rollan E, Flores JM: Epithelioid malignant peripheral nerve sheath tumour in a dog. *J Comp Pathol*. 2004;131: 87-91.
5. Headrick JF, Bentley E, Dubielzig RR. Canine lobular orbital adenoma: a report of 15 cases with distinctive features. *Vet Ophthalmol*. 2004; 7(1):47-51.
6. Mauldin EA, Deehr AJ, Hertzke D, Dubielzig RR. Canine orbital meningiomas: a review of 22 cases. *Vet Ophthalmol*. 2000; 3:11-16.
7. Perez V, Vidal E, Gonzalez N, Benavides J, et al. Orbital meningioma with a granular cell component in a dog, with extracranial metastasis. *J Comp Pathol*. 2005; 133: 212-217.
8. Regan DP, Kent M, Mathes R, Almy FS, et al. Clinicopathologic findings in a dog with a retrobulbar meningioma. *J Vet Diag Invest*. 2011; 23(4):857-862.
9. Reis Jr. JL, Kanamura CT, Machado GM, Franca RO, et al. Orbital (retrobulbar) meningioma in a Simmental cow. *Vet Pathol*. 2007; 44(4):504-507.
10. Tvedten H, Hillstrom A. Cytologic appearance of retinal cells included in a fine-needle aspirate of a meningioma around the optic nerve of a dog. *Vet Clin Pathol*. 2013; 42(2):234-237.

Joint Pathology Center
Veterinary Pathology Services



WEDNESDAY SLIDE CONFERENCE 2015-2016

C o n f e r e n c e 21

13 April 2016

Jey Koehler, DVM, PhD, DACVP
Director, Histopathology Core Laboratory
Department of Pathobiology
Auburn University College of Veterinary Medicine

CASE I: 1888-15 (JPC 4070542).

Signalment: 6-year-old castrated male Yorkshire terrier dog (*Canis familiaris*)

History: Per history provided, Milo is a 6-year-old castrated male Yorkshire terrier dog that was diagnosed with tracheobronchitis for the past month and was placed on antibiotic therapy. The dog developed sudden onset of hindlimb weakness and was unable to walk on both hind limbs. He collapsed acutely, failed to revive when administered cardiopulmonary resuscitation, and was submitted for necropsy.

Gross Pathology: There were no significant gross findings noted.

Laboratory Results: N/A

Histopathologic Description: Brain: Multifocally, expanding the meninges and Virchow-Robins space primarily within the white matter and less severely affecting the

grey matter of the cerebrum, cerebellum and brainstem, are numerous intense inflammatory foci that often coalesce. Inflammatory cells are comprised of large numbers of macrophages, lymphocytes, with fewer plasma cells and neutrophils. The macrophages often appear epithelioid cells and form granulomatous foci that efface and replace neuropil. Within neuropil adjacent to granulomatous foci are large numbers of glial cells (gliosis) and reactive gemistocytic astrocytes. Both lymphocytes and macrophages are arranged in dense and often whirling, perivascular cuffs. Mitoses in the macrophage population are present at 1-3 per high power field (400x) in areas of perivascular cuffs. Endothelium associated with the perivascular cuffing is reactive, and lined by plump and hypertrophied endothelial cells, and vessel walls are infiltrated by the mononuclear cells described above.

Spinal cord: Diffusely expanding meninges and multifocally replacing white and grey matter of the spinal cord are similar



Cerebrum, dog. In cross sections from the cerebrum and cervical spinal cord, the vessels (especially at the interface of the grey and white matter) are accentuated by a perivascular inflammatory infiltrate. (HE, 5X)

inflammatory cells as those described above for the brain sections. Perivascular granulomatous, lymphocytic cuffs are present in neuropil and meninges.

Contributor's Morphologic Diagnosis:

Brain: 1. Severe, multifocal to coalescing lymphohistiocytic encephalitis

2. Severe, diffuse lymphohistiocytic meningitis

Spinal cord: 1. Severe, multifocal lymphohistiocytic myelitis

2. Severe, diffuse lymphohistiocytic meningitis

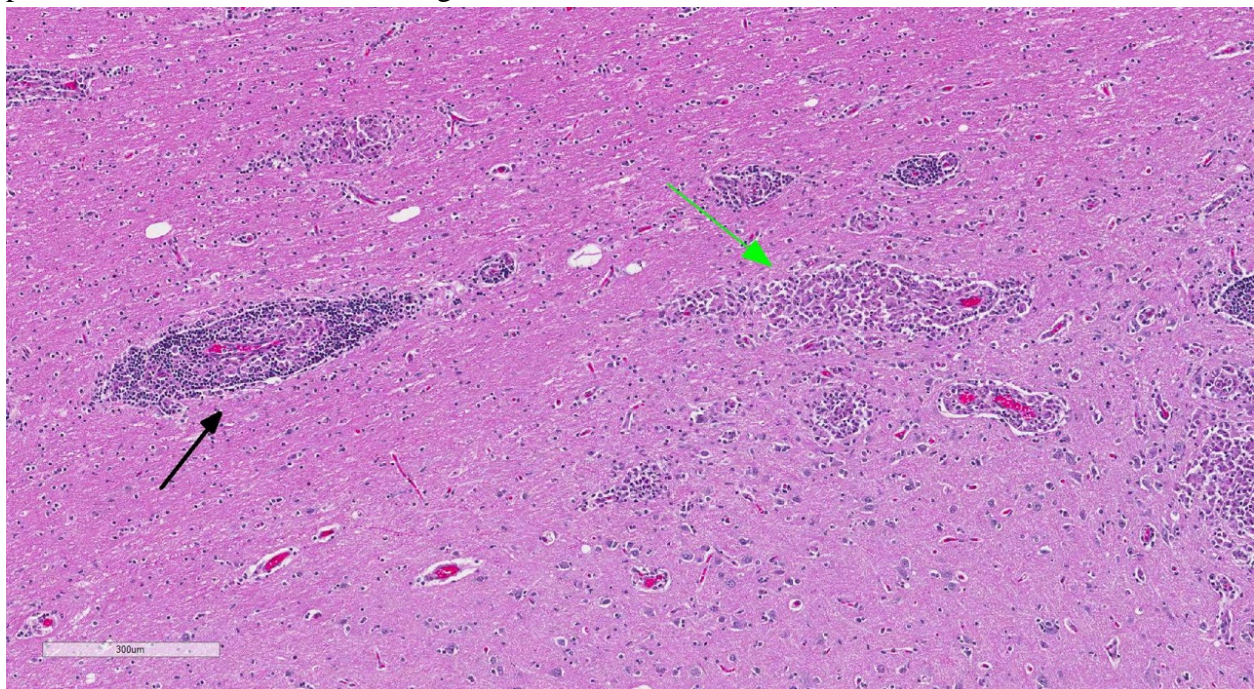
Contributor's Comment: This dog had disseminated granulomatous meningoencephalomyelitis (GME) that affected the brain and spinal cord (and optic nerve, not included on slide). GME is an idiopathic disease that affects the central nervous

system of predominantly young to middle-aged, small toy breed dogs, although age and breed of affected dogs can vary vastly.^{3,4} The disease was first reported in 1978, and represents 5-25% of central nervous system disease of dogs.³ A higher incidence of this disease may be seen in females, and affected dogs are typically mature.² The disease is almost always progressive and is associated clinical signs include ataxia, non-ambulation, paresis, paralysis, as well as a wide range of other neurological signs.² Dogs with GME may develop neutrophilic leukocytosis, with increased protein and cellularity in CSF fluid.² While the disease is normally progressive and prolonged, some affected dogs can die spontaneously.² Grossly, the lesions of GME can be hard to identify, and affected white matter may appear as small foci of malacia.⁴ The disease tends to affect white matter of cerebrum and cerebellum, and occasionally occurs in the

optic nerve and spinal cord. Histological findings of prominent perivascular cuffing of mononuclear cells and discrete granulomatous aggregates are distinctive features of the disease.⁴

GME can be classified as focal, disseminated (multifocal) and ocular.³ The focal type is characterized by coalescing granulomas that form a space-occupying lesion and associated clinical signs, and are more common in the cerebrum and brainstem.³ The disseminated form affects more than one of the following sites: cerebrum, brainstem, spinal cord, cerebellum, meninges and optic nerves.³ The ocular form is associated with optic neuritis and occasionally uveitis, retinal hemorrhage or retinal detachment.³ The exact etiology of GME is unknown, although infectious causes and immune-mediated disease have been proposed. Antemortem diagnosis of GME is typically based on CSF analysis, characterized by increased leukocyte count, mononuclear pleocytosis and increased protein content.³ However, changes can be

variable and may be steroid dependent.³ Definitive diagnosis of the disease is based on brain biopsy.³ Treatment for GME is largely based on immunosuppression with corticosteroid therapy, and azathioprine, cytosine arabinoside, procarbazine, cyclosporine and radiation therapy have more recently been attempted in treatment regime.³ In general, prognosis of dogs with GME is poor. Considering the clinical history of tracheobronchitis in this dog and the nature of inflammatory cells, the differential diagnosis includes canine distemper (*Morbillivirus*) infection. There were no intranuclear or intracytoplasmic viral inclusions present in any of the sections examined to further support a viral etiology in this case. Ancillary testing using immunohistochemistry to label viral antigen in the brain sections would be useful to definitively rule out canine distemper in this case. Fungal or protozoa infection are lower on the differential list as organisms were not observed in any of the examined sections.



Cerebrum, dog. Virchow-Robins spaces are filled by various combinations of histiocytes and lymphocytes (black arrow). Some vessels have a predominantly histiocytic infiltrate (green arrow). (HE, 81X)

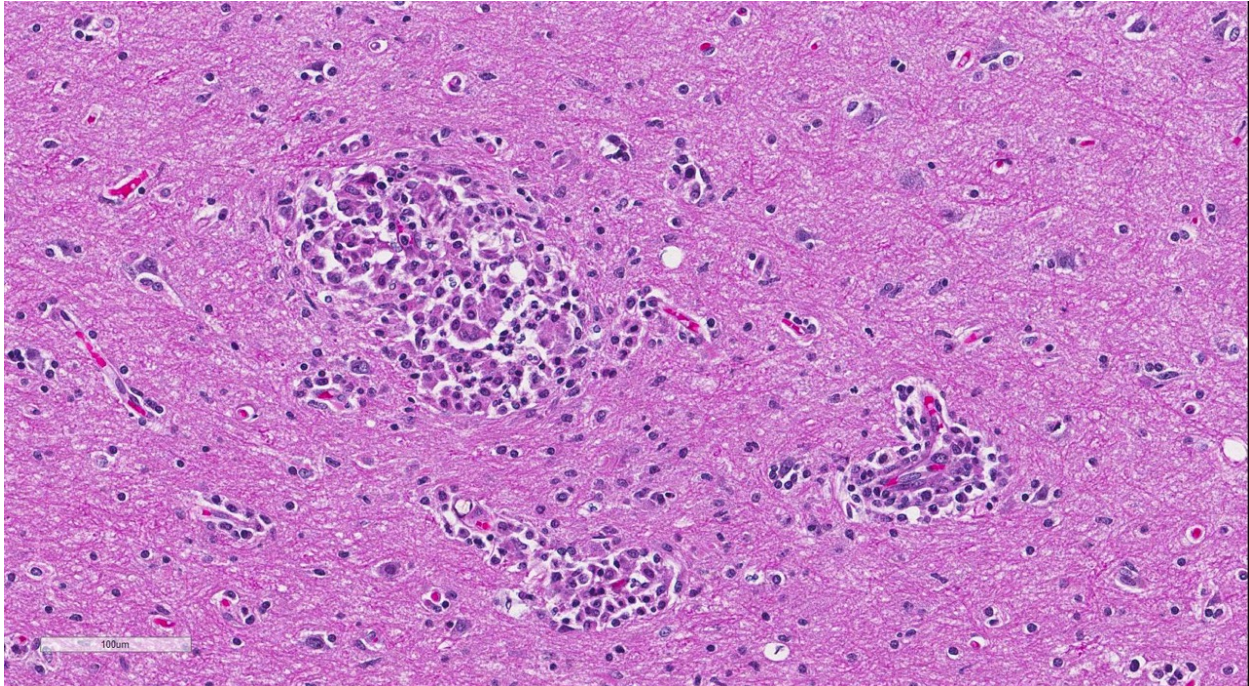
JPC Diagnosis: Brain, cerebrum, brainstem; spinal cord: Meningoencephalomyelitis, lymphohistiocytic, chronic, multifocal, marked.

Conference Comment: In addition to granulomatous meningoencephalitis (GME), other idiopathic inflammatory conditions that affect the nervous system include necrotizing meningoencephalitis (NME) (see case 2 of this conference) and necrotizing leukoencephalitis (NLE). Each of these entities has unique features with reference to breed predilection, histologic lesions, anatomic location and clinical presentation. While NME and NLE are associated with specific dog breeds, GME is not. CD3-positive T-cells appear to play an important role in development of lesions, particularly in GME. CD163-positive macrophages also play an important role in GME where they exhibit a unique, predominantly perivascular distribution.⁵ Histologic findings in GME include granulomatous foci composed of primarily macrophages and lymphocytes, with fewer plasma cells and neutrophils, located in the cerebral white matter, subcortical region, cerebellum, and midbrain. In GME, interleukin 17 (IL-17) levels are often elevated within inflammatory cells (primarily macrophages / microglia) and may contribute to the development of the associated lesions. IL-17 is a component of the Th17 immune response and is produced in some autoimmune conditions, such as rheumatoid arthritis and Crohn's disease, among others. It has been postulated that GME may be represent a delayed type hypersensitivity reaction and that mast cells may play a role in development of early lesions.⁶

Aside from (or in conjunction with) an autoimmune disorder, infectious agents have long been suspected to be involved in the

pathogenesis of GME (and NME), and the phenomenon of molecular mimicry has also been implicated. Infectious agents have not been identified via light microscopy or culture and molecular techniques have failed to identify a viral agent; however, molecular techniques have identified *Mycoplasma canis* (an agent not typically associated with CNS disease) in cases of both GME and NME. To date, the precise role of *M. canis* in the pathogenesis of GME and NME remains unclear.¹ Aside from explanations involving an infectious agent and immune dysregulation, it has also been postulated that GME may represent a lymphoproliferative disorder.⁷ Overall, the common view is that this condition is multifactorial with a complex pathogenesis involving genetic factors, immune dysregulation and environmental factors (i.e. pathogens).^{1,7}

The conference histologic description mirrored the contributor's description above. Additional features described include mild rarefaction and vacuolation of the neuropil adjacent to inflammatory aggregates, and microgliosis (in addition to the astrocytosis noted above). Although many of the astrocytes appear hypertrophied/reactive, the majority have not yet reached the characteristic gemistocytic stage. Low numbers of necrotic neurons are also present, although this is not a prominent feature. Perivascular cuffs consist primarily of lymphocytes, while most of the histiocytes are localized to the neuropil adjacent to perivascular cuffs. The moderator noted that the distinct asymmetric nature of the lesions, particularly within the perivascular cuffs, is a characteristic feature of GME. She also pointed out the vasculocentric nature of the meningeal inflammation and how it is not evenly distributed, which is another common feature of this entity. Conference



Cerebrum, dog. Scattered throughout the parenchyma, there are numerous aggregates of histiocytes. Close inspection of these nodules often reveals one or more vessels contained within it, suggesting that these nodules are likely perivascular cuffs as well. (HE, 120X)

participants briefly discussed differential diagnosis for GME, including viral encephalitis, pointing out that viruses generally result in primarily lymphocytic inflammation. The histiocytic component in GME is an important diagnostic clue, as well as the fact it affects both grey and white matter. The moderator commented that, in general, GME is easier to diagnose in more chronic, severe cases and that it is important to trim in the eyes in suspected cases of GME, as inflammation is often seen surrounding the optic nerve.

Contributing Institution:

Advanced Molecular Pathology Laboratory
Institute of Molecular and Cell Biology
61 Biopolis Drive, Proteos
Singapore 138673

References:

1. Barber RM, Porter BF, Li Q, May M, *et al.* Broadly reactive polymerase chain reaction for pathogen detection in canine granulomatous meningoencephalomyelitis and necrotizing meningoencephalitis. *J Vet Intern Med.* 2012; 26:962-968.
2. Cordy DR. Canine granulomatous eningoencephalomyelitis. *Vet Pathol.* 1979; 16(3):325-33.
3. Emma JO, Merrett D, and Jones B. Granulomatous meningoencephalomyelitis in dogs: A review. *Ir Vet J.* 2005 Feb 1; 58(2):86-92.
4. Maxie MG, Youssef S. Nervous system. In: Maxie, MG, ed. *Jubb, Kennedy and Palmer's Pathology of Domestic Animals.* Vol 1. 5th ed. Philadelphia, PA: Elsevier; 2007: 442-443.
5. Park ES, Uchida K, Nakayama H. Comprehensive immunohistochemical studies on canine necrotizing meningoencephalitis (NME), necrotizing leukoencephalitis (NLE) and granulomatous meningoencephalomyelitis (GME). *Vet Pathol.* 2012; 49(4):682-692.
6. Park ES, Uchida K, Nakayama H. Th1-, Th2-, and Th17-related cytokine and chemokine receptor mRNA and protein

expression in brain tissues, T cells, and macrophages of dogs with necrotizing and granulomatous meningoencephalitis. *Vet Pathol.* 2013; 50(6):1127-1134.

7. Schatzberg SJ. Idiopathic granulomatous and necrotizing inflammatory disorders of the canine central nervous system. *Vet Clin North Am Small Anim Pract.* 2010; 40(1):101-20.

CASE II: UFMG 1 (JPC 4035763).

Signalment: A 2-year-old, intact female Maltese dog (*Canis familiaris*).

History: A 2-year-old, intact female Maltese dog was presented to the veterinarian with a history of acute neurological signs characterized by seizures, constant howling, and circling to the right side. The owner informed that the immunization schedule had been followed. On neurological examination, the dog presented deficit of mental status (apathy and depression), head turn, compulsive circling to the right side and falls to the left side. During ambulation the animal turned away from obstacles, indicating no visual deficit. Abnormal movements and proprioception deficit to the left side were detected. There was also left deficit to menace response and cervical sensibility. A multifocal intracranial lesion involving the telencephalon was suspected. The complete blood count and serum chemistry profiling were unremarkable. Magnetic resonance imaging (MRI) and CSF analysis could not be performed because of the client's refusal. According with breed, age, history and neuroanatomic localization of the lesions, an inflammatory neurological disease of unknown cause was suspected. On the basis of the suspicion, phenobarbital (6mg/kg bid), doxycycline (10mg/kg bid), prednisolone (2mg/kg bid), and A and B

vitamins were prescribed. A re-check five days after the onset of therapy was performed and no changes were detected when thorough clinical examination was performed. On neurological examination, reduction of circling and seizures was observed but there was no improvement in posture, proprioception and menace response. Because clinical signs improved gradually, the initial prescription was maintained. Fifty three days after the first presentation the dog was checked again. The owner reported that the initial dosage of prednisolone was maintained but, arbitrarily the client did not maintained the medicine after three weeks, and the seizures episodes started again after discontinuing the corticoid therapy. The veterinarian detected that all clinical signs mentioned above worsened. A new treatment protocol adding



Cerebrum, dog. At necropsy, there were multiple yellowish areas of malacia throughout the all lobes. (Photo courtesy of: Universidade Federal de Minas Gerais, Escola de Veterinária, Departamento de Clínica e Cirurgia Veterinárias, Av. Antônio Carlos, 6627; 31270-901. Belo Horizonte, MG, Brazil www.vet.ufmg.br)

cyclosporine (6 mg/kg bid) to prednisolone was prescribed. However, ten days later, the clinical signs worsened dramatically. The dog presented severe changes of the mental status (disorientation, aggression and apathy), increased postural deficit, and bilateral deficit to menace response and cluster seizures. Due to the poor prognosis, the owner elected euthanasia.



Cerebrum, dog. There is marked diffuse malacia of the submeningeal grey matter (arrows) (HE, 5X)

Gross Pathology: At necropsy, there was mild asymmetry between the cerebral hemispheres. In the right hemisphere there were multifocal to coalescing depressed, markedly friable and yellowish areas measuring approximately 0.5 to 1.0 cm of diameter. In the frontal lobe there was a locally extensive malacic area measuring around 2.0 cm of diameter. The left contralateral frontal lobe was edematous, slightly yellowish and friable. On the corresponding cut surface of the right frontal lobe, there was partial loss of cortical parenchyma and, demarcation between grey and white matter was not evident. The frontal lobes of both hemispheres were markedly affected followed by parietal and occipital lobes. No gross lesions were observed in the temporal lobe, hippocampus, cerebellum and brain stem. Extraneural

gross lesions included moderate diffuse pulmonary congestion and edema.

Laboratory Results: N/A

Histopathologic Description:

The cerebral cortex showed areas with markedly increased cellularity interspersed with multifocal cavitation, partially filled by numerous Gitter cells, characterizing malacia. Moderate to marked infiltration of cells, such as plasma cells and lymphocytes were observed around vessels and diffuse in the leptomeninges. In addition, the non-cavitation areas were characterized for neuropil vacuolization, neuronal necrosis, neuronophagia, astroglyosis with various gemistocytes, endothelial hyperplasia and hypertrophy. Single or binucleate gemistocytes were more commonly seen adjacent to necrotic areas. These areas were

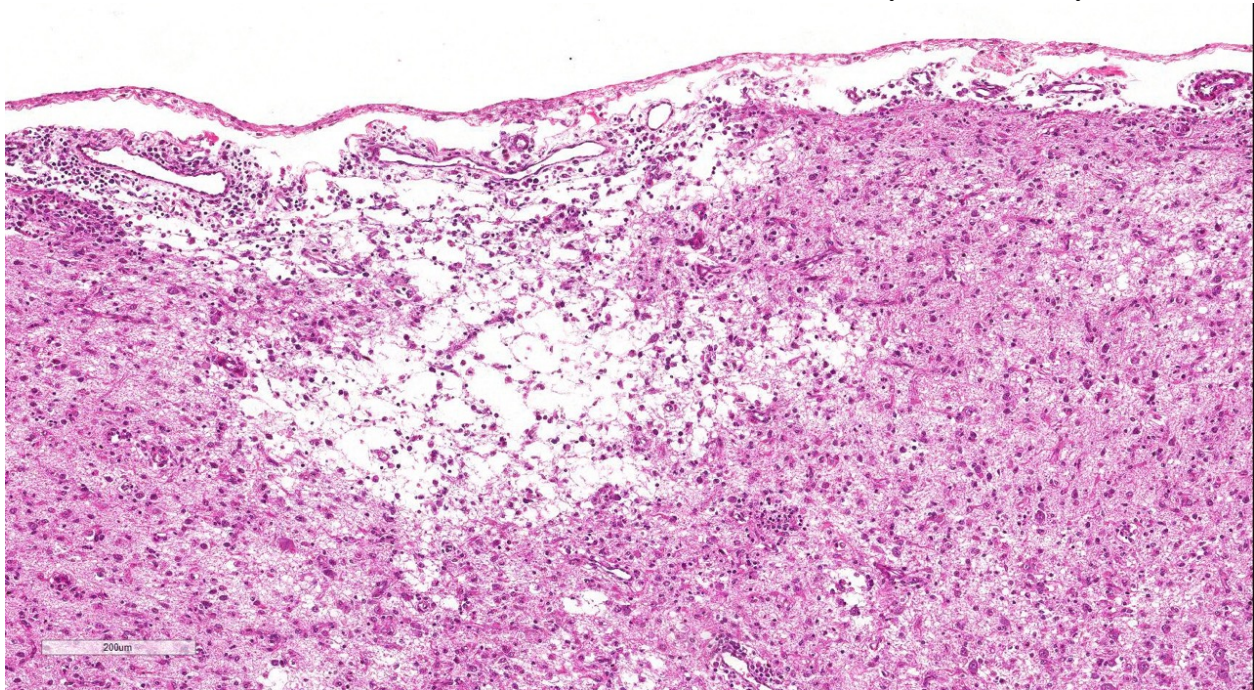
more intense in the frontal and parietal lobes of right side. In the white matter subjacent to the necrotic right frontal cortex there were plasma cells and lymphocytes perivascular cuffs associated to mild vacuolization and axonal degeneration. No lesions were found in the hippocampus, diencephalon (thalamus and hypothalamus), mesencephalon, cerebellum and medulla oblongata. Paraffin blocks of the cerebrum were selected and immunohistochemistry for CD3 (lymphocytes T marker) and CD 79a (lymphocytes B marker) was performed. The immunohistochemical analysis showed that positive CD3 cells were predominant in the perivascular cuffs, leptomeninges and also in the neuroparenchyma. Less numbers of positive CD79a cells were observed in the perivascular cuffs and leptomeninges but they were rarely observed in the neuroparenchyma.

Contributor's Morphologic Diagnosis:

Cerebrum: marked multifocal to coalescing,

necrotizing non-suppurative meningoencephalitis.

Contributor's Comment: Gross and clinical findings were consistent with multifocal to coalescing malacia involving the cerebral cortex. The histopathology allowed the definitive diagnosis of necrotizing meningoencephalitis (NME) characterized by multifocal to coalescing necrotizing non-suppurative meningoencephalitis, affecting the grey matter of frontal, parietal and occipital lobes, predominating in the right cerebral hemisphere. NME is a central nervous system (CNS) nonsuppurative inflammatory disorder of dogs, whose etiopathogenesis is poorly understood. Necrotizing leukoencephalitis (NLE) and granulomatous meningoencephalomyelitis (GME) are also CNS idiopathic inflammatory conditions. Nevertheless, each disease has unique histopathological features.¹³ The NLE is characterized by inflammatory and necrotic



Cerebrum, dog. Higher magnification of necrotic lesions within the submeningeal grey matter. The neuropil surrounding this focus of cavitation is hypercellular with numerous astrocytes, Gitter cells, and extremely prominent vessels. (HE, 130X)

lesions similar to NME, however, the lesions are predominately observed in the white matter. The GME is another idiopathic canine disorder affecting mainly the cerebellum and brainstem. The disease is characterized by nodular granulomatous lesions containing macrophages and epithelioid cells, especially in subcortical regions. In addition, there were perivascular cuffs constituted of lymphocytes, plasma cells, macrophages, and some neutrophils.^{9,13}

NME has been reported in various toy breeds including Pug dogs, Yorkshire terrier, Maltese, Chihuahua, Shih Tzu, West highland white terrier, Boston terrier, Spitz Japanese and Pinscher, Pekingese and French bulldog.^{9,13} NME seems to be more common in females^{5,8} and, has been diagnosed in dogs with six months to seven years of age.¹³ However, the most common age range is from two¹³ to four years.⁵

The clinical signs associated with NME are rapidly progressive and associate to the neuroanatomical localization.¹³ The most common signs include seizures, depression, circling, visual deficit,^{5,6} postural reaction deficits⁴ and vestibule-cerebellar signs.^{6,12} Definitive antemortem diagnosis is challenging because histopathology is mandatory. For most cases, the clinical diagnosis is presumptive, associating clinical signs and neuroanatomic localization, CSF analysis and advanced imaging tests to exclude other causes.^{5,12,13} The prognosis of NME cases is poor due the progressive course of the disease, with lower survival rate in animals with seizures.⁵ The dog of the present study showed clinical signs rapidly progressive and associated with the neuroanatomic localization of the lesions as observed in other studies.¹³ The lesions and clinical signs of most cases of NME are related exclusively to the cerebrum, being an important characteristic for this condition.¹² Detailed neurological

examination allows to determining the sites of the lesions, which are extremely important for presumptive diagnosis and treatment. In addition to neurological examination for supporting de clinical suspicion, is fundamental the epidemiological data, CSF analysis, cross-sectional imaging via computed tomography (CT) scan or magnetic resonance imaging (MRI) of the CNS and infectious diseases testing. Ct-guided brain biopsy and histopathological evaluation of brain tissue may be considered in cases of suspected NME.^{5,13}

An autoimmune pathogenesis has been suggested for NME based on the presence of anti-astrocytic and anti-glial fibrillary acid protein (GFAP) autoantibodies in the cerebrospinal fluid (CSF) of affected dogs.¹⁴ However, similar antibody levels occur in the CSF of dogs with GME, brain tumors and even in some clinically normal dogs.¹⁴ A genomic study in Pugs with NME showed a single strong association with dog leukocyte antigen (DLA) class II, and supports the role of the immune system in the disorder.⁶ Genetic predisposition also has been confirmed in Pug dogs with NME but it is believed there are additional influences contributing to the phenotypic expression of the disease.^{2,6}

The immunohistochemical study showed predominance of T lymphocytes in the leptomeninges, around vessels and in the neuroparenchyma similar to the observed in other studies in dogs with NME.^{7,12} A study using double-labeling immunofluorescence antibody demonstrated predominance of CD3+ T lymphocytes in close proximity or attached to astrocytes, and the cytoplasm and astrocytic processes were positive for IgG in the NME and NLE lesions. The involvement of the autoantibody to astrocytes in the NME cases supports the immune mediated pathogenesis hypothesis however, does not confirm if anti-astrocytic and anti-GFAP antibodies are a primary

cause or a secondary consequence of NME.¹² A recent study showed that viral pathogens are not common in the brain of dogs with NME.¹

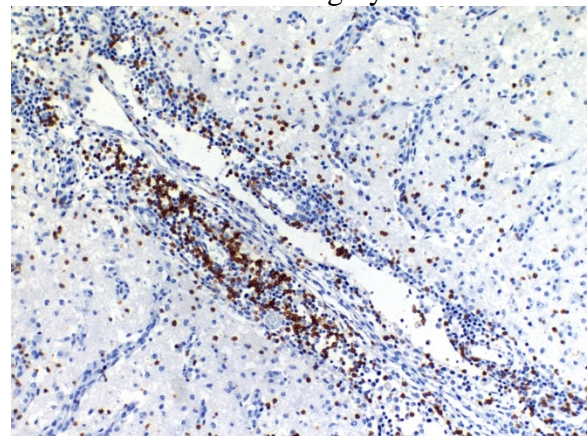
JPC Diagnosis: Cerebrum: Meningo-encephalitis, necrotizing, lymphohistiocytic, multifocal to coalescing severe.

Conference Comment: As mentioned above, a genetic predisposition has been identified in Pug dogs with NME and a genetic susceptibility test is currently available for this breed. Additionally, a potential breed predisposition has also been identified in Maltese dogs, with gene abnormalities similar to what was seen in Pugs, although the degree of gene variation and susceptibility may vary between breeds.¹⁰ The specific genes involved, including those involved with the major histocompatibility complex class II (MHC II), are suspected to play a role in immune system regulation and have been implicated in central nervous system inflammatory conditions in people. The precise role by which MHC II abnormalities contribute to development of this disease is not completely understood, but MHC II molecules play an important role in antigen presentation and determining the reactivity of T cells. Other genes of interest include one that encodes for part of the interleukin 7 receptor, which is important in proliferation and survival of T and B lymphocytes. NME has been postulated to share some pathogenic mechanisms with multiple sclerosis in people and the above described genetic research may provide support for this.¹⁰

Although most commonly associated with small/toy breed dogs, NME has also been reported in a Staffordshire bull terrier.⁴ Other small breeds not mentioned above that

have been documented with NME include Coton de Tulear, Papillon, and Brussels Griffon although it is very uncommon in these breeds and their development of this condition is considered atypical.³ The pathogenesis involved in development of this condition in atypical breeds is unclear as much remains elusive regarding the development, progression and pathogenesis of NME, as well as NLE and GME. In this case, the lesions were fairly characteristic for NME, particularly given the signalment. However, in some early or mild cases in less commonly affected breeds, there may be clinical and/or pathologic overlap with infectious diseases such as *Neospora caninum*, *Toxoplasma gondii* and viruses (e.g., canine distemper virus). Therefore, when the diagnosis is less straightforward but NME is still considered a top differential diagnosis, it is important for the diagnostic pathologist to consider and rule out infectious causes.

The subgross view of this section is striking and the lesions are characteristic for this entity. Within up to 50% of the section, there is loss of differential staining with areas of pallor, drop-out and liquefactive necrosis localized to the grey matter. Within



Cerebrum, dog. CD-3 positive cells predominate within perivascular cuffs throughout the neuropil. (Photo courtesy of: Universidade Federal de Minas Gerais, Escola de Veterinária, Departamento de Clínica e Cirurgia Veterinárias, Av. Antônio Carlos, 31270-901. Belo Horizonte, MG, Brazil www.vet.ufmg.br)

necrotic areas, there is loss of neuropil and increased numbers of microglial cells, lymphocytes, and plasma cells; moderate numbers of gitter cells and hypertrophied astrocytes are also present. There is multifocal perivascular cuffing in the grey matter with affected vessels have reactive endothelium. Spongiosis is present multifocally and necrotic neurons are seen in low numbers. The meninges are multifocally expanded with edema and infiltrated by macrophages, lymphocytes and plasma cells. Conference participants discussed and contrasted the histologic lesion described here to what was seen in the GME case. Ventricular dilation and hydrocephalus ex-vacuo were also described; however, the moderator cautioned against over-interpreting this change in brachycephalic breeds which may normally have some degree of ventricular dilation.

Contributing Institution:

Universidade Federal de Minas Gerais, Escola de Veterinária, Departamento de Clínica e Cirurgia Veterinárias, Av. Antônio Carlos, 6627; 31270-901. Belo Horizonte, MG, Brazil www.vet.ufmg.br

References:

1. Barber RM, Porter BF, Li Q, et al. Broadly reactive polymerase chain reaction for pathogen detection in canine granulomatous meningoencephalomyelitis and necrotizing meningoencephalitis. *J Vet Intern Med.* 2012; 26(4):962-968.
2. Barber RM, Schatzberg SJ, Corneveaux JJ, et al. Identification of risk loci for necrotizing meningoencephalitis in pug dogs. *J. Hered.* 2011;102: 540-546.
3. Cooper JJ, Schatzberg SJ, Vernau KM, Summers BA, et al. Necrotizing Meningoencephalitis in atypical dog breeds: A case series and literature review. *J Vet Intern Med.* 2014; 28:198-203.
4. Estey CM, Scott SJ, Cerda-Gonzalez S. Necrotizing Meningoencephalitis in a large mixed-breed dog. *J Am Vet Med Assoc.* 2014; 245(11):1274-8.
5. Granger N, Smith PM, Jeffery ND. Clinical findings and treatment of non-infectious meningoencephalomyelitis in dogs: A systematic review of 457 published cases from 1962 to 2008. *Vet J.* 2010; 184: 290-297.
6. Greer KA, Schatzberg SJ, Porter BF, et al. Heritability and transmission analysis of necrotizing meningoencephalitis in the Pug. *Res. Vet. Sci.,* 2009; 86: 438-442.
7. Higgins RJ, Dickinson PJ, Kube SA, et al. Necrotizing meningoencephalitis in five chihuahua dogs. *Vet Pathol.* 2008; 45: 336-346.
8. Levine JM, Fosgate GT, Porter B, et al. Epidemiology of Necrotizing Meningoencephalitis in Pug Dogs. *J Vet Intern Med.* 2008; 22: 961-968.
9. Park ES, Uchida K, Nakayama H. Comprehensive immunohistochemical studies on canine necrotizing meningoencephalitis (NME), necrotizing leukoencephalitis (NLE), and granulomatous meningoencephalomyelitis (GME). *Vet Pathol.* 2012, 49 (4):682-92.
10. Schrauwen I, Barber RM, Schatzberg SJ, Siniard AL, et al. Identification of Novel Genetic Risk Loci in Maltese Dogs with Necrotizing Meningoencephalitis and Evidence of a Shared Genetic Risk across Toy Dog Breeds. *PLoS One.* 2014;9(11):e112755.
11. Shibuya MN, Fujiwara K, Imajoh-Ohmi S, et al. Autoantibodies against glial

fibrillary acidic protein (GFAP) in cerebrospinal fluids from Pug dogs with necrotizing meningoencephalitis. *J Vet Med Sci.* 2007; 69(3): 241-245.

12. Spitzbarth I, Schenk HC, Tipold A, Beineke A. Immunohistochemical Characterization of Inflammatory and Glial Responses in a Case of Necrotizing Leucoencephalitis in a French Bulldog. *J Comp Path.* 2010; 142: 235-241.

13. Talarico LR., Schatzberg SJ. Idiopathic granulomatous and necrotizing inflammatory disorders of the canine central nervous system: a review and future perspectives. *J Sm Anim Pract.* 2010; 51: 138-149.

14. Toda Y, Matsuki N, Shibuya M, et al. Glial fibrillary acidic protein (GFAP) and anti-GFAP autoantibody in canine necrotising meningoencephalitis. *Vet Rec.*

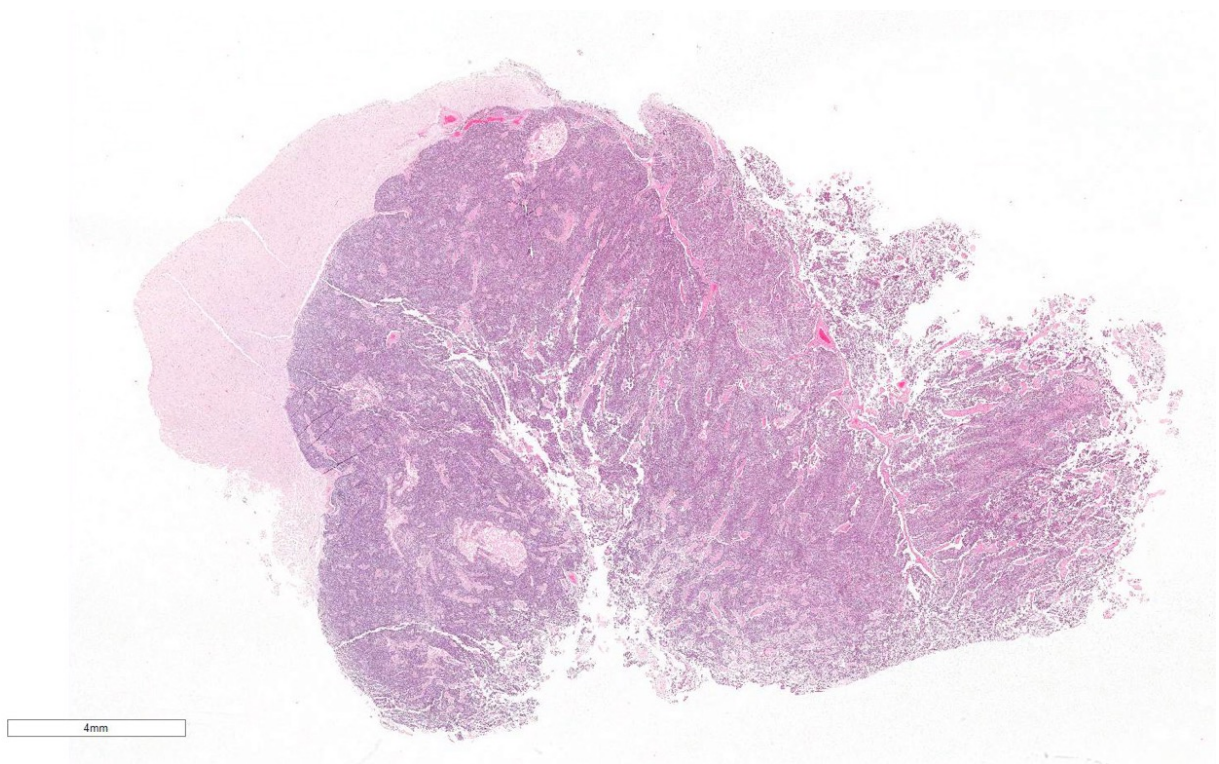
2007; 161(8): 261-264.

CASE III: 11-123787 (JPC 4018117).

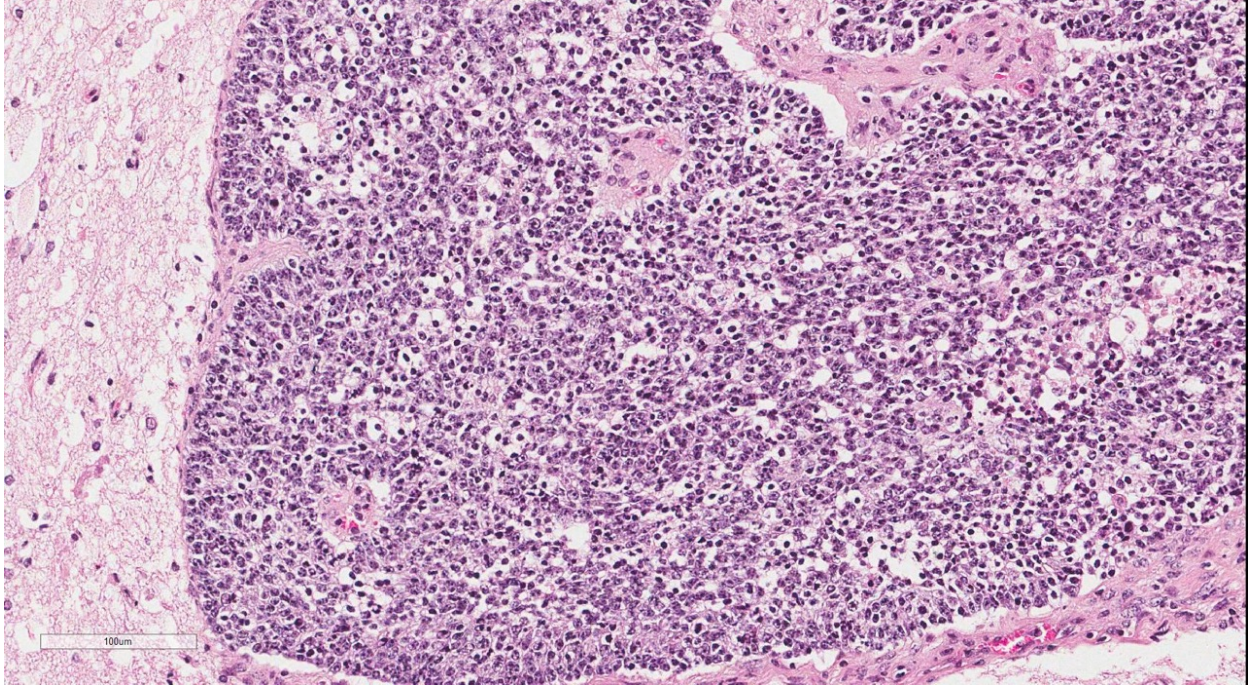
Signalment: Adult female white-tailed deer (*Odocoileus virginianus*).

History: The deer had no fear of humans or vehicles. He had human contact including petting and hand feeding. The animal was euthanized by gunshot wounds to the chest. The head was removed and send intact.

Gross Pathology: The head from the deer was submitted as part of routine Rabies surveillance by New York State Department of Health. A soft, white gelatinous mass effaced the right caudal nasal passage, cribriform plate and extended to involve the



Cerebrum, deer. The olfactory lobe of the cerebrum is compressed and largely effaced by a large, densely cellular neoplasm. (HE, 5X).



Cerebrum, deer. The neoplasm is composed of polygonal cells arranged in nests and cords which often palisade along vessels and the advancing edge of the neoplasm. (HE, 216X)

olfactory bulb of the brain.

Laboratory Results: Brain:

1. Fluorescent antibody test was negative for rabies
2. Immunohistochemistry for chronic wasting disease was negative
3. The brain mass was sent for aerobic bacterial culture and many *Aeromonas* sp. were isolated.

Histopathologic Description:

Brain: Compressing and effacing the neural parenchyma, invading into neuropil in locally extensive areas and extending to cut borders is a fairly well demarcated, large, densely cellular, expansile, variably encapsulated mass composed of sheets of neoplastic cells within an eosinophilic fibrillar background occasionally separated by few large blood vessels. The neoplastic cells are round to polygonal and occasionally palisade around central cores of fibrillary eosinophilic tangles (Homer-Wright rosettes) (Fig. 1), central empty

lumens (Flexner-Wintersteiner rosettes) (Fig. 2) and blood vessels (pseudorosettes) (Fig. 3). Neoplastic cells are approximately 12-15µm in diameter with scant eosinophilic cytoplasm and indistinct cell margins. Nuclei are round with coarsely stippled chromatin and indistinct nucleoli. There is mild anisocytosis and anisokaryosis. Up to 10 mitotic figures are counted in 10 high power (40X) fields. Admixed with the neoplastic cell population are few round 8-10µm diameter cells with hyperchromatic nuclei, variably distinct cell borders and pale vacuolated or scant fibrillar eosinophilic cytoplasm. There are scattered locally extensive areas of necrosis and small foci of hemorrhage. Within the periphery of the mass are few scattered hemosiderin laden macrophages.

Immunohistochemistry was performed on a section of the brain mass. Diffusely, neoplastic cells exhibited moderate to strong cytoplasmic immunoreactivity for neuron specific enolase (NSE) (Fig. 4) and a

subpopulation of the cells showed strong cytokeratin immunoreactivity (Fig. 5).

Contributor's Morphologic Diagnosis:

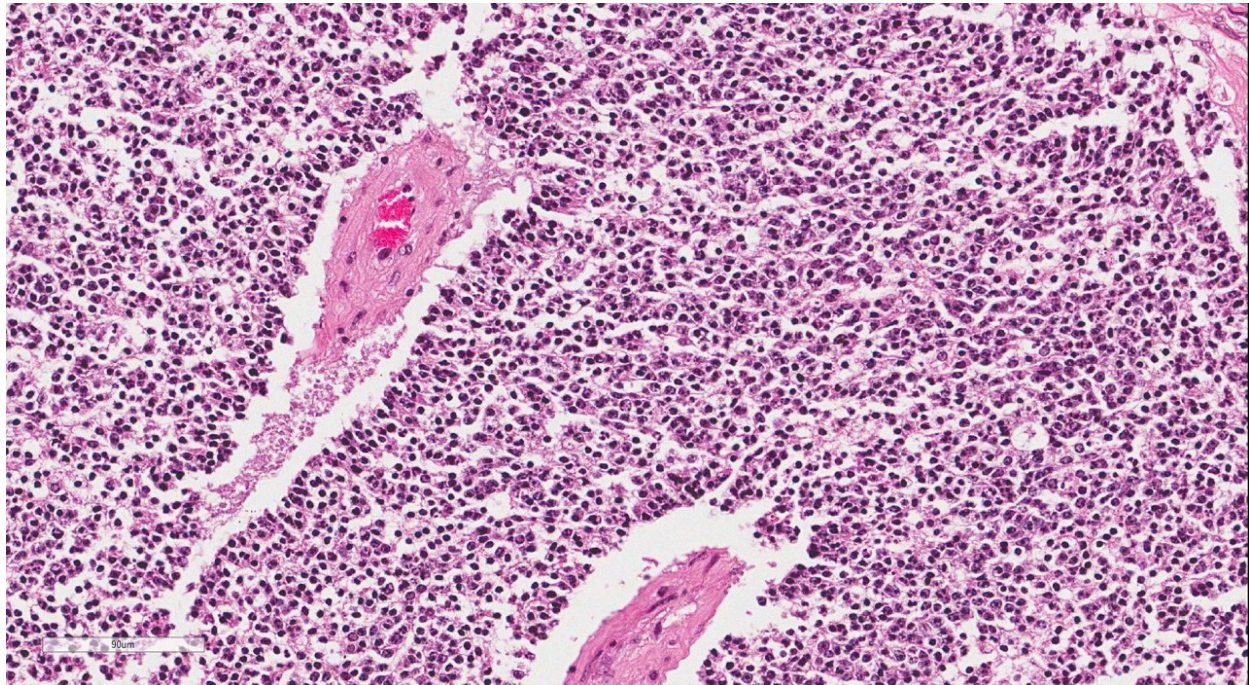
Brain, olfactory lobe: Neuroendocrine carcinoma

Contributor's Comment: The two primary differential diagnoses for this tumor are neuroendocrine carcinoma and olfactory neuroblastoma. These two tumor types have similar histologic features and differentiation often requires ultrastructural analysis and/or immunohistochemistry.

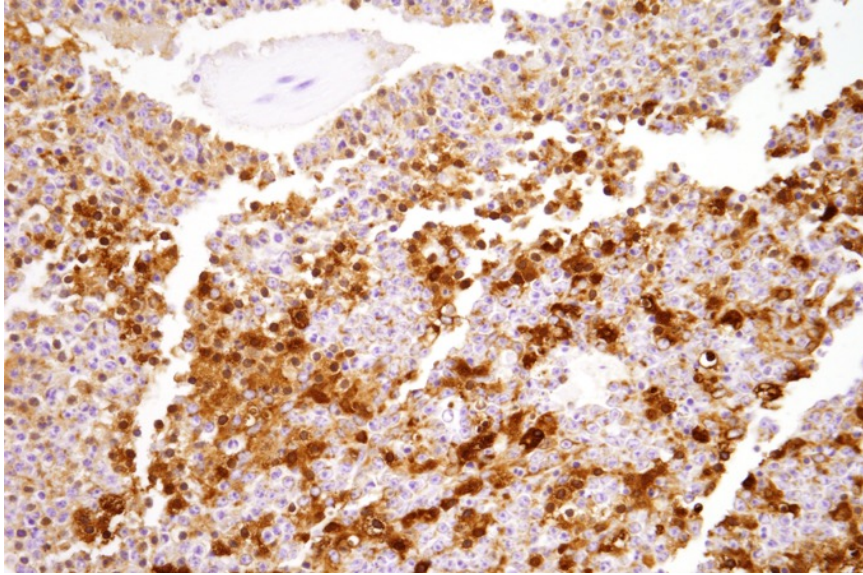
Neuroendocrine tumors are a diverse group of neoplasms derived from cells which (A) produce a neurotransmitter, neuromodulator or neuropeptide hormone, (B) contain dense core granules on electron microscopy and (C) do not have axons or form synapses.¹⁰ Neuroendocrine tumors have been described in the almost every organ and are characterized by a typical pattern of small to medium sized cells with granular eosinophilic chromatin arranged in nests,

cords and packets separated by fine fibrovascular stroma. Rosette formation and peripheral palisading is variably present. Ultrastructurally, tumor cells contain round, membrane bound dense core granules and have distinct intercellular junctions. Cells are argyrophilic (Grimelius positive) and show positive immunoreactivity for neuron specific enolase, chromogranin, cytokeratin and neuropeptides. Nasal neuroendocrine carcinomas have been reported in dogs¹⁴ and horses.¹⁶ In dogs, nasal neuroendocrine tumors have been reported to invade the underlying bone and adjacent sinuses, but not the brain.¹³

Olfactory neuroblastomas (ONB) or esthesioneuroblastomas are rare tumors, believed to be derived from the olfactory neuroepithelium. These tumors arise primarily in the upper nasal cavity and adjacent paranasal sinuses and frequently invade the cribriform plate and the intracranial cavity. Histological features of well-differentiated ONBs include growth in circumscribed lobules separated by richly



Cerebrum, deer. Neoplastic cells form pseudorosettes around blood vessels (and their edematous borders) due to their propensity to form palisades. (HE, 240X)



Cerebrum, deer. Neoplastic cells exhibit strong cytoplasmic positivity for neuron-specific enolase. (anti-NSE, 400X). (Photo courtesy of: Department of Biomedical Sciences, College of Veterinary Medicine, T4 018 Veterinary Research Tower, Cornell University, Ithaca, NY 14853, <http://www.vet.cornell.edu/biosci/pathology/services.cfm>)

vascularized fibrous stroma, or less commonly, a diffuse growth pattern. Pseudorosettes and true rosettes can be found. The neoplastic cells are surrounded by neurofibrillary matrix and have sparse cytoplasm and round to oval nuclei with inconspicuous nucleoli. Nuclear pleomorphism, high mitotic activity and necrosis are frequently observed. Ultrastructural characteristics include dense core neurosecretory granules and neurite-like cell processes with neurofilaments and neurotubules. Like neuroendocrine carcinomas, these tumors are argyrophilic and often show positive immunoreactivity for neuron specific enolase. Synaptophysin, neurofilament protein, class III beta-tubulin and microtubule-associated protein-2 are less frequently detected. Cells are typically not cytokeratin immunoreactive. Olfactory neuroblastomas have been described previously in dogs, cats,^{2, 4, 13} horses⁵ and a cow.¹

Other than cutaneous fibromas, neoplasms are uncommonly reported in white tailed

deer. Central nervous tumors described in white tailed deer include astrocytomas,⁷ ependymomas¹⁰ and a mixed primitive neuroectodermal and rhabdomyoblastic tumor.⁶ Nasal tumors have not been previously reported in white tailed deer, but nasal adenocarcinomas have been described in Persian fallow deer and Eld's deer.^{3,9}

A tentative diagnosis of neuroendocrine carcinoma was made in this case based on cytokeratin immunopositivity, which is a consistent feature of

neuroendocrine carcinomas and uncommon in olfactory neuroblastomas; however, invasion through the cribriform plate and the fibril background of this tumor are more consistent with a diagnosis of olfactory neuroblastoma. A definitive diagnosis would require electron microscopy.

JPC Diagnosis: Cerebrum: Neuroendocrine carcinoma.

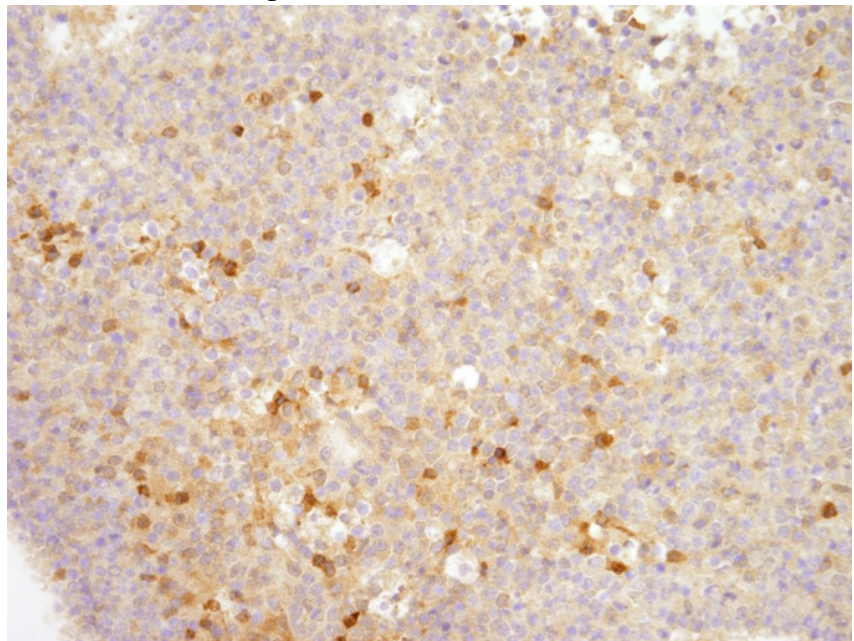
Conference Comment: The conference description was closely aligned with the contributor's description above; however, there was considerable discussion regarding the presence of and types of rosettes, with agreement that the poor fixation in this case gave a false appearance of Homer-Wright and Flexner-Wintersteiner rosettes. The moderator commented on the marked degree of vascular hyalinization and expansion of the perivascular space by dense, hyalinized, bright eosinophilic material. The differential diagnosis list for this lesion included oligodendroglioma in addition to olfactory neuroblastoma discussed above.

Immunohistochemical stains that can be useful in diagnosing oligodendroglioma include cyclic nucleotide phosphatase (CNPase) and oligodendrocyte transcription factor 2 (olig2); the absence of glial fibrillary acidic protein (GFAP) may also aid in the diagnosis.⁸ Other differentials discussed included primitive neuroectodermal tumor and ependymoma. In general, neoplasms associated with the cribiform plate often extend from outside the CNS into the olfactory bulb / frontal lobe as opposed to extending from the brain outward through the cribiform plate.

Primitive neuroectodermal tumors include neuroblastoma, medulloblastoma and neuroblastoma and are composed of 'neuroblasts' and generally arranged in sheets with the presence of Homer-Wright rosettes. Immunohistochemical markers used in the diagnosis of this type of tumor in dogs and cats include neuron-specific enolase (NSE), synaptophysin, a neuron-specific nuclear protein known as neuronal nuclei (NeuN) and neurofilament protein (NFP).⁸ These tumors may have a heterogenous or irregular staining pattern due to the presence of both neural and glial differentiation, which may aid in the diagnosis. Other stains which are reported as positive in some subsets of PNETs include vimentin and S100 among others. Stem cell markers which may be useful include nestin, beta III tubulin and doublecortin. Ependymomas are most often associated with the ventricle in some fashion and

classically have a papillary pattern with ependymal rosette formation, although these features are not present in all cases. These tumors are generally GFAP and vimentin positive.⁸

Neuroendocrine carcinomas are uncommon neoplasms which derive from neuroendocrine cells distributed throughout the body. Other locations for neuroendocrine neoplasms include the gastrointestinal tract, lungs and integument. The most germane differential diagnosis in this case is olfactory neuroblastoma as discussed above, due in large part to overlapping histologic features with neuroendocrine carcinoma. Features which can aid in ultrastructural differentiation include the lack of microtubule containing neural processes in neuroendocrine carcinoma,⁹ as well as the IHC profiles discussed above. A pancytokeratin immunohistochemical (IHC) stain performed at the JPC showed diffuse,



Cerebrum, deer. Some neoplastic cells exhibit strong cytoplasmic positivity for cytokeratin. (anti-NSE, 400X). (Photo courtesy of: Department of Biomedical Sciences, College of Veterinary Medicine, T4 018 Veterinary Research Tower, Cornell University, Ithaca, NY 14853, <http://www.vet.cornell.edu/biosci/pathology/services.cfm>)

strong, cytoplasmic immunoreactivity and a neurofilament IHC was negative, supporting the contributor's diagnosis of neuroendocrine carcinoma.

Contributing Institution:

Department of Biomedical Sciences
College of Veterinary Medicine
T4 018 Veterinary Research Tower
Cornell University
Ithaca, NY 14853
<http://www.vet.cornell.edu/biosci/pathology/services.cfm>

References:

- Anderson BC, Cordy DR. Olfactory neuroblastoma in a heifer. *Vet Pathol.* 1981; 18: 536.
- Brosinski K, Janik D, Polkinghorne A, Von Bomhard W, Schmahl W. Olfactory neuroblastoma in dogs and cats--a histological and immunohistochemical analysis. *J Comp Pathol.* 2012; 146: 152-9.
- Brownstein DG, Montali RJ, Bush M, James AE. Nasal carcinoma in a captive Eld's deer. *J Am Vet Med Assoc.* 1975; 167: 569-71.
- [Cox NR](#), [Powers RD](#). Olfactory neuroblastomas in two cats. *Vet Pathol.* 1989; 26: 341-3.
- Doöpke C, Groöne A, Borstel Mv, et al. Metastatic esthesioneuroblastoma in a horse. *J Comp Path.* 2005; 132: 218–222.
- Holscher MA, Page DL, Powell HS, Kord CE. Mixed primitive neuroectodermal and rhabdomyoblastic tumor in the brain of a wild deer. *J Wildl Dis.* 1974; 10: 201.
- Howard DR, Drehbiel JD, Fay LD, Whitenack DL. Visual defects in white-tailed deer from Michigan: six case reports. *J Wildl Dis.* 1976; 12: 143-7.
- Johnson GC, Coates JR, Winger F. Diagnostic immunohistochemistry of canine and feline intracalvarial tumors in the age of brain biopsies. *Vet Pathol.* 2014; 51(1):146-160.
- Kubo M, Matsuo Y, Okano T, Sakai H, et al. Nasal neuroendocrine carcinoma in a free-living Japanese Raccoon dog (*Nyctereutes procyonoides viverrinus*). *J Comp Path.* 2009;140:67-71.
- Langley K. The neuroendocrine concept today. *Annals New York Academy Sci.* 1994; 733: 1–17.
- Movassaghi AR, Davazdah Emami MR. Ethmoturbinate adenocarcinoma in a Persian fallow deer (*Cervus dama mesopotamica*). *Vet Rec.* 2001; 149: 493-4.
- [Nettles VF](#), [Vandevelde M](#). Thalamic ependymoma in a white-tailed deer. *Vet Pathol.* 1978; 15:133-5.
- [Parker VJ](#), [Morrison JA](#), [Yaeger MJ](#). Olfactory neuroblastoma in a cat. *J Feline Med Surg.* 2010;12: 867-71.
- Patnaik AK, Ludwig LL, Erlandson RA. Neuroendocrine carcinoma of the nasopharynx in a dog. *Vet Pathol.* 2002; 39: 496.
- Sako T, Shimoyama Y, Akihara Y, Ohmachi T, Yamashita K, Kadosawa T, Nakade T, Uchida E, Okamoto M, Hirayama K, Taniyama H. Neuroendocrine Carcinoma in the Nasal Cavity of Ten Dogs. *J Comp Pathol.* 2005; 133: 155-163.
- [van Maanen C](#), [Klein WR](#), [Dik KJ](#), [van den Ingh TS](#). Three cases of carcinoid in the equine nasal cavity and maxillary sinuses: histologic and immunohistochemical features. *Vet Pathol.* 1996; 33(1): 92-5.

CASE IV: WHL 14317601 (JPC 4067276).

Signalment: Adult male fox squirrel (*Sciurus niger*)

Adult female fox squirrel (*Sciurus niger*)

History: Over the course of several days, five squirrels were found dead under a tree at a residence in Colorado. Prior to death, all of the squirrels had similar clinical signs which included hindquarter paralysis, lethargy, and heavy breathing.

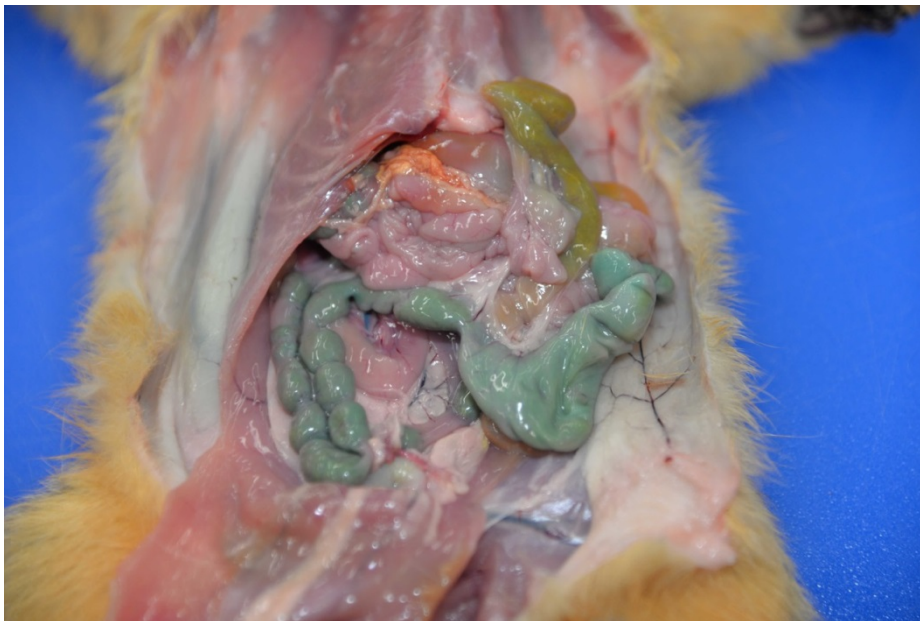
Gross Pathology: Two fox squirrels were presented for postmortem examination in good body condition with minimal autolysis. No evidence of trauma was identified. The adult male squirrel had no significant gross lesions and stomach contents were within normal limits, including grainy yellow-brown ingesta. The adult female had turquoise-green granular material on the fur of the upper lip and similar material within

the stomach. The colonic contents were stained a distinct turquoise-green.

Laboratory Results: Adipose tissue contained desmethylbromethalin.

Histopathologic Description:

Brain, 2 sections (cerebellum and cerebral cortex including hippocampus): Diffusely throughout both sections, the white matter is characterized by moderate to severe extracellular vacuolization. Vacuoles are formed by variably swollen myelin sheaths which occasionally coalesce into large extracellular clear spaces. Dilated myelin sheaths contain normal to minimally swollen axons. Scattered throughout the grey matter of the cerebral cortex and rarely within the hippocampus are low numbers of neurons with degenerative changes, including central chromatolysis and occasional pyknosis. Rare neurons are shrunken, angular, and hypereosinophilic with karyolysis (necrosis). Clefts within the perikaryon of multiple neuronal cell bodies are consistent with fixation artifact.



Colon, squirrel. At necropsy, the colon of one squirrel had bright turquoise green contents. (Photo courtesy of: Colorado State University, Department of Microbiology, Immunology and Pathology, College of Veterinary Medicine and Biomedical Sciences, <http://csu-cvmb.colostate.edu/academics/mip/>)

Contributor's Morphologic

Diagnosis: Cerebellum and cerebral cortex: Vacuolar myelinopathy, severe, diffuse, with mild, multifocal neuronal degeneration and necrosis.

Contributor's Comment:

Bromethalin toxicosis was strongly suspected based on the history and collective gross and histologic findings. This suspicion was



Stomach, squirrel. The stomach of one squirrel had a small amount of turquoise green grainy ingesta. (Photo courtesy of: Colorado State University, Department of Microbiology, Immunology and Pathology, College of Veterinary Medicine and Biomedical Sciences , <http://csu-cvmb.colostate.edu/academics/mip/>)

confirmed by the presence of desmethylbromethalin in the adipose tissue. Desmethylbromethalin is a toxic metabolite of bromethalin, a potent neurotoxin and the active ingredient in a variety of rodenticides. The mechanism of action involves uncoupling of oxidative phosphorylation, resulting in decreased ATP production and diminished Na⁺/K⁺ pump activity.^{9,10} In the CNS, the net result is severe, acute fluid retention and a dramatic elevation in cerebrospinal fluid pressure. Bromethalin is metabolized to desmethylbromethalin through N-demethylation by hepatic mixed-function oxygenases and is excreted predominantly in the bile. The oral LD₅₀ is 2.38-5.6 mg/kg in the dog and 0.4-0.71 mg/kg in the cat.^{3,9} A relative resistance to toxicity has been demonstrated in species unable to metabolize bromethalin to desmethylbromethalin (e.g. guinea pigs with an LD₅₀ of 1000 mg/kg).¹⁰ Short of chemical confirmation, diagnosis of bromethalin toxicosis is based on likelihood

of exposure and development of corresponding clinical signs, including muscle tremors, seizures, dyspnea, hyperexcitability, hind limb ataxia, and paresis to paralysis. Severity and onset (2-14 hours post-ingestion) are dose-dependent.³

Bromethalin is indistinguishable

from anticoagulant rodenticides in appearance and

color, and gross lesions are uncommon. Diffuse white matter vacuolization is the characteristic histologic lesion, and ultrastructural studies have demonstrated intramyelinic vacuoles with separation and splitting of myelin lamellae.^{4,5} Luxol fast blue-periodic acid Schiff stain has demonstrated myelin displacement due to edema with no apparent net myelin loss.⁵ Hypertrophied astrocytes and oligodendrocytes have also been reported.⁵ Vacuolization of the optic nerve occurs in most cases.^{4,5} Similar white matter vacuolization is seen with triethyltin and hexachlorophene neurotoxicosis.^{7,8}

Bromethalin use has increased in recent years in association with new regulations prohibiting residential use of second generation anticoagulant rodenticides. While bromethalin remains readily available for over-the-counter sales, many anticoagulant rodenticides with similar names (e.g. brodifacoum, bromadiolone) have been removed. Thus, bromethalin

toxicity is gaining in importance due to increased popularity of neurotoxic rodenticides.

JPC Diagnosis: Cerebrum and cerebellum, white matter: Vacuolar myelinopathy, diffuse, severe.

Conference Comment: Conference participants discussed this lesion as being very 'quiet' histologically, with minimal if any response to the swelling of myelin sheaths. The moderator discussed how this lesion contrasts with a demyelinating lesion, which manifests histologically as a patchy, less diffuse distribution and with at least some degree of glial response. In this example of bromethalin toxicity, there is a distinct absence of swollen axons and spheroids, and the oligodendrocytes appear quiescent.

The differential diagnosis discussed by participants for a similar histologic lesion in other species included other toxicants, such as hexachlorophene and ammonia, as well as plant toxins seen in various parts of the world, such as *Stypantra* spp. in Australia and *Helichrysum* spp. in Africa. The lesions of bromethalin in the central nervous system of these squirrels also bear resemblance to those of avian vacuolar myelinopathy, which is seen in North America secondary to a cyanobacterial toxin that grows on non-native aquatic vegetation. The condition is frequently lethal and affects various avian species, such as bald eagles and American coots in the southeastern United States.⁶ Another cause of similar white matter specific vacuolar change includes branched-chain alpha-ketoacid decarboxylase deficiency (maple syrup urine disease) in cattle.



Cerebrum and cerebellum, squirrel: The white matter of the corona radiata, corpus callosum, and spinocerebellar tracts, as well as within the cerebellar folia exhibits diffuse pallor. (HE, 5X)

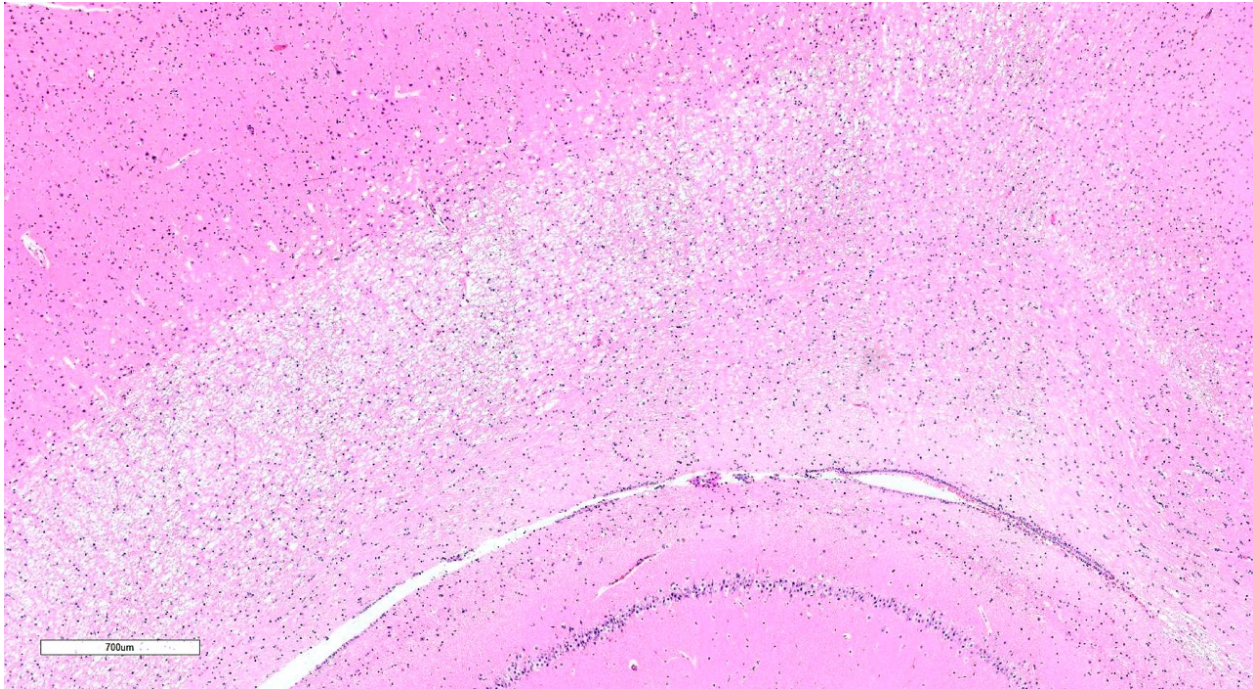
Despite the apparent frequency with which bromethalin intoxication occurs in domestic animals and wildlife species, there are surprisingly few reports in the recent professional literature. In addition to the more acute syndrome discussed above, a paralytic syndrome is also described when concentrations below the LD₅₀ are ingested; it includes ataxia, CNS depression, and paralysis which may develop over a period of days and worsen over a period of weeks.² The acute syndrome has also been reported to occur when smaller doses (below the LD₅₀) are ingested in dogs and may relate to treatment with activated charcoal, which can result in idiosyncratic hypernatremia in rare cases. Dramatic changes in sodium levels can result in CNS associated clinical signs and lesions, including cortical laminar necrosis in cases of salt intoxication; conversely, osmotic demyelination can occur in cases where there is a sudden increase in sodium in a hyponatremic animal. Histologic lesions in osmotic demyelination and the changes seen in bromethalin toxicity can have similarities,

although in osmotic demyelination there is myelin and oligodendrocyte loss which does not occur with bromethalin intoxication.¹

The green-tinged or turquoise coloring seen in the gross image is characteristic of dyes used in certain rodenticides, as well as in some fertilizers and pesticides,² which can make confirmation of bromethalin intoxication challenging.¹ The highest concentration of desmethylbromethalin is usually found in adipose tissue, which is the most important tissue sample for diagnostic toxicology testing in suspected cases of bromethalin intoxication.² Bromethalin is not only lipid-soluble, but also readily crosses the blood brain barrier.¹ Additionally, in cases of mild white matter vacuolation, both light microscopy and ultrastructural examination may not be able to precisely differentiate the changes of bromethalin intoxication from those of autolysis, the latter of which are especially common in wildlife species.² Neuron-specific nuclear protein (NeuN) and glial fibrillary acidic protein (GFAP) may be



Cerebellum, squirrel. The cerebellar white matter contains numerous well-defined vacuoles which impart a diffuse pallor to it. (HE, 80X)



Cerebrum, squirrel. The vacuolated white matter of the internal capsule does not have a cellular infiltrate, as the lesion is primarily intramyelinic edema without axonal destruction. (HE, 80X).

useful in distinguishing subtle changes from autolytic artifact in questionable cases. Decreased NeuN immunoreactivity can indicate neuronal loss and/or metabolic stress and increased GFAP immunoreactivity is indicative of reactive astrocytosis.¹

Contributing Institution:

Colorado State University
Department of Microbiology, Immunology
and Pathology
College of Veterinary Medicine and
Biomedical Sciences
[http://csu-
cvmb.colostate.edu/academics/mip/](http://csu-cvmb.colostate.edu/academics/mip/)

References

1. [Bates MC](#), [Roody P](#), [Lehner AF](#), [Buchweitz JP](#), et al. Atypical bromethalin intoxication in a dog: pathologic features and identification of an isomeric breakdown product. *BMC Vet Res.* 2015; 11(244):1-9.
2. [Bautista AC](#), [Woods LW](#), [Filigenzi MS](#), [Puschner B](#). Bromethalin poisoning in a raccoon (*Procyon lotor*): diagnostic considerations and relevance to nontarget wildlife. *J Vet Diagn Invest.* 2014; 26(1):154-157.
3. [Dorman, DC](#), [Parker, AJ](#), [Buck, WB](#). Bromethalin Toxicosis in the dogs. Part I: Clinical Effects. *J Am Anim Hosp Assoc.* 1990; 26(6): 589-594.
4. [Dorman, DC](#), [Simon, J](#), [Harlin, KA](#), [Buck, WB](#). Diagnosis of bromethalin toxicosis in the dog. *J Vet Diagn Invest.* 1990; 2:123-128.
5. [Dorman, DC](#), [Zachary, JF](#), [Buck, WB](#). Neuropathologic findings of bromethalin toxicosis in the cat. *Vet Pathol.* 1992; 29:139-144.
6. [Haynie RS](#), [Bowerman WW](#), [Williams SK](#), [Morrison SK](#). Triploid grass carp susceptibility and potential for disease transfer when used to control aquatic

vegetation in reservoirs with avian vacuolar myelinopathy. *J Aquat Anim Health*. 2013; 25(4):252-259.

7. Nakaue, HS, Dost, FN, Buhler, DR. Studies on the toxicity of hexachlorophene in the rat. *Tox and Appl Pharm*. 1973; 24: 239-249.

8. O'Shaughnessy, DJ, Losos, GJ. Peripheral and central nervous system lesions caused by triethyl- and trimethyltin salts in rats. *Tox Path*. 1986; 14(2).

9. Peterson, ME. Bromethalin Topical Review. *Topics in Companion Med*. 2013; 28:21-23.

10. van Lier, RB, Cherry, LD. The toxicity and mechanism of action of bromethalin: a new single-feeding rodenticide. *Fundam Appl Toxicol*. 1988 Nov; 11(4):664-72.

Joint Pathology Center
Veterinary Pathology Services



WEDNESDAY SLIDE CONFERENCE 2015-2016

Conference 22

27 April 2016

Cory Brayton, DVM, Ph.D., DACVP
Associate Professor, Molecular & Comparative Pathobiology Johns Hopkins University
School of Medicine Broadway Research Building, Suite 851
733 North Broadway
Baltimore, MD 21205

CASE I: NIEHS-087 (JPC 4017222).

Signalment: 11-month-old B6.129S-*Cybb^{tm1Din}/J* mouse (*Mus musculus*)

History: A breeding colony of B6.129S-*Cybb^{tm1Din}/J* mice were housed in an AAALAC International accredited facility. The mice were housed in static micro isolator cases with *ad libitum* autoclaved food (NIH-31) and beta chip bedding. Mice were provided acidified water due to immunocompromised state. The mice were housed in the same room as B6 immunocompetent mice. Sudden deaths were noted in the colony over a weekend. A total of 87 mice, aged from one to eleven months were affected. Of these, 45 mice were found dead and 19 sick mice were euthanized and necropsied. Twenty males and 38 females were affected.

Gross Pathology: The livers were pale and slightly enlarged. In most of the mice, there



Body as a whole, mouse. The liver was slightly enlarged, and there are multiple tan foci in the liver and lung.

(Photo courtesy of: National Institute of Environmental Health Sciences, Cellular and Molecular Pathology Branch and Comparative Medicine Branch, P.O. Box 12233, Research Triangle Park, NC 27709, <http://www.niehs.nih.gov/research/atniehs/labs/lep/index.cfm>)

were multifocal tan foci in the liver, spleen and lung.

Laboratory Results: From multiple tissues, a pure culture of *Burkholderia* spp. was isolated. The isolate was further

characterized as *Burkholderia cepacia* with PCR. In the blood smears, monocytes contained bacterial rods.

Histopathologic Description: Liver: Multifocally and randomly, there are areas of hepatocyte necrosis containing cellular and karyorrhectic debris and moderate numbers of degenerate neutrophils. Multifocally, many blood vessels contain thrombi. There are large areas of coagulative necrosis surrounding these thrombosed blood vessels. Multifocally, the hepatocyte cytoplasm is vacuolated (glycogen) and, contain clear round vacuoles (lipid). Multifocal portal areas are infiltrated by small numbers of lymphocytes. No bacteria were present in the Gram's stained liver section.

Contributor's Morphologic Diagnosis:

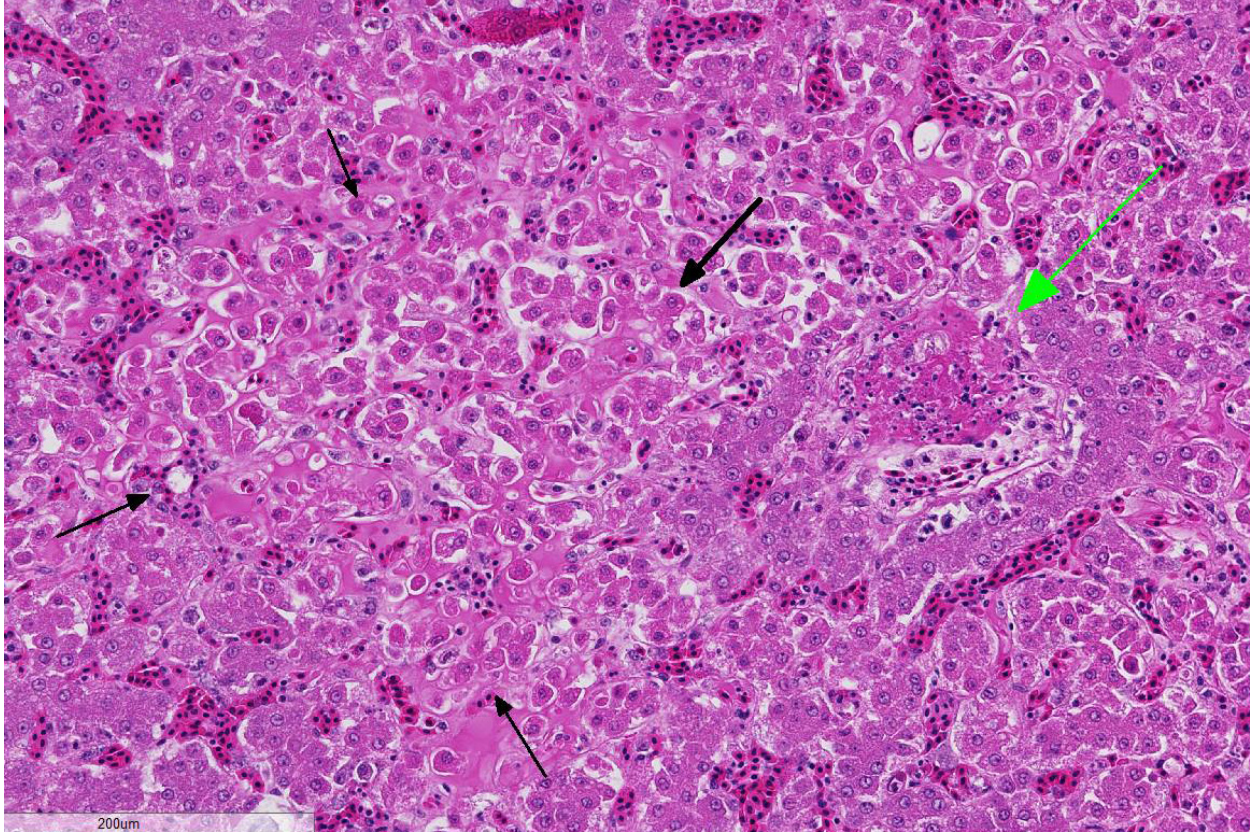
Liver: Hepatitis, necrosuppurative, multifocal, random, moderate with vascular thrombosis.



Liver, mouse. Randomly throughout the section, there are pale foci of necrosis. (HE, 5X).

Contributor's Comment: B6.129S-*Cybb*^{tm1Din}/J mouse is a targeted mutant lacking superoxide production in phagocytes.⁹ 129S6 mice is the embryonic stem cell donor in which cytochrome b-245, beta polypeptide(*Cybb*) targeted mutation(*tm*) was created by Dr. Mary C Dinauer(*Din*)

(<http://jaxmice.jax.org/strain/002365.html>; accessed on August 5, 2011). Superoxide production is critical in host defense. Therefore, mice lacking superoxide production are immunocompromised. This mouse is an animal model for X-linked chronic granulomatous disease in humans.⁹ These mice are susceptible to various bacterial and fungal infections.⁹ Based on the gross lesions in the affected mice differential diagnoses included septicemia, mouse hepatitis viral infection, pox viral infection and Tyzzer's disease. Histologically, the absence of syncytial cells and intracytoplasmic inclusions helped to eliminate the possibility of mouse hepatitis virus and poxvirus infection, respectively. Absence of bacilli in and around the necrotic hepatocytes, eliminated the possibility of Tyzzer's disease. The histologic changes in the current case were consistent with a septicemic process. This was supported by the isolation of bacteria and evidence of bacteremia. *Burkholderia cepacia* complex includes nine members. The bacteria are ubiquitous in nature and can cause pneumonia and septicemia in cystic fibrosis and chronic granulomatous disease patients.^{3,7} In the current outbreak the source of



Liver, mouse. There are multiple areas of coagulative necrosis (black arrows), as well as partially occlusive fibrin thrombi within adjacent vessels. (HE, 181X)

infection could not be determined. Because B6.129S-Cybb^{tm1Din}/J mouse is a model for X-linked CGD,⁹ only male mice should have been affected. However, both males and females were affected in the current case. One possible explanation could be that certain numbers of cells in females can have the mutant X-chromosome resulting in a full expression of an X-linked condition.⁵ Also, spontaneous infections with various pathogens in both males and females have been previously reported in this mouse model.²

JPC Diagnosis: Liver: Hepatitis, necrotizing, multifocal, random, marked with fibrin thrombi.

Conference Comment: *Burkholderia cepacia* complex includes a group of motile, aerobic, gram-negative bacilli that are

ubiquitous in the environment and can be isolated from soil, vegetables and water.¹ They act as endophytic bacteria on certain types of vegetation and have been used as a potential catalysts, involved in the formation of enzymes, used in the creation of alternative energy sources from perennial grasses.⁶ Due in part to the presence of antibiotic resistance mechanisms, they are also important bacterial pathogens in the hospital setting,¹ and are important opportunistic pathogens in cases of septicemia and lung infection in cystic fibrosis patients.⁴ The organism has also been isolated from the deep pyoderma in dogs on immunosuppressive therapy (cyclosporine). In those cases the clinical course was acute and infection was widespread. Because *B. cepacia* is not a commensal on canine skin, it is presumably acquired either from the

environment or within hospitals, although reports of environmental *B. cepacia* in veterinary practices are rare. *B. cepacia* has also been reported to cause subclinical mastitis in dairy sheep.¹

As discussed above, the transgenic mice in this case are deficient in superoxide production in phagocytes. Once phagocytosis of an opsonized particle takes place within a neutrophil, usually via binding of complement or F_c receptors, internal signaling cascades are initiated involving various GTPases and protein and lipid kinases, eventually resulting in release of calcium from the endoplasmic reticulum and production of the oxidative burst within phagolysosomes. The oxidative burst is initiated by formation of the nicotinamide adenine dinucleotide phosphate (NADPH) oxidase, which stimulates generation of superoxide free radicals, critical in microbial killing.⁸ In this case, a mutation in NADPH oxidase is involved in superoxide deficiency and absence of a functional respiratory burst.⁹ Reactions involving superoxide anion result in the formation of hydrogen peroxide, hydroxyl radical and hypochlorous acid as well as peroxynitrate, all of which are important microbicidal agents.⁸

The conference histologic description was very similar to the contributor's description above. Not all sections have prominent fibrin thrombi but in sections with thrombi areas of necrosis appear spatially associated with thrombosed vessels. The differential diagnosis for this lesion includes *Helicobacter hepaticus*, *Salmonella* spp., *Proteus mirabilis* and *Clostridium piliforme* as well as some viral conditions such as mouse hepatitis virus, as mentioned above. Both Gram stains and silver stains failed to identify infectious organisms. Conference participants discussed *B. cepacia* and its various virulence factors including

lipopolysaccharide (LPS), exotoxins, lipases, siderophores and proteases as well as the inherent antibiotic resistance of its cell envelope.⁷

Contributing Institution:

National Institute of Environmental Health Sciences

Cellular and Molecular Pathology Branch and Comparative Medicine Branch

P.O. Box 12233

Research Triangle Park, NC 27709

<http://www.niehs.nih.gov/research/atniehs/abs/lep/index.cfm>

References:

1. Banovic F, Koch S, Robson D, Jacob M, Olivry T. Deep pyoderma caused by *Burkholderia cepacia* complex associated with ciclosporin administration in dogs: a case series. *Vet Dermatol*. 2015; 26:287-e64.
2. Bingel SA. Pathology of a mouse model of x-linked chronic granulomatous disease. *Contemp Top Lab Anim Sci*. 2002;41: 33-38.
3. Coenye T, Vandamme P, Govan JR, LiPuma JJ. Taxonomy and identification of the *Burkholderia cepacia* complex. *J Clin Microbiol*. 2001;39: 3427-3436.
4. Folescu TW, da Costa CH, Folescu Cohen RW, da Conceicao Neto OC, et al. *Burkholderia cepacia* complex: Clinical course in cystic fibrosis patients. *BMC Pulm Med*. 2015;15:158.
5. Kumar V, Abbas A, Fausto N, Aster J. *Pathologic Basis of Disease*. 8th ed., Saunders; 2010:135-182.
6. Leo VV, Passari AK, Joshi JB, Mishra VK, et al. A novel triculture system (CC3) for simultaneous enzyme production and hydrolysis of common grasses through submerged fermentation. *Front Microbiol*. 2016;7:447.

7. Mahenthalingam E, Urban TA, Goldberg JB. The multifarious, multireplicon *Burkholderia cepacia* complex. *Nat Rev Microbiol*. 2005;3:144-156.
8. Myers RK, McGavin D, Zachary JF. Cellular adaptations, injury, and death: Morphologic, biochemical and genetic bases. In: McGavin MD, Zachary JF, eds. *Pathologic Basis of Veterinary Disease*. 5th ed. St. Louis, MO: Mosby Elsevier; 2012:100-101.
9. Pollock JD, Williams DA, Gifford MA, Li LL, D et al. Mouse model of X-linked chronic granulomatous disease, an inherited defect in phagocyte superoxide production. *Nat Genet*. 1995;9: 202-209.

CASE II: AR07-025012 (JPC 4032917).

Signalment: Adult, male, Fischer 344 rat (*Rattus norvegicus*).

History: This rat was euthanized after presenting for rolling and inability to maintain balance.

Gross Pathology: The spleen was dark red, markedly enlarged (9 x 3 x 1.5 cm) and occupied 2/3 of the abdominal cavity, compressing adjacent organs. The surface was irregular and traversed by prominent white-tan fibrous adhesions. The liver was dark red and moderately enlarged.

Laboratory Results: None reported.

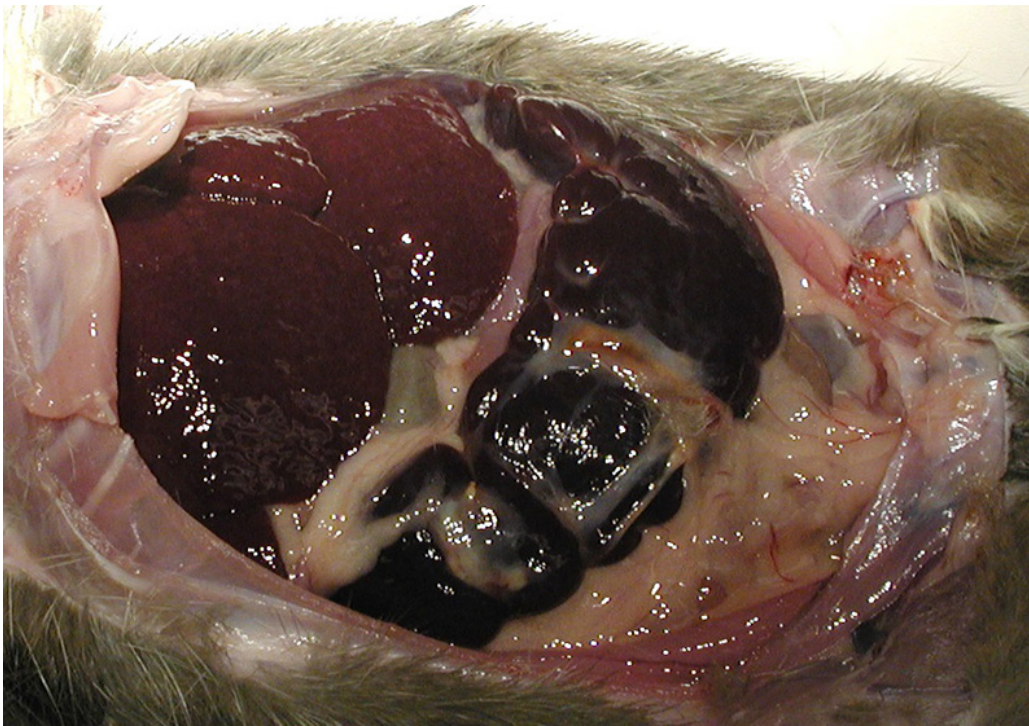
Histopathologic Description: Testis: Testicular blood vessels are filled with neoplastic round cells resembling lymphocytes, with irregularly round, 6-10 micron diameter hyperchromatic nuclei and

scant pale eosinophilic cytoplasm frequently forming thin rims around the nuclei. Mitotic figures are rare. Replacing the testicular parenchyma is another neoplasm, 3 x 4 mm, well demarcated, unencapsulated and multilobular, composed of sheets and packets of round to polygonal cells supported by fine fibrovascular stroma. The neoplastic cells have variably distinct cell borders, abundant eosinophilic finely vacuolated cytoplasm, and oval, central nuclei with finely stippled chromatin and a single, variably distinct basophilic nucleolus. Mitotic figures are rare. The adjacent seminiferous tubules are compressed and shrunken, lined only by Sertoli cells with an absence of germ cells. Some contain rounded germ cells with eosinophilic cytoplasm and nuclear condensation or multinucleated spermatid giant cells. Others are dilated and contain variable amounts of homogeneous eosinophilic material.

Contributor's Morphologic Diagnosis:

1. Testis, vessels: Lymphocytic leukemia (Large Granular Lymphocyte Leukemia)
2. Testis: Interstitial cell tumor
3. Testis, seminiferous tubules: Tubular degeneration and atrophy, multifocal, moderate

Contributor's Comment: Large granular lymphocyte leukemia and interstitial cell tumors are two of the most common neoplasms in aged Fischer 344 (F344) rats. Large granular lymphocyte (LGL) leukemia, also known as mononuclear cell leukemia or Fischer rat leukemia occurs commonly in the F344 rat but is also reported in other strains. It is a rapidly fatal, age-related neoplasia, with a significantly increased risk after 20 months of age.⁴ Clinically, rats can exhibit inactivity, weight loss, pale eyes, icterus, and palpable splenomegaly.⁶



Testis, F344 rat. There is marked splenomegaly with hepatomegaly in an adult Fischer 344 rat. White-tan adhesions multifocally traverse the cobblestoned surface of the spleen. (Photo courtesy of: Wake Forest School of Medicine, Department of Pathology/Comparative Medicine, Medical Center Boulevard, Winston Salem, NC 27157-1040, <http://www.wakehealth.edu/School/Comparative-Medicine/Training-Programs/ACVP.htm>)

Common clinical pathological abnormalities include hemolytic anemia and thrombocytopenia. Gross lesions include a characteristically markedly enlarged, often friable spleen and an enlarged, mottled liver. Enlarged mesenteric lymph nodes and hemorrhage in the lungs, lymph nodes and brain can also be present.⁴

Histologically, LGL leukemia most consistently demonstrates diffuse leukemic infiltration of the red pulp, where the neoplasm is believed to arise, with variable lymphoid depletion.^{4,5} The liver and spleen are generally always infiltrated by neoplastic

LGLs. In advanced stages, a general leukemia is present, and vessels in lymph nodes, lung, and brain are often infiltrated by neoplastic cells. Bone marrow involvement, if present, occurs late relative to involvement of the spleen.⁴ Rats with LGL leukemia can also have focal accumulations of neoplastic lymphocytes,⁷ such as were

observed in the brain in this case, which led to the neurological clinical signs.

Large granular leukocytes have distinctive azurophilic cytoplasmic granules in blood smears; granules are generally not discernible on histology sections.⁵ Well-differentiated LGLs may have reniform nuclei and cytoplasmic granules; poorly differentiated LGLs have few or inapparent granules.⁶ LGL cells are generally pleomorphic and 10-15 microns in diameter. Many studies have demonstrated natural killer cell activity of LGLs, but the exact cell of origin is still not fully understood.^{6,8}



Testis, rat. Within the body of the testis, there is an interstitial cell tumor.

Interstitial, or Leydig, cell tumors are the most common testicular neoplasms in rats, dogs, cats and bulls.^{1,2} Fischer 344 rats have an incidence approaching 100% by 24 months of age.¹ Grossly, interstitial cell tumors tend to be well-circumscribed, tan to yellow-orange, soft masses. There can be multiple tumors and they can be unilateral or bilateral. Histologically, interstitial cell tumors are unencapsulated and composed of uniform round or polyhedral neoplastic cells with abundant eosinophilic finely granular or vacuolated cytoplasm. Peripheral seminiferous tubules are often compressed and show variable degrees of degeneration and atrophy. Nuclei are generally round, centrally-placed and have single nucleoli. Mitotic rates are generally low. Interstitial cell hyperplastic lesions, probably pre-neoplastic lesions, can be more diffuse, occur between tubules rather than replace them, and have a diameter smaller than three seminiferous tubules.¹ A much less common and more pleomorphic proliferative interstitial cell lesion with cellular atypia and invasion of adjacent tissue, including vessels

or the capsule, or with metastases warrants the diagnosis of interstitial cell carcinoma.¹

JPC Diagnosis: 1. Testis, blood vessels: Mononuclear cell leukemia.
 2. Testis: Leydig cell adenoma.
 3. Testis, seminiferous tubules: Degeneration, atrophy and loss with marked aspermatogenesis and spermatid giant cells.

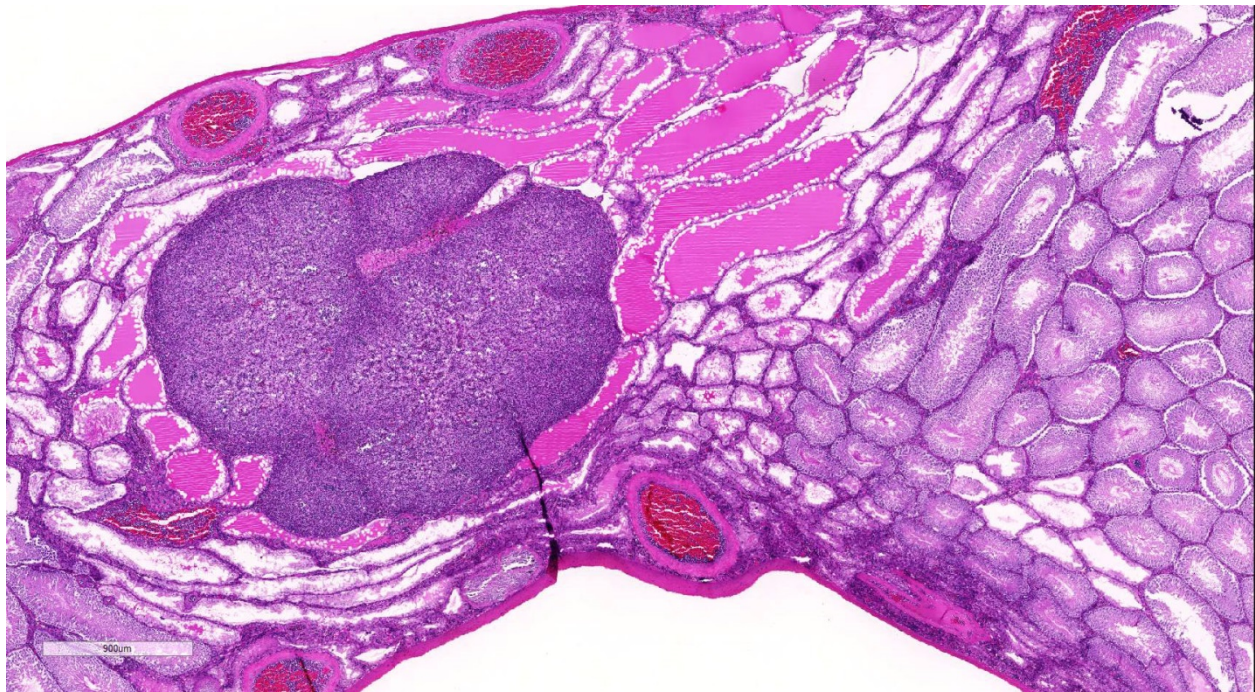
Conference Comment: Conference participants discussed the nomenclature of large granular lymphocytic (LGL) leukemia. We prefer the nomenclature noted above, in agreement with INHAND Project (International Harmonization of Nomenclature and Diagnostic Criteria for Lesions in Rats and Mice). The “granular” descriptor refers to the cytologic appearance of neoplastic cells when stained with a Wright-Giemsa stain; the granules cannot be visualized in histologic sections stained with hematoxylin and eosin. The moderator also mentioned that in some severe cases, extravascular infiltrates of neoplastic cells can be seen as well as circulating cells with mitotic figures. The neoplasm is a heterogeneous, non-B,

non-T cell leukemia with neoplastic cells having natural killer cell activity; cells are negative for the immunohistochemical stain leukocyte common antigen (LCA, CD45). Icterus is often seen in affected animals secondary to hemolytic anemia; the leukemia cells will also phagocytose erythrocytes and their granules can be erythrolytic. Due to the high incidence of this condition in Fischer 344 rats, Sprague-Dawley and Wistar rats (as opposed to Fischer 344 rats) are used more commonly in toxicology studies.

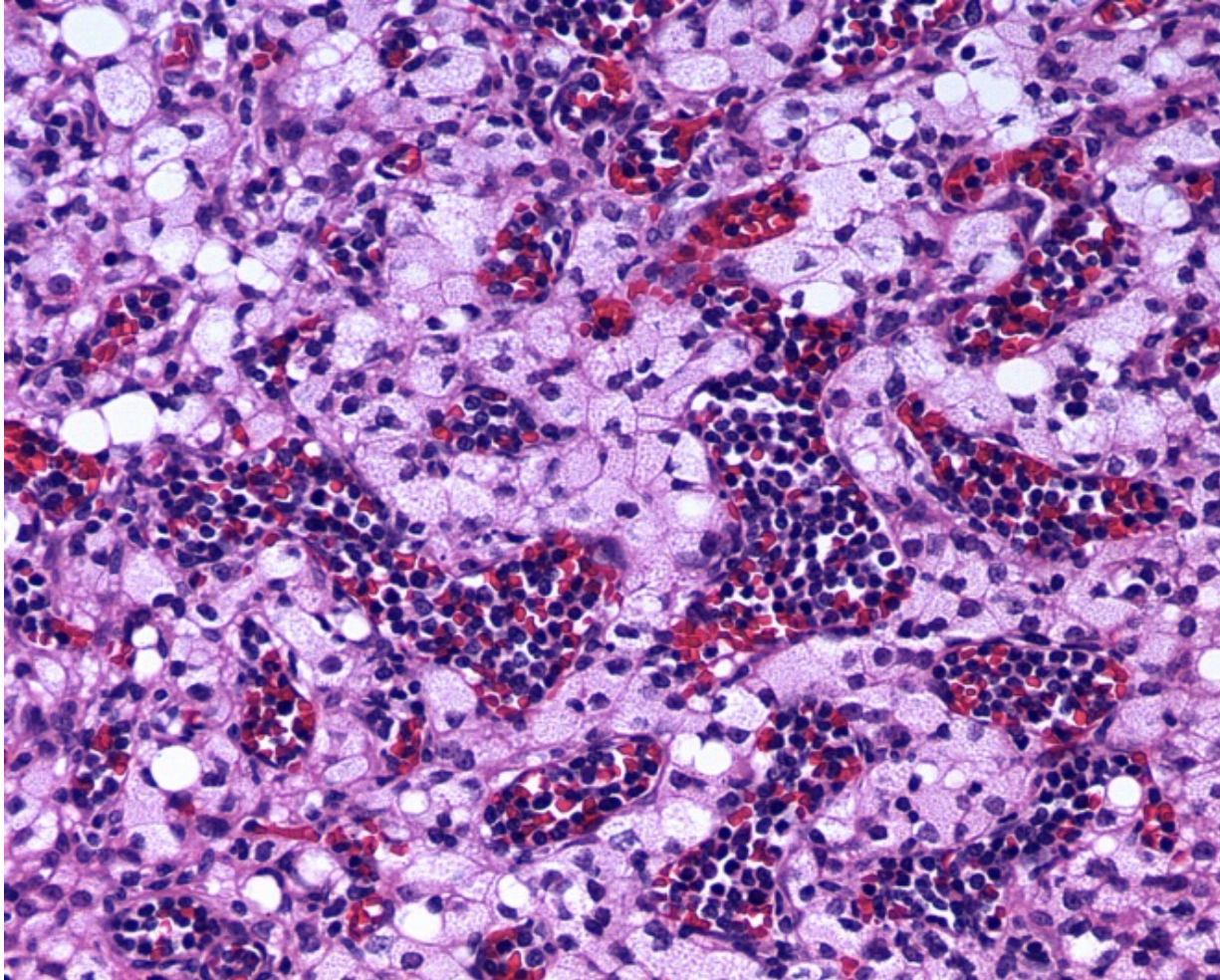
Early diagnosis of LGL leukemia can be challenging, but the presence of leukemia cells in hepatic sinusoids may aid in the diagnosis. Other hepatic changes include nodular regenerative hyperplasia, characterized by centrilobular atrophy and periportal hypertrophy of hepatocytes secondary to anemia-related ischemic hepatocellular injury; endothelial injury may

also play a role in some cases. Splenic congestion, a common and consistent finding, and is postulated to be related to portal hypertension in addition to proliferation of neoplastic LGL leukemia cells in the spleen. The precise cause or pathogenesis of portal hypertension in this condition is unclear.³

As noted in the contributor's comments, Leydig cell hyperplasia is a differential diagnosis for Leydig cell tumor. Neoplastic lesions are considered to be a continuum or progression from hyperplastic lesions in most cases. Unlike hyperplasia, however, Leydig cell tumors will generally demonstrate compression of adjacent testicular parenchyma and neoplastic cells will be larger, with larger nuclei and may (or may not) demonstrate atypia. Hyperplastic lesions may be focal, multifocal or diffuse, with diffuse being most common, and cells may demonstrate prominent vacuolation;



Testis, rat. The tumor is surrounded by ectatic, atrophic seminiferous tubules. The loss of spermatocytes within these tubules has resulted in an overall narrowing of the testis at this location, in spite of the presence of the interstitial cell tumor. (HE, 24X)



Testis, F344 rat. Two neoplastic populations are present in the testis. One fills blood vessels (leukemia) scattered amongst the large polygonal cells with finely vacuolated cytoplasm of the other (interstitial cell tumor). (Photo courtesy of: Wake Forest School of Medicine, Department of Pathology/Comparative Medicine, Medical Center Boulevard, Winston Salem, NC 27157-1040, <http://www.wakehealth.edu/School/Comparative-Medicine/Training-Programs/ACVP.htm>)

however, hyperplastic lesions will not compress the surrounding tissue. Another criterion which may aid in the diagnosis of less straightforward cases is the designation of a proliferative Leydig cell lesion with a diameter of greater than three seminiferous tubules as a neoplasm (Leydig cell adenoma).¹

The pathogenesis of Leydig cell hyperplasia is related to elevated luteinizing hormone levels, paracrine stimulatory factors within the testis or can be secondary to decreased spermatogenesis.¹ Restriction of dietary intake may decrease the incidence of interstitial cell tumor but is not documented

to decrease the incidence of LGL leukemia.⁷ A diffuse distribution of hyperplastic lesions is more common in the mouse as well as in the rat.

Contributing Institution:

Wake Forest School of Medicine
 Department of Pathology/Comparative
 Medicine
 Medical Center Boulevard
 Winston Salem, NC 27157-1040
<http://www.wakehealth.edu/School/Comparative-Medicine/Training-Programs/ACVP.htm>

References:

1. Creasy D, Bube A, de Rijk E, et al. Proliferative and nonproliferative lesions of the rat and mouse male reproductive system. *Toxicol Pathol.* 2012; 40(6):40S-121S.
2. Ladds, PW. The male genital system. In: Jubb KVF, Kennedy PC, Palmer N, eds. *Pathology of Domestic Animals.* 4th ed. London, UK: Academic Press; 1993:471-529.
3. Shiga A, Narama I. Hepatic lesions caused by large granular lymphocyte leukemia in Fischer 344 Rats: Similar morphologic features and morphogenesis to those of nodular regenerative hyperplasia (NRH) in the human liver. *Toxicol Pathol.* 2015; 43(6):852-864.
4. Stromberg PC and Vogtsberger LM. Pathology of the mononuclear cell leukemia of Fischer rats. I. Morphologic studies. *Vet Pathol.* 1983; 20:698-708.
5. Suttie, AW. Histopathology of the spleen. *Toxicol Pathol.* 2006; 34(5):466-503.
6. Thomas J, Haseman JK, Goodman JI, et al. A review of large granular lymphocytic leukemia in Fischer 344 rats as an initial step toward evaluating the implication of the endpoint to human cancer risk assessment. *Toxicol Sci.* 2007; 99(1):3-19.
7. Thurman JD, Bucci TJ, Hart RW, et al. Survival, body Weight, and spontaneous neoplasms in ad libitum-fed and food-restricted Fischer-344 rats. *Toxicol Pathol.*

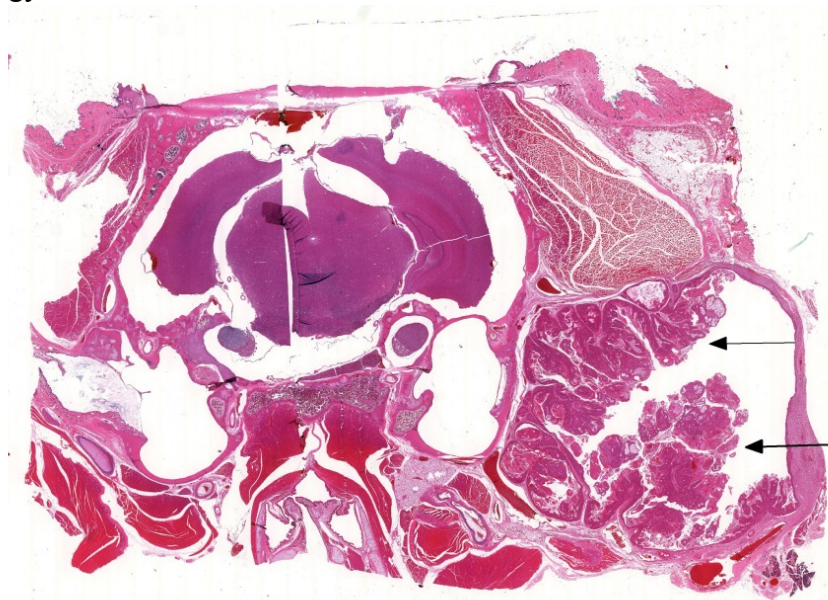
1994; 22(1):1-9.

8. Ward, J. M., and Reynolds, C.W. (1983). Large granular lymphocyte leukemia. A heterogeneous lymphocytic leukemia in F344 rats. *Am J Pathol.* 1983;111(1):1-10.

CASE III: 15-V587 (JPC 4067775).

Signalment: >24 month old, male, Fischer F344 rat (*Rattus norvegicus*).

History: An aged male F344 rat enrolled in a behavior study underwent surgery for the placement of head prosthesis. The animal recovered uneventfully, but 4 weeks following the surgery, a small swelling on the right side of the face was noticed. The swelling increased in size over several days. An aspirate of the mass showed eosinophilic acellular linear material (keratin), non-degenerative neutrophils, histiocytes, lymphocytes, and amorphous debris. The rat was anesthetized and the swelling was lanced and flushed, producing copious



Cross section of head, rat. A large, proliferative mass arises from the squamous lining of the deeper aspect of the ear canal. (HE, 6X).

amounts of purulent and sebaceous discharge. The rat was treated with oral antibiotic therapy (enrofloxacin administered in the drinking water); however, facial swelling was still present and animal's condition deteriorated. Humane euthanasia via intraperitoneal barbiturate overdose was elected by the investigative group.

Gross Pathology: There was an approximately 1 cm diameter, firm swelling at the base of the right ear. There was focal ulceration on the caudoventral aspect of the swelling with adhered bedding material. Both kidneys were diffusely, mildly pale, shrunken and irregular in texture, with pinpoint depressions across the surface. The spleen was approximately twice the normal size with an irregular texture. The liver was diffusely moderately enlarged and irregular. Both testicles were approximately 1.5 times larger than normal and yellow to tan.

Laboratory Results: None

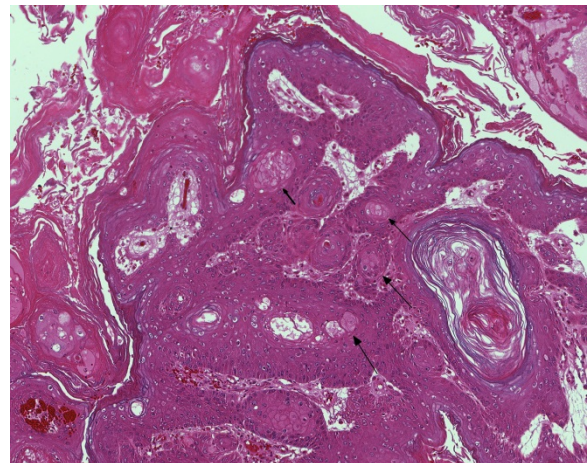
Histopathologic Description:

Extending through the subcutis from the lateral aspect of the bulla is a large, well demarcated, non-invasive, mul-tilobulated and nonencapsulated neoplasm consisting of papillary projections of stratified sq-uamous epithelium supported by expanded fibrovascular cores. The basement membrane is intact. There is diffuse, marked hyperkeratosis with abundant strands of eosinophilic acellular material (keratin) present within the center of the neoplasm. There are multifocal circular areas of lamellated keratin (keratin pearls). Neoplastic cells are well differentiated squamous epithelial cells with variably well delineated cytoplasmic borders and moderate eosinophilic cytoplasm. An ovoid central nucleus with a single nucleolus is present. There is mild to moderate anisocytosis and anisokaryosis. Mitotic

figures are not observed. There is mild, multifocal in-tercellular edema with accentuation of intercellular desmosomes. Multifocal cystic cavities are also present. Sebaceous cells are moderately to markedly enlarged and increased in number, with abundant pale and vacuolated cytoplasm. Extending along the lateral aspect of the neoplasm is a thick layer of mature fibrous connective tissue with mild multifocal extravascular red blood cells (hemorrhage).

Contributor's Morphologic Diagnosis: Zymbal's gland: Squamous cell papilloma with sebaceous hyperplasia and cystic degeneration.

Contributor's Comment: The Zymbal's gland is a multilobulated sebaceous holocrine gland located anterior-ventral to the ear canal in rats and mice, although it is smaller in mice^{5,7} This gland consists of 3-4 lobules which each have intralobular ducts that empty into the excretory duct and then ultimately into the ear canal.^{5,6} Spontaneous neoplasms are rare in rats with an incidence of 1% or less.⁶ Types of neoplasia reported



Ear canal, rat. The mass is composed of papillary projections of squamous epithelium which exhibits normal maturation. There are foci of sebaceous differentiation (arrows) scattered throughout the proliferating epithelium, as well as keratin pearls. (HE, 200X)

include sebaceous cell adenoma, squamous cell papilloma, and carcinoma of sebaceous and/or ductal epithelial origin.⁵ The Zymbal's gland is a target organ of many carcinogenic chemicals,⁴ with an incidence of Zymbal's gland neoplasms in as many as 67% of experimental animals (versus 0% in controls) in some studies.³ Chemicals known to induce Zymbal's gland tumors include 2-Acetylaminofluorine, Tris carbonium pamoate, urethan, heterocyclic amines, benzene, 3-3 dichlorobenzidine, 4-aminostilbene, azoxymethane, methychorlanethrene, and cupferron.⁶

In this case, no history of toxin exposure was present. Despite the large size, a benign tumor was diagnosed given the lack of mitoses and cellular atypia as well as the lack of invasion into the surrounding muscle and subcutis. The tumor was characterized as a papilloma given the exophytic multilobulated growth with prominent fibrovascular core. Marked sebaceous hyperplasia was present, which is reported to be common in cases of squamous cell papilloma of the Zymbal's gland.⁵

JPC Diagnosis: Zymbal's gland: Squamous papilloma with multifocal sebaceous differentiation.

Conference Comment:

Squamous papillomas of the Zymbal's gland originate from the duct epithelium, are composed of stratified squamous epithelium and must be differentiated from squamous cell carcinoma based on absence of invasive growth and cellular atypia. Inflammatory, atrophic and hyperplastic changes are also described in the Zymbal's gland, although their frequency of occurrence varies. The retention of normal tissue architecture aids in differentiating hyperplasia from adenoma. Adenomas will also generally have increased numbers of basaloid cells compared

to hyperplasia, are lobulated, and well defined but not encapsulated. Many of the neoplastic cells demonstrate cytoplasmic vacuolation, akin to mature sebaceous gland cells.⁵ In this case there was considerable discussion during the conference regarding the presence of vacuolated sebaceous cells in this neoplasm; some participants argued the cells which appear vacuolated may actually represent degenerating squamous epithelium. Regardless, glandular proliferation is often associated with squamous papilloma of the Zymbal's gland and thus, if present in this case, would not be surprising and would not change the diagnosis. Zymbal's gland carcinoma is also described and includes such features as pleomorphism, increased mitotic index, squamous differentiation, ulceration and absence of ducts.⁵

In addition to the mammary gland, the Zymbal's gland is commonly assessed in xenobiotic studies in rodents since it is a target organ of many carcinogens. Aside from neoplastic changes, degenerative, necrotic, regenerative and vascular changes are also described in the gland and many of the changes are similar to what is observed in the mammary gland.⁵ Additional tissues which may be sampled in xenobiotic studies include the preputial and clitoral glands, which are also common sites for adenomas in rodents. Degeneration, necrosis and regeneration are often seen in the same gland with repeated toxin exposure. Dilation or cystic degeneration of ducts may also be seen in the Zymbal's gland as a spontaneous aging change in rodents.⁵

Common tumor types in both the F344 and Sprague Dawley rat strains (from the National Toxicology Program historical control database) include mammary gland fibroadenoma, pituitary pars distalis adenoma, thyroid gland C cell adenoma, adrenal medulla benign pheochromocytoma,

and uterine stromal polyp.^{1,2} Mammary gland carcinoma^{1,2} and histiocytic sarcoma are also common tumors seen in Sprague Dawley rats, and large granular lymphocytic leukemia, interstitial cell tumors in males,^{1,2} and mesothelioma originating from the testicular tunic are common in F344 rats.

Contributing Institution:

Department of Comparative Medicine,
School of Medicine
University of Washington, Seattle, WA

References:

1. Dinse GE, Peddada SD, Harris SF, Elmore SA. Comparison of NTP historical control tumor incidence rates in female Harlan Sprague Dawley and Fischer 344/N rats. *Toxicol Pathol.* 2010; 38:765-775.
2. Haseman JK, Hailey JR, Morris RW. Spontaneous neoplasm incidences in Fischer 344 rats and B6C3F₁ mice in two-year carcinogenicity studies: A National Toxicology program update. *Toxicol Pathol.* 1998; 26(3):428-441.
3. Hafez E, Takahashi T, Ogawa H, Sato M, Nakai T, Takasu C, et al.: High susceptibility to zymbal gland and intestinal carcinogenesis in diabetic Otsuka long-evans Tokushima Fatty rats. *J Toxicol Pathol* 2011;24(4):187-193.
4. Haseman JK, Lockhart AM: Correlations between chemically related site-specific carcinogenic effects in long-term studies in rats and mice. *Environ Health Perspect* 1993;101(1):50-54.
5. Rudmann D, Cardiff R, Chouinard L, Goodman D, Kuttler K, Marxfeld H, et al.: Proliferative and nonproliferative lesions of the rat and mouse mammary, Zymbal's, preputial, and clitoral glands. *Toxicol Pathol* 2012;40(6 Suppl):7S-39S.

6. Seely JC: Auditory Sebaceous Glands (Zymbal's Glands). In: Mohr U, Dungworth DL, Capen CC, eds. *Pathobiology of the Aging Rat*. Washington, D.C.: ILSI Press; 1994: 423-433.

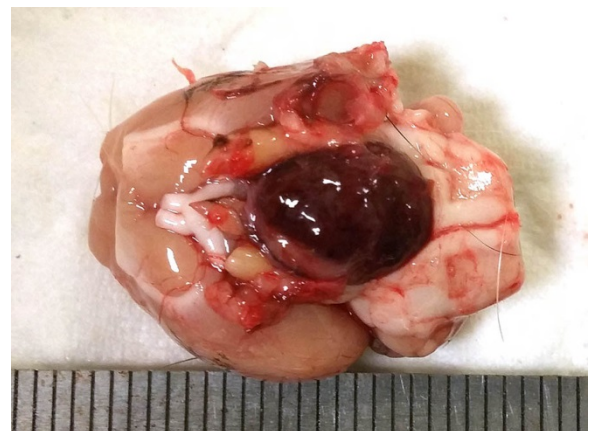
7. Sundberg JP, Nanney LB, Fleckman P, and King LE: Skin and Adnexa. In: Treuting PM and Dintzis SM, eds. *Comparative Anatomy and Histology: A mouse and human atlas*. San Diego, CA: Academic Press; 2012: 433-453.

CASE IV: EX 109 (JPC 4069626).

Signalment: An 18-month-old, female, Long-Evans rat (*Rattus norvegicus*).

History: The investigator noticed a large, firm, subcutaneous mass in the right axilla.

Gross Pathology: At necropsy, a firm, circumscribed and lobulated subcutaneous mass approximately 3.5 cm in diameter, was attached to the skin in the axillary area. On removing the brain, a dark red-brown nodular mass, approximately 1 cm in



Hypophysis, rat. A dark red-brown nodular mass, approximately 1 cm in diameter, replaces the pituitary gland. (Photo courtesy of: Department of Veterinary Resources, Weizmann Institute, Rehovot 76100, Israel, <http://www.weizmann.ac.il/vet/>)

diameter, was present in the ventral aspect of the brain, replacing the pituitary gland.

Laboratory Results: None

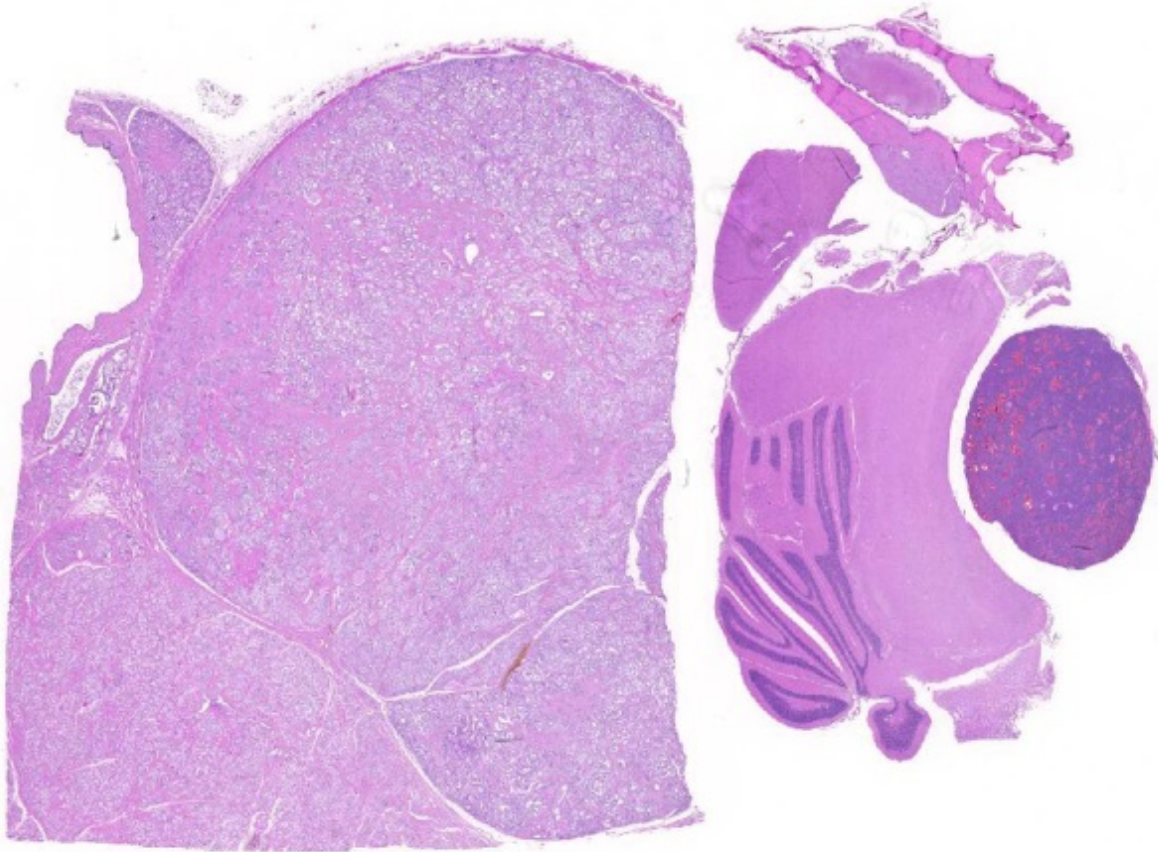
Histopathologic Description:

Axillary mass - Part of a multilobular mass composed of disorganized epithelial proliferation and connective tissue. The neoplastic epithelium forms variably sized acini and tubuli which are aggregated into lobules dissected and separated by moderate to abundant dense, collagen-rich, connective tissue. The neoplastic cells are cuboidal to irregular and arranged as a monolayer; they have moderate to abundant cytoplasm which is often vacuolated. Vacuoles vary from

numerous and small (microvesicular vacuolation) to large, single, lipid vacuoles which lead to significant expansion of the cytoplasm and peripheral displacement of the nucleus. Nuclei are round to slightly irregular, vesicular to finely granular, and have a small nucleolus. There is slight anisocytosis and anisokaryosis. Mitotic figures are not observed. Multifocally, the lumen of acini contains proteinaceous secretory material, which in some cases shows internal layers (corpora amylacea). In other parts of the mass, not submitted, there are large cysts filled with secretory material and lined by epithelial cells as described.



Mammary gland, rat. A firm, circumscribed and lobulated subcutaneous mass approximately 3.5 cm in diameter, was attached to the skin in the axillary area (Photo courtesy of: Department of Veterinary Resources, Weizmann Institute, Rehovot 76100, Israel, <http://www.weizmann.ac.il/vet/>)



Tissues from a rat. Subgross examination of submitted tissues reveals a large multilobular neoplasm replacing the mammary gland (left), and a large neoplasm replacing the pituitary gland (right) (HE, 6X)

Pituitary mass- Compressing the medulla there is a small, discrete, thinly encapsulated and densely cellular nodular mass composed of a uniform population of polygonal cells arranged into solid islands separated by fine fibrovascular stroma. The neoplastic cells have a moderate amount of eosinophilic to lightly amphophilic cytoplasm, relatively indistinct cytoplasmic margins, and round to slightly irregular, vesicular to finely granular nuclei with a small nucleolus. There is anisocytosis and anisokaryosis. A few mitotic figures are observed. At the edge of the mass there are scattered giant karyomegalic cells. There are numerous large, blood-filled spaces lined by neoplastic pituitary cells. At one edge of the mass there are possible remnants of the pre-existing adeno-hypophysis.

Contributor's Morphologic Diagnosis:

Axillary mass: Mammary gland fibroadenoma

Pituitary gland (adenohypophysis): Adenoma

Contributor's Comment: Mammary fibroadenoma: Mammary tumors are one of the most common tumors in old female rats,¹ especially in the SD strain where the incidence of spontaneous tumors often approaches 50% in lifetime studies of control animals.⁴ Most are benign fibroadenoma which are composed of mammary epithelial cells and connective tissue.⁴ The incidence of these tumors varies considerably between different rat strains,

suggesting that genetic background is an important factor in their development. Other factors which influence their occurrence are diet, environment, and in the case of toxicologic studies, the degree of differentiation of the mammary glands, and physiologic and hormonal status at the time of chemical exposure.⁴ Mammary tumors are rare before 1 year of age, and are generally found after 18 months of age.¹ Mammary fibroadenomas also occur occasionally in male rats.⁵

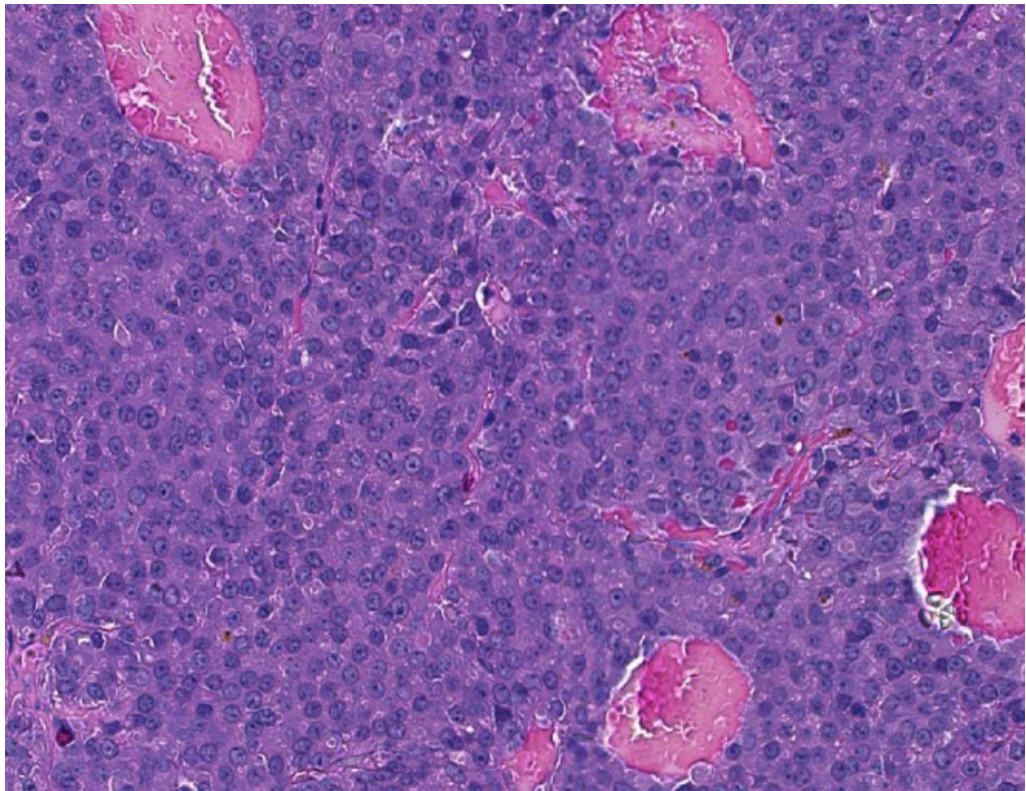
Histologically, the proportion of glandular and connective tissue in fibroadenomas is variable, and this has led to their sub-classification. However, since several subtypes are commonly encountered in a single tumor, this division appears to be of little merit.^{1, 4} Exposure to estrogen and prolonged exposure to prolactin increase tumor frequency, whereas parity and ovariectomy decrease the incidence of mammary gland tumors in rats.^{1,5}

Although increased mammary gland tumors are found in rats with pituitary tumors and high levels of prolactin are considered a contributing factor, a casual effect is difficult to determine.^{1,5} Estrogens induce both pituitary and mammary tumors, and the incidence of both

types of tumors correlates with body weight.¹

Mammary fibroadenomas may become very large, but as a rule, they are only locally infiltrative and rarely metastasize. Surgical excision is possible in pet rats or experimentally valuable animals.⁵ Spontaneous mammary adenocarcinomas are most common in SD rats and uncommon in other strains. They may develop in existing fibroadenoma, but this is rare. They generally do not metastasize.¹

Pituitary adenoma is very common in older rats, especially of the Wistar strain. There is conflicting information in standard references regarding their incidence in other strains: according to Boorman and Everitt¹ they are common in F344 and uncommon in SD, while according to Percy and Barthold⁵ they are common in the SD strain. Some



Pituitary gland, rat. Neoplastic cells are arranged in nests and packets on a fine fibrovascular stroma and there numerous blood-filled spaces throughout the mass. Nuclei exhibit mild anisokaryosis and a low mitotic rate. (HE, 220X)

studies suggest a slightly higher incidence in females. Other than age, genetic background, diet, and breeding history are thought to play a role in tumor development. Reduction of food intake reduces their incidence and, according to one study, mated females are less prone to these tumors than virgin females.⁵ Clinical signs vary from asymptomatic to severe depression, often with incoordination.⁵ The neurologic signs are due to compression of the brain.

Histologically, the hallmark of adenoma is compression of the surrounding parenchyma and sharp delineation at the margins of the nodule. The neoplastic cells are generally larger than normal and have more abundant cytoplasm, which is usually pale or faintly basophilic. The mitotic index is usually low. Often, there are prominently dilated vascular channels which may be lined by endothelial cells or neoplastic pituitary cells; this has been referred to as angiomatous or cavernous pattern. Giant cells and areas of necrosis may be present.³

Most pituitary tumors are thought to arise from the pars distalis and are diagnosed as chromophobe adenomas based on HE-stained sections.^{1,5} Acidophil and basophil tumors have also been described. The diagnosis of chromophobe adenoma provides no information regarding the endocrine status of the tumor.¹ In pituitary tumors studied by immunocytochemistry, prolactin-producing tumors are the most common type,⁵ but growth hormone, ACTH, TSH and FSH-secreting tumors have also been described.¹ Lactation in an aging rat is often a sign of a functional pituitary tumor.¹

Pituitary adenomas should be differentiated from hyperplastic and hypertrophic lesions. In hyperplastic lesions there is proliferation of cells of normal size, no evidence of pseudocapsule formation, and no significant compression of adjacent pituitary tissue.

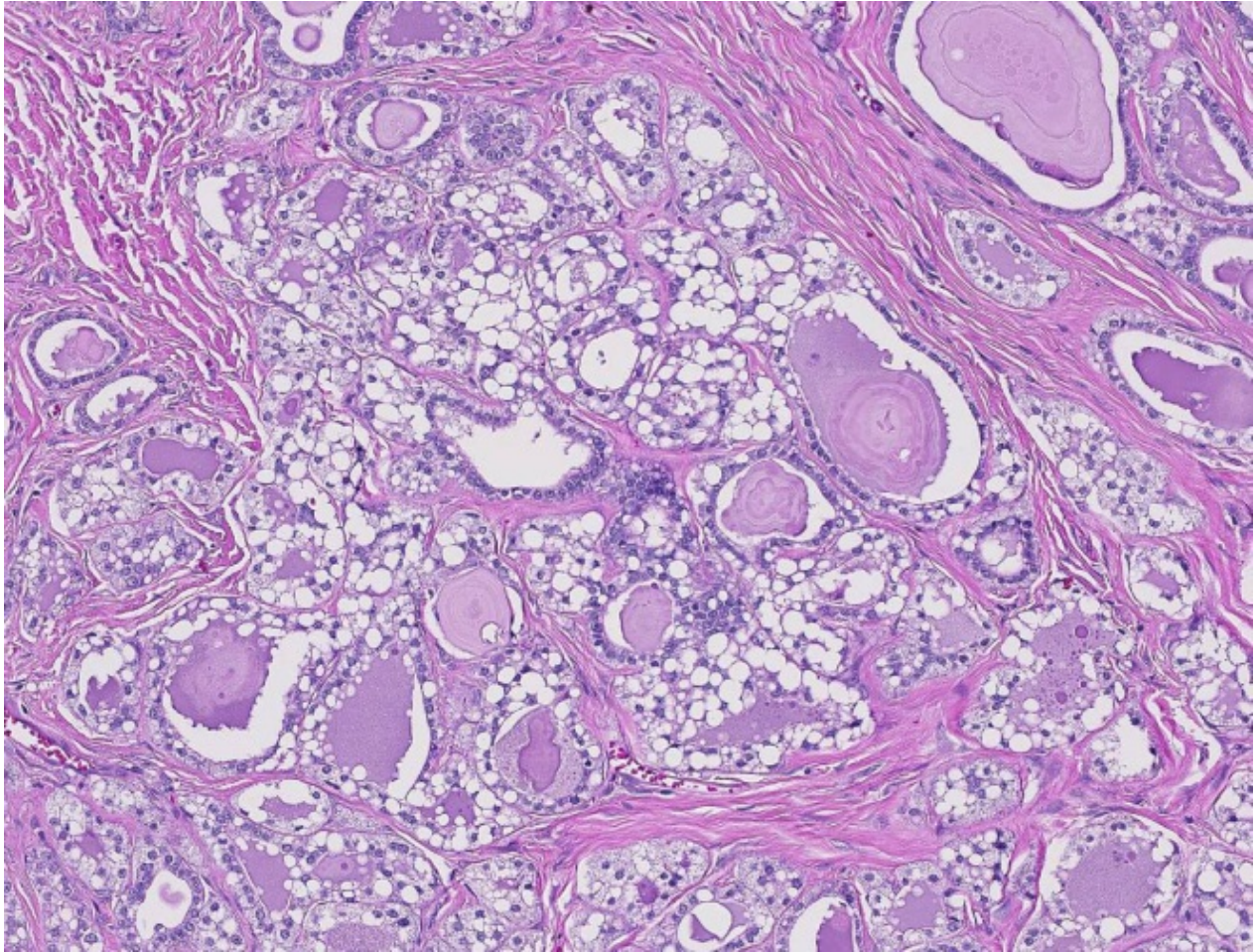
Nodules of hypertrophic cells form islands of large cells without evidence of encapsulation.^{1,3} Pituitary carcinomas are rare and require evidence of invasion or distant metastasis for their diagnosis.

JPC Diagnoses: 1. Pituitary gland: Pituitary pars distalis adenoma.

2. Mammary gland: Mammary fibroadenoma.

Conference Comment: Mammary gland fibroadenoma is one of the most common rat mammary tumors. It is more commonly seen in female rats and has an especially high incidence in Sprague Dawley rats as mentioned above. It is generally well defined and composed of proliferating glandular tissue surrounded by a proliferation of fibrous tissue. Large sections or an entire mammary gland may be involved. It may have a lobular growth pattern with variation in size and composition of individual lobules. Secretory epithelium is arranged in a single layer, and small foci of pleomorphic cells may be present, but mitoses are uncommon. It is differentiated from adenoma by the conspicuous contribution of a fibrous connective tissue component. Adenocarcinoma may arise from within mammary fibroadenoma.⁶ Other less common mammary neoplasms in the rat include ductular carcinoma and cystadenoma.

Another lesion which must be differentiated from benign mammary neoplasia is lobuloalveolar hyperplasia. This condition may be referred to as pseudopregnancy, and is differentiated from neoplasia by maintaining the normal lobular histologic architecture, specifically the relationships among the various mammary tissue components including ducts, glandular epithelium, stroma, and myoepithelium. Cellular pleomorphism is absent; however, focal squamous met-



Mammary gland, rat. Neoplastic cells are arranged in well-defined acini which are filled with variable amounts of purple secretory product. The secretory product is occasionally lamellated (corpora amylacea). Neoplastic cells are columnar with large cytoplasmic vacuoles; accumulation of secretory product within the lumen results in a cuboidal to attenuated morphology of neoplastic cells in many glands. (HE, 123X)

aplasia can occur and hyperplastic lesions may be focal or diffuse.⁶ Diffuse mammary hyperplasia is associated with hormonally-induced physiologic changes during late gestation and lactation. Focal hyperplasia may be accompanied by fibrous proliferation separating acini, but the lobular architecture is maintained and the lesion is not compressive, which aids in differentiating it from mammary fibroadenoma.⁶

Dietary food restriction is known to decrease the incidence of both pituitary and mammary tumors in rats. Lower levels of prolactin are present in rats on a restricted

diet, and prolactin is a primary stimulus for the development of mammary neoplasia in rats. Most rat pituitary neoplasms are prolactin-immunopositive and are postulated to be involved in the development of mammary tumors,² although a definitive link has not been demonstrated in all cases. Furthermore, not all rat pituitary tumors are prolactin positive. Interestingly, reduction in body weight from decreased caloric intake is paradoxically associated with an increase in uterine neoplasia in rats; this effect is postulated to be related to prolactin's influence on function of the ovary and corpora lutea. In the rat prolactin promotes progesterone production in the

corpus luteum post ovulation, which opposes estrogen's promotion of uterine growth. Therefore, a decrease in prolactin results in elevated levels of estrogen, which stimulates endometrial growth.² Long term administration of estrogen to rats also results in prolactin producing pituitary adenomas. These induced tumors may also produce other hormones, such as thyroid stimulating hormone.⁷

Contributing Institution:

Department of Veterinary Resources,
Weizmann Institute,
Rehovot 76100, Israel
<http://www.weizmann.ac.il/vet/>

References:

1. Boorman GA, Everitt JI. Neoplastic disease. In: Suckow MA, Weisbroth SH, Franklin CL, eds. *The Laboratory Rat*. 2nd ed. Elsevier Academic Press; 2006:493-4, 501-2.
2. Harleman JH, Hargreaves A, Andersson H, Kirk S. A review of the incidence and coincidence of uterine and mammary tumors in Wistar and Sprague-Dawley rats based on the RITA database and the role of prolactin. *Toxicol Pathol*. 2012; 40: 926-930.
3. Majka JA, Sollveled HA, Barthel CH, Van Zwiten MJ. Proliferative lesions of the pituitary in rats, E-2. In: *Guides for Toxicological Pathology*. Washington DC: STP/ARP/AFIP; 1990.
4. Mann PC, Boorman GA, Lolloi LO, McMartin DN, Goodman DG. Proliferative lesions of the mammary gland in rats IS-2. In: *Guides for Toxicological pathology*. Washington DC: STP/ARP/AFIP; 1996.
5. Percy DH, Barthold SW. Pathology of laboratory rodents. 3rd ed. Ames IA:Blackwell Publishing; 2007:171-174.
6. Rudmann D, Cardiff R, Chouinard L, Goodman D, Kuttler K, Marxfeld H, et al.: Proliferative and nonproliferative lesions of the rat and mouse mammary, Zymbal's, preputial, and clitoral glands. *Toxicol Pathol* 2012;40(6 Suppl):7S-39S.
7. Takekoshi S, Yasui Y, Inomoto C, Kitatani K. A histopathological study of multi-hormone producing proliferative lesions in estrogen-induced rat pituitary prolactinoma. *Acta Histochem Cytochem*. 2014; 47(4):155-164.

Joint Pathology Center
Veterinary Pathology Services



WEDNESDAY SLIDE CONFERENCE 2015-2016

Conference 23

7 May 2016

CASE I: G10-083313 (JPC 4003029).

Signalment:

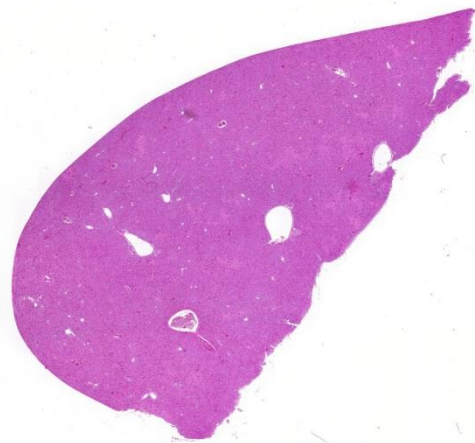
Flock of 20,000 11-week-old commercial meat turkeys, *Meleagris gallopavo*.

History: Flock experienced a spike in mortality. Flock is housed in barn and bedded with a layer of shavings on top of dirt floors. This is the first time this disease has been identified on this farm but the producer does have a second farm where turkeys are also raised and this disease has been a recurring problem on that farm.

Gross Pathology: The submitting veterinarian described swollen livers with yellow streaking and very enlarged dark spleens in the turkeys that were necropsied. Birds also had unclotted blood in the abdominal cavity.

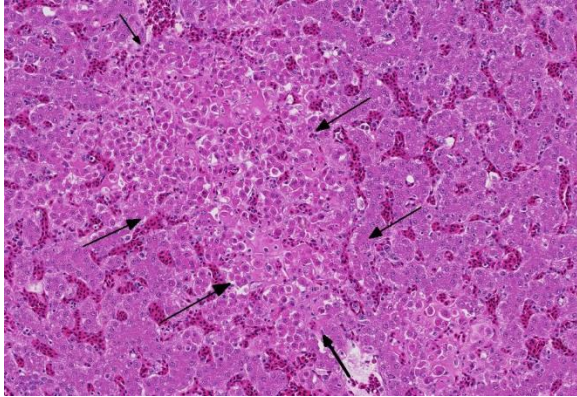
Laboratory Results: 4+ *Erysipelothrix rhusiopathiae* was recovered from a swab of the internal organs.

Histopathologic Description:



Liver, turkey. At subgross magnification, there are randomly scattered areas of pallor. (HE, 5X)

The liver is moderately congested. Multiple variably-sized foci of hepatic necrosis, characterized by individualized, hypereosinophilic hepatocytes with granular or shrunken, hyalinized cytoplasm and either lacking nuclei or containing pyknotic or karyorrhectic nuclei, are closely associated with terminal hepatic veins. Hepatocytes surrounding these necrotic foci are occasionally swollen with pale vacuolated cytoplasm. Multifocally, veins and sinusoids and less frequently small arteries contain



Liver, turkey. Areas of pallor correspond to areas of necrosis (arrows) within which hepatocellular plate architecture is lost and necrotic hepatocytes are rounded up and brightly eosinophilic. (HE, 124X).

fibrin thrombi bearing mats of slender rod-shaped and sometimes gently curved bacteria. Similar appearing bacteria are also free in sinusoids and within activated Kupffer cells, which also contain phagocytized debris including red blood cells. Occasionally the walls of veins and small arteries containing fibrin thrombi have segmental necrosis, with some affected arteries having intramural heterophils and rarely small amounts of nuclear debris.

Contributor's Morphologic Diagnosis:

Liver: Mild, acute, multifocal, hepatic necrosis with necrotizing vasculitis and intravascular fibrin thrombi containing colonies of pleomorphic rod-shaped bacteria.

Liver: Moderate hepatic congestion

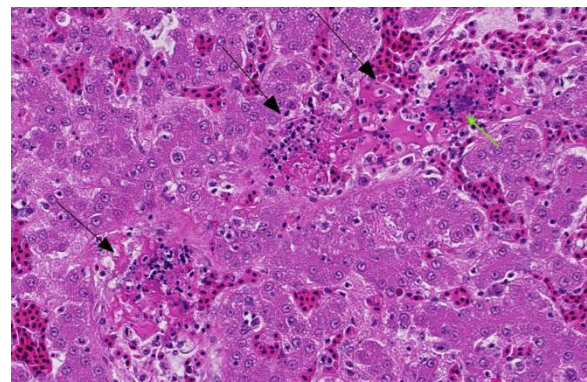
Contributor's Comment: Erysipelas is an acute septicemic disease occurring most commonly in older male turkeys. The differential diagnosis includes other gram-negative bacterial septicemias caused by agents such as *E. coli*, *Salmonella* spp. or *Pasteurella multocida*.² Histologically, the pathology of an *Erysipelothrix rhusiopathiae* infection is different from most

gram-positive agents, first because of the sheer numbers of bacteria present and secondly because of their variable appearance, with slender rod-shaped to slightly curved bacteria aggregating in mats within vessel and capillary lumens and entangled in fibrinous thrombi. Because these bacteria are slow growing, a rapid presumptive diagnosis can also be made by identification of clumps of gram-positive slender straight or slightly curved rod-shaped bacteria from organ or bone marrow smears.²

This case was submitted to the lab in early October which is typical for cases of erysipelas, as outbreaks are reported to occur most often in the late fall or winter. It is thought that the bacteria can persist in the soil and since many grow-out barns for turkeys have dirt floors, the risk of repeat occurrences exists.² In this case, this farm has never experienced an outbreak of erysipelas but the other farm has and it is suspected that there was mechanical transfer of the bacterium from one farm to another.

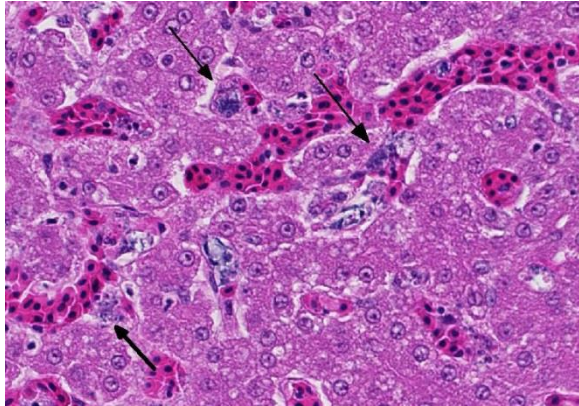
Penicillin is the antibiotic of choice for treating erysipelas. Vaccination using a killed bacterin is an option if the risk of infection is high.²

In humans, the infection caused by *Erysipelothrix rhusiopathiae* is known as



Liver, turkey. Septic thrombi (green arrow) are associated with vasculitis (black arrows) throughout the section. (HE, 150X)

erysipeloid, a skin infection typically localized to fingers and hands and usually preceded by an abrasion or cut. The lesion is actually a cellulitis and is very painful. Systemic effects, such as septicemia and endocarditis can occur but are uncommon.⁶ Most cases of human infection are the result



Liver, turkey. Kupffer cells contain ingested bacilli (arrows). (He, 260X)

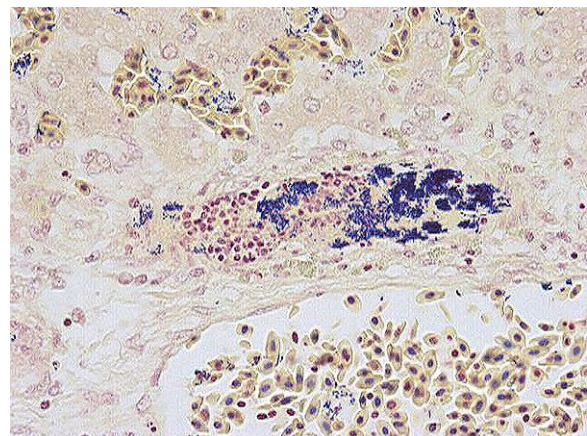
of occupational exposure and those occupations at higher risk include fish handlers, veterinarians, farmers, slaughter plant workers and butchers. Some colloquial names for this condition include fish handler's disease, seal finger and whale finger.

JPC Diagnosis: Liver: Hepatitis, necrotizing, acute, multifocal, random, with septic fibrin thrombi and vasculitis.

Conference Comment: In addition to outbreaks in domestic turkeys, *E. rhusiopathiae* outbreaks have also been reported in laying hens in Europe,³ and sporadically in a variety of other captive and free-ranging birds. The organism is fastidious and able to survive in the environment for extended periods. It may be transmitted by cuts and abrasions or through ingestion. It is generally considered to follow an acute course characterized by septicemia, but a chronic form also occurs in turkeys,¹ which appear to be most

susceptible to infection. In addition to thromboembolism, bacterial endocarditis and joint infections¹ may be seen in affected turkeys, among other signs of septicemia. Thrombosis and hemorrhage are commonly reported in avian species infected with *E. rhusiopathiae*, reflecting the vasculocentric nature of the disease. Grossly, carcasses of affected birds are in good flesh and exhibit organomegaly of the liver, spleen and kidneys, as well as ecchymotic hemorrhages in the subcutis and muscles.¹ Routes of infection include fomites, contaminated soil, insect vectors, asymptomatic carrier animals and contaminated feed.^{3,4}

Although it has been reported, infection in psittacine birds is considered rare. In a case report of infection in a mixed species aviary, lesions included thrombosis, bacterial thromboembolism, necrotizing hepatitis, necrohemorrhagic myocarditis, and hemorrhage.⁴ *E. rhusiopathiae* infection has also been reported in emus, which are large flightless birds that are grouped with other ratites such as ostriches and rheas. Lesions similar to those reported in other species are also seen in emus, including hepatocellular necrosis with absence of an abrupt

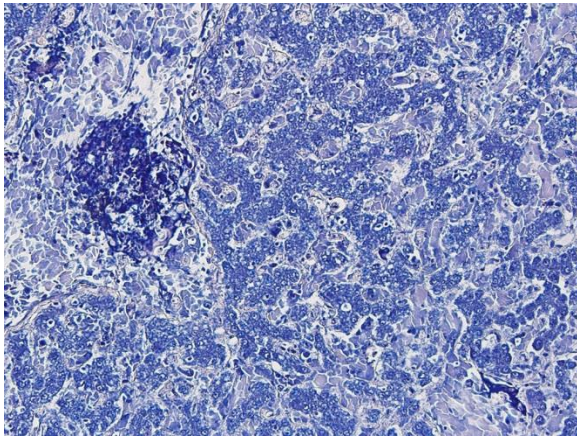


Liver, turkey. Gram-positive bacilli are present within septic thrombi. (Photo courtesy of: Animal Health Laboratory, University of Guelph, Guelph, Ontario, Canada, <http://ahl.uoguelph.ca>)

inflammatory response. Bacteria may be observed in multiple organs, including the kidneys and small intestine as well as the liver; the presence of fibrin thrombi, while prominent in many cases, may be variable.⁵

Contributing Institution:

Animal Health Laboratory, University of Guelph,
Guelph, Ontario, Canada
<http://ahl.uoguelph.ca>



Liver, turkey: A phosphotungstic acid hematoxylin (PTAH) stain demonstrates fibrin thrombi within vessels (left arrow) and within hepatic sinusoids (right arrow). (PTAH, 200X)

References:

1. Bobrek K, Gawel A, Mazurkiewicz M. Infections with *Erysipelothrix rhusiopathiae* in poultry flocks. *World's Poultry Science Journal*. 2013; 69(4):803-812.
2. Bricker JM, Saif YM. Erysipelas. In: Saif YM, ed. *Diseases of Poultry*. 12th ed. Ames, IA: Blackwell Publishing; 2008:909-922.
3. Eriksson H, Bagge E, Båverud V, Fellstrom C, et al. *Erysipelothrox rhusiopathiae* contamination in the poultry house environment during erysipelas outbreaks in organic laying hen flocks. *Avian Pathol*. 2014; 43(3):231-237.

4. Galindo-Cardiel I, Opriessnig T, Molina L, Juan-Salles C. Outbreak of mortality in psittacine birds in a mixed-species aviary associated with *Erysipelothrix rhusiopathiae* infection. *Vet Pathol*. 2012; 49(3):498-502.

5. Morgan MJ, Britt JO, Cockrill JM, Eiten ML. *Erysipelothrix rhusiopathiae* infection in an emu (*Dromaius novaehollandiae*). *J Vet Diagn Invest*. 1994; 6:378-379.

6. Reboli, A, Farrar WE. *Erysipelothrix rhusiopathiae*: An occupational pathogen. *Clin Microbiol Rev*. 1989; 2:354-359.

CASE II: UFMG-2 (JPC 4035761).

Signalment:

Male, Coimbra's titi (*Callicebus coimbrai*)

History: This monkey was kept at the zoological park in Belo Horizonte, Brazil. It was found on the floor in a cage, prostrated and hypothermic. It received emergency therapy with fluids, corticosteroids, glucose, and heating, but died soon after the initial treatment.

Gross Pathology: Grossly, the mesenteric lymph nodes were hemorrhagic, the colon was dilated with multifocal and moderate hemorrhage in the serosa. The colon content was hemorrhagic with a few blood clots, and large amounts of fibrinous exudate. There was sand in the oral cavity, esophagus, and stomach. The heart was mildly dilated. On the surface and cut surfaces of the liver, there was a prominent lobular pattern. Kidneys and adrenal glands were moderately congested.

Laboratory Results: None.

Histopathologic Description: Multifocal to coalescing and severe necrosis associated to



Colon, titi monkey. Colonic contents were hemorrhagic, with clumps of fibrin. (Photo courtesy of: Universidad Federale de Mias Gerais. Avenida Antonio Carlos, 6627. PO Box. 567. Setor de Patologia. Departamento de Clinica e Cirurgia Veterinarias. Escola de Veterinaria. Belo Horizonte, Minas Gerais. Brazil. 31270-901.)

multifocal and moderate hemorrhage was observed in the mucosa of the colon. Myriads of round, 30-50 μm diameter, eosinophilic staining trophozoites were diffusely distributed in the lumen, necrotic mucosa, crypts, and lamina propria of the colon. There was a multifocal and mild inflammatory infiltrate composed of lymphocytes, histiocytes and neutrophils in mucosa and submucosa. Some epithelial cells of the colonic crypts had numerous circular, intensely basophilic cytoplasmic structures, which were interpreted as apoptotic bodies.

Contributor's Morphologic Diagnosis:

Large intestine, colon: Colitis, necrotizing, hemorrhagic, acute, multifocal to coalescing, severe with numerous protozoal organisms consistent with *Entamoeba histolytica*.

Contributor's Comment: *Entamoeba*

histolytica is a protozoan parasite capable of invading the intestinal mucosa. It affects other organs, mainly the liver, causing

amebiasis.⁷ *Entamoeba dispar* is morphologically similar. It also colonizes the human gut, however it has no invasive potential.¹ Both species are found of non-human primates, such as monkeys, orangutans, and baboons.⁵

Most asymptomatic infections found worldwide are now attributed to *Entamoeba dispar*, because it is non-invasive. *E. dispar* is distinct but closely related to *E. histolytica*. This non-invasive species has im-

plications for understanding the epidemiology of amebiasis.³

In humans, amebiasis is more common in developing countries. Bad conditions such as overcrowding, poor education, contaminated water, and poor sanitation favor fecal-oral transmission of amoebas. This disease results in 70 thousand deaths annually. Amebiasis is considered the fourth cause of death due to protozoa.¹¹ A recent study revealed a high prevalence of *E. histolytica* in long-tailed macaques in the Philippines.⁸ Captive monkeys infected with *E. histolytica* is a concern not only for the animal health risk, but also due to the zoonotic nature of the disease.⁴

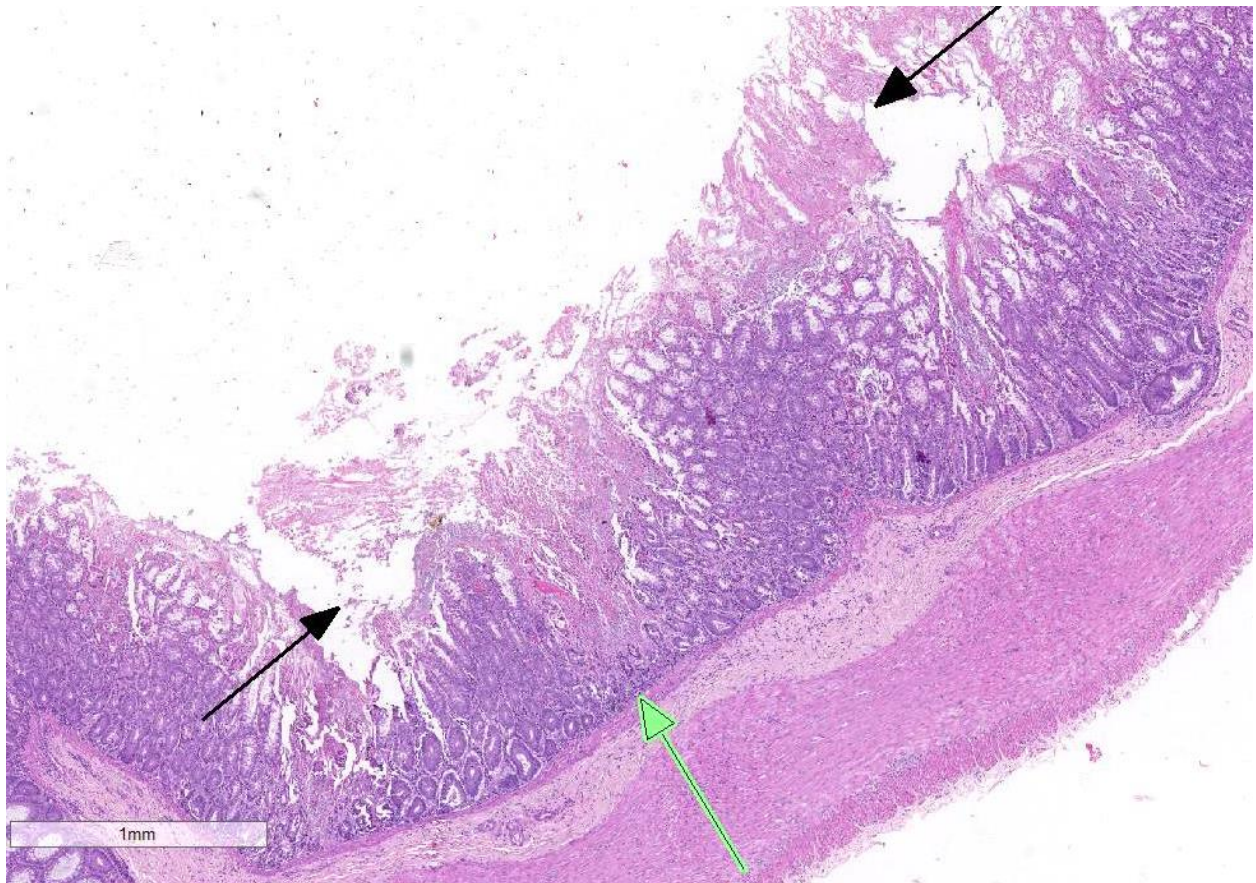
The trophozoite, which is the motile form of *E. histolytica*, lives in lumen of crypts in large intestine, where it multiplies and differentiates into cyst (resistant form responsible for transmission). Cysts are excreted in stools, and may be ingested by a new host through contaminated food or water. Upon ingestion of infective cysts, parasites are released in terminal ileum, with each emerging quadrinucleate trophozoite giving rise to eight uninucleated trophozoites. Trophozoites may invade the colonic mucosa and cause dysentery.³

There are some molecules produced by *E. histolytica* that are related to lysis of the colonic mucosa: adhesins, amoebapores, and proteases. The parasite attachment to colonic mucus blanket is due to a multifunctional adherent lectin, preventing elimination in intestinal stream. Lectins are involved in signaling cytolysis and in blocking the deposition of the injurious membrane attack complex of complement. It may also participate in anchorage of the amoeba to

extracellular matrix during invasion and contribute in the lysis of target cells.³

JPC Diagnosis: Colon: Colitis, necrotizing, acute, multifocally extensive, marked with crypt abscesses, goblet cell loss and numerous amoebic trophozoites.

Conference Comment: *E. histolytica* colonizes the large intestine resulting in



Colon, titi monkey. The proximal 33% of the mucosa of the colon exhibits coagulative necrosis (black arrows), with occasional full thickness necrotic areas perpendicular to the mucosal surface (green arrow). (HE, 18X)

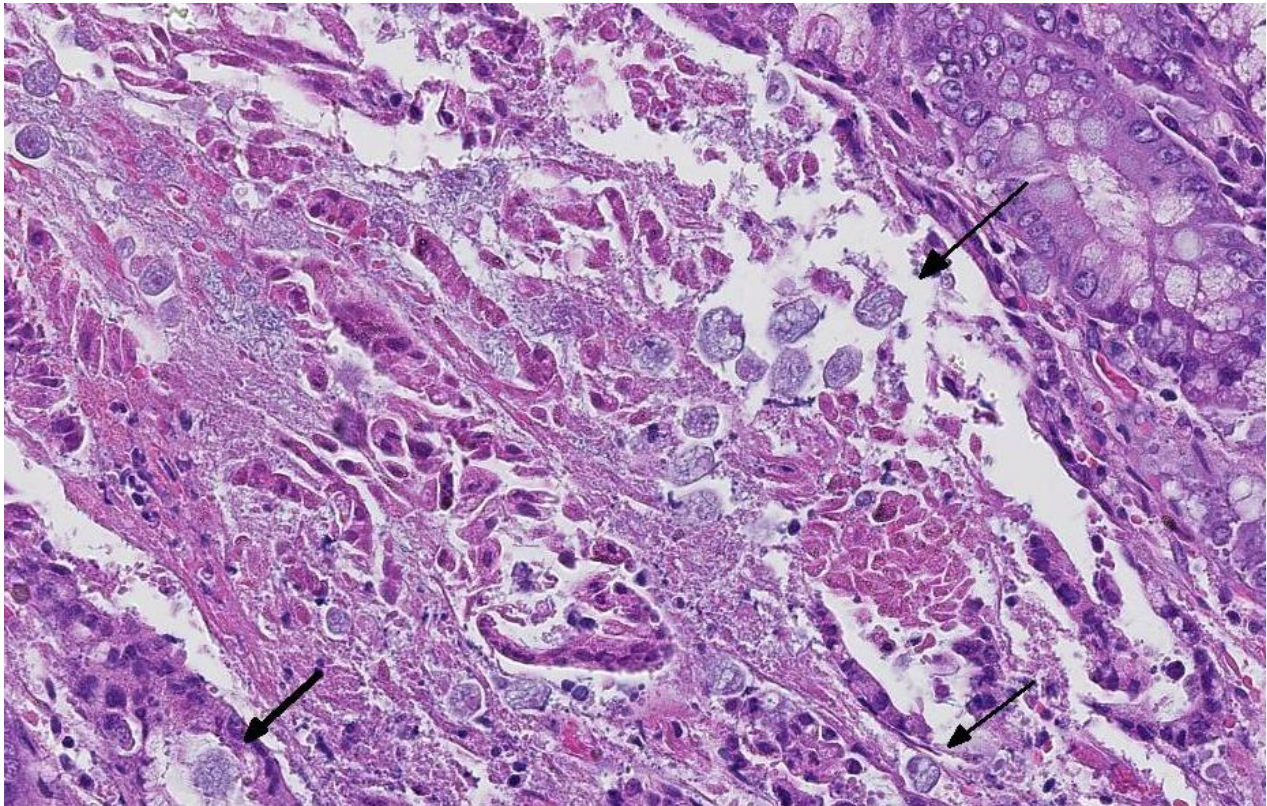
proteoglycans, during invasion process.³ Peptides of *E. histolytica* named amoebapores destroy phagocytosed bacteria from the microbiota that serve as the main nutrient source for the parasite. Whether amoebapores play a role in the cytolytic event has not yet been proven. Proteases produced by the parasite can degrade the

colitis and diarrhea, and in some cases, may result in liver abscesses. *E. histolytica* has two morphogenetic forms: the trophozoite and infectious cyst form. Ingestion of viable cysts initiates infection and subsequent steps are discussed above. The initial attachment to mucosal enterocytes by trophozoites, mediated through adhesins and lectins,

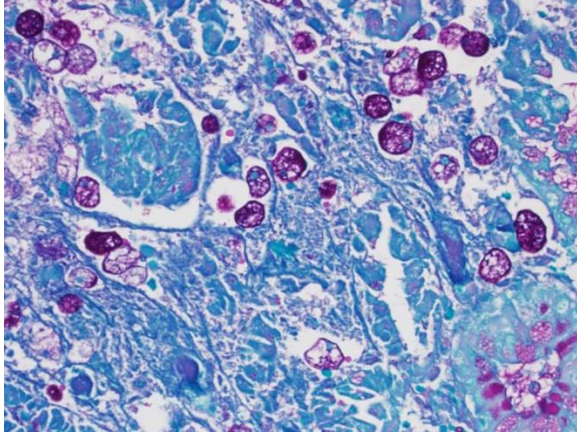
appears to be important in the initial pathogenesis and apparently plays a role in cytotoxic activity.⁶ The host inflammatory response contributes to tissue damage and may help facilitate infection. Important cytokines involved in the host response include IL-8, IL-6 and IL-1 α ; genes involved in cell proliferation also participate in the response to infection. *E. histolytica* destroys host tissue and commonly causes enterocyte apoptosis; trophozoites may ingest host cells following their death. The mechanisms leading to host cell apoptosis are not completely understood, but may involve production of reactive oxygen species and oxidative stress. Other mechanisms which may be involved in cell death include amoebic trophocytosis, where the parasite ingests fragments of host cell, resulting in increases in intracellular calcium and cell death.² Other parasite factors which

are involved in the pathogenesis include production of prostaglandin E₂, which increases sodium ion permeability through tight junctions, as well as secretion of cysteine proteases which digest matrix components such as gelatin, collagen type I and fibronectin. Epithelial barrier disruption also plays an important role in infection.²

E. histolytica trophozoites normally remain in the colonic lumen. However, in some cases, the trophozoites invade the mucosa as well as mural blood vessels and lymphatics, and eventually infect the liver. Ulcerative gastritis secondary to *E. histolytica* infection has also been described in primates that have a sacculated stomach, which is adapted for leaf eating and fermentation. Similarly, *E. histolytica*-associated gastritis may also occur in macropods (kangaroos and wallabies), which likewise have a sacculated



Colon, titi monkey. Necrotic areas within the mucosa contain numerous 15-20 μ m amoebic trophozoites. (HE, 324X)



Colon, titi monkey. Amebic trophozoites stain intensely with periodic-acid Schiff stains (an excellent choice for amebae.) (PAS/Alcian blue counterstain, 400X)

stomach.⁹ Trophozoites are observed in the mucosa and gastric glands, but may also invade to the level of the submucosa, including vessels and lymphatics.⁹

E. histolytica may also cause necrotizing and ulcerative colitis in dogs and cats (likely acquired from a human source) although less commonly than in primates. In cats, *E. histolytica* infection has been associated with severe necrosis of the colon and cecum.^{9,10} It is apparently uncommon for infected dogs to shed infectious cysts.

Contributing Institution:

Setor de Patologia. Departamento de Clínica e Cirurgia Veterinárias.
Escola de Veterinária.
Universidade Federal de Minas Gerais.
Belo Horizonte, Minas Gerais.
Brazil

References:

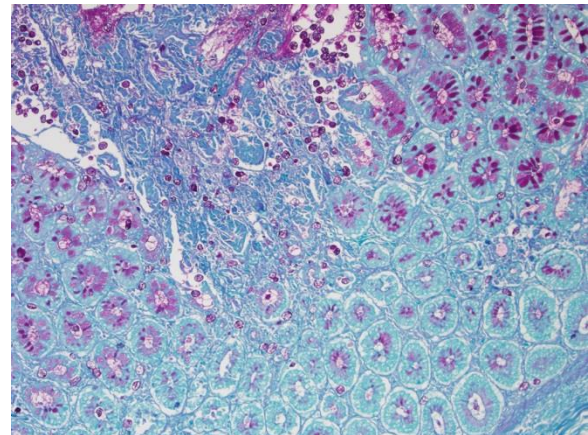
1. Diamond LS, Clark CG. A redescription of *Entamoeba histolytica* Schaudinn, 1903 (emended Walker, 1911) separating it from *Entamoeba dispar* Brumpt, 1925. *J Eukaryot Microbiol.* 1993; 40: 340–344.

2. Di Genova BM, Tonelli RR. Infection strategies of intestinal parasite pathogens and host cell responses. *Front Microbiol.* 2016; 7:256. doi: 10.3389/fmicb.

3. Espinosa-Cantellano M, Martínez-Palomo A. Pathogenesis of Intestinal Amebiasis: From molecules to disease. *Clin Microbiol Rev.* 2000; 13(2):318.

4. Feng M, Cai J, Min X, Yongfeng F, Xu Q, Tachibana H, Cheng X. Prevalence and genetic diversity of *Entamoeba* species infecting macaques in southwest China. *Parasitol Res.* 2013; 112:1529–1536.

5. Feng M, Yang B, Yang L, Fu YF, Zhuang YJ, Liang LG, Xu Q, Cheng XJ, Tachibana H. High prevalence of *Entamoeba*-infections in captive long-tailed macaques in China. *Parasitol Res.* 2011; 109:1093–1097.



Colon, titi monkey. The infiltration of amebic trophozoites into the mucosa causes a downregulation of mucin production by nearby goblet cells. (PAS/Alcian blue counterstain, 100X)

6. García MA, Gutiérrez-Kobeh L, López Vancell R. *Entamoeba histolytica*: Adhesins and Lectins in the trophozoite surface. *Molecules.* 2015; 20:2802-2815.

7. Martínez-Palomo A, Espinosa-Cantellano M. Amoebiasis: new understanding and new goals. *Parasitol Today.* 1997; 14:1–3.

8. Rivera WL, Yason JA, Adao DE. *Entamoeba histolytica* and *E. dispar* infections in captive macaques (*Macaca fascicularis*) in the Philippines. *Primates*. 2010; 51:69–74.
9. Stedman NL, Munday JS, Esbeck R, Visvesvara GS. Gastric amebiasis due to *Entamoeba histolytica* in a Dama Wallaby (*Macropus eugenii*). *Vet Pathol*. 2003;40:340-342.
10. Uzal FA, Plattner BL, Hostetter JM. Alimentary system. In: Maxie MG, ed. *Jubb, Kennedy, and Palmer's Pathology of Domestic Animals*. 6th ed. Vol 2. St. Louis, MO: Elsevier; 2016:98-99.
11. World Health Organization. 1998. The World Health Report 1998. Life in the 21st century: a vision for all. World Health Organization: Geneva, Switzerland.

Figures

Figure 1. Colon, *Callicebus Coimbrai*: hemorrhagic content.

Figure 2. Colon, *Callicebus Coimbrai*: severe necrosis associated to eosinophilic staining trophozoites consistent with *Entamoeba histolytica* (HE 200X).

Figure 3. Colon, *Callicebus Coimbrai*: myriads of round, 30-50 μm diameter, eosinophilic staining trophozoites consistent with *Entamoeba histolytica* in crypts and the lamina propria (HE 400X).

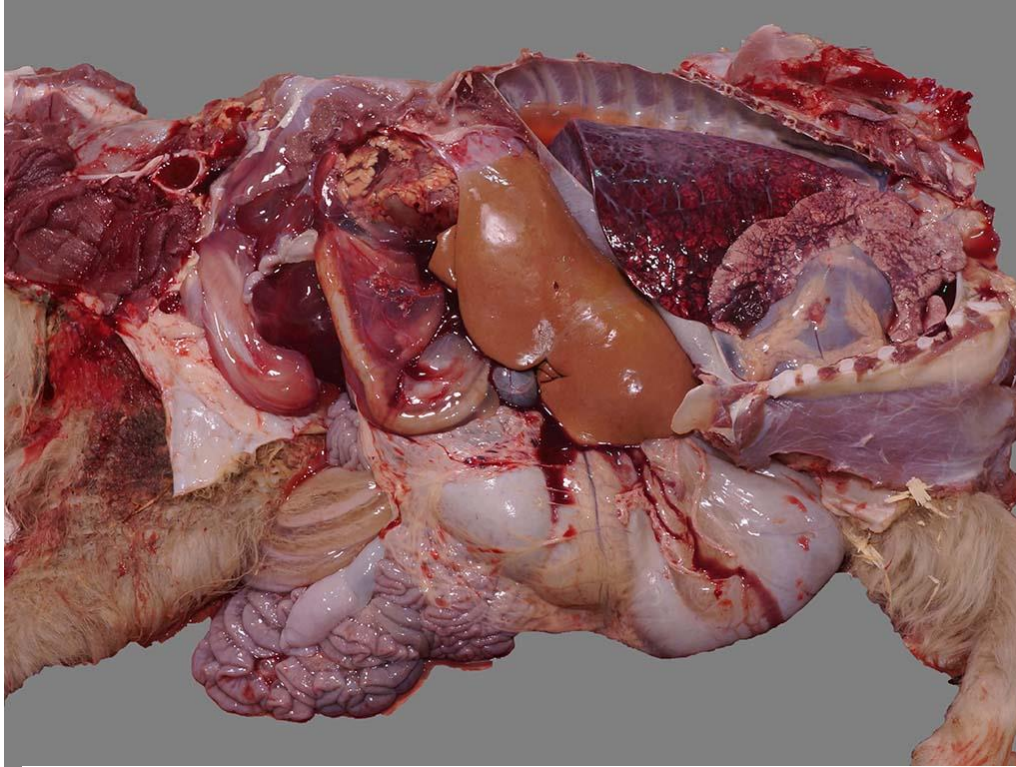
Figure 4. Colon, *Callicebus Coimbrai*: myriads of round, 30-50 μm diameter, eosinophilic staining trophozoites consistent with *Entamoeba histolytica* in crypts and the lamina propria (PAS 400X).

CASE III: D14-043814 (JPC 4066096).

Signalment: 2.5 month old, intact female, Yak (*Bos grunniens*)

History: This yak was bottle-raised from birth and housed in a small pen in the backyard, abutting a building. The yak had an approximately two week history of pica and a one week history of decreased appetite and lethargy, which progressed to loss of a suckle response. The animal developed a fever (104F) and was initially treated with antibiotics and tube feedings of electrolytes and milk at the farm but was referred for suspected laryngeal or pharyngeal trauma based on difficulty tubing and reflux of milk through the nose. On presentation to the referral hospital, the yak was tachypneic (112 rpm) with harsh lung sounds bilaterally and decreased lung sounds ventrally. The yak was markedly azotemic (results below) and was started on intravenous fluids and other supportive care. Thoracic radiographs supported cranioventral pneumonia and a trans-tracheal wash was performed (results below) and antibiotics were initiated. The yak's azotemia did not improve with fluid therapy and the yak was producing minimal urine. The yak developed ascites and a total of 4L was removed via abdominocentesis on the two days preceding euthanasia. The yak did not suckle at any time during hospitalization. The yak was euthanized 7 days after admission to the referral hospital.

Gross Pathology: The abdominal cavity contained 2.5 L of translucent, pale pink to yellow, watery fluid and there was marked perirenal edema with mild to moderate hemorrhage, more pronounced surrounding the left kidney. The kidneys were diffusely pale brown and slightly swollen, with small pinpoint foci of hemorrhage in the cortex, reddening of the corticomedullary junction, and hemorrhage and edema in the adipose tissue of the renal pelvis. There was also



Kidney, yak calf. There was marked perirenal edema with mild to moderate hemorrhage, more pronounced surrounding the left kidney. The liver was diffusely a pale brown. The lungs were red in caudal lobes with interstitial edema, and the cranioventral fields were firm as a result of aspiration pneumonia. (Photo courtesy of: University of Minnesota – Veterinary Diagnostic Laboratory: www.vdl.umn.edu)

marked mesocolonic edema and mild to moderate generalized subcutaneous edema. There were no lesions in the esophagus, pharynx or larynx. The rumen contained a moderate amount of gray opaque liquid and small chips of gray paint. The liver was diffusely pale brown. The thoracic cavity contained 0.3 L of fluid and the pericardium contained 0.1 L of fluid, similar to the abdominal fluid. The lungs were dark red caudally and mottled pink and dark red cranially with diffuse interstitial edema and multiple dark red, firm areas of consolidated lung bilaterally in the cranioventral lung fields, consistent with aspiration pneumonia (foreign material present on histopathology).

Laboratory Results:

Clinical pathology:

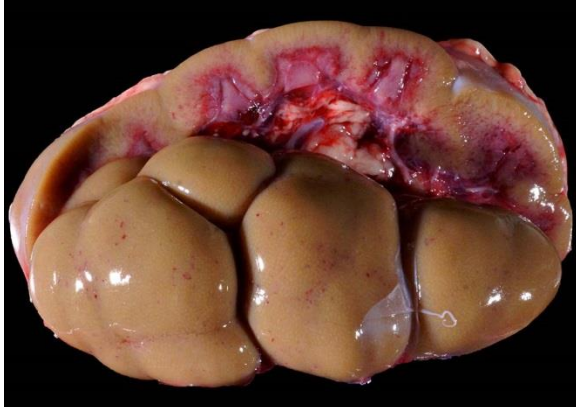
*Reference intervals were not provided for yak; references ranges in parentheses are for cattle tested at the referral hospital for general comparison only
Significantly abnormal values on presentation:
 BUN – 128

mg/dL (10-24)
 Creatinine – 17.1 mg/dL

(0.6-1.3)
 Calcium – 7.6 mg/dL (8.1-10)
 Phosphorus – 11.6 mg/dL (3.4-7.7)
 Total protein – 4.7 mg/dL (6.2-8.9)
 Albumin – 2.8 mg/dL (3.2-4)
 HCT – 18% (25-47)

Values on the day of euthanasia (7 days later):

BUN – 119 mg/dL
 Creatinine – 20.1 mg/dL
 Calcium – 8.2 mg/dL
 Phosphorus – 10.2 mg/dL
 Total protein – 3.4 mg/dL
 Albumin – 1.9 mg/dL
 PCV – 12%



Kidney, yak calf. The kidneys were diffusely pale brown and slightly swollen, with small pinpoint foci of hemorrhage in the cortex, reddening of the corticomedullary junction, and hemorrhage and edema in the adipose tissue of the renal pelvis (Photo courtesy of: University of Minnesota – Veterinary Diagnostic Laboratory: www.vdl.umn.edu)

Microbiology:

Antemortem aerobic culture of trans-tracheal wash: *Pseudomonas aeruginosa*

Postmortem aerobic culture of lung: *Pseudomonas aeruginosa*

Postmortem aerobic culture of kidney, spleen and liver: No growth

Molecular diagnostics:

Kidney was submitted for *Leptospira* species PCR (16s rRNA): negative

Tissue homogenate of lung and spleen was submitted for BVD PCR: negative

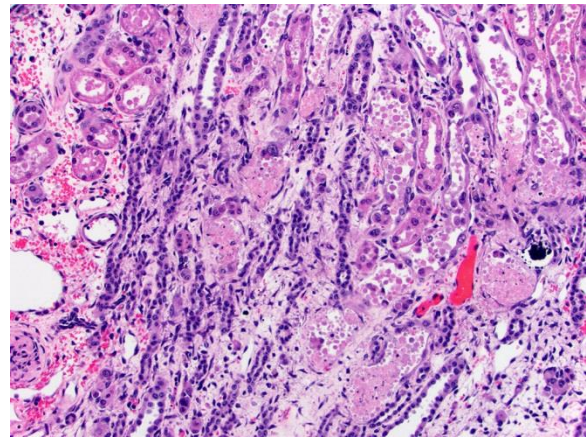
Toxicology:

Liver was submitted for toxic element screen:

Lead detected at 62 ppm (wet tissue basis) (<1 ppm considered normal for cattle, >10 ppm liver lead is consistent with toxicosis)

Histopathologic Description: Kidney – Diffusely affecting the entire cortex, the proximal tubular epithelium is degenerate or necrotic with marked clear cytoplasmic vacuolization (degeneration) of the proximal convoluted tubule (PCT) segments. The

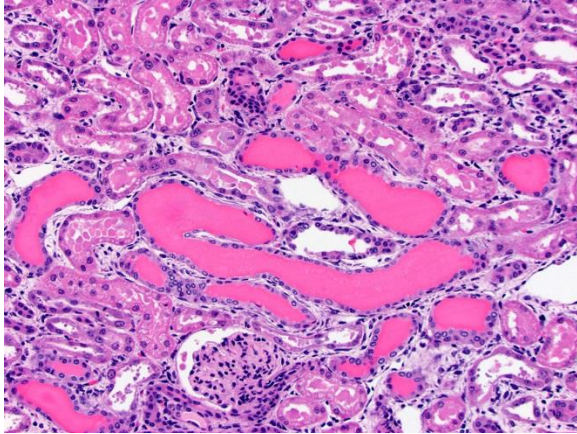
PCT have cuboidal epithelium with a discernible brush border and uniform, basally located nuclei frequently containing aggregates of 2-5 micron diameter, eosinophilic globular material displacing but not marginating the chromatin. Within the PCT lumina, there is eosinophilic material. The plump vacuolated cells of the PCT transition to the proximal straight tubule (PST) segments, which are lined by variably cuboidal to flattened epithelium, often with large nuclei (up to 50 microns in diameter or approximately 3-4 times the size of a normal renal tubular cell) and occasionally multiple nuclei, which contain similar eosinophilic intranuclear material as well as mitoses (interpreted as mixed degeneration and regeneration). There are areas of tubular epithelial necrosis and loss within the PST segment which is characterized by exposure of the basement membrane and numerous cells with pyknotic or karyorrhectic nuclei which are sloughed into the tubular lumen, admixed with small amounts of eosinophilic globular material. There are minimal histologic changes discernible in the



Kidney, yak calf. There is extensive necrosis of tubular epithelium lining the proximal straight tubule. (HE, 100X) (Photo courtesy of: University of Minnesota – Veterinary Diagnostic Laboratory: www.vdl.umn.edu)

medullary components (Loops of Henle, collecting ducts). The distal straight and convoluted tubules (DST, DCT) have uniform cuboidal epithelium with slightly

basophilic cytoplasm, central located nuclei which rarely have eosinophilic intranuclear material but moderate anisokaryosis, no discernible brush border and often have homogeneous pale to brightly eosinophilic material in the tubule lumen (high protein-



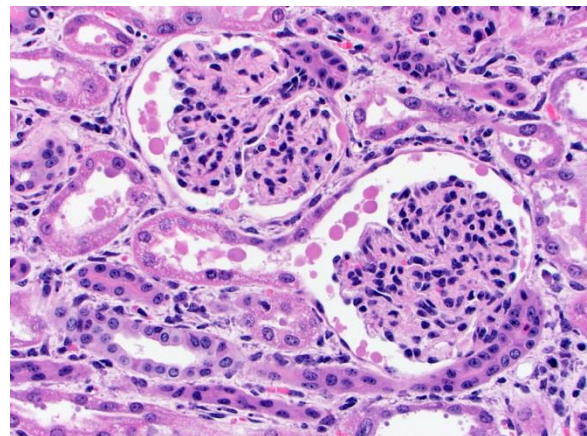
Kidney, yak calf. Distal tubules contain bright pink eosinophilic protein within their lumina. (HE, 200X) (Photo courtesy of: University of Minnesota – Veterinary Diagnostic Laboratory: www.vdl.umn.edu)

content fluid). Occasionally, there are small aggregates of basophilic granular material within the tubular lumina (mineral). The glomeruli are condensed and occasionally have slightly increased pale eosinophilic material expanding the mesangium. The interstitium of the renal cortex is expanded by clear to amphophilic, occasionally granular material (edema fluid) and mildly increased amounts of immature collagen and fibroblasts (fibrosis). There are multiple nodular aggregates of moderate numbers of lymphocytes, smaller numbers of numbers of plasma cells and macrophages within the cortical interstitium. There are multiple small areas of hemorrhage within the perivascular space, interstitium, fibroadipose tissue subjacent to the renal pelvis, and renal capsule. Occasionally the aggregates of eosinophilic intra-epithelial, intra-nuclear material were strongly acid-fast positive and frequently were moderately PAS positive.

Contributor's Morphologic Diagnosis:

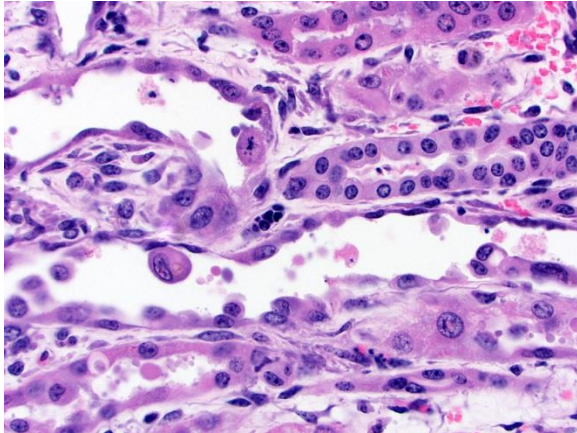
- 1) Kidney, tubules – tubular degeneration and necrosis, diffuse, marked, acute, with intra-epithelial intra-nuclear eosinophilic material (occasionally acid-fast and frequently PAS positive), tubular regeneration, and interstitial edema and hemorrhage
- 2) Kidney – nephritis, interstitial, lymphocytic, multifocal, mild, chronic

Contributor's Comment: This case is an example of acute tubular necrosis in a milk-fed, domestic yak calf (*Bos grunniens*) due to acute-to-subacute lead toxicosis. This animal was exposed to lead by ingestion of lead-based paint (gray paint chips in the rumen) chewed from the siding of the adjacent building. The clinical presentation of ruminants with lead toxicosis is often one of neurologic deficits or altered mentation. Histologically, there may be cerebral edema and laminar necrosis;⁹ however, this yak did not have gross or histologic evidence of notable cerebral edema or necrosis and, other than lethargy and an inability to suckle, was not reported to have neurologic



Kidney, yak calf. Refluxed protein is present within Bowman's space as well as within the proximal segment of the proximal convoluted tubules. (HE, 400X) (Photo courtesy of: University of Minnesota – Veterinary Diagnostic Laboratory: www.vdl.umn.edu)

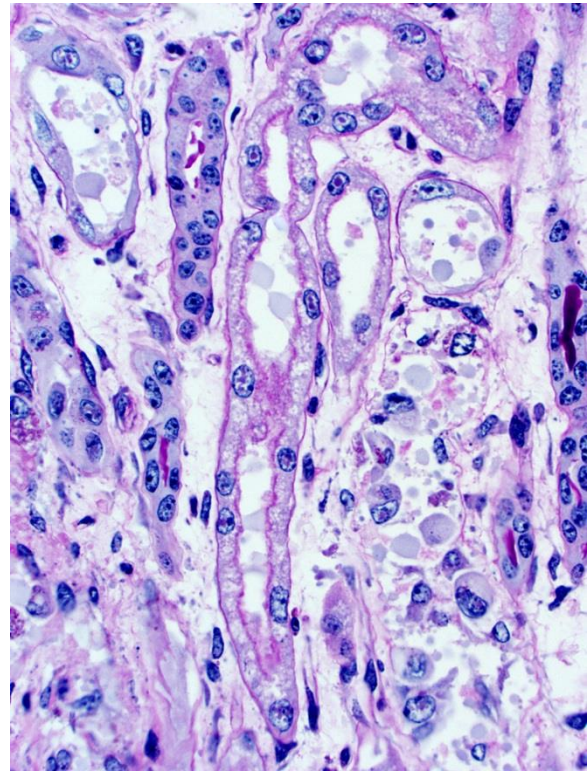
deficits. Peripheral neuropathy, including dysphagia and laryngeal paralysis, has been reported to be a common clinical sign in horses with both acute and chronic lead toxicosis¹¹ and may be the underlying reason for this yak's reported loss of suckle, reflux and aspiration pneumonia which resulted in referral.



Kidney, yak calf. Tubular epithelium contains evidence of necrosis and regeneration including sloughed epithelium and attenuated to plump, often layered epithelium which contains mitotic figures. (HE 600X)(Photo courtesy of: University of Minnesota – Veterinary Diagnostic Laboratory: www.vdl.umn.edu)

Renal changes attributed to lead toxicosis are usually reported to be mild and occasionally evident only as eosinophilic or poorly-staining intranuclear inclusions which are acid-fast positive but, similar to this case, severe nephrosis has also been described in young calves.⁹ The mechanism of renal toxicity of lead is known to involve numerous pathways. Structural mitochondrial degeneration occurs (mitochondrial swelling and distortion of cristae) as well as decreased activity of mitochondrial heme-pathway enzymes,⁵ which interfere with cellular energy production needed to maintain homeostasis and fuel active transport processes vital to renal tubular cell function. Lead also impacts nuclear function through altered gene expression⁵ and is histologically and ultrastructurally evident as lead-protein

inclusion bodies in some cases. Interestingly, not all of the histologically-

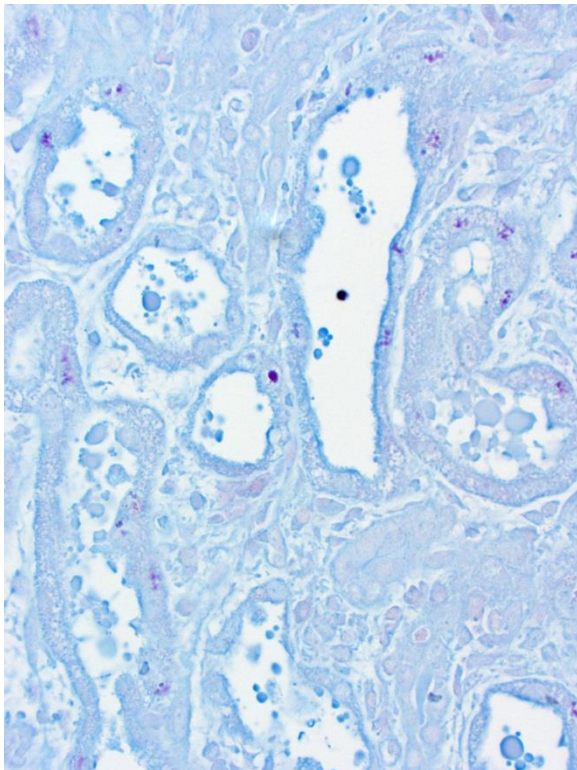


Kidney, yak calf. Nuclei of tubular epithelial cells often contain PAS-positive inclusions. (PAS, 200X) (Photo courtesy of: University of Minnesota – Veterinary Diagnostic Laboratory: www.vdl.umn.edu)

evident eosinophilic intranuclear material in this case was acid-fast positive but the majority was variably PAS-positive, suggesting that many of the inclusions are high in glycogen or other carbohydrate-rich compounds but did not necessarily contain lead complexes. Electron microscopy was performed in this case and solitary or multiple, variably-sized electron-dense inclusions were present in the nuclei of some renal tubular epithelial cells, however the inclusions incorporated less fibrillar material than expected based on previously published reports of lead inclusions.^{3,12} This may be due to the fact that this was a diagnostic case and the tissue was formalin-fixed prior to gluteraldehyde fixation, which may have introduced artifactual changes. Additional

information regarding the composition of inclusions could have been obtained from energy-dispersive x-ray spectroscopy (EDS) but this capability is not available within the electron microscope at the submitting institution. The specificity of renal acid-fast positive inclusions for lead intoxication has been reported to be high in cattle¹³ but renal intranuclear acid-fast inclusions should be further investigated. Other general mechanisms of lead toxicity likely impacting renal function include lead competitively binding in place of calcium, altered calcium regulation, and structural and functional alteration in cellular enzymes.¹⁰

Young animals are known to absorb ingested lead more efficiently than adults⁷ and there are numerous dietary factors known to impact absorption of ingested lead.¹ Many studies on lead absorption are rodent-based; however, studies in cattle



Kidney, yak calf. Inclusions within nuclei of tubular epithelium are often acid-fast. (Ziehl-Nielsen, 100X)
(Photo courtesy of: University of Minnesota – Veterinary Diagnostic Laboratory: www.vdl.umn.edu)

identified significant differences in lead absorption from milk-fed vs. grain and hay-fed calves¹⁵ and in absorption based on levels of lactose in the diet.¹⁴ Calves fed exclusively milk and calves fed elevated lactose levels with grain absorbed more lead than calves not receiving milk or without high levels of lactose supplemented to grain. These diet-related factors may be a major factor for susceptibility in young animals, and in this case the affected yak was on a milk-only diet.

The underlying cause and significance of the lymphocytic interstitial nephritis in this case is unknown.

JPC Diagnosis: 1. Kidney: Tubular degeneration, necrosis, regeneration, and proteinosis, diffuse, marked with tubular casts and intranuclear, eosinophilic inclusion bodies within renal tubule epithelial cells.

2. Kidney: Nephritis, cortical, interstitial, chronic, multifocal, mild.

Conference Comment: In addition to domestic animals, wildlife may also be exposed to lead from various sources. Ingestion of lead is the most common route of exposure, although toxicity due to lead-containing shot is also common (but likely poses a low risk for lead toxicity).⁸

Lead exposure is of particular concern in wild avian species where it may affect a variety of birds ranging from waterfowl to bald eagles. In avian species, lead can inhibit enzymes involved in hemoglobin synthesis and when exposed at high levels, may result in anemia. Lead toxicity is most often a chronic condition and as such, affected birds are often debilitated and in poor body condition.⁶ Gross lesions may include esophageal, ventriculus and proventriculus impaction with food, gall bladder distension, pale streaks in the

myocardium and muscle of the ventriculus indicative of necrosis, as well as pallor of internal organs. Eosinophilic lead inclusions in the nuclei of proximal tubule epithelium also occur in the kidney of birds and, while this finding is specific for lead poisoning, it may not be present in all cases. Although not necessarily specific for lead toxicity, other histologic changes in affected birds may include hepatic hemosiderosis, fibrinoid necrosis of arterioles, encephalopathy and peripheral neuropathy. The highest concentration of lead in birds is found in the bone, liver and kidney; lead levels in bone decline much slower than soft tissues and thus bone serves as a much longer term location of lead deposits.⁶

Lead has no biologic function and although lead can exert its toxic effects via a variety of mechanisms, its competition with calcium in various biologic functions is of particular importance. This can result in various pathophysiologic effects such as inhibition of neurotransmitter release, defects in ion pumps and channels as well as alterations in protein kinase function.⁶ Lead is considered neurotropic, although the precise reason is not well understood; neuronal changes are non-specific and laminar cortical necrosis may be seen in some cases.²

In addition to the central nervous system, lesions also occur in bone. The characteristic lesion is referred to as a “lead line,” which is a band of sclerosis located at the metaphysis of developing bones. It is seen as an early lesion in both children and animals. The lesion consists of persistent mineralized cartilage trabeculae which cannot be effectively resorbed by osteoclasts in spite of their apparent abundance microscopically. Osteoclasts may also contain acid-fast intranuclear inclusions.⁴

We thank the contributor for providing clinical pathology data and gross images with the submission, which enhance the teaching / learning value of the case.

Contributing Institution:

University of Minnesota – Veterinary Diagnostic Laboratory: www.vdl.umn.edu

References:

1. Barltrop D, Khoo HE. The influence of nutritional factors on lead absorption. *Postgrad Med J.* 1975;51(601):795-800.
2. Cantile C, Youssef S. Nervous system. In: Maxie MG, ed. *Jubb, Kennedy, and Palmer's Pathology of Domestic Animals.* 6th ed. Vol 1. St. Louis, MO: Elsevier; 2016:316-317.
3. Choie DD, Richter GW. Lead Poisoning: Rapid Formation of Intranuclear Inclusions. *Science.* 1972;177(4055):1194-1195.
4. Craig LE, Dittmer KE, Thompson KG. Bones and Joints. In: Maxie MG, ed. *Jubb, Kennedy, and Palmer's Pathology of Domestic Animals.* 6th ed. Vol 1. St. Louis, MO: Elsevier; 2016:86.
5. Fowler BA. Mechanisms of kidney cell injury from metals. *Env Health Persp.* 1993;100:57-63.
6. Golden NH, Warner SE, Coffey MJ. A review and assessment of spent lead ammunition and its exposure and effects to scavenging birds in the United States. *Rev Environ Contam Toxicol.* 2016;237:123-91.
7. Kostial K, Kello D, Jugo S, et al. Influence of age on metal metabolism and toxicity. *Env Health Persp.* 1978;25:81-86.
8. LaDouceur EE, Kagan R, Scanlan M, Viner T. Chronically embedded lead projectiles in wildlife: A case series

investigating the potential for lead toxicosis. *J Zoo Wildl Med.* 2015;46(2):438-442.

9. Maxie MG. *Jubb, Kennedy, and Palmer's Pathology of Domestic Animals.* 5th ed. Elsevier Saunders; 2007.

10. Needleman H, Needleman. Lead Poisoning. *Annu Rev Med.* 2004;55(1):209-222.

11. Puschner B, Aleman M. Lead toxicosis in the horse: A review. *Eq Vet Ed.* 2010;22(10):526-530.

12. Richter GW, Kress Y, Cornwall CC. Another look at lead inclusion bodies. *Am J Pathol.* 1968;53(2):189-217.

13. Thomson RG. Reliability of acid-fast inclusions in the kidneys of cattle as an indication of lead poisoning. *Can Vet J.* 1972;13(4):88-9.

14. Zmudzki J, Bratton GR, Womac CW, et al. Lactose and milk replacer influence on lead absorption and lead toxicity in calves. *Bull Environ Contam Toxicol.* 1986;36(1):356-363.

15. Zmudzki J, Bratton GR, Womac C, et al. The influence of milk diet, grain diet, and method of dosing on lead toxicity in young calves. *Toxicol Appl Pharmacol.* 1984;76(3):490-497.

CASE IV: PA5050 (JPC 4033979).

Signalment: 5-year-old, female, Spanish-Boer cross goat (*Capra hircus*)

History: This animal was noted to be acutely disoriented, visually impaired, and intermittently down and twitching. It responded immediately to empirical treatment, but never completely recovered full neurological function and was euthanized two months later.

Gross Pathology: The brain appeared somewhat shrunken on removal from the cranial vault. The cerebral cortex was thinned and discolored, especially in the occipital-parietal region, with areas of clefting and separation from the underlying white matter noted.

Laboratory Results: None

Histopathologic Description:

Sections of occipital-parietal cortex are examined. Each slide contains tissue from the affected animal as well as location-matched cortex from an age-matched control goat. The latter is essentially normal brain for comparison purposes. In the former, there is focally extensive laminar loss of cortical grey matter, significantly diminishing cortical thickness. Although occasional neuronal cells remain present, residual cellularity consists primarily of large, reactive (gemistocytic) astrocytes, activated microglial cells, and phagocytically active macrophages (Gitter cells). Capillary structures are prominent with somewhat swollen endothelium, both in grey



Cerebrum, goat: The cerebrum (at right) is shrunken with marked thinning of the gray matter and blurring of the interface between gray and white matter. (Age and location-matched cerebrum at left.) (Photo courtesy of: Division of Laboratory Animal Resources (DLAR) University of Pittsburgh, <http://www.dlar.pitt.edu/>)

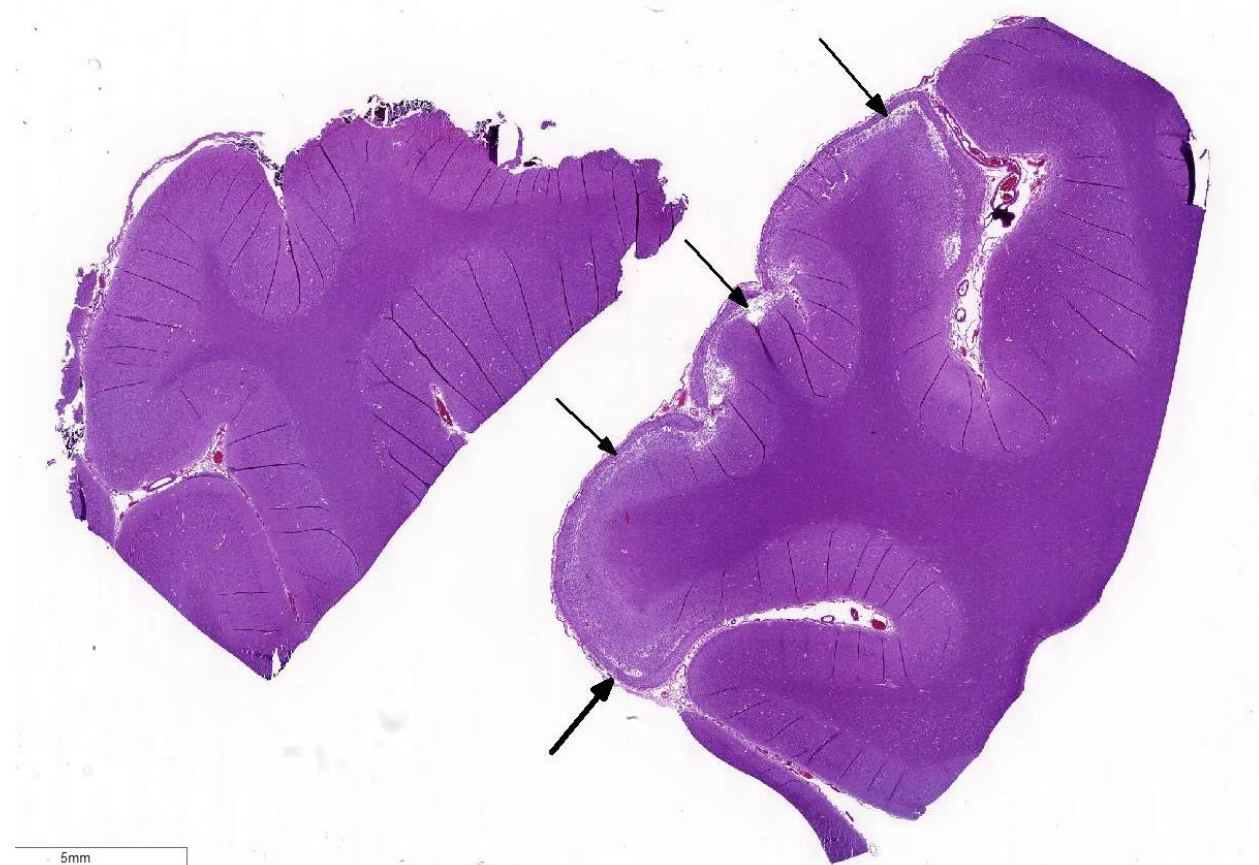
matter and in collapsed, redundant leptomeninges present in the expanded subarachnoid space. Abundant, phagocytically active macrophages are also noted in the latter. The white matter appears slightly hypercellular, probably due to a mild reactive astrocytosis also present in this region. Infrequent pyknotic cells, probably representing necrotic oligodendroglia, are seen due to axonal die back. Mild perivascular lymphocytic cuffing is noted in white matter in some sections.

Contributor's Morphologic Diagnosis:

1) Subtotal laminar cortical necrosis and collapse, severe, with marked extensive residual reactive gliosis, vacuolization and patchy regions of parenchymal separation/clefting, with areas of tissue dropout and meningeal collapse

2) Patchy, mild perivascular lymphocytic cuffing, subjacent white matter, mild (some sections)

Contributor's Comment: The microscopic findings are consistent with polioencephalomalacia (PEM). This is a morphological term used to describe necrosis with softening (malacia) in grey matter of the brain. The condition is described in a surprisingly wide range of domestic animals, both ruminant and carnivores, as well as some non-domestic species.⁹ Wernicke's encephalopathy is the equivalent human disease, which is classically associated with chronic alcoholism. Cattle, sheep and goats are commonly affected ruminants, although a variety of other species are also susceptible. Clinical manifestations of the disease are



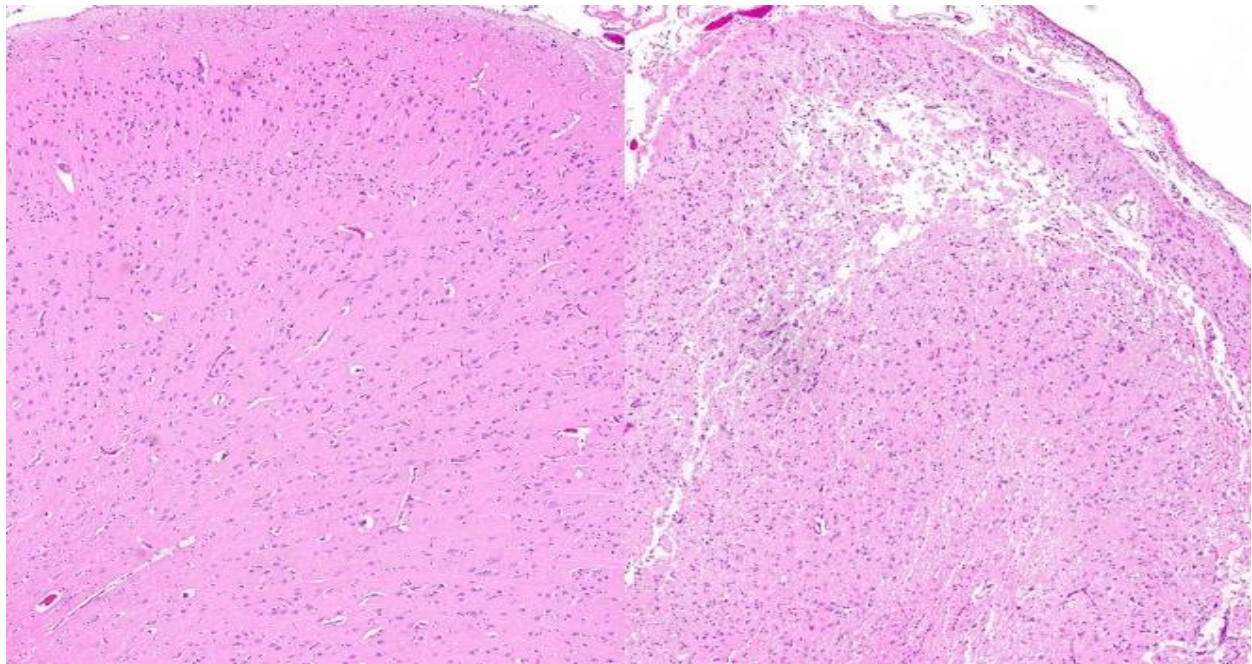
Cerebrum, goat: There is segmental laminar necrosis of the submeningeal gray matter (arrows) (Age and location-matched cerebrum at left.) (HE, 4X)

variable, with animals often presenting with facial twitching, teeth grinding, salivation, blindness, seizures and opisthotonus.⁸ The condition affects primarily young animals, and sheep and goats, as a rule, have a shorter course with fewer survivors. The syndrome is not always fatal; mortality rates are reported at 50-90%, although surviving animals typically have significant neurological deficits, including visual impairment and stupor.⁴ Disease is seen worldwide and is responsible for important economic losses in many countries. The condition is more commonly seen in goats under intensive management conditions when fed more grain concentrate to encourage accelerated growth.⁷

PEM was recognized as a clinical and pathological entity long before specific pathogeneses had been discovered. Originally applied as a diagnosis to cattle and sheep losses in Colorado, the morphological designation of cerebrocortical malacia was subsequently used sy-

nonymously for the specific entity of thiamine deficiency disease. However; it is now known that many cases of PEM in ruminants cannot be ascribed to thiamine deficiency.^{2,3,6} There is often a lack of changes in thiamine concentration in ruminal fluid, tissue and blood in affected animals. Furthermore, there has been a failure to induce the disease by experimentally created deficiencies. The most compelling argument for thiamine's role in PEM had been that administration of it in clinical cases, especially to those early in the disease course, often resulted in recovery. However, this is now believed to be related to improved energy metabolism in the impaired brain, regardless of the inciting cause.^{5,6,7}

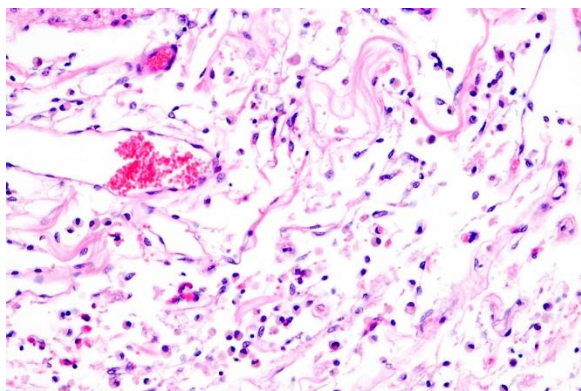
Currently, it is believed that PEM in ruminants can involve a wide range of pathogeneses, including toxic, metabolic, dietary/nutritional and even infectious events. In addition to thiamine deficiency, some of the specific causes of



Cerebrum, goat: Demonstration of laminar necrosis (right) in animal with PEM. (Age and location-matched cerebrum at left.) (HE, 40X) (Photo courtesy of: Division of Laboratory Animal Resources (DLAR) University of Pittsburgh, <http://www.dlar.pitt.edu/>)

polioencephalomalacia in ruminants include sulfur poisoning, lead poisoning, salt poisoning (water deprivation), administration of levamisol or thiamine analogues such as amprolium, ingestion of thiaminase rich plants, and infection with bovine herpesvirus.²

Gross pathological changes are often striking, with the parietal-occipital cortex being most prominently affected. In acute cases, brains may have a swollen appearance and palpable softness, with flattening of gyri and narrowing of sulci. With more prolonged survival, as in this case, there is marked thinning or, in some areas, complete absence of friable, necrotic appearing grey matter, with zones of clefting/separation from underlying white matter visible.⁸ The subarachnoid space is widened, and brains often appear smaller or shrunken. Areas of cerebrocortical necrosis (CCN) can be identified by autofluorescence under UV light, as a consequence of degraded lipoidal material within macrophages or high molecular weight collagen-like material. Although blood pyruvate levels may be elevated,⁴ other serum biochemical analysis is variable and is generally of little value in disease diagnosis.



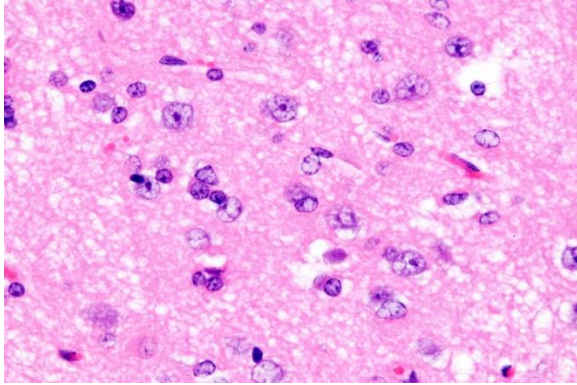
Cerebrum, goat: Remnant gliovascular strands in areas of laminar necrosis in a goat with PEM. (HE, 200X). (Photo courtesy of: Division of Laboratory Animal Resources (DLAR) University of Pittsburgh, <http://www.dlar.pitt.edu/>)

As previously noted, the animal in question responded favorably to thiamine administration upon onset of signs, but continued to have significant neurological and visual deficits after stabilization.

JPC Diagnosis: Brain, cerebral cortex: Necrosis, laminar, multifocal to coalescing, with reactive gliosis.

Conference Comment: The contributor provides an excellent review of polioencephalomalacia, and the aged-matched control provided on the slide increases the teaching / learning value of this case. In ruminants, polioencephalomalacia is usually limited to the cerebrocortical grey matter and has a laminar pattern of distribution, often being referred to as “laminar cortical necrosis.” The lesion in ruminants discussed above shares similarities with salt poisoning in swine and has been documented in cases of lead poisoning in cattle as mentioned in WSC Case 3 of this conference. It is most often a disease of young animals, although older animals may be affected sporadically.

Lesions of PEM vary in severity, depending on various factors such as species, age and duration.¹ Lesions are more severe grossly obvious in animals that survive for a period of time. The cerebral cortex often demonstrates superficial, laminar pallor which will trace the grey-white matter junction and may be most prominent in the gyri. Lesions are bilaterally symmetrical and are apparently more consistent in the caudal cerebral hemispheres. The distribution appears to be related to the area supplied by the middle cerebral artery.¹



Cerebrum, goat: Adjacent to necrotic areas, small numbers of glial cells about neurons. (HE, 400X). (Photo courtesy of: Division of Laboratory Animal Resources (DLAR) University of Pittsburgh, <http://www.dlar.pitt.edu/>

There is some slide variation in the severity of lesions in this case, but in general, it is representative of the classic microscopic lesions of PEM. Polioencephalomalacia does not have a specific etiology, as discussed above, but is often directly or indirectly linked to a deficiency in thiamine. Sulfur-containing compounds have also been implicated in some cases of PEM.¹ There is some question regarding the observed tissue autofluorescence in cases of PEM with some references stating it may originate from substances in mitochondria as opposed to ceroid-lipofuscin pigments.¹⁰

Contributing Institution:

Division of Laboratory Animal Resources (DLAR) University of Pittsburgh, <http://www.dlar.pitt.edu/>

References:

1. Cantile C, Youssef S. Nervous system. In: Maxie MG, ed. *Jubb, Kennedy, and Palmer's Pathology of Domestic Animals*. 6th ed. Vol 1. St. Louis, MO: Elsevier; 2016:309-312.
2. Fabiano JF de Sant'Ana, Claudio SL Barros. Polioencephalomalacia in ruminants in Brazil. *Braz J Vet Pathol*. 2010; 3(1):70-79.
3. Gould DH, Polioencephalomalacia. *J. Animal Science*. 1998;76: 309-314.
4. Koestner A, Jones TC. The Nervous System. In: Jones TC, Hunt RD, King NW ed. *Veterinary Pathology*. 6th ed. Philadelphia: Williams & Wilkins; 1997: 1272-1274.
5. Najarnexhad V, Aslani MR, Balali-Mood Mehdi. The therapeutic potential of thiamine for treatment of experimentally induced subacute lead poisoning in sheep. *Comp Clin Patho*. 2010; 19:69-73.
6. Niles GA, Morgan SE, Edwards WC, The relationship between sulfur, thiamine and polioencephalomalacia – a review. *Bovine Practice*. 2002; 36: 93-99.
7. Smith MC, Sherman DM ed. *Goat Medicine*. 2nd ed. Ames, IA:Wiley Blackwell; 2009: 222-226 .
8. Sullivan ND. The Nervous System. In: Jubb KVF, Kennedy PC, Palmer N eds. *Pathology of Domestic Animals* 3rd ed. Vol 1. New York: Academic Press, Inc.; 1985: 251-256.
9. Summers BA, Cummings JF, de Lahunta A. *Veterinary Neuropathology*. New York: Mosby; 1995:277-280.
10. Zachary JF. Nervous System. In: McGavin MD, Zachary JF, eds. *Pathologic Basis of Veterinary Disease*. 5th ed. St. Louis, MO: Mosby Elsevier; 2012:851.

Joint Pathology Center
Veterinary Pathology Services



WEDNESDAY SLIDE CONFERENCE 2015-2016

Conference 24

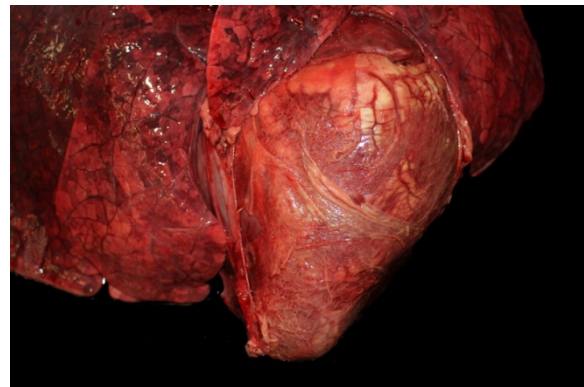
11 May 2016

CASE I: JPC WSC 1 (JPC 4069824).

Signalment: 2 year-old Gyr cow (*Bos indicus*)

History: This 2-year-old, unvaccinated, pregnant cow was down for less than 24 hours. On physical examination, she had increased patellar reflexes in both hind limbs and the left hind leg was swollen and had demonstrable crepitus.

Gross Pathology: A 2x1 cm raised, roughened, hairless area with minimal crusting is on ventral midline over the xiphoid (presumed stephanofilariasis). Subcutaneous crepitus is palpable over the hind limbs, most prominent over the caudal thighs, with a lesser amount palpable on the forelimbs (emphysema). The skeletal muscles of both hind limbs contain large, multifocal to coalescing, dark red to black, dry areas with an odor of rancid butter and occasional clusters of gas bubbles (emphysematous and hemorrhagic myositis), that is worse over the caudal thigh muscles. Similar, less severely affected areas are multifocally found in the skeletal muscle of



Heart, ox. Abundant fibrin covers the myocardium and interior epicardial surface. (Photo courtesy of: Dept Vet Pathobiology, College Vet Med Biomed Sciences, Texas A&M University, <http://vetmed.tamu.edu/vtpb>)

the forelimbs. A moderate amount of subcutaneous, clear, dark red, gelatinous tissue surrounds the gastrocnemius muscles (edema). The dorsal pleural surface contains multifocal to coalescing dark red foci (echymoses). Multifocal to coalescing, 1-100 mm, black foci are on the pericardial sac and jugular vein (petechiae). Covering the epicardium and loosely adhered to the pericardial sac is yellow, friable, fibrillar material (fibrin, fibrinous epicarditis). A 5x3 cm, dark red, irregularly marginated, flat area on the epicardium extends multifocally into the myocardium (myocardial necrosis).



Heart, ox. A 5-3cm irregular dark red area of necrosis is present within the myocardium (at left). (Photo courtesy of: Dept. Vet Pathobiology, College Vet Med Biomed Sciences, Texas A&M University, <http://vetmed.tamu.edu/vtpb>)

Laboratory Results:

Toxic WBCs present on CBC.

Chemistry abnormalities:

[Ca] 6.5 (7.4-11.5 mg/dl); total protein 5.8 (6.5-9.3 g/dl); albumin 2.6 (3-4 g/dl); aspartate aminotransferase 1420 (53-173 U/L); creatinine kinase >16,000 (55-392 U/L); anion gap 21.9 (10-18 mmol/L); fibrinogen 1000 (300-700 mg/dl); leucopenia [WBC] 3800 (4000-12,000).

Cytology:

Smear from a left thigh aspirate: Low cellularity with few, intact, nucleated cells and numerous erythrocytes in a light pink hazy background with many, thick, box-like, bacterial rods often seen in end-to-end pairs. The nucleated cell population is composed of non-degenerate neutrophils, lymphocytes, and monocytes in numbers and proportions consistent with peripheral blood. No overtly neoplastic cells are observed.

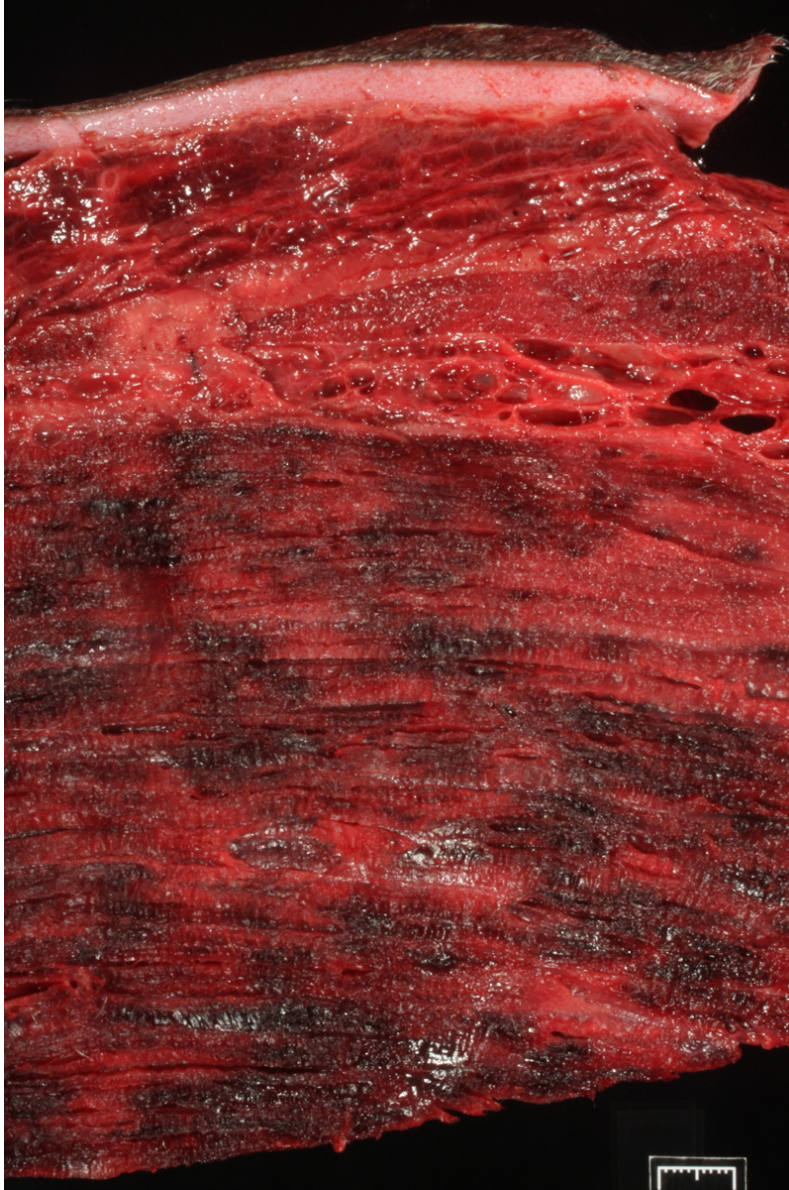
Skeletal muscle FA: *Clostridium chauvoei*-positive

Histopathologic Description: A section of myocardium with epicardial surface is examined. Moving from the epicardium centrally into this inflammatory lesion, the epicardium has an organized fibrin coat with embedded, degenerate neutrophils. The epicardium, epicardial fat and external myocardium have variable amounts of free erythrocytes and degenerating and necrotic neutrophils that dissect and infiltrate tissues. Moving further inside the necrosis, is intense in the cardiomyocytes and neutrophils with more pyknotic nuclei, hyalinized homogeneous cardiomyocytes (necrosis), lysed erythrocytes and fibrin between fibers. The inflammation abruptly stops, and in a central zone (surrounded by the previously described wall of inflammation) the histoarchitecture remains with retention of homogenous fibers separated by fibrillar, pink material (fibrin) and a pale interstitium (edema and lysed erythrocytes) and few, scattered pyknotic nuclei. Clusters and individual bacterial rods with polar spores are seen. At least 10, round to oval, basophilic, approximately 130X250 u, organisms with a <5u wall and numerous, 25u-longX8u-wide, basophilic structures (sarcocyst with bradyzoites) randomly expand cardiomyocytes without tissue response. They are intricately septate.

Contributor's Morphologic Diagnosis:

1. Severe, diffuse, acute, fibrinosuppurative epicarditis; multifocal to coalescing necrohemorrhagic myocarditis with centrally extensive coagulative necrosis, emphysema and abundant, intralesional, gram-positive, spore-forming bacilli (*Clostridium chauvoei*).

2. Multifocal *Sarcocystis cruzi* schizonts/sarcocysts presumed.



Skeletal muscle, ox. Hindlimb skeletal muscles contain multifocal areas of necrosis, hemorrhage, and gas formation. (Photo courtesy of: Dept. Vet Pathobiology, College Vet Med Biomed Sciences, Texas A&M University, <http://vetmed.tamu.edu/vtpb>)

Contributor's Comment: Blackleg is a disease of pastured young animals, especially cattle and sheep, and is often associated with moist pasture in the summer. This is a case of blackleg in a two-year-old cow seen during this year's warm and rainy, late spring. The pathogenesis involves activation of latent *C. chauvoei* in muscle.⁷

Ingested spores replicate in the gut and presumably remain in macrophages with muscle for long periods. Spores are activated by a low oxygen tension in their environment, and the organisms proliferate producing potent, necrotizing toxins and gas. Rapid death with hemorrhagic, crepitant lesions deep in muscles of the pelvic and pectoral girdles are seen. The pathogenesis is recapitulated in the histology with a central zone of coagulative necrosis with individual and clusters of gram-positive bacteria with polar spores and no inflammation that peripherally blends into viable tissue with a zone of primarily degenerate neutrophils and nonlysed erythrocytes. The inciting factor/lesion is not known. When sectioned, the skeletal muscle lesions are seen as dry (coagulative necrosis) areas surrounded by gas, hemorrhage and edema. The various vaccines (polyvalent, 2 to 8-species vaccines) control the disease in endemic areas if timed and applied properly. Although there

are published cases of *C. chauvoei* myositis without extraskletal/visceral lesions,⁶ clostridial myositis can be seen

in the myocardium, tongue and diaphragm.^{2,4,7}

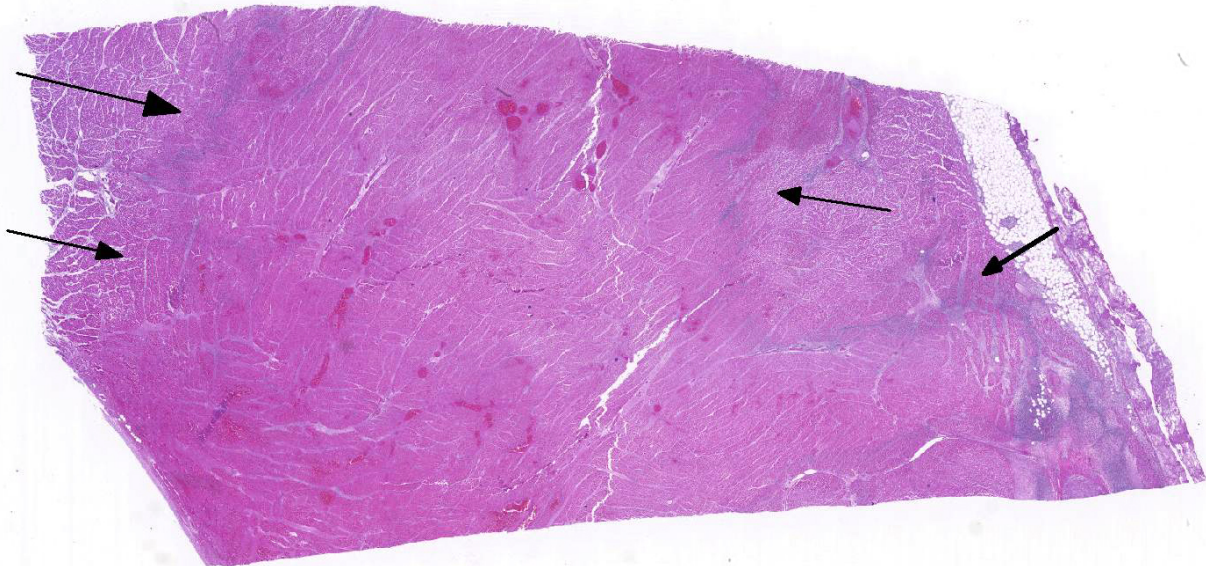
This cow's heart had a fibrinosuppurative epicarditis and when the heart was sectioned, the necrohemorrhagic myocarditis was noted to penetrate the myocardium. Visceral lesions may be small and are missed in cursory necropsies. It is important to note that the visceral sites are heavily used

muscle sites, predisposed to having a lower pO₂. Diagnosis in this case was straightforward because the carcass was fresh, and only *C. chauvoei* was seen with the FA test; however, *C. chauvoei* does not proliferate post-mortem,⁷ and in autolized carcasses, other clostridial species may grow. In making a clostridial diagnosis, four basic aspects/criteria should be considered:¹ a) clinical history, b) post-mortem findings, c) relative numbers of pathogenic organisms seen in the microscopic fields, and d) the postmortem interval. If animals are identified early and treated with antibiotics, they will live several hours longer and will

Sarcocystis (*Sarcocystis cruzi* or *S. hirsuta*) are ubiquitous in cattle muscles, and as seen in this case, the sarcocyst full of bradyzoites does not incite a host response except in cases of eosinophilic myositis.⁵

JPC Diagnosis:

1. Heart: Pancarditis, necrosuppurative and fibrinous, acute, diffuse, severe with necrotizing vasculitis, fibrin thrombi and moderate numbers of bacilli.
2. Heart, myocardium: Sarcocysts, few.



Heart, ox. Subgross image of the area of necrosis within the myocardium (epicardium at left). A line of cellular debris (arrows) delineates the margin. (HE, 5X).

have fibrinous and hemorrhagic transudates covering the pleura, pericardium and peritoneal surfaces (contributor's observation). Such a pleuritis without pneumonia is common with blackleg.

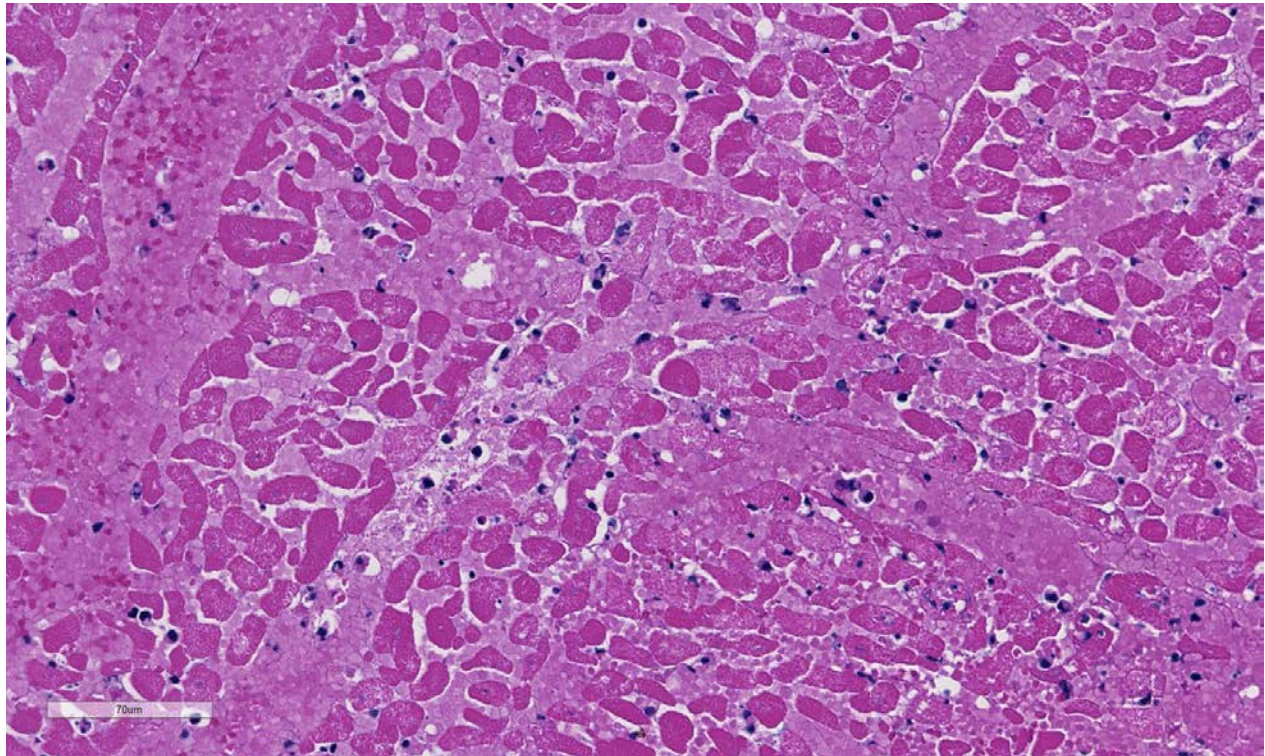
Outbreaks of clostridial myocarditis caused by *C. chauvoei* are reported in calves and sheep.^{3,8} In ruminants, other causes of necrosuppurative (non-traumatic) myocarditis are *Histophilus somni* and listeriosis.⁵

Conference Comment: Once clostridial spores are ingested in the environment, they may remain dormant in the small intestine or germinate and inhabit the small intestine. Spores eventually gain access to macrophages where they spread to muscle and germinate once muscle damage occurs, which creates a low oxygen tension environment. Tissue injury in cases of bl-

blackleg occurs due to necrosis of muscle and supportive tissues due to α and β toxins released from the clostridial organisms. Toxins include oxygen-stable hemolysin, neuraminidase and hyaluronidase, among others. The toxins are released at the site of bacterial replication damaging adjacent muscle and spreading outward through the muscle, supporting tissues and associated vessels.¹¹ Neuraminidase is particularly important as it helps facilitate disease spread.⁹

Other clostridial agents cause disease in a fashion similar to *Clostridium chauvoei*,

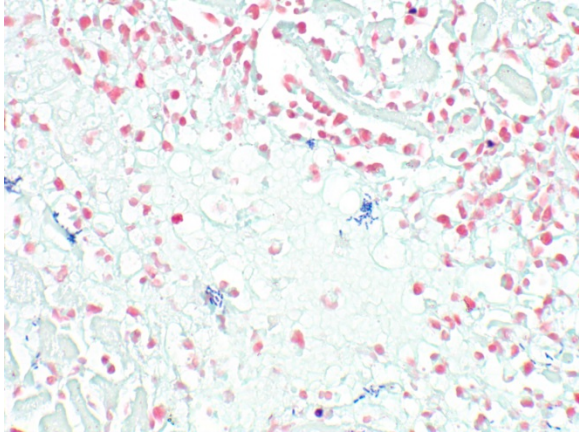
sordelli and *C. novyi*. Malignant edema also has a similar pathogenesis to big head in sheep where wounds of the head sustained during fighting allow germination of *Clostridium novyi* spores followed by release of toxins similar to what is described for blackleg and malignant edema. This results in significant edema in the head and neck region and may extend into the thorax. In black disease, ingested *C. novyi* spores are present in the liver and fluke migration establishes the anaerobic environment needed for spore germination resulting in extensive hepatic necrosis.¹¹



Heart, ox. Large areas of myocardium demonstrate coagulative necrosis. (HE, 320X)

including *C. septicum*, the agent of pseudoblackleg and a potential etiology of malignant edema. As opposed to ingestion, spores of *C. septicum* are often encountered via wound infection. Spores germinate in the anaerobic environment created in the wound, releasing toxins which cause muscle damage similar to what is seen in blackleg.¹¹ Other agents of malignant edema include *C.*

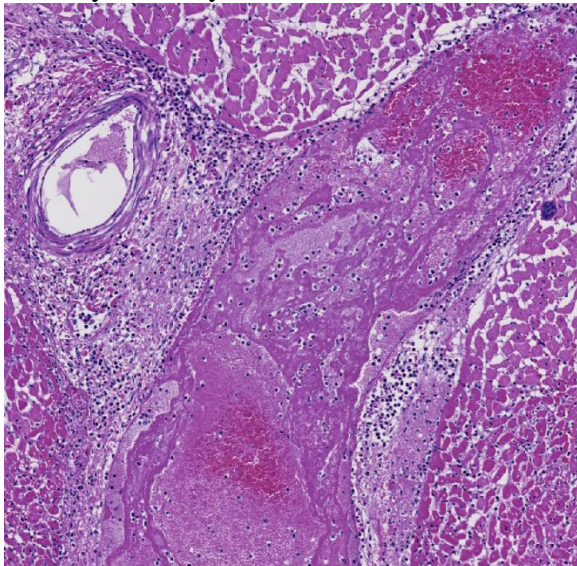
Conference participants commented that although emphysema is commonly seen in this entity, and was present in the excellent gross image provided by the contributor, it is not a prominent histologic finding in the slides provided. Conference participants also noted necrotizing vasculitis as a feature in this case, although it is typically not associated with this entity,¹⁰ as well as the



Heart, ox. Aggregates of robust gram-positive bacilli are scattered throughout the necrotic areas of the section. (Gram, 600X)

presence of fibrin thrombi variably filling vessel lumina and adhering to vessel walls. A tissue Gram stain highlighted bacilli in this slide.

The decreased calcium level in this case is the result of entry of calcium into damaged muscle cells. Albumin is a negative acute phase protein and is decreased in cases of acute inflammation. The increased anion gap is likely due to a combination of lactic acidosis and elevation of renal acids secondary to dehydration. Elevations in as-



Heart, ox. Within the affected areas, occasional veins and lymphatics are occluded by fibrinocellular thrombi. (HE, 80X).

partase aminotransferase and creatinine kinase are secondary to muscle damage. Other agents which may cause necrotizing myositis / myocarditis and were discussed during the conference include *Trueperella pyogenes* which typically results in abscesses and *Bacillus anthracis* which results in the presence of abundant dark, unclotted blood exuding from multiple orifices. Other differential diagnoses discussed include ionophore toxicity, vitamin E /selenium deficiency and eosinophilic myositis.

Contributing Institution:

Dept. Vet Pathobiology, College Vet Med Biomed Sciences, Texas A&M University, <http://vetmed.tamu.edu/vtpb>

References:

1. Batty I, Kerry JB, Walker PD. The incidence of *Clostridium oedematiens* in post-mortem material. *Vet Rec.* 1967; 80: 32.
2. Casagrande RA, Pires PS, Silva ROS, Sonne L, Borges JBS, et al. Histopathological, immunohistochemical and biomolecular diagnosis of myocarditis due to *Clostridium chauvoei* in a bovine. *Ciencia Rural.* 2015; 45:1472-5.
3. Glastonbury JRW, Searson JE, Links IJ, Tuckett LM. Clostridial myocarditis in lambs. *Aust Vet J.* 1988 65:208-209.
4. Malone FE, McFarland PJ, O'Hagan J. Pathological changes in the pericardium and meninges of cattle associated with *Clostridium chauvoei*. *Vet Rec.* 1986; 118: 151-2.
5. Maxie MG, Robinson WF. Cardiovascular system. In: Maxie MG. ed. *Jubb Kennedy and Palmer's Pathology of*

Domestic Animals. Vol 3. 5th edition. Saunders Elsevier: New York; 2007: 41-2.

6. Sojka JE, Bowersock TL, Parker JE, Blevins WG, Irigoyen L. *Clostridium chauvoei* myositis infection in a neonatal calf. *J Vet Diagn Invest*. 1992; 4:201-3.

7. Thompson K. Bones and joints. In: Maxie MG, ed. *Jubb Kennedy and Palmer's Pathology of Domestic Animals*. Vol 1. 5th edition. Saunders Elsevier: New York; 2007:261-4.

8. Uzal FA, Paramidani M, Assis R, Morris W, Miyakawa MF. Outbreak of clostridial myocarditis in calves. *Vet Rec*. 2003; 152:134-6.

9. Useh NM, Nok AJ, Esievo KAN. Pathogenesis and pathology of blackleg in ruminants: the role of toxins and neuraminidase A short review. *Vet Q*. 2003; 25(4):155-159.

10. Valentine BA, McGavin MD. Skeletal muscle. In: McGavin MD, Zachary JF, eds. *Pathologic Basis of Veterinary Disease*. 5th ed. St. Louis, MO: Mosby Elsevier; 2012:907.

11. Zachary JF. Mechanisms of microbial infection. In: McGavin MD, Zachary JF, eds. *Pathologic Basis of Veterinary Disease*. 5th ed. St. Louis, MO: Mosby Elsevier; 2012:195-197.

CASE II: NF-11-604 (JPC 4017089).

Signalment: 2 year old, intact female, Dorper Sheep, (*Ovis aries*).

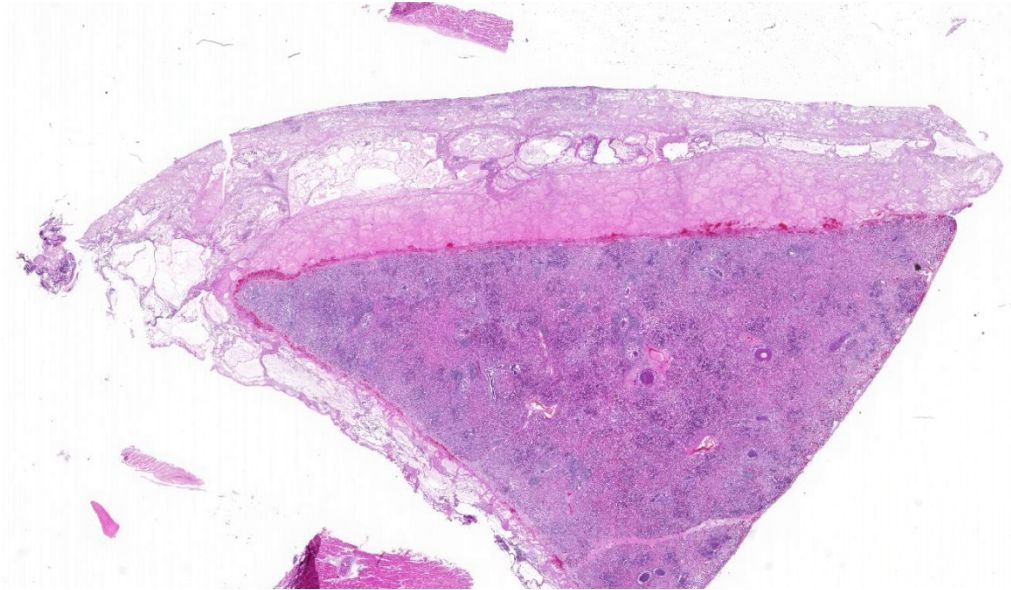
History: This 2-year old intact female Dorper sheep (*Ovis aries*) had a history of weakness, decreased pupillary light reflexes,

abnormal mentation, bloody nasal discharge, dyspnea, and thin body condition (BCS 2/5). The ewe was from a flock of 186 adult animals; 10 of which were found dead.

Gross Pathology: An intact ewe, weighing 33.90-kg was necropsied. The animal was in thin body condition, appeared mildly dehydrated, and was moderately autolyzed. On external examination, there is a small amount of yellow mucoid discharge present on the external nares bilaterally. The conjunctiva and mucous membranes are diffusely pale pink to white. Upon internal examination, the abdominal cavity lacked significant adipose tissue. Pericardial and epicardial fat is also absent. Approximately 50-ml of yellow serous fluid was present within the thoracic and peritoneal cavities. A thick mat of white, friable material (fibrin) is loosely adhered to the pleural surface to the left lung. Fibrin was also present covering the pericardium adjacent to the left lung. The cranioventral left lung is diffusely firm and dark red. On cut section, a moderate amount of white, purulent material oozes from the airways. Diffusely, the caudodorsal aspect of both lungs is mottled red and pink, is rubbery, and fails to collapse. The lumen of the distal 1/3 of the trachea, contained a moderate amount of white, frothy fluid. The tracheobronchial lymph nodes are diffusely enlarged to approximately 2-3 times their normal size. Within the peritoneal cavity, a small focus of hemorrhage is noted surrounding the capsule of the right kidney. Within the abomasum, a single 5-10-cm long, threadlike nematode, consistent with *Haemonchus contortus*, is present. The contents of the colon were scant and soft, green.

Laboratory Results:

Bacterial culture and sensitivity (lung):



Lung, sheep. A wedge shaped section of lung exhibits diffuse parenchymal consolidation and a marked fibrinous pleuritis (top.) (HE, 5X)

Moderate *Mannheimia haemolytica*;
Moderate alpha hemolytic *Streptococcus*;
Few *Trueperella pyogenes*

Qualitative fecal analysis:

Moderate # coccidial oocysts; Many trichostrongyle type eggs; Few *Trichuris* eggs

Histopathologic Description:

Sections of the cranioventral lung consists of severe fibrinosuppurative bronchopneumonia characterized by diffuse necrosis, complete loss of alveolar detail, diffuse filling of alveolar spaces with fibrin, and infiltration of large numbers of viable and degenerate neutrophils, and moderate numbers of multinucleated giant cells. Bronchioles are lined by moderately hyperplastic epithelium and are filled with

degenerate neutrophils and myriad bacterial organisms.

Thick mats of fibrin admixed with large numbers of neutrophils covered the visceral pleura.

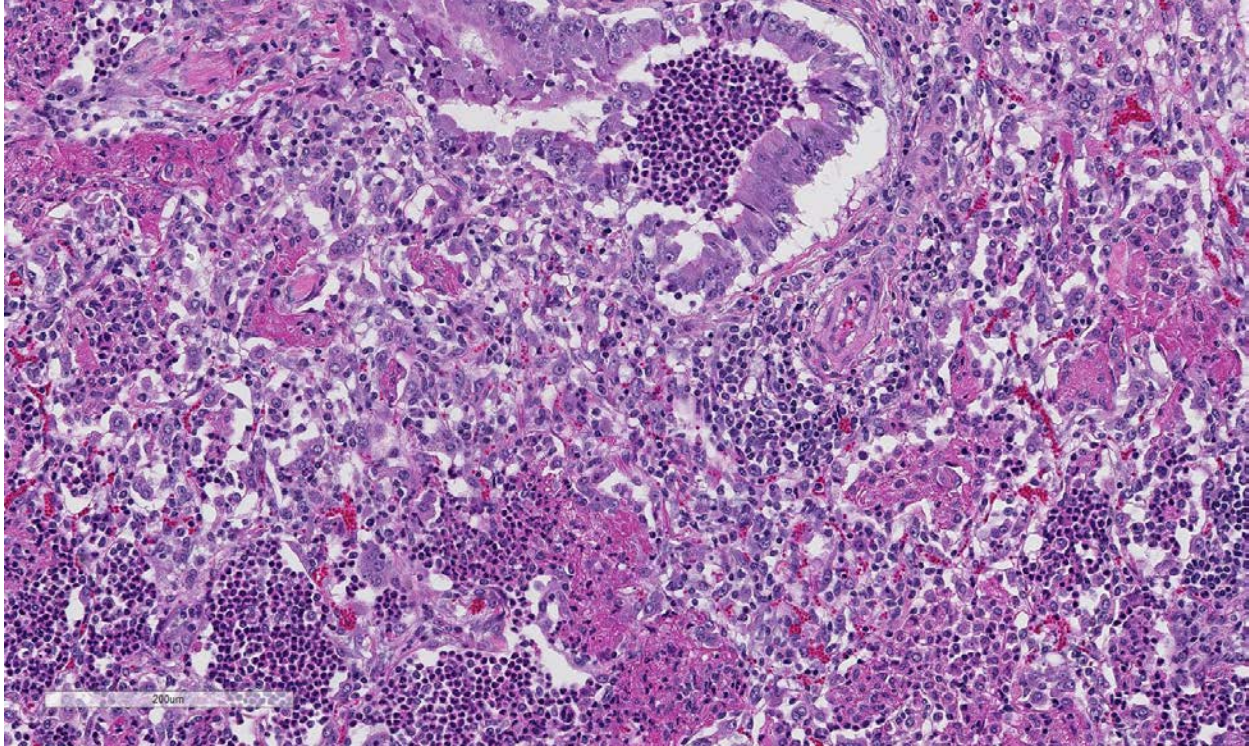
Multifocally, there are large lymphoid cuffs surrounding

airways and blood vessels.

Sections of the caudodorsal lung (not provided) consist of moderate lymphocytic interstitial pneumonia characterized by diffuse thickening of the alveolar septae by lymphocytes, plasma cells, and macrophages. The inflammatory cells also form large lymphoid nodules, which were frequently seen surrounding blood vessels and airways. Mild type II pneumocyte hyperplasia is also present.

Contributor's Morphologic Diagnosis:

Lung: Severe necrotizing and fibrinosuppurative bronchopneumonia, with intralesional bacterial bacilli; Severe, fibrinous pleuritis; Moderate, lymphocytic interstitial pneumonia (caudodorsal lung, not provided).



Lung, sheep. Neutrophils fill airways (top right) as well as alveoli, where they are admixed with variable amounts of polymerized fibrin. There is diffuse type II pneumocyte hyperplasia. (HE, 140X)

Contributor's Comment: The lesions in the (cranioventral) lung are characteristic for an infection with *Mannheimia haemolytica*, which was confirmed by bacterial culture. The isolated *Trueperella pyogenes* most likely represents an opportunistic bacterium.

Mannheimia haemolytica (formerly *Pasteurella haemolytica*, biotype A), a gram-negative coccobacillus, is a common cause of fibrinous and necrotizing pneumonia and pleuropneumonia in cattle, sheep, and goats. Although pneumonic manheimiosis has been most extensively investigated in bovines, pathologic lesions in sheep are essentially similar to those described for cattle, with few differences. In sheep, the disease may be acute or chronic. In the acute form, there may be a hemorrhagic or fibrinonecrotic lobar pneumonia and fibrinous pleuritis, whereas in the chronic form, a fibrinopurulent bronchopneumonia with secondary abscessation

and fibrinous adhesions to the thoracic wall are common. Additionally, serous to serofibrinous fluid may also be seen in the pericardial sac and pleural and peritoneal cavities.⁵

Mannheimia haemolytica is an opportunistic pathogen; it is a normal inhabitant of the nasopharynx and tonsils of cattle and sheep.^{3,7} Although the exact mechanisms are not known, stress or concurrent viral infections may alter the local innate and adaptive immune responses, contributing to the development of disease. The organism also possesses several virulence factors, including leukotoxin (LKT), lipopolysaccharide (LPS), adhesins, capsule, outer membrane proteins, and various proteases which allow promote colonization of the lung and evasion of the host immune response.^{3,5,7}

The roles of LKT and LPS in the pathogenesis of pulmonary manheimiosis

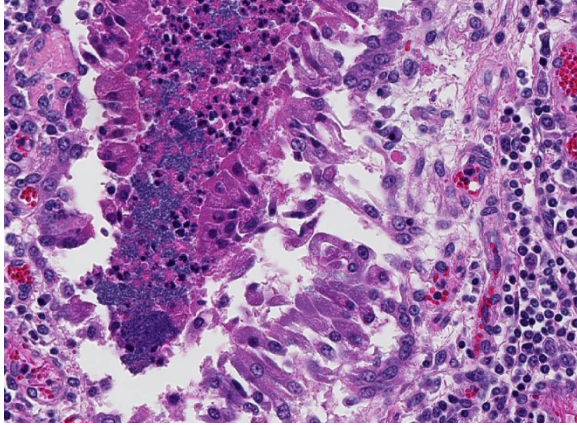
are most well known in bovines with similar effects in small ruminants. LKT is a 102- to 105-kDa protein that is produced by all serotypes during the logarithmic phase of bacterial growth.^{3,5,7} This pore-forming cytotoxin is a member of the RTX (repeats in ToXin) family of toxins. These toxins are genetically related, sharing a highly conserved motif consisting of a series of glycine-aspartic acid nonapeptide repeats in the carboxy terminal third of the LKT protein molecule.⁷ This motif serves two critical functions; it is involved in calcium binding which induces leukocyte toxicity and contains a recognition site required for transport of LKT across biological membranes in bacteria.⁷ Although members of the RTX family of toxins are genetically similar, they differ in the target cell specificity. Other members of the RTX family and their toxins include: *Actinobacillus actinomycetemcomitans* (LtxA), *Actinobacillus pleuropneumoniae* cytotoxins (ApxI, ApxII, ApxIII, ApxIV), *Escherichia coli* alpha hemolysin, *Actinobacillus suis* subs *haemolyticus* toxin (Aqx), *Fusobacterium necrophorum* LKT, *Bibersteinia trehalosi*, and *Bordetella pertussis* hemolysin.⁷

Pneumonia due to *Mannheimia haemolytica* occurs only in ruminants, in part due to LKT-induced effects which are specific for ruminant macrophages, lymphocytes, neutrophils, and platelets.^{3,5,7} The response to LKT is species-specific and dose-dependent. Species specificity is due to the selective interaction of LKT with β 2 integrin LFA-1 (lymphocyte function-associated antigen 1; CD11a/CD18 on target host cells).⁷ At low levels, LKT activates neutrophils and macrophages to stimulate respiratory burst and degranulation, release of proinflammatory cytokines TNF α , IL-1, and IL-8 and histamine from mast cells, and inhibit lymphoid proliferation.⁷ At higher concentrations, leukocytes undergo ap-

optosis, whereas at highest concentrations, LKT causes transmembrane pore formation, cell swelling, and oncotic cell death.^{3,5,7} Pulmonary damage occurs subsequent to the leakage of oxygen free radicals, superoxide anions, lysosomal enzymes, and arachidonic acid metabolites into pulmonary parenchyma.⁷

Pulmonary lesions also occur due to LPS, a molecule composed of polysaccharide side chain (O antigen), lipid A, and inner and outer cores of oligosaccharides. Lipid A is responsible for eliciting endotoxic effects, such as fever and hypotensive shock.¹ It is a potent vasodilator, is directly toxic to pulmonary endothelium, and can recruit neutrophils.^{3,5} LPS stimulates alveolar macrophages to produce proinflammatory cytokines, reactive oxygen and nitrogen intermediates, and other mediators that participate in the inflammatory process, including IL-1 β , IL-8, leukotriene 4, prostaglandin E₂, and TNF α from leukocytes.⁷ An influx of neutrophils occurs secondary to these proinflammatory cytokines and chemotactic mediators. LPS also enhances the effects of LKT.⁷

Although the sections of caudodorsal lung were not submitted, the lesions are worth mentioning as they were most suggestive of ovine lentiviral pneumonia, or maedi-visna (ovine progressive pneumonia). Lentiviruses (Retroviridae) cause slowly progressive inflammation in a variety of tissues, with the lung, CNS, mammary gland, and joint most commonly affected.¹ Syndromes may occur independently or concurrently in any combination. The primary pathologic change is infiltration of lymphocytes into the affected tissues, with occasional formation of lymphoid follicles similar to those seen in lymph nodes.¹ The respiratory form in sheep, *maedi* (“dyspnea in Icelandic) is the most common form in sheep usually greater than 3 years of age. Encephalitis, or *visna* (“fading away” in Icelandic), may present as



Lung, sheep. Large colonies of bacilli are admixed within necrotic debris within airways. (HE, 140X)

ataxia, trembling, and significant weight loss. Mastitis and arthritis also occur, but with little frequency. Small ruminant lentiviruses are primarily transmitted through colostrum or milk, although inhalation of respiratory secretions can occur.¹ In this case, despite the history of neurologic signs, lesions associated with lentiviral infection were not detected in the brain. A commercially available test to confirm this infection is not routinely available, however, given the clinical history and gross and histopathological findings in the lung, lentiviral infection remains a likely differential in this case.

JPC Diagnosis:

1. Lung: Bronchopneumonia, fibrinosuppurative, chronic-active, diffuse, severe with fibrinous pleuritis, multinucleate giant cells, and colonies of bacilli.
2. Lung: Interstitial pneumonia, lymphohistiocytic, multifocal, mild.
3. Heart: Essentially normal tissue.

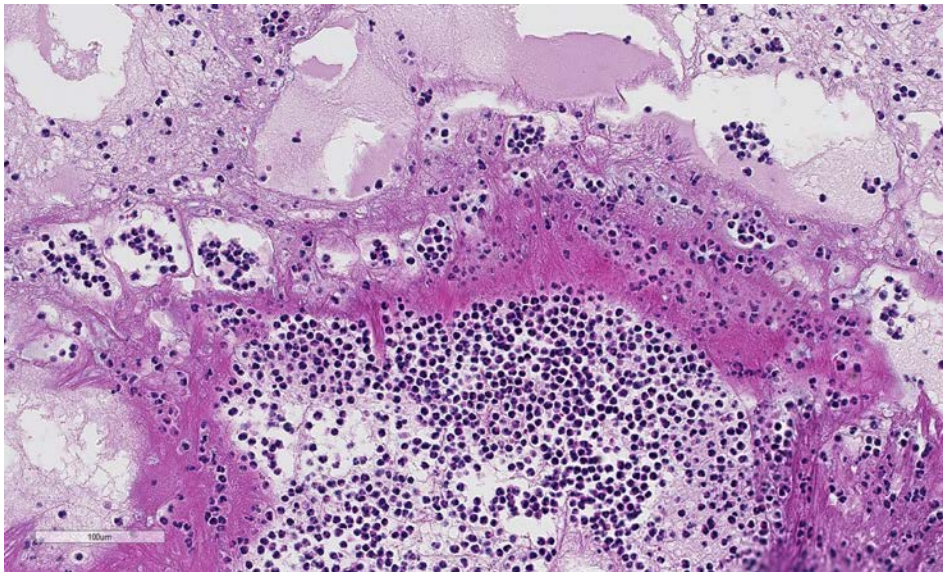
Conference Comment: Ovine pneumonic manheimiosis is a common and economically important disease of sheep;

pulmonary infection is often facilitated by various stressors, including concurrent viral infection. Severe fibrinous and/or suppurative bronchopneumonia is characteristic and fibrinous pleural adhesions may be seen in some severe cases.⁴ Grossly, pulmonary lesions due to *M. haemolytica*, *H. somni*, *B. trehalosi*, *Mycoplasma mycoides mycoides* (small colony variant

) and *P. multocida* may be indistinguishable, as all include a cranioventral, lobular distribution with or without the presence of fibrinous pleuritis, although well-demarcated foci of necrosis will distinguish both *M. haemolytica* and *H. somni*. Albeit characteristically attributed to *M. haemolytica* infection, leukocyte necrosis may also be seen in cases of *H. somni* infection. The presence of suppurative phlebitis with fibrinoid necrosis is more common in cases of *H. somni* infection.² *M. hemolytica* is also a common cause of mastitis in sheep, which can be a problem in both dairy and non-dairy flocks. In addition to *M. hemolytica*, *M. glucosida* may also cause pneumonia and mastitis in sheep. Horizontal transmission is common, with nursing being suggested as the major method of transmission, where the organism is passed to the mammary gland from the nasopharynx of the lamb.⁶

Besides the obvious fibrinosuppurative bronchopneumonia in the submitted sections, there was extensive discussion conference participants also identified a mild interstitial pneumonia with infiltration and expansion of alveolar septa. The mild interstitial component along with occasional albeit prominent cuffing of vessels and small airways by mononuclear inflammatory cells (with a majority of lymphocytes) generated discussion of a concomitant lentiviral infection. Lentiviral pneumonia, as discussed above, was postulated to be present in the

caudal-dorsal sections of lung which were not submitted. Although not conclusive, viral infection may have, or perhaps likely, resulted in a secondary bronchopneumonia in this animal. Ovine progressive pneumonia (maedi-visna) may cause severe interstitial pneumonia with BALT hyperplasia, thickened alveolar septa and peribronchial lymphocytic infiltrates. Alveolar fibrosis and smooth muscle hyperplasia, the latter of which was described in this case, may also be seen.⁴ The presence of multinucleated giant cells within alveoli was perplexing to some conference participants. However, macrophages and multinucleated histiocytes may be seen in more chronic cases of bacterial bronchopneumonia, particularly in areas of abundant fibrin exudation as they



Lung, sheep. The pleura are covered with a 5mm-thick mat of fibrin throughout which are scattered aggregates of neutrophils. (HE, 116X)

help facilitate removal of fibrin.² Many conference participants supposed an etiologic diagnosis of *Pasteurella multocida* in this case due to absence of characteristic leukocyte necrosis with the linear streaming pattern, termed “oat cells,” typically seen in *Mannheimia* infection, as well as the lack of significant epithelial necrosis in airways

(described as a feature of *P. multocida* infections.)

Contributing Institution:

Diagnostic Center for Population and Animal Health
Michigan State University
www.animalhealth.msu.edu

References:

1. Blacklaws BA. Small ruminant lentiviruses: Immunopathogenesis of visna-maedi and caprine arthritis and encephalitis virus. *Comp Immun, Micro, and Inf Dis.* 2002; 35: 259-269.
2. Caswell JL, Williams KJ. In: Maxie MG, ed. *Jubb, Kennedy, and Palmer's Pathology of Domestic Animals.* 6th ed. Vol 2. St. Louis, MO: Elsevier; 2016:544-547.
3. Jeyaseelan S, Sreevatsan S, Maheswaran SK. Role of *Mannheimia haemolytica* leukotoxin in the pathogenesis of bovine pneumonic pasteurellosis. *Anim Health Res Rev.* 2002; 3(2): 69-82.
4. López A. Respiratory system, mediastinum, and pleurae. In: Zachary JF, McGavin MD. eds. *Pathologic Basis of Veterinary Disease.* 5th ed. St. Louis; Mosby Elsevier; 2012:516-517.
5. Mohamed RA, Abdelsalam EB. A Review of Pneumonic Pasteurellosis (Respiratory Mannheimiosis) with Emphasis

on Pathogenesis, Virulence Mechanisms, and Predisposing Factors. *Bulg J of Vet Med.* 2008; 11(3): 139-160.

6. Omaleki L, Browning GF, Allen JL, Barber SR. Molecular epidemiology of *Mannheimia haemolytica* and *Mannheimia glucosidal* associated with ovine mastitis. *J Diag Invest.* 2012; 24(4):730-734.

7. Singh K, Ritchey JW, Confer AW. *Mannheimia haemolytica*: Bacterial-Host Interactions in Bovine Pneumonia. *Vet Path.* 2011; 48(2): 338-348.

CASE III: 2014#2 (JPC 4066678).

Signalment: 5 year-old, castrated male, bovine (*Bos taurus*)

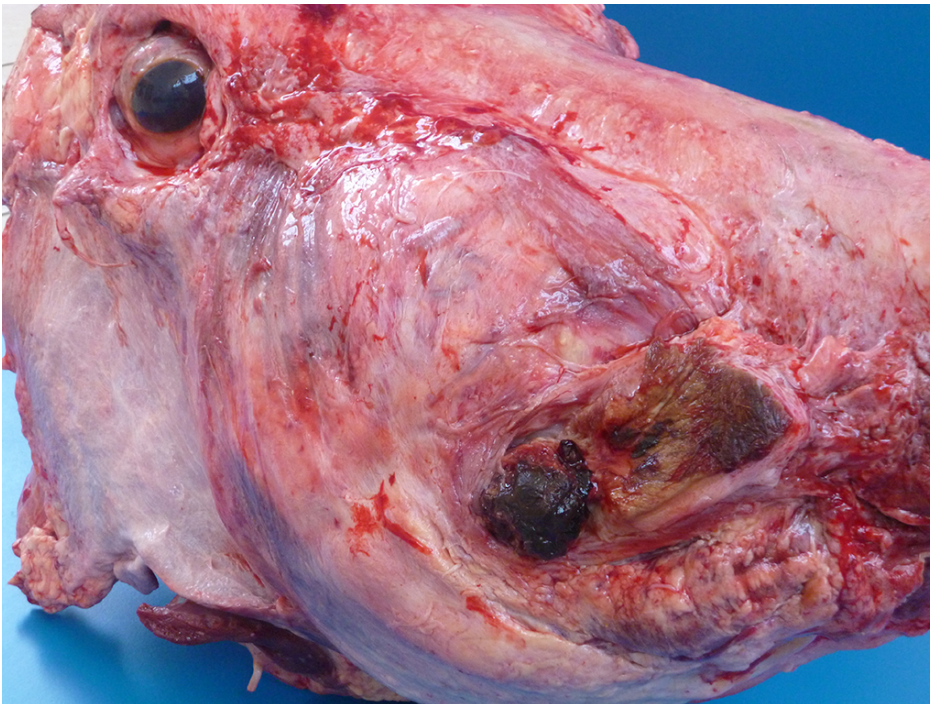
History: The head was deformed by a hard swelling of the right maxilla of several months of evolution that resulted in difficult breathing and weight loss. Due to poor

prognosis, the practitioner advised the owner to send the steer to the slaughterhouse.

Gross Pathology: A 25x12cm hard mass extended from the base of the right ear to around the right eye. In the rostral end of the mass there was a 7x4 cm cavity filled with dark, friable necrotic tissue. At the cut surface of a section in middle part of the bridge of the nose, the nasal cavity was deformed by a mass consisting of bony proliferation. Within the mass, there were focally extensive semisolid (caseous) yellow areas of irregular contour. These areas were surrounded by a dark green halo (necrotic tissue). Extensive firm white fibrotic tissue was also noticed at the cut surface of the lesion. The lesion destroyed the nasal turbinates and markedly displaced the nasal septum to the left.

Laboratory Results: NA

Histopathologic Description: Lesions consist of multiple pyogranulomas surrounded by well-defined and well-differentiated osseous trabeculae. In the center of these pyogranulomas there are structures consisting of an inner mass of filamentous bacilli that stained blue (gram-positive) in the Gram stain. This center is surrounded by strongly eosinophilic radial clubs (Splendore Hoeppli [SH] phenomenon) which are, in turn, surrounded by an inner layer of neutrophils and an outer layer of epithelioid macrophages and



Maxilla, ox. A 25x12 cm hard mass extended from the base of the right ear to around the right eye. In the rostral end of the mass there was a 7x4 cm cavity filled with dark, friable necrotic tissue (Photo courtesy of: Setor de Patologia Veterinária, UFRGS, <http://www.ufrgs.br/patologia/>)

occasionally multinucleated giant cells. Occasionally, these SH structures are mineralized. Extensive fibrous tissue sprinkled with neutrophils, lymphocytes, and plasma cells surrounds the inflammatory reaction and extend into adjacent soft tissues. In some HE-stained sections, weakly basophilic bacilli are seen in the cytoplasm of epithelioid cells, multinucleated giant cells, and in the center of the SH phenomenon; fragments of these structures were also phagocytosed by multinucleated giant cells.

Contributor's Morphologic Diagnosis:

Maxillary pyogranulomatous osteomyelitis, castrated male, mixed breed, bovine.

Etiologic diagnosis: Bacterial osteomyelitis.

Etiology: *Actinomyces bovis*

Name of the condition: Actinomycosis.

Contributor's Comment: Actinomycosis is a pyogranulomatous osteomyelitis that primarily affects cattle and is caused by the gram-positive bacterium *Actinomyces bovis*.⁹ Occasionally other species such as pigs, deer, sheep, goats and horses are affected.⁹ A similar species of bacterium, *A. israeli*, is responsible for the disease in human beings.⁶ The affected bone is thickened from multiple coalescing pyogranulomas that impart to the bone tissue a honeycomb appearance.⁵ The inoculation of *A. bovis* – a commensal organism of the oral cavity – into the oral mucosa of animals can

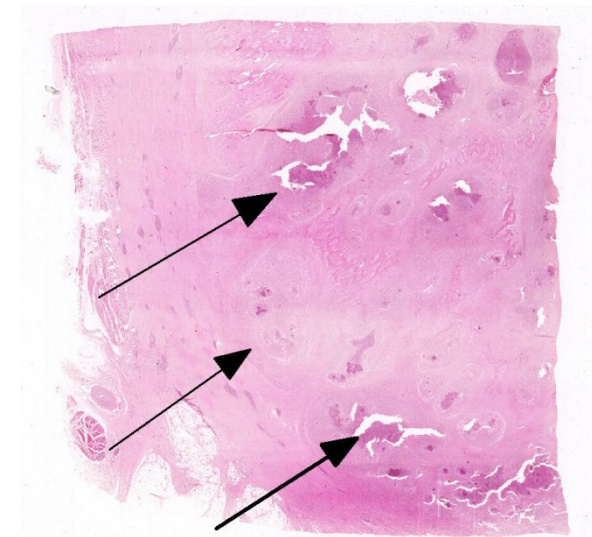


Maxilla, ox. The maxilla and nasal cavity were markedly deformed by a fibrous mass containing multiple foci of yellow caseous necrotic tissue surrounded by a green halo. (Photo courtesy of: Setor de Patologia Veterinária, UFRGS, <http://www.ufrgs.br/patologia/>)

be facilitated by small wounds from hard straw present in the feed, foreign bodies and dental eruption.⁹

Although actinomycosis has been described in cattle at unusual sites such as the penis and in the maxilla, as in the case presented here, the classical presentation in cattle is in the mandible and rarely in the maxilla.^{9,12} It is likely that the reason the mandible is the preferred site is because the direction of vegetal fibers being chewed is downwards forcing the fiber between the teeth and the gums, providing an entrance for the bacterium and resulting initially in a dental alveolitis.

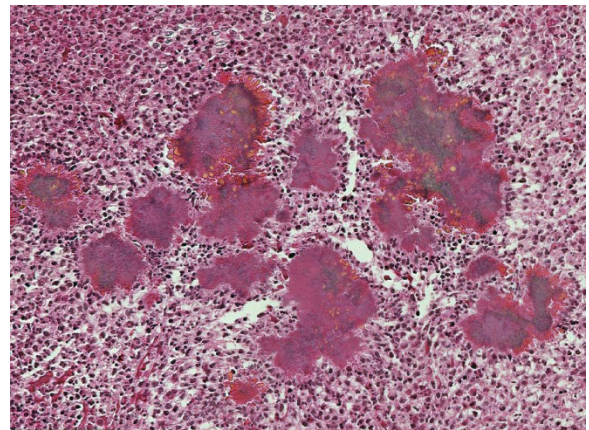
Lesions of actinomycosis grow slowly over time^{5,12} and the involvement of the bone and muscle tissue becomes so marked that it interferes with feeding,⁹ which would explain the emaciation of the ox of this report. In osteomyelitis caused by actinomycosis, initially there is development of suppurative sinus tracts in the medullary spaces of the bone leading to multiple foci of both bone tissue resorption and proliferation. Bone sequestration does not occur; even if the cortical bone is invaded, probably due to the progressive course of



Maxilla, ox. In this decalcified section of the maxillary mass, abundant collagen surrounds areas of necrosis and pyogranulomatous infiltrate (arrows). (HE, 4X)

the disease.⁹ The small granules – known colloquially as sulfur granules – observed grossly at the center of the caseous nodules¹ represents the bacterial colonies and the associated SH phenomenon and are typical of actinomycosis, although can be seen in other pyogranulomatous diseases of cattle such as actinobacillosis and staphylococcosis.⁸

Little is known about the virulence factors of *A. bovis*. The interaction between ligand-



Maxilla ox. Centrally within necrotic/pyogranulomatous areas, there are colonies of small bacilli surrounded by club-shaped brightly eosinophilic Splendore-Hoeppli material. (HE, 256X)

receptor in the target cells, toxins, molecules in the bacterial capsule that compromise phagocytosis, and other factors are probably involved in the pathogenicity of *A. bovis*. It is also probable that *A. bovis* is capable of escaping destruction by neutrophils and macrophages and is capable of colonizing the tissue abscesses. This peculiar resistance of the agent to phagocytosis leads to the formation – around itself – of proteinaceous eosinophilic aggregates consisting of immunoglobulins, which are observed histologically as the SH reaction.¹³ Other bacteria induce similar tissue reactions, particularly *Actinobacillus lignieresii*. However *A. bovis* colonies are larger and the radiating clubs in the SH reaction are shorter and less marked than in actinobacillosis, and

generally localized at the periphery of the colonies.^{4,8,10} Additionally, actinobacillosis is a disease of soft tissues and the microorganisms of *A. lignieresii*, in contrast to those of *A. bovis*, are gram-negative.^{5,8} *Fusobacterium necrophorum* and other bacteria can cause osteomyelitis by direct extension of peri-odontitis; however lesions induced by *F. necrophorum* are usually more destructive and less proliferative.⁹

Grossly, a lesion such as the one described here can be mistaken for - and the lesion was initially interpreted as - a squamous cell carcinoma at the slaughterhouse. Due to great extension of the lesions and the invasive characteristics of the mass reported here, an intranasal squamous cell carcinoma should be in the top of the list as a differential diagnosis at gross examination since this is one of the tumors more frequently observed in the nasal cavity or ruminants.¹¹ At cursory gross examination, the keratin commonly formed in these

tumors may resemble the sulfur granules of actinomycosis.

JPC Diagnosis: Bone: Osteomyelitis, pyogranulomatous, chronic, diffuse, severe, with bone resorption, Splendore-Hoeppli material, and numerous bacterial colonies.

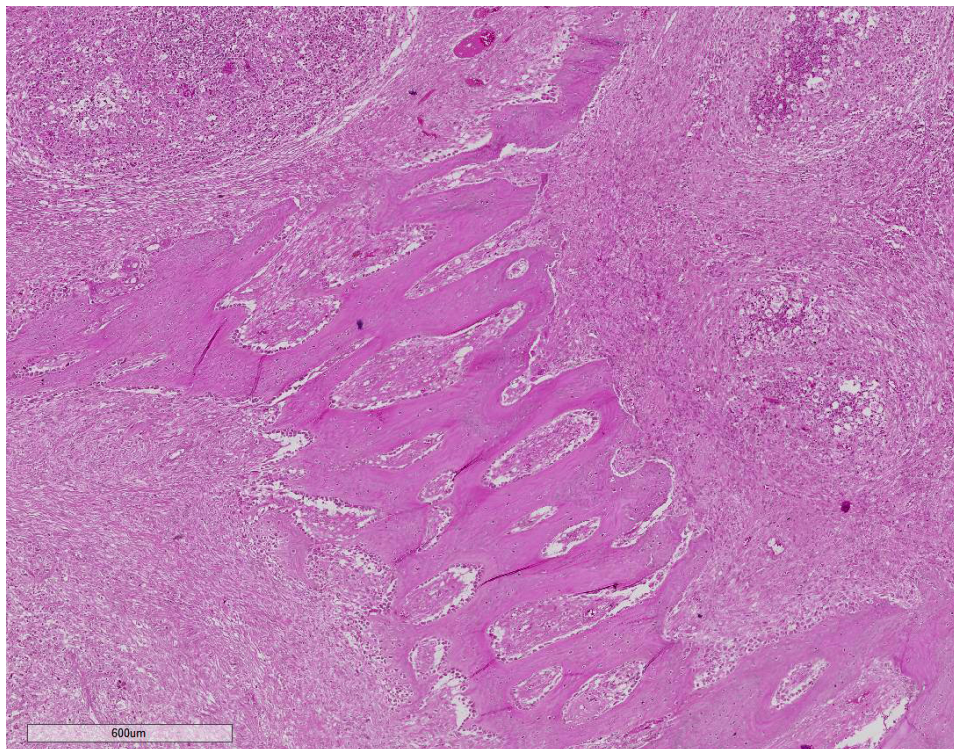
Conference Comment: “Lumpy jaw” not only occurs in domestic species, but also occurs in many wild ungulates, where it can be particularly problematic due to challenges associated with treating an aggressive infection in fractious animals. *Actinomyces bovis* is the most commonly associated agent resulting in pyogranulomatous mandibular (or rarely maxillary) osteomyelitis but bony malformations of the jaw may also occur secondary to periodontal infection. Mandibular osteomyelitis involving the dentition is an important cause of morbidity in older exotic hoofstock, where it has also been

referred to as chronic alveolar osteomyelitis.³

Inciting lesions may include a periodontal or tooth root abscess and/or a chronic pulpitis secondary to enamel or dentin abnormalities.

Anaerobic bacteria can result in persistent dental infections which are challenging to treat successfully resulting in a chronic condition.³

Organisms such as *Fusobacterium necrophorum* and other non-specific



Maxilla, ox. Few trabecular remnants of periosteal new bone are entrapped within the inflammatory lesion. (HE, 35X)

bacteria that result in osteomyelitis as an extension from periodontal infection are generally more de-structive and less proliferative than lesions caused by *A. bovis* but lesions retain some similarities with actinomycosis in location and gross appearance.²

“Lumpy jaw” has also been described in a domestic cat and resembles the condition described in cattle. The cat in that case report did not have a history of trauma and the infection was due to *Nocardia* sp. The mass demonstrated progressive enlargement but was non-painful and initially did not interfere with eating or drinking. The proliferative lesion revealed new bone formation, osteolysis and clusters of filamentous bacteria surrounded by eosinophilic amorphous material and mixed inflammatory cells, predominantly neutrophils. The patient in that report demonstrated poor response to treatment and was humanely euthanized. On sectioning, the enlarged mandible had numerous brown nodules, contained a brownish granular material and had a “honeycomb” appearance,⁷ which is also often used to describe the affected mandible in cases of bovine lumpy jaw. The causative agent was identified as *Nocardia cyriacigeorgica*, which is a relatively new species of *Nocardia* and is apparently a common *Nocardia* sp. pathogen in people. Traumatic gingival introduction was postulated as the source of infection in that case.⁷

Contributing Institution:

Setor de Patologia Veterinária, UFRGS
Porto Alegre RS, Brazil
<http://www.ufrgs.br/patologia/>

References:

1. Brewer JS. Discussion and case history: Actinomycosis. *Iowa St. Univ Vet.* 1956; 18:145-208.
2. Craig LE, Dittmer KE, Thompson KG. Bones and Joints. In: Maxie MG, ed. *Jubb, Kennedy, and Palmer's Pathology of Domestic Animals*. 6th ed. Vol 1. St. Louis, MO: Elsevier; 2016:101.
3. Fagan DA, Oosterhius JE, Benirschke K. “Lumpy jaw” in exotic hoofstock: A histopathologic interpretation with a treatment proposal. *J Zoo Wildl Med.* 2005; 36(1):36-43.
4. Ginn PE, Mansell JEKL, Rakich PM. Skin and appendages, In: Maxie MG. ed. *Jubb, Kennedy and Palmer Pathology of Domestic Animals*. 5th ed. Vol1. St. Louis, MO: Elsevier-Saunders; 2007: 553-781.
5. Grist A. Conditions encountered at bovine post mortem inspection (non parasitic). In: Ibid. eds. *Bovine Meat Inspection*. 2nd ed. Nottingham, UK: Nottingham University Press; 2008: 160-239.
6. Miller M, Haddad AJ. Cervicofacial actinomycosis. *Oral Surg. Oral Med. Oral Pathol.* 1998;85:496-508.
7. Soto E, Arauz M, Gallagher CA, Illanes O. *Nocardia cyriacigeorgica* as the causative agent of mandibular osteomyelitis (lumpy jaw) in a cat. *J Vet Diagn Invest.* 2014; 26(4):580-584.
8. Tessele B, Martins TB, Vielmo A et al. 2014. Lesões granulomatosas encontradas em bovinos abatidos para consumo. [Granulomatous lesions found in cattle slaughtered for meat production.] *Pesq Vet Bras.* 2014; 34:763-769.

9. Thompson K. Inflammatory diseases of bones In: Maxie MG. ed. *Jubb, Kennedy and Palmer Pathology of Domestic Animals*. 5th ed. Vol1. St. Louis, MO: Elsevier-Saunders; 2007: 92-105.

10. Till DH and Palmer FPA. A review of actinobacillosis with a study of the causal organism. *Vet Rec*. 1960; 72:527-543.

11. Wilson DW, Dungworth DL. Tumors of the respiratory tract, In: *Tumors in Domestic Animals*. ed. Meuten DJ. 4th. Ames, IA: Iowa State Press; 2002:365-374.

12. Wilson WG. *Wilson's Practical Meat Inspection*. 7th ed. Oxford, UK: Blackwell. 2005.

13. Zachary J.F. Mechanisms of microbial infections, In: Zachary JF and McGavin MD. eds. *Pathologic Basis of Veterinary Disease*. 5th ed. St. Louis, MO: Elsevier-Saunders. 2012:147-241: 2012.

CASE IV: N14-17 (JPC 4066085).

Signalment: 2 year old Thoroughbred colt (*Equus caballus*)

History: The horse was normal and trained as usual the previous day, but did not consume all of his feed the night prior. The referring veterinarian examined the horse at 11 AM; the temperature was 104.8°F, the heart rate was elevated, and he was reluctant to move. He was treated with Banamine and Bactrim. The horse died spontaneously at 3:30 PM, at which time bloody froth was expelled from both nostrils.

Gross Pathology: The kidneys are bilaterally markedly enlarged. The right kidney weighs 1.85 kg and measures 20 x 19 x 8.5 cm, and the left kidney weighs 1.86 kg

and measures 24.5 x 16 x 7 cm (each kidney is approximately 0.42% of body weight; 0.25% is normal). Bilaterally, the perirenal adipose tissue is mildly edematous. There are widespread multifocal, slightly raised, 1 to 10 mm diameter, tan-yellow foci on the subcapsular surface of both kidneys which occasionally bulge from the capsular surface. The discoloration frequently ex-



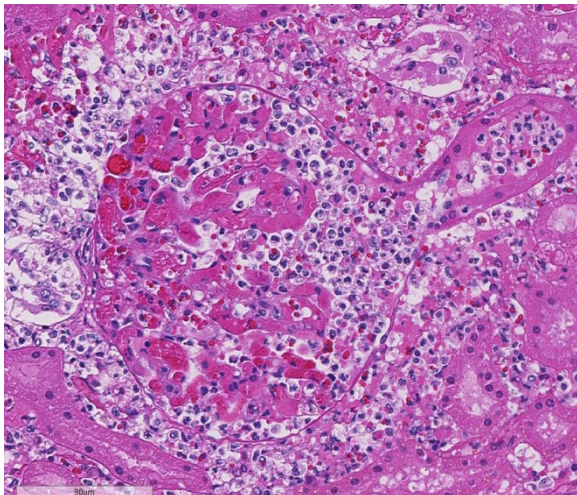
Kidney, foal: At low magnification, there are multifocal areas of cellular infiltration within the renal cortex. (HE, 5X)

tends into the renal capsule and occasionally into the perirenal adipose tissue. The capsules are friable and difficult to peel. Both kidneys moderately bulge on cut surface, and the cortices contain myriad 1mm diameter to 9 x 2 mm yellow-tan foci which occasionally have a cavitated center.

Laboratory Results: Microbiology: Aerobic culture of the kidney yielded heavy growth of *Actinobacillus equuli* ssp. *equuli*.

Histopathologic Description: Predominantly in the cortex, there are multifocal to coalescing, nodular inflammatory infiltrates predominantly of degenerate neutrophils, fewer macrophages, and cellular debris. This infiltrate is often centered on glomeruli, extending into and sometimes effacing the adjacent interstitium and renal tubules. Renal tubules in inflamed areas are sometimes degenerate or necrotic. Larger blood vessels sometimes contain luminal aggregates of fibrin, degenerate and viable neutrophils, cellular debris and erythrocytes; inflammation often extends into the vessel wall (vasculitis). Many foci of inflammation contain aggregates of gram-negative bacilli.

Contributor's Morphologic Diagnosis:



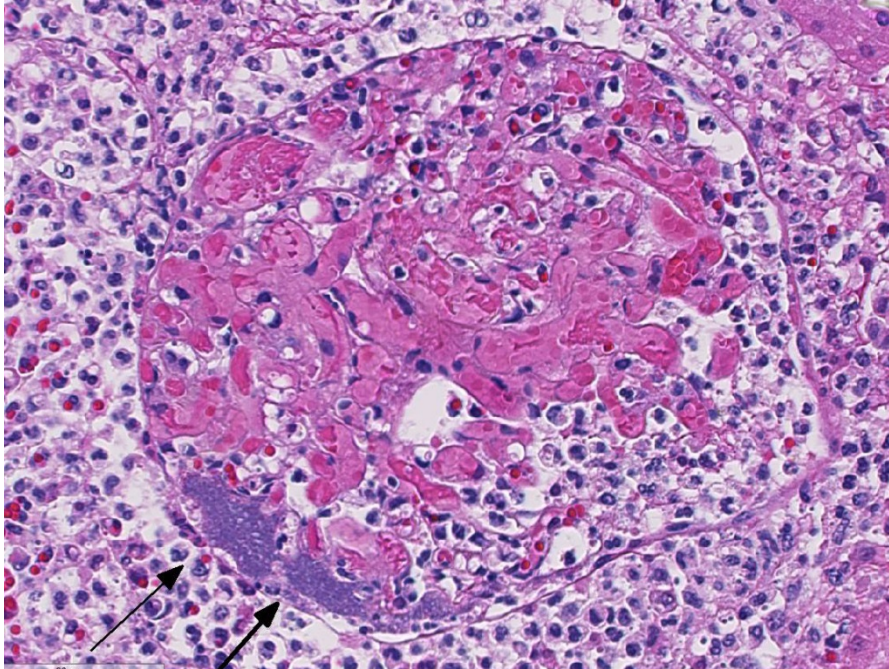
Kidney, foal: Suppurative inflammation is centered on glomeruli throughout the cortex. (HE, 220X)

Embolic nephritis, suppurative, acute, multifocal to coalescing, severe, with intralesional gram-negative bacilli and vasculitis.

Contributor's Comment: The most frequently isolated agent in equine cases of embolic nephritis is *Actinobacillus equuli*, most often secondary to septicemia of foals.⁴ *A. equuli* is a gram-negative bacillus that can be normal flora of the oral cavity, reproductive tract and intestinal tract of horses.^{2,5} It is especially known for its tendency to create microabscesses in the kidneys and other organs.⁴ In foals, *A. equuli* typically causes septicemia, also known as sleepy foal disease.² Septicemic lesions typically include embolic lesions in the kidney, lungs and liver, with lesions also reported in the umbilicus, adrenal gland, and joints.² In adult horses, *A. equuli* has been reported to cause sepsis, nephritis, endocarditis, pericarditis, peritonitis, enteritis, pleuropneumonia, arthritis, periorchitis, and abortion.^{2,3,5} *A. equuli* infections in adult horses are thought to be predisposed by stress or other infections, such as respiratory viruses or salmonellosis.²

JPC Diagnosis: Kidney: Nephritis, embolic, suppurative, multifocal, marked with necrotizing vasculitis and colonies of bacilli.

Conference Comment: Actinobacillosis in adult horses is uncommon and most frequently associated with an underlying disease. There are two subspecies of *A. equuli*, a hemolytic subspecies termed *A. equuli* subsp. *haemolyticus* which is isolated from the normal oral cavity and respiratory tract, and a non-hemolytic form termed *A. equuli* subsp. *equuli*, which also resides in the oral cavity as well as the gastrointestinal tract of adult horses and is the agent of



Kidney, foal: Glomerular capillaries contain fibrin thrombi, and rare, colonies of bacilli within capillary loops or free in Bowman's space (arrows) (HE, 324 X)

In cases of embolic nephritis, bacteria become lodged in glomerular capillaries resulting in the presence of suppurative lesions or abscesses and, in some cases, when emboli are large enough, may occlude arteries resulting in septic infarcts. In septicemic foals that survive for a period of time, microabscesses will be seen in multiple organs and polyarthritis will be present. *A. equuli* may also cause diarrhea and hemorrhagic enteritis in foals.

septicemia in foals.¹ The hemolytic form has been associated with various infections including peritonitis, reproductive failure and respiratory disease. The bacterium possesses an RTX exotoxin known as Aqx that is cytotoxic to equine red blood cells. The non-hemolytic subspecies is more commonly present in cases of septicemia and may also be associated with respiratory disease, embolic nephritis and infection in other organs as well.¹ In septicemic cases, *Actinobacillus* can act as the primary agent or be a secondary infection following other viral or bacterial infections. The presence of endotoxin likely plays a role in the endothelial damage, vasculitis and bacterial emboli which are classically seen in septicemic cases. Although most often associated with foals in conjunction with events such as failure of passive transfer, septicemic lesions such as embolic nephritis, as seen in this case, as well as pneumonia, may be seen in adult horses.¹

A common agent of embolic nephritis in swine, perhaps the most common, is *Erysipelothrix rhusiopathiae*; in cattle the common agent is *Trueperella pyogenes*; and in sheep and goats *Corynebacterium pseudotuberculosis* may be associated with embolic infections.¹ Although uncommon, *A. equuli* infection can be associated with endocarditis or myocarditis in adult horses⁶ and has also been associated with reproductive losses.

Conference participants described the prolific inflammatory infiltrates as being centered on vessels as well as effacing glomeruli, with adjacent tubules being secondarily affected with varying severity. Tubules are multifocally ectatic and variably contain necrotic, sloughed tubular epithelial cells admixed with fibrin, hemorrhage and proteinaceous fluid. Fibrin thrombi with colonies of coccobacilli are occasionally seen in glomerular tufts. Some conference participants interpreted the most severely affected area of the cortex as coagulative

necrosis secondary to infarction due to fibrin thrombi; others attributed the tinctorial change as more consistent with some degree of autolysis. ⁷The differential diagnosis discussed by participants in the case of this horse included *Escherichia coli*, *Klebsiella* sp., *Streptococcus* sp., *Rhodococcus equi* and *Salmonella* species.

Contributing Institution:

University of Florida, College of Veterinary Medicine, Department of Infectious Diseases and Pathology, Anatomic Pathology Service

<http://idp.vetmed.ufl.edu/>

References:

1. Cianciolo RE, Mohr FC. Urinary System. In: Maxie MG, ed. *Jubb, Kennedy, and Palmer's Pathology of Domestic Animals*. 6th ed. Vol 2. St. Louis, MO: Elsevier; 2016:432-433.
2. Layman QD, Rezabeck GB, Ramachandran A, Love BC, Confer AW. A retrospective study of equine actinobacillosis cases: 1999-2011. *J Vet Diagn Invest*. 2014; 26(3):365-375.
3. Matthews S, Dart AJ, Dowling BA, Hodgson JL and Hodgson DR. Peritonitis associated with *Actinobacillus equuli* in horses: 51 cases. *Aust Vet J*. 2001; 79(8): 536-9.
4. Maxie, MG, Newman SJ. Urinary System. In: Maxie MG, ed. *Jubb, Kennedy, and Palmer's Pathology of Domestic Animals*, 5th ed. Vol 2. Edinburgh: Elsevier Saunders. 2007:479-480.
5. Patterson-Kane JC, Donahue JM and Harrison LR. Septicemia and peritonitis due to *Actinobacillus equuli* infection in an adult horse. *Vet Pathol*. 2001; 38(2): 230-2.
6. Robinson WF, Robinson NA. Cardiovascular system. In: Maxie MG, ed. *Jubb, Kennedy, and Palmer's Pathology of Domestic Animals*. 6th ed. Vol 3. St. Louis, MO: Elsevier; 2016:31-42.
7. Uzal FA, Plattner BL, Hostetter JM. Alimentary System. In: Maxie MG, ed. *Jubb, Kennedy, and Palmer's Pathology of Domestic Animals*. 6th ed. Vol 2. St. Louis, MO: Elsevier; 2016:114.

**Joint Pathology Center
Veterinary Pathology Services**



WEDNESDAY SLIDE CONFERENCE 2015-2016

C o n f e r e n c e 25

18 May 2016

Patricia Pesavento, DVM, PhD, DACVP
Professor of Pathology, Microbiology & Immunology
UC Davis School of Veterinary Medicine
Davis, CA

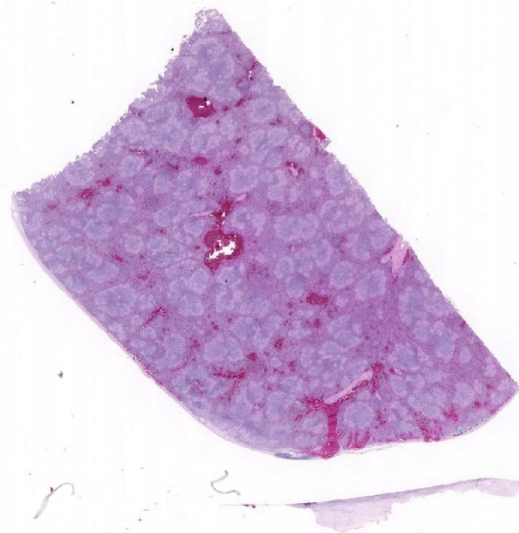
CASE I: H11-003673 (JPC 4021637).

Signalment: 10-week old, male, turkey, (*Meleagris gallopavo*).

History: One of three turkeys found dead without premonitory signs on one day from a large flock of commercial fattening birds. Further individual birds also died over the following two weeks.

Gross Pathology: In good body condition, severe diffuse hemorrhagic enteritis and splenomegaly. Pale mottling of spleen by multifocal 0.5 to 3mm diameter, white, round to irregularly-shaped lesions.

Laboratory Results: No significant bacteria isolated from spleen or small intestine following aerobic and anaerobic culture on blood agar. PCR on splenic samples detected turkey hemorrhagic enteritis virus (THEV).⁷

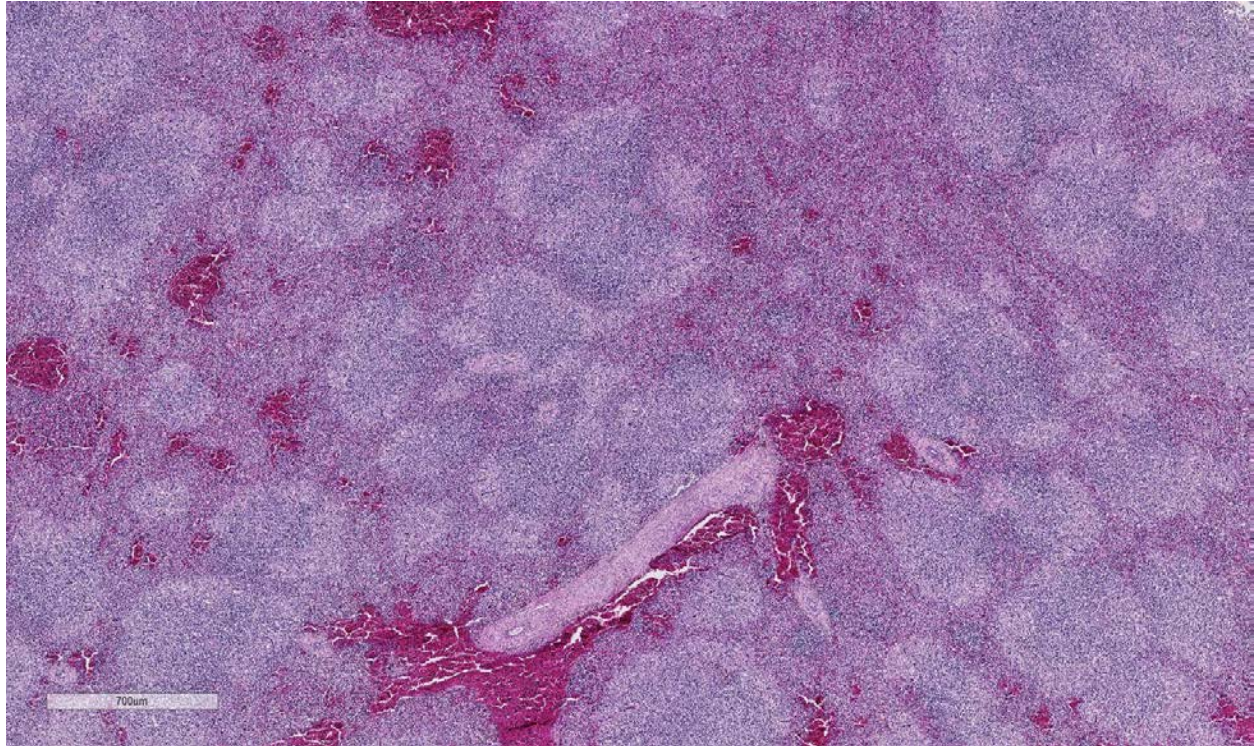


Spleen, turkey. At subgross, this section of enlarged spleen contains numerous coalescing areas of white pulp. (HE, 5X)

Histopathologic Description: Spleen: Multifocal to coalescing areas of necrosis in white pulp area containing eosinophilic amorphous material together with moderate

numbers of admixed heterophils, macrophages, lymphocytes and plasma cells. There is accompanying diffuse severe vascular congestion. Numerous large cells (approximately 15 μm in diameter) contain large nuclei (approximately 12 μm in diameter) which in turn exhibit large basophilic intranuclear inclusions with associated chromatin margination.

resulting in depression, bloody diarrhea, splenomegaly, immunosuppression and death.⁷ The most consistent postmortem finding is splenomegaly with a multifocal to coalescing splenitis with individual cell necrosis and large intranuclear inclusions affecting lymphocytes.^{1, 11} Intestinal lesions and the scale of the mortality depends at least in part on the virulence of the THEV strain.^{9,10} THEV is classified as a type II



Spleen, turkey. White pulp is expanded but hypocellular due to a marked loss of lymphocytes and an infiltrate of large histiocytes. (HE, 18X)

Contributor's Morphologic Diagnosis:

Necrotizing splenitis: acute; multifocal to coalescing; severe, with basophilic intranuclear inclusions consistent with a diagnosis of turkey hemorrhagic enteritis.

Contributor's Comment: The gross and histopathological findings are consistent with a diagnosis of turkey hemorrhagic enteritis (THE) disease of turkeys caused by infection with THEV.¹¹ This was confirmed by PCR. HE affects growing turkeys

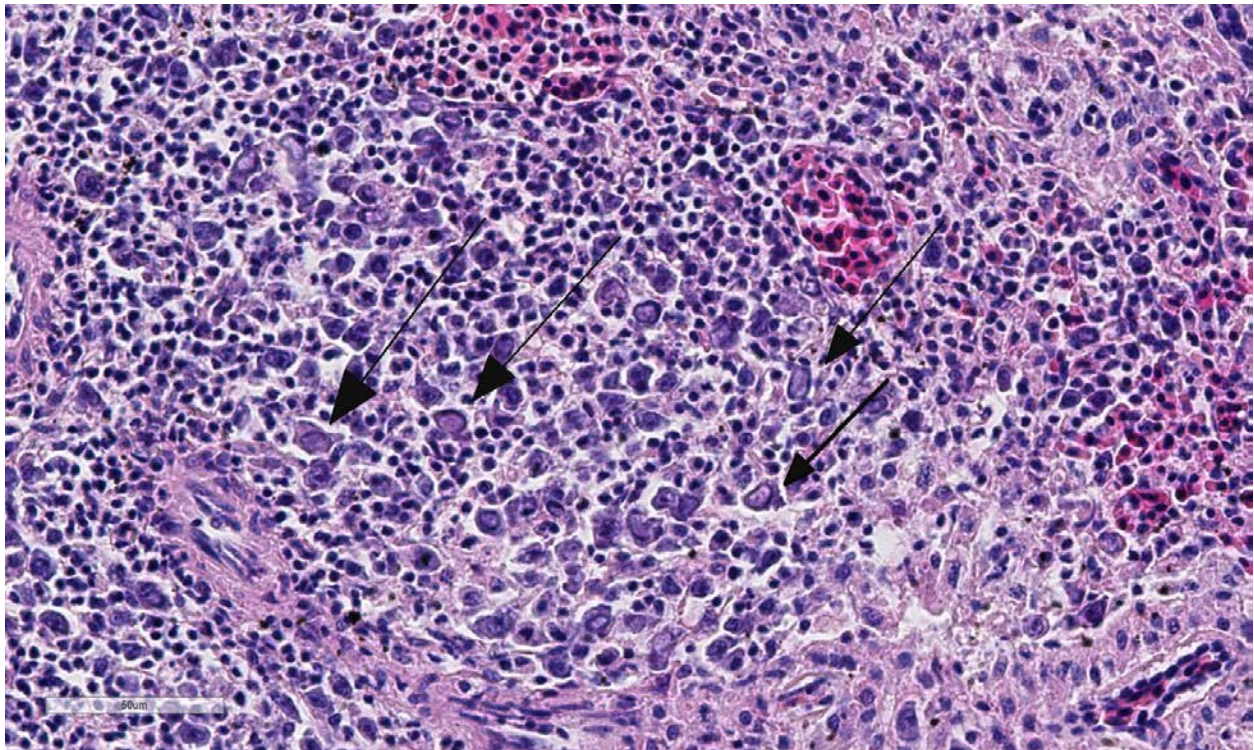
adenovirus, of the family Adenoviridae, and has been further classified as a member of the more recently formed genus *Siadenovirus*.^{1,4,11} It was originally identified in the USA, where it has been widely reported.¹¹ The virus spreads via horizontal transmission including the oral route and rapidly replicates in the spleen of poults.¹² A necrotizing splenitis is frequently described in the splenic white pulp¹³ with targeting of macrophages and particularly IgM-bearing B-lymphocytes.^{12,13} Infected B-lymphocytes and macrophages undergo both necrosis and

apoptosis.⁹ Although the pathogenesis is incompletely understood infection of turkeys with virulent strains of THEV results in hemorrhage into the lumen of the duodenum and jejunum by erythrocytes diapedesis without obvious attendant vascular injury.⁹

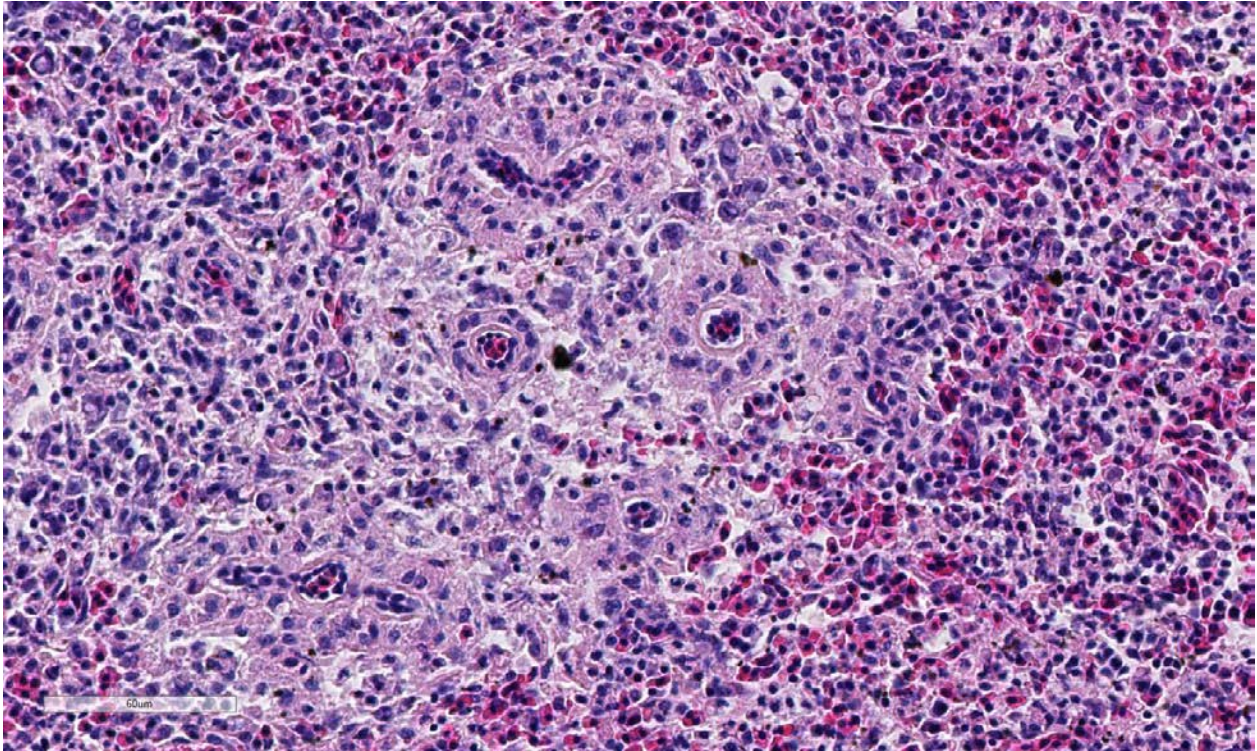
JPC Diagnosis: Spleen: Splenitis, histiocytic, diffuse, severe with lymphoid depletion and intrahistiocytic, intranuclear viral inclusion bodies.

Conference Comment: Adenoviruses in avian or mammalian species may occur as asymptomatic infections or as primary pathogens as seen in this case of THEV. Previously two genera of adenovirus existed, *Mastadenovirus* and *Aviadenovirus*, but the adenoviridae family was revised in 2005 and now includes two additional genera *Siadenovirus* and *Atadenovirus*, the former of which includes THEV.⁶ The *Aviadenovirus* genera, which was previously designated as

group I avian adenovirus, includes many of the pathogenic avian adenovirus diseases including inclusion body hepatitis, quail bronchitis virus and hydropericardium syndrome. *Siadenovirus*, which was previously designated as group II avian adenovirus, in addition to THEV includes MSD in pheasants and “splenomegaly virus” of chickens, another disease very similar to THEV and MSD. This genera is distinguished genetically by the presence of a gene that encodes for sialidase (for which it is named), and also includes an adenovirus of frogs.⁵ *Atadenovirus*, which was previously designated as group III avian adenovirus, includes egg drop syndrome, which is characterized by decreased egg production and thin-shelled eggs; ducks and geese are the natural hosts. *Atadenovirus* also includes viruses which affect mammals and reptiles.^{5,6} Adenoviruses of the *Mastadenovirus* genera include the majority of common mammalian adenoviruses and do not cause disease in avian species.



Spleen, turkey. Histiocytes within splenic white pulp contain large oblong amphophilic to basophilic adenoviral inclusions which peripheralize the chromatin (arrows) (HE, 40X).



Spleen, turkey. Penicilliary vessels within the red pulp are cuffed by several layers of infiltrating histiocytes. (HE, 400X)

The age of affected turkeys is approximately 4 weeks and older, with most infections occurring between 6 – 11 weeks; the course of clinical disease is approximately 7-10 days. Mortality rates may exceed 60%. Due to immunosuppression and secondary bacterial infections or co-infections, such as with *E. coli*, the course of disease and severity of losses can be exacerbated. Infection and recovery, as well as vaccination, provides protection against subsequent challenge.⁸ It is postulated that persistent infection or latency may occur within macrophages or B-lymphocytes in birds infected with avirulent strains of THEV, which are used in live virus vaccines.² The differential diagnosis list for the splenic lesions includes lymphoid neoplasia and bacteremia associated with infections such as *E. coli*, *P. multocida* and *E. rhusiopathiae*.⁸ A similar condition occurs in confinement-raised pheasants of approximately 3-8 months of age due to

infection with an indistinguishable virus, and the condition is known as marble spleen disease (MSD). These two viruses are nearly genetically identical, although the presentation of the disease in these respective species has some distinctions. In pheasants, MSD is characterized by diffuse necrotizing splenitis with hemorrhage and loss of architecture, but generally presents as a respiratory condition in naturally infected birds. Gross lesions may include congested lungs in addition to the splenic changes.⁸ THEV and MSD affect a slightly different age range of fowl but retain many similar features in regards to their effect on the spleen. Macrophages and B lymphocytes are the main target of both THEV and MSD as discussed above and although viral replication chiefly takes place within the spleen, virus may also be found in the intestine, bursa of Fabricius, thymus, liver, kidney and lung.

Conference participants described multifocal areas of pallor characterized by necrosis and loss of B lymphocytes within follicles / white pulp. There is extensive histiocytic infiltration of the spleen, primarily surrounding the vascular tree within the white pulp, and histiocytes frequently contain pale basophilic intranuclear viral inclusion bodies. Inclusion bodies are identified also within morphologically recognizable lymphocytes, although no IHC was performed to definitively establish the range of cell targets. The moderator commented about the histiocytic infiltration around splenic arteries, which is suggestive of the pathogenesis of THEV. The virus has a cytopathic effect on B lymphocytes and also replicates within macrophages, and transient immunosuppression occurs in infection by both virulent and avirulent strains.^{2,8} In response to infection, there is a large influx of macrophages, as well as T-lymphocytes in an attempt to clear the virus.⁸ Conference participants discussed the diagnosis of inflammatory splenitis vs. infiltrative and or necrotizing disease of the spleen. The moderator led a discussion around other features of THEV infection including the rapid clinical course and characteristic presence of hemorrhagic feces just prior to death, for which it is appropriately named. The hemorrhage is thought to be secondary to endothelial disruption and not due to viral destruction.² Grossly, the spleen appears enlarged, friable and mottled.

Contributing Institution:

Veterinary Sciences Centre, School of Veterinary Medicine, University College Dublin,
Belfield, Dublin 4, Ireland
<http://www.ucd.ie/vetmed/>

References:

1. Beach NM, Duncan RB, Larsen CT, Meng XJ, Sriranganathan N, Pierson FW: Comparison of 12 turkey hemorrhagic enteritis virus isolates allows prediction of genetic factors affecting virulence. *J Gen Virol.* 2009; 90:1978-1985.
2. Beach NM, Duncan RB, Larsen CT, Meng XJ. Persistent infection of turkeys with an avirulent strain of turkey hemorrhagic enteritis virus. *Avian Dis.* 2009;53:370-375.
3. Davison AJ, Harrach B: Siadenovirus In: The Springer Index of Viruses, Tidona CA, Darai G, eds. Springer-Verlag: New York, NY; 29-33. 2002.
4. Davison AJ, Benko M, Harrach B. Genetic content and evolution of adenoviruses. *J Gen Virol.* 2003; 84:2895-2908.
5. Fitzgerald SD. Adenovirus infections. In: Swayne DE, ed. *Disease of Poultry*. 13th ed. Ames, IA: Wiley & Sons, Inc; 2013: 289-291.
6. Hafez HM. Avian adenoviruses infections with special attention to inclusion body hepatitis/hydropericardium syndrome and egg drop syndrome. *Pak Vet J.* 2011; 31(2): 85-92.
7. Hess M, Raue R, Hafez HM: PCR for specific detection of haemorrhagic enteritis virus of turkeys, an avian adenovirus. *J Virol Methods.* 1999; 81: 199-203.
8. Pierson FW, Fitzgerald SD. Hemorrhagic enteritis and related infections. In: Swayne DE, ed. *Disease of Poultry*. 13th ed. Ames, IA: Wiley & Sons, Inc; 2013: 309-316.
9. Rautenschlein S, Sharma JM: Immunopathogenesis of haemorrhagic

enteritis virus in turkeys. *Dev Comp Immunol*. 2000; 24:237-246.

10. Saunders GK, Pierson FW, van den Hurk JV. Haemorrhagic enteritis virus infection in turkeys: a comparison of virulent and avirulent virus infections, and a proposed pathogenesis. *Avian Pathol*. 1993; 22: 47-58.

11. Sharma JM. Hemorrhagic enteritis of turkeys. *Vet Immunol Immunopathol*. 1991; 30: 67-71.

12. Suresh M, Sharma JM. Hemorrhagic enteritis virus induced changes in the lymphocyte sub-populations in turkeys and the effect of experimental immunodeficiency on viral pathogenesis. *Vet Immunol Immunopathol*. 1995; 45: 139-150.

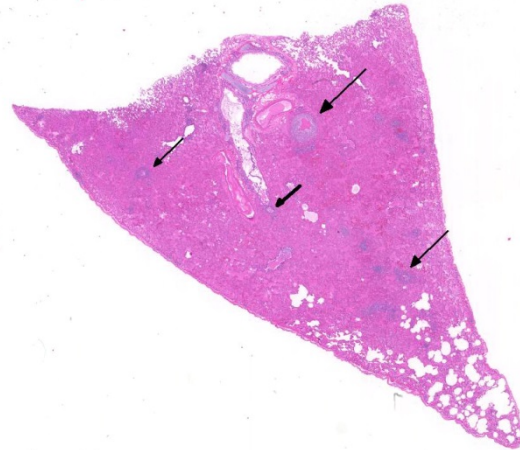
13. Suresh M, Sharma JM. Pathogenesis of type II avian adenovirus infection in turkeys: in vivo immune cell tropism and tissue distribution of the virus. *J Virol*. 196; 70: 30-36.

CASE II: 10-01139 (JPC 3167330).

Signalment: 7-month-old spayed female domestic shorthair cat (*felis catus*).

History: Chronic lethargy, anemia, icterus; presented with low body temperature.

Gross Pathology: Lungs were diffusely reddened, firm and did not collapse. Throughout all liver lobes are 1mm to 3mm pale tan nodules. Similar pale tan nodules from 1mm to 7mm diameter were scattered



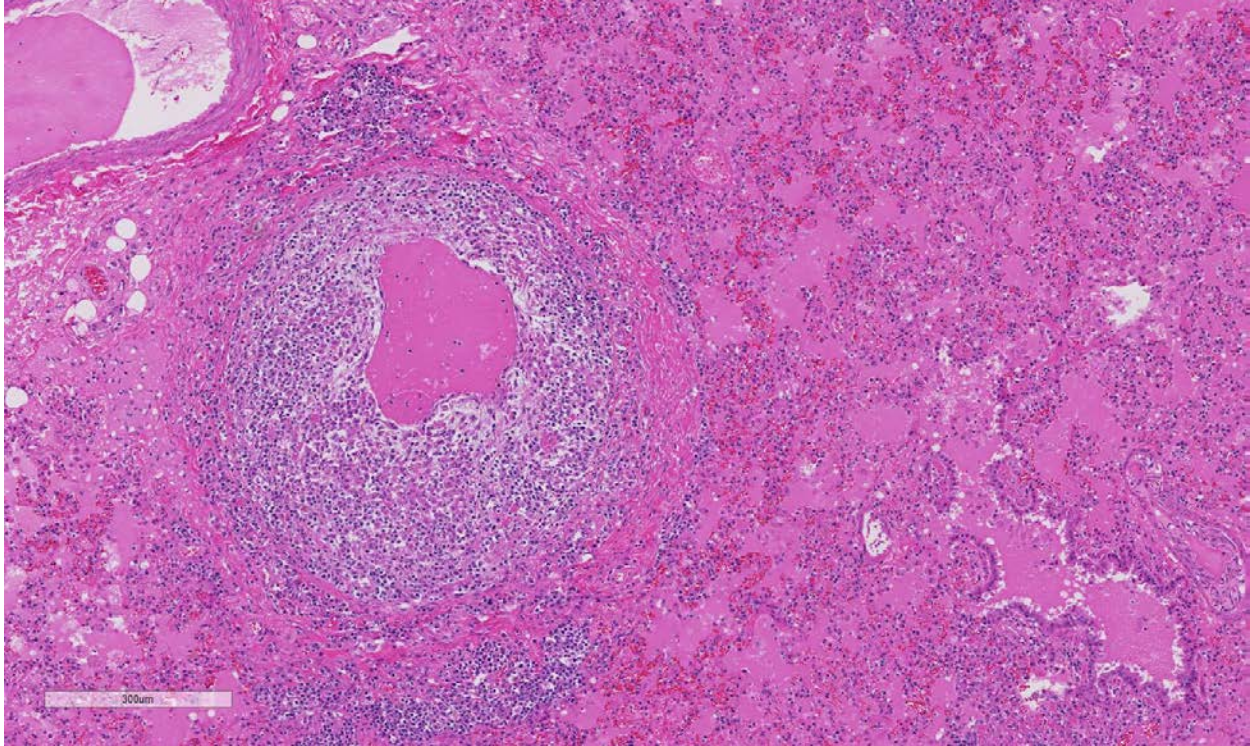
Lung, cat. Subgross examination of the submitted section of lung reveals marked diffuse intra-alveolar edema, and the walls of vessels are prominently expanded by a cellular infiltrate (arrows). (HE, 5X).

throughout the cortex of both kidneys. Mesenteric lymph nodes were enlarged.

Laboratory Results: Total protein - 10.0, albumin 2.1, globulins 7.5, phosphorous 6.8, potassium 3.4, elevated ALP, CK and total bilirubin (1.4).

Histopathologic Description: Blood vessels in the lung are accentuated by inflammatory infiltrates that greatly expand the vessel wall. These infiltrates are composed of macrophages, plasma cells, neutrophils, lymphocytes and occasional Mott cells. Mild fibroplasia is present in the infiltrate also. Vessel lumens are narrowed by the infiltrates. Diffusely, alveoli contain edema fluid and low numbers of macrophages and occasional neutrophils.

Contributor's Morphologic Diagnosis: Lung: Vasculitis/perivasculitis, multifocal, pyogranulomatous with alveolar edema.



Lung, cat. The walls of vessels are markedly expanded up to 10 times by an infiltrate of histiocytes and fewer lymphocytes, neutrophils and neutrophils which effaced the tunica intima and media and extend into the surrounding adventitia and pulmonary parenchyma. Alveoli are filled with edema fluid which is refluxed into adjacent airways. (HE, 71X)

Contributor's Comment: Gross findings in this cat were suggestive of the dry form of feline infectious peritonitis (FIP), and the vascular lesions in the lung were suggestive of those described in cases of FIP. Coronaviral antigen was identified in the vessels by immunohistochemistry.

FIP is one of the leading infectious causes of death in cats from shelters and catteries.⁷ FIP is caused by infection with feline coronavirus (FeCoV) that has mutated to become a pathogenic virus (FIPV). FCoV infections are very common, with up to 90% seropositivity in cats, while FIP morbidity is low, rarely above 5% of infected cats. Most infections with feline coronavirus are sub-clinical, although mild diarrhea and vomiting can occur. The FCoV mutants that cause FIP are either generated within the individual cat, or possibly are acquired externally.

Persistently infected, healthy carriers are believed to be most important in the epidemiology of FIP.⁶ Mutation of the FCoV in the carrier animal generates the FIP virus that is capable of replicating in monocyte/macrophages, resulting in transportation to organs outside of the GI tract, and development of FIP disease. The FCoV mutants also apparently lose their ability to replicate in intestinal epithelium, as they are not recovered from intestinal tissues.² For this reason, it is believed that cat to cat transmission of FIP virus is infrequent; the virus does not readily infect cats under natural conditions because it does not replicate in enterocytes, even though the virus readily infects cats when they are experimentally inoculated by routes other than oral.

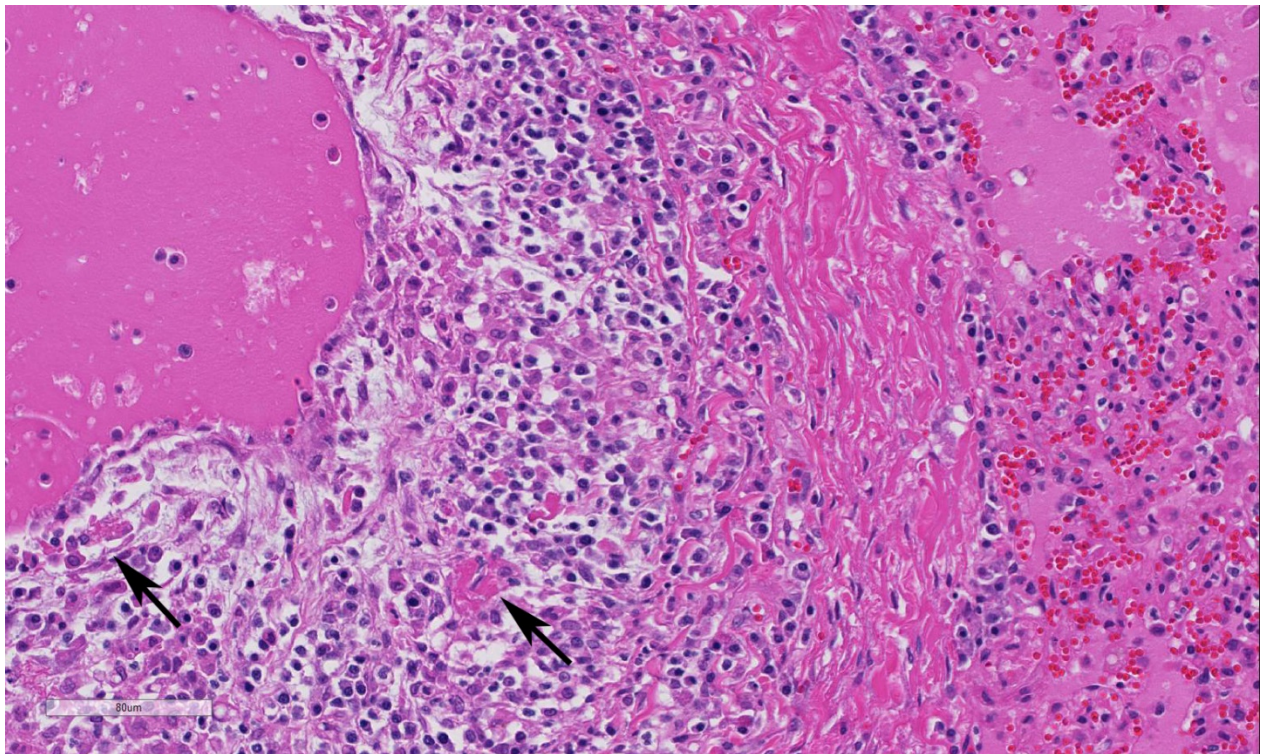
The host immune response largely dictates the lesions of FIP. The immune response to FIP virus is presently understood as follows:

humoral immunity is not important for protection while protective immunity is largely cell mediated.⁷ The type and strength of immunity determines the form that FIP virus infection will take. Cats that develop FIP will have either the wet or dry form depending on whether ineffective cell-mediated or humoral immunity dominates the clinical disease. Strong humoral immunity with very weak or non-existent cellular immunity leads to effusive (wet) FIP. With the effusive form, cats will have up to 1 L of viscous abdominal fluid while pleural effusion is present in about 25% of cases. Humoral immunity with intermediate cellular immunity will manifest as the non-effusive FIP (dry form). With the dry form, the kidneys may be enlarged and nodular with white, firm nodules protruding from the cortex. Foci of inflammation may also be seen in other organs, including the liver and pancreas. The gross lesions of wet versus dry forms are often not distinctly separate,

and much overlap occurs.

Vasculitis and perivasculitis characterize the microscopic lesions of FIP. FIP-induced granulomatous vasculitis occurs in small to medium-sized veins predominantly in the leptomeninges, renal cortex, and eye, but also frequently in the lung and liver.⁴ Vasculitis is characterized as venous and perivenous, macrophage-dominated, circular infiltrates in small veins, and focal infiltrates in larger veins. Neutrophils and T cells represented minorities among inflammatory cells, and B cells mainly occur as peripheral rims around circular granulomatous infiltrates. FIP virus-infected monocytes that become activated and emigrate from vessel lumens into perivenous locations are reported to be unique to the development of the periphlebitis that occurs.

JPC Diagnosis: Lung: Vasculitis,



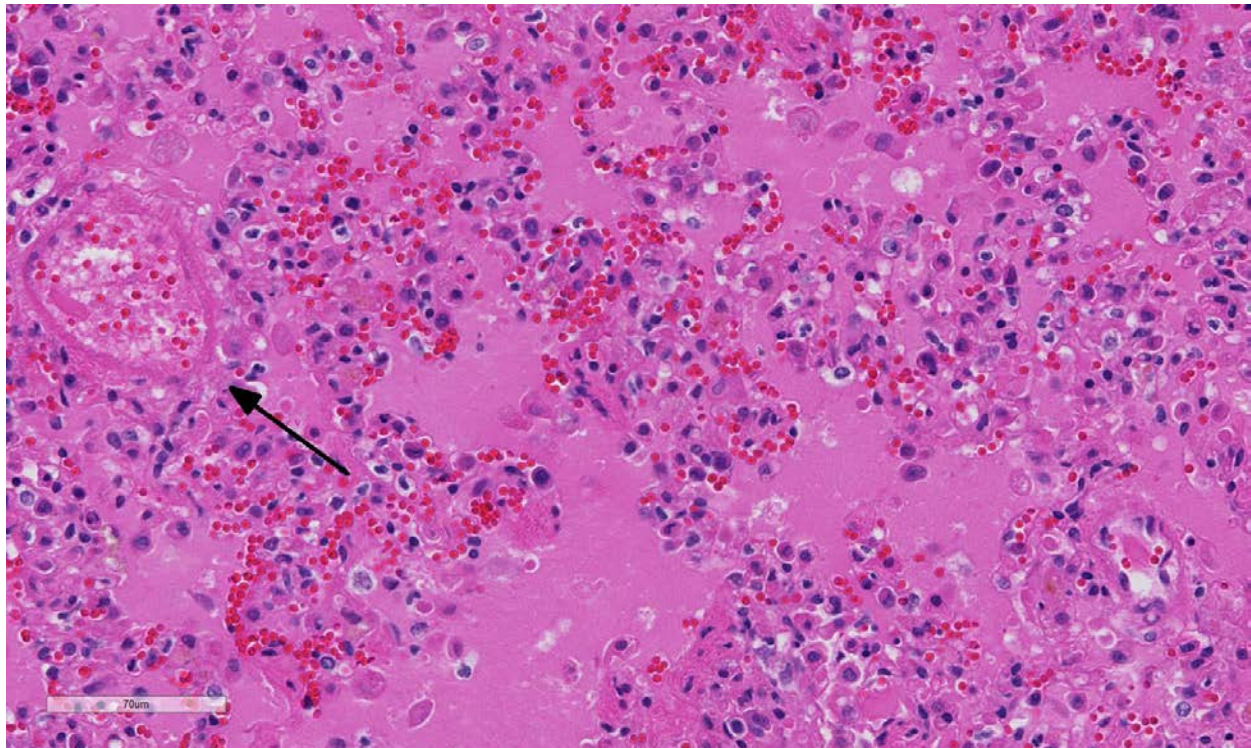
Lung, cat. Higher magnification of the vessel showing the number of infiltrating neutrophils, histiocytes, and lymphocytes as well as the proliferation of fibroblasts and small amounts of brightly eosinophilic extruded protein within the wall (arrows). (HE, 240X)

necrotizing, lymphocytic and histiocytic, diffuse, severe with fibrinoid necrosis and alveolar and interstitial edema.

Conference Comment: Feline coronavirus (FCoV) belongs to the genus *Alphacoronavirus* and species *Alphacoronavirus-1*, along with canine coronavirus and transmissible gastroenteritis virus of pigs. There are two serotypes of FCoV (based on antigenicity) types I and II, and while both may cause feline infectious peritonitis (FIP), type I is more common in the cat population. The serotypes differ primarily in growth characteristics in cell

between type I FCoV and CCoV. Along with homologous recombination, the propensity for frequent variation and mutation of coronaviruses is also based on a high mutation rate (2.0×10^{-6} mutations per site per round of replication) and the sheer size of the genome (26–32 kb).⁹ As is true with many viruses, even a single amino acid mutation and/or recombination events can change viral properties, host range and pathogenicity.

Both feline enteric coronavirus (FECV) and feline infectious peritonitis virus (FIPV) can infect monocytes, but FIPV's are able to sustainably replicate in much higher

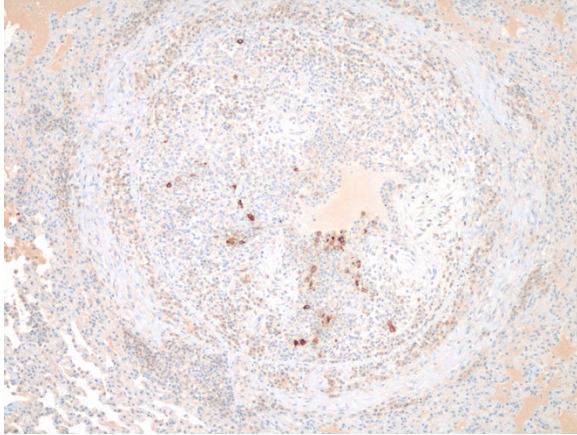


Lung, cat. The walls of thrombosed smaller vessels are diffusely necrotic (arrow), with necrosis within adjacent alveolar walls and flooding of alveoli with edema fluid. (HE, 400X)

culture and in receptor usage, and it is notable that most, if not all, of the experimental work so far has been done on the Type II strains because they grow well in cell culture. Type II FCoVs arose as a consequence of a double recombination

numbers.⁵ However, not all monocytes are permissive to replication of FIPV⁸ and there is variation in individual cats regarding the susceptibility of monocytes to infection and replication, which influences disease susceptibility. It has also been suggested that

monocytes may potentially be the cells where mutation from FECV to FIPV occurs.^{5,8} The precise genetic and mechanistic differences that define changes in viral replication and virulence have not yet been clearly elucidated, but various proteins such as 3c, S, S1 fusion peptide and 7a/b,



Histiocytes within the walls of affected vessels stain positively for feline coronavirus antigen. (anti-FECV, 100X)

among others, appear to play a role.^{5,8} In many cases, these various proteins appear to influence virus infection of, and replication in, monocytes. At least three key events are known in the development of FIP including systemic infection with FIPV, effective FIPV replication in monocytes and activation of those monocytes,⁵ highlighting the critical role of the monocyte response in development of FIP.

There was conference discussion around the use of the terms “wet” and “dry” forms of FIP. Some researchers believe these are a temporal continuum, with the latter being a chronic manifestation, or a post-manifestation of the former. The terms are useful clinically, but we know little about what contributions of the virus and/or host are the bases of the two types of presentations. Lesion distribution in cases of FIP is rather consistent although some degree of individual variation may be observed.

Peritoneal involvement was seen in 75% of cases, often associated with abdominal effusion, and the kidneys, followed by eyes and brain, were most often affected according to one study, and ocular involvement was frequently bilateral.⁵

Antemortem diagnosis of FIP can be particularly challenging. Cytology of abdominal effusion suggestive of FIP contains nondegenerate neutrophils, macrophages, lymphocytes and few plasma cells on a proteinaceous background. Using immunofluorescence or immunohistochemistry to visualize the virus within monocytes of the effusion is considered diagnostic, excepting cases of sequestered granulomas, such as this case. A positive reaction in the Rivalta’s test, used to differentiate transudates from exudates, may increase diagnostic sensitivity when accompanied by cytology of abdominal effusion.³ As discussed above, vascular lesions are generally limited to the small and medium sized veins in affected tissues due to interaction between activated macrophages and endothelium.⁵ In some cases, vascular lesions, which are generally dominated by macrophages, may be replaced by B cells and plasma cells.⁵ This is commonly observed in ocular disease where plasma cells predominate. The clinical course of disease in the wet form is generally much faster than for the dry form and subclinical as well as a protracted or multiphasic course of disease may also be seen. The conference attendees discussed a recent publication that demonstrates theoretical reversal of viremia using pro-tease inhibitors, and clinical trials that are underway to establish whether a rigorous anti-viral therapy could be helpful.¹⁰

Conference participants described the inflammatory infiltrate as being vascular and perivascular in distribution, effecting small

and medium sized vessels, and remarkably circumferential in most affected vessels. The loss of vascular architecture included the entirety of the vessel wall which was markedly thickened by fibrin, both hyalinized and fibrillar, edema, and a mixed population of inflammatory cells, predominantly macrophages. The endothelium is hypertrophic and vascular lumina are narrowed. The moderator stressed the importance of describing vascular changes in detail, specifically with reference to vasculitis; the description should characterize changes within each layer of the effected vessel. Edema fluid fills alveoli in this case, and has refluxed into small and terminal bronchioles, a change which needs to be distinguished from an airway-centric disease (i.e., bronchopneumonia). The alveolar septa and interstitium are mildly expanded by fibrin and edema. There are multifocal areas of alveolar emphysema and few areas of mild fibrinous pleuritis.

Contributing Institution:

Department of Diagnostic
Medicine/Pathobiology College of
Veterinary Medicine
Kansas State University
<http://www.vet.k-state.edu/depts/dmp/>

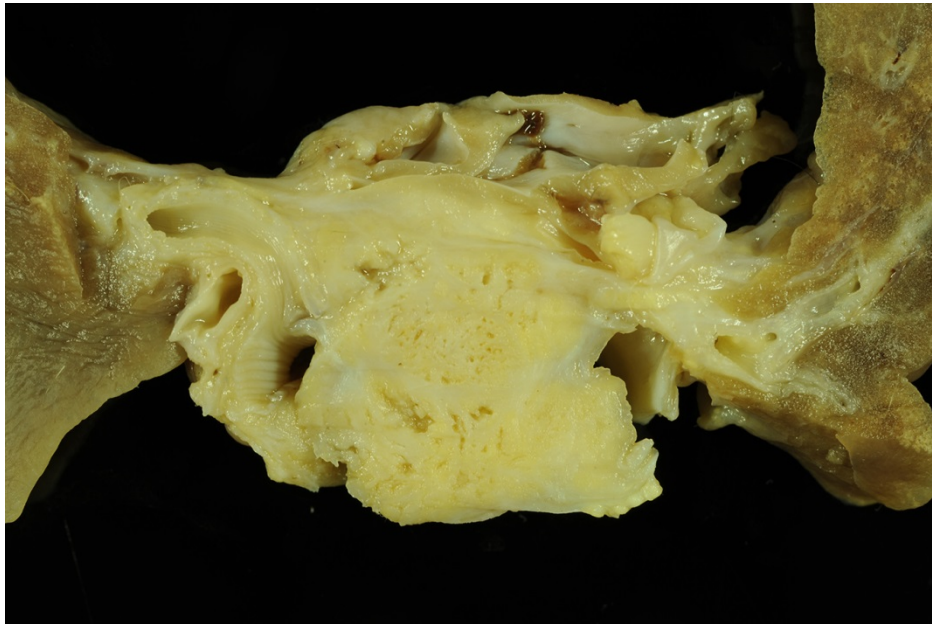
References:

1. Brown CC, Baker DC, Barker IK. Alimentary system. In: Maxie MG, ed. *Jubb, Kennedy and Palmer's Pathology of Domestic Animals*. 5th ed. Vol 2. Saunders Elsevier: New York; 2007: 290-293.
2. Chang HW, deGroot RJ, Egberink HF, Rottier PJM. Feline infectious peritonitis: Insights into feline coronavirus pathobiogenesis and epidemiology based on genetic analysis of the viral 3c gene. *J Gen Virol*. 2010; 91:415-420.
3. Fischer Y, Sauter-Louis C, Hartmann K. Diagnostic accuracy of the Rivalta test for feline infectious peritonitis. *Vet Clin Pathol*. 2012; 41:558-567.
4. Kipar A, May H, Menger S, Weber M, Leukert W, Reinacher M. Morphologic features and development of granulomatous vasculitis in feline infectious peritonitis. *Vet Pathol*. 2005; 42: 321-330.
5. Kipar A, Meli ML. Feline infectious peritonitis: Still an enigma? *Vet Pathol*. 2014;51(2): 505-526.
6. Meli M, Kipar A, Muller C, Jenal K. High viral loads despite absence of clinical and pathological findings in cats experimentally infected with feline coronavirus (FCoV) type 1 and in naturally FCoV-infected cats. *J Feline Med and Surg*. 2004; 6:69-81.
7. Pedersen NC. A review of feline infectious peritonitis virus infection: 1963-2008. *J Feline Med and Surg*. 2009; 11:225-258.
8. Pedersen NC. An update on feline infectious peritonitis: Virology and immunopathogenesis. *Vet J*. 2014; 201(2):123-132.
9. Eckerle LD, Becker MM, Halpin RA, Li K, Venter E, et al. Infidelity of SARS-CoV Nsp14-exonuclease mutant virus replication is revealed by complete genome sequencing. *PLoS Pathog*. 2010;(5):e1000896.
10. Kim Y, Liu H, Galasiti Kankanamalage AC, Weerasekara S, et al. Reversal of the Progression of Fatal Coronavirus Infection in Cats by a Broad-Spectrum Coronavirus Protease Inhibitor. *PLoS Pathog*. 2016; 12(3):e1005531.

CASE III: S 307/14 (JPC 4048846).

Signalment: Few week old, female mongrel dog, canine (*Canis familiaris*)

History: The dog was originally born in Romania. The bitch and her litter were brought to Germany by an animal rights group. The pup showed a 4-week-history of diarrhea and apathy. After 3 weeks the dog developed additionally central nervous signs



Lung, dog: A 3cm yellow-gray mass was present within the pulmonary parenchyma at the level of the tracheal bifurcation. (Photo courtesy of: Setor de Patologia Veterinária, UFRGS, <http://www.ufrgs.br/patologia/>)

including torticollis and ataxia. Finally, it died spontaneously. The mother showed no clinical signs. One other puppy of the same litter developed also diarrhea and apathy and died one week prior to the pup described here. Both puppies received a single vaccination against canine distemper five days before occurrence of the first clinical signs.

Gross Pathology: The dog was in a moderate to poor nutritional condition. In the lung, there was a single white to yellowish-grey mass of 3 cm in diameter at the level of the bifurcation. It was firm with

a granulated cut surface. Focally, there was a yellow greenish suppurative focus. The kidneys showed multiple white foci on the cortical surface. Furthermore, the skin of the abdomen caudally to the umbilicus had multifocal red spots of 0.3 cm diameter and few pustules of approximately 0.2 cm diameter. Brain, spinal cord and intestine were grossly unremarkable.

Laboratory Results: Microbiological culture of lung tissue revealed a moderate content of *Escherichia coli* and mild contents of *Nocardia*-like bacteria and coagulase-negative staphylococci. Identification of the *Nocardia*-like bacteria by sequencing of the 16S rRNA showed 100% similarity to the sequence of *Nocardia veterana*.

Histopathologic Description:

The histologic preparation shows a cross section of the cerebellum and brain stem at the level of the corpus trapezoideum. Multifocally, there are randomly distributed pyogranulomatous foci with centrally destroyed neuroparenchyma. The lesions are composed of moderate amounts of centrally-located degenerated and viable neutrophilic granulocytes surrounded by macrophages with a moderate amount of pale eosinophilic and mildly granulated to foamy cytoplasm with indistinct cell borders. These cells contain one prominent, paracentral, oval to kidney-shaped, basophilic nucleus and are interpreted as epithelioid macrophages. Adjacent to the granulomas moderate pe-

rivasascular infiltration (up to 3 layers) composed of lymphocytes and plasma cells are noted (perivascular cuffing). Vascular endothelial cells display hypertrophy. The meninges also show multifocal, mild lymphocytic infiltration. Mild to moderate microgliosis is characterized by rod-shaped microglial cells. Furthermore, single periventricularly located swollen astrocytes contain intranuclear and/or cytoplasmic, brightly eosinophilic, round inclusion bodies with a diameter of up to 4 μm and occasionally surrounded by a clear halo.

Contributor's Morphologic Diagnosis:

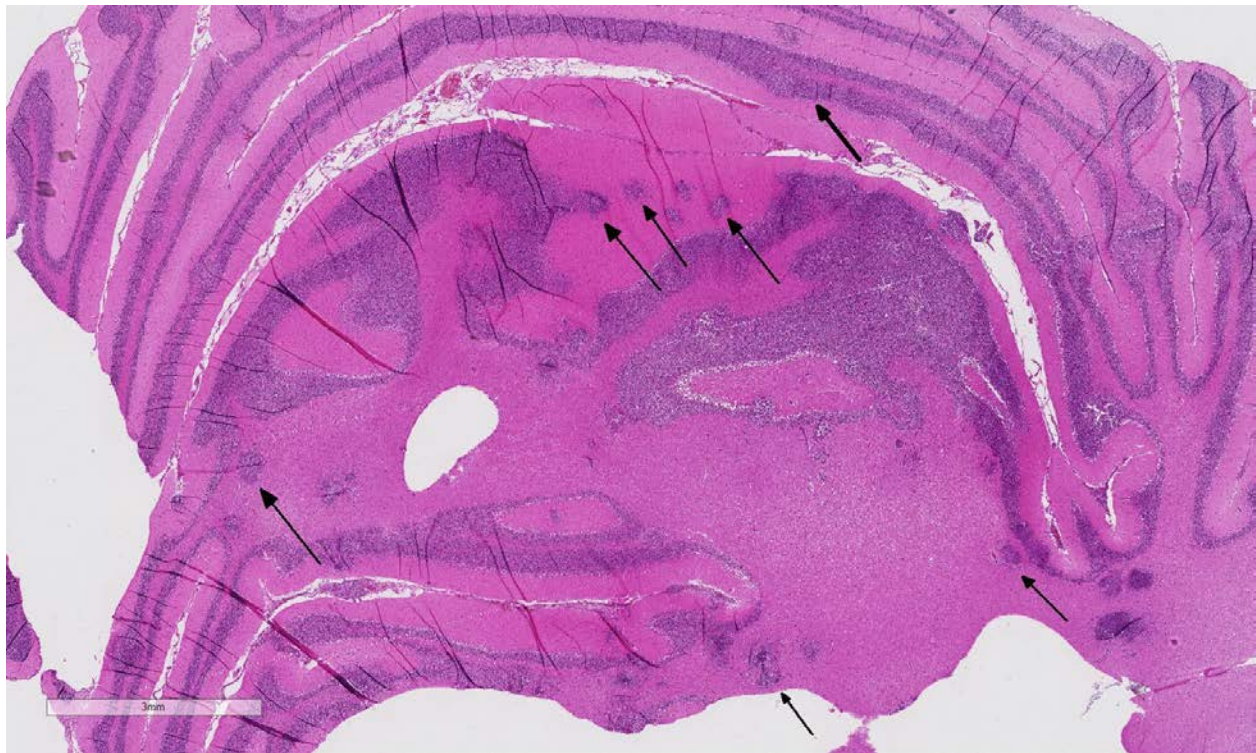
Cerebellum and brain stem:

1. Encephalitis, pyogranulomatous to necrotizing, severe, multifocal, chronic with microgliosis;
2. Periventricular astrocytosis with intranuclear and/or cytoplasmic, viral inclusion bodies;
3. Meningitis, lymphocytic, mild, multifocal, chronic.

Contributor's Comment: The morphologic

findings are consistent with a concurrent infection of canine distemper virus (CDV) and a mixed bacterial infection with the involvement of *Nocardia veterana*.

In addition to the alterations of the brain, the lung revealed a focally severe, chronic pyogranulomatous pneumonia and a non-suppurative interstitial pneumonia with single intranuclear and cytoplasmic, eosinophilic viral inclusions in epithelial cells of bronchioles. The kidneys exhibited a severe, multifocal, chronic, granulomatous to pyogranulomatous nephritis with multifocal arteritis and extensive necrosis. Moderate, multifocal, chronic, pyogranulomatous inflammation was also present in the adrenal gland and the myocardium. However, Ziehl-Neelsen's stain did not reveal convincing evidence of intralesional acid-fast organisms consistent with *Nocardia* sp. However, Grocott's methenamine silver impregnation displayed filamentous bacteria. The skin of the abdomen caudally to the umbilicus revealed a moderate to severe, multifocal, subacute, suppurative to



Cerebellum, dog. There are numerous cellular foci distributed randomly throughout all levels of the cerebellum. (HE, 12X).

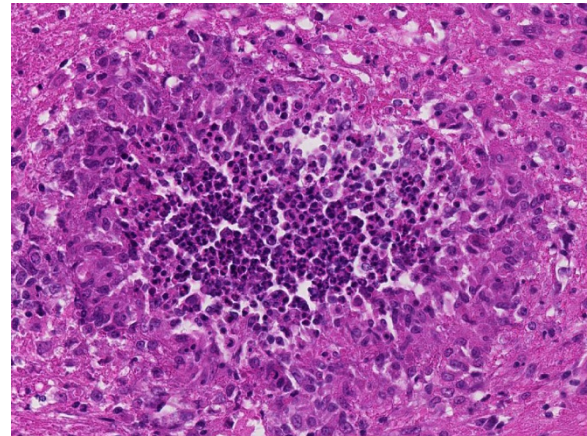
necrotizing dermatitis and inflammation of sweat glands with multifocal formation of pustules and single cytoplasmic, eosinophilic viral inclusions in epidermal cells. Mesenteric lymph nodes displayed severe depletion of lymphocytes and suppurative lymphadenitis. At the time of necropsy, the intestine was unremarkable.

Immunohistochemistry for CDV antigen was positive in epithelial cells of the lung, affected abdominal skin, and in periventricular astrocytes of the brain stem.

Canine distemper virus is a morbilliviral disease of the family *Paramyxoviridae*, including measles virus and rinderpest virus. The host spectrum comprises various species of *Canidae*, *Mustelidae*, *Procyonidae*, *Phocidae*, *Felidae* and other. The virus represents an important infectious disease in many parts of the world. CDV is usually transmitted through inhaled aerosols or close contact. First steps of the pathogenesis include infection of macrophages of the upper respiratory tract or the lung, which migrate to local lymph nodes and tonsils. Afterwards the virus replicates in local lymphoid tissue and spreads throughout the body within 2-5 days after exposure. Manifestations include bronchointerstitial pneumonia, demyelinating disease of the central nervous system, thymus atrophy, ocular disease including conjunctivitis, keratitis, retinitis and optic neuritis, pustular and/or hyperkeratotic cutaneous lesions, dental defects, bone lesions, and abortions.^{4,18} Furthermore, CDV infection leads to profound inhibition of cellular and humoral immune functions resulting in immunosuppression, lymphocyte loss and leukopenia, what boosts susceptibility for opportunistic infections.⁶ Common secondary infections following CDV infection include *Bordetella* sp., adenovirus and *Pneumocystis* sp. infections of the lung as well as toxoplasmosis, Tyzzer's disease, sarcocystosis and

encephalitozoonosis. Secondary enteric infections with *Cryptosporidium* or attaching-and-effacing *Escherichia coli* are also well known.¹⁸ In this case, a secondary mixed bacterial infection with involvement of *Nocardia veterana* led to the pyogranulomatous and necrotizing meningoencephalomyelitis. However, a primary bacterial infection followed by canine distemper cannot be excluded, but is even more unlikely because cases of *Nocardia veterana* described so far in man almost all occurred in severely immunocompromised patients.² The detection of coagulase-negative staphylococci and *Escherichia coli* from lung tissue results most likely from secondary infection with ubiquitously existing bacteria.

Nocardia veterana has been described in 2001 for the first time when it was isolated from bronchial lavage of a human patient with a history of tuberculosis in a veteran's hospital in Australia.¹⁵ *Nocardia* spp. are gram-positive, nonmotile aerobic



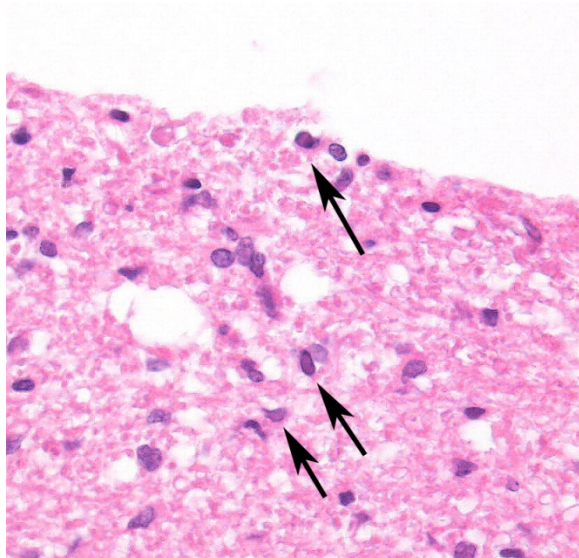
Cerebellum, dog. Hypercellular foci are pyogranulomas, composed of a central core of degenerate neutrophils surrounded by a thick rim of epithelioid macrophages. (HE, 252X)

actinomycetes, which are ubiquitous in the environment and cause a variety of suppurative and granulomatous infections, ranging from cutaneous mycetomas to disseminated systemic diseases.⁵ The

majority of infections are caused by members of the *Nocardia asteroides* complex, which includes *Nocardia asteroides sensu strictu*, *Nocardia abscessus*, *Nocardia cyriacigeorgica* and two clusters closely related to *Nocardia carneae* and *Nocardia flavorosea*.²⁰

Organisms of the *Nocardia asteroides* complex are capable to cause pulmonary, systemic, central nervous and localized cutaneous nocardiosis in man and animals. Infections of bone, eyes, heart, joints and kidneys have also been reported in man as well as mammary gland infections of cows.⁵

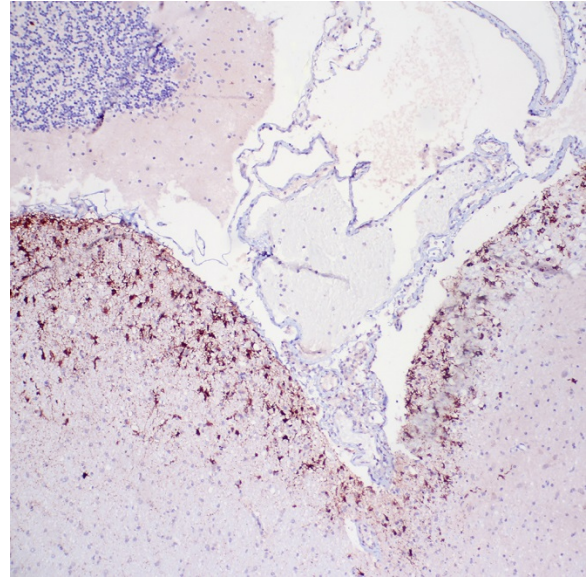
In contrast to *Nocardia asteroides*, infections caused by *Nocardia veterana* are rare and have previously only been reported in man and cows with mastitis in Brazil.¹⁰ In man, *Nocardia veterana* infection is a rare event that is mostly promoted by



Cerebellum, dog. Periventricular astrocytes contain a glassy eosinophilic intranuclear viral inclusion which peripheralizes the chromatin. (HE, 400X)

preliminary immunosuppression.¹⁴ Reported cases include pneumonia in a HIV-infected patient, nodular lymphangitis in a man who was in remission from non-Hodgkin's lymphoma, and a brain abscess in a patient with type 2 diabetes.^{3, 13, 17} Furthermore,

Nocardia veterana infection had caused cutaneous mycetoma in a woman with



Cerebellum, dog. Periventricular astrocytes are strongly cytoplasmically immunopositive for canine morbillivirus antigen. (anti-CDV, 100X).

systemic lupus erythematosus.¹⁶ Single cases of ascitic fluid infection and bloodstream infection in immunocompromised man have also been described in the literature.^{2,10} In cows, *Nocardia* infection of the mammary gland induces severe suppurative pyogranulomatous mastitis.¹⁰ *Nocardia veterana* shows a high rate of multi-resistance to commonly used antibiotic drugs resulting in a failure of conventional antimicrobial agents.^{2,10} It has been shown that high rates of resistance for commonly used drugs in many other *Nocardia* spp. isolated from man exist.²¹

To our knowledge, this is the first report of a systemic bacterial infection associated with *Nocardia veterana* in a dog. These findings emphasize the risk of nocardiosis caused by *Nocardia veterana* in immunocompromised companion animals and a possible transmission from companion animals to immunocompromised man must be considered. Furthermore, sequencing of the 16S rRNA is a suitable tool for defining different *Nocardia* species.^{9,20}

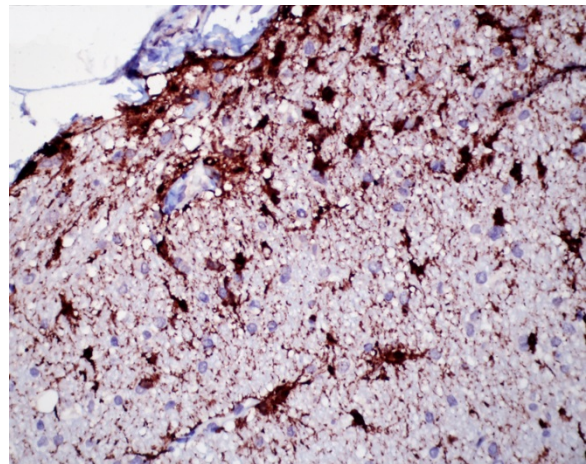
JPC Diagnosis:

1. Cerebellum: Meningoencephalitis, pyogranulomatous, multifocal, moderate with fibrinoid vasculitis.
2. Cerebellum, periventricular astrocytes: Intranuclear viral inclusion bodies, numerous.

Conference Comment: This case serves to highlight the markedly immunosuppressive nature of CDV and the susceptibility to secondary or opportunistic infections, which are quite common as discussed above. CDV infection in dogs has many similarities with measles virus infection in humans. Both viruses enter through alveolar macrophages and dendritic cells, as well as lymphocytes, via the CD150/SLAM molecule and both may result in severe neurologic disease, although neurologic disease is more commonly seen in canine distemper than measles.¹ The demyelinating CNS disease that occurs with CDV infection is said to resemble multiple sclerosis in humans. Additionally, epithelial entry is mediated by the nectin-4 receptor in both viruses.¹ Research has shown that for measles virus infection the period of immunosuppression is generally thought to be weeks to months following infection. The precise mechanisms responsible for this immunosuppression include processes involved in both functional impairment and depletion of immune cells.^{11,12} Interestingly, a recent study using population level data demonstrated that the period of immunosuppression following measles infection may actually be much longer than previously thought, for a period of up to three years where recovered individuals are more susceptible to infectious disease.¹⁹ The cause of this phenomenon is postulated as due to loss of immune memory

lymphocytes due to measles virus infection, which erases previously acquired immunity and has been referred to as “immune amnesia.”^{11, 12,19} This idea is supported by the finding that measles infection resulted in a 2-3 year increase in mortality from other infectious diseases in a population, post measles virus infection.¹⁹ Given the similarities between CDV and measles virus, one wonders if a similar long-term immunosuppressive phenomenon may be observed in CDV infected dogs.

Various neurologic conditions, that are distinctive based on lesion localization and age of onset, may be associated with canine distemper virus (CDV). When the virus infects older dogs, ranging in age from 4-8 years, it can result in a chronic progressive disease referred to as multifocal distemper encephalomyelitis. Histologic lesions



Cerebellum, dog. Higher magnification of CDV-antigen-laden astrocytes. (anti-CDV, 400X).

include a demyelinating leukoencephalomyelitis in the cerebellum and spinal cord.⁷ Old dog encephalitis is separate and rare condition that can slowly progress over a period of 3-4 months and is thought to be due to chronic, subclinical, non-replicating (persistent) infection with CDV. In this condition lesions are localized to the

cerebral cortex, thalamus and midbrain and consist of a necrotizing, non-suppurative encephalitis with prominent perivascular cuffing by lymphocytes in both the grey and white matter. There is demyelination and atrophy of the cerebral white matter, and in some cases intranuclear and intracytoplasmic inclusion bodies may be found in astrocytes. Neuronal changes such as chromatolysis and swelling may be seen in some locations.⁷ Typical lesions of the CNS in classic CDV infection include white matter demyelination which is prominent in the cerebellum and surrounding the fourth ventricle. Lesions are multifocal and there is vacuolation of the neuropil along with myelin loss, and inflammatory infiltrates are rare. Astrocytes often contain intranuclear inclusion bodies, which may be present prior to encephalomyelitis and often persist in the CNS longer than other tissues. Grey matter lesions occur less commonly and may include neuronal necrosis and mononuclear cell infiltration/nonsuppurative encephalitis; inclusion bodies may be identified within neurons of the grey matter when affected.⁸

The conference histologic description was similar to the contributor's description above. The salient features of the section include multifocal pyogranulomas, fibrinoid vasculitis and the presence of intranuclear viral inclusion bodies in periventricular astrocytes. Additionally, the meninges are multifocally expanded by lymphocytes, plasma cells and macrophages and there is mild multifocal expansion of Virchow-Robin space by mononuclear inflammatory cells. There is slide variation with not all slides containing choroid as well as variability in the presence and severity of fibrinoid vasculitis. Not all conference participants identified viral inclusion bodies in periventricular astrocytes, and in general, the distemper lesions in these sections were

extremely subtle. Inclusions were most predictable in the periventricular cells, and were demonstrated in low numbers during the conference. Various differential diagnoses for pyogranulomatous meningoencephalitis were discussed including systemic mycotic infections such as blastomycosis and cryptococcosis. Other considerations include protothecosis and mycobacteriosis.⁷ Silver and acid-fast stains repeated at JPC on the section failed to identify microorganisms. Regardless of the cause for the granulomas in this particular case, pathologists should be concerned about immunosuppression as a predisposing factor in the dissemination of potentially any "secondary" pathogen. The true nature of dual infections (opportunistic vs. polymicrobial) has not been elucidated in most cases.

Contributing Institution:

Department of Pathology, University of Veterinary Medicine
Hannover, Buenteweg 17, 30559 Hannover,
Germany.

<http://www.tiho-hannover.de/kliniken-institute/institute/institut-fuer-pathologie/>

References:

1. Alves L, Khosravi M, Avila M, Ader-Ebert N, et al. SLAM- and nectin-4 independent noncytolytic spread of canine distemper virus in astrocytes. *J Virol.* 2015; 89:5724-5733.
2. Ansari SR, Safdar A, Han XY, O'Brien S. *Nocardia veterana* bloodstream infection in a patient with cancer and a summary of reported cases. *Int J Infect Dis.* 2006;10:483-486.
3. Arends JE, Stemerding AM, Vorst SP, de Neeling AJ, Weersink AJ. First report of a

- brain abscess caused by *Nocardia veterana*. *J Clin Microbiol*. 2011; 49:4364-4365.
4. Baumgärtner W, Boyce RW, Alldinger S, et al. Metaphyseal bone lesions in young dogs with systemic canine distemper virus infection. *Vet Microbiol*. 1995; 44:201-209.
 5. Beaman BL, Beaman L. *Nocardia* species: host-parasite relationship. *Clin Microbiol Rev*. 1994;7:213-264.
 6. Beineke A, Puff C, Seehusen F, Baumgärtner W. Pathogenesis and immunopathology of systemic and nervous canine distemper. *Vet Immunol Immunopathol*. 2009; 127:1-18.
 7. Cantile C, Youssef S. Nervous system. In: Maxie MG, ed. *Jubb, Kennedy, and Palmer's Pathology of Domestic Animals*. 6th ed. Vol 2. St. Louis, MO: Elsevier; 2016:362, 384-385.
 8. Caswell JL, Williams KJ. Respiratory system. In: Maxie MG, ed. *Jubb, Kennedy, and Palmer's Pathology of Domestic Animals*. 6th ed. Vol 2. St. Louis, MO: Elsevier; 2016:575-576.
 9. Chun J, Goodfellow M. A phylogenetic analysis of the genus *Nocardia* with 16S rRNA gene sequences. *Int J Syst Bacteriol*. 1995;45:240-245.
 10. Condas LA, Ribeiro MG, Yazawa K, et al. Molecular identification and antimicrobial susceptibility of *Nocardia* spp. isolated from bovine mastitis in Brazil. *Vet Microbiol*. 2013; 167:708-712.
 11. de Vries, de Swart RL. Measles immune suppression: Functional impairment or a numbers game? *PLoS Pathog*. 2014; 10(12):e1004482.
 12. de Vries, McQuaid S, van Amerongen G, Yuksel S, et al. Measles immune suppression: Lessons from the macaque model. *PLoS Pathog*. 2012; 8(8):e1002885.
 13. Dua J, Clayton R. First case report of *Nocardia veterana* causing nodular lymphangitis in an immunocompromised host. *Australas J Dermatol*. 2013;doi:10.1111/adj.12043.
 14. Godreuil S, Didelot MN, Perez C, et al. *Nocardia veterana* isolated from ascetic fluid of a patient with human immunodeficiency virus infection. *J Clin Microbiol*. 2003; 41:2768-2773.
 15. Gurtler V, Smith R, Mayall BC, Pötter-Reinemann G, Stackebrandt E, Kroppenstedt RM. *Nocardia veterana* sp. nov., isolated from human bronchial lavage. *Int J Syst Evol Microbiol*. 2001; 51:933-936.
 16. Kashima M, Kano R, Mikami Y, et al. A successfully treated case of mycetoma due to *Nocardia veterana*. *Br J Dermatol*. 2005; 152:1349-1352.
 17. Liu WL, Lai CC, Hsiao CH, et al. Bacteremic pneumonia caused by *Nocardia veterana* in an HIV-infected patient. *Int J Infect Dis*. 2011; 15:430-432.
 18. Maxie MG, Youssef S. Respiratory system. In: Jubb KV, Kennedy P, Palmer N, ed. *Pathology of Domestic Animals*. 5th ed. Philadelphia, USA: Saunders-Elsevier; 2007:635-638.
 19. Mina MJ, Metcalf CJ, de Swart RL, Osterhaus ADME, Grenfell BT. Long-term measles-induced immunomodulation increases overall childhood infectious disease mortality. *Science*. 2015; 348(6235):694-699.
 20. Roth A, Andrees S, Kroppenstedt RM, Harmsen D, Mauch H. Phylogeny of the genus *Nocardia* based on reassessed 16S rRNA gene sequences reveals underspeciation and division of strains

classified as *Nocardia asteroides* into three established species and two unnamed taxons. *J Clin Microbiol.* 2003;41: 851-856.

21. Schlaberg R, Fisher MA, Hanson KE. Susceptibility profiles of *Nocardia* isolates based on current taxonomy. *Antimicrob Agents Chemother.* 2014;58:795-800.

CASE IV: 11N2549 (JPC 4032260).

Signalment: 2-month-old intact female Dachshund-cross dog (*Canis familiaris*)

History: The patient was presented to the VMTH with three day history of vomiting, diarrhea, hematemesis and hematochezia. The puppy was adopted few days earlier from a rescue group and received one DHPP vaccine seven days prior to adoption. At admission the patient was severely dehydrated (8-10%) and had pink and tacky mucous membranes. The puppy was weak and ambulatory with diarrhea staining on the perineum. A small amount of bloody diarrhea was expressed during abdominal palpation. The dog was administered IV LRS fluids qs 20 mEqKCl/L and 2.5 % dextrose at 8mls/hr 0.07 mg Ondansetron IV q 12 hrs, 1.4 mg Ranitidine IV q 12hrs, 0.03 mg Buprenorphine IV q 8 hrs, and 70 mg Unasyn IV slow q 12 hrs. The patient did not respond to dextrose boluses and struggled to maintain adequate perfusion. Within 72 hours the dog still had no interest in food, and became stuporous with evidence of severe cranial abdominal pain. At this point, hypoglycemia, hypovolemic shock and possible DIC were suspected. The owners elected humane euthanasia.

Gross Pathology: On gross postmortem examination the dog had depleted fat stores and oral and ocular mucous membranes

were pale. The dorsal aspect of the tongue was multifocally eroded /ulcerated and areas between the erosions were covered by thin, friable, loosely adhered white tan (cotton like) plaque. The abdominal cavity contained approximately 10ml of clear blood tinged watery fluid. The intestinal serosal surface was slightly granular and opaque. The small and large intestine contained yellow-tan mucus.

Laboratory Results: Blood smear demonstrated severe leukopenia with neutropenic left shift. The PCV was 34% and total protein of 5.8. A SNAP test for canine parvovirus was positive on the day of admission.

Histopathologic Description: In a full-thickness transverse section of small intestine, the mucosal architecture was diffusely and circumferentially collapsed with attenuation, blunting and fusion of villi. The superficial mucosa was replaced by a band of eosinophilic cellular and karyorrhectic debris (necrosis). A nearly continuous thick mat of mixed bacteria and yeast covered the



Intestine, dog. At subgross examination, the mucosa is thin and villar architecture is lost. (HE, 5X)

necrotic mucosa. Yeast pseudohyphae had parallel walls and were 2.5 μm in diameter with budding oval to round yeast cells ($\approx 7.5 \times 5.0 \mu\text{m}$ in diameter). The pseudohyphae invaded into various depths of the lamina propria. Crypts were often absent and where present were ectatic and variably lined by attenuated enterocytes and packed with sloughed epithelial cells (crypt necrosis) or lined by hypertrophic and hyperplastic epithelial cells, up to 4 cell layers deep, with increased amounts of cytoplasm, vesicular nuclei, and occasional mitotic figures (regeneration). The lamina propria was expanded by reactive fibroblasts, neutrophils, and rare lymphocytes and plasma cells. Multifocally, intestinal crypts herniated into the severely depleted lymphoid follicles (GALT). The serosal and mesenteric vessels were moderately

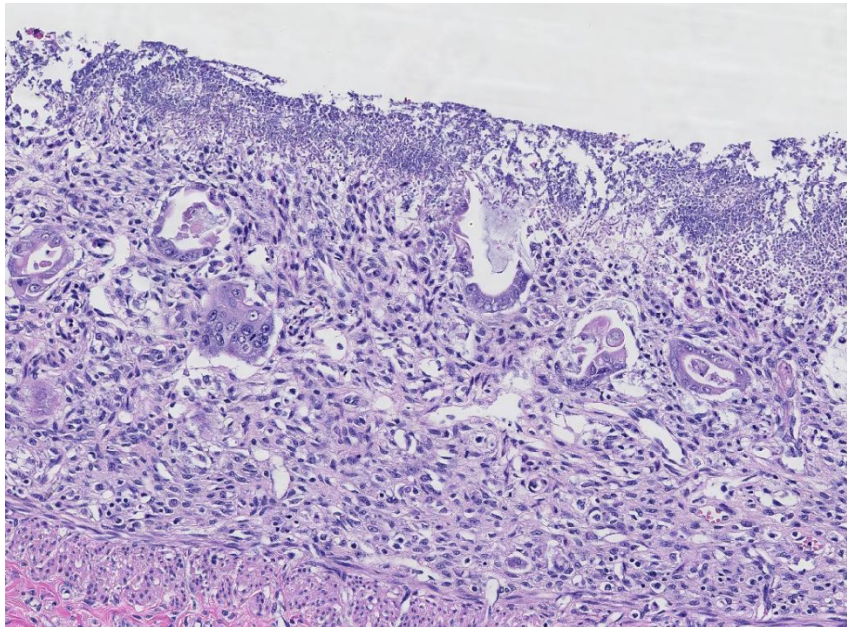
congested, lined by reactive endothelium and contained marginating neutrophils.

Contributor's Morphologic Diagnosis:

1. Small intestine (duodenum, jejunum, ileum): Severe, diffuse, subacute necrotizing enteritis, with colonization of yeast (*Candida* presumed) and mixed bacteria
2. Small intestine (Peyer's patches): Severe diffuse lymphoid depletion

Contributor's Comment: In addition to the necrotizing enteritis, significant findings in this patient also included severely depleted primary and secondary lymphoid organs and severe necroulcerative glossitis with *Candida* yeast and mixed bacterial colonization. The Brown-Brenn (modified Gram) stain highlighted gram-positive bacterial cocci and gram-negative bacterial

rods that colonize the affected areas. A Gomori metheniamine silver stain reveals abundant yeast pseudohyphae and spores. Immunohistochemistry for canine parvovirus (CPV2) was strongly positive in the sections of affected tongue and occasional immunoreactive cells were observed within the necrotic crypts and occasionally in the depleted lymphoid follicles.

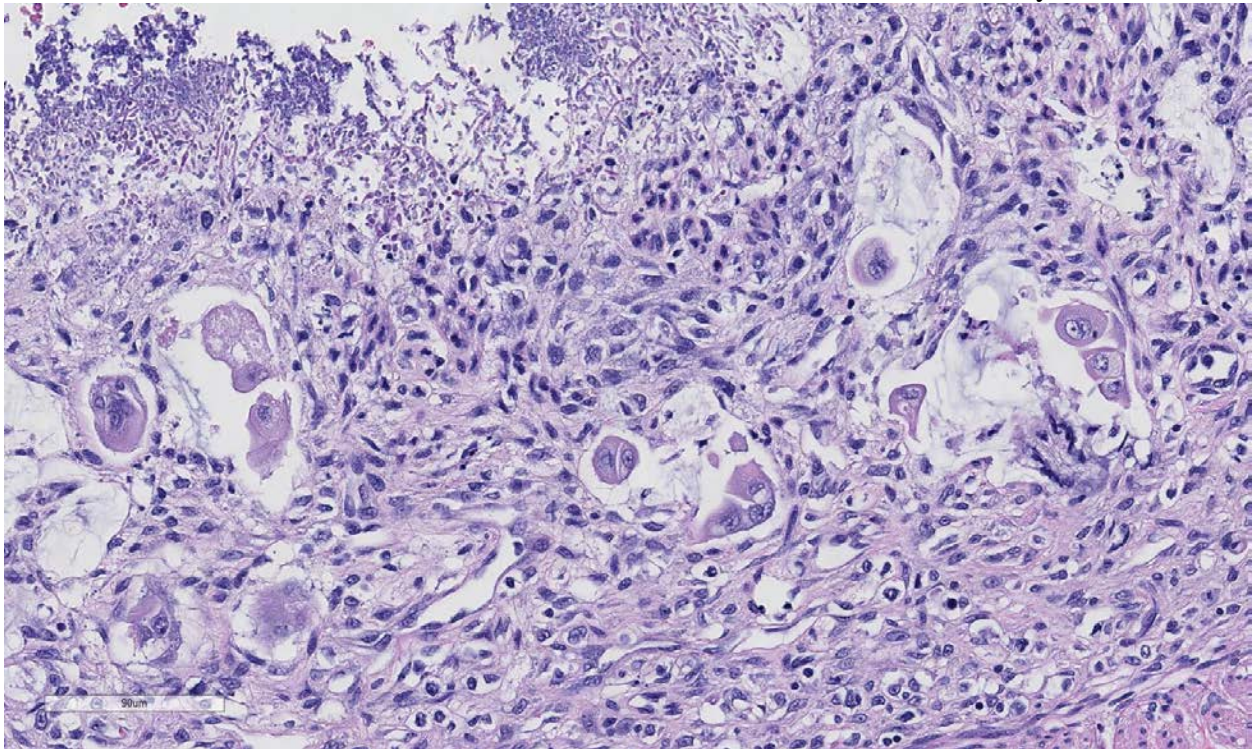


Intestine, dog. There is diffuse villar loss and marked crypt loss, with stromal collapse. There is marked regenerative change and atypia within remaining crypt epithelium. (HE, 88X)

Canine parvoviruses are small non-enveloped DNA viruses that require rapidly dividing cells for replication. They are divided into CPV-1 and CPV-2. CPV-2 is one of the most common causes of infectious enteritis in dogs.⁵ Acute CPV2-enteritis can be observed in dogs of any breed, age, or sex. Long list of predisposed breeds is provided in referenced text.⁷ Since it first appeared in dogs in the 1970s, CPV-2 has a progressive series of recognized antigenic variants that are based on single

host range compared to its predecessor, CPV2.

The mechanism of injury in parvoviral infection is death of rapidly dividing cells such as crypt epithelial cells, lymphocytes and bone marrow cells. Specificity for these mitotically active cells occurs because parvoviruses require a host cell-derived duplex transcription template, which is only available when cells divide, during the S-phase of the cell cycle. Parvoviruses are unable to turn on DNA synthesis in host



Intestine, dog: Higher magnification of bizarre attempts at crypt epithelial regeneration. (HE, 284X)

amino acid substitutions in VP2 gene (most recently CPV2c have emerged and is now distributed worldwide). In dogs, etiologic diagnosis through fecal ELISA is relatively straightforward and effective in recognition of the more recent strains.⁸ The current vaccine series is generally effective regardless of the CPV strain type. It is controversial whether CPV2c is more virulent in dogs, but it does decidedly have an extended

cells, so they must wait for host cells to enter the S-phase of the cell cycle before infecting these cells.⁴

Virus probably infects macrophages or dendritic cells migrating in the mucus layer and on the surface of mucosa.⁴ Virus replicates in these cells and is then spreads via leukocyte trafficking to the lamina propria of the tonsils. Here, additional macrophages and lymphocytes are infected and spread the virus via leukocyte trafficking in

lymphatic and blood vascular systems to regional lymph nodes and systemically to the spleen, thymus, lymph nodes, bone marrow, and mucosa-associated lymphoid nodules such as Peyer's patches of the small intestine.⁴ Virus may also spread as cell-free viremia in lymph via lymphatic vessels to regional lymph nodes. Experimental data suggests that virus spreads to the intestine via the vascular system and not in ingesta via peristalsis.⁴

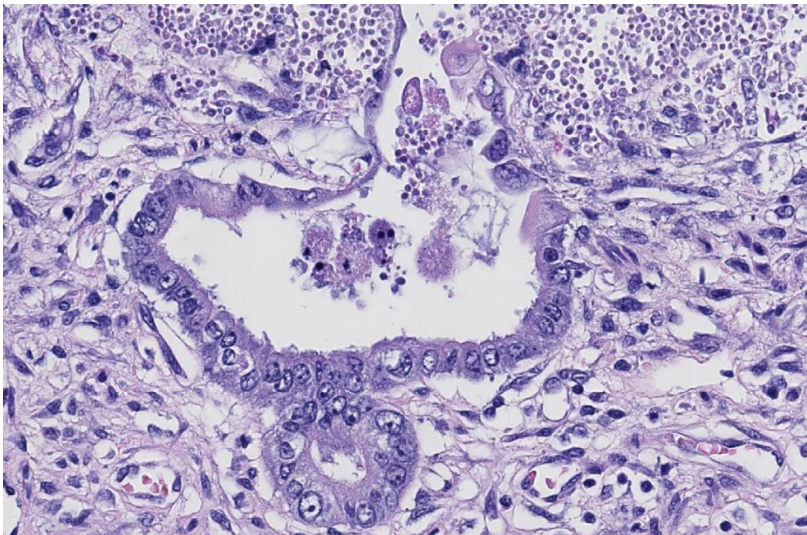
Clinically, CPV in dogs most commonly presents as hemorrhagic enteritis. However myocarditis, thrombosis, bacteremia, and neurological disease have also been reported.^{4,5,7} Two cases of cutaneous disease (erythema multiforme) induced by CPV-2 were recently published.^{3,10} Typically, parvovirus infection peaks after weaning at the age of 4 to 12 weeks, when maternally acquired antibody wanes.² Viral tropism to rapidly dividing cells leads to profound leukopenia and immunosuppression which predispose infected individuals to opportunistic bacterial or fungal infections.⁵ Specifically, in this case, candidiasis and surface bacterial colonization was present.

Candida spp. normally inhabit the alimentary, upper respiratory and genital

mucosae of mammals.⁵ *Candida albicans* and *Candida parapsilosis* are the most common. The mechanism of injury in candidiasis is disruption and death of cells in mucosae caused by inflammation and the concurrent proliferation and invasion of filamentous pseudohyphae and hyphae. *Candida albicans* persists in two forms: yeast (commensal) and filamentous pseudohyphae and hyphae (pathogenic).⁴ Yeast persists in the oropharyngeal cavity by adhering to and colonizing mucosae via ligand-receptor and/or hydrophobic interactions. Yeast ligands include cell wall components, such as mannose, C3d receptors, and mannoproteins, whereas mucosal receptors include fibrinogen, fibronectin, thrombin, collagen, laminin, and vitronectin-binding proteins. The balance between commensalism and disease is tenuous and perturbations of the mucosae and/or changes in the physiologic status of the animal may shift this balance in favor of disease (filamentous pseudohyphal and/or hyphal forms).⁴

Through a process called morphologic (phenotypic) switching, the yeast phase switches to the invasive filamentous phase. Switching appears to occur through inducible chromosomal rearrangements in the genome of the yeast in response to changes in the mucosal environment. Switching is reversible. Under normal conditions, the temperature of mucosae in the oral cavity is near room temperature (25° C). This temperature favors the growth of yeast, whereas growth of the filamentous phase prefers 37° C. Yeast is able to switch this temperature dependence for growth so that the filamentous phase can grow at 25° C.⁴

Pseudohyphae and hyphae of the filamentous phase express



Intestine, dog: Few crypts are widely dilated and contain sloughed necrotic enterocytes admixed with cellular debris (crypt abscesses). (HE, 280X).

new adhesin ligands, secrete hydrolytic aspartyl pro-teinas that injure the mucosa, and invade the mucosae and submucosa in which new groups of adherence receptors are encountered. It appears that a large group of virulence determinates are involved in the process of infection and invasion, but no single factor accounts for virulence and not all expressed virulence determinates may be necessary for a particular stage of infection.⁴

JPC Diagnosis:

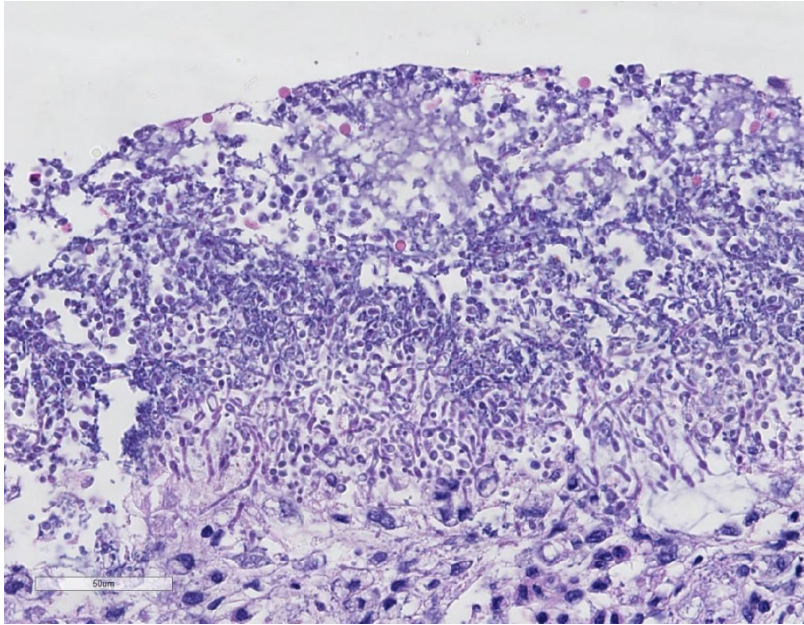
1. Small intestine: Enteritis, necrotizing, diffuse, severe with stromal collapse, crypt loss, abscessation and regeneration.
2. Small intestine, lumen: Yeasts, numerous.

Conference Comment: The contributor provides an excellent review of CPV above. Parvoviruses are common in many wild carnivore populations and result in similar symptomatic disease as seen in domestic animals. However, factors such as virus strain, host and species variations and differences in tissue tropism can result in alterations in disease manifestation and severity.⁶ In general, host ranges are determined by receptor binding, specifically to the transferrin receptor.⁹ Parvoviruses are associated with enteric disease in cats, dogs, mink and calves and are associated with reproductive losses in swine.⁹ In cases of neonatal or *in utero* infection, virus may reproduce in various tissues depending on the replicative status of the organ. This is demonstrated in the cerebellum of infected kittens where infection results in cerebellar hypoplasia and in the myocardium of neonatal puppies, which results in myocarditis. Infection of neonates typically does not result in gastrointestinal disease.⁶

CPV has also been isolated from cats as well as a few species of wild animal such as

raccoons, mountain lions, and cheetahs. In general the disease caused by CPV in cats is much less severe than in dogs and has even been isolated from clinically healthy cats.⁶ Additionally, results from at least one study have suggested that asymptomatic cats can shed CPV for extended periods and may serve as reservoirs for infection of dogs in some cases. In that study cats were documented to be shedding CPV-2a or 2b and not feline panleukopenia virus.¹ CPV-2c, a more recently emerging variant, is able to infect dogs, cats, skunks, foxes and raccoons.⁹ It has become widespread in some areas although there is disagreement regarding the relative virulence as compared to other variants.

Conference participants noted the conspicuous absence of inflammatory cells which is incongruent with the degree of tissue damage and necrosis, and characteristically results from parvo-viral lymphocytolysis and lymphoid depletion as well as lysis of myeloid precursors in the bone marrow. Leukopenia may be extensive in severe cases but a neutrophilia with left shift is often observed during recovery.⁹ Conference participants described mucosal stromal collapse with complete, cataclysmic loss of crypts. Canine parvovirus (CPV) is relatively unique among enteric viruses with its predilection for intestine crypts, and this tropism may be referred to as radiomimetic,⁴ referring to its imitation of the effects of radiation. Other causes of canine enteric disease such as coronavirus or rotavirus, both attack the villus tips and are generally associated with mild, non-fatal disease. Canine distemper virus can infect crypt epithelium but is not described as producing the degree of tissue destruction seen in CPV infection. Pathogenic *Clostridium* spp. generally produce a more hemorrhagic lesion with the presence of bacilli in the necrotic tissue, and the most severe lesions



Intestine, dog. The necrotic mucosal surface is covered by a layer of innumerable yeasts and pseudohyphae (most consistent with Candida sp.) admixed with bacteria. (HE, 368X)

will be in the large intestine.⁹ Conference participants discussed the presence of yeast in this case and most agreed they are an overgrowth or opportunistic infection, secondary to the immunosuppressive virus and change in bacterial flora, and play a minimal role in tissue damage. Classic gross lesions include segmental necrotizing enteritis producing a “red gut” with multifocal Peyer’s patch necrosis. The moderator commented that virus may be identified within germinal centers of Peyer’s patches or mesenteric lymph nodes, but in many severe cases of enteritis virus will be absent from necrotic intestinal epithelium at time of death due to sloughing and loss of enterocytes.

Contributing Institution:

UC Davis College of Veterinary Medicine
<http://www.vetmed.ucdavis.edu/pmi>

References:

1. Clegg SR, Coyne KP, Dawson S, Spibey N. Canine parvovirus in asymptomatic feline carriers. *Vet Microbiol.* 2012; 157(1-2): 78-85.
2. Decaro N, Buonavoglia C. Canine parvovirus--a review of epidemiological and diagnostic aspects, with emphasis on type 2c. *Vet Microbiol.* 2012; 155: 1-12.
3. Favrot C, Olivry T, Dunston SM, Degorce-Rubiales F, Guy JS. Parvovirus infection of keratinocytes as a cause of canine erythema multiforme. *Vet Pathol.* 2000; 37:647-649.
4. Gelberg HB. Alimentary System and the Peritoneum, Omentum, Mesentery and Peritoneal Cavity. In: Zachary JF and McGavin MD. eds. *Pathologic Basis of Veterinary Disease.* 5th ed. St. Louis, MO: Elsevier-Saunders. 2012:322-404.
5. Greene CE. *Infectious Disease of the Dog and Cat.* 3rd ed. Elsevier: Philadelphia, PA; 2006.
6. Hoelzer K, Parrish CR. The emergence of parvoviruses of carnivores. *Vet Res.* 2010;41(6):39.
7. Lamm CG, Rezabek GB. Parvovirus infection in domestic companion animals. *Vet Clin North Am Small Anim Pract.* 2008;38: 837-850, viii-ix.
8. Markovich JE, Stucker KM, Carr AH, Harbison CE, Scarlett JM, Parrish CR. Effects of canine parvovirus strain variations on diagnostic test results and clinical management of enteritis in dogs. *J Am Vet Med Assoc.* 2012;241: 66-72.
9. Uzal FA, Plattner BL, Hostetter JM. Alimentary System. In: Maxie MG, ed. *Jubb, Kennedy, and Palmer's Pathology of Domestic Animals.* 6th ed. Vol 2. St. Louis, MO: Elsevier; 2016:153-156, 185.

10. Woldemeskel M, Liggett A, Ilha M, Saliki JT. Canine parvovirus-2b-associated erythema multiforme in a litter of English Setter dogs. *J Vet Diagn Invest.* 2011;23:576-580.